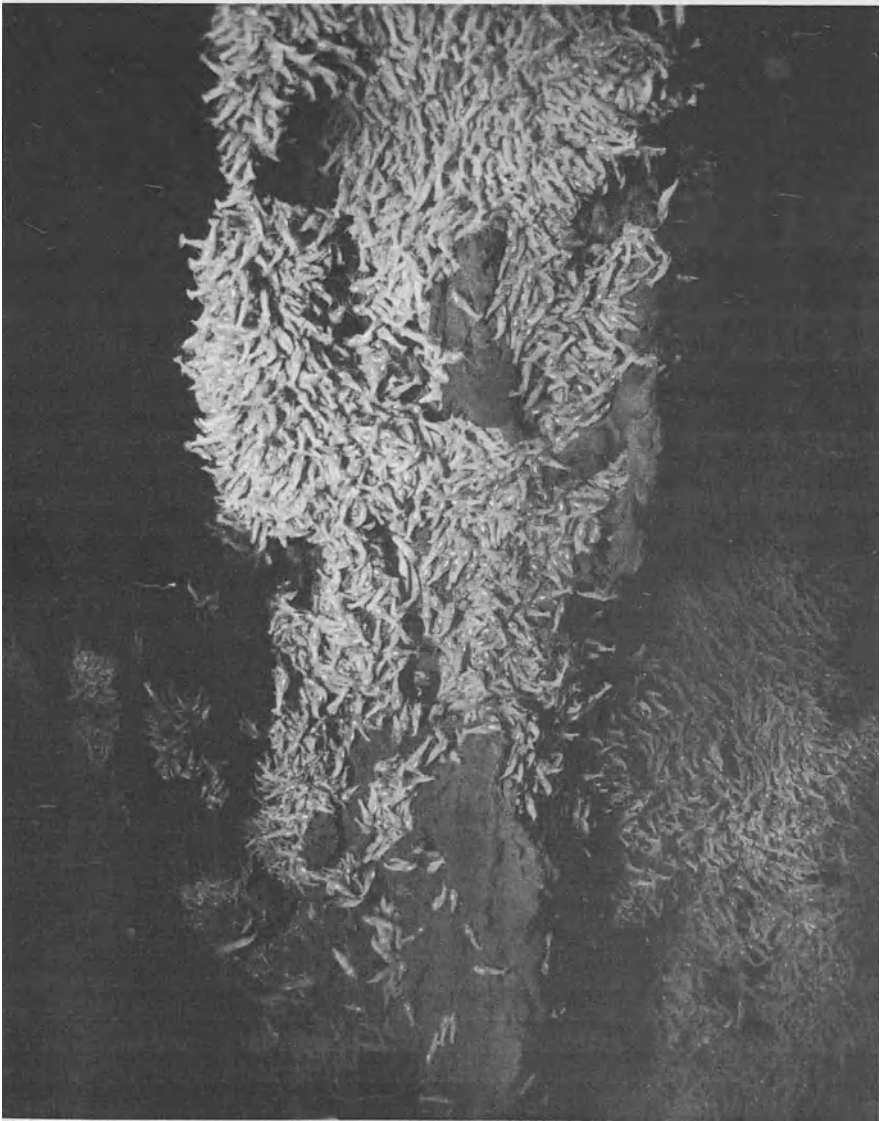A photograph made from the submersible ALVIN in May 1986 during the first dives to observe black smoker geysers that were initially discovered in the Atlantic Ocean by the NOAA VENTS Program in 1985. The photograph shows vent shrimp (individual length 2 to 5 centimeters) of a new variety swarming over a chimney (heigh about 2 meters) built of polymetallic sulfide minerals through which a black smoker geyser is venting. The scene occurs at a water depth of 3,630 meters (12,000 feet) about 3,300 kilometers (1,800 miles) due east of Miami, Florida at the Mid-Atlantic Ridge, a submerged volcanic mountain range that extends along the center of the Atlantic Ocean. The photograph was made by a research team of scientists from the National Oceanic and Atmospheric Administration (NOAA), the Woods Hole Oceanographic Institution (WHOI), and the Massachusetts Institute of Technology (MIT). This photograph, and its caption, were kindly supplied by Dr. P.. Rona, of the Oceanic and Atmosphere Administration (USA), and published in EOS. 18th of November issue (vol. 67, No. 46).

Franco Pirajno

Hydrothermal Mineral Deposits

Principles and Fundamental Concepts
for the Exploration Geologist

With 288 Figures

Professor Dr. FRANCO PIRAJNO
Rhodes University
Department of Geology
Mineral Exploration
P.O. Box 94
Grahmstown 6140
South Africa

Present address:
2/34 Kennedy Street
Maylands 6051
Western Australia

To my parents
Edgardo and Carmen Pirajno

Preface

This book is intended primarily for exploration geologists and post-graduate students attending specialist courses in mineral exploration. Exploration geologists are engaged not only in the search for new mineral deposits, but also in the extension and re-assessment of existing ones. To succeed in these tasks, the exploration geologist is required to be a "generalist" of the Earth sciences rather than a specialist. The exploration geologist needs to be familiar with most aspects of the geology of ore deposits, and detailed knowledge as well as experience play an all important role in the successful exploration for mineral commodities. In order to achieve this, it is essential that the exploration geologist be up to date with the latest developments in the evolution of concepts and ideas in the Earth sciences. This is no easy task, as thousands of publications appear every year in an ever increasing number of journals, periodicals and books. For this reason it is also difficult, at times, to locate appropriate references on a particular mineral deposit type, although this problem is alleviated by the existence of large bibliographic data bases of geological records, abstracts and papers on computers. During my teaching to explorationists and, indeed, during my years of work as an explorationist, the necessity of having a text dealing with the fundamental aspects of hydrothermal mineral deposits has always been compelling.

Metallic mineral deposits can be categorised into three great families, namely: (1) magmatic; (2) sedimentary and residual; (3) hydrothermal. This book deals with the hydrothermal family. Hydrothermal activity, in its broadest sense, is responsible for a very wide range and variety of metallic ore deposits. The intent of this book, however, is not to provide a classification of hydrothermal mineral deposits, for which the reader is referred to Guilbert and Park (1986). The main purpose of this book is to guide the exploration geologist to the most economically and geologically important hydrothermal systems, their possible origin and nature, and the nature of their products, i.e. the ore deposits – and the geotectonic setting in which they occur.

As mentioned above there is today a large number of published works dealing with specific aspects of hydrothermal mineral deposits. In general, a great deal of emphasis is placed on laboratory data, such as experimental studies, isotope systematics and geochemistry. As a consequence, field geological observations have suffered a decline. Many of these works are collected into edited volumes, which treat hydrothermal deposits by

district or regions, environments of ore deposition, or by geological age. Although by no means exhaustive, I have endeavoured to record in this book the fundamentals of the geology of hydrothermal ore deposits, and the most recent conceptual models which, however imperfect or incomplete, attempt to explain their origin. These models are based on the available evidence and clearly, as more information is published, they will need to be refined, modified or changed altogether. In so doing, I have drawn heavily from the published work of specialists and therefore the theories, concepts and ideas presented are the result of many years of research by Earth scientists from all over the world.

Some of the information presented in this book is drawn from unpublished and published works carried out whilst I worked as an exploration geologist in southern Africa, Southeast Asia, Australia, New Zealand and the southwest Pacific islands. Much of the information on southern African deposits was gained during my years as Professor of Exploration Geology at Rhodes University in Grahamstown. During this time, I directed and co-ordinated post-graduate courses in exploration geology, which include field-based studies of ore deposits, their genesis and tectonic settings. This afforded me the unique and pleasurable opportunity of examining and studying a wide range and a great number of mineralised environments, such as only southern Africa can offer. Consequently, two biases – which reflect my experience and provinciality – are discernable in the text. One bias is geographic, as many of the examples discussed are from southern Africa and Oceania. However, I make no apology for this geographical bias, because these land masses are endowed with a wide spectrum of hydrothermal mineral deposits. The other bias is on the selection of topics. These I have chosen largely on the basis of what I believe to be interesting and useful for the explorationist.

Finally, the reader must note that I take full responsibility for the contents of this book. If some of the ideas and concepts taken from the literature have been misrepresented, this was unintentional, and in no way reflects a disregard of the original author(s)' work.

Reference

Guilbert J M, Park C F (1986) The geology of ore deposits. Freeman, San Francisco, 985 pp

Acknowledgements

Lori Wadeson draughted most of the illustrations, while Amanda Butcher read the manuscript and helped with the editing. The last chapter was completed in Perth, Australia, and I wish to express my gratitude to an old friend – Murray Surtees – for having made available the facilities of his office.

My wife, Mariateresa, accompanied, supported and encouraged me throughout this long journey.

<div align="right">FRANCO PIRAJNO</div>

Contents

Part II   Crustal Evolution, Global Tectonics, Hydrothermal Mineral Deposits and Mineral Exploration – Geotectonic and Metallogenic Analysis of Orogenic Belts

Part III   Hydrothermal Processes and Activities – Related Mineral Deposits

Introduction

In the study of hydrothermal mineral deposits, the main objective is a basic understanding of ore genesis processes and the eventual building of models, which would best explain empirical observations, and enable deposit types to fit within the local and global geotectonic frameworks. The information required to achieve this must include: (1) origin and composition of the ore solutions; (2) physico-chemical conditions of solution, transport and deposition; (3) temperature, pressure and depth of ore formation; (4) source of the ore constituents; (5) metasomatic processes; (6) local geology and structure; (7) regional geology and tectonic setting; (8) origin and evolution of the magmas that give rise to hydrothermal processes. This information must be obtained through studies of geological characteristics and field relationships, mineralogy, trace and major element geochemistry of ores and wall rocks. The study of fluid inclusions provides data on the nature of the solutions, temperature, pressure and depth of ore formation, while stable isotope systematics helps in constraining the source of the fluids and tracing their movement through, and interaction with, the crust. Thus, it can be seen that the study of an ore deposit is a multidisciplinary effort. It requires that information be drawn from "outside" disciplines, such as physics, chemistry, mathematics and computer science, as well as the various branches of the Earth sciences.

Regional geological, structural and tectonic studies are of great importance in order to understand the metallogeny of a sector of the Earth's crust. The study of individual deposits and groups of deposits contributes to the understanding of the tectonic and metallogenic framework of an area. Conversely, a clear idea of the tectonic setting and geodynamic history of a region, or an orogen, is extremely important in order to predict the types and styles of mineralisation that may occur. The predictive capacity of regional or global geotectonic perspectives is often underestimated or underutilised.

As mentioned above one of the ultimate objectives is the construction of an ore deposit model. A mineral deposit model describes the essential characteristics of a group or class of mineral deposits. In modelling ore deposits, therefore, all the available information must be considered. The model may or may not include a theoretical component, in which ideas and concepts that attempt to explain the origin of the mineralisation and its relationship with the hosting rocks, are proposed. Genetic models tend to evolve from the simplistic, when the data base is limited, to the complex, as this data base grows. Thus, even those deposits whose genetic processes were seen to be well established may be questioned as more and more data become available. A striking example of this is provided by the conglomerate-hosted Au-U ores of the Witwatersrand basin in South Africa (see Chap. 15). Ore deposit models

are inexpensive but effective tools for mineral exploration and they are useful for the preliminary assessment of the mineral resources of a region.

Each chapter in this book can be considered on a "stand-alone" basis, so that the reader interested in a specific hydrothermal system can simply select the relevant chapter. There are 15 chapters, which are organised into three parts. Part I is an introduction to the nature and types of hydrothermal systems and wall-rock alterations. Part II deals with crustal evolution and the relationship of hydrothermal mineral deposits to the geological evolution of the Earth and it examines the relationship between tectonic settings and hydrothermal mineral deposits. This is accompanied by brief comments on mineral exploration techniques. Part II ends with a chapter on geotectonic and metallogenic analyses of selected areas in southern Africa and Oceania. In Part III hydrothermal processes are treated more specifically and in greater detail, and are accompanied by discussions on selected examples which, in my opinion, best illustrate these processes.

Part III begins with deep-seated magmatic-hydrothermal systems (Chap. 8 on alkali metasomatism; Chap. 9 on greisens). The following chapters reflect the increasing role, with shallowing depth, of meteoric waters in the hydrothermal systems and increasing degrees of water/rock ratios. Thus, Chapter 10 looks at porphyries and skarns, while Chapter 11 examines active and fossil geothermal (epithermal) systems and related volcanic- and sediment-hosted mineral deposits. Kuroko and Precambrian volcanogenic massive sulphide deposits are included in this latter chapter because they represent the submarine equivalent of subaerial geothermal systems. In Chapters 12 and 13 rifting (oceanic and continental) associated hydrothermal activity and mineral deposits are discussed. Oceanic crust environments are examined in Chapter 12 with a discussion on present-day occurrences and their fossil equivalents in the geological record. In Chapter 13 the complex topic of continental rifting and related hydrothermal mineral deposits is examined. It includes examples of present-day mineral deposition in modern rifts. The discussion of deposit types in this chapter encompasses a wide range, from epigenetic to syngenetic, and includes deposits ranging from the Messina breccia pipes, to sediment-hosted massive sulphide deposits, stratiform and stratabound disseminated sulphides and banded iron formations. In most of these deposits the relationship to rifting is based on good evidence, but in a few this is not clear cut and, to add to the problem, there are some deposit types which are of a transitional character. For this reason, it is expedient to consider the rift-related mineralisation in terms of end-member (incipient to advanced) stages of rift evolution.

Low-temperature hydrothermal processes related to the dewatering of sedimentary basins, which result in the formation of carbonate-hosted base metal deposits, are examined in Chapter 14. High-temperature metamorphic processes are examined in Chapter 15, which deals with mesothermal vein lodes of Archean and Phanerozoic age, most of which are economically important by virtue of their precious metal content. Ideas and conceptual models on the genesis of Archean lode deposits have flourished in the last decade and for this reason this topic is treated in greater detail.

I conclude with a brief look at hydrothermal deposits which may have originated through a number of genetic processes. A synopsis of hydrothermal processes in the Earth's lithosphere is given in an Epilogue.

Part I

Nature and Types of Hydrothermal Solutions and Systems

Chapter 1
Water and Solutions

1.1 Introduction

By way of an introduction to the study of hydrothermal mineral deposits, this chapter reviews what we understand of water, its origin on our planet and its significance in terms of planetary, hydrothermal and ore genesis processes. The nature of solutions, solubility, the phenomena of hydrolysis and hydration, redox potential and fugacity are also briefly considered, before continuing with a discussion of the nature of a large group of mineral deposits, whose origin is attributed to the action of hydrothermal solutions.

For a more detailed study of the subject covered during the course of this chapter, the interested reader is referred to the books of Mason (1966), Krauskopf (1979), Masterton et al. (1981), Press and Siever (1982), Holland (1984) and Gill (1989).

1.2 Water: Its Origin and Significance

An oxide of hydrogen, water is composed of two hydrogen atoms and one oxygen atom. It is a volatile polar molecule in which the oxygen atom possesses a weak negative charge and the hydrogen atoms a weak positive charge. The polarity of this molecule is important, making it a good ligand for cations and enabling processes of hydration and hydrolysis (Sect. 1.6). Pure water dissociates according to:

$$H_2O = H^+ + OH^-$$
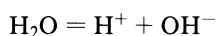
The OH^- ion is known as the hydroxyl group, which commonly enters the structures of a large group of minerals, such as amphiboles and micas.

Perhaps surprisingly water is a minor constituent of our planet. Slightly more than 70% of the surface of the Earth is covered by a thin film of liquid water. In fact if the planet's dimensions are taken in due account, the oceans constitute less than 0.03% of the total mass of the Earth. Nevertheless, water is not an uncommon constituent in other parts of the solar system, where it may be abundant as water-ice in the outer planets. By contrast the "rocky", or terrestrial planets (Mercury, Venus, Earth, Mars) are relatively dry. Water on Earth occurs as a liquid phase in the oceans, rivers, lakes and underground in the pores of the solid surface materials; as a vapour in the atmosphere and as volcanic emissions; as a solid phase in the polar ice

caps and mountain glaciers; and as a chemical constituent of the hydrous minerals in the crust and mantle. All of this water participates in two major geological cycles: the endogenic cycle, which derives its energy from the interior of the Earth, giving rise to tectonic, igneous and metamorphic processes; and the exogenic cycle at and close to the surface, which derives its energy from the Sun, and promotes the interaction of the hydrosphere, atmosphere and lithosphere (hydrologic and weathering cycles).

Juvenile water is that which has never been part of the surface cycle. While its existence may be postulated its detection remains elusive in scientific investigation, because of the obvious contamination with recycled water. One possible way of detecting juvenile water is in those minerals of mantle origin for which a unique isotopic composition must be postulated (Sheppard 1986). Water is a vital constituent of the physical world, being readily found in all three states of matter – liquid, solid and gas. Used as a standard for physical constants, it is a powerful solvent, which carries and deposits substances, and in which life abounds. Life, in the sense that we understand it, most probably originated in water, and to remind us of this, all living things are made up of light constituents of which water is by far the major one.

1.2.1 Planetary Evolution and the Origin of Water

The Earth was formed approximately 4.6 Ga ago. The planets of the solar system closest to the Sun – Mercury, Venus, Earth-Moon system, Mars and the asteroid belt – are rocky and volatile-poor compared to the outer planets. The planets were formed by the collision and cold accretion of nebular grains and larger bodies known as planetesimals, whose compositions differed at different distances from the parent solar nebula. The solar nebula is the raw material of our system, and is estimated to be comprised of a 98% mixture of H_2 and He, less than 2% volatiles (H_2O, CH_4, NH_3, etc), and approximately 0.5% solids containing SiO_2, MgO, FeO, FeS etc. (Lewis and Prinn 1984). Metals, oxides and silicates dominate in the region between Mercury and the asteroids, whereas further beyond water-ice, methane, ammonia and other light materials are more abundant. Nevertheless, comparatively small amounts of these volatiles were present in the accreting rocky debris at the time of the Earth's formation. The newly-formed terrestrial planets were subsequently heated through three main processes: impact energy, gravitational compression and radioactivity. As heat was produced far more rapidly than it could flow out into space, melting began to take place. This initial melting led to the differentiation of the planetary bodies into a series of shells with progressively lighter materials towards their surfaces. On Earth aluminium, silicon, potassium and sodium accumulated as a slag to form the outermost shell (crust) towards the surface, followed by an inner shell (mantle) composed of Fe and Mg silicates with denser and more closely packed crystal structures. The sinking of heavier metallic materials in turn gave rise to the formation of an innermost shell (core), believed to consist mostly of an Fe-Ni alloy. It follows that the Earth's crust has different elemental abundances compared to the whole Earth, as shown in Table 1.1.

Table 1.1. Average composition of sea water in part per thousand (ppt), and as percent of total. (After Mason 1966)

Crust		Whole Earth	
O	46%	Fe	35%
Si	28%	O	30%
Al	8%	Si	15%
Fe	6%	Mg	13%
Mg	4%	Ni	2.4%
Ca	2.4%	S	1.9%
K	2.3%	Ca	1.1%
Na	2.1%	Al	1.1%
other	<1%	other	<1%

A natural consequence of heating and partial melting is volcanic activity that is, the expression of the transfer of heat and mass out onto and towards the surface. It is here that the process of volatile release took place, as it does today through volcanoes and at mid-ocean ridges. Outgassing of water and volatiles, including CO_2, CO, H_2S, H_2, N_2, CH_4, NH_3, HF, HCl, Ar, Ne etc., occurred at a great rate (big burp hypothesis) during this early period of differentiation. Planetary bodies with sufficient gravity, such as the Earth and Venus, and to a lesser extent Mars, were able to retain most of these volatiles, with the exception of H_2 and He which escaped into space. It is calculated that the juvenile volatiles were outgassed during the first 10^8-10^9 years (Pollack and Yung 1980).

On Earth the temperature must have been low enough to allow condensation of water with much CO_2 in solution, and the leaching of other elements from the surface materials. This water collected first of all into pools and then into larger basins to form the oceans. It has been proposed that these larger basins were mare–type basins, such as those formed on the Moon, initially formed by the flux of asteroid-size objects (Frey 1977). Most of the Earth's water took up residence in the oceans, and CO_2 in carbonate rocks, while the other volatiles formed a gaseous shell enveloping the entire planet (atmosphere). Studies in the dating of minerals by ion-probe techniques suggest that some form of continental crust must have been in existence since at least 4.1 Ga (Froude et al. 1983). The presence of sedimentary rocks as old as 3.8 Ga indicate that a hydrosphere and atmosphere must have been well-established since at least that time, suggesting consequences in later developments far more profound than is usually acknowledged by planetary geologists. For example, an unresolved question remains as to whether a granitic crust was formed at one particular early stage or some 500 Ma later, as suggested by the ion-probe dating mentioned above. Equally unresolved is the question of whether the early crust evolved by progressive differentiation of products of partial melting of a solid mantle, or, as seems to be the case for the lunar highlands, by early crystallisation directly from planetary-wide melting. The mass of the Earth' crust relative to the rest of the planet is only about 0.5% and, as pointed out by Taylor and McLennan

(1985), it, like the hydrosphere, may be unique to our planet, since nothing like it has as yet been found on other planets, with the possible exception of Venus. In other words, the retention of a hydro-atmospheric envelope was probably one of the essential ingredients for the development and evolution of a granitic crust. The weathering cycle allowed the accumulation of sedimentary packages, which through metamorphism and partial melting formed crustal melts of granitic composition.

Recent hypotheses on the origin and evolution of the primordial continental crust have been proposed by Kröner (1985) and Lowman (1989). Both these authors envisage an important role for mantle plume (hot spot) volcanism as a crust-building mechanism. Lowman (1989) proposes that an early crust developed by non-plate tectonic global differentiation followed by basaltic underplating and overplating. This basaltic volcanism would have been initiated by basin-forming meteorite impacts at least 4 Ga ago. Kröner (1985) for the building of the early crust, places his emphasis on hot spot volcanism, differentiation and re-melting.

1.2.2 Water – Past and Present

The atmosphere and hydrosphere together make up the gaseous-liquid envelope of the Earth, and, as outlined above, were first formed by the early outgassing of the planet. Condensation of liquid water and its accumulation in low-lying areas, or protobasins, formed the early oceans, which explains the discontinuity of the liquid envelope around the Earth. The hydrosphere comprises all the waters at the surface of the Earth, oceans, lakes, rivers and ice. Present-day oceans cover approximately 366×10^6 km^2, or 70.8%, of the surface of the Earth. The mass of sea water constitutes roughly 98% of the total hydrosphere, and fresh waters the remaining 2%, of which about 22% is groundwater. Approximately 77% of the fresh water is locked up in ice, and less than 1% is surface meteoric water. This makes water a precious commodity.

The history of the hydrosphere and atmosphere is essentially the result of the interplay of volcanic activity, tectonism and the increasing role of biological activity (Holland 1984). Evidence from both terrestrial and marine environments indicates that the salinity of the early oceans had already been established since the formation of the first large bodies of water more than 4 Ga ago. Thus the primeval oceans must have contained significant concentrations of Cl^-, Na^+, Ca^{2+} and Mg^{2+}, with Na^+ and Cl^- being the dominant cation and anion respectively (Holland 1984). That the early oceans were saline is also corroborated by the presence of sedimentary deposits of evaporitic origin in rock sequences of Archean age, such as those of the Warrawoona Group (3.5 Ga) in Australia. In the rocks of this Group, well-developed, rosette-shaped minerals replaced by silica are interpreted to represent casts of evaporite minerals such as gypsum (Holland 1984). There is also by now irrefutable evidence that the oxidation state of the atmosphere was gradually acquired through the geological ages, and that during the first 500 Ma it had at least a mildly reducing character. Evidence from paleosols, the Witwatersrand paleoplacers in South Africa, with their detrital pyrite and uraninite grains, and the banded

Table 1.2. Average abundance by weight of elements in the crust and the whole Earth (After Press and Siever 1982)

Ion	ppt	percent
Cl^-	18.98	55.05
Na^+	10.56	30.61
SO_4^{2+}	2.65	7.68
Mg^{2+}	1.27	3.69
Ca^{2+}	0.40	1.16
K^+	0.38	1.10
HCO_3^+	0.14	0.41
Br^-	0.065	0.19
H_2BO_3	0.026	0.07
Sr^{2+}	0.008	0.03
Total	34.48	99.99

Table 1.3. Chief salts of marine evaporites. (After Krauskopf 1979)

Chlorides	Formula
Halite	$NaCl$
Sylvite	KCl
Carnallite	$KMgCl_3.6H_2O$
Bishofite	$MgCl_2.6H_2O$

Sulphates	
Kainite	$KMgClSO_4.11/4H_2O$
Anhydrite	$CaSO_4$
Gypsum	$CaSO_4.2H_2O$
Polyhalite	$K_2MgCa_2(SO_4)_4.2H_2O$
Kieserite	$MgSO_4.H_2O$

iron formations, suggest an atmosphere poorer in oxygen during the Archean than today.

The composition of sea water is defined by salinity, which is the total amount of dissolved solids per kilogram of water. Table 1.2 gives an average composition of sea water. The precipitates obtained from the evaporation of sea water (evaporites) can constitute important non-metallic orebodies. Leaching of ancient evaporites may influence the composition and precipitation of sulphide species, as is the case for the sulphide brines formed in the Red Sea (see Chaps. 3 and 13). Table 1.3 lists some of the more common and important salts of marine evaporites.

Sea water also contains gases in solution (O_2, N_2, CO_2, Ar, H_2S) as well as a host of other elements including Li, C, Al, Si, P, Ti, V, Mn, Fe, Co, Ni, Cu, Zn, As, Se, Rb,

ATMOSPHERIC CIRCULATION
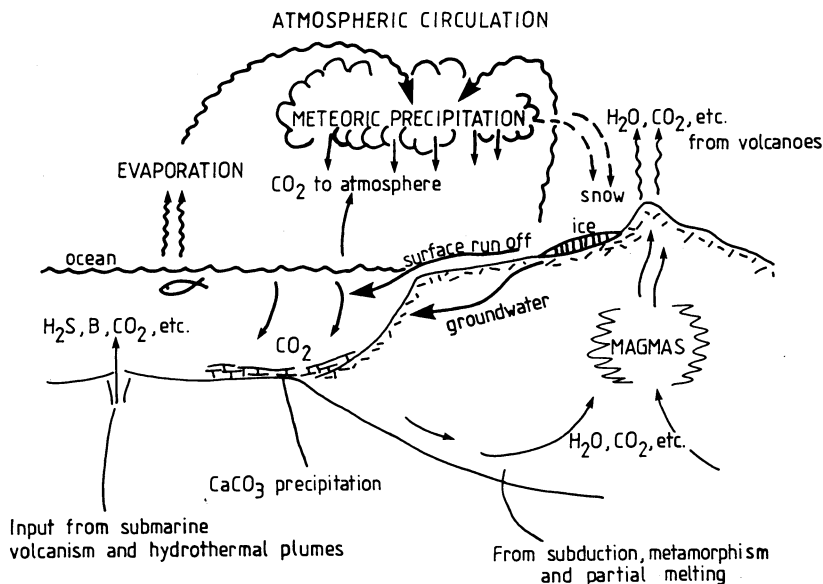
Fig. 1.1. Endogenic and meteoric cycles of H_2O and CO_2 (After Press and Siever 1982)

Mo, I, Ba. Elements such as Au, Ag, Hg, Pb and U are present in even lesser quantities than chloride, carbonate and sulphide species. H_2S may be locally abundant, especially in stagnant organic-rich bottom waters (e.g. Black Sea) and in the areas of mid-ocean ridges.

Meteoric, or terrestrial, waters though minor components of the hydrosphere, are important in that they are responsible for the weathering, erosion and transport of material from the land masses. Figure 1.1 shows the hydrologic cycles from ocean to atmosphere, to land and back to ocean. It is estimated that meteoric water carries some 27.4×10^{14} g of dissolved matter per year. The average salinity of river water is about 100 ppm. Table 1.4 gives the average composition of dissolved solids in river water.

The amount of dissolved solids carried by the rivers annually is but a small fraction of the total mass of solids contained in the sea (49.5×10^{21} g). The material added to the oceans by the rivers is augmented by that from submarine volcanism along the active mid-ocean ridges, which injects the most common anions in the sea (Cl^-, SO_4^{2-}, B, Br). To determine the budget of dissolved matter, it is important to know the average length of time that each element remains in the sea (residence time). This is calculated by dividing the total amount of any one element in solution by the amount introduced each year by terrestrial waters. In terms of this residence time, elements with the highest abundance (Na, Cl, Mg, Ca, K) are found to have the longest residence time, whereas those with lowest abundance (e.g. Fe, Al, Zn, Cu, Mn, Pb, Au, Ag) have the shortest residence time. Figure 1.2 shows the relationship between oceanic residence time of elements and their concentrations, as calculated by Whitfield (1982), who has presented a view of the oceanic dynamic system using

Table 1.4. Average composition of dissolved solids in river water expressed in parts per million (ppm), and as percent of total. (After Mason 1966)

Ion	ppm	wt%
HCO_3^-	58.5	48.6
Ca^{2+}	15	12.5
SiO_2	13.1	11.0
SO_4^{2-}	11.2	9.3
Cl^-	7.8	6.5
Na^+	6.3	5.3
Mg^{2+}	4.1	3.4
K^+	2.3	2.0
NO_3^-	1	0.8
Fe	0.7	0.6
Total	120	100.0
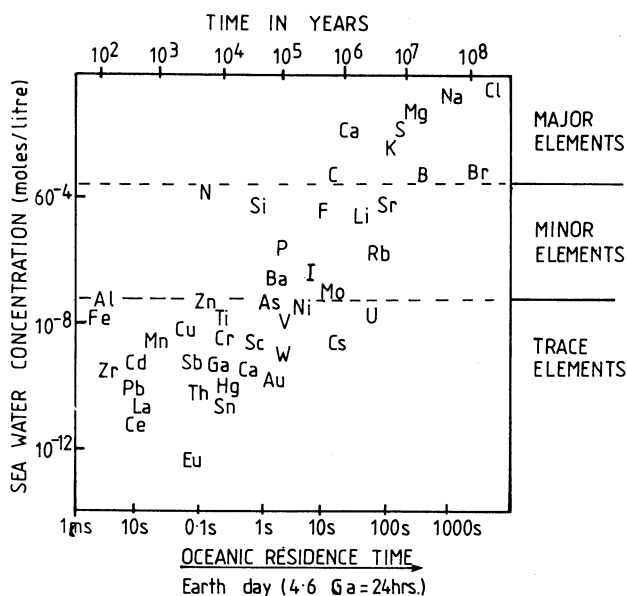
Fig. 1.2. Residence time of elements in oceanic water in relation to concentration (After Whitfield 1982)

the Earth-day method, in which the 4.6 Ga of the Earth's history is compressed into 24 h. At the present rate, rivers transport enough material every "hour" to fill the ocean basins, while every 18 "seconds" the amount of dissolved material transported by rivers would double the amount of salt in the oceans. The longest residence time of the major elements is only about 1 "minute", most of the trace elements remain in

the sea less than 1 "second". Sediments in the sea are less than 1 "hour" old, as the deposited material is continuously subjected to tectonic uplifting and subduction. Despite this dynamic flux, Whitfield points out that geological evidence suggests sea water composition has remained constant for at least 11 "hours", or 2000 Ma. One of the most remarkable characteristics of the oceans is that the concentration of those elements which may be harmful to living organisms (e.g. As, Se, Hg, Pb etc.) does not increase, as might be expected from the annual input from the rivers. Whitfield (1982) explains the chemical budget of the oceans in terms of a steady-state model; in other words, material is added and removed at a constant rate. He also suggests that while the composition of sea water is largely controlled by geological processes, the biotic masses may also influence modern-day seas in their control of the elements' distribution, as indicated by the correlation between the biological importance of an element and its concentration (Fig. 1.2).

Some scientists believe that the composition of sea water has not remained constant throughout the geological ages. Spencer and Hardie (1990), for example, consider that the composition of sea water is controlled by the mixing of two major inputs, namely Na-HCO_3-SO_4 from rivers and Ca-Cl from hydrothermal discharges at mid-ocean ridges. Therefore the concentration of these ionic species in the sea could have varied with time as a function of the intensity of hydrothermal discharges from mid-ocean ridges and climatic changes. These authors argue that a smaller development of mid-ocean ridges would result in lesser fluxes of Ca and Cl and higher solubilities of Na^+, Mg^{2+}, SO^{2-}_4 and HCO^-_3 from river input and viceversa in the case of larger mid-ocean ridges. This would also affect the composition of marine evaporites, in which aragonite rather than calcite and Mg-rich salts would predominate for small ocean ridges fluxes, whilst calcite and K-rich salts would predominate in the other case.

1.2.3 Water in Subduction Zones

It has been calculated that, given the present rate, the entire oceanic crustal mass would be subducted within about 1000 million years, which implies there must be a strong return flow (Fyfe 1978). Endogenic processes are responsible for this continuous return flow, which has very important implications as hydrothermal activity occurs in those regions in which this return flow is most efficient. Large-scale release of fluids (O_2, H_2O, CO_2, S) occurs during subduction as volatile and water-bearing materials are dragged down into the mantle. At depth along the subducting slab, hydrated minerals such as amphibole and mica lose their bound water and other volatiles. During subduction of oceanic lithosphere, re-equilibration to the higher temperature and pressure of amphibolite facies in a region of $20 \times 10 \times 1$ km releases a mass of fluid of some 20 km^3. A proportion of this fluid moves upward through hydrofracturing, or via thrust planes (Fig. 1.3). Fyfe (1978) points out further that in addition to the volatile phases, other elements such as K, Rb, Na, U are also recycled into the mantle. In the mantle wedge above the subducting slab, mantle melts form aided by the release of volatiles. Magmas generated in subduction environments can contain in excess of 0.5% water, and
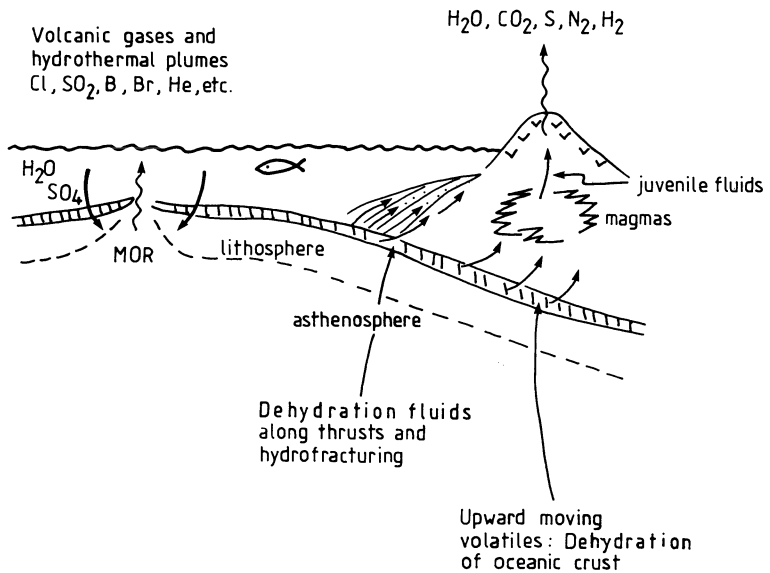
Fig. 1.3. Idealised scheme of circulation of H_2O and other volatiles in the lithosphere-hydrosphere-atmosphere system. MOR Mid ocean ridge

active volcanism at convergent plate boundaries is a powerful contributor of volcanic gases into the atmosphere, mainly H_2O, CO_2 and S. At mid-ocean ridges the uprise of mafic melts probably results in the addition of juvenile gases – including water – into the ocean, although a large amount of sea water is consumed during the penetration of the water in the crust and subsequent hydration reactions. It is estimated that the total addition of juvenile water produced from volcanism and hot springs is about 0.8% of the total quantity of water circulating in the hydrosphere and atmosphere, the remaining 99.2% being recycled water (Mason 1966).

1.2.4 Water in the Crust

Meteoric waters in surface materials constitute groundwater, and their infiltration is controlled by porosity and permeability. Below the groundwater table, rocks are almost completely saturated with water, which deeper down heats to become a brine as it dissolves more and more solids. It is likely that water penetrates to depths of at least 15 km, since geophysical data support the presence of conducting layers at depths of 15–20 km. These layers are interpreted to be an effect of free water in the deep crust, present either as intergranular films, or as water contained in major crustal discontinuities (e.g. underthrust sheets), or both (Taylor and McLennan 1985). The abundance of water at great depths in the crust was confirmed by a Russian drilling programme in shield areas. In the Kola peninsula, for example, zones of hydraulic fracturing and mineralising fluids have been observed at depths

of between 4 and 9 km (see Chap. 2). In the absence of magmatic activity, the origin of this water is thought to be dehydration in the high temperature environment of amphibolite to granulite facies metamorphism in the lower crust. In oceanic areas water probably penetrates to depths of about 8 km.

1.3 Solutions

Ore-forming fluids may occur as molecular solutions, or colloidal solutions.

Hydrothermal fluids are generally assumed to be liquid solutions in which water is the solvent. A true, or molecular solution is defined as a homogeneous system containing a dissolved substance (solute) distributed uniformly in a dissolving substance (solvent). Solutions can exist in all three states of matter: gas, solid or liquid. All gas mixtures are solutions (air, for example); whereas solid solutions are characterised by the substitution or interposing of foreign atoms, or ions, in the lattice sites, or between the lattices of mineral-forming elements. Solids, or gases become solutes when dissolved in liquids. If both components are liquid, it is usual to call the more abundant component the solvent. A solution is said to be saturated if it is in equilibrium with the undissolved solute. Therefore, an undersaturated solution is characterised by a lower concentration of solute with respect to the saturated solution; a supersaturated solution, on the other hand, contains more than the equilibrium concentration of solute. This latter type is usually unstable. There are two types of solute in water: non-electrolytes and electrolytes. In non-electrolytic water solutions the solute dissolves as molecules and therefore they do not conduct electric current. Examples of non-electrolytic solutions are methyl alcohol, or sugar in water. Electrolytic solutions conduct electric current through the dissolved substances which are present as electrically charged ions. NaCl is a typical example which, when dissolved in water, dissociates into its constituent ions:

$$NaCl(s) = Na^+ (aq) + Cl^- (aq).$$

Other examples are:

$$Na_2SO_4(s) = 2Na^+(aq) + SO_4^{2-} (aq);$$

$$HCl (aq) = H^+ (aq) + Cl^- (aq).$$
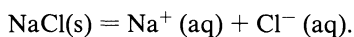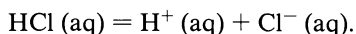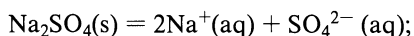
The concentration of solutes in aqueous solutions is expressed as moles of solutes per litre of solution, defined as molarity or molar concentration, and indicated as "M". A mole is the number of a given element's molecules, or atoms, contained in its unit molecular or atomic mass. For example, one mole of O_2 contains 6.022×10^{23} O_2 molecules (Avogadro's number) in exactly 32 g (atomic mass 16 $\times$ 2), and one mole of H_2O contains 6.022×10^{23} H_2O molecules in 18.02 g of H_2O (2.016 + 16.00 atomic masses of H_2 and O respectively). A one-molar solution (1 M) therefore contains one mole (1 mol) of solute per litre of solution.

A colloidal solution is made up of a dispersed phase, solid, liquid or gas, and diffused in a medium which can be either solid, liquid or gas. A review of the general

properties of colloidal systems can be found in Krauskopf (1979, p.120–139), from whom the following is summarised. In ore-forming colloidal systems, solid phases are dispersed in liquid (sol), or gaseous media. The size of the particles is in the range of 10^{-3} to 10^{-6} mm (1000 to 1 μm). Colloidal particles have a very high surface area to volume ratio and behave as electrically charged particles. Their charge is due to adsorption of ions, making colloidal particles repel each other, so that settling is difficult, or impossible. The addition of an electrolyte to the system will neutralise the colloidal particle to enable flocculation (precipitation). When a colloid containing a certain adsorbed ion on its particles, is added to an electrolyte solution consisting of different ions, some of these electrolytic ions will be adsorbed, displacing the original ions, which will then pass into the solution. This is the phenomenon of ion exchange, and an important mechanism in explaining the distribution of cations between solutions and wall rocks. The high concentration of metals in manganese ores can be attributed to adsorption of cations on manganese dioxide sols. Ions that are also commonly adsorbed are H^+ and OH^-. In general, sulphides, silica and manganese dioxide sols are negatively charged, whereas oxide and hydroxide sols are positively charged.

Temperature is an important parameter for colloids in hydrothermal solutions. High temperatures favour flocculation because increased kinetic movements allow the particles to come into contact with one another, and the larger particles thus formed will flocculate (although this is not always true, because gold sols are stable at temperatures of up to 150°C). On a geological time scale colloids are unstable and tend to crystallise, so that the materials examined by the geologist may not show their pristine colloidal state. Amorphous or cryptocrystalline substances with colour banding may have had a colloidal origin. Certain textures of metallic ores in hydrothermal veins and some finely crystalline ores in open cavities are also thought to form from colloidal solutions. Silica in hot springs may also be of colloidal origin. At the Sleeper bonanza Au deposit in Nevada (USA) evidence of colloidal solutions, responsible for the transport of Au and silica, is provided by alternating bands of barren colloform quartz and mineralised opaline quartz (Saunders 1990).

1.4 Solubility and Boiling

Boiling and solubility are instrumental in the separation of components from the solutions, and therefore of great importance in the deposition of ores from hydrothermal fluids.

The solubility of ionic substances is the result of interaction between polar H_2O molecules and the dissolving ions. Solubility depends on: 1) the force of attraction between H_2O molecules and the ions of the solid, which tends to bring the solid into solution; and 2) the force of attraction between oppositely charged ions which will tend to prevent the solid from going into solution. Generalized solubility rules are as follows (Masterton et al. 1981):

NO_3^- All nitrates are soluble.
Cl^- All chlorides are soluble, except for $AgCl$, Hg_2Cl_2.
SO^{2-} All sulphates are soluble except $CaSO_4$, $SrSO_4$, $BaSO_4$, $PbSO_4$, Ag_2SO_4.
CO^{2-} All carbonates are insoluble except those of Group elements (lI, Na, K, etc.).
OH^- All hydroxides are insoluble except Group I elements, $Sr(OH)_2$, $Ba(OH)_2$.
S^{2-} All sulphides are insoluble, except Groups I and II elements.

The above solubility rules illustrate that certain substances are insoluble, particularly the base metal sulphides. This is reiterated by Krauskopf (1979), in what he calls the "dilemma" of hydrothermal solutions. He writes that "most of the familiar ore metals – lead, zinc, copper, silver, molybdenum and mercury – occur directly as sulphides, or as complex minerals containing arsenic or antimony in addition to sulphur. Geological occurrences indicate that these compounds were deposited from solutions in water at moderate temperatures; yet these same compounds in the laboratory are among the most insoluble with which a chemist has to deal. What sort of solutions can be imagined to carry these very insoluble substances in nature?" (Krauskopf 1979, p.393). This question is considered further when we take a look at metal transport and the effects of ligands in Chapter 2.

Both temperature and pressure have major effects on solubility. Usually the dissolution of a solid is an endothermic process, brought about by the necessary absorption of heat to break down the crystal lattice. Hence an increase in temperature ($\Delta H > 0$) increases the solubility and the reaction given below moves to the right:

solid + solvent = solution; $\Delta H > 0$.
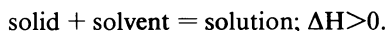
Dissolving a gas into a liquid evolves heat (exothermic) ($\Delta H < 0$), so that:

gas + liquid = solution; $\Delta H < 0$.
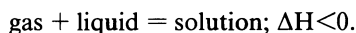
This means that gases become less soluble as temperature increases. Pressure can also have major effects on gas-liquid systems: for a given temperature an increase in pressure increases the solubility of a gas. A pressure rise increases the concentration of molecules in the gas phase, which in turn is counteracted by more molecules entering the solution. The equilibrium of the second equation above also moves to the right. Conversely a drop in pressure will cause the gas to exsolve from the solution. Boiling of a common liquid occurs at a temperature at which its vapour pressure equals the pressure above it. Boiling of a hydrothermal solution takes place for the same reason, with the immediate result that dissolved gases and other volatile compounds, such as CO_2 and H_2S, are removed from the solution. The process of boiling of hydrothermal solutions is important because it results in the precipitation of ore elements (e.g. Au, As, Sb , Ag etc.).

1.5 Acid-Base Nomenclature

A substance is said to be an acid if it produces hydrogen ions (H^+) in water solution, and a base if it produces hydroxide ions (OH^-). This terminology is not to be

confused with the geological usage of acid, basic and alkaline. Silica, being the principal oxide constituent of all rock systems, serves as a basis to determine the acidity of a rock. Thus a high concentration of SiO_2 ($>$ 66 wt.%) defines an acid rock. An intermediate rock contains between 52 and 66 wt.% SiO_2, whereas values of less than 52 wt.% define basic rocks. The basicity of a rock can also be determined by the abundance of metal oxides, such as MgO and FeO; the alkalinity of rocks by the oxides of Na and K. The above geological usage originated many years ago when SiO_2 was considered an acid oxide, and MgO,FeO etc. as basic oxides. This terminology is well-entrenched in the current geological language and is considered useful for practical purposes.

Water, whether pure or in solution, dissociates into a hydrogen cation (H^+) and a hydroxyl anion (OH^-). The dissociation constant of water (Kw) at 25°C is given as:

$$Kw = (H^+) \times (OH^-) = 1.0 \times 10^{-14}.$$

The product (H^+) $\times$ (OH^-) is constant for all water solutions, which at 25°C is always 1.0×10^{-14}; thus the concentration of H^+ or OH^- can be calculated and the acidity or alkalinity of a solution specified (Krauskopf 1979). A neutral solution has equal concentrations of H^+ and OH^-, which is 10^{-7} MH^+. A strong acid has 1 MH^+, and a strong base 10^{-14} MH^+. It is more convenient to express acidity in terms of pH rather than H^+, and this is calculated using a negative logarithmic exponent of the hydrogen concentration according to the formula:

$$pH = -\log_{10}[H^+] = \log_{10} 1/[H^+].$$

Thus a strong acid has a pH of 0, a neutral solution 7, and a strong base a pH of 14.

1.6 Structure of Water – Hydrolysis and Hydration

The structure of the water molecule is of special importance to its chemical behaviour, as discussed in Franks (1982), Neilson and Enderby (1986) and Brimhall and Crerar (1987). It has been determined that the structure of water-ice is analogous to that of tridymite, and that the oxygens in ice are tetrahedrally co-ordinated (the tetrahedron being the building block of all silicate minerals in the Earth's crust). Therefore water appears to have a pseudo-crystalline arrangement similar to the quartz structure, which possibly serves to explain its higher density relative to ice (Paton 1978). The oxygen ion in a water molecule is much larger than the hydrogen ion, with the result that the molecule can be described as a sphere, which – though neutral – has a positive charge on the side of the two hydrogens and a negative charge on the side of the oxygen. Consequently, the isolated molecule has a polar character and behaves in solution like a small magnet. This polar character is the key to the hydration and hydrolysis of silicate minerals, and thus important in weathering and hydrothermal alteration processes.

In the process of hydration water molecules are attracted to and – by virtue of their polar charges – become orientated around other attracting ions, forming hydration shells (Brimhall and Crerar 1987). Dissolution occurs when successive

layers of water molecules completely surround the ion. Polar water molecules can enter crystal lattices and orientate themselves against charged mineral surfaces. Where these molecules come into mutual contact, a lubricated surface is produced, for example clays which become slippery when wet. Water of crystallisation is part of the mineral lattice, as in gypsum ($CaSO_4.2H_2O$), or zeolitic minerals. On heating, this water is given off without breaking the lattice, and can be restored to reform the mineral.

Hydrolysis is the effect of the dissociation of water molecules into H^+ and OH^- ions. The process of hydrolysis is responsible for the breakdown of silicate minerals and involves the addition of H^+ and OH^- to bonding sites in the mineral lattice. Hydrolysis is defined as the reaction between water and the ion of a weak acid or a weak base (Krauskopf 1979, p.37). An example of hydrolysis is the reaction of fayalite with water at neutral pH:

$$2FeSiO_4 + 4H_2O = 2Fe^{2+} + 4OH^- + 2H_2SiO_4.$$
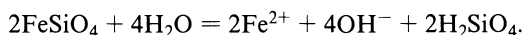
Hydrolysis reactions tend to be accelerated under conditions of low pH, as for example in the vicinity of oxidising sulphide ore bodies. The presence of H^+ ions in acid waters promotes the attack on silicate minerals resulting in the liberation of cations. These cations may remain in the vicinity and become fixed as stable secondary mineral assemblages, while others go into solution and are transported elsewhere. The mobility of these cations under different physico-chemical conditions has important implications for exploration geochemistry and for the evaluation of gossans (Reynolds 1982).

Thus hydrolysis is dependent on the concentration of H^+ ions, and any process which affects their concentration will also affect the speed and intensity of the hydrolysis process. The breaking of molecular bonds by water in a silicate melt, and consequent lowering of viscosity and consolidation temperature is a similar process. Hydrolysis of silicate minerals is very important for hydrothermal alteration, because the hydrogen ions penetrate the silicate lattices where they compete with cations (K, Ca, Na etc) to attach themselves to oxygen ions. The larger concentration of the charge in the hydrogen ions predominates, resulting in the displacement of the cations which are transferred from the silicate into the solution, while H^+ enters the silicate structure, producing in it drastic changes which convert the old silicate into a new mineral, such as sericite or illie. In silicate minerals the presence of the various ions tends to consume more hydrogen than hydroxyl ions, so that if the reaction is to proceed more H^+ ions have to be supplied. Volcanic gases (HCl, H_2S) can provide these H^+ ions and are major acidifying agents during processes of hydrothermal alteration.

1.7 Redox Potential (Eh)

An oxidation-reduction reaction is one in which transfer of electrons takes place from one element to another. The process by which certain elements lose electrons while others gain them can be quantitatively measured. This can be done by

assigning a potential difference to half-reactions, choosing as a standard the half-reaction of the hydrogen couple:

$$H_2 = 2H^+ + 2e^-.$$
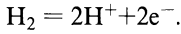
To this half-reaction potential is assigned the arbitrary value of 0 (E= 0.00 V). If the sign is positive, the half-reaction has a greater tendency to release electrons than does the reaction shown above, and the converse is true if the sign is negative. Thus, Cu with an oxidation potential of +0.16 displaces Ag with a potential of +0.22, whereas Zn (−0.76) will displace Cu (+0.16). This means that Zn will release electrons to both Cu and Ag, but Cu only to Ag. Tables of standard oxidation potentials can be found in most chemistry textbooks.

The term redox potential is used as a synonym for oxidation potential and is given the symbol Eh. The redox potential is an important parameter for characterising aqueous solutions and the oxidising and reducing conditions of a geological environment. Conventionally, it is assumed that a high Eh indicates an oxidising system, whereas a low Eh indicates a reducing system. Oxidation involves the loss of electrons, and reduction the gain of electrons. If a copper wire is immersed in a solution of silver nitrate ($AgNO_3$), the copper will dissolve and metallic silver will precipitate. The copper wire releases electrons (e^-) which combine C18 with silver cations in the solution to precipitate neutral metallic silver. This reaction involves oxidation-reduction (redox) and is shown thus:

$$Cu(s) = Cu^{+2} + 2e^-; \quad 2Ag^+(aq) + 2e^- = 2Ag(s).$$
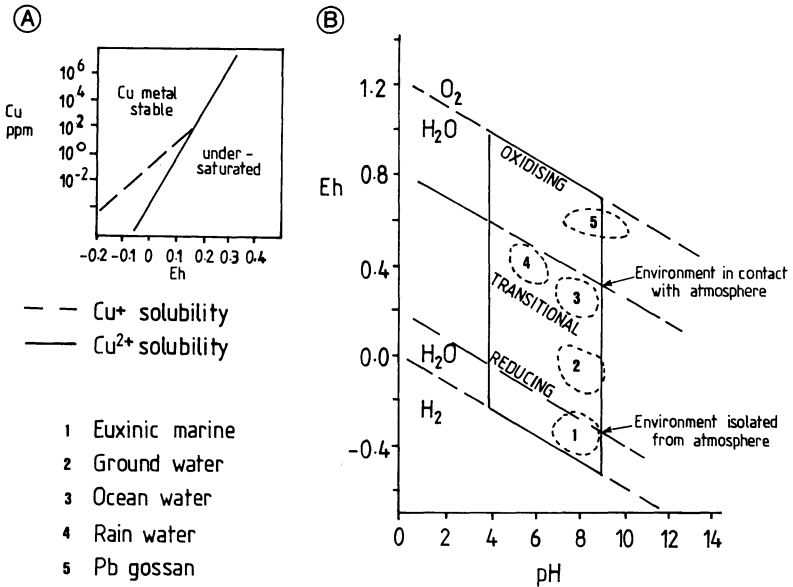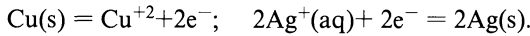
Fig. 1.4A, B. Examples of Eh-pH diagrams. A Solubility of Cu as a function of Eh values (After Rose et al. 1979). B Eh and pH limits of some natural environments (After Krauskopf 1979; Rose et al. 1979)

The net reaction is:

$$Cu(s) + 2Ag^+(aq) = Cu^{+2}(aq) + 2Ag(s).$$
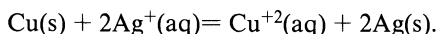
The first equation above is a half-reaction in which electrons are lost, and is therefore oxidation; the second equation is the half-reaction in which electrons are gained, and is reduction. The net result, expressed in the third and last equation, is therefore the oxidation-reduction reaction, in which Cu is the reducing agent and is oxidised, and Ag is the oxidising agent which is reduced. The same can be said for oxidation numbers, where a fictitious charge is given to an ion. Thus, for the net reaction above, Cu is oxidised because its oxidation number is increased from 0 to +2; reduction, on the other hand, results from a decrease in oxidation number, and so Ag is reduced with a decrease in its oxidation number from +2 to 0.

Eh and pH are two important variables which control the mobility of elements in a geological system, and consequently Eh-pH diagrams are useful to show conditions under which processes of oxidation and reduction can occur in nature. Examples of Eh-pH diagrams are given in Fig.1.4.

1.8 Chemical Potential, Chemical Activity and Fugacity

The terms chemical potential, chemical activity and fugacity are frequently used in discussions of hydrothermal alteration involving aspects of physical chemistry, chemical equilibria and thermodynamics.

The chemical potential indicates the capacity of one compound to react with another, and represents a particular energy level for the given compound in a phase. The chemical potential is analogous to gravitational potential energy, in which the stable state is at the lowest potential. The chemical potential can be expressed by the formula:

$$\mu_a = (dG/dX_a)_{P,T}, X_b, X_c, \text{ etc.}$$

In the equation above, the chemical potential μ of a substance a equals the change of an extensive state function G (internal energy, volume, mass) resulting from the addition of small amounts of a, while P,T and all other substances b, c etc remain constant (Best 1982). In a hydrous silicate melt at equilibrium the chemical potential μ of water equals the potential of water vapour, which in turn equals the potential of water in the hydrated minerals (Best 1982).

The activity of a chemical species is denoted by "a" and is approximately proportional to concentration and is expressed as moles per litre. In solid solutions, or mixtures of liquids, chemical activity is related to the mole fraction of the constituent. In gases, chemical activity can be approximated by partial pressure (Rose et al. 1979), and is expressed by:

$$a = m,$$

where m is the concentration and a is the activity coefficient (Hemley and Jones 1964).

Fugacity is a measure of the escaping tendency of a vapour or gas and its departure from ideal behaviour. For example the tendency of liquid water to vaporise or escape into the vapour phase. In a mixture of gases the fugacity f of a gas is proportional to its mole fraction X, or concentration in the mixture, and to the total pressure, according to the relation:

$$f = XP_T.$$

Fugacity is not restricted to gases, but is also accepted as a measure of flow of matter from high to low potentials of solids and liquids. For a more detailed and comprehensive treatment of this topic the reader should consult Carmichael et al. (1974, p.292).

References

Best M G (1982) Igneous and metamorphic petrology. Freeman, San Francisco, 630 pp

Brimhall G H, Crerar D A (1987) Ore fluids: magmatic to supergene. In: Carmichael I S E, Eugster H P (eds) Thermodynamic modelling of geological materials: minerals, fluids and melts. Reviews in mineralogy, vol 17. Min Soc Am, pp 235–321

Carmichael I S E, Turner F J, Verhoogen J (1974) Igneous petrology. McGraw-Hill Book Co 739 pp

Franks F (ed) (1982) Water. A comprehensive treatise. Plenum, New York, 484 pp

Frey H (1977) Origin of the Earth's ocean basins. Icarus, 32:235–250

Froude D O, Ireland T R, Kinny P D, Williams I S, Compston, W, Williams, I R, Myers, J S (1983) Ion microprobe identification of 4,100–4,200 Myr-old terrestrial zircons. Nature (London) 304: 616–618

Fyfe W S (1978) The evolution of the Earth's crust: modern plate tectonics to ancient spot tectonics? Chem Geol 23:89–114

Gill R (1989) Chemical fundamentals of geology. Unwin Hyman, London, 291 pp

Hemley J, Jones W R (1964) Chemical aspects of hydrothermal alteration with emphasis on hydrogen metasomatism. Econ Geol 59:538–569

Holland H D (1984) The chemical evolution of the atmosphere and oceans. Univ Press, Princeton, 582 pp

Krauskopf K B (1979) Introduction to geochemistry, 2nd edn. McGraw-Hill Kogakushu New York, 617 pp

Kröner A (1985) Evolution of the Archean continental crust. Annu Rev Earth Planet Sci 13:49–74

Lewis J S, Prinn R G (1984) Planets and their atmospheres. Origin and evolution Academic Press, New York London, 470 pp

Lowman P D (1989) Comparative planetology and the origin of continental crust. Precambrian Res 44:171–195

Mason B (1966) Principles of geochemistry, 3d edn. John Wiley & Sons, New York, 329 pp

Masterton W L, Slowinski E J, Stanitski C L (1981) Chemical principles, 5th edn. Holt-Saunders international editions, Saunders, Philadelphia, 641 pp

Neilson G W, Enderby J E (1986) Water and aqueous solutions. Hilger, Bristol, 349pp

Paton T R (1978) The formation of soil material. Allen & Unwin, 143 pp Pollack J B, Yung Y L (1980) Origin and evolution of planetary atmospheres. Annu Rev Earth Planet Sci 8:425–487

Press F, Siever R (1982) Earth, 3d edn. Freeman, San Francisco, 613 pp

Reynolds I M (1982) Weathering of ore minerals and textural evaluation of gossans. Unpublished course notes. Rhodes Univ Press Grahamstown, S Afr, 183 pp

Rose A W, Hawkes H E, Webb S (1979) Geochemistry in mineral exploration, 2nd edn. Academic Press, New York London, 657 pp

Saunders J A (1990) Colloidal transport of gold and silica in epithermal precious metal systems: evidence from the Sleeper deposit, Nevada. Geology 18:757–760

Sheppard S M F (1986) Characterisation and isotopic variations in natural waters. Reviews in mineralogy, vol 16. Min Soc Am, pp 165–183

Spencer R J, Hardie L A (1990) Control of sea water composition by mixing of river waters and mid-ocean ridge hydrothermal brines. Geochem Soc Spec Publ 2: 409–420

Taylor S R, McLennan S M (1985) The continental crust: its composition and evolution. Blackwell Oxford, 312 pp

Whitfield M (1982) The salt sea-accident or design? New Sci 94:14–17

Hydrothermal Solutions

2.1 Introduction

A hydrothermal fluid is defined as a hot (ca. $50 - >500°C$), aqueous solution (hydro = water; thermal = hot), containing Na, K, Ca, Cl as major components, as well as many other elements (e.g. Mg, B, S, Sr, CO_2, H_2S, NH_4, Cu, Pb, Zn, Sn, Mo, Ag, Au etc.) as minor constituents (Skinner 1979). The terms fluid and solution are here used interchangeably, although fluid in the strict sense refers to a phase at a supercritical temperature in which a liquid can no longer exist. The pressure required to cause condensation at a given critical temperature is called the critical pressure. There are certain known conditions in nature where a hydrothermal solution is in fact a fluid.

We begin this chapter by having a look at those kinds of waters that may constitute a hydrothermal solution. A brief introduction is given on oxygen and hydrogen isotope systematics and their role in understanding the nature and interactions of hydrothermal fluids and wall rocks. As the only direct observation and sample material of hydrothermal solutions come from fluid inclusions and hot springs, an outline of the characteristics and methodology involved in the study of fluid inclusion is also given. It is emphasised that fluid inclusions provide important insights into the physical and chemical environments of ore deposition. This leads us to a discussion of dissolved constituents, where a series of tables provides some understanding of the composition of natural solutions. The transport of apparently insoluble metals had long baffled chemists until the role of ligands in the dissolution and transport of ore elements – and hence its importance in the study of hydrothermal mineral deposits – was discovered. Various mechanisms of deposition of metals from solutions conclude this chapter.

2.2 Water of Hydrothermal Solutions

The water of hydrothermal solutions can be derived from the following sources: meteoric, sea water, connate, metamorphic, juvenile or magmatic. Most hydrothermal solutions are of mixed origin in which one or more of the above sources can predominate.

Meteoric waters include rain water, lake and river waters, and groundwaters. These waters can penetrate deep into the crust and may become heated and

mineralised, thereby acquiring the properties of hydrothermal solutions. Stable isotope systematics indicate that in volcanic regions the waters of hot springs and pools are largely, if not exclusively, of meteoric origin.

Oceanic crust, in and around mid-ocean ridges, allows penetration of sea water to several kilometres below the sea floor. As a result, the sea water is heated, transformed into a fluid highly enriched with metals and driven by convection, and is subsequently discharged at the sea floor as a submarine mineral-depositing hot spring (Bonatti 1975).

Water trapped during the deposition of sediments and produced during diagenetic reactions is known as connate water, or formation water. It is calculated that some 20% by volume of unmetamorphosed sediments in the Earth's crust consist of pore water (Hanor 1979). It is also widely recognised that hydrothermal fluids can develop during burial diagenesis, and attain high salinities and temperatures. This water is essentially unbound water, that is, not bound in the lattice of rock-forming minerals. Removal of interlayer water from clays, gypsum and organic matter is an important aspect of diagenetic processes. Expulsion of fluids during burial and diagenesis takes place as a result of reduction of porosity, and the volume of water released can be considerable. An average shale can yield 3.5 $\times$ 10^3 litres of water for every 1 m^3 of solid material deposited. Temperatures during diagenesis may range from a few degrees below 0°C up to 250–300°C, but water expulsion during diagenetic changes occurs at temperatures between 90 and 120°C. (Hanor 1979). During the evolution of a sedimentary basin, expulsion of fluids takes place and they migrate upward and towards the margins of the basin, and, where sulphur is added from any source, precipitation of sulphides may occur at favourable sites.

Metamorphic waters are derived from the dehydration of hydroxyl-bearing minerals (bound water) through rising pressure and temperature (metamorphic dewatering). Smirnov (1976) envisaged the presence of a hydrothermal zone ahead of the metamorphic front during prograde regional metamorphism. Henley et al. (1976) suggested that metamorphism could be a source of energy leading to hydrothermal vein mineralisation. The presence of volatile-rich fluids liberated during metamorphism is commonly accepted, and they can be considered as dilute brines generally containing H$_2$O, CO$_2$ and CH$_4$. Direct observation of waters of probable metamorphic origin comes from the Kola peninsula, where the world's deepest well was drilled to a depth of 12 000 m. Between 4500 and 9000 m the well intersected a zone of "disaggregated metamorphic rock", within which abundant hot and highly mineralised water was found. At such depths, this water is likely to be of metamorphic origin released from bound water in rock-forming minerals. Also present in the well were abundant gases such as He, H$_2$, N$_2$, CH$_4$, CO$_2$ and various hydrocarbons, most of which are also believed to have been liberated by deep metamorphic processes (Koslovsky 1984). It is interesting to note that the dehydration of rocks at those depths is accompanied by microfracturing or hydraulic disaggregation. Temperatures of around 180°C were measured at 10 000 m, whereas sulphur isotopic determinations indicate an origin of the sulphur from the mantle. A surprising finding from these results is that the well intersected the Conrad Discontinuity (where density and velocity of seismic waves rise from 2.5 to

2.75 g/cm^3 and 5 to 6 km s^{-1} respectively) which is taken to mark the transition from upper (granitic) to lower crust. This discontinuity, however, is found to be the lower boundary of the disaggregation and hot metamorphic water zones, where the rock returns to its normal density for that depth and water is no longer present. It was further established that in the zone of disaggregation, rock fragments are cemented by sulphides of Cu, Zn, Ni, Fe and Co. These discoveries indicate that gas-water-rock interactions are active at great depths, and that conditions exist for the formation of hydrothermal ore deposits entirely powered by metamorphism (see Chaps. 3 and 15).

Some geoscientists consider juvenile water as that which is assumed to be derived from the mantle. Magmatic waters are those that separate from melts upon cooling, generating a magmatic-hydrothermal system,which is perhaps the most powerful ore-depositing agent. In addition to water, other volatile constituents that may be present in magmas include H_2S, CO_2, SO_2, HCl, B, F, H_2. Water contents of magmas range from as little as 0.2% to as much as 6.5% by weight. The presence and abundance of these volatiles in a magma is generally related to its composition and the source region from which it originated. It is possible, for example, that a B-rich granite may have derived from melts that have interacted with tourmaline-rich metasediments. Further, the relative abundance of one volatile over another (e.g. B/F) may be very important in determining the type of ore deposit that may be formed on exsolution of the volatile fractions from the late stages of consolidation. The evolution of a magmatic-aqueous phase during the solidification of a hydrous magma is discussed in some detail in Chapter 3.

2.3 Oxygen and Hydrogen Isotope Systematics of Hydrothermal Fluids

Analyses of stable (non-radiogenic) isotopes provide useful data for the understanding of the origin, nature and evolution of hydrothermal fluids and their interaction with wall rocks. Since oxygen is the most abundant element, and hydrogen its companion in the water molecule, the ratios of $^{18}O/^{16}O$ and D/H where D is deuterium (^2_1H), the heavy isotope of hydrogen, constitute powerful indicators or tracers of the nature and source of hydrothermal fluids. The theoretical, experimental aspects and reviews of studies of stable isotope systematics can be found in a number of excellent publications. The interested reader is advised to consult Valley et al.(1986), Taylor (1979), Faure (1986) and Bowen (1988). The isotopic values are reported as deviations from an arbitrary standard, which in the case of hydrogen and oxygen is taken to be oceanic water (SMOW, standard mean ocean water) with $\delta^{18}O=0$ and $\delta D=0$. This deviation, indicated by δ is given by the formula:

$$\delta = (R_{sample}/R_{standard} - 1) \times 1000$$

where R is the ratio of the isotopes being considered (e.g. D/H and $^{18}O/^{16}O$). Thus, positive or negative values represent enrichment or depletion with respect to the standard.

Sea water, meteoric water and juvenile water are considered to be "reference waters", in that they have defined isotopic characteristics at their source. Consequently, geothermal, connate, metamorphic and magmatic waters are re-cycled from one or more of these reference waters (Ohmoto 1986). In the study of hydrogen and oxygen isotope systematics, it is important to take into account the "meteoric water line" (MWL). Isotopic variation of meteoric waters is dependent on latitude and elevation, with δD and $\delta^{18}O$ values being lower towards higher elevations and higher latitudes. This is due essentially to less evaporation and therefore less vapour-fluid fractionation, which tends to favour the partitioning of the lighter isotopes into the vapour phase, leaving the fluid enriched in the heavy isotopes. Thus, water condensing from a vapour is enriched in ^{18}O and D relative to the vapour, so that air masses become progressively depleted in the heavy isotopes relative to the initial condensate (Taylor 1979). The linear relationship between δD and $\delta^{18}O$ is defined by:

$$\delta D = 8 \; \delta^{18}O + 10$$

Studies of the isotope characteristics of natural waters by Taylor (1979) and Sheppard (1986); Fig. 2.1) reveal that present-day ocean waters are relatively uniform with δD of $+5$ to -7 per mill and $\delta^{18}O$ of $+0.5$ to 1.0 per mill , and with mean values close to 0 per mill for both D and ^{18}O (SMOW standard). Isotopic values of ancient sea water, as determined through the analysis of minerals that equilibrated with fossil sea water hydrothermal systems, show a progressive increase
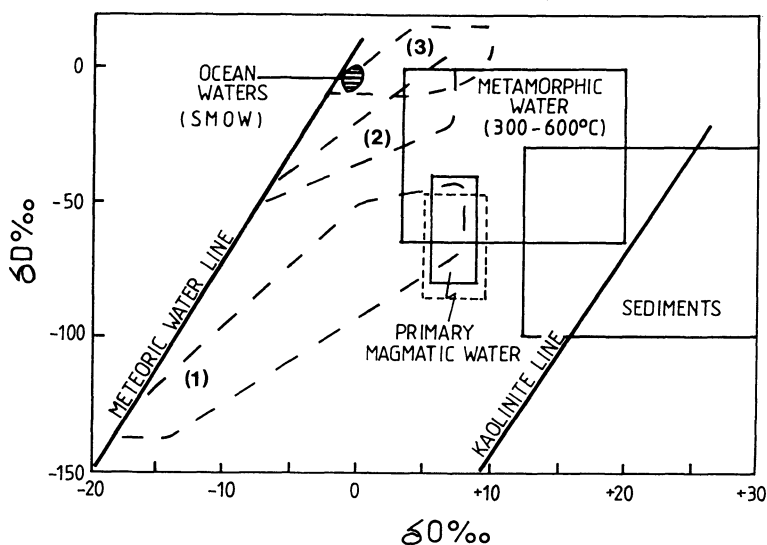
Fig. 2.1. Fields of isotopic compositions of natural waters (primary magmatic, metamorphic, ocean waters). *Long dashed lines* are fields of formation waters in sedimentary basins: *1* Alberta basin; *2* California basin; *3* Gulf Coast basin. *Dashed box* partly superimposed on the box of primary magmatic water, represents "juvenile water" (After Ohmoto 1986). The diagram is taken and modified from Sheppard (1986)

of $\delta^{18}O$ of the sea water since Archean times (-8 to -12 per mill). From 2.5 Ga ago it is calculated that the $\delta^{18}O$ values were between 0 and -3 per mill, and δD of 0 to -25 per mill. Although in no instance can it be stated that truly juvenile water (or for that matter magmatic water) has ever been identified, the nearest D and ^{18}O values are obtained from unaltered igneous and mantle rocks and minerals, using mineral-water isotopic fractionation factors at high temperatures ($>700\,°C$). These give δD values of approximately -50 to -90 per mill and $\delta^{18}O$ of $+5.5$ to $+10$ per mill (Sheppard 1986). The isotopic composition of geothermal waters indicates in all cases a strong meteoric component. The δD values of geothermal waters are more or less the same as those of the local meteoric waters. Modern geothermal waters show an enrichment in $\delta^{18}O$ (^{18}O shift) due to isotopic exchange with wall rocks. The amount of the $\delta^{18}O$ shift increases with temperature and salinity of the fluids, and this probably means that the fluids acquired their heat, and dissolve solids, by interaction with deeply buried and hot rocks (Ohmoto 1986). The $\delta^{18}O$ enrichment is accompanied by a depletion of ^{18}O in the wall rocks. We return to this important aspect of isotope systematics in Chapter 4 with a discussion of the isotopic effects during hydrothermal alteration processes. Connate and formation waters show a wide range of $\delta^{18}O$ and δD. The D values of connate waters show a decrease with latitude, as with meteoric waters. The variations in δD and $\delta^{18}O$ of pore fluids and connate waters are largely dependent on whether the original fluid was sea water or meteoric water. Generally, in pore fluids of oceanic rocks, there appears to be a decrease in δ ^{18}O with increasing depth and salinity. Measurements taken from samples of ocean floor suggest that alteration of basalt with sea water is responsible for this isotopic characterisation of pore fluids (Ohmoto 1986). The δD and $\delta^{18}O$ values obtained from sedimentary basin fluids by contrast show a wide range of values ($\delta D = +20$ to -150 per mill; $\delta^{18}O = +10$ to -20 per mill). Also, in basin brines there seems to be an overall increase in the isotopic values with salinity and temperature, so that brines with the lowest temperature approach the isotopic composition of present-day local meteoric waters.

Metamorphic waters, like juvenile water, are still somewhat unconstrained istopically. They are derived from dehydration of mineral phases during prograde regional metamorphic events, as defined in Section 2.2. Nevertheless, here too the isotopic composition is clearly dependent on the orginal rock type and its history of interaction with fluids. Ohmoto (1986) points out that if volcanic rocks are first altered by sea water, at temperatures less than $200°C$, and then undergo metamorphism, their final $\delta^{18}O$ values could be as high as 25 per mill. On the other hand, if volcanic rocks are altered by meteoric waters, then subjected to high-grade metamorphism, the δD and $\delta^{18}O$ values could be much lower. Metamorphic waters have a range of δD values from 0 to about -70 per mill, and a range of $\delta^{18}O$ from $+3$ to about 25 per mill. Taylor (1979) attributes the wide range of $\delta^{18}O$ to the original values in the metamorphosed rocks. Magmatic waters may have a range of δD and $\delta^{18}O$ values, depending on the source region of the magma in question (I- or S-type for example), as well as the possible isotopic exchanges with wall rocks during the cooling stages of the melt. Isotopic values, determined on the basis of experimental studies of fractionation factors between melts and water, give a range for magmatic waters of $\delta D = -30$ to -75 per mill and, $\delta^{18}O = +7$ to $+13$ per mill (Ohmoto 1986).

2.4 Fluid Inclusions

Fluid inclusions are droplets of fluid trapped in crystals at the time of their growth, or introduced along microcracks and cleavages after crystallisation of the host mineral. They represent samples of hydrothermal fluids, and range in size from a single water molecule up to several millimetres, with an average of about 0.01 mm (Roedder 1979). The number of inclusions in any one crystal can be very high, with a maximum of 10^9 inclusions having been estimated in 1 cm^3. Much interest has been directed to the subject of fluid inclusions over the years, which is covered in a wide number of publications. The present discussion is based largely on the works of: Roedder (1979), from whom a concise review is gained, Guilbert and Park (1985), who provide a general introduction; and the text books by Shepherd et al (1985), Hollister and Crawford (1981) and finally Roedder (1984). These all provide essential reading for the exploration geologist who wishes to acquire a more in-depth understanding of the topic.

Fluid inclusions have many practical uses for the student of ore deposits, providing information on the temperature, pressure, density and composition of the fluids that originated the mineralisation. In terms of their origin, three types of fluid inclusions are recognised, namely: primary, secondary and pseudo-secondary (Fig. 2.2). Primary inclusions are those that became trapped during the growth of the host mineral, and are therefore associated with crystallisation features – such as growth zones; or they may occur isolated due to imperfections of the crystal during its growth (Fig. 2.2). Secondary inclusions are those that form after the growth of the host mineral is completed. They cut across growth zones and even crystal boundaries, and may represent infilling of microcracks by late fluids that might well be unrelated to the ore-forming event. Pseudosecondary inclusions form during the two stages outlined above, and are characterised by their alignment with microcracks that end against a growth zone (Fig.2.2). These definitions are somewhat

GROWTH ZONING
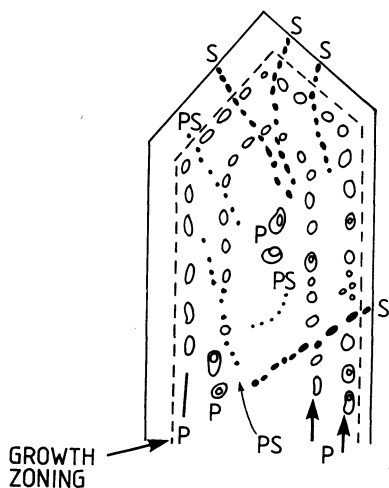
Fig. 2.2. Types of fluid inclusions, and their distribution in a quartz crystal. *P* Primary; *S* secondary; *PS* pseudosecondary (After Shepherd et al. 1985)

TYPE I: LIQUID (L)
monophase

TYPE II: LIQUID >50% (L)
        + VAPOUR <50% (V)
two-phase

TYPE III: VAPOUR >50% (V)
          + LIQUID <50% (L)
two-phase

TYPE IV: VAPOUR ONLY (V)
monophase

TYPE V: LIQUID ± VAPOUR
        + SOLIDS (S) ≤50%
multiphase

TYPE VI: IMMISCIBLE
         LIQUIDS L_1+ L_2
         ± VAPOUR
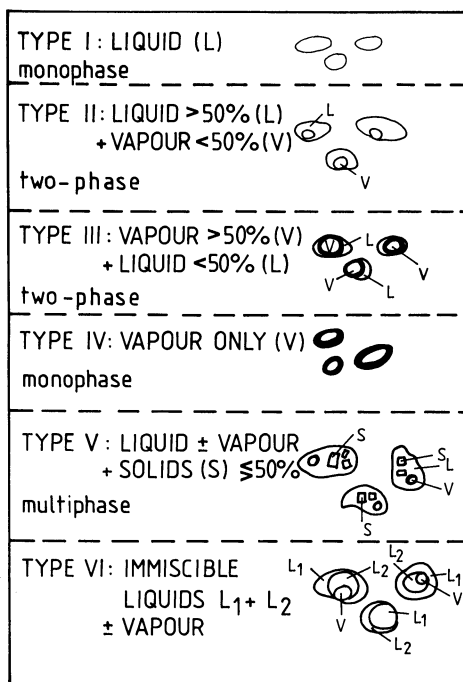
Fig. 2.3. Classification of fluid inclusions observed at room temperature (After Shepherd et al. 1985)

simplistic, and it is often difficult to distinguish between, say, secondary and pseudosecondary, or primary and pseudosecondary inclusions. Tables of empirical criteria for the identification of the genetic types of fluid inclusions are given in Roedder (1979, 1984). In terms of morphology and contents, several important types of fluid inclusions have been described. The classification scheme reported by Shepherd et al. (1985) is summarised below, and diagramatically shown in Fig.2.3.

1. Monophase inclusions: entirely filled with liquid (L).
2. Two-phase inclusions: filled with a liquid phase and a small vapour bubble (L+V).
3. Two-phase inclusions: in which the vapour phase is dominant and occupies more than 50% of the volume (V+L).
4. Monophase vapour inclusion (V): entirely filled with a low density vapour phase (generally mixtures of H_2O, CH_4, CO_2).
5. Multiphase inclusions containing solids (S+L+/−V): contain solid crystalline phases known as daughter minerals. These are commonly halite (NaCl) and sylvite (KCl), but many other minerals may occur including sulphides.
6. Immiscible liquid inclusions: contain two liquids, usually one H_2O-rich and the other CO_2-rich (L_1+L_2=/−V).

In general, the coexistence of types II (L+V) and III (V+L) may indicate that the fluid was boiling at the time of entrapment. In the case of boiling of a one-component system, the gas bubble is the vapour phase of the host liquid; or, in the case of a heterogeneous system, the gas phase exsolves by effervescence. However, it

must be cautioned that the presence of a gas bubble may also indicate immiscibility. This is the case with CO_2 which, if present in the fluids, will separate on cooling (Roedder 1979). The presence of daughter minerals, on the other hand indicates that solids nucleated from an oversaturated liquid solution. It is found that in these hypersaline fluids Na^+, Cl^-, Mg^{2+}, and Ca^{2+} are the most common dissolved ions.

Measurements on fluid inclusions are carried out by means of heating and freezing runs on specially designed microscope stages. Homogenisation of the liquid and gas phases will be seen to occur at a given temperature on heating of the inclusions, when observed under the microscope. This temperature is a lower limit having been obtained at atmospheric pressure, and therefore a pressure correction for the original depth at which the fluids were discharged is necessary. The salinity of the inclusion is determined by first freezing the inclusion and then raising the temperature of the stage, and observing the first and final melt temperatures. The first melt temperature indicates the type of salt (NaCl or MgCl, for example), while the temperature of the last melt indicates the degree of salinity, usually measured in equivalent NaCl.

The liquid of the inclusions is normally an aqueous solution with dissolved ions of Na^+, Cl^-, Ca^{2+}, Mg^{2+}, SO_4^{2-}, HCO_3^{2-}, CO_3^{2-} ions. The concentration of the salts in the solutions ranges from less than 1 wt.% to greater than 50 wt.%. The diagram in Fig.2.4 reflects the range of salinities (wt.% equivalent) and homogenisation temperatures of a range of hydrothermal mineral deposits (Large et al. 1988).

A   FIELD OF DOMINANT CHLORIDE COMPLEXING

B   FIELD OF DOMINANT SULPHIDE COMPLEXING
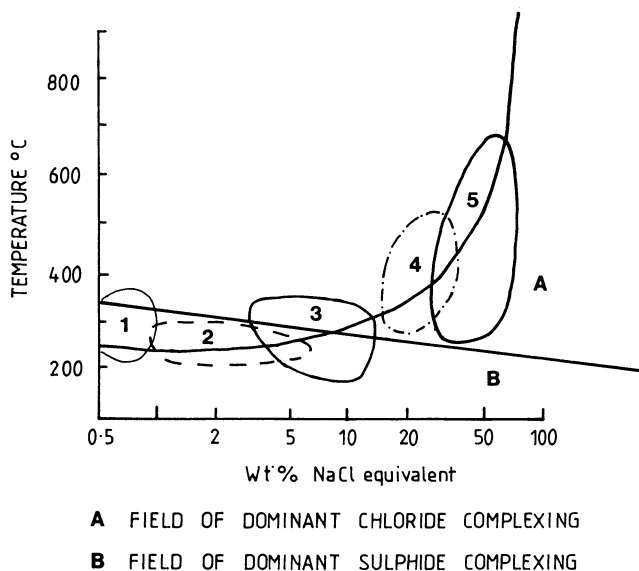
Fig. 2.4A, B. Temperature-salinity fields and mean gradient curve for a range of hydrothermal mineral deposits: *1* Archean lode Au; *2* epithermal Au-Ag; *3* massive sulphide deposits; *4* Tennant Creek Au-Cu, Australia; *5* porphyry Cu-Au deposits (After Large et al. 1988)

2.5 Dissolved Constituents and Metals Partitioning into Hydrothermal Solutions

From the study of fluid inclusions, hot springs and fluids encountered during drilling operations in geothermal areas and oilfields, it is apparent that the amount of dissolved solids in hydrothermal solutions varies from approximately $< 1\%$ to $> 50\%$ by weight.

Some typical compositions are given in Tables 2.1 to 2.3. From the values in these Tables the following observations can be made: (1) Na, K, Cl and Ca are in almost all cases the major components of the solutions; minor components are Sr, Fe, Zn, Mg, Fe, Mn, CO_2, SO_2, H_2S and NH_3; (2) with few exceptions, the most striking feature is that the actual concentration of ore-forming metals in these waters is generally low.

From these Tables it can thus be deduced that metal concentrations in the hydrothermal fluids need not necessarily be high in order to form an ore deposit, and therefore the critical factors for ore deposition must therefore be time and deposition rate. Although difficult to identify with absolute certainty, it is fair to assume that the source of these constituents can be the cooling magmas and/or the rocks through which the solutions pass. The case for Pb is instructive. In a study by Doe and Delevaux (1972) of the sources of Pb in galena ores in southern Missouri, based on the isotopic compositions for this metal, it was found that the Pb is

Table 2.1. Composition of modern and ancient hydrothermal solutions. Data from various sources published in Skinner (1979). All values in parts per million (ppm), unless stated otherwise

Element	Salton Sea	Cheleken Field	Ancient hydrothermal solutions determined from fluid inclusions		
Cl	15.5%	15.7%	8.7%	4.65%	2.95%
Na	5.04%	7.61%	4.04%	1.97%	1.52%
Ca	2.8%	1.97%	8600	7500	4400
K	1.75%	409	3500	3700	6.7%
Sr	400	636	–	–	–
Ba	235	–	–	–	–
Li	215	7.9%	–	–	–
Rb	135	1.0	–	–	–
Mg	54	3080	5600	570	–
B	390	–	< 100	185	–
Br	120	526	–	–	–
I	18	32	–	–	–
NH₄	409	–	–	–	–
SO₄	5	309	1200	1600	1.1%
Fe	2290	14	–	–	8000
Mn	1400	46.5	450	690	–
Zn	540	3.0	1.09%	1330	–
Pb	102	9.2	–	–	–
Cu	8	1.4	9100	140	–

Table 2.2. Analyses of geothermal waters. Data from various sources published in Ellis and Mahon (1977). (1) Iceland; (2) Philippines; (3) Japan; (4) New Zealand; (5) Mexico; (6) Taiwan; (7) Italy. All values in parts per million (ppm), unless stated otherwise

Element	1	2	3	4	5	6	7
Cl	197	1.44%	1219	1625	1.6%	1.34%	4.28%
Na	212	7800	846	950	9062	5490	7.89%
Ca	1.5	219	9.9	28	520	1470	106
K	27	2110	105	80	2287	900	4.83%
Li	0.3	40	4.5	12.2	38	26	380
Rb	0.04	12.5	1.8	0.8	–	12	450
Mg	0.0	0.28	0.02	–	1	131	17
Mn	0.0	–	0.0	0.02	–	40	0.1
Fe	0.1	–	0.05	0.1	0.3	220	0.7
F	1.9	–	3.8	0.8	2	7.0	100
Br	0.45	–	2.5	–	31	–	–
SO_4	61	32	214	17	6	350	16.3%
As	–	28	2.3	–	0.5	3.6	8.3
B	0.6	313	20.51200	14	106	2650	
SiO_2	480	995	425	460	1250	639	–
NH_3	0.1	6.4	0.1	46	21	36	82
CO_2	55	27	56	61	56	2	5850
°C	216	324	200	230	340	245	250
pH	9.6	6.7	8.4	7.4	7.7	2.4	8.5
Depth(m)	650	1947	350	585	1285	1500	1415

Table 2.3. Partial analyses of oil field brines. Data from various sources published in Skinner (1979), analysis (1), and Guilbert and Park (1985). All values in parts per million (ppm), unless stated otherwise

Element	(1)	Ages of source rocks					
		Silurian	Cretaceous			Jurassic	
Cl	1.58%						
Na	5.9%						
Ca	3.64%						
K	538						
Pb	80	10	111	80	226	215	<1
Zn	300	2	357	300	706	39	<1
Fe	298	10	420	298	1060	467	3
Ba	61	11	59	61	1090	504	34
Ca+Na+Ca+K		40%	32%	25.5%	34.4%	48.6%	35.1%

probably derived from the Lamotte Sandstone, which is the main aquifer for the hydrothermal solutions in the district. The Pb is thought to have been transferred from solid solution in the feldspars to the hydrothermal fluid by rock-hot-water

interactions. Other metals such as Zn, Cu, Sn, W are present in various amounts in micas, pyroxenes and amphiboles. Sn and W concentrations of up to 500 ppm have been found in biotites and muscovites (Ivanova 1969; see Chap. 9). The release of the metals may take place either during specific reactions with production of a new mineral phase from the original host, or, simply by a process of ion-exchange reactions.

In summary, evidence suggests that hydrothermal fluids acquire their dissolved constituents by one, or both of two fundamental processes, where: (1) the constituents are released to a fluid by a crystallising magma, and (2) constituents derive from the rock through which the hot aqueous solutions circulate. Finally, Skinner (1979) questions whether or not a rock mass need be abnormally rich in certain elements in order to serve as a source for the elements. For those elements which have crustal abundances of 0.001 to 0.01% (10 to 100 ppm), the rocks need not be enriched. An example is the La Motte Sandstone, above, in which its feldspars provided the Pb to the solutions. Volcanic piles with predominant rhyolite-dacite components will produce Pb-rich ores, because of the abundance of feldspars relative to mafic silicates; yet if andesite-basalt predominate, with an abundance of olivines and pyroxenes, they will yield Cu-rich ores. For those elements such as Sn and Ag, which have very low crustal abundances (less than 10 ppm or 0.001%), a pre-concentration would probably be necessary before solution extraction takes place, although a paucity of reliable data available makes this an uncertain point.

2.5.1 Partitioning of Metallic Elements into Hydrothermal Solutions

Exchange reactions between hydrothermal fluids and rock-forming minerals result in the partitioning of metallic elements into the former. Experimental work (Ilton and Eugster 1990, Ilton 1990) indicates that elements such as Fe, Zn, Cd, Cu and Mn are strongly partitioned into chloride-rich hydrothermal fluids. These elements are leached out of rock-forming mineral sites and enter the fluid phase. A lithosome containing biotite, chlorite, hornblende and feldspars would also contain a substantial proportion of metallic elements. For example, it is estimated that biotite + hornblende + chlorite may contain up to 50% of the Cu in a granodiorite associated with porphyry mineralisation (Greybeal 1973). For more details on the topic of fluid-mineral interactions the reader is referred to the volume edited by Spencer and I-Ming Chou (1990).

2.6 Metal Transport

It has been mentioned previously (Chap. 1) that one of the dilemmas of hydrothermal solutions is the insolubility of most compounds and metals which are nevertheless transported in, and subsequently deposited from them. It was originally believed that certain elements acted as mineralisers; cassiterite (SnO_2), for

example, was thought to have formed according to:

$$SnF_4 + 2H_2O = 4HF + SnO_2,$$
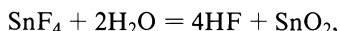
in which F acted as a mineraliser, and that further action by HF generated other minerals such as topaz, tourmaline or fluorite. While the activity of HF is indeed important for the formation of topaz and Sn-W ores, the transport of metals can no longer be explained by the action of mineralisers. Today, the formation of complex ions is invoked to explain the transport of elements in hydrothermal solutions. Complex ions are formed between metals and ligands in solution and are the metals' transporting agents.

2.6.1 Complex Ions and Ligands

A complex ion is a "charged species in which a metal ion is joined by co-ordinate covalent bonds to neutral molecules and/or negative ions" (Masterton et al. 1981). For example, in the complex $Cu(NH_3)_4^{2+}$, where one Cu^{2+} ion combines with four neutral NH_3 molecules, each of the NH_3 contributes a pair of unshared electrons to form a covalent bond with the Cu^{2+} ion. The structure is shown in Fig. 2.5A.

Metals which have the tendency to form complex ions are those that are placed towards the right of the transition series (i.e. Ni, Cu, Zn, Pt, Au, Co, Cr, Mo, W), while non-transition metals (Al, Sn, Pb) form a more limited number of complex ions. The central ion in a complex is a metal cation, and the neutral molecules or anions bonded to the cation are called ligands. The number of bonds formed by the central ion is the co-ordination number. In the case illustrated in Fig. 2.5A, Cu has a co-ordination number of four. Charged complex ions, such as $Cu(NH_3)_4^{2+}$ or $Al(H_2O)_6^{3+}$, cannot exist in the solid state unless the charge is balanced. Thus, $Cu(NH_3)_4Cl_2$, for example, is a complex ion balanced by 2 Cl ions. Therefore the complex ion acts in this case as a cation. Other examples are:

$$Pt(NH_3)_4^{2+} + 2Cl = Pt(NH_3)_4Cl_2 \text{ (complex cation)};$$

$$Pt(NH_3)Cl_3^- + K = Pt(NH_3)Cl_3K \text{ (complex anion)}.$$

If a ligand has more than one bond then it is called a chelating agent (from the Greek chelate, meaning hard). Ligands usually contain atoms of the electronegative elements (C, N, O, S, F, Cl, Br, I). The most common ligands are NH_3, H_2O, Cl^-, OH^-, HS^-. Co-ordination numbers are usually 6, 4 and 2, in that order of frequency. Odd co-ordination numbers are very rare. The co-ordination number also determines the geometry of the complex ions. Thus, for complex ions in which the central ion forms only two bonds the ligands are linear with the bonds directed at 180°.

Metal complexes with co-ordination numbers of 4 form either tetrahedral structures or square planar structures (Fig. 2.5A, B), whereas the octahedral geometry is obtained for ion complexes in which six ligands surround a metal ion (Fig. 2.5C). The interpretation of the nature of the bonding in complex ions is beyond the scope of this book; suffice it to say that two models are considered, based on the electronic configurations of the ion in question. One is the valence bond

A Square planar structure of $Cu(NH_3)_4^{2+}$
B Tetrahedral structure of $Zn(NH_3)_4^{2+}$
C Idealised octahedral complex
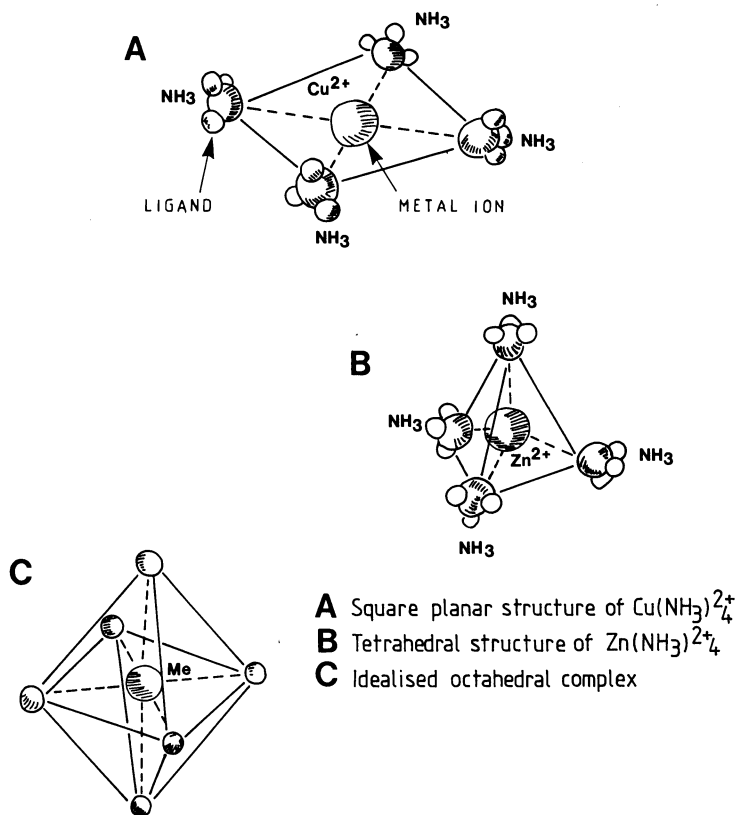
Fig. 2.5A–C. Simplified molecular structures of complex ions (After Masterton et al. (1981)

model and the other is the crystal-field model, the nature of the bonding in the latter case being essentially electrostatic. Details on the nature of complex ions and their role in the transport of transitional metals in hydrothermal solutions can be found in Brimhall and Crerar (1987), and Crerar et al. (1985), from whom the following is summarised.

Metal-ligand interactions are similar to acid-base reactions, with the metal being an electron acceptor and the ligand an electron donor. Metals and ligands can be classified into two important classes: class A, or hard, and class B, or soft. In the former, metals and ligands are highly charged, small and slightly polarisable. Class B, or soft type, is characterised by species that are large, of low charge and are highly polarisable. An important aspect of this classification is that soft metals tend to bind with soft ligands, and hard metals with hard ligands. Table 2.4 lists those metals and ligands which are important in hydrothermal processes, according to their soft or hard behaviour. From Table 2.4 it can be seen that HS^- is a soft ligand and will therefore form strong complexes with Au, Ag, Hg, Cu and Sb (soft metals); whereas weaker complexes will be formed with Pb and Zn, and even weaker still with Sn and Fe.

Table 2.4. Classification of metals and ligands according to Brimhall and Crerar (1987). Hardness decreases to the right; see text for details

	Hard	Borderline	Soft
A	H^+ Li^+ Na^+	Fe^{2+} Co^{2+} Ni^{2+}	Cu^+ Ag^+ Au^+
C	K^+ Rb^+ Cs^+	Cu^{2+} Zn^{2+} Sn^{2+}	Cd^{2+} Hg^+ Hg^{2+}
I	Ca^{2+} Mg^{2+} Ba^{2+}	Pb^{2+} Sb^{3+} Bi^{3+}	$M°$ (metal atoms)
D	Ti^{4+} Sn^{4+} MoO^{3+}	SO_2	
S	WO^{4+} Fe^{3+} CO_2		
B			
A	NH_3 H_2O OH^-	Br^-	CN^- CO
S	CO_3^{2-} NO_3^-		H_2S HS^-
E	PO_4^{3-} SO_4^{2-}		I^-
S	F^- Cl^-		
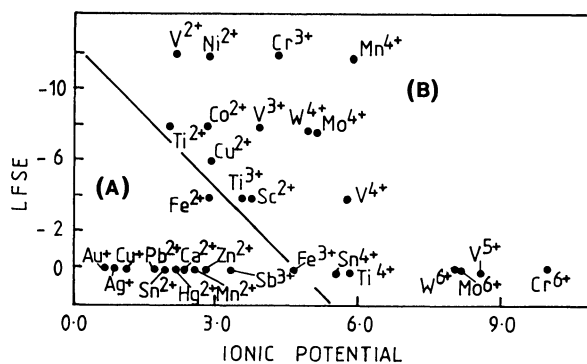
Fig. 2.6. Plot of ligand field stabilisation energy LFSE versus ionic potential, showing discrimination of A field of metal ions that commonly form hydrothermal deposits, and B field of metal ions that less commonly, or rarely, form hydrothermal deposits (After Brimhall and Crerar 1987)

Transition metals show increased hardness at higher temperatures and therefore complexes with intermediate hard ligands such as Cl^- and OH^- become more stable at a given higher temperature. This behaviour is corroborated by experimental evidence which indicates the high stability of chloro complexes at high temperatures, as shown later. Electronegativity, ionic potential and the ligand field stabilisation energy (LFSE; energy that affects the stability and behaviour of transition metal ions in hydrothermal solutions) are considered to be important parameters for the behaviour of transition metals in hydrothermal solutions. A plot of the ionic potential of selected metals versus the LFSE (Fig. 2.6) reveals two distinct fields. In one, are included the ions of those elements that commonly form hydrothermal deposits (low ionic potential and low LFSE); in the other, are the ions of those elements less likely to be found in hydrothermal deposits. Brimhall and

Crerar (1987) find that of the 30 transition metals only Mn, Fe, Cu, Zn, Mo, Au, Ag, W, Hg and Co commonly form sizable hydrothermal deposits, even though this array of elements does not correlate with their crustal abundances. A possible explanation for this is the availability of tetrahedral and octahedral sites in crystallising magmas. High Al_2O_3/alkali ratios appear to favour the octahedral sites in residual melts and hence the concentration of metals in the hydrothermal fluids (Feiss 1978). This ratio, in turn, may be influenced by the presence of volatiles in the magma (see Chap. 8).

2.6.2 Complex Ions in Hydrothermal Solutions

Two classes of complexes are important for the transport of ore metals in hydrothermal solution, namely: sulphide (HS^- and H_2S) and chloride (Cl^-). Both these complexes are capable of transporting large quantities of metals. Other ligands, which are less common, though also important, include OH^-, NH_3, F^-, CN^-, SCN^-, SO^{2-}_4 and also some organic complexes (i.e. humic acid). The comprehensive review of the solubility of ore minerals and complex-forming ligands by Barnes (1979) provides the basis of for the discussion that follows.

The ore-carrying capacity of the fluids is largely determined by the activity of these ligands, rather than the abundance of the metals to which they are bonded. This activity is a function of concentration temperature, ionic strength, pH and Eh. One very important complex is that involving the hydrosulphide ion HS^-. Species such as $Zn(HS)_3^-$ and $HgS(HS)^-$ have been shown to be transported in solution in large amounts. Studies of active hydrothermal systems and epithermal Au deposits indicate that thio-sulphide complexing $(HS)^-$ is in fact the dominant mechanism of transport for Au. Here, Au^+ is complexed by the sulphur ligand HS, which was shown by Seward (1979) at Broadlands, New Zealand, to predominate over chloride complexes at near neutral pH (see Table 2.5).

Thio-complexes of Au^+ up to 300°C and 1500 bar, with pH 3–10 are found to be stable. Au thio-complexing at near neutral pH is defined thus:

$$Au + H_2S + HS^- = Au(HS)_2^- + 1/2H_2.$$
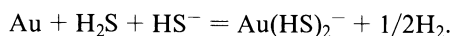
With sulphide complexing, however, the concentration of reduced sulphur atoms in solution must be far greater than that of the metals, if the complexes are to remain stable (Krauskopf 1979; Skinner 1979). It follows that loss of H_2S caused, for example, by boiling will result in an increase in pH, decrease in HS activity, and

Table 2.5. Transport of Au in the Broadlands geothermal system as determined by Seward (1979)

Measured	as Au Cl_2^-	as Au(HS)$_2$
4×10^{-5}	5.6×10^{-6}	1.5×10^{-2}

subsequent precipitation of sulphides and Au, providing this metal is present in sufficient quantities.

Deposition from sulphide complexing can be written as:

$$Me(HS)_3^- = MeS + HS + H_2S \text{ (aq)}.$$
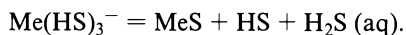
The importance in some hydrothermal systems of chloride complexing is indicated by the abundance of NaCl in fluid inclusions. Aqueous species such as $ZnCl_2$, $CuCl^{2-}_3$, $AgCl_2^-$ form in chloride-rich solutions. Both Barnes (1979) and Krauskopf (1979) report that there is evidence that chloride complexes are more stable than sulphide complexes at higher temperatures (above 350°C). The predominance of sulphide complexing at lower temperatures and chloride complexing at higher temperatures, and their relationships to certain types of ore deposits, are illustrated in Fig. 2.4. In the case of Au, its solubility in chloride solutions is defined thus:

$$Au + H^+ + 2\,Cl^- = AuCl_2^- + 1/2\,H_2.$$
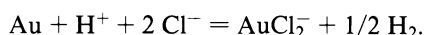
This type of **complexing** for the transport of Au is probably valid in the deeper and hotter regions of magmatic and hydrothermal systems, and in hydrothermal fluids originating during metamorphic dewatering. Deposition of sulphides from chloride-complexed metals takes the form:

$$MeCl_2\text{(aq)} + H_2S\text{(aq)} = MeS + 2H^+ + 2Cl^-.$$
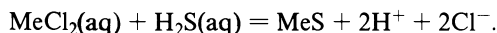
The greater stability of chloride complexes at higher temperatures with respect to sulphide complexing is corroborated by the modelling studies of Ag/Au ratios in hydrothermal solutions by Cole and Drummond (1986). They found that $AuCl^-_2$ complexes dominate at temperatures higher than 250°C and low to moderate pH, thus favouring high Ag/Au ratios in the solution. At temperatures below 250°C sulphide complexing with more Au than Ag predominates, causing lower Ag/Au ratios in the solution.

According to Barnes (1979), deposition of metals from chloride complexes may be due to the following:

1. Increased H_2S concentration;
2. Increased pH (caused by boiling for example);
3. Decreased chloride concentration and decreasing temperature.

The causes of deposition from sulphide complexes are:

1. Pressure release and boiling;
2. Oxidation which decreases the sulphide contents and the pH.

Evans (1987) points out that the actual mechanism of metal transport via complex-forming ligands is by no means clearly understood. One problem is that in order for sulphide complexes to be stable, high concentrations of H_2S are necessary in the fluids – a fact which evidence ascertained from Tables 2.1–2.3 does not appear to support. However, it is possible that S may enter the system at a later stage, for example by reduction of sulphates by organic compounds. If this is true, a mixing model could be considered whereby both chloride and sulphide complexes may be

important as transporting agents for the metallic elements. Sulphide deposition could hence take place according to the reaction:

$$PbCl_2 + H_2S = PbS + 2H^+ \; 2Cl^-,$$
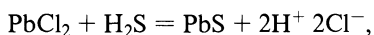
in which galena precipitates on addition of H_2S (Henley et al. 1984, Evans 1987).

2.7 Metal Deposition

Precipitation of the dissolved constituents in hydrothermal fluid can occur as a result of: temperature variations, pressure changes and boiling, reactions between wall rocks and solutions, chemical changes due to mixing of fluids. Temperature changes affect the solubility of sulphides and oxides, as well as the stability of the complex ions (Skinner 1979). It is believed that a fall of just 20°C may be sufficient to cause precipitation. Temperature changes can be caused by mixing of hot solutions with cold near surface waters. This is particularly common and evident at sites where hydrothermal solutions discharge on the sea floor. Here the hot rising fluids with temperatures of up to 350°C mix with sea water of only a few degrees centigrade above zero, resulting in immediate sulphide precipitation which in turn gives rise to the so-called black smoker chimneys. Adiabatic decompression (throttling) also causes rapid temperature drops over short distances, and occurs when the pressure changes from lithostatic to hydrostatic (Skinner 1979). An adiabatic process is one in which no heat flows either into or out of a system sealed off from its surroundings. Since flow of heat in rocks takes time, any process can be adiabatic if sufficiently fast. Thus, rapid compression causes a rise in temperature, and, by the same token, rapid decompression results in a temperature drop.

Pressure changes also cause solubility changes, but need to be substantial (about 1000 bar) for precipitation to occur. One of the most important pressure-controlled phenomena is, of course, boiling. Boiling is the result of a sudden increase in the concentration of the solution and the removal of the volatile constituents, which leaves a residue that is less capable of keeping constituents in solution. It is very important for the precipitation of Au in geothermal systems. In these situations, self-sealing due to mineral deposition (sinter) may be a cause of boiling. Other causes are: increase in temperature, and/or build up of volatiles. If the seal is suddenly breached, say by an earthquake, the immediate drop in pressure results in violent boiling. During boiling H_2, CO_2, etc. go into the vapour phase:

$$HCO_3 + H^+ = CO_2(g) + H_2O$$

and

$$HS + H^+ = H_2S(g)$$
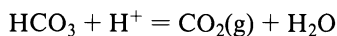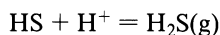
also fO_2 increases, and oxidation $(HS \rightarrow H_2S \rightarrow H_2SO_4)$ and destruction of thiocomplexes $[Au(HS)_2^- - Au^+2(HS)^-]$ will take place, due to the rapid disappearance of the ligands HS.

Thus oxidation within and above the zone of boiling results in the formation of H_2SO_4, decrease in pH and acid leaching (argillic alteration). During this process, electrons are released which reduce the Au^+ to its neutral state Au° causing its precipitation as a native metal. We will return to this process during discussion of geothermal systems in Chapter 11.

Other important mechanisms for the precipitation of the dissolved constituents are chemical reactions between the solutions and wall rocks. Skinner (1979) lists three types of reactions which can be considered important, and which are explained below.

When a hydrothermal solution is acidic, as are the majority, extraction of hydrogen ions from the solution takes place through hydrolysis of feldspars (see Chaps. 1 and 4) and other silicates, which are then transformed into clays (argillic alteration). The loss of H^+ from the solution reduces the stability of chloride complexes and causes precipitation of sulphides, providing S is present to react with the metals liberated from the metasomatised silicates. Another type of wall-rock reaction is the change of oxidation, or valency state, of some metals, most notably Fe, Cu, U. It is known that Fe^{2+} can be transported in solution and that a change from Fe^{2+} to Fe^{3+} causes its precipitation as Fe_2O_3. This is the mechanism invoked for the deposition of banded iron formations (BIF), whatever the causes for oxidation of Fe. Another example is provided by U. This metal is transported in solution as the uranyl ion $(UO_2)^{2+}$, and precipitation occurs when the solutions enter a reducing environment, so that reduction of UO_2^{2+} to UO_2 takes place corresponding to a change in valency from U^{6+} to U^{4+}. Additions of wall-rock components to the solution is a third type of reaction during which precipitation of sulphides may take place. Chemical changes due to mixing of fluids of different components lead to ore deposition.

References

Barnes H L (1979 Solubilities of ore minerals. In: Geochemistry of hydrothermal ore deposits, 2nd edn. John Wiley & Sons, New York, pp 404–410

Bonatti E (1975) Metallogenesis at oceanic spreading centres. Earth Annu Rev Planet Sci Lett, 3:401–431

Bowen R (1988) Isotopes in the earth sciences. Elsevier, London, New York, 647 pp

Brimhall G H, Crerar D A (1987) Ore fluids: magmatic to supergene. In: Carmichael I S E, Eugster H P (eds) Thermodynamics and modelling of geological materials: minerals; fluids and melts. Reviews in mineralogy, vol 17. Min Soc Am, pp 235–321

Cole D R, Drummond S E (1986) The effect of transport and boiling on Ag/Au ratios in hydrothermal solutions: a preliminary assessment and possible implications for the formation of epithermal precious-metal ore deposits. J Geochem Explor 25:45–79

Crerar D A, Wood S, Brantley S, Bocarsly A (1985) Chemical controls on solubility of ore forming minerals in hydrothermal solutions. Can Mineral 23:333–351

Doe R B, Delevaux M A (1972) Source of lead in Southwest Missouri galena ores. Econ Geol 67:409–425

Ellis A J, Mahon W A J (1977) Chemistry and geothermal systems. Academic Press, New York London, 392 pp

Evans A M (1987) An Introduction to ore geology, 2nd edn. Blackwell, Oxford, 358 pp

Faure G (1986) Principles of isotope geology, 2nd edn. John Wiley and Sons, New York, 589 pp

Feiss P G (1978) Magmatic sources of copper in porphyry copper deposits. Econ Geol 73:397–404

Greybeal F J (1973) Copper, manganese and zinc in coexisting mafic minerals from Laramide intrusive rocks in Arizona. Econ Geol 68: 785–798

Guilbert J M, Park C F (1985) The geology of ore deposits. Freeman, San Francisco, New York, 985 pp

Hanor J S (1979) The sedimentary genesis of hydrothermal fluids. In: Barnes H L (ed) Geochemistry of hydrothermal ore deposits, 2nd edn. John Wiley & Sons, New York, pp 137–168

Henley R W, Norris R J, Paterson C (1976) Multistage ore genesis in the New Zealand geosyncline. A history of post-metamorphic lode emplacement. Mineral Depos 11:180–196

Henley R W, Truesdell A H, Barton P B, Whitney J A (1984) Fluid-mineral equilibria in hydrothermal systems. Rev Econ Geol 1. Soc Econ Geol, 267 pp

Hollister L S, Crawford M L (eds) (1981) Short course in fluid inclusions: application to petrology. Mineral Assoc Can, 304 pp

Ilton E S (1990) Partitioning of base metals between silicates, oxides and a chloride-rich hydrothermal fluid. Part II. Some aspects of base metal fractionation during isothermal metasomatism. Geochem Soc Spec Publ 2: 171–178

Ilton E S, Eugster H P (1990) Partitioning of base metals between silicates, oxides and a chloride-rich hydrothermal fluid. Part I. Evaluation of data derived from experimental and natural assemblages. Geochem Soc Spec Publ 2: 157–170

Ivanova G F (1969) Conditions of concentration of tungsten during greisenisation. Geokhimya 1:22–36. (in Russian)

Koslovsky Y E A (1984) The world's deepest well. Sci Am 251:106–113

Krauskopf K B (1979) Introduction to geochemistry. McGraw-Hill Kogakushu, 617 pp

Large R, Huston D, McGoldrich P, McArthur G, Ruxton P (1988) Gold distribution and genesis in Paleozoic volcanogenic massive sulphide systems. In: Bicentenn Gold 88. Geol Soc Aust Abst Ser 22:121–12

Masterton W L, Slowinski E J, Stanitski C L (1981) Chemical principles. Holt-Saunders international edition, 5th edn. Saunders, Philadelphia, 641 pp

Ohmoto H (1986) Stable isotope geochemistry of ore deposits. In: Valley J W, Taylor H P, O'Neil J R (eds.) Stable isotopes in high temperature geological processes. Reviews in mineralogy, vol 16. Min Soc Am, pp 491–559

Roedder E (1979) Fluid inclusions as samples of ore fluids. In: Barnes H L (ed) Geochemistry of hydrothermal ore deposits, 2nd edn. John Wiley & Sons, New York, pp 684–731

Roedder E (1984) Fluid inclusions. Reviews in mineralogy, vol 12. Min Soc Am, 644 pp

Seward T M (1979) Hydrothermal transport and deposition of gold. In: Glover J E, Groves D I (eds) Gold mineralisation. Univ W Aust Ext Serv 3:45–55

Shepherd T, Rankin A H, Alderton D H M (1985) A practical guide to fluid inclusion studies. Chapman & Hall, New York, 239 pp

Sheppard S M F (1986) Characterization and isotopic variations in natural waters. Reviews in mineralogy, vol 16. Min Soc Am, pp 165–183

Skinner B J (1979) The many origins of hydrothermal mineral deposits. In: Barnes H L (ed) Geochemistry of hydrothermal ore deposits, 2nd edn. John Wiley & Sons, New York, pp 3–21

Spencer R J, I-Ming Chou (eds.) (1990) Fluid-mineral interactions: A tribute to H.P. Eugster. Geochem Soc Spec Publ 2, 432 pp

Smirnov I (1976) Geology of mineral deposits. MIR, Moscow, 520 pp

Taylor H P (1979) Oxygen and hydrogen isotope relationships in hydrothermal mineral deposits. In: Barnes H L (ed) Geochemistry of hydrothermal ore deposits, 2nd edn. John Wiley & Sons, New York, pp 236–277

Valley J L, Taylor H P, O'Neil J R (eds) (1986) Stable isotopes in high temperature geological processes. Reviews in mineralogy, vol 16. Min Soc Am, 570 pp

Chapter 3
Hydrothermal Systems

3.1 Introduction

In this chapter the types of hydrothermal activities and systems responsible for the genesis of a wide range of mineral deposits are described. Particular attention is given to what we know of the geometry and physical models of these systems, as inferred from active geothermal areas, or reconstructed from geological observations and laboratory studies. Hydrothermal systems can also be considered in terms of the geotectonic settings in which they occur, and these are discussed in Part II of this volume. The various types of hydrothermal processes, their action on the surrounding lithologies, and their products in terms of mineral deposits are addressed in Part III. Here, the following hydrothermal systems are considered:

1. Shallow to deep-seated, plutonic-related magmatic hydrothermal systems. They generate Sn-W greisen deposits.
2. Volcano-plutonic to subvolcanic and volcanic-related, magmatic-meteoric to predominantly meteoric hydrothermal systems. They are responsible for porphyry mineralisation, skarns, epithermal base and precious metal deposits, as well as several types of vein deposits.
3. Sub-sea-floor hydrothermal systems. These are responsible for the wide range of volcanogenic massive sulphide deposits, as for example the Besshi, Cyprus, kuroko types and the Archean Noranda-type sulphide deposits.
4. Rift-associated hydrothermal systems in sedimentary basins, with or without obvious connection to igneous activity. The sedimentary exhalative stratiform sulphide deposits such as Broken Hill and Mt.Isa in Australia, Gamsberg-Aggeneys in South Africa, or the Sullivan orebody in Canada may have been formed by the action of these systems. To these one may add the Red Sea sulphide deposits, which in turn may show gradational variants with the hydrothermal systems under (3) and (6), depending on the stage of development of the rift setting considered (e.g. incipient to advanced). The geodynamic evolution of rift-related orogens may lead to a time continuum (pre- to post-orogenic) of hydrothermal systems from (3) through to (6).
5. Basinal-diagenetic brines. Examples of their activity are the stratabound carbonate-hosted sulphide deposits. These systems may represent end-members of those under (4).
6. Metamorphism-related hydrothermal systems, mostly due to prograde regional metamorphism (some mixing with meteoric waters can occur). Turbidite-hosted

gold deposits, the Archean lode deposits and perhaps the unconformity-related U deposits, may all be products of this type of hydrothermal activity.

Circulation of hydrothermal fluids in the Earth's crust can occur within a number of geological situations, in which a complex array of transitional conditions can lead to a large number of deposit types and mineralisation styles. For this reason the hydrothermal systems described are essentially end members. This simplification is an expedient to help in the understanding of what are obviously very complex natural systems. The exploration geologist must, however, be cautioned not to apply rigid rules, but to allow for flexibility of thought in dealing with the subject of hydrothermal systems.

Also, it must be remembered that the same "geological situation" may occur in a number of different tectonic settings. Thus, for example, felsic plutonic rocks can occur in magmatic arcs related to subduction, or in certain anorogenic rift settings. It follows that magmatic hydrothermal systems can be activated in both these situations and even produce similar styles of mineralisation.

3.2 Definitions and Types

A hydrothermal system can be loosely defined as the distribution of hot fluids circulating, laterally and vertically at various temperatures and pressures, below the Earth's surface. The presence and movement of these fluids, whether or not they discharge at the surface, constitute hydrothermal activity. A more rigorous definition would have to include the geological situation within which the circulation of fluids is generated and maintained for a period of time long enough to form an anomalous concentration of metallic minerals. Whether this anomalous concentration constitutes an orebody or not is generally artificial, and dictated by the global and/or local social, economic and political framework of organised human societies, at a particular time.

A hydrothermal system consists of two essential components: a heat source (H), and a fluid phase (F). An actively convective hydrothermal cell will consist of: a recharge system (R), a circulation cell (C) and a discharge system (D) (cf. Fig.3.3). A hydrothermal mineral deposit is formed by the circulation of warm to hot fluids (about 50 to > 500°C) that leach, transport and subsequently precipitate their mineral load in response to changing physico-chemical conditions. Mineral deposits are usually formed at the discharge site, whether this is a single conduit, or a series of channelways, or a fine network of small fractures. The rocks within which the deposit is formed undergo varying degrees of hydrothermal alteration, the intensity of which as a rule decreases away from the discharge site(s), and hence from the mineralised body. Alteration takes place because the mineral assemblages in the wall rocks are unstable in the presence of the hydrothermal· fluids, and tend to re-equilibrate by forming new mineral assemblages that are stable under the new conditions. Processes of alteration are examined in some detail in Chapter 4.

A "fossil" hydrothermal system is the result of "frozen-in" hydrothermal activity in a given geological and tectonic setting. For example, a porphyry Cu-Au deposit such as that at Panguna in the island of Bougainville (Papua New Guinea), is the result of a volcano-plutonic hydrothermal system formed in an oceanic island arc setting. Although there may be conflicting opinion amongst geologists as to details of the workings of such a system, there is little doubt that the hydrothermal activity at Panguna was started by magmatic events relating to the emplacement of a volcano-plutonic complex. The gold deposits found in turbidite sequences are also part, or the expression of a portion, of "fossil" hydrothermal systems. In these, however, circulation of the fluids affected a larger sector of the Earth's crust than is the case for a porphyry Cu-Au deposit, and the presence of a metalliferous quartz vein is but the expression of the discharge of fluids in one locale. Base and precious metal deposits in ophiolitic rocks – such as those found in Cyprus, in the Samail ophiolites of Oman, or the Appennines in Italy – are considered the products of fossil hydrothermal systems, whose modern analogues can be found at mid--ocean ridges. Many of the volcanic-associated precious and base metal deposits, both in the subaerial and submarine environments, represent "frozen-in" hydrothermal systems, with their modern counterparts being observed in active geothermal areas in volcanic terranes at modern convergent plate boundaries. Similarly, the sulphide muds forming today in the depressions of the axial zone of the Red Sea may have their analogue in some of the Proterozoic-aged, sediment-hosted massive sulphide deposits. However, not all of the hydrothermal mineral deposits preserved today have a modern equivalent: namely, many of the deposits of Archean age. This is because they were the product of hydrothermal systems activated during particular geotectonic situations, which have not since been repeated. Amongst these one can cite the epigenetic mesothermal Au lodes and BIF-hosted Au mineralisation so commonly found in greenstone belts. In other instances, hydrothermal activity occurs at depths beyond our direct observation. Deep drilling in the continental crust has, however, indicated the presence of hydrothermal fluids circulating along major shear zones at depths of several kilometres.

3.3 Magmatic Hydrothermal Systems Related to Shallow and Deep-Seated Plutonism

These systems are usually generated in H_2O-rich magmas, such as muscovite-bearing granitoids (>8 wt.% H_2O). These magmas tend to crystallise at depths ranging from a few km to over 10 km, and do not usually vent at surface. Although they may, at certain stages, intrude into wet crustal rocks and interact with connate or metamorphic waters (Strong 1981). For the present purpose we are concerned only with the case of a closed system, that is, hydrothermal fluids generated entirely within the body of a cooling magma. As the magma cools and crystallises, H_2O, other volatiles and incompatible elements remain largely excluded from the consolidating mass. Volatile components are at first randomly distributed through-out the upper and central regions of the magmatic body. In this respect Taylor and

Pollard (1988) envisage that during the late stages of magmatic crystallisation, fluids are contained in the interstices of the granitic minerals, in much the same way as "oil in a sandstone...whose movement and accumulation may be controlled by the evolving permeability" (Taylor and Pollard 1988). Eventually, the residual fluid phases may coalesce and concentrate into zones to induce autometasomatism of the igneous parent. In other words, the newly consolidated igneous body "stews in its own juice". This usually begins with a stage of alkali metasomatism (Chap. 8). The aqueous and gas phases exsolved from the magma will form a hydrothermal solution. This leads to a stage of hydrogen-ion metasomatism during which greisen-related deposits may form (Chap. 9). With decreasing temperature and pressure, and the presence of channelways, the fluids may eventually escape into the surrounding country rocks.

3.4 Magmatic-Meteoric Hydrothermal Systems Related to Volcano-Plutonic and Volcanic Complexes

In these situations hydrothermal systems commonly start as described above (Sect. 3.3), in the closed system of a plutonic body. In this case, however, by virtue of its relatively low initial water content, the magma rises closer to the surface and may vent to form a stratovolcano. This is most typical of both porphyry and epithermal systems (Chaps. 10 and 11). The cooling pluton supplies the thermal energy and in the initial stages the fluids. At a later stage, the fluids may be supplied from without by meteoric waters and groundwaters (aquifers). These waters become heated as they are approached by, or descend into the region influenced by the igneous body(ies). Cooling of igneous bodies at depth provides powerful heat engines. The energy of a single granite pluton has been estimated by Fyfe (1987), who calculated that a granite pluton with a volume of 600 km^3, and cooling from 900 to 300°C, could heat about 1000 km^3 of groundwater to 300°C. Meteoric or groundwaters will form convection cells whose activity will last at least until the thermal energy of the cooling igneous rocks has entirely dissipated. This implies clearly that mixing between purely magmatic and meteoric phases is the rule rather than the exception, and indeed in many cases isotopic evidence in modern geothermal systems indicates that meteoric waters may be the sole fluid component. In conclusion, hydrous magmas that consolidate near the surface are likely to generate magmatic-meteoric hydrothermal systems by the action of late residual aqueous fluids, and by the action of meteoric waters that become heated in the vicinity of the intrusive body.

The following discussion focuses first on the development and activity of a magmatic aqueous phase. The next section considers the meteoric hydrothermal systems, using data obtained from the study of modern geothermal fields. While the two systems are treated separately for simplicity, it must be borne in mind that in most instances they form a continuum.

3.4.1 Magmatic Hydrothermal Systems

Aqueous fluids separating from crystallising magmas are usually channelled through fracture systems within the higher portion of an intrusive body, and/or within the surrounding wall rocks. As the role of H_2O in magmas is very important, a brief digression is appropriate at this point, and the reader is referred to Best (1982) or Carmichael et al. (1974) for further details on this topic (see also Chap. 8). Water is by far the most abundant volatile constituent of magmas, especially felsic. Other constituents include H_2S, CO_2, HCl, HF, H_2. The H_2O content of felsic magmas with which hydrothermal activity is connected may range from 2.5 to 6.5 wt.%. The presence of H_2O in a melt has the effect of considerably lowering its viscosity due to the depolymerisation phenomenon. Water-rich silicic melts can be as fluid as basaltic melts. Silicate melts have structures formed by Si^{4+} and Al^{3+} in tetrahedral co-ordination with O^{2-} ions, these O^{2-} ions being commonly shared (bridging) between neighbouring tetrahedra. This linking through the bridging oxygens constitutes a polymerised structure which resembles the crystalline state. H_2O (and other volatiles like B, F, Cl) breaks the oxygen bridges and therefore depolymerises the structure. The bridging is then accomplished by replacing the O^{2-} with $2OH^-$, according to Best (1982):

$$H_2O(a) + O^{2-}(m) = 2OH^-(m),$$
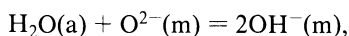
where a = aqueous phase and m = melt phase.

Thus, H_2O is effectively not held in solution as neutral water molecules, but forms hydroxyl OH ions.

Acid volatiles such as H_2S, HCl and HF behave similarly to H_2O in a silicate melt, while CO_2, SO_2 and H_2 do not generally have a solution mechanism like that of water. The solubility of CO_2 in alumosilicate melts is very low compared with that of H_2O and other acid volatiles. CO_2 does not depolymerise the melt. Addition of H_2O to the melt not only breaks the oxygen bridges, but also increases the expansibility of the liquid, consequently allowing entry of the larger CO_2 molecules. Thus, CO_2 solubility increases with increased H_2O contents.

Best (1982) summarises the behaviour and role of H_2O in silicate melts as follows: (1) it depolymerises the melt and reduces its viscosity; (2) it increases diffusion rates; (3) it depresses crystallisation temperatures; (4) it exsolves and expands in the magma, in certain instances causing explosive volcanism. In terms of hydrothermal activity the following points are important: (1) H_2O in subsolidus systems, promotes alteration of higher temperature minerals. (2) Retrograde boiling and separation of an aqueous solution in confined plutonic systems produces pegmatites and mineralised veins.

The concept of boiling in magmas is also important. First boiling is that which occurs in a magma during decompression, causing exsolution of the volatiles due to their decreased solubility resulting from the lowered pressure. Second or retrograde boiling takes place as a result of the enhanced concentration of volatiles due to the effects of crystallisation. The continuous increase of H_2O in the residual melt during crystallisation is such that, at some stage, the pressure in H_2O becomes equal to the confining pressure and retrograde boiling takes place. This retrograde

boiling has the effect of creating a separate aqueous phase (i.e. a hydrothermal solution).

Burnham (1979) examined in some detail the magmatic hydrothermal system generated by the cooling of a hypothetical granodiorite intrusive stock containing 3 wt.% water. The discussion which follows is based on Burnham's article, and reference must be made to the sketches in Fig.3.1A, B and C.

Cooling of the intrusive body is assumed to have taken place in a subvolcanic environment. Therefore, it is implied that during the initial stages of cooling the system is open, allowing the escape of volatiles through fractures above the pluton. At a later stage, the intrusive body becomes a closed system by developing a solidified shell. This stage is shown in Fig. 3.1A, where line S1 represents the boundary outside which the stock is below the solidus temperature. Burnham (1979) further assumes that the maximum temperature in the interior of the stock is 1025° C, that the 1000°C isotherm extends to a depth of 2.5 km, and that this isotherm encloses the portion of the body which is still 90% melt. Upward and outward from the 1000°C isotherm, the H_2O content of the residual melt increases to a zone where the melt is saturated with H_2O at 3.3 wt.%. At this level and up to the solidus line S1, the system is made up of a crystalline assemblage containing pyroxene, a residual melt of granitic composition and the aqueous fluid phase. At greater depths, and always outward from the 1000°C isotherm, hornblende and biotite remain stable at temperatures between 800–900°C and 780–850°C, respectively. Biotite forms by reaction of the residual melt with hornblende, and as a result, silica is enriched in the residual melt and quartz crystallises. These processes lead to saturation with H_2O of the remaining interstitial melt, while the rest of the stock is still largely molten and H_2O-unsaturated. This molten portion becomes enveloped by a zone of H_2O-saturated interstitial melt, which is in turn enclosed by a solidified shell (or carapace in the terminology of Burnham's). The thickness of this H_2O-saturated zone decreases with depth, forming a barrier to the movement of volatiles towards the solidified wall rocks, and thus increasing the vapour pressure within the magma. In the upper portion of the H_2O-saturated zone second boiling occurs, leading to the development of an abundant aqueous phase (Fig. 3.1B).

As depicted in Fig. 3.1B, the mechanical energy developed by the increased vapour pressure overcomes the tensile strength of the rock, as well as the confining pressure, resulting in rapid expansion with fracturing and brecciation (FBx) of the crystalline shell above the H_2O-saturated zone. A further result of this process is the reduction of the fluid pressure, which causes more of the H_2O-saturated interstitial melt to crystallise and to evolve more aqueous fluid phase. This fluid phase will penetrate the overlying fractures, further extending them out and upward by hydraulic fracturing. The near-vertical attitude of the fractures is related to the local stress field, with its maximum principal stress being vertical so that expansion occurs in the direction of the least principal stress, in the horizontal plane. Continued cooling will cause the retreat of S1 to S2 and the H_2O-saturated zone to the deeper levels of the stocks. If the breaching of the H_2O-saturated zone occurs in the thickened upper portions of the zone, where large volumes of aqueous fluid would ordinarily have accumulated, then the formation of breccia pipes is likely (BP in Fig.3.1B, C). Breaching in the thinner and deeper parts of the H_2O-saturated
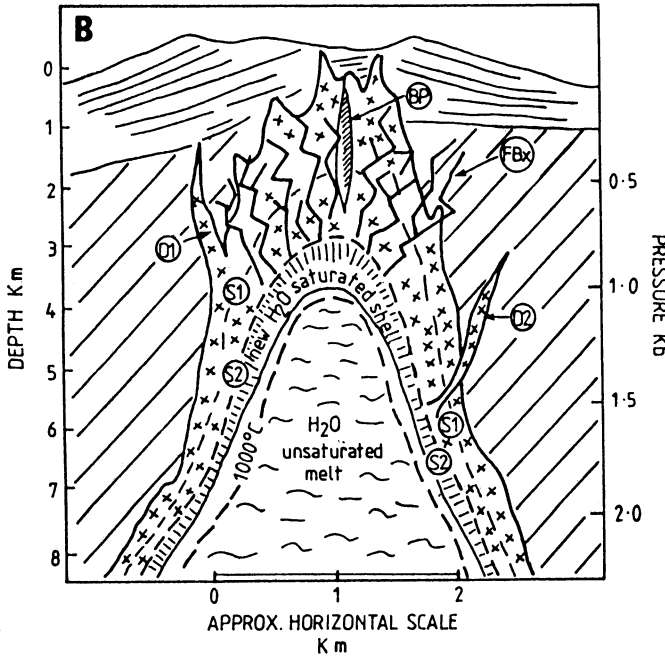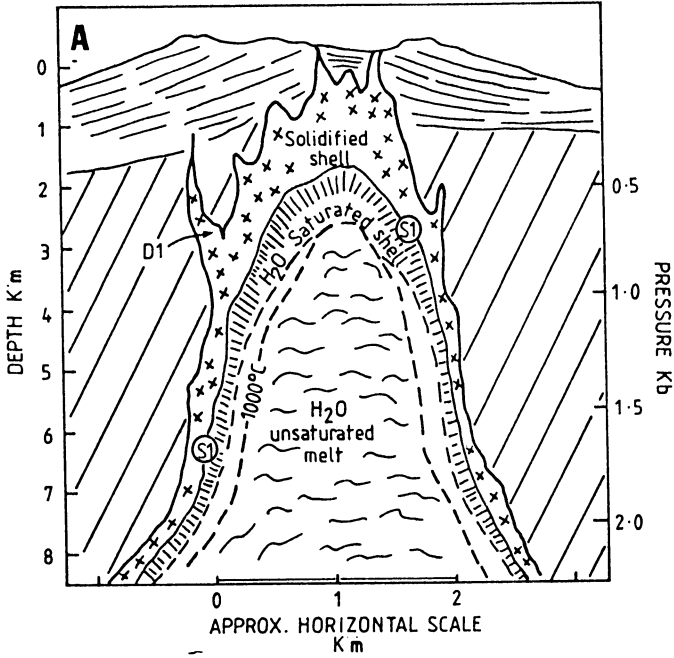
Fig. 3.1A, B
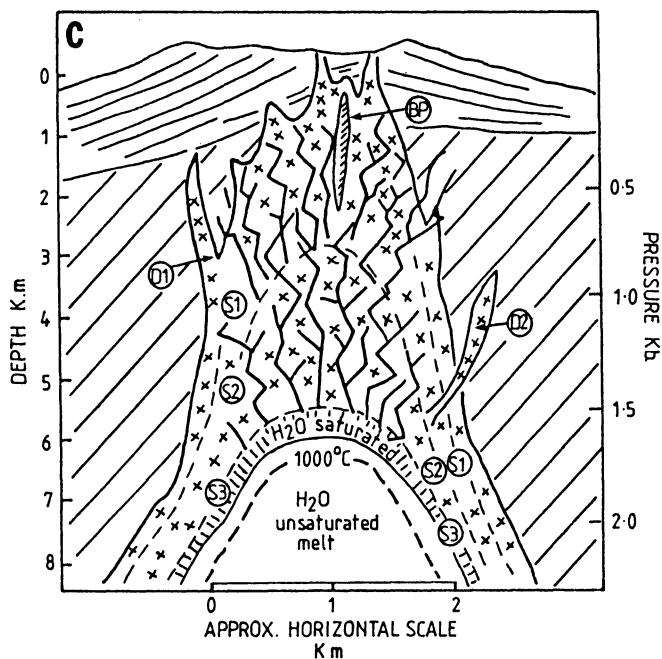
Fig. 3.1A–C. Idealised magmatic hydrothermal system related to the cooling of a porphyry intrusion with a volcanic superstructure. The sequences A to C are explained in the text (After Burnham 1979)

zone, on the other hand will cause plagioclase and hornblende-bearing dykes to emanate from the central and still molten part of the stock (D2 in Fig.3.1B, C). In the stage depicted in Fig.3.1B, the magmatic hydrothermal system has been restored to a situation similar to that prior to fracturing, the only difference being that now the H$_2$O-saturated zone lies at a greater depth. The stockwork zone developed during the stage of second boiling becomes healed by precipitation of silica. Further cooling of the magma leads to a repetition of the processes described above. In the final stage, a complex fracture system is developed above the stock (Fig.3.1C), and this acts as a major channelway for ore-bearing fluids and heat from the underlying and still cooling igneous body. The ore minerals are concentrated in the fluid phases and transported into the network of fractures. Mineralisation is usually associated with late pulses of magmatic hydrothermal activity, and repeated pulses that will lead to the formation of large orebodies. It is theorised that the H$_2$O-saturated zone can expand up to 30% upon complete crystallisation at a depth of 3 km, but not more than 5% at a depth of 5 km (Burnahm 1979). Most of these hydrothermal systems are restricted to the upper parts of the Earth's crust, where rocks are capable of yielding by brittle fracture and penetration of meteoric waters can occur.

Figure 3.2 shows the two stages of the magmatic hydrothermal system and the input of meteoric waters in a plutonic setting of the porphyry type. Typically related to the hydrothermal system just described are alteration features known as potassic,
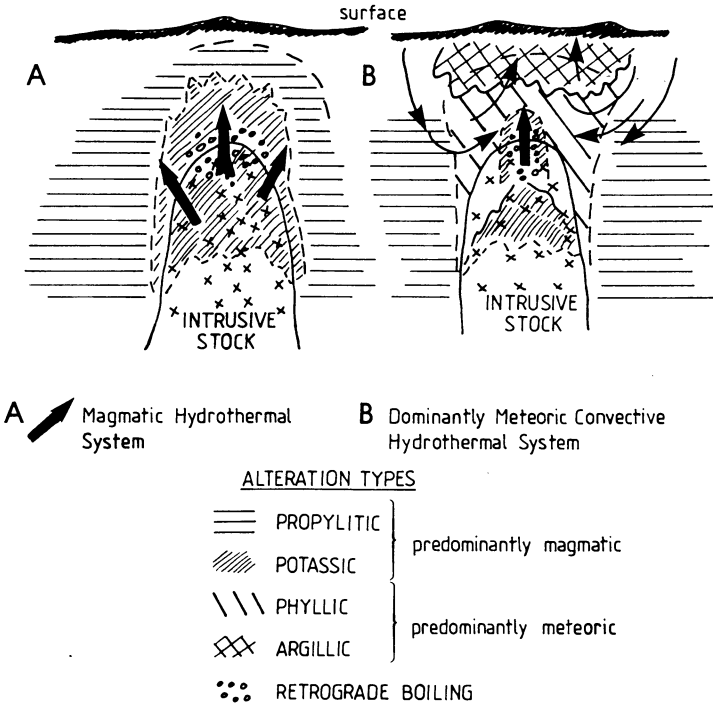
Fig. 3.2. Stages A and B in the development of a magmatic hydrothermal system in a porphyry system, with later input of meteoric water and associated alteration patterns. Drawing not to scale (After McMillan and Panteleyev 1980)

propylitic, phyllic and argillic, all to be described in Chapters 4 and 10. During the magmatic stage, potassic and propylitic alterations (alkali metasomatism) predominate, whereas during the subsequent stages of meteoric water input, hydrogen ion metasomatism (phyllic alteration) predominates. "Collapse" of the hydrothermal system, dominated by meteoric water, results in a stage of acid leaching or argillic alteration.

3.4.2 Predominantly Meteoric Hydrothermal (Geothermal) Systems

The exploration for geothermal energy in regions of high heat flow has contributed a great deal to our understanding of the geology and hydrothermal processes in active geothermal systems and, as a spin-off, our knowledge of ore-forming processes. Active and fossil geothermal systems are associated with areas of volcanic and plutonic activity at convergent and divergent plate margins.

Many of the studies conducted in these areas have in fact focused on the solution, transport and deposition of solute matter from the mineralising solutions. There are many published works on the subject, but for the purpose of the present section the

interested reader is referred to White et al. (1971), Weissberg et al. (1979), Ellis and Mahon (1977) and Henley and Ellis (1983).

The penetration of meteoric waters in the crust of the Earth, via permeable zones down to levels influenced by cooling igneous bodies, results in their interaction either with heated country rocks (conduction), with steam, or directly with hot magmatic fluids. The heated groundwaters, by virtue of their lower density, rise back towards the surface, setting up a thermal convection cell and therefore a geothermal system. Terrestrial geothermal systems are derived from air-saturated meteoric waters that circulate down to depths probably in excess of 5 km, while their activity may occupy a time span of 10^5 to 10^6 years (Henley and Ellis 1983). The surface expression of these geothermal systems are hot springs (chloride-rich, acid sulphate-bicarbonate-rich, dilute chloride waters), steam vents, geysers, mud pools and fumaroles. Geothermal systems are also present on the sea floors, at mid-ocean ridges and around volcanic islands. Section 3.7 looks at these such submarine systems in some detail. The below-surface configuration of a geothermal system varies according to the geological setting, the dominant structures, permeability and hydrology of the region. An idealised "mushroom"-shaped profile of the isotherms above a heat source and the associated convection cell driven by it is illustrated in Fig. 3.3, obtained from well data at Wairakei in New Zealand (Ellis and Mahon 1977). The wall rocks through which the waters circulate are subject to varying degrees and types of hydrothermal alteration which are dependent on a number of factors, including the chemical character of the waters. Ellis and Mahon (1977) point out that the solutes carried by the hot waters may have been acquired from the cooling igneous rocks (magmatic), or could be leached by the fluids through their interaction with the wall rocks, or both.
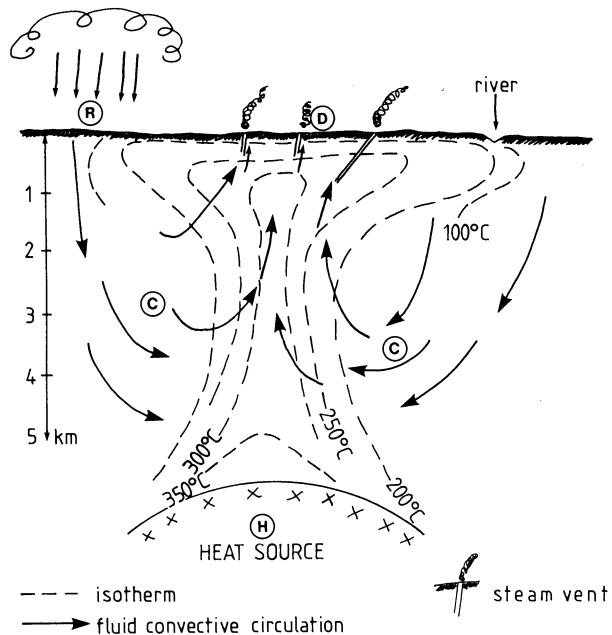
Fig. 3.3. Distribution of isotherms above a heat source, and idealised pattern of fluid convective circulation. H heat source; C convective cell; R recharge; D discharge (After Ellis and Mahon 1977)
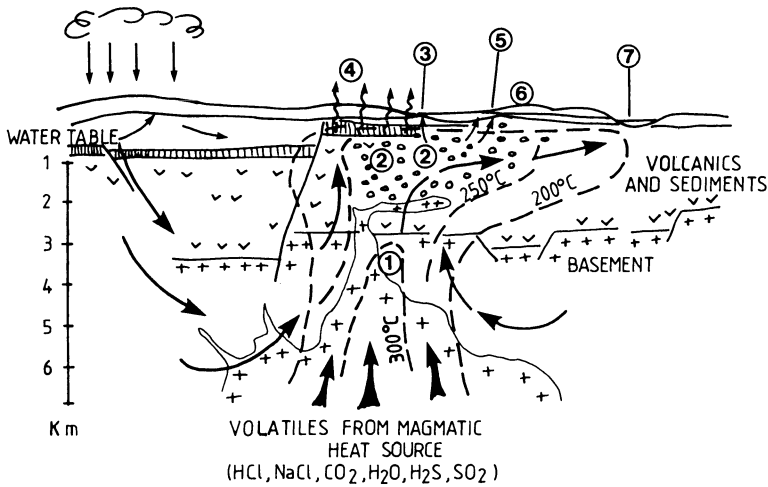
① Isotherms and convective cell of neutral chloride fluids

② Liquid and vapour reservoir

③ Acid-Sulphate-Bicarbonate springs

④ Fumaroles

⑤ Near-neutral pH chloride springs

⑥ Siliceous sinter deposit

⑦ Dilute chloride springs

Fig. 3.4. Caldera-type geothermal system. Fluid convective circulation shown by *thin arrows*; *small circles* indicate approximate extent of liquid-vapour reservoir (boiling zone). See text for details (After Henley and Ellis 1983)

    There are a number of possible scenarios for geothermal systems. Using the works of Henley and Ellis (1983) and Bogie and Lawless (1987) we can consider four principal settings and associated types of geothermal systems. These are: (1) calderas in silicic volcanic terranes; (2) andesitic stratovolcanoes; (3) highland volcanoes; (3) volcanic islands.

    The main features of a geothermal system in a caldera setting are shown in Fig.3.4. Recharge is by meteoric groundwaters, and the heat plus volatiles, including HCl, CO_2, H_2O, etc., are supplied by a buried magmatic system. A convective cell (1) is formed above the heat source, and consists of near-neutral pH chloride water. In the upper levels boiling and separation of steam occur, so that a two-phase zone (liquid + steam) is present near the top of the convective column (2). The development of steam and partitioning of the H_2S into the vapour phase results in steam-heated acid sulphate-bicarbonate waters (3), as well as steaming ground and fumaroles (4) above the two-phase liquid-steam zone. Direct outflow of the near-neutral chloride waters gives rise to boiling alkaline springs (5), from which siliceous sinter is generally deposited (6). Dilution with groundwaters may result in dilute near-neutral chloride springs (7), whereas mixing between the deep near-neutral

chloride and the steam-heated acid sulphate waters will produce oxidising Cl-SO_4 waters.

A characteristic feature of this particular system is its situation within a depression formed by the caldera structure, so that water recharge is more or less at the same level as the discharge, with important implications that will become apparent later. In these systems the development of hydrothermal breccias and sinters is very common, a typical example being the Waiotapu geothermal system in the Taupo volcanic zone in New Zealand (Hedenquist and Henley 1985). The conspicuous development of silica, and its sealing effect, may be partly responsible for the hydrothermal eruptions, though boiling under the siliceous cap with separation and accumulation of volatiles is considered to be the main cause (Hedenquist and Henley 1985). While this particular aspect of modern geothermal systems is covered more thoroughly in Chapter 11, it is nevertheless worthwhile to mention here that Au and other metals are deposited during these boiling events.

The precipitation of silica in the geothermal systems associated with caldera settings, and particularly the formation of extensive sinters (amorphous silica precipitated at the surface by fast flowing hot water), is probably due to two main factors. One is the solubility of quartz at the temperature of equilibration between the water and the wall rocks (180°C). Solubility of quartz increases with temperature, and at high temperatures quartz solubility is decreased in chloride solutions and increased in alkaline solutions (Fyfe et al. 1978). Therefore with subsurface temperature in excess of 180°C, and in chloride waters, the amount of silica may exceed the solubility of quartz, so that precipitation results. The other factor, identified by Bogie and Lawless (1987), is that the silica-charged waters in these low relief areas readily reach the surface and do not outflow as distal springs, as may be the case for stratovolcanoes where the silica is dispersed en route.

In regions of high relief, provided by tall andesitic stratovolcanoes the features of the associated geothermal system differ as shown in Fig.3.5 and discussed below. The convective cell is located deep within the volcanic edifice and possibly its basement (1), and the recharge of the system is from areas of low elevation (2). The centrally situated high relief prevents the discharge of the chloride-rich waters in the areas above the convective up-flow. Instead, due to boiling and steam separation with the presence of H_2S (3), fumaroles and steam-heated aquifers forming acid-sulphate fluids are present high on the volcanic slopes and/or the crater area (4 and 5). It is anticipated here that acid-sulphate waters are the principal cause for acid leaching and argillic type alteration. Also, because of the intensive leaching, rocks may be altered to a porous siliceous residue that is often mistaken for sinter (White et al. 1971). Chloride springs may be found at considerable distances (up to 20 km) along the outlying regions of the volcanic complex (6) (Henley and Ellis 1983). In this case, as previously mentioned, silica is likely to be deposited en route to the distal chloride springs, and sinters are unlikely to form in this setting. However, percolation of acid-sulphate waters and their mixing with the near-neutral reservoir may deposit silica and anhydrite somewhere above the hydrothermal reservoir (Bogie and Lawless 1987).

The third setting considered is that provided by volcanic complexes in highland regions as, for example, in the Andes, or central Papua New Guinea. This is the
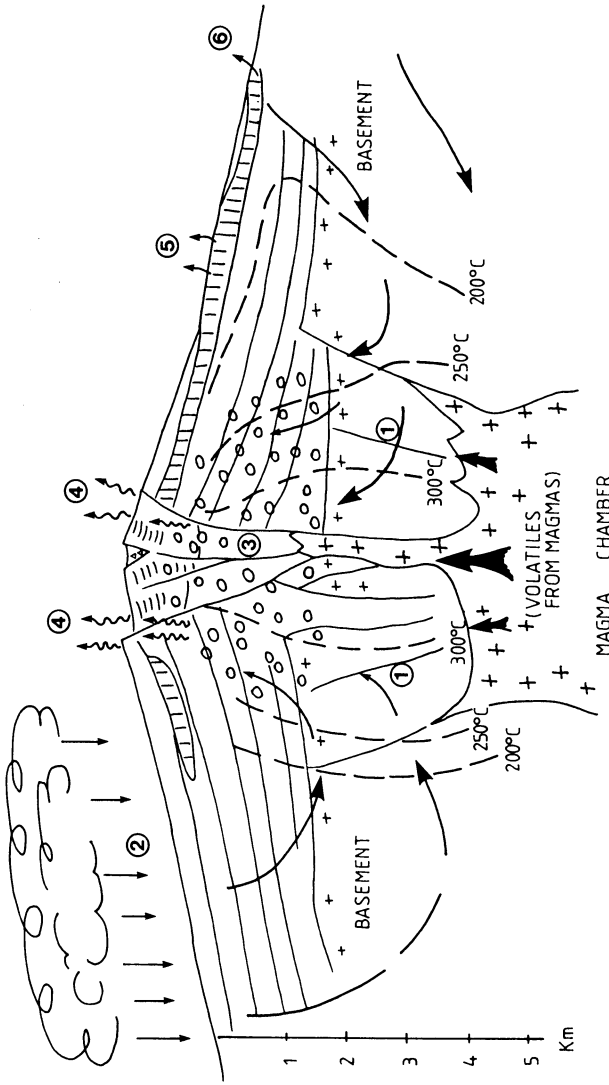
Fig. 3.5. Geothermal system associated with an andesitic strato-volcano. *Symbols* same as those of Fig. 3.4. See text for details (After Henley and Ellis 1983)

① Convective upflow of near-neutral pH chloride fluids

② Meteoric re-charge

③ Liquid-vapour reservoir/oxidation of H_2S

④ Fumaroles and native S

⑤ Sulphate-bicarbonate aquifer

⑥ Distal spring

BASEMENT

MAGMA CHAMBER

(VOLATILES FROM MAGMAS)

200°C 250°C 300°C

Km
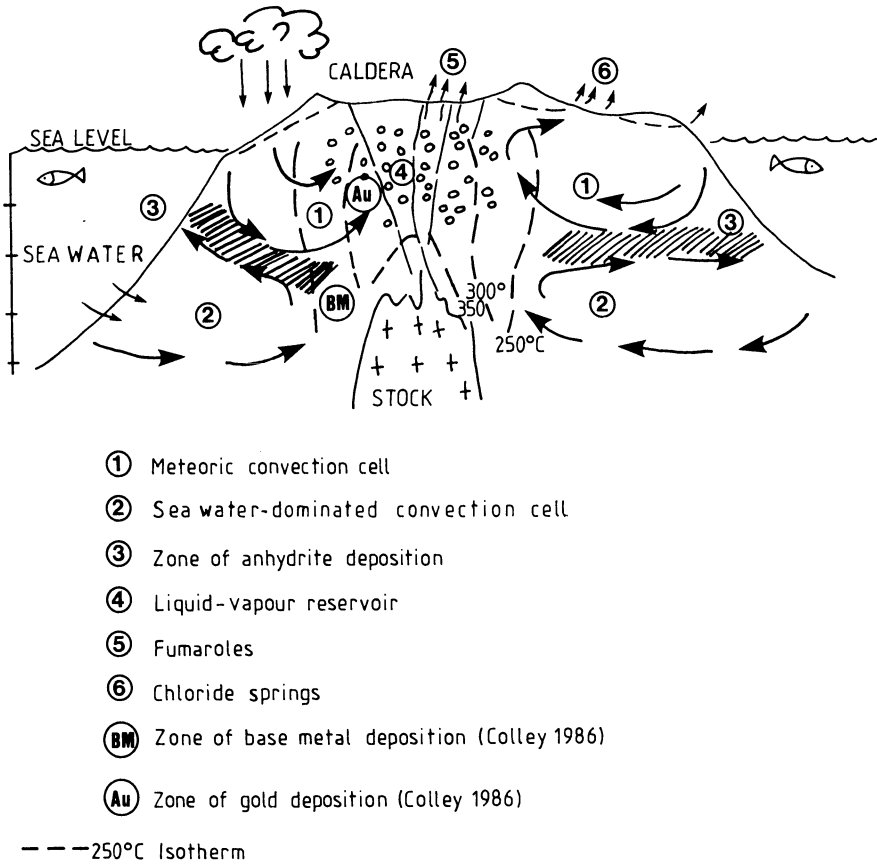
Fig. 3.6. Convective cells associated with a volcanic island. Symbols are the same as those of Fig. 3.4. See text for details (After Bogie and Lawless 1987, Colley 1986)

setting referred to by Bogie and Lawless (1987) as "cordilleran type". The associated geothermal systems share the features of the two types described above (caldera and stratovolcano settings), because here the volcanic edifices are located in high plateau areas, so that recharge is both at high and low elevations. The hydrothermal reservoir is consequently close to the surface but not necessarily laterally confined by inflow of meteoric waters, as in the caldera situations (Bogie and Lawless 1987). Characteristic of these systems may be the presence of maars, due to phreatomagmatic explosions (interaction of groundwater with magma). These may be the sites of important epithermal vein and breccia gold deposits (Sillitoe and Bonham 1984).

   Finally, the setting of volcanic islands, exemplified by the now famous Lihir Island in Papua New Guinea (Chap. 11), is the case of recent island arcs constructed on a predominantly oceanic basement. The principal features of a geothermal system developed in such a setting are shown in Fig. 3.6. The main characteristic in this model is the presence of sea water, which in part may control the hydrology of

the system. Sea water penetration into the flanks of the submerged volcanic edifice will cause fresh water to float upon it on account of the density contrasts (sea water is denser). Thus it is thought that two convective cells are present in this system. One is a cell of fresh water (1) in the upper part of the volcano with a density of less than 1 g/cm^3, located above a cell of sea water-dominated fluid (2) with a density of greater than 1.1 g/cm^3 (Colley 1986). Ordinarily, there would be no mixing at the interface, but any heating of the sea water lens and convection would cause disturbance and limited mixing. This may cause the precipitation of anhydrite along a zone (3) that in time could cause the blockage of sea water recharge. Tectonic activity and boiling may break the anhydrite sealing and the hydrology of the system would be re-established. Fumaroles (5) and chloride springs (6) are present within the caldera and the slopes of the volcanic structure. This model again poses important implications for the exploration of epithermal gold deposits in this setting, because mineral deposition is in part controlled by the peculiar hydrology of the volcanic island (Fig.3.6).

3.4.3 Hot Water-Dominated and Vapour-Dominated Hydrothermal Systems

In a geothermal field, wells may tap either hot water or steam, depending on the balance between heat flow and availability of water in the system (Ellis and Mahon 1977). A model explaining the presence of vapour-dominated systems in geothermal fields such as those of Larderello in Italy and The Geysers in California, was presented by White et al. (1971). These authors attributed the dominance of vapour to diminished permeability due to mineral deposition. In essence, a decreased rate in recharge of water results in more water being "boiled off" than can be replaced by fresh input. Artificially this can be induced in geothermal areas where wells draw off more hot water than can be replaced by natural recharges.

The anatomy of a vapour-dominated geothermal reservoir, according to the model of White et al. 1971, Fig. 7), is summarised here. Above a zone of convective heat transfer by thermal waters (brines), there is a vapour-dominated reservoir enriched in other gases (H_2S, CO_2, etc.) where heat flow is largely by conduction. The vapour-dominated reservoir tends to migrate downward as excess pore water is vaporised. Channels of inflowing groundwaters from the margins of the hydrothermal chamber are continuously narrowed by mineral precipitation (mainly calcite and anhydrite). The vapour-dominated reservoir passes upward into a zone of steam condensation, where clay minerals are being formed and tend to clog pore spaces and channels. However, part of this condensate may move up to the water table, or to the surface as acid-sulphate springs, or may form pools of boiling mud. In addition, vapour from the vapour-dominated reservoir may escape directly at the surface forming solfataric fumaroles (see below). In this dynamic system there is net loss of liquid water, due to diminished inflow caused by mineral deposition (sealing) at the margins of the reservoir,so that liquid water is constantly being replaced by vapour. Continued boiling below the vapour-dominated reservoir tends to produce brines by concentration of solute matter during boiling. Boiling of the brine is also likely to produce superheated steam with respect to pure water at the same pressure.

This causes the brine to become a highly effective agent for heat and mass transfer, because steam boiling off from a brine is superheated by several degrees, depending on and increasing with the concentration of the solutes. Steam-heated aquifers are important for the exploitation of geothermal energy and for the formation of precious metal deposits.

3.4.4 Hot Springs, Mud Pools, Geysers, Crater Lakes and Fumaroles

Transfer of heat and dissolved matter through aqueous and gaseous fluids in volcanic areas is manifested at the surface as hot springs, fumaroles, mud pools and, less commonly, geysers. This section briefly reviews these surface phenomena. Further details may be found in texts of volcanology, such as Williams and McBirney (1979), and the old, but classic book by Rittmann (1962). Ellis and Mahon (1977) provide modern geochemical data. Previous sections have discussed two types of hot springs, namely: acid-sulphate and near-neutral chloride. Other types include carbonate and bicarbonate-rich thermal waters. Selected partial analyses of thermal waters are given in Table 3.1.

Acid-sulphate hot springs are characterised by low pH, due to oxidation of H_2S to H_2SO_4, and are generally low in chlorides, while emanations containing HCl may also be present. Besides H_2S, these thermal waters are enriched with other volatiles (CO_2, NH_3, B), as well as "volatile" metals like Hg, As, Bi and Sn. Acid-sulphate

Table 3.1. Partial analyses of hot spring and thermal pools. All values are given in parts per million (ppm). Data (analyses 1 to 4) from various sources published in Ellis and Mahon (1977). (1) Crater Lake, New Zealand; (2) Kamchatka, USSR; (3) Rotokaua, New Zealand; (4) Champagne pool, New Zealand; (5) Nevado del Ruiz, Colombia (after Sturchio et al. 1988)

Element	1	2	3	4	5
Li	1.6	–	7.8	10.8	3.01
Na	740	1010	990	1070	523
K	79	88	102	102	68.2
Rb	0.4	–	–	1.1	–
Cs	0.1	–	–	2.7	–
Mg	1030	10	11.3	0.4	4.28
Ca	1200	64	11	26	30.5
Fe	900	0.0	–	–	0.02
F	260	0.8	< 1	6.6	0.56
Cl	9450	1684	1433	1770	772
TotalSO_4	10950	83	520	26	38
Total CO_2	–	32	144	55	189
Total SiO_2	852	160	340	–	193
Total B	13.8	39	45	21.9	15.1
Total NH_3	11	–	1.6	0.7	–
Total H_2S	–	–	0.2	1.8	–
°C	–	100	65	99	92
pH	1.2	8.4	2.5	8.0	7.0

thermal waters are generated by condensation of steam and vapours as they rise through cracks and fissures at temperatures below 400°C (Ellis and Mahon 1977). It has been previuosly mentioned that acid-sulphate hot springs occur more commonly on volcanic slopes than basins or caldera structures. They are associated with fumaroles and mud pools.

Alkaline chloride thermal waters are characterised by the presence of Na, K chlorides, silica, bicarbonates, fluoride, ammonia, As, Li, Rb, Cs and boric compounds. The pH, though generally near neutral, can range from 5 to 9 (Ellis and Mahon 1977). These hot springs are commonly found in caldera settings, because the convective column is within easy reach of the ground surface. Siliceous sinters are usually well developed in areas of chloride springs, as the dissolved silica is precipitated for the reasons previously outlined. Siliceous sinters may take on a variety of colours due to Fe oxides and the growth of algae, and their deposits can form spectacular features such as cascades, terraces and mounds. Alkaline chloride waters are also associated with geysers. Geysers are jets of steam-heated groundwaters, whose mechanism of eruption was explained by Bunsen over 100 years ago. They form in areas of restricted groundwater circulation, so that circulating water cannot transfer sufficient heat through the hot springs. The mechanism of geyser jets is based on pressure which is exerted by a column of water on to its deeper levels where boiling temperatures must exceed the levels further up in the column. If the column rises slightly, say, by boiling at a certain level, then the resulting drop in pressure causes boiling at all levels above it. This process continues until there is a general, sudden discharge. It is said that the Waimangu geyser in New Zealand hurled water and rock fragments up to 500 m in the air during the period between 1899 and 1904. Water from geysers contains silica which is precipitated around the orifice as hydrated silica, known as geyserite, and forming mounds and conical structures. Geysers are abundant in Yellowstone National Park, where there are over 200, and in New Zealand and Iceland. They have also been found in Tibet near lake Tengri Nur at 4800 m above sea level, and in the crater of the Socompo volcano in the Atacama region at 6080 m above sea level.

Carbonate-Rich Thermal Waters

Carbonate-rich thermal waters are normally found in areas underlain by calcareous rocks. Travertine is the $CaCO_3$ sinter, its deposition due to exsolution of CO_2 from the waters as they reach the surface. Travertine deposits are abundant in the Latium region, central Italy, from where the name originated (Lapis tiburtina). Because of its light weight and porosity, travertine is an excellent building material, often employed by the Romans. Low-chloride waters may contain bicarbonate in areas of H_2S and CO_2-bearing steam. This steam may condense into an aquifer (Ellis and Mahon 1977). Bicarbonates are formed by reactions with wall rocks.

Crater Lakes

Lakes are not uncommon in the craters of dormant volcanoes. The water of crater lakes absorbs heat and volatiles emanated from the lake floor. Dissolved volatiles

Table 3.2. Average composition of fumaroles at Larderello, Italy. (Rittmann 1962)

	g/kg
H_2O	955.5
CO_2	42.6
H_2	0.88
H_3BO_3	0.30
NH_3	0.30
CH_4	0.15
H_2	0.04

and other components leached from the rocks, including CO_2, HF, HCl, NH_3, SO_2, Ca, Na, Al, Mg, K, Fe, Si, tend to accumulate between eruptions.

Fumaroles

Fumaroles are formed where the influx of groundwater is small and steam readily escapes to the surface. In fact, it is often observed that fumaroles change to acid-sulphate springs, and vice versa, in conjunction with fluctuating groundwater levels, whether seasonal or for other reasons. Solfataras are fumaroles with a high H_2S content, but often the terms solfatara and fumaroles are used interchangeably. Ellis and Mahon (1977) define fumarolic steam as that which derives directly from magma and has not passed through a hot water body. This type of fumarolic steam would contain HCl, CO_2, H_2S, SO_2. Solfataric steam is defined by the above authors as steam boiling from an underground geothermal reservoir, as described earlier. Both types may condense in surface waters (Ellis and Mahon 1977). The temperature of steam spouts varies from 90 to 300°C. Mineral encrustations around the orifices and conduits are common, and include sublimates and compounds formed by reaction of the volatiles with the wall rocks. Common products are chlorides of the alkali metals, ferric chloride, sulphates of the alkali metals and Ca, together with traces of compounds of Cu, Mn, Pb, Zn, As, Hg, Sn. Fumaroles at Mt. Vesuvius were found to contain $PbCl_2$, $FeCl_3$, $CuCl_2$, accompanied by galena, hematite, covellite and even pyrite and chalcopyrite which had formed by reaction with H_2S and H_2O. Ammonium chloride (NH_4Cl) may be locally so abundant that it can be commercially exploited. Also exploitable is native sulphur, formed by the oxidation of H_2S according to:

$$2H_2S + O_2 = 2H_2O + 2S°;$$
$$2H_2S + SO_2 = 2H_2O + 3S°.$$
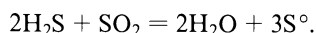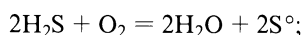
Boric acid, known as sassolite {$B(OH)_3$}, is extracted from the fumaroles of Larderello in Tuscany. Sassolite is also found in the crater of Vulcano in the Eolian Islands. The origin of the element B in the Larderello fumarolic fields, which have an extent of some 200 km², may be related to evaporitic sediments. An average composition of the Larderello fumaroles is given in Table 3.2.

3.5 Sub-Sea-Floor Hydrothermal Systems:
Spreading Centres and Island Arcs

Hydrothermal activity in sea-floor environments around mid-ocean ridges and volcanic islands is very common. In these environments sea water penetrates through fractures above and around a magma chamber, becomes heated and rises towards the sea floor, where it discharges as hot springs along vents and fractures. In this way a hydrothermal convection system is generated. The hydrothermal fluids undergo a series of reactions with the wall rocks, extracting metals and causing alteration. At oceanic spreading centres hydrothermal activity is on such a large scale that for a long time it was thought that the mineralogical changes observed, in what was known as the spilite-keratophyre association of orogenic regions, were the result of regional metamorphism (see Turner and Verhoogen 1960, p.258).

In the last 15 years, studies of the ocean floors by means of submersible crafts have led to some of the most astonishing discoveries ever made by scientific teams. Such discoveries include not only the visual evidence of hot springs actively depositing ore minerals in the submarine valleys of spreading ridges and volcanic islands, but also the totally unsuspected existence of ecosystems and their related organisms. In the context of the present section, the results of these studies published by teams of researchers – particularly from the USA and France – have shed new light on, and provided greater understanding of hydrothermal ore forming processes. This understanding is perhaps one of the most important "tools" to be employed by the exploration geologist, and is especially applicable in the search for and identification of base and precious metal deposits in those areas where the geological record indicates possible previous activity of hot springs in a sub-sea-floor environment. Of particular relevance amongst the contributions referenced in this section are the collection of papers edited by Rona et al. (1983) and the review by Rona (1984). Other references on this subject are given in Chapter 12, where the hydrothermal processes and ore deposition in sub-sea-floor environments are examined and discussed. The present section is concerned with the geometry of hydrothermal circulation in the above-mentioned environments, as deduced from studies of modern and ancient systems. In particular, it examines hydrothermal systems at mid-ocean ridges, at spreading ridges close to land masses, in volcanic islands, and in submarine volcanic constructs such as those postulated for the so-called kuroko-type ore deposits.

3.5.1 Hydrothermal Systems in Spreading Centres

Hydrothermal systems that originate at spreading centres, whether in marginal basins, in mid-ocean ridges, or in narrow oceanic arms, have been recognised in the geological record of the emerged lands. Although Chapter 6 looks more specifically at this topic, it is appropriate to point out here that for several reasons the recognition of sub-sea-floor hydrothermal systems is by no means simple. This is because oceanic crust tends to be destroyed at convergent plate boundaries, so that

only tectonic slices and fragments may survive embedded in a melange of highly tectonised lithologies. In some cases, during the tectonic process known as obduction, whole sections of oceanic crust may be preserved, thereby increasing the possibility of having well-preserved fossil hydrothermal systems, and hence ore deposits. The overall preservation of ancient oceanic crust, or ophiolites, is further constrained by the depth of erosion and therefore the age of the terrane in which it occurs. It is for this reason that we essentially confine our discussion in this section to modern and recent systems.

The geometry of hydrothermal systems in sub-sea-floor environments has been studied by Lister (1983), Sleep (1983) and Taylor (1983), using geological, physical and stable isotopic constraints. Penetration of sea water through oceanic crust results in convective systems which have been modelled to take place as flow in discrete cracks, or as flow in porous media. The discharge of the return flow takes place at localised vents, or clusters of vents, and is episodic in character with a very short life span (usually only a few years). It is estimated that the total mass of water which escapes through a venting system during its average life of 10 years is in the region of some 3×10^{10} kg, or a cube of water with sides of 300 m (Sleep 1983). The venting temperature is around 350 °C. Evidence indicates that sea water circulates and interacts with oceanic rocks to depths of between 5 and 10 km, with overall high water/rock ratios and temperatures probably in excess of 500 °C. In a porous medium the flow of the fluid must be dispersive and slow, so that a parcel of fluid moving laterally or vertically should mix with fluid still retained in the pore spaces. Sleep (1983) points out that there is little evidence of this mixing and therefore fluid flow is more likely to occur through cracks and fractures. Nevertheless, in the case of oceanic crust overlain by land-derived sediments, porosity assumes great importance, as discussed later. Penetration of water into hot rock may take place, according to Lister (1983), by cooling and cracking due to thermal contraction. A "cracking front" advances downward fairly rapidly (several metres a year), thus cooling a large volume of rock within a relatively short time. It is estimated that the cracking front has temperatures varying from about 700 to 450 °C. The cracking front separates a colder permeable region above from the hot rock domain below. Fine-scale cracking of the hot rock is most probably an essential feature for the leaching of ore metals, because the fine cracks expose a very large area per unit volume, allowing substantial interaction between the fluids and the rocks. Also, the precipitation of mineral phases and subsequent sealing of the channels and venting systems explains their short lifetimes, and the opening up of new vents.

The simplified geometry of hydrothermal systems at a mid-ocean ridge in the axial zone and off-axis is shown in Fig.3.7A. The discharge is through vents which are presumed to feed on fracture zones, while recharge occurs along fault scarps near the axial zone. Sea water circulation in oceanic crust was modelled on the basis of field mapping and stable isotopes for the Samail ophiolites in Oman (Taylor 1983). Figure 3.7B shows the geometry of the hydrothermal systems envisaged in this model. Two circulation systems are postulated. An upper system is located above a boat-shaped magma chamber below and extending outwards from the ridge axis. This upper system lies within the pillow lavas and sheeted dyke sectors of the oceanic crust, and is characterised by higher permeabilities and high water/rock

A

① Axis hydrothermal cells
② Off-axis hydrothermal cells
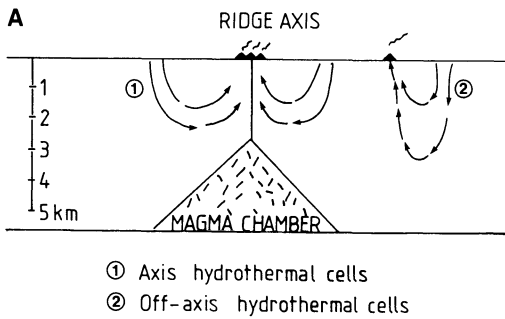
Fig. 3.7. **A** Hydrothermal systems at ridge axis and off-axis, feeding vents on the sea floor (After Sleep 1983). **B** Hydrothermal systems above and below the sides of mid-ocean-ridge magma chamber. See text for explanation; figure not to scale (After Taylor 1983)

B
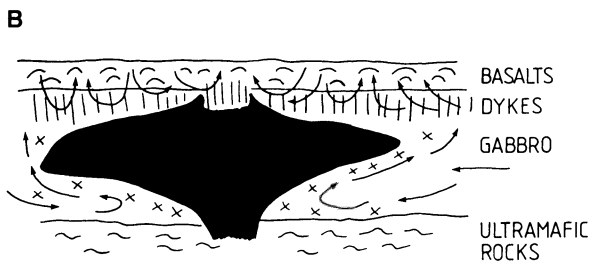
ratios. The lower hydrothermal system is located beneath the "wings of the magma chamber" as shown in the figure, and above the zone of tectonised ultramafics. The latter may develop fractures which overprint the tectonite fabric, and are infiltrated by the descending fluids. The two systems would be generally decoupled for most of their extension, except perhaps in the more distal portions, where mixing of the two could occur (Fig. 3.7B). The lower system is characterised by higher temperature and lower water/rock ratios. Variations of $\delta^{18}O$ through the Samail oceanic crust indicate that ^{18}O enrichment and depletion characterise the upper and lower layers respectively, reflecting the actions of the two operating hydrotermal systems, although "isotopic ageing" produced by the prolonged effects of hydrothermal alteration may tend to mask these isotopic variations (Taylor 1983).

A model of a sub-sea-floor geothermal system is proposed by Bischoff and Rosenbauer (1989). In this model these authors invoke "layered double-diffusive convection", in which a lower brine layer transfers heat and dissolved constituents to an upper sea-water-dominated convective cell (Fig. 3.8A, B). The idea of double-diffusive convection is, at least in theory, well constrained and it has been used to explain certain features of magma differentiation (see e.g. Huppert and Sparks 1984; Irvine et al. 1983). The geometry of the sub-sea-floor coupled two-layer system as envisaged by Bischoff and Rosenbauer (1989; Fig. 3.8A) consists of "nested convection cells" in which the lower cell is formed by a continuously recycled brine located just above the cracking front. This lower brine cell draws heat and dissolved components by circulating through the plutonic rocks, and it transfers heat and part of the solutes to the upper sea-water convective cell across a diffusive interface (Fig. 3.8B). When the upper cell reaches the temperature of 360°C, it rises to debouch
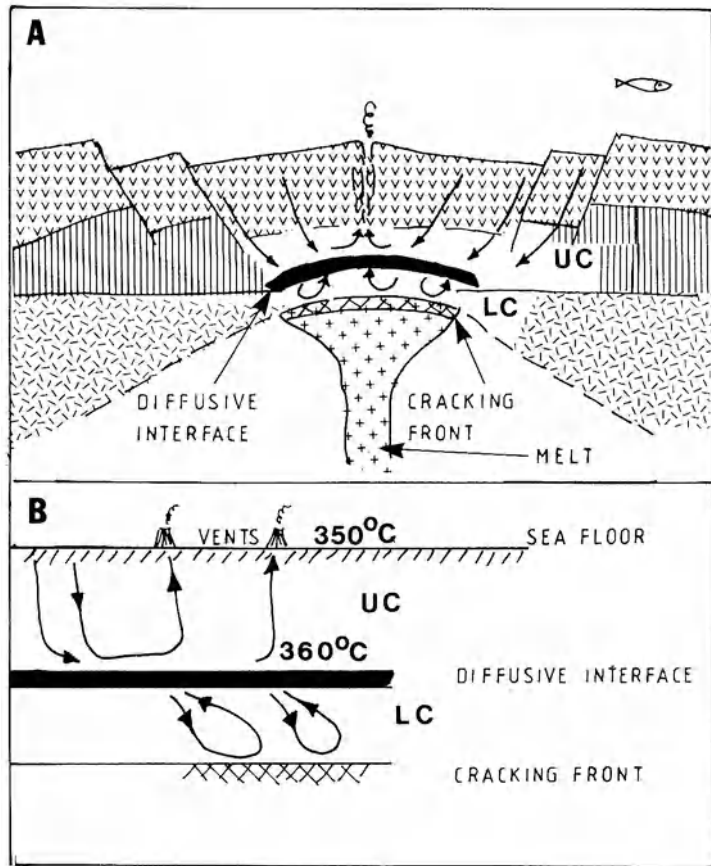
Fig. 3.8A, B. Model of sub-sea-floor geothermal system. **A** Cross-section of oceanic crust and associated convection cells; LC lower brine cell, UC upper brine cell. **B** Detail of double-diffusive convection model; lower cell (LC) transfers heat and solutes to the upper cell (UC) which discharges at the sea floor. $v's$ Basaltic rocks; *vertical lines* sheeted dykes; *random dashes* gabbroic rocks; see Chaps. 6 and 12 for more details (After Bischoff and Rosenbauer 1989)

through vents at the sea floor. The process is used by the authors to explain the salinity variations of the vent fluids. Lower salinity vent fluids are believed to be related to the boiling of the lower brines which results in the dilution of the upper fluids through the transfer of solute-poor vapours into them. Thus, low-salinity vents would coincide with the down-flow regions of the brine cell, while high-salinity vents would correspond with zones of brine up-welling.

So far we have considered circulation of heated sea water below the rock-sea water interface. However, the circulation of ore fluids within the oceanic mass above the hydrothermal vents may also assume great importance in terms of ore genesis processes. This unusual type of hydrothermal system is called a plume, which, due to bottom currents, is normally displaced relative to the underlying source. These plumes are diluted hydrothermal fluids which rise above the vents and can be
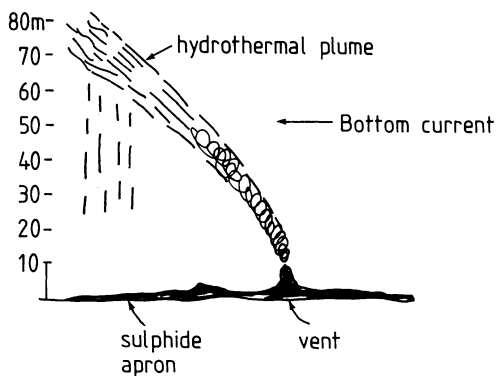
Fig. 3.9. Displacement of submarine hydrothermal plume above a black smoker vent due to bottom currents. The plume is about 80 m high, and sulphide particles settle to form an apron of about 50 m from the vent (After Lonsdale and Becker 1985)

detected by their anomalous temperature with respect to the ambient sea-water. Sonar scanning indicates that the plumes can be sensed up to about 80 m above the emitting vent, while their lateral displacement is detected up to 50 m away. Figure 3.9 depicts a hydrothermal plume inclined approximately 40° above a submarine vent (Lonsdale and Becker 1985). Sulphide particles from the plumes of black smokers (Chap. 12) may settle around the venting area to form an "apron" of sulphide material. Stokes' law governs the settling velocity of particles in a fluid medium. This velocity is proportional to the density difference between the fluid and the particles, to the radius of the particles, gravity, and inversely proportional to the viscosity of the fluid. In general it can be shown that, for a plume height of about 50 m, sulphide particles will settle within radii ranging from 50 to 250 m of the plume (Cathles 1983). Usually substantial sulphide accumulations can only form in quiet conditions, such as those attained in a depression not influenced by bottom currents. On a global scale, the currents' induced lateral shift of the plumes are indicated by the asymmetric distribution, in relation to the ridge axis, of the metalliferous sediments (Fe and Mn oxides) on the sea floor. Also, the displaced distribution of the ^{3}He isotope in sea water is thought to reflect emission from hydrothermal vents on the ridge axis (Edmond and von Damm 1983).

Besshi-type is a comprehensive name given to a class of hydrothermal mineral deposits characterised by massive sulphides emplaced within terrigenous sediments, intercalated with mafic rocks of oceanic affinity. These geological conditions are thought to represent a situation whereby the spreading centre is situated within a narrow oceanic arm between emerged lands nearby, from where abundant clastic sediments are shed off and tend to "swamp" the ridge basaltic rocks. A modern-day example of this particular situation is the Gulf of California, and a possible fossil equivalent is the Matchless Amphibolite Belt in Namibia and its contained massive sulphide deposits (see Chap. 12 and references therein). The seabed of the Guaymas basin in the Gulf of California has been studied by means of sonar scans and submersible craft by Lonsdale and colleagues (Lonsdale et al. 1980; Lonsdale and Becker 1985). In the Gulf of California spreading ridges and transform faults are buried in mud and silt (Fig.3.10). Along a section extending over more than 120 km, well over 100 hydrothermal sites were detected by side-scan sonar. One deposit sampled by dredge was found to contain sulphates (anhydrite and barite), talc,
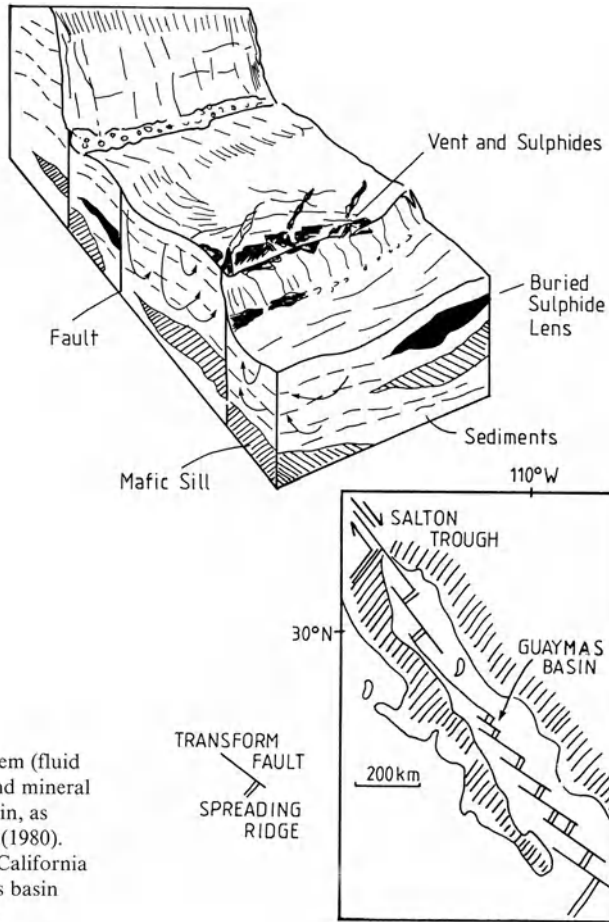
Fig. 3.10. Hydrothermal system (fluid flow indicated by *arrows*), and mineral deposits in the Guaymas basin, as envisaged by Lonsdale et al. (1980). The *inset* shows the Gulf of California and location of the Guaymas basin (After Lonsdale et al. 1980).

calcite, pyrrhotite, sphalerite chalcopyrite and galena, all "soaked in hydrothermal petroleum condensates" (Lonsdale and Becker 1985). The muddy accumulations of the Guaymas basin are in fact rich in planktonic carbon, and this is cracked by the heat of the hydrothermal fluids to form hydrocarbons. The surveying carried out by Lonsdale's team has indicated that the shallowest intrusions of magma are buried in up to 400 m of sediment. From mineralogic and isotope systematics Lonsdale and coworkers deduced the presence of three distinct and superimposed hydrothermal systems. One is characterised by expulsion of pore water following the intrusion of a shallow mafic sill. The discharge is at low temperature (about 100 °C). The other is a deep-seated hydrothermal circulation that cools a magma chamber. This fluid discharges at high temperature through fractures in overlying sills. A third type is due to convection of water within the sediments above a cooling sill, which provides the necessary thermal energy. The high temperature discharges are possibly driven by a magma chamber about 1 km wide and between 3 and 4 km long.

Intrusion of mafic sills into highly porous marine sediments (Einsele et al. 1980) results in decrease of porosity above and below the sill, which drives water away from it. Soon after the intrusion, the temperature at the sill-sediment contact may rise to a maximum 400 °C, and the pore water in that region can reach boiling point. The amount of pore water expelled following the intrusion of the sill may be quite considerable: for example an area of 2 km^2 intruded by sills could expel some 40 $\times$ 10^6 m^3 of pore water. This heated water would then be set into convective motion facilitated by the high permeability of the sediments above the zone of porosity reduction. The hydrothermal fluids can then be channelled along faults and discharge as hot springs at the sediment-water interface.

3.5.2 Hydrothermal Systems in Submarine Volcanic Centres

Fumarolic activity on the sea floor around submerged volcanic structures, or the submerged portions of volcanic edifices, is the expression of volcanogenic submarine hydrothermal systems. Apart from present-day manifestations of this type of activity – such as those in the island of Santorini (Aegean Sea, Smith and Cronan 1983), and Vulcano (Tyrrhenian Sea, Honnorez 1969) – the geological record for these hydrothermal systems is represented, at least in some cases, by the kuroko-type ore deposits. The tectonic setting and general characteristics of these deposits are treated in Chapters 6 and 11 respectively. Here it will suffice to say that the kuroko-type mineral deposits are of epithermal origin, formed within submarine calderas in rifted back-arc settings. As is the case for epithermal subaerial deposits, the kuroko-type deposits appear to form during the late stages of caldera development, through the activity of hot springs and fumaroles taking place along the flanks of rhyolitic domes and/or the depressions of the sea floor. Stable isotope systematics generally confirm that the kuroko ore fluids have a major component of sea water, and the interaction of pore sea water with hot volcanic and subvolcanic rocks generates hydrothermal convection systems. Kuroko-type hydrothermal activity is thought to be characterised by short (a few thousands of years) and vigorous pulses. Modelling of the kuroko hydrothermal systems has been carried out by Ohmoto and Rye (1974), Pisutha-Arnond and Ohmoto (1983) and Cathles (1983). Figure 3.11 shows simple models of convective hydrothermal circulation around a shallow rhyolitic intrusion. These models, based on that of Ohmoto and Rye, postulate some mixing with connate and magmatic waters.

Very interesting and detailed computer-aided modelling was undertaken by Cathles (1983) for submarine geothermal systems, with particular reference to kuroko situations. In his exercise Cathles used a series of calculations, together with geological, geochemical and isotopic data to constrain the convective cooling of a small intrusive body, the related flow of fluids around it and the changes in the chemical and isotopic nature of both fluids and rocks. The results of his modelling are reported here. The author begins by considering the relationship between the size of the igneous intrusion and the total mass of hydrothermal fluid that can be convected by its thermal energy. A simple formula is used to express this relationship:
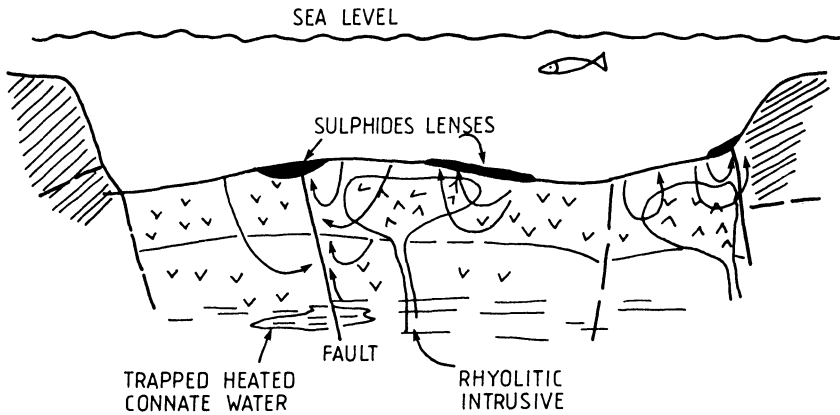
Fig. 3.11. Schematic model of hydrothermal systems in a kuroko-type setting (submarine caldera). See text for explanation. The figure is based on the model proposed by Ohmoto and Rye (1974)

$$M_w = M_i \, C_i/C_w \ln T_0/T,$$

where M_w represents the mass of hydrothermal fluid circulated, M_i the mass of the intrusion, C_i its heat capacity (cal/g/°C), C_w the heat capacity of water, T_0 is the initial difference in temperature between the igneous body and the surrounding environment, and T the temperature difference after cooling to a certain level (i.e. 300°C). If a pluton at a temperature of 700°C is intruded at a depth of 4 km, where the ambient temperature is 100°C and cooled to 300°C, the mass of fluid circulated is 22% of the pluton's mass. If the intrusion is at 1300°C, a mass of hydrothermal solution hotter than 300°C would be about 36% of the pluton's mass. Using the above formula, Cathles' calculations indicate that an intrusion of between 1.5×10^{11} to about 10^{13} tonnes is necessary to account for the metal resources estimated at 4.7 $\times 10^6$ and 4.5×10^6 tonnes of combined Cu + Pb + Zn metals for the Noranda (Canada) and Kuroko (Japan) districts respectively. Also interesting is that the amount of silica deposited at the surface can be used to estimate the size of the intrusion and the amount of fluid involved. Using an example from the Noranda area, where a silicified basalt containing approximately 20% silica is present, and taking into account the solubility of silica in a 300°C solution and the volume of the area affected by the silicification, Cathles estimates that some 2.3×10^{15} kg of hydrothermal solution at above 300°C would have been required to produce this silicification. This in turn requires an igneous mass of about 10^{13} at 700°C. Comparatively small magma chambers (approximately 2 km wide by 3 km high) are considered in modelling their cooling history by convective circulation of fluids. This modelling (see Cathles 1983, Fig.8) indicates firstly that fluids at 600°C should be vented after 5000 years after the intrusive event, and since observation of black and white smokers at mid-ocean ridges indicates venting temperatures of about 350°C, it is concluded that a very hot rock (>350°C) is probably quite impermeable. Permeability is therefore a key factor in that it allows penetration of water and cooling of the igneous body.
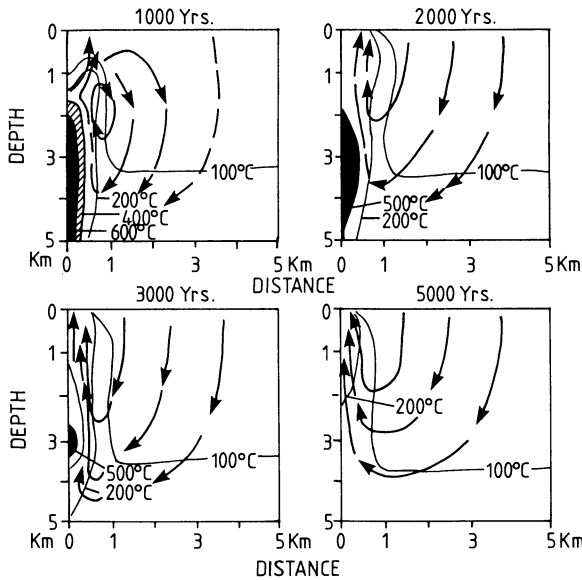
Fig. 3.12. Model of convec-
tive cooling of a magma
chamber, according to
Cathles (1983). Permeability
is taken to be 5 millidarcy.
Arrows indicate fluid flow
(After Cathles 1983)
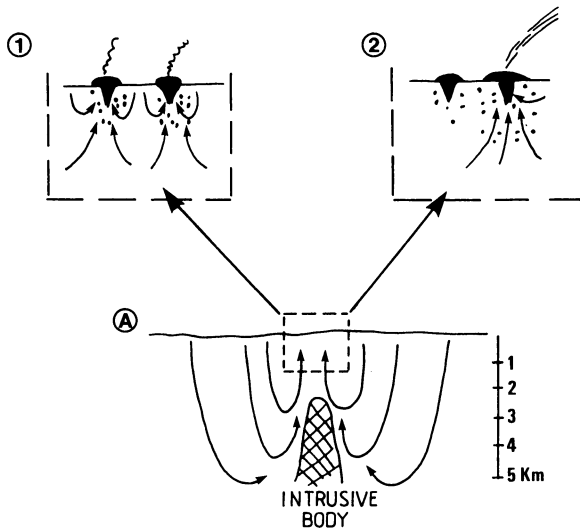
Fig. 3.13. Stages of hydrothermal fluid circulation in a kuroko system (after Cathles 1983). *Stage 1*:
low temperature white smokers, with silica + sulphate deposition and disseminated sulphides.
Anhydrite is deposited at depth. *Stage 2*: high temperature black smokers, with massive and
disseminated (dots) sulphide deposition. One vent *left* is sealed by precipitated mineral phases. A is
the overall view, with the dashed box showing position of *1* and *2* in relation to the whole system

Convective cooling of a magma chamber 1 km wide by 3.25 km high by inflow of
fluids is shown in Fig. 3.12. The flow lines in this figure represent the idealised
geometry of the hydrothermal circulation system. This modelling (Cathles 1983)

shows that initially they move up the temperature gradient, and then back down as they move into the thermal anomaly generated by the pluton. The model also shows that the fluids only gain access to the intrusive mass after it has cooled to approximately 350°C in about 5000 years. During this cooling it is estimated that over 8000 tonnes of solution at a temperature of about 300°C are circulated. Considering the 40-km long Hokoruko basin in Japan, Cathles estimates that the total mass of water vented would have been of the order of 3.3×10^{10} tonnes at a temperature greater than 300°C. The speed with which this water circulates through the entire system is probably around 2000 years (intake and discharge). Finally in Fig. 3.13, two main stages of fluid circulation and ore deposition are considered. Fluids penetrate to a depth of about 5 km and form two convective cells, one nearer the surface and the other deeper down. During the first stage, lower and shallower circulating fluids debouch at the rock-water interface to precipitate sulphates. In stage two, more reduced and higher temperature conditions prevail. The previous vent may have been sealed by mineral precipitation and the fluids vent at a new locale, where they deposit massive sulphides.

3.6 Rift-Associated Hydrothermal Systems in Sedimentary Basins

The study of numerous, economically significant, sediment-hosted base metal sulphide deposits for many years led to a number of ore genesis theories which divided the geological community, worldwide, into three camps. The syngeneticists believed that the ore metals were precipitated from solutions transported in river systems and/or sea water; the epigeneticists held the opposing view that igneous activity and hydrothermal solutions thereof were responsible for the mineralisation. More recently, the diageneticists invoke diagenetic processes as an explanation for the stratigraphically and facies-controlled sulphide disseminations. Certainly, the class of mineral deposits known as sediment-hosted stratiform and stratabound, has naturally brought one to conclude that sediments must have played a role in the processes of ore genesis. The obvious stratiform nature of many of these deposits and their intimate association with sedimentary rocks has given syngeneticists the upper hand for many years. A historical review of these various ideas is not given here, but instead the reader is referred to Stanton (1972), Gustafson and Williams (1981) and Dunoyer de Segonzac (1968).

With the advent of the plate tectonic theory and its corollary of rift tectonics, a number of geoscientists with sound international experience began to recognise that certain views proposed were somewhat provincial, and that no attempt was being made to identify a global common factor or factors. Large (1981) aptly stated that more often than not the many published descriptions and views were "open to tedious semantic arguments". The common factors, it was realised, are that these deposits appear to be related to rifting events (see Raybould 1978), including the inception and geodynamic evolution of sedimentary basins within rifted portions of the crust, the association of the mineralisation with faults that were active at the time, and in some cases, the accompanying igneous activity. Overviews, in terms of

tectonic environments for the sediment-hosted sulphide deposits, by Sawkins (1990) and Mitchell and Garson (1981) are particularly useful and they offer the reader a clear perspective. Also worthwhile is the review by Large (1981), already mentioned, and for a different approach the relevant chapters (14,15 and 20) in Guilbert and Park (1986).

Thus, the popular consensus appears to be that hydrothermal solutions are activated at various stages of the geodynamic evolution of the rifted basins. Hydrothermal fluids begin to form during diagenetic processes and the movement of meteoric waters during early compaction of the sedimentary pile. This is followed by various stages, beginning with the ascent of the fluids along active faults and their discharge, as hot springs to produce chemical precipitates and replacements at the sediment-sea-water interface, to the further development of fluids in the metamorphic environment, as detailed in a later section. Therefore we seem to have a continuum, from early stages of ore deposition during the diagenetic stage, through to the metamorphic stages, not necessarily all present in the same region. The presence of one or more of the products of the type of hydrothermal system would be contingent to the stage of development and state of preservation of the given basin. An important paper by Unrug (1988), to be commented on further later in this section, gives a comprehensive review of the mineralisation in the Lufillian Fold Belt in south-central Africa (see Chap. 7). In this region, Unrug describes various styles of mineralisation (stratiform, vein and skarns) within a unified framework that more or less depicts the entire idealised sequence referred to above (see later). In the sections that follow, some models of hydrothermal systems proposed by a number of workers and based on current geological knowledge, are presented. Firstly, however, it is opportune to outline the types of mineral deposits, whose origin is thought to be related to the hydrothermal systems activated during the evolution of rift structures. These mineral deposits include:

1. Sediment-hosted exhalative stratiform base metal sulphides: These comprise: (a) Pb-Zn-Ba-Cu-Ag such as those of Mt.Isa, McArthur River, Broken Hill in Australia, Rammelsberg in Germany, Aggeneys and Gamsberg in South Africa, Sullivan in Canada; (b) the Cu-Co ± Ag in the Copperbelt of Zambia, Zaire and Angola, Witvlei and Klein Aub in Namibia, White Pine (USA), Coppermine River (Canada), Kupferschiefer (central Europe), Udokan (Siberia).
2. Stratabound carbonate-hosted. These include Pb-Zn ± V of the Mississippi type, Alpine and Irish types (e.g. Tynagh in Ireland) and the Otavi Mountain Land in Namibia.
3. Red Sea brines. These could be the active modern analogue of some of the deposits under (1).
4. East African Rift lakes. Accumulations of metals in the sediments of active continental rift systems may also be analogous to some of the deposits under (1).
5. Finally, it may be mentioned that deposits such as those of Messina in South Africa and Olympic Dam (Roxby Downs) in South Australia, may be a variant of (1). These may provide the "missing link" with an intracontinental magmatic connection, in a rift-setting.

3.6.1 Hydrothermal Systems

Studies of sediment-hosted mineral deposits, and of modern, active rift systems like the Red Sea and the East African rifts, indicate that hydrothermal systems are indeed responsible for their formation. Generally the end members of these systems are: (1) diagenetic low temperature, metalliferous brines that move laterally in the sedimentary basin, driven by lower density and the geothermal gradient; (2) high temperature exhalations, or hot springs issuing from hydrothermal fluids that ascend along graben faults, to exhale at higher levels or at surface, and produce chemical precipitates (exhalites). Thermal energy is provided by igneous intrusions, or by mantle in a crust-attenuated environment. Mixing of the two types of fluids is considered probable in many instances (e.g. Copperbelt in Zambia). We now consider these hydrothermal systems in some detail.

During the evolution of a sedimentary basin, expulsion of fluids takes place as a result of burial, compaction and diagenesis. Diagenetic changes may be an important component of hydrothermal fluids, and in this connection it must be recalled that the boundary between diagenesis and metamorphism is by no means well defined. For practical purposes, diagenesis is essentially a sedimentary process which takes place under physico-chemical conditions not too dissimilar from those found at, or near, the surface, whereas metamorphism involves higher temperatures and pressure. The diagenesis of sediments and its relation to ore forming fluids is comprehensively treated by Hanor (1979), whose article provided much of the information given below.

Expulsion of fluids during burial and diagenesis occurs as a result of reduction of porosity, and the volume of water released can be considerable. An average shale can yield 3.5×10^3 litres of water for every 1 m^3 of solid material deposited (Hanor 1979). Calculations of the volume of water that can be contained in a rock mass subject to burial have been carried out by Fyfe et al. (1978). They consider a prism of sediments 5 km thick and 1 km on a side (5 km^3) with an initial water content of 50%. In this example there would be some 2.5 km^3 of salty water available. The authors also consider that if an element has 1 ppm solubility, then there could be 2.5×10^{15} g $\times 10^{-6} = 2.5 \times 10^9$, or 2500 tonnes, of that element in solution. The composition of basinal waters is characteristic of a given sedimentary basin. Salinity increases with depth in the sedimentary basins, and this is explained by a mechanism of membrane filtration – a process whereby argillaceous sediments allow the passage of neutral molecules (H_2O and H_2S), while preventing the migration of anions and cations, resulting in their downward concentration. Thus, deeper waters become saltier and enriched in cations and anions. Elements that are usually enriched in formation waters are Pb, Zn, Ba, F, Sr and S. The latter is probably derived from bacterial reduction of dissolved sulphates to sulphide during diagenesis. Sulphate is predominant in most formation waters, whereas H_2S is common in oil field gases. In the Cheleken (Caspian Sea) and central Mississippi regions, where there is no evidence of igneous activity, brines have a high metal content. Sources of the metals may be the organic fraction of the sediments and/or the silicate minerals and carbonates (Hanor 1979). The work of Doe and Delevaux (1972) on the isotopic composition of Pb in galena ores from Missouri (see Chap. 2),
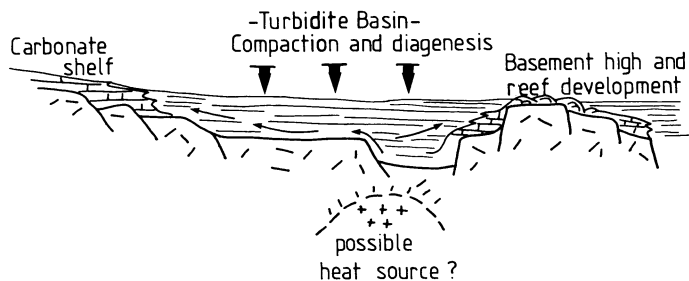
Fig. 3.14. Basin dewatering model (not to scale). Rifted basin is infilled with turbiditic sediments, compaction, dewatering and diagenesis produce metal-bearing fluids that migrate towards basement highs and their associated carbonate-reef complexes (After Guilbert and Park 1986)

revealed that the Pb is derived from the feldspar component of the La Motte sandstone through which the hydrothermal solutions circulated.

Figure 3.14 shows a model of basinal brines movement in continental basins (Guilbert and Park 1986). The brines are generated by diagenesis and compaction, and perhaps heated by a hidden heat source. The brines move updip along the basin flanks towards the basement highs to form low-temperature Pb-Zn deposits of the Mississippi Valley type. A novel idea is proposed by Oliver (1986), who hypothesises that passive continental margin sediments may be compacted, crushed and pushed during collision tectonics. Oliver uses the closure of the Iapetus Ocean and the collision of Africa and North America to form the Appalachian Orogen as a case in point. During the westward thrusting of various terranes on to a continental margin, saline fluids could have been expelled from the buried sediments and moved towards the foreland to the west. These "tectonic brines", according to the hypothesis, were responsible for depositing, in a regional zoning pattern from east to west, coal, gas, oil, and furthest away in carbonate host rocks the Pb-Zn deposits of the Mississippi type (see Chapters 14 and 15). Another case for large-scale brine development and movement is that of the northern platform zones of the Damara Orogen, Namibia, where numerous Cu-Pb-Zn-V deposits, including the world-famous Tsumeb are present. Misiewicz (1988) proposed that diagenetically formed hydrothermal fluids originated by dewatering of the predominantly turbiditic sediments of the northern grabens of the Damara Orogen. These fluids were expelled, and during the late phases of orogenic compressions moved along the length of the grabens, forming a mineralising front several hundreds of kilometres in length. The fluids moved in response to hydraulic gradients in clastic aquifers, along the grabens and towards the basin margins, depositing ore minerals in chemically favourable traps constituted by the carbonate rocks of the northern platform of the Damara Orogen. This example of carbonate-hosted base metal sulphide mineralisation is discussed further in Chapter 14.

A mechanism of episodic dewatering of the sedimentary basin giving rise to a number of pulses of hydrothermal fluids was put forward by Sawkins (1984) to explain the "stacked-lens" nature of some of the "giant" sediment-hosted Pb-Zn deposits in Australia. The hydrothermal fluids generated by this episodic dewater-
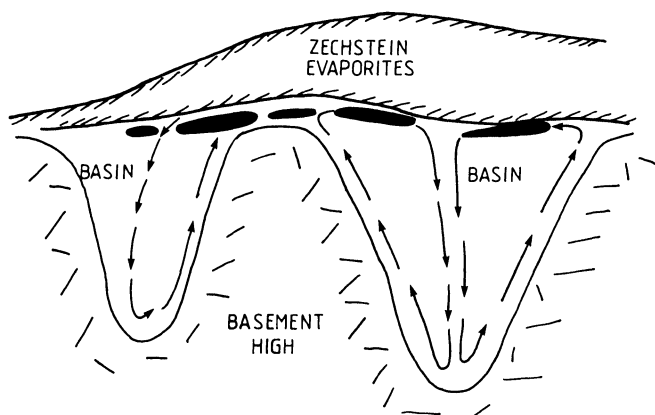
Fig. 3.15. Model of hydrothermal system for the Kupferschiefer Cu-Pb-Zn deposits. Convective cells are formed in the basins, with fluids (*arrows*) migrating up along the flanks of basement highs, and turning over below the Zechstein evaporites, where they form the orebodies (*black*). Drawing is not to scale and is after Jowett (1986)

ing are thought to be moved by tectonic activity such as for example the seismic pumping mechanism of Sibson et al. (1975), discussed later (see Fig.3.29). A particular mode of circulation of sedimentary diagenetic metalliferous brines in basins is proposed by Jowett (1986) for the Kupferschiefer of central Europe. According to this model, shown in Fig.3.15, the diagenetic brines form a convective cell which carries the brines downward into the deep parts of the basin, up along the flanks of the basement highs, and back down into the basin. Metal deposition occurred below the evaporitic sediments of the Zechstein, which is where the brines turn over for the return flow into the basin.

As we have already stated, there is good evidence of a spatial relationship between types of sediment-hosted mineralisation from deeper and hotter towards cooler and higher regions of a sedimentary basin or, in other words, from shale-hosted to carbonate-hosted deposits. This spatial relationship is advocated by Large (1981) and depicted in Fig.3.16. The spatial arrangements and mineralisation styles shown in this figure provide a possible link between the diagenetic and the exhalative theories. Heating of the basinal fluids by a source of thermal energy (mantle?, magmatic?) creates hydrothermal convection in the deep portions of the basin, upward movement and channelling of the fluid along graben faults or other fractures to eventually exhale at, or below the water-sediment interface, where they would precipitate sulphides.

A hypothetical sediment-hosted exhalative sulphide deposit and its progressive zonation away from the point of exhalation as well as its epigenetic and syngenetic facies, is shown in Fig.3.17. An exhalative hydrothermal system formed by large scale (tens of km) convection cells was proposed by Russell (1978) for the sediment-hosted mineralisation in Ireland. This model is shown in Fig.3.18, and consists of a system of "downward excavating cells" in an evolving sedimentary basin. The cells shift deeper towards higher temperatures, becoming larger with time and the
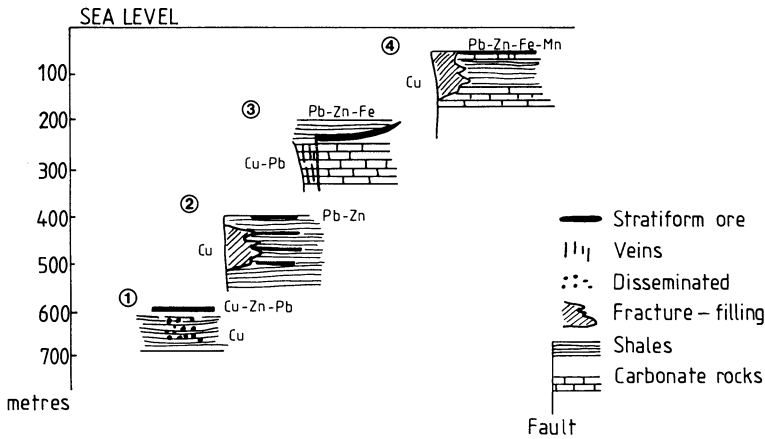
Fig. 3.16. Possible spatial relationships of various types of exhalative startiform and stratabound ore deposits, according to depths in a sedimentary basin. The drawing is not to scale in the horizontal dimension (After Large 1981)
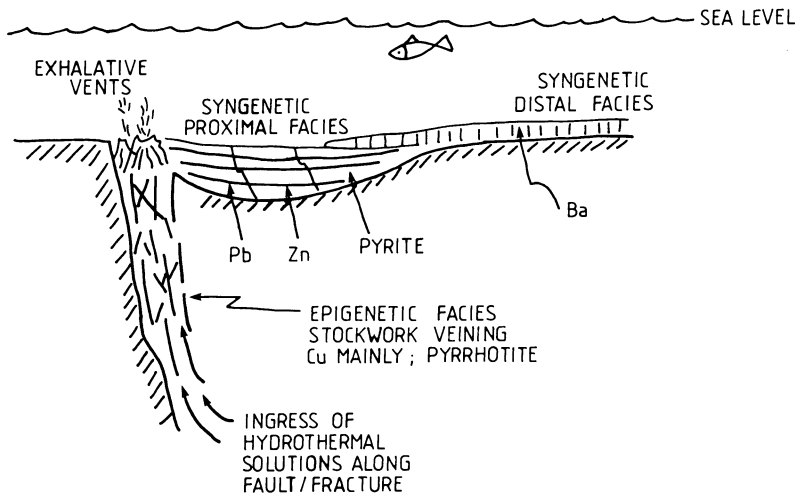
Fig. 3.17. Sediment-hosted exhalative sulphide deposit, showing epigenetic and syngenetic facies, and mineral zonation from the point of discharge of the hydrothermal fluids. The figure is not to scale and is after Large (1981)

progressive evolution of the basin, which allows fractures to move downward as the rock packages become more brittle. In this model there are at least three major pulses, or stages of hydrothermal activity during which different metal abundances result, thus explaining the observed mineral paragenesis of early Fe-Mn-Zn-Pb to mid Zn-Pb-Fe-Mn to late Zn-Pb-Cu-Fe-Mn dominated mineral assemblages.

Plimer (1985, 1986) cites different types of ensialic rifting (failed to successful), mantle degassing, and associated magmatism to explain the development of
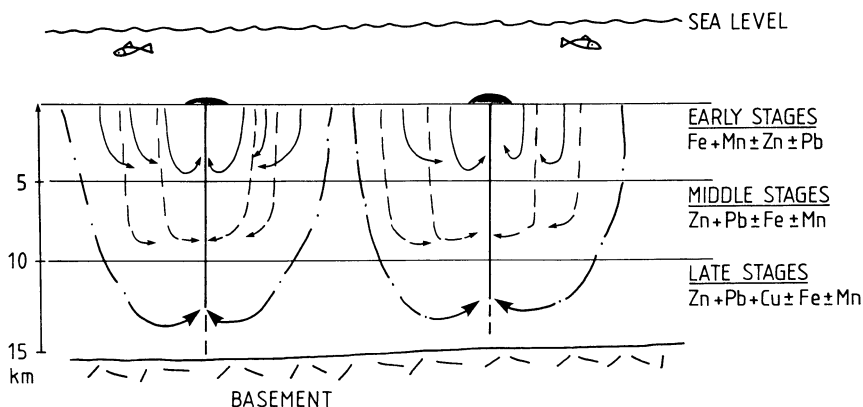
Fig. 3.18. Model of downward penetrating hydrothermal convection cells as proposed by Russell (1978) (After Russell et al. 1981)

complex exhalites at Broken Hill and Mt.Isa in Australia. Details of the geology and mineralisation of these large sediment-hosted metalliferous deposits are given in Chapter 13. Here, Plimer's ideas on the types of hydrothermal systems that might have been involved in the generation of these deposits are outlined. Plimer argues that the Mt.Isa orebodies were formed in an aulocogen-type rift setting, where hypersaline brines formed hydrothermal systems that were focused and exhaled into depressions in the deep grabens, with no magmatic component. Periodic expulsion of the heated brines would have taken place in accordance with Sawkins' views. The brines would have moved along major fractures and faults at high pressure. In contrast, the Broken Hill scenario has an association with bimodal (mafic-felsic) magmatism related to deeper and more successful rifting in a thinner continental crust. Plimer's model assumes mantle fluids enriched in CO_2, F, B, H_2, P, Mn, Fe, Pb, Zn, REE to have risen along the graben faults and to have locally mixed with sea water (Fig.3.19A). Submarine exhalations deposited sulphides and other exhalites containing Si, Zn, Mn, Fe and B-rich minerals on the floor of the rift valleys. Both the regional and local zonations of the Broken Hill setting are interpreted in terms of distance, upward and laterally, from the conduit through which the hydrothermal fluids rose (Fig.3.19B). A similar zonation at the regional scale is observed in Namaqualand (South Africa), for the Aggeneys-Gamsberg exhalative mineral deposits. Plimer's model is disputed by Wright et al. (1987), who disagree with the assumed association with acid volcanics at Broken Hill. They rather interpret these rocks as clastic sediments, and these were possibly the aquifers through which the metal-bearing brines moved during compaction of the largely clastic and porous sedimentary pile. Migration of the fluids along the aquifers and up along basin faults resulted in the trapping of the fluids below an impermeable cap constituted by pelitic rocks.

The abundant and varied mineralisation types of the Pan-African Lufillian orogen of Zambia, Zaire and Angola (see Chap. 7) has been tackled and explained by Unrug (1988) in a model of hydrothermal fluid circulation that combines
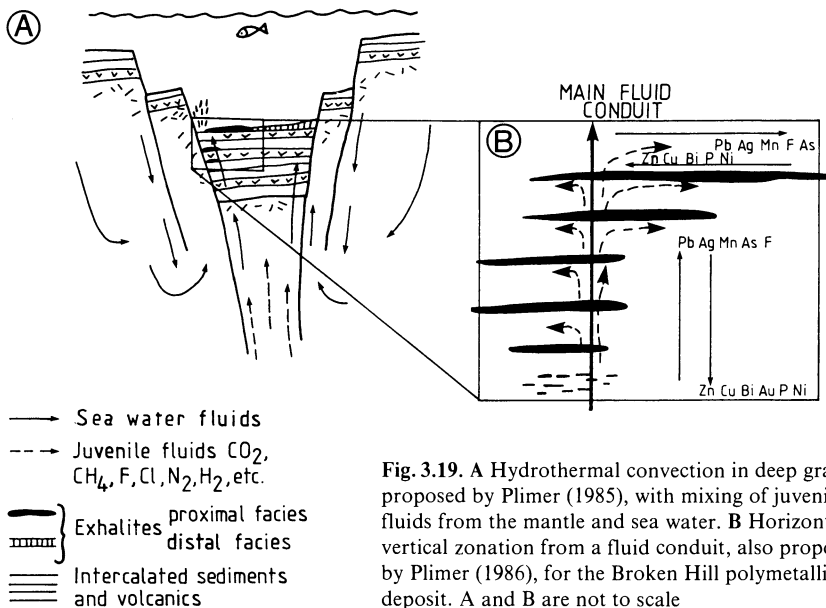
Fig. 3.19. A Hydrothermal convection in deep graben as proposed by Plimer (1985), with mixing of juvenile fluids from the mantle and sea water. B Horizontal and vertical zonation from a fluid conduit, also proposed by Plimer (1986), for the Broken Hill polymetallic deposit. A and B are not to scale

Jowett's (1986) diagenetic brines with deep-seated fluids. Unrug's model, although disputed by Sweeney and Binda (1989) and Garlick (1989), elegantly puts the controversial "Copperbelt" and adjacent areas into a unified framework of rift tectonics, associated basin evolution and hydrothermal fluid development. This model is summarised below (see Unrug 1987, 1988). The stratiform Cu-Co-U-Ni-Au Copperbelt mineralisation (Chap. 13) occurs near the base of a thick stratigraphic succession of the Katangan supergroup. Also present in the succession are other types of mineralisation, including vein and skarn deposits, containing a host of metals such as U, Au, Ag, Pb, Zn etc. The stratiform mineralisation was emplaced before folding and metamorphism, and it is recognised that Cu and Co were probably brought into the basin at a late stage of diagenesis. The temperature of the hydrothermal fluids is estimated to have been between 200 and 250°C higher than the 100–150°C of the brines responsible for the Mississippi Valley-type deposits. Basinal brines were developed in the deepest parts of the basin, and formed convective cells driven by a high heat flow associated with the rifting event that created the basin. These brines probably originated by compaction and dewatering of the thick pelitic sequence of the Lower Kundelungu sequence (Fig.3.20). The thermal gradient forced circulation of the fluids in the aquifers of the Roan Group sediments on the shoulders of the rifted basement blocks. The fluids in turn interacted with the lithologies containing the primary diagenetic sulphides (pyrite mainly) to give rise to the stratiform mineralisation. The fluids in the Lower Roan group were confined by the impermeable overlying units of the Grand Conglomerat, and flowed updip along the basement highs, where they may have overturned (see Jowett 1986) to flow back into the deeper parts of the basin to complete the convection cell. At a later stage, metamorphism, compression and deformation of
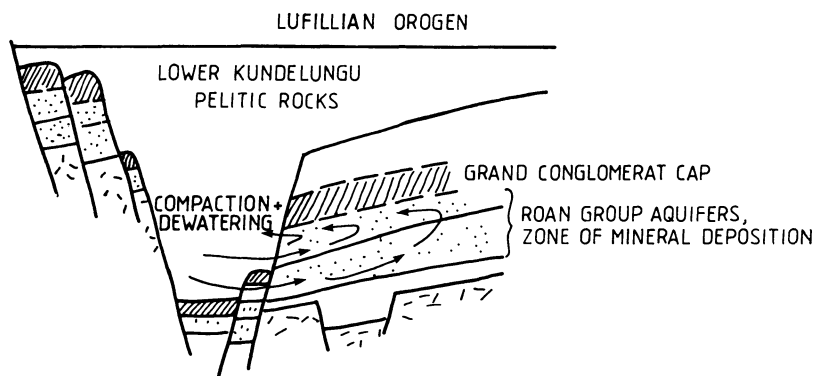
LUFILLIAN OROGEN

Fig. 3.20. Model of fluid circulation in a rift basin of the Lufillian orogen, Central Africa, as suggested by Unrug (1988). Mineral deposits would form below the low permeability cap of the Grand Conglomerat unit within the Roan group aquifer. Section is oriented north-south and is not to scale

the sedimentary sequences produced renewed hydrothermal activity in the form of metamorphism-generated and —driven fluids. These could have formed the vein-type mineralisation also present in the region. Rift-related alkaline magmatism may have been responsible for the skarn mineralisation.

Finally, the interesting sabkha model proposed by Renfro (1974) was elaborated to counteract the discrepancies of the syngeneticists. The latter maintained that metal-bearing fresh waters would mix with sea waters in a restricted basin. Reducing conditions in the restricted water body would cause the metals, which would by now be diffuse in solution, to precipitate along with the incoming sediments on the sea floor. The mineral zonation worked out from the study of the Copperbelt mines (Garlick 1961, Fleischer et al. 1976) was explained as a zonation from shore to sea, with copper sulphides precipitating near the shore (chalcocite-bornite-chalcopyrite) to Fe (pyrite) in the deeper and anoxic waters. Later these metalliferous deposits would be capped by evaporites upon desiccation of the basin. This model suffers from two major drawbacks: (1) the most soluble metals occur in the most basinward position, and the resultant metal zonation requires that transgression should have occurred, whereas in fact the enclosing lithofacies reflect regressive sedimentation; and (2) the metal bearing strata extend into the overlying evaporites and into the oxidised layers below. According to the syngenetic model, the metal facies boundaries should be as sharp as the lithofacies boundaries. Renfro's (1974) "sabkha" model (Fig. 3.21) attempts to explain the association of some stratiform exhalative deposits with evaporitic lithologies, as is the case for the Roan Antelope orebodies of the Zambian Copperbelt and the Kupferschiefer in Germany.

A sabkha is a coastal evaporite flat bordering a body of water on one side and a desert on the other. It differs from a normal evaporite pan in that the depositional environment is subaerial whereas that of an evaporite pan is subaqueous. In a coastal sabkha, groundwater evaporation causes solutes to be deposited at the sabkha surface. This results in a subsurface hydraulic gradient which induces marine water of high pH and low Eh to flow inland towards the sabkha, while
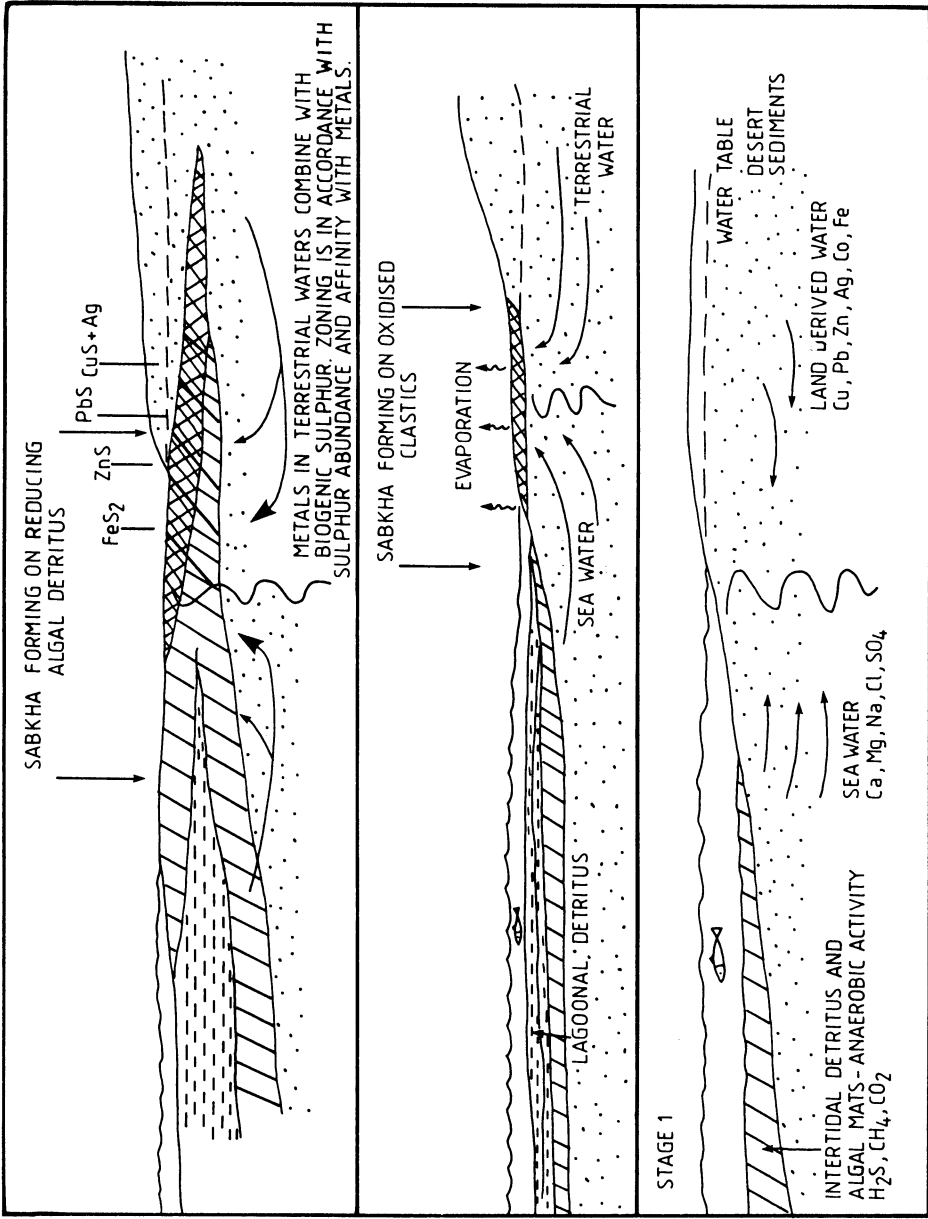
Fig. 3.21. The sabkha model for the genesis of the Copperbelt-type stratiform ore deposits. The model was proposed by Renfro (1974). See text for explanation

meteoric underground water of low pH and high Eh flows seaward. Figure 3.21 depicts the sequences developing from regression-transgression to regression and the creation of a mature sabkha accompanied by precipitation of sulphides, with a zonation dictated by the affinity of the metals with sulphur. The mechanism involved is explained as follows. The body of water adjacent to the sabkha is prolific with blue-green algae. These tend to form algal mats which, upon decay, generate much H_2S, CO_2, CH_4. The landward flowing marine waters are therefore enriched in these constituents, whereas the terrestrial meteoric waters carry traces of Cu, Ag, Zn, Pb and Fe. On transgression, the algal facies will onlap the oxygenated desert sediments, and at the same time the advancing marine water forces the meteoric waters back towards the land. An incipient sabkha forms when sediment supply and subsidence reach a steady state, causing an evaporite suite (aragonite-gypsum-halite) to rest on desert continental sediments. Magnesium from the sea water brine replaces the aragonite to form dolomite. During regression, the algal mat is over-ridden by the evaporites while the trailing edge is buried by desert sediments. The meteoric groundwaters are drawn towards the surface by the strong evaporation, and precipitate sulphides in passing through the decaying algal mat which supplies the necessary H_2S. Metal zoning is from land towards the sea as shown in Fig.3.21.

3.6.2 Hydrothermal Systems in Modern Rift Settings

Red Sea brines

The Red Sea and its coastlines are a large metallogenic province in the making. Following the original discovery in 1965 (Pottorf and Barnes 1983), about 17 hot brine pools – of which at least 7 contain metalliferous sediments – have been identified along the axial zone of the Red Sea rift (Fig.3.22). Numerous Pb-Zn occurrences in Tertiary sediments are situated along both the east and west coasts (Dadet et al. 1970). Many more mineral deposits are present within the general area of the Red Sea rift, and they are all linked with the geodynamic and magmatic evolution of this important part of the Earth's crust. The Red Sea region invites straight comparisons with ancient rift systems and their associated Pb-Zn-Cu-Ag-Ba stratabound and stratiform metal deposits. The hot brine pools and their associated metalliferous sediments show a great diversity in chemistry, temperature, mineralogy and metal content (Fe, Zn, Cu, Ba, Pb, Mn, Ag, Hg, Ga, V). The pools are located at the intersection of east-northeast-trending fractures and transform faults with the median valley of the central rift zone.

The Atlantis II Deep is the best studied of the hot brine pools and has the highest economic potential. Outlined by the 2000 m isobath, it is 14 km long and approximately 5 km wide. Details of the geology and mineralisation of Atlantis II are given in Chapter 13. For the present purpose, it suffices to say that in the Atlantis II Deep, active discharges of hydrothermal fluids have so far formed about 5 km³ of density-stratified brines. A lower brine layer is approximately 150 m thick with high salinity and a temperature in excess of 60°C. The upper brine layer, which is roughly 50 m thick, has a temperature of about 50°C, and led to the discovery of the Deep
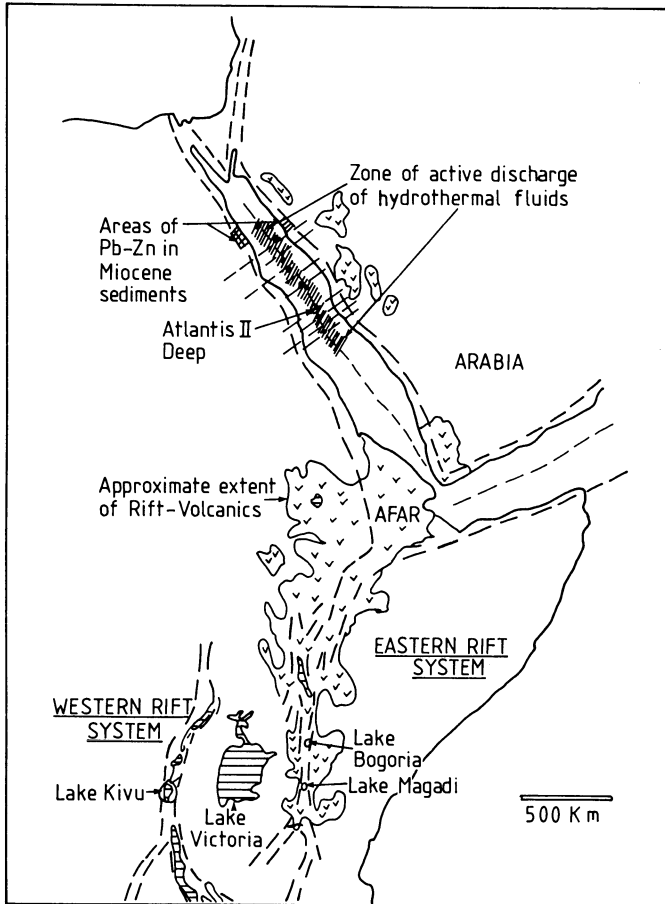
Fig. 3.22. Part of the Cenozoic rift valley system in East Africa, showing the Red Sea metalliferous deposits and location of lakes discussed in the text

(Pottorf and Barnes 1983; Thisse et al. 1983). The lower brine layer is in contact with metalliferous sediments that in turn rest on basaltic rocks. These sediments have been estimated to represent in the region of 50×10^6 tonnes (dry salt-free basis) at 3.4% Zn, 1.3% Cu, 0.1% Pb, 54 g/t Ag and 0.5 g/t Au. The configuration of the hydrothermal system of the Deep is depicted in Fig.3.23. Isotope systematics suggest that the hydrothermal fluids originate as paleo-sea water, which percolates through the evaporite deposits on the shoulders and floor of the rift basin. Leaching of the evaporite minerals (anhydrite and halite) results in high salinities of the fluids. The paleowater is heated by the high local heat flow, and by virtue of its Cl content acquires potential for metal complexing. As this water comes into contact with the recent basalts in the axis of the rift zone, it is heated to a temperature of about 250 °C and it leaches metals from the basaltic layer. The hydrothermal fluid is convected upwards, where at least two fluids can be identified in this part of the circulation

A
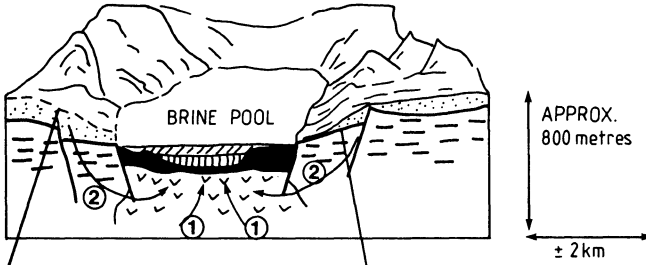
B
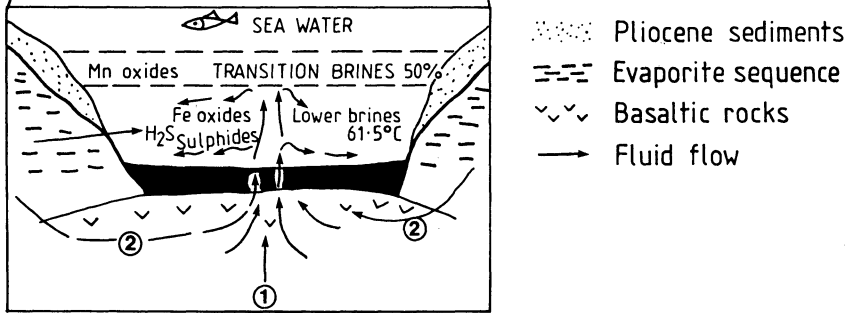
Fig. 3.23A, B. Sketches showing **A** topographic features of a brine pool area, its density stratification, and fluid flow, and **B** detail of A (see text for explanation of details). These sketches are after Pottorf and Barnes (1983) and refer to the Atlantis II Deep

system. Fluid (1) is shallow and relatively oxidised, and with a temperature of less than 250 °C and high salinity. The deeper circulating fluid (2), is more reduced, maintaining a temperature of about 330 °C, which is also of high salinity (Pottorf and Barnes 1983). Subsequent to passing through the basaltic layer, both these fluids discharge in the Deep and mixing occurs. No hydrothermal vents – such as those of the East Pacific Rise – appear to be present, perhaps because vent construction is prevented by the presence of the soft muddy sediments trapped in the pool. The mixed hydrothermal fluids then discharge on to the sea floor where they precipitate metal sulphides, sulphates and silicates. The modified and cooler fluid continues to rise to the density boundary with the upper brine, where it precipitates Fe and Mn oxides.
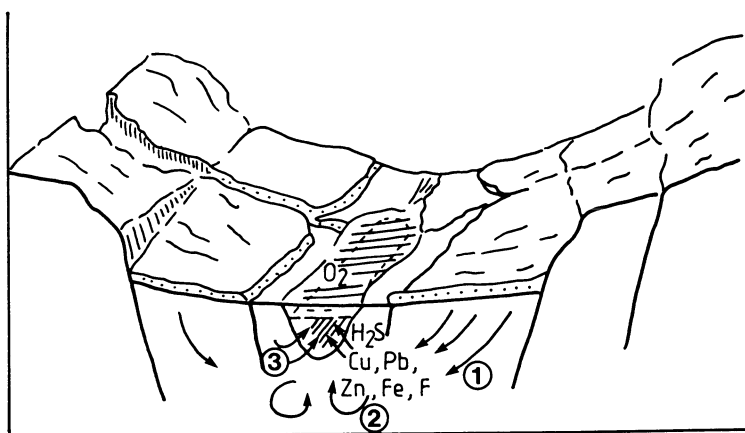
Fig. 3.24. Hydrothermal system of a rift valley lake, modelled on Lake Kivu. *1* Meteoric waters; *2* convective cell; *3* metal-bearing hot springs. The lake is stratified with oxygenated water layers at the top, and an anaerobic zone at depth (After Robbins 1983)

Hot Springs and Metalliferous Deposits in the Lakes of the East African Rift System

High heat flow, hot springs and the presence of organic compounds and metals characterise many of the lakes in East African continental rifts (Fig. 3.22). Studies of these lakes have led Degens and Ross (1976) to conclude that periods of high hydrothermal activity coincide with periods of high rain fall, that metals are leached from the rocks through which the hot fluids pass, and that these fluids form convection cells driven by the volcanic heat. The discharge of hot saline and metalliferous solutions has been investigated in Lake Kivu, Lake Magadi (Eugster 1969, 1986; Degens and Kulbicki 1973; Degens and Ross 1976) and Lake Bogoria (Renaut et al. 1986). A review of the present-day hydrothermal activities in the rift lakes is given by Robbins (1983). Fig.3.24 depicts the type of hydrothermal circulation associated with the rift valley lakes in East Africa (Robbins 1983).

It is estimated that approximately 60000 tonnes of Cu, 270000 tonnes of Pb and 60000 tonnes of Zn have accumulated in Lake Kivu in the last 5000 years (Degens and Kulbicki 1973). Sulphides are formed due to reaction of the metal ions with biogenic H_2S; and zinc metal is carried into solution, combining with S to form spherules of ZnS that are precipitated on the floor of the lake. Robbins (1983) noted that similar spheres of chalcocite are reported from the Nonesuch shale associated with the White Pine stratiform deposit in Michigan (Mid-Continent rift system). Hot springs discharge on the floor of the lake and are thought to originate from meteoric waters that percolate through the volcanic rocks, heated and mixed with volcanic emission of CO_2 and other gases such as H_2, N_2, H_2S and CH_4 (these last two probably of biogenic origin). The high concentration of Na and Cl of the lake's waters are probably controlled by the hydrothermal input into the lake. Lake Kivu sediments are enriched in Mo, V, Pb, Zn, Cu, B and F. The concentration of the last

two elements is particularly high ($B \pm 200$ ppm, F from 0.1 to 0.6%), and their origin is attributed to hydrothermal discharge. Fluorine precipitates as fluorite.

Lake Magadi is an ephemeral alkaline lake where, besides trona ($NaHCO_3$ .Na_2CO_3.$2H_2O$) deposits, the mineral magadiite is present ($NaSi_7O_3(OH)_3$.$3H_2O$). Magadiite precipitates grade along the strike into bedded cherts (microcrystalline silica), and Eugster (1969, 1986) proposed that Na leaching by groundwaters leads to replacement of the magadiite by chert. He also suggested that this replacement in the alkaline environment of the rift lake may be a possible mechanism for the origin of the Proterozoic banded iron formations and their local riebeckite (Na-amphibole) content. Layers of fibrous riebeckite, also known as blue asbestos (crocidolite), may form by reaction of magadiite with Fe-rich minerals. Eugster also reported the presence of Na-Al-Si gels in the lake. Hot springs at Lake Magadi have temperatures of about 86°C and are enriched in Na, HCO_3^-, Cl, K, SO_4, F, SiO_2, P and B. Their total dissolved solids (TDS) range from 10000 to 35000 ppm. The environment of Lake Magadi has been compared to some of the evaporitic sequences in the geological record, such as that of the Duruchau formation in Namibia and the HYC shale of the McArthur River deposits in Australia.

Lake Bogoria (Renaut et al. 1986) lies in a deep half graben of the Kenian rift, and is a saline, alkaline rift lake fed by both surface inflow of waters and some 200 perennial hot springs along the shores and on the floor of the lake. The lake's waters contain Na, HCO_3 and Cl, with variable concentrations of silica. Lower temperature (34–48°C) hot springs have solute concentrations of about 1.0 g/l but with significant SiO_2, F^-, Na^+ and HCO_3^-. High temperature springs (64–98.5°C) have higher solute concentrations (from 4–15 g/l), and have a Na-HCO_3-Cl composition also with high SiO_2 and F. Here, too, it is believed that spring waters are essentially groundwaters or lake water that percolate down through fissures, and are heated by hot volcanic gases (mainly CO_2). Spring deposits consist of travertine mounds and crusts, formed as the result of the removal of CO_2 from oversaturated solutions. The travertine is made up of aragonite and low-Mg calcite, and the mounds are covered by stromatolite algae dated at 4000 years B.P. Opaline silica crusts form around many of the hot springs pools and are accompanied by milky white colloidal silica suspensions and silica gels. Other precipitates include hydrous Na silicates, such as magadiite and fluorite. Hydrothermal alteration of sedimentary rocks and lavas by the hot alkaline water is common, and is characterised by the presence of pyrolusite, opaline silica, quartz, anatase, smectite and illite and zeolites.

3.7 Hydrothermal Systems of Metamorphic and Crustal Origin

Field and laboratory studies of many metamorphic terranes around the world unambiguously demonstrate that fluids in the crust play a critical role in both tectonism and metamorphic reactions. The generation of fluids during metamorphism is also important from the metallogenic point of view, because these fluids have the tendency to migrate towards cooler regions where they may be focused in structurally and/or lithologically controlled locales, forming a class of hydrother-

mal mineral deposits to be discussed in Chapter 15. In this section we examine the origin and movement of fluids, and the possible configuration of hydrothermal systems that can be generated during metamorphism of rock sequences. There is evidence – both direct and indirect – that volatiles and other mobile constituents are, at least in part, generated during metamorphism and move through the crust. Recent deep drilling programmes in the USSR and in Germany have confirmed, by direct observation and by geophysical inference the presence of large-scale movement of crustal fluids at depths of several kilometres (see Kremenetski and Ovchinnikov 1986). The origin, nature and movement of fluids in the Earth's crust are discussed in detail by Fyfe et al. (1978). Amongst the many important works that are relevant to the topic of this section are those of Norris and Henley (1976), Etheridge et al. (1983), Fyfe and Kerrich (1984), Kerrich (1986) and Fyfe (1987), to which the reader is referred.

Some of the principal geological situations in which crustal fluids may be generated and circulated upward to form hydrothermal systems capable of leaching, transporting and depositing ore elements are: (1) regions of prograde regional metamorphism and (2) areas of collision and thrust tectonics. As with all hydrothermal systems, a heat source(s) and fluid phase(s) are needed. Fluid phases originate by metamorphic devolitilisation reactions, although a number of geoscientists believe that in some metamorphic environments the contribution of mantle fluids may also be important. The heat energy necessary to induce dehydration reactions in a rock body can be supplied through a number of sources acting either alone or together over a period of time. These sources may include batholith-scale granitic intrusions, mantle diapirs in zones of crustal attenuation and rifting, or through the juxtaposition by thrust tectonics of hot crust over cooler rocks. Rapid uplift with rising of isotherms of up to 500 °C to within less than 10 km of the surface can also be an important source of heat, for which no igneous activity whatsoever need be present (Craw and Koons 1988). It should be noted that radioactive heat is not considered sufficient to supply enough energy to drive dehydration reactions (Fyfe et al. 1978).

3.7.1 Metamorphism, Metasomatism, Dewatering of Rock Sequences and Fluid Generation

Metamorphism can be defined as "all solid-state changes in fabric and composition of a rock body occurring well beneath the surface of the Earth, but without the intervention of a silicate melt" (Best 1982, p.343). Metamorphic processes can be endothermic (heat is supplied to the system from an external source), or exothermic (heat is evolved by the system). Most dehydration reactions are endothermic, whereas hydration reactions liberate heat. Metamorphism can also be isochemical, if the metamorphosed rocks have retained their original composition with no substantial loss or gain of matter. Metasomatism, in contrast, is the process whereby there is substantial transfer (gain or loss) of matter in a rock body, resulting in significant changes in chemical composition (Best 1982; Chap. 8). Metasomatism requires that large volumes of fluids infiltrate and interact with

the rock bodies. In this discussion endothermic metamorphic processes are considered.

Sedimentary rock sequences may contain large quantities of aqueous fluids within their pore spaces and fractures. Much of this water, whose nature is essentially that of brines, is driven out during compaction and tectonic compression. The movement of these brines in the sedimentary basins, and prior to the onset of metamorphism, may lead to the development of low temperature sulphide and oxide mineralisation in structurally suitable traps giving rise to mineralisation known as the Mississippi Valley type (see Chap. 14). During burial and prograde metamorphism, increasing temperature and pressure activates dehydration reactions, which release water and other volatiles from the lattices of the rock-forming minerals. The materials and minerals responsible for the production of fluids during metamorphism together with representative reactions are discussed in Chapter 15. Intriguing calculations by Fyfe et al. (1978) indicate that an average aluminous pelite will lose 2.7% of water by weight during the transition from the biotite isograd to the K-feldspar isograd. This would correspond to a lake some 300 m deep (!), above a column of pelitic rocks 5 km thick. These fluids, together with connate waters retained in the rock pile, after the initial compaction and consequent loss of permeability are distributed in pore spaces, grain boundaries, grain-boundary defects and microfractures.

The dominant species of fluids in the metamorphic environment are H_2O, CO_2, CO, H_2, Cl, F, S, CH_4, NH_3, inert gases and hydrocarbons. Release of fluids during metamorphism of sediments (pelitic and carbonate rocks), and mafic rocks has been studied by Fyfe et al.(1978), who published fluid release curves for pelitic sediments and mafic rocks. In general, sedimentary rocks contain hydrated and volatile-bearing minerals, such as clays, micas and carbonates. The fluid release curves of Fig. 3.25 represent pelitic rocks at four different geotherms, and show that the quantity of fluids released is a function of metamorphic grade and geothermal gradient. Also, for pelitic sediments release of fluids is a continuous process, with partial melting eventually taking place near the melting curve of granite. For pure phases, such as the assemblage kaolinite + quartz, pyrophyllite would form first, followed by complete dehydration to kyanite and quartz. In this case dehydration is characterised by sharp pulses of fluid release, in contrast to the continuous release with increasing temperature and pressure for the more complex solid solution minerals of pelitic rocks.

3.7.2 Fluid Pressure, Metamorphic Porosity, Impermeable Barriers and Hydraulic Fracturing

In the case of a closed system, the volume of the fluid-filled pores will be reduced during compression, and strains will develop along the grain boundaries with consequent buildup of pressure in the pore fluids. The total effect of this pressure will be against the externally applied pressure, which by necessity is reduced. The effective stress will then represent the difference between applied stress and pore fluid pressure (Phillips 1986). Although it can be expected that the hydrostatic
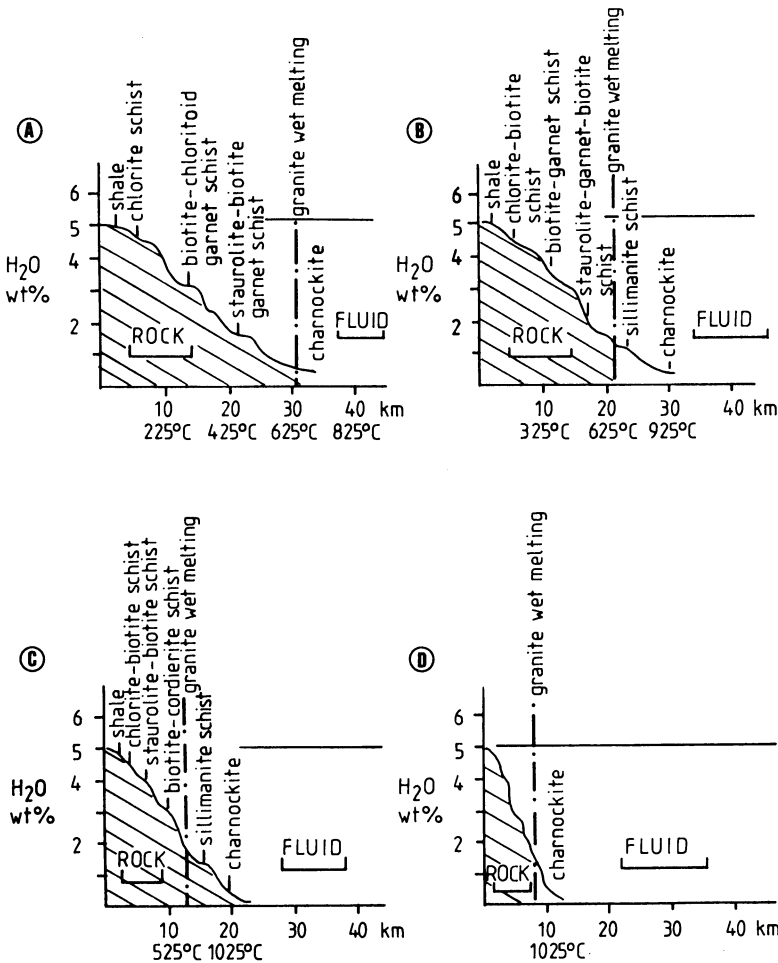
GEOTHERMAL GRADIENTS:

(A) = 20°C km^{-1}

(B) = 30°C km^{-1}

(C) = 50°C km^{-1}

(D) = 100°C km^{-1}

Fig. 3.25. Curves (A–D) of fluid release for pelitic sediments, relating to four geothermal gradients as indicated in the figure (After Fyfe et al. 1978)

pressure of the pore fluids increases with depth, a linear increase is considered simplistic by Fyfe et al. (1978), who draw attention to the spectacular examples of the sudden gushing of brines and crude oil for several tens of m in the air from boreholes, thus demonstrating that those fluids must have been under very high pressure.

The movement of fluids in the crust is related to the permeability of the rocks. Permeability is a parameter which measures the rate of fluid flow through a unit area in a unit time, through given pressure gradient and direction, and is inversely proportional to the viscosity of the fluid (Darcy's law). If pore fluid pressure exceeds the confining pressure and strength of the rock body, hydraulic fracturing will occur and the permeability will increase.

The strength of a rock, or the maximum differential stress ($\sigma_1 - \sigma_3$) that it can withstand in a specific environment, is related to the temperature, confining pressure, fluid pressure and time (Fyfe et al. 1978). The theoretical strength of rocks was modelled by Griffith (1924), who believed that elliptically shaped microscopic flaws occur at random in a homogeneous and isotropic material. If a macroscopic stress is applied microstresses are generated near the tips of the elliptical flaws, and if their long axes are perpendicular to the least principal stress, the flaw can propagate until fracturing occurs. Secor (1968) refined the model by postulating that the flaws are connected by capillaries containing fluid. When propagation occurs, a given flaw increases in volume and the pore fluid pressure decreases, while the fluids in nearby flaws remain unaffected so that a gradient is established and the fluids flow through the capillaries prompting further propagation. According to Fyfe et al. (1978), these microstresses can be so high that they may disrupt and rupture the atomic bonding of the unflawed material so that the flaw propagates. This theory was elegantly demonstrated by means of photo-elastic experiments (Fyfe et al.1978, p.200)

The nature of porosity in the metamorphic environment is considered by Etheridge et al. (1983) in terms of grain boundaries and deformation structures. It seems likely that fluids may reside within tubules, boundary bubbles and films. Etheridge et al. (1983) emphasise that microfractures, and tubules and bubbles along grain boundaries, are highly effective in metamorphic porosity, because they tend to form an interconnecting network. Deformation structures, on the other hand, include microcracks that can propagate from fluids at grain boundaries, porosity arising from mineral reactions (e.g. decarbonation), and macroscopic structures such as foliation and shear zones. The latter constitute major channel-ways for the fluids. Large-scale buoyancy in response to thermal gradients, together with local fluid pressure gradients, mean that fluids tend to move along these structures (Fyfe and Henley 1973, Etheridge et al. 1983).

Impermeable barriers may have an important effect on pore fluid pressure and the movement of connate and/or metamorphic fluids in rock bodies. In a sedimentary sequence, layers of shales or evaporites can constitute efficient impermeable barriers. Impermeable barriers may also form along the zone of mixing between hot rising metamorphic fluids and cooler descending meteoric waters. Their mixing induces precipitation of mineral phases and sealing along this interface zone (Cox et al. 1986). Fyfe et al. (1978) modelled the changes of pore fluid pressure above and below an impermeable layer at a depth of 5 km, in a section of crust 10 km thick. They consider that in that portion of the crust situated below the impermeable layer (between 5 and 10 km), fluids are in a closed system, and will tend to migrate upward until the fluid pressure in the rocks below and adjacent to the barrier builds up to pressures equalling the total vertical pressure. Under these
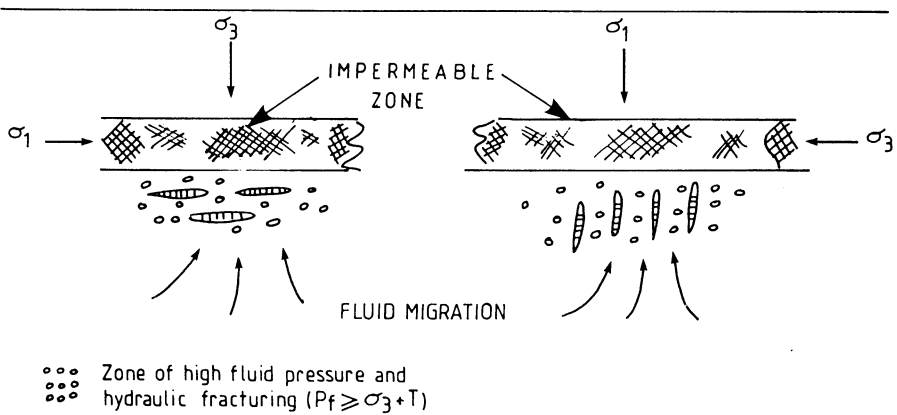
Fig. 3.26. Model of fluid migration and hydraulic fracturing below an impermeable layer in the crust (After Cox et al. 1986)

conditions the fluids would collect in areas of low vertical stress below the barrier to form a "pond-like" body. It is envisaged that the barrier would be breached by hydraulic fracturing, with the fractures extending through to the upper part of the rock sequence (see also Cox et al. 1986). Hydraulic fracturing will occur when the fluid pressure (P_f) exceeds or equals the tensile strength (T) and the least principal stress (σ_3): $P_f > \sigma_3 + T$, and as shown in Fig. 3.26, the attitude of the fractures is a function of the local stress field. Should other impermeable barriers be present in the rock sequence, as they normally would, each of the barriers would cause a rise in the fluid pressure in the closed system below it, followed by fracturing and accumulation of the fluids above it.

In summary, accumulation of the fluids beneath impermeable barriers will result in increased pressure and subsequent escape of the fluid through hydraulic fracturing and through faults and shear zones. Permeability enhancement and/or fracturing of the zone of impermeability by high fluid pressure results in the precipitation of mineral phases and a decrease in pressure. Mineral deposition will in turn result in sealing of the fractures, thus re-establishing the impermeability zone so that the cycle may start again (Cox et al. 1986).

3.7.3 Metamorphic Hydrothermal Systems

Etheridge et al. (1983) developed a model, schematically shown in Fig. 3.27, of large scale convective hydrothermal cells in areas of regional prograde metamorphism. These authors envisage that active fluid circulation occurs above a large heat source, as may be represented by a mantle diapir, for example, which creates a region of crustal melting. Above this, the metamorphic environment may be subdivided into two zones. A lower zone would contain less active circulation: while the upper zone, corresponding to the upper levels of the metamorphic pile, would be affected by more actively convecting fluids. The boundary beween these two zones could
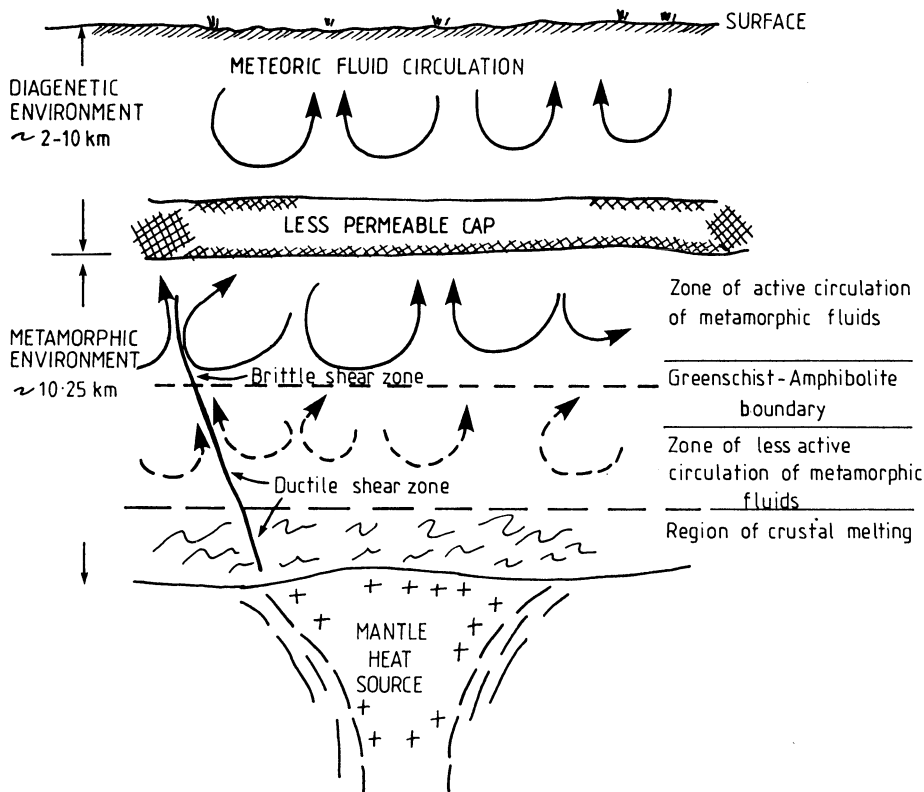
Fig. 3.27. Model of metamorphic fluid generation in the crust in response to a large heat source. See text for explanation (After Etheridge et al. 1983)

correspond to a metamorphic facies boundary such as amphibolite to greenschist. The zones of metamorphic water circulation are confined below a "less permeable" cap, above which is the diagenetic environment where meteoric water circulation predominates. This cap is thought to be formed by sealing, due to precipitation of mineral phases at the interface between the two hydrothermal systems (cool-meteoric from above and hot-metamorphic from below) in a manner somewhat similar to that which happens, perhaps on a smaller scale, in epithermal systems. The "less permeable" cap may be breached by the overpressurised metamorphic fluids by hydrofracturing, as previously discussed. Also, the fluids may in places be channelled through ductile to brittle-ductile shear zones, where mineral deposits would be formed.

The model in Fig. 3.27 is not too dissimilar from that put forward by Fyfe and Kerrich (1984) to explain the ubiquitous gold mineralisation present in the Archean greenstone-granite terranes. Their model postulates extensive dewatering of "wet" metalavas and metasediments by prograde metamorphism triggered by the intrusion of granitic batholiths. This model is a refined version of that of Boyle (1979), who proposed the development of prograde metamorphic facies from
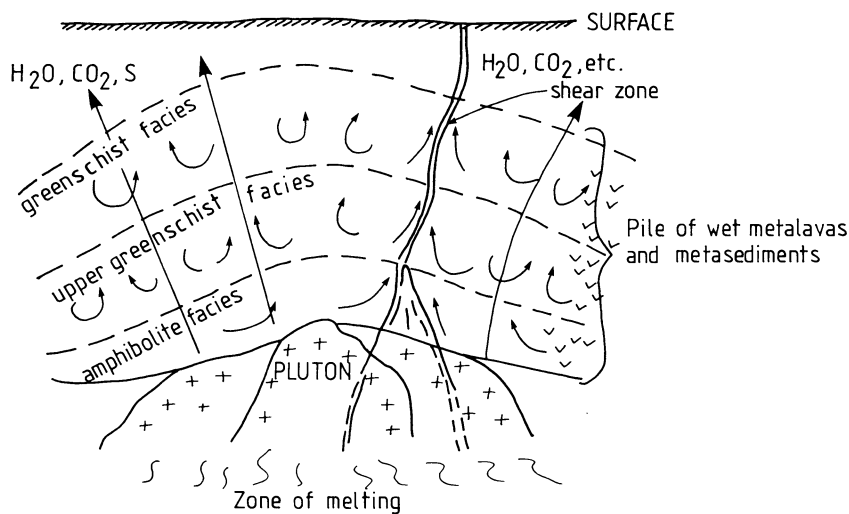
Fig. 3.28. Model of metamorphic facies and development of fluids from progressive dehydration of a wet metamorphic pile. This figure combines the models put forward by Boyle (1979) and Fyfe and Kerrich (1984)

amphibolite to greenschist, with concomitant movement of CO_2, H_2O, S, As and Au from a dehydration front ahead of a large thermal energy source, such as a granodioritic intrusion. Figure 3.28 shows a combined sketch of these two models. A further refinement is the model proposed by Fyfe (1987) who considers the thermal energy input due to underplating of continental crust by mantle melts. Fyfe's model has interesting metallogenic implications, explained by this author as follows.

Underplating of continental crust by mantle melts allows the latter to assimilate crustal components, including greenstone belts. Thus, it is possible to have metal-rich material involved in the heating and degassing of CO_2, H_2O and S from the greenstone rocks. Ore elements could be easily transported upward by these volatiles. Underplating of the base of the crust by mantle melts causes a large thermal anomaly. This would lead to partial melting of the lower crust, the development of acid-intermediate magma and the rise of plutons in the upper crustal levels to depths of about 5 km. Metamorphic degassing would accompany the intrusions. Fyfe (1987) estimates that if greenschist rocks were initially present, with a water content of about 4%, they would be heated to amphibolite facies with a water content of about 1%. If the total volume of the affected zone is 1000 km³, the water evolved from the heating event would be around 100 km³. These fluids would be of low salinity and dominated by H_2O-CO_2. Fluid inclusion studies of many hydrothermal gold deposits associated with metamorphic terranes corroborate this.

All of these models more or less explain the general features and spatial association of most gold deposits in Archean terranes with metamorphic rocks of amphibolite to greenschist facies, as well as their common arrangements around the aureoles of granitic plutons, as is the case for the Barberton greenstone belt in South

Africa. The large-scale CO_2 metasomatism associated with zones of high strain in greenstone belts is also accounted for in these models. The Archean scenario is, however, to be considered in a different light from later systems (Proterozoic and Phanerozoic). Two schools of thought dominated a debate on the origin and development of hydrothermal systems in the early stages of the Earth's geological history, at the Bicentennial Gold '88 conference in Melbourne, Australia. The first – predominantly Australian-school, advocated a major role for fluids of metamorphic and/or mantle origin. These fluids stream upward, leaching, transporting and depositing gold and other metal in areas of greenschist-amphibolite facies within zones of high strain. The second school, with a strong Canadian bias, advocated a genetic and spatial relationship of the mineralistaion with felsic intrusives. In both cases, however, it is clear that most Archean hydrothermal gold deposits are structurally controlled and have an intimate relationship with shear zones and faults. Post-Archean turbidite-hosted gold deposits also have a strong spatial association with greenschist-amphibolite facies metamorphic zones, and with major structural breaks in the crust and in fact share many similarities with their Archean counterparts. Chapter 15 takes a more in-depth look at this issue.

3.7.4 Fluid Paths: Faults, Shear Zones and Thrust Faults

The movement of metamorphic fluids in a rock mass is attained and enhanced by permeability. Permeability is dependent on, and due to, rock type, fractures, foliation, shear zones and faults. Any steeply inclined plane (e.g. foliation) will constitute a pathway for the migration of fluids, and of particular importance therefore are the pipe-like structures formed at the intersection of two planes. According to Norris and Henley (1976), the movement of metamorphic fluids during dehydration of a metamorphic pile may be due to thermal expansion of water and hydraulic fracturing. They emphasise the role of post-orogenic uplift of rock sequences for thermal expansion and transfer of fluids upward and along major fracture systems. Circulating metamorphic fluids are preferentially channelled through pathways determined by breccia, cataclastic or mylonitic zones associated with major faults or structural breaks. The influence of rock type may also be important, either in terms of primary porosity, or because of secondary porosity enhancement due to metamorphic or other processes. Major structural features such as faults, shear zones and thrusts are perhaps the most important channelways – at least in terms of ore deposition – for the movement and focusing of hydrothermal fluids. Large-scale fluid movement is thought to be associated with steep shear zones, because fluids are focused in a highly permeable and restricted zone (Etheridge et al. 1983).

Sibson et al. (1975) invoke seismic pumping as a mechanism whereby large quantities of fluids can move along a fault plane during earthquakes to form hydrothermal mineral deposits. Their model assumes that just before seismic failure along a strike-slip fault a regime of dilation surrounds the area of the focus. This would be due to increasing shear stress by the opening of vertical fractures normal to the least principal stress (σ_3), which in the case of strike-slip faults is horizontal.
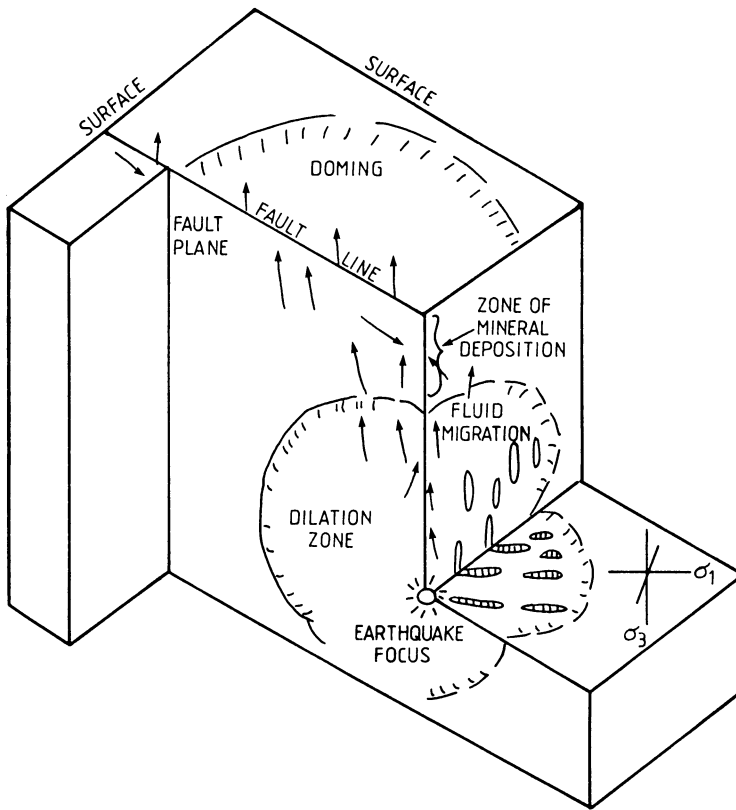
Fig. 3.29. Seismic pumping model of fluid expulsion around a strike slip fault (After Sibson et al. 1975)

Sibson et al. (1975) argue that the development of these fractures allows the fluid pressure to decrease in the region of dilatancy, resulting in fluid movement along these fractures. Fluid pressure then rises again, accompanied by a decrease in the frictional resistance, so that seismic failure takes place with partial stress relief. The result is the expulsion of the fluids upward in the direction of the pressure relief (Fig. 3.29). This flow of fluids takes place along the fault and nearby fractures, and mineral deposition occurs above the dilation zone, as shown in Fig. 3.29. To corroborate their model, Sibson et al. (1975) draw attention to the common observation of hot springs along the active fault. They cite the example of an earthquake in Japan, which resulted from movements along a buried wrench fault about 10 km long. The earthquake was accompanied at the surface by the expulsion for 1 year of some 10^{10} litres of warm brine containing Na, Cl and Ca, and saturated with CO_2. The authors further propose that if the fault intersects a suitable source region, then metals could be leached out by the moving fluids, transported by seismic pumping and deposited above the dilatant zone as illustrated in Fig. 3.29.
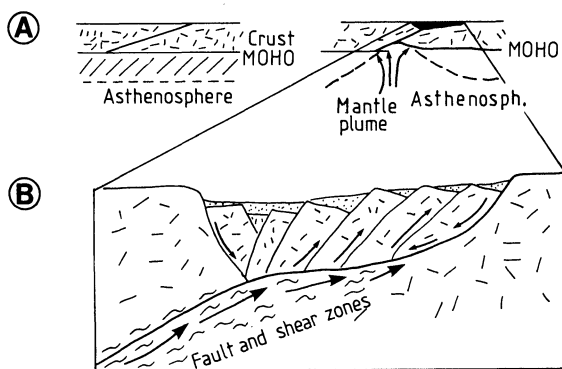
Fig. 3.30. Combined model of hydrothermal fluid flow in detachment zones. *Arrows* indicate fluid movement. A is after Wernicke (1981); B after Reynolds and Lister (1987)

Movement of hydrothermal fluids is also thought to occur along "detachment zones" that separate tectonic "plates" in the metamorphic core complexes of the western USA (Coney 1980, Reynolds and Lister 1987). These detachment zones are low-angle normal faults along which there is strong brecciation and mylonitisation (Fig. 3.30A, B). Hydrothermal alteration and the presence of mineralisation in the tectonic plates testify to the movement of fluids. The upper plate is characterised by potassic (K-feldspar) and hematitic alteration, whereas the lower plate has propylitic-type alteration and is composed mainly of the minerals epidote and chlorite. Reynolds and Lister (1987) proposed that two regimes of fluid flow were present. One, in the upper plate, was associated with meteoric and connate waters; the other, related to the shear zone, migrated from deep-seated regions. The latter fluids could have been derived from either an igneous or a metamorphic source (Kerrich 1986), or even possibly from a mantle source, if one assumes that the detachment zone extends into the mantle above a section of thinned crust, as suggested by Wernicke (1981; Fig. 3.30A).

The role of collision tectonics and thrust faulting in the generation and movement of fluids has been widely recognised in recent years. Hubbert and Rubey (1959, 1960, 1961) were perhaps the first to realise the importance of high fluid pressures for the translation of large overthrust masses. The theory of thrust-related fluid generation and movement is based on the concepts illustrated in Fig. 3.31A, B. A block of crust develops a thrust fault, and a section of this block overrides the other section as shown in the figure. Assuming that the temperature is regularly distributed, e.g. horizontal isotherms and increasing values with depth, then at completion of the thrust movement, the hotter lower zone of the upper section rests above the cooler regions of the lower section. The geothermal gradient shows an inversion of temperature at the boundary between the two sections. This configuration is thermally unstable, and will therefore tend to re-equilibrate with time and re-establish a steady-state geothermal gradient. The thermal disequilibrium may result in the development of convective circulation in the lower underthrust section, and the channelling of fluids above and along the thrust plane (Fig. 3.31C). A more detailed analysis of these effects is descibed by Fyfe and Kerrich (1985), and is summarised below. In major thrusts – such as those described for the Himalayas – with long distances (hundreds of km) and thick plates (15–30 km) involved, thermal
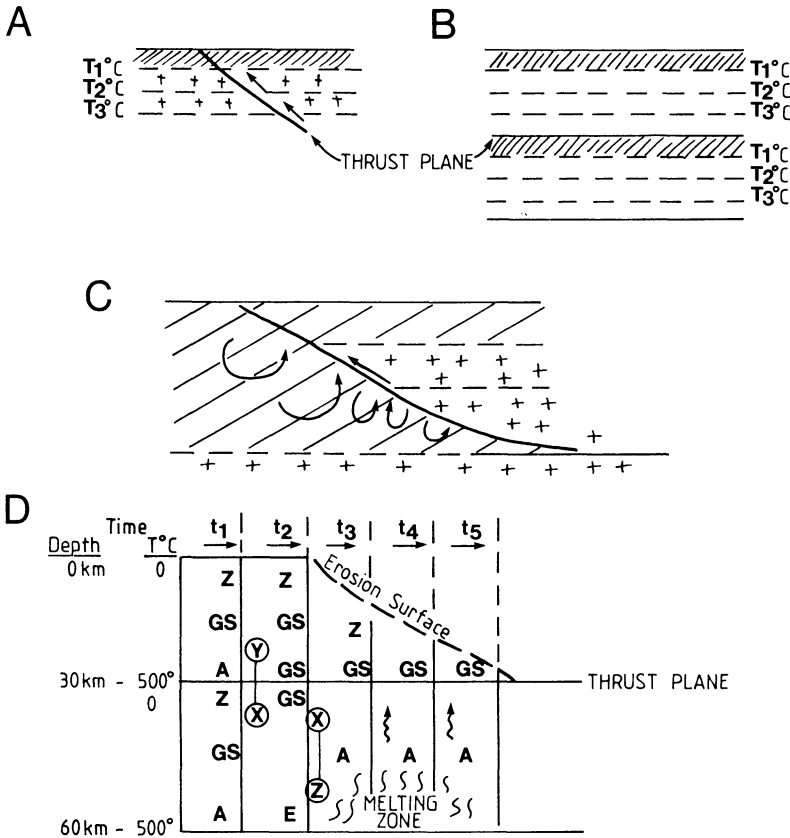
Fig. 3.31A–D. Models of inverted geothermal gradients resulting from thrust tectonics. A and B isotherms in continental crust before and after thrusting respectively (after Open University 1980). C Hotter crust is thrust over cooler water-saturated crust, and hydrothermal convective cells are activated in the underthrust slab. Fluids are focused along the thrust plane (after Etheridge et al. 1983). D Metamorphic zoning attained during continent-continent collision as modelled by Fyfe and Kerrich (1985) and Fyfe (1987); see text for explanation. *GS* greenschist facies; *A* amphibolite facies; *Z* zeolite facies; *E* Eclogite facies

equilibrium is not attained during the time of thrusting (about 100 km in 10^6 years). Thrusting can therefore be considered as isothermal, so that the temperature distribution is as shown in Fig. 3.31D, where one continental block 30 km thick has been thrust upon another. The overthrust continental block is initially hotter than the underthrust block, but with time, equilibrium temperature is determined according to erosion rates and melting at the base. During thrusting, pore water is expelled from the region marked X, and prograde metamorphism occurs over the entire thickness of the underplate. On average it is estimated that about 4% H_2O may be lost from the underplate, and these fluids either penetrate the overthrust plate, or flow along it during thrusting. Penetration of fluids in the overplate is generally by hydraulic fracturing mechanisms, resulting in swarms of veins and

shear zones. Along the zone X-Y the thermal gradient is reversed and retrograde metamorphism occurs in zone Y. The once near-surface rocks will be relatively more oxidised, so that the fluids will tend to oxidise the overplate and, consequently will not precipitate silica but rather dissolve it. Massive veining occurs instead along path Z-X of Fig. 3.31D, with the possible formation of gold deposits. In time, smaller regions of the inverted gradient become present (due to erosion effects), so that even mineralisation processes will eventually progress. Near the thrust surface the most dramatic prograde and retrograde changes occur, including partial melting (time t_3 to t_5 of Fig. 3.31D).

The model for the generation of crustal fluids outlined above was utilised by Le Fort et al. (1987) to explain the origin of Himalayan leucogranites. They associate thrusting on the continental scale – with the inception of inverted metamorphism and the liberation of large quantities of fluids, followed by anatectic melting of crustal material – with the production of geochemically specialised leucogranites. Thrusting, as illustrated above, results in the superpositioning of hot, deep continental crust, over little metamorphosed lithologies. Heating then proceeds from top to bottom, inducing inverted metamorphic grades. Also, during the metamorphism of the lower and colder formations, metamorphic reactions release a large amount of fluids, particularly H_2O and CO_2. The fluids move along and above the thrust inducing melting close to minimum melt compositions.

A special case of fluid systems associated with thrusting is found in the rift-related sediments of the Duruchaus Formation in the Damara orogen in Namibia. This formation consists of metaplaya and metaevaporite sediments, such as tourmalinites and dolomitic rocks, intercalated with metapelites and psmammitic sediments deposited during the incipient stages of rifting. According to Schmidt-Mumm et al. (1987), during the tectogenetic event that formed the Damara orogen, the metaplaya and metaevaporitic sediments were metamorphosed and overthrust by hot crystalline southward-moving nappes. Large volumes of hypersaline and alkaline fluids were derived from the dehydration of this sedimentary sequence. These fluids were channelled along the thrust plane between the basement rocks and the Duruchaus formation, and the high pore pressure produced a number of breccias which broke through the rocks of the Duruchaus formation. These fluids were also channelled along the sole between the Duruchaus Formation and the overlying nappe, producing strong metasomatic alteration and a number of pipes and plugs of quartz vein material, which Schmidt-Mumm et al. (1987) report to have large crystals with faces of up to 50 m.

Another interesting case of metamorphic fluid movement associated with faulting and uplifting has recently been proposed in a number of papers by Craw and co-workers (Craw et al. 1987a, b; Craw and Koons 1988). They postulate infiltration of hot metamorphic fluids to shallow levels of the crust by rapid uplift on the east side of the Alpine transcurrent fault, in the South Island of New Zealand. The H_2O-CO_2-rich metamorphic fluids eventually mix with meteoric waters to precipitate silica and gold (this is discussed further in Chap. 15). The main feature of this model is that a metamorphic-meteoric hydrothermal system can be activated as a result of high heat flow due to rapid uplift which brought hot rocks to shallow levels.

3.7.5 Fluids in Subduction Zones

Subduction of the oceanic lithosphere results in the release of abundant fluids. The release of fluids during subduction and their transfer above the subducting slab has been the subject of several works by Fyfe and his colleagues. Summaries from two key papers of Fyfe (1987) and Fyfe and Kerrich (1985) are given below.

Horst and graben structures present on top of the oceanic lithosphere cause the transportation of their contained pelagic sediments along with normal oceanic crust down the Benioff zone (Fig. 3.32). This suggests that substantial volumes of metal-enriched sediments, and possibly sea-floor volcanogenic massive sulphide bodies will be subducted along with "wet" oceanic crust. As these various lithologies undergo progressive metamorphism, extensive devolitilisation with pulses of high pressure fluids may be produced and expelled by hydrofracturing in the overplate. However, at this stage, the fluids will be cold and incapable of carrying enough solutes to form sizeable mineral deposits. These early stages of the dehydration processes are accompanied by the development of the so-called melange zones. With continued subduction, the descending slab will be heated as it re-equilibrates to the higher mantle temperature. Fyfe (1987) calculates that if the lower 20 km of the slab were to reach amphibolite facies, it would lose approximately 3% water, so that the mass of fluid evolved from a $20 \times 10 \times 1$ km volume would be about 20 km^3. Some of the fluids evolved would travel along the thrust plane, while others would move upward by hydrofracturing. The fluids evolved may attain temperatures of 300 to 600°C, and carry solutes such as silica, Au, Ag and other metals as well as large volumes of CO_2. It is also worth mentioning that the fluids released in this way would cause partial melting of the overlying mantle wedge, which may as a result become enriched in the metallic constituents carried by the fluids. The melts will rise and underplate the crust, producing hybrid magmas which in turn may intrude shallow crustal levels and even erupt at surface, producing the range of hydrother-
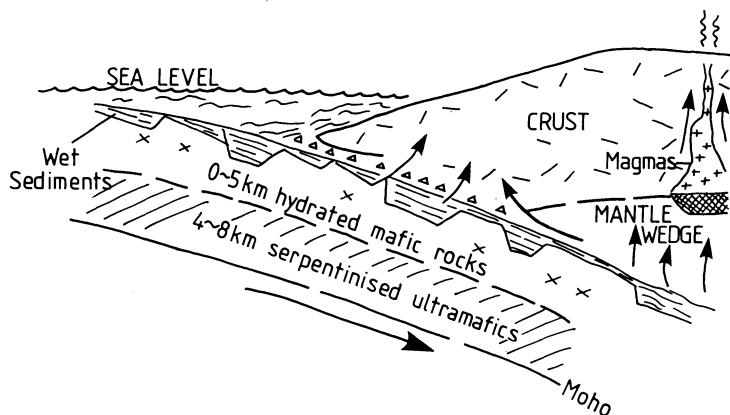
Fig. 3.32. Dewatering and tectonic erosion of a subducting oceanic slab with graben-type structures, infilled with wet sediments, developed during bending of the slab. *Arrows* indicate fluid movement (After Fyfe and Kerrich 1985 and references therein)

mal mineral deposits usually associated with subduction-related magmatism (e.g. porphyry and epithermal systems). We have now come full circle back to the magmatic and magmatic-meteoric hydrothermal systems associated with magmas.

References

Best M G (1982) Igneous and metamorphic petrology. Freeman, San Francisco, New York, 630 pp

Bischoff J L, Rosenbauer R J (1989) Salinity variations in submarine hydrothermal systems by layered double-diffusive convection J Geol 97:613–623

Bogie I, Lawless J (1987) Controls on the hydrology of large volcanically hosted geothermal systems: implications for exploration for epithermal mineral deposits. Proc Pac Rim '87 Congr. Australas Inst Min Metall, Parkville, Victoria, pp 57–60

Boyle R W (1979) The geochemistry of gold and its deposits. Geol Surv Can Bull 280

Burnham C W (1979) Magmas and hydrothermal fluids. In: Barnes L H (ed) Geochemistry of hydrothermal ore deposits, 2nd edn. John Wiley and Sons, New York, pp 71–136

Carmichael I S E, Turner F J, Verhoogen J (1974) Igneous petrology. McGraw-Hill, New York, 739 pp

Cathles L M (1983) An analysis of the hydrothermal system responsible for massive sulfide deposition in the Hokuroko basin of Japan. Econ Geol Monogr 5:439–487

Colley H (1986) Epithermal gold mineralisation associated with Mio-Pliocene volcanism in Fiji. Proc Symp 5 Int Volcanol Congr Auckland, N Z pp 31–36

Coney P J (1980) Cordilleran metamorphic core complexes: An overview. Geol Soc Am Mem 153:7–31

Cox S F, Etheridge M A, Wall J (1986) The role of fluids in syntectonic mass transport, and the localisation of metamorphic vein-type ore deposits. Ore Geol Rev 2:65–86

Craw D, Koons P O (1988) Tectonically induced gold mineralisation adjacent to major fault zones. In: Bicentennial Gold '88, Geol Soc Aust Abstr Ser 22:338–343

Craw D, Johnstone R D, Rattenbury M S (1987a) Gold mineralisation in a high uplift rate mountain belt, Southern Alps, New Zealand. Proc Pac Rim '87 Congr. Australas Inst Min Metall, Parkville, Victoria, pp 95–98

Craw D, Rattenbury M S, Johnstone R D (1987b) Structural geology and vein mineralisation in the Callery River headwaters, Southern Alps, New Zealand. N Z J Geol Geophys 30:273–286

Dadet P, Marchesseau J, Millon R, Motti E (1970) Mineral occurrences related to stratigraphy and tectonics in Tertiary sediments near Umm Lajj, eastern Red Sea area, Saudi Arabia. Phil Trans R Soc Lond Ser A267:99–106

Degens E T, Kulbicki G (1973) Hydrothermal origin of metals in some East African rift lakes. Mineral Depos 8:388–404

Degens E T, Ross D A (1976) Strata-bound metalliferous deposits found in or near active rifts. In: Wolf K H (ed) Handbook of strata-bound and stratiform ore deposits vol 9. Elsevier, Amsterdam, pp 165–202

Doe R B, Deleveaux M A (1972) Source of lead in southeast Missouri galena ores. Econ Geol 67:405–425

Dunoyer de Segonzac G (1968) The birth and development of the concept of diagenesis (1866–1966). Earth Sci Rev 4:153–201

Edmond J M, von Damm K (1983) Hot springs on the ocean floor. Sci Am 248:70–85

Einsele G, Gieskes J M, Curray J, Moore D M, Aguayo E, Aubry M, Fornari D, Guerrero J, Kastner M, Kelts K, Lyle M, Matoba Y, Molina-Cruz A, Niemitz J, Rueda J, Saunders A, Schrader H, Simoneit B, Vacquier V (1980) Intrusion of basaltic sills into highly porous sediments, and resulting hydrothermal activity. Nature (London) 283:441–445

Ellis A J, Mahon W A J (1977) Chemistry and geothermal systems. Academic Press, New York, London, 392 pp

Etheridge M A, Wall J, Vernon R H (1983) The role of the fluid phase during regional metamorphism and deformation. J Metamorph Geol 1:205–226

Eugster H P (1969) Inorganic bedded cherts from the Magadi area, Kenia. Contrib Mineral Petrol 22:1–31

Eugster H P (1986) Lake Magadi, Kenya: a model for rift valley hydrochemistry and sedimentation? Geol Soc Spec Publ 25. Blackwell, Oxford, pp 177–190

Evans A M (1987) An introduction to ore geology, 2nd edn. Blackwell, Oxford, 358 pp

Fleischer D, Garlick W G, Haldane R (1976) Geology of the Zambian Copperbelt. In: Wolf K H (ed) Handbook of stratabound and stratiform ore deposits, vol 6. Elsevier, Amsterdam, pp 223–352

Fyfe W S (1987) Tectonics, fluids and ore deposits: mobilisation and remobilisation. Ore Geol Rev 2:21–36

Fyfe W S, Henley R W (1973) Some thoughts on chemical transport processes, with particular reference to gold. Mineral Sci Eng 5:295–303

Fyfe W S, Kerrich R (1984) Gold: natural concentration processes. In: Foster R P (ed) Gold '82. Spec Publ Geol Soc Zimbabwe. Balkema, Rotterdam, pp 99–128

Fyfe W S, Kerrich R (1985) Fluids and thrusting. Chem Geol 49:353–362

Fyfe W S, Price N J, Thompson A B (1978) Fluids in the Earth's crust. Elsevier, Amsterdam, 383 pp

Garlick W G (1961) The syngenetic theory. In: Mendelsohn F (ed) The geology of the Northern Rhodesian copperbelt. Macdonald, London, pp 146–165

Garlick W S (1989) Mineralization controls and source of metals in the Lufillian Fold Belt, Shaba (Zaire), Zambia and Angola – A discussion. Econ Geol 84:966–968

Griffith A A (1924) The theory of rupture. Proc 1st Int Congr Appl Mechanics, Delft, pp 53–63

Guilbert J M, Park C F (1986) The geology of ore deposits. Freeman, San Francisco, New York, 985 pp

Gustafson L B, Williams N (1981) Sediment-hosted stratiform deposits of copper, lead and zinc. Econ Geol 75th Anniv Vol:139–178

Hanor J S (1979) The sedimentary genesis of hydrothermal fluids. In: Barnes H L (ed) Geochemistry of hydrothermal ore deposits, 2nd edn. John Wiley & Son, New York, pp 137–172

Hedenquist J W, Henley R W (1985) Hydrothermal eruptions in the Waiotapu geothermal system, New Zealand: their origin, associated breccias, and relation to precious metal mineralisation. Econ Geol 80:1640–1668

Henley R W, Ellis A J (1983) Geothermal systems ancient and modern: a geochemical review. Earth Sci Rev 19: 1–50

Honnorez J (1969) La formation actuelle d'un gisement sous-marin de sulfures fuméroliens à Vulcano (mer tyrrhénienne) Mineral Depos 4:114–131

Hubbert M K, Rubey W W (1959) Role of fluid pressure in mechanics of overthrust faulting. Bull Geol Soc Am 70:115–205

Hubbert M K, Rubey W W (1960) Role of fluid pressure in mechanics of overthrust faulting. Bull Geol Soc Am 71:617–628

Hubbert M K, Rubey W W (1961) Role of fluid pressure in mechanics of overthrust faulting. Bull Geol Soc Am 70:1581–1594

Huppert H E, Sparks R S J (1984) Double-diffusive convection due to crystallization in magmas. Annu Rev Earth Planet Sci 12:11–37

Irvine T N, Keith D W, Todd S G (1983) The J-M platinum- palladium reef of the Stillwater Complex, Montana: II Origin by double-diffusive convection magma mixing and implications for the Bushveld Complex. Econ Geol 78:1287–1348

Jowett E C (1986) Genesis of kupferschiefer Cu-Ag deposists by convective flow of rotliengendes brines during Triassic rifting. Econ Geol 81:1823–1837

Kerrich R (1986) Fluid transport in lineaments. Phil Trans R Soc London Ser A 317:219–251

Kremenetsky A A, Ovchinnikov L N (1986) The Precambrian continental crust: its structure, composition and evolution as revealed by deep drilling in the USSR. Precambrian Res 33:11–43

Large D E (1981) Sediment-hosted submarine exhlative lead-zinc deposits – A review of their geological characteristics and genesis. In: Wolf K H (ed) Handbook of stratabound and stratiform ore deposits, vol 9. Elsevier, Amsterdam, pp 469–507

Le Fort P, Cuney M, Deniel C, France-Lanord C, Sheppard S M F, Upreti B N, Vidal P (1987) Crustal generation of the Himalayan leucogranites. Tectonophysics 134:39–57

Lister C R B (1983) The basic physics of water penetration into hot rock. In: Rona P A, Bostrom K, Laubier L, Smith K L (eds) Hydrothermal processes at seafloor spreading centers. Plenum New York, pp 141–168

Lonsdale P, Becker K (1985) Hydrothermal plumes, hot springs, and conductive heat flow in the Southern Trough of Guaymas Basin. Earth Planet Sci Lett 73:211–225

Lonsdale P, Bischoff J L, Burns M, Kastner M, Sweeney R E (1980) A high temperature hydrothermal deposit on the seabed at a Gulf of California spreading center. Earth Planet Sci Lett 49:8–20

McMillan W J, Panteleyev A (1980) Ore deposits models-1 Porphyry copper deposits. Geosci Can 7:52–63

Misiewicz, J (1988) The geology and metallogeny of the Otavi Mountain Land, Damara orogen, SWA/Namibia, with particular reference to the Berg Aukas Zn-Pb-V deposit – A model of ore genesis. MSc Thesis, Rhodes Univ, Grahamstown, S Afr, 143 pp

Mitchell A H G, Garson M S (1981) Mineral deposits and global tectonic settings. Geology Series Academic Press, New York, London, 405 pp

Mottl M J (1983) Metabasalts, axial hot springs, and the structure of hydrothermal systems at mid-ocean ridges. Geol Soc Am Bull 94:161–180

Norris R J, Henley R W (1976) Dewatering of a metamorphic pile. Geology 4:333–336

Ohmoto H, Rye R O (1974) Hydrogen and oxygen isotope compositions of fluid inclusions in the Kuroko deposits, Japan. Econ Geol 69:947–953

Oliver J (1986) Fluids expelled tectonically from orogenic belts: Their role in hydrocarbon migration and other geological phenomena. Geology 14:99–102

Phillips W J (1986) Hydraulic fracturing effects in the formation of mineral deposits. Trans Inst Min Metall, B95:B17–B24

Pisutha-Arnond V, Ohmoto H (1983) Thermal history, and chemical and isotopic compositions of the ore forming fluids responsible for the Kuroko massive sulfide deposits in the Hokoruku district of Japan. Econ Geol Monogr 5:523–558

Plimer I R (1985) Broken Hill Pb-Zn-Ag deposit-a product of mantle metasomatism. Mineral Depos 20:147–153

Plimer I R (1986) Sediment-hosted exhalative Pb-Zn deposits- Products of contrasting ensialic rifting. Trans Geol Soc S Afr 89:57–73

Pottorf R J, Barnes H L (1983) Mineralogy, geochemistry and ore genesis of hydrothermal sediments from the Atlantis II Deep, Red Sea. Econ Geol Monogr 5:198–223

Raybould J G (1978) Tectonic controls on Proterozoic stratiform copper mineralisation. Trans Inst Min Metall 87:B79–B86

Renaut R W, Tiercelin J J, Owen R B (1986) Mineral precipitation and diagenesis in the sediments of the Lake Bogoria basin, Kenia Rift Valley. Geol Soc Special Publ 25. Blackwell, Oxford, pp 159–176

Renfro A R (1974) Genesis of evaporite-associated stratiform metalliferous deposits – A sabkha process. Econ Geol 69:33–45

Reynolds S J, Lister, G S (1987) Structural aspects of fluid-rock interactions in detachment zones. Geology 15:362–366

Rittmann A (1962) Volcanoes and their activity. John Wiley & Sons, New York, 305 pp

Robbins E I (1983) Accumulation of fossil fuels and metallic minerals in active and ancient rift lakes. Tectonophysics 94:633–658

Rona P A (1984) Hydrothermal mineralisation at seafloor spreading centers. Earth Sci Rev 20:1–104

Rona P A, Bostrom K, Laubier L, Smith K L, (eds) (1983) Hydrothermal processes at seafloor spreading centers. Plenum, New York, London, 796 pp

Russell M J (1978) Downward-excavating hydrothermal cells and Irish-type ore deposits: importance of an underlying thick Caledonian prism. Trans Inst Min Metall B87:B168–B171

Russell M J, Solomon M, Walshe J L (1981) The genesis of sediment hosted, exhalative Zinc+Lead deposits. Mineral Depos 16:113–127

Sawkins F J (1990) Metal deposits in relation to plate tectonics, 2nd edn. Springer, Berlin, Heidelberg, New York, 461 pp

Sawkins F J (1984) Ore genesis by episodic dewatering of sedimentary basins: Application to giant Proterozoic lead-zinc deposits. Geology 12:451–454

Schmidt-Mumm A, Behr H J, Horn E E (1987) Fluid systems in metaplaya sequences in the Damara orogen (Namibia): evidence for sulfur-rich brines. General evolution and first results. Chem Geol 61:135–145

Secor D T (1968) Mechanics of natural extension functioning at depth in the earth's crust. Geol Surv Can Paper 68

Sibson R H, Moore J Mc M, Rankin A H (1975) Seismic pumping-a hydrothermal fluid transport mechanism. J Geol Soc London 131:653–659

Sillitoe R H, Bonham, H F (1984) Volcanic landforms and ore deposits. Econ Geol 79:1286–1298

Sleep N H (1983) Hydrothermal convection at ridge axes. In: Rona P A, Bostrom K, Laubier, L, Smith K,L (eds) Hydrothermal pro cesses at seafloor spreading centers. Plenum, New York, pp 71–82

Smith P A, Cronan D S (1983) The geochemistry of metalliferous sediments and waters associated with shallow submarine hydrothermal activity (Santorini, Aegean Sea). Chem Geol 39:241–262

Stanton R L (1972) Ore Petrology. McGraw-Hill, New York, 697pp

Strong D F (1981) A model for granophile mineral deposits. Geosci Can 8:155–161

Sturchio N C, Williams S N, Garcia N P, Londono A C (1988) The hydrothermal system of Nevado del Ruiz volcano, Colombia. Bull Volcanol 50:399–412

Sweeney M A, Binda P L (1989) Mineralization controls and source of metals in the Lufillian Fold Belt, Shaba (Zaire), Zambia and Angola – A discussion. Econ Geol 84:963–964

Taylor H P (1983) Oxygen and hydrogen isotope studies of hydrothermal interactions at submarine and subaerial spreading centers. In: Rona P A, Bostrom K, Laubier L, Smith K L (Eds) Hydrothermal processes at seafloor spreading centers. Plenum, New York, pp 83–140

Taylor R, Pollard P J (1988) Pervasive hydrothermal alteration in tin-bearing granites and implications for the evolution of ore-bearing magmatic fluids. Can Inst Min Metall Spec Vol 39:86–95

The Open University (ed) (1980) Crustal and mantle processes Dalradian case study. Open Univ Press, London, pp 74

Thisse, Y Guennoc P, Pouit G, Nawab Z (1983) The Red Sea: A natural geodynamic and metallogenic laboratory. Episodes 3:3–9

Turner F J, Verhoogen J (1960) Igneous and metamorphic petrology. McGraw-Hill, New York, 694 pp

Unrug R (1987) Geodynamic evolution of the Lufillian arc and the Kundelungu aulocogen, Angola, Zambia, and Zaire. In: Matheis G, Schandelmeier H, (eds) Current research in African Earth Sciences. Balkema, Rotterdam, pp 117–120

Unrug R (1988) Mineralisation controls and source of metals in the Lufillian Fold Belt, Shaba (Zaire), Zambia and Angola. Econ Geol 83:1247–1258

Weissberg B G, Browne P R L, Seward T M (1979) Ore metals in active geothermal systems. In: Barnes H L (ed) Geochemistry of hydrothermal ore deposits, 2nd edn. John Wiley & Sons, New York, pp 738–780

Wernicke B (1981) Low-angle normal faults in the Basin and Range Province: nappe tectonics in an extending orogen. Nature (London) 291:645–647

White D E, Muffler L J P, Truesdell A H (1971) Vapor-dominated hydrothermal systems compared with hot water systems. Econ Geol 66:75–97

Williams H, McBirney, A R (1979) Volcanology. Freeman, Cooper & Co San Francisco, 397pp

Wright J, Haydon R C, McConachy G W (1987) Sedimentary model for the giant Broken Hill Pb-Zn deposit, Australia. Geology, 15: 598–602

Chapter 4
Hydrothermal Alteration

4.1 Introduction

Hydrothermal alteration is a very complex process involving mineralogical, chemical and textural changes, resulting from the interaction of hot aqueous fluids with the rocks through which they pass, under evolving physico-chemical conditions. Alteration can take place under magmatic subsolidus conditions by the action and infiltration of supercritical fluids into a rock mass. At lower temperature and pressure, exsolution of gas and aqueous phases constitute hydrothermal solutions which act on the surrounding rocks, producing changes as the result of disequilibrium, largely due to H^+ and OH^- and other volatile constituents (e.g. B, CO_2, F).

In essence, hydrothermal fluids chemically attack the mineral constituents of the wall rocks, which tend to re-equilibrate by forming new mineral assemblages that are in equilibrium with the new conditions. The process is a form of metasomatism, i.e. exchange of chemical components between the fluids and the wall rocks. Therefore, it is also possible that the fluids themselves may change their composition as a result of their interaction with the wall rocks. The main factors controlling alteration processes are: (1) the nature of wall rocks; (2) composition of the fluids; (3) concentration, activity and chemical potential of the fluid components, such as H^+, CO_2, O_2, K^+, S_2 etc. the so-called operators of Rose and Burt (1979). Henley and Ellis (1983) believe that alteration products in epithermal systems do not depend so much on wall rock composition as on permeability, temperature and fluid composition. They cite, for example, that in the temperature range of 250–280°C, similar mineral assemblages (e.g. quartz-albite-K-feldspar-epidote-illite-calcite-pyrite) are formed in basalts, sandstone, rhyolite and andesite. Other workers, however, emphasise the fundamental role played by the nature and composition of wall rocks in hydrothermal alteration processes, particularly in porphyry systems.

The action of hydrothermal fluids on wall rocks is by infiltration and/or diffusion of chemical species (Rose and Burt 1979). Hydrothermal circulation and the related alteration generally involve large quantities of fluids that pass through a given volume of rocks, which therefore must have considerable permeability in the form of fractures, or connected pore spaces. Small quantities of fluids have lesser, or even negligible effects, as exemplified by metamorphic hydrothermal systems in which the amount of fluids in relation to the rock, i.e. the water/rock ratio (w/r), is small, and the resulting mineral deposits have small or negligible wall rock alteration (Chap. 15). Thus the interaction between H_2O and rocks, and the

intensity of alteration is, inter alia, a function of the water/rock ratio (w/r). This ratio is an important parameter because it affects the degree of exchange with the wall rocks. In hydrothermal systems, w/r ratios may range from 0.1 to 4, with a lower limit obtained when all free water is absorbed as hydrous minerals (Henley and Ellis 1983). Exchange of oxygen isotopes during water/rock interaction permits one to calculate the w/r ratios (see Chap. 2), as discussed by Taylor (1974) for various granitic rocks, in which meteoric waters circulated through a very large volume of rocks. Within this volume the w/r ratio is calculated at between 0.1 to 3.0. Henley and Ellis (1983) report values of 0.7 to 2.0 w/r for the New Zealand geothermal fields.

4.2 Hydrogen Ion Metasomatism and Base Exchange

Hydrolysis and hydration were introduced in Chapter 1. Here, these terms are defined in the context of hydrothermal alteration processes. Hydrolysis, or hydrogen ion metasomatism, is a very important phenomenon involving the ionic decomposition of H_2O into H^+ and OH^-. In hydrothermal alteration, H^+ (or OH^-) is consumed during reaction with the silicate minerals, so that the ratio H^+/OH^- changes. The source of H^+ ions can be subsolidus reactions during alkali metasomatism (see later), water, or acids in the hydrothermal solution. The conversion of anhydrous silicates to hydrous ones (e.g. micas or clays) is a reaction which consumes H^+ and releases metal ions into the solution. This in turn affects the pH of the solution and its power to dissolve or to keep cations in solution. This is related to the dissociation of complexes containing H^+, the degree of association of compounds such as NaCl, and consequently the formation of chloride complexes and the solubility of metallic elements (Guilbert and Park 1986). A typical example of hydrogen ion metasomatism, or hydrolytic decomposition of feldspar, is given by:

$$1.5KAlSi_3O_8 + H_2O = 0.5KAl_3Si_3O_{10}(OH)_2 + K^+ + 3SiO_2 + OH^-;$$
K-feldspar   K-mica   quartz

$$H^+ + OH^- = H_2O.$$
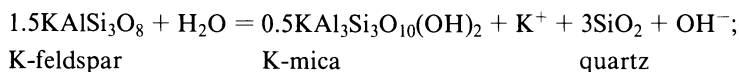
The sum of the first and second reactions gives:

$$1.5KAlSi_3O_8 + H^+ = 0.5KAl_3Si_3O_{10}(OH)_2 + K^+ + 3SiO_2.$$
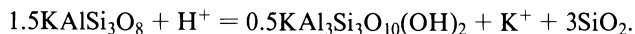
It can be seen from this reaction that K^+ is released and H^+ is consumed. Hydration, the transfer of molecular water from the solution to a mineral, often accompanies hydrolysis. A typical example is the conversion of olivine to serpentine, according to:

$$2Mg_2SiO_4 + H_2O + 2H^+ = Mg_3Si_2O_5(OH)_4 + Mg^{2+}.$$
olivine   serpentine
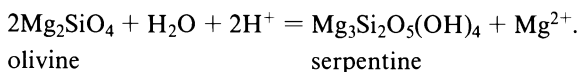
Reactions where a cation is replaced by another in a mineral are called base exchanges, as for example in the conversion of microcline to albite, Na replaces K, which goes into solution:

$KAlSi_3O_8 + Na^+ = NaAlSi_3O_8 + K^+$.
microcline   albite
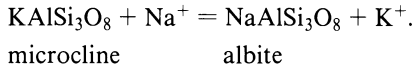
In summary, hydrogen ion metasomatism, hydration and base exchange control the stability of silicate minerals, the pH of the solution, and the transfer of cations into the solution. They are responsible for propylitic, argillic, sericitic or phyllic, and potassic mineral assemblages, which are so typical of hydrothermal mineral deposits. Areas of intense hydrolitic decomposition, or hydrogen ion metasomatism, of silicates, are usually surrounded by propylitic alteration in which hydration phenomena (addition of water and CO_2) are dominant.

4.2.1 Chemical Processes Related to Hydrogen Ion Metasomatism

In this section, hydrogen ion metasomatism and base exchange reactions are considered for: (1) rocks with dominant feldspars; (2) rocks of mafic composition; and (3) Ca-rich rocks and carbonates.

Reactions in Feldspars and K-Mica

Feldspar reactions that occur during hydrogen ion metasomatism are detailed by Hemley and Jones (1964) in their experimental studies with aqueous chloride solutions. Reactions experimentally determined for K- and Na-bearing systems by Hemley and Jones (1964) are considered below:

a) K_2O-Al_2O_3-SiO_2-H_2O system:

The formation of sericite, for example, can be expressed by the following:

$3KAlSi_3O_8 + 2H^+ = KAl_3Si_3O_{10}(OH)_2 + 2K^+ + 6SiO_2$.
microcline   K-mica   quartz

$0.75Na_2CaAl_4Si_8O_{24} + 2H^+ + K^+ = KAl_3Si_3O_{10}(OH)_2 +$
andesine   sericite
                        $+ 1.5Na^+ + 0.75Ca^{2+} + 3SiO_2$.

Other reactions are:

$KAl_3Si_3O_{10}(OH)_2 + H^+ + 1.5H_2O = 1.5Al_2Si_2O_5(OH)_4 + K^+$;
K-mica   kaolinite
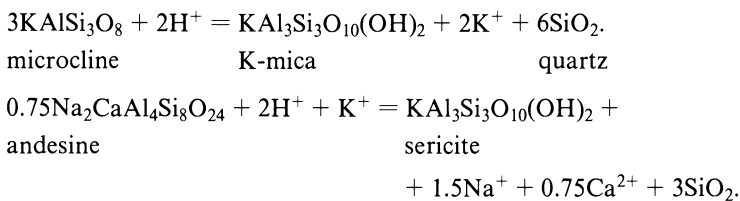
$KAl_3Si_3O_{10}(OH)_2 + H^+ + 3SiO_2 = 1.5Al_2Si_4O_{10}(OH)_2 + K^+$.
K-mica   pyrophyllite
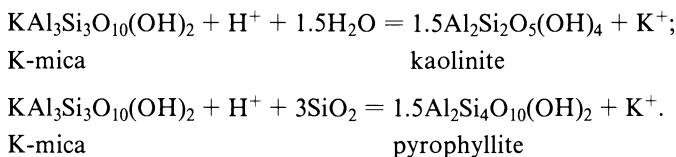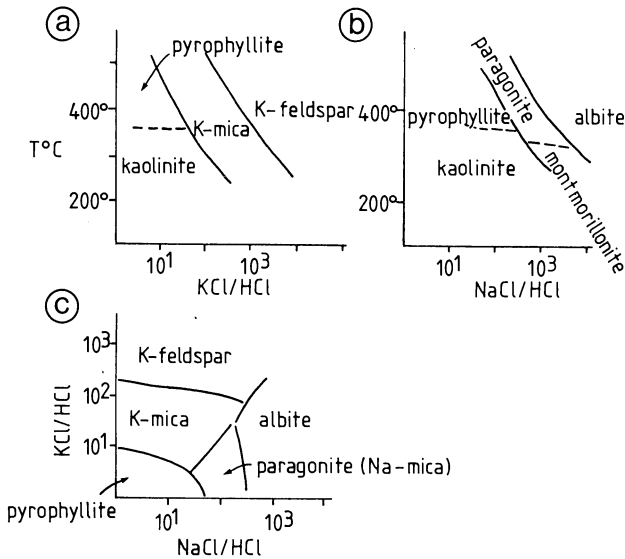
Fig. 4.1. Equilibrium curves experimentally determined in chloride solutions by Meyer and Hemley (1967) for **a** K_2O-Al_2O_3-SiO_2-H_2O system; and **b** Na_2O-Al_2O_3-SiO_2-H_2O system; as a function of temperature. Quartz present and pressure at 1000 bar. **c** K_2O-Na_2O-Al_2O_3-SiO_2-H_2O system at 400° C and 1000 bar total pressure; quartz present (After Meyer and Hemley 1967)

Experimental equilibrium curves for the system considered are shown in Fig. 4.1a. It can be seen that the development of kaolinite is favoured by low temperature and low cation/H^+ ratios.

b) Na_2O-Al_2O_3-SiO_2-H_2O system:

$$1.5NaAlSi_3O_8 + H^+ = 0.5NaAl_3Si_3O_{10}(OH)_2 + 3SiO_2 + Na^+;$$
albite   paragonite

$$NaAl_3Si_3O_{10}(OH)_2 + H^+ + 3SiO_2 = 1.5Al_2Si_4O_{10}(OH)_2 + Na^+;$$
paragonite   quartz   pyrophyllite

$$1.17NaAlSi_3O_8 + H^+ = 0.5Na_{.33}Al_{2.33}Si_{3.67}O_{10}(OH)_2 + 1.67SiO_2 + Na^+;$$
albite   Na-montmorillonite

$$3Na_{.33}Al_{2.33}Si_{3.67}O_{10}(OH)_2 + H^+ + 3.5H_2O = 3.5Al_2Si_2O_5(OH)_4 + 4SiO_2 + Na^+.$$
Na-montmorillonite   kaolinite
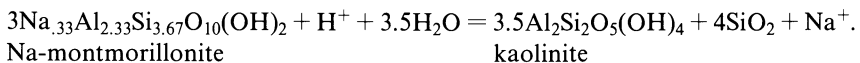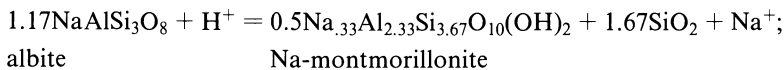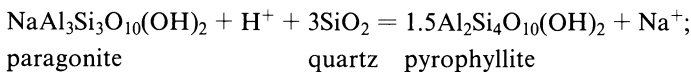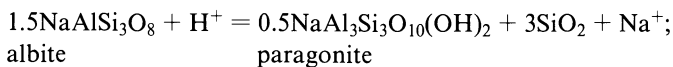
Experimental curves corresponding to the reactions above are shown in Fig. 4.1b. All of these reactions consume H^+ and release cations such as Na^+ and K^+, as well as other metallic elements that may substitute for them in the lattices of the altering silicates. These reactions are sensitive to pressure and temperature changes and the ratios of the components' activities, as shown in the diagrams of Fig 4.1a, b. The combined system illustrating mineral stability relations in the system K_2O-Na_2O-Al_2O_3-SiO_2-H_2O is shown in Fig. 4.1c, in which the boundaries represent both
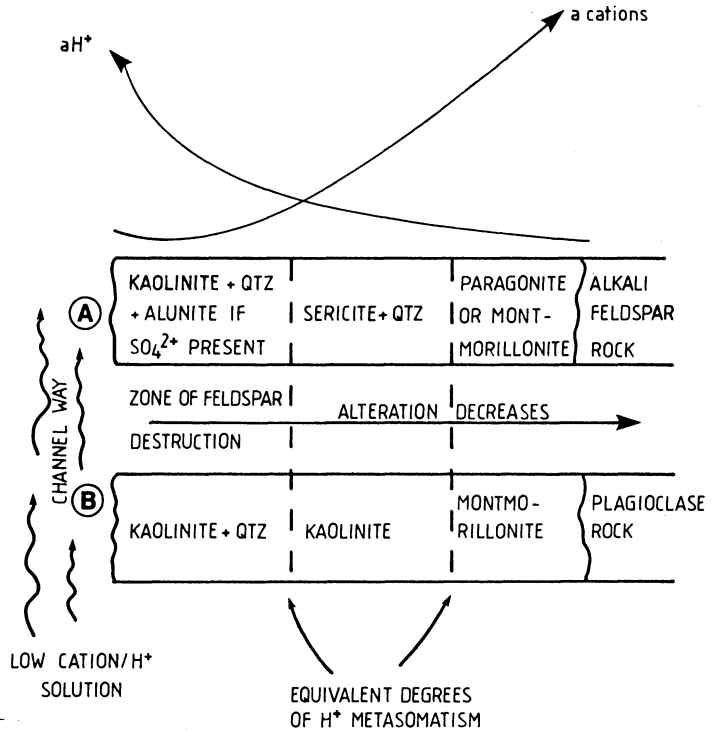
Fig. 4.2A, B. Diagrammatic representation of hydrothermal alteration in rocks containing **A** dominant alkali-feldspar and **B** dominant calcic plagioclase (After Hemley and Jones 1964)

hydrogen ion metasomatism and base exchange reactions, as exemplified by the albite-muscovite boundary, where:

$$3NaAlSi_3O_8 + 2H^+ + K^+ = KAl_3Si_3O_{10}(OH)_2 + 6SiO_2 + 3Na^+.$$
albite   muscovite
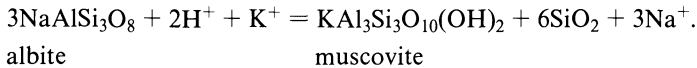
The patterns of alteration of rocks containing dominant feldspars plus quartz are shown in Fig. 4.2. The silica derived by the hydrogen metasomatism of silicates does not crystallise at the site of alteration, but diffuses towards the channelways, while parts of it may remain in the zone of sericite development.

c) K_2O-Al_2O_3-SiO_2-H_2O-SO_3 system:

Hemley and Jones' work does not include systems containing sulphur. In these, oxidation of H_2S leads to the formation of sulphuric acid (H_2SO_4), which is a powerful leaching agent particularly active in the lower temperature regimes of volcanic and subvolcanic environments, as outlined in Chapter 3. Acid leaching is responsible for argillic alteration commonly seen in epithermal mineral deposits and many porphyry systems. Hemley et al. (1969) experimentally studied the above five-component system, involving the stability relations of K-feldspar, muscovite,
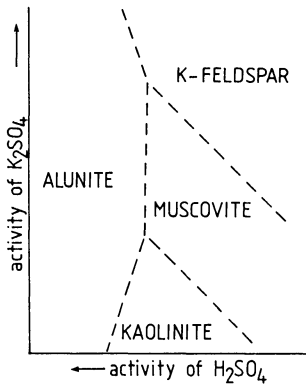
Fig. 4.3. Stability relations of alunite, kaolinite, muscovite and K-feldspar as a function of the activities of K_2SO_4 and H_2SO_4 (After Hemley et al. 1969)

kaolinite and alunite as a function of H_2SO_4 and K_2SO_4 activities. Alunite is a key mineral in the system considered, being an important and common component found in sulphur-rich epithermal gold-silver deposits. Alunite is therefore commonly found associated with hot springs, mud pools and fumaroles in volcanic terranes, where it forms veins, lenticular bodies and masses of rocks almost entirely replaced by it. Spectacular examples of alunite formation can be seen in the Phlegrean fields near Naples and at La Tolfa north of Rome (Italy). Alunite is generally associated with opal, kaolinite, dickite, sericite, pyrophyllite and diaspore. Because of the intense leaching associated with the presence of alunite, a leached zone may be present that is typically porous and siliceous. This silica, however, is residual and should not be confused with sinter material (see Sect. 3.4.2). Reactions relating to Hemley et al.'s experimental work are:

$$KAl_3Si_3O_{10}(OH)_2 + 4H^+ + 2SO_4^{2-} = KAl_3(SO_4)_2(OH)_6 + 3SiO_2;$$
K-mica   alunite

$$3Al_2Si_2O_5(OH)_4 + 2K^+ + 6H^+ + 4SO_4^{2-} = 2KAl_3(SO_4)_2(OH)_6 + 6SiO_2 + 3H_2O;$$
kaolinite   alunite

$$2KAl_3Si_3O_{10}(OH)_2 + 2H^+ + 3H_2O = 3Al_2Si_2O_5(OH)_4 + 2K^+.$$
K-mica   kaolinite
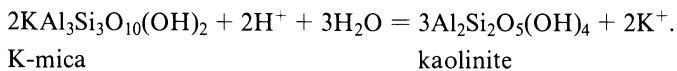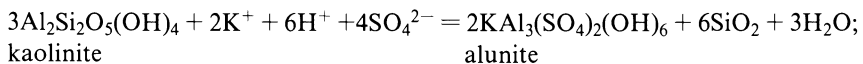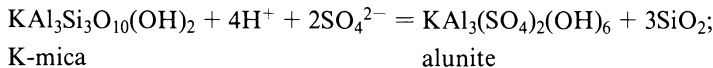
The stability relationships for the above reactions are shown in Fig. 4.3. It can be seen that the K-feldspar-muscovite-alunite invariant point is attained at very high K values, and therefore only rarely occurring in natural systems (Hemley et al. 1969). Alunite is in fact typically found in rocks that have already been subjected to extensive hydrogen ion metasomatism, in which feldspar destruction is followed by the formation of K-mica, clay minerals and pyrophyllite. The reaction involving K-feldspar is:

$$3KAlSi_3O_8 + 6H^+ + 2SO_4^{2-} = KAl_3(SO_4)_2(OH)_6 + 2K^+ + 9SiO_2.$$

Reactions in Fe-Mg Silicates and Alumino-Silicates

Hydrothermal activity in sub-sea-floor environments involves the penetration of sea water through fractures in the oceanic crust. This water becomes heated (Chap. 3), performing a series of reactions (to be examined below) involving mostly hydrogen metasomatism, which causes the fluids to become progressively reduced and enriched in metals removed from the rocks. These metals pass into the solution generally as chloride complexes. The permeability of the oceanic crust facilitates penetration of the sea water over vast areas, so that apart from the actual mineralising system low intensity reactions (especially hydration) result in prograde "ocean floor metamorphism" (Spooner and Fyfe 1973), ranging from zeolite to greenschist facies assemblages containing chlorite, smectite, actinolite, serpentine etc. Within this zone of metamorphism is superimposed the hydrothermal alteration sensu stricto, or " geothermal system metamorphism", of Spooner and Fyfe, which is part and parcel of the mineralisation. The metalliferous solutions are then discharged on the sea floor by hot springs through fractures and vents. In this way disseminated and massive sulphide bodies are formed within the fractured oceanic crust rocks, where one set of reactions occurs, and at, or close to, the sea water-rock interface where another set of reactions take place, depositing in addition to sulphides, Fe and Mn oxides in response to contact of the hydrothermal fluids with cold and oxygenated sea water. In the case of a brine pool, such as those of the Red Sea (Sect. 3.6) precipitation of sulphides dominates, partly because of oxygen deficiency in the sea-floor depression (Bonatti 1978), and partly because of density contrast between the sulphide-bearing brines and sea water (Chap. 12).

A scheme of hydrothermal reactions in a sub-sea-floor environment and their products is illustrated in Fig. 4.4, taken from an excellent article in Scientific American by Edmond and von Damm (1983). In this figure, sea water containing the ions indicated at point 1, penetrates the oceanic crust to form sulphate ($CaSO_4$, point 2). At point 3, several kilometres under the sea floor, reactions occur with the hot mafic rocks. These involve addition of Mg to the mafic rocks, and hydration to form serpentine minerals. In the course of these reactions H^+ is produced, and hydrogen ion metasomatism of the basaltic rocks now takes place, in which H^+ displaces the cations (Fe^{2+}, Mn^{2+}, Cu^{2+}, Zn^{2+} etc.) from the Fe-Mg and alumino-silicate rock-forming minerals, which consequently change to chlorite, clay-type minerals and zeolites. The sea water, in the scheme of Edmond and von Damm, is initially an oxygenated electrolyte solution containing the anions Cl^-, Br^-, CO_3^{2-}, SO_4^{2-} etc. During descent, this water becomes more and more reduced and reacts with the rock-forming silicates. A typical reaction is:

$$11Fe_2SiO_4 + 2SO_4^{2-} + 4H^+ = 7Fe_3O_4 + FeS_2 + 11SiO_2 + 2H_2O;$$
fayalite   magnetite   pyrite

$$2Fe_2SiO_4 + 3H_2O = Fe_3Si_2O_6(OH)_4 + Fe^{2+} + OH^- + H^+.$$
serpentine or talc
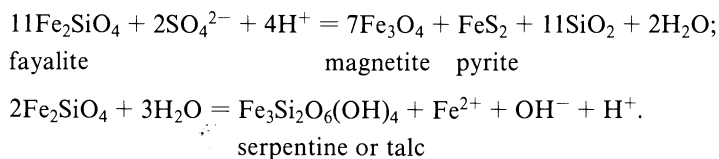
Other reactions between H^+ ions, SO_4^{2-} ions and Fe-silicates produce pyrite and magnetite (point 4), and a solution is subsequently developed that is hot, acidic and
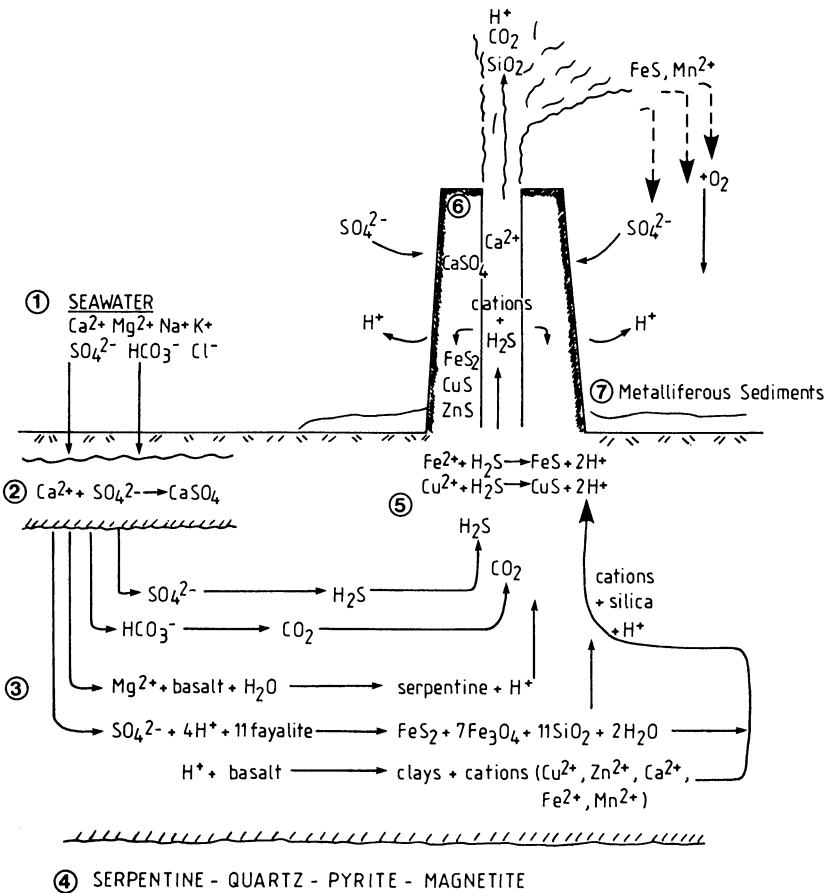
Fig. 4.4. Hydrothermal reactions at a spreading centre. See text for detailed explanation (After Edmond and von Damm 1983)

contains metals (point 5). The solution thus formed rises towards the sea floor where it encounters cold and oxigenated sea water, and precipitation of sulphides and sulphates occurs with the formation of the so-called chimneys (point 7). Some of the Fe-sulphide is carried upwards as a "black smoke", whereas Mn^{2+} and more Fe^{2+} remain in solution to become oxidised and to precipitate laterally away from the smoker's vent, eventually forming a metalliferous sediment. This topic is discussed further in Chapter 12.

Reactions in Ca-Rich Environments

Hydrogen ion metasomatism of carbonate rocks may be expressed by the reaction:

$$CaCO_3 + 2H^+ = Ca^{2+} + CO_2 + H_2O.$$
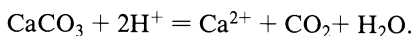
In the presence of silica:

$$2CaCO_3 + SiO_2 + 4H^+ = 2Ca^{2+} + 2CO_2 + SiO_2 + 2H_2O.$$

In systems where CO_2 is present, carbonic acid is formed (H_2CO_3), and its dissociation hydrolyses silicates, forming clays (kaolinite) and liberating silica and metal ions (e.g. Na^+, K^+, Ca^{2+} etc).

We return to the issue of hydrothermal alteration of carbonate rocks in Chapter 10, and later in this chapter when discussing silication.

4.3 Styles and Types of Hydrothermal Alteration

The terminology introduced in this section is frequently used in virtually all aspects of studies on hydrothermal mineral deposits, and is therefore encountered time and again in all subsequent chapters. The terms used to describe and classify hydrothermal alteration can be expressed in the function of: (1) recognised mineral assemblage(s) and (2) chemical changes. In the former, the recognition of mineral assemblages, here intended as an observed specific and characteristic mineral association in the sense of Meyer and Hemley (1967), is primarily carried out through extensive thin-section studies. This leads to a listing of minerals in order of abundance, as advocated by Rose and Burt (1979), or by a general descriptive term reflecting the dominant mineralogy (assemblages), such as argillic, potassic, sericitic etc. Chemical changes indicating the type of chemistry of the fluids involved in the alteration process would include hydrogen ion metasomatism, alkali metasomatism, fluorine and boron metasomatism etc. In addition to the above, the style of alteration takes into account the intensity, form and character of the phenomenon. Here the terminology becomes a little confusing because of its inherent subjectivity. Terms, such as weak, moderate, strong, extensive, pervasive, non-pervasive, are well known and frequently used. These terms essentially refer to the state of preservation of the original rock, how far the alteration process has advanced, both at the single mineral scale and at the regional scale, the overall geometry of the alteration halo and so forth. An empirical and semiquantitative approach is recommended by Guilbert and Park (1986), who propose the use of symbols to characterise the type of alteration. These symbols are listed in Table 4.1 and discussed below.

Table 4.1. Characterisation of alteration types by use of symbols. After Guilbert and Park (1985)

Alteration type	Symbol	Alteration type	Symbol
Greisen	G	Phyllic	S
Potassic	K	Argillic	A
Propylitic	P	Advanced argillic	AA
Silicification	Q	Skarn	SK

Selective pervasiveness and pervasiveness (defined below) would be indicated on scales from 1 to 10, so that pervasiveness 1 would mean that alteration is confined to a veinlet or a thin fracture, whereas 10 would indicate that the entire rock is permeated by the alteration effects. For example, a notation like S-10-4 means a rock in which the minerals susceptible to sericitisation are all affected in about 40% of the rock volume. Another empirical method is that used by Moore and Nash (1974), who determined the sericitic alteration of plagioclases by giving ranks from 1 to 5 for unaltered to completely altered respectively.

It is by now accepted practice that a combination of all or part of the above is normally used in studies of alteration, with emphasis being given to one or the other in accordance with the investigator's methodology, approach and type of research. The terminology and definitions given below in terms of styles and types of hydrothermal alteration are adopted throughout this book.

4.3.1 Styles of Alteration

The main styles of alteration are "pervasive", "selectively pervasive" and "non-pervasive". Pervasive alteration is characterised by the replacement of most, or all, original rock-forming minerals. This results in the partial or total obliteration of the original textures. Selectively pervasive alteration refers to the replacement of specific original minerals, e.g. chlorite replacing biotite, or sericite replacing plagioclase. In this case the original textures are preserved. Non-pervasive alteration means that only certain portions of the rock volume have been affected by the altering fluids. Clearly, then, selectively pervasive alteration falls in this category, as well as fracture or veinlet-controlled alteration. In the latter, as the name implies, the alteration minerals are confined to within a certain distance from a vein or a fracture. The alteration style around the controlling vein or fracture can be pervasive or selectively pervasive. Examples of these styles are shown in Plates 4.9 and 4.10. The "intensity" of alteration, though perhaps a little more subjective, is generally used as a convenient field term, and it can be said to be weak, moderate or strong. Intensity refers to the state of replacement of the mineral phases in a rock, and to the state of textural destruction of the rock in question. Weak, or low, intensity would mean that only a few of the original minerals have been replaced with little or no modification of the original textures (Siems 1984).

4.3.2 Types of Alteration

In this section we follow a discussion on types of alteration essentially based on those recognised and reported by Meyer and Hemley (1967) and Rose and Burt (1979). We are not concerned at this stage with the alteration types and patterns of specific hydrothermal deposits, as these are dealt with in later chapters. Here we examine in a generalised way, types of alteration resulting from the interaction of hydrothermal solutions with wall rocks as revealed and understood from a great variety of hydrothermal ore deposits, and therefore each type discussed
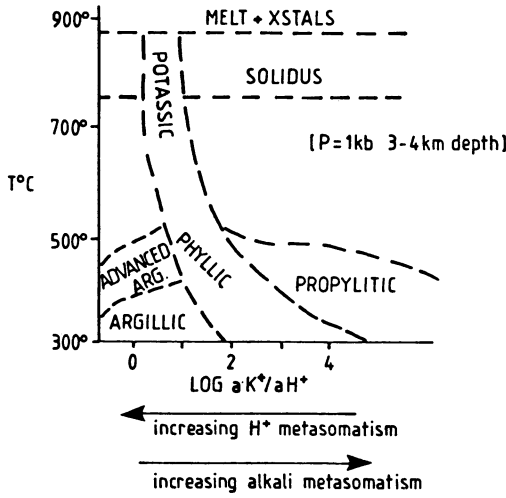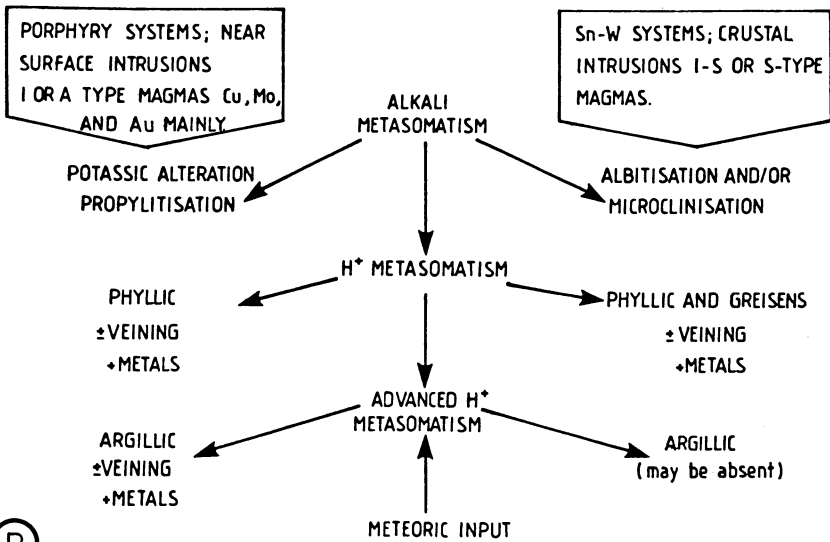
Fig. 4.5A, B. Scheme of idealised evolutionary alteration sequence. A Illustrates types of alteration as a function of temperature, K^+ and H^+ activities (After Guilbert and Park 1985; Burnham and Ohmoto 1980). B Alkali metasomatism liberates H^+, resulting in decreasing alkali/H^+ ratios, and subsequent destabilisation of feldspars and micas, with growth of new mineral phases (greisen and phyllic stages). Advanced H^+ metasomatism is due to meteoric water input into the system, with oxidation and further H^+. Acid leaching and argillic alteration result from this stage

may be applicable only if the proper setting and related deposit type are considered.

    To begin, it is important to reiterate that hydrothermal alteration involves a series of metasomatic processes and base exchange reactions in which the alkali and

H^+ metasomatism is of particular importance, especially in igneous-related hydrothermal systems. Most hydrothermal processes can in fact be related to the activities of alkalies and hydrogen. The connection between a hydrothermal solution and a parent igneous body was introduced in Chapter 3. Here we are mainly concerned with the effects produced on the wall rocks by the chemical changes in a hydrothermal solution as a result of variations in the a_K^+/a_H^+ ratio; i.e. the activities of the K^+ and H^+ ions in the system. This ratio decreases as the system evolves towards lower temperatures and pressures. In other words, with increasing H^+ metasomatism alteration processes would move from alkalic to argillic in a theoretical continuous evolving system. This concept is schematically shown in Fig. 4.5A, B. Consequently, the types of alteration discussed will be in order of decreasing a_K^+/a_H^+ (increasing H^+ metasomatism), and are: (1) alkali metasomatism and potassium silicate alteration in particular; (2) propylitic; (3) phyllic, or sericitic, alteration and greisenisation; (4) intermediate argillic ; (5) advanced argillic.

Alkali Metasomatism, Potassium Silicate Alteration

The interaction with a residual fluid phase evolving from a nearly consolidated igneous mass results in a series of post-magmatic, or subsolidus, changes both within the igneous body and the surrounding country rocks, if they are fractured (open system). These are early high temperature fluids in the range of about 800–600°C, which are derived from a melt in its late stages of crystallisation, and they result in the subsolidus growth of new minerals and exchange reactions. Subsolidus processes include: (1) base exchange reactions in feldspars, specifically Na for K, or, K for Na; (2) changes in the structural state of feldspars; (3) albitisation; (4) microclinisation; (5) growth of tri-octahedral micas. In anorogenic tectonic settings mineralogical changes may include a series of Na-rich amphiboles and F- or B-rich assemblages. We return to this aspect of alkali metasomatism in Chapter 8. Here it will suffice to say that alkaline and highly saline fluids develop during the final stages of consolidation of an igneous mass, resulting in widespread potassic or sodic alteration. Characteristically, alkali metasomatism involves replacement of feldspars and quartz by K-feldspars (microclinisation) or albite (albitisation). These features can be easily identified under the microscope, for example by the presence of relict cores of plagioclases surrounded by K-feldspar, or by criss-crossing thin veinlets of K-feldspar in plagioclase. In the case of albitisation, chess board albite in K-feldspars, intergranular albite at grain boundaries, albite veinlets, etc. are all common. Albitisation of feldspar may in some cases be accompanied by muscovitisation of biotites.

   Potassic alteration is especially common and important in porphyry and epithermal mineralising systems, where it occurs in the high temperature core zones. The minerals characteristic of this alteration are K-feldspar and biotite in porphyries, and adularia in epithermal systems. Potassic alteration is usually accompanied by sulphides (chalcopyrite, pyrite, molybdenite). Anhydrite is a common associated mineral in porphyry environments. Biotite is often green in colour and Fe-rich. Potassium silicate alteration is formed as a replacement of

Plate 4.1. Aspects of hydrothermal alteration exhibited by core specimens of quartz-porphyry rock from the Haib Cu-Mo deposit in southern Namibia. *Top row* shows mainly potassic alteration; reddish-brown spots in specimen on *left* are K-feldspars; specimen in centre has mainly hydrothermal biotite; specimen on *right* has potassic alteration overprinted by later sericitic alteration. *Bottom row* mainly sericitic alteration; specimens on the *left* display potassic alteration (note reddish-brown spots) overprinted by quartz-sericite alteration; light-coloured specimen in *centre* displays pervasive quartz-sericite-pyrite alteration; specimen on *right* displays intense silicification (note patches of bluish opaline quartz)

plagioclase and mafic silicate minerals, at temperatures in the region of 600–450°C. Common assemblages are K-feldspar-biotite-quartz, K-feldspar-chlorite, K-feldspar-biotite-magnetite, accompanied by varying quantities of other minerals such as albite, sericite, anhydrite, apatite, and also occasionally rutile, derived from the breakdown of biotite. The K-feldspars of the potassic zones are characteristically reddish in colour due to minute hematite inclusions. Plates 4.1 and 4.2 illustrate examples of potassic alteration. Figure 4.6a summarises the potassic mineral association on ternary ACF-AKF published by Meyer and Hemley (1967).
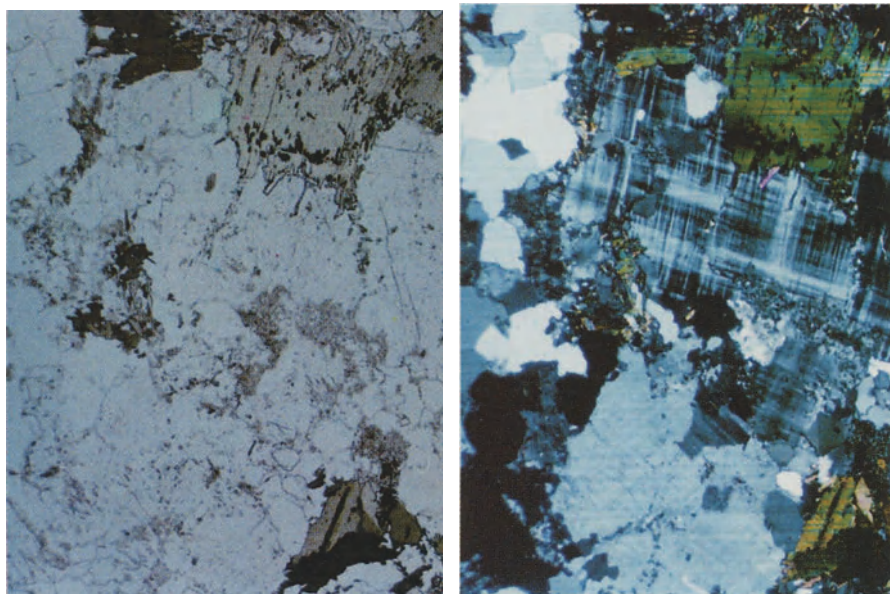
Plate 4.2. Photomicrographs (plane polarised light on *left* and crossed nicols on *right*), showing hydrothermal biotites (*coloured*) and microcline feldspars. Both these minerals are the products of potassic metasomatism and alteration of a quartz-porhyry rock (Haib Cu-Mo deposit, southern Namibia). Width of field is 2 mm

Propylitic Alteration

Propylite is an old term used to describe altered volcanic rocks. Propylitic alteration is characterised by the addition of H_2O and CO_2, and locally S, with no appreciable H^+ metasomatism. Typical minerals are epidote, chlorite, carbonates, albite, K-feldspar and pyrite. In places sericite, Fe-oxides, montomorillonite and zeolite may also be common. The well-defined pressure and temperature stability fields of zeolite mineral species make them important monitors of temperature and depth. This feature is particularly useful in epithermal systems, as it enables the exploration geologist to monitor the proximity to the heat source and boiling zone where higher grades of gold mineralisation may be found. We return to this topic in Chapter 11. In some situations, there can be intense albitisation, chloritisation or carbonitisation, which Meyer and Hemley (1967) prefer to consider separately, reserving propylitisation for weaker H^+ metasomatic effects. Propylitic alteration tends to be more pervasive towards the inner zones of a hydrothermal deposit, or, in other words, towards the heat/hydrothermal source. Outward propylite alteration grades into unaltered rocks, or, where metamorphism is present, into greenschist facies rocks with which propylitic assemblages are equivalent. Figure 4.6b summarises the propylitic mineral assemblages on the ACF-AKF diagrams of Meyer and Hemley. Plates 4.3 and 4.4 illustrate examples of propylitic alteration.
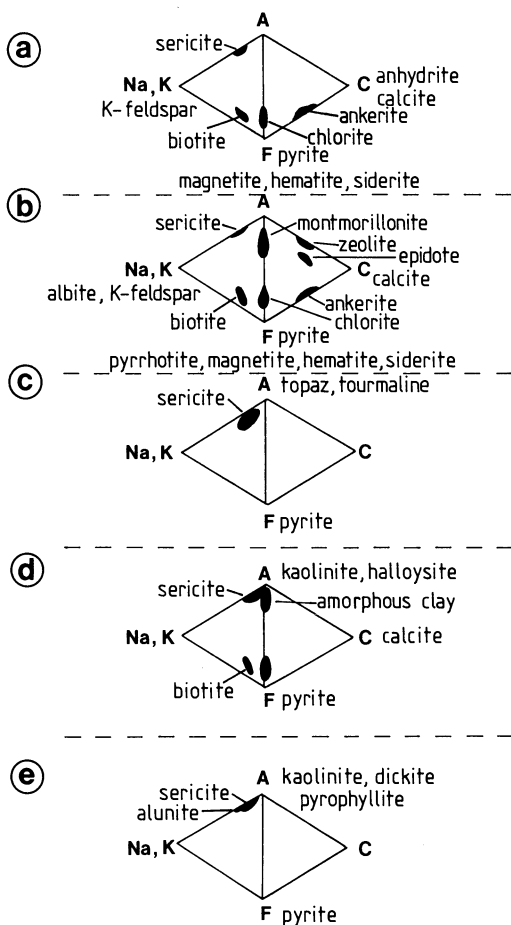
Fig. 4.6a–e. *ACF* (Al$_2$O$_3$-CaO-FeO) *AKF* (Al$_2$O$_3$-Na$_2$O+K$_2$O-FeO) diagrams showing alteration types and related dominant mineral assemblages. **a** Potassium silicate; **b** propylitic; **c** phyllic or sericitic; **d** intermediate argillic; **e** advanced argillic (After Meyer and Hemley 1967)

Phyllic (Sericitic) Alteration and Greisenisation

Phyllic, or sericitic, alteration is typified by the assemblage quartz-sericite-pyrite (QSP). Mineral phases usually associated with QSP alteration are K-feldspar, kaolinite, calcite, biotite, rutile, anhydrite and apatite. This alteration grades into the potassic type by increasing amounts of K-feldspar and/or biotite, and into the argillic type by increasing amounts of clay minerals. Increasing amounts of topaz, tourmaline, quartz and zunyite herald a transition to greisen-type alteration. QSP alteration is one of the most common types of hydrothermal alteration, as it is present in almost all hydrothermal mineral deposits, from Archean volcanogenic massive sulphides and gold quartz lodes to recent epithermal systems. Sericite refers to fine-grained dioctahedral white micas (muscovite, paragonite, phengite, fuchsite, roscoelite). Although sericites are not markedly different from muscovites, they are reported to contain higher SiO$_2$, MgO and H$_2$O, and lower K$_2$O (Deer et al. 1967). Under the microscope sericite may be confused with pyrophyllite, or even phlogopite, and X-ray or microprobe analyses may be necessary to make positive
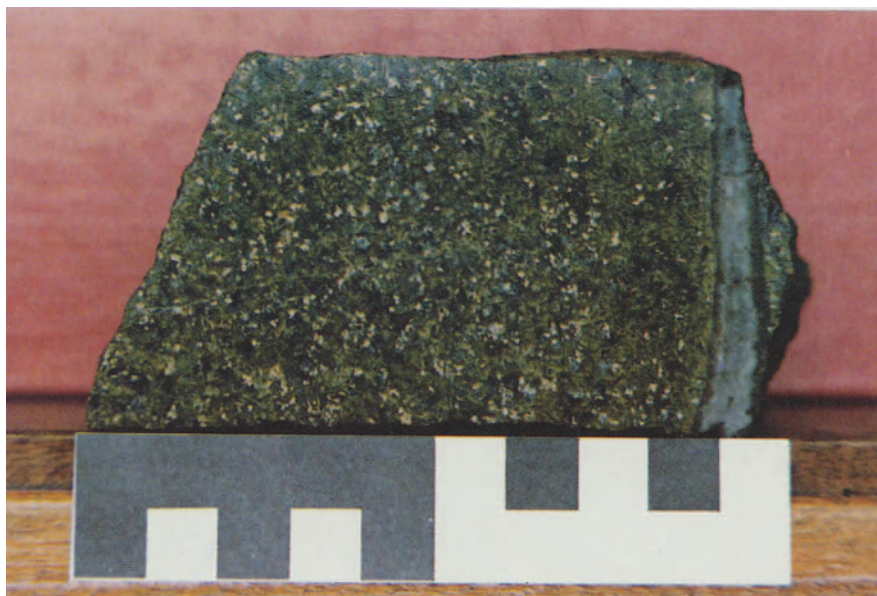
Plate 4.3. Pervasively propylitised sample of feldspar-porphyry rock from the Haib Cu-Mo deposit in Namibia. The *green colour* is due to the presence of chlorite and epidote. Scale bar is in cm
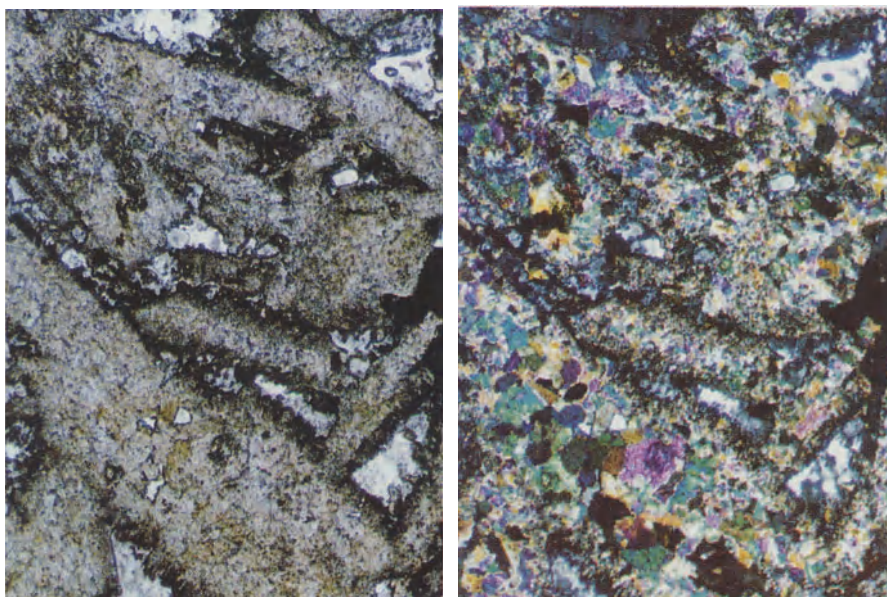
Plate 4.4. Photomicrographs of thin section from specimen shown in Plate 4.3 (*left* is in plane polarised light, *right* is at crossed nicols). Plagioclase phenocrysts are pervasively replaced by an aggregate of chlorite, epidote and quartz. Width of field is 2 mm

Fig. 4.7. Scheme of quartz-sericite-pyrite (QSP) alteration reactions due to advanced H⁻ metasomatism and breakdown of rock-forming silicates. *Downward arrows* indicate elements added; *upward arrows* indicate element released. Al is assumed immobile (After MacKenzie 1983)
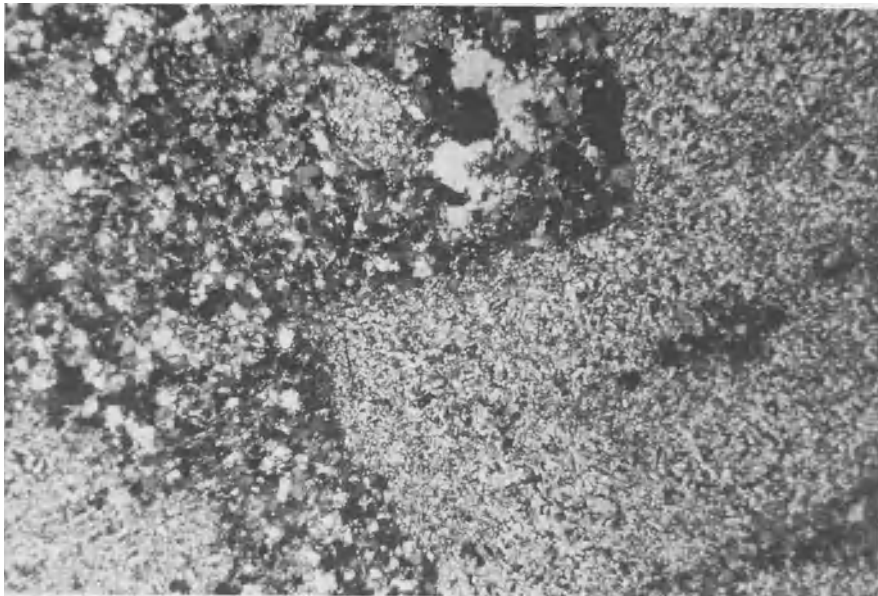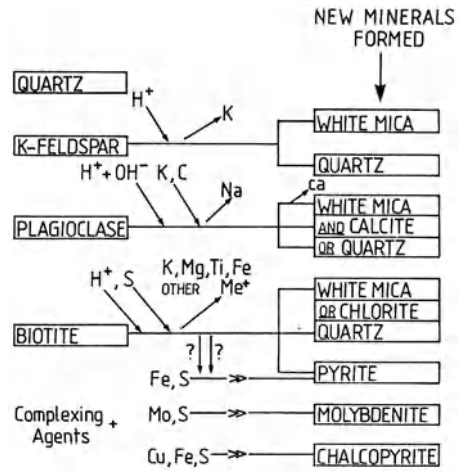
Plate 4.5. Photomicrograph taken at crossed nicols, showing pervasive quartz-sericite alteration of a feldspar porphyry rock. The porphyritic igneous texture is still recognisable. Width of field is 3.5 mm

identification. Hydromuscovites and illites are also associated with this type of alteration; in the former, higher H_2O and K_2O contents are present, whereas the latter is a mica interlayered with clay-type minerals (see Deer et al. 1967). Sericitic alteration is essentially due to the destabilisation of feldspars in the presence of H^+, OH^-, K and S, to form quartz, white mica, pyrite and some chalcopyrite (sulphide
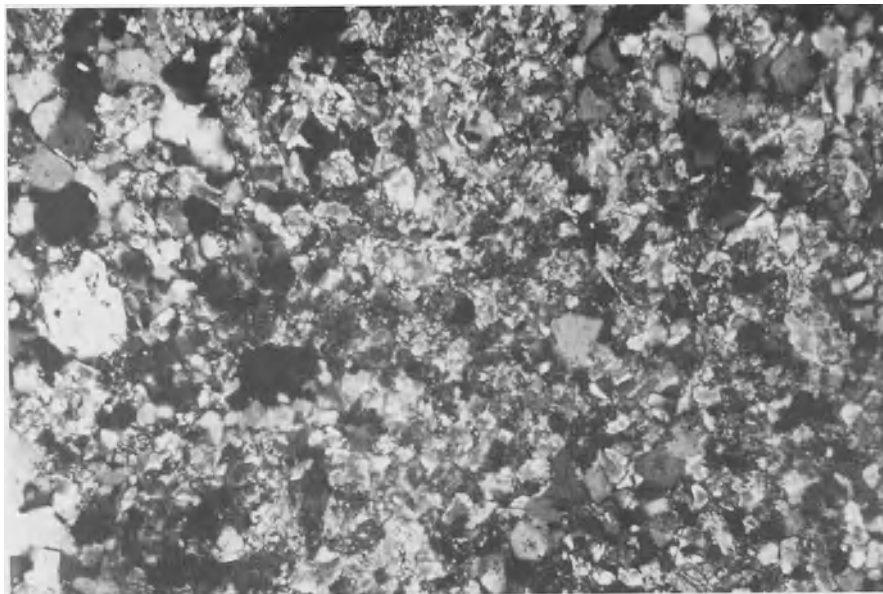
Plate 4.6. Photomicrograph taken at crossed nicols, showing pervasive quartz-sericitic alteration of the same porphyry rock shown in Plate 4.5. Here the original igneous texture is no longer recognisable. Width of field is 0.9 mm

content can be up to 20% by volume). In the process Na, Mg, Ti, Fe and also K are leached out. A scheme of QSP alteration is shown in Fig. 4.7, whilst the mineral assemblages in relation to the ACF-AKF ternary diagram are given in Fig. 4.6c. Examples of sericitic alteration are shown in Plates 4.5 and 4.6.

Greisen, an old Cornish miners' term, refers to a coarse-grained assemblage of quartz-muscovite with varying amounts of topaz, tourmaline, fluorite, oxides (cassiterite, hematite), wolframite, scheelite, and sulphides of Fe, Cu, Mo, Bi, and Cu-Bi-Pb sulphosalts. Although greisen alteration is common in continental porphyry systems, its most favourable environment is a granite stock or sheet emplaced within argillaceous-arenaceous rock sequences, and associated with Sn-W mineralisation. In these situations greisen alteration is usually preceded by Na metasomatism (albitite), during which H$^-$ ions are produced which then initiate the process of greisenisation. This involves the destabilisation and destruction of feldspars and biotites to form the assemblage of quartz + muscovite as shown in Fig. 4.8. The process may be more complicated in mineralised systems, in which there is introduction of B, F, Li. This will result in new series of reactions that may take place to form topaz, tourmaline, and oxide minerals (Plates 4.7 and 4.8). Silicification may accompany greisen alteration during and after, evidenced by the common quartz flooding of the greisen altered rocks. Muscovite preferentially replaces the biotites, and during this process cations locked in the biotite lattice are released into the system, and are possibly responsible for the paragenetically, later associated, metallic mineralisation (Plimer and Kleeman 1986).
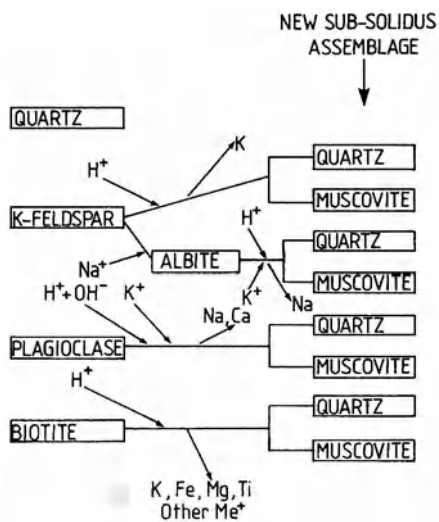
Fig. 4.8. Scheme of greisenisation reactions due to H$^+$ metasomatism with destabilisation of rock-forming silicates. *Downward arrows* indicate elements added; *upward arrows* indicate elements released. Al is assumed immobile (After MacKenzie 1983)
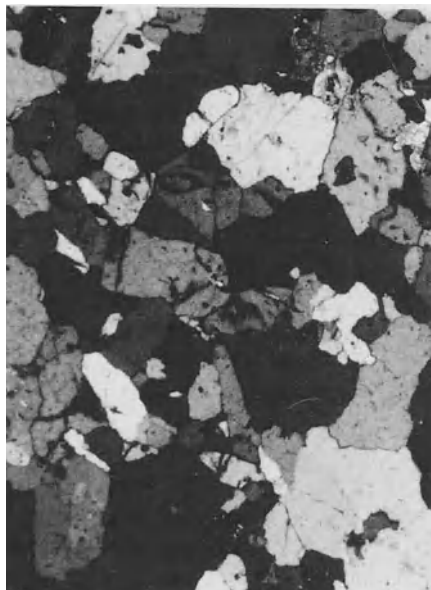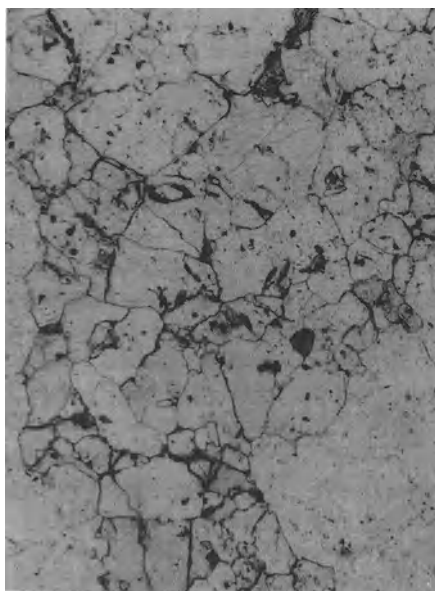
Plate 4.7. Photomicrographs (plane polarised light on *left* and crossed nicols on *right) showing a quartz-topaz greisen assemblage (left* and upper portion of photo is mostly topaz, quartz has lower relief and is on the *lower right*), resulting from the replacement of an original granitic rock (Krantzberg tungsten deposit, Namibia). Width of field is 2 mm

Quartz + muscovite greisens may be followed by progressive stages of F- and/or B-metasomatism, and in the latter case the development of tourmaline may be so extensive that quartz-tourmaline assemblages may dominate altogether. Sub-
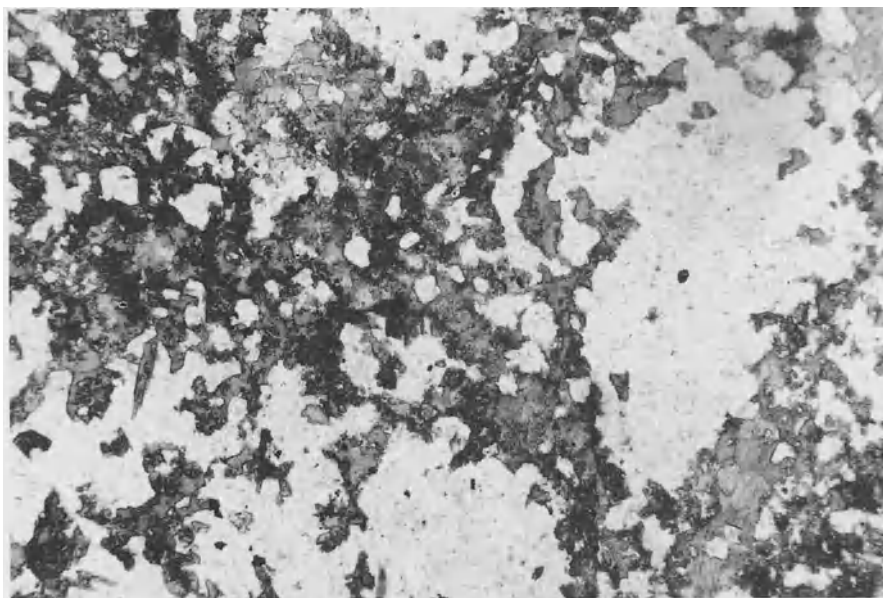
Plate 4.8. Photomicrograph in plane polarised light showing brown pleochroic tourmaline replacing a host granitic rock along grain boundaries and microfractures (Krantzberg tungsten deposit, Namibia). Width of field is 3.5 mm

sequent to greisen alteration, sericitic and argillic types may follow by increased H^+ metasomatic activity.

Argillic Alteration

Argillic alteration is characterised by the formation of clay minerals due to intense H^+ metasomatism (acid leaching), at temperatures of between 100 and 300 °C. This alteration inwardly grades into phyllic zones, whereas outwardly it merges into propylitic ground. This type of alteration is common in porphyry systems, although in older settings like the Haib porphyry Cu-Mo deposit in Namibia (Minnitt 1986) erosion may eliminate evidence of this alteration type. Epithermal environments are typified by extreme acid leaching, and therefore argillic alteration provides a very useful guide to mineralisation. Base leaching of alumino-silicates may result in silica enrichment, so that argillic alteration may in fact grade into zones of silica-rich material. Clay minerals replace principally the plagioclases and the mafic silicates (hornblende, biotite). Amorphous clays such as allophane are also present and replace the alumino-silicate phases. K-feldspar is reported to be a metastable phase. Examples of argillic alteration are shown in Plates 4.9 and 4.10.

Intermediate argillic alteration is defined by the presence of montmorillonite, illite, chlorite, kaolin group clays (kaolinite, dickite, halloysite, hallophane) and minor sericite, while K-feldspar may remain unaltered, and K, Ca, Mg, Na not entirely leached out. Biotite and chlorite may be locally important. Zoning within
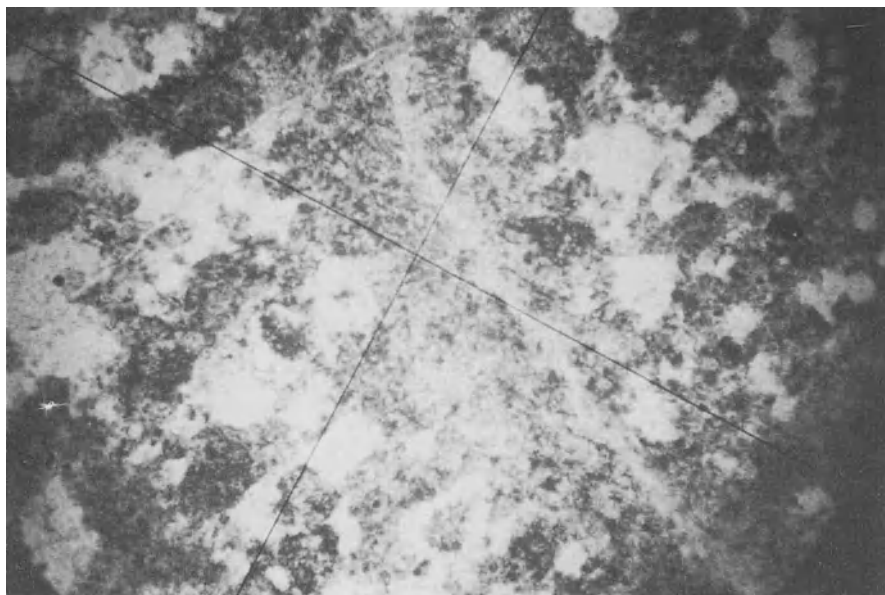
Plate 4.9. Photomicrograph in plane polarised light showing veinlet-controlled argillic alteration (fine greyish material) of porphyry rock (Henderson Mo deposit, Colorado, USA). Width of field is 3.5 mm
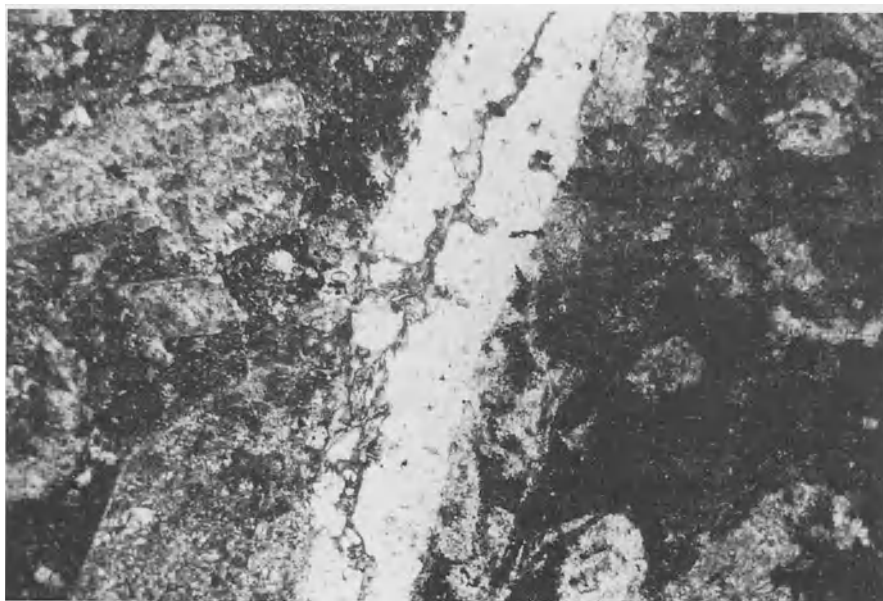
Plate 4.10. Photomicrograph in plane polarised light showing pervasive argillic alteration of andesite rock and cut by a quartz veinlet. A feldspar phenocryst is still recognisable on the *left*, adjacent to the veinlet (Namosi porphyry Cu deposit, Fiji). Width of field is 3.5 mm

Plate 4.11. Intense acid leaching of volcanic rocks. Vulcano, Eolian Islands

the intermediate argillic alteration may be present with kaolinite being closer to the phyllic zone, whereas montmorillonite clays occur in the outer zones. Figure 4.6d shows the mineral assemblage summary on the ternary diagram.

Advanced argillic alteration (Plate 4.11) is due to intense acid attack, and more or less complete leaching of the alkali cations with complete destruction of the feldspars and mafic silicate phases. Dickite, kaolinite, pyrophyllite, barite, alunite and diaspore are the typical mineral phases of this alteration type. In addition, sulphides, topaz, tourmaline and a range of amorphous clays may be present. Sulphide minerals can include covellite, digenite and enargite (high sulphur to metal ratios). Base leaching above 300 °C will produce assemblages containing pyrophyllite, andalusite, quartz, topaz and pyrite. Other associated minerals may include minor amounts of sericite, diaspore, kaolinite, rutile, anhydrite, corundum, zunyite, durmotierite, chloritoid (Siems 1984). Amorphous clays (e.g. allophane) are common in the supergene environment. Advanced argillic alteration is found in porphyry systems, in the inner zones of hydrothermal base and precious metal-bearing veins, and most typically in the high-sulphur epithermal systems. Alunitic alteration is part of advanced argillic alteration, and in the presence of abundant sulphate ions and Al-rich protoliths may become a dominant phase, as mentioned earlier. Alunite group minerals include alunite, natroalunite (Na replaces K), and jarosite (Fe replaces Al). Accompanying minerals are kaolinite, sericite, jarosite, pyrite, barite, hematite, chalcedony and opal. Figure 4.6e summarises the mineral assemblages of the advanced argillic alteration on the ternary diagram.

4.3.3 Other Types of Alteration

Other types of alteration not directly connected with hydrogen ion metasomatism are: tourmalinisation, talc-carbonate alteration, serpentinisation, silicification, silication, fenitisation, hematitisation and Fe alteration, dolomitisation and carbonitisation.

Tourmalinisation

Tourmaline is a complex B-bearing mineral with the general formula $XY_3Z_6B_3Si_6O_{27}(O,OH,F)_4$, where the X site may be taken by Ca or Na, the Y site by Mg and/or Fe^{2+}, (Al + Li) or Fe^{3+}, whilst Al^{3+}, Fe^{3+} or Cr may occupy the Z site (Dietrich 1985). The three end-members of the Mg-Li-Fe tourmaline solid solution series are schorl (Fe-rich), elbaite (Al, Li-rich) and dravite (Mg-rich). The composition of tourmalines may be indicative of the environment in which they originated. For example, the Fe/Mg ratio tends to decrease with increasing distance from a granitic source (Pirajno and Smithies, in press). In general, Fe-rich tourmalines are associated with Sn-W deposits of greisen affinity, whereas Mg-rich tourmalines are found with massive sulphide deposits and stratabound W deposits. "Tourmalinite" is the name given to rocks containing in excess of 15% tourmaline, and is associated with exhalative ore deposits in rift settings (Plimer 1987).

   In Sn-W deposits of greisen affinity, tourmalinised rocks are common. Pervasive to selectively pervasive tourmalinisation usually occurs associated with Sn-W deposits and breccia pipes. In many cases the country rocks surrounding greisenised granite cupolas have disseminated tourmaline, which tends to be particularly abundant in zones of fracturing. Quartz-tourmaline-dominated assemblages form pervasive replacements as well as cross-cutting veins and veinlets. The replacements can be on a very fine scale, so that the most intimate features and textures are perfectly preserved. This type of tourmaline alteration is linked to the emplacement and crystallisation of B-rich granitic magmas, with the possibility that the B-enrichment may have been inherited in a source region containing evaporites or tourmaline-rich protoliths. Tourmaline breccia pipes may also be associated with the crystallisation of "geochemically specialised" granitic magmas, and they result from high volatile pressure exceeding the lithostatic load. At the Krantzgerg W deposit in Namibia, tourmalinisation of the country rocks, hydraulic fractures infilled by tourmaline and breccia pipes are common. These features are related to the emplacement of the B-rich Erongo granite, a peraluminous anorogenic granite (Pirajno and Schlögl 1987). Tourmaline breccia pipes occur associated with porphyry copper deposits, vein type Sn deposits, and as small polymetallic pipes containing W, Cu, Bi, As and Au. Fluid inclusion data indicate that they form at depths ranging from between 1 and 3 km and at temperatures in excess of 300°C from highly saline fluids (Kirwin 1985). At Rooiberg, Transvaal (South Africa), highly mineralised Sn-bearing orbicular pockets occur in sedimentary slabs engulfed in the granitoids of the acid phase of the Bushveld Complex. These pockets contain abundant tourmaline and carbonate minerals, replacing quartz and plagioclase of the host sedimentary rock (Plate 4.12).

Plate 4.12. A Tin-rich orbicular pockets at the Rooiberg A mine, Transvaal, South Africa.

Stratiform tourmalinites are widespread in Proterozoic and Paleozoic sedimentary sequences associated with sediment-hosted massive sulphide deposits, as for example at Sullivan in British Columbia, where a fine-grained quartz-tourmaline rock underlies the ore deposit. Tourmalinites are also present in the Broken Hill areas (Australia), and in Namaqualand (South Africa) (Slack et al. 1984, Plimer 1987). These tourmaline-rich rocks are thought to be the result of submarine exhalations in rift environments, and are therefore neither epigenetic nor of the replacement type. Although this is invariably the case for many of these occurrences, the reader is cautioned against the interpretation of tourmaline-rich rocks, as fine-scale replacements can be deceptive and lead to erroneous conclusions (Plimer 1988; Smithies and Pirajno 1988).

Talc-Carbonate and Talc-Chlorite Alteration

Hydrothermal talc is known to be deposited on the sea floor of the Gulf of California, where it is associated with smectite clays and sulphides. Talc is also present in the Red Sea metalliferous sediments. Talc + carbonate $\pm$ magnetite assemblages of replacement-alteration origin are commonly found in the hydrothermal mineral deposits of Archean greenstone belts. An outstanding example is provided by the Sb-Au mineralisation in the Murchison greenstone belt in South Africa (Antimony line). Here, the Sb-Au mineralisation is associated with massive and widespread structurally controlled talc-chlorite-carbonate alteration. Pearton and Viljoen (1986) believe that this mineralisation is epigenetic, similar in style to

other Archean shear-zone hosted Au deposits (see Chap. 15). The talc-chlorite-carbonate alteration is thought to have originated from metamorphic fluids that were channelled along major structural breaks resulting in the replacement and alteration of the host metavolcanic and metasedimentary rocks. Introduction of vast quantities of H_2O and CO_2 into major structural breaks (shear zones) is possibly a major cause of the widespread regional-scale alteration in Archean settings. Along these structural breaks every stage of replacement and alteration by sericitisation, albitisation, steatitisation (talc) and carbonate (dolomite, ankerite, magnesite) is observed, together with local concentration of pyrite, arsenopyrite and gold (Chap. 15). Talc-carbonate and talc-chlorite alteration processes are therefore due to introduction of H_2O and CO_2. Reactions leading to talc-carbonate alteration were examined in detail by Turner and Verhoogen (1960), and are summarised here:

$$tremolite + 4CO_2 = 2dolomite + H_2Mg_3Si_4O_{12} + 4SiO_2,$$
$$talc$$
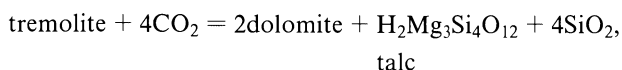
and in the presence of CaO-rich solutions:

$$talc + 2.15CaO + 4.3CO_2 = 2.15dolomite + 0.85MgO + 4SiO_2 + H_2O.$$
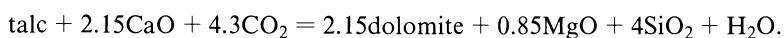
Talc and dolomite may also form directly from serpentinite:

$$2serpentine + 1.23CaO + 2.46CO_2 = talc + 1.23dolomite + 1.77MgO + 3H_2O;$$

$$2serpentine + 3CO_2 = talc + 3magnesite + 3H_2O.$$
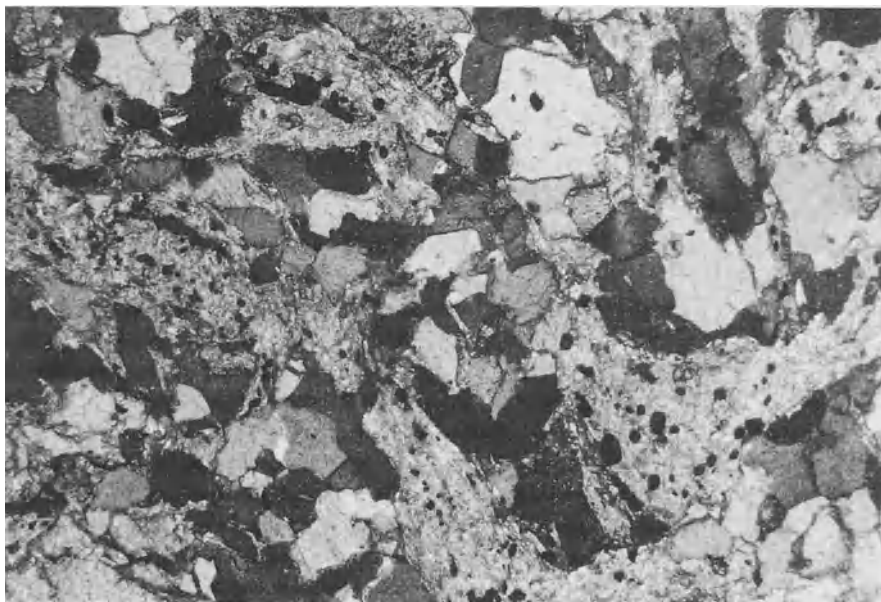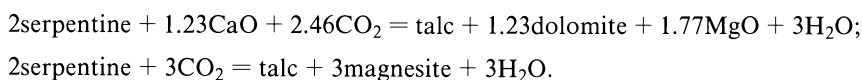
Plate 4.13. Photomicrograph taken at crossed nicols showing talc-carbonate alteration of an original pyroxenite rock. Large crystals are carbonates, fine material is talc. Epoch Ni mine, Zimbabwe. Width of field is 3.5 mm

Other examples of Archean talc-carbonate-chlorite alteration-mineralisation of hydrothermal origin are to be found in Western Australia (see Keays et al. 1982), and in Zimbabwe at the Epoch Ni mine. In the latter, sulphide mineralisation is contained in talc-carbonate and talc-chlorite rocks derived from the alteration of serpentinite and dunite (Pirajno, unpubl. data). The talc-carbonate assemblage includes talc, chlorite, magnesite and dolomite. Talc is by far the most abundant mineral phase (Plate 4.13).

Serpentinisation

This is the most common type of alteration of ultramafic rocks. Serpentine minerals (antigorite, chrysotile and lizardite) are formed from the alteration of olivine and pyroxene by introduction of H_2O and CO_2. Simple hydration however, according to Turner and Verhoogen (1960), is the most likely reaction with no change of volume and removal of MgO and SiO_2:

$$5Mg_2SiO_4 + 4H_2O = 2H_4Mg_3Si_2O_9 + 4MgO + SiO_2.$$

Although serpentinisation can occur at temperatures as high as 500°C, in mid-ocean-ridge settings temperatures of around 250°C are more likely. Ultramafic rocks at mid-ocean ridges undergo serpentinisation as a result of penetration and reaction with sea water. The widespread and regional scale of this phenomenon is such that serpentinisation is considered to be a regional metamorphic process. Tectonic transport of mafic-ultramafic complexes from spreading ridges to continental margins results in high deformation and pressure-related metamorphic processes. Ophiolite is the name given to these rocks, and we return to this topic in our discussion on hydrothermal processes and mineralisation in oceanic crust rocks (Chap. 12). The serpentinites of ophiolitic rocks contain the assemblage of lizardite + chrysotile + brucite ± magnetite. The latter is a common by-product of serpentinisation and is due to expulsion and oxidation of Fe from the silicate lattice. Other important by-products of serpentinisation are metasomatic processes such as albitisation, and the formation of peculiar rocks known as "rodingites". The latter occur as dykes commonly found in the Dun Mountain ophiolite belt in New Zealand (the name derives from the Roding river near Nelson, New Zealand). Rodingites are formed by calc-silicate assemblages (e.g. garnet, clinopyroxene, tremolite-actino-lite, epidote) and together with albitites occur along contacts between serpentinites and country rocks (Carmichael et al. 1974). In some cases rodingite and carbonated serpentinites may be associated with Au, Ag and Co mineralisation (Leblanc and Lbouabi 1988).

Silicification

This is perhaps one of the most common and best known types of hydrothermal alteration. The most common forms of silica are the low temperature α-quartz, or low quartz, the high temperature β-quartz, or high quartz (> 573°C), trydimite, cristobalite, opal, chalcedony. Low quartz is the most common form; cristobalite and trydimite are found in volcanic rocks. Trydimite is especially common as a
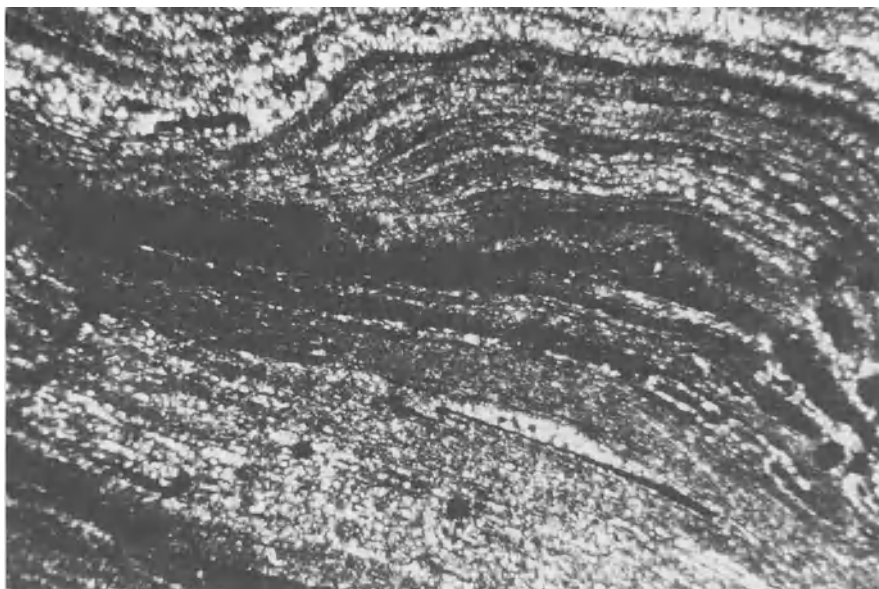
Plate 4.14. Photomicrograph of sinter material (Coromandel, New Zealand) showing fine silica laminations

devitrification product of volcanic glasses, forming intergrowths with alkali-feldspar. Opal [$SiO_2(H_2O)$] which is subsmicroscopic, is associated with sinter deposits and forms colloform crusts in cavities of volcanic rocks. Chalcedony is the principal component of chert and jasper, and is usually red to red-brown in colour. In thin-section, chalcedony appears fibrous or with a typical radial or banded textures. During hydrothermal processes silica may be introduced from the circulating fluids, or it may be left behind in the form of residual silica after leaching of bases. The solubility of silica increases with temperature and pressure (see also Chap. 3), and if the solution undergoes adiabatic expansion silica precipitates, so that in regions of low pressure and temperature it is readily deposited. Siliceous deposits in volcanic areas (sinters) have been mentioned in Chapter 3. Many epithermal mineral deposits, including kuroko types, are characterised by sinters, silica cappings, siliceous breccias, veins and silicification of country rocks. The silica of sinter deposits is usually fine grained, opaline, porous, it forms layers and thin sheets (Plate 4.14), and replaces vegetable matter such as twigs, leaves etc.

Although silica may replace virtually all rock types, silicification of carbonate rocks is perhaps the most common. Jasperoid, or jasperoidal is the term frequently used to refer to epigenetic bodies formed by fine-grained chalcedonic replacements of a pre-existing rock, usually a carbonate (Lovering and Heyl 1974). Precious metal-bearing jasperoidal rocks are an end member of the Carlin-type epithermal gold deposits. These jaspers are fine-grained, vuggy, brecciated and dark grey in colour (Lovering and Heyl 1974). Silicification is common in porphyry copper deposits and in many breccia pipes. At Climax, in Colorado, a barren silica core is

present in the mineralised porphyry system. It is also found associated with greisenised granites as for example at Panasquiera (Portugal), where a silica cap is located near the top of a greisenised cupola (Chap. 9).

Silication

Silication is the replacement of carbonate rocks by silicate minerals, generally through the addition of silica, as in the following reactions:

$$CaMg(CO_3)_2 + 2SiO_2 = (CaMg)Si_2O_6 + 2CO_2;$$

dolomite   diopside

$$CaCO_3 + SiO_2 = CaSiO_3 + CO_2.$$

calcite   wollastonite
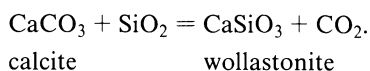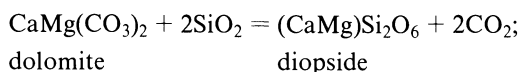
Silication results in skarn rocks, in which the addition of large quantities of silica produces a wide variety of calc-silicate minerals. Alteration mineral assemblages of skarn rocks include Ca, Fe, Mg, Mn silicates, such as epidote, clinozoisite, garnet, clinopyroxene, wollastonite, diopside, vesuvianite, tremolite-actinolite, andradite, grossularite, phlogopite and biotite. Skarns are developed at the contact between plutons and the invaded country rocks, the latter generally being carbonates and, less commonly, Ca-rich silicate rocks. Skarn genesis essentially involves isochemical contact metamorphism and metasomatism, entirely due to emanations from a cooling plutonic body. Retrograde stages of alteration occur towards the final stages of cooling, resulting in more intense hydrothermal activity and precipitation of sulphides and oxides, especially nearer the pluton's contacts. Skarns develop at temperatures of between 650 and 450 °C and at a pressure of 0.3-3 kbar (Einaudi et al. 1981). Skarns are very important because they host a great variety of ores and constitute a distinct class of mineral deposits, whose general characteristics are reviewed in Chapter 10.

Fenitisation

This is a type of alteration which occurs in the aureoles of carbonatites and alkaline complexes. It is essentially a desilication process accompanied by the introduction of Na, K, CO_2, CaO and Al_2O_3. Fenitisation is therefore characterised by the development of alkali pyroxenes (e.g. aegirine), alkali amphiboles (e.g. riebeckite), and alkali feldspars (orthoclase, microcline and albite). The latter are usually coloured red due to the presence of hematite. Affected rocks are called "fenites", derived from the Fen carbonatite where this type of alteration was first documented by Brogger (1921). A plethora of confusing – and difficult to remember – names have been adopted by different authors to describe fenitic rocks. Verwoerd (1966), in an attempt to solve the problem, proposed that the naming of fenitic rocks should be prefixed by the principal mineral component followed by fenite (e.g. orthoclase-aegirine-augite fenite).

Fenites are formed in the country rocks surrounding the alkaline complexes, through stages of progressive metasomatism involving the elimination of free

quartz and the development of alkali mineral phases. Carmichael et al. (1974) attributed these metasomatic effects to residual alkali-rich fluids deriving from the fractionation of alkaline magmas. The fluids are in strong disequilibrium with the country rocks, resulting in haloes of alteration products which in some cases may resemble primary igneous rocks. Fenitisation is considered by many to be a solid-state transformation, due to the expulsion from the igneous complex of hot and highly reactive volatiles and their subsequent infiltration into the country rocks (Best 1982). The spatial relationships of alkaline and carbonatite complexes, their fenitised envelopes and related mineralisation are examined in Chapter 8.

Hematitisation and Fe-Rich Alteration

Hematite, Fe-carbonates (ankerite, siderite), Fe-rich chlorite and Fe-rich amphiboles are often dominant alteration products in a number of important ore deposit types. Unfortunately this type of alteration is not as well documented as it should be, partly because it attracted less economic attention and therefore less research, and partly because the work carried out by company geologists has not been made public due to the strategic nature of some of the related mineral commodities. Hematite impregnations, disseminations and veinlets are associated with the late stages of hydrothermal activity in Sn-W greisen-affiliated mineralising systems. Hematite and chlorite are important gangue and alteration minerals at the giant Roxby Down (Olympic Dam) deposit in South Australia (Roberts and Hudson 1983). In this deposit Fe-rich alteration is associated with mineralisation containing elements such as F, Cu, U, REE, Au.

Particularly interesting is the association Fe-F, (actinolite-fluorite; siderite-magnetite-quartz-fluorite-sulphides), forming unusual mineralising systems related to the acid phase of the Bushveld Complex, Transvaal (South Africa). These mineral deposits are interpreted as distal products of Bushveld granite-related hydrothermal systems (Crocker, 1985). The Vergenoeg hematite and fluorite deposit (Crocker 1985) is an outstanding example of Fe and F metasomatism on a grand scale. The Bushveld granite-related mineralisation is described in Chapter 9; however, for the purpose of this topic it will suffice to say here that the Fe-rich lithologies and mineralisation at Vergenoeg and other localities nearby appear to be the product of a combination of plutonic, volcanic exhalative and metasomatic activities, whose nature is not clearly understood. At any rate, the large and regional scale Fe enrichments observed in these areas have led Crocker to consider a general trend of Fe-Ca-F-CO_2 enrichment, perhaps initially due to immiscibility of magmatic fractions. Exsolution and degassing of HF may have been the leading factor responsible for the massive Fe-F alteration in the region. As HF passes through formerly Fe-rich lithologies (e.g. mafic rocks of the Bushveld Complex), it would leach out Ca and Fe to form fluorite, chlorite, Fe-actinolite and hematite in the uppermost sectors of the system. By pressure loss Fe-actinolite plus HF, CO_2, and O_2 would form magnetite, siderite and fluorite. One of the possible reactions proposed by Crocker (1985) is:

$$4Ca_2Fe_5Si_8O_{22}(OH) + 16HF + 6O_2 = 8fluorite + 10hematite +$$
ferroactinolite
$$+ 32quartz + 10H_2O.$$
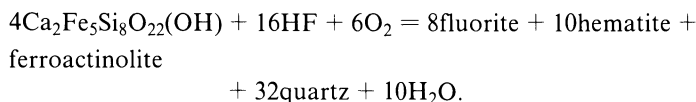
Hematite and chlorite alteration is associated with unconformity-type uranium deposits. This alteration may be accompanied by clay, dolomitisation, silicification and even tourmalinisation. At the Rabbit Lake deposit in Canada (Nash et al. 1981), alteration is characterised by chloritisation (Fe-rich) of mafic minerals, followed by Mg and B-metasomatism, silicification and hematitisation. In the Alligator uranium fields in the Northern Territory (Australia), zones of massive chlorite, quartz and hematite, which are fault-controlled, occur associated with the mineralisation.

In the Brandberg areas (Damara orogen, Namibia) Sn-W vein deposits are locally associated with extensive tourmaline, sericite and hematite alteration. The latter appears to be related to the final stages of the hydrothermal activity. Ferruginisation (mainly siderite) of marble units intercalated with the metapelites hosting the vein mineralisation is also a conspicuous feature (Pirajno and Jacob 1987).

Fe-carbonate alteration is often found in the wallrocks of the turbidite-hosted Au vein deposits. Porphyroblast-like growths of siderite and ankerite give the wall rocks a spotted appearance. Fe-carbonate alteration and chloritisation are also common in gold deposits of Archean age (see below).

Carbonatisation and Dolomitisation

Carbonate alteration of both Ca-rich and silicate rocks involves two basic processes: dolomitisation and carbonatisation. The former is a very common type of alteration of limestones in which cation metasomatism and base exchange take place, whereby Mg^{2+} substitutes for Ca^{2+}, and $CaCO_3$ becomes $CaMg(CO_3)_2$. From the mineralisation point of view, it is important to realise that dolomitisation reactions involve loss of volume (between 6 and 13%, Morrow 1982 a), which enhances the porosity of the rock and hence makes it more receptive to the mineralising fluids. There are several models which attempt to explain dolomitisation and, while it is beyond the scope of this section to provide a detailed review (see e.g. Morrow 1982a, b; Hardie 1987) these include the following: one theory considers that dolomite is an evaporite mineral, and that dolomites are therefore formed by the action of hypersaline brines with high Ca/Mg ratios. In evaporitic environments algae may influence this process, during which dolomite replaces calcite and other evaporite minerals. Another theory, that of mixed waters (known as "dorag", Persian for mixed blood), envisages dolomite being formed by mixing of fresh water with sea water. A third possibility is dolomitisation by burial diagenesis, during which migration of Mg-rich brines and mixing with near-surface brines would take place. A critical appraisal of these theories reveals that in fact none are completely satisfactory (Hardie 1987), but it is nevertheless clear that dolomitisation has an important association with many types of hydrothermal mineral deposits. Dolomitisation is commonly associated with the low temperature Mississippi Valley-type Pb-Zn
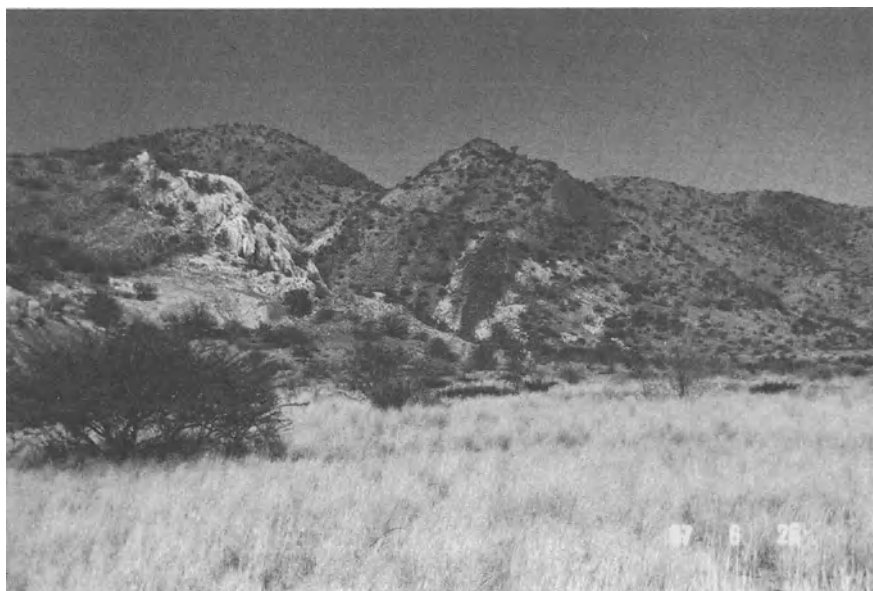
Plate 4.15. Dolomitisation (*white*) of grey calcitic marbles of the Karibib formation, Damara sequence, Namibia. These dolomitised marbles are spatially associated with Au mineralisation (Pirajno and Jacob 1988)

deposits, where this type of alteration seems to have preceded and perhaps favoured the deposition of sulphide minerals (Evans 1987).

Large-scale dolomitisation of marble units of the Karibib formation, Damara sequence, may be related to Au mineralisation in the Central Zone of the Damara orogen in Namibia (Plate 4.15). Although the origin of this very extensive dolomitisation remains uncertain, it may be related to release of CO_2 during metamorphism. Reaction of CO_2 with impure marbles containing actinolite-tremolite minerals, in turn due to high temperature prograde metamorphism, could have produced the dolomite:

$$\text{3calcite} + \text{tremolite-actinolite} + 7CO_2 = \text{5dolomite} + 8SiO_2 + H_2O.$$
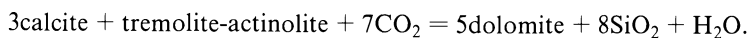
The above reaction is deduced from the mineral associations and relationships present in the dolomitised rocks (Pirajno and Jacob 1988). The relationship of this alteration to Au mineralisation is discussed in Chapter 15. At Mt.Isa (Australia), bodies of silica-dolomite are associated with Cu-Pb-Zn mineralisation, although it seems that this rock is the recrystallised product of siliceous dolomites (see Chap.13).

Mineral deposits of Mississippi Valley affiliation in the "carbonate platform" zone of the Damara orogen (Namibia), such as the famous Tsumeb and Kombat, have spatial relationships with fracture-controlled calcitisation of dolomite, locally accompanied by hematite alteration and silicification. These alteration features are in fact used as major exploration criteria. Carbonate alteration of silicate rocks, in

contrast to dolomitisation, occurs by anion metasomatism with introduction of CO_2. Carbonitisation of mafic rocks is a common type of alteration in the mafic rocks of the Archean greenstone belts, where auriferous quartz veins are present. An outstanding, large-scale carbonate (and Fe), alteration of this type is that of the Golden Mile dolerite in the Kalgoorlie district of Western Australia (Phillips 1986). The hydrothermal alteration of the lithologies of the Golden Mile is divided by Phillips (1986) into three main zones: (1) chlorite zone (chlorite + calcite + ankerite); (2) carbonate zone (ankerite + siderite); (3) pyrite zone (ankerite + muscovite + quartz + albite + pyrite and gold). The reactions envisaged by Phillips are reported below:

1. Actinolite to chlorite:

   6actinolite $+ 12CO_2 + 14H_2O = $ 5chlorite $+$12calcite $+ 28SiO_2$.

2. Chlorite to carbonate:

   chlorite $+$ 6calcite $+ 6CO_2 = $ 6ankerite $+ 4SiO_2 + 4H_2O$;

   chlorite $+ 6CO_2 = $ 6siderite $+ 4SiO_2 + 4H_2O$.

3. Carbonate to pyrite:

   siderite $+ 2H_2S + 1/2\ O_2 = FeS_2 + CO_2 + 2H_2O$.
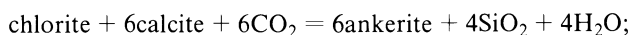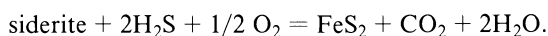
This alteration is thought to be due to syn- to post-metamorphic H_2O-CO_2-rich fluids of low salinity (< 2 wt.% NaCl equivalent), at temperatures of between 350 and 400°C, and pressures of 0.8–2 kbar (Phillips 1986). The Golden Mile alteration-mineralisation is examined in greater detail in Chapter 15.

4.4 Quantification and Monitoring of Hydrothermal Alteration Processes – Data Presentation

Empirical and semi-quantitative approaches to describe hydrothermal alteration have been mentioned in Section 4.3. Studies of equilibria between minerals and hydrothermal fluids necessitate research on thermodynamics, normally carried out at universities and other institutions equipped for such experimental work. The presentation of mineral equilibria, in fact, involves the use of variables such as pressure, temperature, Eh, pH and chemical potential (see Rose and Burt 1979). Acidity-salinity (chemical potential) diagrams have been employed by Burt (1981) to quantify alteration mineral equilibria in greisens and porphyry systems. Activity-activity diagrams are considered to be particularly useful because they allow comparisons between key ions which can be normalised to H^+ (Guilbert and Park 1986). The simplified diagram of Fig. 4.5A, for example, compares temperature to the ratio of the activities of K^+ and H^+. A comprehensive and concise review of the use of activity diagrams in studies of hydrothermal alteration can be found in Rose and Burt (1979, p.188). For the purposes of the exploration geologist, hydrothermal alteration can be relatively easily quantified and described by using mineralogical
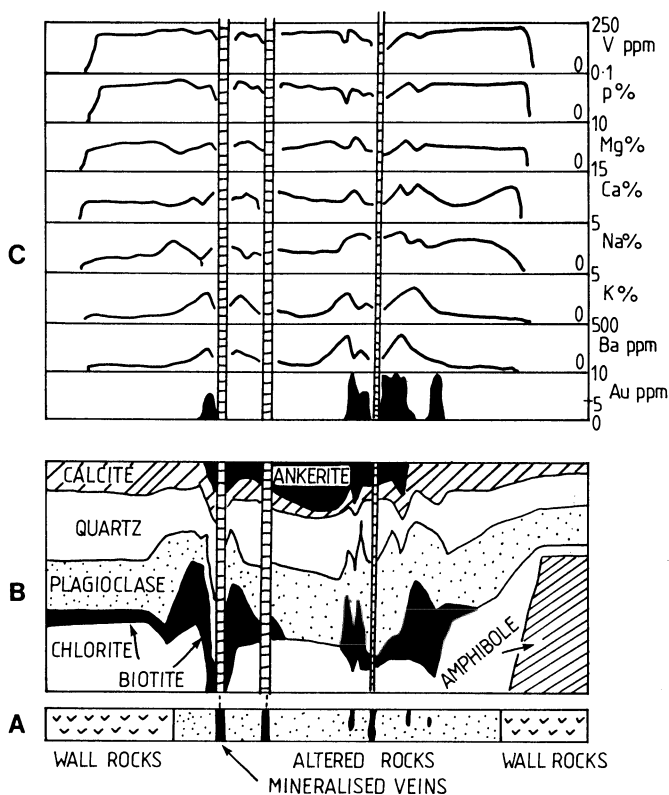
Fig. 4.9A–C. Composite diagram showing **A** simplified geological log; **B** modal mineralogy; **C** geochemical variations; of an Archean auriferous vein system. Data and diagram modified from Phillips and Groves (1982)

and geochemical data. For this, a team of explorationists needs to conduct studies along three fronts. The first is of course detailed field mapping, core logging, etc during which representative specimens of fresh and altered materials are collected. The second comprises mineralogical studies including thin section, X-ray diffraction (XRD) and microprobe work, for the identification of the key mineral assemblages. The third includes major and trace element geochemical analyses. The data obtained in this way can then be evaluated and presented in the form of two-dimensional diagrams. Ideally these should depict both mineralogical and geochemical data.

An example of this type of presentation is shown in Fig. 4.9, in which the volume percentage of each mineral phase, established by point counting of thin sections, is plotted against a suitably simplified geological log. Trace element geochemistry is plotted against the same geological log, thus allowing direct comparison of both mineralogical and geochemical variations in the given mineralising system. More schematic, but equally effective, is the "summary" diagram of Fig. 4.10, where mineralogical and geochemical changes are compared to alteration types.

ALTERATION TYPES

UNALT. ROCK	ARGILLIC	PHYLLIC	ADV. ARGIL.	VEIN

MINERALOGICAL CHANGES

QTZ K-FELDSPAR PLAGIOCLASE BIOTITE HORNBLENDE		+qtz sericite	clays	QUARTZ + SULPHIDES
	Traces sericite + kaolinite	sericite	pyro- phyllite	
	montmorillonite clay kaolinite _ _ _ chlorite _ _ _ _ _ biotite	sericite + pyrite	pyro- phyllite	
	calcite biotite chlorite kaolinite epidote	sericite + pyrite	pyro- phyllite	

GENERALISED CHEMICAL CHANGES

Fig. 4.10. Diagrams depicting a summary of alteration and geochemical changes associated with mineralised veins at Butte, Montana (USA). After Rose and Burt (1979), originally from the work of Meyer and co-workers (in Rose and Burt 1979)

A popular and very useful way of representing alteration data is by plotting gains and losses as percentages relative to the unaltered rock. In this method analytical values and specific gravity determinations are obtained for individual samples, and a horizontal line represents the assumed unaltered rock composition. Gains plot above the horizontal line and losses below it. Examples of this type of study can be found in Camus (1975), who studied the hydrothermal alteration at the El Teniente porphyry Cu deposit, and Ford (1978) who worked on the Panguna Cu-Au porphyry (Chap. 10). One of Ford's diagrams is shown in Fig. 4.11.

A quantitative measure of hydrothermal alteration used by Ferry (1983) is carried out by the calculation of an alteration index (AX). The AX is defined as the total volume of the alteration mineral assemblage, divided by the total volume of all the mineral phases present (including the hydrothermal minerals). This measure of volume percentages is carried out by point counting of thin sections. AX values may range from 0 in the unaltered rock to as much as 0.8 or 0.9 for a pervasively altered
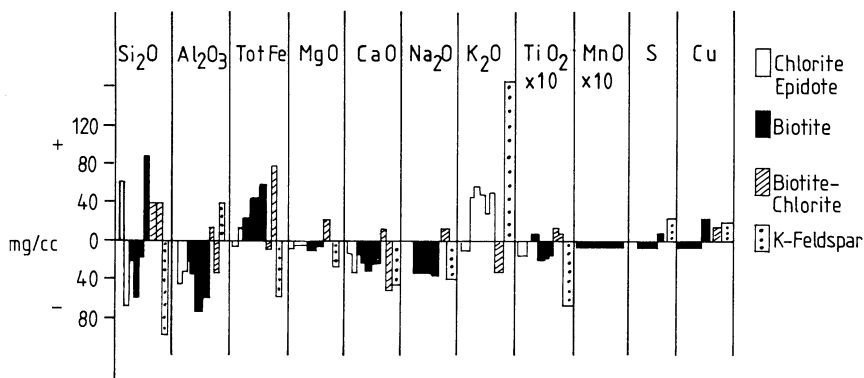
Fig. 4.11. Geochemical changes above and below average unaltered rock (*horizontal line*), during alteration of the Panguna andesite, Bougainville porphyry Cu-Au deposit (PNG). See text for detailed explanation (After Ford 1978)

rock with a few relicts of unaltered minerals. The AX index can then be plotted against suitable geochemical parameters.

Studies of mass transfer accompanying metasomatic processes were conducted by Gresens (1967) and Babcock (1973). They considered composition-volume relationships by developing a set of equations to quantify gains and losses of matter by metasomatic exchanges. Prins (1981) adopted this approach for his work on the fenites of the alkaline and carbonatite complexes of the Damara province, Namibia. The interested reader is advised to consult Prins' work for a useful and instructive example. Gresens' equations allow the calculation of gains and losses in the system by using geochemical analyses and specific gravities of the rocks and minerals in question, rather than the theoretical formulae. In the simplest case of two minerals and two components the following equations were obtained:

$$100 \times [fv\, (gB/gA)\, c1^B - c1^A)] = X_1,$$

$$100 \times [fv\, (gB/gA)\, c2^B - c2^A)] = X_2,$$

where A is the original mineral, B its alteration product, $c1^A$ the weight fraction of component 1 for mineral A (e.g. TiO_2 wt.%), and fv the volume factor. This factor can be greater than 1 in the case of replacement with volume gain, equal to 1 for volume by volume replacement, and less than 1 with volume loss; gA and gB are the specific gravities of minerals A and B; X_1 and X_2 represent the material lost or gained ($X = X_1 + X_2$). The equations above have three variables (fv, X_1, X_2) and if it is considered that replacement is isovolumetric (fv = 1), then only X_1 and X_2 remain to be solved. A simple solution of Gresens' method, using a computer spreadsheet readily simplifying manipulation of the data, is proposed by Grant (1986), to whose paper the interested reader is referred.

Cationic variation diagrams, devised by H. de la Roche and his co-workers (de la Roche et al. 1980), can be used to represent trends and variations in a set of geochemical data, expressed in millications. The R1-R2 plot, where R1 = 4Si-11(Na+K)-2(Fe+Ti) and R2 = 6Ca+2Mg+Al, has been used to classify and study
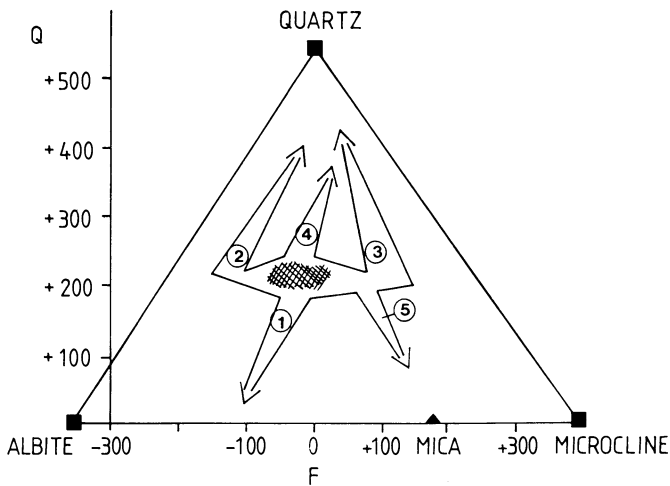
Fig. 4.12. Q-F diagram showing major alteration trends relating to alkaline complexes in Nigeria (after Bowden et al. 1984). Trend *1* is H⁺ metasomatism (greisenisation) and ore deposition in basement rocks. Trend *2* represents greisenisation and silica metasomatism with a slight sodic imprint. Trend *3* represents greisenisation (quartz-topaz-fluorite-mica) developed from microcline-rich rocks (K-metasomatism), with superimposed silica metasomatism. Trend *4* indicates pervasive H⁺ metasomatism of granitoids not affected by earlier metasomatism. Trend *5* (added by the author) represents micaceous greisens. The *central shaded area* is the original alkaline granite

petrogenetic variations of igneous rocks (Batchelor and Bowden 1985). The advantage of this method, according to de la Roche et al. (1980), is that all major cations are combined in one diagram. The QF cationic plot, where $Q = Si/3-(K+Na+2Ca/3)$ and $F = K-(Na+Ca)$, has been used by P. Bowden and J.A. Kinnaird of the University of St.Andrews (Scotland) in their detailed studies of the alteration and mineralisation of the Nigerian anorogenic ring complexes (Bowden et al. 1984; Bowden 1985; Kinnaird 1985). In the QF diagram the data are plotted in relation to mineral "poles" (quartz, albite, microcline and mica). This enables the study of the geochemistry of the alteration processes by monitoring changes in silica and alkali ratios without regard as to how the cations are distributed in the sample considered (Bowden et al. 1984; Kinnaird 1985). An example of QF plot is shown in Fig. 4.12. Calculation of millications from analytical data can be simply achieved using a computer spreadsheet. An example of a millicationic calculation is given in Table 4.2.

4.4.1 Rare Earth Elements in Hydrothermal Alteration Processes

Rare earth elements (REE) include those elements with an atomic number between 57 (lanthanum) and 71 (lutetium). Their similar chemical behaviour is related to the decrease in their atomic volume with increasing atomic number, the so-called lanthanide contraction. Yttrium (atomic number Z=39) is often considered

Table 4.2. Tabulation of millicationic calculation for the construction of de la Roche's diagrams, in this case the Q and F parameters have been calculated (see text for details)

	wt% (1)	Molecular wt% (2)	(1)/(2) (3)	No. of cations (4)	Milli-cations (3)×(4)
SiO_2	56.40	60.09	0.9386	1	938.59
TiO_2	0.86	79.90	0.0108	1	10.763
Al_2O_3	17.50	101.96	0.3433	2	343.27
Fe_2O_3	8.24	159.69	0.1032	2	103.2
MnO	0.04	70.94	0.0006	1	0.564
MgO	5.40	40.30	0.1340	1	133.99
CaO	3.87	56.08	0.0690	1	69.01
Na_2O	2.00	61.98	0.6454	2	64.54
K_2O	3.76	94.20	0.0798	2	79.83
P_2O_5	0.19	110.97	0.0034	2	3.42

$Q = 122.4912$; $F = -53.7154$

together with the REE because of its similar ionic radius to holmium ($Z = 67$). REE with lower atomic numbers are referred to as light REE (LREE), and those with higher atomic numbers as heavy REE (HREE). A detailed review of REE geochemistry is clearly beyond the scope of this book, but the interested reader is recommended to consult the work of Hanson (1980) for a good documentation on the topic of REE studies of igneous systems, the informative short article by Muecke and Moller (1988) and, for a more comprehensive outline, Felsche and Herrmann (1978). For the purpose of graphical presentation, REE abundances are normalised to chondritic meteorite abundances, i.e. each element value in the sample is divided by the corresponding element value in chondrites. The REE abundances in chondritic meteorites are taken to be the base values, and therefore the abundances in the primordial mantle form a horizontal line in the diagram, because it is assumed to be unfractionated. It follows that the REE abundances in the various rock systems show variably shaped curves above that of the primordial mantle, reflecting varying degrees of fractionation. In cases of cogenetic rocks it may be more expedient to normalise the REE to one of the rocks in the sequence, generally the least fractionated (Hanson 1980).

In geological processes REE are variably enriched in magmas, their consolidation products and their residual fluids. Studies of REE abundances in rock systems are especially valuable in the investigation of petrogenetic models. Generally speaking LREE tend to be concentrated in pegmatites and carbonatites, whereas HREE are concentrated in granitic magmas. REE are contained in more than 200 minerals including various phosphates, carbonates, oxides and silicates. Common rock-forming mineral phases containing REE are apatite, zircon, monazite and xenotime. Michard (1989) has studied the REE content of hydrothermal solutions from a number of geothermal fields. She found that the REE concentrations of the hydrothermal fluids are usually very low, but they tend to
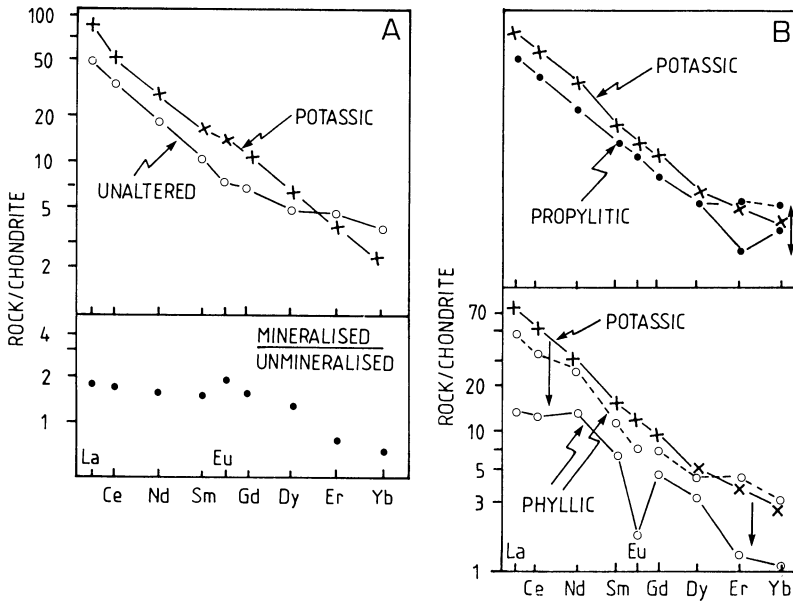
Fig. 4.13A, B. REE distribution for unaltered and altered granodiorite porphyry. See text for explanation (After Taylor and Fryer 1982)

increase as the pH decreases; also, in chloride-rich fluids the REE patterns show distinct positive Eu anomalies.

Little is known of the mobility and transport of REE in hydrothermal solutions. Russian investigators, quoted by Felsche and Herrmann (1978), reported that most REE are transported in alkaline solutions as carbonate, sulphate or fluorine complexes. Precipitation would occur as a result of changes in alkalinity, pressure and carbonate fixation. Also, the HREE form more stable complexes, with a tendency to stay in solution longer than the LREE, and therefore they tend to concentrate in the later products of the hydrothermal activity. In this context, the behaviour of REE during processes of hydrothermal alteration have been investigated by Taylor and Fryer (1980, 1982, 1983). Their results are summarised below and shown in Fig. 4.13. These authors found that REE distribution in unaltered and altered rocks are useful monitors of changing fluid conditions from dominantly magmatic to dominantly meteoric. Changes in REE abundances during potassic alteration in a porphyry system are characterised by LREE increase and HREE depletion (Fig. 4.13A). In the lower diagram of Fig.4.13, the ratio of REE abundances in mineralised to unmineralised rocks shows a decrease from LREE to HREE, and a positive Eu anomaly, indicating this element's enrichment in the hydrothermal fluids. From the propylitic to the phyllic stage of alteration or in other words with decreasing K^+ activity and increasing H^+ metasomatism, the pattern of REE abundances changes. From the potassic to the initial stages of the propylitic event (Fig. 4.13B) there is overall depletion of REE (upper diagram), but less so for the LREE than for the HREE. In the more advanced stages, however, the heaviest

REE are enriched. From the propylitic to the phyllic stage (Fig.4.13B, lower diagram) there is further depletion of the total REE, indicating progressive leaching of the REE with increasing fluid/rock ratios and decrease in pH (increasing H^+). This decrease is more pronounced for the LREE than for the HREE, which are consequently relatively enriched.

In summary, and in agreement with Hanson (1980) and Michard (1989), it is found that in hydrothermally altered rocks the REE abundances are significantly affected only if water is flushed through the system several times. This has important implications, because if the REE patterns are not sufficiently different from those of the unaltered rocks, then the chances of substantial, or rich, mineralisation are poor.

Lottermoser (1990) investigated the mobility of REE during fluid-wallrock interaction in the large and active gold epithermal system in Lihir Island in Papua New Guinea. This system, which is discussed in some detail in Chapter 11, is characterised by a number of zones of hydrothermal alteration and mineralisation. They can be summarised into: (1) a lower potassic-propylitic zone; and (2) argillic and advanced argillic zones. These zones are capped by a sulphide-free oxide zone. Lottermoser's work established that the REE patterns of alteration assemblages in the wall rocks and vein materials display strong mobilisation and fractionation during the hydrothermal processes which characterise an active volcanic ore-generating system. The results of this work, however, show results which contrast with those obtained by Taylor and Fryer (1980, 1982 and 1983), because at Lihir there is progressive addition of LREE from the potassic-propylitic to the argillic zone, with high mobilisation and concentration of HREE characterising the higher levels of the alteration profile. In summary in the Lihir epithermal system the magmatic-hydrothermal component is LREE-enriched, whereas LREE and HREE both are enriched in the meteoric acid sulphate component of the system. As previously suggested, this mobilisation of REE occurs under conditions of large scale fluid flow.

4.5 Oxygen and Hydrogen Isotope Systematics

A brief introduction into the concepts of oxygen and hydrogen isotope systematics, references therein and the definition of the standard notation are given in Chapter 2. Here, we examine the effects of isotopic compositions and variations in hydrothermally altered rocks. Studies of this type have been reported in Volume 69 (1974) of Economic Geology. More recent important works include Criss and Taylor (1986), Ohmoto (1986) and Green et al. (1983).

The study of isotopic compositions is based on systematic variations that occur in natural materials as a result of fluid and rock interactions, and temperature. Isotope exchange reactions take place between fluids, and between these and wall rocks, as for example in the reactions given below:

$$1/2C^{16}O_2 + H_2{}^{18}O = 1/2C^{18}O_2 + H_2{}^{16}O;$$
$$H_2{}^{18}O + 1/2Si^{16}O_2 = H_2{}^{16}O + 1/2Si^{18}O_2.$$
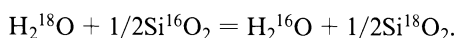
The fractionation factor, a, between CO_2 and H_2O, or SiO_2 and H_2O, is given by the ratio of the isotopes (e.g. $^{18}O/^{16}O$) in the two substances (1 and 2) considered, and determines how much one isotope is enriched in one substance relative to another in per mill fractionation ($10^3 \ln a$). This value is approximated by:

$$\text{delta} = \delta_1 - \delta_2 = 10^3 \ln a_{1-2} = A(10^6 \, T^{-2}) + B,$$

where A and B are constants, and T is the temperature in degrees Kelvin (Faure 1986). The difference in δ-values allows the characterisation of the isotopic interaction between fluids and mineral phases in the wall rocks, and between co-existing mineral phases. Since isotope fractionations are temperature-dependent, while independent of pressure, this allows the determination of isotopic temperatures using fractionation curves. Thus, if two mineral phases equilibrate oxigen with a common fluid, at a given temperature, the difference in their $\delta^{18}O$ is a function of the temperature (Faure 1986). Studies of combined hydrogen and oxygen isotope systematics in hydrothermal systems rely on the different abundances of H and O in rocks and water. This enables the quantification and characterisation of the water-rock interaction, in terms of the H and O exchange between fluid and mineral phases. Therefore, the D/H ratio of the system will be controlled by the water, whereas the $^{18}O/^{16}O$ value is determined by the exchange with mineral phases in which H is only a trace constituent. Consequently the oxygen isotopic composition is affected by the mineral-water interaction resulting in an ^{18}O shift of the fluids from the original value, usually towards higher values (see Fig 2.1). This shift is due to the water attempting to equilibrate with the ^{18}O-rich wall rocks. The amount of shift is related to the ratio of oxygen in the minerals to that of water, to the mineral-water fractionation factor, and hence temperature, and the original isotopic composition of either of the phases (Sheppard 1986). Isotopic interactions are also considered in terms of a closed system (mineral co-existing fluid), or open system (external fluid with increasing fluid to rock ratios) (Gregory and Criss 1986).

Hydrothermal alteration of rocks is accompanied by variations in $\delta^{18}O$ and δD which tend to form zoning patterns around the ore deposit. These patterns are important in determining the geometry of the hydrothermal cell, as well as the size and location of the discharge area (Ohmoto 1986). We examine below some specific examples of isotopic zoning in mineralised and altered rocks. Taylor (1971, 1974) pioneered this type of investigation with his work on the igneous rocks of the Cascade Range (Oregon, USA). This geoscientist analysed hydrothermal minerals and fluid inclusions for their $^{18}O/^{16}O$ and D/H values, and found that shallow intrusions into highly fractured – and therefore permeable – country rocks act as "gigantic heat engines" throughout their evolutionary history. The isotopic signature of the hydrothermal fluids consistently indicated their derivation from meteoric waters. Calculated water/rock ratios show that high ratios are associated with areas of intense alteration and low $\delta^{18}O$ in the rocks. Where less permeable, less meteoric water is available and a larger magmatic component associated with potassic alteration is found to be present. In the particular case of the Tertiary volcanic and intrusive rocks of the Cascade Range, Bohemia mining district, the results of Taylor's work indicated a regular and concentric pattern of $\delta^{18}O$, from low values at the centre to progressively higher values towards the periphery. The areas
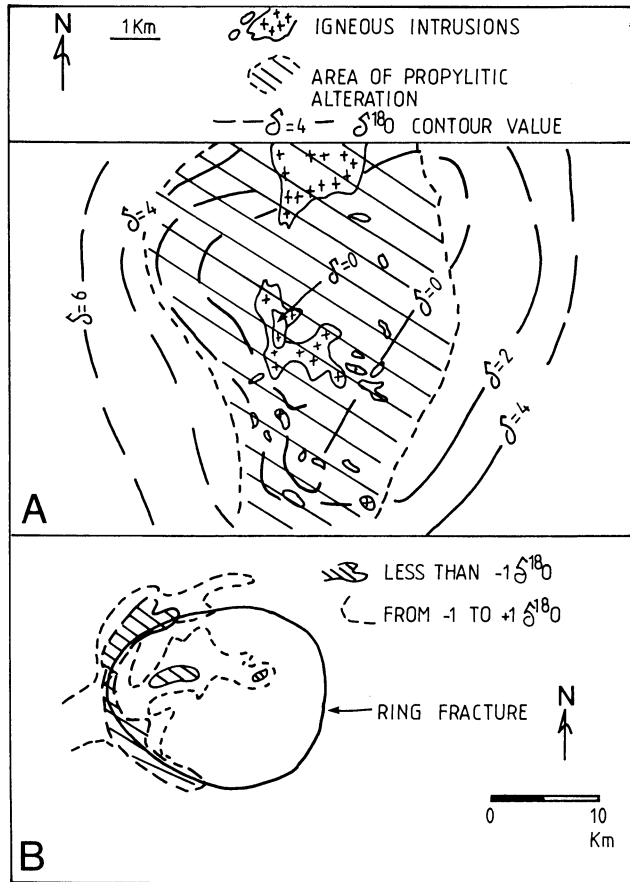
Fig. 4.14. A $\delta^{18}O$ contours in the Bohemia district, Oregon (USA), showing coincidence of low $\delta^{18}O$ values with areas of propylitic alteration (After Taylor 1971, 1974). **B** Contours of whole-rock $\delta^{18}O$ values in the Lake City caldera complex. Note the pronounced $\delta^{18}O$ depletion along the western areas of the ring fracture and inside the caldera, where resurgent rhyolitic volcanism occurred. See text for further comments (After Larson and Taylor 1986)

of lowest $\delta^{18}O$ values coincide with zones of propylitic alteration (Fig. 4.14A). Another instructive example comes from the Lake City caldera, in the mineralised San Juan volcanic field in Colorado. Here a study of stable isotope systematics carried out by Larson and Taylor (1986) revealed the presence of a large fossil hydrothermal system. This work showed pronounced $\delta^{18}O$ depletions along the western rim of a ring fracture, and inside the caldera in an area of rhyolitic resurgent volcanism (Fig.4.14B). These areas correspond to a deeply eroded part of the caldera with intense chloritic and sericitic alteration. The lowest $\delta^{18}O$ values occur along the highly permeable ring fault zone, and also along the southwestern parts of the caldera where epithermal mineralisation is present. High $\delta^{18}O$ values occur in hydrothermal quartz in a quartz-latite dome in the eastern portions of the volcanic

structure. High water/rock ratios, calculated from the isotopic data, are coincident with the zones of low $\delta^{18}O$.

Isotopic studies of whole rock and hydrothermal minerals of volcanics and sediments from the Fukazawa-Kosaka area in Japan – the site of kuroko-type mineral deposits – carried out by Green et al. (1983) revealed systematic variations of $\delta^{18}O$ and δD with alteration and temperature of the sea water interacting with the rocks. The $\delta^{18}O$ values vary from 6.7 per mill in the sericite-chlorite zone (highest temperature of interaction with sea water from about 200-400°C), to 11.1 per mill in the montmorillonite zone (temperature of about 150–300°C), to 16.9 per mill in the zone of zeolitic alteration with the lowest temperature of 25–200°C. A concentric zoning pattern is also found in the footwall rocks, with $\delta^{18}O$ values of 8 per mill in the sericite-chlorite zone up to 500 m from the ore, followed by 8–14 per mill in the montmorillonite zone up to 3 km away, and finally to values in excess of 14 per mill in the peripheral zeolite zone (Green et al. 1983). The authors found that these isotopic variations form a much larger halo than do the distribution of anomalous Cu, Zn, Pb, Mg etc. values in the rocks.

In summary, hydrothermal alteration results in a consistent depletion of $\delta^{18}O$ in the rocks, usually matched by a corresponding enrichment in the hydrothermal solutions, although Criss and Taylor (1986) caution that due to the large fractionation factors between mineral and water, the $\delta^{18}O$ in the low temperature regimes could actually increase by interaction with low temperature waters. The isotope systematics of fluid-rock exchange are ultimately dependent on the initial composition of the fluids, the rock and the temperature.

4.6 Metamorphism of Hydrothermally Altered Rocks

Metamorphism of hydrothermal ore deposits and their wall-rock alteration is not a popular topic of research. For this reason not much is known about the effects of metamorphism on hydrothermally altered rocks. This hiatus in our knowledge of hydrothermal geology, in part, stems from the fact that many hydrothermal mineral assemblages are in first approximation identical to those that occur in metamorphic facies (Table 4.3).

It is clear from the simplified list of minerals given in Table 4.3 that the mineral assemblages, at least from the zeolite through to amphibolite facies, are more or less the same as the hydrothermal minerals of altered rocks. It is, of course, possible that in hydrothermally altered wall rocks, analyses of individual mineral species would reveal subtle compositional differences, such as the Fe/Mg of chlorites, or the Ba content of feldspars. In any case, many processes normally interpreted to be due to regional metamorphism, are in fact hydrothermal alteration effects. Notably this is the case of "sea-floor metamorphism", entirely due to infiltration and reaction of sea water with the oceanic mafic rocks. Although this can be regarded as a case of semantics – after all hydrothermal alteration is a type of metamorphism – it is advisable to try and separate the traditional metamorphic facies from the effects of mineral changes in response to interaction of the rocks with hot fluids. The

Table 4.3. Simplified table of metamorphic facies and corresponding mineral assemblages. After Best (1982)

Facies	Characteristic assemblages
Zeolite	Quartz + laumontite + chlorite
Prehnite–pumpellyite	Prehnite + pumpellyite + quartz
Glaucophone-lawsonite (blueschist)	Glaucophone + lawsonite; jadeite + quartz + aragonite
Greenschist	Albite + epidote + actinolite ± chlorite ± calcite in mafic rocks; pyrophyllite in pelitic rocks
Amphibolite	Hornblende + plagioclase in mafic rocks; kyanite in pelitic rocks
Granulite	Augite + orthopyroxene + plagioclase; Fe-Mg garnet
Eclogite	Feldspar-free assemblages; jadeite-rich clino-pyroxene and pyrope-rich garnet in mafic rocks
Contact metamorphism	Greenschist to amphibolite facies assemblages in contact aureoles of igneous intrusions; andalusite in pelitic rocks

distinction is unfortunately not always clear, as is the case for the extensive, regional scale talc-carbonate, carbonate and sericitic alteration of rocks in Archean greenstone belts (Chap. 15). For our purposes, therefore, metamorphism refers to solid state changes that take place at the regional scale during tectogenetic events (see definition in Chap. 3).

Most mineral deposits, even the more recent ones, that have gone through an orogenic cycle, are metamorphosed to a greater or lesser extent. In the lower grades of metamorphism (up to greenschist facies), the hydrothermal minerals are more or less already equilibrated to the conditions of temperature and pressure, and mineral changes – if any – are not anticipated to be substantial. The propylitic zone (chlorite + epidote ± carbonate ± pyrite) of a porphyry system would be difficult to detect in an area of greenschist facies metamorphism. However, the presence of unusually abundant pyrite, mineral assemblages transitional into sericitic zones, and their restriction to particular areas, may give away the true origin of the minerals in question. Things become considerably more difficult at higher grades of metamorphism (amphibolite to granulite facies). In these conditions it is sometimes difficult even to decide whether a given ore deposit is pre-, syn-, or post-metamorphic. The situation may become even more confused when retrograde metamorphism has taken place. In environments of medium to high-grade metamorphism, fabric and textural studies of the ore minerals and the enclosing lithologies are obviously very important. These studies can establish whether or not the ore minerals were subjected to the same deformation and metamorphic events as the enclosing rocks, taking into due account effects of re-mobilisation and re-crystallisation of the more ductile components (e.g. galena) during metamorphism. Equally important in the search for evidence of hydrothermal alteration in medium-high-grade metamorphic rocks (upper greenschist to amphibolite facies), are studies of whole rock geo-

Table 4.4. Mineral assemblages associated with metamorphosed sulphide orebodies. After Stanton (1982)

Gamsberg, RSA	Broken Hill, AUS	Gorob, Namibia
Sillimanite	Sillimanite	Sillimanite
Fayalite	Fayalite	Kyanite
Clinopyroxene	Staurolite	Staurolite
Orthopyroxene	Hedenbergite	Cordierite
Hedenbergite	–	Anthophyllite
Grunerite	Grunerite	Almandine
Cordierite	Almandine	Biotite
Almandine	Biotite	Muscovite
Biotite	Muscovite	Chlorite
Muscovite	Chlorite	Prehnite
Quartz	Quartz	Quartz

chemistry patterns and mineral chemistry. For example, low K + Na and Al enrichment would be expected in a metamorphosed acid-sulphate alteration zone. Certain key minerals, such as garnet, magnetite, muscovite, chlorite, may reveal unusual concentration and/or ratios of elements (Zn, Ba, Mn, Fe/Mg) which may be indicative of a hydrothermal environment.

The problem of the effects of metamorphism on ore deposits has been investigated for many years by Stanton (1972, 1982, 1983), who concentrated his efforts on the sediment-hosted stratiform massive sulphide deposits. Stanton's work therefore refers to "hydrothermal sediments", rather than wall rock "epigenetic" alteration. Nevertheless, from his work and that of others referred to later, some inferences can be made that may apply to epigenetic alteration.

Stratiform ore deposits are more or less concordant, lens-shaped, and are enclosed in metapelitic lithologies with distinctive metamorphic mineral assemblages, as indicated in Table 4.4. The ore minerals are considered as chemical precipitates deposited with the original sediments. From the viewpoint of an exploration geologist, it must be realised that certain metamorphic assemblages; especially if confined to restricted areas, may indeed represent the metamorphic equivalent of hydrothermal precursor minerals. Table 4.5, also compiled from Stanton (1982), lists a range of minerals usually found in medium-grade metamorphic environments, together with their possible hydrothermal precursors.

In a later and comprehensive paper, Stanton (1989) deals with the topic of the effects of regional metamorphism on chemical sediments. On the basis of detailed geological, mineralogical and geochemical observations, this author explains the intimate relationships in metamorphosed exhalites, between bedded silicate minerals, oxides, sulphides and carbonates, in terms of a "precursor principle". The theory of the precursor principle suggests that the regionally metamorphosed bedded oxides, carbonates, sulphates, sulphides and silicates are derived directly from in situ, low-temperature, sedimentary-diagenetic-alteration precursor minerals and materials and not from Barrovian prograde metamorphic reactions. As the

Table 4.5. Metamorphic minerals, their possible precursors and original hydrothermal materials. Based on Stanton (1982)

Metamorphic minerals	Possible precursors	Possible origin
Chlorite	Montmorillonite	Altered volcanic glass
Muscovite	Illite	Diagenetic illite derived from kaolinite, or epithermal alteration
Almandine garnets	Chamosite	Hydrothermal sediments, oolites
Sillimanite, kyanite, andalusite	Kaolinite, alumino--silicate clays	Acid leaching of sulphate-bearing solutions, epithermal systems
Fibrolite	Halloysite, gibbsite	

precursor principle applies to the economically important family of stratiform exhalative ore deposits, we will briefly review Stanton's ideas on this topic. Although beyond the scope of this book, it is worthy of mention that a major implication of Stanton's precursor principle may involve a re-interpretation of regional metamorphic grades and zones. According to this principle, the regional metamorphic mineral zonations, which are normally attributed to progressively increasing degrees of heat and pressure, are a reflection of the sedimentary facies and associated diagenetic changes. The reader who wishes to learn more on this topic should consult Stanton (1982, 1989)

Exhalative activity on the floor of seas, lakes and lagoons leads to the stratiform accumulations containing various amounts of Fe, Zn, Cu, Pb sulphides, Fe hydrooxides, Ba and Ca sulphates, carbonates, hydrous silica gels as well as a number of clays, chlorites, mixed layer clay-chlorite and zeolites. These accumulations form what is generally known as exhalites or chemical sediments, of which the great occurrences of Proterozoic banded iron formations are perhaps one of the most important examples (see Chaps. 5 and 13). These chemical sediments are subsequently subjected to diagenetic changes and in many cases to regional metamorphism. During the diagenetic and metamorphic phenomena the sulphide, oxides, sulphates and carbonate undergo grain growth and coarsening. Thus, for example, coarse-grained layers of barite and anhydrite are formed from Ba and Ca sulphates, fine cherts or quartzites from the dehydration of hydrous silica gels, while Fe oxides such as hematite and/or magnetite are derived from Fe hydroxides (see later).

Stanton contends that if the above-mentioned transformations do occur for these exhalative materials (as is generally accepted), then the same must be true for those silicate minerals, which are commonly found associated with the stratiform ores (e.g. biotite, garnet, staurolite, pyroxene, amphibole, feldspars and Al-silicate polymorphs). Therefore, as previously indicated, the author questions the validity of the concept that these silicate minerals are formed through a series of metamorphic reactions in response to temperature gradients. The lack of metamorphic diffusion over substantial distances (other than a few millimetres), co-existing

mineral phases at the thin section scale, and textural evidence (e.g. muscovite-biotite or quartz-muscovite assemblages in metamorphic rocks, do not show any evidence of reactions yielding garnet or sillimanite +K-feldspar respectively), imply that metamorphism is isochemical and that "each metamorphic mineral grain now present represents the in situ growth and/or transformation of a pre-metamorphic material of similar overall composition, or that it is one of two or more products of the in situ breakdown of a pre-metamorphic material of appropriate composition. These may be referred to as precursors" (Stanton 1989, p.543).

Common examples of precursor chemical sediment or exhalite and corresponding metamorphosed exhalite include (see also Tables 4.5, 4.6, 4.7): (1) hydrous forms of silica (possibly a gel) in sea floor exhalations changing to cherts; and (2) Fe hydroxides changing to hematite and/or magnetite. In the latter case the dehydration-reduction sequence envisaged is as follows (Stanton 1989, p. 545):

$Fe(OH)_3 \rightarrow FeO.OH + H_2O;$

limonite   goethite

$2FeO.OH \rightarrow Fe_2O_3 + H_2O;$
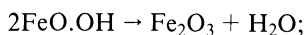
goethite   hematite

$Fe_2O_3 + H_2O + Fe^{2+} \rightarrow Fe_3O_4 + 2H^+.$
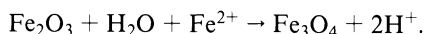
magnetite

In this way the magnetite of banded iron formations and magnetite-quartzites (a common exhalite in many metamorphic terranes) may be formed from the transformation of in situ limonite and goethite. Garnet is often a component of banded quartz-magnetite rocks and as such it may have been formed from a precursor mineral, which could have been a sedimentary-diagenetic Fe-Mn chlorite chamosite. The exhalites of the Broken Hill Pb-Ag-Zn deposits in Australia, are associated with metamorphic minerals such as sillimanite, which may have derived from kaolinite, and gahnite ($ZnAl_2O_4$) derived from a kaolinite with adsorbed Zn and muscovite from illite. Similarly, cordierite is thought to be derived from aluminous clay-chlorite material. The common intergrowths of cordierite-sillimanite are explained as the result of isochemical, in situ metamorphism of clay-chlorite with minor kaolinite-gibsite. In the same way many spinels, of which gahnite ($ZnAl_2O_4$) referred to above is an example, would be formed from clay precursors with adsorbed cations such as Fe^{2+}, Zn^{2+} and Mn^{2+}.

The mechanisms that are thought to be important to explain the regional metamorphic changes of precursor materials are: (1) coarsening and ordering of sedimentary/diagenetic materials such as carbonates, sulphides, clays etc. (2) gel-solid changes, that is the growth of ordered crystal structures from amorphous materials, such as silica gels to cherts, gel goethite to hematite/magnetite; and (3) solid-solid changes of mixed-layer crystal structures that formed during exhalations and diagenesis, such as illite $\rightarrow$ muscovite, kaolinite-gibsite mixed layers $\rightarrow$ sillimanite, kaolinite $\rightarrow$sillimanite, chamosite $\rightarrow$ almandine garnet. Stanton (1989) regards the materials under (1) as simple precursors and those under (2) and (3) as complex precursors.

Table 4.6. Silicate, oxide and sulphide facies mineral assemblages at Aggeneys, South Africa, and their possible precursors. After Ryan et al. (1986)

Facies	Metamorphic assemblage	Possible precursors
Silicate	Quartz, magnetite, grunerite, cummingtonite, fayalite, spessartine garnet	Fe-silicates greenalite, chamosite, stilpnomelane?
Oxide	Magnetite, quartz, garnet biotite	Banded hematite-chert
Sulphide	Quartz, pyrite, pyrrhotite	Quartz and pyrite

The polymetallic, sediment-hosted, exhalative massive sulphide deposits of Aggeneys-Gamsberg in South Africa occur within the Namaqua Metamorphic Complex, a high- to medium-grade province extending along the southern flank of the Kaapvaal craton. The geology and mineralisation of these important deposits are discussed in Chapter 13. Here it will suffice to mention that the original host sequences may have included rhyolitic rocks, volcanic sediments and cherts. At Gamsberg these rocks are metamorphosed to include quartzites, quartz-biotite-muscovite-sillimanite schist (Pella Formation), garnet-pyroxene-amphibolite-magnetite, quartz-sericite-sillimanite schist, quartz-grunerite-garnet, magnetite-quartz-barite (Gams Formation), amphibolites and quartz-muscovite schist. At Aggeneys the ore formation contains quartzite, quartz schist, garnet quartzite, magnetite-quartz-amphibolite, magnetite-barite and baritic quartz schist. Of particular interest is the garnet quartzite (+ cordierite + sillimanite + biotite), because this unit is thought to be the metamorphic equivalent of a siliceous-aluminous precursor feeder zone (McGregor 1986). The mineralised rocks (galena, sphalerite, chalcopyrite, pyrrhotite and pyrite) and their associated mineral assemblages at Aggeneys are therefore the metamorphic equivalent of hydrothermal exhalites of silicate, oxide and sulphide facies, as outlined in Table 4.6. The interpretation of the silicate mineral assemblages of the Gams Formation, and their pre-metamorphic precursors, are given in Table 4.7.

The precursor principle may be applied to epigenetic hydrothermal mineralisation and this may assume great importance in the exploration of volcanogenic base metal and precious metal deposits in terranes of high-grade metamorphism. Aluminous minerals such as clays and chlorite are common products of the hydrothermal alteration of wall rocks during metasomatic exchanges with the mineralising fluids. The occurrence of these minerals in restricted zones implies the presence of hydrothermal fluid conduits (alteration pipes) which underlie volcanogenic deposits. Following deformation and metamorphism it becomes extremely difficult to recognise what could have been an alteration pipe. During metamorphism, the aluminous hydrothermal alteration minerals change to aluminous metamorphic assemblages which include garnet, cordierite and staurolite. Therefore, the recognition of localised high-grade aluminous assemblages may indicate an ancient hydrothermal pipe. We return to this topic in Chapter 12, in the

Table 4.7. Facies and metamorphic assemblages of the Gamsberg deposit, South Africa, and their possible pre-metamorphism precursors. After Rozendaal and Stumpfl (1984)

Facies	Metamorphic assemblage	Precursor mineralogy
Oxide	Quartz, apatite, magnetite hematite, barite	Chert, magnetite, collophane hematite, barite
Carbonate--silicate	Pyroxenoid, garnet, amphibole quartz, pyrrhotite, magnetite	Fe-Mn carbonate, chamosite, chert, quartz, Fe sulphide
Silicate ± carbonate ± sulphide	Quartz, garnet, amphibolite, chalcopyrite, pyrite, pyrrhotite	Chert, quartz, chamosite, Mn-Fe carbonate, Fe sulphide
Sulphide	Quartz, garnet, amphibolite, orthopyroxene, pyroxenoid, olivine, apatite, pyrrhotite, sphalerite, graphite	Pyrrhotite, sphalerite, galena, chert, quartz, Fe-Mn carb., chamosite, organic material
Sulphide	Quartz, sillimanite, muscovite, K-feldspar, pyrite, sphalerite, graphite	Quartz, chert, pyrite, sphalerite, illite, kaolinite, organic material, detrital K-feldspar(?)
Silicate	Quartz, garnet, K-feldspar, clinopyroxene, amphibole, pyrrhotite, pyrite	Quartz, chert, chamosite, Mn-Fe carb., illite, Fe sulphide, detrital K-feldspar(?)
Carbonate ± silicate	Calcite, rhodocrosite, quartz, garnet, K-feldspar, clinopy- roxene, amphibole, magnetite, pyrrhotite	Fe-Ca-Mn carb., chert, quartz, illite, kaolinite, chamosite, magnetite, Fe sulphide

discussion of the massive sulphide deposits on the Matchless Amphibolite Belt in Namibia.

McLeod and Stanton (1984) worked on the mineral chemistry of phyllosilicate assemblages (chlorite + talc ± phlogopite ± biotite and chlorite + muscovite) associated with some of the Paleozoic Pb-Zn massive sulphide deposits of New South Wales and Tasmania (Woodlawn, Captain's Flats, Rosebery, Que River etc.). These deposits are thought to represent the ancient and metamorphosed (green-schist facies) equivalent of the Japanese kuroko-type ores. The authors concluded that these phyllosilicate assemblages derived from precursor clay minerals, such as montmorillonite and illite. More specifically, they consider that crystallisation of chlorite and muscovite could be derived from a reaction of the types: kaolinite + mixed layer illite-montmorillonite, to produce mixed layer illite-dioctahedral chlorite and finally chlorite + muscovite; or, montmorillonite + kaolinitic clay to form illite hydromica + muscovite (McLeod and Stanton 1984 and references therein).

Hemley et al. (1980) investigated mineral equilibria in the system Al_2O_3-SiO_2-H_2O, and their results suggest that minerals commonly found in the argillic zones of hydrothermal deposits can change to phases that are stable at higher temperatures
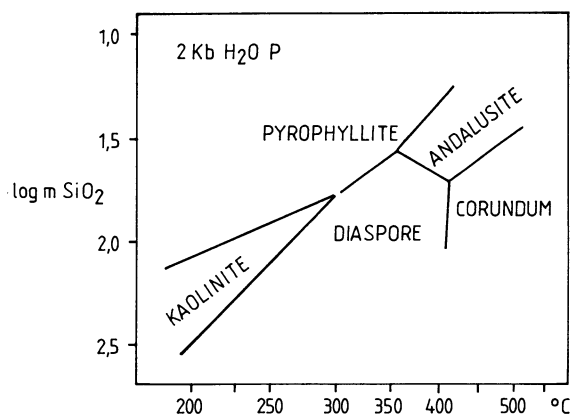
Fig. 4.15. Stability fields of aluminous minerals at 2 kbar water pressure (After Hemley et al. 1980)

and can be found in metamorphic environments. Figure 4.15 refers to the stability of aluminous minerals as a function of temperature and silica activity at 2 kbar. It can be seen that kaolinite is stable at low temperatures, and with increasing silica activity and temperature, pyrophyllite and andalusite come in at progressively higher temperatures. Pyrophyllite has a large stability field, in terms of both silica and temperature. At high silica activity this mineral can be stable up to about 450°C. At lower silica activities, but still at high temperature (250–500°C), diaspore and corundum become stable. The mineral changes of Fig 4.15 are effectively dehydration reactions, as also corroborated by Stanton (1983), who suggested that sillimanite at the Geco stratiform deposit, Canada, is derived from a kaolinitic precursor. The reactions considered by Hemley and coworkers are:

2kaolinite +2quartz = pyrophyllite + H_2O;

2kaolinite = pyrophyllite + 2diaspore;

pyrophyllite + 6diaspore = 4andalusite + $4H_2O$;

2diaspore = corundum + H_2O.
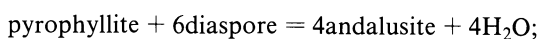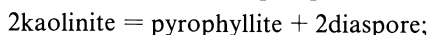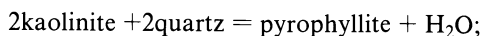
An example of metamorphosed epigenetic hydrothermal alteration comes from a 2000-Ma-old hydrothermal system, in the acid volcanic rocks of the Rooiberg group (Transvaal, South Africa). Here a zone of alteration is characterised by the assemblage dickite-pyrophyllite-quartz-diaspore-zunyite-pyrite. The presence of pyrophyllite and diaspore is interpreted as being due to the low-grade metamorphism of a zone of advanced argillic alteration in an ancient epithermal system (Martini 1988). Another example of documented metamorphism of hydrothermal deposits is afforded by the Fe-Mn-rich lithologies associated with massive sulphide deposits in the southern Appalachians (Georgia, USA). These rocks were subjected to deformation and metamorphism during the Early Ordovician and the Carboniferous, following a collision event with rocks autochthonous to the African craton. The Fe-Mn-rich rocks, Fe formations and enclosing mafic schists are metamorphosed to garnet, kyanite and sillimanite grades (Wonder et al. 1988 and references therein). The petrology and geochemistry of the Fe-Mn-rich rocks, including the so-called coticules or garnet-bearing quartzites, and garnet-bearing Fe formations,

were investigated by Wonder et al. (1988). They found that these rocks originated by the metamorphism of hydrothermal sediments deposited by hot springs on the sea floor. The precursor materials probably contained clays, and Fe and Mn oxides (e.g. todokorite, goethite).

4.7 Detection of Hydrothermal Alteration by Spectral Remote Sensing

Spectral remote sensing has become an important tool for the detection of hydrothermal alteration. The theory of spectral discrimination of rocks and

Table 4.8. Some of the minerals that are typically detected at certain wave lengths in the visible and infrared spectrum

Spectral region	Minerals
Visible and near infrared 0.35 to 1.0 μ	Jarosite, hematite, goethite
Shortwave infrared 1.0 to 2.5 μ	Hydroxyl-bearing minerals: clays, talc, chlorite, alunite, pyrophyllite, jarosite, diaspore, illite, calcite, dolomite
Thermal infrared 8 to 14	Silica, carbonate μ
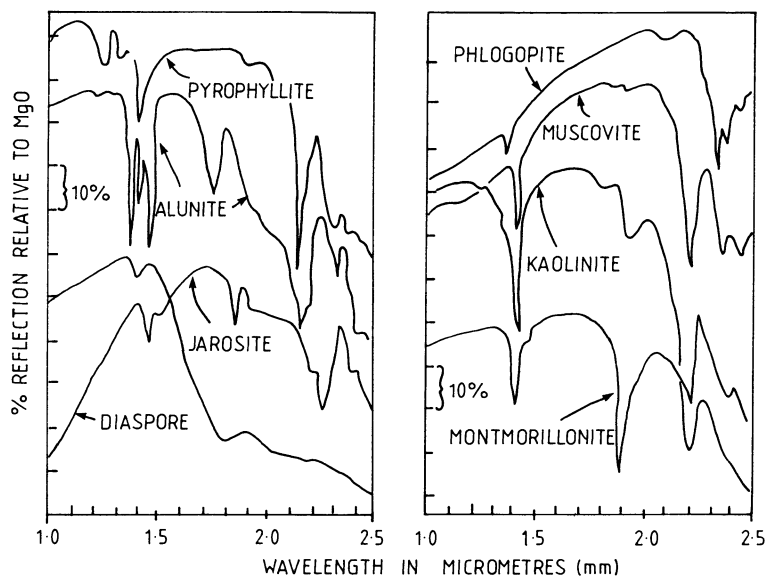
Fig. 4.16. Spectral reflectance of some common alteration minerals (After Hunt and Ashley 1979)
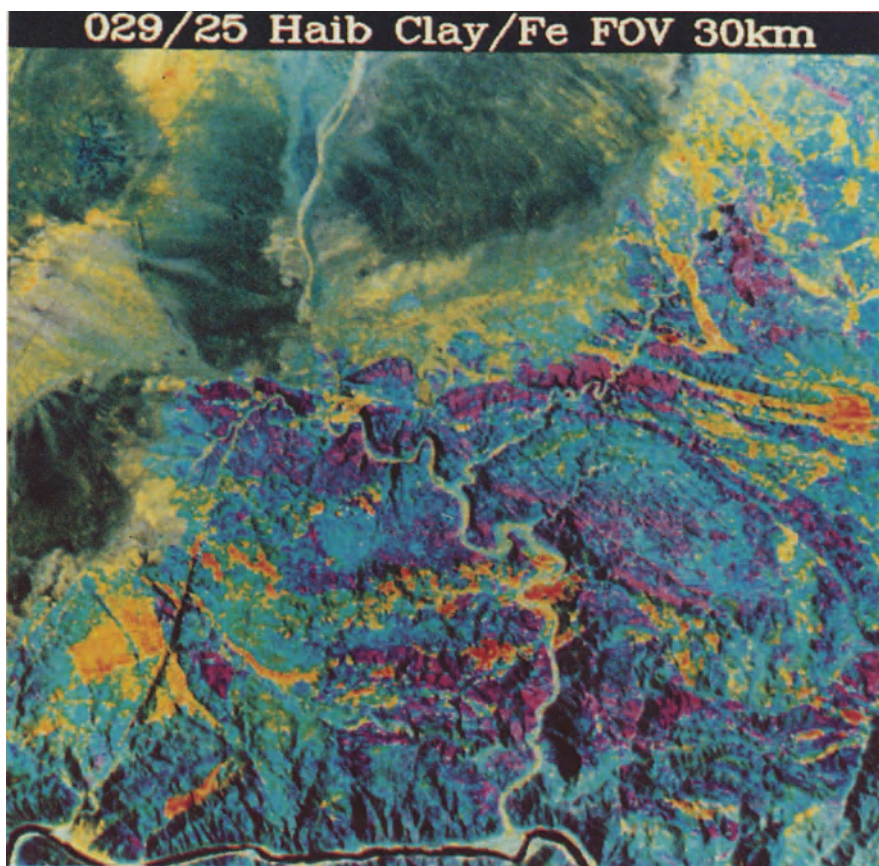
Plate 4.16. Alteration mapping: Digitally enhanced LANDSAT TM image showing sericitic alteration (*red-orange areas in lower centre of image*) at the Haib porphyry Cu-Mo system in southern Namibia. Other *orange-coloured* areas are probably due to a clay signature from rocks of the Karoo Sequence. The system is approximately 2000 Ma old and has well-developed sericitic and potassic alteration envelopes (Minnitt 1986). The image was supplied by Dr. A. A. de Gasparis

minerals is beyond the scope of this book; for principles and details the reader should consult the issue of Economic Geology devoted to remote sensing (vol.78, No.4, 1983), and in particular the papers by Goetz et al. (1983), Whitney et al. (1983) and Gladwell et al. (1983). Other useful publications include Hunt and Ashley (1979), Hunt and Salisbury (1970, 1971), Hunt et al. (1971), and the recent book on remote sensing by Lillesand and Kiefer (2nd edition, 1987).

Details of spectral reflectance of rocks and minerals in the visible to thermal infrared wavelength region are known from field and laboratory work, by recording data with a spectrophotometer (Hunt and Ashley 1979). The detection of spectral reflectance is also obtained by aircraft and spacecraft. The spectral features of altered rocks are a function of electronic and vibrational processes involving Fe and the OH group respectively. Each displays curves with character-

istic slopes and absorption bands that are diagnostic of the surface materials. Table 4.8 gives the three main spectral regions and some of the minerals that can be detected in each.

Spectral features due to vibrational processes are especially useful, as they report OH-bearing minerals that are normally present in hydrothermally altered rocks. For this reason,the short wavelength region between 1.0 and 2.5 μm is ideal for the detection of clays and zones of acid-sulphate alteration with alunite present. Figure 4.16 illustrates an example of near infrared spectra of some typical alteration minerals. In 4.16 it is worth noting that alunite has a well defined, isolated, and therefore diagnostic, absorption band near 1.77 μm. Plate 4.16 shows a LANDSAT TM image of an area north of the Orange River (South Africa, Namibia border) where the Haib porphyry Cu-Mo system is situated (Minnitt 1986). In Plate 4.16 the sericitic alteration associated with this porphyry occurrence is clearly shown by the orange-red areas.

References

Babcock R S (1973) Computational models of metasomatic processes. Lithos 6:279–290
Batchelor R A, Bowden P (1985) Petrogenetic interpretation of granitoid rock series using multicationic parameters. Chem Geol 48:43–55
Best, M G (1982) Igneous and metamorphic petrology. Freeman, San Francisco, New York, 630 pp
Bonatti E (1978) The origin of metal deposits in the oceanic lithosphere. Sci Am 238:54–61
Bowden P (1985) The geochemistry and mineralisation of alkaline ring complexes in Africa (a review). J Afr Earth Sci 3:17–40
Bowden P, Kinnaird J A, Abaa S I, Ike E C, Turaki U M (1984) Geology and mineralisation of the Nigerian anorogenic ring complexes. Geol Yahrb 56:1–68
Brogger W C (1921) Die Eruptivgesteine des Kristaniagebiets IV. Das Fengebiet in Telemarken, Norwegen. Nors Vidensk Akad Oslo Skr Mat Nat 9:408
Burnham C W, Ohmoto H (1980) Late stage processes of felsic magmatism. In: Ishihara S, Takenouchi S (eds) Granitic magmatism and related mineralisation. Soc Min Geol Jpn 8:1–11
Burt D M (1981) Acidity-salinity diagrams – Application to greisen and porphyry deposits. Econ Geol 76:832–843
Camus F (1975) Geology of the El Teniente orebody with emphasis on wall-rock alteration. Econ Geol 70:1341–1372
Carmichael I S E, Turner F J, Verhoogen J (1974) Igneous petrology. McGraw-Hill, New York, 739 pp
Criss R E, Taylor H P (1986) Meteoric-hydrothermal systems. In: Valley J W, Taylor H P, O'Neil J R (eds) Stable isotopes in high temperature geological processes. Reviews in mineralogy, vol 16. Min Soc Am, pp 373–424
Crocker I T (1985) Volcanogenic fluorite-hematite deposits and associated pyroclastic rock suite at Vergenoeg, Bushveld Complex. Econ Geol 80:1181–1200
Deer W A, Howie R A, Zussman J (1967) Rock forming minerals, vol 3. Longmans, London, 270 pp
De la Roche.H, Leterrier J, Grand Claude P, Marchal M (1980) A classification of volcanic and plutonic rocks using R1-R2 diagrams and major element analyses – its relationship with current nomenclature. Chem Geol 29:183–210
Dietrich R V (1985) The tourmaline group. Van Nostrand Reinhold, New York, 300 pp
Economic Geology (ed) (1974) Stable isotopes as applied to problems of ore deposits. Econ Geol 69,6
Economic Geology (ed) (1983) An issue devoted to techniques and results of remote sensing. Econ Geol 78,4

Edmond J M, von Damm K (1983) Hot springs on the ocean floor. Sci Am 248:70–85

Einaudi M T, Meinert L D, Newberry R J (1981) Skarn deposits. Econ Geol 75th Anniv Vol: 317–391

Evans A M (1987) An introduction to ore geology, 2nd edn. Blackwell, Oxford, 358 pp

Faure G (1986) Principles of isotope geology, 2nd edn. John Wiley & Sons, New York, 589 pp

Felsche J, Herrmann, A G (1978) Yttrium and lanthanides. In: Wedepohl K H (ed) Handbook of Geochemistry, vol II/5. Springer, Berlin, Heidelberg, New York, pp 57–71-0

Ferry J M (1983) Regional metamorphism of the Vassalboro Formation, south-central Maine, USA: a case study of the role of fluid in metamorphic petrogenesis. J Geol Soc London 140:551–576

Ford J H (1978) A chemical study of alteration at the Panguna porphyry copper deposit, Bougainville, Papua New Guinea. Econ Geol 73:703–720

Gladwell D R, Lett R E, Lawrence P (1983) Application of reflectance spectrometry to mineral exploration using portable radiometers. Econ Geol 78:699–710

Goetz A F H, Rock B N, Rowan L C (1983) Remote sensing for exploration: An overview. Econ Geol 78:573–590

Grant J A (1986) The isocon diagram – A simple solution to Gresens' equation for metasomatic alteration. Econ Geol 81:1976–1982

Green G R, Ohmoto H, Date J, Takahashi T (1983) Whole-rock oxygen isotope distribution in the Fukazawa-Kosaka area, Hokoruku District, Japan, and its potential application to mineral exploration. Econ Geol Monogr 5:395–411

Gregory R T, Criss R E (1986) Isotopic exchange in open and closed systems. In: Valley J W, Taylor H P, O'Neil J R (eds) Stable isotopes in high temperature processes. Reviews in mineralogy, vol 16. Min Soc Am, pp 91–128

Gresens R L (1967) Composition-volume relationships of metasomatism. Chem Geol 2:47–65

Guilbert J M, Park C F (1986) The geology of ore deposits. Freeman, New York, San Francisco, 985 pp

Hanson G N (1980) Rare earth elements in petrogenetic studies of igneous systems. Annu Rev Earth Planet Sci 8:371–406

Hardie L A (1987) Dolomitisation: A critical view of some current views. J Sediment Petrol 57:166–183

Hemley J J, Jones W R (1964) Chemical aspects of hydrothermal alteration with emphasis on hydrogen metasomatism. Econ Geol 59:538–569

Hemley J J, Hostetler P B, Gude A J, Mountjoy W T (1969) Some stability relations of alunite. Econ Geol 64:599–612

Hemley J J, Montoya J W, Marinenko J W, Luce R W (1980) Equilibria in the system Al_2O_3-SiO_2-H_2O and some general implications for alteration/mineralisation processes. Econ Geol 75:210–228

Henley R W, Ellis A J (1983) Geothermal systems ancient and modern: a geological review. Earth Sci Rev 19:1–50

Hunt G R, Ashley R P (1979) Spectra of altered rocks in the visible and near infrared. Econ Geol 74:1613–1629

Hunt G R, Salisbury J W (1970) Visible and near-infrared spectra of minerals and rocks: I. Silicate minerals. Modern Geol 1:283–300

Hunt G R, Salisbury J W (1971) Visible and near-infrared spectra of minerals and rocks: II Carbonates. Modern Geol 2:23–30

Hunt G R, Salisbury J W, Lenhoff C J (1971) Visible and near-infrared spectra of minerals and rocks: III. Oxides and hydroxides. Modern Geol 2:195–205

Keays R R, Nickel E H, Groves D I, McGoldrick P J (1982) Iridium and palladium as discriminants of volcanic-exhalative hydrothermal, and magmatic nickel sulfide mineralisation. Econ Geol 77:1535–1547

Kinnaird J A (1985) Hydrothermal alteration and mineralisation of the alkaline anorogenic ring complexes of Nigeria. J Afr Earth Sci 3:229–252

Kirwin D J (1985) Tourmaline breccia pipes. Msc Thesis, James Cook Univ, N Queensl, 139 pp

Larson P B, Taylor H P (1986) $^{18}O/^{16}O$ relationships in hydrothermally altered rocks from the Lake City caldera, San Juan Mountains, Colorado. J Volcanol Geothermal Res 30:47–82

Leblanc M, Lbouabi M (1988) Native silver mineralisation along a rodingite tectonic contact between serpentinite and quartz-diorite (Bon Azzer, Morocco). Econ Geol 83:1379–1391

Lillesand T M, Kiefer R W (1987) Remote sensing and image interpretation, 2nd edn. John Wiley & Sons, New York, 612 pp

Lottermoser B L (1990) Rare-earth element and heavy metal behaviour associated with the epithermal gold deposit on Lihir Island, Papua New Guinea. J Volcanol Geothermal Res 40:269–289

Lovering T G, Heyl A (1974) Jasperoid as a guide to mineralization in the Taylor mining district and vicinity near Ely, Nevada. Econ Geol 69:46–58

Martini J E J (1988) As-Zn mineralisation associated with a Proterozoic geothermal system in the Rooiberg Group. S Afr J Geol 91:337–345

McGregor G J (1986) Geology of the Black Mountain orebody. In: Abstr Geocongress '86, Johannesburg. Geol Soc S Afr, pp 1025–1028

MacKenzie I F (1983) Geology and geochemistry of tungsten mineralisation at Doctor Hill and Falls creek, Central Westland, New Zealand. MsC thesis, Victoria Univ, Wellington, 160 pp

McLeod R L, Stanton R L (1984) Phyllosilicate and associated minerals in some Paleozoic stratiform sulfide deposits of south-eastern Australia. Econ Geol 79:1–22

Meyer C, Hemley J J (1967) Wall rock alteration. In: Barnes H L (ed) Geochemistry of hydrothermal ore deposits, 1st edn. Holt Rinehart & Winston, New York, pp 166–235

Michard A (1989) Rare earth element systematics in hydrothermal fluids. Geochim Cosmochim Acta 53:745–750

Minnitt R C A (1986) Porphyry copper-molybdenum mineralisation at Haib river, South West Africa/Namibia. In: Anhaeusser C R, Maske S (eds) Mineral deposits of southern Africa, vol 2. Geol Soc S Afr, pp 1567–1585

Moore W J, Nash J T (1974) Alteration and fluid inclusion studies of the porphyry copper orebody at Bingham, Utah. Econ Geol 69:631–645

Morrow D W (1982a) Diagenesis 1. Dolomite — Part 1: The chemistry of dolomitisation and dolomite precipitation. Geosci Can 9:5–13

Morrow D W (1982b) Diagenesis 2. Dolomite-Part2: dolomitizing models and ancient dolostones. Geosci Can 9:95–107

Muecke G K, Moller P (1988) The not-so-rare earths. Sci Am 258:62–67

Nash J T, Granger H C, Adams S S (1981) Geology and concepts of genesis of important types of uranium deposits. Econ Geol 75th Anniv Vol:63–116

Ohmoto H (1986) Stable isotope geochemistry of ore deposits. In: Valley J W, Taylor H P, O'Neil J R (eds) Stable isotopes in high temperature geological processes. Reviews in mineralogy, vol 16. Min Soc Am, pp 491–560

Pearton T N, Viljoen M J (1986) Antimony mineralisation in the Murchison greenstone belt. In: Anhaeusser C R, Maske S (eds) Mineral deposits of Southern Africa, vol 1. Geol Soc S Afr pp 293–321

Phillips G N (1986) Geology and alteration in the Golden Mile, Kalgoorlie, Econ Geol 81:779–808

Phillips G N, Groves D I (1982) Fluid access and fluid-wallrock interaction in the genesis of the Archean gold-quartz vein deposit at Hunt Mine, Kambalda, Western Australia. In: Foster R P (ed) Proc Symp Gold '82. Geol Soc Zimb Spec Publ 1, pp 389–416

Pirajno F, Jacob R E (1987) Sn-W metallogeny in the Damara Orogen, South West Africa/Namibia. S Afr J Geol 90:239–255

Pirajno F, Jacob R E (1988) Gold mineralisation in the intracontinental branch of the Damara Orogen, Namibia. In: Bicentennial Gold '88, Geol Soc Aust Abstr Ser 23:168–171

Pirajno F, Schlögl H U (1987) The alteration-mineralisation of the Krantzberg tungsten deposit, South West Africa/Namibia. S Afr J Geol 90:499–508

Pirajno F, Smithies R H (in press) The FeO/FeO + MgO ratio of tourmaline: a useful indicator of spatial variations in granite-related hydrothermal mineral deposits. J Geochem Expl

Plimer I R (1987) The association of tourmalinite with stratiform scheelite deposits. Mineral Depos 22:82–291

Plimer I R (1988) Reply to the discussion by R H Smithies and F Pirajno: The association of tourmalinite with stratiform scheelite deposits. Mineral Depos 23:314–315

Plimer I R, Kleeman J D (1986) Major and minor element chemistry of biotites in Mole granite, New South Wales, Australia. Trans Inst Min Metall 95:B1–B5

Prins P (1981) The geochemical evolution of the alkaline and carbonatite complexes of the Damaraland igneous province, South West Africa. Ann Univ Stellenbosch Ser A1 Geol 3:145–278

Roberts D E, Hudson,G R T (1983) The Olympic Dam copper-uranium-gold deposit, Roxby Downs, South Australia. Econ Geol 78:799–822

Rose A W, Burt D M (1979) Hydrothermal alteration. In: Barnes H L (ed) Geochemistry of hydrothermal ore deposits. John Wiley & Sons, New York, pp 173–227

Rozendaal A, Stumpfl E F (1984) Mineral chemistry and genesis of Gamsberg zinc deposit, South Africa. Trans Inst Min Metall 93:B161–B175

Ryan P J, Lawrence A L, Lipson R D, Moore J M, Paterson A, Stedman DP, Van Zyl D (1986) The Aggeneys base metal sulphide deposit, Namaqualand district. In: Anhaeusser C R, Maske S (eds) Mineral deposits of Southern Africa, vol 2. Geol Soc S Afr, pp 1447–1473

Sheppard S M F (1986) Characterization and isotopic variations in natural waters. Reviews in mineralogy, vol 16. Min Soc Am, pp 165–183

Siems P (1984) Hydrothermal alteration for mineral exploration workshop. Lecture Manual, Dep Geol Univ Witwatersrand, Johannesburg, S Afr

Slack J F, Herriman N, Barnes R G, Plimer I R (1984) Stratiform tourmalinites in metamorphic terranes and their geologic significance. Geology 12:713–716

Smithies R H, Pirajno F (1988) Comments on the paper by I Plimer: The association of tourmalinite with stratiform scheelite deposits. Mineral Depos 23:313–314

Spooner E T C, Fyfe W S (1973) Subseafloor metamorphism, heat and mass transfer. Contrib Mineral Petrol 42:287–304

Stanton R L (1972) Ore petrology. McGraw-Hill, New York, 713 pp

Stanton R L (1982) An alternative to the Barrovian interpretation? Proc Australas Inst Min Metall 282:11–32

Stanton R L (1983) The direct derivation of sillimanite from a kaolinitic precursor: evidence from the Geco Mine, Manitouwadge, Ontario. Econ Geol 78:422–437

Stanton R L (1989) The precursor principle and the possible significance of stratiform ores and related chemical sediments in the elucidation of processes of regional metamorphic mineral formation. Phil Trans R Soc London A 328:529–646

Taylor H P (1971) Oxygen isotope evidence for large-scale interaction between meteoric ground waters and Tertiary granodiorite intrusions, western Cascade Range, Oregon. J Geophys Res 76: 7855–7874

Taylor H P (1974) The application of oxygen and hydrogen isotope studies to problems of hydrothermal alteration and ore deposition. Econ Geol 69:843–883

Taylor R P, Fryer B J (1980) Multiple-stage hydrothermal alteration in porphyry copper systems in northern Turkey: the temporal interplay of potassic, propylitic, and phyllic fluids. Can J Earth Sci 17:901–926

Taylor R P, Fryer B J (1982) Rare earth element geochemistry as an aid to interpreting hydrothermal ore deposits. In: Evans A M (ed) Mineralisation associated with acid magmatism. John Wiley & Sons, New York, pp 357–365

Taylor R P, Fryer B J (1983) Rare earth element lithogeochemistry of granitoid mineral deposits. CIM Bull 76:74–84

Turner F J, Verhoogen J (1960) Igneous and metamorphic petrology. McGraw-Hill, New York, 693 pp

Verwoerd W J (1966) Fenitisation of basic igneous rocks. In: Tuttle D F, Gittens J (eds) Carbonatites. Wiley Interscience, Amsterdam, New York, pp 295–308

Whitney G, Abrams M J, Goetz A F H (1983) Mineral discrimination using a portable ratio-determining radiometer. Econ Geol 78:688–698

Wonder T D, Spry P G, Windom K E (1988) Geochemistry and origin of manganese rich rocks related to iron-formation and sulfide deposits, Western Georgia. Econ Geol 83:1070–1081

Crustal Evolution, Global Tectonics, Hydrothermal Mineral Deposits and Mineral Exploration – Geotectonic and Metallogenic Analysis of Orogenic Belts

Chapter 5

Crustal Evolution, Global Tectonics and Mineral Deposits

5.1 Introduction

The theory of sea-floor spreading and the "new" global tectonics, including the more recent ideas on accretionary tectonics, has permitted a much clearer understanding of the genesis of mineral deposits. This understanding is essentially provided by a unifying framework within which processes of ore genesis can be integrated. In this way mineralisation types can be related to time-space positions, in specific lithospheric plate settings, and within continuously evolving crustal geodynamic patterns. The spatial distribution of mineral deposits as related to plate tectonic processes has been widely discussed in many papers, especially during the 1970–1980 decade. Consequently, excellent textbooks on the topic were published soon after, which in spite of subsequent advances in more recent years, remain important texts for providing the geologist with an essential background in the study of mineral deposits. The books referred to are those published by Mitchell and Garson (1981), Hutchison (1983) and Sawkins (1990). Equally important in models of ore genesis is an understanding of the evolutionary trends of mineral deposits through the geological ages. This field of study is obviously connected with the evolution of plate configurations and their interactions through time. The works of Watson (1973, 1978), Reed and Watson (1975), Cloud (1976), Goodwin (1981), Lambert and Groves (1981), Meyer (1981, 1988), Hutchinson (1980), and Windley (1984) all deal with these evolutionary trends.

The question of mineral deposition in space and time hinges on the ore generating processes (magmatic, magmatic-hydrothermal, meteoric-hydrothermal, generation of metamorphic fluids, residual and alluvial accumulations), and their occurrence throughout Earth's history in terms of uniformitarian and non-uniformitarian factors. The former include the effects of pressure, temperature, actions of volatile constituents, mechanisms of solution and transport, and magmatic and metamorphic processes. Factors that have changed throughout time (non-uniformitarian) are: atmospheric influence, the role of the biosphere, radioactivity, lithospheric plate configurations, and tectonic styles. Thus it is clear that some deposits are strictly time-related, as for example U. Others, such as porphyry and epithermal systems, are subduction-related and therefore not so much constrained by time, except in terms of erosion level and hence of preservation potential.

In the following sections, we examine the temporal evolution of mineral deposition as a function of the global geotectonic history.
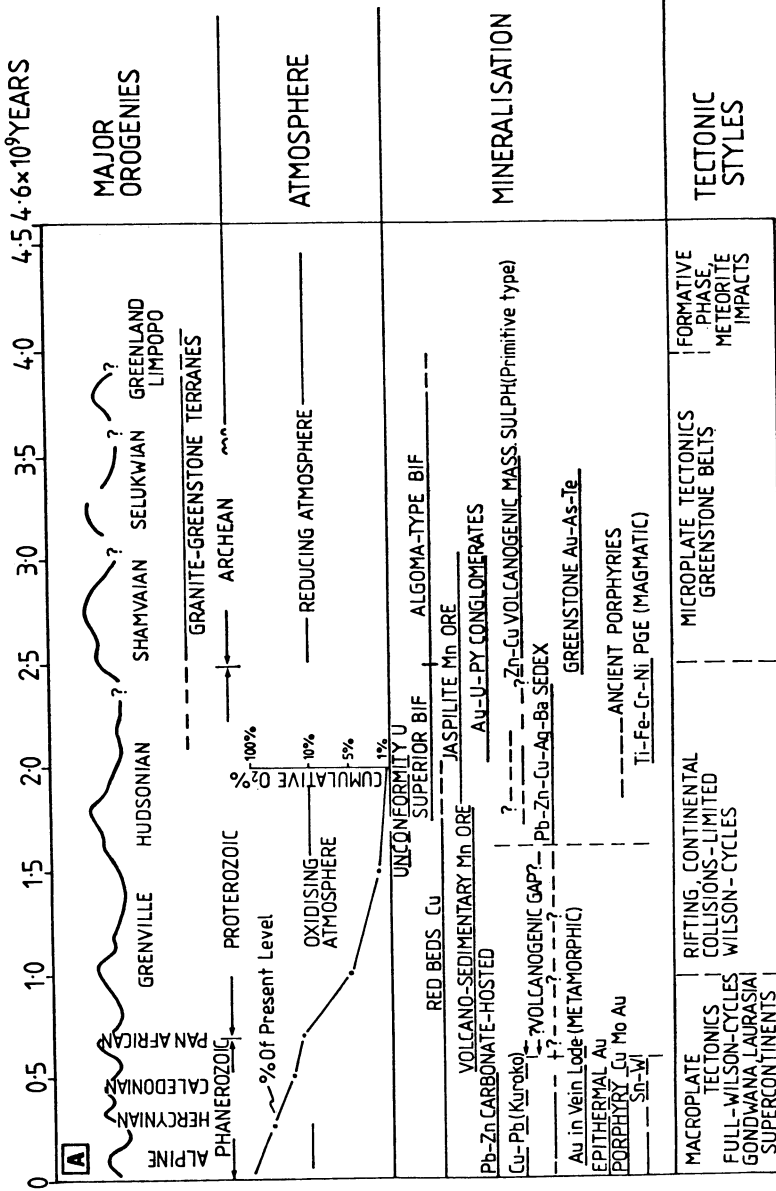
Fig. 5.1A
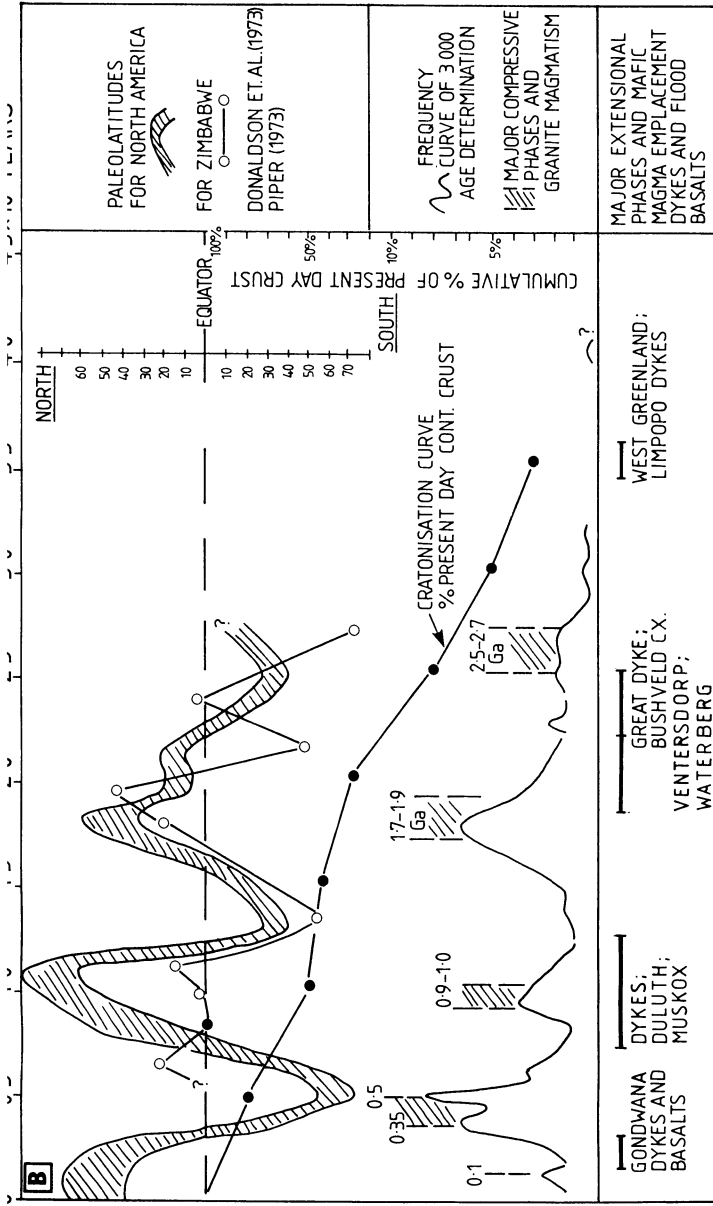
Fig. 5.1A, B. Schematic representation of some of the most important events in the history of the Earth and their relevance to mineral deposition. In **A** the time-dependence of certain mineralising events with tectonic styles and atmospheric oxygenation can be observed. In **B** the possible relationships between palaeomagnetism, global compressive tectonic phases and granite magmatism, the intervening extensional episodes accompanied by mafic magmatism (basic interludes of Read and Watson 1975), are shown. The association, or lack of it, between mineralising and tectono-thermal events can be noted by observing *A* and *B* together, as they are drawn to the same scale. Note, for example, that the "volcanogenic gap" falls between two major periods of granite magmatism and coincides with a "basic interlude". These figures were compiled using data from the following sources: Sutton (1963), Hurley and Rand (1969), Donaldson et al. (1973), Piper (1973), Hunter (1974), Read and Watson (1975), Cloud (1976), Hutchinson (1980), and Windley (1984)

5.2 Tectonic Phases in the Earth's Geological Evolution and Related Metallogeny

Major perturbations within the solid Earth are largely caused by variations in the efficiency of heat transfer and dissipation from the interior of the planet to the surface. These are manifested through tectonic, igneous and metamorphic activities (Meyer 1981). The temporal distribution of ore deposits is therefore a function of these activities, and they in turn are reflected by the frequency of certain metals, and by variations in mineralising environments and ore depositing mechanisms through the geological eras. Summaries of these variations (tectonic cycles, orogenies, magmatism, atmospheric oxygen, metallic accumulations, etc.) are depicted in Fig. 5.1A, B. These figures should be referred to throughout the reading of this section.

The evolution of the Earth's crust can be broadly subdivided into three main stages, which roughly represent the three eons of Archean, Proterozoic (together forming the Precambrian), and the Phanerozoic – this latter eon, representing only about 10% of the recorded geological time. Before proceeding to discuss the patterns of crustal evolution and related metallogeny, it is important to very briefly consider the geological time scale. The chronometric scale defines the geological time boundaries in multiples of a standard year, so that 1 year = 1 a (a stands for annum, Latin for year), 1000 years = 1 ka (k stands for kilo, which is Greek for 1000), $10^6 = 1$ Ma (mega, or 1 million years), $10^9 = 1$ Ga (giga, or 1 billion years). The chronometric subdivisions adopted by the International Union of Geological Science (IUGS) (Sims 1980) are:

- Early Archean   >3500 Ma
- Middle Archean   3500–2900 Ma
- Late Archean   2900–2500 Ma
- Early Proterozoic   2500–1600 Ma
- Middle Proterozoic   1600–970 Ma
- Late Proterozoic   970–570 Ma
- Phanerozoic   570–present

The Archean-Proterozoic transition is generally recognised by the earliest preserved epicontinental basin sedimentary accumulations. However, this boundary is diachronous because cratonic cover sequences began to appear as early as 3 Ga (e.g. Pongola basin in South Africa) and 2.5 Ga elsewhere. The 2.5 Ga boundary coincides with the peak of a global thermal event. The Proterozoic-Phanerozoic boundary is essentially based on the first appearance of exoskeletal invertebrates.

5.2.1 The Archean Eon; Phase of Microplate Tectonics

This phase of our planet's history includes its formative stages, core segregation, major outgassing, meteorite bombardment and the formation of a primeval crust. The main tectonic control is exerted by the thermal regime. Archean heat flow, between 3.8 and 2.5 Ga, is estimated to have been from 2.5 to 4 times its present

value. As a result the lithosphere was presumably thin and somewhat buoyant. Subduction, if any, was probably little developed; rather there was a pattern of small-scale, but nevertheless vigorous, mantle convection which gave rise to a series of small, jostling lithospheric plates. Initially these were made up of mafic and ultramafic rocks. Later, perhaps in response to partial melting of this lithosphere and of the products of erosion of the early consolidated magmas, more felsic material was formed and accreted, leading to the formation of the first sialic microplates. The aggregation of these microplates could have given rise to protocontinents, and eventually to larger near-continental size cratonic areas. These cratons were composed of granitic rocks and greenstone belts.

Crustal Evolution of the Early Archean (ca 4.6 to 3.8 Ga)

Unfortunately no direct evidence is available for the first 800 million years of our planet's history. Modelling of these early stages however, has been aided by the study of the terrestrial-type planets and satellites (Moon, Mars, Venus, Mercury and some of the jovian moons) (Smith 1981; Lewis and Prinn 1984; Lowman 1989). Thus from "comparative planetology", it is thought that the Earth must have experienced a phase of severe meteorite bombardment by basin-forming asteroid-size objects. This bombardment possibly terminated, or abated, at around 4 Ga, and it is considered to have had a very significant effect on the evolution of the early crust, which many workers envisage to have been of mafic-ultramafic composition (Lowman 1989). It is estimated that the protocrust thickness at about 3.9 Ga was somewhere in the range of 5–10 km (Grieve 1980). It has also been suggested that the early crust was a globe-encircling anorthositic layer. The heavy meteorite impacts resulted in pressure release and partial melting of a homogeneous upper mantle with rapid and uniform flooding of the impact-generated basins by basaltic lavas (Frey 1980). As a matter of interest, it is also perhaps worth mentioning that some workers believe that some of the Phanerozoic flood basalt plateaux and rifting events were generated by meteorite impacts (e.g. Alt et al. 1988). Another hypothesis advanced is that remnants of this lunar mare-type volcanism may still exist in some of the Archean greenstone belts.

Nevertheless, a more important effect of the impact basin development was that it allowed hotter and deeper layers to cool rapidly by radiation. Thermal gradients below the basins steepened and would have enhanced whatever convection existed in the upper mantle. It is also plausible that at this stage rapid rifting and breakup of the lithosphere occurred to form a number of small and rapidly moving microplates. Degassing of volatiles released mainly through increased volcanic activity produced the protoatmosphere, leading to condensation of water vapour and the formation of the early oceans (see also Chap. 1). In summary, models of the early Archean suggest that differentiation of the early sialic material led to the development of a protocrust, which was continuously being formed and consumed above vigorously small-scale mantle convection cells (Hargraves 1981, Kröner 1985). Viscous drag subduction led to the development of a re-cycled lithospheric layer of intermediate composition and moderate thickness (10–20 km), decoupled from a still vigorously convecting mantle below.

Crustal Evolution in Mid-Late Archean (ca 3.8 to 2.5 Ga)

Archean rocks are exposed in small areas on all continents as illustrated in Fig.5.2. These regions contain two types of geological terranes: high-grade metamorphism granulite-gneiss terranes, and the low grade metamorphism granite-greenstone terranes. They were formed at different times throughout the Archean and display different characteristics. The "high-grade granulite-gneiss" terranes can occur as linear belts, or isolated remnants within younger cover rocks. These terranes contain three main rock assemblages: quartzo-feldspathic gneiss and migmatites – accounting for almost 80% of the terranes – layered mafic-ultramafic complexes; and suites of metavolcanics and metasediments, the latter including amphibolite, marble, quartzite, micaschist and banded iron formation (BIF). Layered igneous
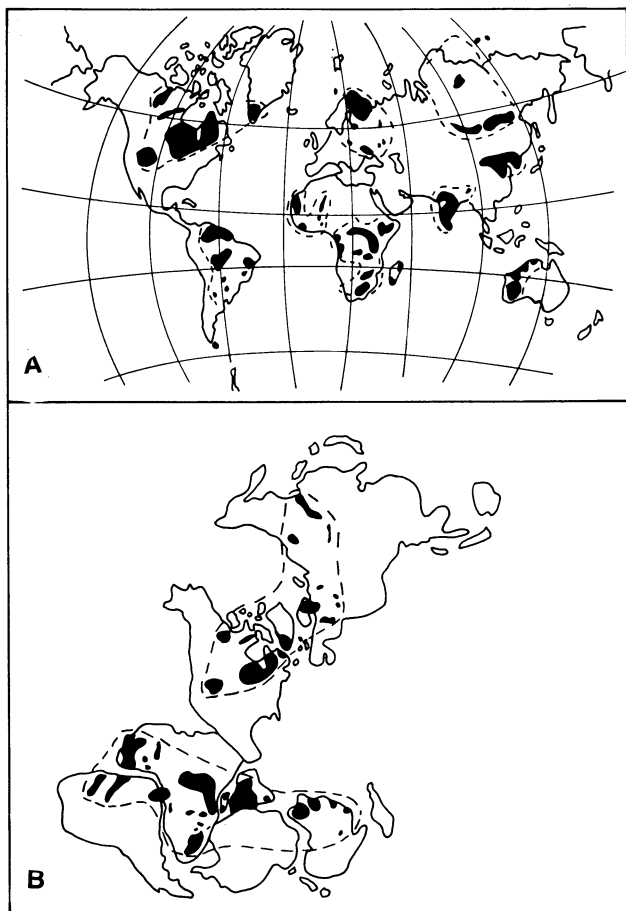
Fig. 5.2A, B. Distribution of Archean provinces (>2.5 Ga) (shown in black) and their possible extent below younger cover (dashed lines): **A** On present-day land distribution; **B** On a reconstruction of the Proterozoic continents. Both illustrations are after Condie (1981)

complexes are distinctive components of most high-grade terranes and may be very large, as for example the Fiskenaesset Complex in southwest Greenland, which has a thickness of 1.5 km and a strike length of about 60 km (Windley 1984). Metamorphic assemblages indicate that some granulite facies rocks were buried at depths of 30–40 km, and their present level is due to substantial uplift (Condie 1981). Also, major shear zones traverse these high-grade terranes and, unlike the granite-greenstone terranes, it appears that the dominant stress regime was subhorizontal and tangential, resulting in major thrusts and recumbent folds. Infolded supracrustal sequences may occur within these high-grade terranes reflecting a variety of progenitors. An example of a well-preserved granulite-gneiss terrane is the Limpopo Belt in southern Africa, separating the granite-greenstone terranes of the Zimbabwe and Kaapvaal cratons (see Tankard et al. 1982).

The "granite-greenstone" terranes form prominent provinces in all continents and they are of particular economic importance in southern Africa, Western Australia, Canada, Brazil and India (Fig. 5.2A, B). Their most striking feature is their worldwide similarities. Mid to Late Archean granite-greenstone terranes are composed principally of granitic and gneissic rocks (80–90%); they surround and locally intrude the volcano-sedimentary greenstone belts which make up the remainder. Greenstone belts worldwide can be grouped into older types (>3 Ga) and younger types (<3 Ga), and they exhibit somewhat different characteristics, probably reflecting a constantly changing thermal regime. Greenstone belts have been defined in different ways, of which the following are two examples: (1) from Lowe and Byerly (1986): "an orogen made up largely of mafic to ultramafic volcanic rocks and their pyroclastic equivalents and epiclastic derivatives, showing intense macroscale deformation but regionally low grades of thermal alteration, and extensively intruded by slightly younger granitoid plutons"; (2) from Vearncombe et al.(1986): "greenstone successions are the non-granitoid component of granitoid-greenstone terranes. Volcanic rocks are an essential component, some of which are usually komatiitic. Sedimentary rocks are commonly present and igneous intrusive units may exist. The greenstone successions are linear to irregular in shape and where linear they are termed belts. The greenstone successions may occur at all metamorphic facies and are heterogeneously deformed. Most greenstone successions are Archean in age".

The main features of the geology of greenstone belts have been summarised by Condie (1981), Windley (1984), and at a workshop held at the Lunar and Planetary Institute, Houston (USA), in 1986. These main features include the following three-fold lithostratigraphic subdivision: (1) a lower ultramafic group, comprising ultramafic to mafic volcanics with broad chemical similarities to mid-ocean ridge basalts, minor pyroclastics and sedimentary rocks; (2) a middle group, including mafic to felsic volcanics, related pyroclastics and sedimentary assemblages; (3) an upper group, dominated by sedimentary, coarse to fine sequences with minor volcanics and BIF components. Numerous hypotheses have been formulated to explain the granite-greenstone terranes with plate tectonic-styled models becoming increasingly popular. Models proposed to explain the origin of greenstone belts can be categorised into three types: extraterrestrial, classical or fixist, plate and/or rift tectonics or mobilists. For more details on the hypothesis of greenstone belt

formation and evolution the reader is referred to Condie (1981), Windley (1984) and Kröner (1981, 1985 and references therein).

The extraterrestrial hypotheses hold that greenstone belts were formed by meteorite impacts, and it has been suggested that the greenstone belts are the equivalent of lunar maria (Green 1972). This model is based on two important facts. One is that the Earth, like all other planets, must have been bombarded by large meteorites, and the other is the high temperature of peridotitic komatiitic magma (1650°C), with the implication that a large amount of melting would be required to produce such a liquid (60–80%). There have, however, been several objections to Green's model. One is that most greenstone belts formed at around 2.9–2.7 Ga, while the last major impact episode was probably around 4.1 to 3.9 Ga. Nevertheless meteorite bombardment did take place and therefore, it must surely have played a role in the protocontinental growth of the early Earth, particularly in localising and accelerating endogenic activity.

The fixists' models date back to MacGregor (1951), who attempted to explain the origin of greenstone belts in Zimbabwe (then Southern Rhodesia). McGregor invoked the diapiric intrusion of granitoids as a major cause of displacement of dense mafic volcanics, erupted on a pre-existing sialic crust. Mantle convection models have been invoked by other workers, such as Fyfe (1978), who proposed that a number of hot spots could have formed at the boundaries of convective upper mantle currents, with production of mafic and ultramafic magmas. Other fixist models are those proposed by Anhaeusser (1971, 1975), involving downsagging of a volcano-sedimentary basin either developed on a thin, unstable oceanic-type crust, or on a thin sialic crust overlying a mafic layer, in which a greenstone belt is formed at the interface of a continental-oceanic crust. In his models, deformation is gravity-induced and accompanied by granite diapirism, which would be derived from the partial melting of the greenstone root zones. Glikson in a series of papers (1972, 1976, 1981), and Glikson and Lambert (1976), emphasised the primitive nature of the lower mafic and ultramafic rocks. In these authors' opinion, the formation of a widespread primitive oceanic crust is the first step towards protocontinental evolution, so that the mafic-ultramafic rocks at the base of the greenstone belts may represent relics of a primordial crust.

The mobilists', or plate and/or rift tectonics, models are based on the controversial assumption that some form of ocean-floor spreading and subduction were operative during the Archean. It is suggested by Bickle and Nisbett (1986) that the best evidence for plate motions is provided by the linear tectonic belts, such as those of the Yilgarn Block of Western Australia, and the large-scale nappe structures recognised in the high-grade terranes as well as in the greenstone belts. Also, they point out that heat loss from the Archean continents, as inferred from metamorphic gradients, is too low by an order of magnitude to be representative of heat loss from the Archean Earth as a whole. They suggest that heat was lost through oceanic regions, as is the case today, which implies that the mid Archean Earth was already divided into oceanic and continental plates. Burke et al.'s (1976) proposal that greenstone belts may represent fossil back-arc basins was followed up by Tarney et al. (1976), who compared the "rocas verde" complex in southern Chile with the development of greenstone belts. This model and that proposed for the
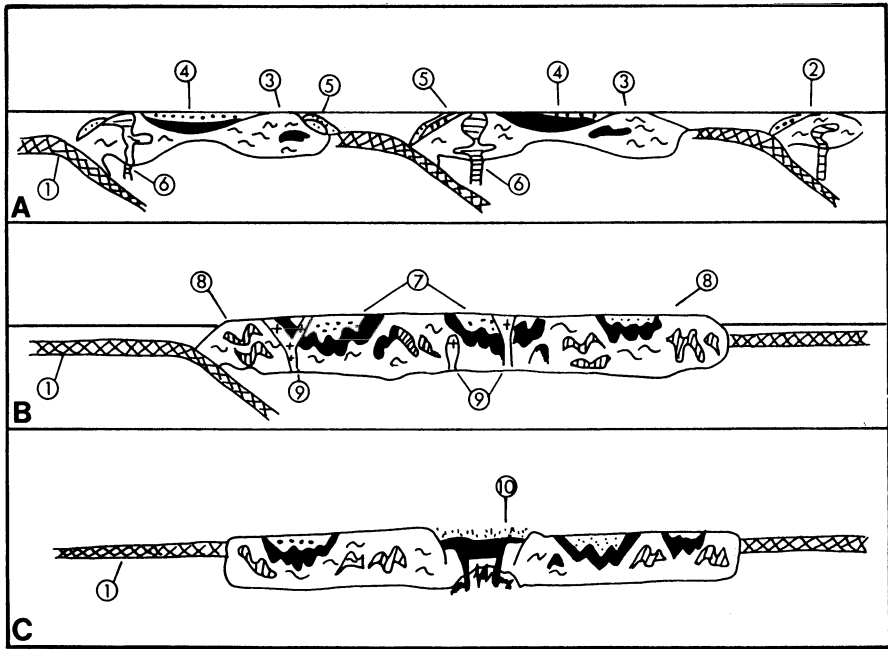
Fig. 5.3A–C. Phases in the evolution of granite-greenstone terranes (After Windley 1984; Tarney et al. 1976). A Island-arc and back-arc marginal basin phase. B Collision of microplates and incipient cratonisation. Au mineralisation predominant. C Rifting phase. Ni-Cu mineralisation predominant. *1* Oceanic crust; *2* island arcs; *3* S-symbol indicates sialic basement (gneissic) with relics of greenstone belts from previous cycles; *4* sediments and lavas in extensional back-arc marginal basins; *5* shelf sediments ; *6* tonalitic magmas of principal arc; *7* greenstone belt; *8* high-grade terranes, gneissic, thrust tectonics, infolded basement and shelf sediments; *9* late K-rich granitoids; *10* rift-related greenstone belt

interpretation of the high-grade terranes as being ancient volcanic arcs (Windley and Smith 1976), for which the Mesozoic batholiths of the Circum-Pacific belt are cited as modern examples, appear to offer a good explanation of Archean crustal evolution. The final plate tectonic model involves the collision and accretion of a number of volcanic arcs and marginal basins which would coalesce to form protocontinents (Fig. 5.3). The two distinct tectonic settings of back-arc marginal basin and magmatic arc areas, would then correspond to greenstone belts and high-grade terranes respectively, as shown in Fig. 5.3. The former has far greater economic importance, because of its better preservation, whereas the high-grade terranes – notwithstanding metamorphism – are the remnants of topographically elevated structures now eroded away.

Other models invoke mechanisms of continental-type rifting. Condie and Hunter (1976) proposed a continental rifting model for the Barberton greenstone belt, where rifting would have occurred in response to an ascending mantle plume. The rift system is partially filled with mafic-ultramafic lavas derived from the plume. As the plume subsides erosion of the rift flanks gives rise to the subsequent volcanic

and sedimentary components of the belt. Sinking of the Barberton succession and renewed plume activity resulted in partial melting and the formation of tonalitic magmas. This tonalitic event would have accounted for the major period of thickening of the Kaapvaal craton.

Another proposal was put forward by Groves and Batt (1984), who studied greenstone belts and their associated metallogeny in Western Australia. These authors classified greenstone belts into platform and rift types based on their volcanic constituents, sedimentary facies, tectonic style and mineral deposits. Their classification is summarised as follows: (1) older (3.5 to 3 Ga), poorly mineralised platform phase belts; (2) rift-related, poorly mineralised belts in older greenstone teranes; (3) younger (3 to 2.7 Ga) platform-phase greenstones with significant mineralisation; (4) rift-related greenstones in younger terranes containing important mineralisation. We return to Groves and Batt's model in Chapter 15.

Kröner (1985) proposes that the evolution of the Archean lithosphere involved incipient rifting which resulted from small-scale convection in the upper mantle. This was followed by various stages of rifting during which greenstone belts were formed. In a final stage, closure of the rift-formed basins and collision resulted in low-angle thrusting, shearing and crustal thicknening (Kröner 1985, Fig. 7). The author goes on to explain the origin of the high-grade terranes as due to low-angle thrusting phenomena which juxtapose upper crustal granite-greenstone terranes with lower crustal high-grade terranes. In the end, as a result of erosion, a strip of high-grade rocks flanking the granite-greenstone terrane is finally exposed.

In the continuing saga of the development of ideas on the evolution of greenstone belts, Groves and his coworkers in a recent paper (Barley et al. 1989) re-interpreted the tectonic evolution of the greenstone belts (Wiluna-Norseman) in Western Australia in terms of a complex interplay of subduction-related tectonics (ensialic volcanic arc, back-arc complex), extension and accretion of tectono-stratigraphic terranes, in a manner similar to that envisaged for the convergent margin of western North America during the Phanerozoic. They also affirm that their new model is compatible with that advocated by Tarney et al. (1976) and implicitly Windley (1984). We return to discuss the evolution of greenstone belts in Chapter 15.

In conclusion, it must be pointed out that a unifying model of greenstone belt formation is still far from being agreed upon. If a unifying model is eventually worked out, this must take into account an evolutionary continuum, at any stage of which a given greenstone belt may have been preserved. Also, each greenstone belt may be exposed at various levels of erosion, which is perhaps why North American geologists tend to favour a granite-related genetic model for greenstone gold mineralisation, since in the Canadian shield it appears that greenstone belts are exposed at a higher level than elsewhere, and this would obviously favour the preservation of high-level hydrothermal systems.

Archean Metallogenesis

The Archean greenstone belts host some of the world's major Ni, Au and base metal deposits. Considerably fewer deposits exist in the high-grade granulite-gneiss terranes, and where present are found within areas of metamorphosed volcanics,

sediments or layered complexes. Examples are the Selebi-Pikwe Ni deposits in Botswana, and the chromite deposits of the Fiskenaesset Complex in Greenland. The major factors influencing Archean metallogenesis are the generation of specific types of acid, basic and ultrabasic magmas, and metamorphism. Following Anhaeusser (1976), we can consider Archean mineral deposits as follows:

1. Ore deposits associated with mafic and ultramafic rocks; Ni-Cu Cr, Au, Fe.
2. Ore deposits associated with mafic to felsic volcanics of calcalkaline character; base metals, Au, Ag, Sb, Fe.
3. Ore deposits associated with pegmatitic rocks; Li, Be, Ta, Sn.

Ore Deposits Associated with Mafic and Ultramafic Rocks

Important Ni-Cu deposits occur as magmatic segregations at, or near, the base of komatiitic peridotite flows in the greenstone belts of Zimbabwe, Canada and Western Australia. It is of particular interest to note here that some Ni deposits in Western Australia are considered to have had a hydrothermal (volcanic-exhalative) origin (Keays et al. 1982). It has been suggested that the sulphide-rich nature of many peridotite magmas may be related to sulphur-rich zones within the mantle (Na'drett 1973). As there is a marked rarity of Ni mineralisation in younger (post-Archean) environments, it is possible that later mantle melts were in fact somewhat depleted in S, unless this element is supplied by an external source and subsequently assimilated by the magmas. A sulphurisation model has been applied to Archean Ni deposits; this involves liberation of Fe, Ni, Co and other siderophile elements in a hot peridotite body and their combining with S supplied from either a volcanic or a sedimentary host (Naldrett 1965). Chromite deposits of Archean age are found in the ultramafics of the Sebakwian group in Zimbabwe, formed by magmatic segregation as cumulate layers in a differentiating ultramafic intrusion. The Archean sedimentary iron formations (BIF, see later) are known as Algoma-type. They have a close spatial and genetic affiliation with Ni sulphide deposits as well as Au and base metal deposits. Algoma-type BIF are relatively thin, discontinuous, and typically exhibit facies changes from oxide to carbonate, silicate and sulphide facies. It is thought that their origin is volcanic-exhalative, with brine solutions vented on the ocean floor in a situation perhaps similar to the present-day rift lakes (see Chap. 3).

Gold is certainly the most economically important commodity of the greenstone belts, where it is found in a large variety of rocks and in different settings. The fundamental questions are the origin of the metal, its transport, and its concentration in its present locales. The gold deposits of Archean greenstone belts are of hydrothermal origin and can mostly be categorised into at least four major groups: (1) deep-seated shear zone and vein deposits; (2) BIF or stratiform-type deposits; (3) disseminated-type deposits; and (4) porphyry-associated deposits. Their origins are highly controversial and models involving metamorphic fluids, volcanogenic-exhalative, and magmatic-hydrothermal are all called upon to explain them. Chapter 15 takes a more detailed look at this aspect of Archean gold ore genesis. For the moment, suffice it to say that most of the Au production in greenstone belts is

derived from shear zone-hosted deposits, and that they are generally in mafic rocks. Also the stratiform gold mineralisation, preferentially developed in Algoma-type BIF, is found associated with volcanic-rich units.

Ore Deposits Associated with Mafic to Felsic Igneous Rocks

Many base metal massive sulphide deposits in Archean greenstones are found in volcanic sequences of calc-alkaline character, and are comparable to the kuroko-type ores (Hutchinson 1973). The Cu-Zn massive sulphide orebodies of the Abitibi greenstone belt in Canada are an important example. They constitute some of the largest massive sulphide masses in the world (Meyer 1988).

They are known as primitive type Zn-Cu-Ag-Au rich ores, and are thought to have formed as chemical precipitates from submarine hydrothermal vents related to
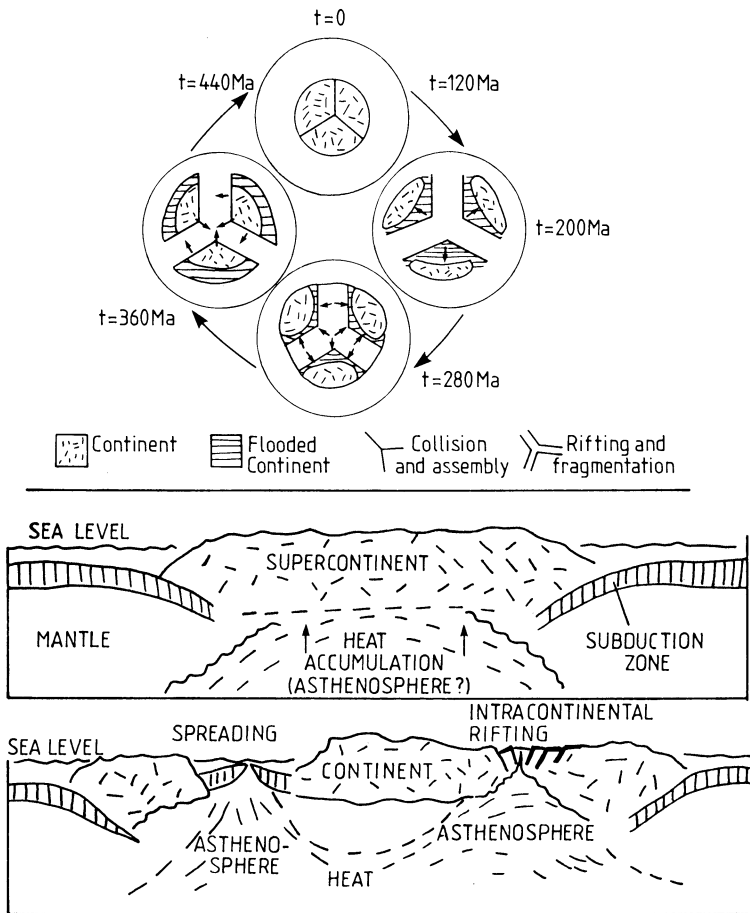
Fig. 5.4. Model depicting the cyclic assembly and fragmentation of a supercontinent, as envisaged by Nance et al. (1988). Accumulation of heat in the underlying mantle is thought to be a prime cause of the initial rifting

felsic volcanic edifices. The overall rock sequences are characterised by cycles of ultramafic-mafic to felsic rocks. Rhyolites mark the end of each cycle and are associated with the sulphide mineralisation. In each cycle the ultramafic-mafic component predominates (up to 70%); however, this component tends to decrease with decreasing age in each subsequent cycle. According to the metallogenic scheme of Groves and Batt (1984), ore deposits are associated with felsic volcanic complexes in platform-stage greenstone belts (an example of which would be the Golden Grove Cu-Zn deposit in Western Australia), and with major calc-alkaline volcanic centres in the rift phase development of the greenstones. We return to these deposit types in Chapter 11.

Mineralisation Associated with Pegmatitic Rocks

Pegmatite fields are common in many Archean terranes. The Bikita pegmatite in Zimbabwe is one of the largest deposits of Li, Cs and Be, and also contains Sn and Ta. The Tanco pegmatite at Bernic lake in Canada is only slightly smaller than the Bikita pegmatite and contains substantial amounts of Li, Cs, Ta, Be and Ga. The giant Greenbushes pegmatite in Western Australia is reputed to contain the largest reserves of Ta in the world, as well as significant quantities of Li, Sn and Nb.

5.2.2 The Proterozoic Eon: Phase of Intraplate Tectonics

The Archean-Proterozoic boundary was a major turning point in crustal evolution and represents a diachronous and transitional period ranging from about 3 Ga to 2.5 Ga. Massive crustal growth, lithosphere thickening, decrease in heat flow and a possible change in mantle convection pattern occurred. The presence of an unconformity is typical, separating highly deformed Archean rocks from little deformed, or undeformed, Proterozoic cratonic sequences. A major thermal event, characterised by large-scale granitic intrusions and metamorphism, is recognised in several continents. This event peaked between 2.6 and 2.5 Ga and is thought to be one of the major crust-forming events in the Earth's history (Moorbath 1977). One of the controversies of Proterozoic crustal evolution is whether the increased cratonisation, coupled to a changed mantle convection system of more regular cells, led to the onset of conventional Wilson-cycle plate tectonics, and the assembly of supercontinents. Palaeomagnetic data indicate that a supercontinent may have been present from about 2.2 to 1 Ga (Piper 1982; Bond et al. 1984). Some workers have theorised that supercontinents have been cyclically forming and fragmenting throughout most of the Earth's history (Nance et al. 1988). Such a theory holds that the aggregation of a supercontinental mass results in the accumulation of heat in the mantle beneath it. This state would eventually result in heat dissipation by means of rifts that break the supercontinent into fragments. The fragments would drift and coalesce again through collision processes and a new supercontinent would again be re-assembled. This cycle, which would take approximately 450 Ma to complete, and also result in major sea level fluctuations, is schematically shown in Fig. 5.4.

Although rift tectonics may have predominated, a number of well-documented Early to Mid Proterozoic "mobile belts" exhibit features closely resembling the Phanerozoic orogens (Kröner 1981). Their deformation by horizontal compression, and the evolution of calc-alkaline assemblages, are indicative of some form of plate movements having taken place during the Proterozoic.

In summary the growth of continental crust at the Archean-Proterozoic boundary (see Taylor and McLennan 1985 for a comprehensive account) clearly heralded a change in tectonic style since the Archean. The increased stability and rigidity of the Archean cratonic masses led to the development of intracontinental rifts, aulocogen and basins, intrusion of dyke swarms and layered complexes, and the formation of linear orogenic belts alongside Archean provinces. Finally, it should be pointed out that while a distinctive period between 1.8 and 1.2 Ga displays little evidence of orogenic cycles, it is characterised by important anorogenic magmatism.

Early Proterozoic (ca 2.5 to 1.6 Ga)

During this period crustal masses of continental, and perhaps even supercontinental, size were formed (see Fig. 5.2B). They are characterised by stable cratons surrounded by "mobile belts". In the stable cratons are found the epicratonic basins, hundreds of kilometres long, infilled with sediments and volcanics, and major igneous layered intrusions. These rocks are the repositories of enormous quantities of Fe, Mn, Au, U, Pt, Cr and Ti.

Southern Africa provides an outstanding example of the early stabilisation of the Archean crust and the development of epicratonic basins, into which accumulated thick sequences of relatively undeformed sediments and volcanics. The basins of the Pongola, Dominion-Witwatersrand, Ventersdorp, Transvaal-Griqualand West, and the Waterberg-Matsap sequences appear to have formed by a succession of rifting events that affected the Kaapvaal province and its western margins (Burke et al. 1985; Clendenin et al. 1988). These epicratonic basins migrated northward, increasing in size with decreasing age, and also display a change in the proportion of volcanic to sedimentary rocks, the older sequences having greater volcanic components than the younger ones. Detailed descriptions of the geology and stratigraphy of the basins can be obtained from Tankard et al. (1982) and Button et al. (1981). The basins' sequences display a cyclic pattern of development, all having commenced with, and frequently terminated by, volcanism. The Dominion Reef, Witwatersrand and Ventersdorp supergroups form the so-called Witwatersrand Triad. The major part of the Pongola, Dominion reef and Ventersdorp supergroups consists of extrusive igneous rocks, whereas that of the Witwatersrand and the overlying Transvaal and Waterberg supergroups is predominantly sedimentary. Other important epicratonic basins with a comparable history occur in Western Australia (Hamersley basin), and in North America. Important Australian examples of Early to Mid-Proterozoic basins include the Kimberley and McArthur basins.

Large transcontinental dyke systems, major layered complexes, and products of anorogenic magmatism are distinctive in this period of the Earth's history. These are

all prime examples of the intrusion (and extrusion?) of mantle-derived melts into a brittle and fractured crust, in response to major thermal relaxation events (a "basic interlude", in the terminology of Read and Watson 1975). Carbonatites and kimberlites were also emplaced during this period of the Proterozoic history. Economically important are the layered complexes such as the Stillwater Complex in Montana (USA), the Sudbury Irruptive on the southern margin of the Superior province in Canada, the Bushveld Igneous Complex in South Africa and the Great Dyke in Zimbabwe. The Bushveld Complex is the largest layered intrusion in the world. It has a thickness of up to 8 km, consists of a peridotite-pyroxenite-gabbro-anorthosite mass with overlying granitic rocks, and was intruded into a structural depression of the Transvaal supergroup. The Complex was heralded by the emplacement of voluminous mafic sills and voluminous eruption of acid volcanics (Rooiberg Felsites), with which there is evidence of associated epithermal-type hydrothermal activity, thus making it one of the oldest known (Martini 1988). For details of the Bushveld geology and mineralisation, the reader should consult the special issue of Economic Geology (Vol. 80, 1985). The Great Dyke of Zimbabwe is 480 km long, and has an average width of about 6 km, is formed by large lopolithic complexes, containing cyclic sequences of peridotite, pyroxenite, anorthositic gabbro and norite, and finally quartz-gabbro. A classic work on the Great Dyke is that of Worst (1960).

Examples of mobile belts whose evolution is explained in terms of Wilson-cycle tectonics include the Canadian Wopmay orogen of Mid-Proterozoic age (Hoffman 1980), the Labrador geosyncline (Dimroth 1981) and the Circum-Superior belt on the southern margin of the Archean Superior province (Baragar and Scoates 1981). The Circum-Superior fold belt is a collection of nine discrete Proterozoic sedimentary-volcanic sequences distributed around the margin of the Archean Superior province in Canada. The Wopmay orogen in the northwest Canadian shield which is between 2.1 and 1.8 Ga old and situated on the west side of the Archean Slave province, is thought to have formed by collision and accretion of a magmatic arc with a continental margin.

In South Africa, the western portion of the Namaqua-Natal mobile belt appears to have formed by the accretion of a number of terranes, involving ocean opening and closing cycles (Hartnady et al. 1985). Further to the north the Irumide orogen, extending from south-central Namibia across to northern Botswana, is, according to Borg (1988) the result of intracontinental rifting developed at a triple junction. The absence in many of these orogenic belts of clear-cut suture zones, containing remnants of oceanic rocks, is not, as considered by some, a shortcoming, because the preservation of recognisable sutures is largely related to erosion levels (Windley 1984).

Early Proterozoic Metallogeny

The Early Proterozoic mineral accumulations are of enormous economic value, and again it is reminded that their nature reflects the general change in tectonic styles and evolution of the crust. Mineral deposits include the bulk of the world's Fe ore (Hamersley and Transvaal basins), Mn ore (Transvaal basin), Au and U (Witwaters-

rand basin), the major base metal Pb-Zn-Ag deposits of the McArthur basin in Australia, the Udokan deposit in Siberia, and those found in the Namaqua Metamorphic Complex in South Africa. The huge Pt, Cr and Fe-Ti reserves of the Great Dyke and Bushveld Complex, and the sulphide Ni deposits of the Sudbury Irruptive form the magmatic component of what must have been a major and global metallogenic epoch in the geological history of our planet.

Sedimentary Fe deposits have a key significance for interpreting the Earth's evolution. Evidence suggests that there are three periods of peak Fe deposition. They are: Mid Archean (3.5–2.9 Ga), Early Proterozoic (2.5–1.9 Ga), and Late Proterozoic (0.75–0.5 Ga) (James and Trendall 1982). The Early Proterozoic deposits were formed in rift-controlled basins near the boundaries of Archean cratons (Windley 1984), and account for almost 90% of the Fe reserves of the world. There are four types of Fe formations: Algoma-type of Archean age, mentioned earlier and associated with greenstone belts; Superior-type of Proterozoic age; Clinton-type and Minette-type of Late Proterozoic and Phanerozoic age respectively. For more information the reader is referred to Appel Uitterdijk and LaBerge (1987), whilst comprehensive reviews on the nomenclature and origins of Fe formations can be found in Kimberley (1989a, b). Kimberley (1989a) defines a Fe formation as a chemical-sedimentary stratigraphic unit containing more than 15% Fe and recognises six Fe formation environments, namely: (1) shallow volcanic platform; (2) metazoan-poor, extensive, chemical-sediment-rich, shelf sea; (3) sandy, clayey, oolitic, shallow sea dotted with islands; (4) deep water; (5) sandy, oolite-poor, shallow sea; (6) coal swamps. The extensive, metazoan-poor shelf sea Fe formation (2) would correspond to the Superior-type, whereas those under (1) and (4) would broadly correspond to the Algoma type. Kimberley (1989a, b) points out that most aspects of Fe formations remain controversial and he does not recommend the use of the acronym BIF for banded iron formations, unless properly defined. In this text, however, we use BIF for the sake of convenience and also because the use of this acronym is well entrenched in the geological terminology.

The origin of the banded iron formations (BIF) has been debated for many years, with genetic scenarios ranging from continental weathering to submarine volcanic exhalations. It is thought that the massive deposition of Fe in the Proterozoic may reflect firstly a change in the source of the Fe and secondly a change from a predominantly reducing to a predominantly oxidising atmosphere. A popular, but often disputed, theory is that O_2 produced by photosynthetic organisms could have been lethal for their survival and therefore oxygen had to be eliminated by inducing oxidation of the readily available Fe^{2+} to Fe^{3+} (oxygen acceptor and sink) (see Cloud 1976). In the end oxygenation prevailed, leading to the present atmospheric oxygen abundance. A model which might explain the huge Fe accumulations is that proposed by Gross (1980). In this model BIF may have developed in a stratified Precambrian ocean with an oxygenated upper layer and a lower anaerobic zone. In this latter zone Fe^{2+} was held in solution, and precipitation occurred during upwelling of the Fe^{2+}-bearing ocean water from the bottom layer into the more oxygenated upper layers. The source of the Fe, however, remains controversial, although it may be speculated that the Fe (and Mn) supply to form the BIF of the Early Proterozoic could have derived from the erosion of continental flood basalts,

which may have overplated the Archean continents in response to the widespread rifting characteristics of this time of the Earth's history. The gradual oxygenation process of the hydrosphere and atmosphere may also have been instrumental in the deposition – also associated with BIF – of enormous quantities of Mn ores, such as those of the Kalahari field in the Northern Cape region in South Africa (see Chap. 13).

By far the most important basins, both in economic terms and shear volume, are the Au-U palaeoplacers of the Witwatersrand in South Africa, which account for 30% of all the Au ever mined (Phillips and Groves 1983). Other similar and equally important basins are those of Elliot Lake in Canada, Jacobina in Brazil, the Tarkwaian sequence of Ghana and the Huronian supergroup in Canada. They contain varying proportions of Au and U, which occur in elongated channel-like bodies in coarse, quartz-pebble conglomerates with abundant clasts and pyrite. These rocks and associated quartzites are of shallow water, fluviatile-deltaic facies, deposited along active, downthrown, fault-controlled margins of a major, asymmetrical, yoked basin (Pretorius 1976a, b). Detailed sedimentological work led by Minter (1978; see also Minter et al. 1986; Pretorius 1986), clearly established the placer origin of these deposits, although, this has recently been challenged by Phillips (1987) and Phillips et al. (1988). The source of the U and Au remains elusive and controversial; various proposals have been put forward, including that they originated from greenstone belts, eroded off porphyry and/or epithermal systems of ancient island arcs. More recently, a theory developed by Hutchinson and Viljoen (1988) invokes a source of pyritic auriferous exhalites formed by submarine hydrothermal discharges along the active faults of the basin.

Early Proterozoic base metal sulphide deposits are hydrothermal volcanogenic and resemble those of the primitive type of the Archean. However, the period between 2 and 1.6 Ga is generally characterised by a marked absence of Zn-Cu-Au volcanogenic deposits, forming a "volcanogenic gap" (Hutchinson 1980; Fig. 5.1), although Rickard (1987) reports the presence of numerous volcanogenic massive sulphide deposits in the Laurasian portion of the Proterozoic supercontinent (Figs. 5.7 and 5.8). These deposits, of which Outokumpu in Finland and Flin Flon in Canada are quoted as examples, were formed during the period 1.8 and 1.9 Ga. They appear to be concentrated in a belt about 8000 km long and 1000 km wide, extending from North America across to northern Europe, in a reconstruction of the Proterozoic supercontinent by Piper (1982; Rickard 1987, Fig.1).

At about 1.8 Ga the large, exhalative sediment-hosted Pb-Zn-Ag deposits were formed. These economically very important deposits are also indicative of the Proterozoic's major change in crustal tectonics, characterised by rifting environments dominated by the deposition of deep water, turbiditic sequences. Some of these stratiform and stratabound deposits are interpreted as having formed in failed rifts (aulocogens), in which exhalative hydrothermal activity was common, although as pointed out by Meyer (1988), these sediment-hosted mineral deposits are not associated with volcanic provinces. However, the dominance of Pb in the deposits is attributed by Meyer to the possible concentration of K-rich felsic rocks in the substratum of the rift-related environments. In this tectonic-depositional environment formed the important 1.7–1.5 Ga shale-hosted McArthur River,

Mt.Isa and Broken Hill deposits (all in the McArthur basin of Australia), and the Aggenays-Gamsberg Pb-Zn-Cu-Ag-Ba deposits of the Namaqua belt in South Africa. The latter occur in rocks metamorphosed to amphibolite facies, and form a series of deposits displaying distinct regional zoning, with Cu-rich ores near the postulated source, Pb in an intermediate position and Zn in a distal basin. The genesis of the Namaqualand deposits is thought to be similar to the Red Sea present-day sulphide brine pools (Rozendaal 1978). Details of some of these deposits and their tectonic settings are examined in Chapter 13.

The layered igneous bodies of the early Proterozoic, as already mentioned, contain large primary magmatic ore deposits of the platinum group elements (PGE), Cr, Ni, Cu, Ti, and V, all deriving from mantle and subcrustal sources. Details of mineralisation in the Bushveld Complex of South Africa can be found in Volume 1 of the Mineral Deposits of Southern Africa (Anhaeusser and Maske 1986), and the earlier mentioned special issue of Economic Geology (1985, v.80).

Carbonatites and other related alkaline complexes of Early-Mid-Proterozoic age may contain economic deposits of Nb (pyrochlore), REE (monazite, bastanaesite), U, and in rare cases – as at Phalaborwa in South Africa – Cu and P. Again in South Africa, Proterozoic kimberlites are diamondiferous.

Mid-Late Proterozoic (ca. 1.6 to 0.6 Ga)

This period of the Earth's history was characterised by at least two important igneous and tectonic events. A distinctive time of crust-forming anorogenic magmatism dominates the Mid-Proterozoic. This magmatism includes the intrusion of major basic dyke swarms and suites of anorthosite-rapakivi granites. The latter were intruded in the Scandinavian region about 1.7 Ga ago, and are aligned with another group in North America with ages ranging from 1.5 to 1.4 Ga (Windley 1984). A similar belt extends across what is now the southern hemisphere, from South America, through Africa and India to Western Australia. The anorthosites consist of more than 90% plagioclase, and are typically associated with adamellites, acid volcanics and rapakivi granites. The latter usually border, and are intrusive into, the anorthosites. This close spatial and chronological relationships between the various igneous components of this great "anorthosite event", suggests bimodal magmatic processes, in other words, the process of magma generation that produced the anorthosites must also have been responsible for the generation of the acidic magmas. The reasons for the generation of these vast amounts of anorthositic magmas is by no means clear. The bimodal association is a feature of anorogenic magmatism, and is thought to be the result of mafic magma underplating of the crust, followed by the melting of the latter to produce acid magmas. Abortive rifting during the Mid-Proterozoic is believed to have controlled the emplacement of a generation of another transcontinental basic dyke swarms, a suite of alkaline intrusives and several large layered igneous intrusions, such as the 1.1–1.2 Ga Muskox complex and the 1.15 Ga Duluth complex. A model relating the emplacement of the anorthosite-rapakivi granites and basic complexes to abortive graben structures was proposed by Bridgwater, Sutton and Watterson (quoted in Windley 1984).

The intracontinental rifting events of the mid-Proterozoic also controlled the location of important epicratonic troughs and grabens, with sedimentary and volcanic accumulations. Alternative interpretations, using a more uniformitarian approach, are that these sedimentary-volcanic accumulations may indicate that they started to form at the trailing edge of stable continental margins, and were then converted into tectonically active margins by the onset of subduction (Windley 1984). Sedimentary-volcanic sequences would then have been laid down in aulocogens, back-arc, or post-collision hinterland basins (Mitchell and Garson 1981). In any case, major rift- and aulocogen-related basins were formed at this time, such as the Keweenawan rift system in the Lake Superior region, and the sedimentary basins of the Belt-Purcell supergroup, where the Sullivan and Coeur d'Alene mineral districts are situated. It is also clear that there are transitional trends in the tectonic styles of the Mid-Late Proterozoic with those of the Early Phanerozoic, as is evident in the Pan African Damara orogen (Chap. 7).

A global system of Late Proterozoic to Early Palaeozoic orogenic belts marks the transition to the Phanerozoic crustal regime and tectonic style of modern plate tectonics. This transition took place between 1.1 and 0.6 Ga. Cordilleran-type geosynclines were developed near the margins of North America and Europe, whereas in the southern continents of Gondwana a great system of geosynclines, all more or less rift-originated, extended from the western and northeastern sides of Africa, South America to Antarctica and Australia (Adelaidean trough). These orogenic belts display variations from typically ensialic types to Wilson-cycle tectonics (Kröner 1981). Passive and active continental margins and island arcs are
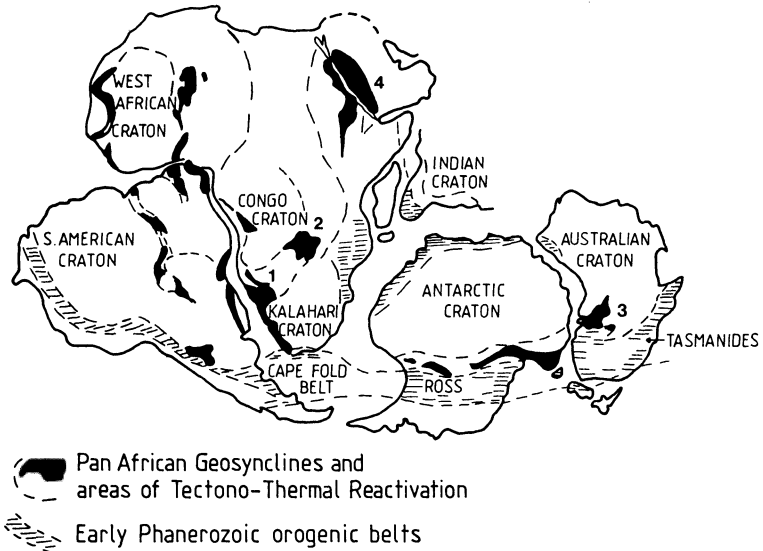
Fig. 5.5. Distribution of Pan African geosynclines (shown in *black*), and Early Phanerozoic orogenic belts, on a pre-drift Gondwana reconstruction. Based on Porada (1985) for the Pan African belts; Morel and Irving (1981) and Read and Watson (1975) for the Phanerozoic belts. *1* Damara Orogen; *2* Lufillian Orogen; *3* Adelaidean trough; *4* Arabian-Nubian shield

recognised. Ophiolites have been identified, especially in West Africa and in the Arabian-Nubian region, testifying to ocean-floor spreading. The transition to the plate tectonic regime was caused by the onset of oceanic crust subduction, which by now was sufficiently dense to enable it to subside. The great system of the Pan-African-Braziliano orogenic belts are shown in Fig.5.5, on a Gondwana reconstruction prior to breakup. In these belts a number of features indicate a mode of origin due to continental rifting, plate collision and accretionary tectonics. This is particularly evident for the geodynamic evolution of the Arabian-Nubian shield. Gass (1981) interpreted the evolution of the Arabian-Nubian region in terms of a number of oceanic island arcs that accreted to one another to eventually form a cratonised mass. At this final stage anorogenic within-plate magmatism occurred, forming ring complexes and other alkaline volcano-plutonic complexes. Several linear mafic-ultramafic zones have been identified and may mark the sutures between the arcs. In the southwestern region of Africa, the Damara orogen originated from a series of rifts from which South America and Africa separated during the breakup of a Late Proterozoic supercontinent. The geodynamic evolution of the intracontinental branch of the Damara orogen appears to have involved the opening and closing of a narrow ocean, and its tectonic history can therefore be broadly summarised into an extensional rifting phase and a compressional collision phase. We return later (Chap. 7) to discuss the evolution and metallogeny of the Arabian-Nubian shield and of the Damara orogen.

Mid-Late Proterozoic Metallogeny

Several distinctive types of mineralisation characterise the Mid-to Late Proterozoic time. Firstly, mineralisation associated with the "anorthosite event" includes significant ores of Sn, Be, W, Zn and Cu. The anorthosite bodies also contain Ti-Fe-V mineralisation of magmatic segregation origin. The alkaline complexes host a variety of elements including U, Th, Nb, Be and the REE. The most important deposits however, are the sedimentary-exhalative stratiform orebodies situated within the basins of rift-related orogens, as for example the 1.5–1.2 Ga Sullivan Pb-Zn deposit in British Columbia. The famous stratiform Cu-Co ores of the Zambian Copperbelt, within the Lufillian orogen of Pan-African age, are responsible for some 20% of the world's Cu production. Of the same age and system of orogenic belts is the giant Roxby Downs (Olympic Dam) polymetallic mineralisation in the Adelaidean belt in South Australia. This deposit, described by Roberts and Hudson (1983) and Reeve et al. (1990), contains Cu-U-Au-Ag and REE, has an areal extent of about 20 km^2 and a thickness of 350 m. To date no convincing genetic model has been proposed, but it is possible that the various mineralisation styles that characterise Roxby Downs may be ultimately ascribed to anorogenic alkaline magmatism in the Adelaidean geosyncline. The Ag-rich deposits of the Coeur d'Alene district in Idaho (USA), within the Belt basin, are thought to be the products of regional metamorphic dewatering and large-scale hydrothermal activity at about 850 Ma (Leach et al. 1988).

   An important new style of mineralisation is seen in Mid-Proterozoic basins. These are the uncomformity-associated U deposits, such as the Ranger, Jabiluka,
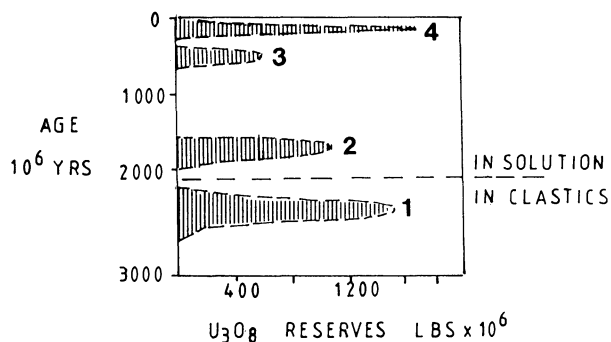
Fig. 5.6. Diagram showing time-bound nature of uranium deposits. *1* Witwatersrand-type conglomerates; *2* Unconformity-related; *3* Shales; *4* Sandstone-hosted and others (After Roberston et al. 1978, quoted in Marmont 1987)

Nabarlek deposits of the Pine Creek geosyncline of northern Australia, or the Rabbit Lake, Key Lake deposits of the Athabasca basin in Canada. In contrast to the earlier U mineralisation of the Witwatersrand and Elliot Lake basins, in which the uranium was mechanically transported as uraninite grains thanks to an oxygen-poor atmosphere, the Proterozoic U mineralisation developed in response to atmospheric oxygenation. This allowed the dissolution of U and its transport as hexavalent uranyl complexes, from either the underlying basement rocks, or the basins' sequences. The U was deposited by circulating hydrothermal fluids of possible meteoric-connate origin, with precipitation occurring near and below an unconformity where these oxygenated fluids encountered a reducing environment such as carbonaceous material (Marmont 1987). The striking time-bound character of U mineralisation is illustrated in Fig.5.6.

5.2.3 The Phanerozoic Eon: Phase of Macroplate Tectonics, Sea-Floor Spreading and Continental Drift

The geodynamic evolution of the Late Proterozoic orogenic belts, such as the Grenville orogen and the Pan-African network of orogens, heralded a new style of tectonism. In fact, towards the end of the Precambrian, declining heat flow produced a lithosphere approaching present dimensions and conditions (about 100 km thick). At this time the increase in negative buoyancy of the oceanic lithosphere, and the rigidity of the plates, led to the inception of modern plate tectonic processes, with sea-floor spreading, Benioff zones and ocean-floor consumption at convergent plate margins. Cordilleran- and Appalachian-type orogens developed at leading and trailing continental margins, and at collision sites, as the Uralide orogen or the ongoing Himalayan and Alpine orogens. Great festoons of intraoceanic, still active, island arcs formed along the western rim of the Pacific ocean. It is not the the purpose of this section to give a comprehensive explanation of the theory of plate tectonics and its corollaries; for details on this the reader is referred to the many

textbooks available today. It is, however opportune to mention some of the "founding fathers" of the theory, and some of the key publications that announced to the geological community this great scientific revolution. A collection of landmark papers edited by J. Tuzo Wilson (1973), reveals the history of the ideas that led to the formulation of plate tectonics by geoscientists such as H.H. Hess, R.S. Dietz, H.W. Menard, and of course J. Tuzo Wilson, who in a series of important articles published in Nature (Wilson 1963, 1965, 1966), described the cyclic opening and closing of the oceans, now called "Wilson cycle". The theory of continental drift, first proposed by Alfred Wegener in 1912, and later championed by the South African Alexander du Toit, could now be recognised as a reality and might be elegantly placed within the framework of the new global tectonics. Other works of the 1970s that are important in the understanding of the new tectonics are Wyllie (1971), the collection of key papers edited by Bird and Isacks (1972), Le Pichon et al. (1973), Tarling and Runcorn (1973).

The Assembly and Breakup of a Supercontinent and Related Metallogeny

The geodynamic evolution of the crust during the latest Proterozoic and the Phanerozoic involved the assembly of a supercontinent, known as Pangea (Figs. 5.7), and its progressive fragmentation, first into two major landmasses – Laurasia and Gondwana – and later into smaller fragments that drifted and collided to eventually form the present day distribution of the continents, in a still ongoing and continuously evolving pattern. There is much that is not entirely understood, not only about the mechanisms of dispersion, but also about the disposition of the continents between the start of the Phanerozoic and the Mesozoic. Geological and geophysical constraints, however, become more certain after this time to permit clearer reconstructions up to the present-day (see de Wit et al. 1988). An understanding of the geodynamics of the assembly and fragmentation with the ensuing orogenic belts created by cycles of subduction, accretion and collision, are indeed of great importance for the exploration geologist, because of the interrelationship with processes of metallogenesis in time and space (metallogenic epochs and provinces). In later chapters we look at these processes as related to specific tectonic settings, and also examine examples of metallogenic and geotectonic analyses of orogenic belts. A detailed account of continental drift, fragmentation and collision of plates during the Paleozoic is provided by Scotese et al. (1979), and a series of paleocontinental maps is available for the entire Phanerozoic (Smith and Briden 1977; Smith et al. 1981), from the Late Proterozoic to the Early Phanerozoic (Morel and Irving 1978) and from the Mid-Devonian to Mid-Tertiary (Irving 1977).

Continental and microplate collisions are now recognised as probably the most important cause of mountain building and orogeny. In the northern portions of the supercontinent – called Laurasia – a more or less continuous system of orogens has been present around the Siberian, European and North American cratons since about 800 Ma ago (Fig.5.7). The Caledonide-Appalachian mobile belt was formed by the opening and closing of a proto-North Atlantic ocean, known as Iapetus. The Caledonide-Appalachian fold belt extends from Britain to the eastern seaboard of the USA, and is explained by ocean-floor spreading, subduction and closure of the
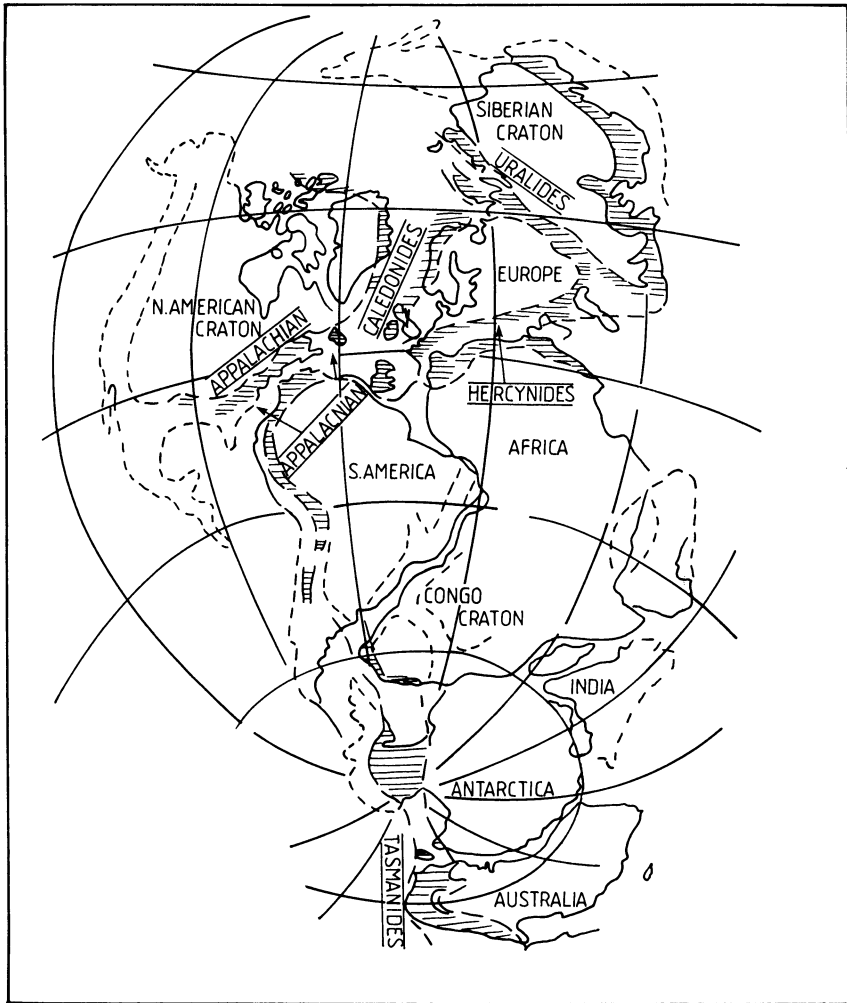
Fig. 5.7. The Laurasian Palaeozoic fold belts on a Pangea reconstruction at 280 Ma (Late Palaeozoic) (After Morel and Irving 1981)

Iapetus ocean (Cook et al. 1979), giving rise to the collision of the North American and European landmasses to form the paleocontinent of Laurentia. The continental mass of Laurasia was thus formed by the collision of up to five smaller continents (Laurentia, Baltica, Siberia, Kazakhstania and China), with the Uralides forming as the result of the interaction between the East European and the Kazakhstan continents. The paper by Zonenshain et al. (1984) gives a comprehensive plate tectonic account of the development of the Uralides.

The mineral deposits of the Caledonide-Appalachian orogen in relation to its geodynamic evolution have been investigated by Swinden and Strong (1976), who noted that within the Appalachian belt there is a zonal disposition of mineral

deposits in linear belts. Mississippi Valley-type Pb-Zn deposits in the west are followed eastwards by ophiolite-hosted Cu-Fe massive sulphides, which are in turn followed by Au deposits and overlapping polymetallic zones of Cu-Pb-Zn-Ag-Au, followed by Sn, W and Mo deposits. This pattern is explained by processes of plate tectonic evolution involving subduction under a continent with Cu-Mo related to a magmatic arc, Au, Pb, Zn and Sb in a subduction-related accretionary complex, Au and base metals associated with sea-floor spreading and the building of island arcs above an intra-oceanic subduction zone. The deposits of Pb-Zn formed in carbonate rocks in a trailing edge of a continental margin (Swinden and Strong 1976). The Hercynian fold belt developed along the southern margin of the Laurasian craton, overlapping in time and space with the Appalachian system (Fig.5.7). The Hercynian belt is thought to have formed as a result of the collision between the Gondwana landmass in the south and the Laurasian continents in the north (Scotese et al. 1979). The tectonic evolution of the Hercynides is a complex affair, involving continental rifting and a system of strike-slip faults deriving from the collision, or indentation, of Gondwana plates against the Laurasian mass (Lefort et al. 1982), in a manner similar to that used to explain the Indian-Asian collision event. One of the most outstanding and characteristic aspects of the Hercynian metallogeny is the presence of granitoid-related hydrothermal systems containing Sn, W and U mineralisation. The development of the Hercynian granite batholiths is the result of the collision tectonics which allowed large-scale generation of crustal melts, with production of post-orogenic two-mica granites. The same tectonic and metallogenic setting is observed along the Himalayan collision front (Le Fort et al. 1987). Other mineral deposits connected with rifting stages in the evolution of the Hercynides are the sediment- and/or volcanic-hosted Cu-Pb-Zn (Rammelsberg, Rio Tinto in the Iberian peninsula), and the carbonate-hosted Pb-Zn deposits.

In the southern portions of Pangea (e.g. Gondwana), orogenic events that had started in the Late Proterozoic continued into the Early Phanerozoic. An active continental margin was present from the western side of the South American craton, around the southwestern part of Africa, the southern margin of East Antarctica, and eastern Australia (Fig. 5.5). The Damara-Lufillian orogenic belts have by this time nearly completed their cycle, with the closure of the South Atlantic to form thrust structures along the northern and southern coastal arms of the Damara orogen. The closure of its intracontinental branch, and further to the northeast the closure and collision of the Lufillian rift systems occurred. In Antarctica the Ross orogen and in Australia the Adelaidean belt also concluded their development, and similarly other intracontinental orogens such as the Mocambique belt and orogenic zones along South India and Sri Lanka. During these late orogenic phases, mineralisation is related to metamorphic and late to post-orogenic granitic events. Both in the Damara and Lufillian belts, for example, mineral deposits of this time are mainly Au and base metal in hydrothermal veins possibly originated by metamorphic fluids, and Sn-W deposits linked to late pegmatites and crustally-derived granitoids. Mineralisation of this period in the Adelaidean orogen is also of the same type, with small hydrothermal vein deposits containing Au and base metal sulphides. In eastern Australia, the Tasman Geosyncline is a major orogenic province at the eastern end of a global systems of orogens along the western and

southern continental margin of Gondwana (Fig.5.5), portions of which are still active today. The Tasman Geosyncline is subdivided into four fold belts (Fig. 5.8): the Lachlan fold belt, the New England fold belt, the Hodgkinson fold belt and the Kanmantoo belt (Palfreyman 1984). Many authors have contributed to unravel aspects of the tectonic history of the Tasman region but partly because of the vastness of the territory, no single description satisfies all the observed features. Some of the works dealing with the Tasman geosyncline include Solomon and Griffiths (1972), Crook (1980), Adams et al. (1985). A time-space tectonic and metallogenic analysis was carried out by Griffiths (1977). A model of the tectonic evolution of the Lachlan belt is discussed in Powell (1983), whilst Murray (1990) provides a review of the Tasman orogenic system and the distribution of mineral deposits in Queensland. The Tasman Geosyncline is very important from the metallogenic point of view, because of the numerous and various contained mineral deposits, most of which are of hydrothermal origin. The geological and tectonic evolution of the Tasman belts can be broadly summarised as follows (Rankine 1987):

1. Development of a marginal sea on oceanic crust, adjacent to the stable Australian Precambrian craton (Kanmantoo belt).
2. Deposition of predominantly deep-water sediments and formation of an island arc to the east (Lachlan fold belt).
3. Arc-continent collision, deformation and emplacement of ophiolites.
4. Granite plutonism in the eastern part, related to both subduction and crustal thickening.
5. Development of multiple volcanic arcs and shallow basinal sequences east of the Lachlan belt (New England fold belt).
6. Formation of the Hodgkinson belt in part synchronous with the New England orogen and deposition of the volcano-sedimentary sequences in the Drummond basin.

Second only to the Archean Yilgarn craton, the Tasman orogens are Australia's richest Au province. In Queensland, important recent discoveries or re-evaluations of high-grade porphyry-epithermal-type Au mineralisation have been made (Morrison 1988). Some of these include the Au deposits of Kidston (Baker and Tullemans 1990), Mt. Leyshon (Paull et al. 1990) and Pajingo (Porter 1990). Numeours other mineral deposits are present from Tasmania in the south right across to north Queensland, and include Cu-Fe, Cu-Mo, Ba-Mn, Ag-Pb-Zn, Sn-W, Sb, mostly of hydrothermal volcanogenic origin or of granitic affiliation. In the final analysis the wealth of the eastern Australian mineral occurrences is linked to a complex interplay of subduction-related environments, and generation of crustal melts in collision and rift-related settings.

Towards the end of the Carboniferous, 280 Ma ago, the continental masses had been rejoined into a Pangea, returning to conditions somewhat similar to those of the Late Proterozoic (Figs. 5.5 and 5.10). The breakup of this Pangea, and in particular of the southern Gondwana continents, began in the Early Jurassic, about 150 Ma ago, leading to the present-day conditions by way of the great Mesozoic-Cenozoic to modern orogenic cycles defined by the Alpine-Himalayan and Circum-
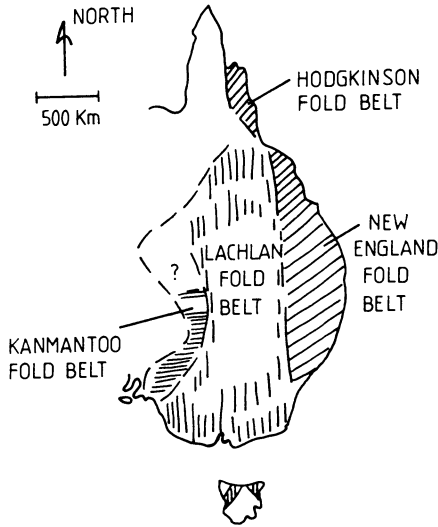
Fig. 5.8. Schematic distribution of the Palaeozoic fold belts in eastern Australia (After Rankine 1987)

Pacific orogenic belts, and a globe-encircling rift-system some 40 000 km long. This is perhaps the most fascinating period of our planet's history, if nothing else from an anthropocentric point of view, since the breakup of the Gondwana and Laurasia landmasses determined new climates, new faunal distribution and biological evolutionary trends culminating first of all in the great explosion of the reptiles, followed by the mammals in ever changing geological and biological systems. Figure 5.8 shows the possible global distribution of the continents about 260 Ma ago, in which Laurasia, forming a northern collection of landmasses, and Gondwana, were united on the northwestern side and separated by the Tethys proto-ocean in the central-eastern regions. This Pangea continental mass was
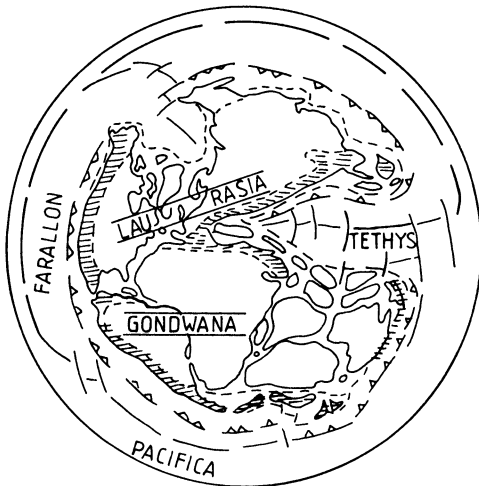
Fig. 5.9. Peripheral orogens (shaded) of the Laurasian and Gondwana continents in the Mesozoic. (After de Wit et al. 1988; Le Pichon and Huchon 1984; Read and Watson 1975)
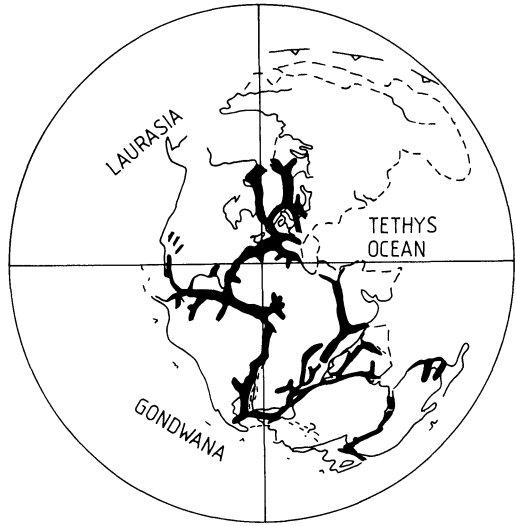
Fig. 5.10. Approximate Mesozoic-Cenozoic rift systems associated with the Pangea continental break-up (After Burke 1977). The network of rifts may be due to a global back-arc-type spreading and rifting accompanied by voluminous outpourings of mafic magmas (Cox 1978). The continental reconstruction is based on the 220 Ma re-assembly by Smith and Briden (1977)

probably concentrated on one hemisphere of the Earth surrounded by oceanic plates on all sides, with active subduction taking place on a grand scale, as indicated in Fig.5.9. From this starting point at least two main theories are advanced by geoscientists as to the next step in the evolution of the Laurasian and Gondwana fragmentations. The first, and perhaps more acceptable of the two (Cox 1978; Le Pichon and Huchon 1984; de Wit et al. 1988), is that the large-scale subduction resulted in vast volumes of oceanic material being dehydrated along Benioff zones. The ascension of great amounts of fluid from the subducting plates would have caused melting of the mantle and the rise of large quantities of mafic magmas to form the great continental flood basalts (e.g. Karoo, Parana-Etendeka etc.), and the emplacement of numerous sills and layered intrusions worldwide along major and extensive rift systems, as shown in Fig.5.10. It is also thought that the continental masses acted as a powerful insulating cap, further enhancing the melting of mantle regions below the above-mentioned rift systems. In another theory, proposed by Alt et al. (1988), it is suggested that oceanic ridges and continental rift systems may have been initiated by meteorite impacts. These impacts would have resulted in pressure release in the mantle by way of deep fractures, with the generation of melts and their upwelling to form hot spots, from which rifting and sea-floor spreading would eventually evolve. These authors compare the inception of the great continental basaltic floods to the lunar maria.

The evolution of mantle plume-generated triple junctions and aulocogens, resulting in continental rifting and subsequent sea-floor spreading is advocated by a number of geologists (Burke and Dewey 1973, Dewey and Burke 1974). Rifting is defined as "places where the entire thickness of the lithosphere has ruptured under tension" (Burke 1977), implying that a rigid crust or plate is a prerequisite for rifting to occur. As advocated by Dewey and Burke (1974), rifting of continental plates may be related to different stages in the Wilson cycle, since an intracontinental rift may either evolve into an ocean basin, or "fail". This is a fundamental concept in the

understanding of the genesis of many hydrothermal mineral deposits. We take a look at the types and mechanisms of rift formation in Chapter 6. Important mineral deposits are related to the formation of rifts from their initial stages of development right through the oceanic stage. Intracontinental hot spots and associated rifting are generally responsible for concentrations of Nb, U, REE in alkaline and carbonatitic complexes, Cu in hydrothermal breccias such as those of Messina in South Africa, Cu-Mo in porphyry-type systems such as those of the Oslo graben in Norway, not to mention the many and important magmatic deposits of Cu-Ni in the mafic complexes.

The Alpine-Himalayan and Circum-Pacific Orogenic Belts, and Related Metallogeny

The Mesozoic-Cenozoic Alpine-Himalayan mountain belts, and the Cordilleran-Andean-Antarctica-New Zealand peripheral system of orogenic belts, developed during the drifting of the continents by subduction, accretion and collision. The Alpine-Hiymalayan belts formed in various stages by the closure of the Tethys ocean and collision of a number of continental plates of Gondwana and Laurasia. The peripheral Circum-Pacific belts, on the other hand, developed largely as a result of the subduction of oceanic crust under continental crust, and by the accretion of microplates on to continental margins. The diverse geodynamic evolution associated with these various settings resulted in different metallogenic histories. The complex geological history of the Alpine-Himalayan belts spans the entire Phanerozoic, involving the interaction of a network of spreading ridges, continental margins, island arcs, and back arc basins, with collision and subduction tectonics still active today.

A number of tentative syntheses depicting the geodynamic evolution of the Alpine sector have been published, and the reader is referred in particular to the work of Dewey et al. (1973). At present the African plate is being consumed in a trench system south of the Aegean arc. Recent and present-day volcanism across the Italian peninsula, the Aegean Sea and Turkey, associated with belts of ophiolites and flysch-type sediments, testify to this continuing evolving and active portion of the Earth's crust. As may be anticipated, the metallogeny related to the Alpine sector is equally complex, and a comprehensive review of European metallogeny can be found in Emberger (1984). Across the Alpine arc, from Italy through the Balkans, to Turkey and the Caucasus mountains, there are Pb-Zn-Ba deposits of rift-related hydrothermal activity, massive sulphides associated with ophiolitic rocks, such as those of Cyprus, porphyry Cu, and numerous occurrences of Sb, Hg and As related to recent epithermal systems connected with arc volcanism. At the time of writing, the latter type of mineralisation is being investigated for Au, and it is possible that new discoveries of this precious metal may soon be announced.

Tectonic syntheses pertaining to the Himalayan sector have been published more recently, thanks to joint Sino-European scientific programmes. In this respect the works of Molnar and Tapponier (e.g. Molnar and Tapponier 1975; Tapponier et al. 1982; Molnar 1984) and those of Le Fort (1986), Coward et al. (1982), Sengör (1979, 1981, 1987), are especially useful. The Himalayan sector is generally considered to

have formed through a complex history of (1) subduction of a Paleo-Tethys sea under a Cimmerian continent (Sengör 1979, 1987); (2) ocean floor spreading in a Neo-Tethys, between it and the northern margin of Gondwana; (3) their closure and collision; (4) the more recent (about 50 Ma ago), northward drift of the Indian subcontinent and; (5) its final collision with the Asian landmass. The latter event produced the indentation tectonics of Tapponier et al. (1982), characterised by long strike-slip faults and rift basins, such as the Baikal system in Siberia. Little is known of the details of the metallogeny of the Himalayan system, and no global syntheses – such as those carried out for the Andes, or the North American Cordilleras – have been published. Porphyry deposits, Sb, Sn-W of greisen affiliation, are, however, known to be present and are perhaps the most common.

The Andean-Cordilleran belt extends across the entire western margin of the Americas, connecting with West Antarctica and New Zealand. Along this margin subduction of oceanic crust occurs under continental margins producing a long array of calc-alkaline volcano-plutonic belts, and back-arc-type extensional basins.

The Andean sector is constructed along the consuming margin between the overriding edge of the South American continent and the subducting Nazca plate. The belt is characterised by an eastward migration of progressively younger volcano-plutonic zones, which coincide with an overall eastward change from tholeiitic to calc-alkaline and to alkaline chemistry. The metallogeny of the Andes shows a zonation in time and space that is clearly related to this eastward magmatic migration. During the Jurassic and the Tertiary, and from west to east, Cu, Cu-Au porphyries of tholeiitic and calc-alkaline affinity, Cu-Mo porphyry of continental affinity, and Au, W, Sb, Sn, Hg, Bi, Ag, Pb deposits associated with more recent volcanism in thicker zones of continental crust, are encountered (Frutos 1982).

The Cordilleras of the North American continent are the product of a very complex interplay of subduction- and rift-related magmatism, extensional and collision tectonics. The recognition of collision, or accretion, of microplates and "suspect terranes" is a relatively recent concept, currently advocated to have operated in many orogens around the Pacific rim (Nur and Ben-Avraham 1982; Howell 1985, 1989) and indeed also being advocated for older orogenic belts, such as the Pan-African belts in the Arabian-Nubian shield (Stoeser and Camp 1985), and the Appalachian orogen (Williams and Hatcher 1982). The theory of the accretion of allochthonous fragments clearly has important implications for the exploration geologist and these are discussed in Chapter 6. For the moment it will suffice to say that "suspect, exotic, allochthonous, or tectonostratigraphic" terranes are terms used to indicate a fault-bounded geological entity characterised by unique stratigraphic, tectonic and metallogenic features that are markedly different from those of neighbouring terranes (Schermer et al. 1984). Various lines of evidence, including palaeontological, structural and palaeomagnetic, indicate that the North American cordilleras from Alaska to Mexico may be a "collage" of about 50 "suspect terranes" (Coney et al. 1980). These terranes collided and accreted to the western margin of the North American cratonic mass during the Mesozoic and the Cenozoic. Movement and dispersion of these terranes is still continuing, notably along the San Andreas fault, and the picture is further complicated by the addition

of volcano-plutonic belts by subduction and back-arc rifting within and across terranes.

The metallogeny of such a geological environment is therefore extremely complex. A careful analysis of these terranes will have to discriminate between deposits formed during the pre-collision tectonic evolution and those formed after their "docking" to the continental margin. Generally, mineral deposits formed before collision would include those that originated by hydrothermal activity on the ocean floor. The North American cordilleras are very rich in mineral resources and include a vast array of porphyry Cu, Cu-Mo, and epithermal Au-Ag deposits, all related to subduction and/or back-arc extensional magmatism. In Alaska are numerous deposits of hydrothermal vein lode-Au mineralisation, probably related to regional metamorphic dewatering, Sn-W mineralisation of granitic affinity, carbonate-hosted Pb-Zn, shale-hosted Pb-Zn-Ba-Ag, and volcanic-sediment hosted Cu-Zn of syngenetic hydrothermal origin (Einaudi and Hitzman 1986).

Thus, it is clear from what has been said of the American Pacific margin orogenic belts that the metallogenic histories of the North American cordilleras and the South American Andean belts are markedly different. In the former, juxtaposition and overlap of distinct metallogenic provinces with no zoning at the regional scale contrast with the overall, comparatively regular, time-space zoning of metals and mineral belts of the Andean region. The different metallogenies of these two great regions of the Pacific rim clearly reflect their tectonic history and geodynamic evolution, knowledge of which is a prerequisite for the exploration geologist in the successful search of new mineral deposits.

Island arcs and their associated submarine trenches are the surface expression of subduction of oceanic crust and related magmatic activity. Modern island arcs, submarine trenches, and active and inactive marginal basins festoon the northern, western and southwestern sides of the Pacific Ocean, extending for over 20 000 km from Alaska to the Tongan islands (Fig. 5.11). The geology, geochemistry and tectonic evolution of the Pacific island arcs are discussed in a volume edited by Coleman (1973), and in a series of papers published in Tectonophysics (vol. 160, No.1/4, 1989). The Pacific island arc volcanism shows systematic petrological and geochemical variations, according to whether the arcs are immature and built entirely on oceanic crust, or progressively more mature with increasing age and amount of continental crust (Windley 1984). Ewart and Bryan (1973) compared the petrology and geochemistry of the intra-oceanic Tongan island arc volcanism with that of the New Zealand arc, which is built on continental crust. Their study reveals that the New Zealand volcanic rocks are enriched in REE and alkalies, have higher K/Rb ratios and initial Sr^{87}/Sr^{86} ratios. Thus, it appears that the amount of continental crust on which the subduction-related arcs are built is important in determining the petrological and geochemical characteristics of the magmatic products. Indeed, there is a continuum of compositions from intraoceanic tholeiitic volcanism to calc-alkaline and alkaline volcanism of continental margins such as the Andes (Brown 1982; Brown et al. 1984; Windley 1984). The metallogenesis of the Pacific island arcs reflects these variations. Cu-Au in porphyry systems, base metals and Au-Ag in kuroko-type deposits, and the recent exciting discoveries of epithermal Au in modern volcanoes are common throughout. In recent years the
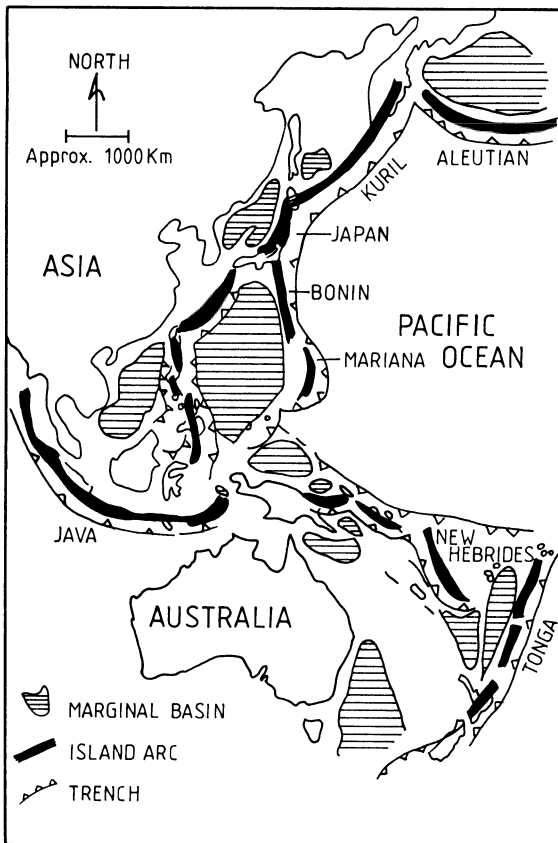
Fig. 5.11. Island arcs, marginal basins and trench systems of the western Pacific (After Dickinson 1973; Karig 1974; Windley 1984); Jolivet et al. 1989)

island arcs of the Pacific have been experiencing mineral exploration activity on an unprecedented scale. The successes of this mineral exploration are due to the recognition of the volcanic-hosted epithermal type of mineralisation which, although recognised by Lindgren (1933) more than 50 years ago, only much later posed any real implication in the field of economic geology.

5.2.4 Conclusions

This brief review of the tectonic evolution of the crust throughout most of the Earth's history indicates that, in terms of metallogenesis, two important aspects must be considered (see Fig. 5.1A, B). Firstly, there are mineral deposits that are formed in non-uniformitarian time and tectonic-style related geological situations. These include both magmatic and hydrothermal mineral deposits, as for example the Archean Ni-Cu sulphides, the Proterozoic Au-U Witwatersrand deposits, the Cr, PGE and Fe-Ti magmatic accumulations, and the giant sedimentary-exhalative rift-related base metal deposits. Secondly, there are the uniformitarian geological

scenarios, which tend to occur at any time of the Earth's history providing that the same set of conditions is present. Uniformitarian mineral deposits include, in general, magmatic-hydrothermal, meteoric-hydrothermal and metamorphic-hydrothermal types, as for example volcanogenic massive sulphides, porphyry and volcanic-hosted epithermal systems, metamorphogenic Au vein lode deposits, and Sn-W mineralisation of granitic affiliation. However, since most of these tend to form near the surface or in high-level hydrothermal systems that through collisional tectonics become topographically elevated, their rapid erosion makes preservation potential poor. The height of mountain ranges is inversely proportional to their age, and their contained mineralisation is indeed reflected in their topographic elevation, as seen in the Andes and the North American cordilleras, and in the very young porphyry and epithermal systems of Papua New Guinea. Nevertheless, in exceptional circumstances some of these deposits may be preserved in the geological record, as for example in Namibia, where one of the oldest porphyry Cu has survived since 2000 Ma ago, or the Roxby Downs deposit in South Australia, conveniently buried under several hundreds of metres of post-mineral sediments.

References

Adams C J, Black L P, Corbett K D, Green G R (1985) Reconnaissance isotopic studies bearing on the tectonothermal history of early Paleozoic and late Proterozoic sequences in western Tasmania. Aust J Earth Sci 32:7–36

Alt D, Sears J W, Hyndman D W (1988) Terrestrial maria: the origins of large basalt plateaus, hotspot tracks, and spreading ridges. J Geol 96:647–662

Anhaeusser C R (1971) The Barberton Mountain Land, South Africa – a guide to the understanding of the Archean geology of Western Australia. Geol Soc Aust Spec Publ 3:103–119

Anhaeusser C R (1975) Precambrian tectonic environments. Earth Planet Sci Lett 3:31–53

Anhaeusser C R (1976) Archean metallogeny in Southern Africa. Econ Geol 71:16–43

Anhaeusser C R, Maske S (eds) (1986) Mineral Deposits of Southern Africa, vol 1, 2. Geol Soc S Afr, 2376 pp

Appel Uitterdijk P W, LaBerge L G (eds) (1987) Precambrian iron formations. Theophrastus, Zographou, Athens, 674 pp

Baker E M, Tullemans F J 1990 Kidston gold deposits. In: Hughes F E (ed) Geology of the mineral deposits of Australia and Papua New Guinea, vol 2. Australas Inst Min Metall Monogr 14, Parkville, Victoria, pp 1461–1465

Baragar W R A, Scoates R F J (1981) The circum-Superior belt: A Proterozoic plate margin? In: Kröner A (Ed) Precambrian plate tectonics. Elsevier, Amsterdam, pp 261–296

Barley M E, Eisenlohr B N, Groves D I, Perring C S, Vearncombe J R (1989) Late Archean convergent margin tectonics and gold mineralization: a new look at the Norseman-Wiluna belt, Western Australia. Geology 17: 826–829

Bickle M, Nisbett E G (1986) Greenstone belt tectonics-thermal constraints. Workshop on the tectonic evolution of greenstone belts. Lunar Planet Inst NASA, pp 1–8

Bird J M, Isacks, B (eds) (1972) Plate tectonics. Selected papers from the Journal of Geophysical Research. Am Geophys Un, Washington D C

Bond G C, Nickeson P A, Kominz M A (1984) Breakup of a supercontinent between 625 Ma and 555 Ma: new evidence and implications for continental histories. Earth Planet Sci Lett 70:325–345

Borg G (1988) The Koras-Sinclair-Ghanzi rift in Southern Africa Volcanism, sedimentation, age relationships and geophysical signature of Late Middle Proterozoic rift system. Precambrian Res 38:75–90

Brown G C (1982) Calc-alkaline intrusive rocks: their diversity, evolution, and relation to volcanic arcs. In: Thorpe R S (ed) Andesites. John Wiley & Sons, New York, pp 437–461

Brown G C, Thorpe R S, Webb P C (1984) The geochemical characteristics of granitoids in contrasting arcs and comments on magma sources. J Geol Soc London 141:413–426

Burke K (1977) Aulocogens and continental breakup. Annu Rev Earth Planet Sci 5:371–396

Burke K C A, Dewey J F (1973) Plume generated triple junctions: key indicators in applying plate tectonics to old rocks. J Geol 86:406–433

Burke K, Dewey J F, Kidd W S F (1976) Dominance of horizontal movements, arc and microcontinental collisions during the later permobile regime. In: Windley B F (ed) The early history of the Earth. John Wiley & Sons, New York, pp 13–129

Burke K, Kidd W S F, Kusky T (1985) Is the Ventersdorp rift system of Southern Africa related to continental collision between the Kaapvaal and Zimbabwe cratons at 264 Ga ago? Tectonophysics 115:1–24

Button A, Pretorius D A, Jansen H, Stocklmayer V, Hunter D R, Wilson J F, Wilson A H, Vermak C F, Lee C A, Stagman J G (1981) The cratonic environment. In: Hunter D R (ed) Precambrian of the southern hemisphere. Elsevier, Amsterdam, pp 501–627

Clendenin C W, Charlesworth E G, Maske S (1988) An early Proterozoic three-stage rift system, Kaapvaal craton, South Africa. Tectonophysics 145:73–86

Cloud P (1976) Major features of crustal evolution. Geol Soc S Afr Vol LXXIX:1–33

Coleman P J (ed) (1973) The Western Pacific island arcs-marginal seas-geochemistry. Univ W Aust Press, Perth, Adelaide, 675 pp

Condie K C (1981) Archean Greenstone Belts. Developments in Precambrian Geology 3. Elsevier, Amsterdam

Condie K C, Hunter D R (1976) Trace element geochemistry of Archean granitic rocks from the Barberton region, South Africa. Earth Planet Sci Lett 29:389–400

Coney P J, Jones D L, Monger J W H (1980) Cordilleran suspect terranes. Nature (London) 288:329–333

Cook F A, Albaugh D S, Brown L D, Kaufman S, Oliver J E, Hatcher R D (1979) Thin skinned tectonics in the crystalline southern Appalachians: COCORP seismic reflection profiling of the Blue Ridge and Piedmont. Geology 7:563–567

Coward M P, Jan M Q, Rex D, Tarney J, Thirwall M, Windley B F (1982) Geotectonic framework of the Himalaya of North Pakistan. J Geol Soc London 139:299–308

Cox K G (1978) Flood basalts, subduction and the breakup of Gondwanaland. Nature (London) 274:47–49

Crook K A W (1980) Fore-arc evolution in the Tasman geosyncline: the origin of the south-eastern Australian continental crust. J Geol Soc Aus 27:215–232

Dewey J F, Burke K C A (1974) Hot spots and continental breakup: implications for collisional orogeny. Geology 2:57–60

Dewey J F, Pitman W C, Ryan W B F, Bonnin J (1973) Plate tectonics and the evolution of the Alpine system. Geol Soc Am Bull 84: 3137–3180

De Wit M J, Jeffery M, Bergh H, Nicolaysen L (1988) Geological map of sectors of Gondwana. Am Ass Pet Geol; Univ Witwatersrand

Dickinson W R (1973) Reconstruction of past arc-trench systems from petrotectonic assemblages in the island arcs of the Western Pacific. In: Coleman P J (ed) The Western Pacific. Univ W Aust Press, Perth, Adelaide, pp 569–602

Dimroth E (1981) Labrador geosyncline: Type example of early Proterozoic cratonic reactivation. In: Kröner A (ed) Precambrian Plate Tectonics. Elsevier, Amsterdam, pp 331–352

Donaldson J A, McGlynn J C, Irving E, Park J K (1973) Drift of the Canadian shield. In: Tarling D H, Runcorn S K (eds) Implication of continental drift to the Earth Sciences. Academic Press, New York, London, pp 3–18

Economic Geology (ed) (1985 A special issue devoted to the Bushveld Complex. Econ Geol 80, 4

Einaudi M T, Hitzman M W (1986) Mineral deposits in Northern Alaska: Introduction. Econ Geol 81:1583–1591

Emberger A (1984) La carte metallogenique de l'Europe et des pays limitrophes 1/2 500000 Un bilan des années 1960–1983 Chron Rech Min 475:51–56

Ewart A, Bryan W B (1973) The petrology and geochemistry of the Tongan Islands. In: Coleman P J
    (ed) The Western Pacific island arcs – marginal seas – geochemistry. Univ W Aust Press, Perth,
    Adelaide, pp 503–522
Frey H (1980) Crustal evolution of the early Earth: the role of major impacts. Precambrian Res
    10:195–216
Frutos J (1982) Andean metallogeny related to the tectonic and petrologic evolution of the
    Cordillera. Some remarkable points. In: Amstutz G C, Goresy El A, Frenzel G, Kluth C, Moh
    G, Wauschkuhn A, Zimmermann R A (eds) Ore genesis – the State of the Art. Springer, Berlin,
    Heidelberg, New York, pp 493–507
Fyfe W S (1978) The evolution of the Earth's crust: modern plate tectonics to ancient hotspot
    tectonics? Chem Geol 23:89–114
Gass I G (1981) Pan-African (Upper Proterozoic) plate tectonics of the Arabian-Nubian shield. In:
    Kröner A (ed) Precambrian Plate Tectonics. Elsevier, Amsterdam, pp 388–405
Glikson A Y (1972) Early Precambrian evidence of a primitive ocean crust and island nuclei of sodic
    granite. Bull Geol Soc Am 83:3323–3344
Glikson A Y (1976) Stratigraphy and evolution of a primary and secondary greenstone: significance
    of data from shields of the southern hemisphere. In: Windley B F (ed) The early history of the
    Earth. Wiley-Interscience, London, pp 257–277
Glikson A Y (1981) Uniformitarian assumptions, plate tectonics and the Precambrian Earth. In:
    Kröner A (ed) Precambrian Plate Tectonics. Elsevier, Amsterdam, pp 91–104
Glikson A Y, Lambert I B (1976) Vertical zonation and petrogenesis of the early Precambrian crust
    in Western Australia. Tectonophysics 30:55–89
Goodwin A M (1981) Precambrian perspectives. Science 213:55–61
Green D H (1972) Archean greenstone belts may include terrestrial equivalent of lunar maria? Earth
    Planet Sci Lett 15:263–270
Grieve R A F (1980) Impact bombardment and its role in proto-continental growth of the early
    Earth. Precambrian Res 10:217–247
Griffiths J R (1977) Geology and metallogeny of the Lachlan orogen, Australia: a time-space
    analysis and preliminary tectonic synthesis. CSIRO Invest Rep 123:42 pp
Gross G A (1980) A classification of iron formations based on depositional environments. Can
    Mineral 18:215–222
Groves D I, Batt W D (1984) Spatial and temporal variations of Archean metallogenic associations
    in terms of evolution of granitoid-greenstone terrains with particular emphasis on the Western
    Australian shield. In: Kröner A, Hanson G H, Goodwin A M (eds) Archean Geochemistry.
    Springer, Berlin, Hedelberg, New york, pp 73–98
Hargraves R B (1981) Precambrian tectonic styles: A liberal uniformitarian interpretation. In:
    Kröner A (ed) Precambrian plate tectonics. Developments in Precambrian Geology, Vol 4.
    Elsevier, Amsterdam, pp 21–51
Hartnady C, Joubert P, Stowe C (1985) Proterozoic crustal evolution in Southwestern Africa,
    Episodes 8:236–244
Hoffman P F (1980) Wopmay orogen: a Wilson cycle of early Proterozoic age in the northwest of the
    Canadian shield. In: Strangway D F (ed) The continental crust and its mineral deposits. Geol
    Ass Can Spec Pap 20:523–549
Howell D G (1985) Terranes. Sci Am 253:90–103
Howell D G (1989) Tectonics of suspect terranes – Mountain building and continental growth.
    Chapman and Hall, London, New York, 232 pp
Hunter D R (1974) Crustal development in the Kaapvaal craton. Econ Geol Res Unit, Univ
    Witwatersrand Inf Circ 83 and 84
Hurley P M, Rand J R (1969) Predrift continental nuclei. Science 164: 1229–1242
Hutchinson R W (1973) Volcanogenic sulfide deposits and their metallogenic significance. Econ
    Geol 68:1223–1246
Hutchinson R W (1980) Massive base metal sulphide deposits as guides to tectonic evolution. In:
    Strangway D W (ed) The continental crust and its mineral deposits. Geol Ass Can Spec Pap
    20:659–684
Hutchinson R W, Viljoen R P (1988) Re-evaluation of gold source in Witwatersrand ores. S Afr J
    Geol 91:157–173

Hutchison C S (1983) Economic deposits and their tectonic setting. MacMillan Press, New York, 355 pp

Irving E (1977) Continental drift since the Devonian. Nature, (London) 270:304–309

James H L, Trendall A F (1982) Banded iron formation: distribution in time and paleoenvironmental significance. In: Holland H D, Schidloswki M (eds) Mineral deposits and the evolution- of the biosphere. Dahlem Worksh Rep. Springer, Beriln, Heidelberg, New York, pp 199–218

Jolivet L, Huchon P, Rangin C (1989) Tectonic setting of Western Pacific marginal basins. Tectonophysics 160:23–47

Karig D E, (1974) Evolution of arc systems in the western Pacific. Annu Rev Earth Planet Sci 2:51–75

Keays R R, Nickel E H, Groves D I, McGoldrich P J (1982) Iridium and palladium as discriminants of volcanic-exhalative hydrothermal, and magmatic nickel sulfide mineralisation. Econ Geol 77:1535–1547

Kimberley M M (1989a) Nomenclature for Iron Formations. Ore Geol Rev 5:1–12

Kimberley M M (1989b) Exhalative orings for Iron Formations. Ore Geol Rev 5:13–145

Kröner A (1981) Precambrian plate tectonics. In: Kröner A (ed) Precambrian plate tectonics. Elsevier, Amsterdam. pp 57–90

Kröner A (1985) Evolution of the Archean continental crust. Annu Rev Earth Planet Sci 13:49–74

Lambert I B, Groves D I (1981) Early earth evolution and metallogeny. In: Wolf K H (ed) Handbook of stratabound and stratiform ore deposits, vol 8. Elsevier, Amsterdam, pp 339–447

Leach D L, Landis G P, Hofstra A H (1988) Metamorphic origin of the Coeur d'Alene base-and precious-metal veins in the Belt basin, Idaho and Montana. Geology 16:122–125

Lefort J P, Audren C L, Max M D (1982) The southern part of the Armorican orogeny: a result of crustal shortening related to reactivation of a pre-Hercynian mafic belt during Carboniferous time. Tectonophysics 89: 359–377

Le Fort P (1986) Metamorphism and magmatism during the Himalayan collision. In: Coward M P, Ries A C (eds) Collision Tectonics. Geol Soc Spec Publ 19:159–172

Le Fort P, Cuney M, Deniel C, France-Laccord C, Shepperd S M F, Upreti B N, Vidal P (1987) Crustal generation of the Himalayan leucogranites. Tectonophysics 134:39–57

Le Pichon X, Huchon P (1984) Geoid, Pangea and convection. Earth Planet Sci Lett 67:123–135

Le Pichon X, Francheteau J, Bonnin J (1973) Plate tectonics. Elsevier, Amsterdam, 300 pp

Lewis J S, Prinn R G (1984) Planets and their atmospheres. Academic Press, New York. London, 470 pp

Lindgren W (1933) Mineral deposits. McGraw-Hill, New York 930 pp

Lowe, D R, Byerly G R (1986) The rock components and structures of Archean greenstone belts: an overview. In: Workshop in tectonic evolution of greenstone belts. Lun Planet Inst, Houston, pp 9–14

Lowman P D (1989) Comparative planetology and the origin of continental crust. Precambrian Res 44:171–(195

Macgregor A M (1951) Some milestone in the Precambrian of Southern Rhodesia. Proc Geol Soc S Afr 54:XXVII–IXXI

Marmont S (1987) Ore deposits models #13. Uncomformity-type uranium deposits. Geosci Canada 14:219–229

Martini, J E J (1988) As-Zn mineralisation associated with a Proterozoic geothermal system in the Rooiberg Group. S Afr J Geol 91:337–345

Meyer C (1981) Ore forming processes in geologic history. Econ Geol 75th Anniv Vol: 6–41

Meyer C (1988) Ore deposits as guides to geological history of the Earth. Annu Rev Earth Planet Sci 16:147–171

Minter W E L (1978) A sedimentological synthesis of placer gold uranium and pyrite concentrations in Proterozoic Witwatersrand sediments. In: Miall A D (ed) Fluvial sedimentology. Can Soc Petrol Geol Mem 5: 801–829

Minter W E L, Hill W C N, Kidger R J, Kingsley C S, Snowden P A (1986) The Welkom Goldfield. In: Anhaeusser C R, Maske S (eds) Mineral deposits of Southern Africa, vol 1. Geol Soc S Afr, pp 497–540

Mitchell A H G, Garson M S (1981) Mineral deposits and global tectonic settings. Academic Press, New York, London, 405 pp

Molnar P (1984) Structure and tectonics of the Himalaya: constraints and implications of geophysical data. Annu Rev Earth Planet Sci 12:489–518

Molnar P, Tapponier P (1975) Cenozoic tectonics of Asia: effects of a continental collision. Science 189:419–426

Moorbath S (1977) Ages, isotopes and evolution of Precambrian continental crust. Chem Geol 20:151–187

Morel P, Irving E (1978) Tentative palaeocontinental maps for the early Phanerozoic and Proterozoic. J Geol 86:535–561

Morel P, Irving E (1981) Palaeomagnetism and the evolution of Pangea. J Geophys Res 86:1858–1872

Morrison G W 1988 Palaeozoic gold deposits of northeast Queensland. In: Bicentennial Gold '88. Geo Soc Aust Abstr Ser 22:91–101

Murray C G 1990 Tasman fold belt in Queensland. In: Hughes F E (ed) Geology of the mineral deposits of Australia and Papua New Guinea, vol 2. Australas Inst Min Metall Monogr 14, Parkville, Victoria, pp 1431–1450

Naldrett A J (1965) The role of sulphurisation in the genesis of iron-nickel deposits of the Porcupine District, Ontario. Can Inst Min Metall Bull 59:489–497

Naldrett A J (1973) Nickel sulfide deposits – their classification and genesis, with special emphasis on deposits of volcanic association. Can Inst Min Metall Bull 76:183–201

Nance R D, Worsley T R, Moody J B (1988) The supercontinent cycle. Sci Am 259:44–52

Nur A, Ben-Avraham Z (1982) Oceanic plateaux, the fragmentation of continents, and mountain building. J Geophys Res 87:3644–3661

Palfreyman W D (1984) Guide to the geology of Australia. Bur Mineral Resour Aust Bull 181, 111 pp

Paull P L, Hodkinson I P, Morrison G W, Teale G S 1990 Mount Leyshon gold deposit. In: Hughes F E (ed) Geology of the mineral deposits of Australia and Papua New Guinea, vol 2. Australas Inst Min Metall Monogr 14, Parkville, Victoria, pp 1471–1481

Phillips G N (1987) Metamorphism of the Witwatersrand goldfields: conditions during peak metamorphism. J Metamorph Geol 5:307–322

Phillips G N, Groves D I (1983) The nature of Archean gold-bearing fluids as deduced from gold deposits of Western Australia. J Geol Soc Aust 30:25–40

Phillips G N, Myers R E, Law J D M, Bailey A C, Cadle A B, Beneke D, Borrego P M D A, Giusti L, Ingle L, Kerr S J, Palmer J A, Ramos Z C D N, Robertson S (1988) Recent advances in the geology of the Witwatersrand goldfields, including the importance of post-depositional processes. In: Bicentennial Gold '88. Geol Soc Aust Abstr Ser 22:319–324

Piper J D A (1973) Geological interpretation of palaeomagnetic results from the African Precambrian. In: Tarling D H, Runcorn S K (eds) Implications of continental drift to the Earth Sciences. Academic Press, New York, London, pp 19–32

Piper J D A (1982) The Precambrian palaeomagnetic record: the case for the Proterozoic supercontinent. Earth Planet Sci Lett 59:61–89

Porada H (1985) Stratigraphy and facies in the upper Proterozoic Damara orogen, Namibia, based on a geodynamic model. Precambrian Res 29: 235–264

Porter R R G 1990 Pajingo gold deposits. In: Hughes F E (ed) Geology of the mineral deposits of Australia and Papua New Guinea, vol 2. Australas Inst Min Metall Monogr 14, Parkville, Victoria, pp 1483–1487

Powell C McA (1983) Tectonic relationship between the late Ordovician and late Silurian palaeogeographies of southeastern Australia. J Geol Soc Aust 30:353–373

Pretorius D A (1976a) The nature of the Witwatersrand gold-uranium deposits. In: Wolf K H (ed) Handbook of stratabound and stratiform ore deposits, vol 7. Elsevier, Amsterdam, pp 29–88

Pretorius D A (1976b) Gold in the Proterozoic sediments of South Africa: systems, paradigms and models. In: Wolf K H (ed) Handbook of stratabound and stratiform ore deposits, vol 7. Elsevier, Amsterdam, pp 1–27

Pretorius D A (1986) The goldfields of the Witwatersrand basin. In: Anhaeusser C R, Maske S (eds) Mineral deposits of southern Africa, vol 1. Geol Soc S Afr, pp 489–494

Rankine G M (1987) Gold metallogeny in Australia. MSc thesis, Rhodes Univ, Grahamstown, S Afr 116 pp

Read H H, Watson J (1975) Earth history, Vol 2, pt 1,2. Compton Pitman, London, 371 pp

Reeve J S, Cross K C, Smith R N, Oreskes N 1990 Olympic Dam copper-uranium-gold-silver deposit. In: Hughes F E (ed) geology of the mineral deposits of Australia and Papua New Guinea, vol 2. Australas Inst Min Metall Monogr 14, Parkville, Victoria, pp 1009–1035

Rickard D (1987) Proterozoic volcanogenic mineralisation styles. In: Pharaoh T C, Beckinsale R D, Rickard D (eds) Geochemistry and mineralisation of Proterozoic volcanic suites. Geol Soc Spec Publ 33:23–35

Roberts D E, Hudson G R T (1983) The Olympic Dam copper-uraniumgold deposit, Roxby Downs, South Australia. Econ Geol 78: 799–822

Robertson D S, Tisley J E, Hogg G M, (1978) The time-bound character of uranium deposits. Econ Geol 73:1409–14(19

Rozendaal A (1978) The Gamsberg zinc deposit, Namaqualand. In: Verwoerd W J (ed) Mineralisation in metamorphic terranes. Spec Publ Geol Soc S Afr 4:235–265

Sawkins F J (1990) Metal deposits in relation to plate tectonics, 2nd edn. Springer, Berlin, Heidelberg, New York, 461 pp

Schermer E R, Howell D G, Jones D L (1984) The origin of allochthonous terranes: perspectives on the growth and shaping of continents. Annu Rev Earth Planet Sci 12:107–131

Scotese C R, Bambach R K, Barton C, Van der Voo R, Ziegler A Y (1979) Palaeozoic base maps. J Geol 87:217–277

Sengör A M C (1979) Mid-Mesozoic closure of Permo-Triassic Tethys and its implications. Nature (London) 279:590–593

Sengör A M C (1981) The geological exploration of Tibet. Nature (London) 294:403–404

Sengör A M C (1987) Tectonics of the Thethysides: orogenic collage development in a collisional setting. Annu Rev Earth Planet Sci 15:213–244

Sims P K (1980) Subdivisions of the Proterozoic and Archean eon: Reconstructions and suggestions by the International Subcommision on Precambrian Stratigraphy. Precambrian Res 13:379–380

Smith A G, Briden J C (1977) Mesozoic and Cenozoic paleocontinental maps. Univ Press, Cambridge, 63 pp

Smith A G, Hurley A M, Briden J C (1981) Phanerozoic paleocontinental world maps. Univ Press, Cambridge, 102 pp

Smith B, Christiansen R L (1980) Yellowstone Park as a window on the Earth's interior. Sci Am 242:84–97

Smith J (1981) The first 800 million years of Earth's history. Phil Trans R Soc London Ser A301:401–422

Solomom M, Griffiths J R (1972) Tectonic evolution of the Tasman Orogenic Zone, eastern Australia. Nature (London) 70:3–6

Stoeser D B, Camp E (1985) Pan-African microplate accretion of the Arabian Shield. Geol Soc Am Bull 96:817–826

Sutton J (1963) Long-term cycles in the evolution of the continents. Nature (London) 198:731

Swinden H S, Strong D F (1976) A comparison of plate tectonic models of metallogenesis in the Appalachians, the North American Cordillera, and the East Australian Paleozoic. In: Strong D F (ed) Metallogeny and plate tectonics. Geol Ass Can Spec Pap 14:441–470

Tankard A J, Jackson M P A, Erikson K A, Hobday D K, Hunter D R, Minter W E L (1982) Crustal evolution of Southern Africa – 3.8 billion years of earth history. Springe, Berlin, Heidelberg, 523 pp

Tapponier P, Peltzer G, Le Dain A Y, Armijo R, Cobbold P 1982 Propagating extrusion tectonics in Asia: insights from simple experiments with plasticine. Geology 10:611–616

Tarling D H, Runcorn S K, (eds) (1973) Implications of continental drift to the earth sciences. Nato Advanced Study Inst, Vol 1, 2. Academic Press, New York, London, 1184 pp

Tarney J, Dalziel, I W D, De Wit M J (1976) Marginal basin "rocas verdes" Complex from S Chile: A model for Archean greenstone belt formation. In: Windley B F (ed) The early history of the Earth. John Wiley & Sons, New York, pp 131–146

Taylor S R, McLennan S M (1985) The continental crust: its composition and evolution. Blackwell, Oxford, 312 pp

Tectonophysics (ed) (1989) Subduction Zones: the Kaiko project. Tectonophysics 160 1/4

Vearncombe J R, Barton, J M, Van Reenen D D, Phillips G N, Wilson A H (1986) Greenstone belts:
    their components and structures. In: Workshop on tectonic evolution of greenstone belts. Lun
    Planet Inst. Houston, pp 19–26
Watson J (1973) Influence of crustal evolution on ore deposition. Trans Inst Min Metall 82:B107–
    B114
Watson J (1978) Ore-deposition through geological time. Proc R Soc London Ser A 362:305–328
Williams H, Hatcher R D (1982) Suspect terranes and accretionary history of the Appalachian
    orogen. Geology 10:530–536
Wilson J T (1963) Evidence from islands on the spreading of ocean floors. Nature (London)
    197:536:538
Wilson J T (1965) A new class of faults and their bearing on continental drift. Nature (London)
    207:343–538
Wilson J T (1966) Did the Atlantic close and then re-open? Nature (London) 211:676
Wilson J T (ed) (1973) Continents Adrift. Readings from Scientific American. Freeman, San
    Francisco, 172 pp
Windley B F (1984) The evolving continents, 2nd edn. John Wiley and Sons, Chichester, 399pp
Windley B F, Smith J (1976) Archean high-grade complexes and modern continental margins.
    Nature (London) 260:671–675
Worst B G (1960) The Great Dyke of Southern Rhodesia Southern Rhodesia. Geol Surv Bull 47
Wyllie P J (1971) The dynamic Earth. John Wiley & Sons, New York, 416 pp
Zonenshain L P, Korinevsky G, Kazmin G, Pechersky D M, Khain V V, Matveenkov V V (1984)
    Plate tectonic model of the South Urals development. Tectonophysics 109:95–135

Chapter 6

Geological Processes and Hydrothermal Mineralisation in Plate Tectonic Settings – Mineral Exploration

6.1 Introduction

The Earth's outer layers, namely, the lithosphere and the asthenosphere have an important role in the mechanisms of plate tectonics. The outermost layer of our planet is the relatively strong and rigid lithosphere – about 100 km thick – broken up into a number of major and minor plates, whose present-day configuration is shown in Fig. 6.1. The boundaries between plates, divergent (rifting, spreading zones), convergent (subduction and collision zones) and transform faults, are the sites of intense geological activity including earthquakes, volcanism, mountain building and of course mineralisation. The lithosphere overlies the asthenosphere, a weak region of the upper mantle about 200 km thick, where temperatures approach melting point. The boundary, which is probably gradational, between these two layers is by no means well defined, and is not to be confused with the crust-mantle boundary which is defined by the Mohorovicic discontinuity. Although the reason for the movement of the lithospheric plates is not entirely understood, it is generally agreed that mantle convective motions, possibly driven by radiogenic heat, may be responsible. The spreading motion of the oceanic crust is indicated by the
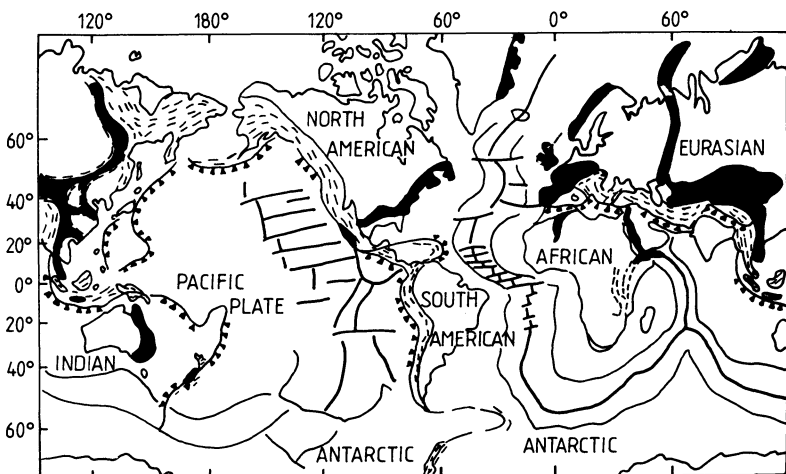
Fig. 6.1. Present-day lithospheric plates. Ocean ridges/spreading zones shown as *thick lines*, transform boundaries as lines that offset ridges, subduction zones are indicated by *barbs on thin lines*; major Palaeozoic (*black*) and Mesozoic (*dashes*) orogenic belts are also shown (After Bott 1982)
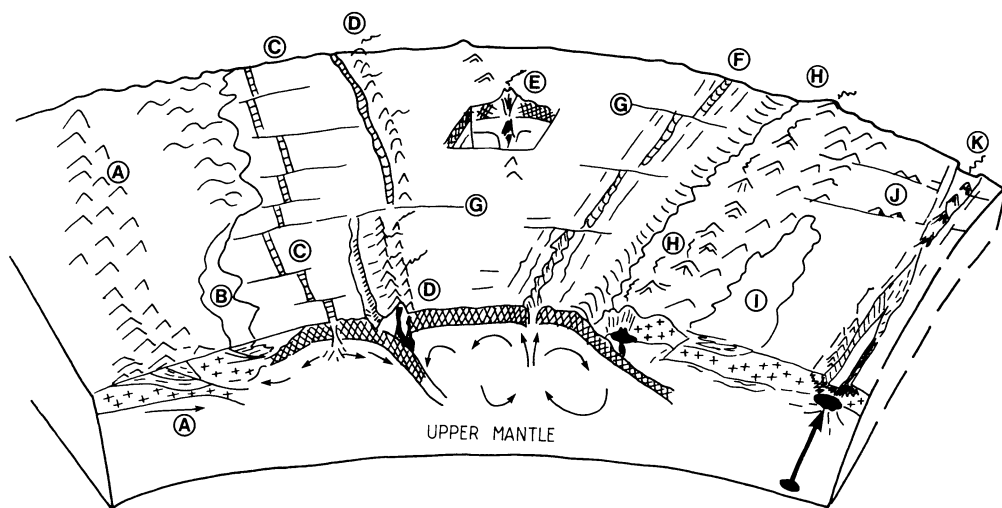
Fig. 6.2. Cartoon (not to scale) showing a segment of the Earth's lithosphere and its major plate tectonic features. *A* Collision orogen and suture zones; *B* passive continental margin; *C* back-arc spreading (marginal basin); *D* intraoceanic island arc; *E* intraplate volcanism (hot spot); *F* spreading centre; *G* transform fault; *H* Andean-type subduction and continental margin; *I* retro-arc (compressional basin); *J* continental extension of transform faults; *K* intracontinental rift (Modified after Hutchison 1983)

characteristic magnetic stripes, symmetrically disposed on either side of a mid-ocean ridge, and first described by Vine and Matthews (1963). In this chapter we examine plate tectonic settings and associated types of hydrothermal mineralisation. A schematic view of plate tectonic settings is shown in Fig. 6.2. It is, however, beyond the scope of this book to provide details of the tectonic settings and the reader is hence referred to those publications listed at the beginning of Chapter 5. We examine below the following plate tectonic environments and settings: (1) extensional tectonics (spreading centres, intracontinental rifts, passive margins and interior basins); (2) compressional tectonics (subduction- and collision-related settings); (3) transform fault settings. Many of the mineralisation types mentioned in this chapter are described in some detail in subsequent chapters. Finally, for each setting and hydrothermal deposits listed, some "hints" on the exploration methods appropriate for the search of the mineralisation in question are given. However, the reader is advised to consult Rose et al. (1979), Beus and Grigoryan (1977), Reedman (1979), Govett (1983) and Smith (1983), for details on exploration techniques.

6.2 Extensional Plate Tectonics

Extensional plate tectonics include mid-ocean spreading centres and intracontinental rifting. The latter may, through various tectonic stages (incipient to advanced), evolve into mid-ocean spreading centres.

6.2.1 Mid-Ocean Spreading Centres

At mid-ocean spreading centres, new lithosphere is formed which consists of mafic material welled up from partially molten asthenosphere, and which forms magma chambers just below the spreading centre. This part of the lithosphere, or oceanic crust, consists of an uppermost layer of basaltic pillow lavas and associated pelagic sediments, underlain and intruded by sheeted dyke systems, passing downward into gabbroic, peridotitic, dunitic and harzburgitic rocks. Once the oceanic crust moves away from the ridge it is either consumed in a subduction zone, or it may be accreted to continental margins, or island arcs. Accreted oceanic crust is known as "ophiolite". This is a term of Greek derivation, meaning snake-rock because of the predominantly green colouration of ophiolitic rocks. Serpentinite is the Latin-derived equivalent but it does not necessarily imply ophiolite. Spreading centres also form in back arc marginal basins (a modern-day example being the Sea of Japan, Fig. 5.11). Although geochemical discrimination has been attempted to differentiate between mid-ocean centres and marginal basin spreading centres, the distinction in ancient systems is by no means clear. Typical cross-sections depicting oceanic crust are shown in Fig. 6.3A, B, bearing in mind that the overall structural configuration
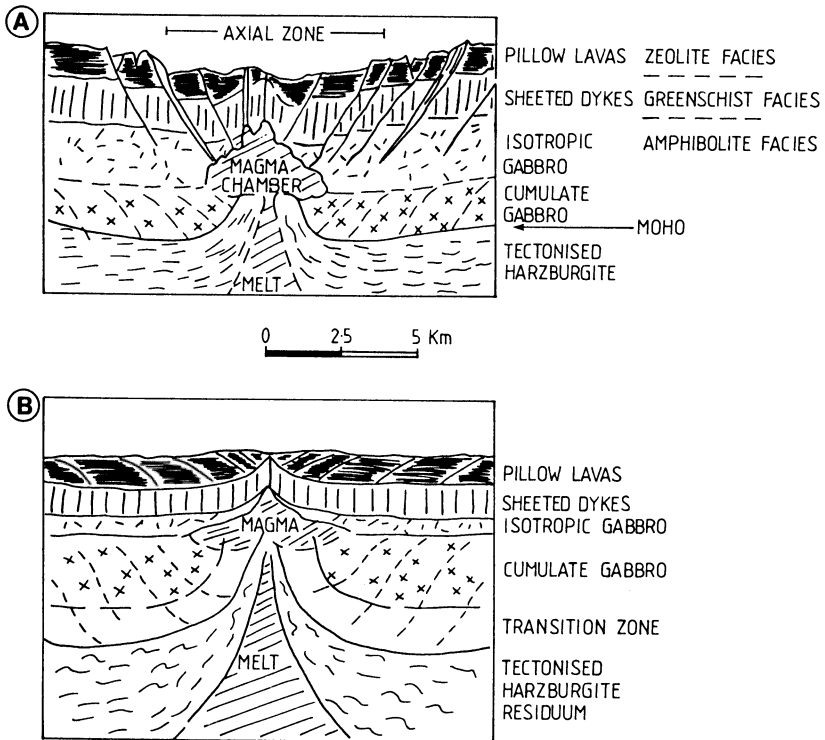
Fig. 6.3A, B. Idealised cross-sections of A slow-spreading North–Atlantic-type mid-ocean ridge and B a fast-spreading East Pacific-type mid-ocean ridge (After Burke et al. 1981)

of a mid-ocean ridge system depends on the rates of spreading, which Fig. 6.3 indicates.

Hydrothermal Mineral Deposits

Ocean floor:

Mid-ocean ridges, and off-ridge axis (sea mounts):

Present-day	Fracture-controlled black and white smokers, and surrounding metalliferous aprons. Principal metal association: Fe-Cu-Zn-Pb-Ba-Au-Ag. Hydrogeneous ferromanganese and phosphate nodules. Metal association: Fe-Mn-Ni-Co-Cu, P, U.
Geological record	Ophiolite-hosted stratiform massive sulphide and epigenetic stockwork feeder zone. Cyprus-type. Principal metal association: Fe-Cu-Zn-Pb-Ba-Au-Ag. Bedded ferromanganese deposits.

Guaymas basin-type (Gulf of California):

Present-day	Smokers vents, metalliferous aprons buried in terrigenous sediments. Metal association: Cu-Zn-Co-Ag.
Geological record	Besshi-type massive sulphide deposits. Matchless belt in Namibia. Sambagawa belt, Japan. Metal association as above.

Mineral Exploration

In present-day ocean-floor mineralisation, geochemical and geophysical techniques are employed for site identification and initial evaluation of the deposits. Echo sounding for sea-floor profiling in conjunction with geothermal scanning to detect temperature anomalies have been effectively used. Systematic bottom sampling by manned or unmanned deep-sea submersibles is a follow-up operation. Samples are analysed for various trace and metallic elements.

The exploration of volcanic-hosted massive sulphide mineralisation of ophiolite affinity involves the use of regional geological exploration, remote sensing, geochemical and geophysical methods. Geological exploration has to concentrate on regions of young orogenic belts and collision plate boundaries (obducted ophiolites or suture zones). The geological evaluation of these terranes is very important because they are generally highly tectonised, fragmented, and frequently metamorphosed. The construction of stratigraphic sections helps to establish the nature and younging directions of the sequence. The regional geological investigation can be aided by remote sensing techniques, which enable the explorer to identify accreted ophiolitic terranes. Lithogeochemistry may be employed to establish the nature of the volcanic rocks, by using for example discriminant diagrams (K, Rb, Sr, LREE are depleted in ophiolite suites). Airborne geomagnetic

surveys provide a valuable mapping aid. Follow-up detailed operations would normally include stream sediment and soil sampling surveys (Cu, Ni, Pb, Zn, Ba, Mn, Mg, Na); element distribution in soils and rocks can detect alteration haloes, since in this type of mineralisation there is a decrease in Na and Mg, whereas Mn, Zn, Cu, Ba, Ni increase in proximity of the mineralised body. Electromagnetic methods have been used successfully to locate subsurface sulphide mineralisation.

The exploration of deposits formed in advanced rifting settings involves remote sensing studies mainly for structural interpretation, and as an aid in area selection. Airborne geophysical methods, such as aeromagnetics survey to detect outcrops or suboutcrops of magnetite-quartzite units in metamorphosed terranes, can be very useful. EM and IP surveys respond well to massive and disseminated sulphide mineralisation in most environments. The application of regional and detailed geochemical surveys, stream sediment and soil sampling, are essential not only to delineate areas of interest but also to establish possible regional-scale metal zonations. These can assist in discriminating distal from proximal mineralising environments (Cu near the source, Zn enrichment indicates a distal zone).

6.2.2 Intracontinental Rifts

Intracontinental rifts can be broadly classified into active and passive, according to whether or not there is involvement of mantle diapirs. In passive systems it is thought that rifting occurs as a result of collisional tectonics (impactogens). The stage of evolution of a rift system, as shown for example in Fig.6.4, is clearly very important in determining the type of associated metallogeny. Burke et al.(1981) recognise the following types of rifts: (1) rifts at continental breakup; (2) convergent boundary rifts; (3) collisional rifts, which include aulacogens and impactogens.

The mechanism of continental rifting involves processes of normal faulting taking place in response to horizontal tension affecting a rigid crustal environment. Stages in the development of an active rift system are as follows (Bott 1981). A mantle diapir rises and collects below continental lithosphere (mantle advection).
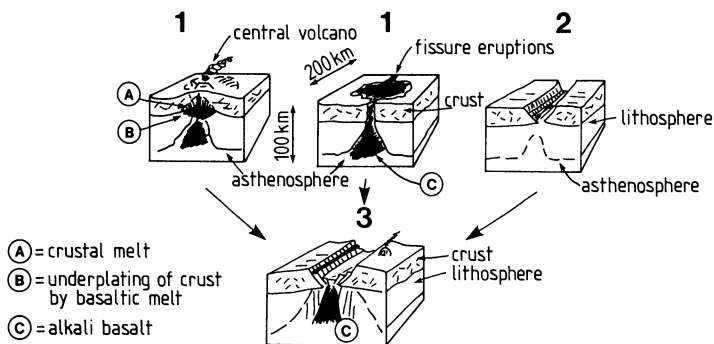
Fig. 6.4. Types of rifts: *1* Active; *2* Passive; *3* Mature rift valley, which may evolve from them (After Burke et al. 1981)
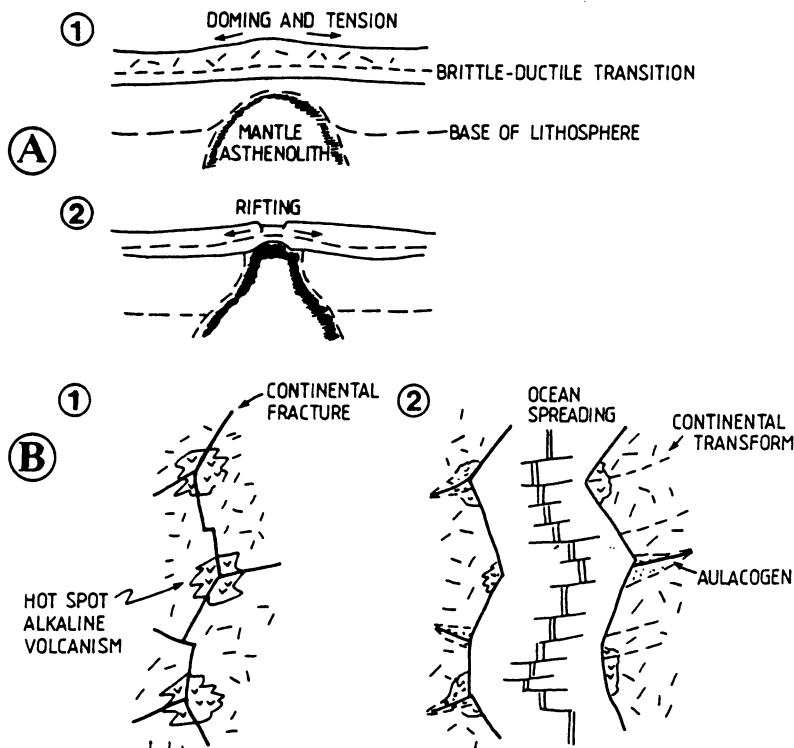
Fig. 6.5. A Heating and thinning of the lithosphere by a mantle asthenolith; uplift and tensional stresses result in rifting (After Bott 1981). **B** Rift-Rift-Rift, or r-r-r junction in continental crust with hot spot volcanism *1*. Advanced South Atlantic-type stage with continental transform faults and aulacogens *2* (After Dewey and Burke 1974)

The overlying lithosphere becomes heated and thinned during isostatic uplift in response to the push exerted by the underlying mantle diapir. Tensile stresses are developed in the upper crust, which cause rupture by normal faulting, and result in a graben-type structure (see Fig. 6.5A). Domal uplift of the crust may result in a triple junction failure, first recognised by Hans Cloos in 1939. A modern-day example of a triple junction is represented by the three-rift arms of the Red Sea, Gulf of Aden and the Afar triangle in Ethiopia. The Red Sea and the Gulf of Aden represent a mature stage of the rifting process where plate accretion is occurring by oceanic spreading. The Afar is the third, and at present failed, arm of the triple junction. The evolutionary processes from an initial "hot spot" to incipient rifting and spreading are illustrated in Fig. 6.5B. Passive rifting may be related to continental collisions, with "aulacogens" representing reactivation of a failed rift system striking at right angle to an orogen; whereas "impactogens" develop as a result of strains set up during a collision event (Burke et al. 1981). Modern examples of the latter are the Rhine graben and the Lake Baikal rift system. Convergent boundary rifts are formed in back-arc areas and may develop into marginal basins, this type of rifting is dealt with in the section pertaining to subduction-related settings.

Rifts serve as major conduits for both magmas and hydrothermal fluids, and it is presumed that the metal associations depend on both magma types and the interaction of the fluids with the volcano-sedimentary sequences. Magma genesis in intracontinental rift environments is therefore related to the ascent of mantle material (asthenolith), and its underplating and melting of the lower crustal regions. Indeed, the effects of mantle asthenolith underplating has been invoked to explain major rifting and continental magmatic events. The mantle plume material would intrude and spread out laterally below the continental lithosphere, causing extensive melting. Extrusion of basaltic magma occurs at first, followed by early "syntectonic" plutons derived from the crustal melts. This part of the cycle is typically alkaline and bimodal, that is, the range of magmatic products is mafic and felsic, with scarce, if any, intermediate products. Continental alkaline magmas are enriched in incompatible elements, H_2O-poor, but rich in "dry" volatiles, such as CO_2, B and F. This is the anorogenic magmatism of continental regions, with the production of A-type granitoids (A= anorogenic or anhydrous, Collins et al. 1982). It is thought by Bailey (1978) that degassing from the deep mantle, particularly C gases and halogens, leads to metasomatism of the upper mantle regions. These regions are subsequently subjected to melting by continued heating and gas fluxing, with thermal uplift, doming and eventual rifting. The abundant presence of "dry" volatile emission in the East African rifts appears to corroborate Bailey's model. Details of the origin and petrogenesis of rift-related magmas can be found in two excellent and authoritative volumes edited by Sorensen (1974) and Fitton and Upton (1987). The magmatic cycle of a rift may end with its closure, resulting in basement reactivation as well as generation of, and late to post-tectonic intrusion of crustal magmas (S-type). Discharge of the metalliferous brines along graben faults results in the formation of stratabound and stratiform ore deposits, and since rifting, magmatism and basin development are all controlled by the same geodynamic processes, the major stratiform and stratabound ore deposits will have a definite tectonic zonation, and, within the confines of the rift structure, will develop preferentially along major fracture systems. As mentioned earlier the Proterozoic eon was a time in the Earth's history in which rifting was a dominant tectonic style due to the assembly of large and rigid continental masses. It is for this reason that terranes of Proterozoic age are the favourite target for rift-related sulphide deposits.

Hydrothermal Mineral Deposits

Continental rifting and aulacogens:

– Breccia pipes, replacement bodies, fissure-lode deposits. Messina-type ore deposits (South Africa). Principal metal association: Cu-Ag-Co-Ni-As.
– Porphyry-type mineralisation associated with subalkaline to alkaline magmas in cauldron or ring structures. Oslo graben type, perhaps Drummond basin (Pajingo) and Georgetown Inlier in Queensland (Kidston). Principal metal associations: Mo-Cu; Au-Ag-Zn-Pb-As.
– Anorogenic granites and ring complexes. Acid phase of the Bushveld Complex, Nigerian and Namibian complexes, Rapakivi granites in Scandinavia. Metal

association: Sn-Nb-Ta-W-U-Th-F-Zn-Cu-REE-Fe. Possibly the Roxby Downs deposit in South Australia may belong to this category.

- Stratiform and stratabound sediment-hosted massive sulphide ore deposits. Broken Hill, McArthur, Mt. Isa (Australia), Sullivan (Canada), Rammelsberg (Europe). Principal metal association: Fe-Pb-Zn-Ag-Cu-Ba.
- Stratiform sediment-hosted. Zambian Copperbelt, Kupferschiefer (Europe). Principal metal association: Cu-Co-Fe-Pb-Zn-Se-Ag-Au.

Advanced stages of rifting:

Red Sea-type setting:

Present-day   Metalliferous brine pools. Principal metal association: Fe-Cu-Zn-Pb-Mn-Ba-Au-Ag.

Geological record   Volcanic-sedimentary-hosted massive sulphide lenses. Aggenays-Gamsberg (South Africa). Metal association as above.

Mineral exploration

The first stage in the exploration of the magmatic-related deposits is the employment of satellite imagery and remote sensing techniques. These may assist in delineating ring structures and linear arrays of volcano-plutonic complexes. They facilitate regional-scale fracture analysis and the detection of zones of crustal weakness, and of dyke swarms. The unusual chemistry and mineralogy (e.g. U- and Th-bearing minerals, high K) of the igneous complexes of rift environments allow the use of airborne geophysical techniques such as radiometric (gamma-ray spectrometry). Geomagnetic surveys are also useful in these settings. A most effective tool in ground techniques, apart from geological reconnaissance and detailed mapping, is the geochemical investigations of rocks and soils. Multi-element analyses can reveal the most fractionated and altered rocks (e.g. high Rb/Sr, Na, K), and good pathfinders include B, F, Rb, Zn and Ba. Studies of alteration patterns, aided by lithogeochemistry, are essential in the early stages of evaluation of the mineralised areas.

The exploration of sediment-hosted massive sulphides also employs an initial stage of satellite and remote sensing investigations to detect major basement faults, sedimentary basins in bounded troughs, and graben structures. Gravity and geomagnetic surveys are employed to delineate basement highs and the presence of magnetite-quartzite horizons, while seismic techniques may help in outlining unconformities. Ground work normally includes carefully integrated geological mapping, basin analysis, stratigraphic and sedimentological studies metamorphism, and geochemical surveys. The latter involve stream sediment, soil and lithogeochemical sampling. Element analyses include Cu, Co, Ag, Pb, Zn. In areas of overburden, pitting and trenching are used for both geological and geochemical information. Also useful in such areas are geobotanical studies (such as the famous copper flower, Ocimum Hombleii de Wild) of the Zambian Copperbelt which has helped many geologists (Horscroft 1961). Detailed EM surveys are occasionally employed for the detection of subsurface massive sulphide bodies.
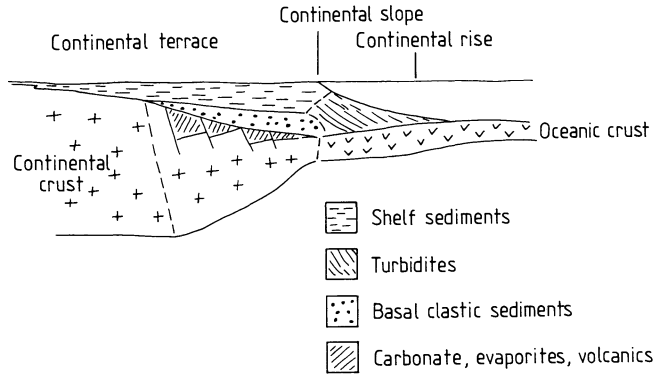
Fig. 6.6. Idealised miogeosynclinal sedimentary prism on Atlantic-type passive continental margin (After Dickinson and Yarborough 1976)

6.2.3 Passive Continental Margins and Interior Basins

Passive continental margins are characterised by thick clastic and chemical sedimentary sequences, and are formed by rifting and advanced ocean-floor spreading. The change from rifting to passive plate margins is transitional. Modern-day examples are represented by the North American eastern seaboard, and the west coast of Africa. The basins are formed by post-rifting subsidence with the deposition of the sedimentary sequences occurring in two main environments: (1) continental shelf (miogeosynclinal) with quartz-arenites, shales (marine and deltaic), carbonates and evaporites; (2) continental rise (eugeosynclinal) with turbidites, shales and greywacke. Usually both continental shelf and rise sedimentary sequences overlie rift-related continental rocks (Fig. 6.6).

Interior basins (Mitchell and Garson 1981), including the Proterozoic basins, are formed within continental areas in rift-related settings. The Proterozoic basins of the Kaapvaal craton in South Africa may have formed as complex, initially passive, impactogen-rift systems. They were possibly the result of collisional events with the Zimbabwe craton in the north (Burke et al. 1985, see also Clendenin et al. 1988). Interior basins generally have sequences consisting of lower and upper coarse clastic-volcanic rocks separated by argillaceous-chemical sedimentary horizons, mainly shales, BIF and carbonates. They overlie a metamorphic basement complex.

Hydrothermal Mineral Deposits

Passive continental margins:

– Carbonate-hosted ore deposits, in fissures, bedding planes, solution cavities. Principal metal association: Pb-Zn-F-Ba-V.

Interior basins:

- Carbonate-hosted epithermal vein deposits at basin margins, type example could be the Pilgrim's Rest mining camp in South Africa (Tyler 1986). Principal metal association: Au-Ag-As-Sb.
- Unconformity vein mineralisation of the Athabasca basin in Canada, and Alligator river in Australia. Principal metal association: U-Fe-Cu-Pb-Co-Bi-Mo-Au-Ag.

Mineral exploration

In the exploration for carbonate-hosted base metal sulphide deposits, a number of unusual factors must be considered, such as a general absence of igneous activity, presence of hydrocarbons and/or evaporites (S source), and the fact that the ore usually occurs on the basin edge, or flanks of basement domes within the basin. Remote sensing investigations and photogeological interpretation – in conjunction with field checks – of selected regions are normally conducted to detect faults, lineaments and other major zones of weakness that may have controlled basin evolution and provided paths of permeability. Karst geomorphology and permeability barriers (e.g. cherts) that may have "dammed" mineralising fluids are some of the features to look for and investigate. Stream sediment and soil sampling with multi-element analysis for Cu, Pb, Zn, and good pathfinders such as F, Ba, Cd, Co are frequently used. Geophysical methods include airborne geomagnetic surveying, as a mapping aid to basement topography for example, IP surveys to detect sulphide zones, and thermal infrared sensing to detect fault or fractures in the carbonate rocks. Unconformity vein type U deposits are explored by using remote sensing and photogeological interpretation combined with field checking in order to note the following parameters: thick intracontinental sequences of relatively undeformed sediments overlying metasediments, and the unconformity between them; areas of basement doming; paleosols (regolith) on unconformity; carbon-rich metasediments and presence of basement source rocks (e.g. pegmatites, calc-silicates, stratabound U etc.). Geochemistry includes stream sediment and soil sampling for U, Pb, Mo, F. Geophysical methods for the exploration of this mineralisation type will obviously include airborne gamma-ray spectrometry on both regional and detailed scales to detect U and Th anomalies. Airborne geomagnetic surveying is sometimes also carried out as a mapping aid. Geological and mineralogical studies of alteration haloes are important once the area of interest has been narrowed down.

6.3 Compressional Plate Tectonics

Compressional and convergent plate margins include subduction- and collision-related settings. The structural configuration of these settings may be complex and depends on a number of factors. Subduction environments, for example, are related, inter alia, to the dip of the Benioff zones and whether the overriding slab is

continental (Andean type) or oceanic (Tonga-Kermadec-type), to cite but two end members. Collision settings are perhaps even more complex because of the variablity of situations that can lead to collision (arc-arc, arc-continent, oceanic plateau-continent, continent-continent and so on).

6.3.1 Subduction-Related Settings

End-member configurations of modern subduction – trench-arc-back-arc systems – are shown in Fig. 6.7A, B. Similar configurations, of a much smaller scale are envisaged for the Archean granite-greenstone terranes, the geotectonic development of which in terms of subduction-island arc-marginal basin was discussed earlier. The relationship of the angle of descent of oceanic crust (dip of the Benioff zone) to plate motions, stress field and magma generation is believed to be instrumental in the type of ensuing magmatism and metallogenesis. As indicated in Fig. 6.7B, a steep angle of descent, as is the case for the modern-day Mariana, or Tonga-Kermadec, subduction systems, is conducive to creating an extensional
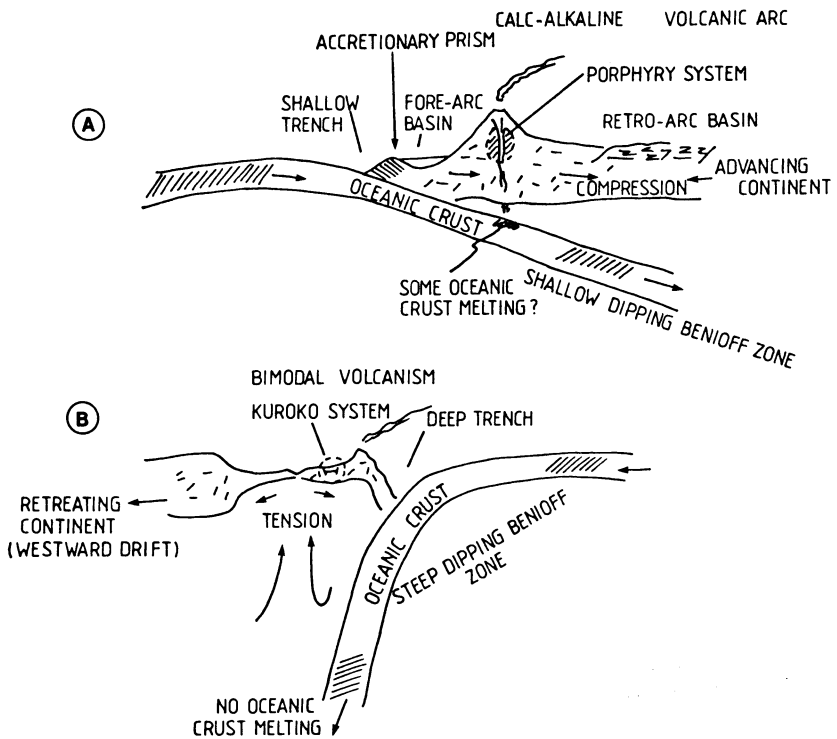
Fig. 6.7A, B. Uyeda's hypothesis of two types of subduction: **A** Chilean-type, with shallow dipping Benioff zone, calc-alkaline magmatism, porphyry-style mineralisation and compression regime behind the arc; **B** Mariana-type steep subduction with generally bimodal volcanism, kuroko-style mineralisation, and tensional regime behind the arc (marginal basin) (After Uyeda 1982)

stress field which would promote the formation of back-arc rift systems and hence hydrothermal massive sulphide deposits of kuroko affinity. By contrast, a shallower subduction zone, such as that occurring under the South American active margin (Chilean-type), would result in a compressive regime behind the magmatic arc, with preferential development of porphyry systems. Furthermore, it is important to note that in Chilean-type subduction systems, accretionary sedimentary prisms in the trench area are well developed, whereas they may be absent in the Mariana-type trench (Uyeda 1982). The implications of this difference in terms of metallogenesis are extremely important, because the presence of a sedimentary accretionary prism is relevant to the formation of epigenetic Au-bearing quartz vein lodes, as explained in Chapter 15. It has also been noted that there is a tendency for the Mariana-type subduction to occur in the western side of the Pacific rim, whereas the Chilean-type occurs in the east (east-facing and west-facing arc systems respectively). This distribution is thought to be related to the westward motion of the lithosphere with respect to the asthenosphere (Dickinson 1978 in Mitchell and Garson 1981; Uyeda 1982). Thus, in an east-facing arc system (western side of the Pacific rim) both subduction direction and lithosphere drift are westward, so that this situation creates a tensional regime behind the arc. This evolves into rifting, generally at the juncture between the arc and the oceanic, or continental, lithosphere, leading to spreading and the formation of a marginal basin. In a west-facing arc system, such as the Andean region, the westward motion of the lithosphere is in opposition to the subduction direction, resulting in a zone of compression behind the magmatic arc (Fig. 6.7B). The situation is not always so simple, however; in the North American continental margin there is both compression and tension, as in the Basin and Range province. The latter appears to be due to the rise of a mantle plume and hot-spot activity in a rift setting (Smith and Christiansen 1980). Thus, behind the magmatic arcs of subdcution zones two tectonic subsettings may occur. One is a back-arc basin in a compressional regime (retro-arc foreland basin, Mitchell and Garson 1981 and references therein); the other is a back-arc basin developed as a result of extensional stresses. They, of far greater importance in terms of metallogenesis than the retro-arc compressional basins, form either behind intraoceanic arcs (Sea of Japan), or behind continental arcs (Basin and Range province of North America) (Fig. 6.8).

Active magmatic arc settings are characterised by seismic activity, high heat flow and calc-alkaline volcanism. Intraoceanic island arcs develop on the overriding plate, parallel to the plate boundary, and those of Phanerozoic to Recent ages may range from hundreds to thousands of kilometres long, and up to 100 km wide. Magma generation occurs in the asthenospheric wedge above the dehydrating subducting slab, producing plutonic rocks ranging in composition from dioritic to granodioritic (I-type magmas). These magmas vent at the surface producing a range of volcanic products from basaltic, andesitic to dacitic. The igneous rocks tend to become more enriched in alkalies and incompatible elements away from the trench, forming a sequence from tholeiites, low-K andesites, dacites (calc-alkaline series) to shoshonites. The petrogenesis of igneous rocks in subduction zones has been investigated, amongst others, by Ringwood (1974, 1985), Wyllie (1981) and Hawkins et al. (1984).
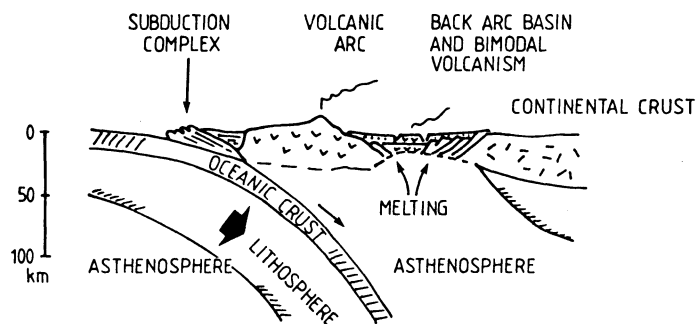
Fig. 6.8. Volcanic arc and back-arc basin with bimodal volcanism similar to Basin and Range province of the USA. After Bally and Snelson 1980)

Andean- or Chilean-type subduction settings form large magmatic arcs thousands of kilometres long. Here, too, volcanic rocks are of calc-alkaline affinity, but are more silicic and intermediate in composition, with basaltic rocks being less abundant than in island arcs. The Andean magmatic arcs are characterised by tall strato-volcanoes built up of andesitic and acid lavas with abundant pyroclastics, mostly ignimbrites. Plutonic rocks comprise a range from tonalites, granodiorite, to quartz-monzonite. The Andean-type igneous rocks also become more evolved and enriched, with distance from the trench, in alkalies and incompatible elements, reflecting increasing depth to the Benioff zone and increasing thickness of the continental crust. Works on the petrogenesis and geochemistry of Andean magmas include Brown (1982), Brown et al. (1984) and Thorpe et al. (1984).

The source and petrogenesis of magmas of subduction zones have great importance not only for the evolution of the magmatic arc in space and time, but also for its metallogenesis, as is so well displayed for the Andean region (Chapter 5). Brown (1982) stressed the importance of the concept of "immaturity" and "maturity" in the development of magmatic arcs. An immature island arc (intra-oceanic) evolves by progressive thickening of its volcanic pile, which in this case is built on oceanic crust. The intra-oceanic island arc becomes more mature when the volume ratio of intrusive to extrusive increases, and likewise their crustal thickness. Brown (1982) used AFM and alkali-lime index plots to illustrate increasing arc maturity for arc magmas ranging from tholeiites to calc-alkaline series. The immaturity to maturity trends, however, are not only developed with time in a given arc, but also in space with distance from the subduction margin. This concept is illustrated in Fig. 6.9. In terms of metallogenesis, the presence and dominance of Cu-Au porphyry systems in intra-oceanic island arcs, and of Cu-Mo porphyries in mature and/or continental magmatic arcs, must clearly correlate with the "maturity" of the arc. In this context the Archean presents an interesting case. Both high- and low-grade Archean terranes have calc-alkaline suites; more specifically, the high-grade terranes contain calc-alkaline tonalitic gneisses, whereas the greenstone belts contain calc-alkaline volcanics. Brown (1982) maintains that the Archean high-grade suites are analogous to modern batholiths, since they contain a gabbro-diorite-tonalite-trondhjemite series very similar to that of modern "immature"
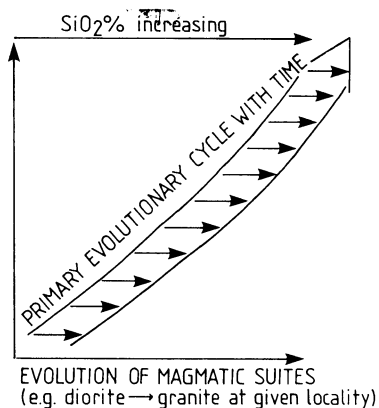
Fig. 6.9. Temporal evolution of igneous suites in Andean-type magmatic arc. (After Brown 1982)

intra-oceanic island arcs. Also, as in modern batholiths, the Archean high-grade tonalites have mantle isotopic signatures, and their origin could be ascribed to "mini-continental plates", in which magmas are generated above fast moving subducting oceanic lithospheric plates. Here, too, the strong Au enrichment of the Archean greenstone belts would substantiate Brown's ideas.

Hydrothermal Mineral Deposits

Subduction-related settings:

Magmatic arcs:

– Porphyry-type Cu-Au, Cu-Mo; Cu-bearing breccia pipes.
– Skarn deposits containing mainly W-Sn-Cu-Zn-Pb.
– Volcanic-hosted epithermal and hot spring deposits with Au-Ag-Hg-Sb-W-S.
– Epithermal vein deposits with Au-Ag, Cu-Au-Ag.
– Carbonate-hosted Au-As-Sb-Hg deposits.
– Sn-W porphyries (e.g. Bolivian tin belt).

Accretionary prism sediments

– Fore-arc felsic magmatism between magmatic arc and trench: vein and skarns containing Cu-Sn-W-Sb-U [e.g.southern Alaska, Sumatra, Japan (?)].
– Mesothermal vein deposits of Au and Ag

Arc-related rift settings:

– Climax-type porphyry Mo-Cu-W-Sn.
– Kuroko-type massive sulphides, Cu-Pb-Zn-Au-Ag.
– Caldera-hosted epithermal and hot spring deposits with Au-Ag-Hg-As-Ba or Au-Te (e.g. Emperor deposit in Fiji).

Archean arc-related settings:

– Algoma-type BIF with Au and base metal sulphides.
– Au mineralisation associated with sodic porphyry intrusives (e.g. McIntyre-Hollinger complex in Canada).
– Volcanogenic massive sulphides (primitive-type, similar to kurokos) with Cu-Zn-Pb-Au-Ag.
– Homestake and Morro Velho type Au deposits in sulphidebearing carbonate Fe formations (Hutchison 1983).
– Talc-carbonate-hosted Sb-Hg-Au Murchison-type mineralisation (South Africa).

Mineral Exploration

In spite of their complexities, the exploration for hydrothermal mineral deposits formed in subduction-related settings follows a common trend. This is essentially due to the fact that most of these deposits are characterised by intense and/or wide haloes of hydrothermal alteration, thus providing the exploration geologist with a signature that is relatively easy to detect. Consequently, exploration is primarily directed at identifying hydrothermal alteration, followed by detailed ground studies including geological, mineralogical, petrological and geochemical work, with the idea of constructing a "model" that can be tested with subsequent subsurface work (e.g. drilling). The reader is reminded that modelling of ore deposits is also applied to other tectonic settings (rifting for example) but on a more regional geological scale. A mineral deposit model combines a number of essential features shared by a group of mineral deposits. In modelling ore deposits, facts and evidence must be evaluated in the light of common factors, using geological, geochemical and geophysical data bases. Consideration of insufficient pieces of evidence may be grossly misleading. Ore deposit modelling is a cheap and highly effective tool for mineral exploration and resource assessment, and its flexibility allows for new evidence to be rapidly evaluated and the exploration philosophy and methodology changed accordingly. High cost techniques for a detailed economic evaluation of the deposit should follow only if a model has been tested and proved correct, even if only on a regional or broad scale.

A first target selection can be rapidly obtained by using remote sensing technology for the detection of volcanic arc terranes, calderas, fracture analyses, and areas of hydrothermal alteration (see Chap. 4). Fieldwork is then undertaken to check on the areas selected, by using geological reconnaissance mapping and preliminary igneous petrological and hydrothermal alteration studies. Regional and detailed scale exploration makes extensive use of stream sediment, soil and rock sampling with multi-element analyses. The advantage of these geochemical methods is that they may still be highly effective even in the case of exploration being constrained by a low budget, because of the usual wide dispersion of metals and the nearly ever present Cu, Pb, Zn, anomalies associated with the mineralisation. Nevertheless, multi-element analyses should include first of all the elements of the ores sought, aided by the numerous pathfinders such as W, Sb, Mo, As, Te, Tl, Hg. It

is a common error to pursue by detailed ground work a, say, Tl or As anomaly in soils or rocks, in the belief that somewhere there must be associated Au. The opposite situation, an Au anomaly associated with anomalous concentrations of Tl or As, is far more worthy of a closer scrutiny.

Geophysical methods are generally used more frequently for massive sulphide deposits (kuroko-type, for example); these include geomagnetic surveys (especially effective for skarns), EM and IP surveys. Radiometric surveys (gamma-ray spectrometry and K^{40} anomalies) may aid in the detection of potassic alteration haloes.

Mineral deposits of Archean arc settings require a slightly different approach, especially because – owing to deformation and metamorphism – hydrothermal alteration patterns may not be as evident as in equivalent modern settings. Greater emphasis is placed on regional and detailed geological mapping with a view to identifying: (1) mafic to felsic volcanic complexes, dome-like rhyolitic units, time breaks in the depositional sequence; (2) BIF horizons. Airborne geomagnetic surveys and EM surveys are frequently used, the former largely as a mapping aid, the latter for massive sulphide detection.

6.3.2 Collision-Related Settings

We introduced the subject of collision and accretion tectonics in Chapter 5. Continent-continent, arc-continent, arc-arc, amalgamation (collision en route) of drifting microcontinents, oceanic plateaux, ridges and seamounts and their accretion on to continental margins have all been recognised in the Phanerozoic geological record, and especially from the breakup of Gondwana onward. Collision events are considered to be a major factor in uplift and mountain building. Young collision belts are characterised by mountains, fold and thrust belts, zones of intense deformation and metamorphism, obducted ophiolites, and intrusion of post-collision crustally-derived granitoids. The entire Alpine-Himalayan orogenic belt was largely formed by the closure of the Tethys oceanic basins, and the collision of a number of microcontinental fragments from the northern edge of the Gondwana continent with the Laurasian continent (Sengör 1987). Also, most of the North American cordilleras, and perhaps parts of the Andean orogen, are believed to have formed by the collision and accretion of a number of terranes that may possibly have originated from the eastern margin of Gondwana (Nur and Ben-Avraham 1982). A number of recent publications dealing with this topic are collected into volumes edited by Hashimoto and Uyeda (1983), Coward and Ries (1986) and Leitch and Scheibner (1987).

Allochthonous fragments of oceanic and continental material are regarded as important additions to the growth of continents (Schermer et al. 1984; Howard 1989). Terrane analyses and recognition is an important tool in order to unravel the tectonic history and the associated metallogenesis of a region. Allochthonous terranes originate by rifting and dispersion from a larger landmass, during drifting the fragments may "amalgamate" before accretion on to a continental margin. From here, however, they can be dispersed and moved along major strike-slip fault systems. At least four major terrane categories are recognised (Schermer et al. 1984):
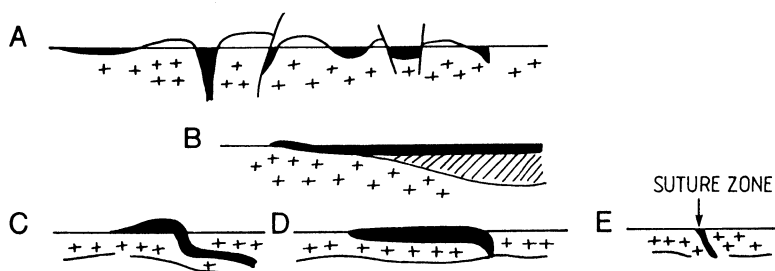
Fig. 6.10A, B. Processes of ophiolite obduction, not to scale). A A once continuous ophiolite sheet partially preserved by folding and faulting; B a continuous well-preserved ophiolite sequence; C and D types of obducted ophiolite sheets; E erosional remnant of obducted ophiolite with small and discontinuous slivers of mafic and ultramafic rocks (suture zone) (After Burke et al. 1981)

(1) stratigraphic terranes with coherent sedimentary record; (2) metamorphic terranes with metamorphic distinguishing characteristics; (3) disrupted terranes with mixed lithologies embedded in serpentinite or greywacke matrix; (4) composite terranes, i.e. those that have been amalgamated prior to accretion.

The closing of oceanic basins, and the accretion of allochthonous terranes, may result in the emplacement of ophiolites by the obduction process. The possible structural configurations resulting from ocean closing and collision of continental masses are illustrated in Fig. 6.10. We have already had occasion to state that the preservation of ophiolitic rocks is a function of the erosion level of a collision belt. In many old terranes, all that remains of a former "suture" is either a line of small slivers of mafic-ultramafic bodies, or, in extreme cases, a zone of shearing.

Crustal collision between two landmasses can take many forms depending on the nature of the leading edges (arc-continent, continent-continent etc.). Figure 6.11 schematically depicts the collision between an Atlantic-type rifted margin and a trench-arc-basin system. The diagram of Fig. 6.11 is a form of template applicable to many published cross-sections of the Alpine-Himalayan orogen. Some of the important features to note in this figure are the retro-arc, fore-arc basins and subduction complex, or accretionary prism (highly deformed sediments interleaved with pieces of oceanic crust material), on the subduction-related margin, and the Atlantic-type rifted basin on the opposing margin. On collision, the sedimentary packages of these basins will form thrust belts, and severely deformed and metamorphosed zones. These geodynamic effects are of great importance because many metalliferous vein lode deposits probably originated through the deformation and metamorphism of these sedimentary piles, whilst thrust faults often act as major avenues for mineralising brines (see Chap. 3). Another important aspect from the metallogenic point of view, is the generation of magmas during the evolution of a collision orogen. Harris et al. (1986) recognise four major groups of igneous rocks as follows (cf. Fig. 6.11): (1) pre-collision igneous rock of calc-alkaline chemistry related to subduction; (2) syn-collision peraluminous leucogranites, derived from the hydrated bases of thrust sheets (see Chap. 3 and Fig. 3.31); (3) late to post-collision calc-alkaline intrusions; (4) post-collision intrusions of alkaline chemistry.
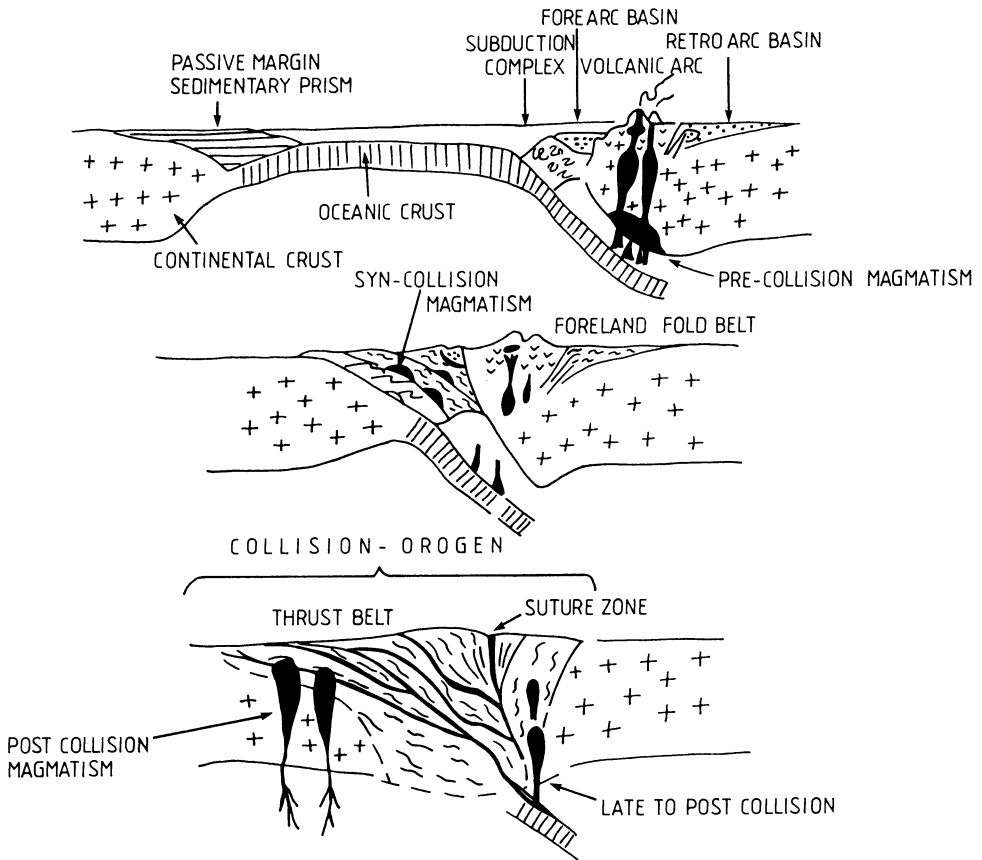
Fig. 6.11. Idealised sketch showing collision process between passive and active margins separated by oceanic crust, accompanied by four stages of magmatism (from pre- to post-collision), see text for details (After Dickinson and Yarborough 1976; Harris 1986)

Hydrothermal Mineral Deposits

Accreted terranes:

– May include all deposits listed in the extensional and compressional tectonic settings.

Suture zones and obducted ophiolites:

– Includes deposits formed in ocean-floor subsettings.

Intracontinental thrust belts and metamorphic belts in accreted terranes:

– Au-Sb-W turbidite-hosted deposits; shear zone-hosted Au-Ag deposits.

Syn- to late-collision igneous terranes:

-   S-type granitic rocks and pegmatite belts containing Sn-W, U, Nb, Be, Sb, and Bi of greisen affiliation.

Archean settings:

-   Although perhaps not strictly part of this category, some of the shear-zone hosted Au deposits of Archean age may be related to collision as well as metamophic events. Nonetheless, it is generally recognised that many of the Archean epigenetic Au deposits are spatially related to crustal scale shear zones (Eisenlohr et al. 1989; Chap. 15).

Mineral Exploration

Fully integrated remote sensing, photogeology and geological reconnaissance mapping are carried out to delineate major crustal lineaments, thrusts, shear zones and sutures. Tectonic modelling and terrane analysis are important tools in the exploration for mineral deposits in collision-related terranes. Geochemical surveys for granite-hosted mineralisation include panning surveys for heavy minerals such as cassiterite and scheelite. Stream sediment and soil sampling with multi-element analyses for Sn, W, U, F. Lithogeochemistry assumes great importance for the establishment of geochemically specialised granites with high background levels of Sn, W, Na, K, high Rb/Sr, low Mg/Li. Hydrothermal alteration studies are conducted on target rocks (granites and their roof zones) to assist in formulating models and/or elemental zoning. Radiometric surveys (gamma-ray spectrometry) and IP are the most common geophysical methods used. Aeromagnetics are used less frequently, mainly as a mapping aid. Highly effective is the use of UV lamps during drainage surveys for the detection of scheelite, a common mineral associated with turbidite-hosted Au deposits. The same geochemical and geophysical method-ology is applied in Archean terranes, perhaps with more emphasis on geological mapping, and studies of metamorphism, hydrothermal alteration and structural analysis.

6.4 Transform Fault Tectonics

There is no generation or destruction of lithosphere at these plate boundaries. A transform fault is a fracture zone that laterally offsets a mid-ocean ridge. Along the offset of the two ridge axis segments the crustal blocks slide past each other. Profiling across these oceanic fracture zones shows that they are formed by a trough, up to 7000 m below sea level, flanked by ridges (transverse ridges, Bonatti and Crane 1984). Compressional or tensional stresses can be set up along transform segments between the ridge axes, if there is a change in the spreading direction. In areas of tension (pull apart), basaltic magma may well up and a new ridge is formed that may propagate itself beyond the transform. It is thought that in this way the opening of

the South Atlantic occurred, from south to north. The tectonic evolution and development of spreading ridges and transform fault systems are discussed by Atwater (1981), Hey and Wilson (1982) and Bonatti and Crane (1984). Transform faults may extend into continental areas and may be associated with the emplacement of anorogenic alkaline complexes as observed in Namibia and Angola. Probably the most significant ore deposit with a clear spatial association to a transform fault is the McLaughlin Au-Hg-Sb deposit (Sawkins 1990 and references therein). In this area there is extensive volcanism associated with geothermal systems. The area of the Salton Sea geothermal system may also be included in the category of transform fault-related settings.

Hydrothermal Mineral Deposits

Oceanic transform faults:

– Limited reported occurrences of Ba and Fe-Mn oxides and hydroxides.

Continental extensions of transform faults:

– Anorogenic complexes may contain Sn-W,Ba,F,REE, U, Th, Nb mineralisation.
– Epithermal and hot spring Au-Ag-Hg-Sb deposits (McLaughlin and Salton Sea in California).

Mineral Exploration

Tracing of transform faults in continental areas is the first step in the exploration of mineral deposits that may be related to this environment. Remote sensing, regional geomagnetic and gravity surveys (existing government maps usually serve the purpose) help to identify these zones. Linear arrays of volcano-plutonic complexes, areas of geothermal activity and hot springs are prime targets to explore further by ground studies, including petrological work, hydrothermal alteration, stream sediment and soil sampling. Multi-element analyses of Sn, W, Ba, F, Nb, U, Cu, Pb, Zn for target areas associated with the anorogenic volcano-plutonic complexes, and Au, Ag, Sb, Hg, Cu, Pb, Zn for epithermal targets are indicated. Airborne radiometric and geomagnetic surveys are the main geophysical techniques employed.

References

Atwater T (1981) Propagating rifts in seafloor spreading patterns. Nature (London) 290:185–186
Bailey D K (1978) Continental rifting and mantle degassing. In: Newman E R, Ramberg I B (eds) Petrology and geochemistry of continental rifts. Reidel, Dordrecht, pp 1–13
Bally A W, Snelson S (1980) Realms of subsidence. Can Soc Petr Geol Mem 6:9–94
Beus A A, Grigoryan S (1977) Geochemical exploration methods for mineral deposits. Applied Publ, Wilmette Ill, 287 pp

Bonatti E, Crane K (1984) Oceanic fracture zones. Sci Am 250:36–47

Bott M H P (1981) Crustal doming and the mechanism of continental rifting. Tectonophysics 73:1–8

Bott M H P (1982) The Interior of the Earth, 2nd edn. Arnold, London, 403 pp

Brown G C (1982) Calc-alkaline intrusive rocks: Their diversity, evolution, and relation to volcanic arcs. In: Thorpe R S (ed) Andesites. John Wiley & Sons, New York, pp 437–461

Brown G C, Thorpe R S, Webb P C (1984) The geochemical characteristics of granitoids in contrasting arcs and comments on magma sources. J Geol Soc London 141:413–426

Burke K C, Kidd W S F, Turcotte D L, Dewey J F, Mouginis-Mark P J, Parmentier E M, Sengör A M C, Tapponier P E (1981) Tectonics of basaltic volcanism. In: Basaltic volcanism on the terrestrial planets. Lunar and Planetary Inst, Houston, Texas. Pergamon Press, New York, pp 803–898

Burke K, Kidd W S F, Kusky T (1985) Is the Ventersdorp rift system of Southern Africa related to continental collision between the Kaapvaal and Zimbabwe cratons at 2.64 Ga ago? Tectonophysics 115:1–24

Clendenin C W, Charlesworth E G, Maske S (1988) An early Proterozoic three-stage rift system, Kaapvaal craton, South Africa. Tectonophysics 145:73–86

Collins W J, Beams S D, White A J R, Chappell B W (1982) Nature and origin of A-type granites with particular reference to south-eastern Australia. Contrib Mineral Petrol 80:189–200

Coward M P, Ries A C (eds) (1986) Collision Tectonics. Geol Soc Spec Publ 19. Blackwell,London, 415 pp

Dewey J F, Burke K C A, (1974) Hot spots and continental breakup: implications for collisional orogeny. Geology 2:57–60

Dickinson W R, Yarborough H (1976) Plate tectonics and hydrocarbon accumulation. Am Ass Petroleum Geol Contin Educ Course Note Ser 1

Eisenlohr B N, Groves D, Partington G A (1989) Crustal-scale shear zones and their significance to Archean gold mineralisation in Western Australia. Mineral Depos 24:1–8

Fitton J G, Upton B J G (eds) (1987) Alkaline igneous rocks. Geol Soc Spec Publ 30. Blackwell, London, 568 pp

Govett G J S (1983) Rock geochemistry in mineral exploration.In: Govett G J S (ed) Handbook of Exploration Geochemistry, Vol 3. Elsevier, Amsterdam, 461 pp

Harris N B W, Pearce J A, Tindle A G (1986) Geochemical characteristics of collision zone magmatism. Geol Soc Spec Publ 19. Blackwell, London, pp 67–81

Hashimoto M, Uyeda S, (eds) (1983) Accretion tectonics in the Circum-Pacific Regions. Proc Intern Sem Accretion tectonics Terra Sci and D Reidel, Dordrecht, 358 pp

Hawkins J W, Bloomer S H, Evans C A, Melchior J T (1984) Evolution of intra-oceanic arc-trench systems. Tectonophysics 102:175–205

Hey R N, Wilson D S (1982) Propagating rift explanation for the tectonic evolution of the northeast Pacific – the pseudomovie. Earth Planet Sci Lett 58:167–188

Horscroft F D M (1961) Vegetation. In: Mendelsohn F (ed) The geology of the Northern Rhodesian copperbelt. MacDonald, London, pp 73–80

Hutchison C S (1983) Economic deposits and their tectonic setting. MacMillan, New York, 355 pp

Leitch E C, Scheibner E (eds) (1987) Terrane Accretion and Orogenic Belts. Geodyn Ser 19. Am Geophys Un; Geol Soc Am, 343 pp

Mitchell A H G, Garson M S (1981) Mineral deposits and global tectonic settings. Academic Press, New York, London, 405 pp

Nur A, Ben-Avraham Z (1982) Oceanic plateaus, the fragmentation of continents, and mountain building. J Geophys Res 87:3644–3661

Reedman J H (1979) Techniques in mineral exploration. Appl Sci, London, 533 pp

Ringwood A E (1974) The petrological evolution of island arc systems. J Geol Soc Lond 130:183–204

Ringwood A E (1985) Mantle dynamics and basalt petrogenesis. Tectonophysics 112:17–34

Rose A W, Hawkes H E, Webb J S (1979) Geochemistry in mineral exploration. Academic Press, New York, London, 657 pp

Sawkins F J (1990) Metal deposits in relation to plate tectonics, 2nd edn. Springer, Berlin, Heidelberg, New York, 461 pp

Schermer E R, Howell D G, Jones D L (1984) The origin of allochthonous terranes: perspectives on the growth and shaping of continents. Annu Rev Earth Planet Sci 12:107–131

Sengör A M (1987) Tectonics of the Thethysides: orogenic collage development in a collisional setting. Annu Rev Earth Planet Sci 15:213–244

Smith B, Christiansen, R L (1980) Yellowstone Park as a window on the Earth's interior. Sci Am 242:84–97

Smith R E (ed) (1983) Geochemical exploration in deeply weathered terrain. CSIRO, Inst Energ Earth Res, Perth

Sorensen H, (ed) (1974) The alkaline rocks. John Wiley & Sons, New York, 622 pp

Thorpe R S, Francis P W, O'Callagahn L (1984) Relative role of source composition, fractional crystallisation and crustal contamination in the petrogenesis of Andean volcanic rocks. Phil Trans R Soc London Ser A 310:675–692

Tyler N (1986) The origin of gold mineralisation in the Pilgrim's Rest goldfield, Eastern Transvaal. Econ Geol Res Unit, Inf Circ 179. Univ Witwatersrand, Johannesburg

Uyeda S (1982) Subduction zones: An introduction to comparative subductology. Tectonophysics 81:133–159

Vine F J, Matthews D H (1963) Magnetic anomalies over ocean ridges. Nature (London) 199:947–949

Wyllie P J (1981) Plate tectonics and magma genesis. Geol Rundsch 70:128–153

Chapter 7

Geotectonic and Metallogenic
Analysis of Orogenic Belts

7.1 Introduction

In this chapter we discuss the geotectonic and metallogenic analysis of the Late
Proterozoic Pan-African orogenic belts of Africa, and the Phanerozoic orogenic
belts of New Zealand. These examples are presented as an integrated modelling of
tectonics and metallogeny as deduced from the available geological, geochemical
and geophysical databases. The usefulness of modelling has already been discussed
in connection with ore deposit types, and here we extend the concept to encompass a
region of the crust that has been subjected to orogen-forming tectonic events, of
which the generation of ore deposits is an integral part. For the present purpose,
however, and also for reasons of brevity, we consider only those deposits that were
formed by hydrothermal activity.

7.2 The P«n-African Orogenic Belts of Africa

A network of Late Proterozoic orogenic belts extends across Africa (including part
of the Arabian peninsula) (Fig. 7.1), eastern and northeastern South America,
across Antarctica and to South Australia (Fig. 5.5), representing a period of
widespread tectonic and thermal activity which took place between approximately
1200 and 450 Ma ago. In Chapter 5 it was mentioned that this period of the Earth's
history is characterised by a transitional regime to a global tectonic style involving
sea-floor spreading on a scale much greater than during the Archean and most of the
Early- and Mid-Proterozoic. In the sections that follow the geological and
metallogenic evolution of the better known Pan-African belts (Arabian-Nubian
shield, Damara Orogen and Lufillian fold belt) are described (Fig. 7.1). These belts
are also chosen to represent diverse geotectonic environments ranging from ocean-
floor spreading, island-arc formation and accretion (Arabian-Nubian shield),
intracontinental rifting with limited ocean opening (Damara belt), to intracontinen-
tal rifting with no development of oceanic crust (Lufillian belt), all ending with plate
convergence and collision.

   The term Pan-African was first coined by Kennedy (1964), who noted the
widespread development of ca. 500 Ma K-Ar radiometric ages in large parts of
Africa and Arabia, which he termed the "Pan-African thermo-tectonic episode".
This early definition has, however, subsequently been used to describe a much wider
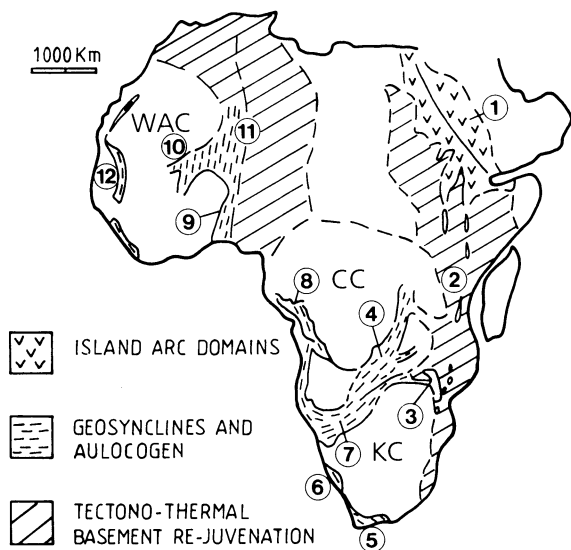
Fig. 7.1. Areas of Pan African tectogenesis in Africa (After Kröner 1979; Porada 1989). *CC* Congo Craton; *KC* Kalahari Craton; *WAC* West African Craton. *1* Arabian-Nubian shield; *2* Mocambique belt; *3* Zambezi belt; *4* Lufillian fold belt; *5* Saldanian belt; *6* and *7* Damara orogen (Gariep orogen and Damara belt respectively); *8* West Congolian belt; *9 10* and *11* Trans-Saharan orogenic belt (Dahomian and Pharusian belts, Gourma aulacogen respectively); *12* West African orogenic belt

spectrum of Late Proterozoic geological processes, and many of the orogenic belts originally considered to have formed ensialically are now recognised to have a plate tectonic origin. There is uncertainty, therefore as to whether the term refers to a thermal event with or without tectonic activity, or to a complete cycle of sedimentary, metamorphic and magmatic episodes spanning the period from approximately 1200 to 450 Ma (Jackson and Ramsay 1980a). Consequently two types of Pan-African mobile belts are recognised. The first type contains regionally metamorphosed magmatic and sedimentary rocks deposited or emplaced between 1200 and 550 Ma, with a final thermal event taking place at around 550 ± 100 Ma, as occurred for example, in the Arabian-Nubian shield, the Damara orogen, the Trans-Saharan (Dahomey-Pharusian belts) orogenic belt and the Lufillian fold belt. In the second type no Late Proterozoic sedimentary and igneous rocks are present, but the belts are characterised instead by reworked older Proterozoic or Archean rocks with or without Pan-African intrusives. Indeed Late Proterozoic tectonic effects may also be lacking, and in some cases, the only reason for designating a given terrane Pan-African is the resetting of the isotopic systems (Jackson and Ramsay 1980a). A major tectono-thermal event did in fact take place throughout much of Africa and Arabia at 550 ± 100 Ma, but this important event usually represents the metamorphic and magmatic terminal phase of a complete orogenic cycle, whose evolutionary time span – though varying from area to area – is as mentioned earlier, generally contained within the period 1200 to 450 Ma.

Recent works, in particular those on the Damara Orogen (Mason 1981; Miller 1983b) and the Arabian-Nubian shield (Johnson and Vranas 1984; Stoeser and Camp 1985; Vail 1985, 1987) show overwhelming evidence for the operation of modern-style plate tectonic processes during the Pan-African event, including the
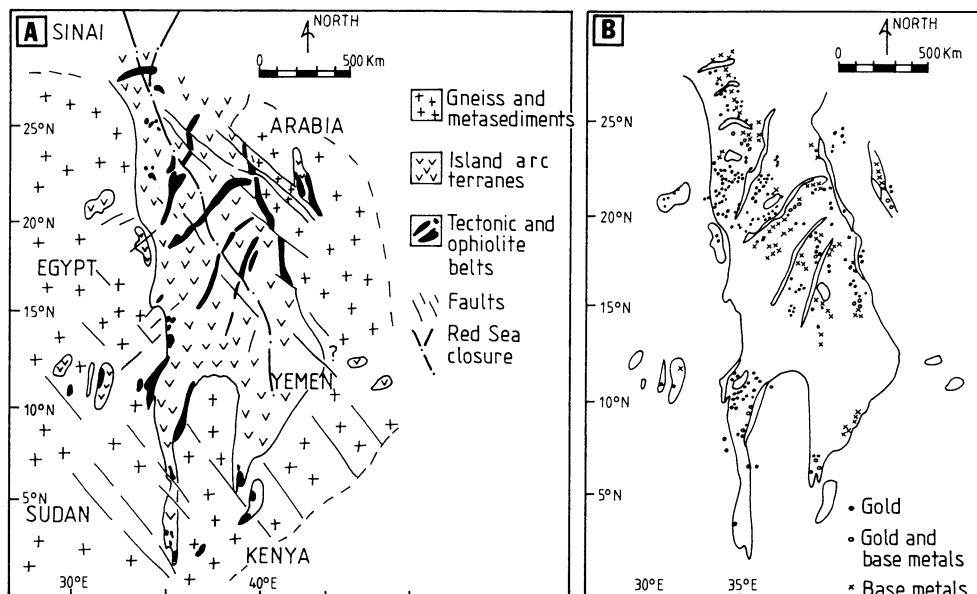
Fig. 7.2. A Geological interpretation of the Late-Proterozoic Arabian-Nubian shield (After Vail 1987). **B** Distribution of Au and volcanogenic base metal + Au sulphide deposits in the Arabian-Nubian shield (After Vail 1987)

occurrence of mineral deposit types characteristic of plate tectonic settings. In conclusion, then, it appears the term Pan-African may be used in one of two ways: (1) to describe the terminal tectono-thermal event at 550 ± 100 Ma, in which case it is used in the sense originally intended by Kennedy (1964); or (2) to describe the full extent of the Late Proterozoic geodynamic evolution in Africa and Arabia (1200–450 Ma). The latter, which seems the most logical use, is adopted here.

7.2.1 The Arabian-Nubian Shield

The position of the Arabian-Nubian shield is shown in Fig. 7.1, and a reconstruction of the geological terranes of the shield prior to the split along the Red Sea rift is illustrated in Fig. 7.2A. The shield occupies extensive areas of northeastern Africa (eastern Egypt, Sinai, northeastern Sudan, parts of Ethiopia and Somalia) and the western side of the Arabian peninsula. It is comprised of a number of geologically distinct terranes, and the general consensus amongst recent workers is that the shield represents a mosaic of accreted Late Proterozoic island arcs. There are many papers dealing with the geology of the Arabian-Nubian shield, and those relevant to the present discussion include: Jackson and Ramsay (1980a, b), Gass (1981), Camp (1984), Vail (1985, 1987), Stoeser and Camp (1985), Kröner (1985) and Pallister et al. (1987).

From the general stratigraphy of the rocks of the shield (e.g. Gass 1981), three major divisions (Lower, Middle and Upper Pan-African) can be made which relate

time, lithologies and tectonic environment. The Lower Pan-African (1200–1000 Ma) is characterised by thick sequences of tholeiitic basalts and andesite of immature island arcs, with greywackes, carbonates and chert. These rocks were intruded by composite batholiths of gabbroic to dioritic composition dated at about 900 Ma. The lower Pan-African rocks are tectonically deformed and metamorphosed up to amphibolite facies. The time span of the evolution of the Lower Pan-African island arcs is not well constrained, and indeed little is known of this period. Jackson and Ramsay (1980b) and Gass (1981) support ages of 1200 to 950 Ma and 1200 to 1000 Ma respectively, while others (Kröner 1985, Stoeser and Camp 1985) provide evidence for ages ranging from 950 to 800 Ma. The Middle Pan-African (1000–650 Ma) is responsible for the bulk of the rocks exposed in the shield, and is characterised by the deposition and emplacement of lithologies that can be defined as belonging to one of two tectonic settings (Jackson and Ramsay 1980b): mature island arcs, or oceanic crust rocks (ophiolites). The former consist of thick sequences of calc-alkaline volcanics (basalt-andesite-dacite-rhyolite) and pyroclastics, interbedded with volcaniclastics, mudstone, chert, quartzite and carbonate. The ophiolitic rocks form linear belts of serpentinised mafic and ultramafic complexes associated with pillow basalts, argillite, tuffs, chert, greywacke and marble. These ophiolite sequences are interpreted as obducted oceanic crust, marking sutures between accreted terranes. Syn- to post-tectonic plutonic rocks of calc-alkaline composition intrude the above sequences, are commonly arranged in linear belts and form some 50–60% of the outcrop. The plutonic rocks tend to become more silica-rich with decreasing age (Gass 1981).

The Upper Pan-African is characterised by accretion and cratonisation, and as such marks the final stage of the Pan-African tectonism in the area. Rocks of this stage include rhyolite and rhyodacitic lavas, with subordinate andesite and pyroclastic deposits. Interbedded with these volcanics are clastic and carbonate (marble) rocks. The volcanics of this period are alkaline to calc-alkaline in nature and are thought to represent emplacement on a thickened crust of continental character (Jackson and Ramsay 1980b). The end of this period is not well established since the region already had a continental character by 600 Ma, although destructive plate margins were in places still active. The cessation of subduction was therefore diachronous. Post-accretion magmatic products represent a change to alkaline-peralkaline plutonic and volcanic magmatism, characteristic of a within-plate setting (Gass 1981). These alkaline igneous rocks may have derived from the partial melting of calc-alkaline crustal protoliths. Post-orogenic granites containing 70–75% SiO_2, 4–5% K_2O and with K_2O/Na_2O = ca. 1, were emplaced along existing lines of weakness. The post-accretion plutonic assemblage consists of: (1) an overwhelming abundance of granite and granodioritic rocks; (2) alkali granites and quartz-bearing alkali-feldpsar syenite; (3) minor gabbro, diorite, monzodiorite, tonalite, syenite and monzonite; and (4) minor nepheline-syenite. The role of this magmatism in controlling magmatic-hydrothermal mineralisation is discussed in Chapter 8.

As previously mentioned, it is widely accepted that the Arabian-Nubian shield was formed through accretion-obduction tectonics of a number of terranes, including domains of volcanic arcs. The general setting has been compared to that of

NUBIAN DOMAIN ◄————————— **ARABIAN DOMAIN** ————►

Ⓐ

PASSIVE MARGIN   ACTIVE ISLAND   TERRANE ACCRETION AND OVERTHRUSTING   EXOTIC TERRANE

NW   SE

Ⓑ   OPHIOLITE OBDUCTION   "DOCKING" AND THRUSTING
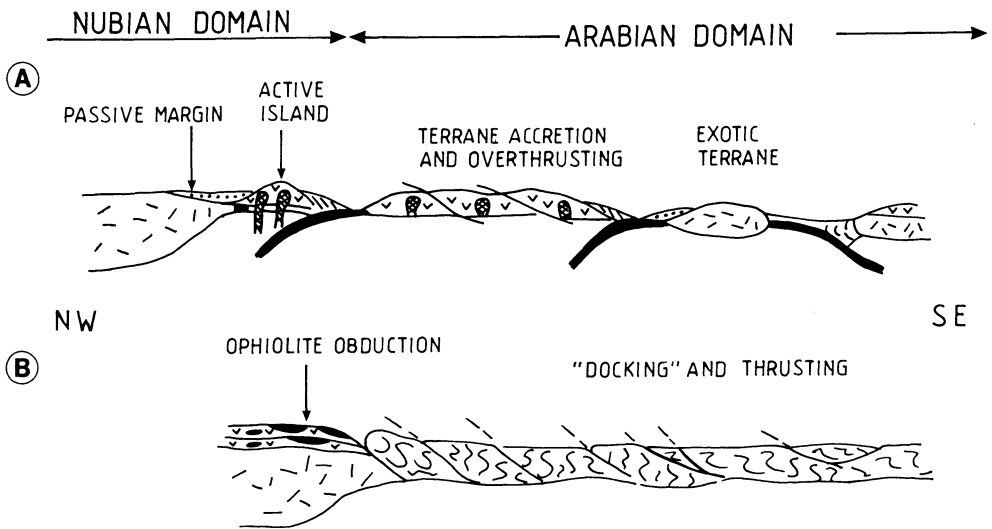
Fig. 7.3A, B. NW-SE idealised section across the Arabian-Nubian shield showing a suggested tectonic evolution and accretion of the Arabian and Nubian domains at 750 Ma **A** and at 640 Ma **B**. See text for more details (After Kröner 1985)

the present-day Indonesian archipelago and the North American cordillera (Kröner 1985). The concept of accretion tectonics and the recognition of the nature of the various terranes is crucial for establishing the mineral potential of a region, and is thus also relevant to any exploration programme. There is some discussion of this subject in Chapters 5 and 6. A model for the tectonic evolution of the Arabian-Nubian shield proposed by Kröner (1985) is shown in Fig. 7.3. Kröner envisages the development of the Arabian and Nubian geological terranes as separate entities until "docking" between the two areas took place sometime between 640 and 600 Ma ago. In the model, a passive continental margin was forming on the Nubian side, while subduction and accretion processes were already underway on the Arabian side. The two environments were, however, separated by an oceanic domain, since continental detritus from the African side did not reach the evolving Arabian arc terranes. Kröner's model shows subduction in the Arabian domain to be mainly westwardly directed, which is in conflict with another model proposed by Stoeser and Camp (1985) for the evolution of the Arabian shield. According to this model, the Egyptian ophiolites were tectonically emplaced and thrust westwards over the continental margin, during marginal basin closure, giving rise to nappe and thrust structures in, and below, ophiolitic melanges (see Fig. 7.3B). However, according to Stern and Hedge (1985), the earliest evidence for ophiolite emplacement occurs between 685 and 665 Ma, yet Kröner (1985) dates volcanic rocks in northern Sudan, which unconformably overlie the ophiolites, at 712 Ma. Thus, notwithstanding timing constraints, terrane accretion and stabilisation of the Arabian shield was probably complete by 630 Ma, while subduction-related accretion continued for another 30 Ma in northeastern Egypt. This possibly marks the final "docking" event,

when the Arabian shield was "welded" on to the Nubian shield to form the Arabian-Nubian shield (Fig. 7.3B).

In summary, it may be said that rifting of a Proterozoic supercontinent (Piper 1982) took place prior to 950 Ma, and between 950 and 630 Ma an ocean basin existed along the northeastern margin of Africa, where active subdcution, island-arc development and accretion of oceanic and continental domains took place. McWilliams (1981) states that, although the core of Gondwana was probably inherited from the Proterozoic supercontinent, Gondwana in its final configuration was assembled between 800 and 650 Ma ago. Given the timing of microplate accretion and stabilisation of the Arabian-Nubian shield, these events appear to represent the accretion of the Arabian part of Gondwana, suggesting that the fundamental nature of the Pan-African events is possibly related to the assembly of Gondwana (Stoeser and Camp 1985). Thus Porada (1989), quoting Piper (1982) and McWilliams, (1981), believes that the Pan-African belt system developed on two major continental fragments – East Gondwana (Australia, India, Antarctica) and West Gondwana (Africa, South America) – and that these collided along a line extending southward from the Red Sea across the Mocambique belt (Fig. 7.1).

Hydrothermal Mineralisation

Hydrothermal mineral deposits of the Arabian-Nubian shield are characteristic of the tectonic environment in which they were formed. The outline of the tectonic history of the shield given in the preceding section enables us to analyse the environmental conditions of ore deposition, since an understanding of these environments is critical to any evaluation of the mineral potential of the region. With this in mind, there are at least three tectonic settings and related hydrothermal mineral deposits that can be considered: (1) hydrothermal deposits associated with ocean-floor spreading; (2) deposits related to subduction and island-arc formation; and (3) deposits related to post-tectonic igneous activity.

Ophiolite suites are common in the Arabian-Nubian shield (Fig. 7.1A) and as they represent segments of obducted oceanic lithosphere offer good targets for base metal mineralisation of the mid-ocean ridge exhalative type (e.g. Cyprus Cu-pyrite), as well as magmatic chromite and nickel sulphide deposits. Only the latter have so far been located in the shield. It must be borne in mind, however, that the ophiolite-hosted exhalative deposits were originally formed in a mid-ocean ridge setting, and that their present location is therefore the result of obduction during plate convergence and collision. Hence they are allochthonous bodies which in most cases have been substantially modified by deformation and metamorphism. Further-more, mid-ocean ridge exhalative deposits are formed within layers 1 and 2 (deep sea sediments and pillow lavas) of the oceanic crust, and as such their preservation potential in an ophiolite suite is lower than the magmatic Cr-Ni deposits of layer 3 (ultramafic rocks).

In the Arabian-Nubian shield the most important metallogenic domains, in terms of frequency and economic importance, are the volcano-sedimentary and plutonic assemblages of the accreted island arc terranes. Volcanogenic base metal sulphide deposits and hydrothermal vein-hosted precious metal deposits are in fact

abundant (Fig. 7.1B), and as such a large proportion of the literature on the metallogenesis of the shield is devoted to these (Sabir 1979; Hakim 1982; Babtat and Hussein 1982; Soliman et al. 1982; Almond et al. 1984; Johnson and Vranas 1984; El-Bouseily et al. 1985; Schellekens 1986). At least three styles of mineralisation have been identified (Sabir 1979). The first is represented by lens-shaped massive sulphides usually hosted by felsic pyroclastic rocks, containing mainly pyrite and sphalerite with variable amounts of chalcopyrite, galena, sulphosalts, oxides and tellurides. The second consists of pipe-like stockwork deposits, occurring within chloritised, sericitised and silicified volcanoclastic assemblages. The main ore minerals are pyrite and chalcopyrite, with minor amounts of sphalerite, galena, cubanite and oxides. The third style is represented by base metal sulphides occurring in a system of quartz veins containing relatively high Au and Ag values.

Although it is clear, from the available literature, that no attempt has been made to classify these ore deposits, the alteration assemblages enclosing the stockworks, and the close association of the mineralisation with rhyolitic rocks and felsic pyroclastics are indicative of kuroko-type deposits. Further, the styles outlined above appear to reflect feeder zones located stratigraphically below the massive sulphide horizons.

Au and Ag mineralisation in the Arabian-Nubian shield occurs primarily in cross-cutting quartz veins within the lithologies of the island arc terranes. The auriferous quartz veins are closely associated with greenschist facies rocks and generally confined to highly sheared granitoids and volcano-sedimentary rocks. The Au occurs as disseminations in ferruginous quartz veins, often associated with minor amounts of pyrite, chalcopyrite and arsenopyrite, and appears to post-date major deformation phases and regional metamorphism. The veins, which are usually less than 1 m thick, are accompanied by sericitic alteration of the wall rocks. This type of mineralisation is best studied in the Red Sea Hills of Sudan, and Almond et al. (1984) propose an origin by leaching and deposition within a hydrothermal system circulating through the shear zones. The abundance of both granitic plutons and mafic-intermediate volcanics makes the actual source of the metals uncertain. Almond et al. (1984) also point out that the heat source required to drive the hydrothermal circulation may be provided by hidden intrusions at depth, with the shear zones constituting zones of weakness controlling the emplacement of the igneous bodies.

The final metallogenic epoch related to Pan-African tectogenesis in the Arabian-Nubian shield is typified by a number of rare element deposits (Nb, Zr, Y, Th, REE, Sn etc. associated with post-tectonic alkali granites (Jackson et al. 1985). This mineralisation represents in most cases the products of alkali metasomatism related to the crystallisation of late stage residual melts. REE provide the most important exploration target associated with these post-orogenic alkali granites, and although no major deposits have been found to date, a number of mineralised complexes have been discussed, details of which are given in Chapter 8.

7.2.2 The Damara Orogen, Namibia

The Damara orogen in Namibia connects to the northeast with the Lufillian fold belt and the Zambezi belt (Figs. 7.1, 5.5). The opening and closing of a proto-South Atlantic (Porada 1979, 1989) caused the development of the Damara-Ribeira orogens along a rift system, whose meeting point is interpreted to be a triple junction situated to the west of the town of Swakopmund in Namibia. Two of the rift arms evolved through an entire Wilson cycle, whereas the third arm – the intracontinental branch of the Damara orogen – which is the area referred to as the Damara belt, was developed from a number of graben-like structures, in one of which there was limited ocean-floor opening. Thus, the Damara orogen comprises a northern and southern coastal arm – these being the remnants on the African side of the two "successful" rifts – and the northeast-trending, 400 km wide, intracontinental branch (the Damara belt; Fig. 7.4). The northern coastal arm is known as the Kaoko belt, which extends along the Atlantic coast, connecting in Angola with the West Congolian belt. The southern coastal arm, also known as the Gariep orogen, links up with the Saldanian belt along the south coast of South Africa (Fig. 7.1). In a series of papers Porada (1983, 1985, 1989) proposes a unified model of geodynamic evolution for the Pan-African belts of southern Africa. In this model, the Damara orogen, as a whole, is the result of a major north-trending rift structure along which the Proto-South Atlantic ocean was formed. This rift propagated from the Gariep orogen northward, then northeastward into the African continent, continuing still further north along the northern coastal branch (Kaoko belt) to join with the West Congolian belt (see inset of Fig. 7.4). Although details of the Proto-South Atlantic Wilson cycle are not known, several lines of evidence indicate that subduction was directed towards the west. The evidence includes: (1) the presence of a thick pile of sheared mafic rocks, possibly ophiolites or a subduction complex, which was thrust from the west over miogeosynclinal rocks on the margin of the Kalahari craton; (2) a thick turbiditic sequence in the northern arm (Kaoko belt), which was thrust from the west over the miogeosynclinal rocks of the intracontinental branch.

The geodynamic evolution of the Damara belt has been a subject of much debate, and for further details the interested reader is referred to the volume published by the Geological Society of South Africa, edited by Miller (1983a), and to the book by Tankard et al. (1982; Chap.9) for a clear and concise overview of the topic. On the basis of structural, tectonic and metamorphic patterns, and stratigraphic and geophysical characteristics, the Damara belt is subdivided into a number of zones (Fig. 7.4). From north to south they are: Northern Platform (NP), Northern Zone (NZ), Central Zone (CZ), Okahandja Lineament Zone (OLZ), Southern Zone (SZ), and Southern Marginal Zone (SMZ). Several models have been proposed to explain the evolution of the Damara orogen in general, and that of the intracontinental branch, or Damara belt, in particular. None of these models, however, can fully explain all of the complex features of the orogen. The models put forward can be grouped into: (1) aulacogen and delamination models in which some form of continental subduction is advocated; (2) models involving ocean-floor spreading and subduction, ranging from a full Wilson cycle to a limited Wilson cycle, in which the opening and closing of a narrow oceanic arm occurred. The weight of the
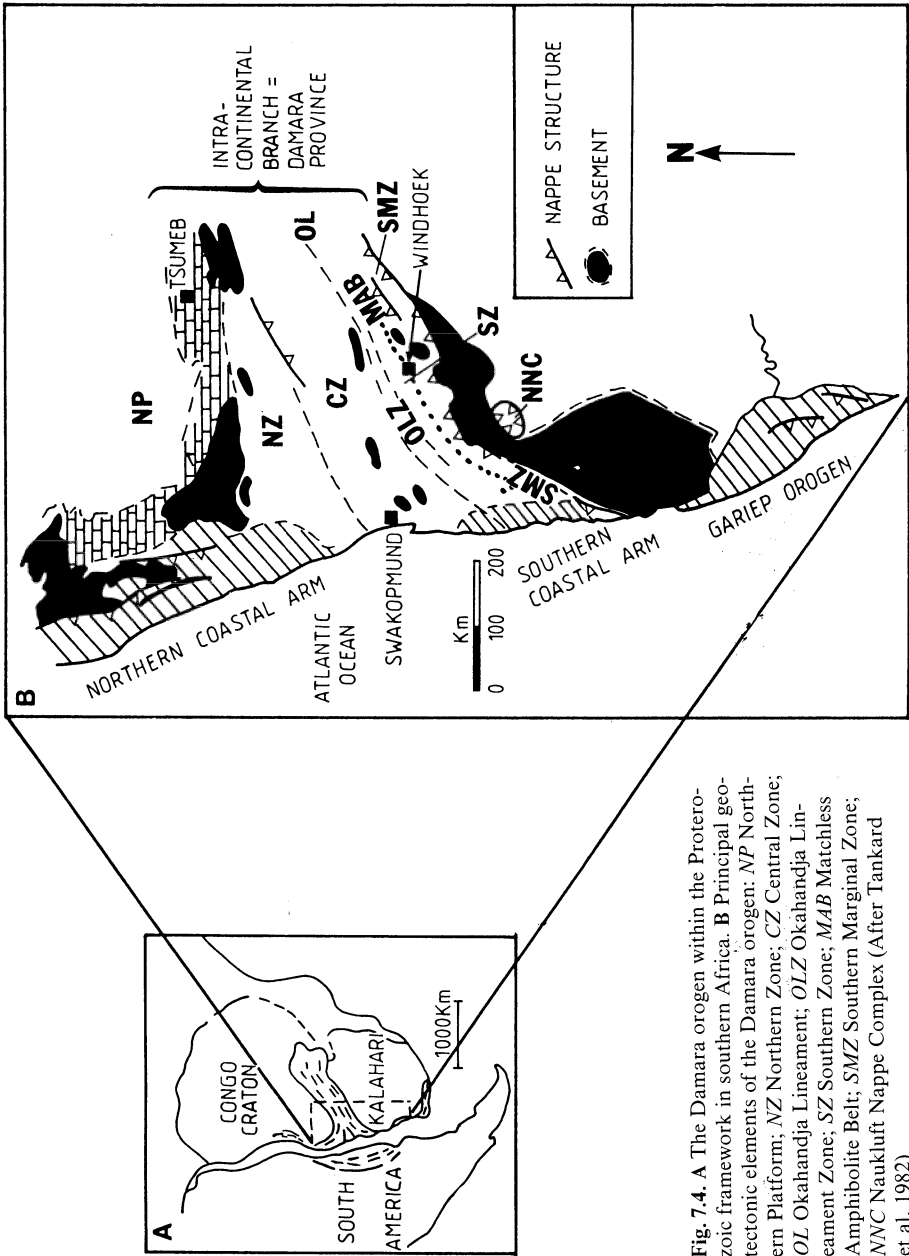
Fig. 7.4. A The Damara orogen within the Protero-zoic framework in southern Africa. **B** Principal geo-tectonic elements of the Damara orogen: *NP* North-ern Platform; *NZ* Northern Zone; *CZ* Central Zone; *OL* Okahandja Lineament; *OLZ* Okahandja Lin-eament Zone; *SZ* Southern Zone; *MAB* Matchless Amphibolite Belt; *SMZ* Southern Marginal Zone; *NNC* Naukluft Nappe Complex (After Tankard et al. 1982)

evidence, particularly that provided by the Matchless amphibolite belt (Breitkopf amd Maiden 1988), favours the latter theory.

Certainly, there is general agreement that the Damara belt developed through stages of rifting, with formation of grabens, and later on by a convergence-collision phase. The last movements to affect the Damara belt are related to the fragmentation of Gondwana during the Mesozoic, when the western continental margin of southern Africa was again rifted. At this time, the separation of southern Africa from South America resulted in the re-activation of pre-existing northeast-trending lineaments with the formation of incipient graben structures.

The Damara lithological record starts with basal clastic rocks, minor volcanics and evaporites of the Nosib Group. These rocks were deposited in the incipient northeast-trending grabens. The Nosib Group is overlain by a thick sedimentary sequence subdivided into the Otavi Group and the Swakop Group, representing two distinct facies. In the north the Otavi rocks comprise stable platform carbonate sediments. In the central and southern parts of the Damara belt the Swakop rocks include facies of trough sedimentation and minor volcanics. They comprise turbidites, carbonates, clastic sediments and mafic volcanics. A regionally extensive, glaciogenic or tectonically-induced mud flow deposit – the Chuos Formation – separates the Otavi Group into the Abenab (stratigraphically lower) and Tsumeb subgroups, and in the Central Zone the Swakop Group into the Ugab (stratigraphically lower) and Khomas subgroups. The Otavi and Swakop sequences are overlain by late-post orogenic molasse-type sediments (Mulden Group to the north, and Nama Group in the central and southern zones).

Magmatism and metamorphism played a major role in the geological history of the Damara belt. Metamorphic events and the most voluminous period of magma generation and emplacement are related to the Pan-African tectono-thermal event that shaped the province between 950 and 500 Ma ago. A second period of magmatic activity took place during the fragmentation of Gondwana between 190 and 120 Ma ago, and continued sporadically until the Tertiary.

The granitoids of the Damara belt were emplaced during three major episodes. The first episode relates to the early phases of rifting, at about 950 Ma, with the emplacement of acid volcanics and volumetrically minor alkaline suites. A second episode took place between 650 and 540 Ma, first with the emplacement of gabbro, diorite and tonalite of I-type affinity during tectonic phases that may have involved limited subduction of oceanic crust. These were followed between 580 and 550 Ma by the emplacement of syn- to late-tectonic biotite-bearing granitoid rocks. The third and last episode of igneous activity took place between 540 and 450 Ma ago accompanying and following continental collision, and a range of granitoids of S-type affinity, including alaskites and two-mica granites, were emplaced. Mafic and ultramafic rocks are present within and along the SMZ, such as the Matchless amphibolite belt, mentioned earlier, the Chuos ortho-amphibolite and various ultramafic lenses (Barnes and Sawyer 1980). These rocks are interpreted to represent a complex suture zone that resulted from the collision of continental plates. Porada (1989) suggested that this zone of mafic and ultramafic rocks may be the southwestern extension of a major sinistral shear structure – the Mwembeshi Shear Zone – which in the

northeast separates the Lufillian fold belt from the Zambezi belt (Fig. 7.7, and see later).

Windley (1984) has drawn attention to the significance of these scattered and irregular igneous bodies as subduction zone material, which, at deep structural levels in eroded orogenic systems, are difficult to recognise because of their tectonised and fragmented nature, the bulk of the original material having been eroded away from the upper levels where ophiolite and associated melange and blue schist rocks may have been present (see Fig.6.10). The Matchless amphibolite belt consists of several lenses and layers of amphibolite and metagabbroic rocks, intercalated within a thick package of predominantly pelitic schist of the Kuiseb formation (Khomas subgroup). The belt is traced more or less continuously for some 350 km and is up to 3 km wide. The attention of several workers has focused on the Matchless belt, as the interpretation of its tectonic setting may help to elucidate the geodynamic evolution of the Damara belt. Field and geochemical evidence, as well as the presence of Besshi-type hydrothermal Cu-Zn ore deposits (Klemd et al. 1987), indicate a rift environment similar to the present-day Red Sea or Gulf of California (Breitkopf and Maiden 1988).

Deformation and metamorphism accompanied the closure of the intracontinental branch, starting sometime between 750 and 650 Ma and continuing up to about 450 Ma with final uplift and cooling. Hartnady et al. (1985) divide the Damara belt into two paired metamorphic belts: a northern Swakop belt of high temperature and low pressure character, and a southern Khomas belt with rock sequences of high pressure and low temperature metamorphic assemblages. Grades of metamorphism deduced from reaction isograds established for pelitic rocks, indicate that the highest temperatures were attained in the southwestern regions of the CZ, where extensive partial melting took place and which roughly coincides with the postulated triple junction area (Miller 1983b). Garnet-biotite and garnet-plagioclase geothermometry, together with detailed microtextural studies (Kasch 1983), indicate that there were two metamorphic episodes: one syntectonic and the other post-tectonic. It is argued, however, that metamorphism was continuous and prograde with peak temperatures of about 580°C and pressures of about 9–10 kbar. At least four deformation events are known to have occurred, resulting in the diverse structural styles in the tectono-stratigraphic zones mentioned earlier. Thus, complex east vergent folds and thrusts characterise the northern coastal branch. The CZ displays spectacular dome and basin structures which pass into the SZ, with marked steep foliations becoming overprinted by progressively lower angle foliations southward. The southern margin of the Damara belt is characterised by thrusts. The spectacular allochthonous Naukluft nappes – the root zones of which are in the Southern Margin of the Orogen in areas of evaporite deposition (Behr et al. 1983; Martin et al. 1983) – were emplaced on older undeformed granitoids.

With the breakup of Gondwana, new and large-scale magmatic events took place in the southern African subcontinent with the voluminous outpouring of the Karoo basaltic lavas. In Namibia, numerous dykes, sills and the basalt-latite-quartz latite rocks of the Etendeka formation along the northwest coast are the remnants of this great thermal event. Between about 145 and 125 Ma ago a number of anorogenic volcano-plutonic ring complexes were emplaced along northeast trends, which are

interpreted as the continental extension of transform faults (Marsh 1973, Prins 1981, Pirajno and Jacob 1987; Fig. 7.6).

The mineral deposits of the Damara belt cover a wide range of types, and have been reviewed by Martin (1978), Miller (1983b), Killich (1986) and Sohnge (1986). The genesis of hydrothermal mineral deposits in the Damara belt can be broadly related to: (1) the extensional phase, with the formation of deposits in intracontinental rifts and in continental shelf environments; (2) the convergence and collision phase accompanied by deformation, metamorphism and the generation of crustal partial melts; (3) the Mesozoic Gondwana breakup event.

Hydrothermal Mineral Deposits Related to Extension

The inception and development of graben structures resulted in two major ore-making processes. Firstly, with high heat flow and the channelling of hydrothermal fluids along active graben faults, and the emplacement of oceanic material in active rifts; and secondly, the infilling of the graben troughs with sediments resulting in the generation of fluids by diagenetic and basin dewatering processes.

To the first can be ascribed the Cu-Zn-Ag massive sulphide mineralisation in the Matchless amphibolite belt. These deposits share the characteristics of the Besshi-type mineralisation of the Sambagawa belt in Japan. They were probably formed by submarine exhalative activity connected with the emplacement of mafic lavas and sills in a deep-water environment being filled with turbidite sediments (Kuiseb Formation). Otjihase, near Windhoek, is the only operating mine in the Matchless belt, although many more deposits of the same type are present in the Matchless rocks. Volcanogenic massive sulphides (mainly pyrite and pyrrhotite) are also found associated with acid volcanics of the early rifting event (Nosib Group).

To the second process belong the sediment-hosted Cu-Ag mineralisation of Oamites in the SMZ, and the carbonate-hosted Cu-Pb-Zn-Ag and V deposits of the continental shelf in the NP zone (Otavi Mountain Land). The origin of these deposits may be due to the generation of hydrothermal fluids during compaction, diagenesis and metamorphism of the thick sedimentary piles accumulated in the graben troughs. Leaching of metals occurred from the sedimentary pile, and also perhaps from basement igneous rocks. The fluids were of temperatures between 150 and 250°C, weakly to moderately saline (up to 20 wt.% NaCl equivalent), and moved along rift grabens, faults and unconformities. The Pb-Zn-Ag mineralisation of the world-famous and currently operating Tsumeb and Kombat mines, is possibly the result of complex hydrothermal systems related to basin dewatering and metamorphism during processes of compressive tectonics (see Chap. 14 for more details).

Hydrothermal Mineral Deposits Related to Convergence and Collision

The convergence-collision phase probably involved large-scale movement of fluids during prograde regional metamorphism and the emplacement of granitoids (Pirajno and Jacob 1988). Most of the hydrothermal mineral deposits are structurally controlled, as they appear to have a clear spatial relationship to

Fig. 7.5. A Part of the intracontinental branch of the Damara orogen, showing tectono-stratigraphic zones and B distribution of Au mineral occurrences and deposits, and other mineral occurrences and deposits of hydrothermal or magmatic-hydrothermal affiliation. See text and Fig. 7.4 for explanation of acronyms; major tectonic lineaments: *UISL* Uis lineament; *OL* Okahandja lineament; *OML* Omaruru lineament
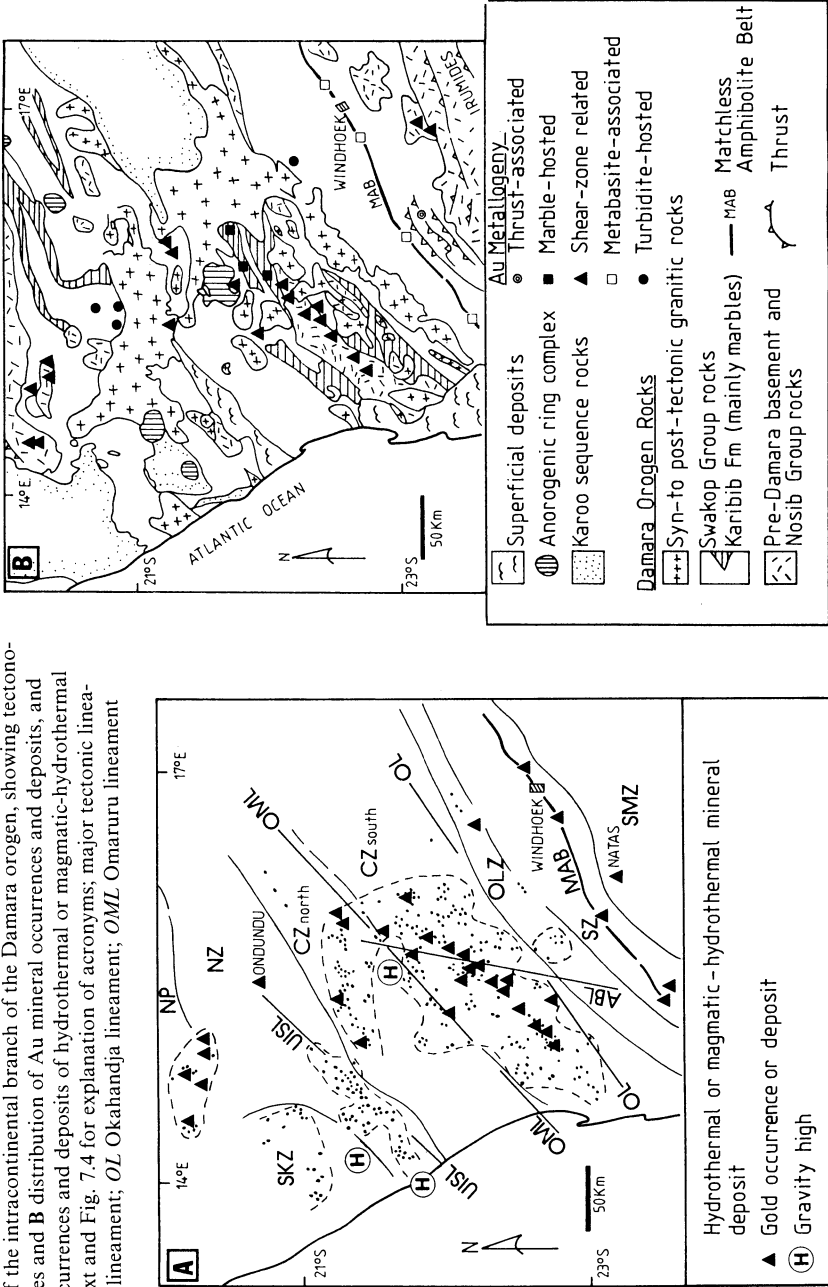
northeast-trending lineaments and postulated graben faults. Also, many of the hydrothermal Au and base metal occurrences are distributed around a major gravity anomaly (Fig. 7.5A), and the zone of crustal anatexis defined by the presence of alaskite bodies, some of which are U-bearing (the currently operating Rossing U mine is the largest of its kind in the world). Another noteworthy feature is that the majority of Au deposits are located within reaction isograds defining areas of upper amphibolite and upper greenschist facies. The nature of the Au metallogeny in the Central Zone of the Damara Orogen is shown in Fig. 7.5B. Hydrothermal Au and other metallic mineralisation were formed along shear zones in basement rocks, in early graben clastic sedimentary rocks and in meta-turbidites, such as the Ondundu deposit. Near the towns of Karibib and Usakos, Au-W-Bi-Cu mineralisation is found in quartz veins hosted in marble rocks of the Karibib Formation. This marble-hosted mineralisation is assuming economic importance with the recently opened mine of Navachab (see Chap. 15). The Karibib Formation consists of metapelites, marbles and calc-silicates, locally intercalated with metabasaltic lavas and pyroclastics. The latter rocks have a geochemical signature indicative of continental rift setting. Field and petrological evidence indicates that the marble-hosted mineralisation may have originated through multistage processes that began during the extensional rifting phase, with Au and other metals being introduced during exhalative activity related to the mafic lavas along the graben faults. Regional metamorphism of dominantly high temperature and low pressure, and deformation resulted in the generation and large-scale movement of CO_2 and H_2O, perhaps derived at least in part from devolatilisation reactions. The effects of the introduction of these fluids can be seen in the widespread hydrothermal alteration that affects the marble units (mainly Ca and Mg metasomatism). It is speculated that during this regional event Au was introduced into areas where the fluids encountered enriched protores, such as the mafic lavas, which in places are known to contain up to 950 ppb Au. Syn- to post-tectonic granitic intrusions followed, generating magmatic-hydrothermal systems that re-distributed some of the previously formed mineralisation within granite-associated vein systems (Pirajno and Jacob 1988; Pirajno et al. 1990).

Other hydrothermal mineral deposits within the NZ, CZ and the Southern Kaoko Zone, near the northwest coast, include hydrothermal quartz veins containing Sn-W mineralisation of greisen affiliation and related to post-tectonic granitic rocks (Pirajno and Jacob 1987). To the south, along the southern margins of the province (SMZ), Pb-Zn, Cu and Au occurrences and deposits are spatially associated with thrust faults, and this mineralisation is also ascribed to ore-bearing brines formed by dewatering processes during prograde metamorphism of the Swakop group sediments (Miller 1983c).

Hydrothermal Mineralisation and the Gondwana Breakup

The emplacement of volcano-plutonic ring-type anorogenic complexes during the drift of South America from Africa and the opening of the South Atlantic, followed lines of reactivation along the continental extension of transform faults (Fig. 7.6). The products of this magmatism are essentially of a bimodal nature, and include
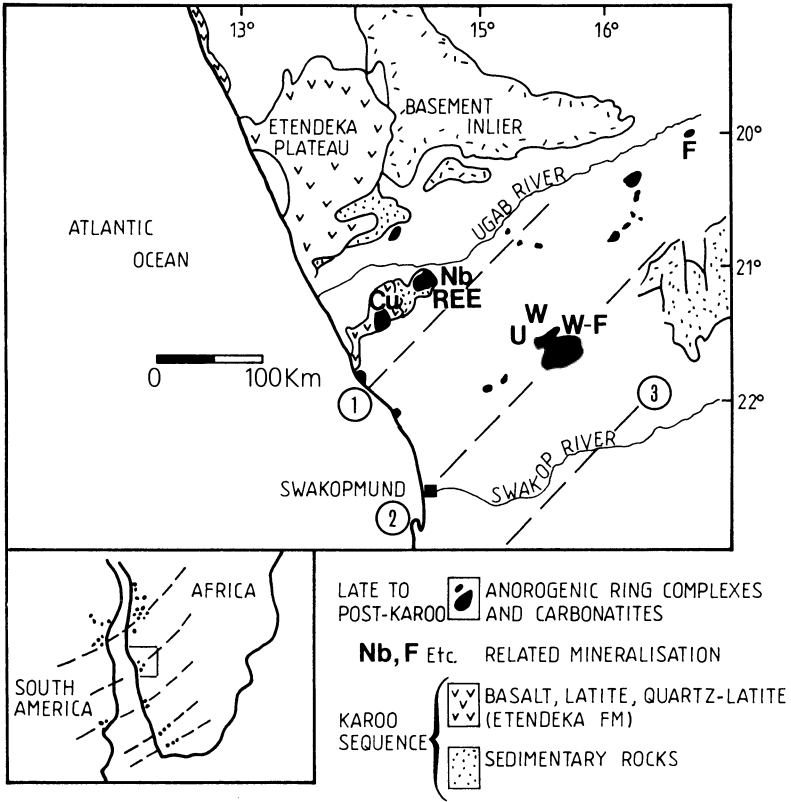
Fig. 7.6. Distribution of Karoo rocks (volcanics and sediments), anorogenic igneous complexes and related mineralisation. *Inset* shows the spatial relationship of the complexes with transform directions in South Africa and South America on a pre-drift reconstruction (After Marsh 1973)

granitic and acid volcanic rocks and differentiated basic complexes. With the former are associated greisen type W-Sn deposits, REE, F, Nb and U mineralisation (Pirajno and Jacob 1987, Pirajno 1990).

7.2.3 The Lufillian Fold Belt

The Lufillian fold belt, together with the Zambezi belt, forms part of the Katanga Orogen. These two belts are separated by the sinistral Mwembeshi Shear Zone (MSZ) (Fig. 7.7). The Lufillian fold belt is preserved in an arcuate zone extending from eastern Angola, through northern Zambia and southern Zaire. The Lufillian sediments were deposited in an intracontinental rift environment, between 950 and 600 Ma ago, on a basement of Early Proterozoic age. Three phases of basin formation are recognised, each corresponding with a period of uplift and fault-controlled subsidence (Unrug 1988). Each phase was accompanied by the deposition of coarse to fine-grained clastic sediments, generally followed by shelf
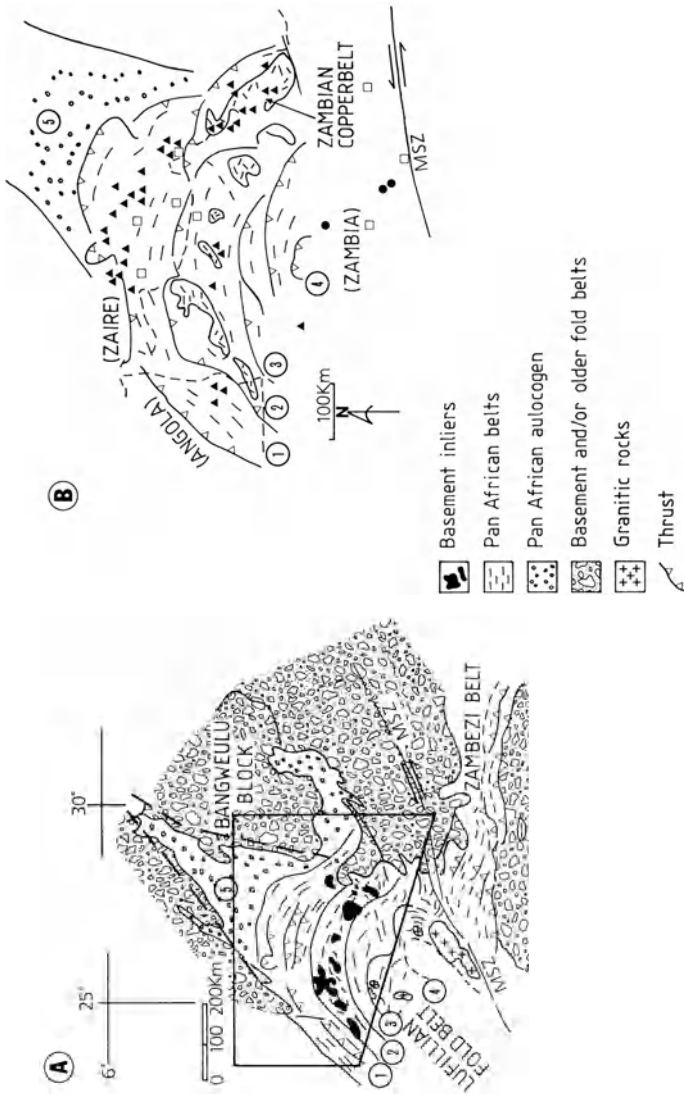
Fig. 7.7. A Schematic geotectonic map of the Lufillian fold belt and part of the Zambezi belt. Modified after Porada (1989). *MSZ* Mwembeshi Shear Zone; *1* to *5* tectonic units discussed in text. **B** Enlarged portion of Lufillian fold belt, (outlined in A showing distribution of main mineral deposits. *Filled Triangles* stratiform sulphide deposits; *squares* vein-type deposits; *filled circles* skarn deposits (After Unrug 1988)

carbonates, and accompanied by minor bimodal volcanism. The sedimentary sequence of the Lufillian belt belongs to the Katanga Supergroup, which includes the Roan Group – lying unconformably on basement rocks – overlain by rocks of the Lower and Upper Kundelungu groups. The Roan rocks include conglomerate, arkose, sandstone, shale and dolomite. A widespread mixtite unit (Grand Conglomerat) – interpreted as a tectonically-induced mudflow deposit – separates the Roan sediments from the overlying Kundelungu rocks. This mixtite unit is the equivalent of the Chuos Formation of the Damara sequence. The Lower Kundelungu rocks consist of volcaniclastic sediments, minor sandstone and carbonate. Another tectonic conglomeratic unit (Petit Conglomerat) separates these rocks from the Upper Kundelungu which is largely made up of mudstone, siltsone and sandstone.

Tectonically, the Lufillian fold belt has been subdivided into a number of units (Unrug 1988, Porada 1989). Porada's subdivision is adopted here (Fig. 7.7), and this comprises: (1) an external arcuate thrust belt; (2) an arcuate chain of basement inliers; (3) a synclinorial belt; (4) a zone of lower Katanga rocks (Katanga High); (5) a northeast-trending aulacogen underlain by Kundelungu rocks.

Three tectono-metamorphic events are thought to have occurred in the Lufillian fold belt. The first two events were relatively minor and correspond with two of the stages of basin formation, whereas the final event – the Lufillian sensu stricto at 656–503 Ma – was responsible for most of the observed deformation and thermal imprint (Cahen et al. 1984). During this event rocks of the Katanga Supergroup were folded and thrust over to the north and northeast. Thrusting involved mainly the Katangan rocks, but in places basement slices were incorporated into the thrust packages. A northeast-trending trough (No.5 tectonic unit above and in Fig. 7.7A) of undeformed clastic sediments coeval with those of the Katanga sequence, and onto which the Katanga sediments were thrust during the Lufillian event, is interpreted as a failed arm of a triple rift system (the Kundelungu aulacogen of Unrug, 1988; or the Shaba aulacogen of Porada, 1989).

Hydrothermal Mineralisation

In the Lufillian fold belt there are numerous hydrothermal mineral deposits containing Cu-Co, Cu, Cu-Co-U, Pb-Zn, and Au. A comprehensive metallogenic analysis of the fold belt has been carried out by Unrug (1988), and his work is summarised below. The distribution of the main mineralised localities is shown in Fig. 7.7B.

Three main types of mineral deposits have been categorised by Unrug (1988); they are: (1) stratiform (Cu, Co, U, Ni); (2) vein-type (Cu, U, Au, Pb, Zn); (3) skarns (Cu). The stratiform deposits are economically by far the most important and form the famous Zambian copperbelt, which together with the Katangan deposits, have reserves of about 150 million tonnes of contained Cu. The stratiform deposits of the Lufillian belt occur primarily in the Roan Group rocks, and are hosted in a variety of lithologies. These deposits, formed prior to folding at about 670 Ma, occur for the most part in the external thrust belt and in the belt of basement inliers (Fig. 7.7.A, B). Some of the more important of these deposits are discussed in detail in Chapter 13.

The vein-type mineralisation post-dates the main deformation period. There are several styles of mineralisation with a great variety of metal associations. Au is present in quartz veins and stockworks associated with shear zones. Pb and Zn sulphides at Kabwe are hosted in carbonate rocks and also contain significant amounts of Cd and Ag. The skarn mineralisation is present only in the innermost tectonic units (Fig. 7.7A, B).

For many years models for the genesis of the stratiform deposits favoured a syngenetic-sedimentary origin for the Cu mineralisation. Recently, however, an epigenetic hydrothermal origin has gained momentum (e.g. Annels and Simmonds 1984, Brown 1984). Unrug's model proposes that the mineralisation formed by convective circulation of basinal brines which replaced early diagenetic pyrite with Cu and Co sulphides. The circulating mineralising fluids were driven by the high thermal gradients associated with rifting, and channelled along permeable horizons in the Roan Group lithologies (see also Chap. 3). The vein-type mineralisation could have resulted from dewatering of the basinal sediments during metamorphism.

7.3 Metallogenic Epochs and Geotectonic Environments of Hydrothermal Mineral Deposits of the Orogenic Belts of New Zealand

The tectonic and metallogenic history of New Zealand has been influenced throughout the Phanerozoic by movements along the active southern margin of Gondwana, and subsequently its fragmentation, which led to the drifting of New Zealand from Antarctica and Australia some 80 Ma ago. The geological framework of the New Zealand microcontinent is the result of geodynamic processes involving accretion of microplates, oceanic crustal fragments and subduction of oceanic crust. Three main tectonic events are recognised: Tuhuan of Palaeozoic age, Rangitata of Mesozoic age, and Kaikoura of Cenozoic age and continuing today (Fig. 7.8). Each of the above-mentioned tectonic events brought about well-defined metallogenic epochs with characteristic mineral deposits. Gold is undoubtedly the dominant metal in all three epochs. The interested reader is referred to the volumes edited by Suggate (1978) for the general geology of New Zealand, and for a comprehensive review of the economic geology of that country Williams (1974) and a recent collection of papers edited by Kear (1989). The metallogeny of New Zealand has been studied and discussed by Pirajno (1980) and Brathwaite and Pirajno (1985), on whose works the present review is based.

7.3.1 Geotectonic Settings of the Tuhuan Orogeny and Related Hydrothermal Mineralisation

The Tuhuan microplate (Fig. 7.9a) is thought to be a portion of a segment of Gondwana, originally joined with Antarctica and southeast Australia. This
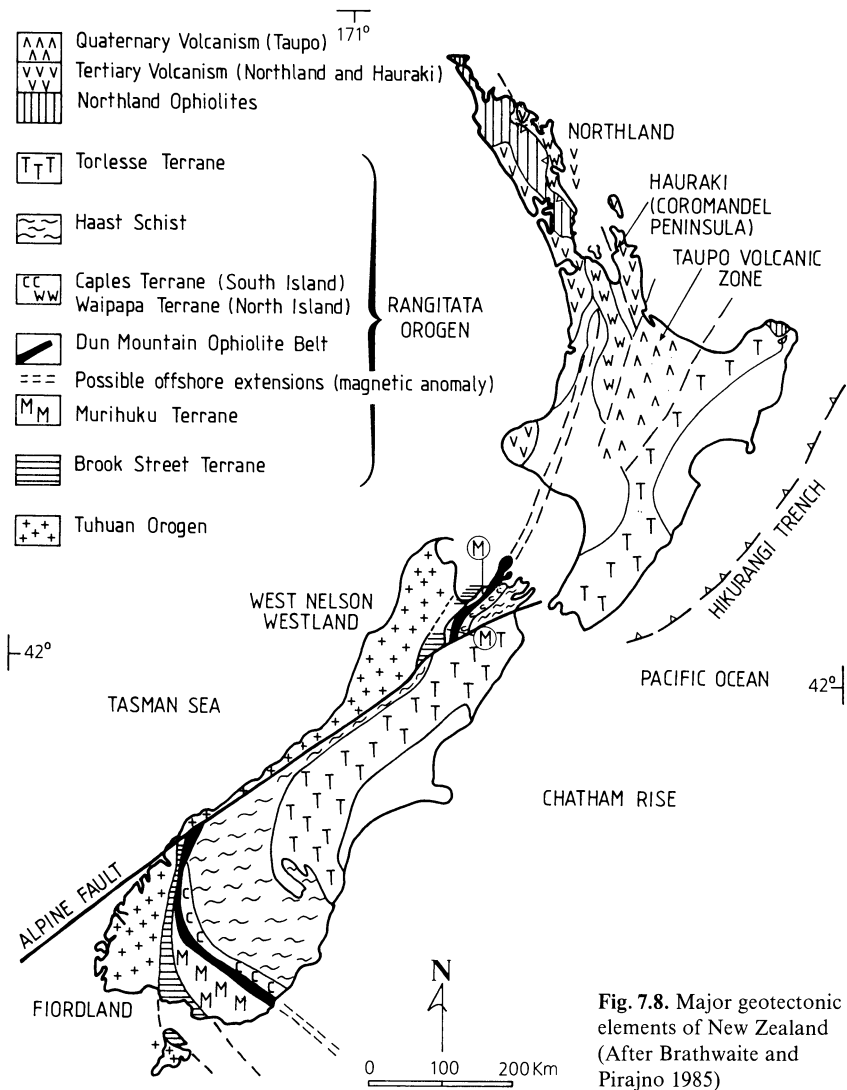
Fig. 7.8. Major geotectonic elements of New Zealand (After Brathwaite and Pirajno 1985)

microplate consists of a number of metamorphosed volcano-sedimentary belts of Lower Paleozoic age intruded by Paleozoic and Mesozoic granitic rocks. The Tuhua microplate is displaced by the Alpine Fault, whose 480 km right lateral shift divides it into two blocks: West Nelson-Westland and Fiordland. The Tuhuan geological terranes are structurally complex, and include a central belt of calc-alkaline volcanics of Cambrian age, interpreted as volcanic arc setting, flanked to the east and to the west by pre-arc and post-arc petrotectonic assemblages, including turbidite and reef facies sequences, a subduction complex, and mafic-ultramafic rocks. The latter may have been part of an ancient oceanic crust, whereas the volcanic arc is allochthonous and in thrust fault contact with the western
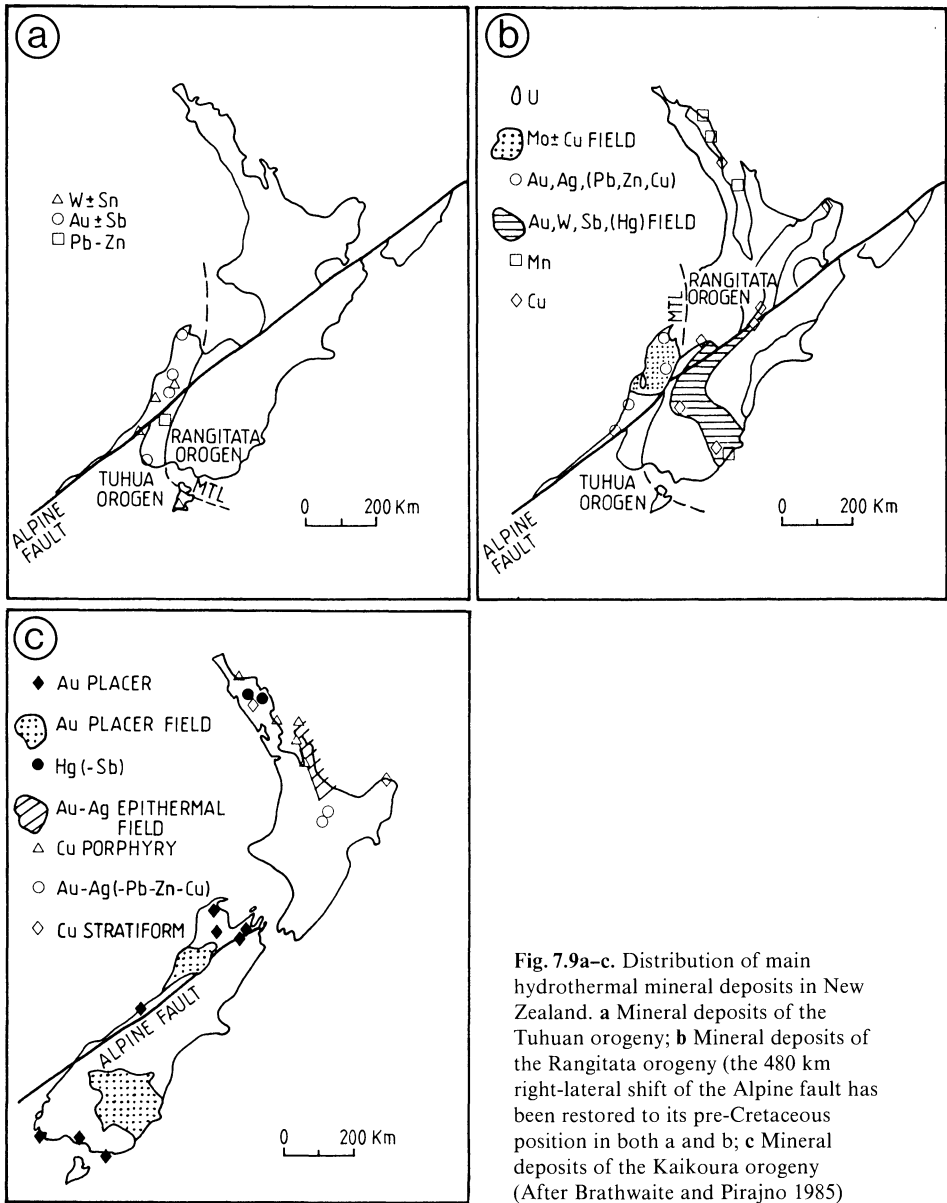
Fig. 7.9a–c. Distribution of main hydrothermal mineral deposits in New Zealand. **a** Mineral deposits of the Tuhuan orogeny; **b** Mineral deposits of the Rangitata orogeny (the 480 km right-lateral shift of the Alpine fault has been restored to its pre-Cretaceous position in both a and b; **c** Mineral deposits of the Kaikoura orogeny (After Brathwaite and Pirajno 1985)

sedimentary belt. During the late phases of the Tuhuan tectonic cycle, compression and metamorphism of the sedimentary and volcanic terranes culminated with the intrusion of granitoids of S-type affinity, between 360 and 280 Ma (Karamea Batholith).

Hydrothermal mineral deposits occur in all the Tuhuan terranes. In the central allochthonous volcano-sedimentary belt, stratabound W (scheelite disseminations)

in marble lenses, and exhalative stratabound Au in a chert-volcanic sequence are present in the West Nelson-Westland block. In Fiordland, stratiform Zn and Cu mineralisation hosted in metasediments and metavolcanics is present. However, by far more important economically are the mesothermal, turbidite-hosted, Au-Sb quartz lodes emplaced in shear zones along fold axes. This mineralisation is considered to be of hydrothermal metamorphic origin, and related to a major greenschist facies metamorphic event of Silurian age. This mesothermal Au-Sb mineralisation has similarities with that of the Ballarat Slate Belt in Victoria, Australia. Greisen-related W (usually scheelite), Sn with minor Au, Mo and Bi are all associated with leucocratic granite cupolas emanating from the Karamea batholith, and intruding into the turbidite rocks.

7.3.2 Geotectonic Settings of the Rangitata Orogeny and Related Hydrothermal Mineralisation

The Rangitata orogen (Fig. 7.9b) is made up of a series of discrete tectonostratigraphic terranes which were accreted onto the eastern margin of the Tuhuan orogen. Subduction processes and accretion of these terranes took place towards the end of the Palaeozoic and lasted for most of the Mesozoic. An important collision event was that which occurred between the Tuhuan landmass in the west and an oceanic plate in the east, carrying an island-arc terrane and fore-arc basin terranes (Brook Street and Murihuku supergroups), and the oceanic crust material that was to form the Dun Mountain ophiolite belt. Aeromagnetic surveys have indicated that the calc-alkaline volcanic arc and the ophiolite belt can be traced for about 1500 km, and are displaced by the Alpine and Campbell right lateral faults for 480 and 330 km respectively (Fig. 7.8). A thick pile of greywacke sediments constitutes the Caples-Waipapa-Haast schist and Torlesse terranes. The Haast schist is a zone of metagreywackes and intercalated metavolcanics, metamorphosed from pumpellyite-actinolite facies in the east to amphibolite facies along the Alpine Fault. The Haast schist rocks are thought to represent a zone of amalgamation, with folding and metamorphism, of the Caple volcaniclastic terrane with the western margin of the Torlesse terrane. Mafic and ultramafic lenses and pods strung out along the Alpine Fault perhaps represent remnants of intervening oceanic material squeezed up during the collision of the Caples-Haast-Torlesse terranes with the rest of the New Zealand landmass, at this time formed by the Tuhuan orogen, island-arc and Dun Mountain ophiolites. Hydrothermal mineralisation at this stage includes a few volcanic-hosted (porphyry to epithermal?) sulphide occurrences in the island-arc setting, pre-collision volcanogenic exhalative Mn- and Cu-pyrite deposits in the Waipapa terrane (Caples terrane equivalent) of the North Island, in the Haast schist and the Torlesse rocks. Syn- to post-collision mineralisation is economically more important, and includes hydrothermal quartz veins with Au-Sb, and W (scheelite), generally in chlorite schist grade rocks. This mineralisation is thought to have formed from fluids originated through the dehydration of the sedimentary pile during metamorphism.

During the late phases (Cretaceous) of the Rangitata tectonic cycle, the emplacement of calc-alkaline granitoids of I-type affinity took place. They intruded

LEGEND : -

	SEPARATION POINT BATHOLITH
	KARAMEA BATHOLITH
	PALEOZOIC ROCKS
	GREENLAND GROUP
	CHARLESTON METAMORPHIC GROUP
▲	PORPHYRY Mo OCCURRENCES
●	GREISEN W (Scheelite) OCCURRENCES
☐	SKARN DEPOSITS
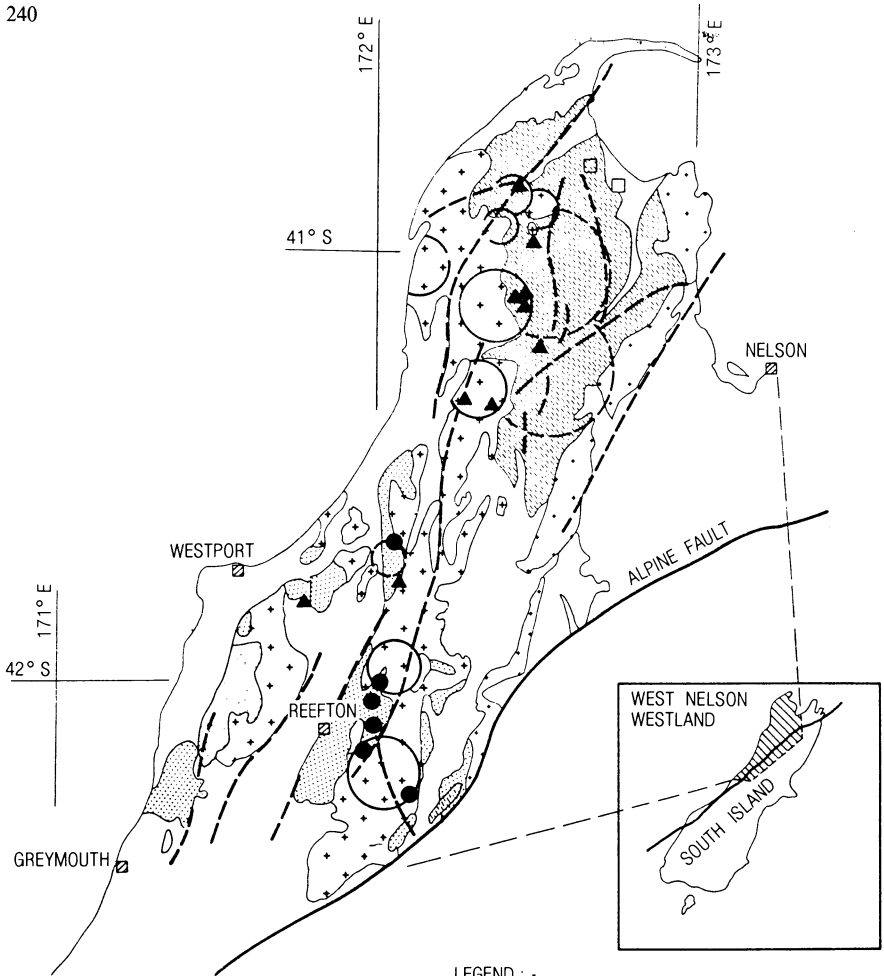
RING STRUCTURES :

○ WELL DEFINED

○ LESS DISTINCT

╱ MAJOR FAULTS

0 10 20 30 40 50 Km

@GEOLOGYBOOKS

along zones of weakness provided by the boundaries between the microplates, but some granitic stocks also intruded the Tuhuan-age Karamea batholith in West Nelson-Westland. These stocks are associated with a number of important porphyry Mo deposits as well as Au-Ag and polymetallic sulphides in quartz vein deposits. Curiously, many of the deposits appear to be spatially associated with well-defined circular structures whose origin is still uncertain (Eggers 1979; Fig. 7.10; and see also Chap. 9).

7.3.3 Geotectonic Settings of the Kaikoura Orogeny and Related Hydrothermal Mineralisation

The Kaikoura cycle (Fig. 7.9c) began in the late Cretaceous, from the end of the Rangitata cycle, and continues today. The principal events are: rifting of the New Zealand microcontinent from Australia and Antarctica, intraplate magmatism in the South Island, obduction of ophiolitic sequences and the establishment of calc-alkaline volcanic arcs in the North Island, from the Miocene to recent. Also, from the Late Miocene and continuing today, are large regional uplifts along the Alpine Fault system, which have formed the Southern Alps mountain range.

In the North Island, slabs of allochthonous volcanics – including seamount structures, ultramafics, and melanges of basaltic lavas and sediments – were tectonically emplaced. In these rocks are found a number of small and dismembered massive sulphide pods (Cyprus-type), and Cu-Pb-Zn-Ba-Au in remnants of sea-floor hydrothermal activity constructs. The subaerial volcanic zones of the Kaikoura cycle in the North Island are economically by far the most important in terms of their hydrothermal mineral potential. The volcanic arcs of Northland, Hauraki (Coromandel peninsula) and the Taupo Volcanic Zone, are ascribed to west-dipping subduction systems due to the convergence of the Pacific and Indo-Australian plates. The Northland and Hauraki volcanic arcs largely consist of andesite-dacite-rhyolitic successions, also including, where exposed by erosion, a few high-level dioritic stocks hosting porphyry Cu mineralisation. Numerous epithermal systems with Hg-Sb-Ag, Au-Ag and base metal sulphides in their deeper levels occur in the Northland and Hauraki arcs respectively. The active Taupo Volcanic Zone is the southern end, present-day expression of the long westerly-dipping, Tonga-Kermadec-Taupo-Hikurangi subduction system. Within the Taupo Zone are at least 20 active geothermal systems that achieved notoriety through the detailed studies of the New Zealand geoscientists who documented them. These geothermal systems contain, and are still in the process of making, Au-Ag-Sb-As-W-Zn-Cu-Pb deposits. The New Zealand fossil and present-day geothermal system are discussed further in Chapter 11. Finally, it is noteworthy that, through the Quaternary glaciations and the current uplift in the South Island, extensive Au

Fig. 7.10. Distribution of metallic deposits of porphyry and greisen affiliation in the West Nelson-Westland province (South Island) and their spatial relationship to circular features

placer deposits were formed from the active erosion of the Au-bearing Tuhuan and Rangitata terranes ("giant placers" of Henley and Adams 1979).

References

Aldrich S (1986) Progress report on a gravity and magnetic investigation of the Messum and Erongo igneous complexes. Commun Geol Surv S W Afr/Namibia 12:47–52

Almond D C, Ahmed F, Shaddad M Z (1984) Setting of gold mineralization in the Red Sea Hills of Sudan. Econ Geol 79:389–392

Annels A E, Simmonds J R (1984) Cobalt in the Zambian copperbelt. Precambrian Res 25:75–98

Babtat M A, Hussein A A (1982) Geology and mineralization of the Jabal Samaran-Jabal Abu-Mushut area, Saudi Arabia. Precambrian Res 16:A8

Barnes S J, Sawyer E W (1980) An alternative model for the Damara mobile belt: ocean crust subduction and continental convergence. Precambrian Res 13:297–336

Behr H J, Ahrendt H, Porada H, Rorhrs J, Weber K (1983) Upper Proterozoic playa and sabkha deposits in the Damara orogen, SWA/Namibia. In: Miller R McG (ed) Evolution of the Damara Orogen of South West Africa/Namibia. Geol Soc S Afr Spec Publ 11:1–20

Brathwaite R, Pirajno F (1985) Metallogenic epochs and tectonic cycles in New Zealand. Geol Carpath 36:293–303

Breitkopf J H, Maiden K J (1988) Tectonic setting of the Matchless belt pyritic copper deposits, Namibia. Econ Geol 88:710–723

Brown A C (1984) Alternative sources of metals for stratiform copper deposits. Precambrian Res 25:61–74

Cahen L, Snelling N J, Delhal J, Vail J R (1984) The geochronology and evolution of Africa. Clarendon, Oxford, 512 pp

Camp V E (1984) Island arcs and their role in the evolution of the western Arabian shield. Geol Soc Am Bull 95:913–921

Eggers A (1979) Large scale circular features in north Westland and west Nelson, New Zealand, possible structural control for porphyry molybdenum-copper mineralisation? Econ Geol 76:2064–2065

El-Bouseily A M, El-Dahhar M A, Arslan A I (1985) Ore microscopic and geochemical characteristics of gold bearing sulfide minerals, El Sid Gold Mine, Eastern Desert, Egypt. Mineral Depos 20:194–200

Gass I G (1981) Pan-African (upper-Proterozoic) plate tectonics of the Arabian-Nubian shield. In: Kröner A (ed) Precambrian Plate Tectonics. Elsevier, Amsterdam, pp 387–405

Hakim H D (1982) A new contribution to the study of gold-silver mineralization at Mahd Ad Dahab, Saudi Arabia. Precambrian Res 16:A22

Hartnady C, Joubert P, Stowe C (1985) Proterozoic crustal evolution in southwestern Africa. Episodes 8:236–244

Henley R W, Adams J (1979) On the evolution of giant gold placers. Trans Inst Min Metall B 88:41–50

Jackson N J, Ramsay C R (1980a) What is the "Pan-African"? A consensus is needed. Geology 8:210–211

Jackson N J, Ramsay C R (1980b) Time-space relationships of upper Precambrian volcanic and sedimentary units in the central Arabian shield. J Geol Soc London 137:617–628

Jackson N J, Drysdall A R, Stoeser D B (1985) Alkali granite related Nb-Zr-REE-U-Th mineralization in the Arabian shield. In: High heat production (HHP) granites, hydrothermal circulation and ore genesis. Meeting St. Austell, Cornwall. Inst Min Metall, London, pp 479–487

Johnson P R, Vranas G J (1984) The geotectonic environments of late Proterozoic mineralisation in the southern Arabian shield. Precambrian Res 25:329–348

Kasch K W (1983) Tectonothermal evolution of the southern Damara orogen. In: Miller R McG (ed) Evolution of the Damara Orogen of South West Africa/Namibia. Geol Soc S Afr Spec Pub 11:255–266

Kear D (ed) (1989) Mineral deposits of New Zealand. Australas Inst Min Metall, Monogr 13, Parkville, Victoria, 225 pp

Kennedy W Q (1964) The structural differentiation of Africa in the Pan-African (± 500 Ma) tectonic episode. Leeds Univ Res Inst Afr Geol 8th Annu Rep Sci Res, pp 48–49

Killich A M (1986) A review of the economic geology of northern South West Africa/Namibia. In: Anhaeusser C R, Maske S (eds) Mineral deposits of Southern Africa, vol 2. Geol Soc S Afr, pp 1709–1718

Klemd R, Maiden K J, Okrusch M (1987) The Matchless copper deposit, South West Africa/Namibia: a deformed and metamorphosed massive sulfide deposit. Econ Geol 82:587–599

Kröner A (1979) Pan-African plate tectonics and its repercussions on the crust of northeast Africa. Geol Rundsch 68:565–583

Kröner A (1985) Ophiolites and the evolution of tectonic boundaries in the late Proterozoic Arabian-Nubian shield of northeast Africa and Arabia. Precambrian Res 27:277–300

Marsh J S (1973) Relationships between transform directions and alkaline igneous rock lineaments in Africa and South America. Earth Planet Sci Lett 18:317–323

Martin H (1978) The mineralisation of the ensialic Damara orogenic belt. In: Verwoerd W J (ed) Mineralisation in metamorphic terranes. Geol Soc S Afr Spec Publ 4:405–416

Martin H, Porada H, Wittig R (1983) Where lies the root zone of the Naukluft Nappe Complex? In: Miller R McG (ed) Evolution of the Damara Orogen of South West Africa/Namibia. Geol Soc S Afr Spec Publ 11:199–208

Mason R (1981) The Damara mobile belt in South West Africa/Namibia. In: Hunter D R (ed) Precambrian of the southern hemisphere. Elsevier, Amsterdam, pp 754–788

McWilliams M O (1981) Palaeomagnetism and Precambrian tectonic evolution of Gondwana. In: Kröner (ed) Precambrian Plate tectonics. Elsevier, Amsterdam, pp 649–687

Miller R McG (ed) (1983a) Evolution of the Damara orogen of South West Africa/Namibia. Geol Soc S Afr Spec Publ 11, 515 pp

Miller R McG (1983b) The Pan-African Damara Orogen of South West Africa/Namibia. In: Miller R McG (ed) Evolution of the Damara orogen of South West Africa/Namibia. Geol Soc S Afr Spec Publ 11: 431–515

Miller R McG (1983c) Economic implications of plate tectonic models of the Damara orogen. In: Miller R McG (ed) Evolution of the Damara orogen of South West Africa/Namibia. Geol Soc S Afr Spec Publ 11: 385–396

Misiewicz J (1988) The geology and metallogeny of the Otavi Mountain Land, Damara orogen, SWA/Namibia, with particular reference to the Berg Aukas Zn-Pb-V deposit – A model of ore genesis. MsC Thesis, Rhodes Univ, Grahamstown, S Afr, 143 pp

Pallister J S, Stacey J S, Fischer L B, Premo W R (1987) Arabian shield ophiolites and late Proterozoic microplate accretion. Geology 15:320–323

Piper J D A (1982) The Precambrian palaeomagneitc record: the case for the Proterozoic Supercontinent. Earth Planet Sci Lett 59:61–89

Pirajno F (1980) Metallogenic provinces, mineral occurrences and geotectonic settings in New Zealand. In: Cresswell M M, Vella P (eds) Proc 5th Int Gondwana Symp, N Z 1980. Balkema, Rotterdam, pp 231–235

Pirajno F (1990) Geology, geochemistry and mineralisation of the Erongo Volcanic Complex, Namibia. S Afr J Geol 93:485–504

Pirajno F, Jacob R E (1987) Sn-W metallogeny in the Damara orogen South West Africa/Namibia. S Afr J Geol 90:239–255

Pirajno F, Jacob R E (1988) Gold mineralisation in the intracontinental branch of the Damara Orogen, Namibia. In: Bicentennial Gold '88, Geol Soc Aust Abstr Ser 23:168–171

Pirajno F, Jacob R E, Petzel V W F 1990 Marble-hosted sulphide and gold mineralisation at Onguati-Brown Mountain, southern Central Zone of the Damara orogen, Namibia. In: Abstr Geocongress '90 Cape Town. Geol Soc S Afr, pp 443–446

Porada H (1979) The Damara-Ribeira orogen of the Pan-African Brasiliano cycle in Namibia (southwest Africa) and Brazil as interpreted in terms of continental collision. Tectonophysics 57:237–265

Porada H (1983) Geodynamic model for the geosynclinal development of the Damara Orogen, South West Africa/Namibia. In: Martin H Eder F W (eds) Intracontinental Fold Belts. Springer, Berlin, Heidelberg, New York, pp 503–542

Porada H (1985) Stratigraphy and facies in the upper Proterozoic Damara orogen, Namibia, based on a geodynamic model. Precambrian Res 29:235–264

Porada H (1989) Pan-African rifting and orogenesis in southern to equatorial Africa and eastern Brazil. Precambrian Res 44: 103–136

Prins P (1981) The geochemical evolution of the alkaline and carbonatite complexes of the Damaraland Igneous Province, South West Africa. Ann Univ Stellenbosch Ser A1 3: 145–278

Sabir H (1979) Precambrian polymetallic sulphide deposits in Saudi Arabia and their metallogenic significance. In: Tahoun S A (ed) Evolution and Mineralization of the Arabian-Nubian shield, vol 2. Pergamon, New York, pp 83–92

Schellekens J H (1986) A Proterozoic island arc-related volcanogenic sulfide deposit near Bahrah, Saudi Arabia. Econ Geol 81: 484–488

Sohnge A P G (1986) Mineral provinces of Southern Africa. In: Anahaeusser C R, Maske S (eds) Mineral deposits of southern Africa, vol 1. Geol Soc S Afr, pp 1–24

Soliman F A, Sharkawi M A, Hussein A A, Gad M A (1982) Geology, geochemistry and mineralization of the Umm Saminki area, Eastern Desert, Egypt. Precambrian Res 16: A38–A39

Stern R J, Hedge C E (1985) Geochronologic and isotope constraints on late-Precambrian crustal evolution in the Eastern Desert of Egypt. Am J Sci 285: 97–127

Stoeser D B, Camp V E (1985) Pan-African microplate accretion of the Arabian shield. Bull Geol Soc Am 96: 817–826

Suggate R P (1978) The geology of New Zealand. Vol 1 and 2. Gov Print, Wellington

Tankard A J, Jackson M P A, Erikson K A, Hobday D K, Hunter D R, Minter W E L (1982) Crustal evolution of southern Africa — 3.8 billion years of earth history. Springer, Berlin, Heidelberg, New York, 523 pp

Unrug R (1988) Mineralization controls and source of metals in the Lufillian fold belt, Shaba (Zaire), Zambia and Angola. Econ Geol 83:1247–1258

Vail J R (1985) Pan-African (late Precambrian) tectonic terranes and the reconstruction of the Arabian-Nubian shield. Geology 13:839–842

Vail J R (1987) Late Proterozoic tectonic terranes in the Arabian-Nubian shield and their characteristic mineralization. Geol J Winter Them Iss 22:161–174

Williams G J (1974) Economic geology of New Zealand. Australas Inst Min Metall Monogr 4, Parkville, Victoria, 490 pp

Windley B F (1984) The evolving continents. 2nd edn. John Wiley & Sons, Chichester, 399 pp

Part III

Hydrothermal Processes and Activities – Related Mineral Deposits

Chapter 8

Alkali Metasomatism and Related Mineral Deposits

8.1 Introduction

Heat-liberating events, such as igneous intrusions emplaced into cool crustal rocks, will result not only in loss of heat to the surrounding environment, but also in the transport of volatile components which are responsible for metasomatic effects. Some of the most impressive of these effects are, for example, skarns (Ca-metasomatism) and tourmalinisation (B-metasomatism). In this chapter we discuss alkali metasomatism in igneous systems, its products, such as albitites and microlinites, and their relationship to mineralising systems. Some important examples of alkali metasomatism and related mineralisation in anorogenic igneous complexes are also given.

Lindgren (1933) described metasomatism as those "processes by which new minerals may take the place of old ones". In this definition any form of replacement, as for example silicification, irrespective of temperature and other environmental conditions, can be considered as a metasomatic process. Ramberg (1952) defined metasomatism as "that process capable of changing the bulk composition of a solid rock". According to Best (1982, p.348), "metasomatism involves major gains or losses of matter, usually made possible by flow of large quantities of fluids through an open rock body along significant temperature and composition gradients". This is a "constant volume replacement", tending to preserve the fabric and textures of the rocks affected. This chapter adopts the latter definition, which, for the present purpose, can be restated: metasomatism is the process whereby elements are exchanged between fluids and adjacent rocks. In the specific context of this chapter, alkali metasomatism involves the transfer of alkali ions – Na and K – from a fluid phase generated during the consolidation of an igneous body, to adjacent rocks.

8.2 Alkali Metasomatism in Continental Igneous Systems

8.2.1 Role of Volatiles in Granitic Magmas

The fundamental importance of the role of volatiles in granitic melts is two-fold. Firstly, they modify the physico-chemical behaviour of the melt and its crystallis-ation products. Secondly as a result of the volatiles' tendency to partition into the residual fluid phases, they are instrumental in the complexing and transporting of

metallic elements, and thus also important in the understanding of ore genesis processes. It is known that the addition of volatiles (B, F, Cl, H_2O) to a mineral assemblage undergoing high-grade metamorphism lowers the melting temperature of the assemblage, and that the addition of volatiles to a melt phase has the effect of lowering its solidus temperature.

The behaviour of volatiles (B, F, Cl) in a melt is similar to that of water, in that they react with the "bridging oxygens" of the silicate tetrahedra by breaking the Si-O bridges and depolymerising the melt (Burnham 1979). In order to fully understand this behaviour, it is necessary to first discuss the relationship of the physical properties of a magma in relation to the atomic structure of silicate melts. Details on this topic may be found in Best (1982), from whom this information is derived. The physical properties of liquids are intermediate between crystalline and gaseous states, and any changes in one of the three states – solid, liquid or gas – is a reflection of the thermal energy of the system. With increasing thermal energy, the motion of the particles increases until loss of cohesion takes place from the crystalline state to the liquid and gas states. Since silicate melts have high electrical conductivity, it is surmised that loosely bound ions must be present in the structure. Thus, a silicate melt is interpreted to be formed by arrays of ions, arranged to form links of Si^{4+} and Al^{3+} in tetrahedral coordination with O^{2-} ions, and creating a silicon-aluminium network, or what is commonly known as a "polymerised structure".

Liquid SiO_2 is formed by a network of Si-O chains, called polymers, and in the Si-O tetrahedra each O bridges two Si ions, and all tetrahedra are interconnected to form a highly polymerised structure. The Si ions are therefore said to be network-forming. In other silicate liquids, such as pyroxenes, there are, in addition to the Si (network-forming cation), network-modifying ions (such as Ca, Mg, Fe, Al etc.). Another difference with the liquid silica is that in liquid pyroxene the Si-O polymers are not as long, because many O do not bridge between two Si, and therefore it is less polymerised, or in other words less viscous.

The effect of H_2O dissolved in a silicate liquid is related to the vapour pressure of H_2O in the system with a reaction of the type (see also Chap. 3):

$$H_2O + O^{2-} = 2(OH)^-.$$
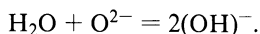
In this H_2O combines with O to form non-bridging hydroxyl ions (OH), breaking the Si-O chain of the melt and reducing polymerisation. The result is a reduction of the viscosity so that the melt then becomes more fluid. This concept is illustrated in
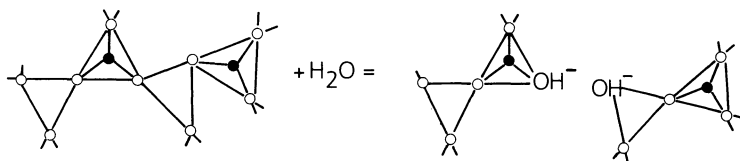
Fig. 8.1. Model of structure of anhydrous silicate melt polymers formed by "network former" Si atoms (*filled circles*), linked to "bridging" oxygens (*open circles*). Addition of water in the melt breaks the polymers through the replacement of the bridging oxygen by two "non-bridging" hydroxyls (After Best 1982)

Fig. 8.1. High temperatures produce the same effect, where the silicate melt structure is loosened as a result of the greater motion of the atoms, which can break free from nearby atoms. In addition, the strong bonds of a highly polymerised melt (high in silica) may be broken under highly applied stress, thus allowing flow.

The presence of volatiles, other than H_2O, in a melt has more or less the same effect as that of water. Both F and Cl produce a distortion of the alumino-silicate structure, resulting in an increase in coordination sites that allow "large, highly charged cations" to form new and high-order structures. Distortion of the Si-O frameworks by F, B, Cl produces octahedral sites capable of accommodating other such elements as Ni, Co, V, Cr etc., although they may already have been incorporated in the early mafic phases. Fractionation processes tend to concentrate volatiles and "incompatibles" such as Sn, W, Mo, Th, U, Zr, Ta, Nb, Hf, and sometimes also Cu, Zn, Pb, in the residual melts for the reasons outlined above. Thus the increase in volatiles not only depolymerises the melt but also provides ligands for complexing trace elements.

In the presence of volatiles the composition of a melt tends to be more alkaline than that formed under volatile-poor conditions. Experimental work reported by Pichavant and Manning (1984) shows that at 1 kbar and near-liquidus temperatures, the addition of B and/or HCl results in a decrease in the Si/alkali and Al/alkali ratios. Therefore both B and HCl cause a transfer of alkalies from the melt to the vapour/fluid phase, although the Na/K ratio may vary. This indicates that Na is leached from melts co-existing with B-bearing vapours, producing in turn an Al- or K-rich silicate melt. In the Q-Ab-Or-H_2O system, changes in the melt composition by addition of B (or F) in a source region undergoing melting are reflected by the shift of the melt composition towards the Q-Or side of the ternary system as shown in Fig. 8.2. There is also experimental evidence that the solubility of H_2O in magmas may be enhanced in B-rich melts (Pichavant 1981), whereas F-rich systems do not appear to have the same effect. The experiments carried out by Pichavant and Manning (1984) indicate that progressive addition of F (between 1 and 4%) and B (between 1 and 4.5%) causes the ternary composition to shift towards the Ab corner (Fig. 8.2). In other words, in the case of magmatic systems that during fractionation and crystallisation are progressively enriched in B, F and Li, there is a concomitant enrichment in the Ab component, while the liquidus temperature is also depressed. Thus, with progressive crystallisation of the volatile-rich melt Na and Si enter easily into a fluid phase. The opposite trend may be observed if the volatiles are removed from the crystallising melt. In this case Ab, or peraluminous minerals, crystallise and the residual melt becomes progressively enriched in Q and Or. This is the K-rich assemblage that is in fact seen to appear under subsolidus conditions (microclinisation, or potassic metasomatism). The removal of the volatiles from the melt can take place either by second boiling, or through the opening of the system by fracturing and adiabatic decompression, leading to boiling and volatile partitioning into the vapour phase. The nature of potassic metasomatism is therefore dependent on the rate of melt-fluid separation. In a closed-system potassic metasomatism is slow, and coarse-grained crystals are likely to form (microcline megacrysts). In a system that has become open by rapid decompression, on the other hand, a "pressure-quenched" intergrowth of quartz + K-feldspar would result, producing
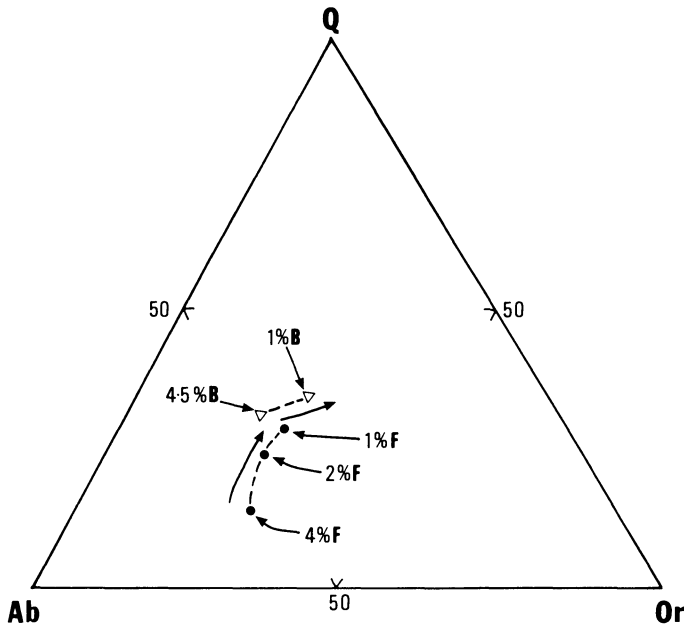
Fig. 8.2. Quartz (*Q*) – albite (*Ab*) – orthoclase (*Or*) composition of granitic rocks containing F and B. The composition of the melt changes (arrows) towards the Q-Or side through extraction of B or F (After Pichavant and Manning 1984)

the type of granophyric texture that is so often observed in granitic systems associated with hydrothermal activity. The effect of F extraction from the melt would be similar to that of B extraction, producing a Na(K)-, Si-, B(F)-rich aqueous fluid.

In summary, increasing volatile content during crystallisation enriches the melt in the Ab content, while the fluid phase is enriched in K (decreasing Na/K in the fluid phase), resulting in transfer of K from fluid to the wall rocks. Conversely when volatiles are lost from the system, the residual melt becomes enriched in Or, while Na is transferred to the fluid phase. K-feldspar crystallises from the melt and Na in the fluid is transferred to the wall rocks.

The evolution of an alkali-rich residual fluid phase from a nearly consolidated igneous body results in a series of post-magmatic and subsolidus growth of minerals, the mineralogical and geochemical evidence of which is compelling (Bowden 1985). Such changes are largely dependent on the intensity of the rock-fluid interaction. The subsolidus processes include: cationic exchange reactions in feldspars, Na for K, or, K for Na (albitisation and microclinisation); changes in the structural state of feldspars.

Other changes involving increasing amounts of H_2O (H^+ metasomatism) and/or "dry" volatiles include: changing compositions of pyroxenes and amphiboles, growths of tri-octahedral micas, aegirine and riebeckite, as well as a series of F- or B-rich mineral assemblages.

++ Microclinised granite (K-Metasomatism)

×× Albitised granite (Na-Metasomatism)

▨ Quartz-albitite

■ Greisenised granite

〰 Country rocks

\|/ Quartz greisen and vein systems
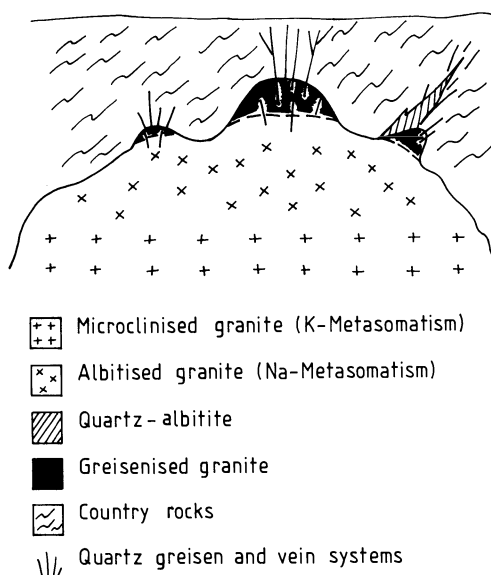
Fig. 8.3. Post-magmatic alkali metasomatism and greisen alteration in granitic rocks (After Beus and Zolashkova 1964)

It must be pointed out that many of the replacement features of subsolidus changes can also be explained by magmatic crystallisation, or unmixing of solid solutions. However, subsolidus reactions are especially developed in the apical zones of plutons, and along fractures or in pods and lenses. Sequences of post-magmatic alteration in granitic rocks and their spatial association with the apical regions of an igneous body are shown in Fig. 8.3. These illustrations are "classics" developed by Russian geoscientists (Shcherba 1970; Smirnov 1976), and have been frequently reported in Western literature.

8.2.2 Textural Features

The mineralogical and chemical composition of rocks affected by alkali metasomatism changes can be monitored both texturally and mineralogically. In igneous rocks there are at least three types of textures that can be attributed to alkali metasomatism. These include: replacement coronas, granophyric textures and perthitic textures.

Replacement coronas refer to the replacement along the margin, and crystal boundaries of ferromagnesian silicates by Na-amphiboles, such as arfedsonite or riebeckite, resulting from the breakdown of fayalite.

There is good evidence from field relationships and geochemical data that granophyric textures, formed by intergrowths of quartz and K-feldspar and encountered in many igneous rocks, are of metasomatic origin. These peculiar intergrowths are usually distinguished by the turbidity of the K-feldspar component. Examples of alkali ion metasomatism is provided by the granophyric intergrowths developing as a result of devitrification of glassy material in ash-flow tuffs and acid lavas.
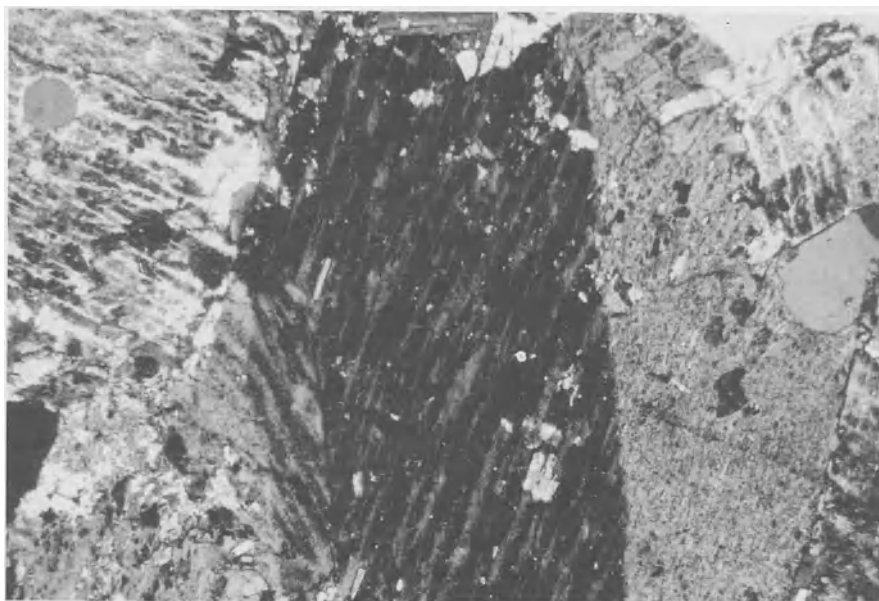
Plate 8.1. Photomicrograph (crossed nicols) showing albitic domains developing in K-feldspar due to Na-metasomatism. This texture is called perthitic. Width of field is 3.5 mm

Perthitic textures of feldspar may in some cases also be indicative of alkali metasomatism, rather than unmixing during cooling of a two-phase assemblage. Replacement of Na for K in feldspars is shown by the presence of albite inclusions in the K-feldspar host (Plate 8.1). These inclusions can occur either as irregular shapes, or as veinlets, and do not follow crystallographic directions, as would be the case for solution unmixing. Microclinisation and K-silicate alteration show features that range from the generation of intermediate to ordered microcline to micas. Order-disorder relationships in alkali feldspar refer to the distribution of Al and Si in the unit cell and its departure from the monoclinic towards triclinic symmetry (obliquity). This obliquity decreases with decreasing temperature and the K content increases. Thus K increases with ordered structures (e.g. towards a sanidine composition), whereas in passing from the ordered towards the disordered structure, Na migrates into the lattice to form distinct domains, giving rise to the perthitic texture. The structure can change back again towards a K-rich domain to form microcline with further decreasing of the temperature (Fig. 8.4). The sequence from high to low temperature feldspar is as follows:

sanidine → orthoclase → perthite (orthoclase + albite) → microcline.
                              (Na-metasomatism)   (K-metasomatism)

Albitites, microclinites, fenites and the core zones of potassic alteration in porphyry systems are the most common products of alkali metasomatism. The following sections focus on albitites, microclinites and fenites, while potassic alteration of porphyry and volcanic systems is examined in Chapters 10 and 11.

Fig. 8.4. Alkali metasomatism of alkali feldspar crystals. 1 Metasomatic Na for K exchange with development of albite domains. 2 Metasomatic K for Na exchange with development of microcline; turbidity results from the presence of minute exsolved hematite inclusions (After Haapala 1986; Kinnaird 1985)
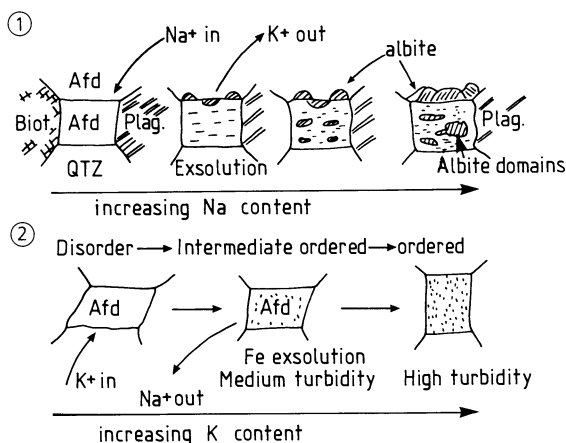
8.2.3 Sodic Metasomatism and Albitites

This aspect of metasomatism is characterised by Na-bearing minerals which are clearly in replacement relationships with primary magmatic minerals. The replacement of alkali feldspar by albite (albitisation or Na-feldspathisation) is the more common form of sodic metasomatism. This replacement may proceed from pre-existing perthites, or by direct replacement of K-feldspar with newly formed albites (Pollard 1983). Albitisation of K-feldspar can be written as follows:

$KAlSi_3O_8 + Na^+ = NaAlSi_3O_8 + K^+$.

(microcline)   (albite)
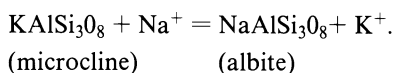
The development of albite-rich rocks is usually associated with "rare element" mineralisation (Nb, Ta, Sn, W, Li, Be). Na-enrichment is accompanied by concentrations of Fe, U, Th, Zr, Nb, Sn, Zn and HREE . Also, Na-metasomatised rocks tend to be enriched with respect to K-metasomatised rocks in Rb, Th, Nb, La, Ce, Hf, Zr, Y (Kinnaird et al. 1985). Several types of albitites have been recognised according to their mineralogy and rock type affected, and are shown in Table 8.1. In general terms albitite is a leucocratic rock made up of albite and quartz and containing some residual primary feldspars (Plate 8.2). Albitisation can affect a large mass of rock, and in some cases, on mobilisation, the albitised material can be injected as apophysis into the country rocks (see Fig. 8.3).

In peraluminous granites, sodic metasomatism is manifested by textural and colour changes, due to coarsening domains in perthite and development of the so-called chessboard texture. Growth of new micas, such as siderophyllite, also takes place. Geochemically the rock is enriched in Nb, Zr, U, Th and REE. Sodic metasomatism in peralkaline granites also brings about textural and colour changes, but these are due to growths of aegirine and arfvedsonite, and replacement of K in perthite by Na (Fig. 8.4), which leads to the development of albitites. Geochemically an enrichment in the same elements as for the peraluminous granites is noted. Albitisation is followed by incipient H^+ metasomatism,

Table 8.1. Chief characteristic minerals associated with alkali granites (After Smirnov 1976)

Type of granitic rock	Chief alteration minerals	Mineralisation
Muscovite-microcline-quartz-albite	Muscovite	Beryl, wolframite, molybdenite, cassiterite, bismuth minerals
Lithionite-mcrocline-quartz-albite-amazonite	Lepidolite, zinnwaldite, topaz	Columbite-tantalite pyrochlore, cassiterite
Biotite-quartz-albite	Biotite	Pyrochlore, zircon, columbite, thorite, xenotime, bastnaesite, molybdenite
Aegirine-albite-microcline	Aegirine	Zircon, xenotime, monazite, yttrialite, fergusonite
Nepheline-bearing microcline-albite	Aegirine, sodic amphibole	Zircon, pyrochlore, sphene, apatite, ilmenite, britholite
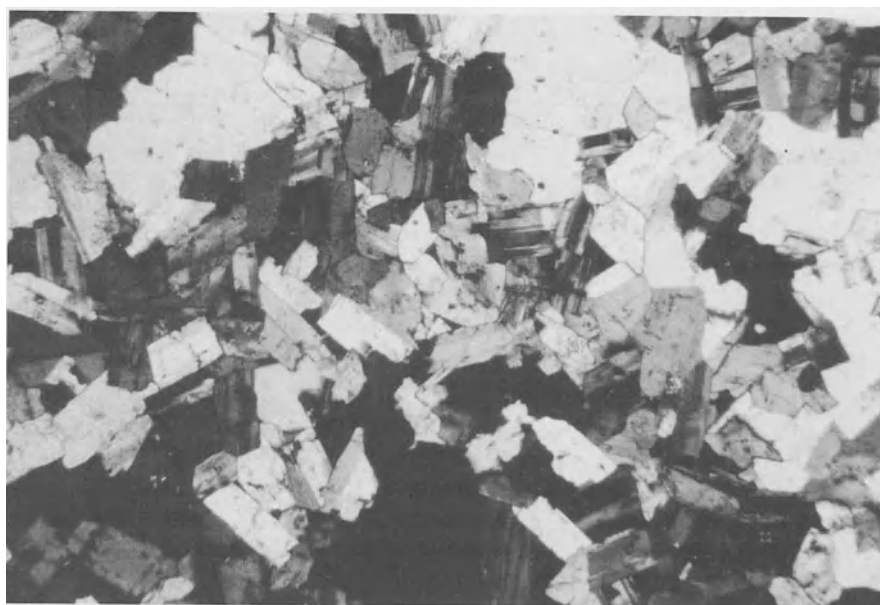
Plate 8.2. Photomicrograph (crossed nicols) of quartz-albitite rock made up of a fine-grained aggregate of quartz and albite crystals. Width of field is 3.5 mm

usually characterised by the growth of sericite and varying amounts of fluorite and topaz.

Experimental work on silicate systems with volatile components such as Li, F, H_2O, and fluid inclusion studies of quartz from sodic granites, can be used to estimate the temperature-pressure conditions of sodic metasomatism. Results

indicate a range of temperatures of between 400 and 600°C approximately, at pressures of 1 kbar or less (Pollard 1983).

8.2.4 Potassic Metasomatism and Microclinites

Potassic metasomatism (or K-feldspathisation or microclinisation) involves K for Na exchange mineral reactions, and is typically represented by the replacement of albitic plagioclase by microcline. Other products of K for Na exchange reactions include the growth of new micas with compositions ranging from annite (Fe^{2+}-rich phlogopite) and amphibole compositions characteristic of Fe^{2+}-rich members (ferroedenite and ferroactinolite) (Bowden 1985).

K-feldspathisation is believed to assume regional proportions and to precede sodic metasomatism (see Fig. 8.3), according to the scheme envisaged by Shcherba (1970), leading to the development of microclinites. Field and petrographic evidence from Nigeria (Bowden et al. 1984) also shows, however, that K-feldspathisation may post-date Na-metasomatism, is generally confined to fractures in the roof zones of granitic plutons, and is related to early stages of vapour separation.

Microclines typically develop in pockets or pods in the roof zones of plutons. Extreme K-feldspathisation may result in a vuggy-textured microclinite due to desilication (Kinnaird 1985). K-metasomatism is characterised by the presence of an intermediate to ordered microcline (Fig. 8.4). Also, during the K for Na exchange, Fe is released from the lattice and oxidised to form minute hematite inclusions
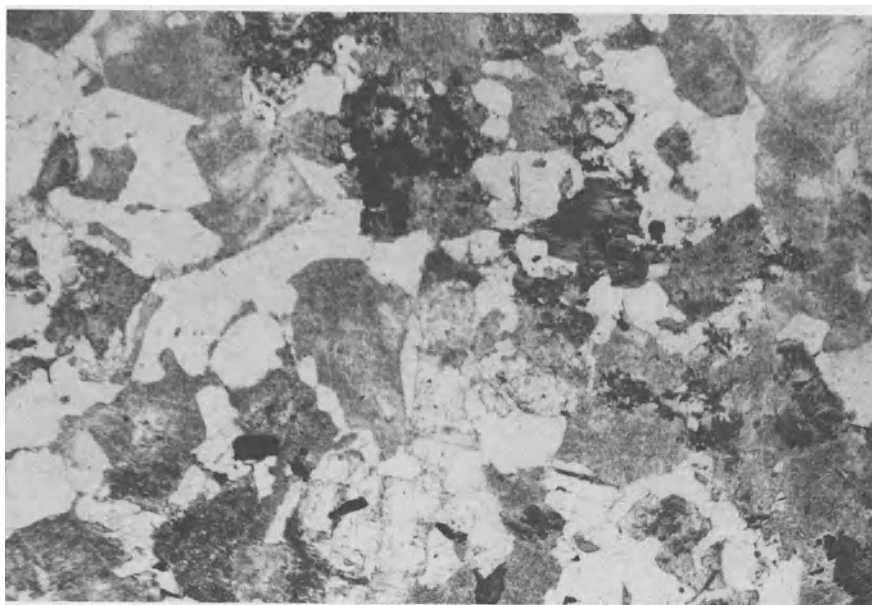
Plate 8.3. Photomicrograph (plane polarised light) showing turbidity of K-feldspar crystals in a K-metasomatised granitic rock. Width of field is 3.5 mm

which give the microclines a distinct reddish colouration in hand specimens (Kinnaird 1985; Kinnaird et al. 1985), whereas in thin-section this phenomenon is manifested by the turbidity of the feldspar crystals (Plate 8.3). K-metasomatism is typically represented by the replacement of albitic plagioclase by microcline or orthoclase. Fluid inclusion work supported by textural evidence for the Nigerian complexes suggests that CO_2 effervescence takes place in the system which enhances the K/H ratio of the remaining fluid, resulting in the development of K-feldspar at the expense of albite (Kinnaird 1985). In an ongoing process of alteration potassic metasomatism is followed by incipient H^+ metasomatism, characterised by the growth of siderophyllite or zinnwaldite aggregates, chlorites, and in some cases kaolinite.

Temperature-pressure conditions for K metasomatism are not well known, but a minimum temperature of 630°C in the Q-Ab-Or system at 1 kbar, with 4% F, is considered possible (Manning 1982; Pollard 1983). Studies of fluid inclusions by Russian workers in K-feldspars indicate a range of temperatures from 320 to 700°C, at 1.2 to 2 kbar. During K-metasomatism Rb, Li, Zn are enriched and Na depleted.

8.3 Alkali Metasomatism in Anorogenic Ring-Type Complexes

Magmatism which occurs in tensional zones of plate interiors is called anorogenic. The nature of this magmatism is generally alkaline with a bimodal range of products (mafic-felsic). More specifically, ring-type igneous complexes are emplaced in stable continental interiors associated with zones of extensions linked with periodic uplifts and subsidence. Some noteworthy examples of magmatic provinces containing ring complexes include Niger-Nigeria (Bowden et al. 1984), Corsica (Bonin 1986), Oslo Graben (Oftedahl 1978), the Nuanetsi-Lebombo area in southern Africa (Cox et al. 1965), and the Damara alkaline province (Prins 1981; Potgieter 1987).

The products of continental alkaline magmatism are volumetrically small. They have high concentrations of incompatible elements and volatiles, especially CO_2, B, F, Cl. The origin of these magmas is by no means certain, except that they are known to form in regions characterised by a thick lithosphere by small fractions of partial melting. It is also envisaged that these magmas may derive from metasomatised parts of mantle material. This metasomatism is thought to be due to mantle outgassing of C with high halogen contents (Lloyd and Bailey 1977; Bailey 1978).

This volatile flux through mantle material lowers the solidus so that liquids would result either from a drop in pressure, or through a local increase in temperature. Discrete mantle plumes or crustal attenuation accompanied by rifting and pressure release are the mechanisms invoked, with the latter gaining favour over the former (Black et al. 1985). Either mechanism could account for the generation and rise of these asthenospheric liquids through conduits which are usually long-lived or re-activated crustal fractures. The enrichments of the alkaline magmas in non-hydrous volatiles, such as CO_2 and halogens, lead to the concentration in the residual melts, during fractionation, of the volatile constituents and elements such as Zr, Y, Nb, U, Th etc.
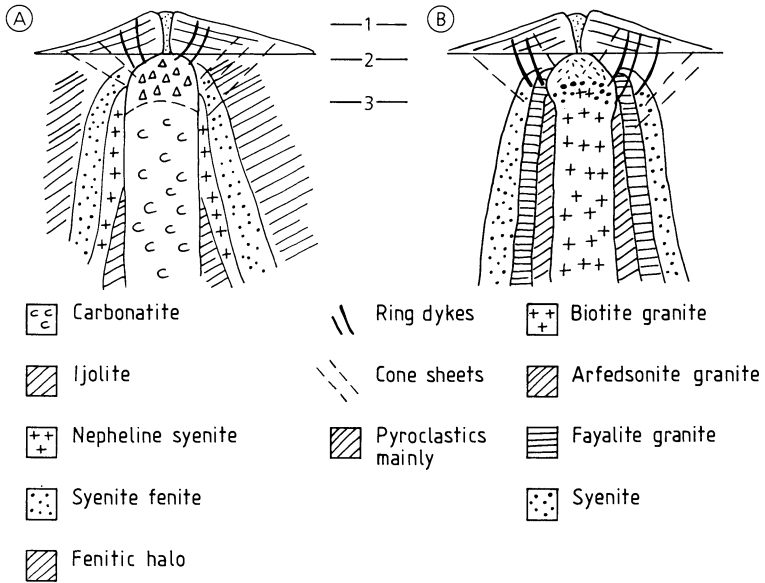
Fig. 8.5A, B. Idealised cross-sections of ring complexes and asssociated volcanic structures. **A** Ijolite-carbonatite type and **B** alkali-granite-syenite type. *1, 2* and *3* Erosion levels common for African complexes; *2, 3,* for example, correspond to erosion levels of complexes in Nigeria and Niger, respectively; see also Fig. 8.6. (After Bowden 1985; Kinnaird and Bowden 1987)

Typical rock associations of alkaline magmatism include: kimberlites, mafic ultrapotassic rocks, syenite-pyroxenite-ijolite-carbonatite assemblages, alkali basalts and peralkaline granite-syenite-gabbro assemblages (Mutschler et al. 1985). According to Bowden (1985), ring complexes can be grouped into: granitic (alkaline granite-syenite-gabbro), alkalic (ijolite-carbonatite) and basaltic-gabbroic ring complexes. Fig. 8.5A, B illustrates idealised cross-sections of alkaline ring complexes of the syenite-pyroxenite-ijolite-carbonatite association, and of the alkaline granite type, respectively. Details of the petrology of the alkaline rocks in general, and ring complexes in particular, are beyond the scope of this discussion. For these the reader is referred to Tuttle and Gittens (1966), Carmichael et al. (1974), Le Bas (1977), Hughes (1982), Black and Bowden (1985), Bonin (1986), and the latest collection of works edited by Fitton and Upton (1987). The ring complexes are generally eroded volcanic centres with a circular shape and characterised by caldera-forming events. The erosion level of the complexes is reflected by the rock types exposed as indicated in Fig. 8.5. In the more deeply eroded structures only the sub-volcanic magma chambers and/or conduits are left exposed. The radii of ring complexes are thought to be proportional to the depth of the magma chamber (Bonin 1986).

Alkaline and ring-type complexes are abundant in Africa, where they are distributed along the East African rift system and roughly around the margins of the Congo, Kalahari and West African cratons, and are aged from 2000 to 25 Ma (Black et al. 1985; Fig. 8.6). During the crystallisation and differentiation of the ring
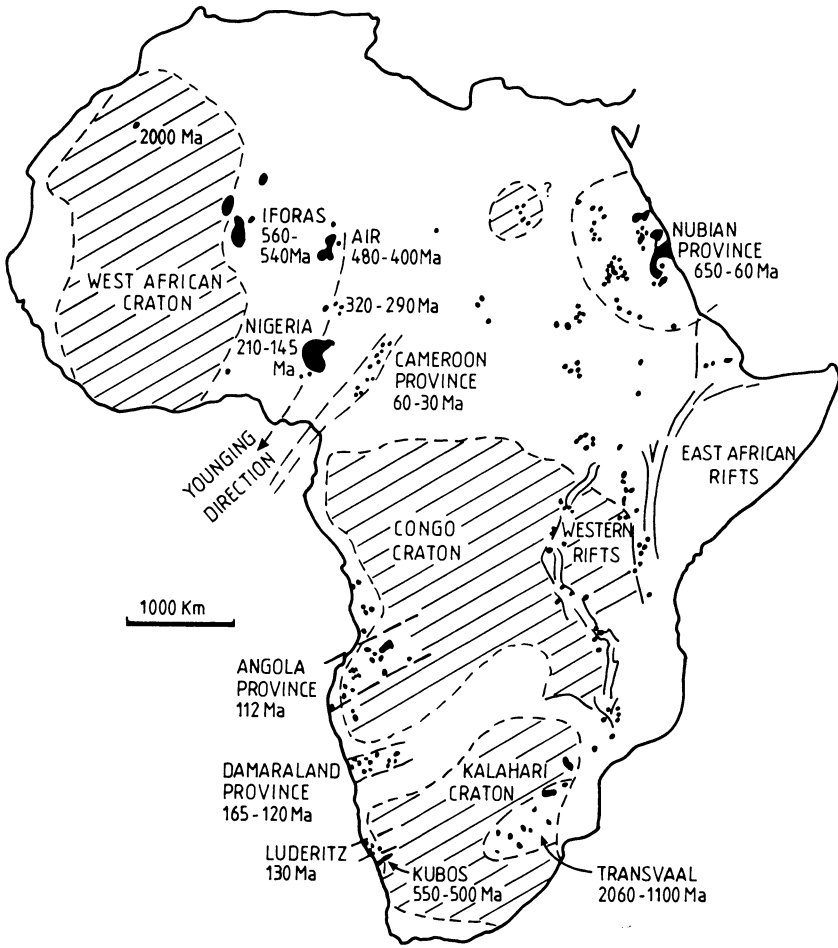
Fig. 8.6. Distribution of major alkaline provinces in Africa. *Dots* indicate single alkaline complexes; *black* areas indicate close clusters of complexes. Note the southwesterly younging direction of the Air-Nigeria provinces (Kinnaird and Bowden 1987). Also note that the older (>1000 Ma) complexes are intracratonic, whereas most others tend to occur along the margins of the cratonic masses (After Black et al. 1985)

complex magmas, peralkaline fluid phases develop which can be retained within the magma, or expelled into the country rocks. The fluids' interaction with the surrounding rocks at subsolidus temperatures induce the metasomatic changes which may extend from a few hundred metres up to several kilometres away from the complex. Studies of the metasomatic and mineralised systems related to ring complexes can be of great importance in the understanding of the geological and geochemical processes related to the partitioning of metals from the alkaline magmas into subsolidus fluids and hydrothermal solutions. Especially important from this point of view are the syenites and alkaline granites. These belong to the spectrum of A-type granitoids (anorogenic, alkaline, or

meta- to peraluminous) (Collins et al. 1982), as distinct from the I and S-types of Chappell and White (1974).

8.3.1 Fenites

One of the most interesting cases of alkali metasomatism is that which takes place around alkaline complexes in stable continental areas. This phenomenon is known as fenitisation, and the rocks affected are called fenites. The name is derived from the Fen carbonatite in Norway where this type of alteration was first documented by Brogger (1921). A plethora of complicated names have been adopted by different authors to describe fenitic rocks. Verwoerd (1966) proposed that the naming of fenitic rocks should be prefixed by the principal mineral components followed by fenite (e.g. orthoclase-aegirine-augite fenite).

Fenites are formed through progressive metasomatism in the country rocks surrounding alkaline complexes. This usually involves the elimination of free quartz (desilication) and the development of alkali mineral phases. Carmichael et al. (1974) attributed these metasomatic effects to residual alkali-rich fluids deriving from the fractionation of alkaline magmas. The fluids are in strong disequilibrium with the country rocks, producing haloes of alteration products, which in some cases may resemble primary igneous rocks. The process is thought to be a solid state transformation due to expulsion from the igneous complex of hot, highly reactive volatiles and their subsequent infiltration into the country rocks (Best 1982). The spatial relationships of alkaline and carbonatite magmas and their fenitised envelopes are illustrated in Fig. 8.5A.

The composition of fenites is dependent on both the nature of the country rocks affected and the igneous complexes from which the fenitising fluids evolve. Fenitic envelopes occur mainly around carbonatites, but other alkaline complexes are also surrounded by alteration haloes with a fenitic character. Since most anorogenic alkali complexes and allied rocks occur in stable continental areas, fenite envelopes are for the greater part found within granitoids and/or basement gneisses. However, fenitisation has also been noted in basic igneous rocks and sedimentary rocks (Verwoerd 1966; Prins 1981). Areas affected by fenitisation may be up to 4 km from the responsible igneous intrusion. Two styles of fenitisation are recognised, one associated with carbonatites; the other with ijolites. Carbonatites form intense K-feldspar fenitisation, whereas ijolite magma is preceded by Na-K fenitisation with the production of aegirine-bearing rocks (Le Bas 1977). Prins (1981) also concluded that K-metasomatism (feldspathisation) is associated with carbonatites, whereas Na-metasomatism (pyroxenisation) is connected with alkaline igneous rocks.

The main geochemical and mineralogical features of fenitic metasomatism are described below, using primarily examples from the African continent. McKie (1966) provided a comprehensive review of the mineralogical and geochemical changes that occur during progressive fenitisation around carbonatites. In the study of the chemical changes that take place during metasomatic alteration McKie (1966) recommended that the analyses be re-calculated in terms of cations combined with 100 anions (O, OH, F). Silica has proved to be a very useful parameter indicative of

alteration (it usually, though not always, decreases with increasing fenitisation), and is therefore expedient to plot cationic values against Si variations.

A complex sequence of progressive geochemical and mineralogical changes was distinguished by McKie (1966) at Oldonyo Dili (Tanzania). Chemical changes during fenitisation show increases in Na, Fe^{3+}, Ca, P, Mn and Mg and decreases in Si, with Fe^{2+}, K, and Al remaining more or less constant (Fig. 8.8). From the geochemistry of several other fenites, McKie (1966) deduced that the fenitising solutions have an oxidising character which he attributed to influx of solutions carrying Fe^{3+}. Mineralogical changes took place in a granitic gneiss composed of microcline, quartz, oligoclase-albite, biotite and garnet. This sequence (Fenite 1 to 10) is summarised here. The earliest stage (Fenite 1) is characterised by strained quartz, microcline-perthite (Or_{94}), and aggregates of magnesio-arfvedsonite replacing biotite. With advancing fenitisation (Fenite 2) quartz becomes unstrained and more common than in the original rock. Oligoclase-albite and orthoclase are abundant, and acicular aegirine intergrown with magnesio-arfvedsonite is also present (Fenite 3). In the following more advanced stages (Fenite 4) albite and aegirine, together with magnesio-arfvedsonite, are common throughout. The presence of calcite is attributed to later solutions distinct from the fenitising fluids. Marginal replacement of microcline by orthoclase, with aegirine-forming veins and aggregates, and quartz greatly reduced, characterise the next stage (Fenite 5). Fenites 6 to 10 are essentially quartz-free. Orthoclase-cryptoperthite, albite, aegirine and magnesio-arfvedsonite become the dominant minerals. Beyond Fenite 8 the dominant orthoclase-cryptoperthite has the composition $Or_{85}Ab_{15}$. Apatite may be locally common, and in places the orthoclase-cryptoperthite is intergrown with aegirine.

The main features of the sequence of mineralogical changes described are the alteration of biotite to magnesio-arfvedsonite and aegirine, the replacement of microcline by orthoclase and that of plagioclase by albite, and the gradual disappearance of quartz. The final product of Oldonyo Dili is a rock composed of orthoclase, aegirine with subordinate albite, magnesio-arfvedsonite and apatite.

The Spitzkoppe alkaline complex (South Africa) has a fenitic halo developed in granitic rocks of the Bushveld Complex. Nepheline and scapolite occur in the fenitised aureole of this complex where early investigators had difficulty in interpreting the nature of the fenitised rocks, suggesting in some cases that they may be magmatic rather than metasomatic. Verwoerd (1966), however, on the basis of textural relationships between minerals – such as the mantling of the augites by Na-amphibole, and the intergrowths of aegirine-augite with nepheline – recognised that they belong to fenitisation of the original igneous assemblages. The original composition of these rocks, whose grain size is preserved following fenitisation, included quartz, hornblende, biotite and magnetite. These minerals reacted with fluids enriched in Na, Al, Fe^{3+}, resulting in the development of aegirine and alkali amphibole at the expense of quartz and ferromagnesian minerals. Fluids containing Si, Al and Na were produced as a result of these reactions, which in turn albitised the surrounding granitic rocks over an area up to 3–4 km wide. Two types of fenite were distinguished in this area by Strauss and Truter (1950). A "red" fenite is composed of turbid microperthite, oligoclase, albite, quartz, aegirine and alkali amphibole. This
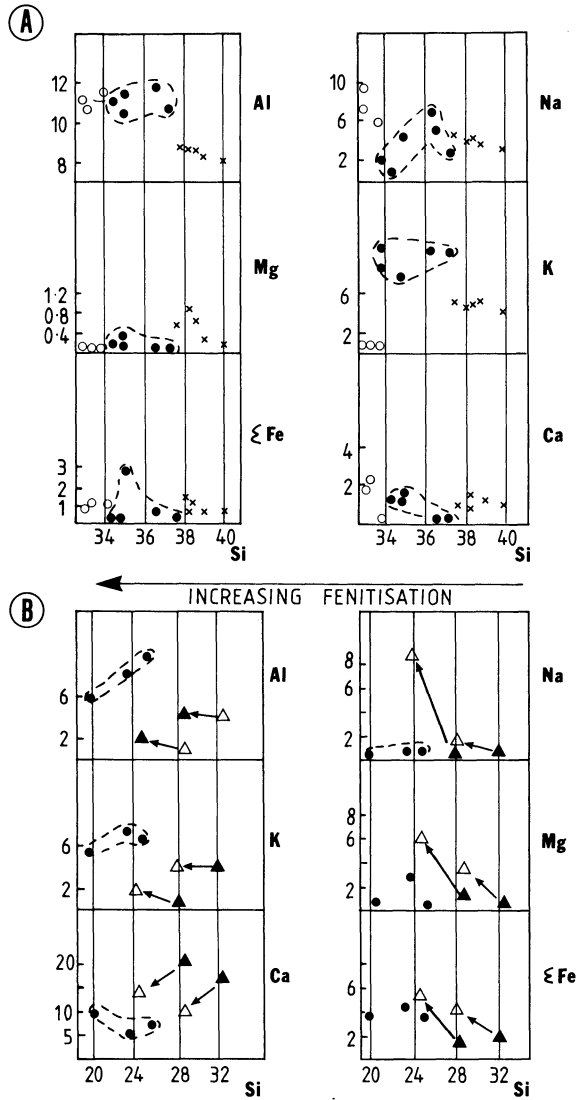
Fig. 8.7A, B. Chemical changes (elemental concentration based on oxygen = 100) with Si (based on a standard cell of 100 anions) attained during metasomatic processes in carbonatite complexes of the Damaraland igneous province, Namibia. A Kalkfeld complex; *black dots* enclosed by dashes are fenitised syenites; *open circles* are trachytic dykes; *crosses* represent fenitised country rocks. B Okorusu complex; *black dots enclosed by dashes* are feldspathic dykes and breccias; *filled triangles* and *open triangles* connected by an *arrow* indicate variations from parent rock to metasomatic pyroxenite (After Prins 1981)

fenite was later affected by a second stage of alteration in which the final products are: microcline-perthite, albite, Na-amphibole, magnetite, apatite, sphene and accessory ziron. A "white" fenite contains microcline-perthite, aegirine-augite, albite, sphene, apatite and magnetite, with no quartz. It is interesting to note that quartz veins present in the Bushveld granophyre within the zone of white fenite are totally replaced by albite.

Prins (1981) studied the chemical changes in the fenitic aureoles of the Kalkfeld and Okorusu alkaline-carbonatite complexes (Namibia). The findings of this author – reported here – are useful to the understanding of the genesis of mineralisation and alteration connected with this type of intraplate anorogenic

magmatism. Examples of variation diagrams depicting these chemical changes are shown in Fig. 8.7A, B.

The Kalkfeld data refer to a pristine wall-rock of granitic composition (Salem granite) and its fenitised products. The main changes involve the enrichment of Na, Al, Mg and total Fe with decreasing Si contents (advancing fenitisation), whereas K and Ca remain nearly constant. Here two important observations were made by Prins (1981). One, that the "trachytic" dykes plotted in Fig. 8.7A may, on the basis of their low Si and high Na, represent mobilised fenites. Two, that the sum of Si + Al + Na + Total Fe is constant for the granitic rocks, leading this author to suggest that this type of metasomatism involves substitutions between the elements so as to preserve the charge balance. The chemical variations at Okarusu (Fig. 8.7B) refer to a metasomatic pyroxenite (pyroxene-fenite) and its parent material which is a calcareous feldspathic sandstone. Here increases in Na, Mg, total Fe, and decreases in Ca and Al versus decreasing Si concentrations are recorded. Feldspathic dykes and breccias (feldspathisation stage), plotted in Fig. 8.7B, show strong Si depletions and are also interpreted as reflecting re-mobilisation. The Kalkfeld syenite-carbonatite complex developed extensive fenitisation both within a primary syenite and within the granitic wall rocks (Salem granite, Damara Orogen). The fenitisation of the granitic rock is characterised by the replacement of quartz by aegirine-augite and Na-amphibole along fractures. The syenite reveals a re-crystallised texture and consists of orthoclase and aegirine-augite.

The Okorusu nepheline-syenite carbonatite complex (Prins 1981), by contrast, developed its fenitic envelope in sedimentary wall rocks, which in their unaltered form contain quartz, feldspar, biotite, calc-silicate and calcite. Fenitisation converted these rocks into a "massive alkali pyroxenite" which retains the sedimentary structures (Prins 1981, p. 205). The pyroxene-fenite consists of alternating bands or layers of pyroxene, and calcite + quartz. Apatite + pyrite + titanomagnetite are also present. During a later stage of alteration biotite and Na-amphibole formed at the expense of the pyroxene. The new pulse of metasomatism introduced K (feldspathisation), resulting in the transformation of pyroxene-fenite and syenite into a K-feldspar-limonite-calcite fenite. The new feldspar forms large crystals, has a maximum ordered structure with a composition of Or_{90-95}, and shows turbidity due to minute hematite inclusions. Flow-structured dykes containing feldspar, limonite, calcite and fluorite are interpreted by Prins (1981) as mobilised feldspathised rocks.

The transfer of elements and the related mineralogical changes associated with the transformation of the unaltered sediments at Okorusu to pyroxene-fenite were calculated by Prins (1981), who used for his calculations the composition-volume equations given by Gresens (1967) and Babcock (1973). For the first set of mineralogical changes and transfer of elements, relating to the early Na-dominated fenitisation (pyroxene-fenite), he assumed constancy of volume. It was found that during metasomatism total Fe, Mg, Na and P were added, whereas K, Mn, Al and Ti remained constant. With some surprise, only a little Si was abstracted, while a large amount of Ca was removed and re-distributed. The weak depletion of Si during the pyroxenisation of the sediments is at odds with the usual desilication observed in fenitised rocks. The author explained the phenomenon by suggesting that the

increase, or decrease, of Si is essentially dependent on the degree of saturation in Si of the fluid relative to the invaded wall rocks. Thus, it is reasoned that if the fluids enter a Si-oversaturated rock body, desilication will occur to establish equilibrium, whereas the opposite will take place if the wall rocks are undersaturated with respect to the matasomatising fluids.

The mineralogical changes and element transfer that took place during the Na-dominated stage (pyroxene fenite) at Okurusu, as calculated by Prins (1981, p. 213), are given below.

$$2\text{anorthite} + 8SiO_2 + 5Fe^{3+} + 4Na^+ + Mg^{2+} + 4H_2O =$$
$$\text{aegirine-augite} + 2\text{albite} + Fe_3O_4 + Ca^{2+} + 8H^+;$$

$$\text{biotite} + 5\text{calcite} + 12\text{quartz} + 3Fe^{3+} + 6Na^+ + 3PO_4^{3-} + 4H_2O =$$
$$\text{apatite} + 6\text{acmite} + 2\text{orthoclase} + Fe_3O_4 + 5CO_2 + 11H^+.$$
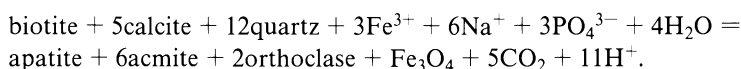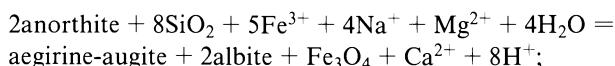
The second stage of fenitisation was K-dominated and allowed the formation of orthoclase. Mass transfer equations were calculated allowing a 20% volume increase for the transformation of the pyroxene-fenite to a feldspathic fenite. Al, K and CO_3 were added, while Fe, Ti, Mg, Na, P remained constant, and Si and Ca were removed. Here feldspathisation is taken to be accompanied by desilication, because of the contrast between the invading fluid (Si-undersaturated) and the host lithology (Si-oversaturated). Silica is therefore removed but is locally re-distributed as chalcedonic breccia fillings associated with calcite.

The equations representing the mineralogical changes and element transfer associated with feldspathisation are shown below (Prins 1981, p. 217):

$$\text{aegirine-augite} + 6\text{quartz} + 3Fe_3O_4 + 4Al^{3+} + 2K^+ + 8CO_2 + 8OH =$$
$$2\text{albite} + 2\text{orthoclase} + 5FeOOH + 6FeCO_3 + CaCO_3 + MgCO_3 + 3H^+;$$

$$\text{aegirine-augite} + 2\text{calcite} + 7\text{quartz} + 4Al^{3+} + 2K^+ =$$
$$2\text{ orthoclase} + 2\text{albite} + 2\text{siderite} + Si^{4+} + Mg^{2+} + 3Ca^{2+}.$$
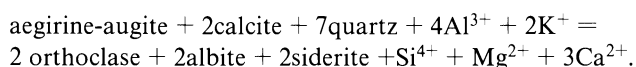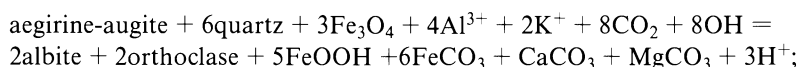
Fenitisation of basic rocks was investigated and reviewed by Verwoerd (1966), using examples from South Africa and Namibia. The chemical changes of basic fenitised rocks around a number of igneous complexes are shown in Fig. 8.8. In geochemical terms fenitisation of basic rocks does not differ much from that of granitic rocks. The removal of Si and addition of K, Na, Ca, Fe, P are the main losses and gains in the system.

Verwoerd (1966) considered these changes to be isovolumetric, with O + OH remaining constant. At Goudini (South Africa) increases in Na, CO_3, Fe and Ti were noted. At higher temperatures of alteration dehydration is accompanied by removal of Al, Ca, Mg and Si. The above chemical changes correspond to a mineralogy essentially dominated by riebeckite and aegirine which replaces pyroxenes. In some places a red-brown (Ti-rich) biotite may replace ferromagnesian minerals in fenitised dolerites.

The Messum igneous complex in Namibia (Korn and Martin 1954) is a large volcano-plutonic structure consisting of a central foyatic intrusion surrounded by gabbroic rocks and pyroclastic products. Fenitisation of the gabbroic rocks is characterised by the replacement of augite by hastingsite, and the introduction of
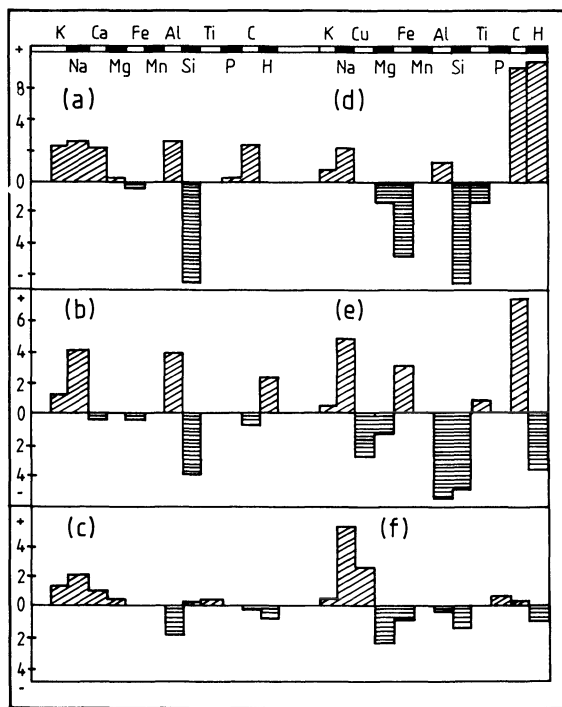
Fig. 8.8a–f. Chemical changes in fenitised basic rocks. Additions and subtractions are above and below the zero line, respectively. a granite to fenite at Fen; b basalt to fenite at Messum, Namibia; c gabbro to fenite at Messum, Namibia; d norite to fenite (stage 1) at Goudini, South Africa; e norite to fenite (stage 2) at Goudini, South Africa; f gabbro to fenite at Spitzkop, South Africa (After Verwoerd 1966)

perthitic alkali feldspar and nepheline, replacing plagioclase. The proportion of orthoclase, nepheline and ferrohastingsite increases in the innermost zones. Sodalite and analcite occur in accessory amounts. The replacement of augite shows the following sequence: augite, sodic augite, magnesiohastingsite, fermaghastingsite, ferrohastingsite.

Composition and Temperature of Fenitising Fluids

Precise temperature, pressure and composition of fenitising fluids are not well understood, but from available data (Woolley et al. 1972; Ferguson et al. 1975; Siemiatkowska and Martin 1975; McKie 1966; Verwoerd 1966; Le Bas 1977; Prins 1981 and others), it can be surmised that the composition of the fenitising fluids ranges from Na + K + CO_2-rich (carbonatitic magmas) to saline brines enriched in Na and/or CO_2. Temperatures of the fluids, based on mineral equilibria, range from 450 °C up to 700 °C (alkaline magmas) with pressure from a few hundred bars up to 5kbar. For the Kalkfeld complex in Namibia, a temperature of under 500 °C is envisaged based on the stability of K-feldspar and aegirine, whereas for the remobilised metasomatic dyke, containing maximum ordered feldspars, a temperature of up to 700 °C is postulated. A lower limit of 200 °C is suggested by the presence of hydrated Fe- and F-bearing minerals.

Data from Prins (1981) and McKie (1966) on the Damaran alkaline-carbonatite complexes reveal that the fenitising fluids have the following characteristics: (1) they

are oversaturated in Si relative to wall-rock sediments, but undersaturated with respect to granitic wall rocks; (2) they are oversaturated in K, Al, CO_2 during the K-dominated stages; (3) they are enriched in Fe, Na, Mg, P; (4) they are undersaturated in Ca; and finally (5) they are generally oxidising in nature (both K- and Na-dominated fenites).

8.4 Mineralisation Related to Alkali Metasomatism

Unusual concentrations of F, P, REE, Zr, Ba, Nb, Th, U, Sn, Ta and W may be present in rocks that have undergone alkali metasomatism in anorogenic ring complexes. These elements may form their own minerals, or they may enter the lattice of rock-forming minerals – such as tri-octahedral micas – that have crystallised in the subsolidus range of temperature and pressure. The processes that lead to the concentration of these elements are therefore linked with the action of the residual alkali-rich fluids. Their concentration either in rock-forming minerals, or in their own mineral species, is largely dependent on the original magma composition and the nature of the source rocks that have melted to produce the given magma. A review of the geochemistry and mineralisation of alkaline ring complexes can be found in a paper by Bowden (1985).

Ring complexes of the ijolite-carbonatite association (Fig. 8.5A) may contain economic concentrations of Nb, P, F, Ba, REE and U. Good examples of this type are the carbonatite complexes in the Transvaal (South Africa) (Crocker et al. 1988), those of the Kola peninsula (USSR), Jacupiranga in Brazil, the numerous carbonatite bodies in Ontario and Quebec (Canada) and the REE orebodies of Mountain Pass in California (Hutchison 1983).

Granitic rocks, in ring complexes of the alkaline granite association (Fig. 8.5B), may contain workable concentrations of pyrochlore, columbite, cassiterite, monazite, zircon, xenotime, fluorite and REE. Pyrochlore preferentially occurs in sodic-metasomatised peralkaline granites, whereas columbite occurs in zinwaldite-albite-rich granites. The anorogenic Brandberg Granite Complex in Namibia (Diehl 1989) for example, is enriched in pyrcchlore in some of its marginal phases (aegirine-granite). Some of the characteristic useful minerals usually associated with alkali (albite-rich) granitic rocks are given in Table 8.1.

The anorogenic biotite granites associated with Sn ± Nb ± Ta ± W have a peralkaline chemistry, are commonly of Late Proterozoic age, and are characterised by high $^{87}Sr/^{86}Sr$ initial ratios (0.718 to 0.722, Hutchison 1983; Pirajno unpubl. data). This mineralisation is well known in the Rondonia province (Brazil), in Niger-Nigeria, in the Arabian-Nubian shield and in west-central Namibia. In all cases the mineralisation appears to be related to the late phases of magmatic differentiation and the development of alkaline-rich fluids, particularly Na. Effects of albitisation can be observed at all scales, from fracture-controlled to pervasive. Albitisation processes are usually followed by, or are nearly contemporaneous with, progressively increasing stages of H^+ metasomatism (greisenisation, see Chap. 9). A marked separation between albitisation and subsequent greisenisation is often difficult to

gauge, and hence the exact association of the mineralising fluids with one or other of the alteration phenomena not always clear-cut. In broad terms it is reasonable to say that the type of mineralisation discussed here begins to take place during the post-magmatic albitisation process, and continues through, and is enhanced during, stages in which there are increasing effects from the H^- metasomatic processes. The origin of the metals is most probably related to the source regions of the magmas. The high Sr initial ratios of the host granitic rocks suggest a crustal source. Field relationships with older stanniferous pegmatites in Namibia, Nigeria and elsewhere (see later), indicate that this crustal source may have been already enriched in these metals.

8.4.1 Mineralisation in Ring Complexes of the Ijolite-Carbonatite Association

Undersaturated alkaline ring complexes are often associated with a core of carbonatite rocks. These peculiar rocks consist largely of carbonates. At least four types are recognised (Le Bas 1977): (1) calcite-carbonatite (coarse-grained varieties are known as sovites); (2) dolomite-carbonatite or berfosite; (3) ferrocarbonatite (ankerite-rich); (4) natrocarbonatite (mainly Na-Ca-K carbonates). Carbonatites usually occur as small plug-like bodies, or as dykes, veins, cone sheets and lavas. That they are of igneous origin is without doubt because they have been observed to occur as lava flows (eruptions of Oldoinyo Lengai in Tanzania). Bowden (pers. comm. 1988) reports that some carbonatites are not entirely magmatic, but may show metasomatic replacement features. In general, carbonatite complexes show a sequence of nephelinite through ijolite to carbonatite (see Fig. 8.5A). The parental carbonatite magma is thought to exsolve out of a phonolitic-nephelinitic melt by liquid immiscibility (Bowden 1985). Alkali metasomatism is therefore instrumental in the production of carbonatites and their contained mineralisation. This mineralisation, however, usually evolves into epithermal systems during the late stages of the magmatic activity. Thus, processes of alkali metasomatism are followed in a continuously evolving system by hydrothermal activity with the development of low-temperature (epithermal) aqueous fluids producing vein-type mineralisation along fractures.

   Mineralisation in carbonatite complexes (see Bowden 1985 for a review) include Ti (perovskite, ilmenite), Zr (zircon), Ba (barite), F (fluorite), P (apatite), Th and U (e.g. uranothorianite). They can also be an important source of Al (nepheline-rich rocks) and, less commonly, Cu, Pb, Zn, Mo and Cu. Carbonatites are also enriched in LREE (light rare earth minerals). There are, according to Bowden (1985), two main associations: apatite-magnetite usually related to sovites and also containing pyrochlore, and REE association with late-stage enrichments of barite, usually found in ankeritic rocks, without magnetite and pyrochlore. Some good examples of carbonatite complex-related mineralisation can be found in South Africa and are briefly reviewed below.
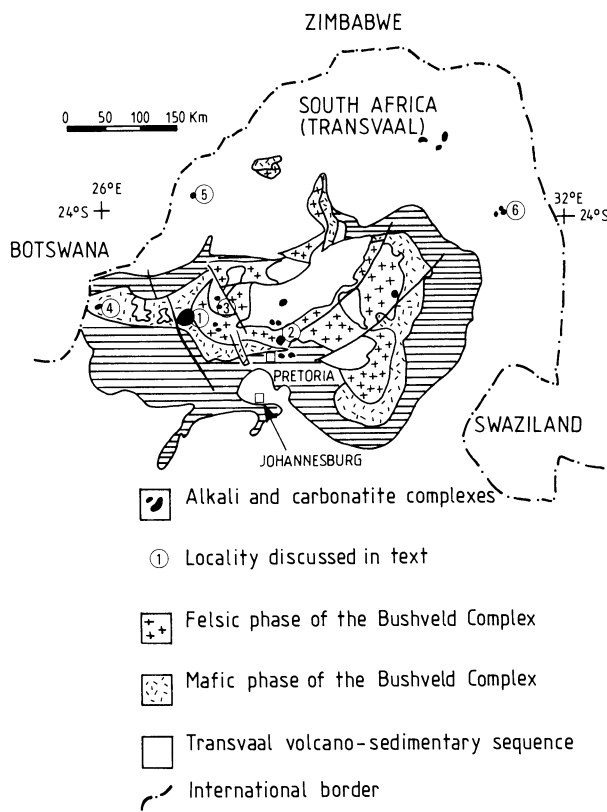
Fig. 8.9. Distribution of ring complexes in the Bushveld province, Transvaal (South Africa). Localities as discussed in the text are as follows: *1* Pilanesberg; *2* Pienaars Rivier; *3* Kruidfontein; *4* Goudini; *5* Glenover; *6* Palabora (After Crocker et al. 1988)

The Bushveld Province, Transvaal (South Africa)

A number of undersaturated, alkali and carbonatite complexes of Mid Proterozoic age (about 1.4 Ga) intrude rocks of the Transvaal basin and Bushveld Igneous Complex (Fig. 8.9). These complexes are concentrated in the central and western areas of the Bushveld Complex-Transvaal basin and their emplacement may have been controlled by a number of northwest-, northeast- and north-northeast-trending, intersecting lineaments or fracture zones. Crocker et al. (1988) published a review dealing specifically with the fluorite resources of the complexes, but also providing the only comprehensive treatise on the allied mineral commodities. It is from their work that most of the information given below is taken. These authors distinguish mineral deposits in alkali complexes (Pilanesberg, Pienaars), and those occurring in carbonatites (Kruidfontein, Goudini and Glenover). In terms of ore type they distinguish the following associations: (1) fluorite-apatite ores of the magmatic-pegmatitic stage; (2) fluorite-apatite-carbonate ores transitional between the magmatic and hydrothermal stages; (3) fluorite-carbonate, fluorite-barite and monomineralic fluorite of hydrothermal vein type. The first and in part, second associations are essentially related to alkali metasomatism and are hence dealt with in this section. The third type of ore association is clearly related to late epithermal

activity that resulted in the development of hydrothermal convection cells and the deposition of quartz vein material, with open space fillings of barite, fluorite and sulphide mineralisation. No apatite is present in this type of mineralisation. It is, incidentally, of interest to note that some of these deposits are at the time of writing being investigated for possible epithermal-type Au mineralisation. The Pilanesberg Complex, which intrudes the western lobe of the Bushveld Igneous Complex, consists of a central zone of white and red foyaite, surrounded by concentric zones of lavas and pyroclastics, followed by a ring of red syenite. Within the Complex there are more than a dozen mineral occurrences, one of which is the Whydhoek deposit containing fluorite and apatite. This mineralisation is associated with coarse-grained (pegmatitic) K-feldspar and aegirine, and is contained in a cylindrical zone developed at the contact between pyroclastics and the red foyaite. In one place the ore is distinctly zoned with an inner fluorite-apatite-aegirine assemblage and an outer pegmatitic apatite-aegirine assemblage. The ore is composed of approximately 40–60% fluorite and 20–30% apatite, with traces of sulphides. In other places fluorite can be seen to occur as an interstitial constituent between the laths of orthoclase in coarse-grained foyaite. Based on textural evidence, Crocker et al. (1988) consider that the fluorite may have crystallised from a low-temperature magmatic melt. Mineralisation of the fluorite-apatite-carbonate association is present at a number of localities. This mineralisation is characterised by lenses, stringers, veinlets and breccia dykes (or tuffisites, thought to be the result of gas streaming). Carbonate minerals are dolomite and calcite.

The Pilanesberg Complex also contains REE mineralisation in the form of the primary mineral britholite. This mineralisation occurs in veins along the contact between a tinguaite ring dyke and a foyaite. The latter also contains disseminated ore. Analysis of concentrates gave 1.56% ThO_2, 0.02% U_3O_8, and 58% of REE oxides (mainly Ce, La, Nd and Pr) (Coetzee 1976).

The Pienaars River Complex is formed by trachytic rocks, various pyroclastic units, syenites, foyaites, phonolites and some minor carbonatite. These rocks are subdivided into three suites, namely: Roodeplaat, Leeuwfontein and Franspoort. Several mineral occurrences are present mostly within the trachytic rocks. At one locality (Wallmannsthal) the mineralisation consists of intergrown fluorite and apatite with minor disseminated pyrite and chalcopyrite; at another, lenses of fluorite-apatite mineralisation are present (Zeekoegat). They are associated with an intrusive foyaite plug emplaced into a quartzite, which as a result was brecciated and alkali-metasomatised with development of orthoclase laths. The fluorite-apatite mineralisation occurs as interstitial grains and clusters up to a few centimetres in size, within the foyaitic rock, which is composed of orthoclase and nepheline set in a matrix of feldspars and amphiboles. In the quartzite rock the fluorite-apatite occurs along the edges of the brecciated fragments.

The Kruidfontein Carbonatite Complex was intruded into dolomitic rocks of the Transvaal sequence. It is a ring structure consisting of an outer zone made up of trachytic, rhyolitic, basaltic and pyroclastic rocks, and an inner zone made up of massive metaberfosite surrounded by a ring of "bedded" metaberfosite and sovite bodies. Crocker et al. (1988) interpret the inner carbonatitic rocks as having originated by metasomatic replacement of pre-existing rocks (mainly pyroclastics),

by ankerite, calcite, K-feldspar and chlorite. Accessory minerals include fluorite, apatite, anatase and magnetite. More recently, however, field and petrological work (Pirajno unpubl. data) indicate that the "bedded" inner carbonatitic rocks are pyroclastic products (air fall tuff and ashflow tuff) of carbonatite volcanism. K-metasomatism is conspicuous in the Kruidfontein Complex. This metasomatism is thought to have been induced by the intrusion of sovite and berfosite plugs and dykes. A ring dyke of reddish-brown, predominantly microclinite, rock is probably the result of the metasomatic replacement of silicate rocks, whose original nature was totally obliterated. At least three types of fluorite mineralisation can be distinguished: (1) primary fluorite, forming disseminated grains in the sovite rocks, and reaching average grades of about 20% CaF_2; (2) secondary fluorite mineralisation is present as replacement bodies in the metaberfosite rocks, where it may reach concentrations of up to 60% CaF_2; and (3) quartz-fluorite veins and fissure fillings. It is of interest to note that, at the time of writing, exploration work by a mining concern has revealed the presence of significant Au values within Fe- and Mn-rich carbonatite vent breccias, debris flow deposits and the K-metasomatised ring dyke material. Submicroscopic Au grains, from 1 to 8 μ in size, occur included in barite, Fe oxides, fluorite and Y-bearing minerals (E. Winter and C. J. van Wyk pers. comm. 1990).

Two other carbonatite complexes studied by Crocker and coworkers are the Goudini Volcano and the Glenover carbonatite complex. In both these complexes metaberfosite rocks are present as a result of strong carbonatitic and alkali metasomatism. In the Goudini volcano metaberfosite contains albite, ankerite and aegirine with subordinate apatite and pyrite. The Glenover complex has apatite-bearing biotite-pyroxenite as well as berfosite-containing fluorite, barite, ankerite, dolomite, calcite, hematite and pyrite. In one area of the Glenover complex within the alkali-metasomatic zone are dykes of fluidised material containing fluorite, apatite and ferric hydrates. This fluidisation is thought to have occurred as a result of degassing along fissures from the underlying magma.

The Palabora Complex (Northeastern Transvaal)

The Palabora Complex (Palabora Intrusive Suite, Frick 1975; Tankard et al. 1982), in northeastern Transvaal, South Africa, was emplaced about 2.1 Ga ago into a basement of Archean gneisses. The Complex is unusual in that its carbonatite member hosts economically viable Cu mineralisation with U and Hf being recovered as by-products. Phosphate is also extracted from apatite disseminations within the pyroxenite members. A simplified geological map of the Complex is shown in Fig. 8.10. Covering an area of about 6 × 2.5 km, it is essentially formed by phlogopite-bearing pyroxenites, pegmatoids and a central carbonatite complex, which includes a core of a rock known as "foscorite" and composed of serpentinised olivine, magnetite, apatite and minor phlogopite. Smaller intrusions of syenitic rocks occur throughout the Complex (Frick 1975). It is not clear whether these potassic rocks were formed through the action of late magmatic fluids or whether they are the products of magmatic differentiation. Frick (1975) believes that the syenitic rocks were formed by differentiation via a trachytic lineage, and also that
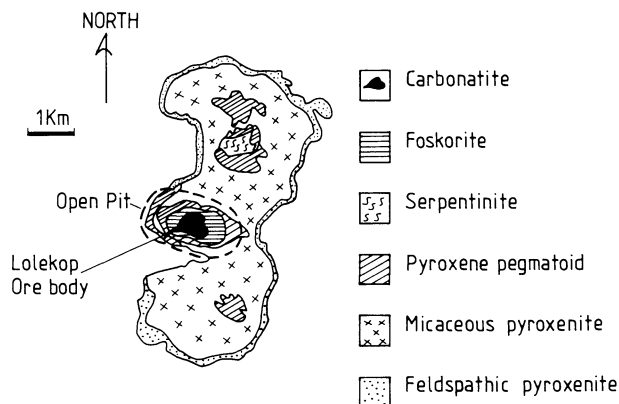
Fig. 8.10. Generalised geological map of the Palabora complex (Palabora Mining Company, 1986)

the carbonatite, was formed by a process of liquid immiscibility from a fractionating magma (Frick 1975).

The Palabora mineralisation consists of Cu with minor magnetite urano-thorianite and baddelyite (ZrO_2) with traces of Hf, all of which are extracted from the central Lolekop carbonatite complex. Apatite and vermiculite are also mined. The Cu mineralisation occurs disseminated within the foscorite, which forms the dyke-like core of the carbonatite. Copper mineralisation is represented by chalcopyrite and bornite, with minor cubanite, pyrrhotite and other sulphides of Cu, Pb, Co and Zn. Vallereite is also present as a late stage phase, mainly along shear zones cross-cutting the ore body. Apatite occurs within the phlogopite-bearing pyroxenite, while magnetite forms up to 50% of the foscorite and is invariably titaniferous, and zoned around the Cu mineralisation.

Other Carbonatite-Related Deposits

Notable alkali metasomatism and carbonatite-related deposits containing apatite, fluorite, pyrochlore, baddelyite, bastnaesite and barite include: the Khibina ring complex in the Kola peninsula (USSR) (Gerasimovsky et al. 1974); Jacupiranga in Brazil, where apatite ore was concentrated by weathering processes; and one of the largest known repositories of REE in the world – that of the Sulphide Queen carbonate body in the Mountain Pass district in California (USA) (Olson et al. 1954), which contains 31×10^6 tonnes of 8.86% rare earth oxides (REO) (Mariano 1989). Other places where this type of mineralisation may also be found are in the Canadian shield, where some 50 carbonatite complexes contain large reserves of Nb (pyrochlore) (see Hutchison 1983 for a brief review). In Inner Mongolia (China) the Bayan Obo deposit is reported to be the largest in the world with reserves of approximately 37×10^6 tonnes of REO (Mariano 1989).

8.4.2 Mineralisation in Ring Complexes of the Alkaline Granite Association

The mineralisation discussed in this section is genetically related to phases of alkali and H^+ metasomatism (greisenisation) in granitic rocks that are part of, and intrude into, ring complexes. These are a class of complexes characterised by rocks of alkaline and felsic compositions. The granitic rocks are generally of A-type affinity, i.e., they are anorogenic, anhydrous and alkaline (Collins et al. 1982). They can also be peraluminous. Ring complexes characteristically occur in continental rift settings. As for the carbonatite complexes, at least two styles of mineralisation can be distinguished in the complexes of the alkaline granite association, namely: pegmatitic pods and disseminations of cassiterite with columbite-tantalite. This mineralisation appears to be entirely connected with post-magmatic activity, in the subsolidus range of pressure and temperature, following the consolidation of nearly all of the magmatic mass (Pollard and Taylor 1986). The temperatures involved in these post-magmatic processes range from 500 to 700°C. The fluids are saline with about 15 wt.% NaCl equivalent, and contain Na, K, Ca and Cl. The mineralising system, however, at some stage may open to the outside, e.g. through fracturing of the roof rocks, evolving further by increasing H^+ metasomatism and input of meteoric waters. Thus, through intermediate stages of H^+ metasomatism (greisen), the mineralising system may reach phases of hydrothermal activity with deposition of fracture-controlled vein quartz and sulphides.

P. Bowden and J. Kinnaird of the University of St. Andrews (Scotland) have carried out detailed investigations on the nature of the fluids of magmatic-hydrothermal systems. They studied in detail the anorogenic ring complexes of Nigeria and their related mineral deposits. The results of their work can be found in Bowden and Kinnaird (1984a, b), Bowden et al. (1984), Bowden (1985), Kinnaird and Bowden (1987). These publications constitute the basis of the information given below on the geology and alkali metasomatism-related mineralisation of the Nigerian province.

Mineralisation of Alkali Metasomatic Origin in the Nigerian Ring Complexes

Alkaline anorogenic magmatism took place between the Ordovician (ca. 430 Ma) and the Jurassic (ca. 110 Ma) in Nigeria (Jos Plateau) and Niger (Air), forming a large magmatic province some 1600 km long and 200 km wide. The age range and progressive younging from north to south are taken to indicate the drift of the African plate over a sublithospheric magmatic plume or hot spot. The emplacement of the complexes was probably controlled by a series of rifts and fractures along northerly and northeasterly trends. Tertiary and Recent volcanic activity is present along a northeasterly trend between the island of Sao Tome' and the Cameroun (Fig. 8.11).

There are more than 50 ring complexes in Nigeria, which vary in size from 2 to 25 km in diameter, are of Jurassic age and were intruded into a basement formed by metamorphic rocks, calc-alkaline and subalkaline granitic rocks and pegmatites (Older Granites) of Pan-African age (900 to 450 Ma). The ring complexes represent the roots of volcanic centres, and consist of mafic to felsic lavas and pyroclastic
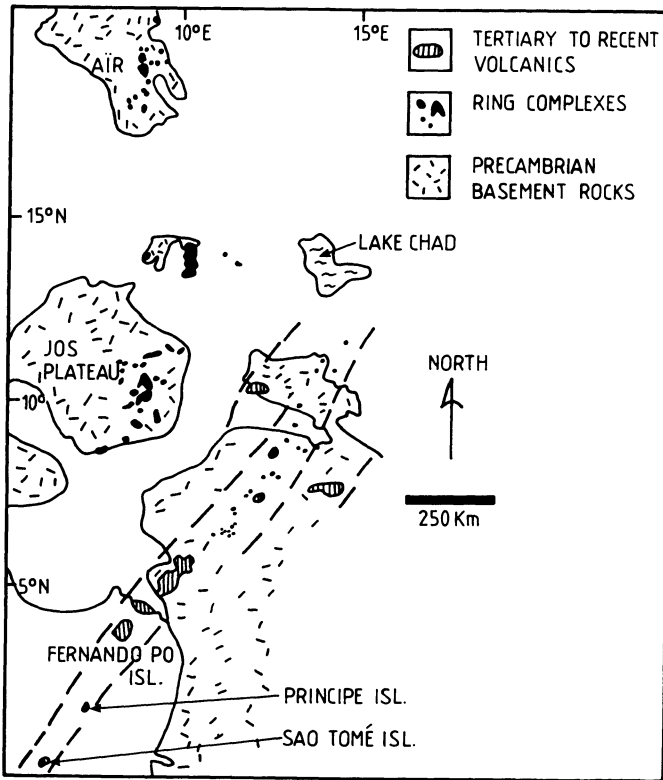
Fig. 8.11. Distribution of alkaline ring complexes in West Africa; Air (Niger) and Nigeria (Jos plateau) provinces of Paleozoic and Mesozoic ages respectively, and the Tertiary to Recent north-east-trending Cameroon line (see also Fig. 8.6). After Hughes 1982; Bowden and Turner 1974)

rocks, the latter being mostly rhyolites and ignimbrites. Rocks of the volcanic pile were intruded by cogenetic, subvolcanic rocks including volcanic feeders (generally quartz-porphyries), cone sheets and ring dykes (rhyolites, porphyries and micro-granites), and granitic rocks (Younger Granites). Discordant high-level granite intrusions were emplaced by stoping through the collapse of a central block, which formed a caldera structure. Younger Granite intrusions appear either as circular stocks, ring dykes or as horizontal sheeted structures, depending on the level of erosion (Jacobson et al. 1958). The granitic rock suite includes about 5% intermediate to basic rocks, which usually form small intrusions ranging in composition from olivine-gabbro to quartz-syenite. At least three granite types have been recognised by Bowden and Kinnaird, namely: (1) peralkaline granite and related syenites, with alkali or calcic amphiboles; (2) peraluminous biotite-alkali feldspar granites and biotite syenogranites; (3) metaluminous fayalite and horn-blende-bearing granitic rocks. A distinct feature of the Younger Granites is their lack of tourmaline. The work of Kinnaird has shown that late stage, subsolidus and post-magmatic alteration processes consist of alkali metasomatism, represented by

sodic metasomatism in peralkaline and peraluminous granites, whereas potassic metasomatism appears to dominate the late stages of consolidation in the biotite granites. These phases of alkali metasomatism are followed by increasing degrees of acid (H^+) metasomatism, represented by greisenisation, phyllic and even argillic alteration processes. Accordingly, the styles of mineralisation, and the mineral associations related to the metasomatic activity of the Younger Granites in the Nigerian ring complexes, can be subdivided into two distinct groups. One group is essentially and almost exclusively associated with alkali metasomatism, comprising late pegmatitic pods with beryl and topaz, and pervasive disseminations of columbite or pyrochlore with cassiterite. The hydrothermal stages, sensu stricto, involving H^+ metasomatism, are characterised by oxide-sulphide assemblages with cassiterite and wolframite in quartz-vein lodes, greisens, stockwork and replacement bodies. This style of mineralisation is treated in the next chapter.

Potassic metasomatism is most noticeable within pods in the cupola zones of biotite granites. It is characterised by the presence of microcline, red in colour due to the release of Fe from the feldspar lattice. Minor disseminations of cassiterite and wolframite, accompanied by monazite, zircon and rutile, are associated with this alteration process. Pegmatitic pods and vugs, formed by smokey quartz and alkali feldspar, are not particularly important in economic terms. They also appear to be related to K-metasomatism, are usually small in size, and are sporadically developed along the marginal zones of the granites. They may contain gem-quality minerals such as topaz and aquamarine.

Late magmatic to post-magmatic disseminations related to sodic metasomatism are concentrated in the apical regions of peralkaline and peraluminous biotite granites. This process results in the pervasive alteration of K-feldspar to albite, formation of aegirine and riebeckite, and desilication and enrichment in REE with the introduction of Nb-bearing fluids. The pyrochlore-columbite $\pm$ cassiterite association is of substantial economic importance in Nigeria, largely because of the development of eluvial and alluvial deposits formed during the erosional unroofing of the granites. Although pyrochlore and columbite occur together, the former is dominant in peralkaline granites, whereas columbite predominates in peraluminous biotite granites. Pyrochlore mineralisation is characterised by disseminations of honey-coloured, U-rich (up to 5% U_3O_8) pyrochlore octahedra, accompanied by Th-rich monazite, U-Th-Hf-enriched zircons, amblygonite, astrophyllite and cryolite (a fluoride of Na and Al). The columbite-bearing granites are more common than those containing dominant pyrochlore. Cassiterite is also present. In some localities columbite is accompanied by REE and U-enriched thorite, xenotime and monazite, as well as zircon, magnetite and ilmenite. In these granites Na metasomatism is characterised by albitisation leading to an albite-protolithionite rock with a fine-grained sugary texture.

Alkaline Ring Complexes of the Arabian Shield

The Arabian-Nubian Shield (Fig. 8.12) includes those pre-Phanerozoic geological terranes whose formation can be broadly related to the Pan-African tectono-
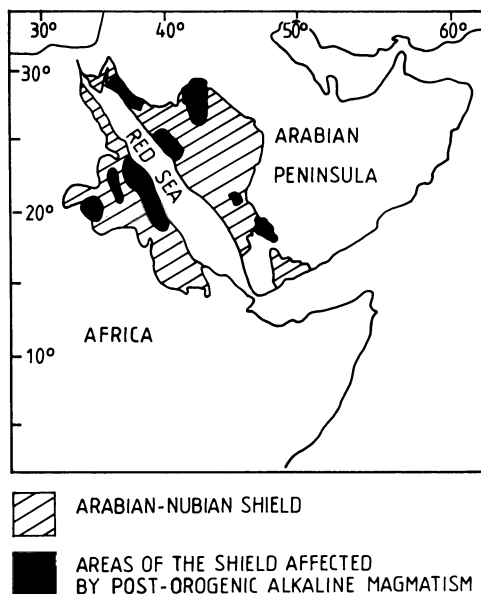
Fig. 8.12. The Arabian-Nubian Shield and approximate distribution of areas of the Shield affected by post-orogenic alkaline magmatism (After Stoeser and Camp 1985; Almond 1979; Vail 1985; Stoeser 1986)

thermal event. A brief review of the geology and mineralisation of the Shield is given in Chapter 7.

There are over 70 intrusions of alkali granites and associated ring complexes in the Arabian Shield, and about 40 in Sudan. The mechanism of emplacement and structure of the ring complexes are similar to those in other parts of the world: building of a central volcanic complex with eruption of initial basic volcanism followed by dominant ignimbrite flows and rhyolitic lavas; and subsequent collapse which forms a caldera with accompanying intrusions of porphyritic ring dykes and stocks of granitic rocks.

In Saudi Arabia, Jackson et al. (1985) recognised the following styles of Nb-Zr-REE mineralisation, all related to phases of alkali metasomatism: (1) disseminations in porphyritic alkali microgranite plutons and stocks; (2) disseminations in aplite-pegmatite sheets in the apical zones and flanks of alkali granite plutons; (3) disseminations in siliceous and pegmatitic pods, as well as veins and breccias in roof zones and wall rocks of the alkali granite plutons. The principal ore minerals are: pyrochlore, columbite-tantalite, monazite, cassiterite, bastnaesite, thorite and zircon. Although to date no major deposits have been identified, five significantly mineralised intrusions have been located in Saudi Arabia, and their grades and tonnages are given in Table 8.2.

8.4.3 Mineralisation Related to Alkali Metasomatism of Pegmatites

In the Damara orogen of west-central Namibia are numerous pegmatites (estimated to number in excess of 2000), some of which are economically important sources of U, Sn, Li, Be, Ta, Cs and Bi (Pirajno and Jacob 1987). The pegmatites of the

Table 8.2. Grades and tonnages of REE mineral deposits in Saudi Arabia (After Drysdall et al. 1984)

Locality	Tonnes	Approximate grades in ppm							
		Nb	Ta	Sn	La	Ce	Y	Th	U
Ghurayyah	440	2.25	212	290	61	144	1.3	399	117
Jabal Tawlah	6.4	3.4	175	381	19	137	5.2	693	8
Umm al Birak	6.6	1.7	121	84	371	800	311	46	28
Jabal Said	23	1.3	82	199	587	1.3	4.2	834	134
Jabal Hamra	18	1.7	146	194	2.6	3.4	1.6	263	75

Damara orogen form a huge field occupying most of the Central Zone and parts of the Northern Zone (refer to Chap. 7 and Fig. 7.4). The uraniferous alaskites are located in that part of the Central Zone where high temperatures of metamorphism were attained, and are thought to have been generated by anatexis of pre-Damara basement gneisses and/or Nosib Group rocks (Jacob 1978). Three major zones of pegmatites are recognised. A northern zone, comprising the northeast-trending Uis-Strathmore belt containing mostly unzoned pegmatites; a central zone, containing the east-west-trending Neneis-Kohero belt of unzoned pegmatites; and a southern zone, formed by the Karibib-Erongo zoned pegmatites. Tin and tantalum mineralisation in the pegmatites of all belts is closely related, spatially and genetically, to albitisation and greisenisation (muscovite + quartz). In almost all cases it can be shown that this predominantly sodic metasomatism is cross-cutting and later than the emplacement of the pegmatites.

The Uis Stanniferous Pegmatite Field

In the northern zone of pegmatites the stanniferous unzoned pegmatites around Uis constitute an important source of Sn and Ta. These pegmatites are part of the northeast-trending Uis-Strathmore belt, which appears to be located in a regional graben structure, marked by a prominent geomagnetic signature, forming the Uis Lineament (Corner 1983). In the Strathmore area (southwest end) the stanniferous pegmatites are enriched in Li and Ta. This regional zonation is attributed to increasing metamorphic grades and depth of emplacement (Sheeran 1984).

The Uis tin mine exploits some of the largest pegmatites in the area with total reserves in excess of 100 million tonnes at grades of about 0.15% Sn, with Ta being recovered as a by-product. The pegmatites are hosted in metasediments of the Kuiseb Formation. The host rocks contain up to 60% tourmaline in the vicinity of the pegmatites, which because of the transgressive nature of the tourmaline disseminations, may be representative of an alteration feature due to intense boron metasomatism (Fig. 8.13). Tourmalinisation is noted up to 200 m away from the pegmatites. Alteration of the wall rocks is not conspicuous, except for the presence of muscovite porphyroblasts in the areas of contact with the albitised and greisenised portions of the pegmatites. Another important feature of the pelitic

SPOTTED SCHIST
SCHIST
QUARTZITE,
CALC-SILICATES

PEGMATITE
ZONE OF TOURMALINISATION
GREISEN
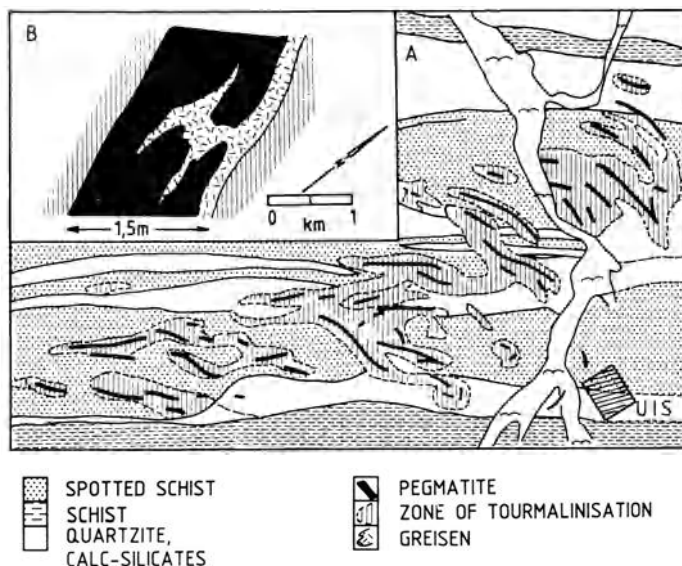
Fig. 8.13A, B. Sketch geological map of the area around Uis (Namibia), showing: **A** distribution of stanniferous pegmatites and associated tourmaline alteration haloes; **B** Inset shows cross-cutting Sn-bearing greisen alteration in pegmatite (After Pirajno and Jacob 1987)

schist in the Uis area is the abundance of "nodules" or "spots". Indeed, this association is a constant feature not only at Uis but also in the other areas (Neneis-Kohero and Karibib-Erongo pegmatites). The zones of spotted schist clearly represent the effects of thermal metamorphism. In thin-section the nodules and spots, which lie haphazardly in a given foliation plane, consist of biotite, quartz, muscovite or sericite, and chlorite. In some cases a core containing cordierite can be discerned. The Uis pegmatites are unzoned and syn to post-tectonic. Although unzoned, the pegmatites may have quartz-enriched cores. Varying in length from 50 to 1500 m with widths of between 1 and 130 m, they are lenticular, linear or sigmoidal in shape. The pegmatites consist of albite, microcline, quartz and muscovite. Other minerals are topaz, garnet, tourmaline, apatite, amblygonite, beryl, tantalite, columbite, cryptomelane, psilomelane, rutile, sphene, lepidolite, calcite, pyrite, chalcopyrite, and of course cassiterite. Cassiterite is abundant in the albitised and greisenised portions of the pegmatites. Albitisation is characteristically pervasive, giving the rock a sugary and fine-grained texture. The greisen material consists of a quart-muscovite assemblage with minor albite. Cassiterite is erraticaly distributed, black in colour with individual crystals varying in size from 1 to 50 mm.

Karibib-Erongo Pegmatite Field

The Karibib-Erongo pegmatites intrude metasediments and granitoids of the Damara orogen, and occupy areas around the Omaruru Lineament and the Erongo

Volcanic Complex (Pirajno and Jacob 1987). These pegmatites are usually well zoned with a quartz core and muscovite-feldspar margins. Mineralisation associated with these pegmatites consists of Li, Be, Cs and Nb-Ta-bearing minerals. They become stanniferous in a restricted zone that is almost coincident with the Omaruru Lineament, whereas others are in close spatial association with the Erongo Volcanic Complex, a ring complex of Mesozoic age (Pirajno 1990). The Brabant pegmatites are intruded into an inlier of Damara granite within the Erongo Complex, with a length of about 500 m and width of between 10 and 20 metres. Zoning is asymmetrical and, from the quartz core outwards, consist of feldspar + quartz + muscovite + tourmaline on the hangingwall side, and zinnwaldite + tourmaline + muscovite on the footwall side. Economic minerals, which include tantalite, cassiterite, zinnwaldite and fluoroapatite, are all associated with cross-cutting bands and patches of albitisation and greisen material. The latter consist of quartz-muscovite-blue tourmaline-fluoroapatite aggregates.

References

Almond D C (1979) Younger granite complexes of Sudan. In: Al-Shanti Ahmad M S (ed) Evolution and mineralisation of the Arabian-Nubian Shield, vol 1. I A G Bull 3. Pergamon, Oxford, pp 151–164

Babcock R S (1973) Computational models of metasomatic processes. Lithos 6:270–290

Bailey D K (1978) Mantle metasomatism, continuing chemical changes within the Earth. Nature (London) 296:525–530

Best M G (1982) Igneous and metamorphic petrology. Freeman, New York, San Francisco, 630 pp

Beus A A, Zalashkova N Y E (1964) Post-magmatic high temperature metasomatic processes in granitic rocks. Int Geol Rev 6:668–681

Black R, Bowden P (eds) (1985) Alkaline ring complexes in Africa. J Afr Earth Sci Spec Iss 3, 1–2

Black R, Lameyre J, Bonin B (1985) The structural setting of alkaline complexes. J Afr Earth Sci 3:5–16

Bonin B (1986) Ring complex granites and anorogenic magmatism. North Oxford Academic, London, 187 pp

Bowden P (1985) The geochemistry and mineralization of alkaline ring complexes in Africa (a review). J Afr Earth Sci 3:17–40

Bowden P, Turner D C (1974) Peralkaline and associated ring-complexes in the Nigeria-Niger province, West Africa. In: Sorensen H (ed) The alkaline rocks. John Wiley & Sons, New York, pp 330–351

Bowden P, Kinnaird A J (1984 b) Petrological and geochemical criteria for the identification of (potential) ore-bearing Nigerian granitoids, vol 9. Proc 27th Int Geol Congr Moscow. VNU Sci Press, Utrecht, pp 85–119

Bowden P, Kinnaird A J (1984 b) The petrology and geochemistry of alkaline granites from Nigeria. Phys Earth Planet Interiors 35: 198–211

Bowden P, Kinnaird, J A, Abaa S I, Ike E C, Turaki U M (1984) Geology and mineralization of the Nigerian anorogenic ring complexes. Geol Jahrb B 56:1–65

Brogger W C (1921) Die Eruptivgesteine des Kristianiagebiets IV. Das Fengebiet in Telemarken, Norwegen. Nors Vidensk Akad Oslo Skr Nat Kl 9:408

Burnham C W (1979) Magmas and hydrothermal fluids. In: Barnes H L (ed) Geochemistry of hydrothermal ore deposits, 2nd edn. John Wiley & Sons, New York, pp 71–136

Carmichael I S, Turner F J, Verhoogen J (1974) Igneous petrology. McGraw-Hill, New York, 739 pp

Chappel B W, White A J R (1974) Two contrasting granite types. Pac Geol 8:173–174

Coetzee C B (1976) Rare earths. In: Coetzee C B (ed) Mineral Resources of the Republic of South Africa. Geol Surv Handb 7:199–201

Collins W J, Beams S D, White A J R, Chappell B W (1982) Nature and origin of A-type granites with particular reference to south-eastern Australia. Contrib Mineral Petrol 80:189–200

Corner B (1983) An interpretation of the aeromagnetic data covering the western portion of the Damara Orogen in South West Africa/ Namibia. In: Miller R McG (ed) Evolution of the Damara orogen, South West Africa/Namibia. Geol Soc S Afr Spec Publ 11:339–354

Cox K C, Johnson R L, Monkman L J, Stillman C J, Vail J R, Wood D N (1965) The geology of the Nuanetsi igneous province. Phil Trans R Soc London Ser A 257:71–218

Crocker I T, Martini J E J, Sonhnge A P G (1988) The fluorspar deposits of the Republics of South Africa and Bophuthatswana. Department of Mineral and Energy Affairs. Geol Surv Handb 11: 131 pp

Diehl M 1989 Geology, mineralogy, geochemistry and hydrothermal alteration of the Brandberg alkaline complex, Namibia. Doctor Thesis, Johannes Gutenberg Univ, Mainz, 148 pp

Drysdall A R, Jackson N J, Ramsay C R, Dough C J, Hackett D (1984) Rare element mineralization related to Precambrian alkali granites in the Arabian Shield. Econ Geol 79:1366–1377

Ferguson J, McIver J R, Danchin R V (1975) Fenitization associated with the alkaline carbonatite complex of Epemba, South West Africa. Trans Geol Soc S Afr 78:111–122

Fitton J G, Upton B G J (eds) (1987) Alkaline igneous rocks. Geol Soc Spec Publ 30. Blackwell, Oxford, 568 pp

Frick C (1975) The Phalaborwa syenite intrusion. Trans Geol Soc S Afr 78:201–214

Gerasimovsky V I, Volkov V P, Kogarko L N, Polyakov A I (1974) Kola peninsula In: Sorenson H (ed) The alkaline rocks. John Wiley & Sons, New York, pp 206–221

Gresens R L (1967) Composition-volume relationships of metasomatism. Chem Geol 2:47–65

Haapala I (1986) Origin of albites in mineralised granites. Proceedings of joint meeting of working group Gp2–4. IGCP Proj 220. BMR Rec 1986/10:22–23

Hughes C J (1982) Igneous petrology. Elsevier, Amsterdam, 551 pp

Hutchison C S (1983) Economic deposits and their tectonic settings. MacMillan, New York, 355 pp

Jacob R E (1978) Granite genesis and associated mineralization in parts of the central Damara belt. Geol Soc S Afr Spec Publ 4:417–432

Jackson N J, Drysdall A R, Stoeser D B (1985) Alkali granite related Nb-Zr-REE-U-Th mineralization in the Arabian shield. High heat production (HHP) granites, hydrothermal circulation and ore genesis. Inst Min Metall:479–487

Kinnaird J A (1985) Hydrothermal alteration and mineralization of the alkaline anorogenic ring complexes of Nigeria. J Afr Earth Sci 3:229–252

Kinnaird J A, Bowden P (1987) African anorogenic alkaline magmatism and mineralisation – a discussion with reference to the Niger-Nigerian Province. Geol J Them Iss 22:297–340

Kinnaird J A, Bowden P, Ixer R A, Odling N W A (1985) Mineralogy, geochemistry and mineralization of the Ririway Complex, northern Nigeria. J Afr Earth Sci 3:185–222

Korn H, Martin H (1954) The Messum Igenous Complex in S.W.A. Trans Geol Soc S Afr 57:83–124

Le Bas M J (1977) Carbonatite nepheline volcanism. John Wiley & Sons, New York, 347 pp

Lindgren W (1933) Mineral deposits. McGraw-Hill, New York, 930 pp

Lloyd F E, Bailey D K (1977) Light element metasomatism of the continental mantle: the evidence and the consequences. Phys Chem Earth 9:389–416

Manning D C (1982) An experimental study of the effects of fluorine on the crystallization of granite melts. In: Evans A M (ed) Metallization associated with acid magmatism. John Wiley & Sons, Chichester, pp 191–203

Mariano A N (1989) Economic geology of rare earth elements. In: Lipin B C, McKay C A, (eds) Geochemistry and mineralogy of rare earth elements. Reviews in mineralogy, vol 21. Min Soc Am, pp 309–337

McKie D (1966) Fenitization. In: Tuttle D F, Gittens J (eds) Carbonatites. Wiley Interscience, New York, pp 261–294

Mutschler F E, Griffin M E, Scott Stevens D, Shannon S S (1985) Precious metal deposits related to alkaline rocks in the north American Cordillera – An interpretive view. Trans Geol Soc S Afr 88:355–377

Oftedahl C (1978) Cauldrons of the Permian Oslo rift. J Volc Geotherm Res 3:343–371

Olson J C, Shawe D R, Pray L C, Sharp W N (1954) Rare earth mineral deposits of the Mountain Pass district, Bernardino County, California. U S Geol Surv Prof Paper 261:1–75

Pichavant M (1981) An experimental study of the effect of boron on a water saturated haplogranite at 1kbar vapour pressure. Contrib Mineral Petrol 76:430–439

Pichavant M, Manning D (1984) Petrogenesis of tourmaline granites and topaz granites; the contribution of experimental data. Phys Earth Planet Int 35:31–50

Pirajno F (1990) Geology, geochemistry and mineralisation of the Erongo Volcanic Complex, Namibia. S Afr J Geol 93:485–504

Pirajno F, Jacob R E (1987) Sn-W metallogeny in the Damara orogen, South West Africa/Namibia. S Afr J Geol 90:239–255

Pollard, P J (1983) Magmatic and postmagmatic processes in the formation of rocks associated with rare element deposits. Trans Inst Min Metall 92:B1–B9

Pollard P J, Taylor R G (1986) Progressive evolution of alteration and tin mineralization:controls by interstitial permeability and fracture related tapping of magmatic fluid reservoirs in tin granites. Econ Geol 81:1795–1800

Pollard P J, Pichavant M, Charoy B (1987) Contrasting evolution of fluorine- and boron-rich tin systems. Mineral Depos 22: 315–321

Potgieter J E (1987) Anorogenic alkaline ring-type complexes of the Damaraland province, Namibia, and their economic potential. Msc Thesis, Rhodes Univ, Grahamstown, 150 pp

Prins P (1981) The geochemical evolution of the alkaline and carbonatite complexes of the Damaraland igneous province, South West Africa. Ann Univ Stellenbosch Ser A1 Geol 3:145–278

Ramberg H (1952) The origin of metamorphic and metasomatic rocks. Univ Press, Chicago 317 pp

Shcherba G N (1970) Greisens. Int Geol Rev 12:114–254

Sheeran D (1984) The geology and mineralization of acid pegmatites. MSc Thesis, Rhodes Univ, Grahamstown, 143 pp

Siemiatkowska K M, Martin R F (1975) Fenitization of the Mississagi quartzite, Sudbury area, Ontario. Bull Geol Soc Am 86:1109–1122

Smirnov V I (1976) Geology of mineral deposits. MIR, Moscow 520 pp

Stoeser D B (1986) Distribution and tectonic setting of plutonic rocks of the Arabian Shield. J Afr Earth Sci 4:21–46

Stoeser D B, Camp V E (1985) Pan-African microplate accretion of the Arabian Shield. Bull Geol Soc Am 96:817–826

Strauss C A, Truter F A (1950) The alkali complex at Spitzkop, Sekukuniland, eastern Transvaal. Trans Geol Soc S Afr 53:81–125

Tankard A J, Jackson M P A, Eriksson K A, Hobday D K, Hunter D R, Minter W E L (1982) Crustal evolution of Southern Africa – 3.8 billion years of earth history. Springer,Berlin, Heidelberg, 523 pp

Tuttle D F, Gittens J (eds) (1966) Carbonatites. Wiley Interscience, New York, 591 pp

Vail, J R (1985) Pan-African (Late Precambrian) tectonic terranes and the reconstruction of the Arabian-Nubian shield. Geology 13:839–842

Verwoerd W J (1966) Fenitization of basic igneous rocks. In: Tuttle D F, Gittens J (eds) Carbonatites. Wiley Interscience, New York, pp 295–308

Woolley A F, Symes R F, Elliot C J (1972) Metasomatised (fenitized) quartzites from the Barralam Complex, Scotland. Mineral Mag 38:819–836

Chapter 9
Greisen Systems

9.1 Introduction

The term greisen refers to an assemblage of quartz + muscovite, accompanied by varying amounts of other distinctive minerals such as fluorite, topaz and tourmaline. Greisenisation is defined by Shcherba (1970) as the high temperature, post-magmatic alteration of rocks by volatile-rich solutions associated with the cooling of granitic intrusives. Burt (1981, p. 832) defines greisenisation as a "hydrothermally altered granitic rock consisting of a mixture of quartz and mica (normally lithian), with variable topaz, tourmaline, fluorite or other F- or B-rich minerals". More specifically, Burt (1981) distinguishes "quartz-topaz, quartz-muscovite or mica-fluorite greisen", defined in terms of the activities of HF and alkalies in alumino-silicate systems.

Greisen systems result from complex, and as yet not completely understood, late- to post-magmatic metasomatic processes that affect and take place within a nearly consolidated granitic body and the adjacent country rocks. These processes involve the concentration of volatile components such as F, B, Li, and the progressive concentration and activity of Na^+, K^+ and H^+ ions in a cooling granite body. Greisen systems are normally associated with Sn, W, Mo, Be, Bi, Li and F mineralisation.

Greisenisation is typically associated with highly fractionated magmas that have intruded into crustal depths ranging from 3 to 5 km, and takes place in the apical portions of granitic intrusive bodies (cupolas), emanating from deep-seated granite batholiths. The highly evolved granitic melts that promote the development of greisenisation phenomena and associated mineralisation are strongly enriched in volatile components, Cl, B, F, and metallic elements, such as Sn, W, Mo, Bi, U, Be. The consolidated enriched products of these magmas are said to be "geochemically specialised". The cause of this specialisation or enrichment is a topic of much debate, with two main schools of thought contending processes of fractional crystallisation versus "geochemical heritage". Magmatic differentiation and fractional crystallisation have been advocated by Lehmann (1982) and Groves and McCarthy (1978). The idea put forward by this school is that in situ fractionation is largely responsible for the significant concentrations of volatiles and trace elements in the residual liquids. These would then accumulate into sheet-like zones in the roof of the fractionating granitic mass. The other school is advocated by Taylor, Pollard and coworkers of James Cook University in Queensland (Australia) (Pollard et al. 1983, see also Eugster 1984). These authors envisage geochemical heritage as the
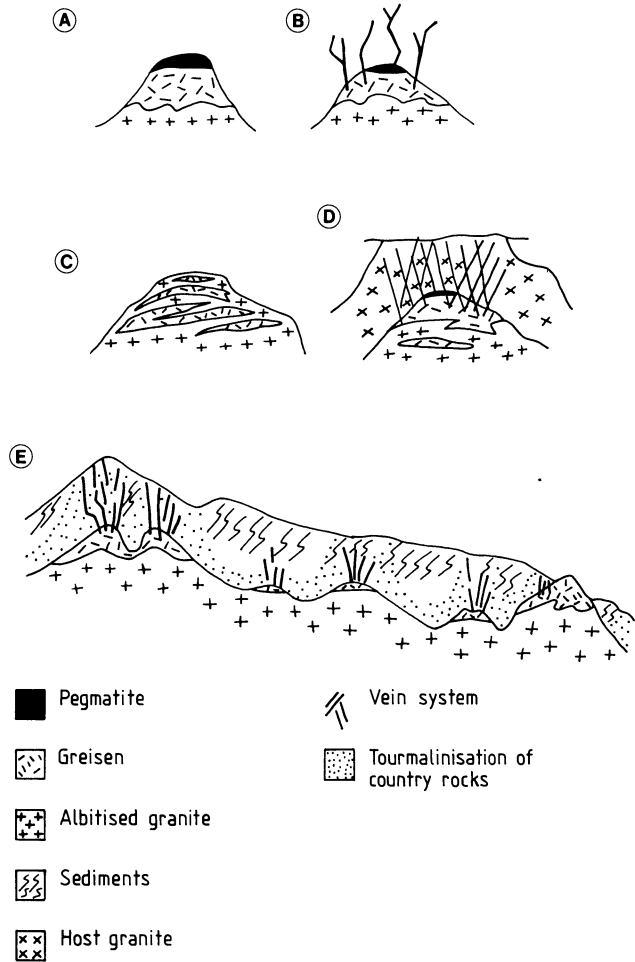
Fig. 9.1A–E. Structural and morphological types of greisen systems. **A, D** and **E** represent end members. (**A** and **B** after Pollard et al. 1988; **C** and **D** after Taylor and Pollard 1999; **E** after Pirajno and Bentley 1985)

main cause of the strong enrichment in volatiles, alkalies and trace elements. Indeed, there are many reasons to believe that the "geochemical specialisation" may have been inherited, or acquired, from the source region where partial melting occurs. In other words, the geochemical heritage is essentially due to the melting of crustal material containing protoliths with unusual contents of Sn, W, U, or, perhaps, containing evaporite sequences enriched in B. It is conceivable that the two theories can be reconciled by postulating that both processes may be operative, i.e. partial melting of enriched crustal material, followed by differentiation and crystal fractionation to further concentrate the volatiles and trace elements in the residual melts.

The morphology of a number of greisen systems is shown in Fig. 9.1. There are two end members: one in which the greisenising fluids are contained within the

granitic cupola (closed system, or endogreisen), and one in which the fluids are channelled along fractures and faults, from within the parent cupola into the country rocks (open system or exogreisens). Transitional situations do exist, and may in fact represent the more common types of greisen systems.

Russian geologists and geochemists have studied greisen rocks in detail, of which good accounts are given by Beus and Zalashkova (1964), Shcherba (1970) and Smirnov (1976). Ivanova (1969) studied the metallic content of greisenised granites and their mineral constituents, while more comprehensive accounts of greisens can be found in Taylor (1979) and Pollard et al. (1988).

In this chapter we examine the main features of greisenisation processes, and the main mineralogical and geochemical attributes of greisen systems. In the final section a number of greisen-related mineral deposits are discussed. These include the deposits formed in F-rich systems in the anorogenic intracontinental setting of the Bushveld Igneous Complex in South Africa, the exogreisen deposits of the Damara Orogen in Namibia, Sn-W deposits in collision-related settings (Panasqueira in Portugal, Southwest England and Cornwall), and the complex endo-and exogreisen systems of Mt. Bischoff in Tasmania.

9.2 Greisenisation Processes

According to Shcherba (1970) the sequence of greisenisation events includes an early alkaline stage, a greisenisation stage and a vein-depositing stage. Smirnov (1976) subdivided the sequence of mineralogical transformations in the endogreisen environment into a progressive stage and a regressive stage, in response to temperature and pH regimes. In endogreisens the earliest stages are typified by alkali metasomatism (Chap. 8), in which albitisation assumes an important role. In general, greisen systems evolve by decreasing alkali/H^+ ratios, resulting in the destabilisation of K-feldspar, plagioclase and micas, and leading to the greisen stage sensu stricto with the replacement of these minerals by quartz and muscovite assemblages (Chap. 4). In some cases muscovite may be very coarse and form thick monomineralic selvages along fractures. Other common mica compositions generated by the greisenising fluids include lithian siderophyllite, protolithionite, zinnwaldite and lepidolite (Kinnaird 1985). Silicification usually takes place during and after greisenisation, and is evidenced by intense quartz flooding and replacements. Muscovite characteristically replaces feldspars and biotite, and the reactions (assuming Al to be immobile) may be written as follows:

$3(KAlSi_3O_8) + 2H^+ = KAl_3(Si_3O_{10})(OH)_2 + 2K^+ + 6SiO_2;$
microcline   muscovite

$3K(Fe,Mg,Ti)_3AlSi_3O_{10}(OH)_2 + 20H^+ = KAl_3Si_3O_{10}(OH)_2 + 2K^+ + 6SiO_2$
microline   muscovite

$\quad + 9(Fe^{2+},Mg^{2+},Ti^{4+}) + 12H_2O;$

$$3KFe_3AlSi_3O_{10}(OH)_2 + 2HCl = KAl_3Si_3O_{10}(OH)_2 + 3Fe_3O_4 + 6SiO_2 + 2KCl + 3H_2.$$
biotite   muscovite
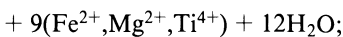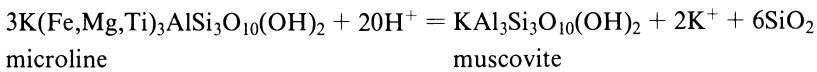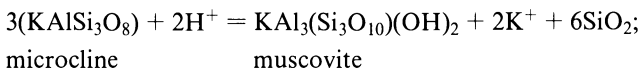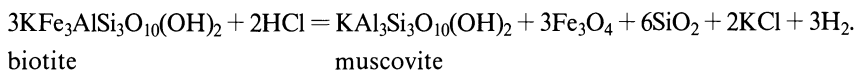
At this point it is pertinent to focus attention on the possible role played by the reactions shown above, in releasing metals into the system. Shcherba (1970), for example, noting that plagioclase and mica are the principal "carriers of rare metals", considered the leaching of the metallic elements from their original sites, in the lattices of these rock-forming minerals, to have occurred during greisenisation processes by virtue of the presence of F and Cl species in the fluids.

Taylor (1979) commented on the Sn content of mineral phases of stanniferous granites (sphene 230–260 ppm, ilmenite 15–80 ppm, biotite 50–500 ppm); whereas, according to Eugster (1984), ilmenites may contain up to 1000 ppm Sn, 100 ppm Mo, 60 ppm W, 1000 ppm Nb, and biotite 1000 ppm Sn, 10 ppm W, 60 ppm Mo, and 100 ppm Nb. Eugster (1984) and Barsukov (1957) asserted that the conversion of biotite to muscovite (see reactions above) is of fundamental importance for the genesis of Sn-W deposits, emphasising the role played by both biotite and muscovite as "excellent hosts" for elements such as Sn, W, Mo etc. The release of these elements from the lattice of micas to form ore minerals is documented by the presence of sulphide and oxide minerals in the cleavage and/or microfractures of the micas in the greisenised granites (Pirajno 1982). Taylor (1979) explains that "a corollary to this concept should be that in the lower zones of Sn-systems the altered rocks should be depleted in Sn values". Indeed this was found to be the case for a greisenised granite in New Zealand (Pirajno 1982).

The structural relationships between the greisenised cupolas and the enclosing country rocks, and their degree of fracturing, determines the type of endo-exogreisen system (Fig. 9.1). Types of greisen alteration within the cupola (endogreisen) and in the country rocks above and around the greisenised granite rocks are shown in Fig. 9.2. A greisenised cupola lodged in a sedimentary sequence containing pelitic and psammatic rocks will form a narrow aureole of contact metamorphism, usually identifiable by the presence of porphyroblastic biotite and, closer to the contacts, cordierite. Spotted schists are a common feature in sedimentary sequences intruded by granitic rocks. Greisenisation overprints the thermal mineral assemblages and is in most cases characterised by the nucleation of muscovite, albite and locally tourmaline. Quartz-sericite, albite and adularia, all of which may occur along fractures, may be associated with quartz vein material containing sulphides and oxides (e.g. pyrite, chalcopyrite, cassiterite, wolframite, scheelite, arsenopyrite, molybdenite etc.). Mineral assemblages generated during greisen alteration of granitic rocks are listed in Table 9.1.

In mafic rocks greisenisation is characterised by the presence of chlorite-talc, phlogopite-actinolite, quartz-plagioclase and quartz-muscovite. Although typical skarns are usually associated with porphyry systems (Chap. 10), some skarns are spatially and genetically associated with greisen-related systems with which all gradations may be observed (Rose and Burt 1979). Greisen alteration of carbonate rocks usually takes place after their skarnification. The greisen solutions are neutralised on contact with the carbonate lithologies, as the anionic species (e.g. F, OH) become fixed by Ca and Al to form fluorite and topaz. An example of
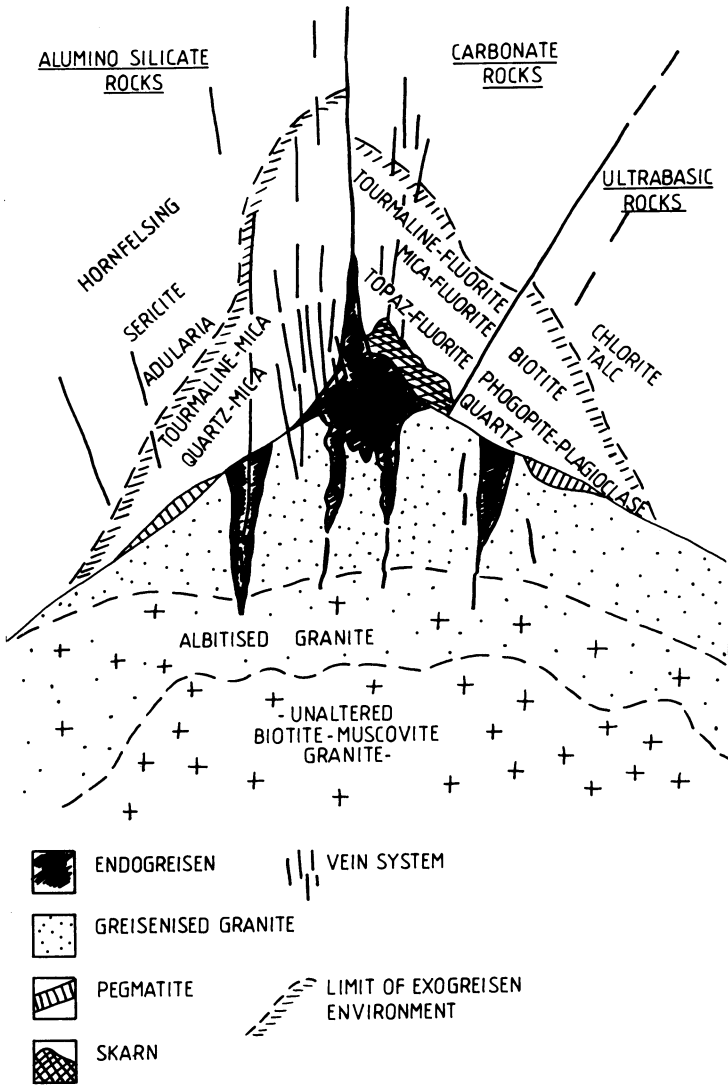
Fig. 9.2. The endo- and exogreisen environments in aluminosilicate, carbonate and ultramafic rocks (After Shcherba 1970)

greisenised carbonate rock (dolomite) is described in a later section which deals with the Mount Bischoff Sn mineralisation. The mineral assemblages typical of greisenised carbonate rocks are shown in Table 9.2.

The sequence of late-post-magmatic processes leading to greisenisation is shown in Fig. 9.3. In this scheme, worked out by Pollard (1983), K-feldspathisation takes place as a result of separation of fluids from a residual granitic melt. This phase leads to a concentration of Na in the melt, resulting in the crystallisation of a Na-rich rock, usually with a high F content (see also discussion in Chap. 8, Sect. 8.2.1). In fact,

Table 9.1. Greisen alteration of granitic rocks (After Kinnaird 1985)

Original rock	Greisen assemblage
Porphyritic plagioclase granite	Chlorite, fluorite, quartz, Li-Fe siderophyllite
Biotite-perthite granite	Chlorite, siderophyllite-protolithionite mica, topaz, quartz
Albitised biotite granite	Sericite, fluorite, siderophyllite-protolithionite mica, quartz, cryolite
Albitite	Fluorite, cryolite, siderophyllite-zinnwaldite-lepidolite mica, topaz, montmorillonite
Microclinite	Li-siderophyllite-protolithionite mica chlorite, quartz and kaolinite

Table 9.2. Greisenisation of carbonate rocks. A and B compiled after Shcherba 1970; C after Wright and Kwak 1989)

Phase	Mineral assemblage
A. Contact metamorphism	Skarn: garnet, vesuvianite, diopside, wollastonite, magnetite
B. Greisenisation of skarnified carbonate rock	1. Fluorite, vesuvianite, magnetite, scheelite, pyrite 2. Mica, fluorite, magnetite, topaz, chrysoberyl, pyrite, scheelite, molybdenite, cassiterite 3. Mica, fluorite, K-feldspar, beryl, phenacite, hematite
C. Greisenisation of carbonate rocks	1. Quartz, topaz, cassiterite, fluorite, sellaite, pyrrhotite 2. Tourmaline, sellaite, fluorite, quartz, cassiterite, phlogopite

Pollard (1983) distinguishes two stages each for K-feldspathisation and Na-feldspathisation, namely, one magmatic and one post-magmatic, as schematically presented in Table 9.3.

Pegmatites may also form at the top of the granite cupolas, and while their relationship to the greisenising fluids is unclear (Pollard et al. 1988), in many cases the pegmatitic material is greisenised and therefore it must be assumed that it forms during a late-magmatic stage, prior to alkali and greisen metasomatism. The enrichment of the residual melt in Na and F results in post-magmatic Na-feldspathisation, or albitisation, which is most common in the uppermost zones of the cupolas and along fractures, where in fact albitites may occur. According to Pollard (1983), this may be due to the enhanced F-content which lowers the solidus, and in so doing allows an extended period of crystallisation that in turn allows the exsolution of an aqueous phase to develop and collect in the apical parts of the granitic cupola. Greisenisation follows the stage of Na metasomatism (Fig. 9.3) during which the circulating hydrothermal fluids are characterised by enhanced

```
LATE-MAGMATIC

                    ┌──────────────────┐
                    │  GRANITIC MELT   │
                    └──────────────────┘
                              │
                              ▼
                ┌──────────────────────────┐
                │ K-FELDSPAR-RICH GRANITE  │
                │   +Na +F -RICH MELT      │
                └──────────────────────────┘
                              │
                              ▼
          ┌──────────────────────────────────────┐
          │  Na-RICH GRANITE (ALBITISATION)      │
          │       WITH HIGH F-CONTENT            │
          │        +AQUEOUS  PHASE              │
          └──────────────────────────────────────┘
                              │
                              ▼
POST-MAGMATIC
               ┌──────────────────────────┐
               │        GREISEN           │
               │   (QUARTZ+MUSCOVITE)     │
               └──────────────────────────┘
                              │
                              ▼
                      SILICIFICATION
                      ALBITISATION II
                     MICROCLINISATION II
```
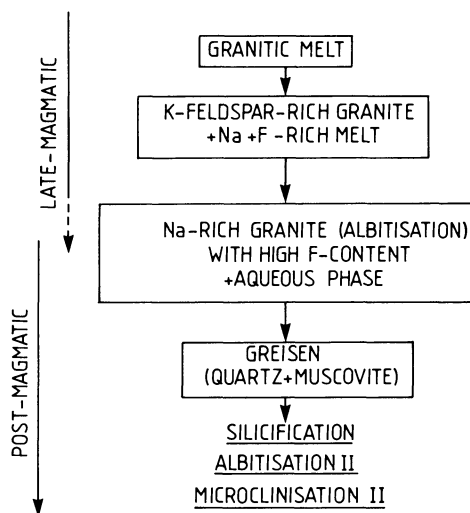
Fig. 9.3. Schematic model of late- to post-magmatic processes leading to greisenisation and post-greisenisation alkali metasomatism (After Pollard 1983)

Table 9.3. Stages of K- and Na-feldspathisation (After Pollard 1983)

K-feldspathisation	Magmatic: K-feldspar-rich granites, pegmatites
	Post-magmatic: microclinisation, K-feldspar megacrysts
Na-feldspathisation	Magmatic: albite granites, aplites, ongonites
	Post-magmatic: albitised granites, albitites

activities of H^+ and of HF, and in which there is wholesale destruction of the granitic mineral components to form greisen assemblages. In open systems – probably with the additional input of meteoric waters – a large amount of H^+ ions are consumed, resulting in mineral assemblages that may include clay minerals such as kaolinite. The silica released by the greisen-forming reactions precipitates to form granular quartz aggregates, quartz flooding and veins. Greisen alteration is the equivalent of quartz-sericite-pyrite alteration of the porhyry systems, and indeed, in many porphyry deposits, greisen alteration may be present (e.g. at Climax in Colorado), merging into quartz-sericite-pyrite so that a clear boundary between the two is not always discernable. Following the phase of greisen alteration, second phases of Na- and K-metasomatism may occur, as indicated by the replacement of greisen minerals (e.g. topaz, muscovite) by albite and new growths of K-feldspars with the notable absence of perthitic feldspars (Pollard 1983). Post-greisenisation alteration is generally related to enhanced hydrothermal activity, that is, increasing H^+ metasomatism, in which meteoric waters may play a substantial role. This subsequent activity results in quartz-sericitic and argillic alteration with illite ± kaolinite, chlorite and carbonate minerals.

Fluid inclusion studies of greisen deposits generally confirm the magmatic origin of the hydrothermal fluids, even though there are cases which have been interpreted by mixing of magmatic with meteoric waters. A review of salinities and homogenisa-

A)

B)
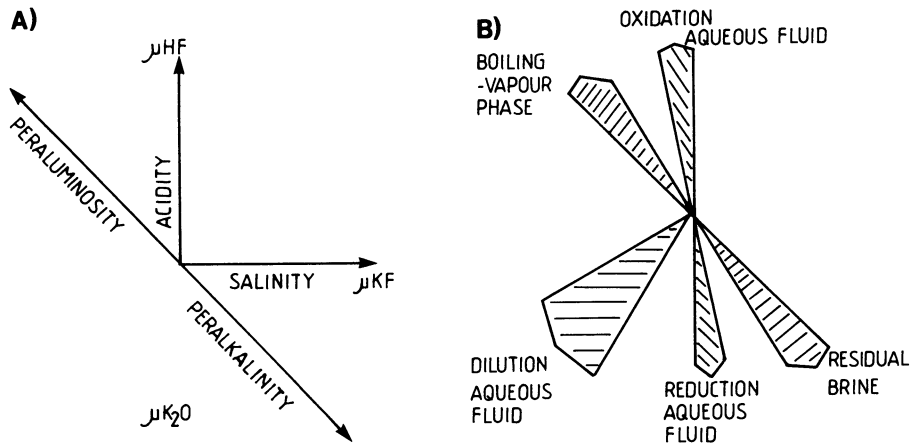
Fig. 9.4A, B. Vector diagrams of Burt (1981), showing trends of **A** alkalinity and aluminosity due to increasing salinity and acidity, respectively and **B** the effects of acidity-salinity in terms of boiling fluids. See text for details (After Burt 1981)

tion temperature of fluid inclusions from greisen-related mineral deposits can be found in Roedder (1984). According to the type of greisen-related deposit (e.g. endogreisen to exogreisen and quartz veins) the nature of the greisenising fluids varies from high (600 to 400°C and >40 wt.% NaCl equivalent) to low (±200°C and 10–15 wt.% NaCl equivalent) temperatures and salinities respectively. Dissolved species include mainly NaCl, KCl and CO_2, but phases such as anhydrite and borax have also been identified.

Burt (1981) studied greisen mineral equilibria in the system K_2O-Al_2O_3-SiO_2-H_2O-F_2O_{-1}, in terms of the activities of HF (acidity) and KF (salinity) (Fig. 9.4). The exsolution of a supercritical fluid phase, its ascent and evolution, marks the inception of the magmatic-hydrothermal activity in a granitic system. In Fig. 9.4A it can be seen that an increase in HF activity ($_\mu$HF) brings about a tendency towards peraluminosity in the magma and H^+ metasomatism (e.g. greisenisation) in the hydrothermal fluids. The opposite is obtained by increasing the salinity (expressed by $_\mu$KF), during which there is increased peralkalinity in the magma, and alkali metasomatism (e.g. feldspathisation) in the fluids. The separation of a liquid phase from a vapour phase (boiling) results in the concentration of the heavier saline species (KCl, NaCl etc.) in the former, and the lighter species (HCl, HF etc.) in the latter (Fig. 9.4B). Consequently, according to Burt (1981), the concentration of acid volatiles in the vapour phase is greatly increased, and this is considered to be the main cause of greisenisation phenomena. These fluids can at various stages be modified by diluting meteoric waters, as testified by the common occurrence of clay minerals, such as in the Cornwall greisen-related mineral deposits. Burt also draws attention to the importance of adding new elements to the system, for example Ca and W. In this case the activity of HF determines the stability of scheelite (lower $_\mu$HF) or wolframite (higher $_\mu$HF) in the system. At low HF activity the formation of scheelite could be as follows:

$$H_2WO_4 + Ca^{2+} = CaWO_4 + 2H^+,$$
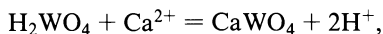
with increasing HF activity scheelite may convert to wolframite according to the following reaction:

$$CaWO_4 + FeO + 2HF = FeWO_4 + CaF_2 + H_2O.$$
scheelite   wolframite   fluorite
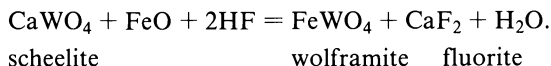
Also, in his work Burt shows that the anorthite content of plagioclase and other calcic phases (e.g. sphene) decreases or becomes unstable as the F-content of the system increases, thus making Ca available to form fluorite. This is confirmed by direct field and mineralogical observations, for example in a low-F greisen-related Sn-W deposit in the Karamea Batholith in New Zealand (MacKenzie 1983), where it is shown that the Ca of the plagioclases was utilised to form scheelite.

In vein-type greisens the hydrothermal processes are at lower temperatures and there appears to be no evidence of boiling. Thus, in the case of greisenisation without boiling, F-bearing micas and topaz would form at high HF activity (Burt 1981). Under conditions of very high F-activity topaz greisens form as a result of the instability of muscovite in the presence of HF as indicated by the reaction shown below for the topaz-rich greisens of Mount Bischoff (Tasmania) (Wright and Kwak 1989):

$$K_2Al_4(Si_6Al_2O_{20})(OH)_4 + 6HF = 3Al_2(SiO_4)(OH,F)_2 + 3SiO_2 + 2K^+ + 4H^+.$$
muscovite   topaz
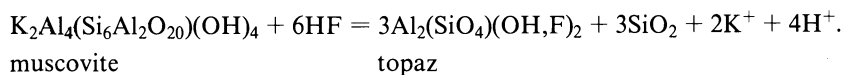
Increase in the activity of H_2O during cooling of the hydrothermal fluids would result in the breakdown of topaz and feldspars to release large quantities of HF, with formation of muscovite and quartz. The release of F, together with the muscovitisation and chloritisation of the biotites at depth, would result in the leaching of metals and their complexing with F and subsequent transport upward in the evolving system. In low-pressure environments, such as in subvolcanic to volcanic areas, the separation of aqueous phases from F-rich magmas causes low-pressure greisenisation. This results in the formation of greisen mineral assemblages, as indicated by the formation of topaz and fluorite in cavities of rhyolitic volcanics and ash-flow tuffs (Burt 1981).

So far, we have considered only the presence of F in a greisen system. However, Li and B also commonly occur, and the main features of B-rich systems as opposed to those enriched in F have been investigated by Pollard et al. (1987). These authors first point out that such environments can occur at either the local or regional scale, and also that there may be mixed situations. The general features of the F-rich and B-rich greisen systems are shown in Fig. 9.5A, B. As previously outlined, F-rich greisen systems are characterised by the presence of fluorite and/or topaz as well as Li-rich micas (e.g. lepidolite or protolithionite). B-rich greisen systems on the other hand, are manifested by abundant tourmaline. In open systems (Fig. 9.5A, 2), this mineral occurs in, and is associated with, breccia pipes, stockworks and veins. These are generally the result of developing high B-rich volatile pressures during the crystallisation of B-rich magmas. In closed systems the granitic cupola contains disseminations of tourmaline and greisen minerals (Fig. 9.5A, 1). In both F- and
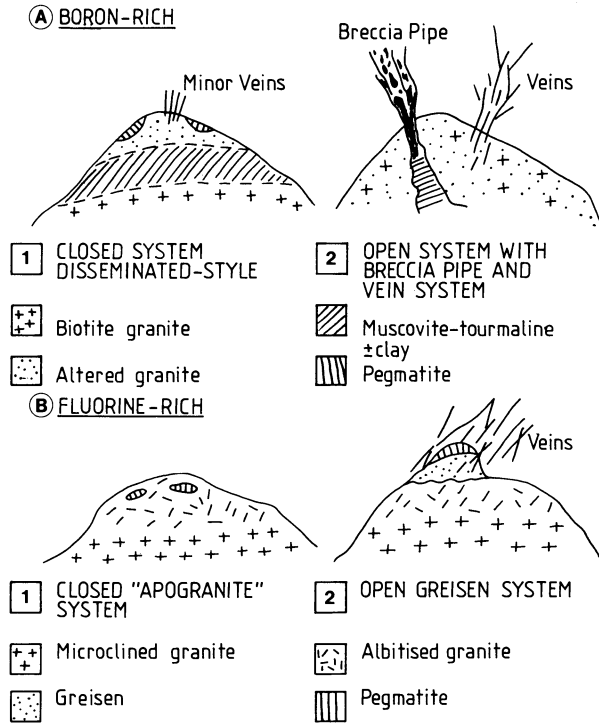
Fig. 9.5. A Boron-rich and B fluorine-rich granitic environments. See text for details (After Pollard et al. 1987)

B-rich systems, other components such as CO_2, Cl and of course H_2O assume importance in terms of granitic melt behaviour during crystallisation and exsolution of hydrothermal fluids (Pollard et al. 1987; see also discussion in Chap. 8).

9.3 Geochemistry

Greisenised granitic rocks are generally characterised by increases in Si, and losses in Al, K and Na, with respect to the parent unaltered granitic body. The breakdown of feldspars during greisenisation processes is thought to be largely responsible for the Na and Al losses and the increase in Si (Kinnaird 1985, see also reactions in Sect. 9.2). The K liberated by the greisenising reactions is taken up by the hydrothermal fluids, probably to generate second-stage K-metasomatism. Kinnaird (1985), in her work on the greisen systems of Nigeria, reports increases in Li, Th, Ce, Y, Sn, Pb, Zn, Fe, W and Cu, as well as enrichment in light REE, in the greisenised rocks. Greisenisation of the Cligga Head granite in Cornwall is also characterised by enrichments in Ca, F, B, Li, Rb, Sn, W and Zn, and depletions in Na, Al, Ba and Sr (Hall 1971). Trace element values for an average granite, and from a "vein-free" greisenised granite cupola and its parent biotite-muscovite granite cupola (Pirajno 1982), are given in Table 9.4.

Table 9.4. Trace element geochemistry of granitic rocks and greisen material. All values in parts per million (ppm) (After Pirajno 1982; A After Turekian and Wedepohl (1961). B Numbers in parentheses indicate numbers of analyses

Element	Average granite	Biotite muscovite granite	Greisenised granite	Greisen material
	A	(2)B	(7)B	(14)B
Li	40	38	52	57
F	850	450	1238	1489
B	10	215	129	94
Rb	170	265	324	378
Sr	100	55	38	36
Ba	840	180	173	179
Nb	21	10	13	17
Zr	175	35	35	34
Ti	1200	240	268	298
Y	40	15	15	15
Cu	10	35	309	402
Pb	19	2	7	9
Zn	39	21	40	96
Ni	4.5	1	1	1
Cr	4	28	45	34
Mo	1.3	0.5	52	29
Sn	3	1	1	6
W	2	3	8	10
Au	0.004	0.008	0.03	0.01
Bi	0.01	1	82	58
Sb	0.2	1	1	1
Th	17	4	6	4

In Table 9.4 it is particularly interesting to note the strong enrichment of the parent biotite granite and its "vein-free" greisenised products, with respect to an average granite, in Bi, Au, W, Cr, Mo, Cu and Zn, and the strong depletions of elements such as Ba, Ti, Y, Ni and Sr.

9.4 Greisen-Related Mineral Deposits

Greisen systems are typically associated with Sn and W mineralisation, usually accompanied by numerous other ore elements such as Cu, Zn, Bi, Mo, F. Common ore minerals are cassiterite, stannite, wolframite, scheelite, arsenopyrite, pyrite, chalcopyrite, molybdenite, sphalerite, bismuth and bismuthinite. Other important minerals are topaz, fluorite and apatite. Most greisen-affiliated Sn and W deposits are spatially and genetically related to S-type granitic rocks, or the ilmenite-type of Ishihara (1977), forming dome-like (cupolas), or ridge-like intrusions. Details of Sn

— Cu + Zn + Pb

— W + Bi

— W + Be + Mo

— Mo + Be + W + Sn

— Sn + Mo

— Zr + Nb + Ta

Granite (±albitised)

Greisen and greisenised granite

Country rock

Quartz vein with greisenised margin
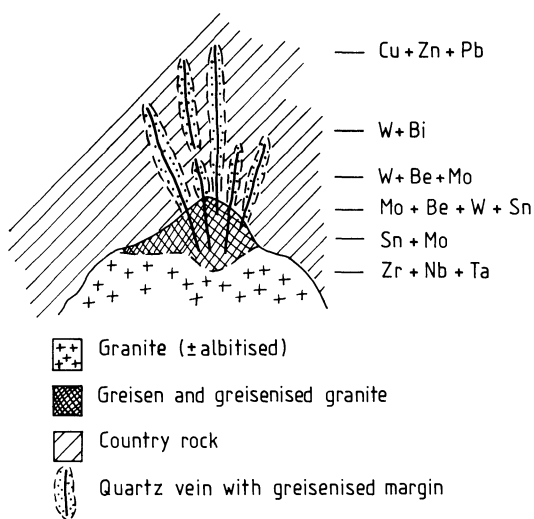
Fig. 9.6. Idealised metal zonation associated with a greisenised granite cupola (After Shcherba 1970)

and W deposits of greisen affiliation can be found in Taylor (1979) and in a recent collection of papers edited by Hutchison (1988).

The general features of greisen-related Sn mineralisation have been discussed by Pollard et al. (1988) and Hosking (1988). This mineralisation occurs as lenses, generally subparallel to the arcuate contacts of the granitic intrusion with the enclosing country rocks. In open systems, fracture-controlled, sheeted veins, and stockworks, emanate from the greisenised granite into the country rocks (Fig. 9.1).

Greisen rocks may have distinct metal zonations. These are usually manifested by a lower zone of Sn + Mo, extending upward and sometimes laterally through W + Bi to Cu, Zn, and Pb (Fig. 9.6). In some cases Au may also be present (Pirajno and Bentley 1985). Yan et al. (1980) describe in detail vertical zonations that apply to the W deposits of China. However these zonations are somewhat idealised, having no general validity, and thus each case has to be assessed separately. Time-paragenetic sequences of greisen-related ore assemblages, on the other hand, appear to follow some general rules that may be applicable to most greisen deposits. Deposition of the ore minerals usually starts with an oxide phase (cassiterite, wolframite), followed by sulphides (pyrite, chalcopyrite, pyrrhotite, arsenopyrite, molybdenite, bismuthinite), and a late, lower temperature, carbonate-oxide stage characterised by calcite, siderite and iron oxides. At Panasqueira (Portugal), for example, the paragenetic sequence consists of an early oxide-silicate stage, a sulphide stage and late carbonate stage (Kelly and Rye 1979). This is discussed in more detail later.

9.4.1 Sn and W Geochemistry in the Greisen Environment – Deposition of Cassiterite and Wolframite

Lehmann (1982) investigated the metallogeny of Sn in granitic fractionation series of mineralised and non-mineralised granites. The geochemical specialisation of the Sn-bearing granites is, inter alia, thought to be controlled by oxidation state of

Sn in the melt, with respect to conditions of high or low oxygen fugacity as determined by the Fe^{+3}/Fe^{+2} ratios. Pollard et al. (1983) however, dispute this. Ishihara (1977, 1981) and Ishihara et al. (1979) classify granitic rocks into magnetite series (more or less equivalent to I-types), and ilmenite series (more or less equivalent to S-types). The hypothesis proposed by these authors with regard to the behaviour of Sn in the granitic melts, is that in the case of magnetite-series granites, characterised by high Fe^{+3}/Fe^{+2} ratios, Sn is in the tetravalent state (Sn^{+4}) and as such may substitute for Ti or Fe, thus entering the lattice of the early crystallising, rock-forming minerals (e.g. sphene, magnetite, hornblende, biotite). Its availability in the remaining liquid fraction would hence be limited, with the further consequence that accumulation of Sn in the residual melt would be insufficient to produce an ore deposit. In the case of the ilmenite-series granites (low Fe^{+3}/Fe^{+2}), Sn is in the divalent state (Sn^{+2}) and as such cannot enter the lattice of the early rock-forming minerals. Under these conditions Sn would be more readily available for accumulation in the residual melts, leading to a Sn-rich, and hence specialised, highly fractionated leucocratic granite. It is of interest to note in this context that studies of worldwide Sn-W and porphyry metallogeny has indicated that I-type/magnetite-series granitoids are generally associated with Cu-Mo porphyry mineralisation, and generated either in the upper mantle or lower crustal levels. On the other hand S-type/ilmenite-series granitoids, which are generally associated with Sn-W mineralisation, are either generated in crustal environments, or, at least, are involved in the interaction with C-bearing metasedimentary rocks (reducing conditions, low oxygen fugacity). The world distribution of these metallic deposits has also indicated that the Cu-Mo porphyries are preferentially confined to subduction-related tectonic settings, whereas the Sn-W deposits of greisen affiliation tend to originate in collisional tectonic settings (Ishihara 1977; Mitchell and Garson 1981; Pirajno 1985).

Cassiterite is the chief ore mineral of Sn and is commonly associated with fluorite and/or tourmaline, suggesting a cogenetic relationship between these minerals and the transporting hydrothermal fluids. Various mechanisms have been proposed for the dissolution and transport of Sn in hydrothermal solutions. According to Paterson et al. (1981) Sn^{+2} readily complexes with F^-, OH^- and Cl^-. Sn transport as a consequence of hydroxyl and hydroxyfluoride complexing is thought to take place in high temperature, alkaline fluids (Eadington 1983). Fluoride and chloride complexes are more significant for the transport of Sn in hydrothermal solutions. It appears that F is more likely to transport Sn in highly saline solutions. Sn is considered to be readily transported as a stannous chloride complex ($SnCl^-$) under conditions of low pH and low fO_2 (Paterson et al. 1981). Precipitation of cassiterite due to the destabilisation of the transporting complexes would then occur either by fO_2 increase, an increase in pH, a decrease in temperature or a combination of these physico-chemical factors. Generally speaking, the conditions which cause precipitation of cassiterite are similar to those for wolframite (discussed below), and it appears that in a Sn-W-bearing solution cassiterite and wolframite would precipitate earlier under slightly more acidic conditions, while scheelite would precipitate later at slightly higher pH levels (neutral to alkaline). Precipitation of cassiterite also depends on the nature of the rocks with which the fluids interact. The metal chloride

solutes are converted to oxides and/or sulphides and HCl and H^+ released (Eugster 1984). Neutralisation of the acid greisenising fluids is readily achieved by their penetration of carbonate rocks; precipitation of cassiterite may be represented as follows (Eugster 1984):

$$SnCl_2 + CaCO_3 + H_2O = SnO_2 + CaCl_2 + CO_2 + H_2.$$
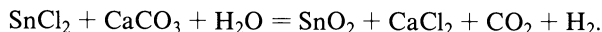
In pelitic rocks it is the conversion of feldspar and biotite to muscovite that may induce precipitation of cassiterite, as mentioned earlier. A possible reaction proposed by Eugster is given below:

$$SnCl_2 + 3KFe_3AlSi_3O_{10}(OH)_2 + 2H_2O = SnO_2 + KAl_3Si_3O_{10}(OH)_2 + 6SiO_2$$
$$\text{biotite} \qquad\qquad\qquad\qquad \text{muscovite}$$
$$+ 3Fe_3O_4 + 2KCl + 4H_2.$$
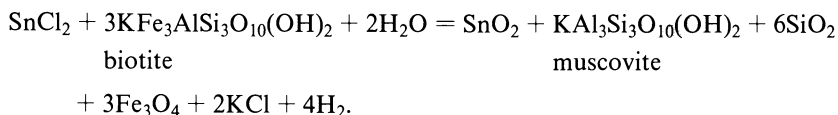
In nature W is found almost exclusively in a hexavalent state (W^{+6}) with oxygen compounds. Thus, there are two principal groups of tungstate compounds known as minerals, namely, wolframite $(Fe,Mn)WO_4$ and scheelite $(CaWO_4)$. Wolframite forms a solid solution series with ferberite $(FeWO_4)$ and huebnerite $(MnWO_4)$. Experimental data (Foster 1977) indicate that W is mobilised in chloride-bearing hydrothermal solutions. Foster (1977) postulated that molecular hexalides (WCl_6) are probably present at near-magmatic temperatures, but with decreasing temperatures and increasing hydration, W is transported as molecular H_2WO_4. With further decreasing temperatures the major W species are ionic $(H_3W_6O_{21})^{-3}$; $(HW_6O_{21})^{-5}$; $(WO_4)^{-2}$). Under these conditions the parameters controlling W transport and deposition are, apart from temperature, fO_2/fS_2, the activities of Ca^{2+}, Fe^{2+} and Mn^{2+} and the pH of the solution (Foster et al. 1978). Scheelite deposition at supercritical (over 500°C and 100 bar) and near-critical temperatures is a function of the temperature variations and the activity of the ratio Ca^{2+}/Fe^{2+}. Assuming a Cl^--rich brine, with high Ca^{2+}/Fe^{2+} ratios, scheelite would be deposited. However, at high fO_2 levels, and where the activity of Fe^{2+} is greater than that of Ca^{2+}, wolframite would be preferentially deposited, whereas at lower fO_2, sulphides will form (Foster 1977, Foster et al. 1978).

The role of F is more important for Sn than it is for W; however, oxyfluoride complexes may be responsible for the transport of W at low temperatures (± 300°C), in cases where the concentration of F in the solution is high (Foster 1977). The role of F in the hydrothermal transport and deposition of W may be dictated by the activities of HF and KF, as proposed by Burt (1981) in terms of his acidity-salinity diagrams (Fig. 9.4). Under conditions of low HF and KF activities scheelite will form, whereas wolframite occupies a field of higher HF and KF values as discussed earlier. This would explain the common association of fluorite and topaz with wolframite mineralisation. Westra and Keith (1981) further substantiated this relationship, noting that scheelite is common (without cassiterite) in calcic magma series which have low F, while in F-enriched calc-alkaline magmas wolframite or huebnerite occur together with Mo and Sn.

9.4.2 Sn Deposits Associated with the Acid Phase
of the Bushveld Igneous Complex, South Africa

The Bushveld Igneous Complex (BIC) is the largest layered intrusion of its kind in the world, comprising vast mineral resources of a number of strategically important commodities (e.g. Cr, platinoids). The BIC underlies an area of approximately 65000 km^2, although of this about 55% is covered by younger sedimentary rocks. Figure 9.7 schematically illustrates the geology of the BIC and the stratigraphic relationships between the component suites. Comprehensive reviews can be found in von Gruenewaldt et al.(1985) and Vermak and von Gruenewaldt (1986). According to SACS (1980), the lithostratigraphy of the BIC consists of three main suites. The Rashoop Granophyre Suite, emplaced about 2090 Ma ago, includes complex lithologies that have formed during an earlier silicic phase, and during the emplacement of the basic rocks (Walraven 1985). The Rustenburg Layered Suite, which is the main, mafic portion of the Complex, and was intruded into the sediments and volcanics of the Transvaal Supergroup some 2050 Ma ago. The Lebowa Granite Suite with approximate ages ranging from 2050 to 2024 Ma comprises a series of cogenetic granitic rocks which intrude all other lithologies and are responsible for the greisen-related deposits discussed below. On a genetic basis, the BIC metallic mineral deposits can be classified into two major groups:

1. Magmatic deposits associated with the Rustenburg Layered Suite containing platinum group elements ($\pm$ Au, $\pm$ Ni, $\pm$ Cu), Cr and V.
2. Hydrothermal deposits associated with the Lebowa Granite Suite, containing Sn, F and minor Cu.

The Sn mineralisation in the second group is of interest in the present context and is discussed below.

The Lebowa Granite Suite represents the final phase of the magmatic activity of the BIC, and its relationship to the BIC lithologies is shown in Fig. 9.7B. It was emplaced as an intrusion of batholithic dimension generally along, or close to, the contact between the Rustenburg Layered Suite rocks and the roof rocks represented by the Rooiberg Felsites (Twist 1985). The Lebowa Suite includes the Nebo Granite, Bobbejankop Granite, Klipkloof Granite and Lease Granite. The Nebo granite is the most abundant, all the others being considered as late-stage fractionated variants (Walraven 1985). The Nebo Granite, which is coarse-grained, is made up of K-feldspar, quartz, plagioclase, hornblende in its lower portions and biotite in its uppermost portions. The Bobbejankop granite is a variety of the Nebo Granite and distinguishable by its reddish colour, miarolitic texture, and the presence of tourmaline clusters. The endogranitic Sn deposits of the BIC occur mostly within the Bobbejankop granite and its roof facies. The Sn deposits of the BIC are grouped into six main camps (Fig. 9.7A), and their postulated relationships with the granitic rocks and surrounding lithologies are shown in Fig. 9.8. Only two mines are currently producing: the endogranitic Zaaiplaats deposit and the exogranitic Rooiberg deposit. The nature of this mineralisation has been reported by Leube and Stumpfl (1963), Hunter (1973), Stear (1977), Crocker (1979, 1986), Coetzee (1986), Pollard and Taylor (1986) and Rozendaal et al. (1986).
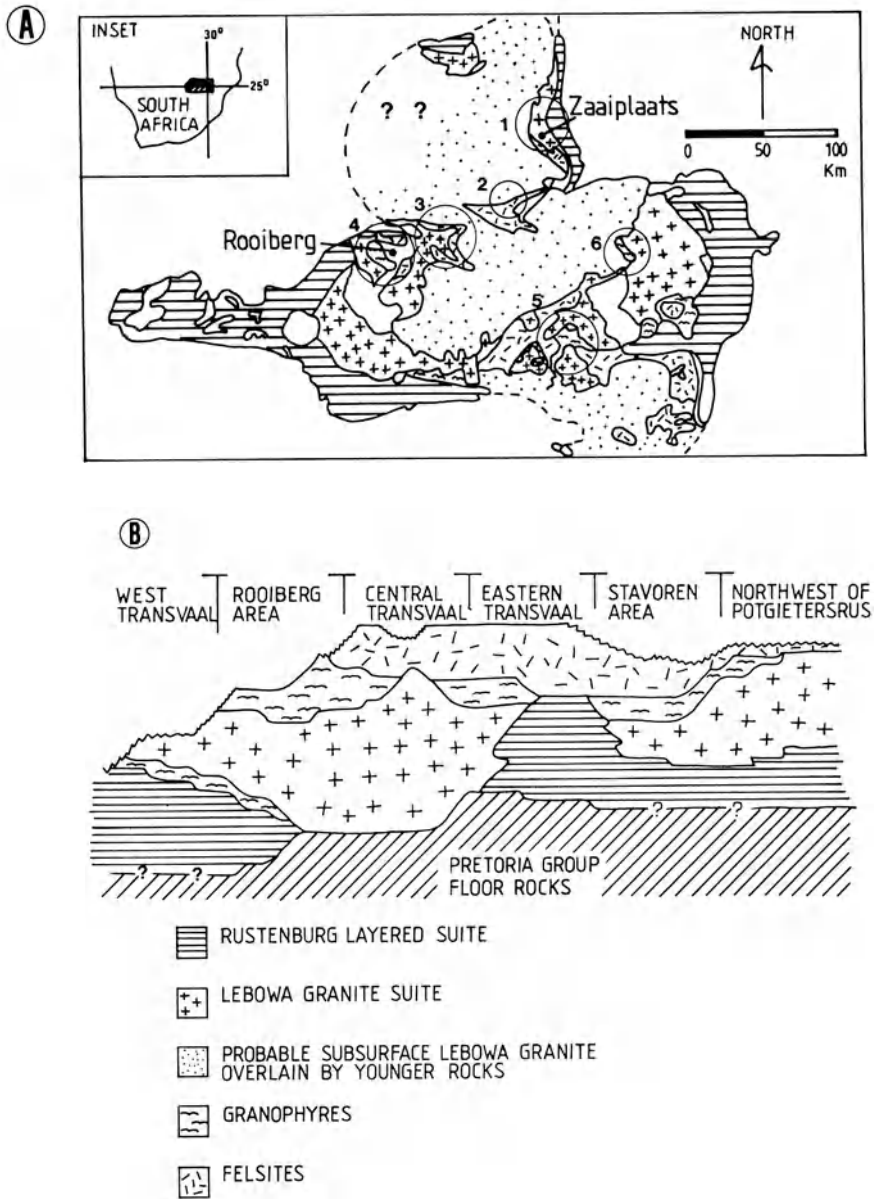
Fig. 9.7. **A** Simplified geological map of the Bushveld Igneous Complex (see also Fig. 8.9), showing the six main areas of Sn mineralisation: *1* Zaaiplaats; *2* Union Tin; *3* Elands; *4* Rooiberg; *5* Moloto; *6* Stavoren (After Walraven 1985; Crocker 1979). **B** Schematic cross-section showing relationships between the main lithostratigraphic units of the Bushveld Complex (After Walraven 1985)

Lebowa granite suite.

Bobbenjankop-Type granite

Shale and arkose of
Pretoria Group

Rooiberg Group felsites

(1) Zaaiplaats mineralisation, pipes and disseminations

(2a) Rooiberg replacement pockets and disseminations

(2b) Rooiberg (Leeupoort) bedding plane and vein
filling

(3) Pipes in granophyre at Stavoren

(4) Stockworks and replacement in felsitic rocks
Union Tin area
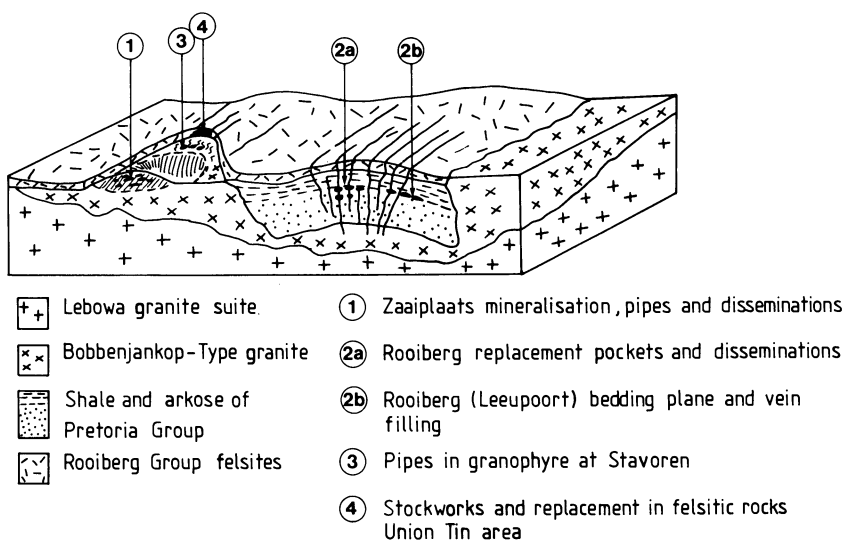
Fig. 9.8. Idealised model depicting the types of Sn deposits related to the Bushveld granites. *1* Zaaiplaats pipes and disseminated mineralisation; *2a* Rooiberg replacement pockets and dissemination; *2b* Rooiberg (Leeuwpoort) bedding plane and vein-filling deposits; *3* pipes in granophyric rocks at Stavoren; *4* Stockworks and replacements in felsite rocks in the Union Tin area (After Stear 1977)

Zaaiplaats

The Zaaiplaats Sn mine is situated some 25 km northwest of the town of Potgietersrus in the Transvaal region (Fig. 9.7A). The mineralisation is confined to the upper portions of the Bobbejankop Granite and within its fine-grained marginal and apical phase, the Lease Granite. The Bobbejankop pluton was intruded as a sheet-like body roughly along the contact between the Rustenburg Layered Suite and its roof rocks represented by the Rashoop Granophyre Suite and the felsite of the Rooiberg Group. The Bobbejankop Granite is deep red in colour, medium-grained, containing quartz and alkali feldspars as patch per-thites, with variable proportions of microcline and albite, which are thought to represent Na- and K-metasomatism of earlier magmatic feldspars (Pollard and Taylor 1986). Biotite is present and invariably altered to chlorite. The Lease Granite is a volatile-rich differentiate of the Bobbejankop granite, and is typically a microgranite with a low content of mafic minerals, which are also chloritised. This granite is bi-textured, that is, it has a coarse-grained phase interlocking with a fine-grained phase. The interlocking coarse materials coalesce to form the overlying pegmatitic zone. The Lease Granite also contains miarolitic cavities, filled with sericite and chlorite, and decreasing with depth. A zone of pegmatite bodies is present on the roof of the Lease Granite at, and near to, the contact with the overlying rocks of the Rashoop Granophyre (Fig. 9.9). The pegmatites are characterised by large quartz and feldspar crystals orientated perpendicular to the contact. The presence of roof pegmatites and the bi-textured nature of the
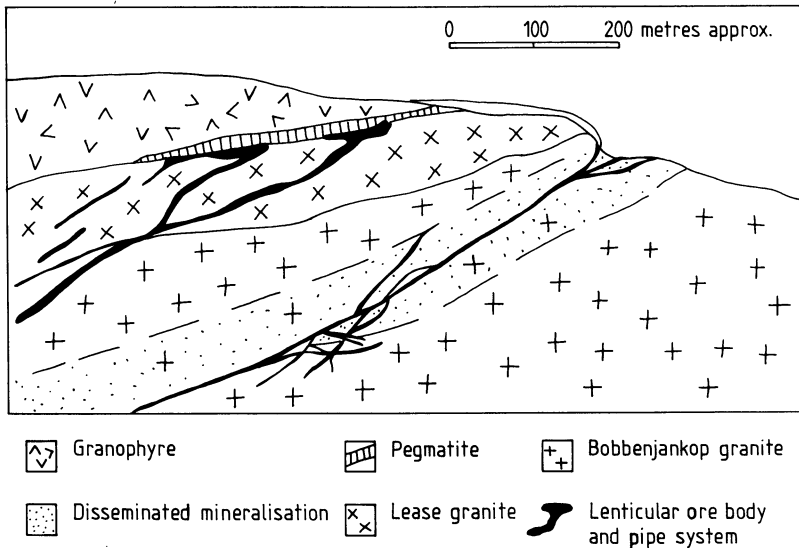
Fig. 9.9. Schematic section through the Zaaiplaats mine area depicting mineralisation styles. Sketch based on Mine handout and Pollard et al. (1988)

Lease Granite may be indicative of a closed mineralising system (R. Taylor pers. comm. 1986).

Three different styles of endogranitic mineralisation are present at Zaaiplaats, including: disseminated orebodies, lenticular orebodies and pipe orebodies. A simplified representation of these three styles is shown in Fig. 9.9. Most orebodies have associated sulphides (chalcopyrite, arsenopyrite, galena, bismuthinite), wolframite, scheelite and even Au (locally up to 2 g/t). Ag is found in grades of up to 150 g/t in the tailing concentrates.

The bulk of the production is obtained from a zone of disseminated cassiterite ore, which is developed within the Bobbejankop Granite some distance below its contact with the Lease Granite. The thickness of this ore zone, as defined by the cut-off grade, is about 10 m, and its average grade about 0.15% Sn. The granite is altered to an epidote-chlorite-sericite assemblage often associated with irregularly shaped vugs up to 25 cm in diameter. These vugs are infilled with cassiterite, scheelite, fluorite, chlorite and sericite. The lenticular orebodies (called "lily pads" by the local miners) occur within the Lease Granite at the base of the pegmatite zone. The lenticular orebodies contain relatively rich mineralisation, with grades of about 0.4 to 0.5% Sn. Extensive albite-sericite and chlorite alteration present within the bodies are considered to have formed by replacement of the Lease Granite by the developing hydrothermal fluids, the pegmatite having acted as a barrier to the upward movement of the fluids (R. Taylor pers.comm. 1986). The lenticular orebodies tend to be funnel-shaped and in places taper downwards into high-grade pipes of small diameter (about 50 cm) (see Fig. 9.9). Pipe-like orebodies, which occur both in the Lease Granite and in the Bobbejankop Granite can be exceptionally rich with grades of up to 30% Sn. The pipes have sharp contacts with the

Plate 9.1. Surface expression of mineralised pipe at Zaaiplaats. Zoning as indicated by the letters is as follows: *A* sericite + cassiterite core; *B* albite + tourmaline intermediate ring; *C* quartz + tourmaline; *D* albitised Bobbejankop granite. The *outer ring* is spray paint

Plate 9.2. Underground exposure of mineralised pipe at Zaaiplaats. Noticeable is the light-coloured sericite + cassiterite core surrounded by a dark tourmaline-rich zone

surrounding granite (Plates 9.1 and 9.2), and range in diameter from several centimetres up to 13 m, the average being 1 to 2 m. Although they have been traced for lengths of up to 1000 m, they are erratic both in distribution and strike and variable in composition. The pipes ramify and exhibit swellings and constrictions. However, there is a tendency for the overall plunge to be in a northwesterly direction, suggesting a vague structural control, and for the more productive pipes to cluster in certain areas of the granite, indicating a relationship between the cassiterite-bearing portions of the pipes and the zones of disseminated mineralisation that are traversed by the pipes (Fig. 9.9). The pipes display a strongly zoned, annular structure, generally consisting of a cassiterite-impregnated sericite-illite core, followed by an intermediate ring of tourmaline, a dark tourmaline (luxullianite)-quartz-feldspar annular zone, grading through a thin albitised zone into the relatively unaltered granite (Plate 9.1). Close examination of the pipes reveals inward-pointing euhedral quartz crystals developed between the albitised granite zone and the luxullianite zone, which is taken to be indicative of open-space filling. Geochemical studies by von Gruenewaldt and Strydom (1985) revealed a distinct geochemical zonation of trace elements around the pipes, with Sn restricted to the pipes, and Cu, Pb, Zn, W and As forming well-defined dispersion haloes around the pipes.

The enigmatic pipes at Zaaiplaats are thought to represent channelways along which hydrothermal fluids moved upwards towards the upper portions of the granite body. Taylor (1979) considered the formation of the pipes to be a possible result of immiscibility of an aqueous phase from the crystallising magma. This aqueous phase would have formed "bubbles" that trailed upwards within the crystallising silicate melt, to become "entrapped by crystallisation before reaching an overlying plumbing system" (Taylor 1979, p.173). In a recent paper published by Pollard et al. (1989), a model of pipe formation has been presented. Their detailed investigation of the mineralogy and textural relationships in one of the main Zaaiplaats pipes has shown that the host granite was subjected to a process of leaching whereby quartz and to some extent feldspar, were removed by very hot solutions. Although the nature of these solutions is not certain, the authors postulate that they were weakly alkaline and contained alkali chloride, fluoride or carbonate complexes that exsolved from the magma in the subsolidus range of temperature and pressure. The dissolution of the quartz and feldspars created zones of permeability, largely formed by vugs, which allowed the movement of the developing hydrothermal fluids. The vugs created by the dissolution process were later infilled by a host of hydrothermal minerals. Minerals deposited in the vugs include quartz, tourmaline, albite, chlorite, cassiterite, scheelite, fluorite, synchisite (a fluorocarbonate containing rare earth elements), calcite and sulphides.

Pollard and Taylor (1986) and Taylor and Pollard (1988) explain the evolution of the magmatic-hydrothermal fluids responsible for the Zaaiplaats mineralisation as follows. The presence of vugs, which occupy 1 to 4% by volume of the granitic rock, and the pervasively altered nature of the granite containing disseminated cassiterite, are evidence of exsolving hydrothermal fluids immediately subsequent to the main crystallisation phase of the silicate melt. Work done by the Taylor-Pollard team in the Herberton tin field of Queensland in Australia indicates that in general magmatic-hydrothermal fluids are developed in situ during the very late stages of

ALBITE -   ──
CASSITERITE -   ──
QUARTZ 1 -   ──
QUARTZ 2 -   ─ ─ ─ ──
QUARTZ 3 -   ── ─ ─ ─ ─
CHLORITE -   ─ ─ ─ ─ ─ ── ─ ─ ─
FLUORITE -   ──────
SERICITE -   ── ──
HEMATITE -   ─ ─ ─ ─ ─ ─ ─ ─ ──
──────────────────────────────►
                  TIME
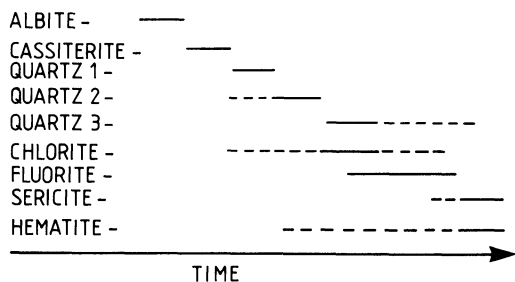
Fig. 9.10. Paragenetic sequence of main vug-infill minerals in the disseminated mineralised zone at Zaaiplaats (After Taylor and Pollard 1988; Pollard et al. 1989)

crystallisation. At Zaaiplaats hydrothermal fluids occupied an extensive system of interstitial cavities, grain boundaries and microfractures, so that the upper portions of the granitic body became a reservoir of magmatic-hydrothermal fluids. A paragenetic sequence of the alteration-mineralisation at Zaaiplaats is shown in Fig. 9.10.

Fluid inclusion studies indicate homogenisation temperatures in the range of 300 to 600°C for highly saline brines, whereas oxygen isotope determinations gave results consistent with fluids of magmatic origin having exchanged with granitic rocks at temperatures of about 350°C (Pollard and Taylor 1986). The model of a magmatic fluid reservoir, as envisaged by these workers, implies that hydrothermal fluid movement is essentially a question of permeability. This in turn is related to the amount and degree of fracturing within the granitic rocks and the adjacent country rocks. Clearly Zaaiplaats is a closed system in which, because of poor permeability, the fluids were contained within the granitic mass (endogreisen). The development of fractures within the entire system may be related either to fluid pressure causing hydraulic fracturing, or to tectonic activity, or both. In orogenic areas both are likely to take place, and the development of vein systems is perhaps more frequent than in anorogenic systems. Fracturing, according to the model outlined above, would result in the tapping of the magmatic-hydrothermal fluids and the establishment of exogreisen vein systems. In orogenic areas, meteoric waters are also more likely to participate in the evolution of the mineralising event by mixing with the fluids of magmatic-hydrothermal origin.

Rooiberg Sn Deposits

The Rooiberg Sn field, situated about 65 km west of Warmbaths (Transvaal) (Fig. 9.7A), was once the largest Sn producer in South Africa. Until 1986 production was from four mines, Hartbeestfontein ("A" Mine, currently active), Nieuwpoort ("B" Mine), Leeuwpoort ("C" Mine) and Vellefontein (Fig. 9.11A). These mines, together with the Union Tin deposit near Naboomspruit, accounted for nearly 90% of the total South African production. At Rooiberg total reserves are about 6×10^6 tonnes grading about 1.3% Sn. The Sn field occurs within the so-called Rooiberg fragment, a gigantic segment or roof pendant of sedimentary and volcanic rocks of the Transvaal Supergroup (Pretoria and Rooiberg Groups), intruded by the Bushveld granites (Lebowa Granite Suite). The intrusion of the sedimentary and volcanic rocks by successive influxes of granitic magma gave rise to horizontally disposed

A
+ Nebo granite
Granophyre
v v Rooiberg felsite
Pretoria GP rocks

NORTH

0   5   10 Km

(A) Rooiberg 'A' Mine
(B) Nieuwpoort 'B' Mine   (V) Vellefontein
(C) Leeuwpoort 'C' Mine
(D) Blaauwbank

B

BLEACHED
HALOES

Tourmaline ± carbonates   Hematite + orthoclase (reddening)

Sericite–ankerite–rich   Cassiterite disseminations in sericitic core

Sulphides and cassiterite   Arkose
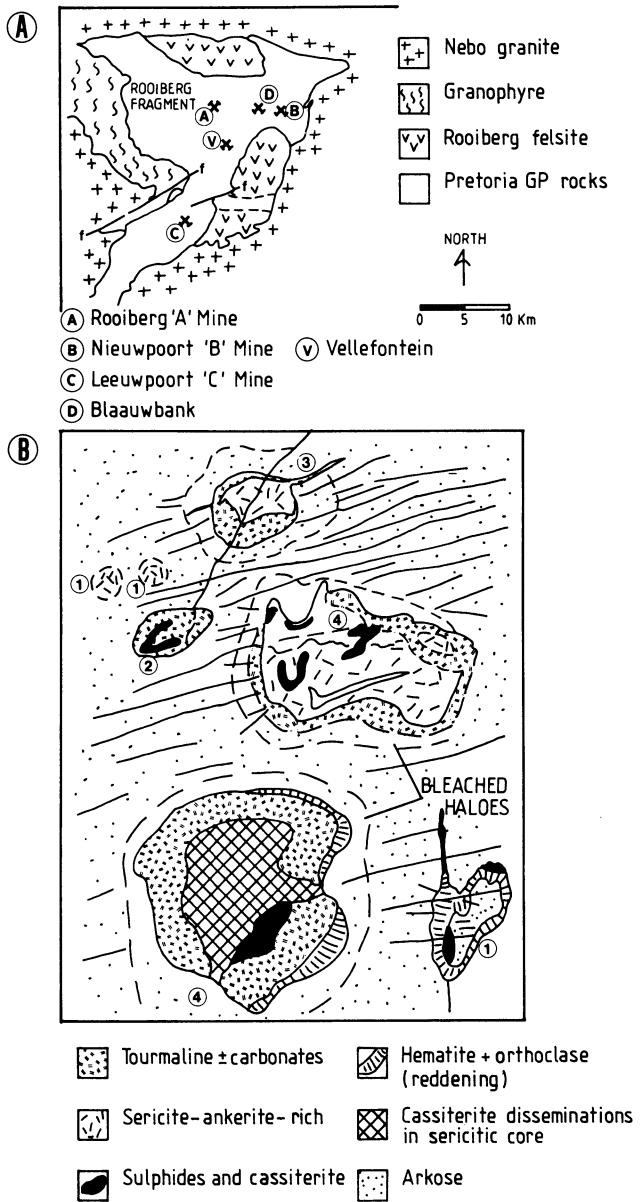
Fig. 9.11A, B. Rooiberg geology and mineralisation. A Simplified geological map of the Rooiberg area, showing location of main Sn deposits. B Rooiberg "A" Mine pockets: *1* embryonic type; *2* nodular; *3* orbicular; *4* complex (After Rozendaal et al. 1986; mine handout; Leube and Stumpl 1963)

Table 9.5. Lithostratigraphy of Rooiberg area (After Rozendaal et al. 1986)

Rooiberg Group	Flow banded felsites	
	Smelterskop Formation (258–1100 m)	Feldspathic quarzite and tuffaceous shales, with interbedded andesitic rocks. Local conglomerates and pebble bands
Pretoria Group	Leeuwpoort Formation (1510–1700 m)	Blaauwbank Shale Member: thinly bedded shales and sandstones, upward fining lenticular arkose and sandstones interbedded with shales and siltstones
		Boschoffsberg Quartzite Member: upward fining sequence of cross-bedded arkose. Coarse-grained units with conglomerates and pebble bands

stress fields within and adjacent to the Rooiberg fragment (Stear 1977). Structurally, the Rooiberg Sn field has the form of a broad east-northeast trending arch, with a superimposed north-west-trending synclinal structure. On the northwestern and southwestern limbs of the arch are two prominent dislocation zones (Kwarriehoek Wrench and South Parallel Fault), one of which – the South Parallel Fault – was probably the main feeder channel for the mineralising fluids. The lithostratigraphy of the Rooiberg fragment is summarised in Table 9.5.

The most important mineralisation occurs within cross-bedded arkosic rocks (Boshoffsberg Quartzite Member) and in the overlying shaly quartzite rocks below the Blaauwbank Shale Member. The latter is thought to have acted as an impermeable barrier to the ascending fluids. Rozendaal et al. (1986) classify the Rooiberg Sn deposits as either conformable or uncomformable. Included in the former are the spectacular "pockets", bedded lodes and stringers, and bedding-plane orebodies, while the uncomformable deposits comprise mineralisation of open-space filling style along fractures and faults.

The bulk of the production comes from the "pocket" orebodies (Plate 4.13), which are best developed at the "A" Mine and confined to a stratabound zone (the "tin" zone). located within a complex of intersecting fissures. These pockets, of varying shape, size and mineral content, are formed along discontinuities in the host rock, including steep hairline fractures, low-angle bedding and/or cross-bedding planes, from which chemical replacement diffused outward. With regard to their shape and stage of development the pockets are referred to as embryonic or incipient, nodular, orbicular (when zoned), or complex (Fig. 9.11B). The alteration-mineralisation associated with the pockets is highly variable. Tourmaline, ankerite, cassiterite and pyrite constitute the main mineral phases, and smaller quantities of chlorite, sericite, chalcopyrite and quartz are also present. Reddening (due to K-feldspar and hematite) of the host arkosic rocks may mark the site of an incipient pocket. The host rocks of the "tin zone" are extensively albitised.

Bedding-plane mineralisation is characterised by fine-grained concentrations of cassiterite, hematite, tourmaline, pyrite, chlorite and ankerite along bedding planes

Plate 9.3. Underground exposure of hydraulic breccia at Rooiberg

of the arkosic rocks. Bedded lodes are economically important and occur as sheet-like, conformable bodies of about 10 to 15 cm thickness. At Vellefontein the cassiterite-bearing bedded lodes are typified by spectacular hydraulic breccias (Plate 9.3), stockworks and stringers. A typical lode is composed of ankerite, tourmaline lenses and country rock fragments. Stringers are filled with carbonate, cassiterite, pyrite and chalcopyrite. Stear (1977) noted that the bedded lodes generally exhibit imperfect mineral banding, with relatively coarse cassiterite and orthoclase usually forming the margins of the lode. Various combinations of the gangue minerals – quartz, ankerite, pyrite, chalcopyrite, chlorite and hematite – constitute the bulk of the lodes. The conformable lodes are spatially related to the uncomformable orebodies. Steeply dipping fractures are characterised by alteration of the wall rocks and networks of tourmaline-rich, locally cassiterite-bearing, hairline fractures, (Rozendaal et al. 1986).

The Rooiberg mineralisation is generally regarded as the product of a granite-related hydrothermal system derived from the Lebowa Granite Suite rocks; in other words, a system not so dissimilar from that at Zaaiplaats, except that in the Rooiberg area the magmatic-hydrothermal fluids had access to the outside in what must have been a large, open system of fractures that probably extended down into the plutonic rocks to tap the magmatic-hydrothermal fluids. Repeated phases of fracturing, perhaps enhanced by the intruding granite, allowed the tapping of continually evolving fluids. Although the origin of the Sn is generally attributed to the Bushveld granitic rocks, it is possible that at least part of the Sn mineralisation may have been leached from the sedimentary and volcanic rocks traversed by the

fluids. This additional step in the formation and evolution of these deposits may well be a common factor in many cases of ore genesis often overlooked, or not seriously considered, by students of ore genesis.

9.4.3 Sn-W Mineralisation at Brandberg West, Damara Orogen, Namibia

Numerous Sn, Sn-W and W deposits are present within the late Proterozoic Pan African Damara orogen (see Chap. 7 for details). These deposits were studied by Pirajno and Jacob (1987) and Pirajno et al. (1987), who geographically grouped them into three major zones. The northernmost of these, in the Brandberg West-Goantagab area, is located in the northern coastal arm of the Damara orogen (Miller 1983). This area occupies the lower Ugab river region, northwest of the Brandberg granite ring-type complex, and extends in an east-northeast direction for some 80 km (Fig. 9.12). It is underlain by turbidite-facies metasediments with intercalated thin marble bands. These rocks are correlative of the Khomas Sub-group formations in the Central Zone of the Damara Orogen. The metasediments are intruded in the east by a large syn- to post-tectonic granitic mass of batholithic proportions. Smaller granite plutons intrude the area in a number of places.

Mineralisation in the Brandberg-Goantagab area is characterised by a number of Sn-W and Sn ($\pm$ Ag and base metals) deposits in quartz vein systems and Fe-rich replacement bodies. These mineralised systems clearly post-date Damara-age fabrics in the host rocks. The nature of the mineralisation suggests that the mineralised systems are related to underlying igneous intrusions. Circular structures, visible on LANDSAT imagery, are present in the area and are associated with quartz veins and, in places, breccias and thermally metamorphosed schists. In fact, at least 8 out of 16 mineral occurrences and deposits are located within or along the margins of these circular structures. The simplified geology of the Brandberg West-Goantagab area, the distribution of the main deposits and circular structures are shown in Fig. 9.12. It is, incidentally, of interest to note that the association of circular structures with mineralisation has been reported from many areas around the world (see, for example, Norman 1982, Chap. 7 and Fig. 7.10). Circular structures are common in the Hercynian orogenic areas in northern Portugal, where they also occur in turbiditic terranes intruded by granitic rocks, and are spatially associated with hydrothermal Sn-W mineralisation (Goinhas and Viegas 1983), such as Panasqueira to be discussed later. Apart from the spatial association, the precise nature of the relationship with the mineralisation is not known and can only be speculated at this stage. It is, however, possible to hypothesise that the circular structures and hydrothermal mineralisation are the effects of the same cause. Degassing of cooling, volatile-rich magma could initiate fracturing of the roof rocks, with the formation of pipe-like structures. All stages of degassing and associated structures may be considered, for example, from incipient to early stages of "pipe" formation with short and curved joints or fractures, to mature stages represented by well-defined ring features (Fig. 9.13). In the late stages of magma consolidation, hydrothermal activity would result in the movement of the fluids through the channelways provided by the ring fractures. The character of the

LEGEND

Sand Cover

Late Karoo Ring-type Complexes

Brandberg :   Doros:

KAROO
SEQUENCE   Lavas and   Breccia   Differentiated
             Sediments   Mafic Rocks
                              Alkaline-granite

                              Hornblende-granite

                              Lava

             Swakop Group   Igneous rocks

DAMARA   Ousis granite
SEQUENCE   Turbidite facies
             meta-sediments
             and marble bands Syn-late tectonic
                              granitoids

                              Mafic rocks

  Circular features

● Vein and/or replacement Sn-W or Sn deposit

▲ Sn ± Ta in Pegmatites

Fig. 9.12. Simplified geology of the Brandberg West-Goantagab area (Namibia), showing distribution of main Sn and Sn-W deposits and circular structures (After Pirajno and Jacob 1987)

hydrothermal Sn-W mineralisation of Brandberg West is consistent with a granitic source, and is most probably the result of greisenisation phenomena related to a hidden granitic cupola at depth. On the basis of Fe/Mg ratios of tourmaline, this
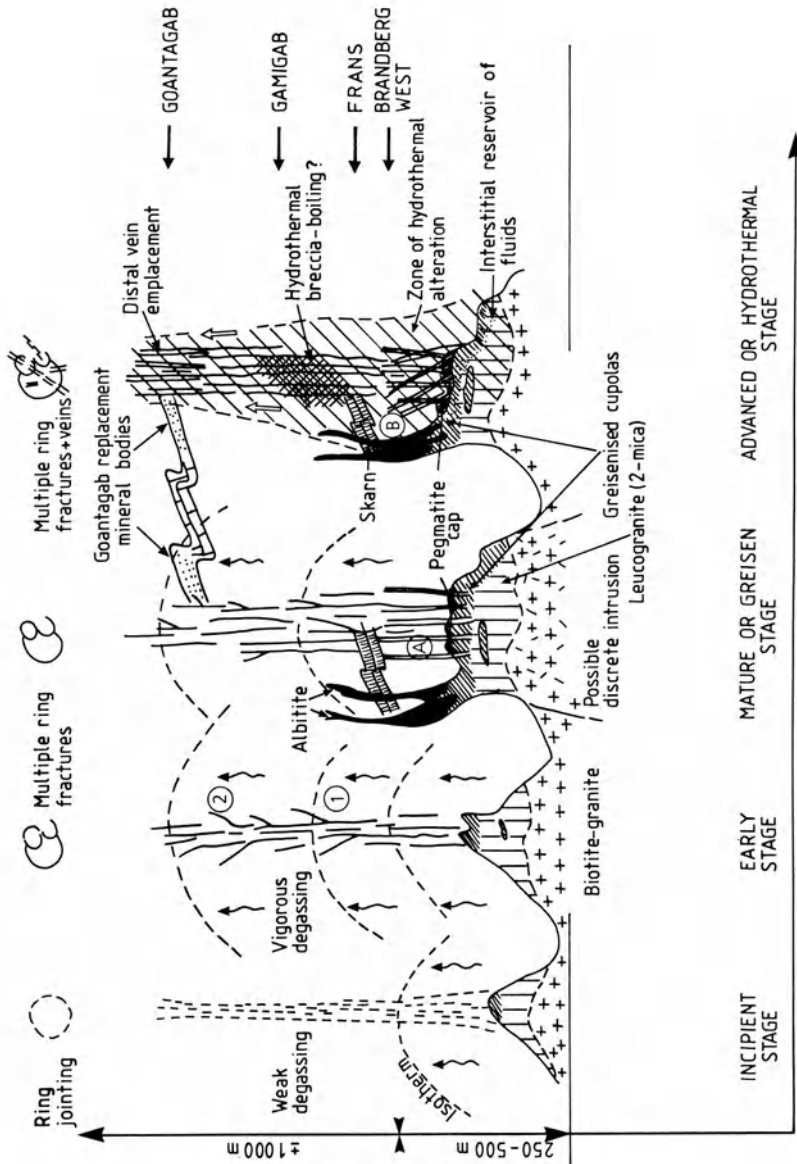
Fig. 9.13. Proposed model to explain the generation of ring structures and Sn-W hydrothermal vein mineralisation in the Brandberg West-Goantagab area. Volatile-rich granitic cupolas intrude the metaturbidite country rocks. Stages of degassing and alteration-mineralisation range from incipient through to advanced (*left* to *right* in the figure), inducing curved fractures and jointing, which in turn result in pipe-like structures, manifested at the surface as variably developed ring fractures. These structures provide the channelways for the mineralising fluids and the subsequent emplacement of vein systems. Brandberg West, Frans, Gamigab and Goantagab are the four main deposits in the area, each showing features which suggest different levels of emplacement above the respective granitic cupolas. *1* and *2* are the cordierite and biotite boundaries of thermal metamorphism respectively. *A* and *B* represent the two alteration-mineralisation events at Brandberg West (greisen and quartz-
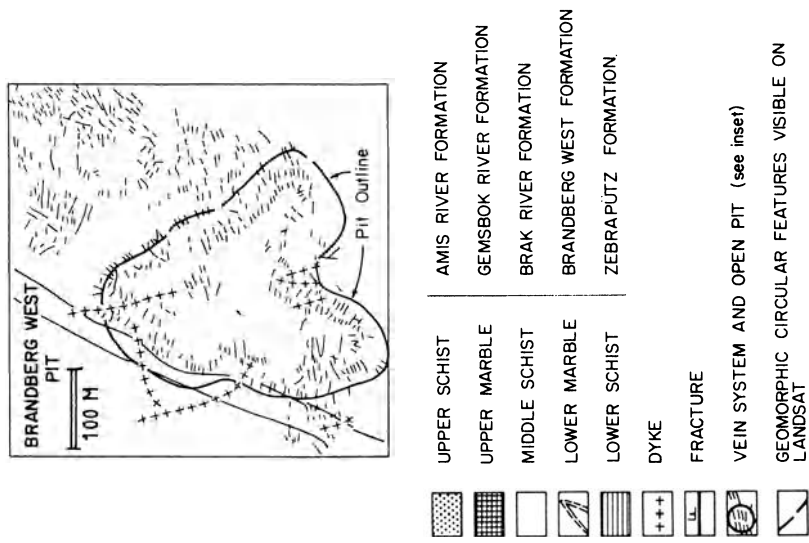
Fig. 9.14. Simplified geological map of the area around Brandberg West, showing the minearilised vein system (After Pirajno et al. 1987)
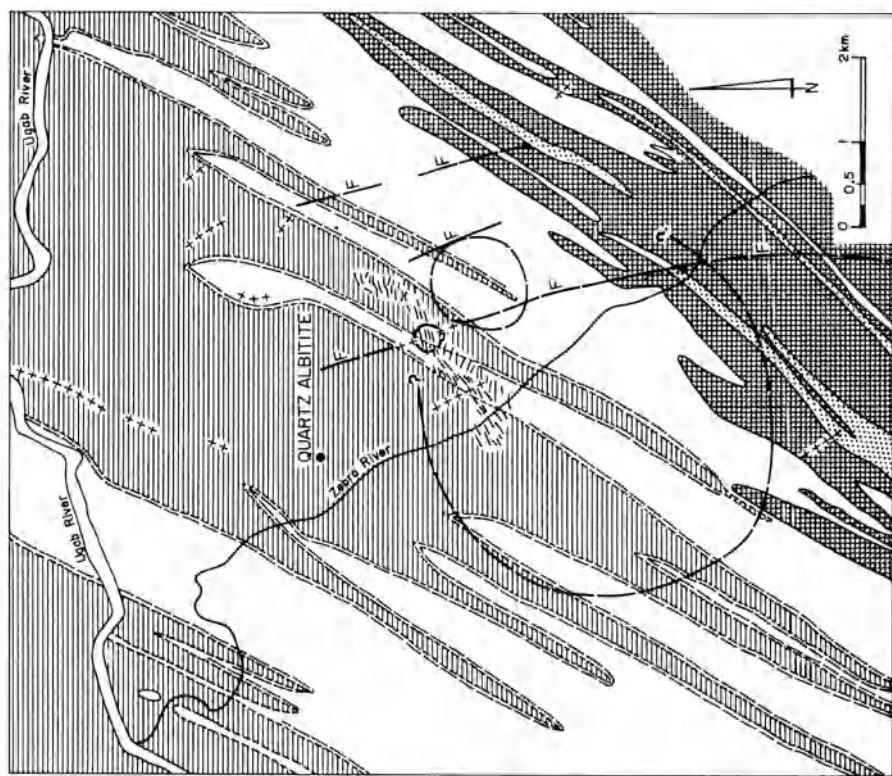
Plate 9.4. Quartz veins cutting across quartz-biotite schist rocks and terminating against the base of overlying marble beds; Brandberg West area, Namibia

mineralisation is considered to be proximal (high Fe/Mg) with respect to other similar occurrences to the east (lower Fe/Mg ratios) (Pirajno and Smithies in press). Figure 9.13 illustrates the model envisaged for the genesis of the circular structures and the Sn-W deposits of the Brandberg West-Goantagab area.

The Brandberg West Sn-W mineralisation is hosted in a number of quartz-vein systems that extend for at least 4 km in a general northeast direction (Fig. 9.14). Mining was carried out as an open-cast operation from 1957 to 1980, during which time some 12 000 tonnes of concentrate were produced, grading about 32% Sn and 19% WO_3. The main lithologies in the area consist of two schist units (Zebraputz and Brak River Formations), separated by a marble unit (Brandberg West Formation; see Fig. 9.14). The base of the sequence is the Zebraputz Formation, also known as Lower Schist, which consists of quartz-biotite schists with minor calc-silicates and quartzite layers. The overlying Brandberg West Formation is represented by the Lower Marble, whereas the Brak River rocks are mainly metagreywacke. In the area surrounding the open pit, the mineralisation is primarily associated with a sheeted vein system (see inset of Fig. 9.14) that can be traced for some 900 m and is about 300 m wide. The quartz veins generally occur in the quartz-biotite schist of the Zebraputz Formation, most of them terminating against the overlying marble unit of the Brandberg West Formation (Plate 9.4). The veins have variable strikes, lengths and thicknesses, and were formed during at least three pulses of ore-bearing fluids and related alteration stages. The vein mineralogy is also varied and complex, quartz being the main vein constituent (70 to 95%), which is usually fractured and accompanied by muscovite, K-feldspar, tourmaline,

QUARTZ–
VEIN

REFERENCE

MUSCOVITE SELVAGE
TOURMALINE – QUARTZ GRAPHITE
MUSCOVITE – QUARTZ
BIOTITE PORPHYROBLASTS
QUARTZ – BIOTITE – CHLORITE SCHIST
CASSITERITE
WOLFRAMITE
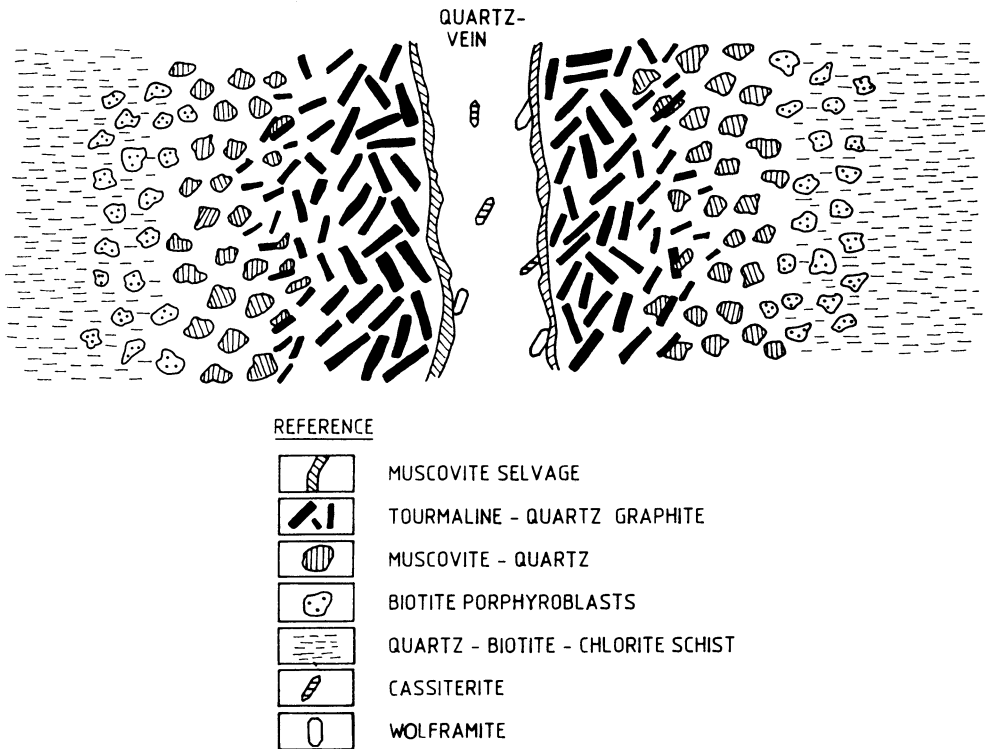
Fig. 9.15. Diagrammatic representation of the hydrothermal alteration of the quartz-biotite schist adjacent to a mineralised quartz vein at Brandberg West. The biotite porphyroblasts are interpreted as a stage of K-metasomatism, whereas the vein selvage formed by muscovite and the muscovite-quartz assemblage in the wallrock are part of the greisen stage

fluorite, graphite, beryl, apatite, cassiterite, wolframite, scheelite, hematite and sulphides (mainly chalcopyrite and pyrite). A typical ore-bearing quartz vein is usually, though not always, bounded by a selvage zone, up to 0.2 m wide, of quartz + muscovite (greisen). Fluorite, topaz, hematite, graphite and cassiterite may also be present. The greisen selvage zone grades into the wallrock through a tourmaline-rich zone. A diagrammatic representation of a quartz vein and the accompanying wall rock alteration is shown in Fig. 9.15. Based on mineralogical, petrological and geochemical studies (Pirajno et al. 1987), a tentative sequence of alteration-mineralisation events can be summarised as follows (see also Fig. 13):

1. Thermal metamorphism is induced by hidden granitic cupolas. Effects of this metamorphism can be seen in the "spotting " of the schist rocks in the area.
2. K-metasomatism, manifested by fracture-controlled development of biotite porhyroblasts (see Fig. 9.15).
3. Greisen stage, characterised by quartz-muscovite ± tourmaline along the same fractures (see Fig. 9.15).
4. Formation of ore-bearing veins (cassiterite ± wolframite).

5. Extensional tectonic event with intense fracturing and dyke emplacement along E-W trends (see Fig. 9.14).
6. Renewed hydrothermal activity, characterised by intense H^+ ions activity and resulting in quartz-sericite alteration, re-opening of the earlier quartz veins, dissemination of cassiterite and fluorite particularly near and along the marble-schist contact and in the marble rocks. Deposition of sulphide minerals also took place during this stage.
7. A concluding stage of hematitisation and carbonate alteration followed, possibly as the result of opening of the system to oxidising meteoric fluids.

The extent of the Brandberg West vein systems indicates that hydrothermal activity was operative on a large scale. The northeast-trending vein system transgresses the lithologies, and was mainly formed by the action of greisenising fluids which were controlled by the intersection of a north-northwest-trending fracture with a circular structure (Fig. 9.14) as well as the marble band which acted as a barrier to the fluids. The greisenising fluids most probably emanated from one or more granitic cupola at depth.

9.4.4 Endo- and Exogreisen Sn Mineralisation at Mount Bischoff, Tasmania

The Mount Bischoff Sn deposit is located in the Waratah district in northwest Tasmania (Australia; Fig. 9.16). From 1872, when the mineralisation was first discovered, up to 1955, about 55000 tonnes of Sn metal were produced from about 5.5 million tonnes of ore, at an average grade of 1.4 %Sn. The published works of Groves and Solomon (1964), Groves et al. (1972), Orr (1977), and Wright and Kwak (1989), augmented by personal observations taken during a drilling programme in the old mine area (Pirajno, unpubl. data 1974), constitute the data base from which the following account is taken.

The Mount Bischoff area is underlain by a sedimentary sequence of Upper Precambrian age, forming an inlier within rocks of the Dundas Trough (Fig. 9.16A). The Precambrian rocks form an anticlinal structure, whose flanks are overlain by Cambrian sediments, in turn overlain by flat-lying sediments and mafic volcanics of Tertiary age. The Mount Bischoff inlier is located between two major Precambrian structural units: the Rocky Cape nucleus to the northwest, and the Tyennan nucleus to the southeast (Fig. 9.16A). Flanking the Tyennan nucleus towards the Mount Bischoff side is the Mount Reid volcanic arc, which is in turn flanked by the Dundas Trough, believed to represent an accretionary prism related to a subduction zone. In the area of the deposit, the stratigraphic sequence from the base upward consists of interbedded shales and sandstones (footwall rocks), followed by a sequence of massive to finely bedded and fine-grained dolomitic rocks (Mount Bischoff dolomite), overlain by interbedded carbonaceous shales, siltstones and sandstones (hangingwall rocks). The Mount Bischoff Sn deposit is characterised by both endo- and exogreisen mineralisation related to granitic intrusives of Devonian age (Meredith Granite Batholith). The adjacent areas, within a radius of about 2 km, contain hydrothermal deposits of Pb-Zn, Pb-Zn-Sb, and Zn-Sn-F, and it is possible
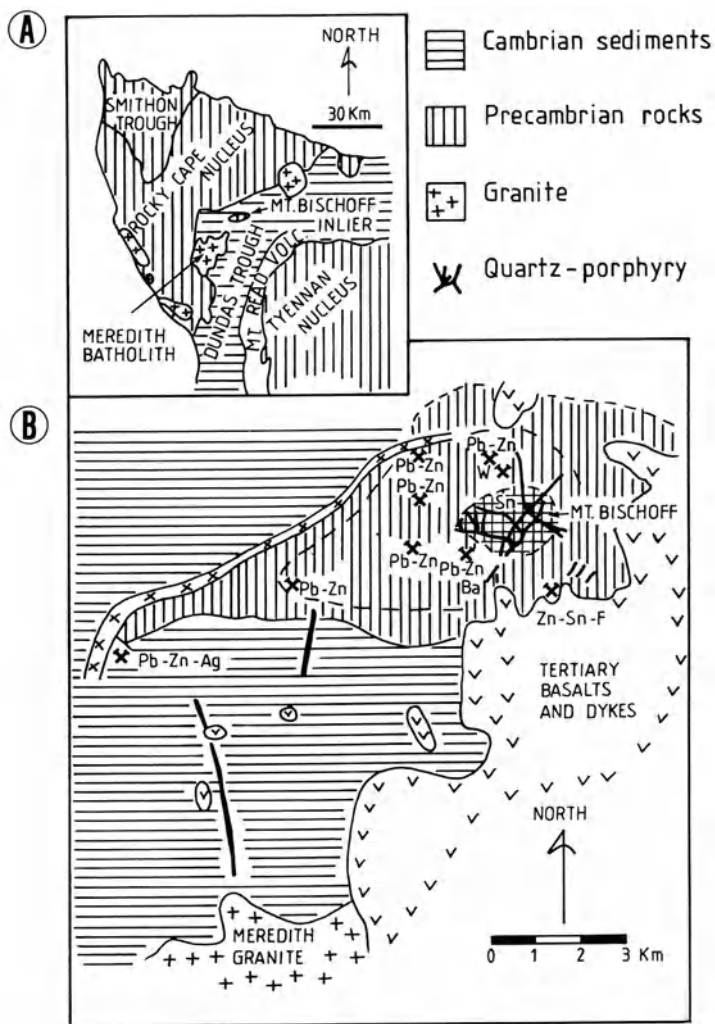
Fig. 9.16. A Geotectonic setting and **B** simplified geological map of the Mount Bischoff area, showing location of mineral deposits (After Orr 1977; Groves and Solomon 1964; Wright and Kwak 1989)

that these are genetically related to the same regional mineralising system that gave rise to the Sn mineralisation at Mount Bischoff. If so, the distribution of these metal deposits may correspond to a regional zoning pattern centred around Mount Bischoff (Fig. 9.16B).

The Meredith Granite Batholith intruded the Precambrian and Cambrian sedimentary rocks along the western side of the Dundas Trough between 350 and 360 Ma ago (end of the Devonian). The Meredith granite covers an area of about 300 km^2, from the vicinity of Renison Bell in the south to within 3.5 km of Waratah. The
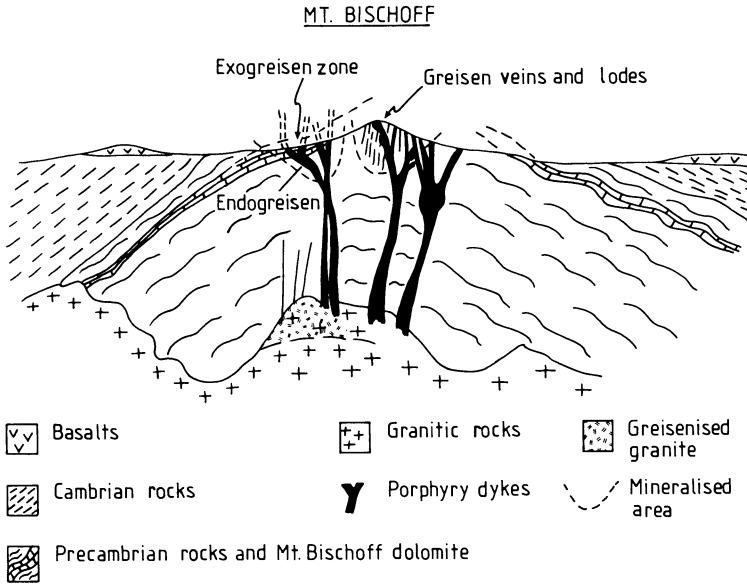
MT. BISCHOFF

Fig. 9.17. Schematic cross-section of the Mount Bischoff area, showing relationship between porphyry dykes and exogreisen mineralisation, and postulated parent cupola. Although not to scale, the depth to the roof of the cupola is thought to be in the order of 1–2 km (After Groves and Solomon 1964; Wright and Kwak 1989)

batholith is of adamellitic composition, having approximately equal amounts of K-feldspar and plagioclase. A modal analysis by Groves and Solomon (1964) gave the following: total feldspar 54.5%, quartz 36.1%, biotite 9%, accessories 0.5%. In the accessory components are included zircon, topaz and tourmaline. The intrusion of the batholith resulted in the emplacement of a number of leucogranite cupolas, one of which is believed to be emplaced at depth below Mount Bischoff into the hinge of the anticlinal structure. It is postulated that quartz-porphyry dykes emanated from the cupola to intrude along tensional fractures (Fig. 9.17). The Mount Bischoff quartz-porphyry dykes, which are about 349 Ma old, are from 5 to 30 m wide and up to 1300 m long. They are preferentially orientated along east-west, northwest and northeast trends. Unaltered dykes contain about 25% quartz, 14% orthoclase, 59% groundmass (orthoclase + quartz + plagioclase) and 2% muscovite. Biotite and tourmaline may also be present.

Mineralisation is associated with the intense greisenisation of both the quartz-feldspar dykes and the Mount Bischoff dolomite, forming endogreisen and exogreisen respectively. Early studies of the Mount Bischoff mineralisation (see Groves and Solomon 1964) subdivided the mineralisation into three types according to the host lithologies. They are: dolomite-ore, quartz-porphyry-ore and ore in the highly contorted shale and siltstones, known as rheomorphic sediment ore, in proximity of the porphyry dykes. In addition, vein-type mineralisation is present and is related to fractures that cut through all lithologies. This is generally a late mineralising event, post-dating the greisen mineralisation. Vein fillings vary
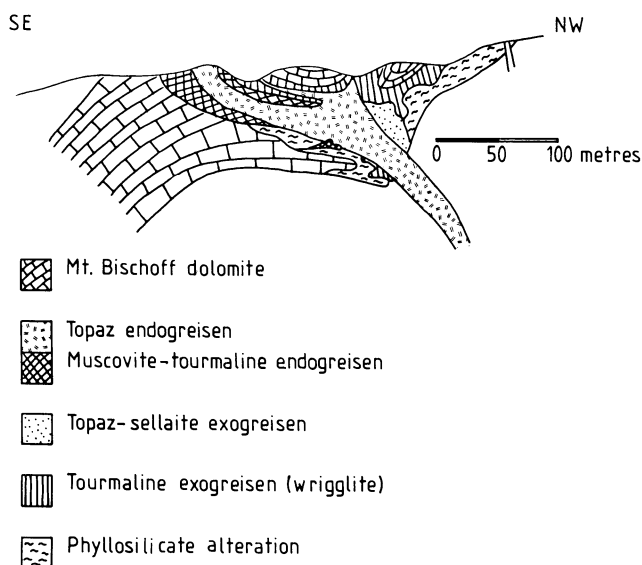
Fig. 9.18. Generalised cross-section of the Mount Bischoff deposit, showing distribution of greisen alteration (After Wright nd Kwak 1989)

considerably, with some common assemblages consisting of quartz + cassiterite, quartz ± tourmaline or topaz, quartz + pyrite + topaz + fluorite + carbonate + sulphides and cassiterite. Veins have been traced for up to 750 m and are from 0.5 to 1 m thick. The greisen phase of alteration was accompanied by cassiterite and minor wolframite mineralisation, and followed by a post-greisen phase of phyllic-type alteration, accompanied by abundant sulphide mineralisation. The distribution of the greisenised rocks is shown in Fig. 9.18. The altered quartz-porphyry (endogreisen) is characterised by three main mineral assemblages (Wright and Kwak 1989), whose chief components are: (1) muscovite + quartz + fluorite + tourmaline ± sphalerite; (2) quartz + topaz ± fluorite ± cassiterite and (3) quartz ± topaz or fluorite. The endogreisen assemblage (2) also contains rare Mg-Na-Al fluoride species, such as sellaite (MgF_2), whereas assemblage (3) is quartz-rich.

The endogreisens were formed through the action of acid fluids, by dissolution and replacement of the quartz and K-feldspar from the dyke material. This acid dissolution, also postulated for the Bobbejankop Granite at Zaaiplaats, created enough permeability to facilitate penetration of the solutions through the dyke rock. The sulphide minerals overprint the greisen assemblages, and, as already mentioned, were precipitated during a post-greisen stage of phyllic alteration, characterised by the incoming of phyllosilicates such as chlorite, and clay minerals in addition to the sulphides. Sulphide minerals include pyrrhotite, arsenopyrite, chalcopyrite, stannite, pyrite, marcasite and bismuthinite.

The exogreisen is developed by the replacement of the dolomitic rocks in contact with and adjacent to the greisenised dykes, as shown in Fig. 9.18. Wright and Kwak (1989) recognise two main exogreisen assemblages: (1) quartz + sellaite + topaz +

cassiterite ± fluorite or pyrrhotite; and (2) tourmaline + sellaite + fluorite + quartz ± cassiterite, phlogopite or hambergite [$Be_2BO_3(OH)$]. The first greisen assemblage (also known as topaz exogreisen) is found in close spatial association with the greisenised dyke. Cassiterite is particularly abundant at the endogreisen-exogreisen contact. Sulphide minerals associated with the topaz-exogreisen are pyrrhotite, arsenopyrite, chalcopyrite, stannite, pyrite, bismuthinite, marcasite and native bismuth. Talc, chlorite and phengite replace the greisen mineralogy and are part of the post-greisen phyllic alteration phase. The second exogreisen assemblage (also called tourmaline exogreisen) surrounds the topaz-exogreisen and is mainly formed by tourmaline + sellaite + fluorite + pyrrhotite, cassiterite, or, quartz and sellaite + pyrrhotite ± cassiterite, fluorite or tourmaline. The tourmaline-greisen is also characterised by a texture known as " wrigglite" which is a fine-scale layering (or banding) that occurs as a result of alternating mineralogies (see also Chap. 10). The tourmaline exogreisen is overprinted by pyrrhotite, talc, phengite, siderite and fluorite, as part of the post-greisen phase of alteration.

A more recent model proposed for the genesis of the mineralisation at Mount Bischoff is that of Wright and Kwak (1989). They envisage that the porphyry dykes acted as the main conduit for the hydrothermal solutions, possibly emanating from both the postulated underlying leucogranite cupola (fragments of leucogranite are found in the dykes) and the dykes themselves. Fluid inclusion studies conducted by Wright and Kwak (1989) indicate that the greisenising fluids had a high salinity (between 40 and 30% of total dissolved salts), with temperatures ranging from about 420 to 340 °C. The greisen fluids were chloride-rich and contained Si, F, B, K, Na, Ca, Mg, Fe, Sn. The temperatures of the post-greisen fluids were in the range of 190 to 120 °C.

In the dykes the solutions boiled and moved into the dolomitic rocks, creating a network of hydrothermally induced fractures and forming the exogreisen assemblages. The authors further envisage that concentrated residual fluids derived from boiling replaced the dolomite with B-rich minerals and gave rise to the observed wrigglite textures. The temporal evolution of the hydrothermal solutions led to a reduction in both temperature and acidity, and produced the post-greisen assemblages. The Sn mineralisation is regarded as a consequence of the neutralisation of the solutions by the dolomite rock with consequent destruction of the topaz phase and deposition of cassiterite.

9.4.5 The Hercynian Sn-W Deposits of Southwest England, Cornwall and Portugal

The Hercynian fold belt of Western Europe marks the site of a major convergence between two continental plates that took place from the Late Devonian to the Upper Permian (a time span of about 150 Ma). The vast amount of geological information accumulated for Western Europe is distributed in many journals, and written in many languages, making the integration of existing knowledge a daunting task. To compound the problem, many areas of the Hercynian belt in Europe have either been covered by younger rocks, or have been re-activated during the Alpine orogeny from the Triassic to the present. The interested reader is advised to consult
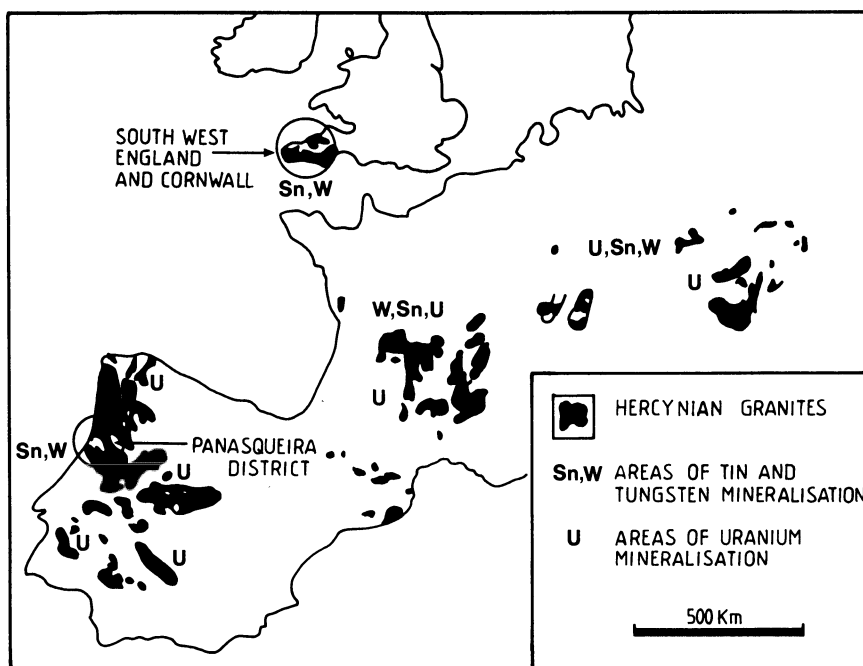
Fig. 9.19. Distribution of Hercynian granitic rocks in Western Europe and associated Sn, W and U metallogeny (After Stemprok 1981; Cuney 1978)

Ellenberger and Tamain (1980), Behr et al. (1984), Lorenz and Nicholls (1984) and Windley (1984), for overviews of the Hercynian events. For the present purpose it is important to stress that Sn-W, as well as U, deposits formed during the Hercynian orogeny are primarily associated with late to post-orogenic batholiths generated during the collisional phases of the geodynamic evolution of the belt (Fig. 9.19).

The Hercynian batholiths consist of calc-alkaline granitoids with associated porphyry feeder dykes and rhyolitic lavas. An important period of granite emplacement appears to have been between 330 and 280 Ma ago. An assessment of much of the major and trace element geochemical data led Floyd et al. (1983) to conclude that the bulk of the Hercynian granitoids were derived from anatexis of lower crustal material, in particular widespread melting of poorly hydrated garnet-bearing granulite which produced large volumes of essentially dry granitic magma. Subsequently, through the assimilation of wet country rock, this magma became water-saturated and crystallised below the surface to form the granite batholiths. The range of compositions seen in individual plutons is explained by local, but minor, variations in source rock composition and/or the degree of melting, together with later differentiation and metasomatism (Floyd et al. 1983). In general the granites have a restricted compositional range, high K/Na ratios, low Fe_2O_3/FeO ratios, and high to intermediate Sr isotope ratios, and a deficiency in hornblende, sphene and magnetite. Therefore the Hercynian granitoids have S-type and/or ilmenite-series affinities. In Southwest England and Cornwall, the granitic rocks are

probably related to collision tectonics, whereas elsewhere in Western Europe it appears that thrust tectonics of the Himalayan type provided the necessary environment to generate granites.

Southwest England and Cornwall

This area, which is along the northern boundary of the Hercynian fold belt, and known as the Cornubian tin field, occupies an area of some 3800 km^2 and coincides with the Cornubian granite batholith (Moore 1982; Fig. 9.20). The area has produced over 2 million tonnes of Sn, 1.3 million tonnes of Cu, 350000 tonnes of Pb, 250000 tonnes of As and 1200 tonnes of W, in addition to minor quantities of Zn, Au, Ag, Sb, U, Ni, Bi, Mo, F, Ba, Sb and Co. Relevant literature includes Jackson (1979), Jackson et al. (1982) and Moore (1982).

The mineralisation is spatially related to the roof and border zones of a series of high level, post-tectonic granitic plutons belonging to the Cornubian batholith and emplaced within turbidite-type metasediments, known locally as "killas". The intrusion of these granites was accompanied by a period of hydrothermal alteration and mineral deposition during which quartz veins containing ores of Sn, Cu, Pb, Mo, As and W were formed. At least six major and several minor masses of granite are discernible, which were emplaced passively by cauldron subsidence and block stoping, and partly by forceful injection. The plutons are composite in nature, roughly circular or ellipsoidal in shape, and have sharp and discordant contacts with the surrounding country rocks. The age of emplacement is 300–260 Ma, with a Rb/Sr isochron of 285 ± 12 Ma. The main stage of mineralisation, which was late (about ± 270 Ma), was associated with pegmatitic veins and granite porphyry dykes. Major fracture systems developed in the roof and margins of the principal intrusions as a result of superimposed hydraulic and existing stress fields, soon after batholith emplacement. These fracture systems controlled the movement of the hydrothermal
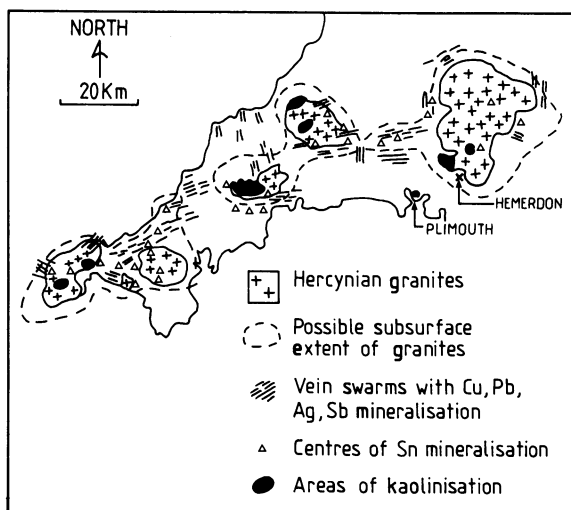
Fig. 9.20. Distribution of granitic rocks and related mineralisation in Southwest England and Cornwall (After Moore 1982)

fluids. Thus vein and fissure systems, together with irregularly shaped replacement deposits of Sn, W, Cu, As ± Pb and Zn, are formed. The distribution of the Sn mineralisation is shown in Fig. 9.20. The above-mentioned mineralisation styles characterise four principal geological environments, namely:

1. Roof of the intrusion: sheeted vein systems, fissure veins, replacement bodies of quartz and tourmaline with cassiterite, wolframite, pyrite, chalcopyrite and arsenopyrite. Intense greisenisation and vein-controlled phyllic alteration.
2. Flank of the intrusion: important for mineralised fissure systems. These are typified by fissure veins with complex multi-stage parageneses of quartz, cassiterite, sulphides with polyphase phyllic, chloritic, tourmaline and feldspathic alteration haloes.
3. Granite contacts: these are important for fissure veins, stockworks and replacement bodies.
4. Outer aureole: areas 2000 to 200 metres outside the granite contacts host mineralised fissure systems with cassiterite, sulphides, tourmaline and phyllic alteration haloes.

Mineral zoning within the vein systems can be very complex, as minerals may have been repeatedly emplaced in some vein systems at different structural levels, with earlier ores being commonly re-mobilised by later hydrothermal fluids. Despite the complexity, a sequence of alteration events can be summarised as follows. Alkali metasomatism (magmatic-hydrothermal fluids), consisting of K-metasomatism followed by Na-metasomatism (albitisation), occurred within and at the margins of the granites. This phase was followed by acid metasomatism (H^+ ion), resulting in greisen development, and by phyllic or sericitic alteration in the more advanced stages. Tourmalinisation was a very important process. Tourmaline replaces the feldspars and biotites and locally overprints the sericitic alteration. Tourmalinisation and silicification are commonly linked. Figure 9.21 depicts the possible sequence of alteration-mineralisation events related to a granite pluton. Isotopic evidence indicates that the hydrothermal circulation was dominated by meteoric waters, and followed a phase of separation by second boiling of hydrous fluids from the plutons, resulting in the fracturing along the flanks of the intrusion. Fluid inclusion studies indicate that the fluids had moderate to low salinities (10 to 20 wt.% NaCl equivalent) and temperatures ranging from 280 to 480°C.

An outstanding example of an endogreisen system is that of the Hemerdon W deposit. "Hemerdon Ball" is a 215 m-high hill about 2 km east-northeast of the city of Plymouth in Southwest England (Fig. 9.20). Mining records in this area date back to the 16th century, and by the 19th century five mines were operating within 3 km of the Hemerdon township. Sn, Cu and Pb were all produced from vein deposits. Since the discovery of China clay deposits (kaolinised granite) around Hemerdon in the 19th century, clay has been extracted almost continuously to the present day. The presence of wolframite at Hemerdon was discovered in 1867, and the deposit was mined during the two World Wars with a total production of about 220000 tonnes of ore. Exploratory drilling from 1977 to 1979 outlined about 45×10^6 tonnes of ore grading 0.17% WO_3 and 0.025% Sn (Mining Magazine 1979). The mineralisation (Pirajno unpubl. data and Hemerdon mine geologists) is contained within a dyke-
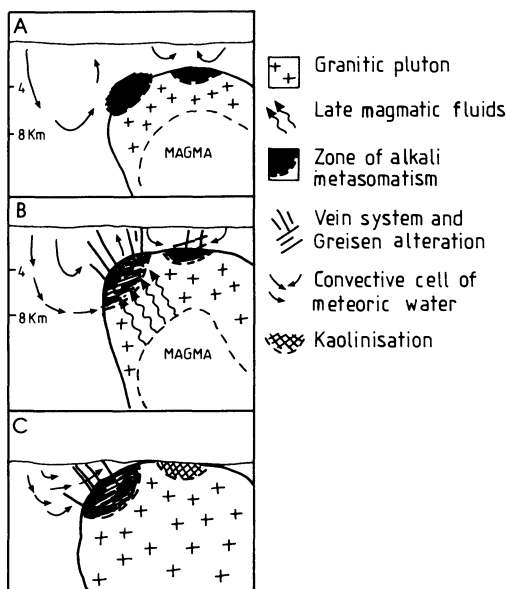
Fig. 9.21A–C. Evolutionary sequence of pluton emplacement, greisen alteration and vein minerali-
sation, as envisaged by Moore (1982). **A** Emplacement of pluton and alkali metasomatism in flank
and roof zones during Permo-Carbonifeorus times. **B** Situation some time later, following influx of
late-magmatic fluids in the flank zone towards an area where a fracture system developed. Meteoric
waters percolate down, leach and transport Sn and other metals. **C** During Late Cretaceous and
Tertiary hot and humid climate, favoured deep weathering which formed the renowned "China-
clay" deposits of this region. Possible rejuvenation of the mineralised vein system as a consequence
of the circulating meteoric waters may also have taken place

like granitic body protruding from the Hemerdon Ball granite outcropping on the
southern flank of the larger Dartmoor granite, to which it is probably connected.
These granites belong to the Cornubian batholith referred to earlier, and intrude
metasedimentary rocks and altered volcanics (killas). It is thought that many of the
granite bodies in the area are connected below the killas, which are, therefore, in
most cases considered as roof pendants. The mineralised granite dyke has a
northeast trend, is approximately 650 m long and 120 to 150 m wide, and is entirely
emplaced within killas country rocks, represented by metamorphosed turbidite
sediments of Devonian age. The granite dyke is made up of K-feldspar, plagioclase,
quartz, biotite and Li-rich muscovite. Sericite, chlorite, kaolinite and illite are
alteration products replacing the primary mineral assemblage. This altered granite
is traversed by three mineralised sheeted vein systems, which locally transgress into
the surrounding metasediments. The latter are tourmalinised, contain hematite and
are intensely fractured. The vein systems have the following attitude and character-
istics:

1. 060° strike, northwest dip – quartz + greisen border
2. 045° strike, 60–70° northwest dip – quartz (no greisen border)
3. 021° strike, vertical dip – quartz + feldspar

Table 9.6. Geochemistry of vein-free granite at Hemerdon.
All values in parts per million (ppm) (Pirajno unpubl. data)

	Range
Sn	30– 70
W	40– 260
As	110– 150
Li	170– 310
F	1700–4300

Wolframite is the main ore mineral, and there are minor quantities of cassiterite and arsenopyrite. The cassiterite tends to occur within the greisenised borders of the quartz veins, and is possibly the earliest ore mineral. This is followed by deposition of quartz + feldspar with wolframite. Minor amounts of pyrite, molybdenite, fluorite and arsenopyrite occur in the southern region of the granite dyke.

Metal and trace element range of values for vein-free granite are given in Table 9.6.

The Panasqueira Sn-W Deposit, Portugal

The Panasqueira Sn-W deposit is situated about 60 km east of the university city of Coimbra, in the Beira Baxia province. Mining in the area dates back to Roman times, but W mineralisation was discovered in 1886. The production of W concentrates from Panasqueira between 1927 and 1976 was about 13 500 tonnes. In 1978 the Panasqueira mine, which is the largest producer of W in Western Europe, produced 1450 tonnes of W concentrate (75% WO_3), 62 tonnes of Sn concentrate (75% SnO_2) and 1100 tonnes of Cu concentrate (22% Cu).

The Panasqueira mining district lies along the southern border of Hercynian granitoids within the so-called Luzo-Oretan geotectonic zone of the Iberian Meseta (Ellenberger and Tamain 1980; Fig. 9.19) The Luzo-Oretan zone is characterised by a substratum of Lower Paleozoic sediments which were subjected to folding and low-pressure metamorphism during early compressive stages of the Hercynian orogeny. The original lithologies in the Panasqueira district were argillites, greywackes and sandstones. Regional metamorphism converted these sediments into biotite-chlorite schist, phyllite and quartzite, grouped under the name of Beira Schists. Thermal contact metamorphism, associated with the emplacement of the Hercynian granites, produced a regionally extensive aureole characterised by "spotting" in the schist rocks. The spots are best developed in the more aluminous units, such as the metapelites, and consist of biotite and chlorite, with lesser cordierite and chiastolite. Calc-alkaline granodioritic to granitic rocks, which are part of the great Hercynian batholith, extend in an arcuate belt from northwestern Portugal, through central Portugal and across to western Spain as far as Segovia. This magmatic event is linked with some of the most important metallogeneses in Europe, including, as well as Sn-W, Cu, Pb-Ag and Pb hydrothermal vein-type deposits (Ziserman et al. 1980).
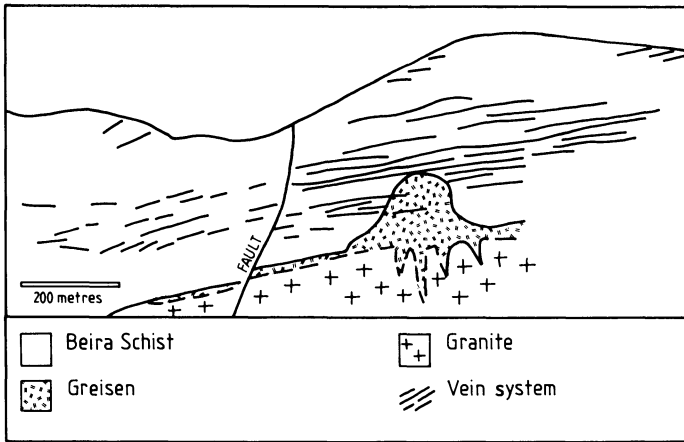
Fig. 9.22. Cross-section of the Panasqueira deposit, showing greisenised granite cupola and attendant subhorizontal vein system (After Oosterom et al. 1984)

Mineralisation in the Panasqueira area is typically of greisen affiliation, probably related to a non-outcropping greisenised granite cupola. A vivid description of the Panasqueira deposit is provided by the closing paragraphs of a pamphlet published by Beralt Tin and Wolfram Ltd. to commerate the 50th anniversary of the company. On page 18 one reads "profitable mineralisation is contained in a sandwich 50 to 60 metres thick, dipping on average 10°, and containing some half dozen irregular and thin veins, of which rarely more than two are payable in any vertical section. Yet this sandwich has a length on the strike varying from half a kilometre at the surface outcrop to a kilometre at places in depth, while the deepest workings are now over two kilometres distant downdip from the surface. Something of the order of 25 millions tonnes of rock has been broken to date". Whilst the general features of the Panasqueira mineralisation are much like other greisen-affiliated hydrothermal vein deposits, it has some unique characteristics the most conspicuous of which is the flat, or nearly flat-lying, attitude of its vein system (Fig. 9.22). An outstanding paper by Kelly and Rye (1979) comprehensively describes the geology of the Panasqueira deposit and reports on the result of detailed studies of fluid inclusions and isotopic work. Other papers dealing with the subject are Kelly (1977) and Oosterom et al. (1984).

The mineralised veins of the Panasqueira deposit range in thickness from a few millimetres to 1 m and can be traced laterally for up to 100 m. As already mentioned, the veins occupy nearly horizontal joint fractures and form a mineralised package over a vertical zone from 100 to 300 m thick. It is thought that the horizontal pre-ore joints were formed by decompression due to erosional unloading. The fissures were occupied by the hydrothermal fluids and opened by hydraulic pressure. The quartz of the vein is coarse-grained and attributed to the slow rate of nucleation, due perhaps to a low degree of saturation of the hydrothermal solutions. The vein system is linked at a depth of about 220 m below the surface, with a greisenised granite cupola. This cupola was probably emplaced through magmatic stoping of

the country rocks, as numerous angular fragments of the hornfelsed schists occur within this granite. The cupola consists of a porphyritic biotite-muscovite granite with K-feldspar megacrysts up to 1 cm long. The porphyritic texture tends to disappear upward and the granitic rock grades into an equigranular endogreisen (quartz + muscovite). A quartz cap occurs at the apex of the cupola (Fig. 9.22), and is interpreted by Kelly and Rye (1979) as a hydrothermal filling of a void formed during contraction of the granitic magma while still in the molten state.

Minerals present in the veins include Fe-rich wolframite (ferberite), arsenopyrite, pyrite, pyrrhotite, sphalerite, molybdenite, cassiterite, scheelite. Numerous other mineral species are present such as oxides, tungstates, carbonates, silicates and even phosphates. Zoning of the ore minerals within the veins is as follows (Kelly and Rye 1979):

1. An inner wolframite + cassiterite zone close to the cupola.
2. An intermediate zone of wolframite mineralisation overlying zone 1 and extending radially outward.
3. An outermost zone of second generation wolframite + cassiterite.

According to Kelly and Rye (1979), the mineralisation sequence in the veins can be subdivided into four main stages:

1. Oxide-silicate stage: quartz, muscovite and tourmaline; accompanied by the main ore minerals, wolframite and cassiterite ± arsenopyrite. Economically, the oxide-silicate stage is clearly the most important since it includes the ore minerals as well as most of the quartz, which comprises 90% of the vein material. Within this stage two substages are recognised. The early muscovite-rich vein selvage, containing minor amounts of tourmaline, cassiterite, topaz and arsenopyrite, and the vein-filling substage, comprising most of the coarse-grained quartz, muscovite wolframite and arsenopyrite.
2. Main sulphide stage: arsenopyrite, pyrite, pyrrhotite, sphalerite, chalcopyrite and stannite. Apatite is also present.
3. Pyrrhotite alteration stage: siderite and marcasite are the main minerals. Minor quantities of sphalerite and pyrite may also occur.
4. Late carbonate stage: dolomite and calcite are the main minerals of this stage. Sulphides may also be present.

Fluid inclusion studies indicate that the mineralising solutions were NaCl-dominated aqueous brines of moderate salinity (5 to 10 wt.% NaCl equivalent), with temperatures in the range of 230 to 360°C. During the late carbonate stage, the temperature of the fluids dropped from 120 to 70°C with salinity values below 5 wt.% NaCl equivalent. $\delta^{34}S$ values of the sulphide minerals from the first three stages fall within a narrow range (−0.1 to −0.9%). These are interpreted to indicate an H_2S-dominated hydrothermal solution of magmatic origin (Kelly and Rye 1979).

References

Barsukov V L (1957) The geochemistry of tin. Geokhimiya 1:41–53

Behr H H, Engel W, Franke W, Giese P, Weber K (1984) The Variscan belt in central Europe: main structures, geodynamic implications, open questions. Tectonophysics 109:15–40

Beus A A, Zalashkova N Y (1964) Post-magmatic high temperature metasomatic processes in granitic rocks. Int Geol Rev 6:668–681

Burt D M (1981) Acidity-salinity diagrams – Application to greisen and porphyry deposits. Econ Geol 76:832–843

Coetzee J (1986) The Lease Granite – a granophyric, miarolitic mineralized granite at the apical region of a tin-tungsten system. Trans Geol Soc S Afr 89:335–345

Crocker I T (1979) Metallogenic aspects of the Bushveld granites: fluorite, tin and associated rare metal-carbonatite mineralisation. Geol Soc S Afr Spec Publ 5:275–295

Crocker I T (1986) The Zaaiplaats tin field, Potgietersrus district. In: Anhaeusser C R, Maske S (eds) Mineral deposits of southern Africa, vol 2. Geol Soc S Afr pp 1287–1299

Cuney M (1978) Geological environement, mineralogy and fluid inclusions of the Bois Noir-Limouzat uranium vein, Forez, France. Econ Geol 73:1567–1610

Eadington P J (1983) A fluid inclusion investigation of ore formation in a tin-mineralized granite, New England, New South Wales. Econ Geol 78:1204–1221

Ellenberger F, Tamain A L G (1980) Hercynian Europe. Episodes 1980:22–27

Eugster H P (1984) Granites and hydrothermal ore deposits: a geochemical framework. Mineral Mag 49:7–23

Floyd P A, Exley C S, Stone M (1983) Variscan magmatism in Southwest England – Discussion and synthesis. In: Hancock P L (ed) The Variscan Fold Belt in the British Isles. Hilger, Bristol, pp 178–185

Foster R P (1977) Solubility of scheelite in hydrothermal chloride solutions. Chem Geol 20:27–43

Foster R P, Mann A G, Armin T, Burmeister B (1978) Richardson's Kop wolframite deposit: a geochemical model for the behaviour of tungsten. Geol Soc S Afr Spec Publ 4:107–128

Goinhas J, Viegas L (1983) Provincia metallogenetica estanifera e tungstenica iberica – consideração sobre as ocorencias de tungstenio em Portugal, sua prospecao e potencialidades. Estud Not Trabalhos 25:147–178

Groves D I, McCarthy T S (1978) Fractional crystallization and the origin of tin deposits in granitoids. Mineral Depos 13:11–26

Groves D I, Solomon M (1964) The geology of the Mt. Bischoff district. Proc R Soc Tas 98:1–22

Groves D I, Martin E L, Murchie H, Wellington H K (1972) A century of mining at Mt. Bischoff, 1871–1971. Tasm Geol Surv Bull 54:310 pp

Hall A (1971) Greisenisation in the Granite of Cligga Head, Cornwall. Proc Geol Ass 82:209–230

Hosking K F G (1988) The world's major types of tin deposits. In: Hutchison C S (ed) Geology of tin deposits in Asia and the Pacific. Springer, Berlin, Heidelberg, New York, pp 3–49

Hunter D R (1973) The localization of tin mineralization with reference to southern Africa. Mineral Sci Eng 5:53–77

Hutchison C S (ed) (1988) Geology of tin deposits in Asia and the Pacific. United Nations Economic and Social Commission for Asia and the Pacific. Springer, Berlin, Heidelberg, 718 pp

Ishihara S (1977) The magnetite-series and ilmenite-series granitic rocks. Min Geol 27:293–305

Ishihara S (1981) The granitoid series and mineralisation. Econ Geol 75th Anniv Vol, pp 458–484

Ishihara S, Sawata H, Arornsuwan S, Busaracome P, Bungbrakearti N (1979) The magnetite series and ilmenite series granitoids and their bearing on tin mineralisation, particularly of the Malay peninsula region. Geol Soc Malay Bull 11:103–110

Ivanova G F (1969) Conditions of concentration of tungsten during greisenization. Geokhimiya 1:22–32

Jackson N J (1979) Geology of the Cornubian tin field, a review. Geol Soc Malay Bull 11:209–239

Jackson N L, Halliday A N, Sheppard S M F, Mitchell J G (1982) Hydrothermal activity in the St. Just mining district, Cornwall, England. In: Evans A M (ed) Metallization associated with acid magmatism. John Wiley & Sons, Chichester, New York, pp 137–179

Kelly W C (1977) The relative timing of metamorphism, granite emplacement and hydrothermal ore deposition in the Panasqueira District (Beira Baixa, Portugal). Comun Serv Geol Port 61:239–244

Kelly W C, Rye R O (1979) Geologic, fluid inclusion, and stable isotope studies of the tin-tungsten deposits of Panasqueira, Portugal. Econ Geol 74:1721–1822

Kinnaird J A (1985) Hydrothermal alteration and mineralization of the alkaline anorogenic ring complexes of Nigeria. J Afr Earth Sci 3:229–252

Lehmann B (1982) Metallogeny of tin: magmatic differentiation versus geochemical heritage. Econ Geol 77:50–59

Leube A, Stumpfl E F (1963) The Rooiberg and Leeuwpoort tin mines, Transvaal, South Africa. Econ Geol 58:391–418

Lorenz V, Nicholls I A (1984) Plate and intraplate processes of Hercynian Europe during the late Paleozoic. Tectonophysics 107:25–56

MacKenzie I F (1983) The geology and geochemistry of tungsten mineralisation at Doctor Hill and Falls Creek, Central Westland, New Zealand. MSc Thesis, Victoria University, Wellington, 160 pp

Miller R McG (1983) The Pan-African Damara Orogen of South West Africa/Namibia. Geol Soc S Afr Spec Publ 11:431–515

Mining Magazine (ed) 1979 Hemerdon – Britain's largest tungsten deposit. Min Mag 141:342–351

Mitchell A H G, Garson M S (1981) Mineral deposits and global geotectonic settings. Acad Press, New York, London, 405 pp

Moore Mc M (1982) Mineral zonation near the granitic batholiths of southwest and northern England and some geothermal anologues In: Evans A M (ed) Metallization associated with acid magmatism, vol 6. John Wiley & Sons, Chichester, New York, pp 229–241

Norman J W (1982) The origin of metals: a speculation. Min Mag 146:226–229

Oosterom M G, Bussink R W, Vriend S P (1984) Lithogeochemical studies of aureoles around the Panasqueira tin-tungsten deposit, Portugal. Mineral Depos 19:283–288

Orr D (1977) Mt. Bischoff tin deposit. 25th Int Geol Cong, Sydney, Excursion Guide, vol 31A, pp 27–31

Paterson D J, Ohmoto H, Solomon M (1981) Geologic setting and genesis of cassiterite-sulfide mineralization at Renison Bell, western Tasmania. Econ Geol 76:393–438

Pirajno F (1982) Geology, geochemistry, mineralisation, and metal zoning of the McConnochie greisenised granite, Reefton district, Westland, New Zealand. N Z J Geol Geophys 25:405–425

Pirajno F (1985) Porphyry Mo and greisen W metallogeny related to the Karamea Batholith, South Island, New Zealand. N Z J Geol Geophys 28:187–(191

Pirajno F, Bentley, P N (1985) Greisen-related scheelite, gold and sulphide mineralisation at Kirwans Hill and Bateman Creek, Reefton District, Westland, New Zealand. N Z J Geol Geophys 28:97–109

Pirajno F, Jacob R E (1987) Sn-W metallogeny in the Damara Orogen, South West Africa/Namibia. S Afr J Geol 90:239–255

Pirajno F, Petzel V F W, Jacob R E (1987) Geology and alteration-mineralization of the Brandberg West Sn-W deposit, Damara Orogen, South West Africa/Namibia. S Afr J Geol 90:256–269

Pirajno F, Smithies R H (in press) The FeO/FeO + MgO ratio of tourmaline: a useful indicator of spatial variations in granite-related hydrothermal mineral deposits. J Geoch Expl

Pollard P J (1983) Magmatic and postmagmatic processes in the formation of rocks associated with rare-element deposits. Trans Inst Min Metall 92:B1–B9

Pollard P J, Taylor R G (1986) Progressive evolution of alteration and tin mineralization:controls by interstitial permeability and fracture-related tapping of magmatic fluid reservoirs in tin granites. Econ Geol 81:1795–1800

Pollard P J, Taylor R G, Cuff C (1983) Metallogeny of tin: magmatic differentiation versus geochemical heritage – a discussion. Econ Geol 78:543–545

Pollard P J, Pichavant M, Charoy B (1987) Contrasting evolution of fluorine- and boron-rich tin systems. Mineral Depos 22:315–321

Pollard P J, Taylor R G, Cuff C (1988) Genetic modelling of greisen-style tin systems. In: Hutchison C S (ed) Geology of Tin Deposits in Asia and the Pacific. Springer, Berlin, Heidelberg, New York, pp 59–72

Pollard P J, Taylor R G, Tate N M (1989) Textural evidence for quartz and feldspar dissolution as a mechanism of formation for Maggs Pipe, Zaaiplaats tin mine, South Africa. Mineral Depos 24:210–218

Roedder E (1984) Fluid inclusions. Reviews in Mineralogy, vol 12. Min Soc Am, 644 pp

Rose A W, Burt D M (1979) Hydrothermal alteration. In: Barnes H L (ed) Geochemistry of hydrothermal ore deposits, 2nd edn. John Wiley & Sons, New York, pp 173–235

Rozendaal A, Toros M S, Anderson J R (1986) The Rooiberg tin deposits, West-Central Transvaal. In: Anhaeusser C R Maske S (eds) Mineral deposits of southern Africa, vol 2. Geol Soc S Afr, pp 1307–1328

Shcherba G N (1970) Greisens. Int Geol Rev 12:114–255

Smirnov V I (1976) Geology of mineral deposits. MIR, Moscow, 520 pp

SACS – South African Committee for Stratigraphy (1980) Stratigraphy of South Africa, pt 1 (Comp. L.E.Kent) Lithostratigraphy of the Republic of South Africa, South West Africa/ Namibia, and the Republics of Boputhswana, Transkei and Venda: Handb Geol Surv S Afr 8, 690 pp

Stear W M (1977) The stratabound tin deposits and structure of the Rooiberg fragment. Trans Geol Soc S Afr 80:67–78

Stemprok M (1981) Tin and tungsten deposits of the west central European Variscides. Proc 5th IAGOD Symp. Stuttgart, pp 495–512

Taylor R G (1979) Geology of tin deposits. Elsevier, Amsterdam, 543 pp

Taylor R G, Pollard P J (1988) Pervasive hydrothermal alteration in tin-bearing granites and implications for the evolution of ore-bearing magmatic fluids. Can Inst Min Metall Spec Vol 39:86–95

Turekian K K, Wedepohl K H (1961) Distribution of the elements in some major units of the earth's crust. Bull Geol Soc Am 72:175–192

Twist D (1985) Geochemical evolution of the Rooiberg silicic lavas in the Loskop Dam area, southeastern Bushveld. Econ Geol 80:1153–1165

Vermaak C F, Von Gruenewaldt G (1986) Introducion to the Bushveld Complex. In: Anhaeusser C R Maske S (eds) Mineral deposits of southern Africa, vol 2. Geol Soc S Afr, pp 1021–1030

Von Gruenewaldt G, Strydom J H (1985) Geochemical distribution patterns surrounding tin-bearing pipes and the origin of the mineralizing fluids at the Zaaiplaats tin mine, Potgietersrus district. Econ Geol 80:1201–1211

Von Gruenewaldt G, Sharpe M R, Hatton C J (1985) The Bushveld complex: Introduction and review. Econ Geol 80:803–812

Walraven F (1985) Genetic aspects of the granophyric rocks of the Bushveld Complex. Econ Geol 80:1166–1180

Westra G, Keith S B (1981) Classification and genesis of stockwork molybdenum deposits. Econ Geol 76:844–873

Windley B F (1984) The evolving continents. John wiley & Sons, New York, 399 pp

Wright J H, Kwak T A P(1989) Tin-bearing greisens of Mount Bischoff, northwestern Tasmania, Australia. Econ Geol 84:551–574

Yan M B, Wu Y L, Li C T (1980) Metallogenic systems of tungsten in Southeast China and their mineralisation characteristics. Soc Min Geol Jpn Spec Iss 8:215–222

Ziserman A, Bertraneu J, Jaujou M (1980) European Mineral Wealth. Episodes 1980:33–35

Chapter 10

Porphyry Systems and Skarns

10.1 Introduction

Metallic ore deposits related to porphyry systems encompass a wide variety of types that can be characterised in terms of geotectonic setting, metal content, hydrothermal alteration pattern and the nature of the associated granitoids and wall rocks. Porphyry systems are universally typified by three main features: (1) presence of veins and veinlets forming stockworks, within which are disseminated sulphides of Fe, Cu, Mo, Pb and Zn, as well as native Au, and minerals of W, Bi and Sn; (2) the mineralisation is spatially and genetically related to intrusive bodies, of which at least one has a distinct porphyritic texture (hence the name porphyry); (3) large volumes of rocks are affected by hydrothermal alteration-mineralisation. The size of porphyry deposits may vary from several million tonnes up to a few billion tonnes, with grades ranging from as little as 0.2% Cu up to 2% Cu (porphyry Cu), 0.01 to 0.5% Mo (porphyry Mo), and for those containing Au, this metal's tenors range from fractions of ppm up to a few ppm. The tonnages and grades of a number of selected porphyry deposits are given in Table 10.1. Since the advent of the plate

Table 10.1. Approximate grades and tonnages of selected porphyry deposits (a) 1, After Gilmour (1978); 2 Guilbert and Park (1986); 3 Sillitoe and Gappe (1984); 4 Hall et al. (1990)

Deposit	Tonnage (t) and grade	Country	Reference a
San Manuel	480×10^6 t @ 0.77% Cu	Arizona USA	1
Climax	480×10^6 t @ 0.2% Mo	Colorado USA	1
Quartz Hill	1.3×10^9 t @ 0.15% Mo	Alaska USA	2
Tirad	ca 500×10^6 t @ 0.4% Cu, 0.4 g/t Au	Philippine	3
Libo	210×10^6 t @ 0.28% Cu, 0.25 g/t Au	Philippine	3
Santo Tomas	320×10^6 t @ 0.47% Cu, 0.5 g/t Au	Philippine	3
Frieda River	ca 860×10^6 t @ 0.5% Cu, 0.3 g/t Au	Papua New Guinea	4

tectonic theory much has been written on porphyry deposits. The literature reports on porphyry Cu, Cu-Mo, Mo, W, Cu-Au and porphyry Sn deposits, while Guilbert (1986) prefers the general name of "porphyry base metal deposits" (PBMD). The country rocks intruded by the igneous bodies may include carbonate units, and they, as a result of thermal and metasomatic exchanges with the fluids that emanate from the intrusions, will form skarn-type ore deposits. Although not all skarns are affiliated with porphyry systems (see Chap.9), this chapter mainly considers those skarn deposits which are.

The literature dealing with porphyry deposits is copious, and as such it would be arduous to enumerate even a fraction of the works produced. Among the many important contributions the reader is referred to: Hollister (1978), Titley and Beane (1981) and Beane and Titley (1981) for reviews; the collection of papers edited by Friedrich et al. (1986), Hollister et al. (1975), Hollister (1979), Titley (1982) for the North American deposits, Sillitoe (1970, 1972, 1976, 1981, 1986) and Sillitoe and Gappe (1984) for the South American and Philippine deposits; a Special Issue of Economic Geology (Vol. 73, No.5, 1978) is devoted to porphyry deposits of the Pacific islands and Australia; Laznicka (1976) reports on the porphyry deposits of the USSR. Later in this chapter we examine a number of selected examples of porphyry and skarn deposits.

10.2 Tectonic Settings

Porphyry systems generally occur at convergent plate margins and in rift-related settings. The global distribution of porphyry deposits is shown in Fig. 10.1. At convergent margins porphyry deposits form above subduction zones at continental margins and at intra-oceanic island arcs. An example of the former are the Andean porphyries, and of the latter the Pacific island porphyries. These systems are generally associated with quartz-monzonite, granodiorite or diorite, of typical calc-alkaline sequences. They contain Cu with subordinate Au and Mo. In rift-related settings at least three situations are recognised by Sillitoe (1980) as being conducive to porphyry mineralisation (Fig. 10.2). One is in a back-arc rift setting following cessation of subduction in which alkaline granitic rocks of A-type chemistry and associated rhyolites predominate, examples of which include Climax and Urad-Henderson in Colorado; another is within a rift zone forming during the initiation of a Wilson cycle (intracontinental rifting) and finally within a rift developing in an overthrust plate following continental collision. Here, too, A-type magmatism is predominant and ring complexes common – an example being the Mo deposits of the Oslo graben in Norway, to be discussed in a later section. Rift-related porphyry systems are generally associated with granitic rocks or quartz-monzonite and contain Cu + Mo, Mo ± W.

The spatial and temporal distribution of porphyry deposits (Fig. 10.1) has important implications for their metal association (Sillitoe 1986). The genesis and evolution of porphyry systems are strictly associated with the magmatic events related to the plate boundaries mentioned above, and hence their coincidence with
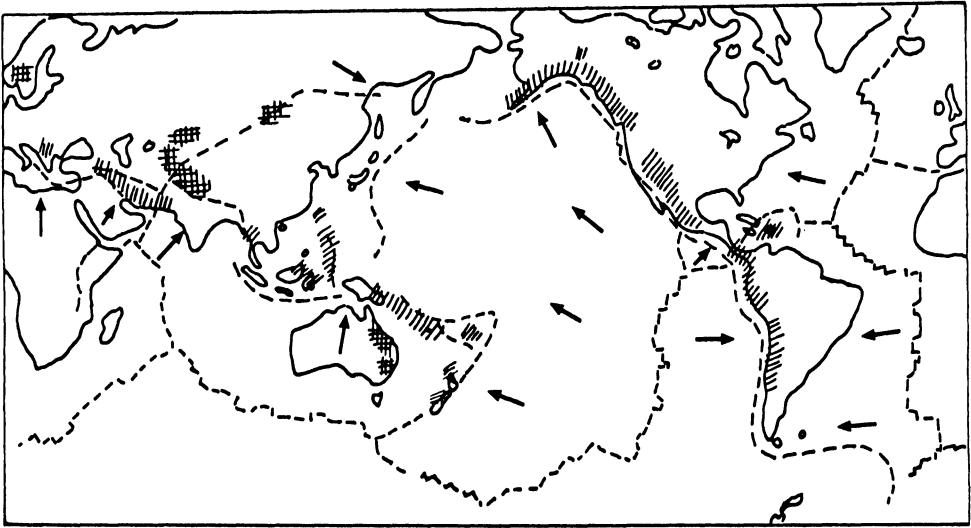
Fig. 10.1. Distribution of Paleozoic (*cross-hatched*) and Mesozoic-Cenozoic (*shaded*) porphyry provinces of the world, and their relationship to modern plate boundaries (*small dashed lines*). *Arrows* indicate direction of plate movement
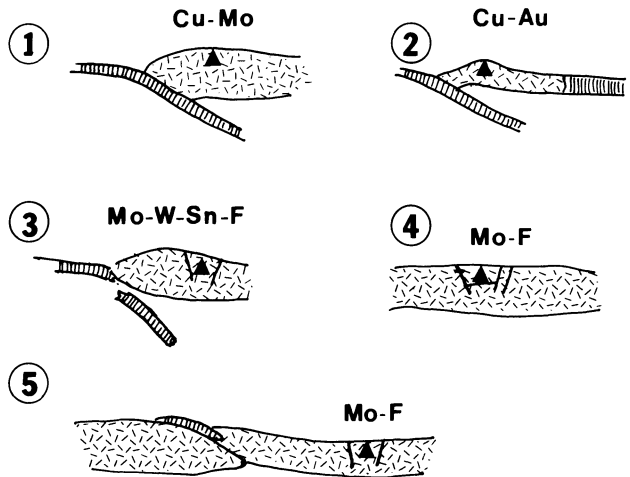
Fig. 10.2. Geotectonic settings of porphyry systems. Position shown by *small triangle*; dominant metals shown. *1* Subduction zone at continental margin (Andean-type); *2* subduction zone at island arc; *3* back-arc rift setting formed after cessation of subduction; *4* intracontinental rift zone; *5* rifting associated with continental collision (After Sillitoe 1980)

orogenic belts. The origin and source of the metals such as Cu, Mo and Au has been debated by many authors. The problem may be considered in terms of Cu/Mo ratios, or of the relative Cu-Au-Mo contents. There are two schools of thought: one envisages that the metals originated in the source region of the magmas, with

subsequent assimilation of continental crust and scavenging of metals. In essence this school purports that the Cu/Mo ratio decreases with increasing thickness of the sialic crust and distance from the Benioff Zone. High Mo and high silica would indicate a thick sialic crust. The Andean belt is cited as an example of this variation (see Hollister 1978; and Titley and Beane 1981). Crustal sources of metals would include sedimentary and volcanic rocks, pre-existing mineralised bodies and the granitic rocks. By contrast high Au, or high Cu/Mo ratios would indicate a thin and more mafic crust, the Pacific island porphyry deposits being an example of this category. In this case the source of the metals would be provided by the more mafic components of the crust such as oceanic crust and the predominantly dioritic plutons.

The second school of thought theorises that a subcrustal source might be involved and is the prime supplier of the metals. Sillitoe (1986) uses the central Andean porphyry province to argue this case and his theory is briefly reported here. This author notes that the spatial distribution of the porphyry deposits in the central Andes shows a marked parallelism with the axis of the Peru-Chile trench, thus indicating a relationship to subduction processes. Furthermore Sillitoe contends that the Cu/Mo ratios do not appear to have any relationship to crustal thickness as is supposed by the first school. Neither there appears to be any relationship with the time distribution of the Cu/Mo ratios. The metal sources are therefore believed to include the subducted oceanic crust (including the sedimentary material of layer 1, the upper mantle wedge above the Benioff Zone and possibly the zone of underplating by the rising mafic melts beneath the crust.

10.3 Classification of Porphyry Systems

There are many types of porphyry systems in terms of tectonic setting, morphology and structure, composition and patterns of alteration-mineralisation, and therefore it is almost impossible to formulate any one model to generally describe a porphyry system. Each type of system, however, is a variation of the same theme, this being the intrusion of a high level porphyritic granitoid body. The differences and unique features exhibited by individual deposits reflect the influence of regional and local geological variables. With this in mind some generalisations can nevertheless be made, and the models described below serve as a good starting point for an exploration geologist investigating a porphyry system.

Sutherland Brown (1976) and Nielsen (1976) classified porphyry systems of the Canadian cordillera on the basis of their morphology and position in the crust into: (1) plutonic; (2) hypabyssal or phallic; and (3) volcanic. Following the same criteria, McMillan and Panteleyev (1980) classify porphyry systems into: plutonic, volcanic and classic, and this classification is also adopted here (Fig. 10.3). The plutonic system (Fig. 10.3 A) is characterised by a lack of obvious concentric mineral zoning and has broad, diffuse zones of weak mineralisation. The plutons are multiphase and form large batholitic complexes of calc-alkaline chemistry. Breccias are common and are associated with late-stage dykes. Tourmaline may be common in

LAVAS AND PIROCLASTICS

PORPHYRY STOCKS / PLUTONS

BASEMENT ROCKS

SKARN MINERALISATION IN CARBONATE ROCKS

SULPHIDE MINERALISATION

EPITHERMAL VEINS   DIATREME / BRECCIA
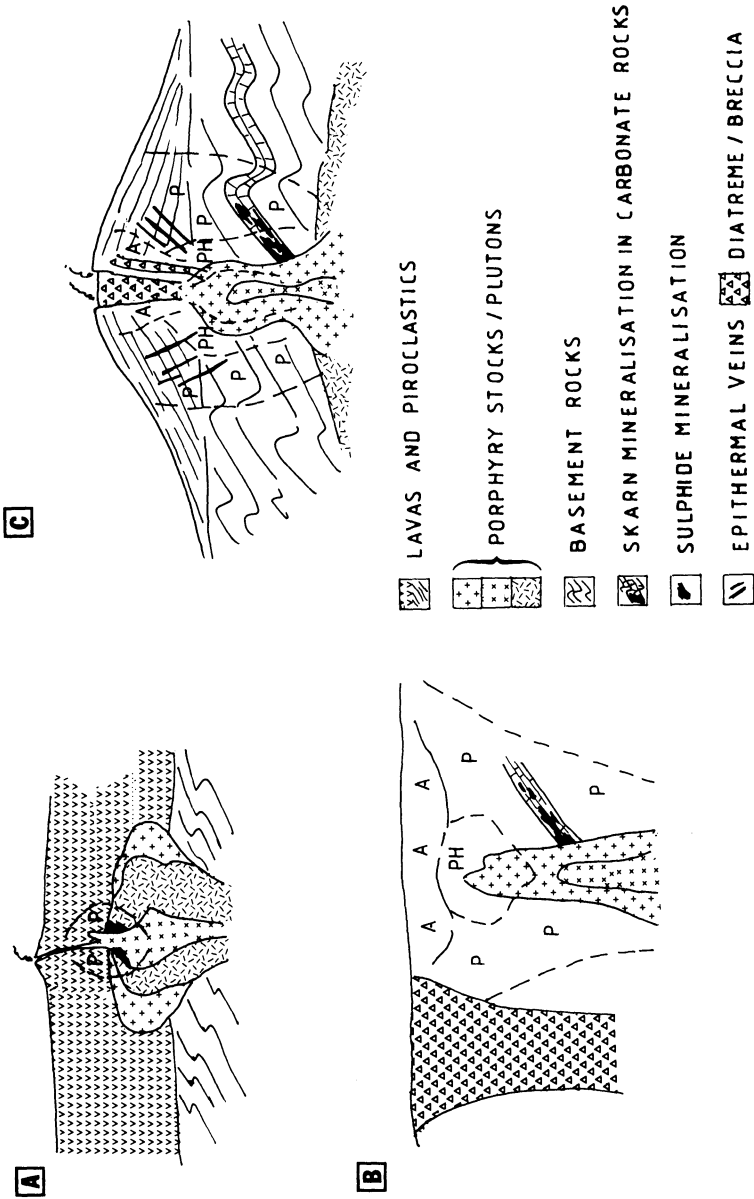
Fig. 10.3A–C. Idealised models of porphyry systems. **A** Plutonic type; drawing not to scale. Depth to top of pluton is approximately 5–6 km (after MacMillan and Panteleyev 1980). **B** Classic type; drawing not to scale. Vertical extent to upper portions of the porphyry stock may be approximately 0.5 to 1.5 km (After Sillitoe and Gappe 1984). **C** Subvolcanic type; drawing not to scale. Vertical extent from top of volcano to upper portions of porphyry stock may be approximately 3–4 km (After Sillitoe 1973). Alteration: *A* argillic; *P* propylitic; *PH* phyllic

the breccias. Alteration is fracture-controlled to pervasive and characterised by well-developed phyllic and argillic types, while potassic alteration is localised. Mineralisation is typically associated with stockworks and sulphide zoning shows progressive Fe enrichment outward from chalcopyrite to bornite to outlying pyrite-rich zones. Molybdenite contents are variable.

Classic systems (Fig. 10.3B) consist of post-orogenic composite stocks with typical porphyritic textures and a complex array of plugs, diatremes, breccias and dykes. They have a small areal extent (0.5–2 km^2) but large vertical dimensions. Potassic, phyllic and propylitic alterations are developed as shells around the intrusions. Mineralisation also occurs as shells – a weakly mineralised core in which pyrite is a dominant sulphide, surrounded by successive zones dominated by molybdenite, chalcopyrite and finally pyrite. The volcanic type (Fig. 10.3C) represents the near-surface expression of orogenic granitic rocks that have intruded a cogenetic volcanic pile. McMillan and Panteleyev (1980) distinguish calc-alkalic types and alkalic types. Calc-alkalic types are represented by small plugs (0.2–10 km^2), sheets or dykes emplaced in a subvolcanic environment. These igneous bodies have a small core of potassic alteration with phyllic and/or argillic alteration developed locally, whereas propylitic alteration is widespread. Mineralisation is predominantly Cu-Mo, forming lenses or irregularly shaped orebodies. The ore contains chalcopyrite, bornite and molybdenite. The alkalic types are characterised by high-level plugs generally linked to underlying mesozonal batholiths. Alteration is potassic overprinted by propylitic, followed again by alkali metasomatism, which is mainly sodic and/or potassic. These are generally Cu-Au deposits in breccias and/ or highly fractured rocks. Locally there may be development of magnetite and apatite. Mineral zoning consists of chalcopyrite + magnetite and bornite grading outwards to a pyrite halo.

Finally, a category of porphyry systems, first proposed by Sillitoe et al. (1975), is that of subvolcanic-related Sn-Ag mineralisation in Bolivia, which is dealt with in the last section of this chapter. Volcanic-associated Sn mineralisation considered to be of the porphyry Sn-type has also been reported from China (Guiqing 1988; Zhunggi et al. 1988). The chief characteristic of these systems is the absence of potassic alteration and the complex metal associations such as Sn-Ag-Sb-Pb.

10.4 Hydrothermal Alteration and Mineralisation

Hydrothermal alteration and mineralisation are essential features of porphyry systems. They form more or less concentric shells centred on the productive intrusions. The effects of hydrothermal alteration and mineralisation extend into a large volume of wall rocks around and above the intrusives. The nature of the fluids responsible for the alteration-mineralisation phenomena has been investigated by Taylor (1974) and Sheppard (1971), who examined the D/H and δO^{18} isotopic composition of key minerals in order to determine the origin of the H_2O involved in the mineralising solutions. These studies revealed that most hydrothermal biotites exhibit an isotopic composition indicative of an igneous origin, but in some biotites

there is evidence of later exchange with meteoric waters. It was also found that the oxygen and hydrogen isotopic composition of clay minerals and sericite is dependent on their geographic position, leading to the conclusion that they were formed by fluids with a strong meteoric component.

The action of magmatic and meteoric fluids in porphyry systems has been described by Guilbert (1986, p. 199) as the "summation of many continuous, time-staged processes rather than a single event". Magmatic waters are first exsolved from the crystallising porphyry intrusion (see Chap. 3 and Fig. 3.1). These early magmatic-hydrothermal solutions form at temperatures ranging from 750 to 450 °C and at depths of between 5 and 1 km below the surface. The action of these waters is essentially confined to the apical portions of the intrusive stock and immediate surrounding areas. The early magmatic-hydrothermal fluids are generally succeeded by convective fluids of meteoric origin, with which they mix at first until the magmatic component relating to that particular intrusion tends to disappear completely. Meteoric-hydrothermal fluids of porphyry systems have temperatures ranging from 450 to 250 °C and form at depths of between approximately 1 and <0.5 km. The study of fluid inclusions in porphyry systems indicates that there are, broadly speaking, three classes of fluids (Beane and Titley 1981): (1) hypersaline fluids with up to 40 wt.% NaCl equivalent and homogenisation temperatures of 750 °C or greater; (2) high salinity fluids, with approximately 10 to 25 wt.% NaCl equivalent and homogenisation temperatures of between 600 and 250 °C; and (3) low salinity fluids with less than 10 wt.% NaCl equivalent and homogenisation temperatures of between 400 and 200 °C. Integration of isotopic, fluid inclusion, petrological and field data suggest that the hypersaline fluids are largely magmatic-derived. Fluid inclusion data also suggest that boiling and condensation occurred within these hypersaline magmatic fluids.

In summary, from these studies the picture emerges that the earliest fluids are exsolved from cooling magmas over a protracted period of time, and they ascend and circulate through both the producing cooling intrusive and adjacent fractured wall rocks. During this time increasing amounts of meteoric-derived convective

Table 10.2. Chief characteristics of Lowell-Guilbert and diorite models of porphyry systems (After Hollister 1978)

	Lowell-Guilbert model	Diorite model
Intrusive type:	Quartz-monzonite porphyry, quartz-diorite porphyry	Sienite porphyry Diorite porphyry
Alteration:	Potassic (orthoclase-biotite, orthoclase-sericite); phyllic (quartz-sericite-pyrite); argillic; propylitic (chlorite-epidote)	Potassic (biotite-orthoclase, orthoclase-chlorite); propylitic (chlorite-epidote ± albite)
Mineralisation:	Pyrite, chalcopyrite, bornite, molybdenite, rare Au	Pyrite, magnetite, chalcopyrite, bornite rare molybdenite, important Au
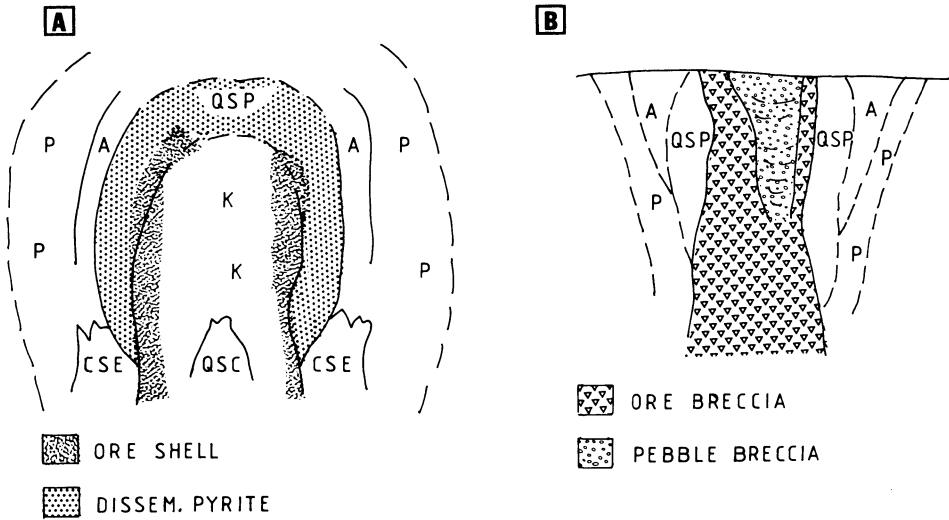
Fig. 10.4A, B. Lowell-Guilbert models of alteration-mineralisation zonal patterns related to a quartz-monzonite porphyry system **A** and **B** a breccia-type porphyry system (after Hollister 1978). Drawings not to scale. Alteration: *K* potassic; *A* argillic; *QSP* phyllic (quartz-sericite pyrite); *P* propylitic; *CSE* chlorite-sericite-epidote ± magnetite; *QSC* quartz-sericite-chlorite ± K-feldspar (After Lowell and Guilbert 1970)

waters are drawn into the system, at first mixing with the endogenous fluids and later dominating the entire hydrothermal system. It is important to realise in this context that the permeability of the wall rocks controls the access of the convecting meteoric fluids. The action of the hydrothermal solutions on the surrounding rocks produces the alteration-mineralisation patterns of porphyry systems which depends on the nature of the fluids, wall-rock and intrusive compositions, and, as mentioned above, permeability.

Perhaps some of the most significant contributions to the understanding of porphyry mineral deposits are the works of Lowell and Guilbert (1970) and Guilbert and Lowell (1974), together with the formulation of the well-known Lowell-Guilbert model. This model is based essentially on the San Manuel-Kalamazoo porphyry system in Arizona, augmented by observations carried out in 27 other porphyry deposits in North America. There are, however, many variations of, and departures from the Lowell-Guilbert model, due to the different compositions of the intrusive porphyry bodies, whether they are silica-rich and alkalic or alkalic-calcic, or silica-deficient and more calcic. Thus, two main models may be considered: the Lowell-Guilbert model (or quartz-monzonite model) and the diorite model (Hollister 1978). The chief characteristics of these models are given in Table 10.2 and shown in Figd. 10.4 and Fig. 10.5. In addition, the alteration-mineralisation of carbonate wall rocks constitute the skarn-type deposits with distinct mineral assemblages and zoning patterns, to be discussed in a forthcoming section.

10.4.1 Lowell-Guilbert Model

This model, known also as the quartz-monzonite model, is somewhat of an oversimplification, but nevertheless useful. The earliest alteration is due to the effects of alkali metasomatism (generally potassic, but can also be sodic) within and around the productive intrusive porphyry body. This constitutes a core of potassic alteration which gives way to a more diffuse zone of propylitic alteration. This stage is characterised by disseminated and veinlet-type sulphide mineralisation. At later stages, and as a result of the incursion of meteoric waters, phyllic and argillic alteration overprint the early alkali-metasomatic effects causing a re-distribution of the sulphide mineralisation (Guilbert 1986). The essential features of the Lowell-Guilbert model are reported below and shown in Fig. 10.4A.

The hydrothermal alteration zones form more or less concentric shells around the potassic zone, around which are distributed the phyllic or quartz-sericite-pyrite zone, the argillic zone and the propylitic zone. The "potassic" minerals that typify the zone are orthoclase and biotite. The potassic zone contains the assemblage quartz + K-feldspar + biotite + sericite + anhydrite + pyrite + chalcopyrite + bornite ± magnetite ± molybdenite. As mentioned previously, such an assemblage is ascribed to late-magmatic-hydrothermal fluids. This alteration is generally pervasive and characterised by the replacement of primary biotite and feldspars. K-feldspar forms microveinlet fillings as well as replacement of primary feldspars. Hydrothermal biotite occurs as microfracture fillings accompanied by chalcopyrite and anhydrite, as sparse to massive replacement of plagioclase, as euhedral crystals almost identical to primary biotites, and as pervasive replacement of groundmass feldspars. The altered porphyries display a smokey-grey colour and the "ore shell" is typically contained within the outer limits of the potassic core.

The phyllic zone, known also as quartz-sericite-pyrite (QSP) zone, surrounds and overlaps the potassic zone. Contacts between the phyllic and potassic zones are gradational. This alteration is caused by the leaching of Na, Ca and Mg from the alumino-silicate minerals (Titley and Beane 1981). Phyllic alteration is characterised by the assemblage of quartz + sericite + pyrite ± chlorite ± rutile ± chalcopyrite. Fe is leached out of the primary mafic silicates to form mainly pyrite. Sericite predominates in the inner portions of the zone, while clay minerals and hydromicas become more abundant towards the outer portions. Sericite pervasively replaces all the primary silicates often forming a felted texture; faint vestiges of cleavage and twin planes, in places, indicate the presence of former silicates, although towards the inner margins of the zone relics of K-feldspars may still be recognisable. Pyrite can reach up to 30% by volume and forms veinlets and granular disseminations. Chalcopyrite may be present in subordinate amounts. Silicification is prominent and, according to the authors, well beyond that expected from the breakdown of primary minerals, suggesting perhaps that some silica comes in with later solutions. Contacts between the phyllic and argillic zones are gradational and indistinct.

The argillic zone is characterised by the presence of clay minerals (argilla means clay in Latin) such as illite, kaolinite and montmorillonite. During this phase of alteration acid conditions prevail and leaching of cations is extensive. Plagioclase

is converted to kaolinite near the ore shell and to montmorillonite further away. K-feldspar shows minor replacement by kaolinite and/or sericite. Pyrite, though less common than in the phyllic zone, may also be present. Intermediate argillic alteration refers to the presence of minerals such as montmorillonite, illite, chlorite, hydromicas and, locally, kaolinite. The formation of these minerals is related to the availability of limited amounts of K, Ca and Mg (Beane and Titley 1981). Advanced argillic alteration refers to more or less complete acid attack with the formation of kaolinite-dickite and varying amounts of diaspore, alunite, amorphous silica, more rarely corundum and pyrophyllite. Beane and Titley (1981) point out that in many cases the argillic alteration reported for some porphyry deposits is actually supergene alteration, and this is often associated with chalcocite mineralisation. Pyrite, chalcopyrite and bornite are the main sulphide species associated with the argillic alteration.

The propylitic zone is the largest of the alteration shells forming a wide halo in the country rocks around the porphyry intrusives, and as such is relatively easy to detect in the early stages of mineral exploration. However, the exploration geologist must bear in mind that the propylitic zone is the equivalent of, and can be easily confused with, greenschist facies metamorphism. The propylitic zone grades into the argillic zone. The main assemblage consists of chlorite + epidote + pyrite + calcite ± clay minerals. Chlorite and carbonate generally replace biotite along cleavages, whereas epidote and calcite occur as fine granules in plagioclase, or associated with montomorillonite replacing amphiboles. Pyrite is abundant and chalcopyrite rare. Deeper zones of alteration are indicated by the presence of K-feldspar + sericite and by disseminations of magnetite, chalcopyrite, pyrite and some molybdenite.

Tourmaline may be present in some porphyry deposits of the quartz-monzonite type and is usually associated with breccia pipes (a special issue of Economic Geology – vol.80, No. 6, 1985 – is devoted to mineralised breccias and breccia pipes). Although present in the North American and some of the Pacific deposits, breccia pipes are characteristic of the Andean region where they may be economically important. At El Teniente (Chile) two tourmaline breccia pipes, up to 1.3 km in diameter, contain Cu and Mo ore. Tourmaline may also occur in the argillic, propylitic, phyllic and potassic zones where it preferentially replaces the ferromagnesian minerals (Hollister 1978).

Hollister (1978) also considers a model of porphyry system which he calls "breccia-type" (Fig. 10.4B). The alteration-mineralisation is related to a large breccia pipe in which B-bearing fluids may play an important role and are responsible for the introduction of early tourmaline + quartz + pyrite, followed by Cu mineralisation. The alteration sequence is similar to the Lowell-Guilbert model (central potassic zone followed by phyllic, argillic and propylitic zones). The potassic minerals (orthoclase and biotite) and sulphides, characteristically may occur as cementing material for the breccia clasts. A pebble breccia may be present within the central portions (Fig. 10.4B) and is characterised by extensive argillic alteration, crude graded bedding and the presence of rounded fragments which include ore material. Pebble breccias are formed during a post-mineral stage by continuing meteoric-hydrothermal activity.

Apart from the quartz associated with the alteration mineral assemblages discussed above, silica is an important constituent of porphyry systems. It occurs as quartz veins and veinlets, as jasper and/or chalcedony replacing silicate minerals and carbonate country rocks. The porphyry Mo deposits of the North American Cordillera (e.g Climax in Colorado) have, in addition to the usual alteration-mineralisation shells, greisen-type alteration. This is usually spatially and genetically related to a late granitic intrusion. The zones of hydrothermal alteration of the Climax-type deposits (Hollister 1978, Guilbert and Park 1986) can be summarised as follows: (1) greisen zone; (2) quartz-K-feldspar, quartz-topaz; (3) phyllic with a topaz-magnetite subzone; (4) argillic; (5) propylitic. More details of this type of porphyry deposits are given in a later section.

10.4.2 Diorite Model

Porphyry systems associated with intrusives of dioritic or syenitic composition have alteration-mineralisation patterns that differ substantially from systems associated with more felsic granitic rocks to which the Lowell-Guilbert model is more applicable. The mafic character of both the intrusive rocks and the surrounding comagmatic volcanics plays an important role in the mineralogical and geochemical aspects of hydrothermal alteration and mineralisation. Thus, for example, the phyllic alteration is either lacking or poorly developed, whereas potassic and propylitic alteration zones are more prominent (Table 10.2). This type of porphyry system is usually found in island arcs built on oceanic or thin continental crust.

The alteration-mineralisation patterns of diorite-model porphyries are characterised by potassic and propylitic zonal sequences related to the effects and role played by the K^+ and H^+ ions in systems of high Na_2O/K_2O ratios and generally low in silica (Hollister 1978). The diorite model, shown in Fig. 10.5, consists of two successive shells of potassic (inner) and propylitic (outer) alteration. The potassic
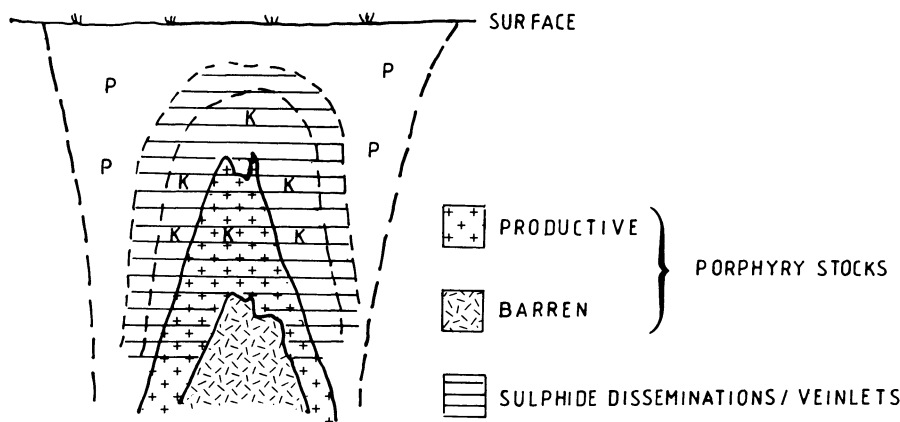
Fig. 10.5. Diorite model; drawing not to scale. Alteration: *P* propylitic; *K* potassic. See text for details (After Hollister 1978)

alteration is characterised by dominant biotite and chlorite with little or no K-feldspar. Chlorite replaces sericite in the diorite model, while albite, which may be present, takes the place of orthoclase. Phyllic alteration, if present, is generally weakly developed. Propylitic alteration which is characterised by the assemblage chlorite + epidote + albite + carbonate is paragenetically later than, and replaces, the potassic assemblages.

In diorite-type porphyries chalcopyrite disseminations are important and tend to accompany the potassic zone. The chalcopyrite to pyrite ratio is close to unity (Beane and Titley 1981), whereas the chalcopyrite to bornite ratio is equal to, or less than, 2 (Hollister 1978). Magnetite is a common constituent of diorite-type porphyries, and pyrrhotite may also occur.

10.4.3 Alteration-Mineralisation of Carbonate Wall Rocks (Skarns)

Skarns are calc-silicate rocks formed by replacement of carbonate lithologies either during regional metamorphism or by contact metasomatic processes related to igneous intrusions. The word "skarn" was originally used by Swedish miners to indicate Fe-rich calc-silicate gangue material. A brief digression into the termin-ology and classification of skarns is useful before proceeding with the main purpose of this section, which is to review skarn-type alteration-mineralisation related to porphyry environments. The terminology and classification of skarns adopted here are those of Einaudi et al. (1981), Einaudi (1982a, b) and Einaudi and Burt (1982).

The first distinction made by Einaudi (1982a) is between reaction skarns and ore skarns. The former, of limited extent, are formed along shale-limestone contacts during metamorphism. The latter, as the name implies, are the skarns that contain mineralisation, and are formed as a result of infiltration of fluids derived from igneous intrusions. A classification of skarns should take into consideration both the rock type and the mineralogical association of the replaced lithology. The terms endo- and exoskarns refer to the skarnification of igneous or aluminous rocks and carbonate rocks respectively. In our case we consider only the exoskarns, subdivided by Einaudi (1982a) in terms of their calc-silicate mineral assemblages into calcic skarns and magnesian skarns. Calcic skarns, which are formed by replacement of limestones, contain minerals such as garnets (andradite-grossularite series), clinopyroxenes (diopside-hedenbergite series), wollastonite, scapolite, epi-dote and magnetite. Magnesian skarns result from the replacement of dolomitic rocks and are typified by minerals such as diopside, forsterite, serpentine, magnetite, talc in silica-poor environments; and talc, tremolite-actinolite in environments richer in silica. Silica-pyrite skarn is a third type which relates to a stage of alteration-mineralisation associated with some porphyry deposits (see later). Skarnoid is a term used in connection with garnet-rich rocks whose origin is uncertain. From the economic point of view skarns are classified in terms of their metal association, and the following classes are considered: Fe skarns, W skarns, Cu skarns, Zn-Pb skarns, Mo skarns and Sn skarns. The chief characteristics of these skarns are given in Table 10.3A, B, and for more details the reader is referred to the works of Einaudi and coworkers cited above as well as Kwak (1987) and the Special

Table 10.3. Chief characteristics of skarn deposits. (A) Non-porphyry-related skarns; (B) porphyry-related skarns (After Einaudi et al. 1981; Einaudi and Burt 1982)

A.	Fe	W	Sn-W	Mo
Size ($\times 10^6$) (tonnes)	5–200	0.1–2	0.1–3	<0.1–?
Grade	40% Fe	0.5% W	0.1–0.7% Sn	±0.1% Mo
Associated metals	Cu, Co, Au	W, Mo, Cu, Zn, Bi	Sn, F, W, Cu, Zn	Cu, U, W, Bi
Igneous rocks	Gabbro, syenite, diorite	Quartz-diorite, quartz-monzonite	Granite	Granite, quartz-monzonite
Ore minerals	Magnetite, chalcopyrite, cobaltite, pyrrhotite	Scheelite, molybdenite, chalcopyrite, sphalerite, magnetite, pyrite, bismuth	Cassiterite, scheelite, sphalerite, pyrrhotite, magnetite, pyrite, arsenopyrite	Molybdenite, pyrrhotite, chalcopyrite, pyrite, bismuthinite, magnetite, bornite, arsenopyrite, sphalerite
Early minerals	Ferrosalite, grandite, epidote, magnetite	Ferrosalite, hedenbergite, grandite, idocrase, wollastonite	Idocrase, spessartine, andradite, datolite	Garnet, pyroxene, wollastonite, idocrase, olivine
Late minerals	Amphibole, chlorite, ilvaite	Spessartine, almandine, grandite, biotite, hornblende, plagioclase	Amphibole, mica, chlorite, tourmaline, fluorite	Amphibole, epidote, actinolite, chlorite

B.	Cu	Zn-Pb
Size ($\times 10^6$) (tonnes)	1–400	0.2–3
Grade	1–2% Cu	9% Zn, 6% Pb ± 15 g/t Ag
Associated Metals	Mo, Zn, W, Ag	Ag, Cu, W
Igneous rocks	Graodiorite, quartz-monzonite, stocks, dykes and breccia pipes	Granite, diorite, syenite, stocks and dykes
Ore minerals	Chalcopyrite, pyrite, hematite, magnetite, pyrrhotite, molybdenite, tennantite	Sphalerite, galena, pyrrhotite, pyrite, magnetite, chalcopyrite, arsenopyrite
Early minerals	Andradite, diopside wollastonite	Mn-hedenbergite, andradite, spessartine, rhodonite
Late minerals	Actinolite, chlorite, montmorillonite	Mn-actinolite, ilvaite, chlorite, rhodocrosite

Issue of Economic Geology (1982, Vol.77, No.4) for further details. Here we are mainly concerned with porphyry-related skarns which generally include the Cu- and Zn-Pb types. However, the reader must bear in mind that many of the features discussed here for porphyry-related skarns may also be applicable to other classes of skarns. Examples of Sn and W non-porphyry-related skarns are also briefly discussed in a later section.

Tectonic Settings

Skarns occur in most tectonic settings where there is magmatism and development of carbonate lithologies (Einaudi et al. 1981). Most skarn classes, and particularly those of the porphyry-related types are related to convergent plate boundaries, ranging from oceanic island arcs to continental margins. Rift settings and anorogenic magmatism tend to produce skarns of the Sn-W class.

In oceanic island arcs intermediate to mafic plutonic rocks may interact with reef limestones to produce magnetite-rich skarns. Einaudi et al. (1981) report that the main characteristic of skarns in this environment are their association with gabbro and diorite plutons, Na-metasomatism, Fe-rich compositions and the presence of Co, Cu and Au. These features would reflect the primitive, oceanic nature of the crust and wall-rock plutons. Cu skarns, Zn-Pb and W skarns are commonly formed in more mature magmatic arcs constructed on continental crust. They are associated with granodiorite, quartz-monzonite stocks, or diorite and granodiorite plutons (see Table 10.3B). Depth of emplacement is also important. W skarns appear to be related to batholiths emplaced at depths of between 5 and 15 km. Intermediate to shallow-depth magmas (1–6 km) give rise to porphyry stocks with less extensive contact aureoles, and the associated skarns are sulphide-rich with Cu, Cu-Fe, Pb-Zn, and minor Mo, Au and Ag. W and Mo would become dominant in I-type magmas which have interacted with continental crust rocks. Crustal-derived magmas emplaced in rifting environments may produce skarns of the Sn-W class with a host of other elements such as Be, B, F, Bi, Cu, Zn, Sn and U (Kwak 1987).

Porphyry-Related Skarns

The alteration-mineralisation of carbonate rocks in the environment of porphyry systems constitutes a class of skarns characterised by being both economically important and the largest base metal sulphide skarn deposits. Porphyry-related skarns, whose features generally correspond to Cu and Zn-Pb skarns (see Table 10.3B), have been studied in detail by Einaudi (1982a, b), and the results of his work, which focussed mainly on the North American deposits, are summarised in this section.

The nature of the ore-bearing skarns in the porphyry environment depends largely on the carbonate content of the replaced units, their permeability and structural features. The alteration-mineralisation styles also depend on the hydrothermal and metasomatic processes involved. These are responsible for the formation of the various types of skarns which Einaudi (1982a, b) calls: hornfels skarnoid, calcic skarns, magnesian skarns and silica-pyrite skarns. Hornfels skarnoids

originate by decarbonation and dehydration of the carbonate units without addition of components. They include wollastonite-rich lithologies developed from silica-rich limestones, and diopside hornfels developed from calcareous siltstones; calc-silicate hornfels containing quartz, tremolite-actinolite, epidote, plagioclase and diopside are commonly formed in calcareous shales. Calcic skarns are the dominant type in the porphyry systems of North America. They contain epidote, garnet $\pm$ clinopyroxene, wollastonite $\pm$ garnet $\pm$ idocrase $\pm$ clinopyroxene forming a zoned pattern from the productive intrusive outward, in the order given above. These anhydrous mineral assemblages are, at later stages and with decreasing temperatures, replaced by hydrous silicates, sulphides, oxides and carbonate minerals. The mineralisation in this system consists of sulphide and oxide disseminations, veins and massive replacement of the carbonate rocks at the skarn front. It shows a distinct zoning pattern consisting of pyrite $\pm$ chalcopyrite nearest the contact with the intrusive and associated with garnet-rich skarns, to pyrite + chalcopyrite $\pm$ magnetite associated with garnet-pyroxene skarn, to bornite + chalcopyrite $\pm$ magnetite (garnet-wollastonite skarn), to sphalerite + chalcopyrite $\pm$ magnetite $\pm$ pyrite (marble zone). This zoning is interpreted by Einaudi to be due to decreasing Fe outward from the pluton. More details on zoning are discussed later.

Magnesian skarns are usually derived from dolomitic rocks and characterised by the common presence of magnetite, while other typical minerals may include serpentine, forsterite and talc. These skarns are rich in magnetite but have relatively low sulphide contents. Silica-pyrite, mentioned previously, is "a common alteration feature associated with sulphide deposition in carbonate rocks of some porphyry copper districts" (Einaudi 1982b, p.192). Silica-pyrite forms during phases of advanced hydrogen ion metasomatism of the pluton, such as phyllic and argillic alteration stages. Silica-pyrite skarns are characterised by pyrite, quartz, various forms of silica (in some areas opal and cristobalite, in others chalcedony and jasper), clay minerals (montmorillonite, nontronite), chlorite and talc.

Skarn Formation

The subject of replacement of carbonate rocks by silicate minerals was introduced in Sect. 4.3.3 (Chap. 4) on silication, which was said to result in the formation of skarn rocks (sensu lato). Skarn genesis involves a series of processes related to, and correlated with, the late magmatic and hydrothermal events of a pluton intruding sedimentary rocks. The emplacement and cooling of the plutonic mass is accompanied by contact metamorphism and metasomatism in the wall rocks (see Chap. 3, Sect. 3.7.1 and Chap. 8 for definitions of metamorphism and metasomatism). Thus, the formation of skarns involves stages of isochemical metamorphism and metasomatism. Towards the final phases of cooling a retrograde stage occurs, during which the early skarn assemblages are destroyed and replaced by hydrous minerals. Effectively, these stages of skarn formation correspond with the early potassic and later phyllic and argillic alteration in the porphyry intrusive stock or pluton. Skarns develop in temperatures ranging from between 700 and 200 °C and at pressures of between 0.3 and 3 kbar. The metasomatic fluids have salinities which range from 10 to about 45 wt.% NaCl equivalent. The hydrothermal solutions
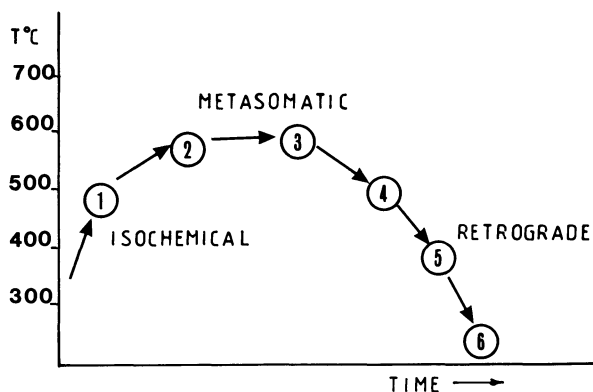
Fig. 10.6. Stages of skarn development as a function of time and temperature. See text for details (after Brown et al. 1985). *1* calcite, diopside; *2* calcite, diopside, wollastonite, idocrase, grossular; *3* andradite, diopside-hedenbergite, epidote, high-Mo scheelite; *4* quartz, chalcopyrite, low-Mo scheelite; *5* amphibole, calcite, epidote, quartz; *6* zeolites

originated from the magma in the early stages with an increasingly meteoric component during the retrograde stages, as also observed for, and compatible with, the porphyry mineralising solutions.

In summary, the formation of skarns can be related to three main stages (Fig. 10.6): (1) isochemical thermal metamorphism; (2) metasomatism; and (3) retrograde hydrothermal alteration. The diagram of Fig. 10.6 refers to a study of W (scheelite) skarns at Pine Creek in California by Brown et al. (1985). At this locality the carbonate protolith contained calcite, dolomite, quartz, K-feldspar and organic material. This protolith underwent progressive devolatilisation which produced the mineral assemblage of calcite + diopside + K-feldspar + sphene + graphite (isochemical stage). Following the cooling of a quartz-monzonite pluton, H_2O-rich fluids were expelled and moved up along the structural break provided by the contact of the carbonate rocks with the pluton. These fluids reacted with the carbonates to release Ca and CO_2, some of which diffused back towards the pluton, forming an endoskarn. Infiltration of the metasomatising fluids into the carbonates formed Fe-poor silicates and Fe-rich garnet and pyroxene (metasomatic stage). A light green outer skarn zone was formed containing calcite + diopside + wollastonite + idocrase + garnet + fluorite. The scheelite-bearing skarn contains garnet + pyroxene + epidote. Amphibole minerals, epidote, quartz and zeolites characterise the retrograde stage.

Metamorphic and metasomatic reactions of skarns involve the systems CaO-MgO-SiO_2-H_2O and CaO-Al_2O_3-Si_2O-CO_2-H_2O (Einaudi et al. 1981). Some typical reactions are given below:

tremolite + 3 calcite + 2 quartz = 5 diopside + CO_2 + H_2O;

9 hedenbergite + $2O_2$ = 3 andradite + 9 quartz + magnetite;

3 hedenbergite + S_2 = andradite + 3 quartz + FeS_2;

andradite $+ 3\,CO_2 + 2S_2 = 2FeS_2 + 3$ quartz $+ 3$ calcite $+ 3/2O_2$;

2 andradite $+ 4S_2 = 6$ wollastonite $+ 4FeS_2 + 3O_2$.
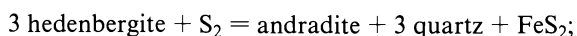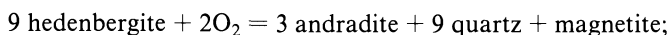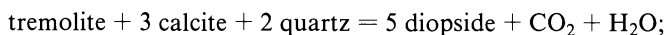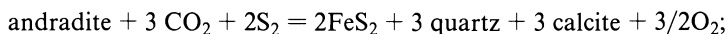
Carbonate rocks are decomposed according to the reaction:

$CaCO_3 + 2H^+ = Ca^{2+} + CO_2 + H_2O$.

Garnets and pyroxenes are important components of skarns. Their zoning and various generations are a function of the changing physico-chemical conditions of the fluids. For this reason microprobe analyses of garnets and pyroxenes are important in establishing the nature and type of skarns. Ternary plots of the compositional distribution of garnets and pyroxenes (spessartine-grandite-andradite and johansenite-diopside-hedenbergite respectively) can be used to characterise the class of skarns. Porphyry-related Cu skarns are characterised by the presence of andradite and diopside, whereas the grossularite-hedenbergite association is more typical of W-bearing skarns (Einaudi and Burt 1982).

The mechanism of skarn genesis is explained by Smirnov (1976) with the diffusion-infiltration theory, reported by Einaudi et al. (1981) under the name of bimetasomatic diffusion. The latter authors also mention other processes for the development of skarns. Einaudi and Burt (1982), for example, consider infiltration to be the main mechanism of skarn genesis. All, however, refer to large-scale transfer and/or exchange of components during high temperature regimes.

The diffusion-infiltration theory, first formulated by a Russian geoscientist, D.S. Korzinskii, holds that skarns result from a system with imbalanced chemistry, developed in hot aqueous solutions which impregnate both the intrusive igneous rocks and the carbonate lithologies on either side of the contact. This leads to the formation of endo- and exoskarns, mentioned previously. Elements are dissolved from both sides and the solution tends to homogenise by diffusion from areas of high concentration to areas of low concentration. Exchange reactions take place along these diffusion fronts between the solutions and the enclosing lithologies. Due to the different mobilities of the elements concerned, their concentrations in the solution would fall toward the diffusion front at different rates giving rise to well-developed zoning and distinct mineral paragenesis. Smirnov (1976) considers four groups of compounds and elements in order of decreasing mobility. They are: (1) H_2O and CO_2; (2) S, Cl, K, Na; 3) O, Si, Ca, Mg, Fe; 4) P, W, Al. Furthermore, three temperature stages are distinguished (Smirnov 1976, p.183): (1) a high temperature stage with pyroxene + garnet and pyroxene + epidote; (2) an intermediate temperature stage with two substages, one characterised by epidote + actinolite, and the other with epidote + chlorite; (3) a low temperature stage is subdivided into six substages with prehnite, pumpellyite, calcite + albite, calcite + quartz + sericite + chlorite, calcite + quartz + sericite + dolomite, and zeolite. These stages roughly correspond to those shown in Fig. 10.6.

A sequence of events of skarn genesis in a porphyry-related system is summarised below and depicted in Fig. 10.7. Firstly, the intrusion of a pluton results in contact metamorphism of the carbonate wall rocks. This stage involves decarbonation and dehydration reactions to form diopside and wollastonite skarns. The timing of this stage would correspond with the crystallisation of the pluton's margins following
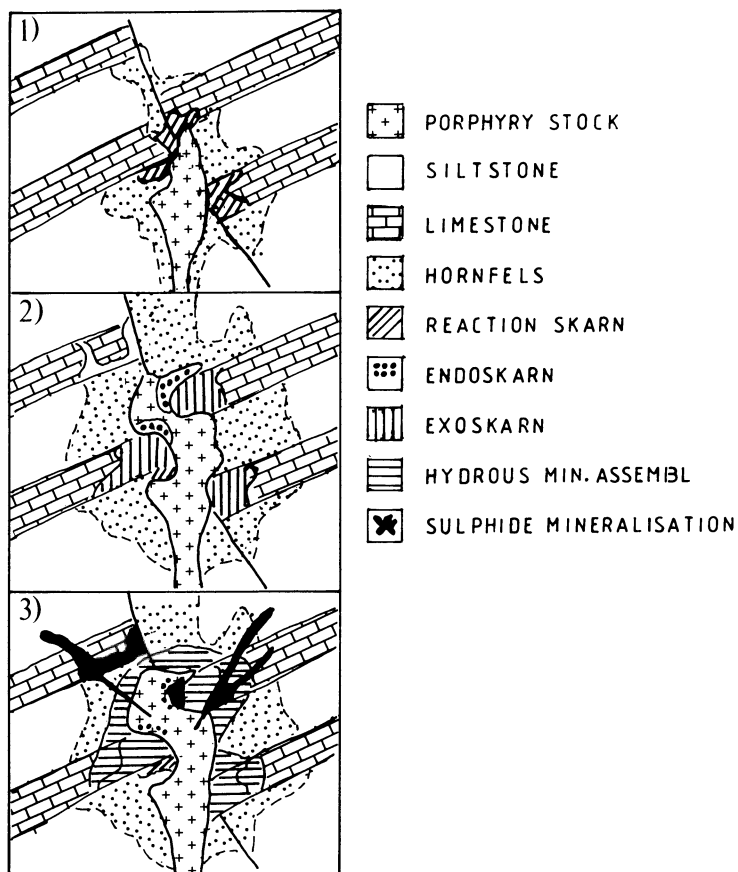
Fig. 10.7. Stages of skarn formation (after Einaudi et al. 1981; see also Figs. 10.6 and 10.8). 1 Isochemical stage with hornfelsing of non-carbonate units and development of reaction skarns in carbonate rocks; 2 Metasomatic stage with development of exo- and endo-skarns; 3 Retrograde stage with formation of hydrous minerals, massive sulphide veins and destruction of earlier skarns

the intrusion of the melt phase into the sedimentary lithologies. The temperature range is from 900 to 500°C. Metasomatic fluids, which are released from the partially solidified intrusion, infiltrate into and along fractures of pluton and country rocks. This is the stage of potassic alteration and disseminated chalcopyrite mineralisation in the plutonic rocks. This stage corresponds to the movement of the fluids outward into the structural breaks of the country rocks (fractures, contacts, permeable horizons) to form early skarn facies consisting of andradite, magnetite and sulphides. The temperature range is from approximately 600 to 400°C.

The next phase is one of ore deposition in the ongoing skarn development: andradite is replaced by magnetite, quartz, pyrite and calcite; while diopside skarn is replaced by actinolite, calcite quartz with some chalcopyrite. This corresponds to the waning stages of potassic alteration and the beginning of the quartz-sericite-
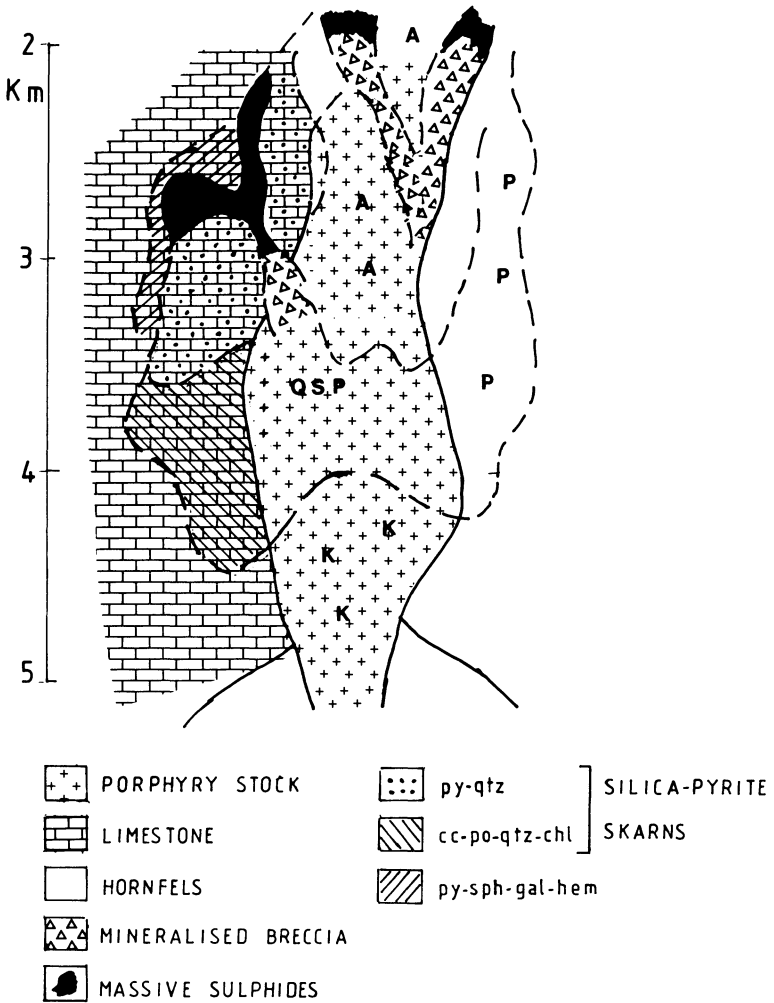
Fig. 10.8. Idealised zonal patterns of alteration-mineralisation in a porphyry-related skarn deposit of the lode type (see text) (after Einaudi 1982 b). *py* pyrite; *po* pyrrhotite; *sph* sphalerite; *gal* galena; *cc* chalcocite; *hem* hematite; *qtz* quartz; *chl* chlorite. Alteration: *A* argillic; *QSP* phyllic; *P* propylitic; *K* potassic

pyrite alteration in the pluton with concomitant Cu $\pm$ Mo mineralisation. The range of temperatures is from 500 to 300 °C.

The final stage (retrograde alteration) involves the destruction of the skarn assemblages and is characterised by the deposition of clay minerals (kaolinite, montmorillonite, nontronite), chlorite, calcite, quartz, hematite, pyrite and/or locally silica-pyrite. Mineralisation largely consists of pyrite, sphalerite, galena and tennantite. These sulphides tend to form veins. This stage of skarn destruction or retrograde alteration coincides with late phases of quartz-sericite-pyrite and argillic

alteration of the porphyry intrusion and is therefore dominated by the incursion of meteoric waters in the system.

Ore deposition in the sequence above is, in broad terms, classified by Einaudi (1982a) on a morphological and textural basis into two styles, namely: disseminated mineralisation and lode mineralisation. The former coincides with the early phases of skarn genesis (potassic event in the porphyry stock), and the latter more or less with sericitic, silicification and argillic alteration of the porphyry pluton. These two styles may occur in the same deposit. Lateral and vertical zoning of both disseminated and lode mineralisation styles may be present and is related to the distance from the porphyry pluton (Figs. 10.7 and 10.8). The nature of the zoning also depends on the nature of the replaced lithologies (e.g. limestone, calcareous siltstone). In the disseminated mineralisation styles, a zone of bornite + chalcopyrite + magnetite closest to the intrusion is followed by an intermediate zone of pyrite + chalcopyrite, a peripheral pyrite ± chalcopyrite ± tennantite ± sphalerite ± galena, hematite and/or magnetite. A distal zone occurs within the carbonate rocks and contains pyrite + chalcopyrite + magnetite ± sphalerite ± tennatite ± pyrrhotite. In the lode style of mineralisation the following zonation from the intrusive contact outward may be present: a zone of pyrite + digenite + enargite ± Sn-Bi-W minerals; an intermediate zone of pyrite + bornite + chalcopyrite + tennantite ± sphalerite; a peripheral zone of pyrite + chalcopyrite + tennantite + sphalerite + galena ± hematite; a distal zone within the carbonate rocks of pyrite + bornite + chalcopyrite + tennantite + sphalerite + galena ± magnetite or hematite.

The alteration and mineralisation of carbonate rocks in the porphyry environments displays very complex features reflecting the variability of both the geological materials and the physico-chemical properties of the hydrothermal solutions. The above review is clearly generalised and focuses on the common features of porphyry-related skarn deposits. The exploration geologist should be aware that individual deposits will display many variations of the common theme.

10.5 Mineral Deposits of Porphyry Systems

This section looks briefly at a selection of porphyry base metal deposits (including skarns). The examples given are representative of island-arc settings (Panguna and Ok Tedi in Papua New Guinea), continental Andean-type margin (Chuquicamata and El Teniente in Chile), back-arc rifting (Climax and Urad-Henderson in Colorado) and rift setting (Mo deposits in the Oslo graben Norway). Short reviews of porphyry-related skarns in the western USA, Sn and W skarns in Tasmania and of the porphyry Sn deposits of Bolivia are also included in this section.

10.5.1 Panguna and Ok Tedi Porphyry Cu-Au Deposits, Papua New Guinea

The Panguna and Ok Tedi Cu-Au deposits are located in the southwest Pacific islands of Bougainville and Papua New Guinea, within a consuming margin
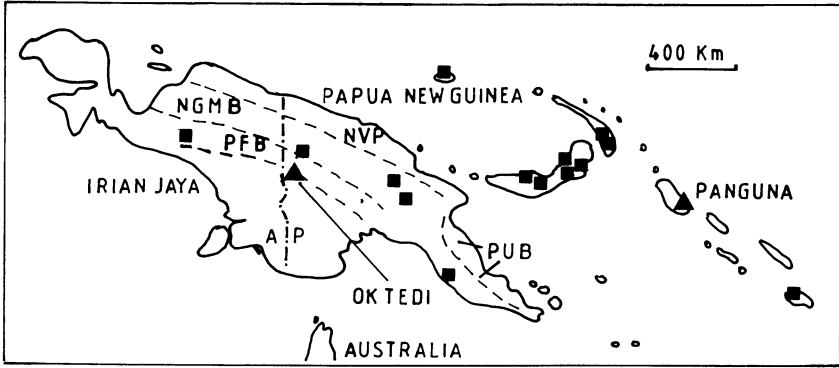
Fig. 10.9. Simplified geology and distribution of main porphyry deposits (*squares*) and location of Panguna and Ok Tedi (*triangles*) in Irian Jaya and Papua New Guinea (after Hill and Hegarty 1987; Titley 1975). *NVP* Northern Volcanic province; *NGMB* New Guinea Mobile Belt; *PFB* Papuan Fold Belt; *AP* Autralian Platform; *PUB* Papuan Ultramafic Belt

between the Indo-Australian and the Pacific plates (Figs. 10.1 and 10.9). In detail the plate tectonic setting of the region is characterised by a complex interplay of a number of small plates to the north and northeast of mainland Papua New Guinea, such as the Caroline plate, the Bismarck and Solomon plates. Subduction, formation of volcanic arcs, continental collision with the northern margin of Australia and the accretion of island arcs, are part of the complex tectonic history of the region (see Chap. 5 and Fig. 5.11). While numerous porphyry systems have been discovered in the Papua New Guinea region, only a few are currently active mines. Nevertheless, all of these deposits are of considerable scientific interest as they are geologically very young all having been formed from the Miocene to Recent.

The region in question is subdivided into a number of tectonic provinces (Dow 1975, Hill and Hegarty 1987) which are, from south to north: the Australian Platform, the Papuan Fold Belt, the New Guinea Mobile Belt, the Papuan Ultramafic Belt and the Northern Volcanic Arc (Fig. 10.9). The Australian Platform constitutes a stable Precambrian to Paleozoic basement of granitic and metamorphic rocks overlain by shallow marine and lacustrine sediments of Jurassic to Holocene age. The Papuan Fold Belt, which is included in this subdivision, lies along the northern margin of the platform. Many porphyry Cu deposits are associated with this Belt. The New Guinea Mobile Belt contains a thick sequence of geosynclinal sediments intruded by mafic to felsic plutonic rocks. This belt is part of a collision zone between the Australian continent in the southwest and island-arc systems to the northeast. Ophiolitic rocks mark the site of collision and obduction with the Northern Volcanic Arc to the north. The Northern Volcanic Arc continues eastward into the New Britain and Solomon island arcs which are part of the Melanesian oceanic province (Dow 1975). A comprehensive work on the geology and mineral deposits of Papua New Guinea can be found in Rogers and McKee (1990).

Panguna

This is the largest Au-rich porphyry Cu deposit known and was discovered in 1964 following regional and detailed geochemical sampling. An evaluation drilling programme totalling some 67 000 metres and carried out over a period of 4 years delineated primary ore reserves of approximately 944×10^6 tonnes at 0.48% Cu, 0.56 g/t Au and 3 g/t Ag. These drill-indicated grades, however, turned out to be somewhat conservative, and in 1977 the average grade was calculated at 0.68% Cu, 0.9 g/t Au and 1.9 g/t Ag. Details of the Panguna deposit can be found in Baumer and Fraser (1975), Ford and Green (1977), Baldwin et al. (1978), Ford (1978), Eastoe (1978) and Clark (1990). These works provided the basis for the following discussion.

Panguna is located on Bougainville island which is part of the Solomon Islands, a Late Cenozoic volcanic arc. Bougainville is underlain by Cenozoic andesitic and basaltic rocks, associated volcaniclastics and limestones. A number of younger dioritic and granodioritic stocks intruded this sequence during the Pliocene and Pleistocene. The Panguna deposit is centred on a complex of three porphyritic quartz-diorite and granodiorite bodies which are intrusive into the Panguna Andesite member. The intrusive stocks are marginal differentiates of the large equigranular Kaverong quartz-diorite, with ages of 4 to 5 Ma, itself containinig weak fracture-controlled alteration-mineralisation. The leucocratic quartz-diorite, the biotite-granodiorite and the biotite-diorite are the three strongly fractured, altered and mineralised stocks, while the Biuro granodiorite (3.4 Ma) and the plug-like Nautango andesite (1.6 Ma) post-date the mineralising event (Fig. 10.10A).

Approximately one third of the ore is contained within the Panguna andesite member, the remainder being in the three intrusive stocks in which well-mineralised intrusive and collapse breccia zones are present. The ore minerals occur associated with steeply dipping veins and fracture fillings, and as fine disseminations in the altered areas. Ore minerals are chalcopyrite and lesser bornite and associated Au and Ag. Gold occurs as submicroscopic particles of the native metal and Au values vary sympathetically with Cu. Recent studies indicate that most of the Au is contained within the lattice of chalcopyrite and bornite. Other sulphide and oxide species include pyrite, magnetite, hematite and traces of molybdenite. In general terms the Cu ore tends to increase with an increase in the proportion of veining, whereas disseminated ore increases with the more pervasive alteration. Also in the Panguna andesite the Cu content tends to decrease with distance from the intrusive contacts. Reconstruction of hydrothermal alteration geometry is complicated by the presence of multiple and overlapping alteration types. Potassic and propylitic alteration are dominant features, while argillic and phyllic alteration are important only in small areas (Fig. 10.13B). Potassic alteration forms a zone, within which are the higher Cu grades, and which is centred on the mineralised biotite-granodiorite and the leucocratic quartz-diorite. Potassic alteration in the Panguna andesite is mainly represented by a zone of secondary biotite surrounding the porphyries. The Kaverong quartz-diorite and the intrusive stocks display potassic assemblages of biotite + chlorite + K-feldspar + magnetite ± anhydrite, or biotite + K-feldspar + chlorite, as in the leucocratic quartz-diorite. Phyllic and argillic alterations are
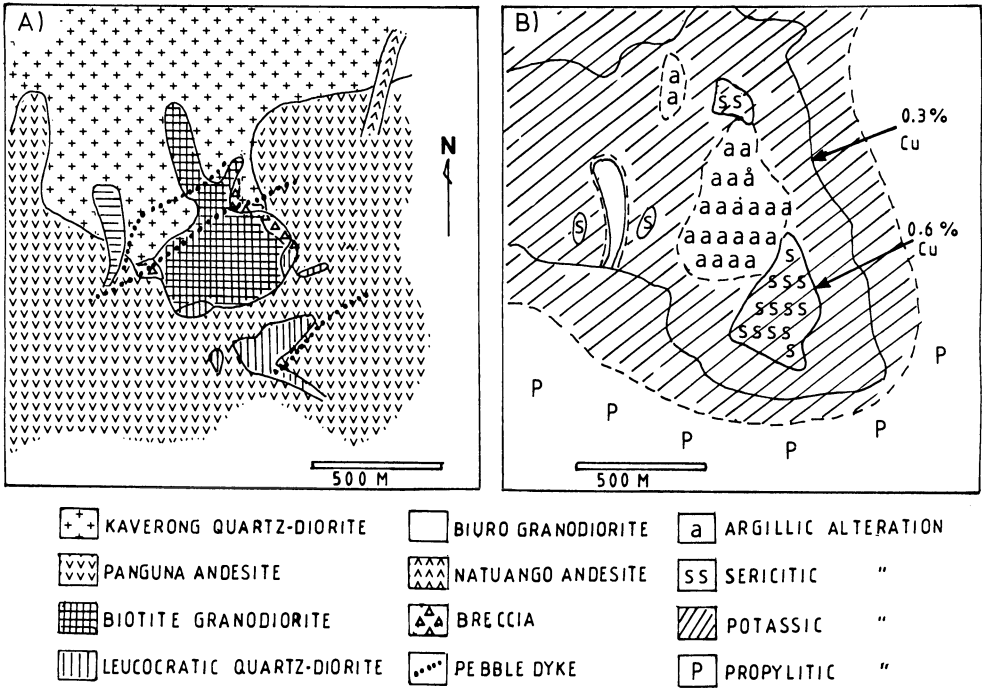
Fig. 10.10. A Simplified geology of Panguna porphyry Cu-Au deposit (after Ford and Green 1977). B Alteration patterns of the Panguna Cu-Au deposit (After Ford 1978)

confined to the biotite-granodiorite and consists of chlorite + sericite + clay minerals. Propylitic alteration surrounds the potassic zone, and in the Panguna andesite consists of chlorite, epidote, pyrite, calcite, albite and K-feldspar.

The alteration-mineralisation events started with a magmatic-hydrothermal stage with potassic alteration and Cu mineralisation, followed later by an influx of a cooler meteoric-dominated hydrothermal fluid which was feldspar-destructive and caused phyllic and argillic alteration. The Cu and Fe sulphides were deposited by boiling of the magmatic-hydrothermal solutions which had between 30 and 76 wt.% salts (NaCl + KCl) and temperatures ranging from 700 to 350°C and pressures of 200–300 bar, equivalent to approximately 2–3 km of depth. The meteoric-dominated fluids had a salinity of about 10 wt.% NaCl equivalent and resulted in the deposition of pyrite, quartz and clay at a temperature of approximately 300°C. Supergene oxidation produced a number of secondary minerals such as chrysocolla, dioptase, malachite, cuprite, chalcocite, covellite and native Cu. The secondary ore grades are only a little higher than the primary ore.

Ok Tedi (Mt. Fubilan)

The Ok Tedi deposit is located in the extreme northwest of the province of Papua, near the border with Irian Jaya (Fig. 10.9). Discovered in 1968, the deposit has been investigated and evaluated by a number of mining concerns. A recent estimate of the
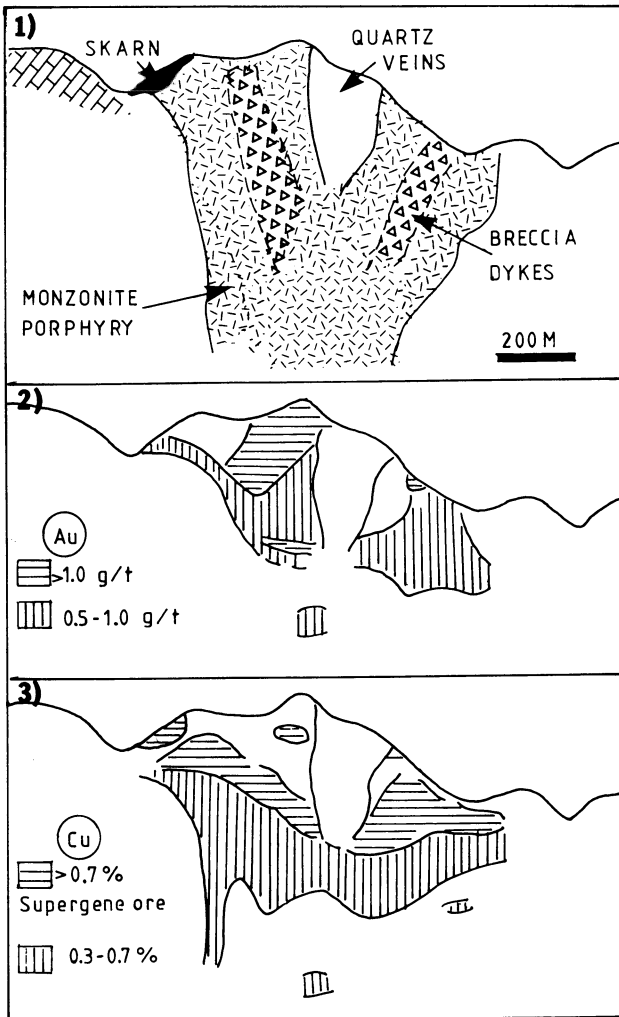
Fig. 10.11. Simplified cross-sections of the Ok Tedi Cu-Au deposit showing *1* geology; *2* Au distribution and *3* Cu distribution (After Davies et al. 1978)

ore reserves and resources is based on data gained from a total of 210 drill holes (Pintz 1984). Ore reserves are estimated to be 355 x 10^6 tonnes at an average grade of 0.7% Cu and 0.59 g/t Au; a leached ore cap contains about 3×10^6 tonnes at 2.08 g/t Au; and 29×10^6 at 1.2% Cu and 1.6 g/t Au of skarn ore (Rush and Seegers (1990). Additional resources include 192×10^6 tonnes at 0.4% Cu and 0.3 g/t Au and 51×10^6 of skarn ore at 1.46% Cu (Pintz 1984). Information on this deposit is taken from Bamford (1972), Davies et al. (1978), Pintz (1984) and Rush and Seegers (1990).

The Ok Tedi deposit is situated within the west-northwest-trending Papuan Fold Belt at the northern edge of the Australian Platform and therefore at the leading edge of the Australian continental plate. During the Late Pliocene a monzonite-

diorite complex (Fubilan stock) intruded into sedimentary rocks of Upper Cretaceous to Miocene age. The sediments, which include siltstone, sandstone and a 300-m thick limestone member, are structurally deformed around the Fubilan stock. The mineralisation occurs mostly within a monzonite porphyry intrusive phase centred on Mount Fubilan and measuring approximately 900 m in a north-south direction and 850 m in a east-west direction. Bamford (1972) subdivided the mineralisation into two broad categories, namely: (1) disseminated hypogene and supergene sulphides; and (2) skarns and massive magnetite-sulphide mineralisation (Fig. 10.11).

Disseminated hypogene sulphide mineralisation is related to a zone of strong potassic alteration of a monzonite rock, characterised by biotite, brown phologo-pite, rutile and minor K-feldspar. No other alteration type is present except for minor clay-sericite associated with a central massive quartz stockwork plug. Sulphides occur as disseminations and veinlet fillings and include chalcopyrite, bornite with lesser pyrite, marcasite and minor molybdenite. Chalcocite and covellite replace the primary sulphides and become dominant in a supergene cap which occurs below a leached zone containing low Cu values (0.05%) but high in Au (1–3 g/t).

Several skarn deposits are developed at lithological boundaries and in limestone wall rocks. The Gold Coast skarn is a body of massive magnetite, massive sulphides and calc-silicate containing high Cu grades. Magnetite skarn are characterised by granular magnetite, tremolite and diopside with veins of chalcopyrite and pyrite. Massive sulphide skarn contains pyrite, pyrrhotite and minor chalcopyrite. Calc-silicate skarn is made up of an assemblage of diopside + grossularite-andradite with veinlets of pyrite and chalcopyrite.

10.5.2 Porphyry Cu-Mo Deposits in Chile

The Andean continental margin contains numerous porphyry Cu-Mo deposits (Figs. 10.1 and 10.12). We have mentioned that these porphyry systems are genetically related to calc-alkaline magmatism in response to subduction of oceanic crust under the continental margin of the South American continent. The spatial and temporal relationship of mineralising systems in the Andean margin is briefly dealt with in Chapters 5 and 6 and further reviews can be found in Frutos (1982) and Sillitoe (1986 and references therein).

The geological evolution of the central and southern Andes from the Paleozoic onward is characterised mainly by the development of a magmatic arc at a convergent margin formed by the Farallon, Nazca and American plates. The entire magmatic system evolved from the initial stages of an ensimatic arc in the Lower Paleozoic to advanced and present-day stages of a magmatic arc of continental affinity. During the Mesozoic and Cenozoic, a migration of the magmatism towards the east occurred along regional belts parallel to the coast and hence to the trench and subduction zone. The emplacement of the Chilean porphyry deposits is therefore related to Mesozoic and Cenozoic calc-alkaline magmatic activity, which resulted in a continuous belt of granodioritic intrusions, andesitic lavas and

WEST FISSURE

FORTUNA GRANODIORITE

CHUQUI PORPHYRY

ELENA GRANODIORITE

ANDESITE

MIGMATITE

PALEOZOIC

MONZOGRANITE

SOUTH

AMERICA

CHUQUICAMATA

EL TENIENTE

1000 KM

1 KM

N

PIT OUTLINE

1000 M

ALTERATION

K-FELDSPAR + BIOTITE

K-FELDSPAR

K-FELDSPAR + SERICITE

QUARTZ-SERICITE

SUPERGENE CLAYS

EPIDOTE-CHLORITE

Fig. 10.12. Simplified geology and
hydrothermal alteration zoning at
Chuquicamata porphyry Cu deposit.
See text for details (after Ambrus
1978; Kirwin unpubl. *Inset* shows
distribution of porphyry deposits
and location of Chuquicamata and
El Teniente in South America

associated lithologies. Initial $^{87}Sr/^{86}Sr$ ratios of between 0.703 and 0.706 in the Chilean calc-alkaline rocks are indicative of a strong mantle component and tend to confirm mantle and/or lower crust involvement. By comparison the porphyry deposits of the North American Cordillera (including Climax types) have initial $^{87}Sr/^{86}Sr$ ratios of between 0.705 to 0.710 (Kestler et al. 1975; White et al. 1981). The ten most important Chilean porphyry deposits contain approximately 120×10^6 tonnes of Cu metal and about 30×10^6 tonnes of Mo metal (Frutos 1982). The two largest deposits are Chuquicamata (stockwork type) and El Teniente (breccia-type), which together contain approximately 60% of the total reserves, and are described in this section. Another important deposit is El Salvador (Gustafson and Hunt 1975). In the Chilean deposits the Cu/Mo ratios vary from 100:1 to 10:1 and therefore Mo is recovered as a by-product.

Chuquicamata

This deposit (and the nearby Exotica deposit) is located in northern Chile, 230 km northwest of the town of Antofagasta. The name is derived from an ancient local tribe known as the Chucos, and the "land of the Chucos" is in fact Chuquicamata. Although records of mineralisation in the region date back to the time of the Spanish conquistadores, it was not until 1915 that the first mining operations commenced. The discovery of the Exotica orebody (Mortimer et al. 1977), some 3 km to the south, was made accidentally while drilling the waste dumps for the recovery of leached Cu (Kirwin, unpubl. data). Ore reserves of Chuquicamata are in the region of 1.8×10^9 tonnes at 1.1% Cu and 0.12% Mo, making it one of the largest porphyry deposits in the world.

The primary Cu-Mo mineralisation occupies an area 12 km long and approximately 800 m wide, within an elongate granodioritic porphyry complex (Chuqui porphyries) which intruded into Jurassic granodiorites and Paleozoic granitic and metamorphic rocks during the Early Oligocene (Fig. 10.12). To the east the Chuqui porphyries grade into the Elena granodiorite, and the orebody to the west is separated from the Fortuna granodiorite by a major fault structure known as the West Fissure which, as discussed later, may have played an important role during and after the emplacement of the Chuqui porphyries. These porphyries are granodioritic in composition and at least three types can be distinguished (Ambrus 1978): (1) the East Side porphyry containing phenocrysts of plagioclase, K-feldspar and biotite; (2) the West Side porphyry composed of quartz, plagioclase and biotite set in a fine-grained groundmass; and (3) the Banco porphyry which appears to be a mixed phase of (1) and (2).

Three stages of alteration and mineralisation are recognised (Ambrus 1978). The earliest hydrothermal activity resulted in potassium-silicate alteration and the deposition of pyrite-molybdenite-chalcopyrite in various types of quartz veins. The main hydrothermal stage is represented by a pervasive quartz-sericite-pyrite alteration and forming the richest hypogene ore containing abundant pyrite with lesser bornite, chalcopyrite, sphalerite and enargite. This phyllic alteration grades eastward into a zone of propylitic alteration with albite, chlorite, specularite and epidote (Sillitoe 1973). The latest mineralising stage took place close to the West

Fissure, is associated with argillic alteration and produced veinlets containing pyrite, enargite, sphalerite, galena and tennantite. The zonal pattern of hydrothermal alteration is shown in Fig. 10.12. Molybdenite is found in quartz veinlets, as individual grains from 1 to 10 mm, or as clusters disseminated in quartz and generally concentrated near the vein margins. Pyrite and chalcopyrite are the associated ore minerals. The so-called blue veins have a narrow halo of "feldspar-destructive" alteration with fine disseminations of molybdenite. Composite quartz veins up to 0.5 m in thickness contain coarse molybdenite and grade into irregular quartz masses and pods. Nearly one third of the total Mo content of the deposit occurs as coarse-grained, curved and elongated bunches of crystals along fracture surfaces (Puig-Pichuante 1986). On the basis of the asymmetric alteration pattern, Sillitoe (1973) envisages a displacement of approximately 3 km along the West Fissure with the resulting elimination of a great portion of the altered and mineralised zone.

Leaching, oxidation and secondary enrichment were important ore-forming processes, and much of the production of Cu metal is in fact derived from the zone of supergene enrichment. The supergene zone occupies an area of 3.5 km in a north-south direction, with an average width of 500 metres and thickness of approximately 400 m. A leached capping with less than 0.10% Cu is followed by irregular masses of antlerite, brocantite and atacamite (approximate grade of 1.5% Cu). This is underlain by enrichment zones of chalcocite and chalcocite + covellite (approximately 18% Cu), and finally an elongate and deeper covellite enrichment zone (10–15% Cu) which appears to be spatiallly associated with the West Fissure. Many of the supergene minerals at Chuquicamata are unique and owe their preservation to the unusual and extreme arid conditions of the Atacama desert. A number of sulphates, nitrates, chlorides, iodates and iodides occur within a few metres from the surface (Kirwin, unpubl. data). Oxidation of molybdenite leads to lindgrenite $[Cu_3(Mo_4)_2(OH)]$ which, as the most important Mo oxide, is more abundant in zones where the Cu oxides are stable. In the upper levels extreme acid conditions result in the leaching of lindgrenite to ferrimolybdite $[Fe(MoO_4)_38H_2O]$ (Ambrus 1978).

El Teniente

The El Teniente deposit owes its name to the discovery by a fugitive Spanish army lieutenant in 1706, but the first official records of production are dated at 1819 (Howell and Molloy 1960). The ore reserves of El Teniente are approximately 4000 $\times 10^6$ tonnes at 1.16% Cu and about 0.02% Mo (Ambrus 1978), but in spite of its size and economic importance few works have been published on the El Teniente deposit (Lindgren and Bastin 1922, Howell and Molloy 1960, Camus 1975, Ambrus 1978). The present account is based on Camus (1975) and unpublished notes by D. Kirwin.

El Teniente is situated approximately 100 km southeast of Santiago (Fig. 10.12 inset) within a major north-south-trending volcano-sedimentary belt of Cretaceous age intruded by quartz-diorite plutons and related dacitic volcanic rocks. The mine area is underlain by great thicknesses of lava flows, pyroclastics and sediments

which are intruded by intermediate to felsic intrusive rocks. The ages of these rocks range from Upper Cretaceous to Quaternary, the oldest formation being the Coya-Machale (Upper Cretaceous) which consists of folded sediments, andesite and pyroclastics some 3000 m thick. Above this is the Farellones Formation (Paleocene to Eocene) which is subdivided into three members in the mine area. The lowest member is from 1400 to 1000 m thick, is made up uniquely of andesitic rocks which are also the main host of the mineralisation; the middle member is 800 m thick and made up of epidotised andesites and interacalated lacustrine sediments; the upper member consists of basalt and andesite lavas with some pyroclastics. During the Pliocene quartz-diorite, dacite porphyry, the Braden Formation (pipe breccia) and latite porphyry were emplaced. Breccia pipes occurring at El Teniente and further south along the volcano-sedimentary belt are associated with, and contain fragments of, the dacite porphyries.

Mineralisation and alteration are associated with the quartz-diorite-dacite intrusive complex and the mineralised area is cut by the Braden Formation, which is a brecciated inverted-cone structure surrounded by a margin of breccia some 20 to 40 m thick (Fig. 10.13). The diameter of the breccia pipe varies from 1300 m at surface to 650 m at a depth of 1600 m below surface. The pipe consists of rounded to subangular mineralised fragments, ranging in size from a few centimetres to 3 metres and set in a rock-flour matrix. No clast-size preferential distribution is recognised, but graded bedding is seen in the upper levels of the pipe. The surrounding marginal breccia is made up of angular fragments cemented by a tourmaline-quartz-sulphide matrix. Fragments of this marginal belt are also found in the Braden Formation pipe, indicating that they are pre-pipe age. Another breccia occurs in the upper parts of the quartz-diorite intrusive and extends vertically for about 350 m. In this breccia, fragments of quartz-diorite from a few millimetres to about 30 cm exhibit a lack of relative movement and are set in a matrix of tourmaline and sulphides. Pebble dykes of post-mineralisation age occur in the upper levels of the deposit and are spatially related to the Braden Formation pipe.

Three hypogene alteration phases and one supergene phase have been recognised. The hypogene phases are: potassic, phyllic and propylitic. The supergene phase is mainly argillic. Potassic alteration affects a large portion of the deposit and is characterised by K-feldspar and biotite. The mineralisation is mainly associated with this phase of alteration. While phyllic alteration affects all rocks it is best developed in the quartz-diorites, where quartz and sericite are the chief minerals, but tourmaline, anhydrite, chlorite and pyrophyllite may also be present. The propylitc zone contains chlorite, epidote, calcite, magnetite, anhydrite and tourmaline. Propylitisation is only observed in the Farellones andesites and the quartz-diotite. Tourmaline, an important component of the El Teniente alteration assemblages, is related to two distinct events: (1) the emplacement of the quartz-diorites and (2) the emplacement of the breccia pipe. It occurs as fine to coarse disseminations, as fracture fillings and as matrix in the breccias. Hypogene sulphides form a zonal pattern in the north and central parts of the orebody with bornite at the core surrounded by a zone of chalcopyrite $\pm$ pyrite grading into a marginal zone of pyrite. Other sulphides and ore minerals are molybdenite,
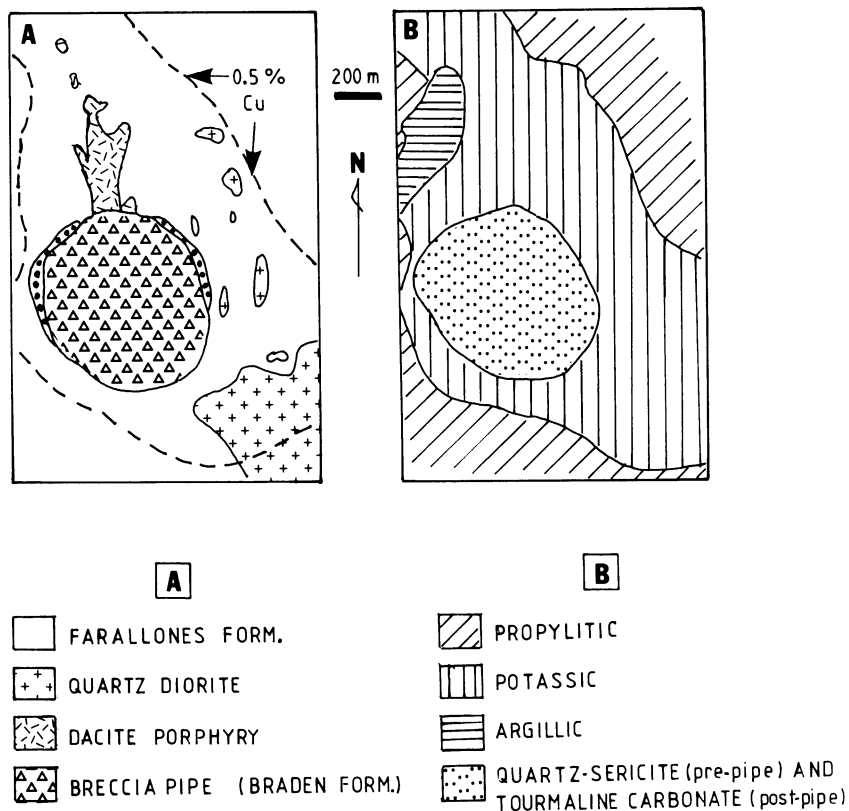
Fig. 10.13. A Simplified geology and B alteration pattern of the El Teniente porphyry Cu deposit at 5 Level. See text for details (After Camus 1975)

tennatite, hematite, magnetite and enargite. Molybdenite which is associated with quartz veins, occurs throughout the deposit but is most highly concentrated at the intrusive contacts.

The genesis of the El Teniente mineralisation is related to the emplacement of stocks, their cooling, retrograde boiling, hydraulic brecciation and the activities of magmatic and meteoric hydrothermal systems. Metals were probably transported in highly saline brines and deposited in veins and veinlets within the surrounding fractured rocks. As with other porphyry systems the potassic phase of alteration-mineralisation is linked to the activity of a magmatic hydrothermal system, while the phyllic, argillic and perhaps the propylitic phases were genetically related to influx of meteoric waters.

10.5.3 Porphyry Mo Deposits of the Colorado Mineral Belt

The largest resources of Mo in the world come from the Colorado Mineral Belt situated within the Rio Grande rift system. The porphyry Mo deposits of this area are thought to constitute a class of their own, known as Climax type, and are characterised by porphyry intrusives enriched in silica and alkalies and with an A-type chemistry. They are therefore distinct from the subduction-related quartz-monzonite-hosted porphyry Cu-Mo systems such as those of the Andean continental margin, or those of the North American cordillera, as for example the Endako Mo deposit in Canada (Kimura and Drummond 1969, Kimura et al. 1976). There are three major groups of porphyry Mo deposits: Urad-Henderson, Climax and those of the Mt. Emmons area (Fig. 10.14). In this section the Urad-Henderson and Climax deposits are described briefly; further details may be found in the works of Wallace et al. (1978), Woodcock and Hollister (1978) and White et al. (1981).

The Colorado Mineral Belt is approximately 400 km long and 15 to 60 km wide, extending in a northeast-southwest direction across Precambrian and Phanerozoic rocks (Fig. 10.14). The Belt is in the Rocky Mountains region of the USA along the eastern margin of the North American Cordillera. Phanerozoic rock sequences from Cambrian to Quaternary were deposited on the Precambrian basement. Magmatic activity during the Laramide orogeny resulted in a series of events which culminated in the emplacement of a variety of volcanic, subvolcanic and plutonic rocks penetrating both basement and Phanerozoic sequences. Metallogeny in the region is related to these magmatic episodes, which are thought to be related to a back-arc rift geotectonic setting (Sawkins 1990). The Laramide magmatic activity came in two major pulses – one in the Cretaceous, and one in Oligocene times – during which lines of weakness in the old Precambrian crust were reactivated, providing the pathways to the ascending magmas. The mineralising events are all related to granitoid stock intrusions of Tertiary age. The origin of the ore-forming magmas is
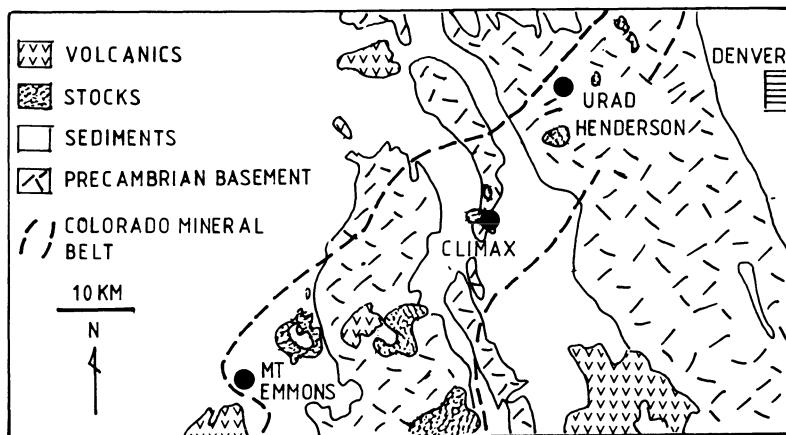
Fig. 10.14. Simplified geological map of the Colorado Mineral Belt showing location of main porphyry Mo deposits (After Wallace et al. 1978)

not clear, but on the basis of initial Sr isotope ratios it is thought to be related to source regions of mantle partial melting as well as the interaction of mantle-derived melts with the lower crust. Differentiation of enriched A-type magmas results in the formation of highly fractionated F-rich melts which separate and intrude into the upper crustal levels. High F contents enable the development of late stage hydrous and potassic melts into which Mo and other incompatible elements are partitioned (White et al. 1981). Vapour saturation results in the formation of stockworks above the intrusion (see Chap. 3 and Fig. 3.1), and large amounts of incompatible-enriched (e.g. Mo, F, Si and S) fluids are therefore directly exsolved from the magmas, released into fractures within the intruding stocks and the surrounding rocks. Various lines of evidence indicate that the fluids were expelled at depths ranging from approximately 600 to 3000 m below surface (White et al. 1981).

Urad-Henderson

The Urad and Henderson are separate orebodies, but the Urad-Henderson Mo deposit, located some 75 km west of Denver, forms the world's second largest concentration of Mo metal. Ore reserves of the Henderson orebody were estimated to be around 300×10^6 tonnes at an average grade of 0.3% Mo. The Urad orebody was partially destroyed by geological events following its development, and the remaining reserves of approximately 14×10^6 tonnes at 0.2% Mo have been mined out. The Henderson orebody occurs deep within the Red Mountain at about 1200 metres below the summit. The surface expression of the Urad mineralisation had been recognised since the early 1900s through the presence of ferrimolybdite along a mineralised fault which cuts the orebody. After 2 years of exploration drilling, during which about 45 holes had been completed, results were not considered promising. In 1965, the last hole, which was authorised to close the programme, intersected one of the largest hidden orebodies in the world. The discovery of the Henderson mineralisation is an outstanding tribute to geological ingenuity and persistence as well as management acumen.

The geological events that led to the development of the Urad-Henderson porphyry Mo system include a complex sequence of igneous and hydrothermal activities. Figure 10.15 shows time-composite sketches depicting the history of porphyry stock emplacement and related mineralisation (Wallace et al. 1978). The igneous bodies in order of emplacement are called: Tungsten Slide unit, East Knob unit, Square quartz-porphyry, Red Mountain porphyry, Urad porphyry, Primos porphyry and Henderson granite (Fig. 10.15). All are aged between 27 and 21 Ma and intrude the Precambrian Silver Plume granite (1.4 Ga). The Urad orebody is believed to have extended for at least 1000 m in the vertical sense, but as previously mentioned it was destroyed by the intrusion of the Red Mountain porphyry stock. Mineralisation consists of fine-grained molybdenite with minor fluorite, pyrite, galena, sphalerite and huebnerite, contained in veinlets from 1 to 20 mm wide forming extensive stockworks. Hydrothermal alteration is complex and typified by a variety of assemblages reflecting not only the nature of the fluids but also that of the wall rocks affected. Broadly speaking at least two stages of alteration are recognised by Wallace et al. (1978): a main stage and a late stage. The main stage is a
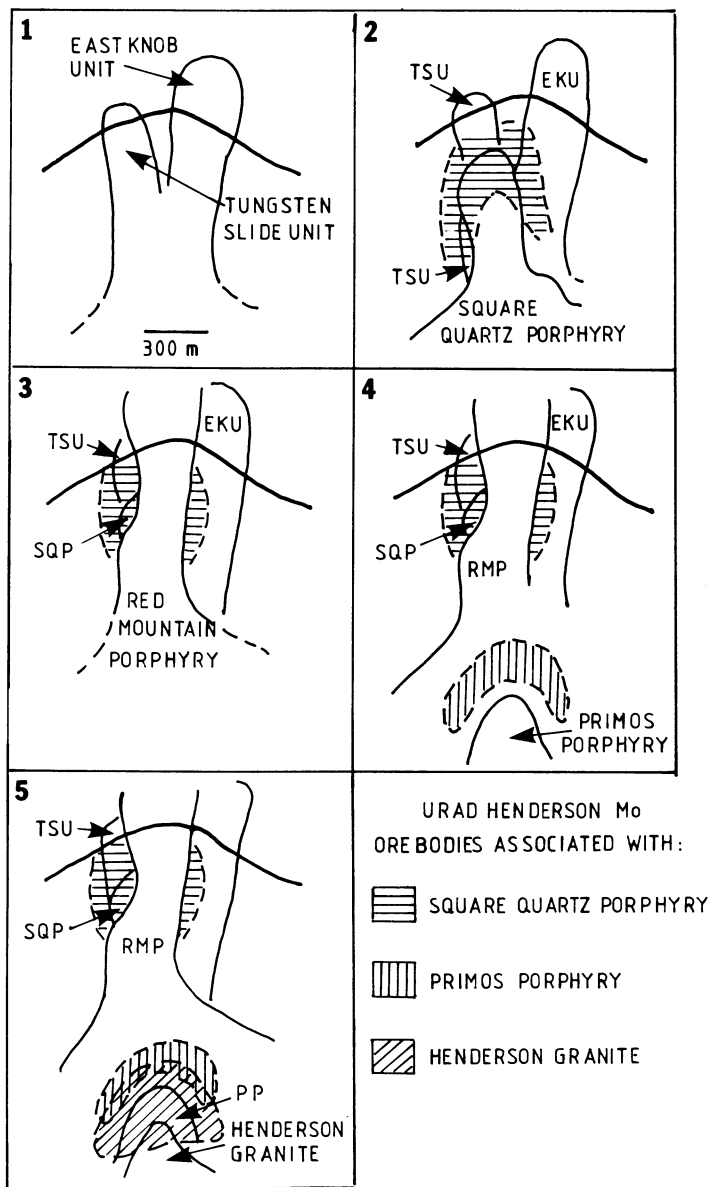
Fig. 10.15. Generalised time-sequence of magmatic and mineralising events of the Urad-Henderson porphyry Mo deposit. 1 Intrusion of Tungsten Slide Unit *TSU* and East Knob Unit *EKU; 2* Square Quartz Porphyry *SQP* is emplaced and is associated with a first pulse of alteration-mineralisation; 3) intrusion of the Red Mountain Porphyry *RMP* and partial destruction of the *SQP* orebody; 4) Primos Porphyry *PP* intrudes at depth and form another Mo orebody; 5 the Henderson Granite intrudes into the *PP* and a third Mo orebody is formed and overlaps that formed by the *PP* intrusion. Scale is in panel 1 (After Wallace et al. 1978)

major alteration sequence which progressed upward and outward from the deepest and central area of potassic alteration, called the K-feldspathised zone with a biotite subzone, a quartz-topaz zone, quartz-sericite-pyrite and argillic zones, all enclosed in a large halo of propylitic alteration which is exposed at the surface. The late stage of alteration includes a greisen zone and a lower argillic zone which overlap the lower portions of the main stage alteration sequence. More details on the hydrothermal alteration are given, following the discussion of the Climax deposit.

Climax

The Climax Mo deposit is located on the Continental Divide about 160 km by road from Denver. Although mineralisation in the area was first discovered in 1879, it was not until World War I, when Mo became a useful alloy metal, that mining began. Ore reserves at Climax were of the order of 483×10^6 tonnes (see also Table 10.1) at an average grade of about 0.2% Mo, of which 185×10^6 tonnes were as open cut ore and about 298×10^6 tonnes as block-cave ore. W, Sn and pyrite have been recovered as by-products. A comprehensive description of Climax can be found in Surface et al. (1978). The Climax igneous complex includes a series of four major intrusive pulses, each of which was accompanied by hydrothermal activity. Three distinct orebodies related to the first three intrusions were generated; these are, in order of decreasing age: the Ceresco orebody, most of which has been eroded off, and the Upper and Lower orebodies. Post-mineralisation movement along the Mosquito Fault to the west was up to about 2600 metres and it is believed that perhaps part of the Ceresco orebody might be located at depth along the west side of the fault. The mineralisation in the two upper orebodies consists of two ore zones each, an upper W-rich zone and a lower Mo-rich zone. In the Upper orebody W and Mo mineralisation overlap. Ore minerals are molybdenite, huebnerite ($MnWO_4$), cassiterite and pyrite. Quartz-molybdenite veinlets, which also contain topaz and fluorite, form the famous Climax stockwork system. The stockworks are most common in the zones of potassic alteration, although the two events are separated in time. In a typical quartz-molybdenite veinlet (range of thickness is from 0.5 to 20 mm) molybdenite is irregularly distributed along the margins of the veinlet, whereas the centre is occupied by a closely packed mosaic of fine quartz grains. Some veinlets consist almost entirely of molybdenite and pyrite.

Hydrothermal Alteration of the Climax and Urad-Henderson Deposits

Patterns of alteration-mineralisation in these porphyry systems are complex due to the superposition of multiple intrusive and hydrothermal events. Considering only one event, the pattern of alteration common to most porphyry Mo deposits is idealised in Fig. 10.16. Details of hydrothermal alteration are best known from comprehensive studies of the Henderson deposit at Red Mountain, where five major zones of alteration are recognised (White et al. 1981). A potassic alteration zone coincides with the 0.3% Mo cut-off boundary of the Henderson ore and is characterised by the total replacement of plagioclase by K-feldspar, giving rise to an equigranular groundmass of K-feldspar and quartz. K-feldspar veinlets are locally
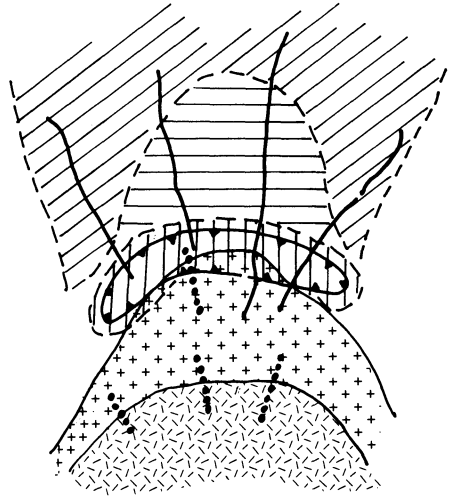
LATE PORPHYRY STOCK

EARLY PORPHYRY STOCK

ARGILLIC ALTERATION

QUARTZ SERICITE ALTERATION

POTASSIC ALTERATION

ORE SHELL

BASE METAL, Mn,F VEINS

GREISEN VEINS

Fig. 10.16. Generalised model of porphyry Mo system and associated hydrothermal alteration patterns (After Mutschler et al. 1981)

present. A quartz-sericite-pyrite zone has a bell shape possibly reflecting temperature variations during the alteration process. This zone is characterised by the replacement of K-feldspar and plagioclase by sericite, by the presence of optically continuous quartz overgrowth and by abundant pyrite. Where pervasive the original igneous textures are completely destroyed. An upper argillic zone displays selective replacement of plagioclase by montmorillonite, kaolinite and sericite, while K-feldspar remains relatively unaltered; biotites are replaced by sericite, rutile, pyrite, carbonate and fluorite. A lower argillic zone occurs at the base of the orebody and is represented by the replacement of all K-feldspars by kaolinite. The propylitic zone is well developed in the Precambrian Silver Plume granite. This alteration zone is typified by the mineral assemblage chlorite + epidote + calcite + clay + sericite. The outer boundary of the propylitic zone is taken to be where primary biotite is replaced by chlorite. Five additional alteration zones of lesser extent are: vein and pervasive silica zones, magnetite-topaz zone, garnet zone and a greisen zone. The latter contains quartz-muscovite and topaz as the main minerals and occurs around quartz-molybdenite veinlets and below the Henderson ore zone.

The garnet zone (spessartine) is associated with a late stage of Pb-Zn-Mn hydrothermal event (see Fig. 10.16).

Fluid inclusion data indicate that the Mo mineralisation was formed at temperatures of between 650 and 500°C from fluids of high salinity (in excess of 30 wt.% NaCl equivalent and up to 65 wt.%), at depths of approximately 1500–2500 m at Henderson. White et al. (1981) consider the presence of features such as crenulate quartz layers, replacement of albite by orthoclase, graphic intergrowths, presence of mineralised layers of pegmatites and F-bearing minerals as important clues as to the origin, separation, accumulation and escape of the hydrothermal solutions. The origin of crenulate quartz layers, for example, is explained by these authors as due to rhythmic fluctuation in the pressure of H_2O and F in the system. The replacement of albite by K-feldspar may be related to the upward concentration of volatiles and the separation of an aqueous fluid from the silicate melt with K-partitioning preferentially into the fluid phase, so that it reacted with albite causing its replacement. The authors also noted the spatial association of graphic intergrowths (quartz-alkali feldspar) with molybdenite mineralisation and again interpret this feature in terms of separation of a H_2O-rich fluid. Pegmatites, pods and dykes are common in the Climax-type system and occur near the roof zones. They include accessory minerals such as fluorite, molybdenite and REE minerals. In this respect the presence of pegmatites in the roof zones is a feature similar to that of the Sn-W systems described in Chapter 9.

10.5.4 The porphyry Mo Mineralisation of the Oslo Graben, Norway

Chapter 6 (and references therein) referred, inter alia, to the grouping of continental grabens and rift zones according to their tectonic setting at the time of their inception, and the important role played in facilitating the emplacement of magmas and the channelling of mineralising fluids. One of the many Phanerozoic rift systems is the Oslo Graben where porphyry Mo mineralisation has been recognised and is found associated with the porphyritic phase of biotite granites at several localities (Geyti and Schonwandt 1979; Schonwandt and Petersen 1983).

The Oslo Graben is part of the post-Hercynian rift system which extends beneath the North Sea. The evolution of the Oslo Graben began as a passive rift system later followed by extensive Permian magmatic activity which included initial basaltic volcanism, the eruption of latitic lavas and the formation of ring complexes characterised by central volcanoes and cauldron subsidence. Lastly, the emplacement of composite bodies of biotite granite, monzonite and syenite took place. Hydrothermal alteration and Mo mineralisation were discovered as a result of mineral exploration which was started on the basis of a conceptual model of porphyry-style mineralisation (Geyti and Schonwandt 1978). Two important localities of porphyry Mo mineralisation are in the Glitrevann and Hurdal igneous complexes where the mineralisation is closely associated with granitic rocks (Schonwandt and Petersen 1983). The mineralisation of the Glitrevann complex is briefly discussed below.

The Glitrevann complex is a ring-type volcano-plutonic structure consisting of rhyolite and rhyolitic ignimbrite associated with basaltic volcanics. The eruption of voluminous ash-flow tuffs caused the collapse of the volcanic structure and the formation of the Bordvika cauldron. This was followed by further eruption of rhyolite porphyries basaltic lavas and ash-flow tuffs. A phase of intrusive activity followed with the emplacement of syenitic ring dykes and the intrusion of a composite granitic stock (Schonwandt and Petersen 1983). This stock consists of three units, namely: aplitic granite, and black and grey quartz-feldspar porphyries. Mo mineralisation is associated with hydrothermal alteration at Bordvika where the host rocks are rhyolite and quartz-feldspar ignimbrite which acted as a cap to the underlying aplitic granite. Molybdenite, accompanied by pyrite and fluorite, occurs in quartz vein stockworks within a zone of sericitic alteration. Geyti and Schonwandt (1979) mapped four zones of alteration (potassic, sericitic, argillic and propylitic) and likened the system to the Climax porphyry Mo deposit type. At Bordvika potassic alteration is not common and consists of K-feldspar veinlets associated with quartz, pyrite and molybdenite. Sericitic alteration with up to 10% by volume of pyrite is very prominent and widespread. Where pervasive, the original feldspars are completely destroyed and the sericitised rock becomes fine-grained and white in colour. Sericitic alteration is also found as millimetre-wide haloes around mineralised veins. Argillic alteration is mainly kaolinite and montmorillonite occurring as dusty replacements of feldspar crystals. Petrographic criteria were used to distinguish between sericitic and argillic alteration. Where sericite completely replaces feldspars and constitutes a substantial proportion of the groundmass the rocks are considered to be affected by sericitic alteration. Intense "dusty" replacement of feldspars with little or no replacement of groundmass material is taken to indicate argillic alteration. Propylitic alteration, which occurs outside the zone of argillic alteration and is poorly developed, is characterised by the assemblage of chlorite + calcite + epidote ± fluorite in veinlets and as cavity fillings.

10.5.5 Skarn Deposits in the Western USA

Skarn deposits in the western states of the USA are porphyry Cu-related. The majority of these Cu skarns are located in Arizona, the most important region for porphyry Cu deposits, but important deposits also occur in Nevada (Yerington) and in Utah (Bingham, one of the largest known Cu skarns). The Bingham and Yerington deposits are briefly discussed in this section. The Cu skarns of the western USA are associated with Cenozoic calc-alkaline magmatic arcs related to complex subduction processes along the west coast of the USA (Cordilleran belt). It is thought that the strong pulse of magmatism and related porphyry systems during the Tertiary coincides with an increase in spreading rates along the East Pacific Rise, and changes in the angle of dip of the Benioff zone (Sawkins 1990).

The Cu skarns of the western USA are associated with highly fractured subvolcanic granodiorite to quartz-monzonite porphyry displaying varying degrees of potassic and sericitic alteration. The intrusive stocks were emplaced at depths of between 5 and 1 km. Cu-skarns are of the calcic type and mineralisation consists of

sulphide (2–15%) and Fe oxide (ca. 10%) disseminations, veins, and massive replacement of marble rocks at the skarn front. Ore reserves range from less than 1 to ca. 400×10^6 tonnes at grades of approximately 1% Cu with Au, Ag, Mo, Pb and Zn being recovered locally as by-products.

Bingham

The Bingham deposit in the state of Utah is the largest known Cu-skarn deposit, and one of the largest porphyry Cu in the world. The skarn ore reserves are about 150×10^6 tonnes at 1.3% Cu, 0.03% Mo and 12 g/t Ag (Einaudi et al. 1981). The discussion that follows is based on Lanier et al. (1978), Atkinson and Einaudi (1978) and Reid (1978).

   In the Bingham mine area a Mid-Tertiary composite stock, intruded along a northeast-trending fault direction, consists of early monzonite, followed by quartz-monzonite and late quartz-latite porphyry. This composite stock was intruded into a sequence of sedimentary rocks of Upper Carboniferous age, consisting of older units of feldspathic orthoquartzite and calcareous quartzite (Butterfield Peaks Formation) and younger units of limestone, calcareous sandstone, and quartzite (Bingham Mine Formation). The intrusive stock contains primary mineralisation at an average grade of approximately 0.65% Cu. An early stage of Mg-Si metasoma-tism formed diopside in quartzite and in silty limestone beds, and wollastonite in cherty limestone, up to 1500 m and 600 m from the stock respectively. A trace amount of sulphides accompanied this early metasomatic event, which was synchronous with the emplacement of the quartz-monzonite porphyry. Actinolite-biotite alteration of diopside along sulphide-bearing fractures in quartzite, and garnet alteration of wollastonite-bearing marble, constitute the main-stage mineral-ising event, which was synchronous with the potassic alteration of the intrusive stock. The mineralised skarns vary in thickness from 15 to 60 m. The main-stage skarn consists of brown andradite, diopside, magnetite and chalcopyrite superim-posed on the early-stage wollastonite up to 450 m from the porphyry intrusion. The main-stage of ore deposition culminated with the alteration of andradite to various mixtures of calcite, quartz, hematite, magnetite, siderite and sulphides. In the wollastonite zone, yellow-green garnet is accompanied by chalcopyrite and bornite with minor sphalerite and galena. Pyrite/chalcopyrite ratios decrease from the outer margin of the andradite-diopside zone towards the intrusive contact and at depth. A late-stage alteration phase produced pyrite, chlorite, montmorillonite, sericite, talc and opal.

Yerington (Mason Valley)

The Yerington district, western Nevada, is located within a belt of Jurassic intrusive rocks comprising a northern granodiorite batholith and a southern quartz-monzonite batholith. These are separated by Triassic-Jurassic volcanic and volcaniclastic-sedimentary rocks forming an east-west-trending zone about 8 km long and 3 km wide (Einaudi 1982a). The district is an area of major porphyry Cu systems with possible total resources in excess of 1000×10^6 tonnes of Cu ore,

including the Yerington, Ann Mason, Bear-Lagomarsino and MacArthur porphyry Cu deposits. Mason Valley is one of several Cu-skarn deposits in the district (Einaudi 1977).

The Mason Valley Cu-skarn deposit occurs within a thick sequence of volcano-sedimentary rocks of Triassic age. The lower half of the sequence is composed of metamorphosed andesite and rhyolite lavas, breccias and sediments, whereas the upper portion consists largely of massive limestone, thin-bedded black calcareous shale and siliceous volcaniclastic rocks. The limestone beds are the host of numerous small Cu skarns located on the outer margins of a hornfels-skarnoid aureole. The distribution of the metasomatic rocks and mineral zoning indicate that the Yerington batholith, to the north, rather than the other batholith to the south, is responsible for the skarn mineralisation. The Jurassic Yerington batholith rocks include granodiorite intruded by quartz-monzonite and younger quartz-monzonite porphyry dykes. The youngest rocks in the area are Tertiary rhyolite-dacite volcanics.

The carbonate rocks are not in direct contact with the porphyry plutons but are located some 3 to 4 km from the outermost edge of the porphyry Cu mineralisation. The large mass of granodiorite effectively shielded the carbonate rocks from direct contact with the porphyry Cu plutons. This spatial separation resulted in a mild retrograde alteration-mineralisation event, rendering it difficult to correlate alteration-mineralisation events between the intrusive and the sedimentary rocks. Two episodes of metasomatic and hydrothermal activity have been recognised (Einaudi 1977, 1982a). An early episode produced garnet-pyroxene hornfels near the batholith contact and recrystallisation to hornblende hornfels facies further out. Garnets of the hornfels rocks belong to the grossularite-andradite series, whereas the pyroxenes belong to the diopside-hedenbergite series. The second episode involved the brecciation of the early hornfels and the development of chalcopyrite-pyrite-bearing skarns.

Formed in limestone, the skarn extends along a contact zone with tuffaceous rocks for about 600 m, with an average width of 65 m. The skarn zone dips about 70° W, parrallel to bedding. The skarn consists of a footwall zone and a hangingwall zone – the former being made up largely of garnet and containing pyrite and chalcopyrite (1–5% by volume), the latter consisting of garnet and pyroxene and approximately 20% pyrite and chalcopyrite. The hangingwall skarn is late relative to the footwall skarn and is developed along the outer edge of the footwall zone. The zoning in the hangingwall skarn outward from a centre-line towards the dolomitic marble is: garnet + pyroxene, pyroxene and tremolite + talc at the contact with the dolomitised marble. This zonal pattern reveals that the direction of the metasomat-ising fluids was southward away from the batholith contact and along the faulted and brecciated limestone-tuff contact. In the later stages the fluids infiltrated along bedding planes in marble rocks, forming the hangingwall skarns.

10.5.6 Other Types of Skarn Deposits

For the sake of completion and by way of comparison, selected examples of non-porphyry-related skarns are considered in this section. Important W skarn deposits of Mid- to Late Cretaceous age, located in Canada (North West Territories, Yukon), are the MacWilliam Pass (MacTung) deposit containing about 30×10^6 tonnes of ore at 0.95% WO_3, and the Canadian Tungsten (CanTung) deposit with approximately 4×10^6 tonnes at 1.5% WO_3. CanTung is one of the largest producers of scheelite in the world. Both deposits are hosted in carbonate units of the Lower Paleozoic within the thermal aureole of quartz-monzonite stocks. Details of these Canadian deposits can be found in Einaudi et al. (1981), Dick and Hogson (1982) and Mathieson and Clark (1984).

The Sn-W Moina deposit, the W skarn of King Island and the Cleveland Sn deposit (Tasmania, Australia) are chosen here as examples for a more detailed discussion, based on the works of Kwak and Askins (1981) (Moina deposit), Kwak and Tan (1981) (King Island), Collins (1981) (Cleveland) and Einaudi et al. (1981). For more details the reader is referred to the above, the Special Issue of Economic Geology devoted to the geology and mineral deposits of Tasmania (vol.76, No.2, 1981) and to Kwak (1987).

In Tasmania there are several skarn deposits which may represent a continuum between deposits dominated by high temperature skarn minerals and those of lower temperature sulphide replacement type. The Moina and King Island deposits are examples of the former, while the latter are represented by the Sn deposits of Rennison Bell, Cleveland and Mount Bischoff. A description of the Mount Bischoff deposit is given in Chapter 9.

Moina Sn-W deposit

The Moina skarn deposit contains $25-30 \times 10^6$ tonnes of ore at an average grade of 0.15% Sn, and is located near the margin of the Dolcoath granite in north Tasmania. The area is underlain by Ordovician sedimentary rocks capped by Tertiary basalts. The Ordovician sediments comprise the Moina sandstone (altered to quarzite) conformably overlain by the Gordon limestone (altered to marble). The Dolcoath granite, of Devonian age, is not in contact with either the limestone or the skarn, but is separated by about 200 m of Moina sandstone. Kwak and Askins (1981) interpret the mineralising fluids to have been channelled along fracture zones through the Moina sandstone, damming up at and near the contact with the overlying limestones to form the skarn deposits. The east-west-trending fractures, filled with Sn-W-bearing quartz veins, along the Bismuth Creek fault probably provided the plumbing system for the access of the fluids. The skarn unit extends for more than 1 km and is up to 100 m thick. It is divided into a lower granular skarn unit and an overlying "wrigglite" skarn unit. The granular skarn is further divided into a pyroxene-rich type, a garnet-rich type and a wollastonite-rich type. All three are enriched in F, Sn, Fe, W and Cl. Wrigglite (see also section on Mount Bischoff in Chap. 9) is a dark, fine-grained rock with an irregular laminar pattern of alternating light and dark laminae up to 0.5 mm

wide, which are closely related and parallel to fractures. The primary mineralogy of the wrigglite skarn is magnetite in the dark laminae and vesuvianite and fluorite in the light laminae. The skarn unit as a whole carries up to 25% F, 0.6% Sn, 0.5% W, 0.2% Be, 27.5 Zn and 4.5 g/t Au. Primary skarn may be altered to form amphibole and/or sulphide-rich zones in which Sn value are low. Replacement of wrigglite skarn by base metal sulphides, Fe sulphides and hematite is generally close to the Bismuth Creek fault. It is interesting to note that Kwak and Askins (1981) report Sn to be contained as a solid solution in garnet as well as very fine cassiterite.

The genetic model for the Moina deposit as worked out by Kwak and Askins is summarised below. The intrusion of the Dolcoath granite produced a dense hornfels unit and metamorphosed the sandstone and limestone to quartzite and marble respectively. At the same time metasomatism produced the granular calc-silicate skarn. Aqueous fluids evolved from the crystallising pluton and were trapped below a solid carapace and the dense hornfels rocks. Rupturing of the carapace, perhaps by fluid overpressure, led to a pressure drop, and boiling (fluid inclusion evidence suggests a temperature range from 300 to 500°C) produced an acidic and volatile-rich (HF, HCl, H_2S) vapour phase and basic saline phase. The vapour phase greisenised the granite and the hornfels, while the fluids were channelled along faults and fractures, eventually replacing the marble rocks to form skarns higher up in the sequence. The laminations of the wrigglite skarn remain complex and at least five models in numerous papers have been proposed in an attempt to explain this phenomenon (Kwak and Askins 1981). One of these models interprets the rhythmic nature of the wrigglite laminae as possibly due to a mechanism similar to that which produces Liesagang rings. The mechanism of Liesagang rings, though still poorly understood, probably involves diffusion of ions from supersaturated colloidal (?) solutions.

King Island W (Scheelite) Deposit

The King Island mine is located in the southeastern part of the island (off the northwestern tip of Tasmania). Three orebodies originally contained about 14×10^6 tonnes of ore grading 0.8% WO_3 (Einaudi et al. 1981). The local geology consists of a sandstone-siltstone unit overlain by dolomitic siltstone and shale of the Grassy Group of upper Proterozoic to Lower Cambrian age. This in turn is overlain by a Mid(?) Cambrian volcanic sequence comprising lavas and pyroclastics, which was intruded by two granitic stocks: the Grassy granodiorite and the Bold Head adamellite (lower Carboniferous-Devonian). In the vicinity of these intrusions the Grassy Group sediments, which are metamorphosed and metasomatised, are locally known as the Mine Series. This succession is, from the bottom upwards: lower biotite-hornfels, lower metavolcanics, finely banded hornfels and marble, C-lens skarn unit (separated into an upper and lower unit by barren marble), pyroxene-garnet ± biotite hornfels, upper biotite hornfels and upper metavolcanics. The Mine Series at the Dolphin orebody, on the northern margin of the Grassy granodiorite, strikes approximately parallel to the contact and dips from 30 to 60° towards the pluton.

The W ore mineral is a Mo-bearing scheelite (powellite) which occurs as inclusions in, and interstitially to, andradite garnet. Most of the scheelite mineralisation occurs in the C-lens skarn, although some is found in the marble in the interbedded footwall rocks. The mineralogy of the primary skarn is garnet + pyroxene + scheelite, on which is superimposed a secondary assemblage of ferro-hastingsite + epidote + calcite + quartz + Fe sulphides + scheelite + molybdenite. Thus two generations of scheelite are recognised: one (Mo-rich) formed by high temperature solutions (500°C near the pluton's contact to 300°C at approximately 500 m away); the other formed as a result of the dissolution of the Mo-rich scheelite and subsequent re-distribution as Mo-poor scheelite and molybdenite. This latter constitutes most of the King Island ore.

Cleveland Sn Deposit

The Cleveland mine is located in the northwest of Tasmania about 60 km west of Moina. Ore reserves in 1978 were approximately 1.3×10^6 tonnes at 0.69% Sn and 0.24% Cu (Collins 1981). The local geology consists of a near-vertical to steep, northwest-dipping and northeast-trending volcano-sedimentary sequence of Cambrian age. The three main stratigraphic units in the mine area are: the Deep Creek volcanics (mainly spilitic basalt and interbedded pyroclastics, argillite and chert), the Halls Formation (shale, limestone, chert, greywacke, pyroclastics and basalt) and the Crescent Spur sandstone (essentially a turbidite sequence). Dykes, sills and larger masses of dolerite and gabbro intrude this sequence. The Late Devonian Meredith granite crops out about 4 km south of the mine area with its contact aureole extending up to 2.5 km in plan from the contact which is not seen at the Cleveland mine.

The Sn-Cu orebodies occur in a series of sub-parallel, near-vertical, sulphide lenses within the Hall Formation. They are off-set by a series of subparallel reverse faults. The mineralisation consists of fine- to medium-grained quartz + tourmaline + fluorite + chlorite with pyrrhotite, chalcopyrite, cassiterite and stannite. The mineralisation commonly exhibits fine compositional banding (average 2–5 mm thick) parallel to bedding in the cherts, and this is interpreted as replacement of primary bedding. The mineralogy within the ore lenses defines four distinct zones which are centred around a stockwork zone of quartz + fluorite + wolframite + molybdenite + cassiterite, and this occurs in the structural footwall of the sulphide lenses. In the hangingwall of the lenses the Deep Creek volcanics are extensively altered. The genesis of this ore deposit can be summarised as follows. The deposition of Deep Creek volcanics and the overlying Crescent Spur sandstone took place in Early Cambrian and was followed by the intrusion of mafic rocks. Deformation during the Early-Mid Devonian resulted in the vertical attitude of the sequence and the formation of fractures. In Late Devonian and Early Carboniferous intrusion of the Meredith granite occurred. During a late phase of intrusion, hydrothermal fluids at temperatures of approximately 500°C were exsolved from the granite. These passed upward into the early Cambrian succession through fractures to form the early stockwork system. This was followed by dissolution and replacement of the limestone beds which formed the sulphide lenses.

10.5.7 Porphyry Sn Deposits in Bolivia

Bolivia accounts for approximately 13% of the world's tin production (Mining Annual Review, 1985). Most of this comes from a well defined metallogenic province, the Sn belt, which extends for about 800 km throughout the length of the Eastern Cordillera of Bolivia (Fig. 10.17A, B). The Eastern Cordillera is a plutonic arc of granodioritic to granitic batholiths which were emplaced during two magmatic events. One took place in the Early Mesozoic (199–180 Ma), the other in the Tertiary (19–8 Ma) (Schneider and Lehmann 1977; Hutchison 1983). These two magmatic events are also responsible for two main episodes of mineralisation in the Cordillera. The first, of Triassic-Jurassic age, consists of auriferous quartz veins, W-Sb-Hg mineralisation and base metal and Sn deposits. The second is of Miocene-Pliocene age and is represented by Sn-Ag mineralisation.

The Sn belt can be subdivided into a northern sector, or Cordillera Real region, and a central-southern sector (Fig. 10.17B; Sillitoe et al. 1975), separated by the so-called Arica's elbow where the eastern Andean Cordillera changes from a northwest to a north-south trend. The northern sector, characterised by Mesozoic batholithic Sn-W mineralisation, is more deeply eroded than the central-southern sector which has only exposed the later Tertiary igneous rocks and is therefore characterised by Sn-Ag subvolcanic mineralisation. In the Bolivian Sn belt three main types of deposits have been identified (Schneider et al. 1978): (1) manto-type (stratabound) deposits of Lower Paleozoic age, in the northern and southern sectors; (2) vein
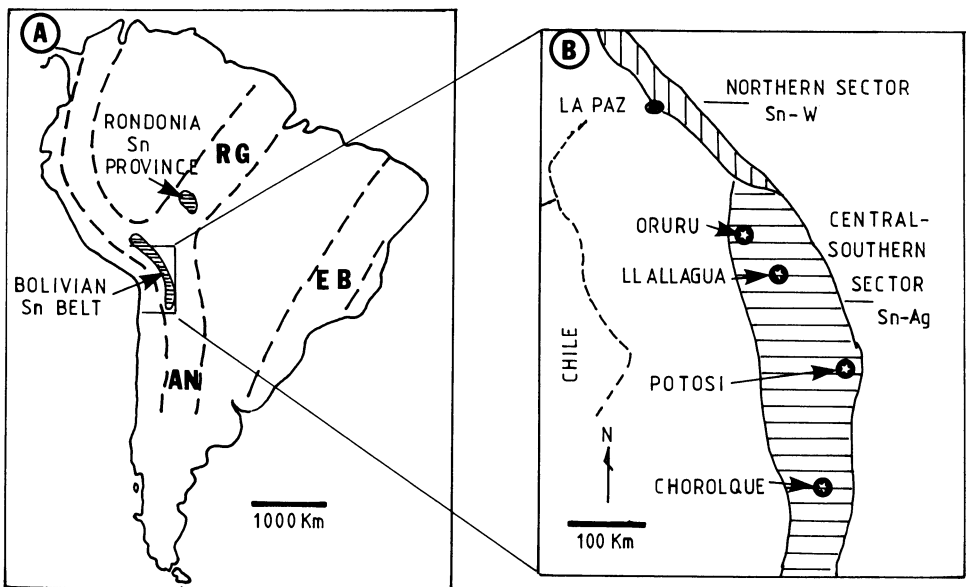
Fig. 10.17. A South American tin belts (after Schneider and Lehmann 1977; Schuiling 1967). *AN* Andean belt; *RG* Rondonia-Guyana belt; *EB* East Brazilian belt. **B** Bolivian tin provinces and location of major deposits (After Sillitoe et al. 1975)

ARGILLIC ALTERATION

SERICITIC ALTERATION

PROPYLITIC ALTERATION

QUARTZ LATITE PORPHYRY

LATE Sn-Ag-BEARING VEINS
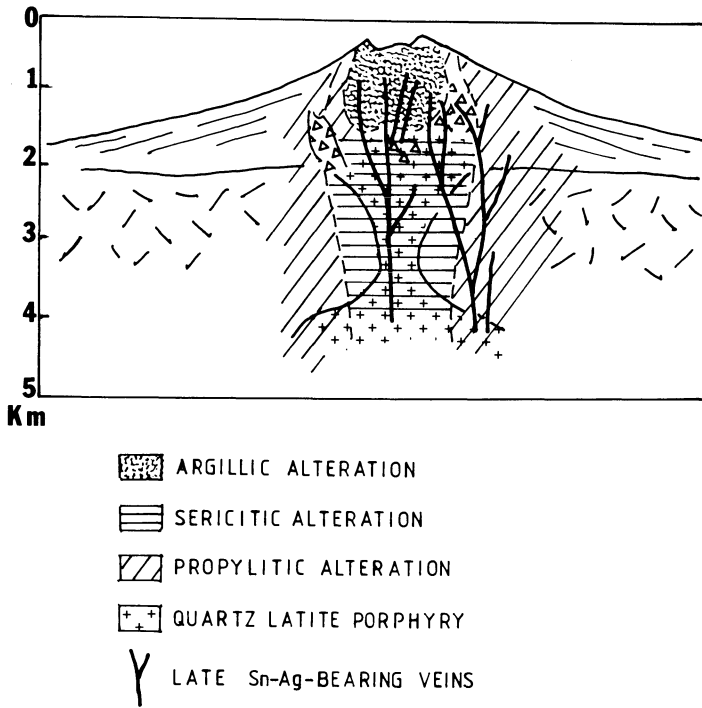
Fig. 10.18. Model of subvocanic porphyry Sn deposit of the Bolivian province (After Sillitoe et al. 1975)

deposits (Triassic-Jurassic age) confined to the northern sector and hosted within a Lower Paleozoic sedimentary sequence intruded by the Mesozoic batholiths; (3) Tertiary Sn deposits in the southern sector associated with subvolcanic intrusions which are further divided into two subtypes (Villapando 1988): one includes vein deposits characterised by complex Bi-As-Pb-Zn-Cu parageneses; the other, which is the main subject of this section, consists of breccia pipes and vein systems characterised by Ag-rich parageneses.

The porphyry Sn deposits in the central-southern sector of the Bolivian Sn belt account for about 75% of that country's Sn production. In this region the igneous rocks form small isolated stocks, dykes and larger volcanic structures. Ignimbrite sheets of peraluminous chemistry are present but post-date the mineralisation (Ericksen et al. 1990). The major deposits are those of Llallagua, Potosi, Oruru and Chorolque (Fig. 10.17B). Sillitoe et al. (1975) and Grant et al. (1980) compared these deposits to porphyry coppers and concluded that the two types share many similarities. An idealised model of the porphyry Sn deposits according to the above authors is shown in Fig. 10.18. These deposits are centred on small calc-alkaline stocks of intermediate composition and have the form of inverted cones. Coeval volcanics are locally preserved adjacent to some deposits. Stockworks were probably formed by hydrothermal brecciation processes which overlapped in time with pulses of mineralising events. The stocks and adjacent wall rocks have

undergone pervasive hydrothermal alteration in which a mineralised core of veins and breccias with quartz-tourmaline (cf. Fig. 10.18) is surrounded by a zone of sericite, pyrite and tourmaline with minor cassiterite. This assemblage gives way to an outer zone of propylitic alteration characterised mainly by chlorite. Argillic alteration and silicification may occur in the upper portions of the system within remnants of the volcanic edifice. In contrast to porphyry Cu systems, potassic alteration is absent in the porphyry Sn deposits.

In most deposits the stockwork mineralisation is cross-cut by a system of veins that carry high-grade Sn and other metals, notably Ag, for example at Potosi. The ore and gangue minerals are cassiterite + quartz + tourmaline ± pyrite which occur as disseminations and in veinlets forming mineralised zones of approximate cylindrical shape with considerable vertical extent (at least 700 and up to 1150 m at Potosi). Ore grades range from 0.3 to 0.4% Sn. At Llallagua, the Salvadora quartz-latite porphyry stock has approximate dimensions of 1700 × 1050 m and was intruded into folded Paleozoic sediments with some isolated outcrops of rhyolitic tuffs occurring about 2 km to the north. The mineralisation consists of stockwork veins with cassiterite, pyrite and pyrrhotite; disseminated cassiterite in hydrothermal breccias; and lode ore of quartz + cassiterite, forming a subparallel system which is currently exploited and is the main ore producer. At Potosi the Cerro Rico quartz-latite stock is approximately 1700 × 1200 m at the surface, conical in shape and pinches out to a dyke at depth. Alteration is pervasive throughout the stock with sericitic and tourmaline alteration at depth and silicification near the surface. Clay and alunite occur as a late stage alteration in the form of veinlets that cut the mineralised veins. Mineralised veins form a sheeted system containing Sn and Ag ores. Ore mineral paragenesis (Sillitoe et al. 1975) indicates an early stage of quartz + pyrite + cassiterite with minor arsenopyrite and wolframite + bismuthinite at deeper levels; an intermediate stage with cassiterite + chalcopyrite + tetrahedrite + stannite and a late stage containing cassiterite and "ruby silver" (pyrargyrite), jamesonite + boulangerite.

Ore Genesis and Origin of the Sn

Assuming similarity between porphyry Cu systems and porphyry Sn deposits then a similar genetic model is deemed appropriate. It is probable, however, that the porphyry Sn deposits were emplaced at shallower depths than the porphyry Cu, because they have features indicative of a volcanic environment. Fluid inclusion data indicate depths of formation betweem 800 and 5000 m, depending on the proportions of lithostatic and hydrostatic pressure, but, for the above reasons, a depth of approximately 1000–2000 m is favoured (Sillitoe et al. 1975). Ore genesis involved the evolution of high temperature (± 500°C) and high salinity (± 30–40 wt.% NaCl equivalent) magmatic fluids, later followed by meteoric hydrothermal convection systems. The earliest hydrothermal activity produced widespread brecciation and intense hydrothermal alteration. This was followed by vein emplacement with at least three main stages of mineralisation which can be summarised as: (1) quartz-cassiterite stage, during which cassiterite deposition appears to have taken place at temperatures of between 300–250°C;

(2) sulphide stage; and (3) a stage of late veinlets with clay minerals or fluorite and siderite.

Dating of the different types of deposits indicates metallogenic epochs of Sn mineralisation within the Bolivian belt as a whole. These deposits appear to be genetically related, with the manto type representing the precursors to vein deposits formed during the Mesozoic magmatic event, and to the subvolcanic porphyry types formed during a later tectono-magmatic reactivation in the Tertiary (Schuiling 1967; Schneider and Lehmann 1977; Villapando 1988). The question of the origin of the Sn, however, still remains (see Hutchison 1983 for a detailed discussion). A look at Fig. 10.17A shows that the distribution of the Sn deposits falls within three main belts (Schuiling 1967): (1) the Andean belt of which the Bolivian deposits are part; (2) the East Brazilian belt; (3) the Rondonia-Guyana belt. We can also see from this that the Bolivian belt is situated near the intersection of the Andean and Rondonia-Guyana belts. Dating of the granites and pegmatites associated with the Sn mineralisation from French Guyana and Rondonia gives ages of between 1200 and 940 Ma respectively (Schuiling 1967) thus constituting a Precambrian epoch(s) of Sn mineralisation. It is possible that the manto-type deposits were derived from this mineralisation by erosion of the uplifted Precambrian shield during the development of the Andes (Schneider and Lehman 1977). The concept of "metallogenic heritage" would appear to be substantiated by systematic variations of elements such as W, Zr and Hf in the cassiterites (Schneider et al. 1978, Dulski et al. 1982). Furthermore, Hutchison (1983) noted that the intersection of the Bolivian belt with the Rondonia-Guyana belt may represent a triple junction, with the latter representing a possible aulacogen structure. Magma generation in this area could therefore have involved Sn-enriched protoliths. This possibility is corroborated by recent studies conducted on the peraluminous igneous rocks of the Bolivian Sn province (Ericksen et al. 1990). The results of these studies suggest that Sn-rich magmas were responsible for the emplacement near the surface of the peraluminous igneous rocks with which the Sn mineralisation is genetically associated.

It may also be speculated that there is a similarity between the South American situation and that of the Pan-African Damara orogen in Namibia, where Sn-bearing pegmatites (and U-bearing alaskites) are found in the intracontinental branch of the orogen close to a postulated hot spot or triple junction (see Chap. 7).

References

Ambrus J (1978) Chuquicamata deposit. In: Sutulov A (ed) International Moylbdenum Encyclopedia 1778–1978, Vol 1. Resources and Production. Intermet, Santiago de Chile, pp 87–93

Atkinson W W, Einaudi M T (1978) Skarn formation and mineralization in the contact aureole at Carr Fork, Bingham, Utah. Econ Geol 73:1326–1365

Baldwin J T, Swain H D, Clark G H (1978) Geology and grade distribution of the Panguna porphyry copper deposit, Bougainville, Papua New Guinea. Econ Geol 73:690–702

Bamford R W (1972) The Mount Fubilan (Ok Tedi) porphyry copper deposit, Territory of Papua and New Guinea. Econ Geol 67:1019–1033

Baumer A, Fraser R B (1975) Panguna porphyry copper deposit, Bouganville. In: Knight C L (ed) Economic Geology of Australia and Papua New Guinea. 1 Metals. Australas Inst Min Metall, Parkville, Victoria, pp 855–866

Beane R E, Titley S R (1981) Porphyry copper deposits. Part II. Hydrothermal alteration and mineralization. Econ Geol 75th Anniv Vol, pp 235–269

Brown P E, Bowman J R, Kelly W C (1985) Petrologic and stable isotope constraints on the source and evolution of skarn-froming fluids at Pine Creek, California. Econ Geol 80:72–95

Camus F (1975) Geology of the El Teniente orebody with emphasis on wall rock alteration. Econ Geol 70:1341–1372

Clark G H (1990 Panguna copper-gold deposit In: Hughes F E (ed) Geology of the mineral deposits of Australia and Papua New Guinea, vol 2 Australas Inst Min Metall Monogr 14, Parkville, Victoria, pp 1807–1816

Collins P L F (1981) The geology and genesis of the Cleveland tin deposit, Western Tasmania: Fluid inclusion and stable isotope studies. Econ Geol 76:365–392

Davies H L, Howell W J S, Fardon R S H, Carter R J, Bumstead E D (1978) History of the Ok Tedi porphyry copper prospect, Papua New Guinea. Econ Geol 73:796–809

Dick L A, Hogson C J (1982) The MacTung W-Cu (Zn) contact metasomatic and related deposits of the Northeastern Cordillera. Econ Geol 77:845–867

Dow D B (1975) Geology of Papua New Guinea. In: Knight C L (ed) Economic Geology of Australia and Papua New Guinea. 1 Metals. Australas Inst Min Metall, Parkville, Victoria, pp 823–835

Dulski P, Moeller P, Villapando A, Schneider H J (1982) Correlation of trace element fractionation in cassiterites with the genesis of the Bolivian metallotect. In: Evans A M (ed) Metallization associated with acid magmatism. John Wiley & Sons, New York, pp 71–83

Eastoe C J (1978) A fluid inclusion study of the Panguna porphyry copper deposit, Bougainville, Papua New Guinea. Econ Geol 73:721–748

Economic Geology (ed) (1978) Porphyry copper deposits of the southwestern Pacific islands and Australia. Econ Geol 73, 5

Economic Geology (ed) (1981) An issue on the geology and mineral deposits of Tasmania. Econ Geol 76, 2

Economic Geology (ed) (1982) A special issue devoted to skarn deposits. Econ Geol 77, 4

Einaudi M T (1977) Petrogenesis of the copper-bearing skarn at the Mason Valley mine, Yerington District, Nevada. Econ Geol 72:769–795

Einaudi M T (1982a) Description of skarns associated with porphyry copper plutons. In: Titley S R (ed) Advances in geology of the porphyry copper deposits, southwestern North America. Univ Arizona Press, Tucson, pp 139–184

Einaudi M T (1982b) General features and origin of skarns associated with porphyry copper plutons. In Titley S R (ed) Advances in geology of the porphyry copper deposits, south-western North America. Univ Arizona Press, Tucson, pp 185–209

Einaudi M T, Burt D M (1982) Introduction, terminology, classification and composition of skarn deposits. Econ Geol 77:745–754

Einaudi M T, Meinert L D, Newberry R J (1981) Skarn deposits. Econ Geol 75th Anniv Vol, pp 317–391

Ericksen G E, Luedke R G, Smith R L, Koeppen R P, Urquidi B F (1990) Peraluminous igneous rocks of the Bolivian tin belt. Episodes 13:3–8

Ford J H (1978) A chemical study of alteration at the Panguna porphyry copper deposit, Bougainville, Papua New Guinea. Econ Geol 73:703–720

Ford J H, Green D C (1977) An oxygen and hydrogen isotope study of the Panguna porphyry copper deposit, Bougainville. J Geol Soc Aust 24:63–80

Friedrich G H, Genkin A D, Naldrett A J, Ridge J D, Sillitoe R H, Vokes F M (eds) (1986) Geology and metallogeny of copper deposits. Spec Publ 4, Soc Geol Appl Min Depos. Springer, Berlin, Heidelberg, New York

Frutos J (1982) Andean metallogeny related to the tectonic and petrologic evolution of the Cordillera Some remarkable points. In: Amstutz G C, El Goresy A, Frenzel G, Kluth C, Moh G, Wauschkuhn A, Zimmermann R A (eds) Ore genesis – The State of the art. Springer, Berlin, Heidelberg, New York, pp 493–507

Geyti A, Schonwandt H K (1979) Bordvika a possible porphyry molybdenum occurrence within the Oslo province, Norway. Econ Geol 74:1211–1220

Gilmour P (1978) Grades and tonnages of porphyry copper deposits. In: Titley S R (ed) Advances in geology of the porphyry copper deposits, southwestern North America. Univ Arizona Press, Tucson, pp 7–35

Grant J N, Halls C, Sheppard M F, Avila W (1980) Evolution of the porphyry tin deposits of Bolivia. In: Ishihara S, Takenouchi S (eds) Granitic magmatism and related mineralization. Mining Geology. Soc Min Geol Jpn Spec Iss 8:151–173

Guilbert J M (1986) Recent advances in porphyry base metal deposit research. In: Friedrich G H, Genkin A D, Naldrett A J, Ridge J D, Sillitoe R H, Vokes F M (eds) Geology and metallogeny of copper deposits. Soc Geol Appl Min Depos Spec Publ 4:196–208

Guilbert J M, Lowell J D (1974) Variations in zoning patterns in porphyry ore deposits. Can Inst Min Metall Bull 67:99–109

Guilbert J M, Park C F (1986) The geology of ore deposits. Freeman, New York, 985 pp

Guiqing L (1988) Geological characteristics of the ignimbrite-related Xiling tin deposit in Guandong Province. In: Hutchison C S (ed) Geology of tin deposits in Asia and the Pacific. UN Econ Soc Commiss Asia Pac. Springer, Berlin, Heidelberg, New York, pp 495–506

Gustafson L B, Hunt J P (1975) The porphyry copper deposit at El Salvador, Chile. Econ Geol 70:857–912

Hall R J, Britten R M, Henry D D 1990 Frieda river copper-gold deposits. In: Hughes F E (ed) Geology of the mineral deposits of Australia and Papua New Guinea, vol 2. Australas Inst Min Metall Monogr 14, Parkville, Victoria, pp 1709–1715

Hill K C, Hegarty K A (1987) New tectonic framework for PNG and the Caroline plate: implications for cessation of spreading in back-arc basins. In: Pacific Rim Congr '87. Australas Inst Min Metall, Parkville, Victoria, pp 179–182

Hollister V F (1978) Geology of the porphyry copper deposits of the western hemisphere. Am Ins Min Metall Pet Eng, 219 pp

Hollister V F (1979) Porphyry copper-type deposits of the Cascade Volcanic Arc, Washington. Mineral Sci Eng 11:22–35

Hollister V F, Anzalone S A, Richter D H (1975) Porphyry copper deposits of southern Alaska and contiguous Yukon Territory. CIM Bull 68:104–112

Howell F H, Molloy J S (1960) Geology of the Braden orebody, Chile, South America, Econ Geol 55:863–905

Hutchison C S (1983) Economic deposits and their tectonic setting. MacMillan, London, 315 pp

Kestler S E, Jones L M, Walker R L (1975) Intrusive rocks associated with porphyry copper mineralization in island arc areas. Econ Geol 70:515–526

Kimura A T, Drummond A D (1969) Geology of the Endako molybdenum deposit. CIM Bull 62:699–708

Kimura A T, Bysouth G D, Drummond A D (1976) Endako. CIM Spec Vol 15:444–454

Kwak T A P (1987) W-Sn skarn deposits and related metamorphic skarns and granitoids. Developments in economic geology 24. Elsevier, Amsterdam, 415 pp

Kwak T A P, Askins P W (1981) Geology and genesis of the F-Sn-W (Be-Zn) skarn (wrigglite) at Moina, Tasmania. Econ Geol 76:439–467

Kwak T A P, Tan T H (1981) The geochemistry of zoning in skarn minerals at the King Island (Dolphin) mine. Econ Geol 76:468–497

Lanier G, John E C, Swanson A J, Reid A, Bard C E, Caddey SW, Wilson J C, (1978) General geology of the Bingham mine, Bingham Canyon, Utah. Econ Geol 73:1228–1241

Laznicka P (1976) Porphyry copper and molybdenum deposits of the USSR and their plate tectonic settings. Trans Inst Min Metall 85:B14–B32

Lindgren W, Bastin E S (1922) Geology of the Braden mine, Rancagua, Chile. Econ Geol 17:75–99

Lowell J D, Guilbert J M (1970) Lateral and vertical alteration-mineralization zoning in porphyry ore deposits. Econ Geol 65:373–408

Mathieson G A, Clark A H (1984) The CanTung E Zone scheelite skarn orebody, Tungsten, Northwest Territories. A revised genetic model. Econ Geol 79:883–901

McMillan W J, Panteleyev A (1980) Ore deposits models. 1. Porphyry copper deposits. Geosci Can 7:52–63

Mining Annual Review 1985 Bolivia. Mining Journal, London, pp 337–389

Mortimer C, Munchmeyer C, Urqueta I (1977) Emplacement of the Exotica orebody, Chile. Trans Inst Min Metall 86:B121–B127

Mutschler F E, Wright E G, Ludington S, Abbott J T (1981) Granite molybdenite systems. Econ Geol 76:874–897

Nielsen R L (1976) Recent developments in the study of porphyry copper geology: a review. In: Sutherland Brown A (ed) Porphyry deposits of the Canadian Cordillera. Can Inst Min Metall Spec Vol 15:487–500

Pintz W S (1984) Ok Tedi – Evolution of a third world mining project. Mining Journal Books, London, 206 pp

Puig-Pichuante R (1986) Molybdenum mineralisation with emphasis on porphyry systems. Genesis and exploration. MSc Thesis, Rhodes Univ, Grahamstown, S Afr, 105 pp

Reid J E (1978) Skarn alteration of the Commercial Limestone, Carr Fork area, Bingham, Utah. Econ Geol 73:1315–1325

Rogers R, McKee C (1990 Geology, volcanism and mineral deposits of Papua New Guinea In: Hughes F E (ed) Geology of the mineral deposits of Australia and Papua New Guinea, vol 2 Australas Inst Min Metall Monogr 14, Parkville, Victoria, pp 1689–1701

Rush P M, Seegers H J (1990 Ok Tedi copper-gold deposits In: Hughes F E (ed) Geology of the mineral deposits of Australia and Papua New Guinea, vol 2 Australas Inst Min Metall Monogr 14, Parkville, Victoria, pp 1747–1754

Sawkins F J (1990) Metal deposits in relation to plate tectonics, 2nd edn. Springer, Berlin, Heidelberg, New York, 461 pp

Schneider H J, Lehmann B (1977) Contribution to a new genetical concept on the Bolivian tin province. In: Klemm D D, Schneider H J (eds) Time and stratabound ore deposits. Springer, Berlin, Heidelberg, New York, pp 153–168

Schneider H J, Dulski P, Luck J, Moeller P, Villapando A (1978) Correlation of trace element distribution in cassiterites and geotectonic position of their deposits in Bolivia. Mineral Depos 13:1(19–122

Schonwandt H K, Petersen J S (1983) Continental rifting and porphyry-molybdenum occurrences in the Oslo region, Norway. Tectonophysics 94:609–631

Schuiling R D (1967) Tin belts on the continents around the Atlantic Ocean. Econ Geol 62:540–550

Sheppard S M F (1971) Hydrogen and oxygen isotope ratios in minerals from porphyry copper deposits. Econ Geol 66:515–542

Sillitoe R H (1970) South American porphyry copper deposits and the new global tectonics. Resumenes Primer. In: Congr Latinoamericano, Lima, Peru, pp 254–256

Sillitoe R H (1972) A plate tectonic model for the origin of porphyry copper deposits. Econ Geol 67:184–(197

Sillitoe R H (1973) The tops and bottoms of porphyry copper deposits. Econ Geol 68:799–815

Sillitoe R H (1976) Andean mineralization: a model for the metallogeny of convergent plate margins. In: Strong D F (ed) Metallogeny and plate tectonics. Geol Assoc Can Spec Pap 14:59–100

Sillitoe R H (1980) Types of porphyry molybdenum deposits. Min Mag 142:550–553

Sillitoe R H (1981) Regional aspects of the Andean porphyry copper belt in Chile and Argentina. Trans Inst Min Metall 90:B15–B36

Sillitoe R H (1986) Space-time distribution, crustal setting and Cu/Mo ratios of central Andean porphyry copper deposits: metallogenic implications. In: Friedrich G H,Genkin A D, Naldrett A J, Ridge J D, Sillitoe R H, Vokes F M (eds) Geology and metallogeny of copper deposits. Geol Soc Appl Min Depos Spec Publ 4:235–250

Sillitoe R H, Gappe I M (1984) Philippine porphyry copper deposits: geologic setting and characteristics. CCOP Proj Off UNDP Tech Support for Regional Offshore Prospecting in East Asia, pp 1–88

Sillitoe R H, Halls C, Garnt J N (1975) Porphyry tin deposits in Bolivia. Econ Geol 66:215–225

Smirnov V I (1976) Geology of mineral deposits. MIR, Moscow, 520 pp

Surface V, Brumbaugh R L, Smith R P (1978) Climax molybdenite deposits. In: Sutulov A (ed) International molybdenum encyclopedia 1778–1978, Vol 1. Resources and production. Intermet, Santiago de Chile, pp 95–107

Sutherland Brown A (1976) Morphology and classification. In: Sutherland Brown A (ed) Porphyry deposits of the Canadian Cordillera. Can J Earth Sci Spec Vol 15:44–51

Taylor H P (1974) The application of oxygen and hydrogen isotope studies to problems of hydrothermal alteration and ore deposition. Econ Geol 69:843–883

Titley S R 1975 Geological characteristics and environment of some porphyry copper occurrences in the southwest Pacific. Econ Geol 70:499–514

Titley S R (ed) (1982) Advances in Geology of the Porphyry Copper Deposits Southwestern North America The University of Arizona Press Tucson

Titley S R, Beane R E (1981) Porphyry copper deposits. Part I. Geologic settings, petrology, and tectogenesis. Econ Geol 75th Anniv Vol, pp 214–235

Villapando A (1988) The tin ore deposits of Bolivia. In: Hutchison C S (ed) Geology of tin deposits in Asia and the Pacific. UN Econ Soc Commiss for Asia and the Pacific. Springer, Berlin, Heidelberg, New York, pp 201–215

Wallace R S, McKenzie W B, Blair R G, Muncaster N K (1978) Geology of the Urad and Henderson molybdenite deposits, Clear Creek County, Colorado, with a section on a comparison of these deposits with those at Climax, Colorado. Econ Geol 73:325–367

White W H, Bookstrom A A, Kamilli R J, Ganster M W, Smith R P, Ranta D A, Steininger R C (1981) Character and origin of Climax-type molybdenum deposits. Econ Geol 75th Anniv Vol, pp 270–316

Woodcock J R, Hollister V F (1978) Porphyry molubdenite deposits of the North American Cordillera. Mineral Sci Eng 10:3–18

Zhunggi Y, Shenyu W, Guoxin L (1988) Volcanic activity in Xiling mine area, Guandong Province, and its genetic relationship with tin and polymetallic sulphide deposits. In: Hutchison C S (ed) Geology of tin deposits in Asia and the Pacific. UN Econ Soc Commiss for Asia and the Pacific. Springer, Berlin, Heidelberg, New york, pp 505–521

Fossil and Active Geothermal Systems – Epithermal Base and Precious Metal Mineralisation (Including Kuroko-Type Deposits)

11.1 Introduction

In regions of high heat flow, thermal convection dominates the behaviour of groundwaters or sea water in permeable and/or fractured crust, thus generating geothermal systems. Terrestrial geothermal systems are derived from air-saturated meteoric waters which penetrate the crust to regions influenced by cooling magmas (Henley and Ellis 1983). Submarine geothermal systems are, by contrast, characterised by sea water convection cells which are also heated by cooling magmas at depth. This chapter takes a look at terrestrial geothermal systems and at a category of submarine systems related to submerged volcanic structures at convergent plate boundaries. The following chapter looks at geothermal activity associated with mid-ocean ridges.

In terrestrial geothermal systems the circulation of hot waters can reach depths of approximately 5 km, lasting from tens of thousands up to about 2 million years. Near-surface temperatures are approximately 50–100 °C, reaching 350–400 °C in the subsurface environment. These low to moderate temperatures, together with pressure, are the main reason for the use of the term epithermal, with which the mineral products, ore deposits and occurrences produced during these geothermal activities are widely known. The thermal energy which is transferred towards the surface is derived in part from the cooling magmas and in part from cooling of the wall rocks. For the Yellowstone geothermal system, for example, it is calculated that crystallisation of about 0.1 km^3 of rhyolitic magma and its cooling of 300 °C, together produce enough energy to account for the vigorous discharge of hot springs in the area (Fournier 1989). Most solutes are transferred to the circulating waters from the wall rocks through which they pass, and most of the gas components are probably derived from the underlying cooling magmas.

Active geothermal systems are commonly found in areas of recent tectonic and igneous activity at plate boundaries. Most geothermal fields are in fact associated with volcanic structures – in particular calderas – at both convergent margins (volcanic arcs) and intracontinental divergent boundaries (rift valleys). In volcanic areas the preferred association is with andesitic, dacitic and rhyolitic centres rather than basaltic (Ellis 1979). Geothermal systems may or may not vent at surface. Some of the surface expressions include hot springs, geysers, mud pots and fumaroles. The subsurface geometry of the hydrothermal circulation of a geothermal system varies according to the geological setting, the dominant structures, and the permeable and impermeable zones in a given area (see Chap. 3). Convective flow is usually vertical

or near-vertical and is often controlled by faults and/or fractures, although in the presence of flat-lying permeability barriers the circulating fluids may be forced to move laterally.

In general, discharge of fluids at the surface is represented by near-neutral chloride-rich hot spring waters, or it may be characterised by acid-sulphate boiling pools. The latter are generally related to steam that separates from deeper chloride-rich boiling fluids in vapour-dominated systems resulting in fumarolic activity containing CO_2 and H_2S (see Chap. 3 and later). Bicarbonate-rich waters are common in areas where carbonate rocks are present. Deeper in the system, beneath the levels of boiling and atmospheric oxidation, waters are usually slightly alkaline (pH 6–7) and weakly saline. Isotope systematics indicate that the waters of geothermal systems are dominantly of meteoric origin with a possible minor component being derived from magmatic sources. Again for the Yellowstone system it is estimated that all the chloride waters discharged by the hot springs could be derived from about 0.2–0.4% magmatic and 99.6–99.8% meteoric waters (Fournier 1989). Metal-rich precipitates in many cases characterise the surface expressions of the geothermal systems, as for example the much publicised Taupo geothermal fields in New Zealand, and the Steamboat Springs geothermal area in Nevada (USA). These surface precipitates may contain ore-grade metalliferous concentrations of Au, Ag, W, As, Sb and Tl, and are generally associated with relatively large deposits of amorphous siliceous material (sinters) which form around chloride-rich hot springs. Elements such as Cu, Pb, Zn, Te and Bi are by contrast concentrated at deeper levels. Thus, it is clear that geothermal systems have distinct metal zonations with respect to depth, as discussed later. Metal contents of geothermal discharge water and chemical precipitates are given in Table 11.1. The striking feature of these discharge waters is their poor metal content compared with the strong concentration in the precipitates (by a factor of up to 10^6), as may be the case for Au and Ag. As mentioned in Chapter 2, some of the critical factors for this enrichment must be time and depositional rates. In this respect an interesting calculation first published by Weissberg et al. (1979) shows that the discharge water of one borehole contained 0.04 $\mu g l^{-1}$ Au, so that 32×10^6 g of Au would be contained in 800 km^3 of discharge water (1 tonne of H_2O = 1 m^3). Given that a natural discharge rate of 1.6×10^6 kg/h (or 0.014 km^3 yr^{-1}) was recorded at Wairakei, then some 800 km^3 of thermal water would pass through the system in 57000 years. In 300000 years a total of 4200 km^3 of water would circulate through the system, and, given a suitable rate of deposition, an orebody containing 168×10^6 g of Au could result. Similar calculations carried out by Browne (1986) indicate that those of Weissberg et al. may, in fact, be conservative. On the basis of the Au content in scales deposited during discharge from a well, Browne (1986) estimated a concentration of 1.5 g/t Au in the aquifer, and envisaged that it would take only 1500 years to transport 32×10^6 g of Au through the system. Since geothermal fields are known to have been active for between 1 and 2 million years, the implications of these estimates, even if taken conservatively, in consideration of less efficient deposition rates, are obvious.

The exploration for geothermal energy received great impetus in the 1960s and 1970s as a result of the increased oil prices and the political uncertainties in the oil-

Table 11.1. (A) Metal analyses of surface water and precipitates at Broadlands (after Weissberg et al. 1979), and Waiotapu geothermal areas (after Hedenquist 1983 and references therein). Values in parts per million (ppm). (B) Spectrographic analyses of precipitates at Steamboat Springs, Nevada, USA (after White 1985). Values in parts per million (ppm)

A	Broadlands surface water	Champagne pool orange precip.	Yellow-orange mud	Sinter terrace	Subsurface siliceous breccia	Subsurface wall-rock
Au	0.00004	80	0.03–0.08	2.3	0.05	0.05
Ag	0.0007	175	0.5–10	2.0	2.5	1.5
As	5.7	2%	11–12%	3500	100	–
Sb	0.2	2%	750–800	440	55	< 5
Tl	0.007	320	50–110	40	< 5	–
Hg	0.0004	170	11–13	16	< 1	–
Cu	0.0009	–	–	< 5	95	45
Pb	0.0013	15	–	5	2600	3000
Zn	0.001	50	–	5	1.3%	4100

B	Siliceous mud	Sinter	Opaline sinter	Metastibnite-opal; well No. 4
Au	15	1.5	0.3	60
Ag	150	1	2	400
As	700	50	150	600
Sb	1.5	1.0	700	0.2
Tl	700	70	10	2000
Hg	100	30	2	80
Cu	20	1	15	> 2000
Pb	7	–	–	400
Zn	50	0.2	15	> 2000

producing countries. The result of this exploration, particularly in New Zealand, the USA, southern Europe and Japan, was of incalculable benefit to our knowledge of hydrothermal activity, processes of solution, transport and deposition of metallic elements, effects of water-rock interaction, and in a broader sense, the ore-forming processes related to the geothermal systems. There is much literature on the subject, but for the present purpose the reader is referred to White (1955, 1974, 1981), Weissberg (1969), Ellis and Mahon (1977), Weissberg et al. (1979), Ellis (1979), Seward (1979a, b) and Henley and Ellis (1983).

Similarities between the active geothermal systems and epithermal precious and base metal ore deposits were noted many years ago by Lindgren (1933). It is now widely recognised that epithermal deposits are essentially the result of the interaction of geothermal waters with wall rocks and that many epithermal deposits in the geological record are in fact the fossil equivalent of ancient geothermal systems. Nowhere is this in greater evidence than in New Zealand, where subduction-related volcanic arcs, such as the active Taupo Volcanic Zone and the Coromandel peninsula volcanics of Miocene-Pliocene age and associated Hauraki goldfields, afford a unique opportunity for examining active and fossil epithermal

systems geographically adjacent to one another (see Chap. 7, Fig. 7.9 and subsequent discussion on the geology and mineralisation of these areas). Useful publications dealing in particular with epithermal deposits formed in terrestrial geothermal systems can be found in Tooker (1985) and Berger and Bethke (1985), while several papers on epithermal systems of the Pacific areas are published in the Proceedings of the 1986 International Volcanological Congress (Symposium 5), the Pacific Rim '87, the volumes of extended abstracts of the Bicentennial Gold '88 and Hedenquist et al. (1990).

   In this chapter we look at such features of geothermal systems as the types of epithermal mineral deposits formed within them, their host environments, hydrothermal alteration, transport and deposition of metals and their zoning. Submarine geothermal systems, such as those that develop in submerged calderas, are also treated. There is discussion of some of the major active geothermal areas (Taupo Volcanic Zone, New Zealand and Salton Sea in California) and epithermal mineral deposits that were formed in ancient geothermal systems. These include the Au-Ag and base metal deposits of the Coromandel peninsula in New Zealand, the epithermal deposits of Papua New Guinea, and those of the Carlin-type deposits in the western USA. We conclude with a discussion on kuroko-type epithermal mineralisation, and take a look at examples from both the Archean and the Phanerozoic.

11.2 General Characteristics of Epithermal Systems

The increased price of Au, together with the unstable political situation in South Africa – the largest producer of this metal in the world – generated an upsurge in the exploration for epithermal precious metal deposits, and a proliferation of papers on the subject during the last decade. While, on the one hand, contributing a great deal to our understanding and knowledge of these mineral deposits, this has also caused some confusion with terminology and the proposed conceptual models. In this section we look at end-member geological models which, although generalised, are nevertheless useful to the exploration geologist. Here, we define epithermal deposits as those formed at low to moderate temperatures (between approximately 50 and 350°C) and pressures, from dominantly meteoric hydrothermal fluids which are weakly saline (<1 to approximately 5 wt.% NaCl equivalent). Although epithermal deposits are mostly volcanic-hosted and clearly related to volcano-plutonic activity, there is nevertheless a category of sedimentary-rock-hosted epithermal deposits which appear to have some connection to igneous activity. Epithermal mineralisation has a number of common and distinctive features, such as the presence of fine-grained chalcedonic quartz, calcite, quartz pseudomorphs after calcite (probably indicative of boiling fluids), and hydrothermal breccias. The elemental association is also characteristic, with ore elements such as Au, Ag, As, Sb, Hg, Tl, Te, Pb, Zn and Cu. Ore textures include open-space filling (characteristic of low pressure environments), crustifications, colloform banding and comb structures. The deposits, which are formed from the surface to approximately 1.5 km below the

Table 11.2. (A) Approximate tonnage and grade of hot spring (HS), vein-type (V) and disseminated replacement (DR) epithermal deposits of the USA (after Silberman and Berger 1985 and references therein). (B) Approximate tonnage and grade of some Chilean vein-type (V) epithermal deposits (after Camus 1985). (C) Approximate geological reserves of adularia-type (Ad) epithermal deposits in Papua New Guinea (after Rogerson and McKee 1990)

A

District/mine	Type	Tonnes $\times 10^6$	Au g/t	Ag g/t
Round Mountain, Nevada	HS	177	1.3	–
McLaughlin, California	HS	20	5	–
Paradise Peak, Nevada	HS	9	11	145
Comstock Lode, Nevada	V	17	13	325
Creede, Colorado	V	4.5	0.9	527
Goldfield, Nevada	V	5	24	9.5
Carlin, Nevada	DR	10	9	–
Pinson, Nevada	DR	6.8	± 5	–

B

District/mine	Type	Tonnes $\times 10^6$	Au g/t	Ag g/t
El Indio	V	3.3	12	141
El Bronce de Petorca	V	2.5–3	8–10	20
Sierra Overa	V	0.15–0.2	10–50	–
San Cristobal	V	0.2	4	50

C

Area	Type	Tonnes $\times 10^6$	Au g/t	Ag g/t
Porgera	Ad	78	3.7	–
Misima Is.	Ad	62	1.35	20
Wau	Ad	0.46	1.8	–
Hidden Valley	Ad	37	2.1	31

surface, are typified by veins, stockworks and disseminations. These features, which may occur either together or as single entities, constitute deposits generally easy to mine as open cast or shallow underground operations, with relatively large tonnages and low Au + Ag grades, or small tonnages and high Au + Ag grades. Table 11.2A, B and C provides examples of the tonnages and grades of epithermal precious metal ore deposits. Owing to the surface and near-surface environment of this mineralisation, the age of epithermal systems range from those that are forming in present-day geothermal fields to those of Tertiary age. Epithermal deposits of Mesozoic and Paleozoic age, though not common, have been reported, such as those in the Drummond Basin in Queensland (Cunneen and Sillitoe 1989;
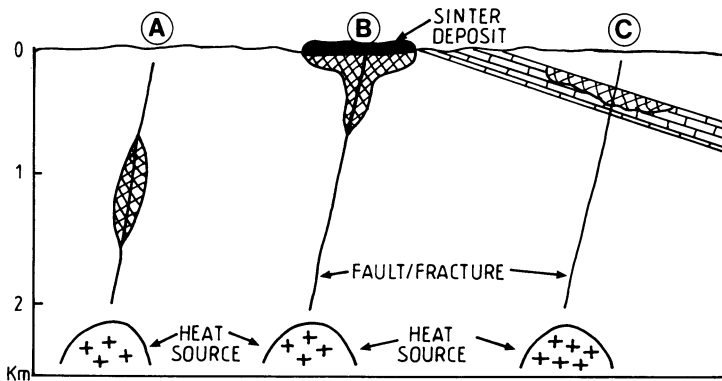
Fig. 11.1. Schematic representation of the three types of epithermal mineralisation (*cross-hatched areas*). *A* Open-vein type, in which boiling and hydrothermal deposition occur mainly at depth. *B* Hot spring-type with open-vein type at depth; boiling and hydrothermal deposition occur at and near the surface. *C* Sediment-hosted disseminated and replacement type occurs when the geothermal fluids interact with chemically reactive carbonate rocks

White et al. 1989). The preservation potential in the geological record of epithermal systems can thus be said to be poor, and only in special circumstances may they be preserved.

11.2.1 Main Types of Epithermal Deposits

Ore minerals and alteration assemblages, host lithologies and associated volcanic rocks assist in defining the types and styles of epithermal mineralisation. In this respect the works of Buchanan (1981) and Berger and Eimon (1982) are important in providing a workable classification and general characteristics of epithermal mineralisation. Based on the above, epithermal systems can be classified into hot-spring type, open-vein type and disseminated-replacement type (Fig. 11.1), the first two possibly forming a continuum from surface chemical precipitates to deep veins and fissure fillings. Erosion plays an important role in that often only a few veins are exposed, representing the remnants of what could have been an extensive epithermal system.

Hot Spring Type

Hot spring type epithermal systems, which are formed at or near the surface, are characterised by siliceous cappings (sinter) passing downward into a zone of silicified material and stockwork veins, and into a zone of hydrothermal brecciation. Hydrothermal breccias are formed as a result of boiling or hydrothermal eruptions. The silica cap is usually brecciated, and in places explosion craters or maars are present with associated fall-out sedimentary aprons. Figure 11.2 shows a schematic cross-section of a hot spring type epithermal deposit. Dominant element

50 metres approx.

▤ Sinter deposit

▦ Silicified zone, opaline or porous silica-rich zone; disseminated Au,As,Sb,Ag mineralisation

▨ Boiling zone (hydrothermal brecciation), low-angle veins; Au,Ag,As

▧ Vein system: quartz-sulphide (Cu,Pb,Zn) veins in lower levels; stockworks in upper levels with Au, Ag,As,Sb,Tl

▽ Hydrothermal breccia and explosion crater

S－－－ Base of silicification
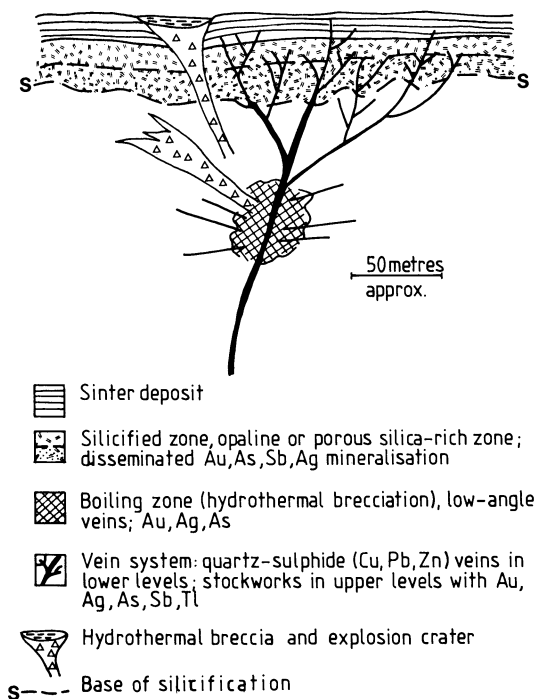
Fig. 11.2. Schematic cross-section of hot spring-type epithermal deposit; see text for details (After Berger and Eimon 1982)

association is Au-Ag-As-Sb-Hg-Tl with minor Cu-Pb-Zn in the deeper levels. The mineralisation is low grade and in the form of disseminations and stockworks just below the silicified cap, although it can reach high grades in hydrothermal breccias and associated vein systems corresponding to the boiling zone. The upper portions of the silica cap are usually barren, but some native sulphur, Au and cinnabar mineralisation may be present. Below the zone of silicification hydrothermal alteration is of the argillic type. Free Au occurs with quartz and adularia in veins, stockworks and disseminations in permeable host rocks. This mineralisation is characterised by its fine-grained size and low overall sulphide content and therefore scarcity of base metals. Episodes of brecciation are important in hot spring deposits because they can be related to rapid pulses of precious metal deposition. As is discussed in more detail later, explosive brecciation occurs wherever the silica cap acts as a seal. This allows the fluids to reach sufficient pressure to rupture the cap, the sudden pressure release causing the fluids to boil, with subsequent mineral deposition and re-sealing of the cap, so that the process may start again. For this reason it is often difficult in trying to work out the number of brecciation episodes that have taken place in a hot spring deposit. The zone of hydrothermal breccia (Fig. 11.2) has a number of low-angle veins that branch off and connect with quartz-sulphide stockworks above and around them (Berger 1985).

An example of hot spring mineralisation is the Round Mountain Au deposit in Nevada (Tingley and Berger 1985).

Higher
levels of
metal
deposition

High grade "Bonanza"-ore
Au + Ag

Lower levels
of metal
deposition

Approx. base of Au-Ag
mineralisation

Argillic alteration

Silicification

Hydrothermal breccia and stockwork

Zone of electrum, Ag-sulphides and
base metal sulphides

Main vein zone with dominant pyrite
and base metal sulphides
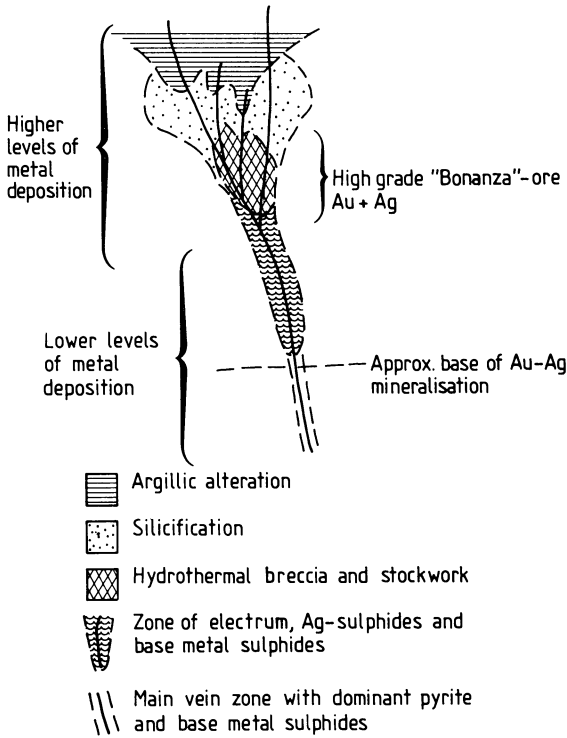
Fig. 11.3. Schematic cross-section
of open-vein type epithermal
deposit, showing two levels of
mineralisation; see text for
details (After Berger and Eimon
1982)

Open-Vein Type

The downward extensions of hot spring deposits, or in other words their feeder
zones, are effectively an example of open-vein type deposits. Open-vein type
epithermal deposits are also known as bonanza, vein and lode type (Silberman and
Berger 1985). They differ from the hot spring type in that mineral deposition occurs
at deeper levels, has higher sulphide and base metal contents, substantial vein
widths, higher grades but lower tonnages. Dominant element association is Au-Ag-
As with minor Se, Te, Cu, Pb and Zn. Figure 11.3 illustrates a model of epithermal
vein system with two levels of mineralisation, and Fig. 11.4 depicts a combined hot
spring vein-type epithermal system. In general the veins are vertically zoned. A
typical vein may consist of agate and clay near the surface, passing downward into
quartz, calcite, adularia and precious metals. The precious metal ore zone has a
restricted vertical interval, usually between 350 and 100 m. At the base the ore grade
decreases while the base metal contents increase, and minerals such as galena,
sphalerite and less commonly chalcopyrite and/or pyrrhotite become important
mineral phases at depth. Quartz continues to be present while calcite is reduced in
volume. The veins within the precious metal zone typically consist of quartz, calcite
and adularia, and may contain ore minerals such as pyrite, arsenopyrite, native
gold, argentite, electrum and tellurides. Other minerals which may be present in
various amounts include: tetrahedrite, fluorite, barite, stibnite, realgar, rhodocro-
site, as well as the above-mentioned base metal sulphides. Native gold constitutes
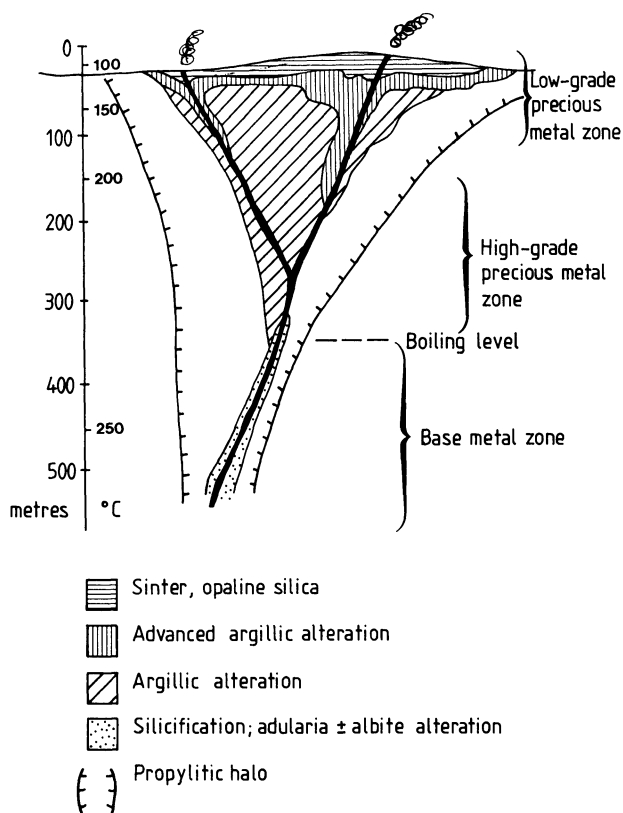
Fig. 11.4. Schematic cross-section of a hot spring depositional model passing downward into an open-vein type system, according to Buchanan (1981). The surface sinter material may contain opal, cristobalite, cinnabar and some pyrite. The zone of advanced argillic alteration is characterised by alunite, kaolin, pyrite. Clay minerals generally form a halo along the vein structure. Illite occurs mainly in the higher levels, passing downwards to a sericite + adularia assemblage. The propylitic zone contains chlorite, illite, carbonate, montmorillonite and pyrite; epidote predominates in the deeper sectors. Ore minerals in the low-grade precious metal zone are native gold, pyrite, stibnite, realgar, cinnabar. In the high-grade precious metal zone ore minerals include mainly electrum, argentite, pyrargyrite. The base metal zone contains pyrite, chalcopyrite, galena

the most important ore mineral, followed by the tellurides, while other complex Au minerals are of lesser importance. The sulphide minerals – in particular pyrite and arsenopyrite – may contain important amounts of Au, which tends to increase towards the surface. In the open-vein epithermal systems the bulk of the mineralisation is confined to major veins, with low-grade stockwork and disseminated zones commonly found in the upper sectors of the system, usually where there is a major change in the attitude of the veins. The ore shoots (a payable zone within the vein in which a combination of width and grade allow stoping), which rarely fill the entire vein structure, usually form isolated zones within the vein (Buchanan 1981). As is common with most vein-type deposits, they are related to structural

features, such as the intersection of fractures, changes in attitude, zones of stress release etc.

The Vatukoula Au deposit in Fiji (Ahmad et al. 1987a, b; Anderson et al. 1987), and most of the precious metal deposits of the Hauraki goldfield in New Zealand (Brathwaite et al. 1989), can be considered as examples of open-vein type.

Disseminated-Replacement Type

Disseminated replacement-type epithermal precious metal deposits, schematically illustrated in Fig. 11.5, are commonly associated with carbonaceous and carbonate host rocks. This type of deposit is relatively common in the Basin and Range province of the USA and is characterised by distinctive mineralogical, geochemical, structural and lithological attributes. Disseminated replacement-type epithermal deposits are also known as Carlin-type because most of their general features are well developed at the Carlin mine in Nevada (discussed later). These deposits have an overall tabular shape and fine-grained ore minerals with an element association consisting of Au-As-Sb-Hg-Tl. They have relatively large tonnages and low grades (Table 11.2A). The fine nature of the mineralisation and restricted geographic distribution of these deposits have encouraged several mining concerns to look for similar deposits in other parts of the world.

APPROX.
200 metres

Permeable carbonate beds

Disseminated Au mineralisation

Acid leached and oxidised zone

Pre-ore dyke

Barite-calcite vein

Silicified halo around fault

Flow of geothermal fluids

Oxidising surface waters
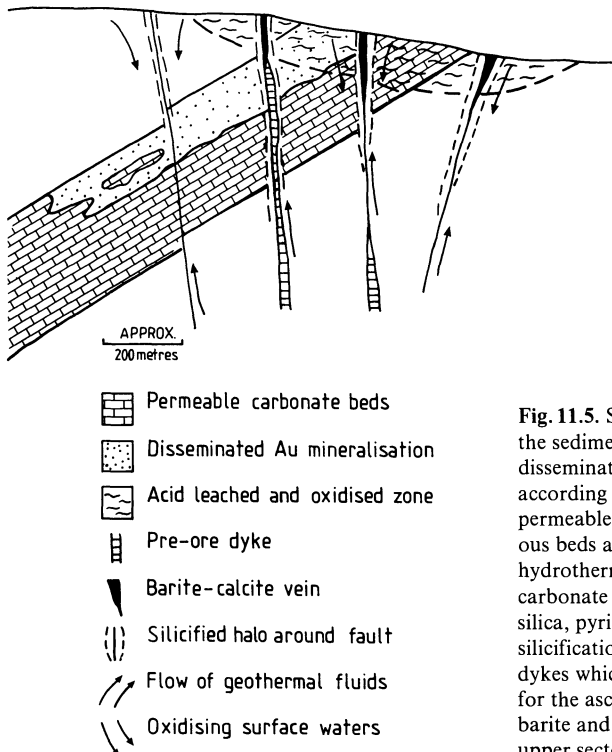
Fig. 11.5. Schematic representation of the sediment-hosted replacement and disseminated-type depositional model, according to Radtke et al. (1980). The permeable carbonate and/or carbonaceous beds are chemically reactive, and the hydrothermal solutions dissolve the carbonate components and precipitate silica, pyrite and Au. There is strong silicification along the faults and/or dykes which have served as channelways for the ascending fluids. Late-stage barite and calcite veins form in the upper sectors of the faults

In disseminated-replacement epithermal deposits the ore commonly begins along faults which have a silicified halo, and extends into carbonate rocks to form the main and primary ore zone. The ore zone within these sedimentary rocks is characterised by extensive silicification and fine disseminations of pyrite and Au with varying amounts of quartz, calcite, dolomite, clay minerals, barite and K-feldspar. The carbonate host rocks may contain up to 0.5% by weight of organic C. The primary ore passes upward into a zone of argillic alteration (acid leaching) and supergene oxidation (Fig. 11.5).

11.3 Volcanic-Hosted Epithermal Deposit Types

Morphology, alteration mineral assemblages and the nature of the volcanic environment (see Figs. 3.4, 3.5 and 3.6) provide further constraints on the characterisation of volcanic-hosted epithermal mineralisation.

Sillitoe and Bonham (1984), for example, have modelled volcanic-related mineralised systems (mostly of the epithermal range) in terms of their relationship to volcanic systems and related landforms. They distinguish deposit types related to andesitic strato-volcanoes, Valles-type calderas, high-silica rhyolite domes and maar-diatreme complexes. Andesitic strato-volcanoes may host, within the upper portions of the stocks feeding the volcanic structure, Cu-Mo $\pm$ Au porphyry. Upward and within the volcanic edifice there may be epithermal veins containing Au, Ag, Cu, Pb and Zn, Au and Ag in breccias and native S in the crater area. Valles-type calderas may host vein deposits of Cu, Pb, Zn, Au and Ag just above the magma chamber, and ring-fracture-controlled stockworks and disseminations of Au, Ag, Hg, U, Li, Be in intracaldera tuffs and/or moat-fill sediments. Rhyolite flow domes could have Au, Ag, Pb, Zn, Cu vein deposits, and near-surface breccias and disseminations of Au and Ag associated with siliceous precipitates. Finally maar-diatreme systems would be characterised by hydrothermal breccias containing Au and Cu, and perhaps stockwork-disseminated Au mineralisation hosted by maar lake beds and/or tuff rings. An example of diatreme-hosted Au-Ag deposits is that of Montana Tunnels in the USA, reported on by Sillitoe et al. (1985).

In terms of alteration mineral assemblages, as well as the nature of the volcanic environment, epithermal systems have been considered as follows (Silberman and Berger 1985; Bonham 1986; Heald et al. 1987; Henley and Berger 1988): (1) quartz-adularia, adularia-sericite, or low-sulphur types; and (2) quartz-alunite, acid-sulphate, or high-sulphur types.

Quartz-adularia, adularia-sericite or low-sulphur types refer to epithermal systems that are generally associated with caldera structures of acid volcanic terranes (see Fig. 3.4), in which hydrothermal activity is characterised by deep meteoric circulation of predominantly chloride-rich fluids, with a pH ranging from 5.5 to 6.5, and temperatures of 250–350°C (Hedenquist and Lindqvist 1985). Near the surface, in the hot spring zone, the host rocks are silicified and contain adularia, albite, calcite and dolomite. This grades into argillic-type alteration with kaolinite, illite, sericite and/or chlorite, illite, smectite, calcite and zeolites. Propylitic alteration follows and affects fairly wide areas. The alteration mineralogy in or

adjacent to veins, stockworks and fractures includes quartz, adularia, calcite, dolomite, Mn-bearing carbonates and silicates, minor fluorite and barite. Ore minerals include native Au, electrum, As, Sb and Hg sulphides, Ag sulphosalts, selenides and base metal sulphides.

Quartz-alunite, acid-sulphate or high-sulphur types may occur in caldera settings, but appear to be more characteristic of strato-volcanoes related to calc-alkaline magmatism (see Fig. 3.5). Near-surface hydrothermal circulation is characterised by acid-sulphate-rich, or mixed acid-sulphate-chloride-rich, fluids, with pH values ranging from 2 to 5, and temperatures of between 100 and 180°C. The origin of the acid nature of these fluids (explained in Chap. 3, Sect. 3.4.2) is essentially due to the inability, in places, of deep chloride-rich fluids to discharge at the surface. However when they reach the boiling level, volatiles such as CO_2 and S compounds (SO_2 and H_2S) are partitioned into the vapour phase. The steam thus produced will heat levels of aquifers forming acid-sulphate and/or CO_2-rich (bicarbonate) waters. Localised mixing of chloride-rich with acid-sulphate or bicarbonate waters occurs. Oxidation of H_2S results in the development of H_2SO_4 and native S (Henley and Ellis 1983; Hedenquist and Browne 1989). Figure 11.6 schematically illustrates the various types and nature of the geothermal fluids in volcanic areas and the associated dominant alteration (acid-sulphate and adularia-sericite).

The main effects of the circulation of predominantly acid-sulphate fluids is the intensive acid leaching of wall rocks leading to various stages of intermediate to advanced argillic alteration and the deposition higher up (usually in the crater of the volcanic edifice) of native S, the presence of boiling mud pools, warm to hot springs, and abundance of kaolinite and alunite. Typical advanced argillic mineral assemblages are represented by: quartz + alunite + kaolinite, quartz + pyrophyllite + zunyite + diaspore, quartz + alunite + sericite, quartz + alunite + native S + barite (Bonham 1986). Argillic alteration grades outwards to widespread propylitic alteration. Ore minerals include pyrite, enargite, native Au and S, barite near the surface; enargite-luzonite series, tetrahedrite-tennantite series, Ag sulphides and sulphosalts, native Au, Bi minerals, tellurides and Pb-Zn sulphides and barite in deeper levels.

Bonham (1986) also considers an alkalic subtype of the epithermal system which is characterised by Au-tellurides and associated with alkaline igneous rocks such as syenite, trachytes and phonolites. The alkali subtype occurs in a variety of volcanic environments including maar-diatreme and calderas (see Mutschler et al. 1985). The main mineralogical features of this subtype (Bonham 1986) are: quartz + fluorite + adularia + carbonates + roscoelite vein assemblages surrounded by a narrow alteration envelope of adularia + carbonate + sericite + pyrite + smectite + illite + roscoelite, and followed by a zone of propylitic alteration with disseminated pyrite.

11.3.1 Epithermal Systems of Submerged Volcanic Structures

There is evidence of present-day hydrothermal activity from a number of subduction-related volcanic arcs. The intermediate to acidic composition of this volcanism, the totally or partly submerged caldera structures, and the nature of the
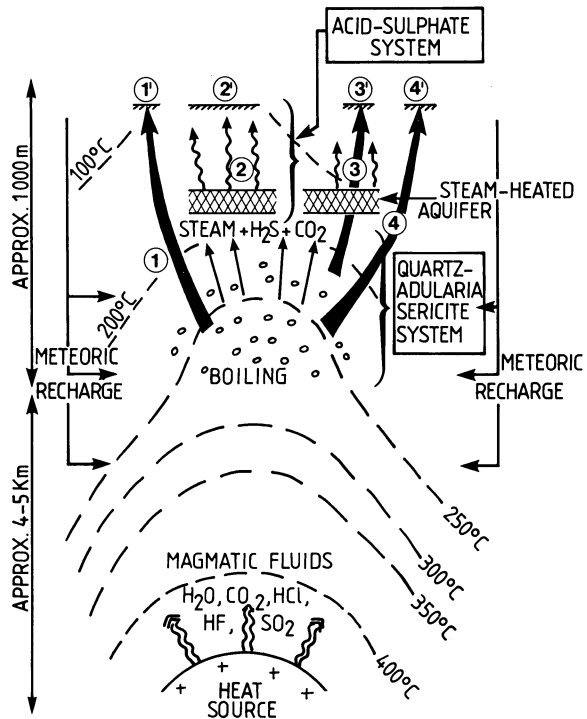
Fig. 11.6. Idealised representation of the main types and nature of geothermal fluids. This figure is based on Hedenquist and Lindqvist (1985) and Hedenquist and Browne (1989). Note that the upper sector is expanded with respect to the lower one. The types of geothermal fluids (see text for details) are: *1* chloride-rich fluids, *1'* near-neutral chloride boiling spring; *2* acid-sulphate fluids, *2'* acid-sulphate springs, fumaroles and mud pools; *3* CO_2-rich fluids, *3'* bicarbonate hot springs; *4* chloride-rich fluids, *4'* dilute chloride warm springs. Chloride-rich fluids are usually associated with quartz-adularia-sericite systems and with siliceous sinters; acid-sulphate fluids are associated with varying degrees of acid leaching (argillic alteration); bicarbonate waters are commonly responsible for the precipitation of extensive deposits of carbonate material such as travertine. In this case the CO_2 may have been acquired from the surrounding lithologies (e.g. limestones). The magmatic fluids component is assumed, but the actual measure of its input is not known and is isotopically difficult to detect once the incursion of large quantities of meteoric waters has taken place

chemical precipitates suggest an environment similar to that of the kuroko ore deposits (discussed in a forthcoming section). Good examples are provided by the islands of Vulcano in the Tyrrhenian Sea and Santorini in the Aegean Sea.

Vulcano is one of the seven volcanic islands of the Aeolian arc which is related to a zone of active subduction southeast of, and below, the Calabrian region, marking a convergent boundary between the European and African plates. The Aeolian volcanism is characterised by explosive activity which resulted in the construction of rhyolitic and dacitic domes (Barberi et al. 1974, Ellam et al. 1988). At Vulcano the growth of a strato-volcano was followed by explosive cycles of activity and the development of caldera structures formed by rhyolitic and trachytic lavas and pyroclastics. The present fumarolic activity is distributed in the crater area at La
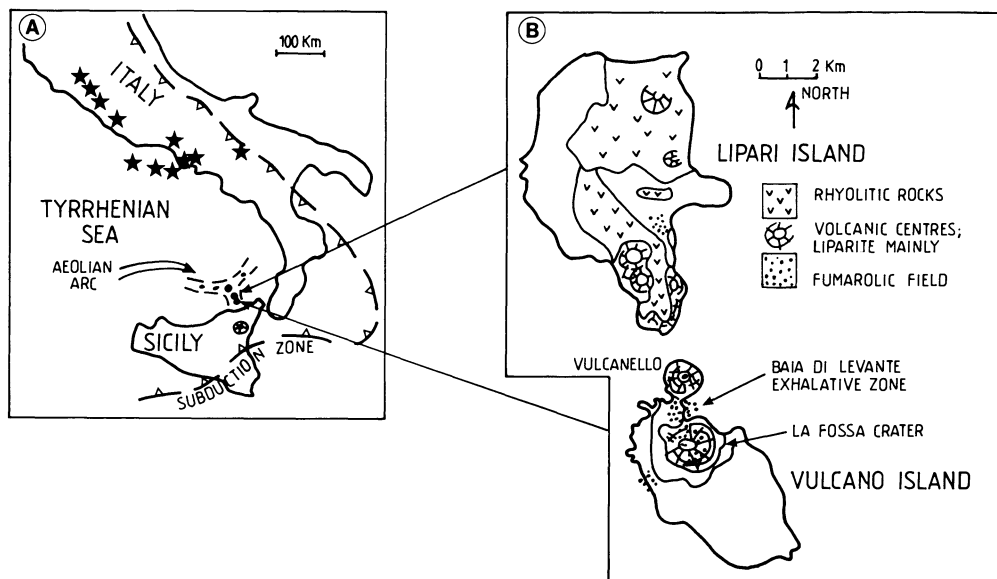
Fig. 11.7. **A** The Aeolian island arc and other recent volcanic centres (stars) in Italy. **B** The islands of Lipari and Vulcano and their most recent volcanic centres. Exhalative activity is currently taking place on the sea floor between La Fossa crater and Vulcanello (after Honnorez 1969). Acid-sulphate alteration is predominant at La Fossa and Baia di Levante, where pyroclastics and lavas are pervasively altered to clays and alunite minerals. La Fossa last erupted during 1888–1890

Fossa, and between it and the Vulcanello vent to the north along the sea shore in the Baia di Levante (Fig. 11.7). The presence of a shallow magma chamber has been suggested beneath the narrow channel separating Vulcano from Lipari, and the commonly observed near-surface seismicity is interpreted as being due to gas explosions in cavities above the magma chamber, subsequently evolving into fumarolic activity at the surface (Barberi et al. 1974). In the Baia di Levante, active emissions form a submarine geothermal field with temperatures of between 60 and 110°C. These emissions are rich in CO_2 with minor H_2S (Martini et al. 1980). Two types of aquifers have been suggested: a lower, seawater-dominated aquifer is that of the Baia di Levante submarine zone; the other is a meteoric water-dominated aquifer which is acid-sulphate-rich and feeds the fumaroles of the La Fossa crater (Fig. 11.7). Thus, it is thought that they represent two separate convective cells with local mixing. The submarine fumaroles precipitate Fe, Cu, Zn and Pb sulphides (Honnorez 1969). Intense hydrothermal alteration of surface pyroclastics has resulted in the development of masses of clay and chalcedony with disseminations of pyrite and chalcopyrite (Vallette and Picot 1981). A series of boreholes drilled for geothermal exploration (Faraone et al. 1986) revealed the presence of hydrothermal breccias and intensely altered lavas above a monzogabbroic intrusion. Lava fragments are altered and cemented by montmorillonite, calcite, anhydrite, chlorite and abundant silica. The upper part of the intrusion also displays a potassic alteration assemblage with K-feldspar + biotite ± epidote ± chlorite ± calcite ± pyrite.
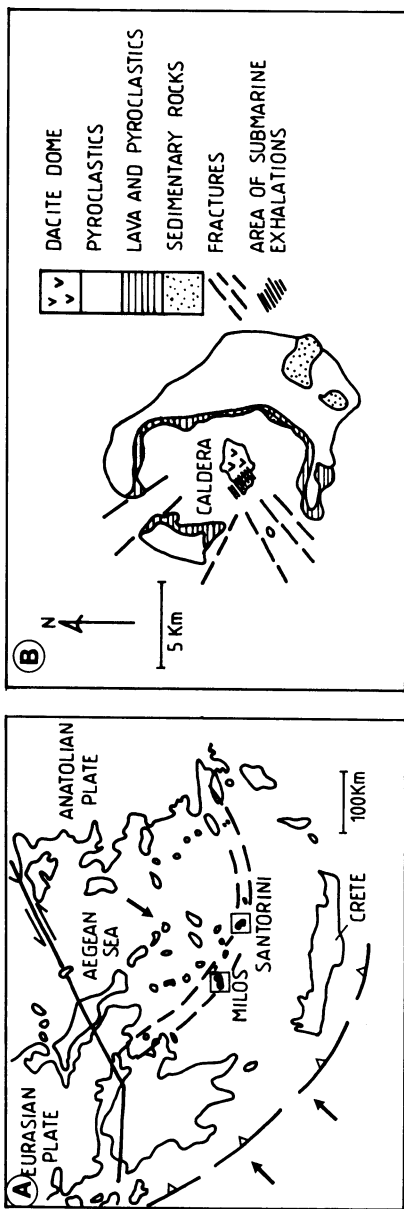
Fig. 11.8. A The Aegean volcanic arc and location of the islands of Santorini and Milos (after Hauck 1988). B The Santorini partially submerged caldera; the two small islets in the central part of the caldera are Palea and Kameni, which are part of a dacitic dome structure (after Smith and Cronan 1983; Bullard 1984). C Schematic cross-section through the islets of Palea and Kameni showing the postulated hydrothermal convection responsible for the deposition of the Fe-rich muds on the sea floor (After Arvanitides et al. 1988)

The Hellenic (or Aegean) volcanic arc comprises a series of calc-alkaline volcanoes related to the interaction of the African plate with the Aegean-Anatolian microplates (Fig. 11.8A). The islands of Santorini (or Thera) are part of this arc, and are the remnants of a partly submerged caldera built up through a succession of effusive and explosive (dacite and related pyroclastics) cycles of volcanic actvity from Late Pliocene to historical times. The present morphology is due to a major eruption which took place in about 1400 B.C., resulting in the collapse of the caldera. It is thought that it was this great eruption that caused the destruction of the Minoan civilisation which at that time thrived on the island of Crete some 110 km to the south. It has also been suggested that the legend of Atlantis, told by Plato in 395 B.C., may in fact refer to this eruption (see Doumas 1978; Bullard 1984), and indeed recent archeological findings appear to corroborate this.

Hydrothermal discharge on the sea floor has been reported from a number of sites around the islands of Palaea and Nea Kameni, located in the central area of the submerged caldera (Fig. 11.8B). These islands are made up of dacitic flows and domes which rise some hundreds of metres above the sea floor (Arvanitides et al. 1988). Metalliferous sediments at the discharge sites contain up to 30–40 wt.% of Fe_2O_3, abundant opaline silica and minor quantities of Cu, Mn, Ba and Zn (Smith and Cronan 1983, Arvanitides et al. 1988). The predominance of Fe in this submarine epithermal system has been explained by extensive oxidation of H_2S emanating from a degassing magma at depth (Fig. 11.8C). The resulting acid-sulphate-rich fluids attack the dacitic lithologies predominantly leaching out Fe which is the most abundant metallic element in these wall rocks. Smith and Cronan (1983), who carried out detailed investigations on the geochemistry of the Santorini metalliferous sediments, found that the hydrothermal component of these sediments is determined by the relative proportions of hydrated Fe oxides, Mn oxides and silica. They also found a zonation in the elemental abundances of these oxides and distinguished two main zones as follows: (1) an inner exhalative zone with hydrated Fe oxides (containing Fe, Mn, Cu, Zn, Pb, Mo, V, Sc, Ba and Hg) and silica; (2) an outer exhalative zone with hydrated Fe oxides (+ Fe, Mn, Zn, Mo and Ba).

Approximately 100 km west-northwest of Santorini is the volcanic island of Milos which is also part of the Aegean volcanic arc (Fig. 11.8A). On this island sulphide-sulphate deposits are present. This mineralisation has features that are considered typical of kuroko-type ore deposits (Hauck 1988). The deposits, of Pleistocene age, consist of Mn-Ba ores, siliceous ore, gypsum ore and barite ore. Sulphide minerals include galena, sphalerite, chalcopyrite, bornite, pyrite, covellite, pyrargite and proustite. Sulphur isotope determinations by Hauck (1988) confirm that the S mostly originated from seawater sulphate and the temperature of ore formation ranged from 220 to 260°C. The ore elements are thought to have been leached from the volcanic pile by interaction with circulating hot seawater.

11.3.2 Hydrothermal Alteration

Hydrothermal mineral phases that develop in epithermal systems are a function of temperature, pressure, rock type, nature of the circulating fluids (such as pH,

Table 11.3. Chief hydrothermal alteration assemblages of epithermal systems. (A) Alteration assemblages related to near-neutral, chloride-rich geothermal fluids (after Hedenquist and Lindqvist 1985). (B) Alteration assemblages related to CO_2-rich geothermal fluids (after Browne and Ellis 1970; Browne 1978). Inferred temperatures approximately the same as in Table 11.3A. (C) Alteration assemblages related to acid-sulphate geothermal fluids (after Hedenquist and Lindqvist (1985)

A

Alteration type	Mineral assemblage (+ key minerals; ± accessories)	Inferred temperature (°C)
Potassic	Adularia + biotite + magnetite ± epidote ± chlorite ± muscovite	> 320
Sericitic	Sericite + quartz ± sulphides ± oxides	> 220
Argillic	Smectite or interlayered illite smectite ± sulphides ± zeolites ± quartz ± calcite	< 200
Inner propylitic	Epidote + actinolite ± chlorite ± illite	> 300
Propylitic	Epidote ± chlorite ± illite ± sukphides	> 250

B

Alteration type	Mineral assemblage (+ key minerals; ± accessories)
Advanced argillic	Kaolinite + alunite ± opal
Sericitic	Sericite + quartz + calcite ± chlorite ± adularia
Potassic	Adularia + albite ± sericite ± calcite ± quartz ± chlorite
Propylitic	Calcite + chlorite + quartz ± albite ± adularia

C

Alteration type	Mineral assemblage (+ key minerals; ± accessories)	Inferred temperature (°C)
Advanced argillic (high temperature)	Pyrophyllite + diaspore + andalusite ± quartz ± sulphides ± tourmaline ± enargite–luzonite	250–350
Advanced argillic (low temperature)	Kaolinite + alunite ± chalcedony ± quartz ± pyrite	< 180

activities of CO_2, H_2S) and water/rock ratios (Browne and Ellis 1970). Following Henley and Ellis (1983), and Hedenquist and Browne (1989) we consider the hydrothermal alteration in epithermal systems in terms of interaction of (1) near-neutral chloride fluids; (2) CO_2-rich fluids; and (3) acid-sulphate fluids.. A summary of alteration types and related hydrothermal minerals are given in Table 11.3A, B, C.

Alteration Related to Near-Neutral Chloride- and CO_2-Rich Fluids

Common alteration assemblages related to deep chloride-rich and near-surface CO_2-rich geothermal fluids (Table 11.3A, B) that interact with intermediate to acid volcanic wall rocks are albite + adularia ± wairakite ± sericite ± epidote usually derived from plagioclase precursors. Biotites alter to chlorite ± sphene ± epidote, pyroxenes and amphiboles alter to mixtures of sericite + chlorite + sphene + quartz ± pyrite. Groundmass material may change to aggregates of quartz + sericite + calcite ± zeolites ± sulphides ± chlorite. Fracture and vein filling minerals include quartz, calcite, sericite, adularia, zeolites (laumontite, wairakite), chlorite, epidote and sulphides, such as pyrite and pyrrhotite (Hedenquist and Browne 1989). The detailed studies of active geothermal systems by Hedenquist (1983, 1986) and Hedenquist and Browne (1989) indicate that adularia and albite do not appear at depths where the temperature is less than 180°C, and that increasing alteration (e.g. increasing water/rock ratios) tends to produce a progression from unaltered plagioclase through albite to adularia. Sericite, white mica or hydromuscovite and quartz are common alteration products of both primary and hydrothermal feldspars, of groundmass material and of mafic phenocrysts. Hedenquist and Browne (1989) found that the K content of the sericites tends to increase with depth and temperature, thus approaching the composition of muscovite. Zeolites include species such as mordenite, laumontite and wairakite and are temperature-sensitive, as discussed later. Calcite, present especially in cavities and fractures, also occurs as fine to large blades (up to several centimetres), which in many instances are replaced by silica ("bladed silica"). This platy, or bladed, habit of calcite in epithermal systems is taken to indicate deposition from a boiling fluid.

Alteration Related to Acid-Sulphate-Rich Fluids

In the lower temperature range ($<$ 180°C) the chief mineral phases related to acid-sulphate geothermal fluids are kaolinite, alunite, cristobalite, gypsum, opal, native S, quartz and sulphides. Pyrophyllite, diaspore and andalusite are stable at temperatures in excess of 250°C, and possibly even greater than 350°C, as in the case of andalusite (Table 11.3C, see also Fig. 4.15). Barite, anhydrite and hydrated Fe oxides may also be present in the lower temperature range.

Siliceous Precipitates, Self-Sealing and Hydrothermal Breccias

Precipitation and re-distribution of silica is one of the most common features of hydrothermal activity. The behaviour of silica in hydrothermal solutions has been investigated in detail by Fournier (1989). In general the solubility in water of various forms of silica (amorphous silica, opal, cristobalite, chalcedony and quartz) increases with temperature in the range of 10 to 100 ppm for temperatures of $<$ 50–100°C, and up to 1000 ppm above 300°C; thereafter, solubility of silica decreases. The silica of epithermal environments is largely derived from alumino-silicate minerals, quartz and volcanic glass. Supersaturated silica solutions are facilitated by rapid cooling such as that due to decompressional boiling, or by dissolution of

siliceous rocks by acid solutions (Fournier 1989). Silica supersaturation promotes precipitation of amorphous (opaline) silica at temperatures of approximately 140° C, and near-neutral chloride-rich solutions generally deposit at the surface large quantities of amorphous silica, forming aprons of sinter material (see Chap. 3). Amorphous silica is unstable and with time forms chalcedony, or fine-grained quartz. Present-day sinters typically show finely banded or non-planar laminated structure (see Plate 4.14). Other small-scale structures perpendicular to the laminae may also be present. These have tubular or columnar shapes, which in some cases have been interpreted as having originated from the growth of bacterial stromatolites (Walter et al. 1972). Clearly, then, the presence and recognition of sinter material are indicative of a paleosurface and therefore of a fossil geothermal system.

Addition, or re-distribution, of silica in boiling zones, together with calcite and feldspar, may result in the development of an impermeable barrier or, as is commonly known, the system becomes self-sealed (Facca and Tonani 1967). An impermeable barrier created by self-sealing is considered to be a major cause of hydrothermal eruptions. This is achieved by a combination of the gradual build-up of volatile pressure and of seismic activity which induces rupturing of the sealed zone, resulting in sudden decompression and subsequent eruption. Many breccia pipes are thought to form in this way. Hydrothermal fracturing is a manifestation of the same phenomenon at greater depths, where fractures form as a result of the decompression of high fluid pressure when this exceeds the confining pressure by an amount equal to the tensile strength of the rock (see Chap, 3). Hedenquist and Henley (1985), who have studied in some detail the origin of hydrothermal eruptions and their relationship to deposition of minerals and precious metals, do not favour large-scale self-sealing in a geothermal field, but rather envisage localised sealing. This would result in the diversion of the fluid flow through fractures, kept open by tectonic activity, either within or laterally to the zone of sealing. These authors, however, contend that local sealing can produce eruptions in a sequence which they subdivide into a pre-eruption phase, a crater-formation phase and a post-eruption phase. In the first of these three phases the hot geothermal fluid cools and depressurises as it rises towards the surface, until at a given temperature and pressure it boils. Silica is deposited as quartz below approximately 100 m and as chalcedony above this depth. During boiling, volatiles such as CO_2 and H_2S partition into the vapour phase. CO_2 (and H_2S) loss leads to a pH increase in the residual fluids which causes precipitation of calcite. There is discussion of boiling in Section 11.4. Thus, the precipitation of quartz, calcite and other phases (e.g. adularia) results in decreasing permeability in the upper sectors of the system, although as mentioned previously, continuing tectonic activity keeps channels open for most of the time. Nevertheless when localised sealing occurs, exsolved gases accumulate below the seal until the total pressure exceeds the lithostatic pressure plus tensile strength of the rocks inducing hydraulic fracturing. This can rapidly expand and propagate upward, eventually triggering an eruption. The hydrothermal conduit and crater become a locus for the deposition of precious metals, even in the aftermath of the eruption, and an ore deposit, spatially and temporally associated with hydrothermal breccias, may thus form (Hedenquist and Henley 1985).

Geochemical Variations in Altered Rocks

Geochemical variations in altered wall rocks are clearly a reflection of the mineralogical changes induced by their interaction with circulating fluids. In epithermal systems, general element variations in the wall rocks are losses of Na, Ca, Ti and Ba and gains in K, Si, Rb, Sc, Ga, Sr, As, Sb, Ag, Au, Sn, Tl and W. Transfer of elements takes place from alumino-silicate, ferromagnesian minerals and the groundmass material (glass or crystalline matrix). Where CO_2 is present, carbonic acid is formed (H_2CO_3) and reaction with aluminosilicates will liberate H^+, causing reactions such as those schematically shown below (see Chap. 4 for details) to follow with liberation of cations in solution and deposition of silica:

K-feldspar + H^+ → illite + K^+ + SiO_2;

Na-feldspar + H^+ → montmorillonite + Na^+ + SiO_2.
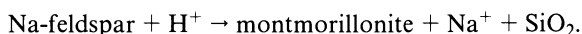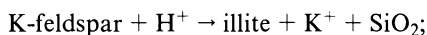
Light Stable-Isotope Systematics

An introduction to isotopic studies of hydrothermal solutions is provided in Chapter 2, and the effects of isotopic variations in hydrothermally altered rocks are discussed in Chapter 4. Details of light stable-isotope systematics of epithermal systems are reported by Field and Fifarek (1985) and Criss and Taylor (1986). These studies refer to the fractionation of the isotopes of oxygen and hydrogen between fluids and mineral phases in the wall rocks. This fractionation, which is the result of the mass differences of the isotope species, is dependent on temperature but independent of pressure. The oxygen and hydrogen isotopic composition of chloride-rich geothermal fluids as compared to meteoric waters shows a strong enrichment in $\delta^{18}O$ values (^{18}O shift), while the δD values remain constant. The amount of ^{18}O shift appears to be directly proportional to temperature and inversely proportional to water/rock ratios. On the other hand, the isotopic composition of acid geothermal fluids, in addition to the ^{18}O shift, also shows an enrichment in the δD values (Criss and Taylor 1986, Figs. 6 and 7). The observed ^{18}O shift is found to be matched by a corresponding depletion of the $\delta^{18}O$ values in the wall rocks, which is interpreted as being due to isotope-exchange reactions between ^{18}O-depleted fluids and ^{18}O-enriched wall rocks (see Fig. 4.14).

11.3.3 Mineral and Metal Zoning

Henley and Ellis (1983) have reported on mineral zoning with increasing temperature. They quote an example of the alteration of volcanic glass which, with increasing temperature, is altered to opal, smectite, calcite and zeolite to mixed layer clays. The composition of zeolite minerals is affected by successively high temperature, from heulandite at about 100°C, through laumontite (150–200°C) to wairakite (up to 300°C). A summary of the temperature range of hydrothermal minerals is shown in Fig. 11.9. Bird et al. (1984) have shown that mineral zoning with increasing temperature and depth reflect progressive dehydration of calc-
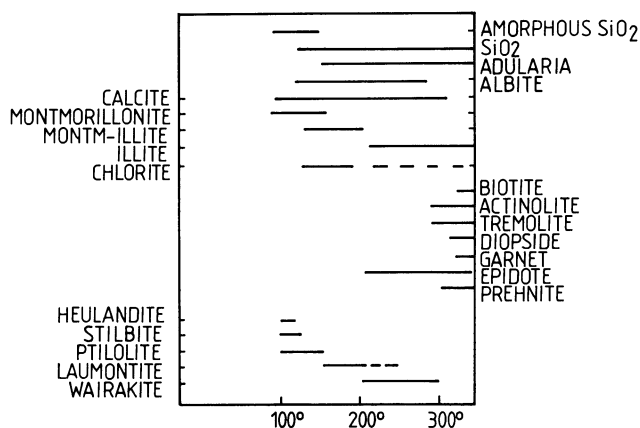
Fig. 11.9. Temperature range of alteration minerals in epithermal systems (After Henley and Ellis 1983)
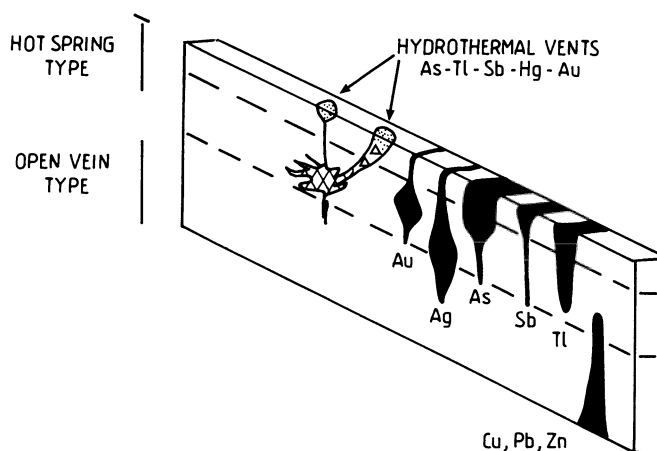
Fig. 11.10. Idealised representation of metal zoning in epithermal systems (After Berger and Eimon 1982)

silicate minerals, whereby the amount of zeolitic and structural water in the calc-silicate assemblages decreases. These authors found systematic changes in the mineralogy and texture of deltaic sediments (Cerro Prieto and Salton Sea) which have interacted with geothermal fluids. In order of increasing depth and temperature the following zones occur: (1) montmorillonite + kaolinite (150°C); (2) illite + chlorite zone (150–180°C to 230–250°C); (3) calc-silicate zone with epidote, prehnite, actinolite, Ca-pyroxene (230–250°C to > 350°C); (4) biotite zone (325–350°C). The geometry and boundaries of the alteration zones closely follow the configurations of the isotherms of the geothermal system, and the general zoning patterns are similar to those that form in low-pressure contact metamorphic rocks (Bird et al. 1984).

Epithermal deposits display characteristic metal zoning with depth. Base metal sulphides (Cu, Pb and Zn) in the deeper parts of the system grade upward to zones containing Au-Ag, at or near the surface As-Sb-Hg-Tl, as previously indicated (Figs. 11.2, 11.3 and 11.4). Figure 11.10 shows a typical metal zonation as reported by Berger and Eimon (1982).

11.4 Transport and Deposition of Precious Metals in Epithermal Systems

The role of complex ions and ligands in the dissolution, transport and deposition of metals is introduced in Chapter 2. Experimental geochemistry applied to problems of ore deposition has contributed a great deal to the understanding of the mechanisms involved in metal speciation and solubility in hydrothermal fluids. Apart from those works referenced below, the reader is referred to Volume 53 of Geochimica et Cosmochimica Acta (1989), in which a number of papers deal with the results of experimental studies of hydrothermal processes.

Dominant, and geologically important, ligands for metal transport are Cl^- (chloride), HS^- (thio-sulphide) and OH^-. Minor ligands, in the sense that they are either of low abundance, unstable or weak, are NH_3, S^{2-}, SO_4^{2-}, F^- and HCO_3^-. The last two, however, become important ligands for the transport of metals, such as Sn in greisen systems (F^-) and U in the weathering environment (HCO_3^-). It must be noted that at temperatures in excess of 350°C complexes in aqueous solutions are neutral, while below this temperature charged complexes predominate. Nevertheless, the most common and efficient ligands for the dissolution and transport of metals are the chloride and sulphide complexes. Chloride complexes, which predominate in high salinity fluids and at high temperatures (in fact their solubility increases with increasing temperature), preferentially tend to complex base metals and Ag. Sulphide complexing, on the other hand, predominates in low salinity fluids (i.e. geothermal fluids), is less dependent on temperature and is especially favourable for complexing Au and, depending on physico-chemical conditions, Ag (see later). The "soft", or class A, and the "hard" or class B, behaviour of metals and ligands (also discussed in Chap. 2) predicts that strong complexes are formed by complexing agents and metals of the same class (see Table 2.4).

Precipitation of metals from hydrothermal solutions takes place whenever the transporting complex is destabilised and as a result the solubility of the metal in question is greatly reduced. A number of factors induce destabilisation of metal complexes, including: (1) temperature decrease; (2) pressure loss and/or boiling; (3) changes in the redox state of the solution; (4) reduced activity of complexing ions (i.e. S or Cl).

Hydrothermal breccias and fluid inclusion studies have shown that boiling is a very important process for ore deposition in epithermal systems. It must be remembered, however, that fluid mixing is also an important process for the deposition of ore minerals. Boiling temperatures increase with salinity and decrease with increasing concentration of volatiles in the fluid. The important effects of

boiling are the partitioning of volatiles (CO_2, H_2S, H_2, SO_2, CH_4 etc.) into the vapour phase. The release of CO_2 causes a rise of the pH in the remaining solutions, while their salinity increase as a result of H_2O steam loss. Loss of H_2S destabilises sulphide complexes (see later) and changes the oxidation state of the remaining liquid, as for example:

$$H_2S \text{ (aq)} \rightarrow H_2S \text{ (g)};$$

$$Me (HS)_3^- \rightarrow MeS + HS^- + H_2S \text{ (g)};$$
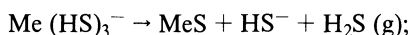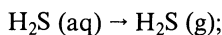
where MeS is metal sulphide precipitate.

Oxidation processes involve the following reactions (Barnes 1990):

$$2HS^- + 2O_2 \rightarrow H_2S + SO_4^{2-};$$

$$H_2S + 2O_2 \rightarrow 2H^+ + SO_4^{2-};$$

$$HS^- + 2O_2 \rightarrow H^+ + SO_4^{2-};$$
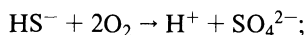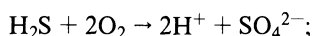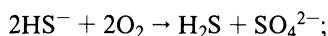
$$Me(HS)_3^- + 4O_2 \rightarrow MeS + 3H^+ + 2SO_4^{2-}.$$
$$\text{(ore)} \quad \text{(acid)} \quad \text{(sulphate)}$$

The pH increase associated with loss of CO_2 results in the decrease in the concentration of metals, therefore boiling and pH changes are effective depositing mechanism for chloride-complexed metals which are subsequently deposited as mineral phases, while metals that are sulphide-complexed are deposited as native metals (Cole and Drummond 1986).

Transport of Au and Ag in hydrothermal solutions occurs dominantly as chloride and sulphide complexes. In epithermal systems Au is transported in the +1 and +3 states as either chloride or bisulphide complexes (see also Chap. 15). Seward (1979a) has shown that complexing reactions for Au in the +1 state are:

$$Au^+ + H^+ + 2Cl^- = AuCl^-_2 + 0.5H_2;$$

$$Au^+ + H_2S + HS^- = Au(HS)^-_2 + 0.5H_2;$$
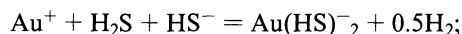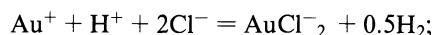
Loss of H_2S during boiling results in increased activity of S^{2-} and HS^- in the remaining solutions, in turn leading to more dissolution of Au and its transport in solution by sulphide complexing. The continuing oxidation of H_2S meanwhile forms H_2SO_4 which attacks alumino-silicates (acid-leaching), releasing electrons into the system which destabilise the sulphide complex (e.g. Au^+ gains electrons), according to the reaction shown below:

$$Au(HS)^-_2 = Au^\circ + 2HS^-.$$
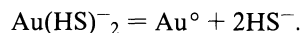
The cycle discussed above is schematically illustrated in Fig. 11.11.

In epithermal systems Ag is transported in the +1 state as a chloride complex ($AgCl^-_2$) and is deposited either as Ag° or as a sulphide. The ratios of Ag/Au are important in determining the type of dominant complexing and the expected nature of the epithermal system (Cole and Drummond 1986). Thus, systems with Ag/Au ratios less or equal to 1 tend to be dominated by native Au and electrum, sulphide complexing of Au is dominant, and temperatures are less than 250°C. Systems
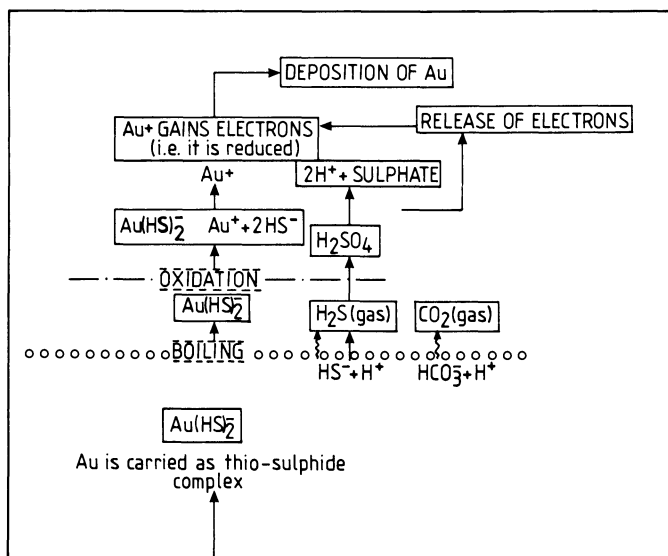
Fig. 11.11. Model depicting the breakdown of Au-carrying thio-sulphide complexes as a result of boiling and oxidation. (After Seward 1979a; Hedenquist 1983; Henley and Ellis 1983; Rossiter 1984)

where Ag/Au ratios are greater than 1 are characterised by argentite, base metal sulphides, sulphosalts, and electrum, with only minor Au. In this case chloride complexing is dominant and the temperatures are greater than 250 °C. In summary, precipitation of Au takes place in response to changes in temperature, pressure, pH, Eh and the activity of reduced S. It is possible that the same type of complexing may also be prevalent for other metals such as As, Sb and Hg. Chloride complexing is further especially important for Ag and base metals (Pb, Zn, Cu) in higher temperature regions.

Figure 11.12 (A,B, C) illustrates the dominant conditions in which Au and Ag are transported. The diagrams were constructed for a temperature of 250 °C, considering S and Cl activities that best approximate natural conditions in geothermal systems (Gammons and Barnes 1989; Shenberger and Barnes 1989). It can be seen from Fig. 11.12A that Au is highly soluble as $AuCl_2^-$ when in equilibrium with hematite, and that the $Au(HS)_2^-$ complex is stable under alkaline conditions, however, a drop in pH (arrow 1), or in aO_2 (arrow 2), will cause destabilisation and Au precipitation. In this diagram it is also important to note that the highest solubility field for Au coincides with the stability field of pyrite, indicating that this metal is transported in equilibrium with pyrite. This is corroborated by the observed common association in nature of pyrite and Au (Shenberger and Barnes 1989). Precipitation of Au may therefore occur by mixing of a reduced fluid with oxygenated waters (i.e. meteoric), or with any other oxidised environment. Au deposition by oxidation is given by:

$$2Au(HS)_2^- + H_2O + 7.5O_2 \rightarrow 2Au + 6H^+ + 4SO_4^{2-}.$$
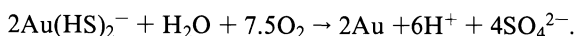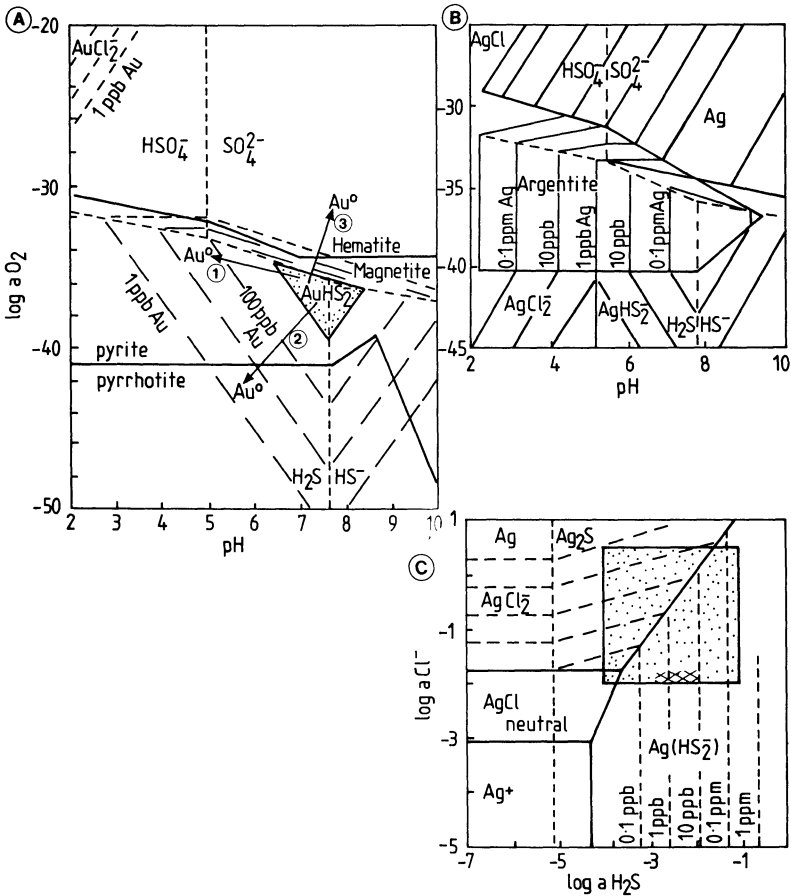
Fig. 11.12A–C. Diagram showing dominant chemical conditions (oxidation state, pH, activities of S and Cl), for the transport of Au and Ag in hydrothermal systems (see text for details). A Diagram constructed at 250°C, total sulphur activity $= 0.01$ m and total chloride activity $= 0.1$ m, which roughly corresponds to a salinity of 2 wt.% NaCl equivalent. Note that the highest solubility of Au is attained by $Au(HS)_2^-$ complexing in the stability field of pyrite and at pH values between 7 and 8; Au is also soluble as $AuCl_2^-$ but at high O_2 fugacity (hematite stability field) (after Shenberger and Barnes 1989). B Solubility of Ag at 250°C, as a function of pH and oxidation state, total sulphur and chloride activities as at A; minimum solubility is at pH 5 at the boundary between chloride (lower pH) and sulphide complexes (higher pH), also note that the maximum solubility field is in equilibrium with the argentite (Ag_2S) field (after Gammons and Barnes 1989). C Ag solubility at 250°C, pH $= 6$, as a function of chloride and H_2S activities, whose limits in natural systems are indicated by the *shaded area*; the *cross-hatched* field indicates the range for epithermal deposits; note that native Ag and argentite can precipitate at high chloride activity (upper left corner of diagram) (After Gammons and Barnes 1989)

Reduction, on the other hand, may take place if the fluid interacts with graphite- or organic material-bearing rocks. Another cause of Au precipitation is a reduction in the activity of the S species in the system, due for example to boiling and/or precipitation of sulphide minerals (Shenberger and Barnes 1985). At 100°C the stability field of $Au(HS)_2^-$ is much smaller than that shown in Fig. 11.12A for 250°

C, which implies that the solubility of the metal is reduced, and hence precipitation may also take place during cooling of the solution. The phase diagrams shown in Fig. 11.12B, C refer to the stability conditions of Ag as a function of pH, the activities of Cl and S, and oxidation state, at a temperature of 250 °C. In Fig. 11.12B it is seen that in high oxidation states and low pH, chloride complexing is dominant, and that $Ag(HS)_2^-$ is stable under more reducing conditions and pH values ranging from near-neutral to alkaline (Gammons and Barnes 1989). Figure 11.12C shows that the predominance of chloride versus sulphide complexing depends on the relative activities (and hence concentrations) of Cl and S species in the system. The shaded area illustrates the likely field for natural ore solutions (Gammons and Barnes 1989).

11.4.1 Boiling Depths and Metal Zoning

In this section we look at the effects of boiling in terms of Ag/Au ratios and related metal zoning, following the theoretical modelling carried out by Cole and Drummond (1986) whose results are discussed here. As mentioned above Ag/Au ratios can be important as exploration guidelines in establishing the nature of the system as well as elucidating metal enrichment and zoning. In their modelling Cole and Drummond assume a constant pressure gradient of 175 bar per 1 km of depth. Boiling is dictated by the initial temperature, salinity, volatile concentration and pH. Their calculations show that a Au ore grade of 30 g/t requires "10^6 m of boiling solution" for a system with 10 % porosity, densities of 1.0 and 2.7 g/cm^3, for solution and rock, respectively, and a Au enrichment of 1 ppb/m of boiling solution. Thus, if the flow path to the point of deposition is 1 km, it would require 1000 cycles of fluid turnover associated with the boiling process to produce the above tenors of Au mineralisation. However, if boiling is violent as in a hydrothermal eruption, then metal deposition would occur instantly on a small volume of rock. The depth of boiling becomes shallower with either decreasing temperature and/or CO$_2$ concentration for a given salinity. For example at a content of tot CO$_2$ of 1 mol, salinity of 1 mol, initial boiling depth is 1050 m at 300 °C, 930 m at 250 °C and 850 m at 200 °C, assuming a constant pressure gradient of 175 bar/km. If, on the other hand, tot CO$_2$ is lowered, the fluid pressure is also lowered and the depth of boiling decreased. Thus, for example, for a solution at 250 °C, pH = 5, salinity 1 mol and tot CO$_2$ of 0.1 mol, the boiling depth is 290 m. The important point to consider here, as a result of these calculations, is that there is a general increase in the rate of Au and Ag deposition towards the top of the boiling interval, and this coincides with a change in Au complexing from chloride to sulphide. The result is the well-known metal zoning of epithermal systems. A summary of the relationships between the various parameters considered and metal zoning is shown in Table 11.4. The relationship between the vertical extent of the mineralisation, initial CO$_2$ concentration and precious metals deposited during boiling, is illustrated in Fig. 11.13. The modelling results of Cole and Drummond show that boiling systems with low CO$_2$ exhibit mineralisation along a narrow vertical interval, but with high Ag and Au grades and small alteration haloes, because of the lower volatile concentrations and therefore

Table 11.4. Dominant metal zoning for boiling hydrothermal solutions in the temperature range of 200–300 °C. BM = base metal sulphides, Ag = argentite; temperatures, pH, total H_2S and total CO_2/total H_2S are at initial conditions before boiling (after Cole and Drummond 1986)

Zoning	Ag/Au	°C	pH	tot H_2S	tot CO_2/tot H_2S
BM/Ag→Au	< 0.1	200–250	5–6	0.1–0.001	< 100
BM→Ag→Au	0.001–10	200–250	5–6	0.1–0.001	< 1000
BM→Au→Ag	1–100	200–250	4–5	0.001–0.00001	> 100
BM→Ag/Au	10–1000	250–300	5–6	0.001–0.00001	> 1000

Fig. 11.13. This diagram shows a plot of ore deposition versus the concentration of CO_2, constructed on the basis of data for five boiling epithermal systems. Theoretical trends of vertical extent of deposition are shown for 3 mol NaCl (*curve 1*) and 1 mol NaCl (*curve 2*), boiling conditions at 250 °C, total H_2S activity = 0.001 m. The diagram, after Cole and Drummond (1986), indicates that lower CO_2 contents result in high grades over short vertical intervals (see text and also Table 11.4)
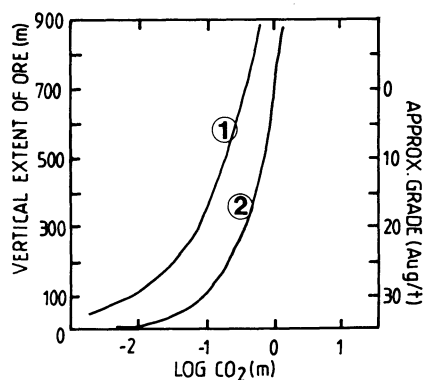
less acid leaching. Thus, the relationships of vertical ore extent, CO_2 and grade show a distinct zoning pattern: a zone of precious metals above a zone of base metal sulphides (see also Table 11.4), which is consistent with observations. Above the zone of precious metal deposition the exsolved gases (CO_2 and H_2S) and H_2O vapour either continue to rise and emerge out of the system as hot springs, fumaroles etc., or they condense and mix with groundwaters. Silica deposited by the boiling solutions occurs above the mineralised intervals to form the surface sinter deposits.

11.5 Active Geothermal Fields

The distribution of present-day active geothermal systems along both convergent and divergent plate boundaries reflect their relationship to magmatism, and ultimately, to heat transfer from the Earth's interior. Reviews of the better known geothermal fields are provided by Weissberg et al. (1979) and White (1981). The latter author lists active geothermal systems as: Hg-depositing, epithermal precious metals and base metal-dominated. The Red Sea brine pools and mid-ocean ridge geothermal systems are included in the base metal-dominated category. To White's list should be added the East African rift geothermal fields with their predominantly alkaline chemistry. The latter are discussed briefly in Chapters 3 and 13. As stated at

the beginning of this chapter here we are concerned with geothermal systems that are associated with convergent plate boundaries, including both terrestrial (or continental) systems and submarine systems related to submerged volcanoes of calc-alkaline arcs. We now examine two important geothermal fields, namely, those associated with the Taupo Volcanic Zone in New Zealand and the Salton Sea in the USA.

11.5.1 Geothermal Systems of the Taupo Volcanic Zone, New Zealand

The Taupo Volcanic Zone (TVZ) is a 25- to 50-km-wide depression which extends for about 300 km north-eastwards across the central part of the North Island (see Fig 7.8). Accounts of the geology, tectonism and volcanic history of the TVZ can be found in Cole (1981, 1984, 1986) and Cole and Lewis (1981). A collection of papers dealing with the TVZ geothermal fields is provided in Henley et al. (1986).

Evidence from gravity surveying indicates that this depression has been down-faulted between 2 and 4 km. The TVZ comprises calc-alkaline volcanics that have been erupted from five major centres such as Rotorua, Okataina, Maroa and Taupo, of predominantly acidic composition, and the Tongariro centre at the southwest end of predominantly andesitic composition (Fig.11.14A). The TVZ continues off-shore in the northeast, with a number of volcanoes such as White Island, Whale island etc. Rhyolites and ignimbrites are predominant in the acid volcanics with minor andesite, dacite and basalts all less than 1 Ma old. Major structures of the TVZ are north-northeast-trending active normal faults, which are probably related to subsidence of the Mesozoic greywacke basement. Other structures include north-west-trending faults probably related to the Hauraki volcanic region to the northwest and ring faults which are related to the multiple calderas of the rhyolitic volcanic centres. The TVZ represents a marginal basin which formed behind a primary magmatic arc of andesitic-dacitic composition related to the subduction of the Pacific plate beneath the Indian plate along the Hikurangi trench off the east coast of the North Island (Cole 1984).

Geothermal Systems

The central part of the TVZ is characterised by an average heat flow several times greater than normal, which is probably caused by hydrothermal convection systems that are manifested at the surface in more than a dozen major fields (Fig. 11.14). In turn, these convection systems are probably the result of thermal energy derived either from the cooling of underlying magmas, or by mantle material intruded below the attenuated crust of the marginal basin. The location of the TVZ geothermal fields is controlled by the intersection of secondary faults with the main north-northeast-trending structures. The geothermal fields on the eastern side are the youngest, while those on the western side are either extinct or nearly extinct. The surface manifestations include hot springs, geysers, mud pools, steaming ground and fumaroles. At Wairakei, 8 km north of Lake Taupo, geothermal steam is utilised to generate electricity which supplies up to 20% of the power requirements

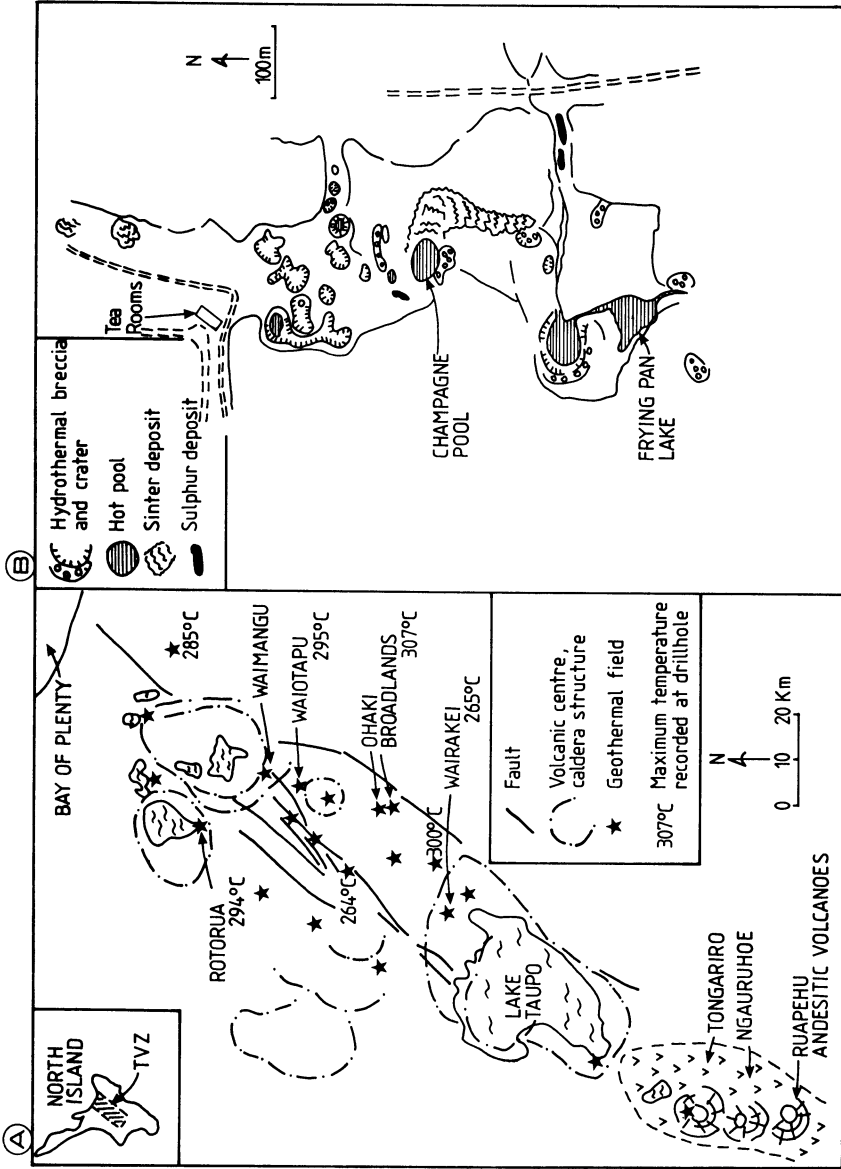**Fig. 11.14.** A Geothermal fields of the Taupo Volcanic Zone, North Island, New Zealand (after Weissberg 1969; Hedenquist and Lindqvist 1985). **B** Part of the Waiotapu thermal area, an active ore-making system (After Hedenquist 1983)

@GEOLOGYBOOKS

of the North Island. Precious metal ore-grade precipitates are actively forming from hot springs, as well as drillhole discharges in a number of these fields such as those of Waimangu, Waiotapu, Ohaki-Broadlands and Rotokawa (Weissberg 1969; Ewers and Keays 1977; Seward 1979b; Weissberg et al. 1979; Hedenquist and Henley 1985). In general, the geothermal waters are neutral to slightly alkaline and have low metal concentrations (see Table 11.1A). Although stable-isotope studies have shown that these geothermal fluids are primarily of meteoric origin, it has been pointed out that a contribution of magmatic fluids, perhaps of up to 10%, would be isotopically undetectable. Such a contribution, if originally at approximately 2 wt.% NaCl, could account for all of the chloride and up to 30% of the heat budget for a system like Wairakei (Henley and Ellis 1983).

A major feature of the Ohaki-Broadlands area is a 60-m diameter thermal pool, filled with water of neutral to mildly alkaline pH at a temperature of about 95°C, and essentially of a dilute NaCl-bicarbonate composition. The pool is lined by a greyish-white sinter material. In 1957 a flocculent red-orange precipitate appeared in these waters and was eventually incorporated into the marginal sinter. This precipitate was found to be composed of an amorphous Sb sulphide with anomalous concentrations of Au, Ag, Tl and As (Weissberg et al. 1979). At Broadlands a greywacke basement is overlain by subhorizontal layers of ignimbrite, pumice breccia, dacite, rhyolite and other pyroclastic deposits (Huka Fall Formation). Thermal activity in the area commenced approximately 0.5 Ma ago, with maximum temperatures in the order of 300°C (Browne and Ellis 1970). Ewers and Keays (1977) found the following metal zoning: (1) higher concentrations of Tl, As, Au and Sb near the surface; and (2) greater abundance at depth of Bi, Se, Te, Ag; with Pb, Cu and Zn increasing towards the higher temperature zones. Sulphides are represented mainly by pyrite and smaller quantities of sphalerite, galena and chalcopyrite. The sulphides occur as veinlets in the more massive and impermeable rocks, and as disseminations in the more porous and permeable lithologies. Ewers and Keays (1977) conclude that As, Sb, Tl and Au may be held within the pyrite lattice, whereas Se, Te, Bi and Ag may be preferentially contained within the base metal sulphides. Extensive zones of propylitisation, silicification and argillic alteration surround fissures and fractures through which the fluids move. Propylitic alteration is characterised by dominant chlorite and calcite, and the argillic zones have interstratified illite-montmorillonite. Vein and vein margin material include quartz, adularia and sericite. Pyrite and sphene are ubiquitous in all alteration types.

Covering an area of roughly 18 km^2, the Waiotapu geothermal field (Fig. 11.14B) is the largest in New Zealand, and its major features include Champagne Pool, sinter deposits and several craters formed by hydrothermal eruptions (Hedenquist 1983). The area is underlain by ignimbrites, air-fall pyroclastics and lake sediments. Dacitic and rhyolitic volcanic structures are also present. Thermal activity comprises discharges of acid-sulphate and chloride-rich (Champagne Pool) waters as well as mixed acid-sulphate-chloride springs (Frying Pan area). Mineralisation is especially prominent at Champagne Pool where an orange precipitate has high concentrations of As, Sb, Au and Ag (Table 11.1A). The Pool fills a hydrothermal eruption crater at least 40 m deep from which, according to Hedenquist, the eruption is believed to have occurred some 900 years ago.

Hydrothermal Eruptions

As mentioned above, the Waiotapu field is characterised by numerous craters and pools which represent vents from which hydrothermal eruptions have occurred in the past. While some of these vents continue to discharge thermal waters (Champagne Pool), others have been flooded by groundwaters (Ngakoro Lake) (Hedenquist and Henley 1985). The vents are surrounded by deposits of eruption breccias which are typified by variable clast abundance, size and angularity as well as a poorly sorted matrix-supported texture and absence of primary volcanic material. These eruptions occur when self-sealing takes place, which allows an increase in fluid pressure. Hedenquist and Henley (1985) propose a mechanism in which it is envisaged that a seal need only develop locally, with the boiling fluids being diverted to surface via open fractures. In this situation gases which collect in the fracture beneath the seal become compressed so that the pressure at the seal increases (see also Sect. 11.2.4). Rupture of the seal occurs either by hydraulic fracturing or by tectonic activity, the compressed gases rapidly expand and an eruption takes place.

11.5.2 Salton Sea, California, USA

The Salton Sea geothermal field occurs near the southeastern edge of the Salton Sea, on the north slope of the Colorado river delta. It is near the axis of a major structural trench that extends northwestward from the Gulf of California. The depression is a rift in the San Andreas fault system in a highly fractured and structurally complex region. The field is one of several within the Imperial Valley (USA) and the Mexicali Valley (Mexico), where the Cerro Prieto geothermal system is situated. Details of the Salton Sea system may be found in McKibben and Elders (1985) and McKibben et al. (1988). The Salton Sea geothermal field is currently being developed as a source of electric power, and it has also been estimated that mineral recovery from a 1000 MW power plant could produce between 14 and 31% of the Mn requirement in the USA.

The lithologies in the Salton Sea area include an alternating sequence of fluvial and lacustrine deltaic deposits of Pliocene-Pleistocene age with a thickness of about 4500 m above the basement. Within the field, a number of Late Quaternary domes of rhyolitic rocks are aligned roughly northeast for a distance of approximately 8 km, nearly perpendicular to the main structural trends. Sills and dykes have been intersected in drillholes. The sedimentary rocks have been progressively metamorphosed to greenschist facies by burial and thermal metamorphism; this thermal activity is probably related to buried intrusive rocks. The chloride- and metal-rich brines, containing up to 26 wt.% of dissolved solids, have temperatures of 300°C at 1000 m and 365°C at depths of 2000–3000 m. Hydrological studies have established that groundwater flow is from the southeast, and that, based on Cl/Br ratios which are three times higher than sea water, all subsurface waters in the Imperial Valley are Colorado River waters (White 1981). It has also been suggested that the Pb of the brines is possibly leached from the Colorado River sediments by interaction with the

thermal brines (McKibben and Elders 1985). Geochemical and isotopic studies have indicated the presence of two distinct geothermal fluids: one is a deep hypersaline metamorphic brine; and the other a low-salinity fluid of shallower origin (McKibben et al. 1988).

Textural features and distribution of Fe sulphides indicate a broad zoning as a function of temperature and depth. Thus, there are three zones of mineralisation in the Salton Sea field. The first occurs at depths of less than 760 m, where the Fe sulphides form fine-grained disseminations in an essentially unaltered host rock; the second zone, which occurs at depths of greater than 760 m, is characterised by extensive alteration of the sediments; the third zone occurs at depths of approximately 1000 m and forms fracture and pore space fillings in sandstone and siltstone. The genetic processes that account for this mineralisation include diagenesis (temperatures of less than 250°C), metamorphism (200–300°C) and hydrothermal activity, which accounts for the fracture fillings with ore minerals such as chalcopyrite, sphalerite, pyrite, pyrrhotite and galena. The host rocks are altered and the alteration assemblages include calcite, quartz, adularia, epidote, anhydrite, chlorite and actinolite. There are two types of vein assemblages (McKibben and Elders 1985). One is sulphide-carbonate-silicate with minerals such as chalcopyrite + sphalerite + calcite + epidote ± adularia ± pyrite ± quartz ± galena. The other is hematite-silicate-sulphide-sulphate and contains principally hematite + epidote ± chalcopyrite ± pyrite ± anhydrite.

A model by McKibben et al. (1988) to explain the mechanisms of brine upwelling and mineral deposition, proposes that an intrusion caused the expulsion of reduced connate fluids in an upper zone of low-salinity fluids, forming the first type of veins discussed above. With the rise of the thermal front, hypersaline brines ascend from depth to interact with moderate- to low-salinity fluids in the upper zones, forming the second type of veins. On cooling of the geothermal system, oxidised surface waters are drawn in and form the late-stage hematite veinlets. The authors further speculate that if the hypersaline brines of the Salton Sea system were to vent in a body of water, the development of a stratiform metalliferous deposit could result.

In 1962, over a 3-month period, fluid discharge from boreholes at temperatures of 130–170°C precipitated several tonnes of sulphide minerals and opaline silica having a bulk composition of up to 20% Cu, 7% Ag, and 7% Fe (Weissberg et al. 1979). An estimate of the size and content of the brine reservoir by White (1981) gives the following: 5×10^6 tonnes (t) of Zn metal, 9×10^5 t of Pb, 1.2×10^5 t of As, 6×10^4 t of Cu, 2×10^4 t of Cd and 1×10^4 t of Ag, contained in a brine volume of about 11.6 km^3 to a depth of 3 km and with a mean reservoir temperature of 300°C.

11.6 Volcanic-Hosted Epithermal Mineral Deposits

There are many important districts of epithermal mineral deposits in the world, some of which have been long known, while others have been discovered only recently, and others still are currently being evaluated at the time of writing, as a result of an unprecedent worldwide exploration effort for precious metals in the

epithermal environment. Some of the more important and better known epithermal districts are those in the North American continent, such as those of the western USA (e.g. Colorado, Nevada, California) (Berger and Bethke 1985; Tooker 1985), the Canadian Cordillera (British Columbia) (Panteleyev 1986), the numerous Ag-rich epithermal deposits of Mexico (see Special Issue of Economic Geology Vol. 83, 1988), and the epithermal districts of the Andean regions, in which those in Chile are of particular importance, where a number of recent and important discoveries have been made (e.g. the El Indio deposit, see Table 11.2B, and Siddeley and Araneda 1986). On the opposite side of the Pacific Ocean, a substantial number of precious metal epithermal deposits are present in the young volcanic terranes from New Zealand (Kear 1989), the Fijian islands, Papua New Guinea, Indonesia, Borneo, Taiwan, Philippines through to the well-known kuroko districts of Japan (Ohmoto and Skinner 1983; Proceedings Pacific Rim '87; Bicentennial Gold '88 Abstracts Volumes; Hedenquist et al. 1990). Epithermal mineralisation has also been located in the older volcanic terranes of Eastern Australia (Queensland) (several papers published in the Proceedings of Gold '86 Symposium and the Bicentennial Gold '88 Abstracts Volumes). Exploration activities are, at the time of writing, also being focused along the Tertiary to Recent volcanic arcs of southern Europe, from Italy through to Turkey, along the complex convergent margin between the African plate and the European microplates.

11.6.1 Hauraki Goldfields, Coromandel Peninsula, New Zealand

A substantial number of epithermal precious and base metal deposits, as well as porphyry deposits are distributed from the Great Barrier island in the north, across the Coromandel peninsula through to its southernmost reaches at Te Puke, for a total distance of approximately 200 km (Fig. 11.15). Relevant details on the geology and mineralisation of the Hauraki, or Coromandel Volcanic Zone and its related mineral deposits can be found in Skinner (1986), Christie and Brathwaite (1986), Brathwaite et al. (1989), Brathwaite and Pirajno (in prep.), and the comprehensive work of Williams (1974). The account that follows is essentially based on the work of the above authors (see also Chap. 7).

Geological Setting

The Hauraki Volcanic Region is one of several magmatic arcs of Tertiary to Quaternary age (ca. 20 Ma ago to present-day) that characterise the northern and central parts of the North Island, and were formed during stages of subduction and collision tectonics between the Pacific plate in the east and the Indian plate in the west (Ballance 1976). The Hauraki Volcanic Region (Coromandel Volcanic Zone) consists of a thick pile of acid-intermediate volcanic and intrusive rocks of calc-alkaline affinity, which were emplaced on a faulted basement of Jurassic greywackes and argillites (Manaia Hill Group).

The volcanic sequence of the Hauraki Region comprises the Coromandel Group of Lower Miocene to Lower Pliocene age including dioritic intrusives, andesitic and
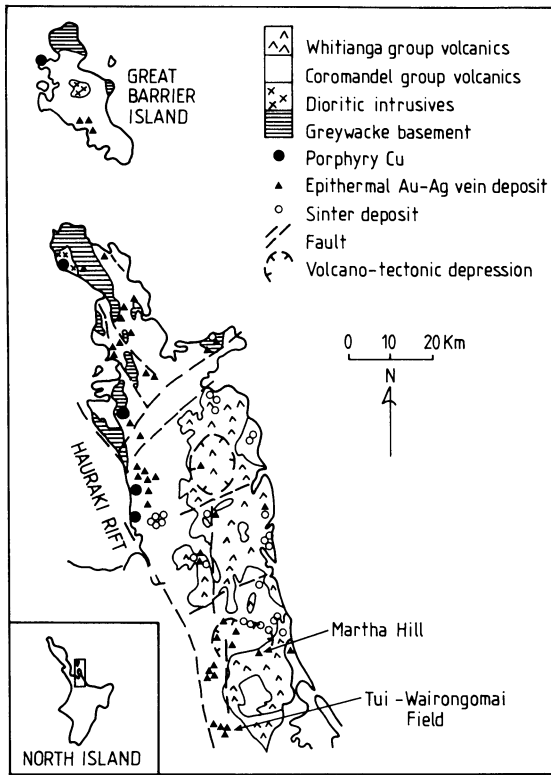
Fig. 11.15. The Hauraki volcanic region, Coromandel Peninsula and Great Barrier Island, and distribution of porphyry systems and epithermal vein deposits. Sinter occurrences are also shown; these are related to the Whitianga volcanism and are not, or at least only weakly mineralised (After Williams 1974; de Ronde 1986; Brathwaite et al.1989)

dacitic volcanics, and porphyry dykes. These are overlain by, but locally overlap in time with, rocks of the Whitianga Group of Upper Miocene to Pliocene age, comprising predominantly ignimbrites, dome-forming rhyolites, and various pyroclastics and sediments. The Coromandel peninsula is bounded on the west by a graben structure (Hauraki Rift) filled with sediments and volcanics of Quaternary age. The regional and dominant trend of the Peninsula is north-northwest, with main fault directions along northeast and northwest trends. Volcano-tectonic depressions have been recognised in the eastern sectors of the peninsula and are infilled with the volcanics of the Whitianga Group. One of these structures is the Waihi depression, a near-circular structure about 8 km in diameter, with which are spatially associated a number of epithermal deposits (Fig. 11.15).

Mineralisation

The mineral deposits of the Hauraki Volcanic Region are genetically related to the subvolcanic and volcanic magmatism. Most epithermal vein deposits are hosted by the earliest andesites (Early-Mid-Miocene), whereas volcanics of Mid to Late Miocene are generally unmineralised. Minor mineralisation is associated with the

rhyolitic rocks of the Whitianga Group. The mineralisation of the Hauraki region comprises porphyry Cu deposits and epithermal Au-Ag and base metal deposits.

The porphyry mineralisation is the oldest (ca. 18–16 Ma) and can be found in the Great Barrier Island, at Paritu almost on the northernmost tip of the Coromandel peninsula, and further south near Thames on the western side of the peninsula (Fig. 11.15). This porphyry mineralisation is associated with quartz-diorite and grano-diorite dykes and stocks which have been exposed owing to uplift and erosion along the western part of the Hauraki region. Cu mineralisation consists of chalcopyrite and pyrite disseminations and veinlets, locally forming stockworks. Molybdenite and wolframite may occur as minor ore constituents. In the Ohio Creek prospect, near Thames, a central zone of quartz-sericite-pyrite alteration contains, in addition to Cu, low Au grades (about 0.3 g/t). At Paritu, 5 km south of Cape Colville, quartz-diorite and granodiorite plutons which have intruded rocks of the basement are accompanied by numerous cogenetic dykes. Hydrothermal alteration is locally pervasive and includes propylitisation, silicification and chloritisation of both intrusive and country rocks. The porphyry system in the Great Barrier island occurs in the north (Miner's Head) where basement rocks consisting of highly contorted greywacke and argillite have been intruded by small stocks and dykes of intermediate to acid composition. The mineralisation, which was known since 1837, and hosted in brecciated greywacke adjacent to a dacitic stock, consists of pockets and veinlets of pyrite and chalcopyrite. During the period between 1857 and 1867 some 50 000 tonnes of ore were worked giving 2300 tonnes of hand-picked ore assaying 15% Cu. Modern-day exploration however, failed to locate economically viable mineralisation.

The epithermal deposits of the Hauraki goldfields are of the quartz vein type, the majority of which are hosted in andesite and pyroclastics and to a lesser extent in rhyolitic rocks. The veins are widest in massive andesites, whereas in rhyolitic rocks thin quartz veinlets and silicified breccia zones are more common. They are structurally controlled along fracture and fault systems with dominant northeast-erly and northerly trends. The longest vein has a strike of approximately 4.5 km, while the widest is the Martha lode attaining a thickness of 30 m in places. The more common dimensions, however, are in the order of a few hundred metres of strike length and from a few centimetres to about 5 m wide. Although some deposits form isolated quartz veins, most form systems of subparallel veins. An excellent account, both historical and geological, of individual deposits may be found in Williams (1974), while the results of more recent work have been published in the volumes edited by Henley et al. (1986) and Kear (1989).

The quartz veins of the Hauraki epithermal systems are open-space fissure fillings often displaying crustiform banding. Vein minerals apart from quartz include calcite, quartz pseudomorphs after calcite, manganiferous carbonates, adularia, siderite, barite and anhydrite. Pyrite is a common sulphide mineral; electrum and native Au constitute the chief economic ore minerals. Acanthite, pyrargyrite, Au and Ag selenides and tellurides are locally present. In the deeper levels, and consistent with the general character and zoning of epithermal mineralisation, the veins may contain significant quantities of base metal sulphides such as sphalerite, chalcopyrite and galena, as well as pyrite. Other ore minerals

include arsenopyrite, Sb, Bi, Se, Te sulphides and sulphosalts. The vein mineralisation is accompanied by non-pervasive to pervasive hydrothermal alteration of the wall rocks. Extensive zones of propylitic and clay alteration commonly surround the veins. Propylitic assemblages include chlorite and calcite, whereas argillic assemblages are characterised by interstratified illite-montmorillonite, illite and chlorite. Quartz, adularia and sericite can be found in the altered country rocks adjacent to the veins. Pyrite and sphene are ubiquitous minerals. Rabone (1975) mapped in detail zones of progressive alteration in andesitic rocks in the Waitekauri area. Relating these zones to north-northeast-trending faults, he recognised four main zones of progressive alteration based on mineralogical changes which are easily discernable under the microscope. Rabone's results, being of general application, are summarised here.

In Zone 1, unaltered to weakly altered andesite is composed of hypersthene, augite and plagioclase phenocrysts in a groundmass of andesine microlites, pyroxene and intergranular felsitic material. At this stage the hypersthene is partially or totally altered to chlorite. In Zone 2 the andesitic rock is weakly to moderately altered. Chlorite develops from both hypersthene and augite, with total to partial replacement of these mineral phases. In a more advanced stage carbonate replacement of chlorite begins to take place. Plagioclase shows incipient alteration along cleavage planes to chlorite and clay minerals. The chloritisation process releases silica which is deposited in the groundmass. Moderate to strong alteration occurs in Zone 3, where augite is totally replaced by clay minerals, sericite, epidote and carbonate. Locally, microfractures are filled with albite. Hydrothermal biotite appears here, while in the more advanced stages chalcedonic quartz starts to replace the carbonate. In dacitic rocks hornblende is at first replaced by carbonate and later by quartz and hematite. Intense alteration characterises Zone 4 in which the original textures are almost completely obliterated. Quartz, clay minerals and pyrite are the dominant minerals in andesite, while in dacite the earlier hydrothermal minerals are replaced by quartz and hematite, and plagioclase by adularia. The intensity and frequency of the carbonate minerals is taken to be an indication that the altering solutions are CO_2-rich. These alteration zones usually follow the trend of the veins, the alteration being pervasive and strong where a vein system occurs.

In summary, therefore, hydrothermal alteration of the Hauraki epithermal systems is characterised by outer zones of weak to advanced propylitic alteration in which chlorite, calcite, quartz, pyrite and illite are dominant. Accessory minerals include adularia, albite and epidote. Pervasive silicification with quartz, adularia, sericite, pyrite and sphene surrounds the quartz veins. Argillic alteration, which usually occurs above the propylitic areas, consists of illite-smectite, interlayered illite-smectite, kaolinite, quartz, chlorite and pyrite. Advanced argillic alteration has been found in only a small number of localities, such as at Thames, and is represented by alunite, kaolinite, pyrophyllite, diaspore and dickite mineral assemblages.

Fluid inclusions and stable isotope systematics suggest that the epithermal systems of the Hauraki goldfields were generated by deep circulating hydrothermal fluids of low salinity (ca. 4 wt.% NaCl equivalent), with temperatures in the order of 200–300°C. Oxygen isotope ratios of fluid inclusions indicate that this hydrother-

mal fluid was probably meteoric water similar to that circulating in the geothermal fields of the Taupo Volcanic Zone. A magmatic input for the Hauraki hydrothermal fluids has been inferred from the C isotopic ratios of calcites as well as the presence of CO_2 in the fluid inclusions. Thus, the overall model for the Hauraki mineralisation is that of meteoric convective cells with a minor magmatic component, driven by the thermal energy provided by subjacent subvolcanic intrusions of acid to intermediate composition. In the sections that follow we discuss examples of hot spring (sinter)-associated mineralisation, of precious metals vein-type and of base metals vein-type mineralisation.

Sinter-Associated Hg and Au-Ag Mineralisation

There are numerous sinter deposits in the Hauraki goldfields, many of which are found associated with the rhyolitic volcanism of the Whitianga Group, and are therefore largely confined to the eastern side of the Coromandel Peninsula (Fig. 11.15). Williams (1974) reported that some of these sinters are weakly auriferous, and indeed mineral exploration work led by the present author in the 1970s near Whangamata and further north in the Kaoutunu peninsula, has confirmed this. In the latter area, sinter deposits cap zones of quartz veins and associated stockworks emplaced in basement greywacke and andesites of the Coromandel Group. The sinter material is a massive cryptocrystalline chalcedony of white, reddish or black colour, which forms lens-shaped deposits, in places containing carbonaceous material, plant relics and moulds. Samples of this sinter material assayed between 0.1 and 0.5 g/t Au, 0.1 and 14 g/t Ag. The sinter deposits grade downward into silicified brecciated zones and stockwork veining in the country rocks. Williams (1974) drew attention to Au-bearing, strongly silicified and sinterous rhyolitic rocks in the Neavesville area. At this locality rhyolitic lithic tuff overlying black shales shows intense silica flooding as well as quartz-adularia-sericite alteration and stockwork veining in a zone (about 50 m thick) known as The Bluffs (Barker 1989). Visible mineralisation consists of pyrite disseminations, veinlets and framboidallike grains. Au is present as a few tenths of a gram per tonne up to about 4 g/t. Recent exploration has failed to indicate economic mineralisation, although Barker (1989) reports ongoing work in this area.

About 8 km north of the town of Thames, on the western side of the Coromandel peninsula, cinnabar and associated minor sulphides are present in sinter material in andesitic pyroclastics and lacustrine sediments (Watson 1989). Values of up to 26% Hg have been recorded. In addition to cinnabar, other sulphides include pyrite, marcasite, arsenopyrite and stibnite.

The Martha Hill Au-Ag Vein Deposit

The Martha Hill deposit is situated at Waihi, in the southern sectors of the Coromandel peninsula (Fig. 11.15). The Martha Hill mine was closed in 1952 after approximately 11×10^6 of ore had been extracted since 1889. A total of 2.4×10^8 g of Au and 8.1×10^8 g of Ag was recovered during this time. The recognition of mineralised ground (quartz vein stockworks) between the nearly mined out lodes

CLAY AND ASH BEDS

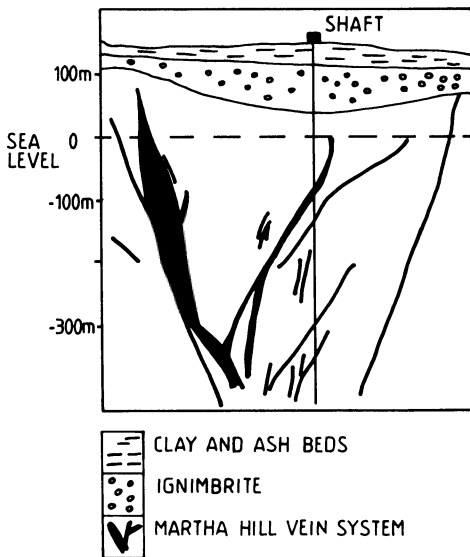IGNIMBRITE

MARTHA HILL VEIN SYSTEM

Fig. 11.16. The Martha Hill epithermal vein system; see text for details (After Williams 1974)

led to a re-appraisal of the mine from 1973 onward. In the 1980s a series of angled holes were drilled totalling approximately 13 400 m. At the time of writing, the mine is being developed and production due to commence shortly. Ore reserves amount to approximately 10×10^6 tonnes at 2.6 g/t Au (Brathwaite et al. 1986).

The geology and mineralisation of the Martha Hill deposit have been studied by Brathwaite et al. (1986), and Brathwaite and McKay (1989), from whom this discussion is derived. The deposit is located on the rim of a circular structure that may represent a buried caldera. The mine area is underlain by andesitic, dacitic and rhyolitic lavas and pyroclastics of the Coromandel group which host the vein system. These lithologies are overlain by a blanket of pumice breccia, ignimbrite and ash material belonging to the Whitianga Group. The quartz vein system, which has a general northeasterly trend, consists of a number of subparallel quartz veins which locally develop into an anastomosing pattern (Fig. 11.16). Stockworks and smaller veins occur between the major lodes. The largest lode is the Martha Lode, roughly 1600 m long and up to 30 m wide. The veins are sulphide-bearing, consisting mainly of milky quartz, banded chalcedonic quartz and calcite. Sulphide minerals include pyrite, sphalerite, galena, chalcopyrite and acanthite. Electrum is the Au-bearing mineral with an average Ag content of about 38%. Two types of sulphide-bearing quartz veins have been reognised: (1) a sulphide-poor Au- and Ag-bearing grey quartz; and (2) a banded crustiform quartz with sphalerite + pyrite + chalcopyrite + galena + acanthite + electrum.

Hydrothermal alteration is characterised by a quartz-adularia-illite type which surrounds the quartz veins and passes into an outer zone of propylitic alteration consisting mainly of chlorite and calcite. As mentioned previously (Rabone 1975), this alteration is ranked into three classes of weak, moderate and strong, and the intensity of the alteration is greatest in the vicinity of the veins. Strong alteration of andesite is typified by silicification and by quartz + illite + adularia + sphene +
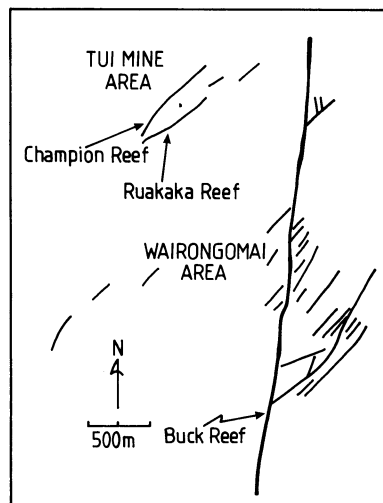
Fig. 11.17. The Tui-Wairongomai vein system; see text for details (After Williams 1974)

pyrite assemblages. Brathwaite et al. (1986) and Brathwaite and McKay (1989) conclude that the Martha Hill deposit was formed by low salinity (0.2 to ca. 4 wt.% NaCl equivalent) CO_2-bearing fluids with temperatures of about 220–270 °C. They further note that the formation of the Martha Hill vein system was controlled by tectonism with repeated fracturing and dilation, and by a sustained geothermal system with high water/rock ratios and repeated sealing and fracturing. Although there is no direct evidence of a heat source in the form of a subjacent intrusion, a genetic relationship with rhyolitic volcanism is inferred on the basis of similarities of hydrothermal minerals with a nearby rhyolite-associated Au deposit.

Tui-Wairongomai Au-Ag and Base Metal Deposits

The Tui-Wairongomai Au-Ag and base metal field is situated near the township of Te Aroha in the south of the Coromandel peninsula (Fig. 11.15). The Tui mine was the only sizeable base metal mine ever to operate in New Zealand. Mineralisation of this area has been studied and reported on by a number of geoscientists including Wodzicki and Weissberg (1970), Robinson (1974), Williams (1974) and more recently Bates (1989).

The Tui-Wairongomai area is underlain by propylitised andesite, dacite and pyroclastic rocks of the Coromandel Group. The quartz vein system is controlled by a conjugate stress pattern, in which two sets of fractures intersect one another at angles of between 20° and 50° (Fig. 11.17). One set strikes a few degrees east of north and is nearly vertical, while the other has a northeast trend with steep dips to the northwest and southeast. The largest vein (Buck Reef), along the northerly trend, is approximately 4.5 km long with widths of between 1 and 30 m. The thickest sections, which were named "quartz blows" by the old prospectors, tend to occur at the intersection of the Reef with the northeast-trending veins. The vein material is massive white to grey quartz and contains, locally, little free Au and pyrite. The

northeast-trending vein system forms two groupings of veins. One is to the northwest of the Buck Reef where the Tui Mine (Champion and Ruakaka lodes) is located; the other (the Wairongomai veins) is mostly on the east side of the Reef. These veins have strike lengths of 150 to 200 m, and thicknesses of 0.1 to 10 m. The vein material is massive quartz with minor calcite, locally brecciated and including fragments of andesite. Each main vein is accompanied by smaller veins and veinlets of just a few centimetres thick. The northeast-trending vein system at both Tui and Wairongomai is characterised by base metal mineralisation accompanied by varying amounts of Au and Ag. In all cases the mineralisation consists of bands and lenses of galena, sphalerite, chalcopyrite and pyrite, usually concentrated near the footwall areas.

The Tui Mine was established on two main veins, namely, the Champion Reef and the Ruakaka Reef, both hosted by a sequence of massive andesite quartz-andesite, ignimbrite and tuffs. The Champion Reef is about 1 km long and from 0.1 to 6–7 m wide in its central tracts. The Ruakaka Reef, also about 1 km long and up to 8 m wide, differs from the former in that it is highly brecciated and includes fragments of volcanics. Minor quartz veins and veinlets lace the country rocks between the two reefs.

The reefs intersect in the upper levels of the mine, converge to the southwest and then diverge with depth to the northeast. The nature of the vein material indicates a complex history of movements, brecciation and mineralisation. Vein mineralogy of both reefs consists of sphalerite, galena, pyrite, chalcopyrite, marcasite, barite, hematite and kaolinite, in addition to quartz. Minor amounts of tetrahedrite and cinnabar may also be present. The mineralisation consists of coarse-grained sulphides, mainly sphalerite-galena-chalcopyrite-pyrite, which form lenticular masses, seams or stringers, generally located at or near the hangingwall side of the veins. The mineralised zones are discontinuous and irregular in both strike and thickness. A good-sized ore lens may reach a maximum length of 30 m and width of 10–15 m. Mineral zoning is present both across and along the strike. It is not clear, however, whether or not vertical zoning is present because of the masking effect of supergene minerals such as covellite, chalcocite, cuprite, anglesite, malachite and azurite. In the Ruakaka Reef an outer shell of pyrite + chalcopyrite envelopes a zone of quartz, followed by a zone of galena + sphalerite and an innermost zone of chalcopyrite and kaolinite (Robinson 1974). Textural relationships of ore and gangue minerals suggest that following faulting and brecciation, quartz + pyrite + chalcopyrite were deposited first. Renewed fault movement and brecciation were again followed by mineral deposition, this time of galena + sphalerite, a second generation of pyrite + chalcopyrite, then pyrite + chalcopyrite + tetrahedrite. Lastly, hematite + barite + kaolinite were deposited in the remaining available spaces (Wodzicki and Weissberg 1970). Potential ore reserves estimated by the present author during his work in the area (Pirajno unpubl. data) are approximately 0.36×10^6 tonnes, at less than 10% combined metals (Cu, Pb and Zn). Taking into account the mined-out ore, the total tonnage was probably, in the order of 0.5×10^6 tonnes. Assays of composite vein material are given in Table 11.5. Bates (1989) estimates that at the time of its closure the mine contained approximately 0.14×10^6 tonnes grading 4% Pb, 5.5%

Table 11.5. Assay values of mineralised zones at Tui-Wairongomai field, Coromandel, New Zealand. Pirajno (unpubl. data). All values in parts per million (ppm), unless otherwise stated; – not detected

Location:	Galena Lode	Hopper Reef	Champion Lode (5-level)	Champion Lode (5-level)	Ruakaka Reef (5-level)
Sample:	Sulphide band	Sulphide band	Sulphide band	Quartz gangue	Sulphide band
Cu%	0.98	0.20	0.48	0.04	1.15
Zn%	13.8	24.0	2.4	0.40	35.0
Pb%	11.1	22.0	1.35	0.50	0.07
Hg	4.1	1.0	5.4	1.7	21
Ag	56.7	79.4	8.5	99.2	8.8
Au	1.98	0.28	0.6	22.4	–
Cd	800	1500	190	22	2200

Zn and 0.5% Cu. Au and Ag were obtained mostly from the Pb concentrates in which grades were 312 g/t Ag and 6 g/t Au.

Hydrothermal alteration is strongest in proximity of the veins. Wodzicki and Weissberg (1970) described four zones which are similar to those outlined in the section on epithermal Au-Ag deposits above. Broadly speaking, in Zone 1, andesitic rocks are little altered with pyroxene changing to chlorite, magnetite and pyrite. Zone 2 is characterised by adularia replacement of plagioclase. Sericite replacing K-feldspar with minor amounts of calcite, epidote, pyrite and quartz are the main features of Zone 3. In Zone 4, adjacent to the quartz veins, rocks are bleached to almost white, and the mineral assemblage is quartz + sericite + chlorite + calcite + pyrite.

Sulphur isotope studies (Wodzicki and Weissberg 1970, Robinson 1974) suggest that the S (δ^{34}S per mill values from 0.0 to 3.3) is in part magmatic and in part originating from the Jurassic basement rocks. Calibration curves for the temperature dependence of S-isotope fractionation between sulphides were used by Robinson (1974) to determine the temperature of formation of mineral pairs from Tui. The results of this study indicate temperatures of 400 ± 80°C for the pyrite-chalcopyrite pair, 360 ± 60°C for pyrite-galena, 320 ± 60°C for sphalerite-galena, and 280 ± 30°C for chalcopyrite-galena. The origin of the Tui-Wairongomai mineralisation is thought to be related to the activity of rhyolitic and dacitic magmas. These provided the heat source to a fairly large system of convecting meteoric waters, which leached metals from the Jurassic basement rocks. The mineralising fluids were channelled in structurally favourable sites and deposited ore minerals by open space-filling.

11.6.2 Epithermal Au in Lihir Island, Papua New Guinea

Lihir Island is one of the volcanic islands of the New Ireland province, where a number of shoshonitic alkaline volcanoes were formed during the Miocene to

Recent, as a result of a southwest subducting oceanic plate (Kilinaialu trench). Lihir is part of the Tabar to Feni group of Pliocene-PLeistocene volcanic islands which lies some 50 km northeast of New Ireland. A large Au deposit was first discovered in 1982 on coastal bluffs along the eastern side of the island. A detailed drilling programme was implemented soon after, and subsequently, an open-cutable Au deposit – known as Ladolam – was outlined, with total reserves of oxide and sulphide ore of approximately 173×10^6 tonnes grading between 2 and 3.5 g/t Au. Most of the Au occurs as refractory ore to a depth of 200 m. The Ladolam deposit is hosted by hydrothermal breccias formed in the roof zone of a monzonite stock emplaced about 0.35 Ma ago (Davies and Ballantyne 1987). Apart from press and stock exchange releases at the time of writing, only few publications have appeared on Lihir. The following account is based on Davies and Ballantyne (1987), Plimer et al. (1988) and Moyle et al. (1990).

On Lihir island at least three volcanic centres are recognised – Kinami, Huniho and Luise – all of which were built on older volcanic rocks. The Luise volcano hosts the Ladolam deposit and is characterised by an elliptical caldera measuring approximately 6×4 km and is open to the sea, forming the Luise Harbour. Lithologies at the surface include latite, andesite and trachyte lava flows, tuffs and breccias. Subsurface rocks intersected by drilling are a biotite-pyroxene monzonite porphyry stock, and smaller bodies – possibly apophysis – of plagioclase-hornblende porphyry and syenite-trachyte porphyry. The Ladolam deposit consists of four main orebodies, namely: Lienetz, Minifie, Coastal and Kapit. Moyle et al. (1990) recognise two main phases of hydrothermal alteration. One is related to an earlier subvolcanic porphyry system, which, based on a reconstruction of the volcanic edifice, must have originally lied at approximately 1000 m below the summit crater. This porphyry style alteration is characterised by potassic (K-feldspar ± biotite) and propylitic (chlorite ± albite ± epidote ± calcite ± magnetite ± amphibole) assemblages. This alteration style now occurs at a depth of about 100 m below the surface. The second phase of hydrothermal alteration-mineralisation is epithermal, lies above the former, overprints the porphyry system in the upper zones of the deposit and contains the Au mineralisation. The epithermal alteration consists of three types: advanced argillic, argillic and phyllic. Advanced argillic alteration is characterised at the surface by a leached, white, porous material formed by skeletal silica + kaolinite + alunite, locally known as white rock. This grades at depth into a pyrite-alunite-silica rock. Argillic alteration generally forms a zone below and around the advanced argillic zone. At the surface this alteration is characterised by orange-brown limonitic or grey-white pyritic clays. The argillic alteration assemblage consists of kaolinite ± smectite ± illite. The zone of phyllic alteration is developed mainly at depth and is represented by the assemblage illite ± K-feldspar ± silica. It is of interest to note that the floor of the Luise caldera is characterised by a magnetic low and this is attributed to destruction of magnetite by hydrothermal alteration (Moyle et al. 1990)

The ore mineralogy of the Ladolam deposit is dominated by pyrite and marcasite, occurring as disseminations and veinlets. Other, but minor, ore minerals include magnetite, rutile, chalcopyrite, pyrrhotite, galena, sphalerite, covellite and arsenopyrite. A little molybdenite is present in the zone of potassic alteration.

Sulphosalts are also present and are represented by tetrahedrite, tennantite, luzonite, and enargite. Au occurs included as particles within the pyrite, chalcopyrite and arsenopyrite. Free Au is present in the oxide ore.

Hydrothermal breccias of various types are common and crackle breccias, fluidised and explosion breccias have been distinguished in addition to the important breccia horizon known as the "boiling zone", which is also the host to the mineralisation. Breccias are common in the potassic zone and are cemented by anhydrite + carbonate + quartz veins. According to Davies and Ballantyne (1987), this constitutes an anhydrite-sealed zone. The boundary between the argillic and potassic zone constitutes the Boiling Zone referred to earlier. The boiling zone is in turn characterised by a distinctive clast-supported breccia consisting of angular fragments in between which anhydrite, quartz, calcite, adularia and sulphides occur.

Nature of the fluids and ore genesis

Plimer et al. (1988) propose that the plutonic core of the Luise caldera was highly charged with volatiles (mainly H_2O, CO_2, H_2S), resulting in a large explosion. They also speculate that sea water, which could have entered the magma chamber, may have added to the already high volatile content and perhaps even promoted the explosive activity. Light stable-isotope systematics obtained from quartz, carbonate, kaolinite and sulphates suggest that the hydrothermal fluids were of meteoric origin, while S isotopic data would indicate that the source of S was probably both magmatic and sea water. Extensive boiling of near-neutral, chloride-rich brines resulted in extensive loss of H_2S to the vapour phase producing acid-sulphate steam-heated fluids, consequent argillic alteration and the destabilisation of sulphide Au complexes possibly in the manner outlined in Section 11.3. Plimer et al. (1988) suggest that in addition to boiling, mixing of fluids was also responsible for the precipitation of Au and this metal was possibly leached from the S-rich alkaline basaltic rocks by the chloride-rich geothermal fluids.

Moyle et al. (1990) regard the Ladolam mineralisation as a volcanic-hosted epithermal deposit sharing the characteristics of both acid sulphate and adularia-sericite type (Heald et al. 1987). They believe that the Au mineralisation was formed by the circulation of large volumes of S-rich neutral chloride fluids, which on boiling exsolved H_2S and deposited Au. The evolution of the system is summarised into three stages. In the first stage the Luise stratovolcano was intruded by alkaline stocks whic caused the formation of porphyry-type hydrothermal alteration with weak Cu-Mo ± Au mineralisation. Stage two was characterised by the formation of the caldera structure (possibly due to an explosive event) and the anhydrite-calcite breccia. The sudden release of pressure caused by the caldera-forming event caused boiling of the fluids and precipitation of Au. Breaching of the caldera by sea water resulted in the cementing of the brecciated rocks by anhydrite and calcite. The main geothermal system was developed during stage three as a result of sealing of the breccia from the sea, so that recharge of the system was mainly by meteoric waters. The geothermal system thus formed resulted in the dissolution of the anhydrite-calcite stockwork, increasing permeability and continued hot spring activity with boiling and Au precipitation. The final present-day scenario is that of a roughly

layered system constituted – from top to bottom – by zones of advanced argillic, argillic, phyllic alteration overlying a zone of anhydrite-calcite stockwork above a porhyry-style zone of potassic alteration. The entire epithermal system to the top of the porphyry zone is approximately 200 m thick.

Fluid inclusions studies carried out on anhydrite, calcite and quartz indicate temperatures ranging from 120 to 340°C, with two ill-defined groupings at 140–150° C and 200–220°C, and salinities of 3.8 wt.% NaCl equivalent. Fluid inclusions were found to contain CO_2, H_2S and CH_4. Analyses of fluid samples revealed a Au content less than 1.5 ppb, while scales from pipes assayed up to 2.8 ppm Au.

Active thermal acid-sulphate springs present in the Luise caldera, have a pH of 1–2 and contain CO_2, N_2, O_2, H_2S and H_2. Sinter deposits are formed from these springs and consist of opaline silica-kaolinite-alunite-native S-marcasite. Sinter material precipitated from near-neutral chloride springs consists of pyrite-opaline silica.

11.7 Sediment-Hosted Epithermal Deposits

Sediment-hosted, disseminated precious metal deposits are hydrothermal replacement bodies related to fossil geothermal systems. Au and Ag deposits of this type occur in the western USA, the largest concentration being in the states of Nevada and Utah (Fig. 11.18). The geological area hosting these deposits is the Basin and Range province, situated between the Colorado plateau in the east and the Sierra Nevada in the west. The Basin and Range province is generally referred to as a back-arc basin formed by extensional tectonics which followed the cessation of subduction and arc volcanism. Evidence of Late Cenozoic extension is provided by the presence of bimodal (basalt-rhyolite) volcanism and the development of normal faults. Precious metal mineralisation appears to be related to hydrothermal processes associated with this tectono-thermal event. Hot springs and geothermal systems associated with the Tertiary volcanism are still active today. The sediment-hosted epithermal Au and Ag deposits are Tertiary in age, shallow-seated, and spatially related to normal faults, which are generally occupied by pre-ore dykes (Radtke et al. 1980). Important structural controls are intersections between high-angle normal faults and minor fractures with brecciated, permeable, thin-bedded carbonate units. The orebodies are tabular, stratiform and irregularly shaped masses, passing upward into zones of argillic alteration (acid leaching) and supergene oxidation. They extend to unknown depths below the zone of oxidation. The geometry of the mineralised zones is a function of the permeability and the nature of the bedding of the host lithologies, but in all cases it is assumed that the mineralised zones have structurally controlled feeders. Madrid and Bagby (1988) distinguish three main types of geometry based on examples from: Carlin (lateral replacement emanating from a main feeder), Pinson (peripheral fractures) and Preble (upward and lateral replacement).

Dykes and sills of fine-grained quartzo-feldspathic igneous rock are commonly present and clearly pre-date the mineralising events. Their occurrence indicates the
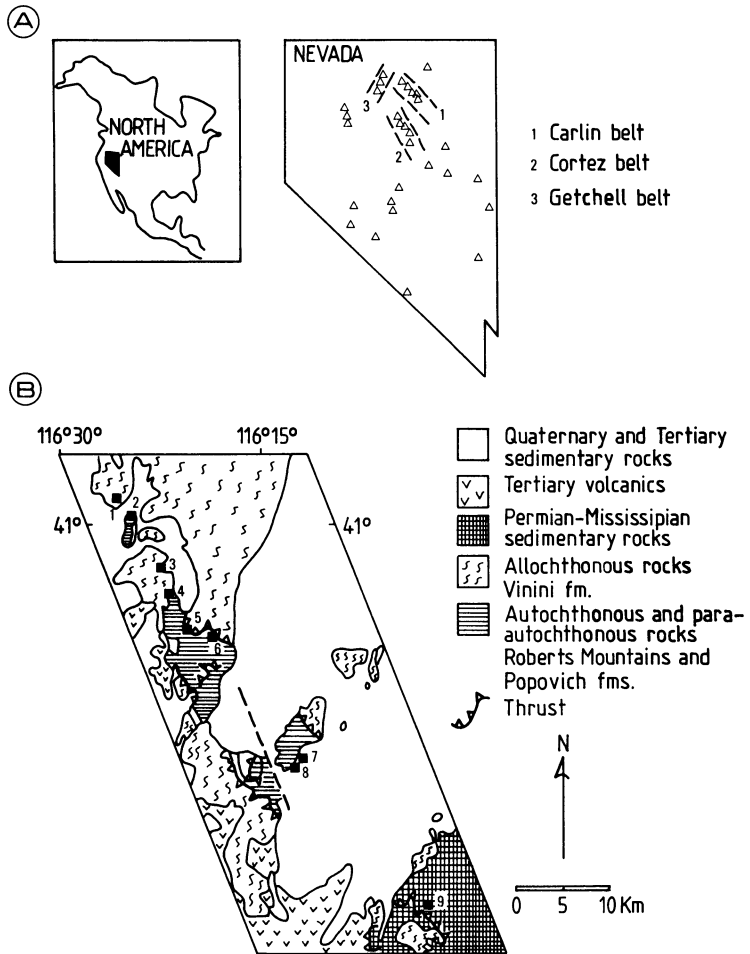
Fig. 11.18. A Locality map showing distribution of sediment-hosted disseminated precious metal deposits in Nevada, western USA (after Bagby and Berger 1985). **B** Simplified regional geological map of the Carlin Belt and distribution of the main sediment-hosted disseminated precious metal deposits: *1* Dee; *2* Bootstrap; *3* Goldstrike; *4* Blue Star; *5* Bullion Monarch; *6* Carlin; *7* Gold Quarry; *8* Maggie Creek; *9* Rain (After Bagby and Berger 1985)

probable presence of subjacent granitic rocks, which may have been the heat source for the hydrothermal convection systems responsible for this mineralisation. As discussed later in this section, there may be a genetic relationship between subjacent igneous rocks and the Au mineralisation. The mineralisation is hosted by dark to grey, thin-bedded, siliceous, argillaceous, dolomitic limestones (Radtke et al. 1972). The carbonate rocks also have varying amounts of organic carbon (Radtke and Dickson 1974). The primary ore usually consists of a fine-grained carbonaceous carbonate rock, impregnated with fine-grained silica and containing sparse pyrite disseminations (Radtke and Dickson 1974). In hand specimen it is often difficult to

distinguish between the ore and the unmineralised rock. Pyrite occurs as micro-scopic grains less than 0.005 mm in diameter and as much as 90 % of the Au occurs as sub-rounded grains no larger than 0.001 mm. In these sediment-hosted deposits the distinctive metal association (Au, As, Sb, Hg, Tl) is similar to that of the geothermal metal precipitates previously discussed. Hydrothermal alteration is prominent in these deposits, the main types being argillic alteration near the surface, silicification and dolomitisation. Silicification is particularly well developed along fault zones in the vicinity of the mineralisation. Tonnages and grades of the sediment-hosted precious metal mineral deposits are highly variable, ranging from less than 1×10^6 tonnes up to 160×10^6 tonnes, with Au tenors from a fraction of g/t up to 10 g/t (Bagby and Berger 1985).

Fluid inclusion studies indicate that the temperature and pressure during ore deposition ranged from surface hot spring conditions (100 °C) to about 225 °C and 30 bar. At Carlin, temperatures and salinities of the fluids were approximately 175 to 200 °C and from 3 to 15 wt. % NaCl equivalent (Radtke et al. 1980).

11.7.1 Mineral Belts and Deposit Types of Nevada, USA

The location of known major sediment-hosted, disseminated precious metal deposits is shown in Fig. 11.18. The geological characteristics, orebody data, alteration and structural details can be found in Bagby and Berger (1985). Other important contributions are those of Radtke and Scheiner (1970), Radtke et al. (1972, 1974, 1980), Radtke and Dickson (1974), Rye et al. (1974), Berger (1980) and Rye (1985).

Most of these deposits occur along major mineral belts, namely: the Carlin, Cortez and Getchell belts (Fig. 11.18A). An important aspect of the regional geological setting of these deposits is their spatial relationship to the Precambrian basement, accreted allochthonous terranes and major thrust faults (Bagby and Berger 1985). Although the majority of the deposits occurs within the area of accreted allochthonous terranes, they are not necessarily underlain by the allochth-onous rocks. The Carlin Belt includes the Rain, Gold Quarry, Maggie Creek, Carlin, Bullion Monarch, Blue Star, Gold Strike, Bootstrap and Dee deposits (Fig. 11.18B). The belt, with a northwest trend, cuts across the north-trending regional fabric defined by the east-directed Roberts Mountain allochthonous terrane, which in turn overlies the Precambrian basement. This terrane is composed of interbedded cherts, shales and siltstones with minor volcanics and carbonates. Windows of autochthon-ous rocks form the eastern assemblage rocks of Lower Paleozoic age, which include predominantly carbonate rocks with minor shales and siltstones. Rocks of both assemblages are hosts for the mineralisation, but it is the autochthonous carbonate assemblage rocks that are the most important. The Carlin Belt is not only identified by the alignment of tectonic windows in the Roberts Mountain Allochthon and the ore deposits, but also by igneous stocks and dykes of Cretaceous to Tertiary age (Radtke et al. 1980; Bagby and Berger 1985). In addition, the belt is defined by a series of broad, magnetic anomalies which suggests the presence of subjacent intrusions (Roberts et al. 1971). Hydrothermally altered and mineralised granitic

stocks occur in the Carlin-Dee sector of the belt, indicating both that the mineralisation post-dates pluton emplacement and that the hydrothermal fluids used the same regional structures that served as controls for the emplacement of the Mesozoic igneous rocks. The Cortez Belt is defined by the alignment of the Gold Acres, Cortez, Horse Canyon and Tonkin Springs deposits in north-central Nevada. The lithologies of this belt include: laminated silty carbonaceous limestone of the Roberts Mountain Formation of Silurian-Devonian age (autochthonous), silty carbonaceous limestones of the Wenban Limestone Formation of Devonian age (autochthonous), siltstones and cherts of the Ordovician Vinini Formation (allochthonous), and altered mineralised igneous rocks of Tertiary and Mesozoic age. At Cortez the disseminated mineralisation is possibly genetically related to a 34-Ma-old, altered and mineralised, biotite-quartz-sanidine porphyry. Similarly, altered and mineralised dykes of Oligocene age occur at the Gold Acres and Horse Canyon, suggesting that the mineralisation event took place at least either during, or soon after, the Oligocene.

Other types of mineralisation in the Cortez area include Ag in manto replacement and fissure veins in the Cambrian Hamburg dolomites, Ag-Pb-Zn-Cu-Au veins in the Wenban Formation and a Jurassic quartz-monzonite (Wells et al. 1969). The Buckhorn epithermal vein Au deposit occurs along a fault zone within Pliocene andesitic-basalt lavas, east of the Gold Acres deposit; bedded barite mineralisation is present within the Ordovician sedimentary rocks. The Getchell Belt is defined by the northeast alignment of the Preble, Pinson and Getchell deposits. The belt is localised along the fault-bounded eastern margin of the Basin and Range-type Osgood Range Mountains. Several rock formations occur in this belt and are the hosts for Au as well as W and Ba mineralisation. Major hosts for the disseminated Au mineralisation are: variably calcareous and siliceous shales and thin-bedded limestones of the Cambrian Preble Formation (autochthonous), thin-bedded limestone and siltstone of the Ordovician Comus Formation (autochthonous), and the Cretaceous Osgood Mountain granodiorite which intrudes the above formations with development of W-bearing skarns. Granodiorite and dacitic dykes associated with the Osgood pluton are altered and mineralised in the vicinity of the sediment-hosted precious metal deposits.

Classification of the Sediment-Hosted Disseminated Au-Ag Deposits

Since its discovery in the early 1960s, the Carlin deposit has lent its name to a style of fine-grained disseminated mineralisation hosted by carbonate rocks. The discovery and development of more deposits in the 1970s made it apparent that the "Carlin-type" was probably an end member of a group of deposits that displays considerable variations in their geological, mineralogical and geochemical characteristics, although there are many similarities that allow the broad definition encoded in the heading above. Thus, Bagby and Berger (1985) have defined two deposit-type subsets, namely: (1) Jasperoidal-type; and (2) Carlin-type. For each of these types there are Au- and Ag-rich end-members. The jasperoidal subset includes those deposits in which Au and Ag are generally hosted in jasperoidal or quartz veins and silicified wall rocks. The term jasperoid refers to an epigenetic body composed by

fine-grained, chert-like, siliceous replacement of a pre-existing rock. Most jasperoid bodies are structurally controlled by high-angle normal faults and by the contact between carbonate rocks and shales. Therefore ore zones in the jasperoidal types are commonly limited to narrow shear zones, and along the contact of carbonate rocks with the overlying shale beds adjacent to high-angle faults. The Carlin subset deposits are those wherein the Au and Ag are more or less evenly distributed in the host rocks which do not always appear to be silicified. Ore zones in this type are pod-like and extend tens of metres away from the faults. There is a complete gradation between the two sub-sets, and a deposit classified as jasperoidal may have exploration potential for Carlin-type and vice versa. Thus, the two subsets are end members and are considered to be a useful concept for both regional- and district-scale exploration programmes.

Jasperoidal-Type Subset

The Pinson and Preble deposits are considered as Au-rich representative of this type. They occur in the Getchell belt, along the eastern flank of the Osgood Mountains in Humboldt County, Nevada. The Pinson deposit contains approximately 3×10^6 tonnes at 4.1 g/t Au, whereas the Preble deposit has 1.2×10^6 tonnes grading about 3.1 g/t Au. The structural geology of the Osgood Mountains is very complex and is characterised by thrust faults and high-angle faults. The dominant control of the Getchell belt deposits is the Getchell fault system, which has been traced for over 40 km along the eastern side of the Osgood Mountains.

At Preble, the Cambrian age Preble Formation is the host rock for the Au deposit, consisting mainly of calcareous and carbonaceous phyllitic shale with interbedded, finely laminated limestone. Most of the ore is hosted by the phyllitic shale (Fig. 11.19A). At Pinson, the allochthonous Camus Formation overlies the Preble Formation in a thrust relationship. The Camus Formation consists of intercalated thin beds of siltstone and limestone with two massive limestone units up to 50 m thick. The majority of the mineralisation is contained in the lower limestone unit which is silicated to diopside and tremolite (Antoniuk and Crombie 1982).

At Preble the ore zone occurs along a shear zone parallel to bedding. Hydrothermal alteration of the host phyllitic shales mainly involves major addition of silica. Jasperoid veins cut the Preble Formation limestone, whereas silica replacement of the limestone and shale rocks forms massive jasperoid bodies. The finely disseminated ore at Preble correlates with this silicification. Dolomitisation of the limestone is also common near high-angle faults. Supergene alteration has resulted in a prominent zone of oxidation to a depth of about 60 m. Au occurs mostly with sulphides and Fe oxides after pyrite in the unoxidised and supergene zones respectively. In addition to pyrite, other sulphides include arsenopyrite, marcasite, chalcopyrite and sphalerite (Bagby and Berger 1985). At the Pinson deposit the mineralisation is of two types (A and B), both of which are related to intense silicification within a normal fault zone. The A zone is of higher grade (approximately 5.8 g/t Au) and it occupies a 20-m wide northeast-trending shear zone in which the Camus Formation rocks have been completely replaced by jasperoid. The lower grade B zone (approximately 2.5 g/t Au) is less silicified than
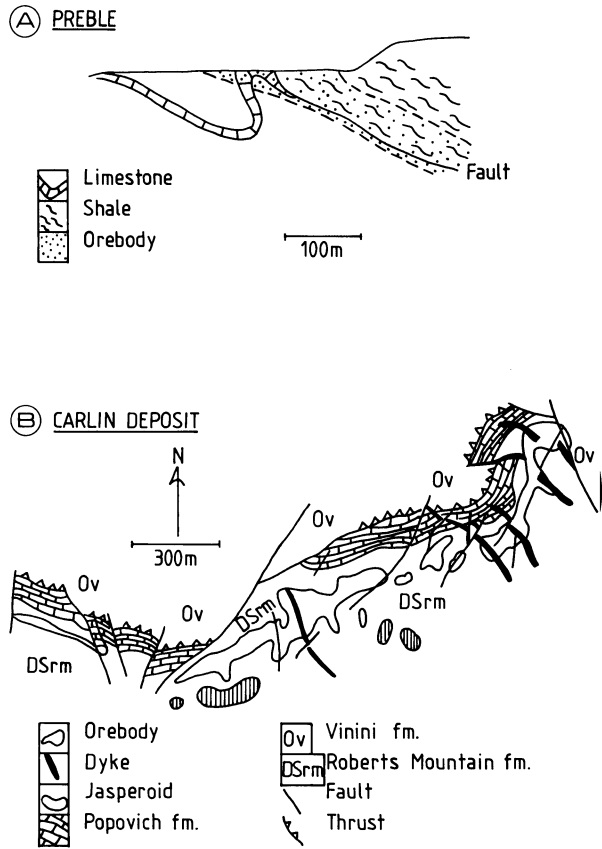
Fig. 11.19. A Schematic cross-section of the Preble deposit (after Bagby and Berger 1985). B Simplified geology and distribution of orebodies at Carlin (After Radtke et al. 1980)

the A zone and occurs along a fault in which the Au mineralisation is associated with limonite and kaolinite. The general mineralogy at Pinson consists of Fe oxides with remnant pyrite, marcasite and fine Au (less than 5 μm) which occurs as a free phase associated with quartz and, to a lesser extent, pyrite. In common with most other sediment-hosted precious metal deposits in Nevada, at Preble and Pinson there is a strong geochemical correlation of Au with Hg, As and Sb.

Carlin-Type Subset

The Carlin deposit is situated in northern Eureka County, Tuscarora Mountains, Nevada. A brief history of the discovery of the deposit, its mining, leaching and milling operations is given by Jackson (1983). The deposit contains approximately 10×10^6 tonnes grading about 10 g/t Au. The geological characteristics of the deposit have been published by Radtke et al. (1980), Adkins and Rota (1984), Dickson et al. (1979) and Bagby and Berger (1985) which constitute the data base for the present discussion.

The Carlin orebodies consist of tabular and irregularly shaped zones in the upper portions of the autochthonous Roberts Mountains Formation of Silurian age (Fig.

11.19B). This Formation strikes northeast and dips beneath the Roberts Mountains Thrust which is the oldest and most prominent structure in the area. Numerous high-angle faults of various ages disrupt this thrust fault. All these structures are considered to pre-date the mineralising event, the high-angle normal faults clearly served as channels for the hydrothermal solutions, resulting in the shattering and brecciation of the upper portions of the Roberts Mountains Formation, which was also chemically favourable and suitably positioned for ore deposition. It appears that the Roberts Thrust has had no influence on ore deposition, while the normal fault zones are only sparsely mineralised. The upper portions of the Roberts Mountains Formation are composed of two main facies of carbonate rocks. One consists of well-laminated, argillaceous to arenaceous dolomite with a high content of organic carbon (up to 0.8 wt.%); the other is characterised by thin-bedded arenaceous rock with a low content of organic carbon (0.2–0.4 wt.%). The rocks of the first type appear to have higher permeability, making them more suitable both for the dissolution of carbonate and for the introduction of the hydrothermal fluids (Radtke et al. 1980). Igneous rocks in the Carlin pit occur as fault-filling dykes (Fig. 11.19B) of dacitic or quartz-latitic composition. In the district, however, numerous dykes and two granodioritic to dioritic stocks of Late Jurassic and Early Cretaceous age are present. The mine dykes are altered and locally mineralised.

The mineralisation occurs in several stratigraphic zones defining a northeast trend of about 2.8 km and forming three recognisable mine units: the Main Ore Zone, the East Ore Zone and the West Ore Zone. Since the ore is difficult, if not impossible, to distinguish from waste, ore control is totally dependent on assay values. The unoxidised ore is classified into five types: normal, siliceous, pyritic, carbonaceous and arsenical (Radtke et al. 1980). Normal ore accounts for nearly 60% of the total unoxidised ore, in which some 25 to 50% of the original calcite was removed by the hydrothermal solutions, while small amounts of pyrite, fine quartz, Au, Hg, Tl, Sb and As were introduced. Small amounts of Au are associated with organic carbon. Siliceous ore, which accounts for approximately 5% of the primary mineralisation, contains large amounts of introduced silica and grades from normal type to jasperoidal type. Most of the Au occurs on the surfaces of fine-grained pyrite, while small amounts of very fine Au are dispersed in the hydrothermal quartz grains. Stibnite, realgar and pyrite are the sulphide minerals present in this ore type. Pyritic ore (5–10% of the primary ore) is characterised by the high pyrite content (up to 10% by volume). Pyrite occurs as euhedral to subhedral grains forming disseminations or small veinlets. Locally pyrite forms clusters of framboidal-like structures associated with organic material and quartz. Some of this framboidal pyrite is coated by Au. Small quantities of other sulphides include realgar, stibnite, sphalerite, galena, molybdenite and chalcopyrite. Hydrocarbons are also present as dissemination in the rock matrix. Carbonaceous ore, which makes up approximately 15–20% of the unoxidised ore, contains between 1 and 5 wt.% organic carbon, is dark grey to black in colour and has small veinlets of hydrocarbons and other organic material. In addition to pyrite the carbonaceous ore also contains realgar, orpiment, stibnite, cinnabar, sphalerite, galena and a mineral called carlinite (Tl_2S). Au occurs both with the carbonaceous material and as coatings on pyrite grains. Arsenical ore constitutes 5–10% of the primary ore and contains high concentra-

tions of As (0.5–10 wt.%), mainly as realgar and orpiment. Au occurs associated with the carbonaceous material, as coatings on the surface of pyrite grains and as inclusions in realgar. The arsenical ore also contains unusually high concentrations of Hg, Sb and Tl, together with a wide variety of sulphides and sulphosalts.

Organic carbon compounds which occur in the unoxidised Au-bearing carbonate rocks at Carlin – and in fact in many of the other disseminated sediment-hosted precious metal deposits in Nevada – consist of veinlets, seams and particles of amorphous carbon, hydrocarbons and a substance resembling humic acid (Radtke and Scheiner 1970). The precise nature of the Au-carbon association is not clear. It is currently believed, however, that the organic material was introduced with the main-stage hydrothermal solutions. In terms of ore genesis, it appears that the role of the carbonate rocks is of far greater importance due to the replacement of calcite grains by silica containing pyrite and micron-sized Au grains. The removal of the calcite therefore created the necessary permeability for the silica-rich ore fluids.

The main hypogene hydrothermal alteration at Carlin – as distinguished from the supergene alteration – is characterised by decalcification, argillisation, silicification and pyritisation, which more or less correspond to stages of hydrothermal activity. These stages include an early hydrothermal stage, a main and late
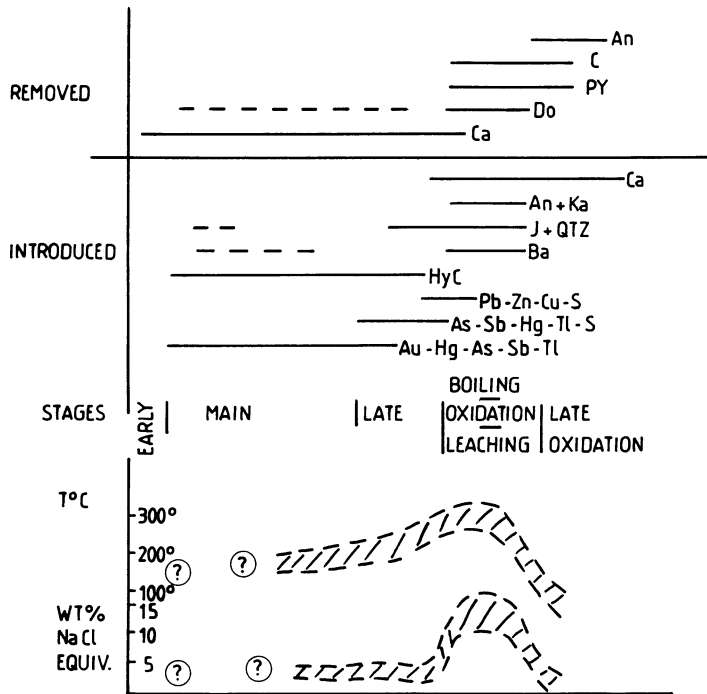

Fig. 11.20. Mineral paragenesis (*top diagram*) of the Carlin deposit. *An* Anhydrite; *C* organic carbon; *py* pyrite; *Do* dolomite; *Ca* calcite; *Ka* kaolinite; *J* jasperoid; *QTZ* quartz veins; *Ba* barite; *HyC* hydrocarbons. Temperature and salinity trends (*bottom diagram*) are approximate, thickness of curves indicates range of values (After Radtke et al. 1980)

hydrothermal stage, an acid-leaching stage, and, finally, a stage of supergene oxidation. A paragenetic sequence of alteration-mineralisation is shown in Fig. 11.20. Decalcification represents the earliest stage of alteration in which carbonate minerals were selectively removed and re-distributed. The initial penetration of the fractured rocks was probably made by low temperature fluids which dissolved the calcite, resulting in the increase of permeability previously mentioned. Argillisation accompanied the pre-Au decalcification stage, resulting in the formation of clay minerals. Silicification was a bulk replacement process at Carlin and is closely related to the introduction and concentration of the Au mineralisation. Pyritisation is common to most deposits of this type. Pyrite-rich rocks are locally auriferous and the pyrite grains contain Au in cavities and fractures. There appear to be two stages of pyrite formation, the second generation of pyrite being associated with the Au mineralisation.

Post-Au mineralisation hydrothermal activity is the acid-leaching stage which resulted in the prominent alteration of the upper portions of the ore zones. This stage is characterised by the effects of the oxidation of H_2S exsolved during boiling of the fluids towards the end of the main-stage mineralising event (Fig. 11.20) During this phase most of the remaining calcite together with large amounts of dolomite, were removed from the host lithologies (upper portion of the Roberts Mountains Formation and lower parts of the Popovich Formation). Organic carbon compounds and pyrite were oxidised and removed, and kaolinite and anhydrite thus developed.

Following the cessation of hydrothermal activity, rocks and ores underwent supergene alteration brought about by cool meteoric waters. Supergene alteration is deepest along faults and lithological/formation contacts. The oxidised ore contains varying amounts of quartz, clay (illite, kaolinite and montmorillonite) and dolomite. Small particles of Au are scattered through the rock and locked in fine-grained quartz, with lesser amounts associated with the secondary Fe oxides and clays.

11.7.2 Nature of Fluids and Ore Genesis

The precise nature and origin of the mineralising fluids responsible for sediment-hosted epithermal deposits remain uncertain. Several studies have attempted to resolve this issue and summarised below are the results of some of these studies, which are largely based on isotopic and geochemical data.

Stable isotope systematics (Dickson et al. 1979, Radtke et al. 1980) for the Carlin materials support a meteoric source for the hydrothermal fluids which contained sedimentary sulphur and carbon. The δD values of fluid inclusions are strongly negative (-139 to -160 per mill), suggesting that major amounts of meteoric water were present during the alteration processes, and, since the timing of this alteration spanned the ore-forming event, it is concluded that the mineralising fluids were also of meteoric origin. The $\delta^{34}S$ values of different sulphides average $+11.4$ per mill, which is close to the average of $\delta^{34}S$ of $+13$ per mill for the diagenetic pyrite in the Roberts Mountains Formation rocks. This would indicate that the S in the Carlin

deposit was probably derived by dissolution of the diagenetic sulphides in the Formation. The $\delta^{13}C$ values of hydrothermal calcite also indicates that the carbon in the ore fluids was derived from the host rocks. Recently Hofstra et al. (1991), using geochemical, fluid-inclusion and stable-isotope data from jasperoidal, barite and calcite and chemical-reaction-path modeling, determined that mixing of two fluids and sulphidisation were responsible for the Au mineralisation of the Carlin-type deposits in the Jerritt Canyon district in Nevada. These authors propose that one fluid was "evolved" meteoric water, enriched in CO_2 and H_2S, characterised by δD of ca. −111 per mill, $\delta^{18}O$ of ca. 5 per mill and with a temperature of 225°C, and a salinity of 6 wt.% NaCl equivalent. The other fluid was dilute "unexchanged" meteoric water characterised by δD of ca. −118 per mill, $\delta^{18}O$ of ca. −16 per mill and with temperatures of less than 200°C. Hofstra et al. (1991) believe that the Au was transported as a sulphide complex which broke down by reacting with the Fe content of the wall rocks, precipitating Au according to the reaction:

$$Au(HS)_2^{-1} + FeO + H^+ \rightarrow FeS_2 + Au + H_2O + 0.5H_2,$$
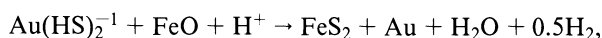
where FeO is the reactive Fe contained in the wall rocks. It is interesting to note that sulphidisation of Fe-rich lithologies as a Au precipitating mechanism is also advocated to explain some of the Au mineralisation in Archean lode deposits (see Phillips et al. 1984; Chap. 15).

Finally, in the regional context, Sillitoe and Bonham (1990), using examples from Bau in eastern Sarawak (Borneo) and Bingham in Utah (USA), propose that the sediment-hosted disseminated Au mineralisation may have been contributed by magmatic-hydrothermal solutions. These authors propose that sediment-hosted Au deposits occur in the peripheral regions of porphyry intrusions containing base and precious metal mineralisation. In their model, fluids originate from a porphyry Cu-Mo-Au, moving along steep faults, along which porphyry dykes emanating from the igneous stocks are also emplaced. The movement of the mineralising fluids along these steep faults results in the formation of Zn-Pb-Ag ± Au carbonate-replacement skarns, nearer the intrusion, and of sediment-hosted epithermal Au-Sb-As deposits in distal areas. Jasperoidal material would be deposited within these faults above and distal to the metal deposits (Sillitoe and Bonham 1990).

11.8 Kuroko-Type Mineral Deposits

Hydrothermal mineralisation of the kuroko type belongs to the general category known as volcanogenic massive sulphide deposits. They are related to submarine volcanism, but occur in a variety of tectonic settings. Volcanogenic massive sulphide deposits have been classified in terms of their metal content (Franklin et al. 1981), geological environment (Sangster and Scott 1976), composition of host rocks and tectonic setting (Sawkins 1976, 1990). The latter enables a clearer subdivision, and to a large degree encompasses the criteria used in other classification schemes. Thus, if we adopt the plate tectonic approach of Sawkins, we can distinguish three main types of volcanogenic massive sulphide deposits: (1) kuroko-type, which forms in

subduction-related settings (island arcs); (2) Cyprus-type, formed at mid-oceanic, or back-arc spreading centres; and (3) Besshi-type, which also form at spreading centres, but is sediment-hosted because of the proximity of these centres to landmasses. In this section we confine our discussion to the kuroko-type massive sulphide deposits, while the other two are treated in the following chapter. The name kuroko, which litterally means "black ore" in Japanese, has taken on a much wider meaning from its original restriction to the massive sulphide mineralisation whose type occurrences are in Japan.

Precambrian volcanogenic massive sulphide deposits, such as those that occur in the Archean greenstone belts of Canada (Noranda-type), have been considered as an ancient analogue of the kuroko deposits. Hutchinson (1980), however, recognises them to be a separate class of deposits which he calls "primitive type". The distinction between the Phanerozoic kuroko deposits and the volcanogenic massive sulphide deposits of Precambrian age is essentially one of metal contents, with Pb appearing to be a dominant metal in the former while it is scarcer in the latter. Thus, the metal association of the Phanerozoic volcanogenic massive sulphide deposits is $Zn - Pb - Cu \pm Au \pm Ag$, while the Precambrian deposits are dominated by $Zn - Cu \pm Au \pm Ag$. The time distribution of the volcanogenic massive sulphide deposits is shown in Fig. 5.1A and discussed in Chapter 5, where the possible presence of a volcanogenic gap between approximately 1.7 and 0.5 Ga is considered. Although the Phanerozoic kuroko-type deposits and the Precambrian deposits (Noranda- or primitive-type) share many similarities, they are, nevertheless, treated separately because of certain inherent differences, other than their metal content, due to their diverse ages and settings.

11.8.1 Kuroko Deposits

The kuroko polymetallic massive sulphide deposits form at the discharge site of submarine hydrothermal systems associated with caldera structures. They are of Phanerozoic age, and associated with subduction-related volcanic arcs. They may be considered the submarine equivalent of the subaerial epithermal systems discussed in the preceding sections. Fluid inclusion data, in fact, indicate that kuroko ores form at temperatures ranging from 100 to approximately 330°C (Pisutha-Arnond and Ohmoto 1983). According to Ohmoto and Takahashi (1983), kuroko mineralisation requires relatively deep marine conditions (>1000 m), because in shallower environments boiling solutions would result in the dispersion of the mineralisation with the subsequent development of veins and/or disseminated sulphides. Examples of present-day mineralised systems that have strong similarities to kuroko-type deposits are discussed in Section 11.2.3. The kuroko deposits – such as those of the well-known Hokuroko district in Japan – are related to bimodal volcanic sequences generally consisting of tholeiitic basalts at the base followed upwards by dacite, rhyodacite, rhyolite and related pyroclastic rocks. This bimodal sequence is usually superimposed on calc-alkaline volcanic piles typical of magmatic arcs formed above subduction zones. Sillitoe (1982) proposes inter-arc and back-arc extensional settings for most kuroko-type deposits, characterised by

rifting and dominant bimodal volcanism. Rifting of an island arc could, according to Sillitoe (1982), occur as a result of oblique subduction, and it is also possible that this rifting may evolve into a marginal basin. An intracontinental extensional environment is also considered by Sillitoe (1982) for rhyolite-hosted massive sulphide deposits that are generally associated with bimodal sequences, such as those of Bathurst, New Brunswick in Canada, Captains Flat and Woodlawn in Australia, and the Iberian pyrite.belt.

The association of massive sulphide ore deposits with caldera structures and resurgent rhyolite domes has been noted by several authors (e.g. Sillitoe 1980, Ohmoto and Takahashi 1983). The most important role of caldera formation is thought to have been the consequent creation of depressions, which became the loci for discharging hydrothermal fluids. In addition, faulting associated with caldera formation is largely responsible for providing channelways for the circulating fluids. In most cases the mechanism of caldera formation is preceded by voluminous eruptions of pyroclastic material, resulting in the rapid emptying of the magma chamber and subsequent collapse of the volcanic structure. Kuroko-type deposits usually occur in clusters, each of which is associated with a caldera structure. They also tend to occur along particular stratigraphic intervals within a volcanic sequence, such as the final stages of major pulses of volcanic activity.

Kuroko massive sulphide deposits are thought to form through discharge of hydrothermal solutions which take place on depressions on the sea floor and along the flanks of rhyolitic domes (Eldridge et al. 1983). Horikoshi (1969) believes that hydrovolcanic explosions occur on the flanks of rhyolite domes, and are followed by fumarolic activity, and the deposition of sulphides which may be subsequently transported and deposited in topographic lows. It must be pointed out, at this juncture, that the density and pressure of the hydrothermal solutions in relation to the density and hydrostatic pressure of the sea water at the point of discharge, are important factors in determining the style and morphology of the kuroko orebodies. We may consider three cases. In the first, the hydrothermal fluid density and pressure are greater than the surrounding medium, the ore solutions are injected into the sea water and the resulting mineralisation is dispersed over a fairly wide area, forming layered horizons. In the case of kuroko mineralisation, the orebodies would then be largely composed of sulphates with minor sulphides. In the second case, the density and pressure of the ore solutions are at near equilibrium with the surrounding medium, resulting in the formation of well-zoned, stratabound black and yellow ores under relatively stable conditions. In the third case, the ore fluids have density and pressure less than the surrounding sea water; thus veins and stringer deposits form instead of massive sulphide and sulphate bodies. We return to the relationship of fluid dynamics and the morphology of ore deposits in Chapter 12.

A typical cross-section through a kuroko deposit is shown in Fig. 11.21A, and its evolutionary stages are shown in Fig. 11.21B. In models of kuroko ore genesis, leaching of metals from the wall rocks is generally implied; however, more recent studies indicate that the metals are, at least in part, derived from high level plutonic bodies underlying and possibly feeding the volcanic system (Urabe et al. 1983). Stable isotope systematics confirm that kuroko ore fluids have a major
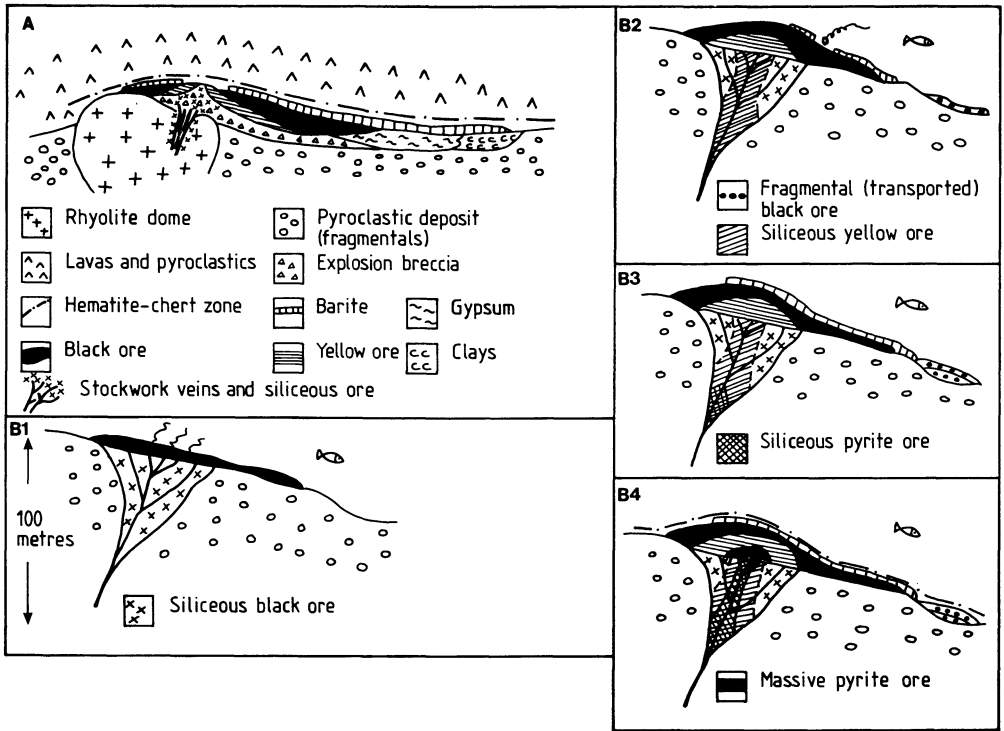
Fig. 11.21. A Idealised cross-section of a kuroko-type deposit (after Sato 1974). B1 to 4 depict the evolutionary stages in the development of a kuroko orebody; legend same as in A, except where otherwise stated; see text for details (After Eldridge et al. (1983)

component of sea water, but mixing with magmatic waters is nevertheless not entirely excluded.

Alteration and Mineralisation

Hydrothermal alteration of kuroko mineral deposits is characterised by intense K and Mg metasomatism which results in alteration assemblages dominated by chlorite, quartz and sericite. Silicification and zones of clay alteration are also prominent and may grade away from the mineralisation into regional greenschist metamorphic assemblages. A measure of the degree of alteration for kuroko deposits is proposed by Ishikawa et al. (1976), who define an alteration index in terms of the ratio between elements enriched and elements enriched plus depleted; for example:

$$\text{A.I.} = \frac{\text{MgO} + \text{K}_2\text{O}}{\text{Na}_2\text{O} + \text{K}_2\text{O} + \text{CaO} + \text{MgO}}.$$

In detail hydrothermal alteration mineral assemblages are complex. Shirozu (1974) distinguished four main zones of alteration which, from the margins towards the
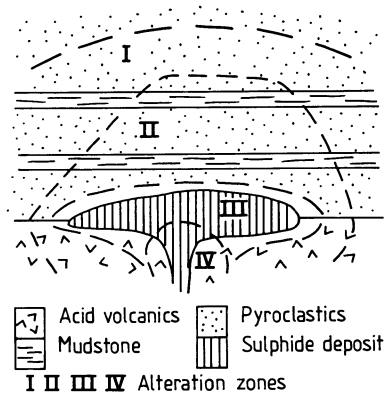
Fig. 11.22. Alteration zones associated with a
kuroko massive sulphide deposit. Explanation
of zones I to IV are given in the text
(After Shirozu 1974)

core of the mineralisation, are: zone I characterised by the assemblage montmorillo-
nite + zeolite + cristobalite; zone II consists of sericite + sericite-montmorillonite +
Fe-Mg chlorite + albite + K-feldspar + quartz; zone III is characterised by clay
alteration within and around the mineralisation, and contains sericite + interstrati-
fied montmorillonite-sericite + Mg-chlorite and quartz; zone IV surrounds the
central part of the mineralised body and it displays strong silicification, with quartz
+ sericite + Mg-rich chlorite. The spatial disposition of zones I to IV around the
massive sulphides is shown in Fig. 11.22.

A time-space model of hydrothermal alteration proposed by Pisutha-Arnond
and Ohmoto (1983) is summarised and discussed below. From the margins towards
the core of the mineralisation, alteration zones and mineral assemblages are as
follows: (a) a zeolite zone with Mg-Na montmorillonite, clinoptilolite, mordenite,
saponite and crystobalite; (b) a zeolite zone with first appearance of analcime,
calcite, illite, and quartz; (c) a Mg-Ca montmorillonite zone ; (d) a transitional
mixed-layer illite-montmorillonite zone; and (e) a zone of sericite and Mg-rich
chlorite.

The two zeolite zones (a and b) are interpreted to be the product of diagenesis,
with zone (a) changing to zone (b) at deeper stratigraphic levels. The early diagenetic
stages are primarily due to pore sea water reacting with the glass component of the
volcanic rocks, resulting – according to Pisutha-Arnond and Ohmoto (1983) – in a
substantial increase of total dissolved salts in the solutions. Following this
diagenetic stage and with the onset of hydrothermal activity, the zeolite zone
assemblages change laterally towards the core zone (e.g. towards the main central
conduit and massive sulphides), to the assemblages outlined in (c), (d) and (e). The
spatial arrangement (a) to (e) also reflects a time sequence, with assemblage (a) being
the earliest and (e) the latest at a given point. These mineralogical characteristics,
together with the related chemical changes, are the result of heated sea water-rock
interactions. Hydration and cation exchange reactions typify the alteration zones,
and the stability relations between alteration minerals are largely a function of pH,
temperature and the activities of the cations involved (e.g. Mg, Ca and Na). Cation
exchanges between smectite and fluids result in the increase of Ca and decrease of
K and Mg in the pore fluids. The Ca gained by the fluids is then used to form

sulphates and carbonates. In the late diagenetic to early hydrothermal stages and with increasing temperature, the organic matter present in the marine sediments may release CO_2 which further enhances the formation of carbonate.

As the hydrothermal system becomes more active, high temperature fluids ascend through fractures towards the discharge zone, reacting with the zeolite minerals present, to form the mineral assemblages of the Mg-Ca montmorillonite zone. This process results in a halo of Na depletion around the deposits. With further increase of the temperature ($> 250°C$) of the fluids, Ca-montmorillonite becomes unstable and is replaced by expandable mixed-layer clays, montmorillonite, illite and sericite. At this point sulphide minerals are precipitated on the sea floor (Pisutha-Arnond and Ohmoto 1983). They are the black ore (kuroko), consisting predominantly of sphalerite and galena, with minor quantities of tetrahedrite, barite and chalcopyrite. As the temperature reaches approximately 300°C, with the introduction of hotter fluids, all of the montmorillonite and most of the plagioclase are converted to sericite and sericite + chlorite. The fluids of this stage are Cu-rich and therefore the dominant sulphide becomes chalcopyrite, or yellow ore (oko in Japanese). Chalcopyrite replaces the earlier sulphides in the lower parts of the sulphide deposit. The ingress of fluids with temperatures in excess of 300°C results in the deposition of pyrite, which dissolves the earlier chalcopyrite and forms the pyrite-rich lowermost portion of the massive sulphide deposit. As the fluids become cooler precipitation of ferruginous cherts and barite takes place at the top of the massive sulphide deposit.

The distribution of the alteration-mineralisation zones is therefore clearly related to a time-space continuum of fluid discharge, and the mineralogical and metal zoning is generally well defined for most kuroko systems, although it must be realised that not all of the zones described below are necessarily present in a given deposit. This may be further complicated in systems where more than one episode of mineralisation has taken place. Thus, in an idealised kuroko system, there are six main ore zones (cf. Fig. 11.21A, B), namely: (1) Keiko, or siliceous ore, the silicified portion of the footwall consisting of a quartz vein stockwork and/or silicified zones containing pyrite and lesser amounts of chalcopyrite, sphalerite, galena and barite; (2) Oko or yellow ore, which transitionally overlies the keiko zone, and consists mainly of pyrite with varying amounts of chalcopyrite, sphalerite, minor barite and gypsum; (3) kuroko or black ore, transitionally overlying the oko ore and consisting of sphalerite, galena, chalcopyrite, tetrahedrite-tennantite, barite; bornite, electrum and complex Ag sulphosalts may also be present and generally increase towards the top of the orebodies; (4) a barite zone overlies the kuroko ore, followed by (5) a zone of ferruginous chert (tetsusekeiei), which is the uppermost part of the deposit and is composed of cryptocrystalline quartz, hematite and minor quantities of barite with traces of sulphides; (6) a sekko or gypsum zone, composed mainly of anhydrite and gypsum, with minor chalcopyrite, pyrite and clay minerals, occurs laterally and below the kuroko ore.

Homogenisation temperatures of fluid inclusions indicate a wide range of temperature for the ore solutions, from approximately 100 to 330°C, with salinities of 3.5 up to 6 wt. % NaCl equivalent. More specifically the yellow ore minerals were precipitated at the highest temperature (ca. 330°C), while the black ore minerals

were formed at temperatures of between 200 and 330°C (Pisutha-Arnond and Ohmoto 1983).

The size of kuroko orebodies, though variable, is generally small. A workable funnel-shaped orebody may have dimensions of $300 \times 100 \times 50$ m. Tonnages of individual orebodies vary from a few thousands of tonnes to slightly more than 1×10^6 tonnes. Grades are also variable, but typically have the following ranges: Cu 0.5–2%; Pb 0.5–2%; Zn 2–10%; Au 0.5–6 g/t; Ag 20–1000 g/t; $BaSO_4$ 20–50%.

Lithogeochemical Variations

Major and trace element variations in the environment of kuroko systems can be a great aid to the exploration geologist. The distribution of major and trace elements, both at the regional and local scale, has been found to show useful systematic variations with respect to the central core zone of the mineralised system, as would be expected in view of the distinct mineral and metal zoning that characterises the kuroko deposits. These geochemical variations can be particularly useful in tropical areas where the intense weathering often makes it difficult to recognise hydrothermally altered rocks.

Geochemical work carried out by Lambert and Sato (1974), for example, has shown that silica is strongly enriched and Na depleted in the innermost zones (zones III and IV of Shirozu 1974); K, on the other hand is usually enriched in zones II, III and IV, so that a progressive increse in the K/Na ratios is observed towards the mineralised areas over distances of hundreds of metres.

Detailed major and trace element lithogeochemical studies both at regional and "mine scale" have been conducted by Rugless (1983a) on a kuroko-type deposit at Wainaleka, Fiji, to be described later. This worker collected rock chip samples for regional studies, and used channel samples of outcrops and drillcore for "mine scale" studies. Rugless' work revealed some interesting elemental variations associated with both hangingwall and footwall rocks, as well as the mineralised zone. His findings are summarised here.

On the regional scale distinctive geochemical trends occur. K, Rb and Mn are depleted up to approximately 1 km below the mineralisation, whereas Mg is enriched in the same area. Rb and K, however, are strongly enriched in the mineralised area. Na, Ca and Sr exhibit strong depletion 200–300 m below the mineralisation, corresponding to the zone of most intense alteration. The Wainaleka deposit occurs within anomalous trends defined by Cu, Pb, Ag, Co and Zn. The altered rocks are generally characterised by Ca and Na depletion and Fe, Mg and K enrichment (Fig. 11.23).

At the "mine scale", weakly altered hangingwall rocks (andesite, sodic rhyolite and pyroclastics) show enrichment in Mg, Ca, Na, Fe, Mn and Sr, and depletion in K and Rb up to 50 m above the mineralised and unmineralised footwall rocks. The Cu, Ag, Zn and Pb contents are all enhanced, and K and Rb depleted in the hangingwall rocks. The mineralised lens and the adjacent feeder (or stringer) zones have, as expected, enrichment in Cu, Zn, Pb, Fe, Cr and Ag down to 20 m below the hangingwall contact. In the footwall rocks, depletions of Na, Ca, Mn, Sr, and enrichment of K and Rb relative to the hangingwall rocks are observed.
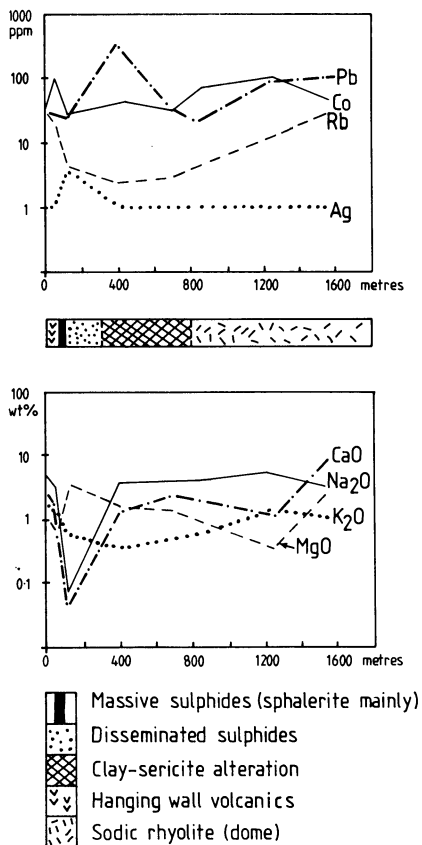
Fig. 11.23. Regional lithogeochemical variations in the Wainaleka area, Viti Levu, Fiji. The Wainaleka kuroko-type mineralisation is in an area characterised by tropical weathering, which renders recognition of rock types and hydrothermal alteration difficult. Lithogeochemistry can be of considerable aid in an exploration programme aimed at the detection of a hydrothermal ore deposit characterised by well-developed mineral and metal zoning, such as a kuroko-type deposit. In the diagrams of this figure note the strong enrichment in Pb, Co, Rb, Ag, K, Mg and the strong depletion in Ca and Na, near or up to a few hundred metres from the mineralisation (After Rugless 1983a)

Massive sulphides (sphalerite mainly)
Disseminated sulphides
Clay-sericite alteration
Hanging wall volcanics
Sodic rhyolite (dome)

The Kuroko Deposits of Japan

The kuroko deposits of Japan have been well studied and documented by several workers, because of their young age (16–11 Ma) and lack of significant deformation and metamorphism. For details the reader is referred to Tatsumi (1970), Lambert and Sato (1974), Ishihara (1974) and Ohmoto and Skinner (1983).

The Japanese kuroko deposits occur within the Green Tuff belt (Fig. 11.24), which is thought to have resulted from the tectonic and igneous activity that formed the Japan Sea and the Japanese island arc during the period from about 65 Ma ago to the present (Ohmoto 1983). The onset of the back-arc extension in Japan is postulated to be related to the steepening of a northwesterly dipping subduction zone beneath the Japanese island arc 65 Ma ago (Outer Honshu province). Subduction of oceanic crust below the Outer Honshu province resulted in calc-alkaline magmatic activity in the inner zone of the province. Continued magmatic activity, uplift and back-arc spreading in the Yamato basin between 25 and 5 Ma ago was accompanied by bimodal volcanism, subsidence and caldera formation in the inner Honshu and Yamato provinces (Ohmoto 1983). Kuroko-type deposits were formed during this period within the deep marine basins that
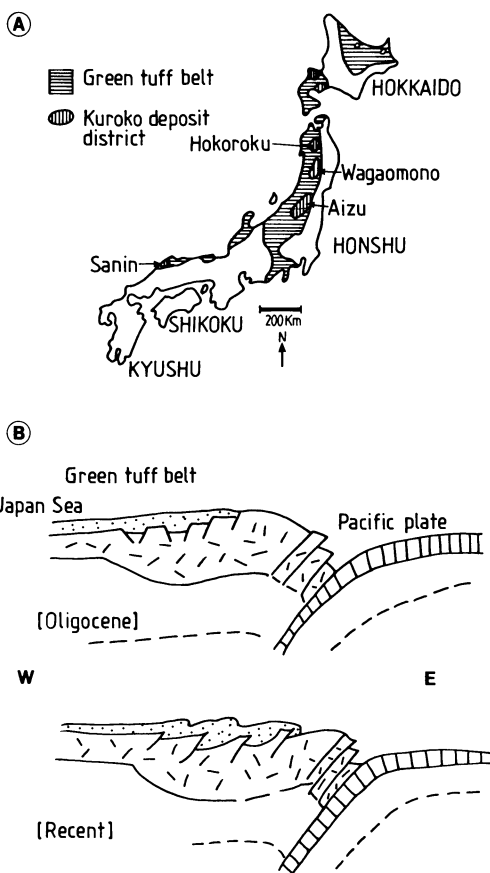
Fig. 11.24. A The Green Tuff belt of Japan and distribution of districts containing kuroko massive sulphide and sulphate (gypsum and barite) deposits (after Sato (1974). B The tectonic evolution of the Green Tuff Belt during the Oligocene to Recent (After Fuji 1974)

resulted from rapid subsidence. The deposits were localised by calderas within these basins.

Numerous massive sulphide and barite deposits of Miocene age occur in the Hokkaido and Honshu islands of Japan. The Okoruku district (Honshu) is particulary well endowed with kuroko deposits (Fig. 11.24).

As an example of Japanese kuroko mineralisation we look at some of the key geological features of the Shakanai deposit, located about 4 km from the town of Ohdate, Akita Prefecture. Information on this deposit can be found in Ohtagaki et al. (1974), with additional data reported here, obtained from D. Kirwin (unpubl. data). The Shakanai mine area comprises a cluster of 11 orebodies, outlined by 763 surface drillholes. Total reserves are approximately 30×10^6 tonnes. In 1976 production was in the region of 26000 tonnes of ore per month grading 2.5% Cu, 4.2% Zn, 1.3% Pb, 75 g/t Ag and 0.7 g/t Au.

In the mine area, the 500-m thick Shakanai Formation consists of mudstone, brecciated rhyolite and pyroclastics in its lower part (first 250 m), and brecciated rhyolite and dacite with associated pyroclastics in its upper part. The orebodies are situated within the upper part of the Formation at the contact with the overlying
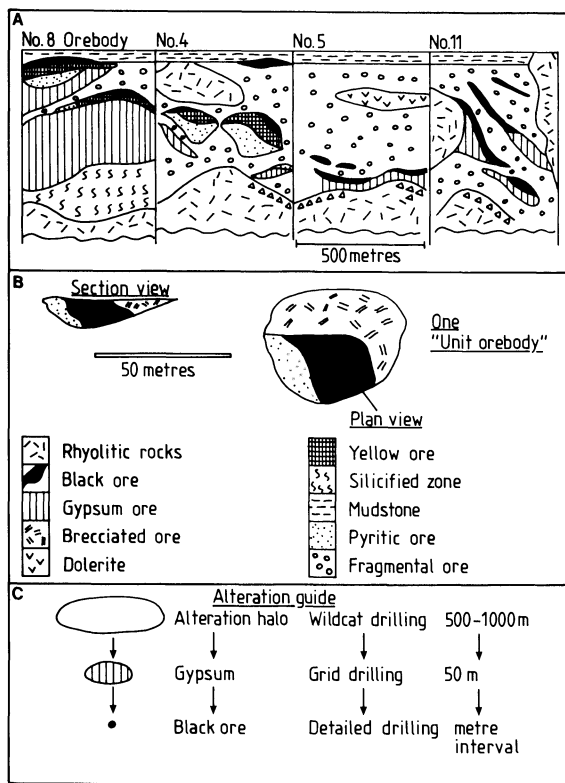
Fig. 11.25. A Idealised cross-section of selected parts of the Shakanai mineralised area showing geological succession and stratigraphic position of orebodies. Each panel represents a horizontal distance of approximately 500 m and a vertical dimension of about 600 m (after Kirwin, unpubl.). B The No. 1 orebody at Shakanai is composed of a number of "units", characterised by fragmental and brecciated ores in addition to black ore; the drawing illustrates one of these "units" (after Ohtagaki et al. 1974). C Hydrothermal alteration is used as an exploration guide; the drawing illustrates the ratio of the alteration halo to the size of the black ore zone and the drilling intervals used to progressively narrow down the target-area (After Kirwin, unpubl.)

Sainokami Formation which includes mudstone, pyroclastics and minor rhyolites. Intrusive rocks include chloritised dolerite sills and dykes which cross-cut both formations. Several rhyolite or dacite bodies of uncertain age are present, of which two phases are altered and mineralised, while a third and later dacitic body is unaltered.

The mineralisation at Shakanai is well zoned with black ore at the top, followed downward by yellow ore, siliceous ore and gypsum ore at the bottom. The disposition of some of the ore lenses and their stratigraphic position is shown in Fig. 11.25A. The No. 1 orebody consists of a number of "unit" bodies of black ore interbedded with mudstone and pumiceous tuff (Fig. 11.25B). The massive black ore is composed of fine-grained sphalerite, galena and barite with minor quantities of chalcopyrite, pyrite, bornite, germanite, argentite and tetrahedrite-tennantite. Native Au is associated with galena. This ore grades into brecciated ore composed of round black ore fragments, less than 1 metre in diameter, in a matrix of clay. At about 100 m from this orebody is another black ore lens constituting the No. 3 orebody. The No. 2 orebody is essentially composed of gypsum in footwall tuffs surrounded by sericitic alteration. Gypsum ore consists of alabaster, anhydrite, satinspar and clay, with grades of approximately 30% $CaSO_4$. The No. 4 orebody, which is the largest of the cluster, is composed of three main zones of yellow ore with

minor amounts of marginal black ore forming small pods in clay-altered tuffs. The upper portions of the yellow ore consist of graded aggregates of chalcopyrite, pyrite, sphalerite and quartz. The remaining lower portions of this ore zone consist of pyrite breccias with stockworks of chalcopyrite and pyrite. The No. 11 orebody is formed by three stacked ore lenses hosted in tuffs. The lower zone contains black ore and gypsum, the middle zone Cu-rich black ore, and the upper zone is formed by mixed yellow and black ore. Hydrothermal alteration surrounding the ore zones is characterised by Mg-chlorite, sericite and montmorillonite. Al-chlorite occurs in the footwall gypsum zones. The footwall volcanics show varying degrees of diagenetic alteration represented by minerals of the zeolite group such as mordenite and heulandite. Alteration zoning is used as a guide by the local geologists to locate orebodies. Wildcat drilling at 500 to 1000 intervals is normally carried out to locate alteration, and a 50-m grid then is laid out for follow-up drilling operations in order to locate the ore (Fig. 11.25C).

Kuroko-Type Deposits in Fiji

Important mineral deposits in the Fiji islands are the epithermal Au deposits of Vatukoula (Ahmad et al. 1987a, b; Anderson et al. 1987) and Mount Kasi (Taylor 1987), the Namosi porphyry Cu system (Waisoi) and the Cu-Zn-Pb-Au-Ag volcanogenic massive sulphide Undu deposits (Colley and Rice 1975; Fig. 11.26). Rhyolite-hosted massive sulphide deposits of the Undu Group in Fiji are good examples of kuroko-type mineralisation. These deposits tend to occur near the top of the volcanic complexes and within felsic pyroclastic rocks which mark the end of
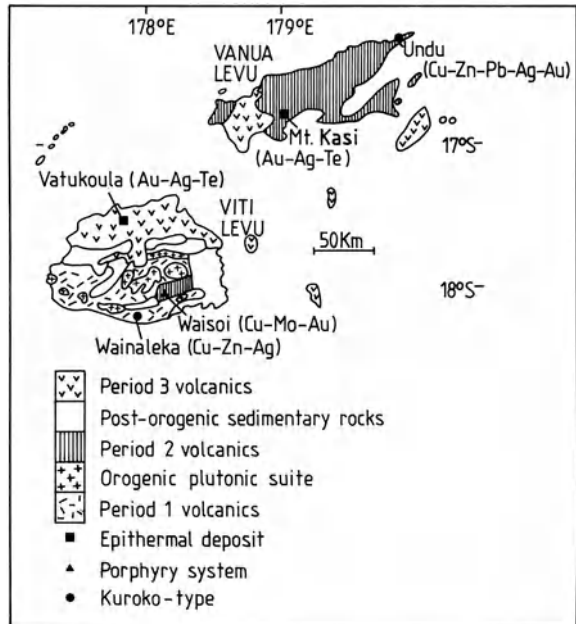

Fig. 11.26. Simplified geology of the Fiji islands and location of main mineral localities (After Colley and Greenbaum 1980; Rugless 1983a)

a volcanic cycle from mafic to felsic. They were formed about 5 Ma ago within caldera structures resulting from bimodal volcanism triggered during the early stages of the opening of the back-arc Lau Basin. The Wainaleka occurrence is a small volcanogenic massive sulphide deposit located in the island of Viti Levu, Fiji. The deposit has all the classic features of kuroko-type mineralisation, besides its metal content, which is Pb-poor and Zn-rich. The deposit was the subject of two research theses by Mroczeck (1982) and Rugless (1983b). Ore reserves are approximately 10^5 tonnes grading 1.5% Cu, 5% Zn and 10 g/t Ag.

The Fiji islands (Viti Levu and Vanua Levu) are situated in a tectonically complex area of the south west Pacific, between two active plate boundaries delimited by the Vamatu Trench in the west and the Tonga Trench in the east (Fig. 11.26). The tectonic evolution of the Fiji platform area is summarised from Rugless (1983a, b), Colley and Greenbaum (1980) and Carney and MacFarlane (1978). The Fijian platform is formed by sialic crust which may have evolved from the mantle during a sequence of subduction processes. No rocks older than the Tertiary are exposed, and the islands themselves were formed in the Tertiary and Quaternary during at least three major volcano-plutonic cycles which took place during pre-orogenic, orogenic and post-orogenic tectonic phases. The pre-orogenic phase (First Volcanic Period, Late Eocene to Lower Miocene) resulted in the emplacement of rocks of a tholeiitic island-arc assemblage. The orogenic phase (Second Volcanic Period) took place during the Late Miocene with the emplacement of a typical calc-alkaline suite consisting of basalt, andesite, dacite, rhyolite and associated volcanoclastics. The post-orogenic phase (Third Volcanic Period), from the Pliocene to Pleistocene, is characterised by tholeiitic to alkali basalt and shoshonite volcanism, which appears to be more typical of intraplate oceanic island volcanism.

During the pre-orogenic period a thick sequence of mafic to felsic volcanics, associated breccias and volcanoclastics (Wainamala sequence) were deposited. It is within this sequence that the Wainaleka deposit is situated. The orogenic period is marked by strong tectonic activity and the intrusion of plutonic rocks, including tonalite, trondhjemite, minor gabbro, microdiorite. The end of this period is characterised by andesitic volcanism and the accumulation of volcanoclastic sediments. During this calc-alkaline, dominantly-andesitic volcanism, the Namosi porphyry Cu system and the Undu occurrences were formed. Colley and Greenbaum (1980) draw attention to the evolutionary sequence of mineral deposition with tectonism and igneous activity. Thus, the Cu-Zn Wainaleka deposit represents an early phase of mineralisation hosted in primitive island-arc volcanics, and it is in this respect that Rugless notes that the deposit can be compared to the Precambrian-style kuroko mineralisation (see later). The Namosi porphyry Cu deposit is associated with an andesitic strato-volcano of the Second Volcanic Period. The Cu-Pb kuroko-type Undu deposit occurs in dacitic volcanics also of this period, and the metallogenic cycle is concluded with the Au-Ag-Te epithermal mineralisation (Vatakoula and Mount Kasi) which is associated with alkali and shoshonitic volcanics of the Third Period.

The Wainaleka Cu-Zn Deposit

The Wainaleka area is underlain by a bimodal volcanic suite overlying basement rocks, belonging to the Wainamala Group (First Volcanic Period). These basement rocks, which are typical of oceanic crust, consist of intercalated spilitic tholeiitic basalt and pelagic mudstone. The overlying volcanics are thought to belong to an island-arc succession consisting of tholeiitic basalt, andesite, sodic rhyolite, pyroclastics and volcanoclastics. In the prospect area the basement oceanic rocks are intruded by a rhyolitic complex about 6 km long and 1.5 km wide. The complex, composed of sodic rhyolite flows, welded tuffs, lithic tuffs, minor andesite and basalt, is overlain by mafic to intermediate volcanoclastic rocks. Hydrovolcanic explosions are postulated to have occurred along the flanks of the rhyolitic dome, accompanied by hydrothermal alteration-mineralisation that resulted in the genesis of the Wainaleka deposit.

The Wainaleka mineralised lens is about 100 m long, 5 m wide and 120 m deep. The mineralisation has a clear mineralogical zoning with a sphalerite-rich top, underlain by massive pyrite grading into disseminated chalcopyrite and sphalerite. The whole forms a stratabound massive sulphide lens contained within a fragmental unit. Underlying the stratabound lens is a poorly defined stringer, or stockwork, pyrite-chalcopyrite feeder zone. Barite is absent but gypsum occurs as veins laterally to the disseminated mineralisation. Sulphide ore minerals include pyrite, sphalerite, chalcopyrite, tetrahedrite-tennantite, galena, enargite, bornite, covellite and marcasite. A ferruginous zone, containing sulphide clasts, occurs above the mineralised lens. Hydrothermal alteration of the domal complex and adjacent country rocks is extensive. Rugless (1983a, b) distinguishes four zones of alteration (given in the inverse order of Shirozu's zones mentioned earlier). Zone 1 is a quartz-sericite assemblage closely associated with the mineralisation and characterised by the almost complete obliteration of the volcanic textures. This alteration extends for about 2 km from the upper contact of the fragmental unit and for some 300 m below the sulphide lens. Drillhole data enabled further subdivisions within Zone 1, of which five types are identified. Type 1 forms a 20–25-m-wide zone associated with the mineralised lens and the feeder zone. This type displays intense silicification characterised by a microcrystalline quartz mosaic with interstitial sericite. Illite and interstratified sericite-montmorillonite are also present. Type 2 is quartz-sericite-clay alteration peripheral to type 1, and is effectively the main type of alteration in Zone 1. Type 2 grades into Type 3, which is represented by the assemblage quartz + chlorite. X-ray-diffraction analyses indicate that this chlorite is Mg-rich with Fe contents increasing away from the mineralised lens. This feature, Mg/Fe ratio, increases towards the ore lens and can therefore be utilised as an aid to lithogeochemical exploration. Type 4 is represented by a jasper + chlorite assemblage peripheral to Type 3. Jasper is crypto-microcrystalline quartz associated with limonite and chalcedony. Type 5 is gypsum + chlorite alteration which occurs peripherally to the feeder zone. Mg-chlorite and illite are also present.

Zone 2 is represented by clay + sericite alteration in which relic textures can still be discerned. It surrounds Zone 1 and forms a halo some 4 km long and 0.8 km wide. Zone 2 alteration affects most of the lithologies of the domal complex. In the altered

rhyolite resorbed quartz phenocrysts can be discerned; plagioclase laths show incipient alteration to sericite and clay. The groundmass is re-crystallised microcrystalline quartz and clay. Zone 3 consists of clay + carbonate + chlorite + epidote alteration within the domal complex and underlying country rocks. It extends for approximately 1 km below the mineralised lens. In this zone volcanic textures are generally preserved, and the rhyolite shows quartz phenocrysts and plagioclase with incipient clay alteration. Carbonate is present as patches and veinlets in the groundmass, while chlorite and epidote replace the mafic minerals. Zone 4 is represented by the assemblage chlorite + albite + carbonate + epidote + zeolite in the mafic lithologies; montmorillonite + carbonate in the felsic lithologies. This is a type of propylitic alteration extending for at least 500 m above the ore lens.

11.8.2 Precambrian Volcanogenic Massive Sulphide Deposits

Precambrian (primitive-type, or Noranda-type) kuroko-style massive sulphide deposits are formed in ensimatic island arcs and are hosted in calc-alkaline sequences which range from tholeiites at the base to andesite-dacite-rhyolite at the top. Volcanic rocks include lavas and associated pyroclastic rocks (fragmentals) generally associated with immature volcanoclastics (Hutchinson 1980). Many deposits of this type occur in Archean greenstone belts and in the Early Proterozoic. Good examples are Noranda, Kidd Creek and Flin Flon in Canada (Spence and de Rosen-Spence 1975; Walker et al. 1975; Franklin et al. 1981), and Golden Grove in Western Australia (Ashley et al. 1988). Less commonly this "primitive type" (Hutchinson 1980) of kuroko-style mineralisation is also found in Phanerozoic island arc terranes such as the deposits in the Canadian Paleozoic terranes of Newfoundland (Thurlow et al. 1975) and New Brunswick (Jambor 1979), and the Wainaleka deposit described above. As mentioned previously, the main difference with the Phanerozoic Japanese-style kurokos is the metal association which, for the Precambrian deposits, is essentially Cu-Zn-rich with higher Ag/Au ratios. Another important difference between the Precambrian-type and the younger kuroko deposits is that the former contain a much smaller proportion of felsic volcanics. In the Abitibi greenstone belt of Canada, for example, felsic rocks constitute less than 4% of the entire volcanic pile. These differing proportions of mafic and felsic rocks may account for the metal associations and the observed increase in Pb content of the volcanogenic deposits with decreasing age.

The Canadian volcanogenic massive sulphide deposits are hosted by felsic and mafic volcanics and typically occur close to small, locally steep-sided, felsic domes composed of rhyolitic and fragmental rocks and quartz-feldspar porphyries. The domes are usually underlain by rhyolitic dykes, and subvolcanic intrusions of tonalitic and trondhjemitic compositions may be present in the footwall stratigraphy – as, for example, at Noranda, Sturgeon Lake, Matagami, Flin Flon and Bathurst. The presence of pillow lavas, graded bedding, great lateral extent of the lava flows, and paucity of pyroclastic material are all indicative of submarine conditions. The general lack, or scarcity, of oxide facies rocks such as sulphates (barite and gypsum) or banded iron formation rocks may be indicative of an
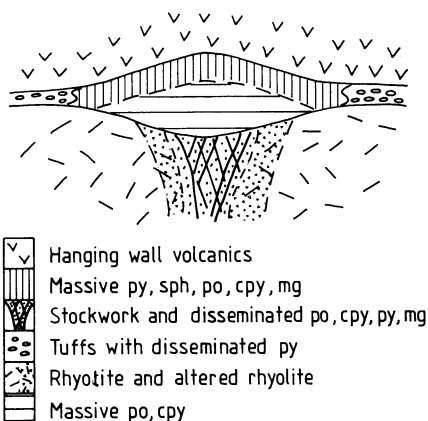
Fig. 11.27. Idealised cross-section of an Archean (kuroko-type) volcanogenic massive sulphide deposit (after Franklin et al. 1981 and references therein). *py* Pyrite; *sph* sphalerite; *po* pyrrhotite; *cpy* chalcopyrite; *mg* magnetite

- Hanging wall volcanics
- Massive py, sph, po, cpy, mg
- Stockwork and disseminated po, cpy, py, mg
- Tuffs with disseminated py
- Rhyolite and altered rhyolite
- Massive po, cpy

oxygen-deficient environment. The deposits display a close association with coarse acid pyroclastic rocks (colloquially called "mill rock", Sangster and Scott 1976). The orebodies are nearly circular or lensoid in shape and contain greater than 50% by volume of sulphides (Fig. 11.27). The size of the deposits in terms of tonnage and grades, although variable, is much greater than the younger kuroko orebodies. The Golden Grove deposit in Western Australia, for example, has reserves of 21×10^6 tonnes grading 1.2% Cu, 8.2% Zn, 0.6% Pb, 1 g/t Au and 67 g/t Ag (Ashley et al. 1988); the Millenbach deposit in the Noranda district contained reserves of about 2×10^6 tonnes grading 3.5% Cu, 3.6% Zn, 33 g/t Ag and 0.6 g/t Au (Simmons 1973). These massive sulphide deposits are underlain by footwall breccia zones or pipes shaped as an inverted cone, with sulphides occurring as disseminations and veinlets (stringer ore) (Fig. 11.27). The footwall pipes, interpreted as the feeder channels for the mineralising fluids, are fairly well defined and vertically extensive. In the Vauze deposit (Spence 1975), for example, the alteration pipe extends over 1000 m below the massive sulphide lens. Many pipes appear to be structurally controlled by faults and/or fractures. Alteration patterns are largely confined to the footwall pipes – unlike the younger kurokos – and are characterised by chlorite, sericite, silica and carbonate assemblages. The Millenbach pipe, Noranda, exemplifies a typical alteration sequence, with its chlorite-rich core which is surrounded by a halo of sericite and an outermost silicified zone. The chloritic alteration of the pipes is therefore the most prominent feature of the Precambrian volcanogenic deposit. Thus, chloritic alteration and Mg-metasomatism are the main features of these deposits, and in extreme cases this may lead to cordierite or anthophyllite rocks, locally known as "dalmatianite" because of their spotted appearance. Important chemical changes in the alteration pipes are enrichments in Fe and Mg and depletions in Ca, Na, Si and K.

The Noranda Deposits of the Abitibi Belt, Canada

The Abitibi greenstone belt is approximately 750 km long and between 150 and 100 km wide. It comprises 11 major mafic-to-felsic volcanic piles or complexes, within
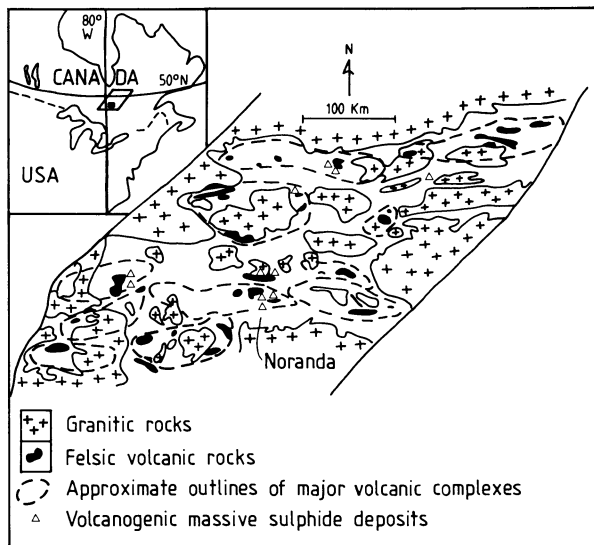
Fig. 11.28. The Abitibi greenstone belt, Canada, and the distribution of the major volcanic complexes and volcanogenic massive sulphide deposits (After Sangster and Scott 1976; Franklin et al. 1981)

which are the important volcanogenic massive sulphide deposits of the Noranda, Timmins and Matagami Lake mining camps (Fig. 11.28).

The Blake River Group of the Noranda area – consisting of felsic lavas and pyroclastics – hosts the Vauze, Millenbach, Horne, Norbec, Amulet, Lake Dufalt and Waite deposits from which some 90×10^6 tonnes of ore have been extracted (Spence and de Rosen-Spence 1975). The ore deposits occur within a steeply dipping series of folded and faulted rhyolitic rocks, and the mineralisation is associated with sequences of rhyolite lavas, breccias, tuffs and quartz-porphyry intrusions. A network of dykes of dioritic composition intrude the sequence and locally completely surround the mineralised zones. Five zones of rhyolitic rocks mark succesive periods of volcanic activity. The ore deposits and underlying chloritic pipes occur near the top of the rhyolitic formations and are associated with domes and explosive breccias. There is evidence of fragmentation of the sulphides prior to their being covered by later lavas. The Vauze deposit (Spence 1975; Spence and de Rosen-Spencer 1975) is associated with a rhyolite breccia located on the flank of a domal structure. In this deposit two types of ore are recognised: (1) massive stratiform lens on the flank of the dome, known as the B1 Zone; and (2) a steeply plunging pipe with disseminations and stringers of sulphides (B2 Zone), accompanied by chloritic and sericitic alteration.

The massive sulphide lens (B1 zone) has a length of approximately 140 m, with an average thickness of about 2 m thinning out towards the edges where it merges with mineralised chert. The lens overlies a rhyolite breccia and is overlain in turn by an andesite flow. In this massive sulphide lens three main subzones of sulphide mineralisation are distinguished. The first is a massive sulphide subzone consisting of pyrrhotite, chalcopyrite, pyrite and sphalerite. It is crudely banded and thickest towards a postulated discharge vent area where it consists almost exclusively of chalcopyrite. Gangue material is composed of chlorite, quartz and carbonates. This

massive ore grades into a breccia of sulphide clasts mixed with rhyolite fragments, which forms the second subzone of mineralisation. The third subzone stratigraphically overlies both the massive and brecciated subzones and consists of sulphide-bearing cherty tuff. It thickens away from the vent and is overlain by andesite. Within the chert layer pyrite, sphalerite and minor chalcopyrite occur as discontinuous layers.

The B2 ore zone consists of two pipe-like shoots of sulphide mineralisation which occur in a more or less circular zone of strongly chloritised and sericitised rock. The mineralisation, which is concentrated mainly in these two shoots, consists of disseminations and stringers of mainly pyrite and chalcopyrite, with minor sphalerite, bornite, pyrrhotite, magnetite, Ag and Au. Pyrite and chalcopyrite are associated with the more pervasive chloritic alteration towards the centre of the pipe.

Important points to consider in formulating a genetic model for the Canadian deposits are the stratiform and stratabound nature of the massive sulphide; their stratigraphic position at a time break within the depositional sequence; association of the ore with fragmental rhyolitic rocks and a dome-like structure; and the lateral and vertical zoning. In summary, the following sequence of events is envisaged. The ore-bearing hydrothermal solutions moved up along and through channelways of fractured rock, forming what now appears as a breccia pipe and causing alteration mainly in the form of Mg metasomatism, subsequently depositing sulphides as disseminations and veinlets. The emergence of the mineralising solutions from a vent on the flank of the rhyolitic dome resulted in the precipitation of sulphide layers as lenses along the steep sides of the dome. Slumping of the sulphide material along these steep sides resulted in the formation of the breccia ore zones. With time, this hydrothermal activity waned with the concomitant impoverishment in their metal content, causing the deposition of siliceous layers (chert) covering the sulphide mineralisation. Renewed volcanism resulted in the outpouring of pillowed lava flows which covered the massive sulphide deposit.

References

Adkins A R, Rota J C (1984) General geology of the Carlin gold mine. In: Johnson J L (ed) Exploration for ore deposits of the North American Cordillera. Field Trip Guide Book, Ass Expl Geochem Reg Symp, Reno, Nevada, pp 17–23

Ahmad M, Solomon M, Walshe J L (1987a) The formation of the quartz-gold-telluride veins of the Emperor Mine, Fiji. In: Proc Pac Rim Congress '87. Australas Inst Min Metall, Parkville, Victoria, pp 1–4

Ahmad M, Solomon M, Walshe J L (1987b) Mineralogical and geochemical studies of the Emperor gold telluride deposit, Fiji. Econ Geol 82:345–370

Anderson W B, Antonio M, Davis B, Jones G, Settefield T, Tua P (1987) The Emperor epithermal gold deposit, Vatukoula, Fiji. Proc Pac Rim Congress '87. Australas Inst Min Metall, Parkville, Victoria, pp 9–12

Antoniuk T, Crombie D R (1982) The Pinson Mine, a Carlin-type gold deposit. Can Min J 103:61–65

Arvanitides N, Galanopoulos V, Kalogeropoulos S, Skamnelos G, Papavassiliou C, Paritsis S, Bostrom K (1988) Drilling at Santorini volcano, Greece. EOS, Am Geophys Un 69:578–579

Ashley P M, Dudley R J, Lesh R H, Marr J M, Ryall A W (1988) The Scuddles Cu-Zn prospect, an Archean volcanogenic massive sulfide deposit, Golden Grove district, Western Australia. Econ Geol 83:918–951

Bagby W C, Berger B R (1985) Geologic characteristics of sediment-hosted, disseminated precious-metal deposits in the Western United States. Rev Econ Geol 2:169–202

Ballance P F (1976) Evolution of the upper Cenozoic magmatic arc and plate boundary in northern New Zealand. Earth Planet Sci Lett 28:356–370

Barberi F, Innocenti F, Ferrara G, Keller J, Villari L (1974) Evolution of the Aeolian arc volcanism (Southern Tyrrhenian Sea). Earth Planet Sci Lett 21:269–276

Barker R E G (1989) Neavesville gold-silver prospect recent exploration. Australas Inst Min Metall Monogr 13. Parkville, Victoria, pp 57–58

Barnes H L (1990) Hydrothermal fluids and the deposition of ore minerals, with emphasis on gold, silver and copper. Course Notes; Economic Geology Research Unit. Univ Witwatersrand, Feb 1990

Bates T E (1989) Te Aroha goldfield Tui and Wairongomai gold/ silver/base metal prospects. Australas Inst Min Metall Monogr 13. Parkville, Victoria, pp 79–88

Berger B R (1980) Geological and geochemical relationships at the Getchell mine and vicinity, Humboldt County, Nevada. Soc Econ Geol Field Trip Guide 111:135

Berger B R (1985) Geologic-geochemical features of hot spring precious-metal deposits. In: Tooker E W (ed) Geologic characteristics of sediment- and volcanic-hosted disseminated gold deposits – search for an occurrence model. US Geol Surv Bull 1646:47–53

Berger B R, Eimon P (1982) Comparative models of epithermal gold-silver deposits. Soc Min Eng Reprint 82–13:25 pp

Berger B R Bethke P M (eds) (1985) Geology and geochemistry of epithermal systems. Rev Econ Geol 2

Bird D K, Schiffman P, Elders W A, Williams A E, McDowell SD (1984) Calc-silicate mineralization in active geothermal systems. Econ Geol 79:671–695

Bonham H F (1986) Models for volcanic-hosted epithermal precious metal deposits: a review. In: Proc Symp 5 Int Volcanol Congr, Auckland, N Z, pp 13–17

Brathwaite R L, McKay D F (1989) Geology and exploration of the Martha Hill gold-silver deposit, Waihi. Australas Inst Min Metall Monogr 13. Parkville, Victoria, pp 83–88

Brathwaite R L, Pirajno F (in prep) Metallogenic Map of New Zealand. N Z Geol Surv Bull. Govt Print, Wellington

Brathwaite R L, McKay D F, Henderson S (1986) The Martha Hill gold-silver deposit, Waihi. In: Proc Symp 5 Int Volcanol Congr, Auckland, N Z, pp 19–23

Brathwaite R L, Christie A B, Skinner D N B (1989) The Hauraki goldfield. Regional setting, mineralisation and recent exploration. Australas Inst Min Metall Monogr 13. Parkville, Victoria, pp 45–56

Browne K L (1978) Hydrothermal alteration in active geothermal fields. Earth Planet Sci Ann Rev 6:229–250

Browne K L (1986) Gold deposition from geothermal discharges in New Zealand. Econ Geol 81:979–983

Browne P R L, Ellis A J (1970) The Ohaki-Broadlands hydrothermal area, New Zealand: mineralogy and related geochemistry. Am J Sci 209:97–131

Buchanan L J (1981) Precious metal deposits associated with volcanic environments in the southwest. In: Dickinson W R, Payne W D (eds) Relation of tectonics to ore deposits in the South Cordillera. Ariz Geol Soc Digest 14:237–262

Bullard F M (1984) Volcanoes of the Earth. University of Texas Press, Austin, Texas, 629 pp

Camus F (1985) Geologia de los yacimientos epitermales de oro en Chile y posible modelo idealizado. In: Frutos J, Oyarzun Munoz R, Pincheira Munez M (eds) Geologia y recursos minerales de Chile. Univ Press, Concepcion, Inscr 63765, pp 653–690

Carney J N, MacFarlane A (1978) Lower to middle Miocene sediments on Maewo, New Hebrides, and their relevance to the development of the outer Melanesian arc system. Bull Aust Soc Expl Geophys 9:123–130

Christie A B, Brathwaite R L (1986) Epithermal gold-silver and porphyry copper deposits of the Hauraki goldfield – a review. In: Henley R W, Hedenquist J W, Roberts P J (eds) Guide to the

active epithermal (geothermal) systems and precious metal deposits of New Zealand. Monograph series on mineral deposits 26. Gerbruder Bornträger, Berlin, pp 129–145

Cole D R, Drummond S E (1986) The effect of transport and boiling on Ag/Au ratios in hydrothermal solutions: a preliminary assessment and possible implications for the formation of epithermal precious-metal ore deposits. J Geochem Expl 25:45–79

Cole J W (1981) Genesis of lavas of the Taupo Volcanic Zone, North Island, New Zealand. J Volc Geotherm Res 10:317–337

Cole J W (1984) Taupo-Rotorua depression: an ensialic marginal basin of North Island, New Zealand. In: Kokelaar B P, Howells M F (eds) Marginal basin geology: volcanic and associated sedimentary and tectonic processes in modern and ancient marginal basins. Geol Soc London Spec Publ 16:109–120

Cole J W (1986) Volcanism in the Taupo Volcanic Zone In: Henley R W, Hedenquist J W, Roberts P J (eds) Guide to active epithermal (geothermal) systems and precious metal deposits of New Zealand. Monograph series on mineral deposits 26. Gebruder Bornträger, Berlin, pp 23–28

Cole J W Lewis K B (1981) Evolution of the Taupo-Hikurangi subduction system. Tectonophysics 72:1–21

Colley H, Greenbaum D (1980) The mineral deposits and metallogenesis of the Fiji Platform. Econ Geol 75:807–870

Colley H, Rice C M (1975) A kuroko-type ore deposit in Fiji. Econ Geol 70:1373–1386

Criss R E, Taylor H P (1986) Meteoric-hydrothermal systems. In: Valley J W, Taylor H P, O'Neil I R (eds) Stable isotopes in high temperature geological processes. Reviews in Mineralogy, vol 16. Am Min Soc, pp 373–424

Cunneen R, Sillitoe R H (1989) Paleozoic hot spring sinter in the Drummond Basin, Queensland, Australia. Econ Geol 84:135–142

Davies R M, Ballantyne G H (1987) Geology of the Ladolam gold deposit Lihir island, Papua New Guinea. In: Proc Pac Rim '87 Congr. Australas Inst Min Metall, Parkville, Victoria, pp 943–949

De Ronde C E J, (1986) The Golden Cross gold-silver deposit. In: Henley R W, Hedenquist J W, Roberts P J (eds) Guide to the active epithermal (geothermal) systems and precious metal deposits of New Zealand. Monograph series on mineral deposits 26. Gebruder Bornträger, Berlin, pp 165–184

Dickson F W, Rye R O, Radtke A S (1979) The Carlin gold deposit as a product of rock-water interaction. Proc 5th IAGOD Sympos 2. Stuttgart, pp 101–108

Doumas C (ed) (1978) Thera and Aegean World. 2nd Int Sci Congr. Santorini, Greece

Economic Geology (ed) (1988) A special issue devoted to the geology and mineral deposits of Mexico. Econ Geol 83, 8

Eldridge C S, Barton P B, Ohmoto H (1983) Mineral textures and their bearing of formation of the kuroko orebodies. Econ Geol Monogr 5:241–281

Ellam R M, Menzies M A, Hawkesworth C J, Leeman W P, Rosi M, Serri G (1988) The transition from calc-alkaline to potassic orogenic magmatism in the Aeolian islands, southern Italy. Bull Volc 50:386–398

Ellis A J (1979) Explored geothermal systems. In: Barnes H L (ed) Geochemistry of hydrothermal ore deposits. John Wiley & Sons, New York, pp 632–683

Ellis A J, Mahon W A J (1977) Chemistry and geothermal systems. Academic Press, New York, London, 392 pp

Ewers R G, Keays R R (1977) Volatile and precious metal zoning in the Broadlands geothermal field, New Zealand. Econ Geol 72:1337–1354

Facca G, Tonani F (1967) The self-sealing geothermal field. Bull Volcanol 30:271–273

Faraone D, Silvano A, Verdiani G (1986) The monzo-gabbroic intrusion in the island of Vulcano, Aeolian archipelago, Italy. Bull Volc 48:299–307

Field C W, Fifarek R H (1985) Light-stable isotope systematics in the epithermal environment. Rev Econ Geol 2:99–128

Fournier R O (1989) Geochemistry and dynamics of the Yellowstone National Park hydrothermal system. Ann Rev Earth Planet Sci 17:13–53

Franklin J M, Sangster D, Lydon J W (1981) Volcanic-associated massive sulfide deposits. Econ Geol 75th Anniv Vol, pp 485–627

Fuji K (1974) Tectonics of the Green Tuff Region, Northern Honshu, Japan. Min Geol Spec Issue 6:251–260

Gammons C H, Barnes H L (1989) The solubility of Ag_2S in near-neutral aqueous sulfide solutions at 25 to 300°C. Geochim Cosmochim Acta 53:279–290

Hauck M B (1988) Kuroko-type ore deposits on the Aegean Islands, Greece. In: Friedrich G H, Herzig P M (eds) Base metal sulphide deposits. Springer, Berlin, Heidelberg, New York, pp 216–228

Heald P, Foley N K, Hayba D O (1987) Comparative anatomy of volcanic-hosted epithermal deposits: acid-sulphate and adularia-sericite types. Econ Geol 82:1–26

Hedenquist J W (1983) Waiotapu geothermal field. Excursion handout notes on epithermal environments in New Zealand. Pt 2. Individ Geotherm Fields. Int Volcanol Congr, Auckland, N Z, pp F1-F16

Hedenquist J W (1986) Geothermal systems of the Taupo Volcanic Zone: their characteristics and relation to volcanism and mineralisation. R Soc N Z Bull 23:134–168

Hedenquist J W, Browne P R L (1989) The evolution of the Waiotapu geothermal system, New Zealand, based on the chemical and isotopic composition of its fluids, minerals and rocks. Geochim Cosmochim Acta 53:2235–2257

Hedenquist J W, Henley R W (1985) Hydrothermal eruptions in the Waiotapu geothermal system, New Zealand: origin, breccia deposits and effect on precious metal mineralization. Econ Geol 80:1640–1666

Hedenquist J W, Lindqvist W P (1985) Aspects of gold geology and geochemistry. Contrib Econ Geol Res Unit. James Cook Univ, Queensland

Hedenquist J, White N C, Siddeley G (eds) (1990) Epithermal gold mineralization of the Circum-Pacific: geology, geochemistry, origin and exploration, I. J Geochem Spec Issue 35, 447 pp

Henley R W, Berger B R (1988) Advances in the understanding of epithermal precious metal deposits. In: Bicentennial Gold '88. Geol Soc Aust Abstr Ser 22:277–283

Henley R W, Ellis A J (1983) Geothermal systems ancient and modern: a geochemical review. Earth Scie Rev 19:1–50

Henley R W, Hedenquist J W, Roberts P J (eds) (1986) Guide to active epithermal (geothermal) systems and precious metal deposits of New Zealand. Monograph series on mineral deposits. Gebruder Bornträger, Berlin, 211 pp

Hofstra A H, Leventhal J S, Northrop H R, Landis G P, Rye R O, Birak D J, Dahl A R 1991 Genesis of sediment-hosted disseminated-gold deposits by fluid mixing and sulfidization: Chemical-reaction-path modeling of ore-depositional processes documented in the Jerritt Canyon district, Nevada. Geology 19:36–40

Honnorez J (1969) La formation actuelle d'un gisement sous-marin de sulfures fumarolliens Vulcano (Mer Tyrrhenienne), Pt 1: les mineraux sulfures des tufs immergés faible profondeur. Mineral Depos 4:114–131

Horikoshi E (1969) Volcanic activity related to the formation of kuroko-type deposits in the Kosoku district, Japan. Mineral Depos 4:321–345

Hutchinson R W (1980) Massive base metal deposits as guides to tectonic evolution. In: Strangeway D W (ed) The continental crust and its mineral deposits. Geol Ass Can Spec Pap 20:659–684

Ishihara S (ed) (1974) Geology of kuroko deposits. Min Geol Spec Issue 6, 435 pp

Ishikawa Y, Sawaguchi T, Iwaya S, Horiuchi M (1976) The delineation of prospecting target for Kuroko deposits based on modes of volcanism of underlying dacite and alteration haloes. Min Geol 26:105–117

Jackson D (1983) Carlin Gold: a Newmont money generator keeps on renewing itself after sparking the rebirth of gold mining in Nevada. Eng Min J 184:38–43

Jambor J L (1979) Mineralogical evaluation of proximal-distal features in New Brunswick massive sulfide deposits. Can Miner 17:649–664

Kear D (1989) Mineral deposits of New Zealand. Australas Inst Min Metall Monogr 13. Parkville, Victoria, 225 pp

Lambert I B, Sato T (1974) The kuroko and associated deposits of Japan: a review of their features and metallogenesis. Econ Geol 69:1215–1236

Lindgren W (1933) Mineral deposits. McGraw-Hill, New York, 930 pp

Madrid R J, Bagby W C (1988) Gold occurrence and its relation to vein and mineral paragenesis in selected sedimentary-rock hosted, Carlin-type deposits in Nevada. In: Bicentennial Gold '88. Geol Soc Aust Abstr Ser 22:161–166

Martini M, Piccardi G, Cellini Legittimo P (1980) Geochemical surveillance of active volcanoes: data on the fumaroles of Vulcano (Aeolian Islands, Italy). Bull Volc 43:255–263

McKibben M A, Elders W A (1985) Fe-Zn-Cu-Pb mineralization in the Salton Sea geothermal system, Imperial Valley, California. Econ Geol 80:539–559

McKibben M A, Andes J P, Williams A E (1988) Active ore formation at brine interface in metamorphosed deltaic lacustrine sediemnts: the Salton Sea geothermal system, California. Econ Geol 83:511–523

Moyle A J, Doyle B J, Hoogvliet H, Ware A R (1990) Ladolam gold deposit, Lihir island. In: Hughes F E (ed) Geology of the mineral deposits of Australia and Papua New Guinea, vol 2. Australas Inst Min Metall Monogr 14. Parkville, Victoria, pp 1793–1805

Mroczeck C R (1982) Some aspects of the mineralisation of the Wainaleka massive sulphide prospect, Fiji. MSc Thesis, Victoria Univ, Wellington, N Z, 94 pp

Mutschler F E, Griffin M E, Scott Stevens D, Shannon S (1985) Precious metal deposits related to alkaline rocks in the North American Cordillera: an intrepretive review. Trans Geol Soc S Afr 88:355–377

Ohmoto H (1983) Geological, paleontological and tectonic studies, Pt 1. Geologic history of the Green Tuff Region. Econ Geol Monogr 5:9–23

Ohmoto H, Takahashi T (1983) Geological, paleontological and tectonic studies, Pt 3. Submarine calderas and kuroko genesis. Econ Geol Monogr 5:39–54

Ohmoto S, Skinner B J (eds) (1983) The kuroko and related volcanogenic massive sulfide deposits. Econ Geol Monog 5, 604 pp

Ohtagaki, T, Tsukada, Y, Hirayama, H, Fujioka, H, Miyoshi, T (1974) Geology of the Shakanai mine, Akita Prefecture. Min Geol Spec Issue 6:131–140

Panteleyev A (1986) A Canadian cordilleran model for epithermal gold-silver deposits. Geosci Can 13:101–111

Pisutha-Arnond V, Ohmoto H (1983) Thermal history, and chemical and isotopic compositions of ore-forming fluids responsible for kuroko massive sulfide deposits in the Hokoruku district of Japan. Econ Geol Monogr 5:523–558

Plimer I R, Andrew A S, Jenkins R, Lottermoser B G (1988) The geology and geochemistry of the Lihir gold deposit, Papua New Guinea. In: Bicentennial Gold '88. Geol Soc Aust Abstr Ser 22:139–143

Rabone S D C (1975) Petrography and hydrothermal alteration of Tertiary andesite-rhyolite volcanics in the Waitekauri Valley, Ohinemuri, New Zealand. N Z J Geol Geophys 18:239–258

Radtke A S, Dickson F W (1974) Genesis and vertical position of fine-grained disseminated replacement-type gold deposits in Nevada and Utah, USA. Proc 4th IAGOD Symp 1:71–78

Radtke A S, Scheiner B J (1970) Studies of hydrothermal gold deposition: Carlin gold deposit, Nevada: the role of carbonaceous material in gold deposition. Econ Geol 65:87–102

Radtke A S, Heropoulos C, Fabbi B P, Scheiner B J, Essington M (1972) Data on major and minor elements in host rocks and ores, Carlin gold deposit, Nevada. Econ Geol 67:975–978

Radtke A S, Dickson F W, Rytuba J (1974) Genesis of disseminated gold deposits of the Carlin type. Geol Soc Am Abst Programmes 1:239–240

Radtke A S, Rye R O, Dickson F W (1980) Geology and stable isotope studies of the Carlin gold deposit, Nevada. Econ Geol 75:641–672

Roberts R J, Radtke A S, Coats R R, Silberman M L, McKee E H (1971) Gold bearing deposits in north-central Nevada and south-western Idaho, with a section on periods of plutonism in north-central Nevada. Econ Geol 66:14–33

Robinson B W (1974) The origin and mineralisation of the Tui mine, Te Aroha, New Zealand, in the light of stable isotope studies. Econ Geol 69:910–925

Rogerson R, McKee C 1990 Geology, volcanism and mineral deposits of Papua New Guinea. In: Hughes F E (ed) Geology of the mineral deposits of Australia and Papua New Guinea. Australas Inst Min Metall Monogr 14. Parkville, Victoria, pp 1689–1701

Rossiter R D (1984) Epithermal gold deposits: their geology and genesis. MSc Thesis, Rhodes Univ, Grahamstown, 132 pp

Rugless C S (1983a) Lithogeochemistry of Wainaleka Cu-Zn volcanogenic deposit, Viti Levu, Fiji, and possible applications for exploration in tropical terrains. J Geochem Explor 19:563–586

Rugless C S (1983b) Geology and geochemistry of Wainaleka copper zinc deposit, Viti Levu, Fiji. PhD Thesis, Univ NSW, Sydney, 187 pp

Rye R O (1985) A model for the formation of carbonate-hosted disseminated gold deposits based on geologic, fluid inclusions, geochemical, and stable-isotope studies of the Carlin and Cortez deposits, Nevada. US Geol Surv Bull 1646:35–42

Rye R O, Doe B R, Wells J D (1974) Stable isotope and lead isotope study of the Cortez, Nevada, gold deposit and surrounding area. US Geol Surv J Res 2:13–23

Sangster D F, Scott S D (1976) Precambrian stratabound massive sulphide ores of North America. In: Wolf K H (ed) Handbook of strata-bound and stratiform ore deposits, vol 6. Elsevier, Amsterdam, pp 129–222

Sato T (1974) Distribution and geological setting of the kuroko deposits. Soc Min Geol Jpn Spec Issue 6:1–10

Sawkins F H (1976) Massive sulphide deposits in relation to geotectonics. In: Strong D F (ed) Metallogeny and plate tectonics. Geol Ass Can Special Pap 14:221–240

Sawkins F H (1990) Metal deposits in relation to plate tectonics, 2nd edn. Springer, Berlin, Heidelberg, New York, 461 pp

Seward T M (1979a) Hydrothermal transport and deposition of gold. In: Glover J E, Grove D I (eds) Gold Mineralisation. Univ W Aust Extens Serv Publ 3:45–55

Seward T M (1979b) Modern hydrothermal systems in New Zealand and their relation to gold mineralisation processes.In: Glover J E, Grove D I (eds) Gold Mineralisation. Univ W Aust Extens Serv Publ 3:56–64

Shenberger D M, Barnes H L (1989) Solubility of gold in aqueous sulfide solutions from 150 to 350° C. Geochim Cosmochim Acta, 53:269–278

Shirozu H (1974) Clay minerals in altered wall rocks of the kuroko-type deposits. Min Geol Spec Issue 6:303–311

Siddeley G, Araneda R (1986) The El Indio-Tambo gold deposits, Chile. In: Proc Gold '86 Symp. Toronto, pp 445–456

Silberman M L, Berger B R (1985) Relationship of trace element patterns to alteration and morphology in epithermal precious-metal deposits. Rev Econ Geol 2:203–232

Sillitoe R H (1980) Are porphyry and kuroko-type massive sulphide deposits incompatible? Geology 8:11–14

Sillitoe R H (1982) Extensional habits of rhyolite-hosted massive sulfide deposits. Geology 10:403–407

Sillitoe R H, Bonham H F (1984) Volcanic landforms and ore deposits. Econ Geol 79:1286–1298

Sillitoe R H, Bonham H F (1990) Sediment-hosted gold deposits: distal products of magmatic-hydrothermal systems. Geology 18:157–161

Sillitoe R H, Grauberger G L, Elliott J E (1985) A diatreme-hosted gold deposit at Montana Tunnels, Montana. Econ Geol 80:1707–1721

Simmons B D (1973) Geology of the Millenbach massive sulphide deposit, Noranda, Quebec. Can Inst Min Metall Bull 66:67–73

Skinner D N B (1986) Neogene volcanism of the Hauraki Volcanic Region. R Soc NZ Bull 23:21–47

Smith P A, Cronan D S (1983) The geochemistry of metalliferous sediments and waters associated with shallow submarine hydrothermal activity (Santorini, Aegean Sea). Chem Geol 39:241–262

Spence C D (1975) Volcanogenic features of the Vauze sulfide deposit, Noranda, Quebec. Econ Geol 70:102–114

Spence C D, De Rosen-Spence A F (1975) The place of sulfide mineralization in the volcanic sequence at Noranda, Quebec. Econ Geol 70:90–101

Tatsumi T (Ed) (1970) Volcanism and ore genesis. Univ Press, Tokyo, 448 pp

Taylor G P (1987) Breccia formation and its relation to gold mineralisation at Mt Kasi, Fiji. In: Proc Pac Rim '87 Congr. Australas Inst Min Metall. Parkville, Victoria, pp 597–601

Thurlow J G, Swanson E A, Strong D F (1975) Geology and litho-geochemistry of the Buchans polymetallic sulfide deposits, Newfoundland. Econ Geol 75:130–144

Tingley J V, Berger B R (1985) Lode good deposits of Round Mountain, Nevada. Nev Bur Min Geol Bull 100:62 pp

Tooker E W (ed) (1985) Geologic characteristics of sediment-and volcanic-hosted disseminated gold deposits. Search for an occurrence model. US Geol Surv Bull 1646, 150 pp

Urabe T, Scott S D, Hattori K (1983) A comparison of foot-wall rock alteration and geothermal systems beneath some Japanese and Canadian volcanogenic massive sulfide deposits. Econ Geol Monogr 5:345–364

Vallette J N, Picot P (1981) Les dépots fumaroliens terrestres et marins de l'Ile de Vulcano (Italie). Bull Volcanol 44:11–29

Walker R R, Matulich A, Amos A C, Watkins J J, Mannard G W (1975) The geology of the Kidd Creek mine. Econ Geol 75:80–89

Walter M R, Bauld J, Brock T D (1972) Siliceous algal and bacterial stromatolites in hot springs and geyser deposits of Yellowstone National Park. Science 178:402–405

Watson D P (1989) The geology, mineralisation and field relationships of the Kauaeranga cinnabar deposits. In: Kear D. (ed) Mineral deposits of New Zealand. Australas Inst Min Metall Monogr 13. Parkville, Victoria, pp 63–66

Weissberg B G (1969) Gold-silver ore-grade precipitates from New Zealand thermal water. Econ Geol 64:95–108

Weissberg B G, Browne P R L, Seward T M (1979) Ore metals in active geothermal systems. In: Barnes H L (ed) Geochemistry of hydrothermal ore deposits. John Wiley & Sons, New York, pp 738–780

Wells J D, Stoiser L R, Elliott J E (1969) Geology and geochemistry of the Cortez gold deposit, Nevada. Econ Geol 64:526–537

White D E (1955) Thermal springs and epithermal ore deposits. Econ Geol 50th Anniv Vol, pp99–154

White D E (1974) Diverse origin of hydrothermal ore fluids. Econ Geol 69:954–973

White D E (1981) Active geothermal systems and hydrothermal deposits. Econ Geol 75th Anniv Volume, pp 392–423

White D E (1985) Summary of the Steamboat Springs geothermal area, Nevada, with attached road-log commentary. US Geol Surv Bull 1646:79–87

White N C, Wood D G, Lee M C (1989) Epithermal sinters of Paleozoic age in north Queensland, Australia. Geology 17:718–722

Williams G J (1974) Economic Geology of New Zealand. Australas Inst Min Metall Monogr 4. Parkville, Victoria, 490 pp

Wodzicki A, Weissberg B G (1970) Structural control of base metal mineralisation at the Tui Mine, Te Aroha, New Zealand. NZ J Geol Geophys 13:610–630

Chapter 12
Hydrothermal Processes in Oceanic Crust
and Related Mineral Deposits

12.1 Introduction

Following a brief review of the main physiographic features of the ocean floor and the nature and structure of the oceanic lithosphere, this chapter looks in some detail at the hydrothermal processes which take place as a result of sea water percolation into large sectors of the oceanic crust in the mid-oceanic regions. It further examines the mineral deposits that result from this activity, both in the present-day sea floor and in the geological record (ophiolite belts). Excluded from this discussion are the hydrogenous sea-floor deposits of Mn-rich nodules, which are believed to form by direct precipitation of metals from sea water, although the metal components are possibly derived from the hot springs that issue at mid-ocean ridges, and are subsequently dispersed in sea water.

The reader is reminded that there are many other hydrothermal systems that discharge at, or close to, the sea-floor. Most of the hydrothermal systems that occur in regions of high heat flow, such as island arcs (for example, the kuroko systems (discussed in Chap. 11) and rift-related settings (Chap. 13), share similarities with those that are formed at sea-floor spreading centres. As pointed out in the beginning of Chapter 3, the evolutionary stages of a rift system have to be taken into account. An incipient rift may initially form a narrow sea way, for example the Red Sea, in which hydrothermal discharge at several sites results in syngenetic metalliferous deposits. The presence of oceanic crust in these early stages of opening is confined to narrow strips, or it has not yet made its appearance on the sea floor. We take up this topic again in a section discussing the development and closure of an ocean basin.

An understanding of the nature, composition and structure of the oceanic lithosphere has been largely obtained from geophysical techniques. Profiles of the sea-floor and the construction of bathymetric charts are obtained by the use of single and multibeam echo sounding. The side-scan sonar imaging system, in conjunction with the multibeam echo sounding, provides images of the ocean floor and its main structural features. Cross-sections of the oceanic layers are obtained from refraction and reflection seismic surveys. Recently, beautiful global maps of the oceans showing, relative to the scale, the detailed topography of the ocean floors, have been produced by means of bathymetric measurements from orbiting satellites (e.g. SEASAT). This technique surveys the surface of the oceans by radar altimeters with a precision of a few centimetres. Small variations in the shape of the ocean surfaces in relation to the geoid (surface of equal gravity) are determined by the topography of the floor, as the force of gravity gives the geoid undulations which

correspond to topographic highs and lows of the ocean floor. This radar survey filters out the effects of the motions of the sea, caused by currents, wave actions, barometric pressure etc. The use of both manned and unmanned submersible crafts since the 1960s has provided us with direct observations of the sea-floor and its geological phenomena, particularly the discharge of hot springs in the axial regions of mid-ocean ridges. Deep sea drilling has also contributed much to the data base, where probing hundreds of metres into the sea-floor has provided geological records that could be compared with that of on-land oceanic sequences. Nevertheless, the most complete lithological and stratigraphic successions are provided by these on-land oceanic sequences, that is, the ophiolite complexes (see Chap. 6). Accordingly, for a more complete understanding of igneous and metamorphic processes and the products of hydrothermal activity in oceanic crust environments, we turn to the study of ophiolitic rocks.

Suggested literature for the reader who is interested in marine geology and details of the sea-floor and the evolution of ocean basins, includes Kennett (1982), Seibold and Berger (1982) and a book by the Open University oceanography team (Open University 1989). A collection of Scientific American papers entitled *The Ocean* (Scientific American 1969) makes excellent reading on a wide range of topics concerning the oceans of the Earth.

12.2 Physiography of the Ocean Floor

A typical profile of the ocean floor, for example across the Atlantic ocean, clearly shows at least three principal elements in the morphology of this oceanic area, namely: continental margins, comprising a continental shelf, slope and rise; the abyssal plains; and the mid-ocean ridge. The continental margins of the Atlantic Ocean are called Atlantic-type, or aseismic or passive margins, developed initially from the rifting of a continental mass. The Red Sea represents the early stages in the making of an ocean, in which the sea has invaded the opening created by the rifting of a continent. A profile across the Pacific Ocean shows a rather different picture in which some new physiographic elements can be seen. The Pacific margins, which are of the active type and very much seismic, indicate on-going tectonic and magmatic activity, which is topographically expressed by deep submarine trenches and festoons of volcanic islands. The collision of oceanic and continental plates in the Pacific gives rise to Chilean-type margins, whereas collision of two oceanic plates gives rise to the Mariana-type margins, which, as explained in Chapter 6, result in different types of subduction zones (see Fig. 6.7). Other important physiographic features to be found in all oceans are transform faults, fracture zones and seamounts. Together with the mid-ocean ridges, they constitute very important areas in terms of ore-making processes, owing to their permeability which allows the ingress of large amounts of sea water, and to their associated magmatic activity which provides the heat source for the convective circulation of heated sea water.

In addition to the above features, the ocean basins are also characterised by the presence of plateaux, some of which are remnants of volcanic chains, or

accumulation of basaltic material formed at hot spots or spreading centres (Nur and Ben-Avraham 1982). There are, however, many oceanic plateaux – particularly in the Pacific – whose origins are not clear. Some of these may be pieces of continental crust, or microcontinents, which have become isolated and submerged following the fragmentation of larger continental masses. The Chatham Rise and Campbell Plateau, east of New Zealand, form part of a submerged microcontinent, the western portion of which is made up of the islands of New Zealand at the boundary between the Pacific plate and the Indo-Australian plate. Several of these oceanic plateaux constitute allochthonous terranes after they have "docked" to a continental margin. This topic is discussed in more detail in Chapters 5 and 6.

A view of an ocean basin with oceanic ridges, transform faults, seamounts and trenches is schematically represented in Figs. 6.1, 6.2 and 12.6.

12.2.1 Mid-Ocean Ridges

The most conspicuous topographic features of the ocean basins are the mid-ocean ridges (the word "ridge", however, does not do justice to what is effectively the longest mountain range on the planet Earth). They extend through all the oceans for a total length of approximately 75 000 km at an average depth of 2500 m below sea level, with widths of up to 1000 km and heights above the surrounding sea-floor ranging from approximately 1000 to 3000 m. The mid-ocean ridges usually occur in the middle part of an ocean basin (hence the adjective "mid"), except in the Pacific Ocean where they are for the most part confined to the northeast and eastern parts of the basin. Only in one place does the mid-ocean ridge have a terrestrial expression, and that is Iceland, an island which straddles, and is part of, the mid-Atlantic ridge system. The ridges are characterised by a highly rugged topography and are formed by a ridge crest and ridge flanks, which extend more or less symmetrically for hundreds of kilometres, on either side of the crest. Within the ridge crest a central rift valley, 1 to 2 km deep and up to 30–35 km wide, may occur. These median rift valleys are characterised by a series of inward-facing escarpments up to a few hundreds of metres high. The deepest part of a rift valley forms the inner floor, which is a flattish area where accumulation of lava flows takes place. However, the development of the rift valleys is a function of the rate of spreading. The mid-ocean ridge in the Atlantic has an average spreading rate of 1 to 2 cm yr^{-1} (slow-spreading centre) and the resulting median rift valleys are well developed and deep. By contrast, in the Pacific ocean where spreading rates are of the order of 5 to 8 cm yr^{-1} (fast-spreading centre), the resulting ridge profiles are smoother and much less rugged, and the median rift valley may be absent altogether. The mid-ocean ridges are seismically and volcanically active, particularly in the axial regions, where new crust, which is in fact created as magma is injected and poured out on the sea-floor, which then spreads apart. Most of the sub-sea-floor hydrothermal discharges occur in the axial regions.

Mid-ocean ridges are interrupted by "discontinuities" of which MacDonald and Fox (1990) recognise at least four types (first-, second-, third- and fourth-order discontinuities). Transform faults (discussed below) are first-order discontinuities.

In fast-spreading centres a second order discontinuity is formed by overlapping spreading centres which offset the ridge by a few kilometres. In slow-spreading centres these overlaps result in a bend of the rift valley. Third- and fourth-order discontinuities are characterised by small overlaps, in the order of hundreds of metres, and/or slight deviations of the ridge axis (MacDonald and Fox 1990). According to these authors the origin of these discontinuities could be related to breaks or inhomogeneities of magma supply. On the basis of gravity and seismic data, they suggest that molten mantle material rises from depths of 30 to 60 km to form shallow-seated magma chambers from which melts are intruded into fractures of the oceanic lithosphere eventually to form dykes or to erupt onto sea-floor. The magma chambers are lenses of molten rock situated above a zone or reservoir of partial melts. Discontinuities are formed in those areas where magma chambers and reservoirs are small and deep ($>$ 3 km), whereas below the ridge axis they occur at shallower depths (between 1.5 and 3 km).

12.2.2 Transform Faults and Fracture Zones

The ocean floor is cut by numerous fracture zones which can be seen on modern oceanic maps as parallel lines that usually transect the mid-ocean ridges at right angles, thereby indicating the direction of sea-floor spreading (see Fig. 12.6). The ridge axes are, in fact, offset by transform faults, along which the lithospheric plates slide past each other. Transform faults terminate at the end of each offset spreading ridge, and beyond these points the fault becomes a fracture, as no slip movement occurs since the fracture is, by this stage, entirely situated in one plate. The transform faults therefore also mark plate boundaries, which together with their fracture zone extensions, form small circles centred on the rotation pole of the lithospheric plates. Fracture zones can extend from several hundreds of kilometres up to a few thousand, and can be up to 100 km wide. They also have an irregular topography characterised by escarpments and troughs. "Leaky" transform faults are those along which generation of new crust takes place by virtue of the fact that they are oblique to the direction of spreading. In this case as the plates slide past each other the transform fault has to open in order to accomodate the new geometry, thus allowing melts to rise into the opening. Transform faults can continue into continents, such as is the case for the transform boundary between the Pacific and the North American plate. Here along the Gulf of California, this transform boundary becomes the Salton trough, and further to the north the much publicised San Andreas fault. As described in Chapter 11, the Salton trough is the site of intense on-land hydrothermal activity, and submarine hydrothermal activity has been discovered at a number of sites in the Gulf of California (Guaymas basin, discussed later; see also Fig. 3.10). Fracture zones can also continue into continental areas, where they may become the site of intracontinental alkaline volcanism, as is observed in southwestern Africa (Angola, Namibia, South Africa) where numerous alkaline complexes, carbonatites and kimberlites tend to occur along the on-land continuation of fracture zones in the South Atlantic (Marsh 1973; Prins 1981).

12.2.3 Seamounts and Volcanic Chains

Seamounts and volcanic chains are an important part of the ocean floor picture. Ocean floor volcanoes form off the ridge axis, and during sea-floor spreading ride along with the lithospheric plate. In so doing, some of these volcanoes may reach close to, or even emerge above the sea level, thus forming islands. However, as the plate continues its movement it cools and subsides, so that the volcanic island once again becomes submerged. These sunken island volcanoes are characterised by their flat tops, which are probably due to wave erosion, and as such are known as guyots and often occur as scattered isolated structures in the abyssal plains. The origin and nature of seamounts are not entirely understood, one of the questions being, for example, whether they are the product of eruptions from fractionating magma chambers that are decoupled from the main chamber beneath the axis, or whether in fact they are connected with it. In the latter case, the magma feeding the seamount is drawn from the more fractionated sides of the axis chamber from which more primitive melts are derived. This issue is not entirely academic because seamounts are clearly important for the production of hydrothermal deposits, as is detailed later.

Chains of seamounts – such as the Emperor Seamount Chain and the Hawaiian Ridge, or the Tuamoto Archipelago in the Pacific – are volcanic chains that are thought to form above stationary hot spots. As the oceanic plate moves over the hot spot it carries away the volcanic edifice that was constructed upon it. Age relationships for the Emperor Seamount Chain (the age of the volcanoes increases away from the currently active Hawaiian island towards the north-northwest and northwest) appear to corroborate this idea (Moberly and Campbell 1984; Thomas-Crough 1984). The "elbow" that marks the junction between the Emperor chain and the Hawaiian ridge is an effect of the change in the direction of spreading. The Walvis Ridge in the South Atlantic is thought to represent the trace of a hot spot (Schilling et al. 1985), and it is further thought that hot spot tracks in general are possibly the site of the initial rifting which begins the life cycle of an ocean basin (Duncan 1981; Morgan 1983).

12.3 Birth, Life and Death of an Ocean Basin

We have mentioned that mid-ocean ridges are constructive margins, where new oceanic crust is more or less continuously created by the upwelling of magma in the axial rift valleys. As it is assumed that the size of the Earth has remained practically constant for most of its geological history, the creation of new crust at the spreading centres must be counterbalanced by the destruction of an equal amount of crustal material. This takes place in zones of subduction (as we have seen in Chaps. 5 and 6), along which the oceanic crust with its sedimentary cover plunges into the mantle. The present-day oceanic crust is characteristically young, in fact no older than the Jurassic (about 150–160 Ma), as for example in the north-northwest of the Pacific ocean and along the eastern seaboard of North America. It has been noted that the

Fig. 12.1. Depth-age relationship, observed (*shaded*) and theoretical (*solid line*). The theoretical curve is calculated assuming that the oceanic litosphere thermally contracts as it cools and moves away from the axis of the spreading centre (After Open University 1989)
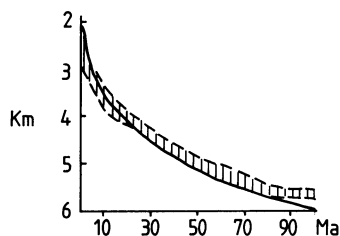
depth of an ocean basin increases with distance from the ridge axis and with the age of the lithosphere. More specifically, the average depth away from the ridge may be expressed as a linear relationship, which varies with the square root of the age of the oceanic crust (Fig. 12.1). From this figure the approximate age of the oceanic crust can be determined if the depth, corrected for sediment cover, is known. However, as is clear from Fig. 12.1, the age-depth relationship is not applicable beyond an age excceding 100 Ma, because on reaching thermal equilibrium the curve tends to reach a constant value. Further limitation is that the fast-spreading ridges are deeper than slow-spreading ridges (Open University 1989). From this it is clear that the oceanic crust of a fast-spreading ridge will have a greater volume than that created by a slow-spreading ridge; also, during episodes of fast spreading, the sea level has to rise because of the bulging lithosphere (Kennett 1982).

There are several lines of evidence to indicate that throughout the history of our planet oceans have formed and disappeared in a series of geotectonic cycles, of which a brief discussion is given in Chapter 5. Figure 12.2 illustrates the evolution of an ocean basin which begins with the inception of rifting in a continental mass, from its embryonic stage, through to its young, mature and terminal stages, and finally to the relics of former oceanic crust, as shown by ophiolitic rocks along suture zones.

The East African rift valleys are zones of crustal extension and uplift heralding a rupture of the crust and its eventual spreading. The next stage is characterised by young, narrow sea arms bound by subparallel coast lines. The Red Sea and the Gulf of Aden are modern-day examples of this stage of ocean development. The widening of the rift between the Arabian peninsula and Africa probably began some 20 Ma ago and is continuing today. The reconstruction of the fit between the two shore lines is remarkable, except for the Afar Triangle which is overlapped by the southwest corner of Arabia. During these initial stages shallow, and locally ephemeral, marine basins form, and if the climatic conditions are right, evaporation of these lake-size seas will result in the deposition of great quantities of evaporites. This is indeed the case for the Red Sea, where evaporites up to 4 km thick are present along the flanks of the rift. As mentioned in Chapter 3 and described in Chapter 13, the presence of evaporites may play a very important role in the genesis of sulphide orebodies. From this young Red Sea stage follows a mature stage, in which an ocean basin develops with an active mid-ocean ridge. This is the stage of the Atlantic Ocean today. Most geoscientists agree that in all probability the Atlantic Ocean did not exist 150 Ma ago and that it was the rifting and fragmentation of the Pangea supercontinent which began in the Mesozoic that eventually led to the opening and
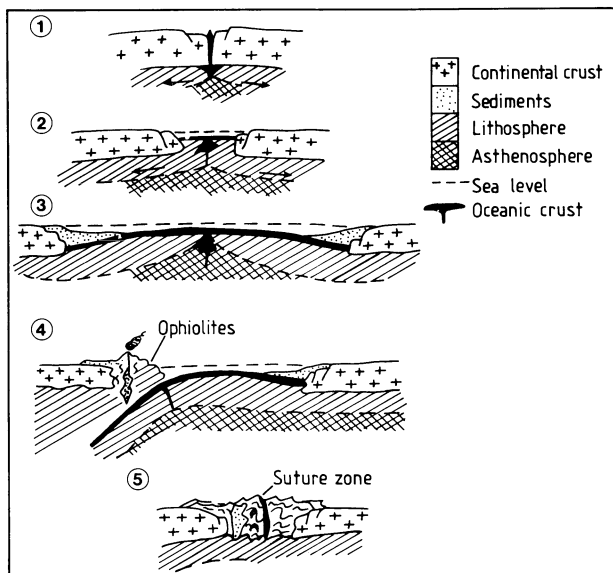
Fig. 12.2. The birth, life and death of an ocean basin. *1* A rift is formed in continental crust, and is characterised by graben structures and bimodal continental magmatism; present-day examples are the rift valleys of the East African rift system. *2* Splitting of the continental crust forms an elongate sea basin, evaporites and terrigenous sediments accumulate; a present-day example of this stage is the Red Sea. *3* Sea-floor spreading continues and an oceanic basin is formed, sedimentation takes place at the passive continental margins; this is the stage of the Atlantic ocean. *4* The ocean basin begins to close, a subduction zone is developed and a magmatic arc forms on the overriding continental margin, oceanic crust material is intruded into wedges of trench sediments (accretionary subduction complex) forming belts of melange and ophiolites; some parts of the Pacific Ocean could be represented by this stage (e.g. Andean margin); the two continental margins continue to move towards each other, in a situation that could be compared to the movevemnt of India towards Eurasia during closure of the Tethys Ocean. *5* Collision takes place and the opposing continental masses are "sutured", with only fragments of oceanic material being squeezed along the line of collision (suture zone); the ocean basin is now completely closed. Re-opening can occur and the cycle is repeated

development of the ocean as we see it today. Prior to this, another ocean existed – namely, the Iapetus – the opening and closing of which led to the formation of the Caledonides, Hercynides and the Appalachian orogens (Chap. 5). The Atlantic has passive, aseismic margins in which sedimentary rocks, including reef carbonates, turibidites and evaporites, predominate. A more mature, or even declining stage is characterised by fast-spreading ridges, subduction zones and magmatic arcs. The Pacific Ocean is clearly representative of this stage of ocean development. Closure of the ocean basin is the final or terminal stage, during which shrinking, uplift and collision with the rising of young mountain ranges, take place. The Mediterranean Sea, Black Sea and Caspian Sea, together with the Alpine-Caucasus-Elburs mountain ranges, may be representative of this stage today. These seas are possibly the remnants of the great Thethys, an east-west-trending ocean that separated the Laurasian continents in the north from the Gondwana continent in the south. The

movement of these two large landmasses towards each other led to the gradual disappearance of Thethys during a number of complex geotectonic events, briefly reviewed in Chapter 5. Finally, as collision continues, all bodies of water disappear, mountain ranges rise and develop further, so that all that remains of the former ocean are the so-called suture zones, in which slivers of oceanic crust are preserved. The Indus suture in the Himalayas is an example of this stage.

12.4 Oceanic Lithosphere and Ophiolites

We have mentioned that knowledge of the structure and nature of the oceanic lithosphere is derived from geophysical, deep-sea drilling, direct observations by submersible crafts, and the study of ophiolitic rocks. The integration of the data thus obtained has enabled the construction of models of oceanic lithosphere such as those shown in Figs 6.3 and 12.3. With reference to Fig. 12.3, the upper portion of the oceanic lithosphere, the oceanic crust proper, is formed by basaltic and gabbroic rocks which are the products of consolidation of upwelling mantle partial melts. The rest of the lithosphere, beneath this zone of mafic rocks is essentially the refractory residue of these partial melts that have been injected into the already consolidated crust and erupted at the surface. The separation between these two zones is marked by the Mohorovicic discontinuity, or Moho, which lies at a depth of approximately 7–10 km depending on the distance from the ridge. Below the refractory layer, that is, the lower lithosphere boundary, is the pristine upper mantle material, or asthenosphere, which extends down to about 300 km, and in which temperatures approach the melting point and lateral flow can occur on account of its plastic behaviour. Owing to its rheological properties the asthenosphere is identified with a low velocity zone, or attenuation of P- and S-seismic waves.

It is beyond the scope of this book to detail the igneous processes and various petrogenetic models that have been proposed to account for the nature and compositions of the rocks that compose the oceanic lithosphere. For this the reader is referred to Burke et al. (1981), Best (1982), Hughes (1982), Wilson (1989) and the collection of specialised papers edited by Toksoz et al. (1980), Gass et al. (1984) and Beccaluva (1989). For the present purpose it will suffice to say that generation of magma at mid-ocean ridges takes place by adiabatic decompression of the asthenospheric mantle material, which rises below the ridge and partially melts to produce magmas of basaltic composition. There is evidence that zoned magma chambers may be present just below the ridge axis. According to Burke et al. (1981), olivine cumulates are deposited near the magma supply axis, which grade into clinopyroxene-rich cumulates and into clinopyroxene-plagioclase cumulates towards the edges of the chamber. The size, shape and depth of the magma chambers, as shown in Fig. 6.3 and previuosly mentioned, probably differ in slow- and fast-spreading ridges. The magma chamber more or less continuously injects molten material along fissures, which consolidates to form dykes and feed the eruption of lavas on the ocean floor. The mid-ocean ridges are in fact, the site of almost continuous volcanic activity. In contrast, the volcanism of off-axis submarine
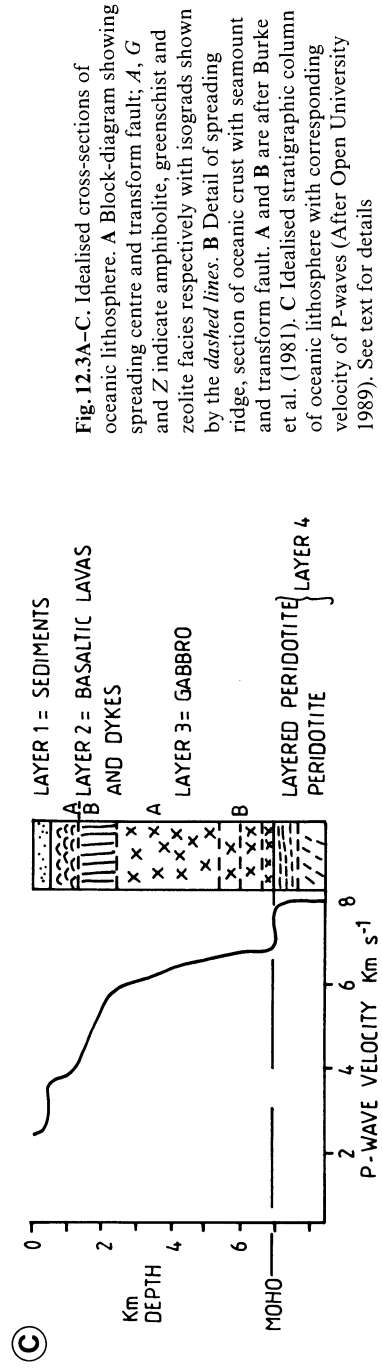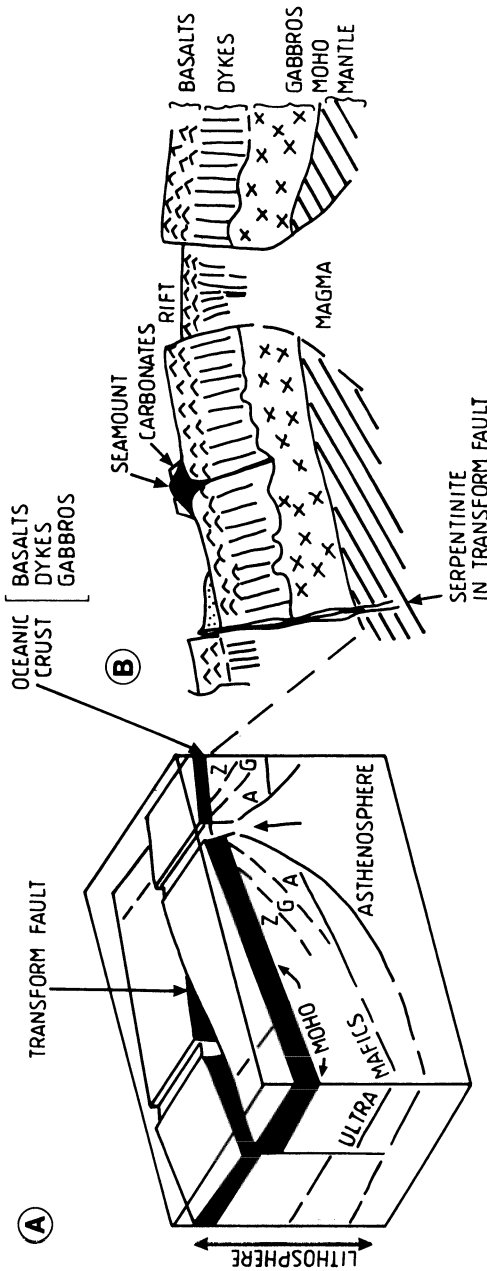
Fig. 12.3A–C. Idealised cross-sections of oceanic lithosphere. A Block-diagram showing spreading centre and transform fault; *A*, *G* and *Z* indicate amphibolite, greenschist and zeolite facies respectively with isograds shown by the *dashed lines*. B Detail of spreading ridge, section of oceanic crust with seamount and transform fault. A and B are after Burke et al. (1981). C Idealised stratigraphic column of oceanic lithosphere with corresponding velocity of P-waves (After Open University 1989). See text for details

volcanoes (guyots) is short-lived, substantiating the idea that the feeding magma chambers are decoupled from the asthenospheric mantle and as such may evolve independently.

Above the magma chamber is a zone of dykes – a sheeted dyke complex – which is in turn overlain by the basaltic lavas. The cooling and crystallisation of the chamber melt produces gabbroic rocks at the top and along the sides, with layered gabbros at the bottom. These in turn pass below the Moho into depleted harzburgite and lherzolite (upper mantle peridotite), which has led to the subdivision of the oceanic lithosphere into the four layers (Fig. 12.3) described below.

Layer 1 is the veneer of unconsolidated oceanic sediments, including clays, siliceous and calcareous oozes. This layer is on the average about 0.5 km thick, but is absent at the ridge crest, with the possible exception of local basins. The oceanic sediments of layer 1 thicken away from the ridge areas towards the continental margins. The thickness of the oceanic sediments can reach 5 km beneath parts of the continental rise bordering the Atlantic Ocean (Bott 1982). Layer 2, comprising the basaltic lavas and dykes, is further subdivided into layer 2A (basaltic pillow lavas and sheet lava flows) and 2B (dykes). Layer 2 is between 1 and 2.5 km thick and characterised by P wave velocities of between 3.4 and 6.2 km s^{-1} (Bott 1982). The composition of the basaltic lavas, usually labelled MORB (mid-ocean ridge basalts), is variable and depends on a number of factors, which Wilson (1989) summarised as follows: composition of the source mantle; degree of partial melting (about 20% partial melting is required to produce primitive compositions), depth of melting, magma segregation; and fractional crystallisation. Layer 3, which is the main oceanic layer, is between 3 and 7 km thick and characterised by P wave velocities of between 6.4 and 7.7 km s^{-1} (Bott 1982). It may also be subdivided into layers 3A (isotropic gabbro) and 3B (layered gabbros), which are probably partially metamorphosed to amphibolite and greenschist facies (see later). The Moho occurs at an average depth of 7 km, and is marked by a steep P wave velocity jump at the base of layer 3, from the values above to about 8.15 km s^{-1} (Bott 1982). Layer 4 is constituted by an upper section of layered peridotite passing downward into unlayered peridotite, dunite, harzburgite etc.

The preservation of oceanic crust in the geological record is poor, because, as pointed out in the previous discussion on the life cycle of an ocean basin, this crust tends to be destroyed in subduction zones. However, tectonic slices and fragments may survive during collision tectonics by the process of obduction, and along the sutures that mark the line of collision between two lithospheric plates with intervening oceanic crust (see Chap. 6 and Fig. 6.10). These sequences of oceanic crust rocks on land are the ophiolites, recognition of which is sometimes made difficult by the depth of erosion. This is substantiated by the observation that ophiolites are scarce in rocks older than the Phanerozoic. Where ophiolitic rocks are present in terranes older than the Phanerozoic, then high-grade metamorphism and deformation may add further complications. For example, Light (1982) reports that the possible collision between the Kapvaal and Zimbabwean cratons in the Limpopo province of southern Africa is marked by a suture zone characterised by riebeckite-bearing mafic and ultramafic rocks. At deeper levels this suture is represented by mylonites, pseudotachylites and slivers of serpentinite. The best

chance for a relatively good preservation of ophiolites in Phanerozoic terranes is by obduction (Fig. 6.10). A well-documented example is provided by the Papuan Ultramafic Belt (Davies 1971; Davies and Jaques 1984). But what precisely is an ophiolite, and how is it defined? In 1972, participants of the Penrose Conference agreed to define an ophiolite as follows (Penrose Conference Participants 1972): "Ophiolite refers to a distinctive assemblage of mafic to ultramafic rocks. It should not be used as a rock name or as a lithologic unit in mapping. In a completely developed ophiolite the rock types occur in the following sequence, starting from the bottom and working up: Ultramafic complex, consisting of variable proportions of harzburgite, lherzolite and dunite, usually with a metamorphic tectonic fabric (more or less serpentinised). Gabbroic complex, ordinarily with cumulus textures commonly containing cumulus peridotites and pyroxenites and usually less deformed than the ultramafic complex. Mafic sheeted dyke complex. Mafic volcanic complex, commonly pillowed. Associated rock types include (1) an overlying sedimentary section typically including ribbon cherts, thin shale interbeds, and minor limestones; (2) podiform bodies of chromite generally associated with dunite; (3) sodic felsic intrusive and extrusive rocks. Faulted contacts between mappable units are common. An ophiolite may be incomplete, dismembered, or metamorphosed, in which case it should be called a partial dismembered, or metamorphosed ophiolite. Although ophiolite generally is interpreted to be oceanic crust and upper mantle the use of the term should be independent of its supposed origin". Indeed, with regard to the last paragraph of the Penrose Conference definition, it must be cautioned that more recently, on geochemical and age-relationships evidence, it seems that most ophiolite sequences are thought to represent parts of the oceanic crust created in marginal basins. Details of the geology, petrology and tectonism of ophiolitic rocks can be found in Coleman (1977). The distribution of ophiolites worldwide is shown in Fig. 12.6.

12.5 Heat Flow, Oceanic Crust Metamorphism and the Nature of Related Hydrothermal Solutions

The topic of sub-sea-floor hydrothermal activity is introduced in Chapter 3, which discusses the geometry of hydrothermal convection cells in oceanic crust (Figs. 3.7, 3.8, 3.9 and 3.10). General aspects of hydrothermal alteration are considered in Chapter 4, and Chapter 6 looks briefly at the hydrothermal mineral deposits associated with oceanic crust in the context of global tectonics. There is much literature on the various aspects of sub-sea-floor hydrothermal activity and associated mineralisation, and in additon to the references given in this chapter, relevant works are referenced in Chapters 3, 4, and 6. Comprehensive reviews are provided in Rona (1984, 1986, 1988), and details of the geology, geochemistry and mineralisation of sea-floor environments can be found in Bonatti (1975), Rona et al. (1983) and Barrett and Jambor (1988).

Oceanic crust rocks are well endowed with mineral deposits, ranging from magmatic segregations to hydrothermal. The former comprise podiform chromite

Fig. 12.4. Theoretical heat flow curve (*solid line*) and observed heat flow values (*shaded curve*) as a function of oceanic crust age (e.g. distance from spreading centre). Heat flow units are expressed in μ cal cm^{-2} s^{-1} (After Kennett 1982). See text for details
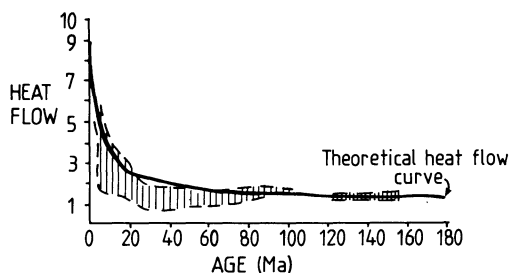
deposits associated with tectonised peridotite of the upper mantle. Disseminations of Ni $\pm$ Pt sulphides, Fe-Ti oxides and Au are also associated with tectonised peridotites. The hydrothermal mineral deposits of the oceanic crust, discussed here, are confined to the upper layers (generally layers 1 and 2, and less commonly layer 3). In the sections that follow we look first at heat flow and ocean floor metamorphism, and continue with a description of the nature, composition and general characteristics of the sub-sea-floor hot springs and related mineral deposits.

12.5.1 Heat Flow and Oceanic Crust Metamorphism

The temperature gradient in rocks of the mid-ocean ridge areas, particularly in the axial regions, is responsible for a flux of heat flow which is transferred upward both by conduction and convection. Convective transfer is due to the upward movement of heated sea water, that is, hydrothermal circulation. Figure 12.4 illustrates the theoretical and observed profiles of heat flow measurements in oceanic rocks. These measurements (which refer to the rate of conductive heat loss per unit area) indicate, firstly, that the heat flow at mid-ocean ridges is substantially greater than elsewhere in the crust; secondly, that the heat flow profiles show an exponential decay with increasing age, and therefore distance from the ridge. Thirdly, and most importantly for our purposes, there is a considerable discrepancy between the observed and theoretical plots, the former being constantly lower than the latter, at and near the ridges. It is concluded that the "missing" heat is caused by the contribution of the hydrothermal circulation of sea water which effectively acts as a coolant.

The percolation of sea water in oceanic crust occurs primarily, at mid-ocean ridges, transform faults and along fracture zones. At mid-ocean ridges cold sea water penetrates the numerous fractures of the oceanic crust layers 2 and 3. Heating of sea water takes place by conductive exchange with the warm to hot rocks, and by mixing with heated waters rising from the regions above the magma chamber. The heated sea water becomes a hot brine which reacts with the mafic rocks. Consequently, with increasing temperature and pressure (as is detailed later), these mafic rocks become metamorphosed to greenschist, amphibolite and serpentinite. This is called ocean floor metamorphism, or hydrothermal metamorphism, which is effectively a form of hydrothermal alteration. There are major exchanges between sea water and the essentially anhydrous mafic rocks, involving mainly hydration, cation exchange and carbonation (Spooner and Fyfe 1973; Andrews and Fyfe 1976).

Table 12.1. Chemical analyses of basaltic rocks "before" and "after" hydrothermal metamorphism
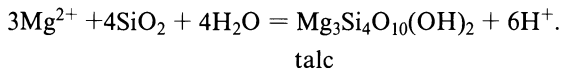
	(1)[a]	(2)[a]	(3)[a]
SiO_2	46.98	42.54	49.34
TiO_2	1.25	1.91	1.49
Al_2O_3	16.58	15.25	17.04
Tot Fe	11.37	12.38	8.81
MnO	0.14	0.05	0.17
MgO	13.31	17.72	7.19
CaO	2.45	0.40	11.72
Na_2O	1.20	0.07	2.73
K_2O	0.03	0.09	0.16
P_2O_5	0.24	0.22	0.16
H_2O	6.80	8.84	1.27
Rb	1	–	10
Sr	64	–	130
Ba	20	5	14
V	228	436	–
Cr	229	150	297
Co	57	42	32
Ni	111	100	97
Cu	21	7.5	–
Zn	62	48	–
Y	32	–	43
Zr	97	–	95
Nb	3.3	–	–

[a] (1) Average of 4 analyses of Mid-Atlantic-Ridge basalts; (2) average of 3 analyses of experimental metabasalts after reaction with sea water at 300 °C at high water/rock ratios; (3) average unaltered tholeiitic basalt. Analyses in (1) and (2) are after Mottl (1983), (3) is after Hughes (1982). Values in wt.% for major oxides and parts per million (ppm) for trace elements; – not analysed or not detected.
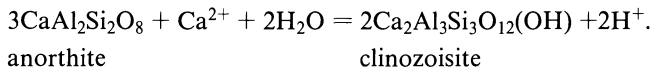
Numerous experimental studies on basalt-sea-water interaction, conducted using a range of temperatures and water to rock ratios, corroborate that substantial mass transfer occurs. This is characterised by cation fixation and hydrolysis reactions which increase in intensity with increasing temperature and water/rock ratios (Mottl 1983; Rosenbauer and Bischoff 1983; Seyfried and Janecky 1985). The water/rock ratio is defined as the total mass of water that passes through the system, in the unit time, divided by the total mass of rock in the system considered (Mottl 1983). Transfer of Mg, SO_4^{2-}, Na and Cl occurs from sea water to oceanic crust, while leaching and mass transfer of Li, K, Rb, Ca, Ba, Cu, Fe, Mn, Zn and Si takes place from the oceanic crust to the solutions (Rona 1984; Table 12.1). One of the most important aspects of basalt-sea-water interaction is the removal of Mg^{2+} from sea water, after which this cation becomes included in mineral phases such as smectite, chlorite and tremolite-actinolite. The transfer of Mg^{2+} takes place as $Mg(OH)_2$, and after its reaction with the rock-forming silicates (e.g. pyroxenes), H^+ is liberated and enters the solution thereby increasing its acidity (pH decreases). This, in turn, produces further changes due to H^+ metasomatism, during which the H^+ exchanges

for cations, such as Ca and K, releasing them into the hydrothermal fluid (see Chap. 4 for more details of H^+ metasomatism). In addition to Mg^{2+}, Na^+ is also removed from sea water, generally at temperatures less than 300°C and water/rock ratios of between 5 and 10 (Mottl 1983). The transfer of Na^+ to the solution is largely responsible for the formation of analcime and albite. Removal of Mg^{2+} and Na^+ is counterbalanced by the leaching of Ca^{2+} from the basalt. At temperatures greater than 150°C, K^+ and SiO_2 are leached from the mafic rocks. Experimental evidence indicates that SiO_2 exceeds quartz saturation at temperatures from 150 to 500°C, thereby causing precipitation of quartz. Some typical metasomatic reactions that take place during the hydrothermal metamorphism of basaltic rocks are given below (Seyfried et al. 1988):

Mg metasomatism:

$$3Mg^{2+} + 4SiO_2 + 4H_2O = Mg_3Si_4O_{10}(OH)_2 + 6H^+.$$
$$\text{talc}$$

Ca metasomatism:

$$3CaAl_2Si_2O_8 + Ca^{2+} + 2H_2O = 2Ca_2Al_3Si_3O_{12}(OH) + 2H^+.$$
anorthite   clinozoisite

Na metasomatism:

$$2Na^+ + 4SiO_2 + CaAl_2Si_2O_8 = 2NaAlSi_3O_8 + Ca^{2+}.$$
$$\text{albite}$$
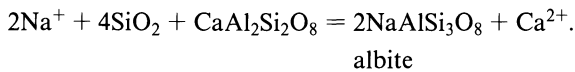
Other mineral reactions in sea-floor rocks are discussed in Chapter 4 and shown in Fig. 4.4.

Prograde metamorphic assemblages of sea-floor rocks range from zeolite facies in the low temperature regime to amphibolite facies at higher temperature and pressure. Metamorphosed mafic rocks derived from hydrothermal metamorphism were known as "spilites" – a term which is still in use, and refers to rocks showing a basaltic texture in which a greenschist mineralogy is developed by secondary processes (Coleman 1977, Hughes 1982 and references therein). Spilitic lavas consist of sodic plagioclase, augite or its altered products (actinolite, chlorite-epidote) and Fe ore. The classic spilites of the literature are often associated with rocks of sodic rhyolitic composition – known as keratophyres – and with marine sediments (Turner and Verhoogen 1960). These altered rocks constituted what was known as the "Steinmann trinity", or the orogenic series, namely: radiolarian chert + spilite + serpentinite. This association – found to be common worldwide – was recognised to be similar to sequences put together from the study of sea-floor rocks, until eventually the whole was set into a unified model of sub-sea-floor magmatic and hydrothermal processes (Spooner and Fyfe 1973).

As stated above, hydrothermal metamorphism is related to the convective circulation of heated sea water, the effects of which increase progressively downward in the crust and as such can be considered as a form of prograde thermal metamorphism, distinct from the dynamo-metamorphic effects which take place

during the tectonic emplacement of the oceanic crust onto a continental margin. This is an important facet that must be kept in mind when examining ophiolitic sequences. The products of hydrothermal metamorphism of oceanic crust, from layer 2 (pillow lavas) to the upper portions of layer 3 (gabbro), range from zeolite to greenschist to epidote-amphibolite facies. Oxygen isotope systematics from the Samail ophiolite complex (see later) indicates that only small amounts of sea water reach the base of layer 3, where the fluids reach a temperature of about 400°C and about 400 bar pressure (Taylor 1983, Seyfried et al. 1988).

Exposure of the basaltic rocks to cold sea water results in their oxidation and the subsequent production of zeolites (sea-floor weathering). Zeolite facies rocks occur at the margins of the ocean ridges where hydrothermal processes take place at temperatures of less than 200°C. Greenschist facies rocks are generally confined to the axial regions of the mid-ocean ridges where the temperature of hydrothermal processes is in excess of 200°C and can reach up to 400°C (Rona 1984). Characteristically, the oceanic rocks tend to preserve their original igneous textures after being metamorphosed. Considering a primary mineral assemblage of the mafic rocks represented by glass-olivine-clinopyroxene-plagioclase, the changes that occur during hydrothermal metamorphism were determined by Kawahata and Furuta (1985) for oceanic rocks at the Galapagos spreading centre. They distinguished three zones of metamorphism as a function of depth and temperature. The mineralogy of these zones is summarised below. Glassy material is replaced by smectite in zone 1 (surface to a depth of about 900 m), and by chlorite with minor actinolite, serpentine and talc in zones 2 and 3 (900–1100 and 1100–1350 m respectively). Olivine is replaced by saponite in zone 1, and by chlorite in zone 2, while serpentine and talc are present in zone 3. Clinopyroxene remains as a relict in zone 1, but is replaced by actinolite and chlorite in zones 2 and 3. Plagioclase relicts persist throughout zone 1 and are replaced by chlorite, albite and quartz in zones 2 and 3. Abundant vein material is also formed, especially in zones 2 and 3, and includes smectite, chlorite, Ca-zeolites, quartz and chlorite.

By comparison, the metamorphic mineral assemblages as determined in a sequence of ophiolitic rocks from Liguria, Italy, allow us to see deeper into the crust (probably bottom of layer 2 and top of layer 3). They include (Spooner and Fyfe 1973): (a) albite + smectite + hematite + calcite + sphene ± chlorite; (b) albite + chlorite + pumpellyite + hematite + calcite + sphene ± smectite; (c) albite + chlorite + pumpellyite + sphene ± hematite ± calcite; (d) albite + epidote + pumpellyite + actinolite + chlorite + sphene ± hematite ± calcite; (e) albite + epidote + pumpellyite + actinolite + hornblende + chlorite + magnetite + sphene ± calcite. Assemblages (a) to (d) refer mainly to layer 2, while assemblage (e) refers to the lower parts of layer 2 and upper portions of layer 3. Studies of ophiolites also indicate that epidote-rich zones (epidosites) may form at the base of the sheeted dyke complex and near the presumed top of the magma chambers (Seyfried et al. 1988 and references therein). These epidote-rich rocks also contain quartz and chlorite and are characterised by the complete obliteration of the igneous textures. The above authors consider that epidosites represent the fossilised residue of a reaction zone, permeated by hot and ascending hydrothermal fluids with high water/rock ratios.

Fig. 12.5. A Mineral species that characterise the hydrothermal metamorphism in oceanic crust rocks as a function of depth and temperature; *LAU* laumontite; *SMEC* smectite; *CHL* chlorite; *AB* albite; *QZ* quartz; *EP* epidote; *ACT* actinolite (After Coleman 1977 and references therein)
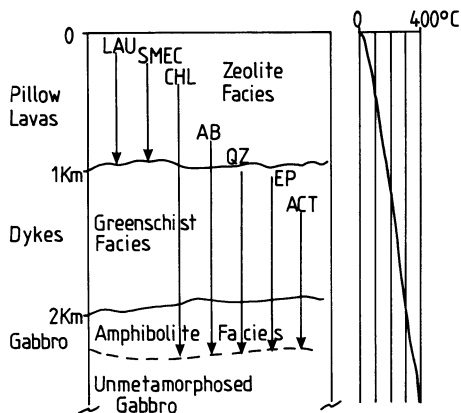
In layer 4 (peridotite and allied rocks) hydrothermal metamorphism results in serpentinisation mainly, which is essentially a process of hydration and is discussed in Chapter 4. The transformation of the ultramafic rocks into serpentinites produces a decrease in the density and a change in the rheological properties of these rocks, which makes them behave plastically. They are, as a result, intruded, or "squeezed" in the cold state along fractures and "leaky" transform faults (Fig. 12.3). For this reason serpentinites are often associated with synkenematic brecciation, cataclasis and mylonitisation. Metasomatic rocks known as rodingites commonly accompany serpentinites, briefly discussed in Chapter 4, where it is also mentioned that they may be associated with Ag and Co-Fe mineralisation.

Figure 12.5 illustrates the distribution of the metamorphic minerals with depth and increasing temperature. Corresponding variations in $\delta^{18}O$ values, for which, according to the findings of Taylor (1983) in the Samail ophiolitic rocks, a general depletion is noted with depth. Large variations of $\delta^{18}O$ are observed from their magmatic value of + 5.7 per mill, to values in excess of +12 near the base of the section. These variations are interpreted as due to a wide range of water/rock ratios and therefore hydrothermal metamorphism of the rocks.

12.5.2 Nature and Composition of the Hydrothermal Solutions

Spooner and Fyfe (1973) calculated that the cooling from 1200 to 300 °C of 1 km^3 of mafic magma can heat about 3 km^3 of sea water to 300 °C. The oxygenated and alkaline sea water, with a pH of about 8, becomes a reduced (pH 4–6), Cl-rich brine capable of leaching and transporting significant quantities of metals (Andrews and Fyfe 1976). As described above, the high temperature solutions (200–400 °C) leach out of the mafic rocks, elements such as Li, K, Rb, Ca, Ba, the transition metals (Cu, Fe, Mn, Zn), and Si. Keays (1987) contends that at least part of the ore-forming metals, in particular precious metals, may be leached out from the magmatic sulphides disseminated in the mafic and ultramafic rocks of layers 3 and 4. Addition of volatile phases (He, F, Hg, S, B, H and CH$_4$) to the hydrothermal fluids may also

occur from the mantle. They may originate either from the degassing of the underlying magma chambers, or indirectly as by-products of the hydrothermal alteration of the mafic rocks (Rona 1984). Transport of metals and S in the solutions is probably by chloride complexes in the higher temperature fluids and by thio-sulphide complexes in the lower temperature range, with the S largely being derived from reduction of SO_4 from sea water. Huston and Large (1989) who studied the chemistry and behaviour of Au in the volcanogenic massive sulphide deposits from Tasmania and elsewhere, showed that Au is transported as $Au(HS)_2^-$, while metals such as Ag, Pb and Zn are transported as chloro-complexes during the early stages of fluid evolution (200–250°C). These metals precipitate as a result of oxidation by mixing with sea water, and reduced S activity. As the fluids reach higher salinity and temperatures of 300°C or more, chloride complexing takes over and Au is transported as $AuCl_2^-$, as are Cu and other metals. Precipitation occurs as a result of pH increase and decrease in both temperature and fO_2 (reducing conditions). For this reason, the authors contend, Au is often associated with pyrite-chalcopyrite stringers and massive lenses, which replace the earlier sulphides at the base of volcanogenic sulphide deposits. The upper parts of the sulphide deposit, on the other hand, are dominated by lower temperature Zn-Pb-Ag-rich sulphide assemblages, and, in the event that Au is present, then it would have been transported by sulphide complexing. The two associations, Cu-Au and Zn-Pb-Ag-Au are usually mutually exclusive. While the chemical modelling of Huston and Large (1989) is specifically directed at kuroko-type deposits, its general principles may well be applicable also to mid-ocean-ridge hydrothermal systems.

The chemistry of hydrothermal fluids, venting at four sites in the East Pacific Rise (EPR) at 21° N, has been determined by von Damm et al. (1985), the results of whose work is summarised here (Table 12.2). Mn, Fe, Co, Cu, Zn, Ag, Cd, Hg, Pb, and As are all to a greater or lesser degree enriched in the EPR hydrothermal solutions. Li is found to be enriched in all four vent areas, whereas Na is enriched at one locality and depleted in the other three. The Na depletion is considered by the authors as due to the formation of albite from anorthite at depth in the system, so that by the time the fluids reach the sea-floor they are depleted in this metal. By contrast, the conversion of albite to chlorite higher in the system is possibly the reason for the Na enrichment in one of the vents. Experimental evidence indicates that Na is leached from the rocks and taken into solution at water/rock ratios greater than 10, to be taken up by the wallrocks at ratios less than 10 (Open University 1989). Cl, like Na, is both enriched and depleted in the solutions; although the behaviour of Cl is not entirely clear, it is possible that a sink for this element is provided by its substitution for hydroxyl groups (OH). Also, about 10% loss of water by hydration could account for both the Na and Cl depletion in the solutions. K and Rb values, while found to be somewhat variable, are generally higher than sea water. The generally low concentrations of these elements may be a function either of original composition of the mafic rocks or of the uptake of these metals to form mineral phases, or both of these. Ca is enriched in the solutions by variable amounts, in some cases Ca showing only a small increase. Low Ca concentrations are attributed to precipitation of Ca-silicates at depth, such as epidote. As previously indicated, Ca is released into the solution during H^+ metasomatism

Table 12.2. Elemental contents of typical vent hydrothermal fluid at 350°C of the East Pacific Rise and that of normal sea water (After Open University 1989, p.100)

	Hydrothermal solution[a]	Sea water[a]	EPR solution[b]	Basaltic rock[b]
Cl	17300	19500		
Na	9931	10500	+/−	+/−
Mg	−	1290	−	+
SO_4^{2-}	−	905		
H_2S	210	−		
Ca	860	400	+	−
K	975	380	+	+/−
Sr	8	8	+/−	+/−
Si	600	3	+	−
Li	6	0.18	+	+/−
Rb	2	0.12		
Ba	5–13	0.02	+	+
Zn	7	0.005		
Fe	101	0.002	+	−
Mn	33	0.0004	+	−

[a] Values in parts per milllion (ppm); − not detected.
[b] The changes in solution chemistry are indicated in terms of gains and losses of elements compared with an altered basaltic rock as reported by von Damm et al. (1985); + indicates gain, − loss and +/− indicate both a loss and a gain, generally depending on temperature.

and albitisation of the anorthite molecule, or during the conversion of epidote to chlorite. von Damm et al. (1985, p.2204) point out that the Ca cycle is a complex one with "numerous source and sink reactions available".

Mg is depleted in all vent solutions which is in agreement with an assumed end-member solution value of zero. Mg and sulphate, in fact, show a negative correlation with temperature, and extrapolation to the zero values of Mg and SO_4 intersects the temperature axis at 350°C, which is considered to be an end-member solution (Edmond et al. 1979; von Damm et al. 1983). Ba is enriched in all solutions examined, but the concentration of this element may be underestimated due to the precipitation of barite in the chimneys (see later). Silica is enriched in the solutions and its presence is largely controlled by the solubility of quartz in the system, which is dependent on temperature and pressure. The Si content of the solutions in the EPR shows a regular decrease from north to south in the four vents examined by the authors, which is thus interpreted as indicating an increase in the depth of the hydrothermal circulation. Using the measured Si content, temperature of the EPR vents, solubility curves of quartz as a function of temperature and pressure, and by removing the pressure of the water column (2500 m = 250 bar), von Damm and co-authors were able to estimate the pressure and depth at which the fluids are in equilibrium with quartz. They found pressures of between 300 and 600 bar, corresponding to depths of 0.5 to 3.5 km below the sea floor. Total S occurs as the two species of SO_4 and H_2S. The latter is present in all the vent solutions examined, while, as stated previously, sulphate has zero concentration in the end-member solution (Table 12.2).

The behaviour of S in the hydrothermal solutions is both complex and critical. The S cycle is determined by the presence of two sources and two sinks (von Damm et al. 1985). The source of S resides in both sea water and the mafic rocks, while sinks are provided by the deposition of sulphates (barite, anhydrite) and its precipitation as sulphides. The S that is contained in the fluids discharged at the sea-floor is derived from both sea water sulphate and mafic rocks. S-isotope systematics are also difficult to interpret because sea water sulphates contains +20 per mill $\delta^{34}S$, while basaltic S has 0 per mill $\delta^{34}S$. During reduction of sulphate to sulphide the first sulphide formed will have near 0 per mill values of $\delta^{34}S$, so that if the sulphate is partially reduced the resulting $\delta^{34}S$ will have a range from 0 to +20 per mill. S-isotope measurements by Kawahata and Shikazono (1988) indicate a range of values for $\delta^{34}S$ of between + 1.7 and + 5.8 per mill in sulphide samples, and of between + 0.5 and + 4.6 per mill in the H_2S of the hydrothermal fluids of the EPR. Kawahata and Shikazono (1988) conclude that about 11% of the S is contributed by sea water and 89% by the basaltic S. Reduced S is clearly important for the transport of metals, as discussed earlier in this chapter and in Chapter 11. At any rate, S is used up in the precipitation of sulphides and sulphates, which contribute to the build up of the mineralised mounds and chimneys to be discussed in the following section.

12.6 Tectonic Settings, Sub-Sea-Floor Hydrothermal Processes, Hot Springs and Their Mineral Deposits

In common with other hydrothermal systems, a sub-sea-floor hydrothermal system consists of a heat source (the underlying magma chamber), a recharge area, circulation cell and sea-floor discharge (see Figs. 3.7 and 3.8). The heated sea water, having become an ore solution, is discharged as a hot spring on reaching the sea-floor. The ascending ore solutions and their surface discharge constitute an ore-making system. When considering the extent of mid-ocean ridges around the globe, one realises that we are, most likely, in the presence of one of the most powerful and extensive mineralising systems in the planet. Unfortunately, its magnitude is not reflected in the geological record for the reason already stated: namely, poor preservation potential due to collision tectonics. Figure 12.6 illustrates the worldwide distribution of ophiolite belts, within which potential fossil systems of sub-sea-floor mineralisation occur, and the distribution of present-day sites of hydrothermal discharge along the mid-ocean spreading centres. In the latter it is clear, as pointed out by Rona (1984), that the distribution of discharge sites is an artifact of our knowledge, and many more could be expected to be added as submarine exploration continues. The hydrothermal mineral deposits that are formed at sea-floor spreading centres include massive stockworks and disseminated sulphides and sulphates, metalliferous encrustations and accumulation of metalliferous sediments in topographic depressions. The ore metals include mainly Fe, Cu, Zn, Mn, Au, Ag and Ba.

There are four main geological environments where oceanic crust-related hydrothermal mineralisation occurs: (1) in the axial zones (rift valley) of a spreading
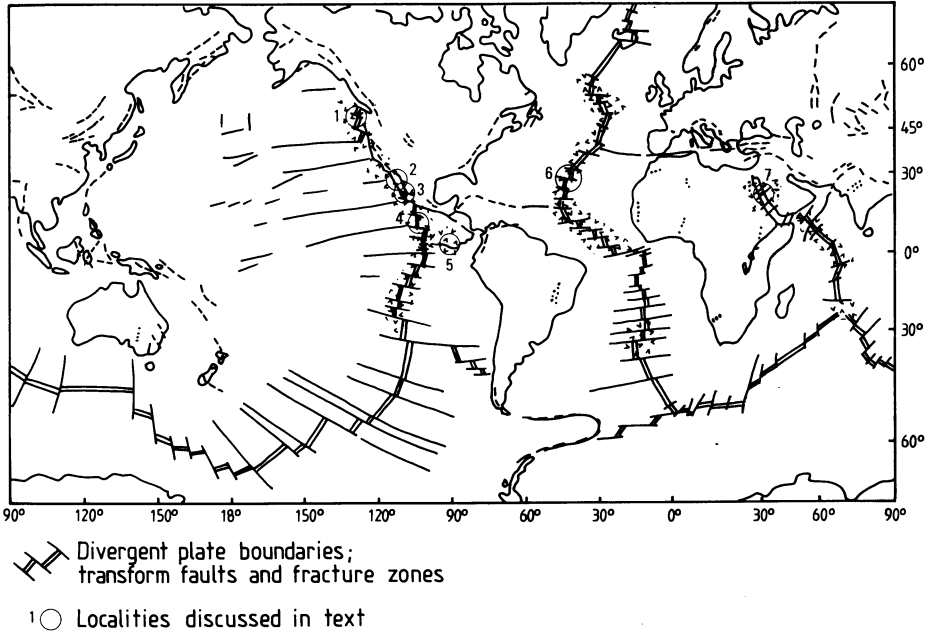
Fig. 12.6. Distribution of ophiolite belts of Mesozoic and Paleozoic ages (*dashed lines*), and of Upper Proterozoic age (approximately 540–1200 Ma, *dotted lines*). *Shaded areas* (random V's) over spreading centres indicate portions that have been, and are being, explored. Localities mentioned and/or discussed in text are *1* Juan de Fuca ridge; *2* Salton Sea; *3* Guaymas basin; *4* East Pacific Rise; *5* Galapagos spreading centre; *6* TAG hydrothermal areas; *7* Red Sea (After Coleman 1977; Rona 1986, 1988)

ridge; (2) at off-axis seamounts; (3) on the ridge flanks where there may be a thin sedimentary cover; and (4) away from spreading centres where there is a substantial thickness of deep-sea sedimentary material. Fe- and Mn-rich clays are typical of the latter situation, and these clays may also contain trace amounts of other metals such as Ni, Cu and Co. The origin of the metalliferous clays is not clear, but it is thought that they may be related to distal deposition of particulate matter issued from the sea-floor hot springs at mid-ocean ridges and/or localised hydrothermal activity.

In the sections below we focus on the mineral deposits formed at spreading ridges (on- and off-axis). We look first at the various types of hydrothermal mineral deposits, together with their morphology, nature and relationship to the tectonic setting. The basis of this discussion is provided by the comprehensive reviews of Rona (1984, 1988). We continue with brief descriptions of individual discharge sites such as those of the East Pacific Rise, the Atlantic spreading centres and the Guaymas basin in the Gulf of California.

12.6.1 Tectonic Settings

The nature of the mineralising systems that are formed in the environments of oceanic crust and the size of their mineral deposits are largely dictated by the tectonic setting, stage of opening of an oceanic basin and the rate of sea-floor spreading. Rona (1988) points out that sulphide deposits at slow-spreading centres tend to be larger than those at fast-spreading centres, because of the longer residence time of a parcel of oceanic crust within the region of high heat flow. Thus, we consider slow, intermediate to fast spreading ridges within the framework of early and advanced stages of opening of ocean basins. In each of these situations local conditions must also be considered, such as depth to magma chamber, thermal gradient, permeability, the geometry of the convective system and timing of geological events. Geophysical evidence suggests that magma chambers at slow-spreading ridges (<2 cm y^{-1}, e.g. Atlantic) are at depths ranging from 3 to 10 km, while at intermediate to fast-spreading ridges (>2 cm y^{-1}, e.g. Pacific) the magma chambers appear to be much closer to the sea floor, at depths of between 1 and 3 km.

Slow Spreading and Early Stages of Opening

This situation, illustrated in Fig. 12.7A, is characterised by a narrow sea bounded by rifted continental margins. The Red Sea is an ocean basin in its early stages of opening, locally floored by basaltic rocks along narrow sectors corresponding to its axial regions from which slow spreading is currently active. The shoulders of the Red Sea rift consist of continental sedimentary rocks including thick evaporite beds. In this situation, hydrothermal solutions have high salinities due to the presence of the evaporites (Chap. 3 and Figs. 3.22 and 3.23 for details). Fe-Cu-Pb-Zn sulphides precipitate under reducing conditions in restricted basins forming pool-like stratified sulphide deposits. Polymetallic sulphates, silicates, oxides, hydroxides and carbonates precipitate at the interface between the hypersaline solutions and the overlying normal sea water. A more comprehensive description of the Red Sea mineralised pools is given in Chapter 13. It is worth noting that a dispersion halo of Mn-Cu-Zn-Hg enrichment may occur for a radius of up to 10 km around a mineralised basin (Rona 1984).

Slow Spreading and Advanced Stages of Opening

Figure 12.7B illustrates a cross-section at a slow-spreading mid-ocean ridge, such as the Trans-Atlantic Geotraverse field (TAG) in the Atlantic Ocean. Hydrothermal circulations is within linear sections of the axial rift are cross-cut by transform faults. Discharges, which occur along fractures and faults in the walls of the rift valley, also impregnate talus material forming a breccia with a mineralised matrix. In a TAG-type hydrothermal deposit the mineralisation consists of Fe and Mn oxide accumulations and encrustations, possibly followed at depth by stockwork veins containing Fe-Cu-Zn sulphides. Recharge is higher up on the shoulders of the central rift valley as shown in the figure. Transform faults constitute a related subsetting, in which disseminations and veins of Fe-Cu sulphides may be present
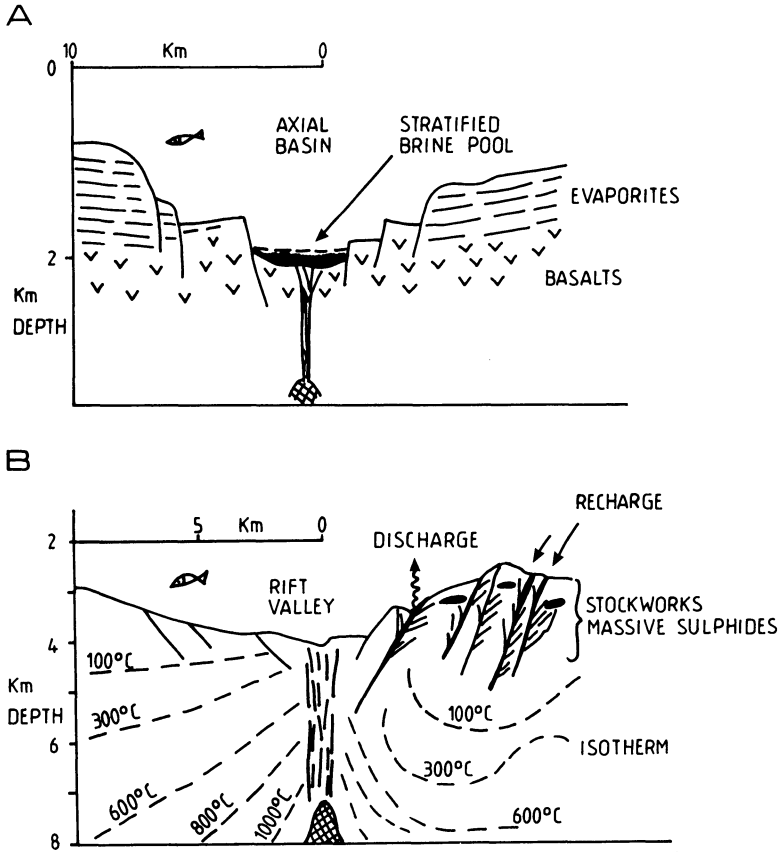
Fig. 12.7A, B. Slow-spreading centres. A Early stage of opening; narrow sea arm bounded by continental crust (e.g. Red Sea); a basin is formed in the axial zone in which hydrothermal fluids are discharged and form a stratified deposit, characterised by a lower zone of metalliferous muds and sulphides and an upper zone of oxides, hydroxides, silicates and sulphates. B Advanced stage of opening; crestal area of a mid-ocean ridge transected by transform faults (e.g. TAG area); hydrothermal discharge is along faults in the walls of the rift, forming encrustations of Fe-Mn oxides and sulphide stockworks. The matrix of talus material along the fault scarps may become impregnated with sulphides. Note bending of isotherms due to cooling effect of convecting sea water (After Rona 1984)

along the wall of the offset segments. A dispersion halo of Mn, Fe, Cu and Zn can extend up to 4 km from the active vents (Rona 1984).

Intermediate to Fast Spreading and Early Stages of Opening

In this setting a narrow oceanic arm is bounded by continental areas and the active spreading centres are segmented by numerous "en echelon" transform faults. An example of this setting is the Gulf of California (Guaymas basin, to be discussed later; see also Fig. 3.10). Abundant terrigenous and/or biogenic sediments are
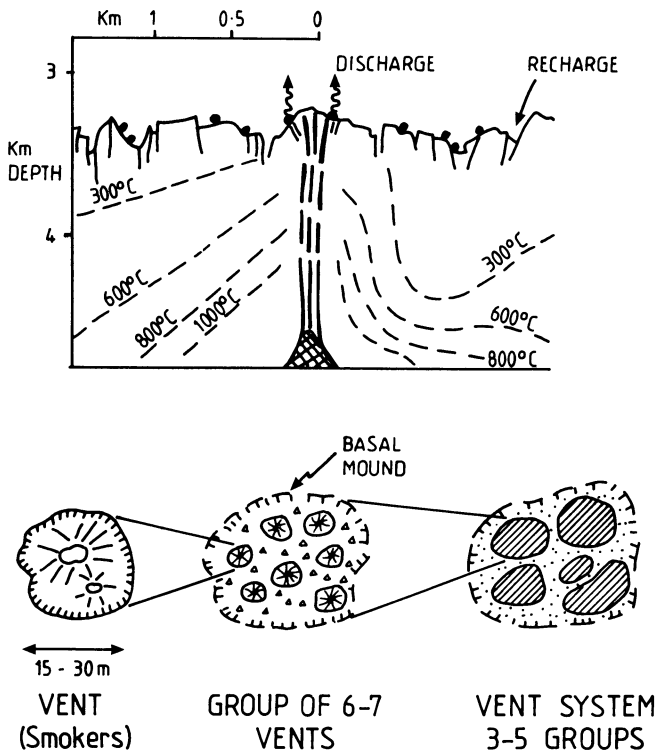
Fig. 12.8. Intermediate to fast spreading ridge and advanced stage of opening (e.g. East Pacific Rise). Sulphide deposits (clusters of smokers and mounds) are shown by the *black dots*; bending of isotherms as in Fig. 12.7 (after Rona 1984). At the *bottom* of the figure a schematic representation of a group of smokers and a smokers system is shown

deposited in these basins, resulting in the rapid burying of the mineralised zones. Heat sources are thought to be cooling dykes and sills emplaced into the wet sedimentary pile. The mineralisation consists of metallic oxides, silicates, sulphides and sulphates which accumulate along fault scarps and on the sea-floor. Massive and disseminated sulphide bodies occur within the sedimentary column.

Intermediate to Fast Spreading and Advanced Stages of Opening

This is the setting best represented by the East Pacific Rise (EPR) and illustrated in Fig. 12.8. Here, there are numerous hydrothermal fields in which discharge of fluids takes place along linear zones (faults), and at point sources, located within an inner zone of active extension in a terrain characterised by horst-graben structures. Hydrothermal vents (smokers) may form bands 20–500 m wide and up to 6 km long. The vents rise up to 10 m on a base with a diameter of 15 to 30 m, and may be arranged in groups of six or seven. These, in turn, may form a vent system containing three to five groups, as schematically illustrated in Fig. 12.8. Massive sulphide and stockwork deposits are formed containing mainly Fe-Cu-Zn-Ba-Ag.

12.6.2 Hydrothermal Processes and Types of Sulphide Deposits

Hydrothermal processes at oceanic spreading centres are considered in terms of temperature and volume of flow (Rona 1984). Away from spreading centres, and at temperatures of less than 200°C, diagenetic and "weathering" processes dominate with the formation of zeolite metamorphic facies. Closer to the spreading centres, however, low-temperature ($<$ 200°C) hydrothermal alteration or metamorphism, as outlined previously, also consists of zeolite facies mineral assemblages. At temperatures of between 200 and 400°C, hydrothermal processes are associated with greenschist facies metamorphic assemblages. In terms of volume of flow, a distinction is made between sea water- and rock-dominated systems. In the former, the mass ratios between sea water and rock are high, in other words, a large volume of water passes through fractures and cracks in layers 2 and 3 of the oceanic crust. This large flow volume allows the necessary chemical reactions that result in the conversion of sea water into an acid- and metal-transporting ore fluid. In rock-dominated systems, by contrast, the water/rock ratios are low and the resulting solutions only slightly acid and metal-poor. Consequently it follows that in low-temperature, rock-dominated systems, the hydrothermal processes are of low-intensity and scarce importance in terms of ore deposition. High-temperature, seawater-dominated systems are characterised by high-intensity hydrothermal activity which is a very effective ore-forming system (Rona 1984).

The ascent of the metal-rich solutions along channelways occurs through decreasing temperature and pressure gradients. Separation of liquid and vapour phases (critical point) for a 350°C solution is at a pressure of about 1500 bar. However, boiling does not occur at depths below sea level of more than 2000–1500 m, or $>$200–150 bar pressure (1 bar = a water column 10 m high). Boiling could nevertheless take place at shallower depths where the adiabatic curve for the ascending fluids intersects the liquid-vapour curve for sea water (Delaney and Cosens 1982; Bonatti 1983). Mixing of these primary solutions with sea water (which is alkaline, oxidising, and at temperatures of approximately 2°C) causes the rapid precipitation of disseminated stockworks and massive sulphides along the route of the fluids, and at the sea floor, under predominantly reducing conditions. Under more oxidising conditions various Fe-rich silicates, Fe and Mn oxides and hydroxides, sulphates and carbonates are precipitated above the sulphide zones and further away from the vents. The injection of hydrothermal plumes into the water column (see Fig. 3.9) will result in the precipitation of amorphous ferric oxide particulate matter with high colloidal adsorption capacity. It is therefore possible that this will cause the scavenging of Fe and Mn as well as other metals from the sea water. Flocculation would thus follow, causing metalliferous sediments to be deposited distally from the discharge sites.

The discharge of the primary solutions on the sea-floor occurs through vents or chimneys (more popularly known as smokers), of which there are two types: black and white. In black smokers the fluids, which emerge at temperatures of approximately 350°C, are characterised by black clouds of sulphide material which precipitates immediately as the hot fluid comes into contact with the cold sea water (about 2°C). Sulphides include pyrrhotite, pyrite, sphalerite, chalcopyrite, cuban-

ite, digenite etc. Primary solutions, discharging through white smoker chimneys at temperatures of between 100 and 350°C, precipitate white clouds of barite and silica with minor pyrite. The chimneys can grow by several centimetres per day and the fluid velocity is from tens of cm s^{-1} in white smokers to 2–3 m s^{-1} in black smokers. The activity of an individual smoker is usually short, as the feeding channels become sealed by the deposition of minerals, until a new channel opens up and a new smoker chimney is formed (see later). Estimates of the heat flux from black smokers suggest a life span of between 1 and 10 years (MacDonald et al. 1980). It appears that the two types of smokers are end members of a continuum of warm to hot sea-floor springs (Open University 1989, p. 102). It is theorised that the transition from low- to high-temperature emissions occurs in response to the sealing of the channelways by mineral deposition, which reduces permeability and hence isolates the flow of the hot fluids towards the surface. This then causes the fluids, which cannot mix with the cold sea water, to become hotter, until they manage to emerge as black smokers. It is possible, therefore, that these hydrothermal vents may evolve with time from a warm-water vent to a white smoker, and finally to a black smoker. This is a hypothetical evolution which may also be related to the depth of penetration of the fluids into the oceanic crust towards the cracking front above the magma chamber.

Figure 12.9A schematically illustrates a model of sulphide deposit (mound) formed by a vent system which, as previously stated can be formed by several chimneys. A cross-section of a smoker is shown in Fig. 12.9B.

On the basis of the aforesaid, a classification of the types of sulphide deposits at sea-floor spreading centres can be made. Bonatti (1983) distinguishes the following types, based on their timing and position within the enclosing medium: (1) pre-discharge deposits; (2) syn-discharge deposits; (3) post-discharge deposits; and (4) intrasedimentary deposits. Pre-discharge deposits consist of disseminations and stockworks mainly; as the name implies this type of sulphide mineralisation is formed by precipitation of sulphides (pyrite and chalcopyrite mainly) from the solutions along fractures (channelways) en route to the surface; in other words, they are epigenetic. Syn-discharge deposits are represented by the massive sulphide, sulphates, metal oxides, hydroxides and metal silicates vent accumulations. Massive sulphides include pyrite, pyrrhotite, chalcopyrite, sphalerite and wurtzite; sulphates are barite and anhydrite; metal oxides and hydroxides are goethite, todokorite and birnessite, which are precipitated by oxidation of the discharge fluids around the vents; metal silicates may precipitate from the solutions by reaction of silica with Fe to form Fe-smectites and/or talc. Post-discharge deposits (syngenetic), are further categorised by Bonatti (1983) into diluted and concentrated subtypes. Diluted deposits are mainly oxides and hydroxides which tend to be kept in solution for a long time so that they are diluted with sea water. In this system the less soluble components, e.g. Mn, will eventually be precipitated on the sea-floor. The concentrated subtypes are represented by the stratified sulphides, oxides, hydroxides and silicate accumulations in structural depressions under reducing to oxidising conditions (e.g. Red Sea deeps). The main sulphides are sphalerite, chalcopyrite and pyrite; sulphates are anhydrite and barite; Fe-smectite, silica and manganosiderite are other mineral phases present in these systems. Intrasedimentary deposits, in
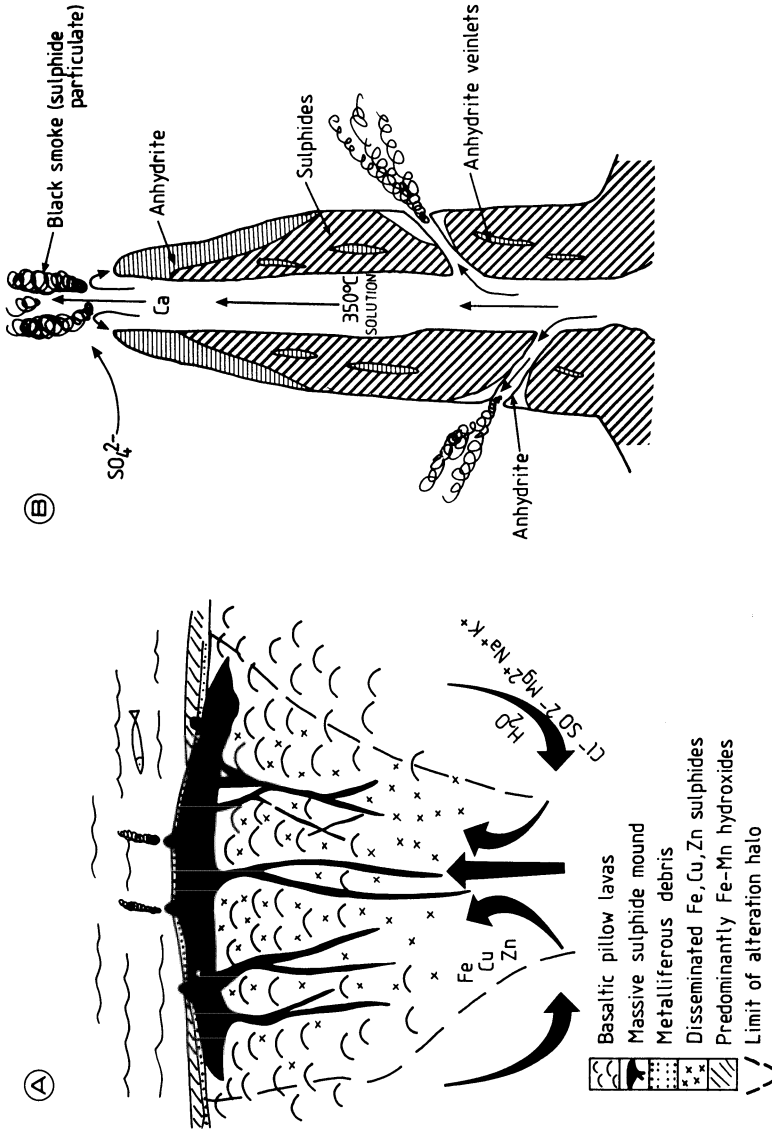
Fig. 12.9. A Schematic representation of cross-section of sulphide mound; see text for details (after Embley et al. 1988). B Cross-section of black smoker; anhydrite precipitates first forming a "leading edge", followed and replaced by hotter solutions which deposit sulphide material (After Edmond and von Damm 1983)
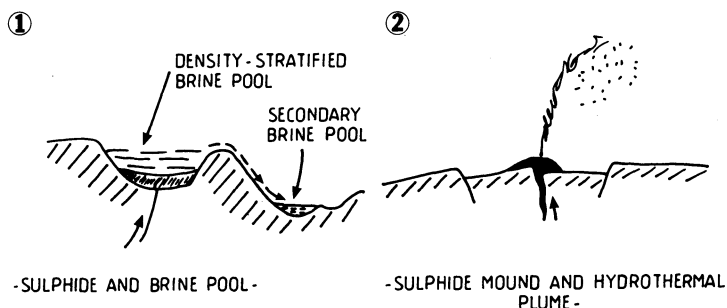
Fig. 12.10. Schematic representation of two main types of submarine hydrothermal sulphide deposits. 1 Density stratified sulphide and brine pool with spillover into a secondary pool by gravity flow; this is the case of density (and salinity) of the solutions being greater than sea water. 2 Sulphide mound and plume of hydrothermal particulate material; this is the case of density of the solutions being less than sea water (After Sato 1972; Rona 1988)

spreading centres near landmasses, are those in which sulphide precipitation occurs either at the sea water-sediment interface, or within the sedimentary column.

Up to this stage in our discussion it has become apparent that the mineral deposits formed by the venting of hydrothermal fluids at spreading centres can occur either as mounds or as pool-like stratified accumulations, as illustrated in Fig. 12.10. The shape of the deposits is essentially related to the dynamics of the discharging fluids (Sato 1972, Rona 1988). Hydrothermal solutions that are less dense than sea water tend to rise as buoyant plumes up to 300 m above the vents, and their equilibrium level is primarily related to the flux of the vent. This is the case for both the Pacific and Atlantic discharge sites, where the salinities of the solutions are usually close to that of sea water. Salinities of the fluids discharging in the EPR range from 2 to 4.9 wt.% NaCl equivalent, about 4 wt.% in the Guaymas basin, and in the Juan de Fuca ridge vents they reach salinities of approximately 7 wt.%. In the brine pools of the Red Sea the discharging fluids are extremely saline (range is from 4 to 32 wt.% NaCl equivalent) and therefore much denser than sea water. The discharging solutions tend to accumulate in submarine depressions and are density-stratified, as indicated in Fig. 12.10 (see also Fig. 3.23). It must be reiterated that the range of salinities varies in space and time, with higher salinities (and temperatures) usually being found deeper in the crust and in the early stages of the developing ore solutions; a general decrease both in the salinity and temperature of the fluids also occur with time. However, certain factors may serve to alter this simple evolutionary trend, for example, the presence of evaporites in the path of the moving fluids (Rona 1988).

12.6.3 Sub-Sea-Floor Hydrothermal Mineral Deposits

Exploration of the mid-ocean ridges, by submersible craft, in the Pacific and Atlantic Oceans has led to the discovery of numerous hot spring systems, many of which have resulted in the deposition of ore grade mineralisation. A history of the

discoveries and studies of sub-sea-floor mineralisation can be found in Rona et al. (1983 and references therein). Some of the highlights of this history are summarised below. The first discovery and retrieval of hydrothermal material from a seamount located off the axis of the East Pacific Rise (EPR) was reported in 1966. In 1972 the first submarine hydrothermal field was discovered in the mid-Atlantic ridge by the NOAA Trans-Atlantic Geotraverse project (TAG), while the first direct observation of active hydrothermal vents and the discovery of new biological communities and ecosystems, associated with the deep-sea hot spring environment, were made in 1977 by the crews of the ALVIN submersible. Mounds of massive sulphide deposits were observed and sampled by an international team of geoscientists using the submersible CYANA at the EPR near 21° N latitude. As a result of these and subsequent exciting discoveries made during many dives in the 1980s, our knowledge of sea-floor spreading, magmatic, hydrothermal processes and ore genesis has increased considerably.

As could be expected, the size of ocean-floor-hosted mineral deposits is highly variable and, as mentioned previously, a function of a number of factors, such as residence time of the discharging solutions, rate of spreading (a parcel of crust can be fairly quickly removed from the area of hydrothermal circulation in a fast-spreading ridge), and structural traps. The largest deposits are most likely those at the slow-spreading Red Sea axis, where a 10-km basin has an estimated 94×10^6 tonnes of metalliferous sediment (dry, salt-free weight; Rona 1988 and references therein). In this, the average metal contents are approximately 20–30% Fe, 0.4% Cu, 4% Mn, 1.7% Zn, 2% Ba, 180 ppm Ag and 0.5 ppm Au. Mound-shaped sulphide bodies in the Atlantic can reach dimensions of 200 m width and 40 m height, with an aggregate tonnage probably in excess of 1.5×10^6 tonnes (Rona 1988). Approximate metal contents have the following ranges: 0.01–40% Cu, 0.01–36% Fe, 0.01–52% Mn, 0.01–6.5% Zn, up to 150 ppm Ag and 16 ppm Au. In the northeast Pacific seven active mounds, up to 400 m in diameter and 60 m high, and which occur within terrigenous sediments, may each contain some 1×10^6 tonnes of ore material containing approximately 0.42% Cu, 36% Fe, 0.12% Mn, 3.5% Zn, 1.5% Ba, and about 5 ppm Ag and 0.15 ppm Au.

Below is a brief description of some of the hydrothermal fields that have been reported in a number of publications. We examine the fields of the EPR, TAG and those of the Guaymas basin, and also look at the hydrothermal fields associated with submarine volcanoes (seamounts). Their locations are shown in Fig. 12.6.

The East Pacific Rise (EPR)

The EPR is an active, fast-spreading (approximately 10–16 cm y^{-1}) mid-ocean ridge which separates the Pacific, Nazca and Cocos lithospheric plates. The areas that have been studied in some detail are located between 11 and 13° N latitude and between 17 and 21° N latitude. The works of Francheteau et al. (1979), Hekinian et al. (1980, 1983), Haymon and Kastner (1981), Hekinian and Fouquet (1985), Fouquet et al. (1988) and Graham et al. (1988), form the basis of the present discussion.

Near 13° N, a large number of hydrothermal deposits extending over an area approximately 20 km long and 150 m wide, and along a section of the axial zone of
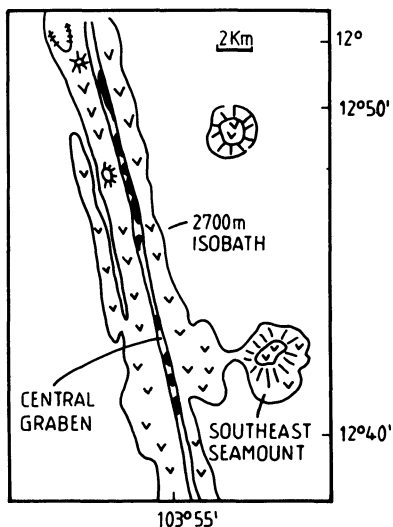
Fig. 12.11. Sketch map of the East Pacific Rise around 12° 50' N latitude; see text for details. *Black areas* indicate hydrothermal fields (After Hekinian and Fouquet 1985)

the mid-ocean ridge, together with a substantial mineral deposit located on a nearby seamount, have been explored (Fig. 12.11). The EPR at 13° N is characterised by an axial graben, 600 to 200 m wide and about 20 to 50 m deep, and bounded by normal faults. The average water depth at the graben floor is 2630 m. About 6 km east of the axis are two volcanic edifices (seamounts) which rise 350 (southeast seamount) and 250 (northeast seamount) m above the sea floor. Basaltic rocks in the axial zone consist of three main morphological types, namely: (1) elongated collapsed lava lakes, located in the centre of the graben; (2) lobate lava flows, occurring on the sides of the lava lakes; and (3) pillow lavas which occur in the graben, along fault scarps and at the top of the ridge. In general, the on-axis basaltic rocks have more primitive compositions (low Ti, high Mg and Ca) than those on the seamounts (enriched in Ti and K, and poorer in Mg).

The on-axis deposits form conical constructs (chimneys or smokers), up to 25 m high, arranged in clusters about 50 m in diameter. They are made up largely of Fe, Cu and Zn sulphides. The active and non-active chimneys have an early coating of anhydrite and Fe sulphides which is thought to act as an insulant, thus enabling the precipitation of higher temperature sulphides in the centre of the chimney. The succession of mineral phases observed towards the centre of a smoker is marcasite, Zn-sulphide, pyrite $\pm$ chalcopyrite $\pm$ pyrrhotite.

The off-axis deposit is located on the southeastern seamount and is about 800 $\times$ 200 m; by assuming a depth of 1 m, an average specific gravity of 3 g/cm^3, this deposit would contain approximately 0.5 $\times$ 10^6 tonnes of ore material. The hydrothermal material of this deposit has been categorised into four groups: (1) Fe-rich massive sulphides, consisting of pyrrhotite, colloform and layered pyrite, Zn and Cu sulphides, opal and barite; (2) Fe-Cu massive sulphides; (3) silica-rich sulphides, consisting of dark grey material containing sulphides in various stages of replacement and dissolution by silica-rich fluids (the main sulphide phases are chalcoyrite, digenite, bornite and idaite); (4) Fe-hydroxides, which are the major
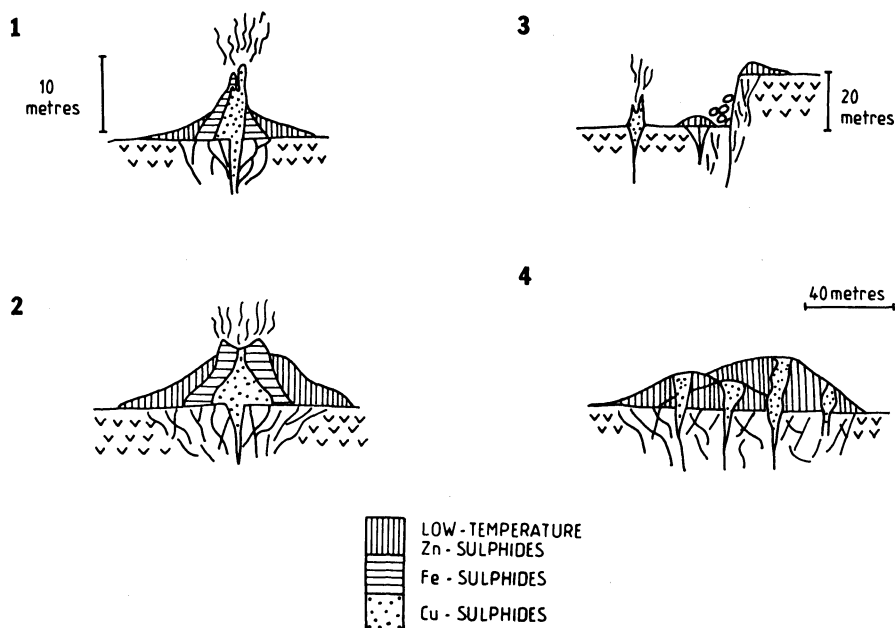
Fig. 12.12. Schematic representation of the evolution of sub-sea-floor sulphide constructs. 1 Low-temperature phases of Fe and Zn sulphides are deposited on the sea floor, these may inlcude at first, pyrite, marcasite, colloform pyrite, silica, followed by Zn-sulphide and more pyrite. Mineral constructs begin to form (chimneys, or smokers if they are actively venting). A subsequent pulse of deposition results in the precipitation of Fe and Cu sulphides at higher temperatures. 2 At this stage hydrothermal venting begins to decline, but localised discharge, at lower temperature, results in the further building up of the chimney with Fe-rich phases. 3 Fracturing and collapse of the mineral construct may follow, while emission from a new vent begins nearby. 4 Illustration of the type of massive sulphide mound that may form in an off-axis situation; the mound is made up of a series of lens-shaped bodies formed by low-temperature Zn-Fe phases and high-temperature Cu-rich phases and underlying stockwork (for details on the makeup of an individual chimney see Fig. 12.9B) (After Hekinian and Fouquet 1985)

constituents of this seamount deposit, cover the massive sulphides and form interstitial material in the pillow lavas. Hekinian and Fouquet (1985) believe that the off-axis seamount mineralisation is formed by a more extended and lower temperature hydrothermal event than the on-axis deposits. Also, the discharge of hydrothermal fluids on seamounts may form lenses of sulphides which accumulate on top of one another to form more extensive deposits (Hekinian and Fouquet 1985). The Fe-hydroxides appear to have formed as alteration products of the sulphide minerals. The alteration of chalcopyrite to goethite is prominent and is associated with chalcocite as an intermediate product. Co-bearing phases are locally present as inclusions in pyrite and chalcopyrite.

The general succession in these massive sulphide deposits (on- and off-axis) is colloform pyrite, pyrite ± pyrrhotite ± Zn-sulphide, chalcopyrite, marcasite, opal. This paragenesis indicates that there may have been three stages of deposition:

Table 12.3. Selected metal analyses of hydrothermal material from the EPR near 13° N[a]

	Cu-rich chimney	Zn-rich chimney	Massive sulphide	Silica-rich sulphide
Cu (wt.%)	2.6–31.6	2.92–0.32	7.9–0.77	1.82
Zn (wt.%)	0.25–0.04	41.7–14.0	0.07–0.03	0.05
Fe (wt.%)	15.0–30.6	14.75–26.45	41.25–44.9	19.05
Pb	26–2	2391–948	146–129	307
As	45–0	184–1253	43–101	84
Ag	6–0	186–79	13–5	9
Se	90–241	0–15	335–48	110
Co	500–160	50–30	3000–500	600
Cd	12–4	557–815	5–3	0

[a] Values are in parts per million (ppm) unless otherwise stated. Where two values are given, they represent the margin and core of a chimney, respectively (After Hekinian and Fouquet 1985).

massive sulphide stage, silica-rich stage and weathering of sulphides. The evolution of the sulphide constructs formed on both on- and off-axis is illustrated in Fig. 12.12, and bulk analyses of the hydrothermal material are given in Table 12.3.

A number of submersible-based investigations (ALVIN and CYAMEX) led to the discovery of a large hydrothermal field near 21° N latitude. The hydrothermal field in this part of the EPR is formed by a zone, 1.5 km wide, fractured and faulted horst-graben terrain. The field consists of both active and inactive vents and associated sulphide mounds and chimney constructs. The sulphide mounds include accumulated sulphide debris which overlie the basaltic lavas, extend over areas of 15 × 30 m and are up to 2 m high. The mounds are cross-cut by networks of tubular structures, 0.5 to 3 cm in diameter, which are interpreted as fossilised worm tubes and mineralised channels. These tubular structures have alternating lamellae of pyrite, hydrous amorphous silica, hydrous Fe oxide, sphalerite, gel-like wurtzite and small lenticles of clay material. On top of the basal mound are the chimneys which, if active, are called smokers. Black smokers emit, at several cm s^{-1}, dark clouds of precipitates consisting of pyrrhotite, pyrite and sphalerite suspended in hot water at a temperature of about 350°C. The black smokers consist of an exterior zone made up of anhydrite, gypsum, sphalerite, pyrite, pyrrhotite, wurtzite and covellite; and an interior zone made up of chalcopyrite, cubanite and bornite (see also Fig. 12.12). White smokers are cooler (<300°C), have slower flow rates, emit amorphous silica, barite and pyrite, and are built of the material mentioned above plus sphalerite, wurtzite, marcasite and sulphur. The white smokers are also characterised by the presence of numerous organisms including clams, mussels and vestimentiferan worms that essentially survive on chemosynthetic products derived from H_2S, NH_4^+ and Fe^{2+}, which are used as a source of energy by chemosynthetic microorganisms (Grassle 1983). Non-active chimneys have an interior zone made up of sphalerite, sulphur, pyrite, chalcopyrite, wurtzite, marcasite, galena, bornite, cubanite and chalcocite. The exterior zone consists of amorphous silica, barite, goethite, natrojarosite and corundum. Fallout from the smokers and their

fragmentation result in sulphide and sulphate sediments which accumulate to form part of the basal mounds. Bulk analyses of sulphide material give the following range of metal values: 0.20–1.5% Cu, 0.05–50% Zn, 83–480 ppm Ag, up to 640 ppm Pb, 700 ppm Cd and 500 ppm Co. High levels of Au (up to 9600 ppm) and Pt (up to 1.17%) have been detected by electron microprobe analyses of wurtzite gel material, pyrite, marcasite and chalcopyrite.

The Guaymas Basin, Gulf of California

In this area (see Fig. 3.10), where spreading ridges and transform faults systems are buried in mud and silt, a number of hydrothermal deposits have been studied by Lonsdale et al. (1980), Lonsdale and Becker (1985) and Peter and Scott (1988). Side-scan sonar surveys of the Guaymas basin, determined the presence of two active spreading segments known as Northern Trough and Southern Trough delimited by transform faults. In the Northern Trough a deposit containing mainly talc and pyrrhotite was discovered (Sea Cliff hydrothermal deposit), while more than 120 discharge sites are located in the Southern Trough, a 30-km-long axial rift valley, characterised by fault scarps. The basin floor is covered by biogenic and turbiditic sediments about 500 m thick. These sedimentary accumulations are rich in planktonic carbon, which is "cracked" to form hydrocarbons by the heat of the hydrothermal activity (Edmond and von Damm 1983).

The hydrothermal deposits of the Guaymas basin are especially important in that they provide a possible comparison with a style of mineralisation popularly known as Besshi-type. This type of hydrothermal mineral deposit is characterised by massive sulphide lenses, generally Cu-Zn-rich, formed within terrigenous sedimentary sequences associated with intercalated sills and flows of basaltic rocks, and which are thought to provide the heat source responsible for the hydrothermal activity (see also Chap. 3; Fox 1984). The surveying carried out by Lonsdale and Becker (1985) indicated that the shallowest intrusions of magma occur below a cover of sedimentary material about 400 m thick. The sites of hydrothermal discharge in the Southern Trough form clusters, with several clusters forming a hydrothermal field. At each site hydrothermal constructs include chimneys, mounds and spires, locally clogged up by tube worms. Some chimneys are composed of a mixture of anhydrite and pyrrhotite. Condensed hydrocarbons are associated with spires of barite in anhydrite-sulphide mounds. Others have their orifices sealed by horizontal precipitates of anhydrite, barite, calcite and sulphides. These horizontal caps force the fluids to discharge downward, precipitating more anhydrite. During their underwater observations, the researchers occasionally punctured the floor covered by hydrothermal material, resulting in hot hydrothermal fluid being emitted at temperatures of about 300°C. The chimneys grow to a height of up to 5 m, on mounds that are between 5 and 25 m high, until they become unstable and collapse. This, in turn, causes the broken vent to re-open and to start discharging again; a new chimney is once more formed which grows until it collapses. The end result is that the sea floor is strewn with talus of hydrothermal material which contributes to the building of a mound. Other types of constructs are columns 10–50 m wide and 25 m high, with smaller vents at their summit. The whole
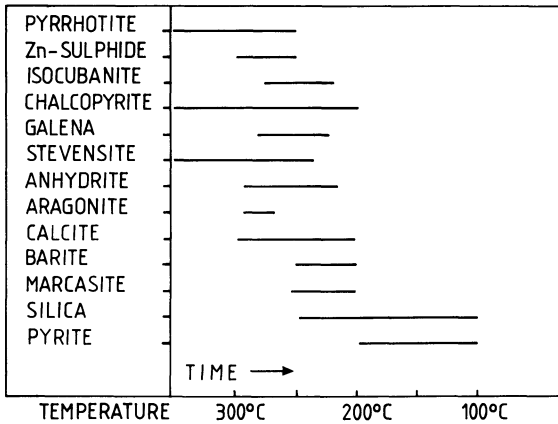
Fig. 12.13. A generalised time-temperature paragenetic sequence of sea floor hydrothermal deposit in the Guaymas basin (Gulf of California) (After Peter and Scott 1988)

hydrothermal field is therefore made up of clusters of active and inactive mounds, embedded in sheets of cemented talus material.

The sulphide mineralogy of the Guaymas deposits consists of pyrrhotite, marcasite, pyrite, sphalerite, wurtzite, isocubanite and chalcopyrite. Anhydrite, barite, calcite, silica, stevensite (a Mg-smectite), Fe oxides and clays constitute other important mineral phases of these deposits (Peter and Scott 1988). The mineral distribution differs between mounds and chimneys and between active and inactive chimneys. Marcasite occurs only in mounds, while chalcopyrite and wurtzite are found in the spires; amorphous silica and barite are more abundant in the mounds than in the spires. Anhydrite is usually absent in inactive constructs because this mineral, which is precipitated in sea water at temperatures greater than 140°C, becomes unstable at lower temperatures. $\delta^{34}S$ values for the sulphate minerals range from $+ 20.7$ to $+ 26.4$ $\delta^{34}S$ per mill, and this S-isotopic composition is interpreted as having derived from the reduction of sea water sulphate in the vent fluid (Peter and Scott 1988). The presence of calcite in the system is interpreted as due to CO_2 degassing from the vent fluids. The mineral paragenesis of the Guaymas submarine deposits is shown in Fig. 12.13 and a selected number of analyses given in Table 12.4.

On the basis of mineralogical studies and isotope systematics the presence of three distinct but superimposed hydrothermal systems have been inferred. One is characterised by the expulsion of pore water in the wet sediments, following the intrusion of a shallow sill (see Chap. 3). The discharge is at a temperature of about 100°C. The second system is a deep-seated hydrothermal circulation above a magma chamber. This fluid discharges at high temperatures through fractures in overlying sills. The third type of hydrothermal system is thought to be due to convection of hot water within the sediments above a cooling sill. Lonsdale and Becker (1985) conclude that the low-temperature vents, resulting from pore-water expulsion, will deposit barite and minor sulphides. The source of Ba is possibly the diatom-rich sediments. The high-temperature discharges would be largely responsible for the deposition of sulphide material (mainly sphalerite and chalcopyrite).

Table 12.4. Selected and partial chemical analyses of hydrothermal material from the Guaymas submarine hot spring deposits[a]

	(1)	(2)	(3)	(4)	(5)
SiO_2	31.1	50.0	34.6	5.94	41.4
TiO_2	0.10	0.13	0.08	0.23	–
Al_2O_3	0.11	3.12	0.28	0.79	0.28
MgO	0.61	26.39	0.12	2.57	0.55
CaO	24.2	0.05	7.0	0	0.15
P_2O_5	0.02	0.11	0.02	0.03	–
CO_2	17.5	0.3	5.0	0.1	0.2
BaO	11.5	1.80	13.3	48.8	11.6
LOI	5.39	14.6	18.1	12.5	–
Fe	1.32	2.22	12.59	0.34	12.8
Zn	0.23	0.86	1.58	0.26	0.43
Cu	0.06	0.28	0.23	0.05	0.16
Pb	0.13	0.4	0.91	0.03	0.47
Mn	0.50	0.11	0.41	0.008	0.01
Ag	16.8	19.5	353.2	53.8	97.4
Au	0.046	0.1	0.22	0.093	–
Cd	4	41	67	19	22
As	67.0	24.0	280.0	38.0	–
Mo	–	6	–	29	17
Sb	17.0	140.0	490	–	–

[a] (1) base of inactive light grey chimney; (2) green-brown mound material; (3) sulphide-rich, dark grey inactive spire; (4) greenish-coloured mound material; (5) mound with crust of orange-brown Fe oxide. Values are expressed in wt %, except for Ag, Au, Cd, As, Mo and Sb which are expressed in parts per million (ppm). After Peter and Scott (1988).

A model for the formation of the Guaymas hot spring constructs, as worked out by Peter and Scott (1988), is summarised here. Venting of fluids on the sea-floor begins with the precipitation of stevensite (Mg-smectite), anhydrite and pyrrhotite around the margins of the vents. This forms an impermeable crust which subsequently fractures and allows the fluids to form spire structures. The mineral constructs continue to grow upwards and outwards at the sea-floor-sea water interface, which results in less mixing of sea water with the hot fluids, thus allowing the precipitation of the sulphides. As venting continues, the walls of the constructs become thicker and the fractures tend to be sealed by mineral deposition, so that the fluids become hotter and more sulphides precipitate and replace earlier mineral phases. When the central orifice of a chimney is sealed, the fluids escape laterally forming spires. Amorphous silica is precipitated as the system cools. Clusters of tube worms and other organisms play a role in the mineral deposition by insulating the vent fluid from the cold ambient sea water, promoting deposition of sulphides, as indicated by sulphide-replaced tube worms. The mounds are thought to be constructed in a manner analogous to chimneys but with the addition of detritus derived from the collapse of the spires and chimneys.

TAG Hydrothermal Field at 26° N Latitude

This is an active hydrothermal field on the mid-ocean ridge in the Atlantic Ocean, between the Atlantis (in the north) and the Kane (in the south) fracture zones (Fig. 12.6). The field, which has been the focus of several studies since its discovery in 1972 (Rona 1980, Thompson et al. 1985, 1988), covers an area of approximately 100 km^2 mostly along the eastern wall of the rift valley between two short transform faults. This wall rises for about 2000 m above the rift valley floor, and it forms a series of steps due to normal block faulting. These faults are probably the channelways for the fluids, and it is theorised that the geometry of the block-faulted terrain is such that sea water is forced to percolate downward in the valleys and upward along the walls and rises, where an exceptional number of faults and fractures are present subparallel to the rift valley floor (Rona 1980; Thompson et al. 1985). The TAG field comprises an area of low-temperature discharges along the higher slopes of the eastern wall and a high-temperature discharge zone lower down, where the east wall and the rift valley floor, closer to the axis of the mid-ocean ridge. South of the TAG field a recent discovery of another high temperature hydrothermal field, called the Snakepit, was made in 1985 (Thompson et al. 1988). TAG and the Snakepit are the only two high-temperature hydrothermal fields so far discovered on the slow-spreading Mid-Atlantic ridge.

The low-temperature zone of TAG consists of massive stratiform deposits of Mn- and Fe-oxides and Fe silicates (nontronite), from about 1 metre to 15–20 m across. The high-temperature field consists of a black-smoker system approximately at a depth of 3600 m, and is located on oceanic crust estimated to be 0.1 Ma old. The smokers are on a large outer mound 580 m wide, on which is a smaller inner mound about 250 m wide. The entire structure is approximately 80 m high. The outer mound is formed by basaltic talus and blocks of massive sulphides covered in carbonate ooze material. The inner mound has steep walls about 30 m high and composed of weathered massive sulphide debris. On the mound are inactive and active chimneys, as well as various organisms (crabs, gastropods, eels and worm tubes); chimney structures are up to 10 m high and are located on a construct about 30–40 m in diameter. Discharge of black clouds takes place from fissures at the base of the chimney structures, and the researchers reported that the whole system appears enveloped in a dense cloud of smoke (Thompson et al. 1988). One of the active chimneys of this central structure is composed of an exterior zone of pyrite ± marcasite; and chalcopyrite + anhydrite ± pyrite ± marcasite in the interior. Other chimneys emit white smoke and are composed of mixtures of sphalerite and anhydrite on the outside, and sphalerite ± chalcopyrite ± pyrite ± anhydrite on the inside. The inner parts of these chimneys are characterised by a network of discharge channels lined with chalcopyrite, pyrite and sphalerite. Other mineral phases of the high-temperature TAG hydrothermal system include Fe oxides, orange to red in colour, and they are similar to those found in the low-temperature field. Anhydrite and aragonite are the main sulphate and carbonate phases respectively. The TAG inner mound is estimated to contain some 5×10^6 tonnes of ore material (Thompson et al. 1988).

The Snakepit field is located at approximately 23° N latitude and lies in the axial zone of the rift valley, on a volcanic ridge made up of pillow basalts. The field itself is characterised by ridges, 20–30 m high and about 100 m long, parallel to the volcanic ridge. They are composed of sulphide talus and chimney material and the areas between the ridges are covered by metalliferous sediments, mainly pyrrhotite, chalcopyrite, marcasite and pyrite. Active black and white smokers are present on these ridges with solution temperatures measured at 350–335°C and 226°C, respectively. The chimneys are made up of an outer portion of fibrous pyrite ± marcasite, and inner pyrrhotite ± chalcopyrite ± pyrite, or outer pyrite + anhydrite, and inner sphalerite + pyrite ± marcasite. The talus material consists of inner pyrite + marcasite and outer native S + jarosite + Fe oxides.

Hannington et al. (1990) investigated the effects of sea water weathering on a TAG massive sulphide deposit consisting of a central black smoker system and an apron of sulphide talus with distal metal oxides. The authors found that acid conditions, with pH of 3.6 to 5.5, prevail due to the reaction of sulphides with sea water. Gossanous Fe oxides, secondary Cu sulphides, native Cu and native Au are formed during submarine weathering. Au contents of up to 23 ppm tend to occur towards the outer limits of the oxidation zone, where Au chloride complexes are broken down as a result of pH increases.

Sub-Sea-Floor Mineralisation Associated with Seamounts

We have previously mentioned seamounts, their possible origin and discussed the occurrence of sulphide deposits on the southeastern seamount on the EPR. Hydrothermal discharges on seamounts have been recorded and investigated at a number of sites at mid-ocean ridges, namely the 21° N EPR (Alt et al. 1987), the Juan de Fuca ridge (Canadian American Seamount Expedition 1985); in the Hawaiian Chain (Malahoff et al. 1982); and in the Tyrrhenian Sea (Minniti and Bonavia 1984).

Two seamounts (Larson's Seamounts), located about 20 and 30 km west of the EPR at 21° N, have hydrothermal deposits within caldera-like structures (Alt et al. 1987). Larson's Seamounts, including the Red Volcano and the Green Volcano, are about 700 m high and of tholeiitic composition. Both are characterised by the presence of semicircular calderas approximately 2 km in diameter, within which are a number of small cones, or nested small craters. Alt et al. (1987) identified four types of hydrothermal material: massive sulphides, material containing opal-barite-atacamite, Fe and Mn oxides and clay minerals. In Green Volcano sulphide chimneys and mound deposits, Fe-Mn sediments and crusts, together with massive deposits of opal-barite occur in the crater inside the caldera and on the caldera rim. In Red Volcano Fe-Mn red-orange muds and crusts, nontronite and talc occur within the caldera. The sulphide material includes spherulitic marcasite and pyrite, chalcopyrite, covellite and Zn sulphide. Illite, opal, chalcedony and barite are also present in the chimney material. Sulphides are locally replaced by Fe oxyhydroxides which, together with jarosite, natrojarosite, and opal intergrown with barite and atacamite, occur in fractures, pores and cover surfaces. The association opal-barite-atacamite is probably due to

oxidation of primary Cu sulphides. Fe and Mn oxides and silicates include goethite, amorphous Fe oxyhydroxide, birnessite, todokorite, nontronite and Fe-rich talc. The latter forms aggregates of spherules and sheafs in veinlets and fractures. Most of the non-sulphide materials are the result of either oxidation of sulphides or low-temperature (170–30°C) hydrothermal precipitates. The authors conclude that the hydrothermal deposits of Green and Red Volcanoes were formed between 140000 and 70000 years ago and are related to the volcanic activity of the seamounts.

A breached caldera, about 7 km × 3 km, characterises the Axial Seamount on the Juan de Fuca ridge, in the Pacific Ocean (Canadian American Seamount Expedition 1985). In the flat floor of the caldera a number of small depressions, 15–25 m wide and up to 30 m deep, extend for about 300 m along a north-south fissure. Along this fissure hydrothermal vents discharge fluids at temperatures of approximately 29–35°C, although extrapolation to the end-member primary fluid gives a value of 532°C. A few chimney structures are present in the vicinity of this north-south fissure. Sulphides, amorphous silica and barite are the main constituents of the hydrothermal deposit. Sulphide phases are sphalerite, marcasite, pyrite, wurtzite and traces of galena and tetrahedrite. Chemical analyses of two samples give 10–28% Zn, 0.1–0.3% Cu, 0.1–0.6% Pb, 14–15% Ba, 233–342 ppm Ag, 110–740 Cd, 32–45 ppm Mo and 470–1300 ppm Mn.

The Loihi Seamount, located at the southernmost end of the Hawaiian hot spot track, is an active submarine volcano (Malahoff et al. 1982). The volcanic edifice, similar to the subaerial Hawaiian volcanoes, is characterised by an elongated caldera, within which are two craters and two associated rifts. Hydrothermal deposits in the Loihi volcano consist of yellow-brown goethite-Fe-montmorillonite-nontronite, occurring as precipitates on talus material. They are thought to represent the alteration products of high-temperature sulphide assemblages which may occur at depth. Although small chimney-like constructs have been noted and photographed, they could not be sampled.

In the Tyrrhenian Sea, Minniti and Bonavia (1984) report the presence of hydrothermal mineralisation associated with the Palinuro seamount, a submarine volcanic edifice to the north of the Aeolian island arc. The nature of the volcanic products of this seamount (within plate basaltic rocks of alkaline to tholeiitic affinity) suggests a marginal basin setting. Sampling of the crater of the Palinuro seamount revealed massive sulphide mineralisation consisting of tennantite-tetrahedrite, luzonite and lesser amounts of pyrite, barite, native Ag, bismuthinite and stibnite. The authors argue that this unusual mineral assemblage is reminiscent of that which characterises the high level portions of porphyry systems.

Sub-Sea-Floor Mineralisation in a Back Arc Spreading Centre

Fouquet et al. (1991a, b) discovered a number of active hydrothermal fields in a spreading centre of the back-arc Lau basin, in the southwest Pacific. The Lau basin, situated west of the Tonga-Kermadec subduction zone and associated Tofua volcanic arc (see Fig. 5.11), is being formed by behind-arc spreading between the Lau ridge in the west and the Tonga ridge in the east. Along the Valu Fa spreading

centre, southwest of the island of Tonga, there are at least four active hydrothermal fields, characterised by low- to high-temperature discharges of hydrothermal fluids depositing Fe-Mn oxide encrustations, sulphates (white smokers) and sulphides (black smokers). One of the most active and extensive of these discharge areas is the Vai Lili hydrothermal field. The Vai Lili field was traced for approximately 400 m along strike and is 100 m wide. Hydrothermal discharges occur at temperatures ranging from 400 to 320°C in black smokers, whilst white smokers discharge occurs at temperatures of 320 to 250°C. The solutions are extremely acid with measured pH values as low as 2. Active smokers can be up to 17 m high and are surrounded by talus of sulphide material. In some localities the sulphides are overlain by Fe-Mn oxides crusts. Hydrothermal plumes rise up to 200 m above the sea-floor. Compared with MOR-type hydrothermal discharges the Vai Lili solutions contain unusual concentrations of B, Ba, Zn, Pb, As and Cd. Fouquet and coworkers were able to sample a cross-section through a massive sulphide deposit. From top to bottom the deposit consists of: (1) active smokers and talus of chimney material containing barite, anhydrite, chalcopyrite and sphalerite; (2) porous material made up of barite, sphalerite, galena, tennantite and native Au; (3) massice Cu-rich sulphides; (4) stockworks in altered andesitic rocks with veinlets of chalcopyrite, silica, barite and sphalerite.

The authors consider the setting of the Lau basin to be intermediate between oceanic and continental back-arc environments. This and the nature of-the mineralisation suggest that the massive sulphide deposits of the Vai Lili hydrothermal field may have some similarities with, or is transitional to kuroko-type massive sulphide deposits.

Chimneys and Mounds in the Geological Record

The descriptions of sub-sea-floor hydrothermal constructs have logically resulted in an attempt to recognise similar structures in ancient hydrothermal mineral deposits which are thought to have formed in the same way. Fragments of black smoker chimneys have been recognised by Oudin and Constantinou (1984) in the brecciated ore of the Troodos massive sulphide deposits in Cyprus (to be described later). Fossil chimneys and mounds have also been recognised in the 360-Ma-old sulphide and barite sedimentary-exhalative deposits in Ireland, namely, at the Tynagh Pb-Zn deposit (Banks 1985), and at one of the Silvermines orebodies (Boyce et al. 1983). In the latter, a fossil hydrothermal mound has been recognised in an open-pit barite deposit. However, the Silvermines fossilised hydrothermal constructs show marked differences from those typical of a mid-ocean-ridge setting, being smaller, composed almost entirely of pyrite, with minor sphalerite and barite, and having a distinct S-isotopic signature. The differences noted by the authors are ascribed to the diverse tectonic settings and hence the environment of the hydrothermal discharge (see Chap. 14). The Irish deposits are thought to have formed by hydrothermal discharge in a structural depression or brine pool, at temperatures of approximately 150°C. Sulphur isotope determinations (δ^{34}S of between -18 and -42 per mill) of fossil tubes suggest the involvement of microorganisms which have reduced sea-water sulphate.

Pyritic fossil worm tubes have been reported from the Bayda sulphide orebody of the Samail ophiolite (to be described later) in northern Oman (Haymon et al. 1984). These fossil worms are chracterised by moulds and casts preserved in massive sphalerite and pyrite with some quartz. The tube-like fossils are 1 to 5 mm in diameter, are randomly oriented and have concentric mineral layering from pyrite, on the exterior, to quartz (or void), to pryite, sphalerite and quartz. The authors compared these fossilised tubes with the worm-tube structures of the EPR.

Finally, in the Matakaoa Volcanics, North Island (New Zealand), an allochthonous block of oceanic crust of Tertiary age contains small pods of Au-bearing barite and sulphide mineralisation. The study of this mineralisation revealed structures reminiscent of sub-sea floor chimneys (Pirajno 1980).

12.7 Oceanic Crust-Related Hydrothermal Mineral Deposits

In this section we look at some examples of hydrothermal mineral deposits, the genesis of which is generally recognised to have been in an oceanic crust environment, at or near a spreading centre. We describe the deposits of the Samail ophiolites in Oman, the Cyprus Cu deposits, which have been used as one of the type examples for a category of deposits known as volcanogenic massive sulphides, and the Besshi-type Cu-Zn-Ag deposits of the Matchless Amphibolite Belt of the Damara orogen in Namibia.

12.7.1 Massive Sulphide Deposits of the Samail Ophiolite, Oman

Since 1975 a multidisciplinary research and exploration programme has been conducted by various British, French and American universities and institutions, in the Oman mountains in the Arabian peninsula. This work, which was primarily directed at evaluating the mineral resources of the region, also provided invaluable information on the geology, geochemistry, tectonism and ore genesis in ophiolitic rocks. Further, the data gained from this multidisciplinary study permitted an in-depth comparison between the Oman ophiolite mineral deposits and those that are generated at spreading centres. There are several publications dealing with aspects of the geology, geochemistry and mineralisation of the Samail ophiolite; those that provided the basis for the following discussion are Fleet and Robertson (1980), Smewing et al. (1984), Coleman (1984), Ixer et al.(1984), Alabaster and Pearce (1985) and Nehlig and Juteau (1988). A special issue of Tectonophysics (Vol. 151, Boudier and Nicolas 1988) is devoted to the ophiolites of Oman.

The Samail ophiolite is situated in northern Oman, on the east-southeastern side of the Arabian peninsula (Fig. 12.14A, inset). It forms a well-defined belt which is part of a great ophiolite system that extends from the Mediterranean Sea across Turkey and the Middle East, and marks the boundary, or the suture zone, along which the Tethys Ocean closed towards the end of the Cretaceous period. The igneous stratigraphy of the Samail rocks fits the definition of ophiolites as given by
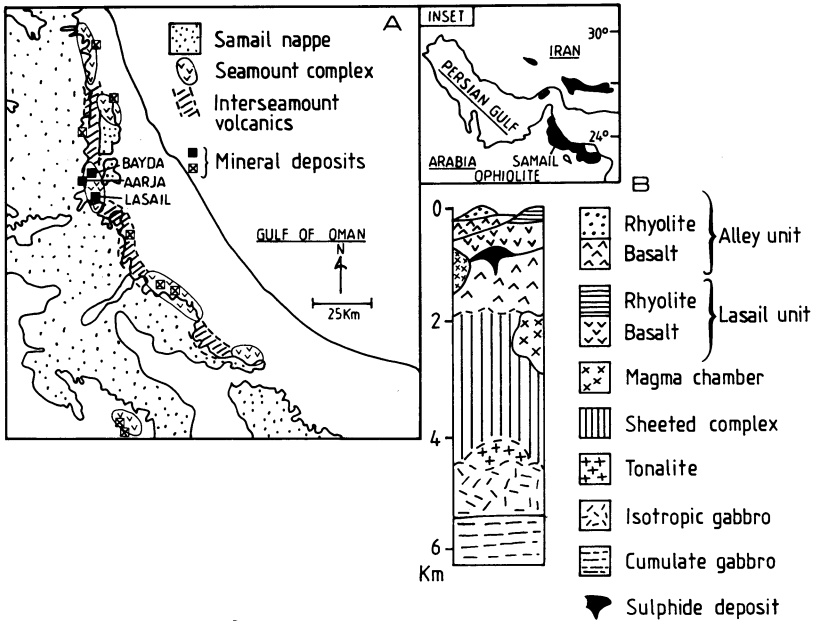
Fig. 12.14. **A** Sketch map showing location of Samail ophiolite (*inset*) and distribution of associated hydrothermal mineral deposits. *Black squares* indicate deposits discussed and/or mentioned in text. **B** Simplified stratigraphy of the Samail ophiolite (After Alabaster and Pearce 1985)

the Penrose Conference participants in 1972, and is essentially made up of a plutonic sequence and a sheeted intrusive complex, followed upward by a sequence of lavas and metalliferous sediments. Alabaster and Pearce (1985) explain the magmatic history of the region in terms of distinct volcanic units and associated high-level intrusives (Fig. 12.14B). The Geotimes Unit, consisting of basaltic pillow lavas up to 1.5 km thick, forms the volcanic basement upon which later units accumulated. Geochemical and petrological data suggest that the Geotimes Unit is part of a fractionation trend from cumulate gabbro, through isotropic gabbro, tonalite and trondhjemite of the Main Plutonic Sequence. It is argued that the Geotimes Unit may have formed the crust of a marginal basin rather than an open ocean. The Lasail Unit overlies the Geotimes Unit and consists of mafic to felsic lavas up to 750 m thick. This Unit is cut by andesitic cone sheets which appear to centre over a major intrusion, the Late Intrusive Complex, forming a closed system with a gabbro-diorite-trondhjemite fractionation sequence. The Alley Unit consists of basaltic pillow lavas and minor rhyolitic rocks, related to high-level gabbroic plutons. The last igneous event produced the Clinopyroxene-phyric Unit, made up of basaltic lavas fed by mafic and ultramafic intrusions. The work of Alabaster and Pearce (1985) reveals a coherent picture of ocean floor hydrothermal and ore genesis processes in the Lasail area, and is thus a good example of comprehensive geological work, the kind which should be implemented by exploration geologists.

In the Lasail area hydrothermal metamorphism produced mineral assemblages characteristic of greenschist facies, chlorite and albite, interpreted as being the result

of a multipass fluid flow beneath a sedimentary cover. The Geotimes Unit displays an alteration assemblage of brown smectite + chlorite + albite + calcite + quartz + Fe hydroxides ± actinolite ± epidote ± sphene ± prenhite ± stilbite. Albitisation of the feldspars is typical in the Unit; chlorite is particularly abundant, whereas prehnite and epidote are usually found only in vesicles and veinlets. Traces of jasper and sulphides are locally present and a zone of stockwork veining is believed to represent the feeder to the Lasail massive sulphide deposit. The Lasail basalts have an alteration assemblage of epidote + chlorite + albite + prehnite + quartz + calcite ± actinolite ± sphene ± pyrite ± laumontite ± Fe hydroxides. Chlorite and epidote usually replace the olivines, while albite ± prehnite ± epidote replace the plagioclases. Chlorite, epidote and prehnite are also abundant in the groundmass. Clinopyroxene is the only relict mineral to have survived alteration. The Lasail Unit is interpreted to represent off-axis volcanic seamounts developed on oceanic crust. The alteration assemblage that characterises the basaltic rocks of the Alley Unit includes stilbite + celadonite + albite + chlorite + smectite + calcite ± mesolite ± quartz ± Fe hydroxides. Albite replaces plagioclase and is in turn replaced by the zeolite minerals. The Clinopyroxene-phyric Unit has an alteration assemblage of chlorite + epidote + albite + smectite ± prehnite ± calcite ± sphene ± Fe hydroxides.

The predominance of albite and chlorite is indicative of widespread greenschist facies, which in present-day oceanic crust is restricted to hydrothermal discharge zones. Analyses of chlorites and zeolites show a uniform composition for these minerals and this too contrasts with oceanic greenschist rocks in which the chlorites, for example, show strong variations in Mg/Fe ratios. Alabaster and Pearce (1985) advocate a "sealed, multipass hydrothermal system", due to repeated fluid circulation through the crust. The greenschist facies assemblages are thought to represent prograde metamorphism, while the assemblages containing zeolites and clay minerals possibly represent retrograde reactions due to the cooling phases of the hydrothermal system. The seal of the convective circulation could have been provided by the sedimentary cover of radiolarian mudstones, pelagic sediments and volcanoclastics.

The distribution of the Samail mineral deposits is shown in Fig. 12.14A. There are numerous Fe-Mn-rich sediments which occur as lenses intercalated in the lavas of the Geotimes Unit. These metalliferous sediments are red-brown in colour, composed mainly of radiolarians, and contain quartz, hematite, goethite, Mn oxyhydroxides, carbonates (calcite, dolomite, ankerite), epidote, pumpellyite, apatite and natroalunite (Karpoff et al. 1988). Two end members are considered by Karpoff et al. (1988), Fe-Mn types and Si-Ca types, the former having a greater recognisable hydrothermal component than the latter which contain more biogenic materials.

Economically more important are the massive sulphide deposits (see Fig. 12.14A), such as those of the Lasail area, where three main deposits have been identified: Lasail, Aarja and Bayda, described by Ixer et al. (1984). All three are pyrite-rich, but contain enough chalcopyrite and sphalerite to attain the necessary ore grades for Cu. The larger Lasail deposit has about 8×10^6 tonnes of ore, Aarja approximately 3×10^6 tonnes, and Bayda 0.75×10^6 tonnes; all with an average Cu grade of approximately 2% (Ixer et al. 1984). The Lasail massive sulphide deposit

is approximately 50 m thick and extends to a depth of at least 200 m. The mineralisation consists of a massive sulphide saucer-shaped lens underlain by a stockwork of quartz-pyrite-chlorite in the Geotimes footwall lavas. The massive sulphide lens consists mainly of pyrite with intercalations of chalcopyrite, magnetite-hematite $\pm$ chalcopyrite bands. Minor quantities of sphalerite, marcasite, bornite and traces of cubanite, pyrrhotite, mackinawite and carollite are also present. The gangue mineralogy includes quartz, calcite, chlorite, epidote and gypsum. The massive sulphide lens is overlain by gossan material containing Fe oxides and hydroxides, jarosite, kaolinite, malachite, azurite and native Cu. Geochemical analyses of drill core, reported by Ixer et al. (1984) indicate the following ranges of metal values: 0.44–21.4% Cu, 14–245 ppm Pb, 0.02–19.7% Zn, 3–522 ppm Mo, 18–544 ppm Co. Geological evidence suggests that rocks of the Lasail Unit may represent off-axis volcanic seamounts (Alabaster and Pearce 1985), and the mineralogical and geochemical character of the Lasail mineralisation points to certain differences with typical on-axis mineralisation. Ixer et al. (1984) suggest that some of these differences are the higher pyrite content, the overall Zn and Cu depletion, and the higher Co content of pyrites of the Lasail mineralised material compared to the on-axis mineralisation. Pyrites of mineralised material associated with seamounts may contain up to 17% Co (Hekinian et al. 1983), whereas pyrites from the EPR and the Juan de Fuca ridge have Co contents of less than 40 ppm (Ixer et al. 1984). `

12.7.2 The Cu Deposits of Cyprus Island

Copper (cuprum) may have derived its name from the island of Cyprus, or vice versa. What is certain, however, is that Cu has been mined on Cyprus since ancient times ($\pm$ 3000 B.C.).

The Cyprus Cu deposits – from which, in addition to Cu, pyrite, and occasionally Zn and precious metals are recovered – having undergone only minor metamorphism and deformation are ideally suited for study. For this reason they have been used as a type example of ophiolite-hosted volcanogenic massive sulphide deposits. The geology, geochemistry and tectonic evolution of the Cu deposits of Cyprus are described in the works of Govett and Pantanzis (1971), Robertson (1975), Constantinou and Govett (1972) and Constantinou (1980), and reviewed by Franklin et al. (1981). The main geological feature, and the host of the Cu deposits, is the Troodos Igneous Complex, one of the best exposed and documented ophiolite complexes of the world (Fig. 12.15). It represents the exposed portion of a much larger igneous complex that probably extends beneath most of the island. Although unanimously recognised as an ophiolite, the precise origin of the Troodos Complex remains a matter of controversy. It may be part of oceanic crust thrust up to its present position from a mid-ocean-ridge in the Tethys Ocean, or it may be an off-axis part of the Tethyan oceanic crust, or it may be part of a back-arc marginal basin.

The Complex has been divided into: (1) The Troodos Plutonic Complex; (2) Sheeted Intrusive Complex; and (3) Troodos Pillow Lavas. The Plutonic Complex is
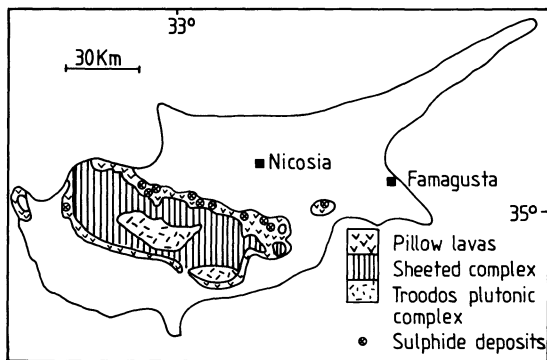
Fig. 12.15. Simplified geology of the Troodos Igneous Complex, Cyprus, and location of main massive sulphide deposits (After Searle 1972)

composed of ultramafic rocks, including harzburgite and dunite, interpreted as depleted mantle material, and a gabbroic suite, including peridotite and pyroxenite, intepreted as components of the magma chambers that fed the overlying basalts. The gabbroic rocks and part of the overlying Sheeted Intrusive Complex are correlated with layer 3 of the typical oceanic lithosphere sequence. The upper part of the Sheeted Complex, which consists almost entirely of dolerite dykes, and the overlying pillow lavas of tholeiitic basaltic composition, are correlated with layer 2 of oceanic crust. The Troodos Complex is overlain by marls and limestones which are correlated with layer 1.

The Sulphide Orebodies

The sulphide mineralisation is restricted to the Troodos Pillow Lavas, which consist of three units: Upper and Lower pillow lavas and the Basal group. This mineralisation occurs as massive sulphides and stockworks forming clusters of three or more bodies in five major mining districts. More than 90 orebodies are known, their size varying from about 50000 tonnes to 20 million tonnes, and Cu grades ranging from 0.3 to 4.5%. Reconstruction of the orebodies shows that they are saucer-shaped, and most of them characterised by a distinct vertical zoning comprising, in downward succession, an ochre horizon, a zone of massive ore (Zone A), a pyrite-silica zone (Zone B) and a stockwork zone (Zone C; Fig. 12.16). Zone A massive ore is the most economic and comprises two structural types: conglomeratic ore and hard-compact ore. The former is made up of spheroidal, or pillow-shaped, blocks of sulphide material in a gritty matrix of sulphide grains. The size of the blocks tends to increase downward with a concomitant decrease in the matrix material. The increase in the matrix material affects tonnage calculations on account of its lower specific gravity. Hard-compact ore underlies the conglomeratic ore and comprises large blocks of sulphides separated by fractures, several centimetres wide, along which there is a soft and friable pyrite. The dominant ore mineral is pyrite, of which three paragenetic types are recognised. Pyrite I, which is euhedral to subhedral; pyrite II is anhedral and overgrows pyrite I; and pyrite III occurring as colloform bands mainly in the conglomeratic ore. Chalcopyrite and minor sphalerite are more abundant in the conglomeratic ore, and are rare in the
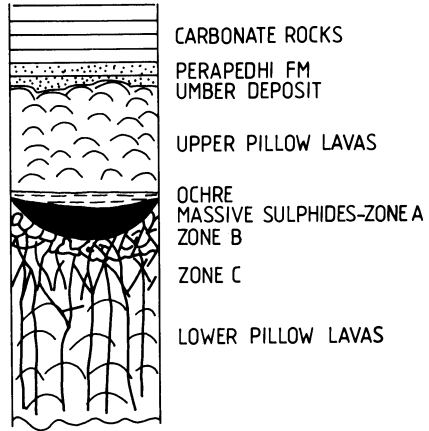
Fig. 12.16. Schematic section through a typical Cyprus-type sulphide deposit and its relationship to overlying lithologies (After Hadjistavrinou and Constantinou 1982)

compact ore where they occur as inclusions along the pyrite growth zones. The pyrite-silica zone (Zone B) is characteristically very hard, and, in addition to pyrite, has small and variable amounts of chalcopyrite and sphalerite. The silica component is represented by quartz, chalcedony and red jasper. The stockwork zone (Zone C) has been found by drilling to extend to depths greater than 700 m. It contains small amounts of chalcopyrite and sphalerite, mostly confined to pyrite veins. Pyrite, on the other hand, occurs as veins and veinlets and is disseminated throughout the lavas, which are intensely silicified. The stockworks pass downward into hydrothermally altered and mineralised lavas in which the pillow structures are still recognisable. The hydrothermal mineral assemblage is quartz-chlorite-epidote-illite-kaolinite. Zeolites (laumontite, celadonite, mordenite) are common in both Lower and Upper pillow lavas. Deeper down, chlorite, albite, epidote, calcite and pyrite become the dominant alteration minerals.

Ochre material, conformably overlies the ore (Fig. 12.16) and is a Mn-poor, Fe-rich, bedded deposit with varying proportions of chert, tuffaceous material and limestone. Ochre contains bands or fragments of sulphides and is enriched in Cu and Zn, with low Ni/Co ratios (<1). It should not be confused with umber, which is a fossiliferous, fine-grained Mn-Fe-rich sediment, with high Ni/Co ratios (>1). Umber lies unconformably above the sequence of pillow lavas and at the base of the overlying sedimentary sequence.

Geological evidence indicates that the lavas that host the sulphide mineralisation were erupted in an environment where oceanic crust was generated. Hydrothermal alteration and the nature of the mineralisation are consistent with sub-sea-floor hot spring activity in which pyrite is the dominant primary mineral with lesser quantities of chalcopyrite and sphalerite. As described earlier for the Samail deposits this may be indicative of an off-axis origin. After formation of the sulphide mineralisation, oxidation of pyrite at the sea water-mineralisation interface produced H_2SO_4, causing acid leaching of pyrite I. This leaching process resulted in the vertical zonation of the ore, from an upper zone of complete leaching, through a zone of partial leaching (conglomeratic ore), to a lower zone where leaching was minimal (compact ore). Some of the products of leaching were lost to sea water, while some

were precipitated as secondary sulphides in a zone of secondary enrichment within the conglomeratic ore. The degree to which secondary enrichment progressed was largely dependent on the precipitation and removal rates of the Fe hydroxides because, as layers of the Fe hydroxides accumulated on top of the sulphides, these were protected from further oxidation. The Fe hydroxides are now preserved as layers of ochre material. Continuing volcanic activity deposited fresh basalts over the sulphide mineralisation, and when volcanism ceased oceanic weathering resulted in the formation of umbers, and thereafter a normal marine sedimentary sequence began to accumulate.

Cyprus-type massive sulphide deposits that are exposed at the surface may be found by locating the gossan outcrops, which are often enriched in precious metals. According to the model of sub-sea-floor mineral deposition, blind deposits should only be sought beneath fresh lavas because altered basalts, with traces of sulphide mineralisation, would indicate a stratigraphic position below a previously eroded massive sulphide deposit. Lithogeochemistry may be a useful exploration tool, as suggested by Govett and Pantazis (1971), who showed that Cu is anomalous in the lavas of mineralised areas. However, the anomalous Cu is to be found only in the interpillow material. In the same areas Zn and Co may be anomalous in the centre of pillows whilst Ni is depleted. The distribution of these trace elements are attributed to secondary processes. The identification of ochre, which may be distinguished from umber by differences in trace element geochenistry (e.g. Cu/Zn or Ni/Co ratios), would be a good pathfinder for shallow deposits. The Cyprus-type massive sulphide deposits provide good targets for electrical geophysical techniques such as E.M., I.P or resistivity.

12.7.3 The Cu Deposits of the Matchless Amphibolite Belt, Namibia

The Matchless Amphibolite Belt (MAB) occurs in the Southern Zone of the intracontinental branch of the Damara orogen, Namibia (Chap. 7 and references therein; Fig. 7.4). The MAB is clearly visible in LANDSAT imagery (Plate 12.1) as a dark northeast-trending line, extending for about 350 km from the southwest in the Namib desert to the northeast in the highlands around the city of Windhoek.

Rocks of the MAB include amphibolite, metagabbro, minor talc schist, quartz-sericite schist and chlorite schist, conformably intercalated within quartz-biotite schist, garnet, staurolite and kyanite schist of the Kuiseb Formation (Khomas Subgroup, Damara Sequence; Plate 12.2). The metasedimentary rocks are indicative of terrigenous-dominated sedimentation in a deep and narrow trough (Khomas Trough), which may have been underlain by oceanic crust. The mafic rocks of the MAB form discontinuous lenses within the metasediments (see Fig. 12.17), aggregating a total exposed width of approximately 3 km. Attention has focused on the MAB because the interpretation of the nature of its lithologies may help in elucidating the tectonic setting of the Belt and hence the geodynamic evolution of the Damara orogen as a whole. Three tectonic settings have been considered: intracontinental, oceanic and one of small and restricted ocean basins where spreading was active. The amphibolites have been interpreted as metalavas of
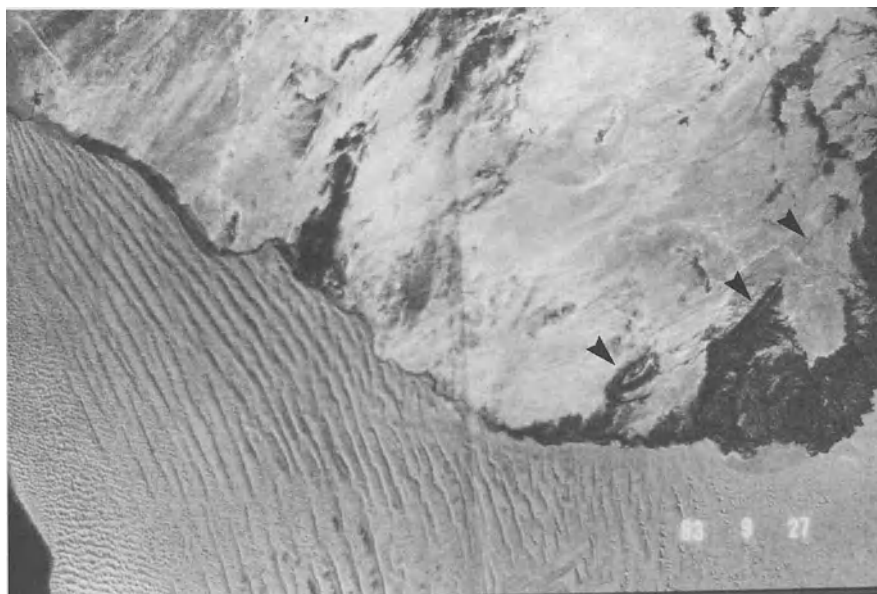
Plate 12.1. LANDSAT imagery of the Namib desert, Namibia. The *lower part* of the image shows the north-south-trending sand dunes of the Namib, separated by the Kuiseb river from the exposed portions of the Damara orogen, the Matchless amphibolite belt is visible as a thin *dark line (arrows)*, with its typical fold closure (*arrow*) at its southwest end (see Figs. 12.17A and 12.19)

tholeiitic composition with petrological and geochemical affinities to mid-ocean ridge basalts (MORB). However, there is evidence for a syn-sedimentary submarine extrusive origin for the amphibolites, such as interfingering with the metasediments and their common association with magnetite quartzite, whose precursor lithology was probably a chemical sediment formed near hydrothermal discharge vents. Also, the position of the MAB, high in the Kuiseb stratigraphy, together with the lack of evidence of a tectonic melange and recognisable sheeted dykes, do not suggest that the MAB is a typical ophiolite. Breitkopf and Maiden (1988) and Klemd et al. (1989) have interpreted the tectonic setting of the MAB on the basis of the trace element geochemical signature of the mafic rocks and the character of the associated sulphide mineralisation. These authors consider that along the length of the MAB – and the Khomas trough – there may be at least two main tectonic subsettings. One is in the western sector of the Belt, where the Gorob and Hope Cu deposits are located (Fig. 12.17A), in which the mafic rocks show degrees of fractionation compatible with within-plate basalts. This is shown by their Ti, Ti/Cr and FeO/MgO ratios, which are higher, and Ni/Ti ratios, which are lower, than the mafic rocks of the other subsetting in the central and eastern sectors. In the eastern sector MAB rocks have compositions consistent with mid-ocean-ridge tholeiitic basalts. The Matchless, Otjihase and Ongambo Cu deposits occur in this eastern sector (Fig. 12.17A). Thus, the scenario envisaged is one of extensional tectonics, characterised by continental rifting with thinning and stretching of the crust, which resulted in the
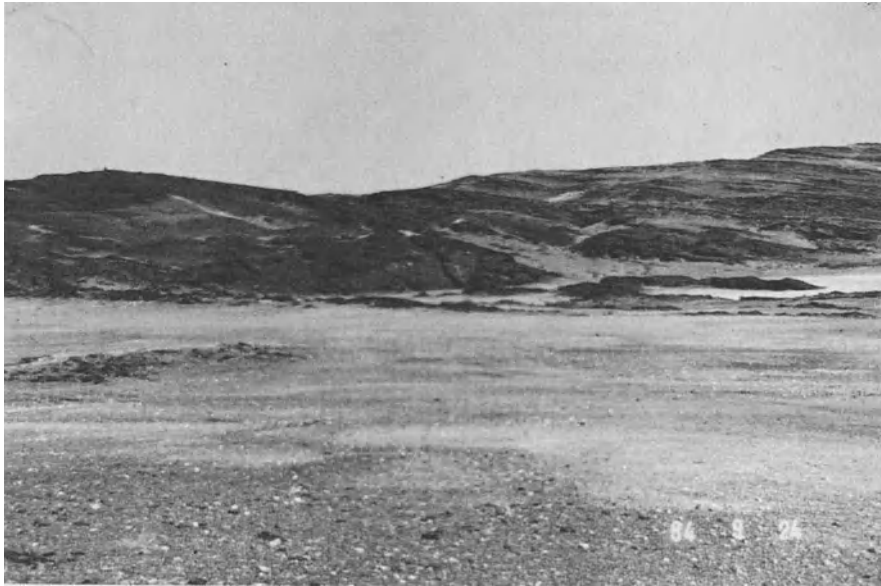
Plate 12.2. Panoramic view of the Matchless amphibolites near Gorob (looking west). Amphibolites are the dark rocks on *centre and left side* of the plate, and associated Kuiseb metapelites (light grey rock) on the *right*
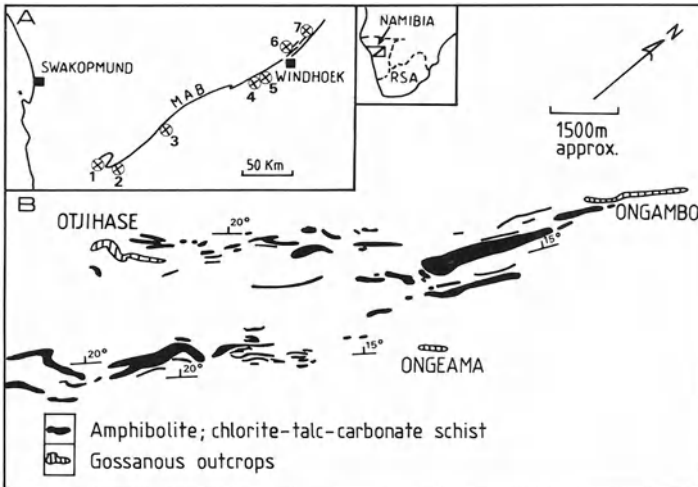
Fig. 12.17. A Schematic representation of the Matchless Amphibolite Belt (MAB) in the intracontinental branch of the Damara Orogen, Namibia, and location of associated massive sulphide deposits, (see also Figs. 7.4, 7.5A and Plate 12.1). *1* Hope; *2* Gorob; *3* Niedersachsen; *4* Matchless; *5* Kupferberg; *6* Otjihase; *7* Ongeama and Ongambo. After Breitkopf and Maiden (1988). **B** Distribution of the Matchless amphibolite and allied lithologies around the Otjihase, Ongeama and Ongambo sulphide deposits near Windhoek (After Viljoen and Viljoen 1975)

development of a series of small, elongated basins or troughs. In the western sectors the basins were formed above the thinned and stretched continental crust in which mafic magmas ascended and fractionated within this crust. In the central sectors there was possibly less continental crust, as suggested by the systematic variations in Ti, Ni, Cr, Fe and Mg indicated above. According to this model, a basin in the eastern sector of the Khomas trough was probably floored by oceanic crust, and mafic magmas were being injected into wet and unconsolidated terrigenous sediments. The western basin could have been formed by strike-slip movements which resulted in a pull-apart basin (Breitkopf and Maiden 1988). The authors also contend that the size of the associated massive sulphide deposits appears to correlate with the stage of opening of these basins. The larger deposits (Matchless, Otjihase) are located in the eastern basin floored by oceanic crust, and the smaller (Gorob, Hope) in areas underlain by continental crust.

Mineralisation

A number of massive sulphide deposits containing Cu $\pm$ Zn $\pm$ Ag $\pm$ Au, occur along the MAB (Fig. 12.17A). These include Gorob, Hope, Luigi and Vendome in the southwestern part of the Belt, Niedersachsen in the central part and Matchless, Kupfeberg, Otjihase, Ongeama and Ongambo in the northeast, near Windhoek. The MAB mineralisation has been reported by Goldberg (1976), Killick (1983), Admanson and Teichmann (1986), Klemd et al. (1987) and Klemd et al. (1989). In this section we look at the Otjhase and Gorob deposits.

Dynamothermal metamorphism has obliterated the original structures and bedding of the sedimentary layers; intense compression of the MAB and Kuiseb Formation rocks resulted in isoclinal to recumbent folding and the development of a dominant penetrative S_2 foliation which dips to the northwest. The shape and present attitude of the massive sulphide bodies, which are cigar-shaped and have steep northerly plunges, reflect the deformation history of the area. Mineral lineations are present which parallel the ore shoots and as such provide a useful guide for the intepretation of geophysical surveys and for the establishing of drill targets (see Fig. 12.19B).

Otjihase

The Otjihase deposit is located 20 km northeast of Windhoek, capital city of Namibia. Ore reserves are approximately 16×10^6 tonnes at 2% Cu, 0.3–0.6% Zn, 9–10 ppm Ag and 0.35–0.5 ppm Au. The mineralisation is hosted in quartz-biotite schists of the Kuiseb Formation, but in the vicinity of the orebodies the host rocks also include garnetiferous quartz-biotite schist and chlorite schist, talc-carbonate schist and actinolite schist. The rocks strike northeast, dipping northwest at about 15°. North- and northeast-trending faults occur in the area and have divided the deposit into different fault-bounded blocks. Surface expressions of the mineralisation are characterised by four distinctive gossanous magnetite quartzite outcrops which can be traced for a distance of at least 1.5 km (Fig. 12.17B). These outcrops are up to 12 m thick and have a downdip extent of about 4 km. The gossan material
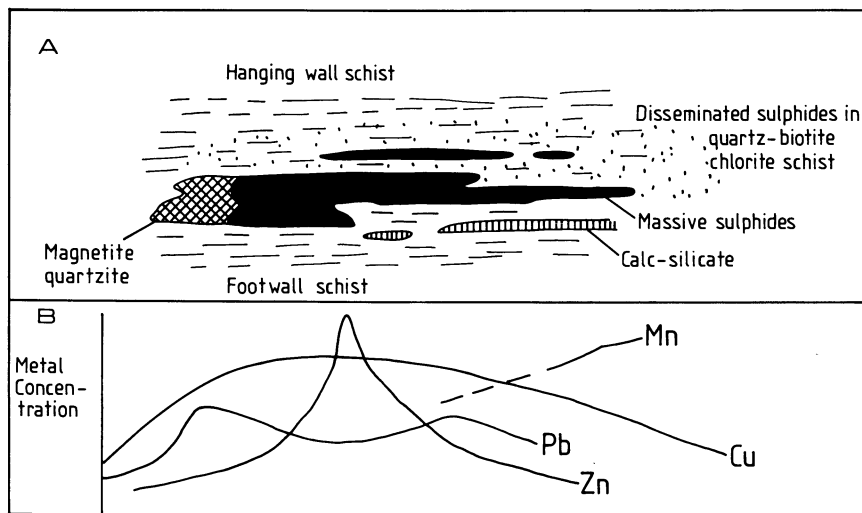
Fig. 12.18. A Schematic cross-section of a Otjihase-type orebody and **B** semi-quantitative relative lateral distribution of selected metals; see text for discussion. Based on information provided by A. Thomson, mine geologist

is red-brown in colour and consists of leached limonite, goethite and siliceous material in which Cu values are only about 0.1%. Oxidation of the sulphide zones extends down to a depth of about 50 m in places, where there is an abrupt change to sulphides without a zone of secondary enrichment. The mineralisation is situated some 300–200 m structurally, and possibly also stratigraphically, above the MAB rocks (Fig. 12.17B). The main orebody is narrow, elongate and lenticular, and is known as the northern oreshoot. As already mentioned, an important feature both of the Otjihase deposit (and of Gorob) is that the plunge of the long axis of the ore shoots is defined by a prominent D2 mineral lineation, which parallels the direction of minor fold axes seen on the surface in the footwall magnetite quartzite. The northeastern limit of the orebody is sharp and represents a possible fold closure, while on the southwestern side the ore zone interfingers with schists and the cutoff is determined by assay values. The hangingwall contact is usually transitional, whereas the footwall contact is sharp. Therefore a footwall contour map provides a useful picture of the mineralisation and also aids in stope planning. The orebody averages 2.5 m in width, but may locally thicken to 7 m. A representative cross-section of an ore lens of the Otjihase deposit is shown in Fig. 12.18 A.

Goldberg (1976) divided the ores into massive, disseminated and stringer. The massive ore is composed of more than 80% sulphides and 20% magnetite quartzite gangue. Sulphides are fine- to coarse-grained and form massive bands composed of pyrite + chalcopyrite or alternating bands of pyrite and chalcopyrite. Disseminated ore contains up to 50% sulphides in a gangue of sericitised chlorite-biotite schist and magnetite quarzite. Stringer sulphides form narrow veins of either pyrite or chalcopyrite.

The mineralisation consists of pyrite and chalcopyrite mainly, with varying minor quantities of sphalerite, galena, pyrrhotite and electrum. Ag and Au are also associated with the chalcopyrite. The sulphides form disseminations in magnetite quartzite and quartz-biotite ± chlorite ± garnet ± feldspar schist and as massive bodies in association with the above lithologies. Metamorphism and deformation have substantially modified the orebodies with noticeable boudinaging of the magnetite quartzite, flowage of the more ductile schists, and doubling-up of layers which have resulted in local thickening of the orebodies. Annealing of the sulphide grains has resulted in the development of coarse-grained sulphide aggregates and mosaics. Because of deformation it is difficult to recognise pristine vertical and lateral zonations within the ore lenses. Looking at the representative cross-section of Fig. 12.18A and the semi-quantitative geochemical profiles along the mineralisation (Fig. 12.18B), two interpretations may be advanced, depending on whether the mineralisation was formed as a convex lens, or mound, or as a sulphide pool (see discussion in Sect. 12.6.2). In the first case, (as suggested by the mine geologists) (A.Thomson pers. comm. 1989), the entry point of the hydrothermal solutions was at the site of the magnetite quartzite, which would then represent the waning stage of the sulphide deposition, with the sulphide lenses occurring laterally to the magnetite-quartzite. In this case, the present footwall would also be the stratigraphic footwall. The other possibility is that the original mineralisation was formed in a structural depression as in a brine pool. The magnetite quartzite would still represent waning hydrothermal activity, but would have formed in the oxygenated environment above the sulphide pool. In this case the magnetite quartzite would represent the stratigraphic top with the whole ore lens, as seen now, lying on its side, with the stratigraphic footwall on the right-hand side of Fig. 12.18A.

Hydrothermal alteration is not readily apparent, either mineralogically or geochemically, because of metamorphism and deformation. However, in their study of the Matchless ore lenses, Klemd et al. (1989) have proposed that the chlorite-quartz ± ankerite schist, with intercalated bands of magnetite quartzite and lenticles of sulphides at the immediate structural hangingwall of the orebody, may represent an original footwall feeder zone, and therefore the sequence would be overturned. In their model, the magnetite quartzite is interpreted as the metamorphosed equivalent of a ferruginous cherts deposit around the exhalative vents on the sea-floor. By contrast, the pyrite-quartz-muscovite (or sericite) rocks, which occur in the structural footwall are interpreted as exhalites forming as a result of waning hydrothermal activity, and they appear to decrease in number away from the mineralisation, that is, upward in the stratigraphic hangingwall. Geochemically, the assumed footwall feeder zone rocks show depletions in Na, Ca and Sr, and enrichment in Rb, Ba, Fe and S as well as Cu, Zn and Pb. The local exploration geologists (T.Smalley and D.Corbett pers. comm. 1990), however, do not support the model proposed by Klemd et al. (1989), but instead regard the magnetite quartzite bands as the top of the mineralised system, in which case the sequence would be the right way up (Smalley 1990).
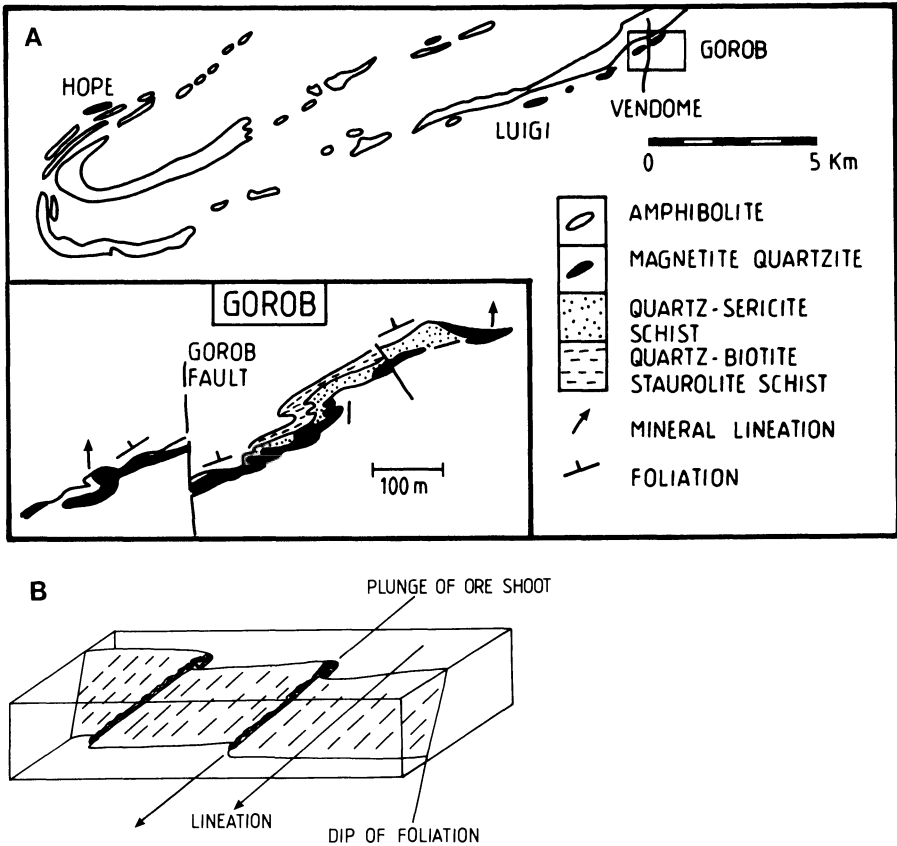
Fig. 12.19. A Sketch map of the southwest end of the Matchless Belt, Namibia, showing distribution of sulphide deposits and detail of the Gorob prospect (after Killick 1983). **B** Block diagram showing location of ore shoots in drag-fold closures and plunge of lineations; see text for details

Gorob

The Gorob prospect is located at the southwestern end of the MAB (Plate 12.1), where a number of similar deposits occur around a major synform which closes to the west near the Hope deposit (Fig. 12.19A). The latter deposit was subjected to high grade contact metamorphism resulting from the intrusion of the Donkerhoek granite to the north. The Gorob deposit is separated by approximately 200 m of quartz-biotite schist from the base of the MAB rocks in the north. The surface expression of the deposit is a gossanous outcrop of magnetite quartzites and quartz-sericite schist, stained by secondary Cu minerals such as malachite and chrisocolla. The gossanous outcrops dip approximately 45° to the northwest. Drilling revealed that the ore shoots are contained in drag-fold closures that parallel a prominent D2 mineral lineation which indicates the plunge of the shoots at 45° towards 356° (Fig. 12.19B). Below the level of oxidation, pyrite is the dominant sulphide followed by chalcopyrite, pyrrhotite, sphalerite, galena and rare molybdenite (Killick. 1983).
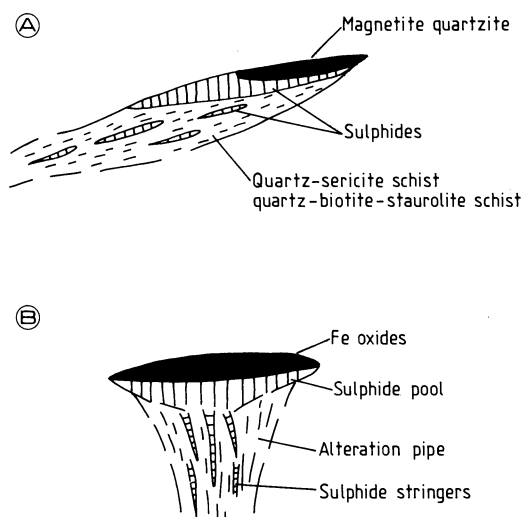
Fig. 12.20A, B. Reconstruction of an idealised mineralised lens at Gorob (Pirajno unpubl. data). **A** Observed field relationships of a deformed mineralised lens showing the succession of magnetite quartzite, sulphide mineralisation (gossan) and a zone of quartz-sericite schist and quartz-biotite-staurolite schist enclosing sulphide lenses and stringers. **B** Reconstructed mineralised lens, based on the interpretation that the quartz-sericite and quartz-biotite-staurolite schists represent the metamorphic equivalent of a siliceous and potassic alteration envelope containing sulphide stringers (possible feeder channels to the mineralised lens)

Killick (1983) also reported a metal zoning from a Cu-rich hangingwall to a Zn-rich footwall, as well as a sharp footwall contact and a gradational hangingwall contact as observed at Otjihase. This would indicate that the younging direction is towards the south and that in the Gorob area the succession is probably overturned. A reconstruction of an idealised mineralised lens at Gorob is shown in Fig. 12.20.

Comparison with Besshi-Type Deposits and Ore Genesis

The affinity of the MAB massive sulphide deposits with Besshi-type deposits (Fox 1984) is generally accepted (Breitkopf and Maiden 1988; Klemd et al. 1989). These deposits are formed when a ridge axis is proximal to a source of terrigenous sediments, so that the axial region is rapidly covered in silty material. The ascending magmas probably do not make it to the sea-floor but are intruded into the sedimentary material as sills (see Fig. 3.10), with the hydrothermal convection cells developing above the intruded sill, which acts as a heat source. These features distinguish Besshi-type deposits from the volcanic-hosted massive sulphides of the Cyprus-type. Besshi-type ores are usually tabular in shape, or cigar-shaped where deformed. The metal association is typically Cu-Zn ± Ag ± Co, and Sn, Mo and W may be enhanced, possibly due to the nature of the sedimentary host rocks. Carbonate material of exhalative origin is usually present, and, as in the Matchless Belt, oxide-silicate Fe formation (metamorphosed to magnetite quartzite) may also

occur. Three S isotope analyses of sulphide samples (pyrite and chalcopyrite) returned $\delta^{34}S$ values of $+7.9$, $+8.9$ and $+9.4$ per mill (J.A. Kinnaird pers. comm. 1990), which compare well with the S isotopic composition of a sulphide deposit in a "sedimented ridge crest" in the Northern Juan de Fuca ridge (Franklin et al. 1990). Here these authors reported $\delta^{34}S$ values ranging from $+6$ to $+15$ per mill, which are interpreted to be the result of interaction of hydrothermal fluids with sediments in the sub-sea-floor environment (Franklin et al. 1990).

The Besshi deposits occupy a tectonic setting which is transitional between rift-related sedimentary exhalative, the Red Sea rift setting (to be discussed in the Chap. 13) and the Cyprus-type volcanic-hosted massive sulphide deposits. In the classification adopted by Rona (1988) for present-day oceanic crust-related mineralisation, the sediment-hosted deposits of the Salton Sea area, Guyamas basin in the Gulf of California, Bauer Deep on the east flank of the EPR and many others cited by Rona (Rona 1988, Table 1, p. 440–442) could all be the equivalent of the Besshi-type deposits of the geological record. Fox (1984) listed a number of Besshi-type deposits, ranging in age from the Lower Proterozoic to the Upper Paleozoic. They include the type area in Japan, known as Sambagawa belt (Upper Paleozoic), with the Besshi mine containing 33×10^6 tonnes at 2.6% Cu, 20 ppm Ag and 0.05% Co; the deposits of the Outokumpu region in Finland (lower Proterozoic), with the Kerretti mine (31×10^6 at 3.5% Cu, 0.5% Zn, 0.12% Co, 10 ppm Ag and 1 ppm Au) and the Vuonos mine (6.6×10^6 tonnes at 2.1% Cu, 1.2% Zn, 0.11% Co, 38 ppm Ag), and others in Canada, USA and Norway (Fox 1984, Table 1).

As mentioned previously, sea water-dominated hydrothermal convection cells develop in the semi-consolidated sediment pile above mafic intrusions, discharging as submarine hot springs at the sea-floor. Ferruginous cherts are characteristically developed and generally cap the sulphide mineralisation. Carbonate lenses or layers in the silty sediments are formed perhaps from the dissolution of organic material by the convecting fluids. Ferruginous cherts are the precursor rocks of magnetite quartzite and the carbonates are possibly the precursor rocks of the calc-silicate lenses (hornblende-garnet) commonly seen intercalated with the Kuiseb schist. The quartz-sericite schists associated with the MAB deposits are possibly the metamorphosed equivalent of clay-rich altered sediments.

The MAB and its environs constitute a prime target for the discovery of new base metal deposits, and, at the time of writing, mineral exploration is stepping up in this very interesting area.

References

Adamson R G, Teichmann R F H (1986) The Matchless cupreous pyrite deposit, South West Africa/Namibia. In: Anhaeusser C R, Maske S (eds) Mineral Deposits of Southern Africa, Vol 2. Geol Soc S Afr, pp 1755–1760

Alabaster T, Pearce J A (1985) The interrelationship between magmatic and ore-forming hydrothermal processes in the Oman ophiolite. Econ Geol 80:1–16

Alt J C, Lonsdale P, Haymon R, Muehlenbachs K (1987) Hydrothermal sulfide and oxide deposits on seamounts near 21 N, East Pacific Rise. Geol Soc Am Bull 98:157–168

Andrews A J, Fyfe W S (1976) Metamorphism and massive sulphide generation in oceanic crust. Geosci Can 3:84–94

Banks D A (1985) A fossil hydrothermal worm assemblage from the Tynagh lead-zinc deposits in Ireland. Nature (London) 313:128–131

Barrett T J, Jambor J L (eds) (1988) Seafloor hydrothermal mineralization. Can Mineral Spec Issue 26, 888 pp

Beccaluva L (ed) (1989) Ophiolites and lithosphere of marginal seas. Chem Geol 77:165–398

Best M G (1982) Igneous and metamorphic petrology. Freeman, San Francisco, 630 pp

Bonatti E (1975) Metallogenesis at oceanic spreading centers. Earth Planet Sci Rev 3:401–431

Bonatti E (1983) Hydrothermal metal deposits from the ocean rifts: a classification. In: Rona P A, Bostrom K, Laubier L, Smith KL (eds) Hydrothermal processes at seafloor spreading centers. Plenum, New York, pp 491–502

Bott M H P (1982) The interior of the Earth: its structure, constitution and evolution. Arnold, London, 403 pp

Boudier F, Nicolas A (eds) (1988) The ophiolites of Oman. Tectonophysics Spec Issue 151

Boyce A J, Coleman M L, Russell M J (1983) Formation of fossil hydrothermal chimneys and mounds from Silvermines, Ireland. Nature (London) 306:545–550

Breitkopf J H, Maiden K J (1988) Tectonic setting of the Matchless Belt pyritic copper deposits, Namibia. Econ Geol 83:710–723

Burke K C, Kidd W S F, Turcotte L, Dewey J F, Mouginis-Mark P J, Parmentier, E M, Sengör A M C, Tapponier P E (1981) Tectonics of basaltic volcanism. In: Basaltic volcanisn on the terrestrial planets. Lunar Planet Inst (ed), Houston. Pergamon, New York, pp 803–898

Canadian American Seamount Expedition (1985) Hydrothermal vents on an axis seamount of the Juan de Fuca ridge. Nature (London) 313:212–214

Coleman R G (1977) Ophiolites. Springer, Berlin, Heidelberg, New York, 229 pp

Coleman R G (1984) Ophiolites and the tectonic evolution of the Arabian peninsula. Geol Soc Special Publ 13:359–366

Constantinou G (1980) Metallogenesis associated with the Troodos ophiolite. In: Panayioutou A (ed) Ophiolites. Int Symp Cyprus 1979, Proc Cyprus Minist Agric Nat Resourc, pp 663–674

Constantinou G, Govett G J S (1972) Genesis of sulphide deposits, ochre and umber of Cyprus. Trans Inst Min Metall 81:B34–B36

Davies H L (1971) Peridotite-gabbro-basalt complex in eastern Papua: an overthrust plate of oceanic mantle and crust. Bur Mineral Resourc Aust Bull 128 48 pp

Davies H L, Jaques A L (1984) Emplacement of ophiolite in Papua New Guinea. Geol Soc Spec Publ 13:341–349

Delaney J R, Cosens B A (1982) Boiling and metal deposition in sub-marine hydrothermal systems. Mar Techn Soc J 16:62–65

Duncan R A (1981) Hotspots in the southern oceans an absolute frame of reference for motion of the Gondwana continents. Tectonophysics 74:29–42

Edmond J M, von Damm K (1983) Hot springs on the ocean floor. Sci Am 248:70–85

Edmond J M, Measures C, McDuff R E, Chan L H, Collier R, Grant B, Gordon L I, Corliss J B (1979) Ridge crest hydrothermal activity and the balances of the major and minor elements in the ocean: the Galapagos data. Earth Planet Sci Lett, 46:1–18

Embley R W, Jonasson I R, Perfit M R, Franklin J M, Tivey M A, Malahoff A, Smith M F, Francis T J G (1988) Submersible investigation of an extinct hydrothermal system on the Galapagos ridge: sulfide mounds, stockwork zone, and differentiated lavas. Can Mineral 26:517–539

Fleet A J, Robertson A H F (1980) Ocean-ridge metalliferous and pelagic sediments of the Semail Nappe, Oman. J Geol Soc London 137:403–422

Fouquet Y, Auclair G, Cambon P, Etoubleau J (1988) Geological setting and mineralogical and geochemical investigations on sulfide deposits near 13 N on the East Pacific Rise Marine. Geology 84:145–178

Fouquet Y, von Stackelberg V, Charlou J L, Donval J P, Erzinger J, Foucher J P, Herzig P, Mühe R, Sokai S, Wiedicke M, Whitechurch H (1991a) Hydrothermal activity and metallogenesis in the Lau arc basin. Nature (London) 349:778–781

Fouquet Y, von Stackelberg U, Charlou J L, Donval J P, Foucher J P, Erzinger J, Herzig P, Mühe R, Wiedicke M, Soakai S, Whitechurch H (1991b) Hydrothermal activity in the Lau back-arc basin: sulfides and water chemistry. Geology 19:303–306

Fox J S (1984) Besshi-type volcanogenic sulphide deposits a review. CIM Bull 77:57–68

Francheteau J, Needham H D, Choukroune P, Juteau T, Seguret M, Ballard R D, Fox P J, Normark W, Carranza A, Cordoba D, Guerrero J, Rangin C, Bougault H, Cambon P, Hekinian R (1979) Massive deep-sea sulphide ore deposits discovered on the East Pacific Rise. Nature (London) 277:523–528

Franklin J M, Goodfellow W D, Lydon J W, Jonasson I R, Davis E E (1990) Middle valley; a major center of hydrothermal activity in a sedimented ridge crest, Northern Juan de Fuca Ridge. Abstracts with Programs. Geol Soc Am Annu Meet, Dallas, p A9

Franklin J M, Sangster D M, Lydon J W (1981) Volcanic-associated massive sulfide deposits. Econ Geol 75th Anniv Vol:485–627

Gass I G (1982) Ophiolites. Sci Am 247:108–117

Gass I G, Lippard S J, Shelton A W (eds) (1984) Ophiolites and oceanic lithosphere. Geol Soc Special Publ 13. Blackwell, Oxford, 413 pp

Goldberg I (1976) A preliminary account of the Otjihase copper deposit, South West Africa. Econ Geol 71:384–390

Govett G J S, Pantanzis T M (1971) Distribution of Cu, Zn, Ni and Co in the Troodos pillow lava series, Cyprus. Trans Inst Min Metall 80:B1327–B1346

Graham U M, Bluth G J, Ohmoto H (1988) Sulfide-sulfate chimneys on the East Pacific Rise, 11 and 13 N latitudes. Part I: mineralogy and paragenesis. Can Mineral 26:487–504

Grassle J F (1983) Introduction to the geology of hydrothermal vents. In: Rona P A, Bostrom K, Laubier L, Smith K L (eds) Hydrothermal processes at seafloor spreading centers. Plenum, New York, pp 665–676

Hadjistavrinou Y, Constantinou G (1982) Cyprus. In: Dunning, F W, Mykura W, Slater D (eds) Mineral deposits of Europe, Vol 2. Inst Min Metall, London, pp 255–277

Hannington M D, Hall G E M, Vaive J (1990) Acid pore fluids from an oxidising sulfide deposit on the Mid-Atlantic ridge: implications for supergene enrichment of gold on the sea-floor. Abstracts with programs. Geol Soc Am Ann Meet, Dallas, p A42

Haymon R M, Kastner M (1981) Hot spring deposit on the East Pacific Rise at 21 N: preliminary description of mineralogy and genesis. Earth Planet Scie Lett 53:363–381

Haymon R, Koski R A, Sinclair C (1984) Fossils of hydrothermal vent worms from Cretaceous sulfide ores of the Samail Ophiolite, Oman. Science 223:1407–1409

Hekinian R, Fouquet Y (1985) Volcanism and metallogenesis of axial and off-axial structures on the East Pacific Rise near 13 N. Econ Geol 80:221–249

Hekinian R, Fevrier M, Bischoff J L, Picot P, Shanks W C (1980) Sulfide deposits from the East Pacific Rise near 21 N. Science 207:1433–1444

Hekinian R, Fevrier M, Avedik F, Cambon P, Charlou J L, Needham H D, Raillard J, Boulegue J, Merlivat L, Moinet A, Manganini S, Lange J (1983) East Pacific Rise near 13 N: geology of the hydrothermal fields. Science 219:1321–1324

Hughes C J (1982) Igneous petrology. Elsevier, Amsterdam, 551 pp

Huston D L, Large R R (1989) A chemical model for the concentration of gold in volcanogenic massive sulphide deposits. Ore Geol Rev 4:171–200

Ixer R A, Alabaster T, Pearce J A (1984) Ore petrography and geochemistry of massive sulphide deposits within the Semail ophiolite, Oman. Trans Inst Min Metall 93:B114–B124

Karpoff A M, Walter A V, Pflumio C (1988) Metalliferous sediments within lava sequences of the Samail ophiolite (Oman): mineralogical and geochemical characterization, origin and evolution. Tectonophysics 151:223–246

Kawahata H, Furuta T (1985) Sub-sea-floor hydrothermal alteration in the Galapagos spreading center. Chem Geol 49:259–274

Kawahata H, Shikazono N (1988) Sulfur isotope and total sulfur studies of basalts and greenstones from DSDP hole 504B, Costa Rica rift: implications for hydrothermal alteration. Can Mineral 26:555–565

Keays R R (1987) Principles of mobilization (dissolution) of metals in mafic and ultramafic rocks. The role of immiscible magmatic sulphides in the generation of hydrothermal gold and volcanogenic massive sulphide deposits. Ore Geol Rev 2:47–63

Kennett J (1982) Marine Geology. Prentice-Hall, Englewood Cliffs, 813 pp

Killick A M (1983) Sulphide mineralization at Gorob and its genetic relationship to the Matchless Member, Damara Sequence, SWA/ Namibia. Geol Soc S Afr Spec Publ 11:381–384

Klemd R, Maiden K J, Okrusch M (1987) The Matchless copper deposit, South West Africa/ Namibia: A deformed and metamorphosed massive sulfide deposit. Econ Geol 82:587–599

Klemd R, Maiden K J, Okrusch M, Richter P (1989) Geochemistry of the Matchless metamorphosed massive sulfide deposit, South West Africa/Namibia: wall-rock alteration during submarine oreforming processes. Econ Geol 84:603–617

Light M P R (1982) The Limpopo Mobile Belt: a result of continental collision. Tectonics 1:325–342

Lonsdale P, Becker K (1985) Hydrothermal plumes, hot springs, and conductive heat flow in the Southern Trough of Guyamas Basin. Earth Planet Scie Lett 73:211–225

Lonsdale P, Bischoff J L, Burns V M, Kastner M, Sweeney R E (1980) A high-temperature hydrothermal deposit on the seabed at a gulf of California spreading center. Earth Planet Sci Lett 49:8–20

MacDonald K C, Fox P J (1990) The Mid-Ocean Ridge. Sci Am 262:42–49

MacDonald K C, Becher F, Spiess F N, Ballard R D (1980) Hydrothermal heat flux of the "black smoker" vents on the East Pacific Rise. Earth Planet Scie Lett 48:1–7

Malahoff A, McMurtry G M, Wiltshire J C, Yeh H-W (1982) Geology and chemistry of hydrothermal deposits from active submarine volcano Loihi, Hawaii. Nature (London) 298:234–239

Marsh J S (1973) Relationships between transform directions and alkaline igneous rock lineaments in Africa and South America. Earth Planet Sci Lett 18:317–323

Minniti M, Bonavia F F (1984) Copper-ore grade hydrothermal mineralization discovered in a seamount in the Tyrrhenian sea (Mediterrenean): is the mineralization related to porphyry-coppers or to base metal lodes? Marine Geol 59:271–282

Moberly R, Campbell J F (1984) Hawaiian hotspot volcanism mainly during geomagnetic normal intervals. Geology 12:459–463

Morgan W J (1983) Hotspot tracks and the early rifting of the Atlantic. Tectonophysics 94:123–139

Mottl M J (1983) Metabasalts, axial hot springs, and the structure of hydrothermal systems at mid-ocean ridges. Geol Soc Am Bull 94:161–180

Nehlig P, Juteau T (1988) Deep crustal seawater penetration and circulation at ocean ridges: evidence from the Oman ophiolite. Mar Geol 84:209–228

Nur A, Ben-Avraham Z (1982) Oceanic plateaus, the fragmentation of continents, and mountain building. J Geophys Res 87:3644–3661

Open University (1989) The ocean basins: their structure and evolution. Open Univ, London, and Pergamon, New York, 171 pp

Oudin E, Constantinou G (1984) Black smoker chimney fragments in Cyprus sulphide deposits. Nature (London) 308:349–352

Penrose Conference Participants (1972) Penrose Field Conference Ophiolites. Geotimes 17:24–25

Peter J M, Scott S D (1988) Mineralogy, composition, and fluid-inclusion microthermometry of seafloor hydrothermal deposits in the southern trough of Guaymas Basin, Gulf of California. Can Mineral 26:567–587

Pirajno F (1980) Sub-seafloor mineralisation in rocks of the Matakaoa Volcanics around Lottin Point, East Cape, New Zealand. NZ J Geol Geophys 23:313–334

Prins P (1981) The geochemical evolution of the alkaline and carbonatite complexes of the Damaraland Igneous Province, South West Africa. Ann Univ Stellenbosch Ser A1 3:145–278

Robertson A H F (1975) Cyprus umbers: basalt-sediment relationships in a Mesozoic ocean ridge. J Geol Soc London 131:511–531

Rona P A (1980) TAG hydrothermal field: Mid-Atlantic Ridge crest at latitude 26 N. J Geol Soc London 137:385–402

Rona P A (1984) Hydrothermal mineralization at seafloor spreading centers. Earth Sci Rev 20:1–104

Rona P A (1986) Mineral deposits from sea-floor hot springs. Sci Am 254:66–75

Rona P A (1988) Hydrothermal mineralization at oceanic ridges. Can Mineral 26:431–465

Rona P A, Bostrom K, Laubier L, Smith K L (eds) (1983) Hydrothermal processes at seafloor spreading centers. Plenum, New York, 796 pp

Rosenbauer R J, Bischoff J L (1983) Uptake and transport of heavy metals by seawater: A summary of the experimental results. In: Rona P A, Bostrom K, Laubier L, Smith K L (eds) Hydrothermal processes at seafloor spreading centers. Plenum, New York, pp 177–198

Sato T (1972) Behaviour of ore-forming solutions in sea-water. Min Geol 22:31–42

Schilling J G, Thompson G, Kingsley R, Humphris S (1985) Hotspot migrating ridge interaction in the South Atlantic. Nature (London) 313:187–191

Scientific American (ed) (1969) The Ocean. Freeman, San Francisco

Searle P L (1972) Mode of occurrence of the cupriferous pyrite deposits of Cyprus. Trans Inst Min Metall 81:B189–B197

Seibold E, Berger W H (1982) The sea-floor. An introduction to marine geology. Springer, Berlin, Heidelberg, New York, 288 pp

Seyfried W E, Janecky D R (1985) Heavy metal and sulfur transport during subcritical and supercritical hydrothermal alteration of basalt: Influence of fluid pressure and basalt composition and crystallinity. Geochim Cosmochim Acta, 49:2545–2560

Seyfried W E, Berndt M E, Seewald J S (1988) Hydrothermal alteration processes at mid-ocean ridges: constraints from diabase alteration experiments, hot spring fluids and composition of the oceanic crust. Can Mineral 26:787–804

Smalley T J (1990) The Matchless West Extension cupreous pyrite deposit, Namibia; a field-based study. In: Abstr Geocongress '90 Cape Town. Geol Soc S Afr, pp 514–517

Smewing J D, Christensen N I, Bartholomew I D, Browning P (1984) The structure of the oceanic upper mantle and lower crust as deduced from a northern section of the Oman ophiolite. Geol Soc Spec Publ 13:41–54

Spooner E T C, Fyfe W S (1973) Sub-sea-floor metamorphism, heat and mass transfer. Contr Mineral Petrol 42:287–304

Taylor H P (1983) Oxygen and hydrogen isotope studies of hydrothermal interactions at submarine and subaerial spreading centers. In: Rona P A, Bostrom K, Laubier L, Smith K L (eds) Hydrothermal processes at sea-floor spraeding centers. Plenum, New York, pp 83–139

Thomas Crough S (1984) Seamounts as recorders of hot-spot epeirogeny. Geol Soc Am Bull 95:3–8

Thompson G, Mottl M J, Rona P A (1985) Morphology, mineralogy and chemistry of hydrothermal deposits from the TAG area, 26 N Mid-Atlantic Ridge. Chem Geol 49:243–257

Thompson G, Humphris S E, Schroeder B, Sulanowska M, Rona P A (1988) Active vents and massive sulfides at 26 N (TAG) and 23 N (Snakepit) on the Mid-Atlantic-Ridge. Can Mineral 26:697–711

Toksoz M N, Uyeda S, Francheteau J (1980) Oceanic ridges and arcs. Developments in geotectonics, Vol 14. Elsevier, Amsterdam, 538 pp

Turner F J, Verhoogen J (1960) Igneous and metamorphic petrology. McGraw-Hill, New York, 694 pp

Viljoen R P, Viljoen M J (1975) ERTS-1 imagery: an appraisal of applications in geology and mineral exploration. Mineral Sci Eng 7:132–168

Von Damm K L, Edmond J M, Grant B, Measures C I (1985) Chemistry of submarine hydrothermal solutions at 21 N, East Pacific Rise. Geochim Cosmochim Acta 49:2197–2220

Von Damm K L, Grant B, Edmond J M (1983) Preliminary report on the chemistry of hydrothermal solutions at 21 North, East Pacific Rise. In: Rona P A, Bostrom K, Laubier L, Smith K L (eds) Hydrothermal processes at seafloor spreading centers. Plenum, New York, pp 369–390

Wilson M (1989) Igneous Petrogenesis. Unwin Hyman, London, 466 pp

Chapter 13

Hydrothermal Mineral Deposits
of Continental Rift Environments

13.1 Introduction

In Chapter 6 (Sect. 6.2.2) we introduced the subject of continental rifts and aulacogens, and their related mineral deposits. In this chapter, we take a more detailed look at rifting phenomena, their possible causes, mechanisms, magmatic activity, sedimentation, time and space distribution, associated hydrothermal processes and mineral deposits.

At least four types of rift environments may be considered: (1) rifting at oceanic spreading centres; (2) back-arc rifting; (3) continental intraplate rifting; and (4) rifting related to continental collisions (impactogens). The first two are often difficult to separate in the geological record; they result in the creation and emplacement of oceanic crust which is discussed in Chapter 12. In this chapter we are concerned with continental intraplate rifting and impactogens.

It is obvious, as far as hydrothermal mineral deposits are concerned, that a continuum of deposit types must exist between the inception of rifting through to the more advanced stages of rift development. Only through careful and detailed geological work on the structural, sedimentary (basin analysis) and magmatic aspects of extensional tectonics, can one determine the nature of rifting and whether the geological record under study indicates a continental rift environment at an early, intermediate or advanced stage of development. These studies must clearly help in establishing the nature and type of hydrothermal deposits that may be present. The task is by no means easy, and a large component of such a study must rely upon published works. For the purpose of this chapter (and Chap. 14), we adopt the concepts and classification employed by Sawkins (1982, 1990) which although somewhat arbitrary, they are nevertheless useful for both the characterisation of mineral deposits and the building of conceptual models that can be utilised in mineral exploration.

The following works deal with general and detailed aspects of extensional tectonics and rifting: Bott (1981), Neumann and Ramberg (1978), Palmason (1982) and a special issue of Tectonophysics edited by Morgan and Baker (1983a). These publications, together with Sawkins (1982, 1990), provide the basis for most of the following sections.

13.2 Continental Rifting

Rifting is a process whereby linear fault-bounded troughs develop in response to doming and horizontal extensional stresses which result in thinning of the lithosphere. Rifts are associated with high heat flow, seismic activity, volcanism and hydrothermal activity. As outlined in Chapters 6 and 12, beginning with a triple junction, a continental rift may develop into an oceanic basin, with various stages of transition from continental to oceanic. One of the triple junction arms may penetrate a continent without developing further, thus constituting a failed arm or aulacogen. The great rift system extending from the Red Sea to southern Africa provides an example of these transitional stages, and is discussed later.

Studies of rift environments from both the geological record and modern, active rifts suggest, firstly, that in all cases lithosphere thinning does occur, and secondly, that asthenospheric mantle material occurs below the rift in the sublithosphere region. Continental rift systems are usually associated with broad uplifts, or doming, of the crust, as observed in the East African region and in the Basin and Range province, both of which are nearly 2000 m above sea level (Bott 1981). The causes and mechanisms of this crustal doming and thinning remain uncertain and controversial. Three main mechanisms have been invoked (Morgan and Baker 1983b): (1) thermal thinning and subsidence; (2) lithospheric stretching; and (3) asthenospheric diapirism.

Uplift and thinning of the lithosphere may occur by heating from a sublithospheric heat source, such as a mantle plume, or hot spot. The process may be aided by degassing from the mantle (Bailey 1983). Lithosphere stretching may also be caused by extensional stresses generated during plate movement; however, Morgan and Baker (1983b) point out that while this mechanism may explain the subsidence of rift floors, it fails to account for the doming which appears to precede rifting. In the mechanical thinning model (passive rifts), asthenospheric material may upwell beneath the stretched lithosphere due to decompression melting and/or diapirism. It is also argued that regional stress fields which induce rifting may be generated during collision of lithospheric plates (impactogens). The prime example of a collision-generated rift system is that produced in the Siberian platform where the world's deepest rift valley – the Baikal rift zone with a vertical displacement of up to 8 km (Hermance 1982) – is thought to have formed as a result of the collision of India with Eurasia. The third hypothesis, which perhaps commands more support, is that of asthenospheric diapirism (active rifts). Passive and active rifts are schematically illustrated in Figs. 6.4 and 6.5. The underlying principle of the active-rift hypothesis is that hot and less dense asthenosphere underlies a denser mantle lithosphere. In this way a diapir is formed which tends to rise by virtue of its density contrast with the overlying lithosphere. Although the origin of the hotter and less dense asthenospheric mantle material is far from clear, it has been suggested that it may be generated by thermal instabilities at the core-mantle boundary and/or by mantle convection. Plume or hot spots are therefore thought to be one of the chief causes of doming, triple junctions, aulacogens and rifting (see discussion in Chap. 6, Fig. 6.5, and references therein).

In summary, lithosphere thinning and continental rifting may result from one of two basic mechanisms involving the passive and active role of mantle upwelling. The former is exemplified by the Baikal and Rhine rift systems, both of which occur in front of the collision line between the Gondwana continents and the Eurasian landmass. In these rift systems, differential stresses set up in the crust as a result of plate interactions, generated rifting and its associated limited magmatism. In the other case, active involvement of mantle diapirs is seen as the major cause of doming and rifting, and this is usually preceded and accompanied by volcanic activity. This appears to be the case for the East African rift system. Active rifting is possibly also the main cause of continental breakup (Sawkins 1990).

13.2.1 Geophysical Signatures of Continental Rifts

Anomalous gravity, seismic, magnetic and heat flow signatures characterise modern rift structures. These have been used to study and model rifting processes (see Morgan and Baker 1983a). Seismically active areas in Africa are concentrated in the Red Sea, Gulf of Aden and the East African rift system. Epicentres along the East African rifts have a scattered distribution and extend into Precambrian cratonic areas, possibly indicating re-activation along ancient zones of weakness. Seismicity in the Australian continent, for example, gives an indication of ancient rift zones (Sykes 1979). Thus, east of the Gawler block, earthquake epicentres occur along the Adelaide geosyncline, where intracontinental rifting was active in the Proterozoic. Epicentres occur in the Canning basin, between the Pilbara and Kimberley cratonic blocks, where ancient rifting was probably initiated in the Archean; and along the western and eastern margins of the Archean Yilgarn shield of Western Australia, where faulting is currently active and is associated with continental margin rifting which was possibly started during the breakup of Gondwana.

Seismic soundings have been used to profile subsurface layering and have helped in the demostration of lithospheric thinning. An important geophysical signature of active rifts is the low velocity and attenuation of seismic waves. This is explained by high crustal temperatures and the presence of partial melts. High surface heat flow is characteristic of modern rifts, as in East Africa, the Baikal rift system, and the Rio Grande rift of the USA. Residual negative gravity anomalies associated with rift structures are attributed to the presence of upwelling, low-density, partial melts. Domal regions of the East African rift system are characterised by broad Bouguer anomalies with short wavelength and axial positive highs (de Rito et al. 1983). The regional mass deficiency is attributed to a thinned lithosphere caused by the rise of lower density asthenospheric material, or the emplacement of a low-density large laccolithic body at a high level. The short-wavelength axial residual positive anomalies are on the other hand, thought to coincide with voluminous basaltic intrusions. The spreading arms of the Afro-Arabian rift system – the Red Sea and Gulf of Aden – are by contrast characterised by broad positive Bouguer anomalies, presumably because denser mantle material rises to generate oceanic crust at the developing spreading ridges. Magnetic anomalies within the Red Sea and the Gulf of Aden are consistent with sea-floor
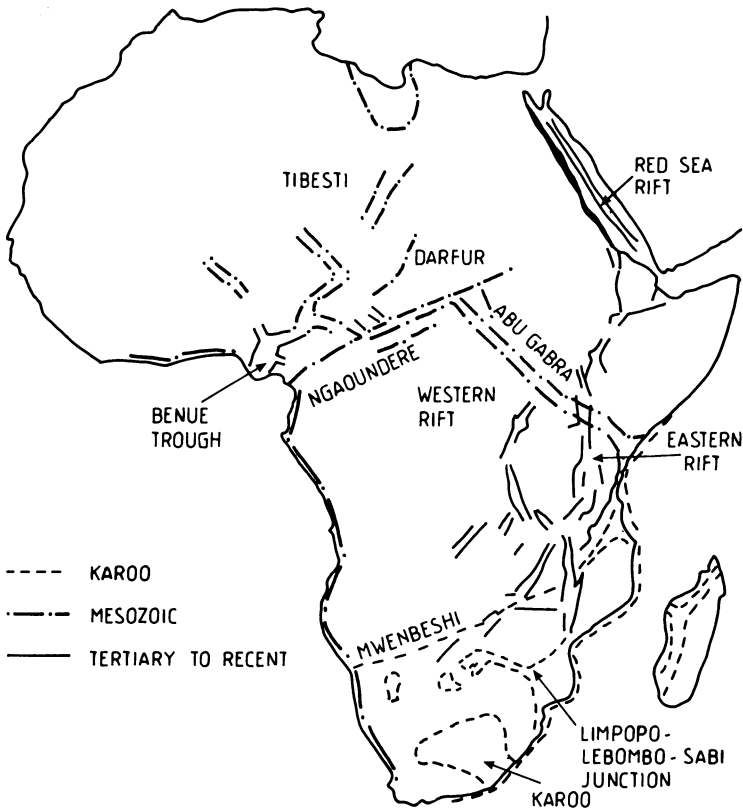
Fig. 13.1. The Phanerozoic rift systems of Africa. Three major rift system are recognised to have developed since the Early Mesozoic: *dashed lines* Karoo rifting, associated with the breakup of Madagascar and Antarctica from the southeastern margin of Africa; *dotted-dashed lines* Mesozoic (Cretaceous) rifting associated with the opening of the South Atlantic ocean and the breakup of South America from Africa (Central African Rift System); *black lines* Tertiary to Recent rifting associated with the opening of the Red Sea and the formation of the East African Rift System (After Browne and Fairhead 1983; Fairhead and Green 1989; Lambiase 1989)

spreading, while paleomagnetic data demonstrates the episodic nature in the evolution of continental rifting (Girdler 1983).

Many cratonic basins appear to be associated with ancient rifts, and these are commonly characterised by positive linear Bouguer gravity anomalies which may be the equivalent of the axial positive gravity highs found in modern rifts. De Rito et al. (1983) attribute the subsidence of basins as a response to isostatically uncompensated mass excess due to axial mafic igneous intrusions. Gravity anomaly patterns have outlined a major rift system in Central Africa (Bermingham et al. 1983; Browne and Fairhead 1983). The Darfur, Tibesti and Hoggar domal uplifts have been compared to the domal regions of the East African system in Kenya and Ethiopia. The former are thought to represent an earlier stage of development than the East African uplifts. The Darfur dome is characte-

rised by a regional negative Bouguer anomaly without the axial positive high. Two arms of the Central African rift system are the north-northeast-trending Ngaoundere rift and the Abu Gabra rift which trends southeastward to join the Kenyan rifts, north of Lake Victoria (Fig. 13.1). These rift arms have broad regional positive Bouguer anomalies and as such are compared with the Red Sea and the Gulf of Aden arms. Bermingham et al. (1983) interpret the anomaly patterns to indicate that rift processes associated with these two African rift systems are distinctly different. The regional positive anomalies are associated with extensional tectonics, causing stretching and necking of the crust and lithosphere, while the regional gravity anomaly is associated with active domal uplift. In a three-arm rift system, two arms are characterised by extensional tectonics, and occur as subsiding sedimentary rift basins which may progress to an oceanic stage with development of passive continental margins (Abu Gabra, Red Sea). The uplifted north-trending domal arm of Darfur, on the other hand, would remain as a third, and "failed," rift arm which could develop into an aulacogen. The Central African rift system lacks seismicity, however, possibly as a consequence of the very slow rate of rifting.

13.3 Magmatism and Metamorphism Associated with Rifting

Igneous activity associated with rifting events spans a wide range of magmatic products in which both crust and mantle may act as sources. The variety of igneous rocks is essentially related to the particular stages in the development of a rift system. A thorough discussion of the magmatism of continental rift zones may be found in Wilson (1989), while further literature is provided by Fitton and Upton (1987; see also discussion in Chap. 6, Sect. 6.2.2). The peculiar nature and variety of rift magmatism makes its study particularly interesting. In addition, although many of the rift-related magmatic products (such as carbonatites) are volumetrically ·minor, the study of their petrogenesis places very important constraints on the understanding of mantle processes and magma generation.

   Two main theories attempt to explain rift magmatism. One holds that, as the continental lithosphere thins – whether passively or actively, as described previously – asthenospheric material rises and decompresses to generate a partial melt; the amount of melt is dependent on a number of factors, such as the initial temperature of the asthenosphere. The other theory maintains that rift magmas are generated through processses of mantle degassing and metasomatism (see later). In the former view a mantle plume, or asthenolith, upwells below the thinned crust, which it underplates. The crust becomes heated above its solidus and melts giving rise to a range of hybrid magmas of silicic composition. Underplating of the continental crust by mantle melts could explain the sequence of magmatic events in a rift setting. At first, subalkaline to alkaline basaltic rocks are extruded via a network of feeder dykes. This is followed by bimodal magmatism (felsic-mafic) derived from the regions of crustal melting and continuing extrusion of mantle melts. The effects of asthenolith underplating has been invoked to explain major rifting and magmatic

events such as in the intracontinental branch of the Damara orogen in Namibia (Chap. 7).

The wide spectrum of magmatic products of rifting environments must take into account the continental flood basalts, which herald the inception of major rifting events. An outstanding example of continental flood basalts is the Karoo-Etendeka (southern Africa), Parana and Antarctic provinces which, together with the Deccan, were erupted just prior to the breakup of the Gondwana supercontinent in the Mesozoic. The Etendeka province in Namibia and the Parana in Brazil and Argentina heralded the rifting and opening of the South Atlantic Ocean. The magmatic products of these provinces are typified by compositionally uniform subalkaline dolerite feeders and basaltic lavas, locally intercalated with silicic ignimbrites (e.g. Etendeka province).

Fracture patterns more or less parallel to rift axes usually provide the pathway to the emplacement of mafic dykes, which probably feed overlying lava fields. Swarms of dolerite dykes are found emplaced in rift-related fracture systems throughout geological time, and are known from the early Proterozoic, when rifting occurred in Archean shields, in Greenland, Canada, Australia and southern Africa, up until the present with the East African rifts (see also Chap. 5 and Fig. 5.1).

A review on the relationship between rifting and the voluminous effusions of continental flood basalts is provided by White and McKenzie (1989). As discussed previuosly, uplift, or doming, is thought to be the result of ascending mantle plumes, which White and McKenzie (1989) estimate to be about 150 km in diameter. A mantle plume rises and is deflected laterally by the overlying lithospheric plate. This results in the formation of a "mushroom" head of hot mantle material some 1500 km across. The lithospheric regions above this mushroom head are mechanically lifted resulting in the doming of the crust. These domes, or crustal swells, may have diameters of 1500 to 2000 km and uplifts of 1000 to 2000 m. Temperatures in the head of mantle material are 100–200°C greater than the normal asthenosphere. Huge quantities of basaltic melts are then generated by decompression, as the melt rises to fill up the space beneath stretched and thinned lithosphere. Basaltic lavas are erupted and flow laterally and down from the uplifted regions thus forming the extensive basaltic plateaus. A crucial point in the model of White and McKenzie is that rifting could occur at any point within the continental dome and not necessarily just above the plume. Rifting along outlying areas of the dome would result in the tapping of magmas of diverse nature generated by different degrees of partial melting. The authors quote the example of the British Tertiary igneous province which, they contend, was caused by "localised rifting above the mushroom head of anomalously hot mantle produced by the plume centered beneath Greenland" (White and McKenzie 1989, p. 7703).

Magmatic activity in rift zones is, however, different from continental flood basalts and related dyke swarms. Rift magmatic products include subalkaline to alkali basalts, basanite, nephelinites, carbonatites and ultrapotassic rocks (Wilson 1989). Alkali ring complexes, composed of saturated and undersaturated igneous products, are also common. Rift-related magmas are enriched in incompatible elements, such as Ti, P, Y, Nb, Ba, K, Rb, Zr, Th, U, F and REE. There is increasing evidence that the source of continental rift magmas is metasomatised mantle.

Mantle metasomatism is advocated by Bailey (1978, 1983, 1987), who points out that rift zones are in fact characterised by unusual quantities of volatile emissions, especially CO_2, H_2O, F and Cl. It is also hypothesised that rifting may localise mantle degassing (essentially C, H and O), causing a flux of volatiles which would in turn cause partial melting of the metasomatised mantle material with the production of incompatible element-enriched magmas. Degassing of the mantle may occur in pulses, and may be related to core activity and interaction of the core-mantle boundary layer. Subduction zone magmatism is a variant, in that streaming or fluxing of volatiles to produce melting is probably related to degassing of the subducted slab (sediments + mafic rocks). The upward flux of volatiles causes melting above the subduction zone with production of calc-alkaline magmas.

Bailey (1983) compares the igneous activity of oceanic and continental rifts, considering it in terms of plate movements and mantle processes. Bailey (1983, 1987) shows that whereas oceanic rifts are caused by the separation of two plates with a moving rift line, continental rifts are characterised by a rift within one plate, with slow or negligible opening. More importantly, in this author's view, is that in the case of oceanic rifts there is permissive upwelling of asthenospheric mantle and its melt products into the space provided by the shifting plates, leading to strong decompression melting, and the relatively compositionally uniform and voluminous production of MORB. The mantle sources are depleted in large ion lithophile elements (LILE) and mantle xenoliths are not found in the igneous products of ridge magmatism. In continental rifts, although an anomalous sublithospheric low-density mantle may be present, as suggested by geophysical signatures, its source is not clear and there is no space for permissive emplacement. As already stated, rift magmatism is highly variable, alkaline and volatile-rich. Geochemical evidence indicates that mantle sources are enriched in LILE prior to melting, and metasomatised mantle xenoliths are frequently found in rift igneous products. Bailey concludes that the cause of uplift and magmatism in the two end-member cases of rifting – oceanic and continental – is the permissive release of asthenospheric material into mid-ocean ridges, whilst release of volatile elements from the mantle, and their fluxing through the subcontinental lithosphere, is responsible for metasomatism and partial melting in regions of continental rifting.

Two main factors are seen to influence continental rift magmatism. One is the fracturing of continental crust which allows degassing of a large area in the mantle with the channelling of the volatiles through a narrow zone (Fig. 13.2). The second factor is that the channelling of the volatiles through the rift zone "focuses heat and builds up the level of incompatible elements by metasomatism along the channelways in the overlying mantle and crust" (Bailey 1983, p.590). Melting would occur in the subcontinental lithospheric mantle, which is metasomatised along the channels through which the volatiles are moving. These mantle melts would rise as diapirs and form magma chambers. Diapirs may locally underplate and partially melt the crust to produce localised silicic melts. As a point of interest it is worth mentioning that the origin of kimberlites and lamproites, which are occasionally the carriers of diamonds, may also be related to sudden and massive degassing – primarily CO_2 – phenomena, thought to occur at great depth (approximately 100–200 km).
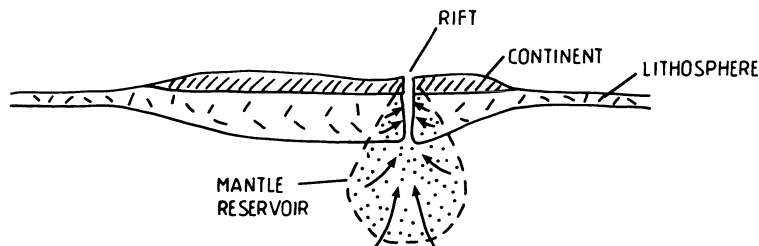
Fig. 13.2. Model to explain igneous activity in continental rifts (after Bailey 1983). In this model igneous activity is thought to originate from a large mantle reservoir (*dot pattern*), fracturing of the continental crust allows the escape of volatiles from the reservoir, resulting in the concentration of heat and volatiles in the lithosphere and subsequent partial melting

Diamonds would be present only if the magma ascends through regions within the stability field of diamond (Wyllie 1980; Bailey 1984).

If separation of the lithosphere occurs, a continental rift evolves into an oceanic basin and at this point asthenospheric mantle may begin to penetrate into the rifted spaces. Bonatti (1985) has analysed the transition from continental to oceanic rift in the Red Sea. On the basis of geophysical observations, the axial zone of the Red Sea can be divided into four sectors, which from north to south are: northern region, transitional region, multi-deeps region and rift valley region (Fig. 13.20). The transitional region is characterised by axial troughs and deeps, separated by zones with no rift valley with a thick sediment cover. Bonatti (1985) envisages a "punctiform initiation of sea floor spreading". His theory is that in the axial troughs, oceanic crust is initially emplaced in a hot spot, situated within a zone of tensional stresses, and from this spot an oceanic rift segment propagates. The initial break by oceanic crust material is made in thinned continental crust which would at this stage be characterised by numerous dyke injections. Propagation from a spot would give rise to a spreading segment, which would join with the spreading segment propagating from another spot. In the case of the Red Sea the overall propagation proceeded northward from the rift valley sector, where there is active oceanic spreading, to the multi-deeps region where a number of pool-like troughs (deeps, some of which are hydrothermally active, see later) occur, to the transitional region, and finally the northern region in which high amplitude magnetic anomalies suggest that it is floored by thinned and dyke-injected continental crust.

The "punctiform" model of Bonatti (1985) therefore envisions upwelling of mantle diapirs at given points, which according to the author, appear in the transitional region to be regularly spaced, at approximately 50–km centres. The spacing would be the result of density/viscosity sinusoidal instability between the mantle diapirs (low density and viscosity) and the surrounding medium. This instability would "evolve into a pattern of wavelength-spaced injections of lower density fluid into the denser layer above" (Bonatti 1985, p.36).

13.3.1 The Nature of Igneous Activity in Rift Systems

A review of the igneous activity in ancient and recent rift systems is given by Williams (1982), who compares the tectonomagmatic evolution of the Paleozoic Oslo rift with the Cenozoic Rio Grande rift and the East African rift systems. Magmatism in the Rio Grande Rift (see later) is of a complex nature and is typically bimodal, characterised by basaltic and silicic compositions. In this section, however, we examine the magmatism of the East African rift system, which is by far the most abundant and varied. Mention is made of the Oslo rift in Chapter 10 in connection with porphyry mineralisation.

Igneous Activity in the East African Rifts

The wide compositional variations of rift magmas are exemplified by the igneous products seen in the East African rift system (see Fig. 3.22). Bailey (1983) divides the spectrum of alkaline volcanics into an alkali basalt association and a nephelinite association. The former is characterised by alkali-olivine basalt, basanite, hawaiite, mugearite, trachyte, rhyolite and peralkaline trachyte-rhyolite-ignimbrite series. The nephelinite association includes nepheline-trachyte, phonolite, carbonatite and kimberlite. All of these types are erupted from fissures or central volcanic complexes.

The Afar triple junction highlights the change and the transition between magmatism of a continental rift environment to that of an oceanic stage. This transition is considered to have taken place in a number of stages (Barberi and Varet 1978). In the first – continental rift valley stage, in the lake region of the Ethiopian rift – tensional tectonics allowed the widespread fissure eruption of basaltic lavas. Felsic products were erupted from central volcanoes which are developed at the intersection of the main rift trend with transverse lines of weakness. The magmas are alkaline and enriched in light REE. The second stage is characterised by the transition to an embryonic oceanic spreading – southern Afar at the northern termination of the Ethiopian rift – in which tectonic and volcanic activity occurs along a narrow axial graben. Fissure basaltic activity predominates, while central volcanism becomes less common. The magmas are moderately enriched in light REE. Development of a proto-oceanic spreading structure is the third stage – northern and central Afar – and is characterised by a narrow rift valley with fissure-type volcanism. Basaltic rocks, of tholeiitic composition with REE patterns of chondritic affiliation, are the only products. The final stage is an oceanic rift – Gulf of Aden – in which oceanic crust is formed by the eruption of basalts with only minor Fe-enriched intermediate lavas.

The Ethiopian rift valley connects the Afar triangle with the Kenyan sector of the East African rift system. One of the active volcanic areas of the Ethiopian rift is Tullu Moje (Bizouard and Di Paola 1978). Here, two distinct and unrelated magma series are recognised. One is a K_2O-rich series with basalt, hawaiite and trachyte, which are thought to have derived from one another by fractional crystallisation. Olivine is present in rocks of this series and shows increasing Fe contents with increasing degrees of fractionation. The other series is K_2O-poor, and includes

comendite and trachy-rhyolites, which are characterised by the presence of orthopyroxene instead of olivine. These rocks do not appear to be related by processes of crystal fractionation.

The Kenyan rift province (eastern branch of the East African system) is characterised by a wide spectrum of Na-rich igneous rocks amounting to some 220 000 km^3 (Baker 1987). In this province volcanism began about 30 Ma ago and continues today. The magmatic activity shows variations in both time and space, from the western flank to the central parts and to the eastern flank of the rift, as well as from a northern sector to a southern sector. In the western flank of the northern sector nephelinites and carbonatites were emplaced between 24 and 10 Ma ago. In a pre-rift depression voluminous eruptions of alkali basalts and phonolites took place. This volcanism changed to less alkaline compositions with the development of bimodal basalt-trachyte volcanoes, calderas and eruptions of ignimbrites. During the Plio-Pleistocene on the eastern flank of the rift fissure, volcanism resulted in a chain of monogenetic alkali basalt cones, shield volcanoes and large central volcanoes (Mt. Kenya, Kilimanjaro), while within the rift, recent volcanism is characterised by eruptions of trachyte and alkali rhyolite and basalt-trachyte calderas. In the southern sector, the rift zone has scattered nephelinite-carbonatite complexes emplaced during the stages of half-graben and graben development (Baker 1987).

13.3.2 Metamorphism in Continental Rifts

High heat flow and geophysical information, obtained from the study of recent and modern rifts, such as the Rhine Graben and the East African rift system, is consistent with the presence of high temperatures associated with lithospheric thinning across rifted regions. The high crustal temperatures attained in rift environments must produce conditions of prograde metamorphism (high temperature/low pressure). Indeed, extension and continental rifting are believed to be responsible for the development of high temperature/low pressure metamorphic terranes (Wickham and Oxburgh 1985; Sandiford and Powell 1986). It is generally recognised that metamorphic rocks exhibit pressure-temperature-time (P-T-t) paths which reflect increasing heat flux, crustal thickening due to tectonic convergence, and cooling due to erosion. The geometry of extension, crustal thinning and the associated convective heat transport dictates the nature and conditions of metamorphism. Lower crustal temperatures in rift environments may reach high enough values to promote partial melting, and the uprise of partial melt in the crust may promote high temperature metamorphism at higher crustal levels (Sandiford and Powell 1986). The extent of thermal metamorphism, that is, regional or local, is considered to be dependent on the nature and extent of the extensional regime. Thus, it is possible that only metamorphism of limited extent would occur within the areally restricted linear graben structures. By contrast, in extensional regimes such as that responsible for the Basin and Range province in the USA, regional-scale metamorphism is expected to occur (Sandiford and Powell 1986).

Clearly, studies of rift-related regional metamorphism can only be conducted in ancient examples of rift settings; conversely, the recognition of high temperature/ low pressure mineral assemblages may help in determining the presence of an ancient extensional tectonic regime. This type of work has been conducted in the Pyrenees by Wickham and Oxburgh (1985) and Wickham and Taylor (1987). Another example of rift-related regional metamorphism is provided by the intracontinental branch of the Damara orogen, discussed briefly in Chapter 7.

High temperature/low pressure Hercynian metamorphosed basement rocks in the eastern Pyrenees have been exposed during the Alpine uplift in the Tertiary. As there is no evidence of collision tectonics in this area, Wickham and Oxburgh (1985) concluded that the metamorphism in question could only have developed in a zone of continental rifting. One of the areas studied is the Trois Seigneur massif, which is characterised by a sequence of pelitic and carbonate rocks of Cambrian to Silurian age. Gradational and prograde metamorphic grades can be observed from chlorite-sericite schist, andalusite schist, andalusite-sillimanite mica schist to biotite-sillimanite schist and gneiss (migmatites), and finally, to a peraluminous granitic rock. The onset of melting in this sequence is thought to correspond with the first appearance of the migmatitic rocks for which a temperature of approximately 700° C and pressure of 3–3.5 kbar have been estimated on the basis of experimental studies and petrographic evidence. The metamorphism of the precursor sedimentary rocks occurred under water-rich conditions and the generation of granitic melts from the pelitic rocks. The pressure and temperature curve calculated for the Trois Seigneur massif indicates a geothermal gradient of $80-100°C$ km^{-1}, with melting taking place at an approximate depth of 14–15 km, at the temperature and pressure given above. Various lines of evidence also indicate that, as metamorphism in the lower parts of the sedimentary sequence was in progress, sedimentation in the rift basin was still continuing at the surface.

Stable isotope systematics ($^{18}O/^{16}O$) have been used to establish the origin and depth of penetration of hydrothermal fluids during this regional metamorphism of the Hercynian crust in the Pyrenees (Wickham and Taylor 1987). The $\delta^{18}O$ values are homogeneous in the upper level metasedimentary sequences (Zones 1 and 2, +14 to +16 per mill and +10 to +12 per mill respectively, in pelitic rocks), whereas in the gneissic rocks of the lower level (Zone 3) $\delta^{18}O$ range from +6 to +22 per mill. The $\delta^{18}O$ values of the schist rocks and migmatites of Zone 2 are uniform and much lower than those of low-grade carbonate and shale of Zone 1. The authors interpret these variations to the interaction and circulation of surface-derived metamorphic pore fluids in the upper crustal levels (Zones 1 and 2), while the heterogeneous $\delta^{18}O$ values of the underlying gnessic rocks of Zone 3 would reflect much lower fluid interaction. Melting occurred at the base of the sedimentary sequence, perhaps in response to heating caused by the intrusion of mafic melts. The authors consider the presence of late-stage granodioritic bodies to be the result of this lower crustal melting. Some of these granodiorites may have fed surface volcanism in the paleorift zone.

13.4 Basin Formation and Volcano-Sedimentary Sequences in Continental Rifts

The evolution of continental rifts, from incipient graben structures to proto-oceanic and oceanic sea-floor, is accompanied by the development of sedimentary basins. Rift-related sedimentary basins host a variety of hydrothermal mineral deposits including vein-type, stratabound and/or stratiform disseminated and massive sulphide deposits. Comprehensive studies of basin geology can be found in Dickinson and Yarborough (1976) and Bally and Snelson (1980). The evolution of sedimentary basins has been modelled by McKenzie (1978). For the present purpose it is useful to adopt the classification of sedimentary basins employed by Dickinson and Yarborough (1976).

Extensional tectonics and crustal rifting result in the formation of sedimentary basins which can be categorised into three main end members: (1) basins formed during the incipient stages of continental rupture; (2) basins formed during more or less complete continental separation, accompanied by sea-floor spreading, and with oceanic crust intervening between the rifted margins; (3) basins formed during transform faulting or the rifting of magmatic arcs. The first group includes two related types: (a) intracratonic basins, in which the basement is constituted by attenuated continental crust; examples of this type of basin are the Proterozoic sedimentary basins of the Kaapvaal craton in South Africa (e.g. Transvaal and Witwatersrand); (b) aulacogens (referred to previously), which form wedge-shaped rift structures that may be floored by oceanic, continental or transitional crust. An example of aulacogen is the Benue Trough, extending northeastward from the Gulf of Guinea, and representing the failed arm of a triple junction Cretaceous rift system, from which South America and Africa separated. In the Benue Trough the accumulation of sediments is estimated to reach a thickness of 10 km. Other examples are provided by some of the graben structures of the Late Proterozoic Damara orogen, and the Kundelungu aulacogen (see Figs. 7.4 and 7.7). The second group of basins may include the following: (a) proto-oceanic basin, formed by a narrow belt of oceanic and/or transitional crust, between two continental margins, so that sedimentation in the basin is influenced by the flanking continental margins; modern examples of this situation are the Red Sea and the Gulf of California, while, as an example from the geological record we can cite the Khomas trough of the Damara orogen, which is floored in part by the Matchless Amphibolite Belt of oceanic crust affinity (Chap. 12); (b) miogeoclinal basins, formed along rifted, passive continental margins, these include continental terrace and shelf deposits at the edge of the continental block, and continental rise turbidite deposits at the edge of the ocean basin (see Fig. 6.6); the present-day Atlantic seaboards of North America and West Africa are representative of this type of basin. The third group of basins includes: (a) pull-apart structures formed as a result of oblique-slip movements (a transform boundary) between two laterally moving blocks; (b) interarc basins which form during rifting of a magmatic arc; forearc and retroarc basins occur on the subduction and continental side, respectively (see Fig. 6.11).

There are three principal mechanisms that can cause subsidence of the crust and the development of a sedimentary basin (Dewey 1982). They are: (1) thinning of the lithosphere; (2) cooling of the lithosphere; and (3) loading of the lithosphere. McKenzie (1978) proposes that mechanisms (1) and (2) combine to form a two-stage subsidence model in which a protobasin is formed by rapid extensional subsidence due to stretching of the lithosphere, and this is followed by slow thermal subsidence, as the asthenospheric mantle wedge below the protobasin cools and sinks back to isostatic equilibrium. If stretching is sufficient, bimodal volcanics may be extruded during the initial stages of subsidence, and these may accentuate the subsidence by loading.

13.4.1 The Stratigraphic Record of Proterozoic Basins in South Africa

Four economically important supracrustal successions on the Kaapvaal craton (South Africa) are the Pongola, Witwatersrand, Ventersdorp and Transvaal-Griqualand West Supergroups. For an overview of the geological history of these basins the reader is referred to Tankard et al. (1982). These are volcano-sedimentary sequences which developed from the beginning of the Proterozoic onward as a result of cratonic stabilisation at the end of the Archean. The Archean-Proterozoic boundary is drawn at the time of craton stabilisation, which occurred diachronously worldwide between 3 and 2 Ga. Cratonisation was accompanied by thickening of the continental crust and intracratonic basin-forming events (see also Chap. 5 and references therein). In South Africa cratonisation began as early as 3 Ga ago, and intracratonic basins were formed on the Kaapvaal and Zimbabwe cratons between 3 and 1.5 Ga. The South African basins were developed along a system of north- to northeast-trending grabens which, starting with the Pongola basin at around 3 Ga, formed progressively larger and northward-migrating depositories. The geodynamic evolution that led to the formation of the Kaapvaal intracratonic basins is open to speculation, but it is generally agreed that grabens may have formed in response to stresses generated during tectonic interaction between the Kaapvaal and Zimbabwe microplates. One proposal by Burke et al. (1985) is that, at least for the Ventersdorp basin, rifting was originated by the collision of the Kaapvaal and Zimbabwe microplates. Another idea, based on evidence of thrust tectonics in the Witwatersrand basin, and suggested by Barton et al. (1986), is that this basin was formed by Himalayan-type continental collision. Clendenin et al. (1988), on the other hand, speculate that the three sequences of the Witwatersrand, Ventersdorp and Transvaal are part of a rift system formed during oblique collision of the Kaapvaal and Zimbabwe cratons. This hypothesis is examined further later in this section.

Accumulation in the South African intracratonic basins consisted of lavas and sediments, the latter tending to increase in volume with the age of the basins. The Transvaal-Griqualand West Supergroups represent remnants of the same succession, now exposed in two separate structural basins, which developed after the deposition of the volcano-sedimentary sequences. The simplified stratigraphic columns for each of these basins are shown in Fig. 13.3. Dolomites and banded iron formations make their first widespread appearance in these basins. The Pongola and
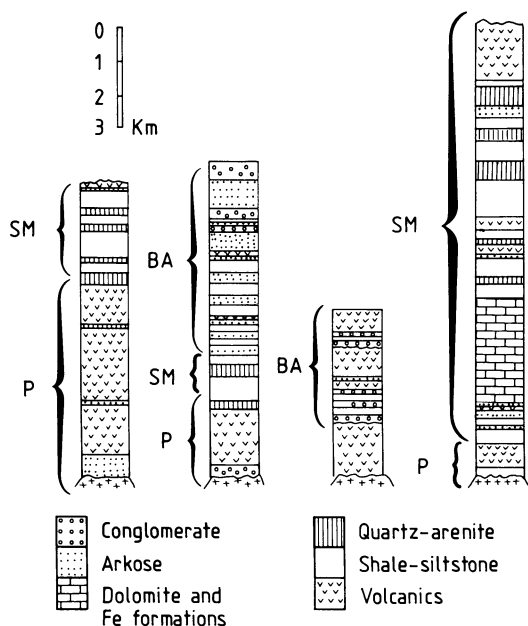
Fig. 13.3. The stratigraphy of the early Proterozoic Supergroups of South Africa. *P* protobasin sequence; *SM* shallow marine sequence; *BA* braided alluvial and alluvial fans (After Bickle and Erikson 1982)

Witwatersrand Supergroups fit the McKenzie model of basin evolution well. Both evolved through a recognisable protobasin stage, represented by volcanic-dominated sequences (Nsuze and Dominion Groups). The thick volcanic sequence of the Pongola Supergroup is attributed to higher geothermal gradients, which allowed more volcanics to be extruded than in the later basins. The volcanic sequences are overlain by sediments of shallow marine, tidal and fluvial origin, which were deposited during the thermal stage of basin subsidence. The Ventersdorp and Transvaal-Griqualand West Supergroups do not fit the McKenzie model. The Ventersdorp stratigraphy is wholly dominated by volcanics, and the sedimentary sequence may either have been eroded off, or perhaps never deposited in the first place. The Transvaal Supergroup, on the other hand, has a volcanic sequence at its base (Wolkberg-Buffalo Springs Groups), but this is considered too small to represent a protobasin of the greater Transvaal-Griqualand West basin. We return to the Transvaal-Griqualand West basin later in connection with its contained Fe and Mn deposits. In the model of Clendenin et al. (1988), mentioned above, it is envisaged that the volcano-sedimentary sequences of the Wiwatersrand, Ventersdorp and part of the Transvaal supergroups, considered together may represent a three-stage rift evolution, which would fit the McKenzie's model. According to the authors, a pre-graben stage would be represented by the early volcanic extrusions of the Dominion Group, followed by sedimentation of the West and Central Rand Groups. The pre-graben stage would have been terminated by the extrusion of the Ventersdorp basaltic lavas (Klipriviersburg Group). A basin-forming graben stage was heralded by the emplacement of the bimodal volcanics of the Platberg Group (Ventersdorp), and after a period of sedimentation this stage closes with more extrusions of basaltic lavas (Allenridge Formation, Ventersdorp). Finally, rocks of
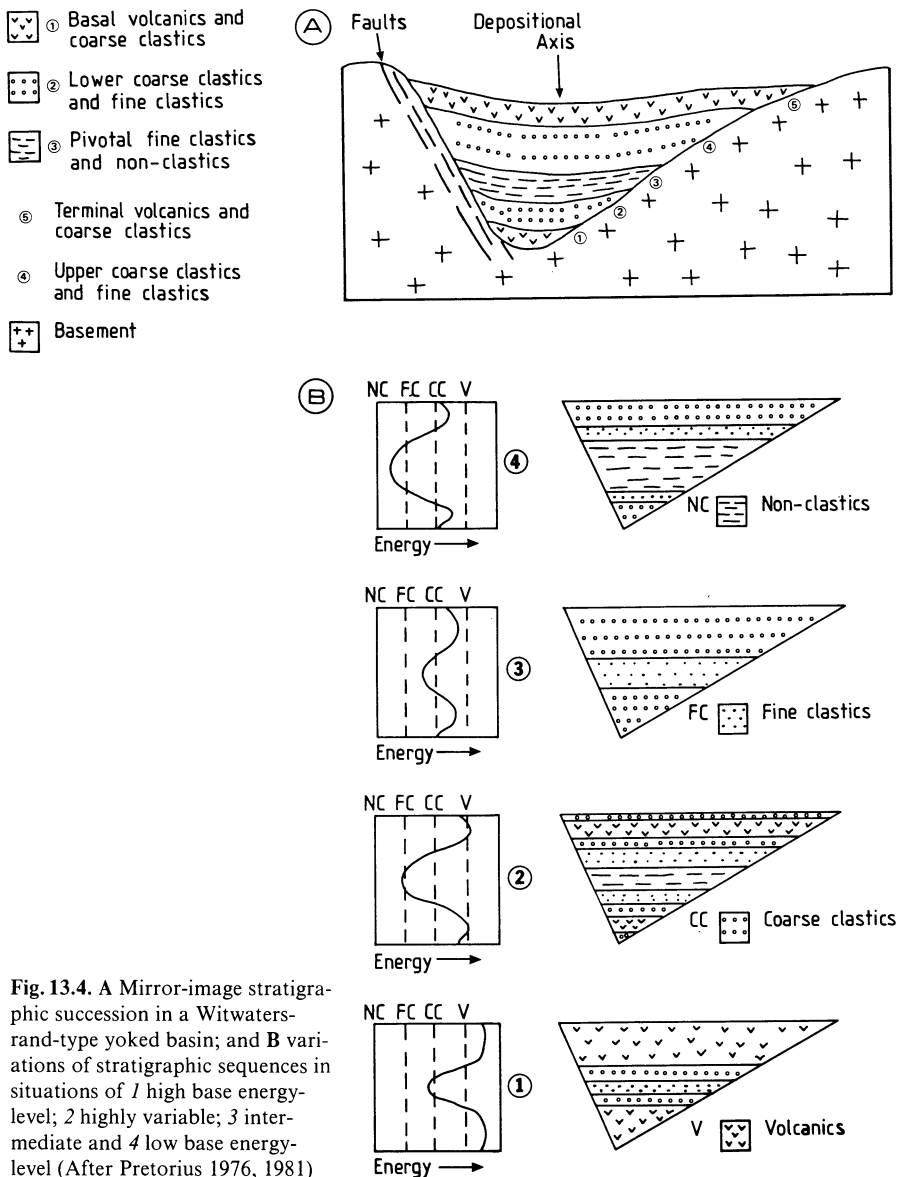
Fig. 13.4. A Mirror-image stratigraphic succession in a Witwatersrand-type yoked basin; and B variations of stratigraphic sequences in situations of *1* high base energy-level; *2* highly variable; *3* intermediate and *4* low base energy-level (After Pretorius 1976, 1981)

the Black Reef Quartzite Formation and of the Chuniespoort group of the Transvaal sequence would represent a post-graben stage due to thermal subsidence. Taking the Witwatersrand as a main example, Pretorius (1976, 1981) presented a generalised model of a stratigraphic succession of an Early-Mid Proterozoic yoked basin in South Africa. He observed that all the Proterozoic basins are characterised by the same general geometry of yoked basins (Fig. 13.4A), with the depositional axes (depocentres) oriented east-northeast. He further noted that basin develop-

ment was characterised by a cyclical pattern, in which basal volcanics and coarse to fine clastic rocks have their counterparts in a reverse sequence, in terminal volcanic and coarse to fine clastic sequences. This repetition takes place about pivotal fine clastic and non-clastic rocks, which are located more or less at the centre of the basin succession (Fig. 13.4A). The geometry and gross mirror image of the stratigraphic sequences suggested by Pretorius may reflect stages of opening and closing of graben-related geotectonic cycles. The sequence of volcanics, coarse clastics, fine clastics, non-clastics, and the dominance or absence of one or other of these lithological groups, would reflect a range of conditions from high to low base energy levels (Fig.13.4B). The volcanic rocks extruded in the basins have a general alkali-rich continental tholeiitic affinity, although the basal members may have komatiitic compositions. Bimodal volcanics (mafic-felsic) are also present and are best developed in the Ventersdorp basin.

Button (1976), who compared the Transvaal basin with the Hamersley basin in Western Australia, found that they show remarkably similar features and history of development. Both basins are characterised by a general stratigraphic succession consisting of basal volcanic and clastic units followed upward by chemical sediments, and finally by an upper, thick sequence of clastic rocks. The lower volcanics and clastic rocks include basaltic extrusives and pyroclastics, arenites, argillites, greywackes and minor dolomites. The chemical sedimentary units contain principally dolomite, chert and BIF and locally minor volcanic rocks. The upper clastic units comprise shaly sediments, sedimentary breccias, arenites, stromatolitic carbonates and basaltic to intermediate volcanic rocks.

13.4.2 The Stratigraphic Record of Aulacogens

Aulacogens are failed rifts in the sense that they did not develop into oceanic basins. The term aulacogen (from the Greek aulax, meaning furrow) refers to wedge-shaped rift structures, characterised by thick sedimentary successions, formed at the re-entrants of orogenic belts into continental platforms. Aulacogens were first recognised by the Russian geologist, Nikolai Shatski (Hoffman et al. 1974), as long sediment-filled troughs striking into the Russian cratonic platform. The formation of aulacogens thus requires the presence of stable continental crust and it is for this reason that they are not known in the Archean. Dickinson and Yarborough (1976) consider aulacogens as structures intermediate between intra-cratonic and oceanic basins. According to these authors, aulacogens – unlike intracratonic basins – are more or less symmetrical in transverse profile, and their flanks are initially active fault-controlled hinge lines. A model of aulacogen evolution is illustrated in Fig. 13.5A. The infill of aulacogens reflects their tectonic history, and this may include at least two distinct volcano-sedimentary successions in which the sedimentary component is derived from opposite directions. One succession consists of basal mafic to alkaline volcanics, immature to mature clastic sediments and carbonates accumulated into the trough from the adjacent continental block. The other is largely derived from the orogenic belt that forms at the mouth of the aulacogen (Fig. 13.5A) and consists of marine and non-marine

[1Km
10Km

Carbonate and mudstone
Mudstone and turbidites
Arkose
Olistostrome
Volcanics
Quartzite or sandstone
Fanglomerate
Basement
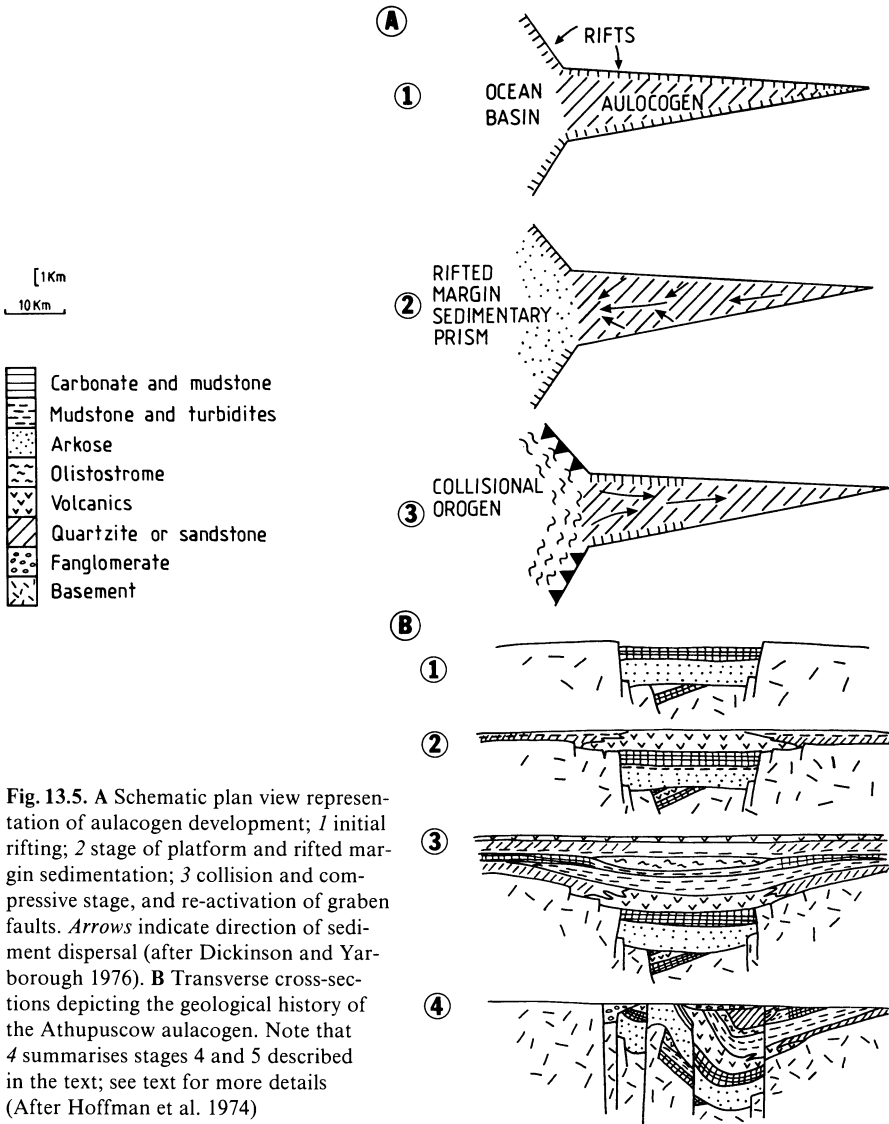
Fig. 13.5. A Schematic plan view represen-
tation of aulacogen development; *1* initial
rifting; *2* stage of platform and rifted mar-
gin sedimentation; *3* collision and com-
pressive stage, and re-activation of graben
faults. *Arrows* indicate direction of sedi-
ment dispersal (after Dickinson and Yar-
borough 1976). B Transverse cross-sec-
tions depicting the geological history of
the Athupuscow aulacogen. Note that
4 summarises stages 4 and 5 described
in the text; see text for more details
(After Hoffman et al. 1974)

clastics. The geological history of an aulacogen may be concluded with its closure
and collision, with development of thrust tectonics from the orogenic belt at its
mouth, as illustrated in Fig. 13.5A.

North American Aulacogens

Hoffman et al. (1974) studied and compared North American aulacogens with
similar, modern structures in Africa such as the Benue Trough and the Afar
depression, mentioned previously. In the Canadian shield two important aulaco-

gens are the Athapuscow and the Bathurst aulacogens, striking into the Archean Slave and Churchill provinces respectively. The geological history of these aulacogens is complex including phases of subsidence, graben formation, mild compression and re-activation in the form of transcurrent movements. In the Athapuscow aulacogene five stages of development are recognised (Fig. 13.5B; Hoffman et al. 1974). A graben stage consists of three main phases of volcano-sedimentary accumulation, including: (1) approximately 1000 m of dolomite, overlain by pyritic slate, basaltic and gabbroic rocks, capped by cherty dolomite; (2) a quartzite phase with cross-bedded arkose, glauconitic quartzite and ash-fall tuffs forming monotonous sequences up to 1600 m thick. These sediments were deposited by braided rivers that flowed down the axis of the rift valley towards the continental margin as indicated in Fig. 13.5A; (3) a dolomitic phase constituted by alternations of dolomitic shale and cherty stromatolitic dolomite and beds of orthoquartzite possibly derived from fault scarps. The second stage is a transitional one, characterised by accumulation of sediments on to the adjacent platform to the northeast. These sediments include cross-bedded quartzite overlain by siltstone for a total thickness of approximately 700 m. Within the aulacogen area up to 1400 m of acid and mafic volcanics were emplaced. In the third stage, downwarping of the trough resulted in the accumulation of flysch-like sediments consisting of red and green shales with thicknesses of between 350 and 1450 m at the platform end (northeast) and the geosynclinal (southwest) end of the aulacogen respectively. Other lithologies include carbonate rocks and conglomerates. Always in this third stage are stromatolitic limestone and dolomite deposited in shallow water, with deep-water correlatives (southwest end of the trough) consisting of rhythmically thin-bedded limestone, calcareous shale and greywacke. At the platform edge are stromatolitic mounds up to 80 m across and 20 m high, whereas a large olistostrome made up of angular blocks of stromatolitic dolomite and limestone, chaotically arranged in a mudstone matrix, occurs in the trough area. A sequence, up to 450 m thick and containing turbidites and local pillow lavas, overlies the olistostrome units. The fourth stage was one of mild compression, which resulted in some deformation of the aulacogen volcano-sedimentary sequence. During the fifth stage, up to 4000 m of clastic sediments were deposited unconformably on the older rocks.

Recent work by Hoffman (1987) resulted in a re-assessment of the geological history of the Athapuscow terrane. This is now believed to have been involved in a collision event along a major transform structure (Great Slave Lake shear zone) between the Slave craton and the North Keewatin terrane.

Aulacogen-Like Troughs of the Damara Orogen, Namibia

The depositional environments of the intracontinental branch of the Pan African Damara orogen in Namibia are interpreted as being characteristic of aulacogen-like troughs. As briefly discussed in Chapter 7 (see Fig. 7.4), the orogen is made up of an intracontinental branch and two coastal arms, whose relationship has been likened to a triple junction and setting similar to the Athapuscow aulacogen referred to above. According to Porada's (1983) interpretation, the intracontinental branch

comprises three main northerly and northeast-trending, graben and half-graben systems which formed in response to continental stretching. The presence of the Matchless Amphibolite Belt in one of the central-southern rifts indicates that a certain amount of ocean-floor spreading did occur in one of the rifts (see also Chap. 12). Approximately 1000–900 Ma ago, these grabens filled with terrestrial, predominantly fluviatile and locally lacustrine or playa-like sediments, and in the northern and central rifts various volcanic rocks of acid to alkaline character were erupted. These rocks belong to the Nosib Group, which appears to be confined to the rift structures. In the southern rift, evaporite sequences are characterised by dolomitic and pelitic sediments containing evaporite minerals pseudomorphosed by metasomatic reactions involving K, Na, B and Cl ions (Behr et al. 1983). The pseudomorphing minerals include microcline, scapolite, dolomite, albite and tourmaline. Tourmaline is interpreted to have originated from borates formed in playa lakes. We recall that in Chapter 4 mention is made that hypersaline fluids may form as a result of the deformation and metamorphism of these evaporitic sediments. The graben stage was followed by a subsidence stage during which the members of the Swakop Group were laid down. Two major successions were deposited during the subsidence stage. One is of miogeosynclinal facies, or platform succession, with predominantly dolomite and limestone rocks (Otavi group); the other, of eugeosynclinal facies (sensu lato), forms a thick sedimentary accumulation (Swakop Group) which includes carbonate rocks, diamictites (Chuos Formation) and turbidite deposits. Part of the latter are the rocks of the Kuiseb Formation – a thick flysch-like sequence consisting of carbonate, quartzite and pelitic rocks, locally intercalated with mafic volcanics. The sedimentary successions of the subsidence stage were laid down during at least two marine transgressions. The first marine transgression, coming in from the Atlantic side, affected the rifts and rift shoulders. A second transgression phase started with rapid differential crustal downwarping which led to the development of a wide basin between the Congo and Kalahari cratons (see Fig. 7.4). The Chuos diamictites (see Chap. 14) have also been interpreted as mass flow deposits which possibly reflect this phase of rapid subsidence. The differential subsidence in the central graben of the orogen resulted in a shelf (on the northern side of the graben) and deep basin (on the south side) configuration (Porada 1983). Dolomite and limestone were deposited on the shelf (Karibib Formation) while thick accumulations of calcareous turbidites took place in the basin (Tinkas turbidites).

The final phase (late- to post-orogenic) in the history of the Damara rifts consisted of closure, collision, metamorphism and granitic magmatism. This led to uplift, resulting in molasse-type sedimentation (Mulden and Nama Groups).

13.4.3 The East African Rift System

The East African Rift System forms a north-northeast-trending zone, approximately 4000 km long, extending from the Afar to the Zambezi river (Fig. 13.1). Reviews and articles on the African rifts, associated basins and sedimentation can be found in Frostick et al. (1986) and McConnell (1972). The East African Rift

System consists of a series of discontinuous grabens and half-grabens characterised by differential uplift, normal faulting, alkaline volcanism, geothermal activity, and development of basins and lakes. In several places the pattern of the rift system reflects Precambrian basement structures. There is a close relationship between areas of domal uplift and provinces of alkaline magamtism. The domal uplifts, or swells of the continental crust, occur as independent centres in the order of 1000–500 km across (Le Bas 1971). The domal uplifts are transected by graben structures along linear or radiating patterns. In some sectors of the rift system the rate of uplift and erosion of the domes is greater than the accumulation of volcanics. In the northern part of the system, from Kenya and the Ruwenzori mountains, to the Afar in Ethiopia, the rifts are characterised by Cenozoic to Recent volcanism, whereas in the southern sectors volcanic activity is much more limited, or altogether absent. Observations in modern rifts (Reading 1986) indicate that where the rate of volcanic activity exceeds that of rifting, the basins are predominantly filled with volcanics and their derived sediments. Where moderate to high rates of volcanic activity occur, then shallow lakes tend to form, while where volcanism is minor or absent, deep rift lakes are formed. Thus, Reading (1986) classifies the basins of the East African Rift System in: (1) volcanically filled (e.g. the Gregory rift, south of Lake Turkana); (2) volcanic-dominated rift basins with lakes (e.g. the Turkana depression); and (3) non-volcanic rift basins (e.g. Lake Malawi and Lake Tanganyika).

As previously mentioned, the various segments of the East African rifts tend to follow pre-existing Precambrian discontinuities. This is best illustrated by the division of the rifts in the Tanzanian province into western and eastern rifts which swing around the Tanzanian craton (Fig. 13.1). The Albert and Edward rifts follow the trends of Archean and Early Proterozoic orogenic belts, whereas the Gregory and Ethiopian rifts of the eastern branch follow the meridional trends of the Mocambique mobile belt. The Luangwa rift valley in Zambia follows the trend of Irumide mobile belts, continuing across the Lufillian arc towards the Okavango rift system in Botswana. The latter is still active and follows Irumide and Damaran trends, illustrating in fact that these rift structures occur along re-activated old lineaments. The Luangwa valley is largely filled with sediments of Karoo age, and other Karoo-aged sedimentary basins occur around the Zimbabwean craton. Sedimentation in the rift valleys consists mainly of fluvial-lacustrine sequences. Alluvial fans, delta plain or flood plain and lakes are the main sediment repositories. Playas, or basins with internal drainage, are also present. The western rift system is characterised by a number of basins, some of which are occupied by present-day lakes filled with up to 2 km of sediments. Rift lakes have warm and high-salinity waters, fed in part by hot mineral springs and in part by ephemeral runoff. Little terrigenous sediments are fed into these lakes, in which sediments are generally laminated organic oozes, clays and carbonates. Carbonates occur as chemical precipitates, or as biologically derived stromatolitic carbonates.

Continental evaporitic successions may develop from coastal sabkhas and playa lakes. Evaporites are characterised by deposits of gypsum, anhydrite and halite, derived from brines which become concentrated by evaporation, until precipitation of these minerals occurs. In the East African rifts a famous evaporite basin is the

Danakil depression in the Afar area. The basin was at one time connected, through a restricted opening, with the Red Sea, but became isolated by the extrusion of lava flows in the Tertiary and Holocene. The Danakil depression contains thick deposits of anhydrite, halite and potash minerals.

13.4.4 The Rio Grande Rift (USA)

The Rio Grande Rift consists of a series of grabens, which occur along the eastern side of the Colorado plateau and extend for approximately 900 km in a northerly direction from the state of Colorado to Mexico. The famous Valles caldera (New Mexico) is situated in this rift. Rifting began approximately 30–27 Ma ago; however many of the recent rift faults are probably re-activated ancient structures that date back to the Precambrian, Paleozoic and Laramide orogenies (Williams 1982). Uplifting of up to 1000 m occurred during the Miocene and Pliocene. No initial doming has been recognised for the Rio Grande Rift, and prior to rifting, sediments and volcanics of Cenozoic age accumulated on broad depressions during the Late Eocene (Williams 1982). In the Colorado sector the Rio Grande Rift comprises a narrow, northern zone (Arkansas Valley) and a wider southern basin (San Louis Basin), which borders the San Juan volcanic field. These basins are filled with mafic lavas and pyroclastic beds intercalated with alluvial material. In New Mexico the rift system is characterised by a series of en-echelon basins offset by complex transverse structures, which give the system an overall south-southwest trend. In southern New Mexico, the rift is most extensive and widens into a northerly trending series of parallel basins and ranges, which extend southward for approximately 250 km. West of the town of Socorro, the rift separates into the southwest-trending San Augustine basin. Large volumes of basaltic andesite, rhyolitic ash-flow sheets, with high initial Sr-isotope ratios, and therefore a lower crustal origin, developed in localised areas between 35 and 26 Ma. This was followed by a pause in the volcanic activity during the Mid Miocene (20–12 Ma), after which volcanism increased and was concentrated in the areas between Socorro and the Jemez mountains, in northern New Mexico, where the Rio Grande Rift transects northeasterly-trending lineaments. This volcanism is typically bimodal (basalt-rhyolite) with low initial Sr-isotope ratios, perhaps indicating that the horizontal extension and the volcanic activity of this stage was a response to mantle diapirism. The basin-fill sedimentary record is well studied in the Espanola basin, in the northern part of New Mexico. In this basin are Plio-Pleistocene alluvial sediments, which overlie and intercalate with tuffaceous sediments derived from the adjacent volcanic fields. These sediments, in turn, are underlain by sandstone, shale, conglomerate and volcaniclastic material of Eocene-Oligocene age (Williams 1982).

   The tectonomagmatic evolution of the Rio Grande Rift followed a complex pattern, which is difficult to unravel, and on which there is no general agreement. Broadly speaking, however, it appears that an initial, or pre-rift, basaltic andesite and interbedded high-silica ash-flows volcanism (thought by some authors to be related to back-arc extension) was followed, after the Miocene "lull", by bimodal volcanism, which is more typical of intraplate extension. Horizontal extension led to

EARLY PROTEROZOIC

MID-LATE PROTEROZOIC   RIFTS AND AULOCOGENS

EARLY PALEOZOIC   RIFT ZONES
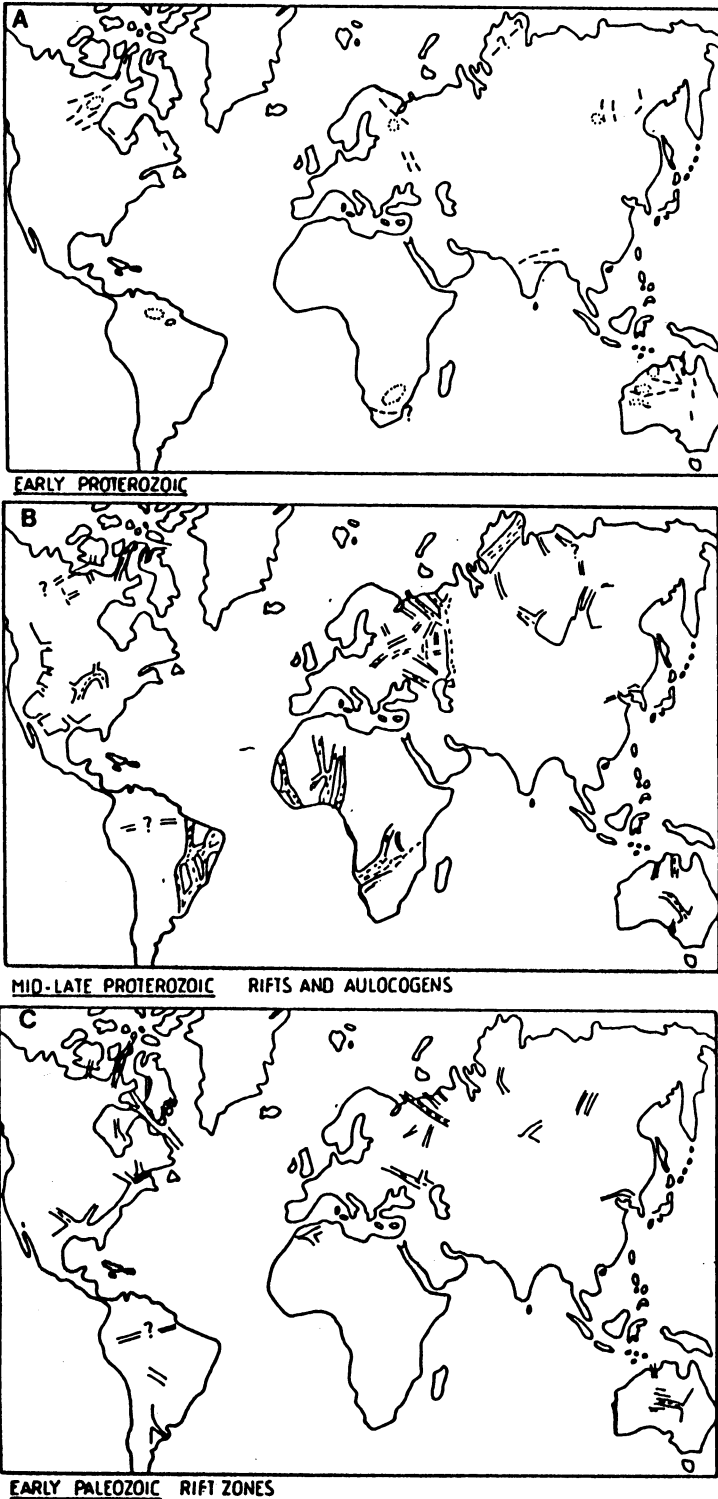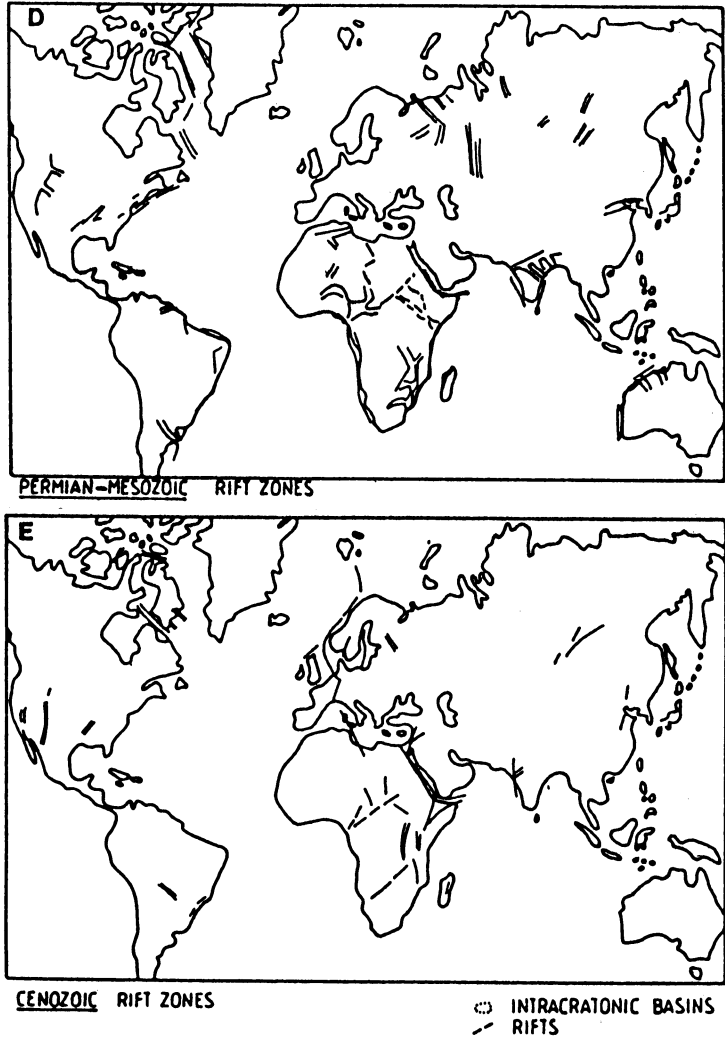
Fig. 13.6A–C

Fig. 13.6A–E. Temporal and spatial distribution of rift structures on present-day configuration of the Earth's continents. A Rifts and intracratonic basins of the early Proterozoic; B Rifts and aulacogens of mid-late Proterozoic; C Rift zones of the early Paleozoic; D Rift zones of Permian-Mesozoic age; E Cenozoic rift zones (After Milanovski 1983)

the inception of basins into which extensive sedimentary sequences were deposited. Thus, a complex interplay of tectonic activity, block-faulting, basin formation and sedimentation and volcanism characterise the history of this rift system.

13.5 Continental Rifting in Space and Time – Hydrothermal Mineral Deposits

Continental rifting has been a major geological process in the Earth's crust since the Proterozoic. Milanovoski (1983), who has reviewed the development of rifts in the Earth's history, distinguished five major epochs of rifting and crustal extension: Archean, Early Proterozoic, Late Proterozoic, Paleozoic and Mesozoic-Cenozoic. However, in terms of hydrothermal mineral deposition related to continental rift structures, we consider of importance the rifting events that took place since the Early Proterozoic. Figure 13.6 (A-E) illustrates the spatial and temporal distribution of rifts and rift-like structures on the present-day land-ocean configuration of the surface of the Earth. Clearly, continental rifts that evolved into ocean basins will have portions of the rifted margins as coastlines, as can be seen in Figs. 5.5, 5.7, 5.10 and in Fig. 13.6D. The rift structures shown in Fig. 13.6 have varied greatly in their evolutionary history, geometry, associated lithologies, and subsequent closure, deformation, metamorphism and thermal events. Temporal aspects may be considered in terms of global geological history, or in terms of the geodynamic evolution of the individual rift structures. Figure 13.7 is a schematic representation of the temporal evolution of extensional structures and related mineral deposits from the Early Proterozoic to the Mesozoic and Cenozoic. As mentioned above, mineral deposit types, within an individual rift, are related to the geodynamic evolution of the rift structure. Thus, there will be syn-rift, late- and post-rift mineral deposition. Chapter 3 reviewed models of hydrothermal convection systems related to phases of syn- and late-rifting development, and these are illustrated in Figs. 3.14 to 3.24. Post-rift stages are characterised by compression, deformation, metamorphism and granitic magmatism. Hydrothermal mineral deposits formed during this stage of rift evolution are related to the movement of metalliferous brines of crustal, metamorphic or igneous origin. This type of hydrothermal activity is considered and discussed in Chapter 15. In this section we adopt the principles used by Sawkins (1982, 1990), and consider rift-related mineralisation within a framework of incipient, intermediate and advanced stages of rifting.

13.5.1 Early Stages of Continental Rifting

During the early stages of continental rifting (hot-spot related according to Sawkins), mineral deposits are typically of magmatic-hydrothermal affiliation and include Sn, W, Nb, U, REE, Cu and Mo related to anorogenic igneous complexes. These deposit types are discussed in Chapters 8, 9 and 10. Hydrothermal breccias containing Cu sulphides (Messina, South Africa), or Fe-rich breccias with

polymetallic hydrothermal mineralisation, exemplified by the Roxby Downs giant deposit of South Australia, may be considered as belonging to incipient continental rifting. Geothermal activity associated with rift lakes, such as that which characterises the East African system, also belongs to the category of incipient rifting.

13.5.2 Aulacogens and Troughs – Intermediate Stages of Continental Rifting

Aulacogens and troughs are formed during stages of rifting that we can consider as intermediate between the East African system and the more advanced stages involving incipient ocean-floor spreading. These continental rift-related basins are characterised by bimodal (felsic-mafic) magmatism and thick clastic sedimentary sequences, within which a spectrum of mineral deposit types may occur. In the phase of rift development considered here there is no involvement of oceanic crust. Broadly, there are at least three major categories of mineral deposits which are formed within aulacogenes and troughs as defined above: (1) sedimentary-exhalative (sedex) stratabound/stratiform massive sulphide deposits; (2) sediment-hosted stratabound/stratiform disseminated Cu-rich deposits; and (3) native Cu in flow tops and interflow sediments of basaltic lavas.

The term stratabound refers to mineralisation which may be either concordant or discordant, but which is nevertheless confined to a particular stratigraphic horizon. Stratiform refers to mineralised bodies with a layer-like geometry, i.e. they are well developed in two dimensions. Stratiform orebodies are also stratabound, but the reverse is not necessarily true; thus, native Cu mineralisation in the flow tops of basaltic lavas is stratabound but not stratiform.

The sedimentary exhalative (sedex) sulphide deposits are illustrated in Figs. 3.16 and 3.19, which depict an idealised time-space evolution of mineralising systems in a rift structure, from deeper and higher temperature to shallower and lower temperature. Exhalative sulphide deposits in aulacogens and troughs are stratabound and/or stratiform and appear to include a number of end-member types characterised by metal association and host lithologies. Exhalative stratabound/stratiform massive sulphide deposits are formed by the discharge of metalliferous brines rich in Cu, Pb, Zn, Ag and Ba. The composition of these brines, however, depends on the nature of the crust and the host lithologies, such as volcanic-dominated or sedimentary-dominated or volcano-sedimentary, and hence the type of rifting involved. Plimer (1986), for example, examines the Australian Cu-Pb-Zn massive sulphide deposits in terms of characteristic metal associations and zonations, and the associated lithologies (see Chap. 3). Thus, Plimer (1986) considers the volcanic-hosted Broken Hill-type to be related to rift zones with typical bimodal magmatic activity, and the ascent of mantle-generated fluids rich in CO_2, F, P, Mn, Fe, Pb, Zn etc. (see Fig. 3.19). The Broken Hill Pb-Zn-Ag-Cu deposits are spatially associated with a host of other hydrothermal mineral deposits such as stratabound Cu-Au, W, epigenetic Pb-Ag, Cu-Ag, Cu-Ni-Fe and Pt deposits, and pegmatitic Sn-Ta, U, Nb, Be and Sn deposits. By contrast, sediment-hosted Mt. Isa sulphide mineralisation includes Pz-Zn ores and brecciated sediment-hosted Cu ores, and there appears to be a spatial and genetic association

Table 13.1. Selected stratabound/stratiform sedimentary-exhalative massive sulphide deposits. Data after Laznicka (1981); data for Aggeneys, Gamsberg and Rosh Pinah after mine geological staff

Deposit	Dominant metals	Approximate tonnage ($\times 10^6$)/grade	Age/dominant host lithology or facies
H.Y.C.-McArthur River; Northern Terr. Australia	Zn, Pb	2/10% Zn 4% Pb	Lower Proterozoic/ marine platform sed.
Mt.Isa; Queensland, Australia	Zn, Cu, Pb Ag	90/6.9% Pb 6.3% Zn, 3% Cu	Lower-Mid-Proter./ sedimen. ± volc.
Lady Loretta; Queensl. Australia	Pb, Zn, Ag Ba	9/18% Zn, 6.7% Pb, 109 g/t Ag	Lower Proterezoic./ sedimen. ± volc.
Broken Hill; New South Wales; Aust.	Pb, Zn, Ag	180/15% Zn, 10% Pb, 160 g/t Ag	Lower-Mid-Proter./ sedimen. ± volc.
Aggeneys; South Africa	Pb, Zn, Cu	225/1–3.5% Pb, 0.5– 2.4% Zn, 10–50 g/t Ag	Mid-Proterozoic/ volcano-sedimen.
Gamsberg; South Africa	Zn, Pb, Ba	150/7.4% Zn, 0.55% Pb	Mid-Proterozoic/ volcano-sedimen.
Sullivan; British Colum. Canada	Pb, Zn, Ag, Sn	175/6.4% Pb, 5% Zn, 60 g/t Ag	Upper Proterozoic/ sedimentary
Rosh Pinah; Namibia	Zn, Pb, Cu, Ba		Upper-Proterozoic/ volcano-sedimen.
Rammelsberg; Germany	Zn, Pb, Cu, Ag, Ba	22/19% Zn, 9% Pb, 1% Cu	Devonian/sedimen. ± volcanic
Meggen; Germany	Zn, Pb, Ba	60/10% Zn,	Devonian/sedimen.
Bathurst-New Castle; New Brunswick, Can.	Zn, Pb, Cu, Ag, Au	22/5% Zn, 1.9% Pb, 0.4% Cu	Ordovician/volc.- sedimentary

with Mississippi Valley-type (carbonate-hosted) Pb-Zn deposits. In contrast to the Broken Hill type, the exhalites associated with the Mt. Isa-type lack P, F, Mn, Fe and base metals. Plimer concludes that the Mt. Isa mineralisation is related to convective hydrothermal systems generated in failed rifts (aulacogen) coeval with maximum tectonic activity and highest geothermal gradient. The hot saline brines, with a high metal-carrying capacity, would have leached metals from the enclosing sedimentary lithologies, and exhaled in oxygen-deficient pools. A number of exhalative stratabound/stratiform massive sulphide deposits are listed in Table 13.1.

Sawkins (1989) considers the formation of the "giant" Pb-Zn-rich exhalative sediment-hosted massive sulphide deposits of Broken Hill, McArthur, Mt. Isa in Australia, Aggenays-Gamsberg in South Africa, and Sullivan in Canada, being somehow related to anorogenic felsic magmatism. This author relates the large abundance of Pb in these deposits with the availability of Pb-rich material, due to

CENOZOIC			SEA FLOOR SPREADING	
MESOZOIC	SANDSTONE U;		GONDWANA BREAKUP	ATLANTIC-TYPE PASSIVE MARGIN
PALEOZOIC				
	CARBONATE-HOSTED Pb-Zn			BACK ARC BASIN
570				
TRANSITION AND LATE PROTERO-ZOIC	RED SEA-TYPE SEDEX DEPOSITS Cu-Pb-Zn		WILSON CYCLES	
				RED SEA RIFT
1000				
	STRATABOUND DISSEMINATED SULPHIDES Cu-Co; Cu-Ag UNCONFORMITY U		RED BEDS AND COPPERBELT TYPE BASINS	YOKED BASIN (see fig. 3.20)
			EXTENSION AND RIFTING	
1600 MID PROTERO-ZOIC	SEDEX MASSIVE SULPHIDES Cu-Pb-Zn-Ag-Ba UNCONFORMITY U		AULOCOGENS	ATHUPUSCOW TYPE BASIN (see fig. 13.5)
2000			EPICONTIN-ENTAL SHELF BASINS	
EARLY PROTERO-ZOIC	SUPERIOR-TYPE BIF Fe-Mn; Pb-Zn-F			TRANSVAAL-HAMERSLEY TYPE BASIN (Button 1976) (see text)
2500	PLACER Au-U		CLASTIC-DOMINATED YOKED BASINS	WITS-TYPE BASIN (see fig. 13.4)
LATE ARCHEAN	ALGOMA-TYPE BIF			
2900 MID ARCHEAN	ALGOMA-TYPE BIF AND Au			BACK ARC BASIN IN GREENSTONE BELTS (see fig. 5.3)
			GREENSTONE BELTS	
3500 EARLY ARCHEAN				

Fig. 13.7. Temporal evolution of rift structures and related syn-rift mineral deposits

abundant feldspar-bearing rocks, such as crustal granitoids, and dacitic-rhyodacitic volcanics and extensive pyroclastics of anorogenic tectonic settings and their derived clastic sedimentary units. Sawkins further suggests that the sedimentary exhalative massive sulphide deposits are formed during more advanced phases of rifting with respect to the disseminated Cu-rich sulphide deposits.

Table 13.2. Selected stratabound/stratiform disseminated sulphide deposits. Data after Laznicka (1981); data for Klein Aub after mine geological staff

Deposit	Dominant metals	Approximate tonnage ($\times 10^6$)/grade	Age/dominant host lithology or facies
Kupferschiefer-Mansfeld-Sanger-hausen; Germany	Cu, Zn, Ag Pb, Co	67/2.9% Cu, 1.8% Zn, 191 g/t Ag	Permian/contin. marine (lagoon)
Kupferschiefer-Richelsdorf; Germany	Cu, Zn, Pb, Co, Ag	53/2% Cu, 1.3% Zn	Permian/contin. marine (lagoon)
Udokan; Siberia USSR	Cu	300/3% Cu	Lower-Proterozoic/ deltaic-lagoon
Klein Aub; Namibia	Cu, Ag		Upper-Proterozoic/ volcano-sedimen.
Nchanga; Zambia	Cu, Co	377/4.1% Cu, 0.1% Co	Upper-Proterozoic/ delta-lagoon-shal. marine
Mufulira; Zambia	Cu, Co	285/3.5% Cu, 0.13% Co	Upper-Proterozoic/ lagoon-intertidal
White Pine; Michigan, USA	Cu, Ag	600/1.2% Cu	Mid-Proterozoic/ contin. marine-lagoon
Pine Point; North West Terr. Can.	Zn, Pb	40/6% Zn, 2.4% Pb	Devonian/Carbon.- -evaporite platf.

Sediment-hosted stratabound disseminated Cu-Ag and Cu-Co deposits are found in the Irumide and Lufillian orogenic belts in south-central Africa (see Chap. 7 and later section), in the Kupfschiefer in central Europe, in the Stuart Shelf of the Adelaidean geosyncline, in the Keweenawan rift in the Lake Superior region (White Pine deposit), and at Udokan in Siberia. In contrast to the sedex type these deposits are more typical of syn-rifting events, in situations characterised by subaerial evaporitic to shallow depositional environments. The stratiform, sediment-hosted disseminated Cu-Co sulphides of the Copperbelt type appear to occur in continental "yoked" basins (see Fig. 13.7), and are also spatially associated with a host of other hydrothermal metalliferous deposits (see Chap. 3) which are formed during late to post-rifting phases of basin development. These Cu deposits are generally hosted by reduced carbonaceous horizons deposited in playa lake or lagoonal environments, during phases of low tectonic activity. The metalliferous brines (diagenetic-hydrothermal to basinal hydrothermal brines) would permeate the porous continental sediments and the metals would be precipitated in previously conditioned reduced horizons, forming disseminations rather than massive concentrations of sulphides. Models of hydrothermal systems proposed to explain the origin of these deposits are discussed in Chapter 3 and illustrated in Figs. 3.15, 3.20 and 3.21. Table 13.2 lists some selected disseminated Cu-sulphide deposits related to shallow marine-continental facies in yoked basins.

Uranium mineralisation, commonly associated with continental clastic sediments, is found spatially associated with the unconformity separating basement rocks from the overlying sedimentary sequences. Unconformity- and vein-type U mineralisation commonly occurs in the same rift environments that host the stratabound disseminated sulphide deposits. Uranium mineralisation in this situation does not have a relationship with igneous activity, although an indirect association is expected if the U metal is derived from crustal sources such as anatectic, anorogenic granitoids, or the products of differentiated alkaline melts. The development of uraniferous brines early in the sedimentary history of a yoked basin would allow the re-distribution of the geochemically mobile U by groundwater movements. Under these conditions roll-front-type U deposits would be formed. Vein-type or unconformity-type U deposits, on the other hand, are associated with extensive alteration zones and unusual metal associations, and for this reason are probably related to focused hydrothermal fluids of late- or post-rift stages associated with regional geothermal gradients, metamorphism and, perhaps, granite intrusions. Unconformity-type U deposits are examined in Chapter 15.

13.5.3 Advanced Stages of Rifting

In this book we consider advanced stages of rifting as those in which the rift structure is floored by transitional or oceanic crust. The term transitional is meant in the sense that Bonatti (1985) has used it to describe the floor of the Red Sea. Massive sulphide deposits that form at mid-ocean ridges represent the ultimate phase of hydrothermal mineralisation in the spectrum of rift-related deposits, and these are described in Chapter 12. As Sawkins (1982) points out, it can be argued that the Red Sea brine pools should also be regarded as concentrations of sulphides in an oceanic environment, and as such the Red Sea-type deposits would be a variant of the mid-ocean ridge sulphide mineralisation. However, the Red Sea is an example of a rift system transitional to becoming an ocean basin. Therefore, given the gradational and transitional nature of most mineralising systems, the inclusion in this chapter of the Red Sea deposits is dictated by reasons of expediency.

Carbonate-hosted Pb-Zn deposits, also commonly known as Mississippi Valley type, and including variants such as the Irish and Alpine types (Sawkins 1990), are probably formed in epicontinental basins at continental margins (see Fig. 3.14), or in carbonate platforms along the shoulders of the graben structures (e.g. Northern Platform of the Damara orogen, Namibia). These low-temperature deposits do not appear to be connected with igneous activity. Irish-type deposits are spatially associated with graben faults along which the mineralising fluids have travelled. As such, they could represent a transitional phase to the stratiform/stratabound massive sulphides of incipient rifts (see also Fig. 3.16). Chapter 14 takes a look at the carbonate-hosted deposits.

Finally, also in this category of rifting, we may include the accumulations of Fe- and Mn-rich sediments, which are considered to be chemical precipitates, and which occur throughout the geological ages from Archean to Recent. Algoma-type (Archean) and Superior-type (Proterozoic) banded iron formations (BIF) are

economically important, the latter being repositories of huge quantities of Fe and Mn, such as those of the Hamersley (Western Australia) and Transvaal (South Africa) basins (see Fig. 13.7). Aspects of BIF geology are briefly introduced in Chapter 6. There is evidence that these basins may have formed during rifting events that affected stable cratonic areas as indicated by the common association of thick sedimentary units and bimodal basaltic-rhyolitic volcanism. We return to this topic later in the chapter.

13.6 Hydrothermal Mineral Deposits in Incipient Rifts

In this section we take a look at some examples of mineralising systems – both ancient and modern – that are related to hydrothermal activity within incipient continental rifts. The first is the Messina Cu-bearing hydrothermal breccias in South Africa. These deposits occur in the Limpopo arm of the Limpopo-Lebombo-Sabi triple junction, possibly initiated during the Mesozoic, and characterised by numerous dyke intrusions and a number of igneous complexes (Nuanetsi Igneous Province). The second example deals with the Olympic Dam Cu-U-Au deposit in South Australia, where Late Proterozoic rocks of the Adelaidean Supergroup were deposited in a shallow intracratonic basin, and host a number of Zambian Copperbelt-type stratiform Cu deposits. The size and importance of these particular deposits are, however, completely overshadowed by the giant Olympic Dam deposit, whose precise nature is not well known, but it is possible that its origin may be related to magmatic activity within a setting of incipient continental rifting. Third, and last, we discuss hydrothermal activity in the modern rift setting represented by the western branch of the East African Rift System.

13.6.1 The Messina Cu Deposits, South Africa

The Messina Cu deposits are hosted in Archean high-grade metamorphic rocks of the Limpopo province. This province is a zone of polymetamorphic rocks which separates the Zimbabwe and Kaapvaal cratons (see Tankard et al. 1982; Fig. 13.8A). The Messina deposits occur along the northeast-trending Messina Fault, a splay fissure from the Dowe-Tokwe fault. Details of these deposits can be found in Jacobsen and McCarthy (1975, 1976), McCarthy and Jacobsen (1976), Jacobsen et al. (1976), Sawkins (1977), Ryan et al. (1983) and Bahnemann (1986). Although the age of the mineralisation is somewhat controversial, the weight of the evidence favours a Karoo age (Permo-Carboniferous to Jurassic-Cretaceous), and hence a relationship to the events that shaped the Limpopo-Lebombo-Sabi triple junction (Fig. 13.8A). The Karoo events are characterised by continental sedimentation and aborted rifting which resulted in thick sedimentary and volcanic successions (Truswell 1977). The breakup of the Gondwana continent in the Mesozoic was heralded and accompanied by the huge outpourings of Karoo basaltic lavas. It is estimated that the Karoo lavas reached a thickness of approximately 10 km,

537

Fig. 13.8A–C. Simplified maps of the distribution of Karoo igneous and sedimentary rocks in the Limpopo-Lebombo-Sabi triple junction region in A southeastern Africa, and B the Messina-Nuanetsi area (after Cox 1970). C The distribution of breccia pipes and Messina-type hydrothermal Cu deposits and their spatial relationship to the Messina fault (After Jacobsen and McCarthy 1976)

@GEOLOGYBOOKS

covering some 2×10^6 km^2 of the southern African subcontinent. The Mesozoic igneous activity was also characterised by numerous, but volumetrically minor, injections of alkaline igneous rocks (including the diamondiferous kimberlites) which were largely emplaced along ancient and well established trends. Sedimentary basins were formed in the Limpopo and Sabi areas into which the Karoo sediments accumulated.

The Karoo igneous rocks of the Lebombo-Sabi monoclines and the Nuanetsi Igneous Province (Cox 1970) were erupted approximately 194–190 Ma ago along major zones of crustal weakness forming the Limpopo-Nuanetsi-Sabi triple junction which is clearly defined by the distribution of the Karoo sedimentary rocks swarms of dykes and volcanic rocks (Fig. 13.8A, B). The Lebombo and Sabi monoclines form the southern and northeastern arms of the rifted continental margin, while the Nuanetsi igneous rocks extend in a west-southwesterly direction along the "failed" arm of the rift to the east along the Archean Limpopo province. The volcanic rocks form a bimodal suite including thousands of metres of basaltic lavas and rhyolitic volcanics, which attain their best development in the Lebombo monocline. At the meeting point of the Lebombo and Sabi arms is the Nuanetsi Igneous Province (southeast Zimbabwe and northern Transvaal). The Nuanetsi province is made up of mafic and felsic volcanics and alkaline intrusive rocks arranged in a synclinal structure (Nuanetsi syncline). Ring complexes and carbonatites are also present (Jacobsen and McCarthy 1975). Of particular interest in the present context is the presence of widespread hydrothermal alteration, especially around Messina, characterised by sodic and CO_2 metasomatism.

The Messina Hydrothermal Mineralisation

The mineralisation is hosted within granulite-facies gneisses, amphibolites, quartzites and biotite-garnet gneisses of the Archean Beit Bridge supracrustals, and the Bulai and Singelele granite gneisses. From southwest to northeast along the Messina Fault, there are five main orebodies: Campbell, Harper, Messina, Spence and Artonvilla (Fig. 13.8B, C). Mineralisation in these deposits occurs as elongate, and more or less conformable, lodes (Artonvilla and Spence), or as discordant lodes, fissure veins and breccia pipes (Campbell, Harper and Messina). Breccia pipes, veins and lodes are all undeformed and post-date any penetrative fabric in the area.

At Artonvilla the mineralisation is accompanied by intense hydrothermal alteration, which is mostly confined to structural discontinuities within cordierite-biotite-garnet gneiss and pyroxene granulite. Orebodies of disseminated sulphides have a distinct concentric zonation of alteration and ore minerals. Sericitisation marks the outer zone, while progressing inward alteration changes to albitisation, chloritisation and epidotisation, with corresponding zoning of pyrite, chalcopyrite, bornite, chalcocite and occasional native Cu in the centre. Geochemically, these zones are characterised by increasing K_2O (sericitisation) which decreases sharply inwards, whilst SiO_2, Al_2O_3, and Na_2O increase. The orebodies are planar and dip at about 45° to the southwest. The main ore minerals are chalcopyrite, bornite and chalcocite. The Messina and Harper orebodies are hosted by the Singelele granite gneiss and Beit Bridge metaquartzites, with the mineralisation being associated with

fissure systems related to the Messina Faults. Numerous lodes are present and, more importantly, large and irregular breccia pipes. Nine breccia pipes have so far been recognised in the Messina area, of which three have been mined (Campbell, Harper and Messina). The pipes range in diameter from 10 to 300 m, with vertical extents of approximately 1.5 km, and are bounded by contacts which follow a pre-existing regional jointing pattern. The size of the breccias changes along the pipe from a macrobreccia system at depth to progressively finer breccias towards the apex. Hydrothermal alteration of the wall-rock gneiss mantles the breccia columns. An outer zone of sericitised gneiss grades inwards to albite, and finally to an assemblage of zoisite and quartz immediately around the brecciated contacts (Jacobsen et al. 1976). The outer alteration zone has a bleached appearance, with sericite replacing plagioclase and quartz. In the albitised zone, albite replaces the earlier sericite and the wall-rock mineral components (quartz and feldspars), imparting a characteristic red colouration to the altered rock. The innermost alteration zone, together with the breccia fragments, is buff coloured and contains zoisite, quartz and epidote. The zoisite changes from white-yellow to brown as the mineralisation is approached, a feature used in underground borehole exploration (J. Twidale pers. comm. 1985). In the deeper levels, where the pipes may be uneconomic, chlorite, specularite, calcite and zeolites occur in late-stage cavity fillings. Sulphide mineralisation shows a vertical zonation, with pyrite ± chalcopyrite ± molybdenite in the apical areas, grading downwards to chalcopyrite + bornite and to bornite + chalco-pyrite ± native Cu in the deeper levels. Rich pods of ore may contain over 4% Cu, but more usually tenors range from 1 to 1.5% Cu.

The Harper mineralisation is associated with breccias in the splay fissure which branches off the Messina Fault, and with cross-fissures in the metaquartzite host rocks, thus forming a boxwork-styled mineralisation (Fig. 13.9A, B). The miner-alogy and zoning of the ore is similar to that of the breccia pipes. The Campbell mine is also hosted by the Singelele granite gneiss and Beit Bridge metasediments. This mineralisation occurs very close to the intersection of the Messina and Dowe-Tokwe faults, which dip steeply towards each other. The granite gneiss in the wedge-shaped area between the two faults is traversed by a number of fractures which are mineralised with bornite, chalcocite and chalcopyrite. The ore shoots converge towards the West Lode breccia pipe, which is 550 m below the surface and is transected by the Messina fault at depth, with a displacement of approximately 80 m. The main difference from the other pipes is that the sulphide mineralisation is confined to the periphery of the pipe.

The irregularity of the orebodies makes the estimation of the ore reserve extremely difficult. However, until 1985, known reserves were approximately 6×10^6 tonnes at 1.1% Cu. An unusual method of ore reserve estimation is employed by mine geologists, in which the coarse-grained nature of the ore is relied upon. Sections along an exposed underground face are measured in detail and the proportions of the various ore minerals estimated. The percentage of Cu is then calculated for each section on the basis of the known Cu content of each ore mineral (e.g. chalcocite 79.7%, bornite 55.5% and chalcopyrite 34.6%). Over the years, this method has proved to be remarkably reliable.
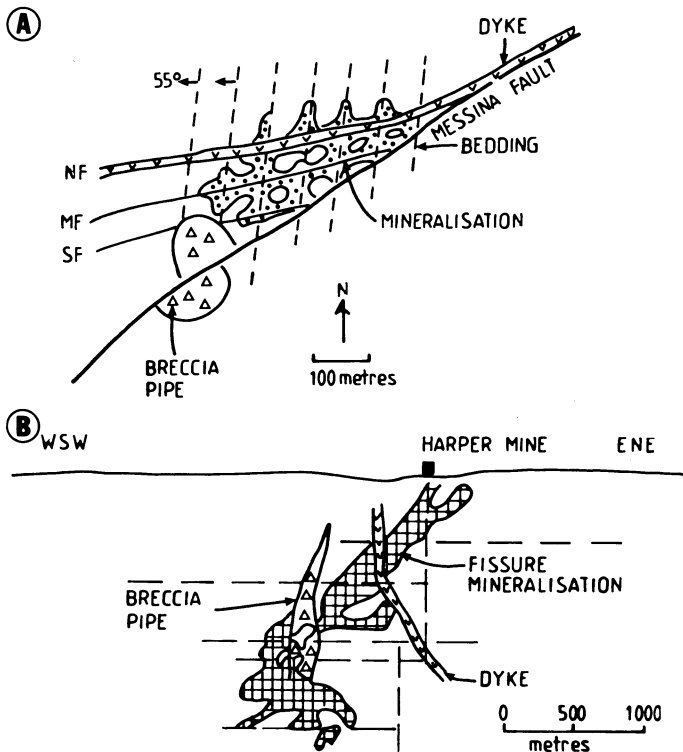
Fig. 13.9. A Schematic representation of the spatial association of the mineralisation with the Messina Faults and allied splay fissures, at the Harper mine. The fissure-related mineralisation plunges at 55° in the plane of bedding. *NF* North Fissure; *MF* Middle Fissure; *SF* South Fissure. B Cross-section of the Harper orebody in the plane of the Messina Fault, showing both fissure and breccia-type mineralisation (J. Twidale, pers. comm. 1983)

Age and Ore Genesis

The precise age of the mineralisation is not known. Age limits are provided by pre- and post-minerlisation mafic dykes which yield K-Ar ages of approximately 1800 and 185 Ma respectively. Jacobsen and McCarthy (1976), McCarthy and Jacobsen (1976), Jacobsen et al. (1976) and Sawkins (1977) all agree that the Messina Cu mineralisation could be genetically linked to the Nuanetsi Igneous Province, emplaced approximately 206 Ma ago. There are several lines of evidence pointing to this conclusion. The mineralisation, which post-dates the tectonic fabric of the host rocks; the alkaline and fenite-like nature of the hydrothermal alteration around the deposits; the mineralised bodies, which are aligned along an extension of the Nuanetsi rocks, and indeed the areal extent of the Nuanetsi ring complexes which decreases towards the southwest, suggesting that there is less unroofing towards Messina. This would indicate that similar intrusive complexes may lie below the Messina orebodies. Sawkins and Rye (1979) demonstrated that the mineralising fluids were of low temperature (210–120°C) and weakly saline (1–26 wt.% NaCl

equivalent), and of probable meteoric origin. One genetic model (Sawkins 1977) envisages leaching of Cu from overlying Cu-rich basalts of possible Soutpansberg age (approximately 1700 Ma) by meteoric fluids. A hydrothermal convective cell could have been activated by the high heat flow, normally associated with rifting, near and along the Messina fault. In another model (Jacobsen et al. 1976), Cu would have derived from late stage fluids associated with evolving alkaline magmas. The fluid ascended along joints, reacting with the wallrocks and causing considerable increase in vapour pressure, which at the highest point of the column led to hydraulic fracturing and the formation of breccia pipes. A combination of these two models is possible; the heat, metals and early fluids could have derived from alkaline intrusives at depth, with later superimposition of heated meteoric waters.

13.6.2 Olympic Dam (Roxby Downs), South Australia

The Olympic Dam Cu-U-Au deposit is located approximately 650 km north-northwest of Adelaide (Fig. 13.10). At the time of writing the only comprehensive published accounts of this mineralisation can be found in Roberts and Hudson (1983), Roberts (1986) and more recently Oreskes and Einaudi (1990) and Reeve et al. (1990). The Olympic Dam, an unusual hydrothermal deposit, with an unusual
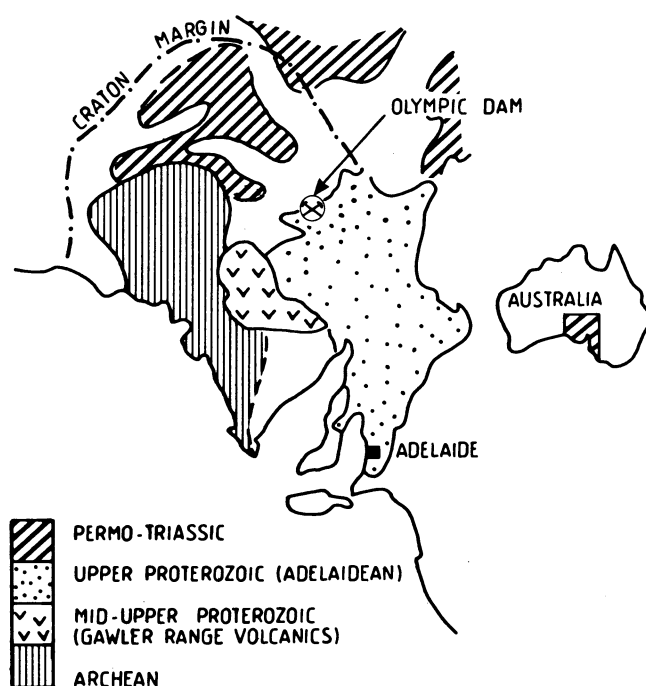
Fig. 13.10. Simplified geological map of the southern part of South Australia, showing the location of the Olympic Dam (Roxby Downs) deposit (After Roberts and Hudson 1983)

metal association (Cu-U-Au-Ag-REE-Ba-F), is set in a rift-related environment, and it contains probable ore reserves in the order of 450×10^6 tonnes at 2.5% Cu, 0.08% U_3O_8, 0.6 g/t Au and 6.0 g/t Ag. The deposit occurs in the Stuart self region, hosted in Mid-Proterozoic basement rocks, which are overlain by flat-lying Upper Proterozoic to Cambrian sedimentary rocks (Fig. 13.10). In the Olympic Dam area the basement rocks include a basal anorogenic, A-type, K-feldspar granite, within which is a northwest-trending graben, approximately 7 km long and 4 km wide. This granite was overlain by conglomerates and tuffaceous sediments of the Gawler Range Volcanics. These rocks are now preserved in a fault-bounded block in the centre of the deposit. The graben and the Olympic Dam mineralisation have no surface expression, being covered by 350 m of flat-lying post-mineral sediments. Thus, the discovery of the Olympic Dam deposit is considered to be a tribute to both geological ingenuity and management acumen. The rocks within the Olympic Dam graben are all, to a greater or lesser degree, hydrothermally altered. Pervasive alteration is characterised by hematite, chlorite, silica, carbonate and sericite. The age of the deposit is probably between 1.4 and 1.3 Ga, which is some 200 Ma younger than the hosting alkali feldspar Olympic Dam granite.

During the initial work on this deposit the mineralisation was considered to be characterised by an older stratabound type and a younger transgressive type (Roberts and Hudson 1983). The stratabound mineralisation is confined to clastic sedimentary units and characterised by the sulphide assemblage bornite + chalcopyrite + pyrite, associated with hematite, carollite, uranium, and REE minerals. The sulphide mineralisation occurs as disseminations, replacement, cavity filling and as fine layers. The gangue mineralogy consists of hematite, quartz, sericite, fluorite, barite, rutile and minor amounts of tourmaline and anhydrite. Also, the stratabound mineralisation contains clasts of banded siderite, spherulites of Fe-rich material (siderite, chlorite etc.) and hematite. The transgressive mineralisation is characterised by the sulphide assemblage of chalcocite + bornite, which occurs as veins and irregular lenses in breccia units. The sulphide ore minerals are associated with hematite and fluorite.

Oreskes and Einaudi (1990) have re-interpreted the geological and mineral evolution of the Olympic Dam deposit on the basis of detailed underground mapping and core logging. A summary of their work and interpretation is given here. The deposit is characterised by a number of hematite-quartz breccia dyke-like bodies which correspond to the transgressive mineralisation type of Roberts and Hudson (1983). These breccia bodies are up to 100 m wide, host the Cu-U mineralisation and form a zone elongated in a northwest direction (possibly a pre-existing fault), which measures approximately 2.5 by 1.5 km along a strike length of greater than 5 km. Oreskes and Einaudi recognise two main types of breccias: heterolithic and hematite-quartz microbreccia. They are arranged in a zonal pattern which begins with brecciated granite at the periphery of the deposit, passing into the heterolithic breccia and hematite-quartz microbreccia in the central portions. The heterolithic breccia consists of fragments, less than 10 cm in diameter, of hematite and granite in a matrix of quartz + hematite + sericite + siderite + chlorite. Breccia clasts include fluorite, siderite, barite and pyrite. In places the heterolithic breccias contain fragments of sedimentary material of which at least three facies are

recognised: bedded hematite, laminated barite and volcaniclastics. Heterolithic breccias grade into hematitic microbreccias and fine-grained massive hematite-quartz. It is important to note that hematite euhedra replace original feldspars and carbonate minerals. Veins are also present and contain fluorite, barite, siderite, hematite and sulphides. REE, U and Au are present in substantial amounts in these breccias. The chief U minerals are coffinite, pitchblende and brannerite; the REE minerals include monazite, xenotime, bastnaesite [$(Ce,La)CO_3(F,OH)$] and florencite [$CeAl_3(PO_4)_2(OH)_6$], which are associated with sericite, hematite and fluorite. Au and Ag occur mainly as native species. The REE abundance is correlated with increasing hematite content of the breccias. Deposition of the REE phases occurred throughout much of the hydrothermal activity at Olympic Dam, with HREE characterising the final stages. The formation of the breccias implies large-scale movement of fluids, which in places resulted in fluidisation, as testified by the presence of hematite spherulitic structures. The presence of sedimentary barite and hematite as fragments and minor pods in the upper parts of the deposit suggest a surface and/or near-surface exhalative activity.

Textural relationships and the distribution of the sulphides indicate firstly that they were deposited during the late stages of the mineralisation event and secondly that they are zonally arranged around the central hematitic core which is nearly devoid of sulphide mineralisation. Outward from this barren core sulphide assemblages are characterised by bornite + chalcopyrite to distal chalcopyrite + pyrite.

The origin of the mineralised breccia bodies is thought to be the result of hydrothermal brecciation associated with extensive Fe-metasomatism of the Olympic Dam granite, which possibly took place at depths of 1 or 2 km below the Proterozoic paleosurface. The authors point out that the entire alteration-mineralisation-breccia system can be viewed as an interplay of ongoing mechanical brecciation and the metasomatic replacement of the host granite. The genesis and evolution of the Olympic Dam deposit, according to Oreskes and Einaudi (1990), is related to the upward streaming of hydrothermal fluids along steep faults and fractures. Early hydrothermal activity resulted in intense sericitic (with minor hematite) alteration, followed by the major brecciation and alteration-mineralisation event. This stage was characterised by large-scale hematite replacement and deposition accompanied by fluorite, siderite, barite and REE phases. Fe-Ba-REE-Th-Y-CO_2-F enriched hydrothermal fluids circulated in the subsurface and locally exhaled at the surface with the deposition of baritic and baestnaesite-rich sediments. At the same time ongoing tectonic activity resulted in the erosion of the breccias bodies and of the altered granite with the formation of bedded hematitic and quartz-sericite sediments. At depth brecciation and mineralisation continued with further deposition of REE minerals and the begining of sulphide precipitation. Collapse of the upper parts of the breccia system followed, while hydrothermal activity decreased in intensity resulting in the main episode of Cu-Fe sulphide mineralisation. Supergene enrichment in the form of chalcocite ore occurred as a result of surface weathering during the Proterozoic. Finally, erosion and sedimentation took place, and approximately 700 Ma ago the Olympic Dam deposit was buried by sediments thus allowing its preservation.
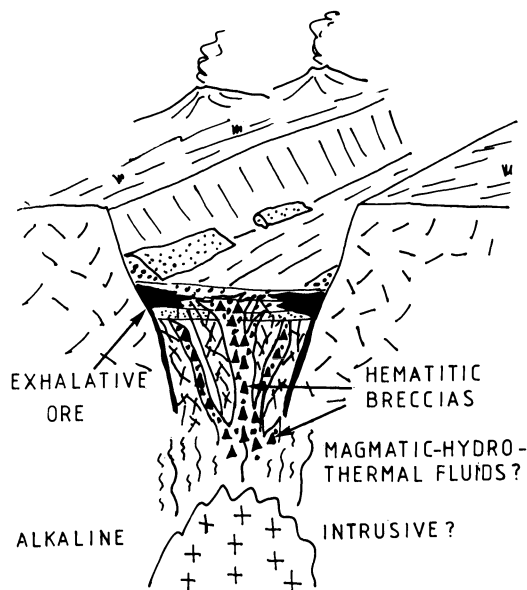
Fig. 13.11. A schematic representation of a conceptual model for the genesis of the Olympic Dam mineral deposit and its possible relationship to an underlying alkaline intrusive

The evolutionary history of the Olympic Dam deposit is obviously complex and as yet little understood. Nevertheless, it is clear that it was formed in an extensional continental environment and that at least two mineralising pulses or events were responsible for the exhalative and hematitic breccia mineralisation. Fluid inclusion data suggest that both were formed from fluids of similar salinity (7 wt.% NaCl equivalent) and composition but with different temperatures (approximately 160 °C and 240 °C respectively) (Roberts and Hudson 1983). The unusual metal association, Fe-rich alteration, the presence of F, Ba and REE, suggest a relationship with alkaline igneous activity. A cartoon depicting a possible scenario for the Olympic Dam ore deposit is shown in Fig. 13.11.

13.6.3 Hydrothermal Activity in the Tanganyika Trough, East African Rift System

The occurrence and nature of hot springs and metal deposits in the lakes of the East African rifts are described in Chapter 3 (see Fig. 3.24). In this section we take a look at a recent discovery – reported by Tiercelin et al. (1989) – of sublacustrine thermal springs and associated deposits of massive sulphide mineralisation.

The Tanganyika trough is part of the western branch of the East African rifts, and the newly discovered hydrothermal sites are located in the northern sector of the trough at the intersection of north-south fractures and a major northwest-trending strike-slip fault system. The high heat flow associated with the strike-slip fault system may be related to hydrothermal convection beneath the Lake. Tiercelin et al. (1989) report the presence of three sites of hydrothermal activity on the west side of northern Lake Tanganyika: Pemba, Cape Banza and Cape Kalamba. At Pemba, hydrothermal activity occurs on land and under water to about 50 m depth. On

shore, sulphide and quartz veins form stockworks in the fractured basement rocks along a zone approximately 100 m long. The mineralised zone consists of kaolinised material containing pyrite, quartz and natroalunite. Hot water (65°C), H_2S and CH_4 exhale under water from sandy sediments. Sulphide blocks are also present and consist of pyrite and marcasite, associated with quartz, kaolinite and barite. This sublacustrine mineralisation is thought to be forming by interaction of the exhalations with microorganisms. At Cape Banza several hydrothermal vents are observed at a water depth of about 10 m. The discharging fluids have temperatures of 70 to 80°C and a flow rate of 1 to 3 l/s. Small chimney-like structures through which the fluids discharge are made up of aragonite and pyrite.

The model of hydrothermal circulation proposed by Tiercelin and co-authors involves low-temperature meteoric waters and/or lacustrine water recharge, heating from igneous intrusions in the axial zones of the trough and discharge of the fluids through the thick (approximately 6 km) organic-rich sedimentary deposits in the lake. The organic-rich sediments constitute a trap for the metals and also contribute to hydrocarbon formation. The fluids discharge at the bottom of the lake at temperatures of approximately 80–65°C, but it is inferred that at depths of 1 or 2 km, temperatures may exceed 300°C.

The implications of this discovery are far-reaching in that they could provide a modern analogue for at least some of the rift-related stratabound/stratiform sulphide deposits.

13.7 Hydrothermal Mineral Deposits in Aulacogens and Troughs at Intermediate Stages of Rifting

In this section we examine examples of volcano-sedimentary exhalative massive sulphide deposits, and continental stratiform sediment-hosted disseminated sulphide deposits. Selected examples of these deposit types are given in Tables 13.1 and 13.2. In the former group we look at the McArthur River and Mt. Isa deposits in Australia, and the Aggeneys-Gamsberg deposits in South Africa. In the stratiform disseminated sulphide group we examine the Klein Aub Cu-Ag deposit in Namibia, and briefly review the Cu-Co deposits of the Zambian Copperbelt, the White Pine Cu deposit and the stratabound native Cu mineralisation in the lavas of the Keewanawan rift in the USA.

13.7.1 McArthur River and Mt. Isa, Northern Australia

The McArthur River and Mt. Isa Zn-Cu-Pb-Ag deposits are located in the Northern Territory and northwest Queensland respectively. They are part of a number of large sediment-hosted massive sulphide deposits, including Hilton and, further south in New South Wales, the Broken Hill deposit, situated in Proterozoic rifts (Fig. 13.12). The McArthur River deposit lies on the eastern margin of the north-trending Batten Trough, whilst Mt.Isa and the close-by Hilton deposit are located
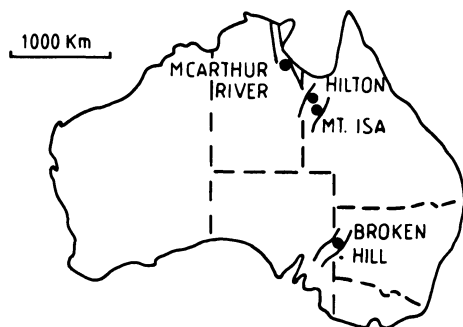
Fig. 13.12. Location of the major sediment-hosted massive sulphide deposits in Australia

further to the south in a northeast-trending trough. The Mid-Proterozoic sediments within the Batten trough are essentially unmetamorphosed, whereas those to the south around Mt. Isa have undergone several periods of deformation and are variably metamorphosed. Approximate ore reserves for these deposits are given in Table 13.1. There is much literature on these deposits, and the present discussion is based on Solomon (1965), Murray (1975), Mathias and Clark (1975), Lambert (1976), Walker et al. (1977), Williams (1978a, b), Finlow-Bates (1979), Rye and Williams (1981) and Gulson et al. (1983).

McArthur River

The McArthur River deposit was discovered by a field assistant in 1955 and the initial drilling, carried out in 1959, delineated a mineralised zone approximately 1.65 km long, 1 km wide and 50 m thick. Development of this major deposit has been hampered by metallurgical problems due to the very fine-grained nature of the ore; hence, only a substantial increase in base metal prices, and improved recovery of the metals, would make the deposit a viable mining proposition. The stratigraphic succession in the vicinity of the mineralisation represents a major transgression from subaerial red dolomitic siltstone of the Tooganinie Formation through intertidal and shallow marine carbonates of the Emmeruga and Teena Formations, to deeper water sediments of the Barney Creek Formation. Subsequent regression is represented by shallow-water and intertidal carbonates of the Barney Creek Formation and the overlying Reward Formation. The major orebody at McArthur River is the H.Y.C. (Here is Your Chance) orebody which occurs in the H.Y.C. pyritic shale of the Barney Creek Formation. This unit was laid down in a sea-floor depression (Bulbarra depression), whose development was controlled by syn-depositional movements along the Western and Emu faults. The H.Y.C. orebody (Fig. 13.13A) can be divided into seven mineralised beds separated by interore beds. The ore zones are thin laminae of fine-grained pyrite, sphalerite and galena interbedded with shale and tuffaceous shale. These beds show features of penecontemporaneous deformation, such as slumping. The interore beds consist of more dolomitic material. East of the H.Y.C. a different style of mineralisation occurs in four smaller orebodies, which are discordant and resemble a Mississippi Valley-type deposit. The host rocks of these orebodies are dolomites of the
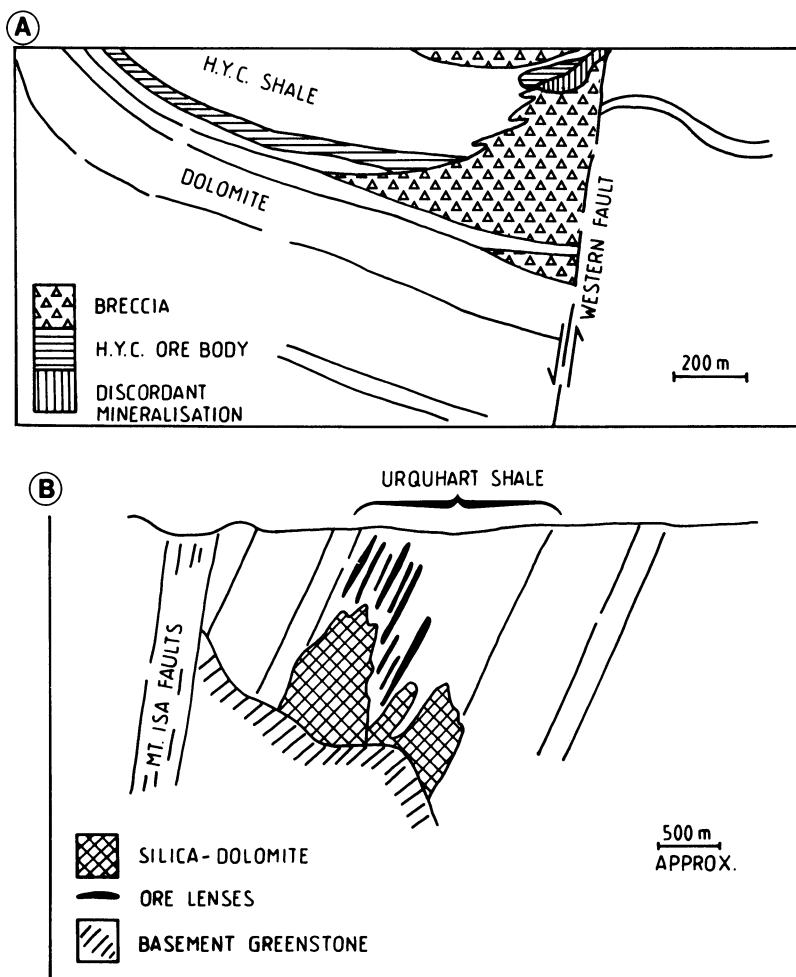
Fig. 13.13A, B. North-facing, schematic cross sections of A the McArthur River and B Mt. Isa deposits (After Walker et al. 1977 and Plimer 1986 respectively)

Emmeruga and Cooley Formations, thought to represent either an algal reef complex or a near-shore carbonate bank. Coarse-grained sulphides, represented by pyrite, sphalerite, galena, chalcopyrite, bornite, marcasite and tetrahedrite, occur associated with dolomite gangue in veins and stockworks of brecciated host rocks and show textures of open-space filling.

The main sulphides of the McArthur deposits are pyrite, sphalerite and galena, with lesser quantities of chalcopyrite, tetrahedrite, arsenopyrite, marcasite, chalcocite and covellite. Pyrite shows some distinct morphologies which, in conjunction with S-isotope systematics, have been used to explain the genesis of the sulphide mineralisation. Pyrite occurs in three main forms: (1) euhedral to rounded crystals, between 2 and 5 µm in size, which were deposited first and occur as fine

dissemination or laminae; (2) spherical pyrite in the size range of 5 to 20 μm; (3) framboidal shapes. The interpretation of pyrite morphologies and S-isotope systematics is not simple; it has been suggested that the pyrite was formed in two stages: (1) by a hot metal-rich, but S-poor, brine which dissolved early diagenetic pyrite; and (2) re-deposition of pyrite on the earlier grains by the new S-enriched solution.

The base metal sulphides are zonally distributed, showing decreasing Cu/Pb + Zn ratios from the Emu Fault towards the H.Y.C. orebody (Fig. 13.13 A). This zoning, therefore, suggests that the mineralising fluids were possibly introduced along the Emu Fault and spread out away from it. $\delta^{34}S$ values for sphalerite and galena increase westward from the Emu Fault, a feature which has been interpreted as due to cooling of the ore solutions away from the conduit represented by the Fault. The conformable nature of the ore, and its early diagenetic structures suggest a syngenetic origin for the H.Y.C. orebody. Lambert (1976) favours a model in which Fe, Cu, Pb and Zn are introduced in the form of reduced sulphur complexes, from which the sulphides are precipitated as a result of physico-chemical changes on discharge into sea water. The fluids could have developed from the heating of sea water in a rift environment in the manner suggested in Chapter 3 (see Figs. 3.17–3.19). The interore beds of brecciated dolomitic material are thought to represent turbidites that interrupted what would otherwise have been a continuous mineralised sequence. The discordant mineralisation would have been deposited as the mineralising fluids moved through the shallow-water facies rocks, on their way towards the Bulbarra depression. Because of the similarity of this mineralisation with Mississippi Valley-type deposits, Williams (1978a, b) proposed an epigenetic model for their genesis involving metal- and sulphate-rich solutions emanating from fault zones and reacting with the dolomitic rocks. In any case it is generally agreed that both the conformable and discordant deposits were formed from the same mineralising fluids which flowed from the Emu Fault (Rye and Williams 1981).

Mt. Isa

The Mt. Isa and Hilton Pb-Zn-Ag deposits (Fig.13.12) are hosted by the Urquhart Shale Formation, which is thought to be a correlative of the H.Y.C. shale at McArthur River. The Urquhart Shale Formation occurs in the upper part of the Mt. Isa Group, consisting of a thick sequence of shale, dolomitic siltstone, tuffaceous material and siltstone units. The Urquhart Shale Formation includes well-bedded carbonaceous, dolomitic, quartzo-feldspathic siltstone, dolomite and tuffite.

At Mt. Isa there are 16 ore horizons, each of which may be up to 35 m thick. The mineralisation extends for some 1600 m along the strike, discontinuously across a stratigraphic width of approximately 1200 m and downdip for about 700 m (Hutchison 1983). A schematic cross-section of the Mt. Isa mineralisation is illustrated in Fig. 13.13B. The major ore minerals, occurring as distinct concordant bands, include galena, sphalerite, freibergite, pyrite and pyrrhotite, with minor amounts of chalcopyrite, marcasite, arsenopyrite and tetrahedrite. Gangue minerals are Fe-dolomite, quartz, albite, microcline, chlorite, sericite and phlogopite. Folding has deformed the orebodies, and the re-mobilisation of sulphides

during deformation events has resulted in enrichment of the mineralisation in fold hinges.

Immediately adjacent to the Pb-Zn-Ag orebodies are large, non-stratiform Cu orebodies, which are confined to a silica-dolomite facies of the Urquhart Shale. The silica-dolomite consists of crystalline dolomite, re-crystallised shale and brecciated siliceous shale. The silica-dolomite orebody extends for about 2600 m and is 530 m wide at its thickest point near the greenstone basement contact. The Cu ore, which occurs as disseminations and vein fillings within the silica-dolomite rocks, includes pyrite, pyrrhotite and chalcopyrite, with minor amounts of arsenopyrite, marcasite, galena, sphalerite and a number of Co-As species. The major gangue minerals are siderite and quartz, with minor and localised talc, chlorite and K-feldspar. Chalcopyrite forms veins and irregular aggregates, usually associated with coarse-grained pyrite. Locally, bands of fine-grained chalcopyrite are associated with fine-grained framboidal pyrite. The Cu grades decrease away from a massive sulphide pod, situated on top of the greenstone unconformity (Fig. 13.13B).

One interpretation for the genesis of the Mt. Isa orebodies is that the Cu orebodies were formed syngenetically at the same time as the stratiform Pb-Zn-Ag ores, and that the silica-dolomite facies of the Urquhart Shale formed in a near-shore algal reef environment which was sheared and re-crystallised during later deformation. As for the McArthur River deposit, the mineralisation may have formed by ascending mineralising solutions along channelways – probably a fault zone – which were active during deposition of the sediments. The Cu mineralisation could have been precipitated nearest the source of the fluids, with Pb, Zn and Ag further away from it, as illustrated in Figs. 3.17 and 3.19. An alternative hypothesis, proposed by Swager (1985), considers a hydrothermal-epigenetic origin for the Cu mineralisation in the silica-dolomite, temporally separated from the stratiform Pb-Zn-Ag mineralisation. According to Swager (1985), the silica-dolomite was formed during hydrothermal replacement processes coeval with a D3 deformation event. On the basis of microstructural evidence three stages of alteration-mineralisation are recognised: (1) silicification and dolomite re-crystallisation; (2) dolomitisation; and (3) chalcopyrite + pyrite + quartz + chlorite deposition. Thus, in conclusion, it is possible that the Mt. Isa mineralisation resulted from two temporally distinct events. One, the stratiform Pb-Zn-Ag mineralisation, could have been formed during rifting by the movement of hydrothermal solutions activated by the high heat flow in the rift environment. The other, Cu and silica-dolomite, would be the result of a much later hydrothermal event connected with deformation and metamorphism.

13.7.2 The Sediment-Hosted Exhalative Massive Sulphide Deposits in the Namaqualand Metamorphic Complex, South Africa

Four major base metal sulphide deposits, Broken Hill, Black Mountain, Big Syncline – constituting the Aggeneys group – and Gamsberg are found in the Bushmanland subprovince of the Namaqua Metamorphic Complex (NMCʃ in the western Cape, South Africa (Fig. 13.14A). The Gamsberg deposit has been studied
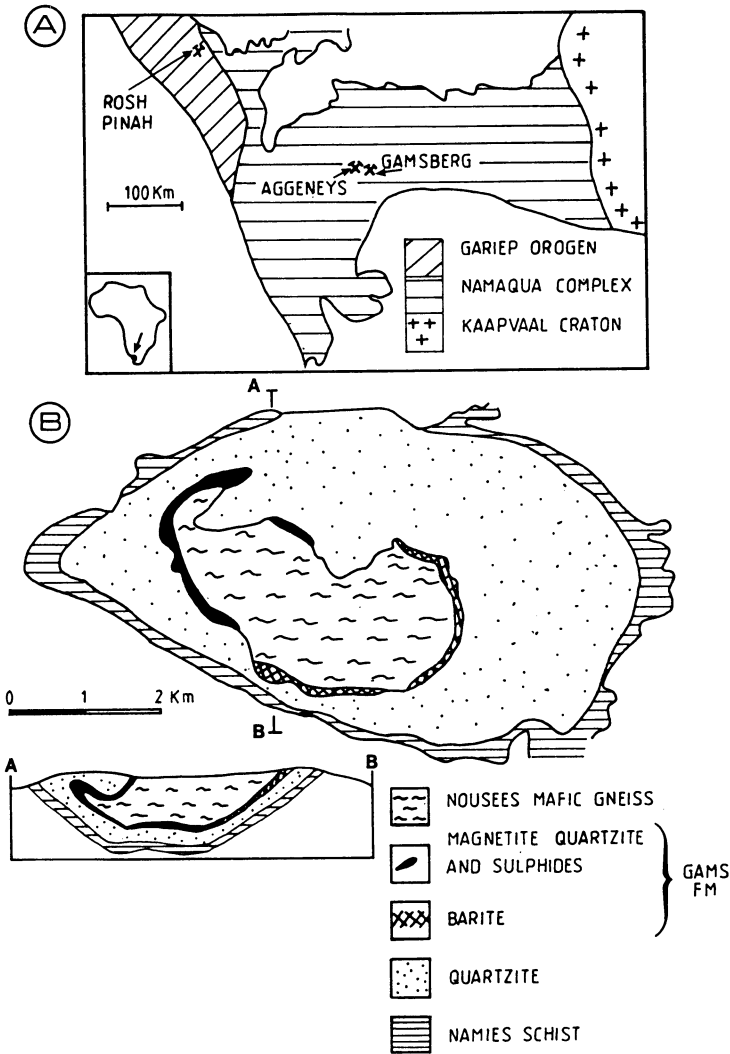
Fig. 13.14. A Location of the Aggeneys-Gamsberg deposits in the Namaqua Metamorphic Complex, South Africa. To the northwest is the Rosh Pinah deposit in the Pan African Gariep orogen, a continuation of the southern coastal arm of the Damara orogen (Namibia); this deposit is hosted by carbonate rocks and is thought to have formed in a rift environment similar to that of

by Rozendaal (1986), and details of the Aggeneys orebodies can be found in Ryan et al. (1986), McGregor (1986) and Smith (1986).

The NMC forms most of the crystalline basement of southwestern South Africa, with a complicated geological history that culminated with the Namaqua event at 1.3 to 1.1 Ga (Tankard et al. 1982). The NMC is constituted by an amalgamation of intensely deformed and high-grade metamorphic terranes, divided into a number of
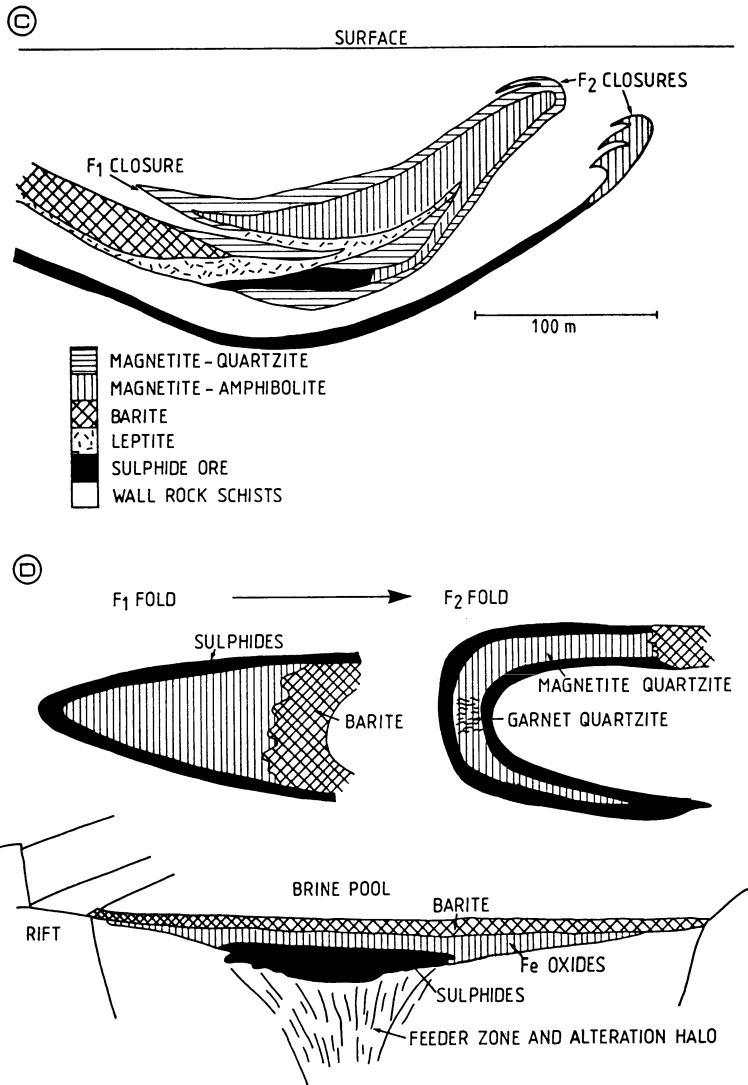
Aggeneys and Gamsberg. **B** Simplified geological map of the Gamsberg inselberg and section across the sulphide mineralisation (after Rozendaal (1986). **C** Schematic cross-section of the Black Mountain orebodies (Aggeneys). **D** A possible reconstruction of the Aggeneys mineralisation prior to F1 and F2 folding. **C** and **D** are after Ryan et al. (1986)

subprovinces, whose general characteristics can be found in Hartnady et al. (1985). In the area of the mineralisation, rocks of the Bushmanland sequence are exposed in a series of inselbergs, with the best section through the succession occurring at Gamsberg, the lithostratigraphy of which is given in Table 13.3.

The basal Haramoep Gneiss, informally known as Pink Gneiss, has an unknown precursor, although recent work appears to indicate that it may have had an acid

Table 13.3. Lithostratigraphy of the Bushmanland Group at Gamsberg (After Rozendaal 1986)

	Formation	Member	Lithology
Bushmanland	Nousees Mafic Gneiss		Amphibolite, quartz-feldspar-amphibole gneiss, pyroxene-plagioclase-quartz fels Quartz-muscovite schist, quartzite bands, conglomerate lenses, feldspathic schist
Group	Gams	C	Garnet-pyroxenoid rhythmite, pyroxenoid-amphibole-garnet-clinopyroxene rock, quartz-garnet-amphibole-magnetite rock, magnetite-hematite quartzite with inter-calated barite
		B	Mineralised quartz-sericite-sillimanite schist and quartz-grunerite-garnet rock
		A	Quartz-garnet-feldspar-clinopyroxene rock, carbonate-quartz-garnet-clinopyroxene marble, garnet-pyroxene-amphibole rock
	Pella Quartzite		Quartzite, conglomerate, quartz-biotite-muscovite-sillimanite schist, quartz-muscovite schist, massive milky quartzite
	Namies Schist		Quartz-biotite-muscovite-sillimanite schist, quartzite bands, sillimanite lenses
	Haramoep Gneiss		Pink granite-gneiss

volcanic parentage, and may perhaps have formed extensive ignimbrite sheets. On this basis, and together with other evidence, such as the bimodal composition of the gneissic rocks, the Bushmanland sequence is interpreted as a volcano-sedimentary sequence which was part of an evolving rifting system (Moore 1989; Willner et al. 1990). The Namies Schist and the Pella quartzite are interpreted as units of argillaceous and arenaceous sediments respectively (Rozendaal 1986). However, based on geochemical evidence, Willner et al. (1990) interpret the sillimanite and corundum-bearing rocks of the Namies schist as having originated from the metamorphism of Al-rich clays and hydroxides associated with unusual exhalative products enriched in B, F and P. The precursor rocks are therefore interpreted as belonging to high-Al hydrothermal alteration systems which preceded the metallif-erous event that gave rise to the sedex deposits of Aggeneys and Gamsberg. The Namies schist and Pella quartzite are overlain by the ore-bearing horizon, namely the Gams Formation. At the top of the sequence the Nousees Mafic Gneiss is interpreted as a unit of arenaceous sediments and basaltic lavas. Because of the isolated nature of the inselbergs, it is not possible to prove the correlation between the sequence at Gamsberg with that in the Aggeneys area. Such a correlation, however, is inferred, because of the massive sulphide deposits which are almost certainly genetically related, as indicated by the regional metal zonation (see later).

The Gams Formation is therefore regarded as the ore-bearing horizon at both Gamsberg and Aggeneys (Fig. 13.14B, C).

The Gams Formation is comprised of fine-grained pelitic and calcareous metasediments, characterised by a prominent banding and high concentration of Fe and Mn. At Gamsberg the Formation is divided into the A, B and C members (Table 13.3), which probably represent various facies of a precursor banded iron formation lithology. Thus, the A member may represent silicate and carbonate facies, the B member the sulphide facies and the C member a mixed silicate, oxide and carbonate facies. Barite occurs in the C member above the sulphide horizon and is currently mined as a small-scale operation on the east side of the Gamsberg structure (Fig. 13.14B). A discussion on the precursor lithologies of the metamorphosed rocks at Gamsberg and Aggeneys is given in Chapter 4 and summarised in Tables 4.6 and 4.7. Each of the base metal deposits is preserved in a synclinal fold structure, and in spite of intensive exploration work, the structural complexity of the local geology is still not completely understood. At Broken Hill, two orebodies merge together and are interpreted as being the two limbs of a single isoclinally folded unit, but the different Pb/Zn ratios in the upper and lower orebody indicate that this may not be the case. An alternative interpretation proposed by P. Smith (pers. comm. 1989) is that the two ore zones are two distinct sulphide deposits which were separated by an influx of clastic sediments. A greater concentration of Cu in the upper orebody suggests that the sequence is inverted. A possible reconstruction of the Aggenaeys mineralisation prior to deformation is illustrated in Fig. 13.14D.

In all four deposits the main sulphide minerals are chalcopyrite, sphalerite, galena, pyrite and pyrrhotite; other minerals present are marcasite, hematite, magnetite, ilmenite, graphite, barite and various silicates. There is a zonation from the Cu-rich Zn-poor Black Mountain deposit in the west, to the Zn-rich, Pb-poor Gamsberg deposit in the east, as is evident from the ore reserves and grade figures given in Table 13.4 and illustrated in Fig. 13.15. This zonation is interpreted by Rozendaal (1986) as being related to the distance from the source of the mineralising fluids. The nature of the ore ranges from undeformed, well-banded sulphides, to fine-grained sulphide breccias, to coarse-grained re-crystallised sulphides.

Gossans occur above all four deposits in the Aggeneys-Gamsberg area. They vary from an orange-brown jasperoidal material with well-developed boxworks to a black magnetite rubble with no signs of mineralisation. At Gamsberg the gossan

Table 13.4. In-situ ore reserves and grades of the Aggeneys and Gamsberg base metal deposit (After Rozendaal 1986; Ryan et al. 1986)

Deposit	Tonnage (10^6)	% Cu	% Pb	% Zn	g/t Ag
Black Mountain	82	0.75	2.67	0.59	29.8
Broken Hill	85	0.34	3.57	1.77	48.1
Big Syncline	101	0.04	1.01	2.45	12.9
Gamsberg	150	–	0.55	7.41	6.0
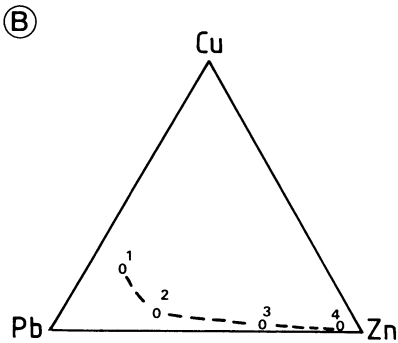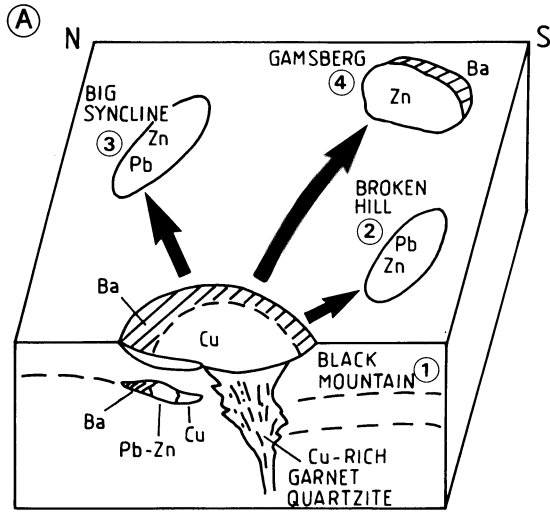
Fig. 13.15. A Schematic representation of the genesis and metal zoning of the Aggeneys-Gamsberg base metal sulphide deposits. The garnet-quartzite beneath Black Mountain is interpreted as an alteration zone around a channelway through which mineralising fluids ascended and discharged in a structural depression. Dispersion of fluids, shown by the *arrows*, resulted in sulphide and oxide accumulation in other structural depressions at increasing distances (Broken Hill, Big Syncline and Gamsberg) from the vent area (Black Mountain) (cf. Fig. 12.10). B Ternary plot showing relative proportions of metal contents for the Aggeneys-Gamsberg deposits (*numbers* correspond to those in A; refer also to Table 13.4)

contains up to 7.7% Pb and only 0.3% Zn, thus demonstrating the greater mobility of Zn in the oxidised environment.

Ore Genesis

The stratiform and banded nature of the orebodies, and the intimate association with the Fe formation, suggest that the mineralisation is of syngenetic origin. The Aggeneys-Gamsberg deposits are considered to be associated with an intracontinental rift environment, although Sawkins (1990) points out that they may also have formed on a passive continental margin. The ores form when hydrothermal solutions rich in Fe, Cu, Pb and Zn are introduced into the submarine environment. The physico-chemical changes that occur as the fluids discharge onto the sea floor result in the precipitation of base metal sulphides, as discussed in Chapter 12. The hydrothermal fluids are envisaged as either metal-rich brines developed from formation waters, or modified highly saline sea water. The heat source to drive the

hydrothermal system was probably related to the presence of rift-related magmas. The main channelway along which the hydrothermal fluids gained access to the region is thought to have been a regional fault. A possible channelway is believed to have passed near Black Mountain, because of the regional zonation referred to above, and the presence of a cross-cutting Cu-rich garnet-quartzite zone beneath the Black Mountain orebody. This zone has been interpreted as a hydrothermal alteration surrounding a feeder vent. The scenario envisaged is that fluids were introduced along this channelway and then dispersed across the sea floor away from the Black Mountain vent. The sulphides precipitated in local depressions on the seafloor, perhaps in the manner illustrated in Fig. 12.10A. The Cu/Pb/Zn ratios now reflect the distance of each depression from the vent area, thus explaining the lack of recognisable feeder channels, stockworks or alteration zones (Fig. 13.15).

Exploration

The exploration for sediment-hosted exhalative massive sulphide deposits of the NMC involves principally geophysical and geochemical methods. Airborne magnetic surveys are the chief regional exploration technique, as soil geochemistry is either ineffective or difficult to interpret, due to the cover of the Kalahari sands. The airborne survey is ideal for the detection of the Fe-rich horizons that host the massive sulphide mineralisation, and where magnetite-rich gossans are present they are easily located. The identification of a target area is followed by geochemical surveys which include detailed soil geochemistry and the analysis of the Fe-rich rocks with a view to discriminating between base metal gossans and barren ironstones. Structural mapping is also important in order to attempt to elucidate the structural complexities of the area and to determine the plunge direction of potential mineralised horizons.

13.7.3 Stratabound Cu-Ag Deposits of the Irumide Belt in Southern Africa

In southern Africa a number of Proterozoic tectonic provinces, or mobile belts, are situated between the Kalahari shield in the south and the Angola-Kasai shield in the north (Fig. 13.16). The ages of the Proterozoic mobile belts in Africa cluster around 1.9 Ga (Eburnian-Ubendian), 1.1 Ga (Kibaran/Irumide) and 0.6 Ga (Pan-African). The period from 1.4 to 0.9 Ga is one of great importance in Africa, during which the Kibaran and Irumide tectogens were formed and overprinted older mobile belts. The northeast-trending Irumide belt is a complex zone comprising basement, granite intrusions, clastic sequences and bimodal volcanics emplaced in fault-bounded grabens. The belt extends from southern-central Namibia, across northern Botswana to the northern margin of the Zimbabwean craton (Fig. 13.16), where it meets the Zambezi rift and is intersected by the Lufillian belt. The Botswana portion of the Irumide belt is covered by much younger rocks and its geology remains therefore speculative. The Irumides are best exposed, relatively undeformed and little metamorphosed in south-central Namibia, along the northwestern margin of the Kalahari craton. Recent studies and interpretations of the geological evolution
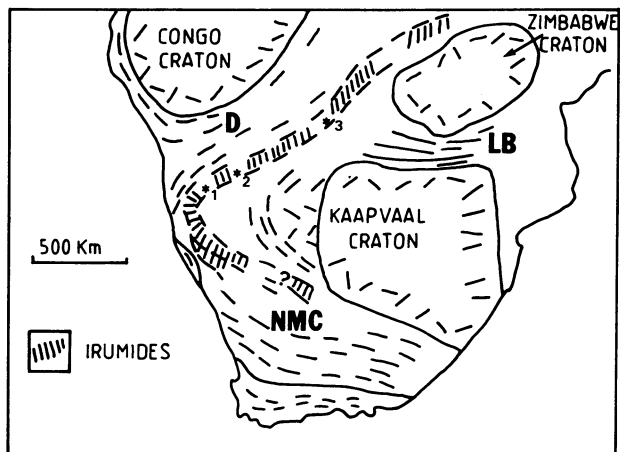
Fig. 13.16. Location of stratabound Cu-Ag deposits of the Irumide belt in southern Africa. *1* Klein Aub; *2* Witvlei; *3* Lake N'Gami. *LB* Limpopo Belt; *NMC* Namaqua Metamorphic Complex and Natal Belt; *D* Damara orogen (After Borg and Maiden 1987)

of the Namibian Irumide belt and its contained stratabound Cu-Ag deposit have been carried out by Borg and Maiden (1986, 1987) and Borg (1988), on whose works the following discussion is based.

The Irumide volcano-sedimentary sequences in Namibia and Botswana accumulated in a number of troughs or basins during the Mid-Late Proterozoic. Seven of these basins are the Koras, Sinclair, Klein Aub, Dordabis, Witvlei, Ghanzi and Lake N'Gami. The volcano-sedimentary sequences, which are typical of rift environments, rest on older basement of igneous and metamorphic rocks, and comprise bimodal volcanics of rhyolitic and basaltic compositions, conglomerates, sandstones, shales and carbonate rocks. Stratabound Cu-Ag mineral deposits occur in the Klein Aub, Dordabis, Witvlei and Lake N'Gami basins. Of relevance to the present discussion is the Klein Aub basin, near the town of Rehoboth, south of Windhoek. The volcano-sedimentary succession of the Klein Aub basin is approximately 11 km thick, comprising three main units: (1) acid extrusives with intercalated coarse clastic sediments; (2) basic extrusive and red beds; and (3) shallow marine deposits. The first unit comprises rhyolitic porphyry and pyroclastics, the nature of which suggests a caldera-type volcanism. The acid volcanics (Nuckopf Formation) are associated with lenses of continental coarse sediment (Grauwater Formation). The second unit unconformably overlies the first and comprises basic volcanic rocks and a thick sequence of coarse continental red beds (Doornpoort Formation). A change to marine conditions is indicated by rocks of the third unit, which include pyritic sandstone, shale and stromatolitic carbonate rocks (Klein Aub Formation); these rocks have been subjected to lower greenschist facies metamorphism and deformation, during the collisional phases of the Damara orogen to the north. The succession was folded and a well-developed slaty cleavage dips at 70° to the north-northwest. Mineralisation in the Klein Aub basin occurs as native Cu in the brecciated flow top of the basaltic lavas of the Doornpoort

Formation and in shear zones in hydrothermally altered lavas, and as stratabound disseminated Cu-Ag in pyritic sediments of the Klein Aub Formation.

The thermotectonic evolution of the Klein Aub basin, as worked out by Borg (1988), is of general interest because it offers insights in terms of rift tectonic evolution and related mineral deposits. Three phases have been recognised. In the first phase, crustal extension and thinning were accompanied by a high heat flow regime which caused partial melting of the lower crust. Felsic magmas were produced, resulting in high-level intrusions and extrusion of acid volcanics. This is a stage of block faulting and formation of grabens. During the second phase, the graben faults penetrated deep below the crust into the mantle, causing the upwelling and extrusion of basaltic lavas. Erosion of the uplifted faulted blocks supplied coarse clastic sediments which accumulated into narrow depressions. The third phase is characterised by thermal subsidence and a marine transgression. In other basins, lakes were formed during this subsidence. Low-energy sediments were deposited in these shallow waters in which bacterial activity resulted in the formation of pyritic shales and sandstones. In the regional context the Irumide grabens formed an extensive rift system (Koras-Sinclair-Ghanzi rifts) (Fig. 13.16) around the southwestern, western and northwestern margins of the Kalahari craton (Kaapvaal, Limpopo and Zimbabwe provinces). In Late Proterozoic times rifting shifted to the north, producing the Pan-African Damaran and Lufillian rift systems. This northward shift is interpreted by Borg (1988) as a possible southward movement of the African plate over a hot spot.

The Klein Aub Cu-Ag Deposit

The Klein Aub mine is located approximately 180 km south of Windhoek. In 1986 production was 19000 tonnes per month with an average head grade of 2% Cu and 40 g/t Ag, yielding 375 tonnes of Cu and 600 kg of Ag. Details of the geology of the Klein Aub deposit can be found in Ruxton (1986). The Klein Aub Formation, which is host to the Cu-Ag deposits, comprises a sequence about 3700 m thick, containing, from the base upward, conglomerate, red-brown quartzite, conglomerate with interbedded quartzite, shale, calcareous shale with lenses of limestone and fine-grained purplish quartzite. The Formation is separated by an unconformity from the underlying lithologies of the Doornpoort Formation. The Cu-bearing basaltic lavas of the Doornpoort Formation have been dated at approximately 1.1 Ga. The basement is block-faulted and in the vicinity of Klein Aub it forms a paleotopographic high, which supplied sediments into the fault-bounded Klein Aub basin. The stratigraphic column in the mine area is shown in Fig. 13.17A.

The stratabound mineralisation occurs in a number of stacked bands (Fig. 13.17B) in fine-grained, locally calcareous, laminated siltstone and argillites. Cross-bedded sandstone-siltstone units normally occur beneath the mineralised bands. A reverse oblique fault, with strike- and dip-slip components, truncates the mineralised bands downdip to the south. The fault is almost bedding-parallel and dips southwards slightly more steeply than the mineralised bands. Borg and Maiden (1987) recognise two types of mineralisation: one, which constitutes 60–70% of the ore, occurs along cleavage planes or bedding-plane fractures, the other occurs in a

A

(dotted)	FINE-GRAINED BROWN QUARTZITE		
(beads)	BRECCIA ZONE	KLEIN AUB FM	
(wavy)	QUARTZITE, ARGILLITE, LIMESTONE MINERALISATION (Cu-Ag)		SINCLAIR GROUP
(beads/dots)	CONGLOMERATE, QUARTZITE WITH BASALTIC HORIZONS	DOORNPOORT FM	
v v v v	ACID VOLCANICS	GRAUWATER FM	
+ + +	GRANITE AND GNEISS	BASEMENT	
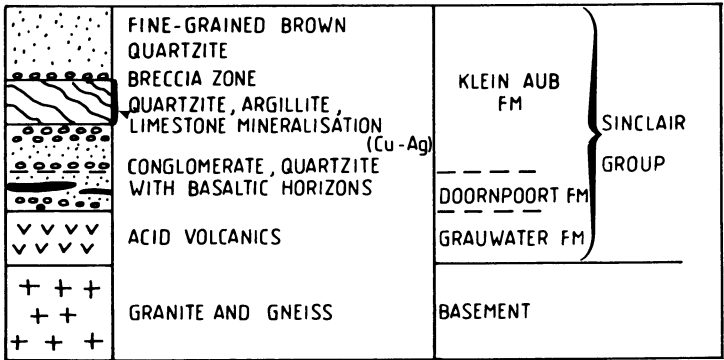
B
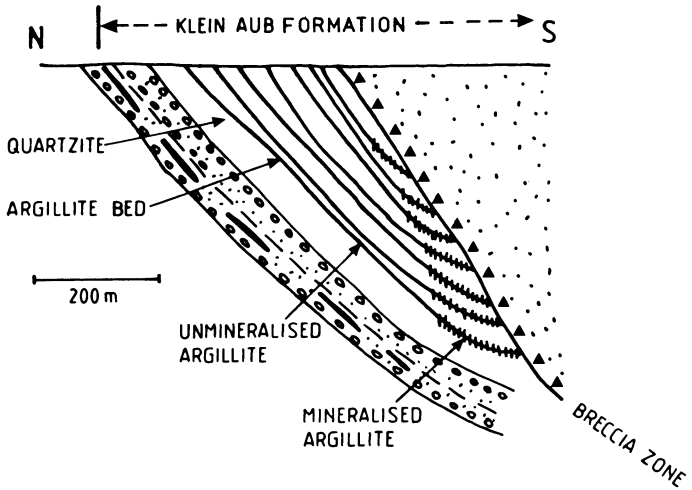
Fig. 13.17. A Schematic stratigraphic column for the area around Klein Aub; **B** schematic cross-section of the Klein Aub Formation showing relationship of mineralised argillite beds and a Breccia Zone, which marks the presence of a strike-slip fault

finely disseminated form in the host units. Tregoning (1977) also observed mineralised veins cutting across bedding planes at steep angles. Although the fault zone itself is not mineralised, it is noted that the tenors of the mineralised bands tend to decrease away from the fault. The main ore mineral is chalcocite; subordinate amounts of hematite, pyrite, chalcopyrite, bornite, digenite, covellite and rare native Cu are also present. Although there is a consistent raltionship between Cu and Ag, the mode of occurrence of Ag is not clear. Studies by Tregoning (1977) suggest that Ag may be contained in the lattice of the Cu minerals, or it may be associated with hematite.

Both syngenetic and epigenetic models have been proposed to explain the origin of the Klein Aub mineralisation. The former envisages the transport of Cu into the basin with synsedimentary precipitation caused by reducing conditions. The

stratabound and finely disseminated nature of some of the mineralisation is cited as evidence in favour of the syn-sedimentary origin. Tregoning (1977, 1987) proposes a syn-sedimentary origin with later remobilisation during deformation and metamorphism, which would account for the discordant mineralisation. However, these models fail to account for the decreasing tenors away from the fault. Borg and Maiden (1987), on the other hand, favour a multistage ore genesis involving leaching of Cu and other metals from the underlying basaltic lavas, which are locally mineralised with native Cu in the amygdales of the flow tops. These authors postulate four main stages. In the first there was extrusion of the basaltic lavas and sedimentation of red beds in an environment of basement uplift and block faulting. In the second stage a marine transgression took place, with the change from oxidising continental conditions to a reducing shallow marine environment. At this stage organic S would have formed diagenetic pyrite, and some syn-sedimentary Cu sulphides may also have formed. The third stage, which involved compaction and basin dewatering, resulted in the upward movement of fluids, which leached metals from basement rocks (also enriched in Cu and other metals, such as Au), red beds and basaltic rocks. The fluids would have precipitated Cu on contact with the S-bearing sediments. The final stage would have involved devolitilisation reactions during deformation and metamorphism, with the production of hot fluids. These fluids could have leached more Cu from the basaltic lavas, precipitating Cu in the pyritic beds. The hydrothermal alteration of the basalts is used as evidence that hydrothermal solutions interacted with them. The strike-slip fault provided the main channelway for the movement of the Cu-bearing fluids. This scenario is similar to that discussed in Chapter 3 for the Zambian Copperbelt, and for the stratabound Cu mineralisation of the Keweenawan rift, to be described later.

Grade control is carried out by chip sampling and by visual estimation through painting the ore zone with a cream-coloured paint that changes to shades of blue proportionally to the intensity of the Cu mineralisation.

13.7.4 The Zambian Copperbelt

The stratiform Cu deposits of the Zambian Copperbelt, together with the related mineralisation in neighbouring Zaire, form one of the great metallogenic provinces of the world, containing some 1.5×10^9 tonnes of ore averaging 3% Cu, with locally significant Co (Sawkins 1990). In 1974, eight major mines produced some 750 000 tonnes of copper concentrate making Zambia the fourth largest producer in the world. Most of the Cu mined in Zambia is located in well-defined sedimentary horizons of the Late Proterozoic Katanga Sequence which is part of the Lufillian fold belt (Fig. 13.18). A brief review of the geological history of this belt and its related mineralisation is given in Chapter 7, and models of hydrothermal systems that attempt to explain the genesis of the Copperbelt mineralisation are given in Chapter 3 and shown in Figs. 3.20 and 3.21. The stratiform Cu orebodies occur in 900-Ma-old sediments of the Lower Roan Group, Katanga Supergroup, unconformably overlying Archean granitic and gneissic basement rocks. The principal host rocks are euxinic argillaceous rocks, arkose and quartzite. The unconformity is
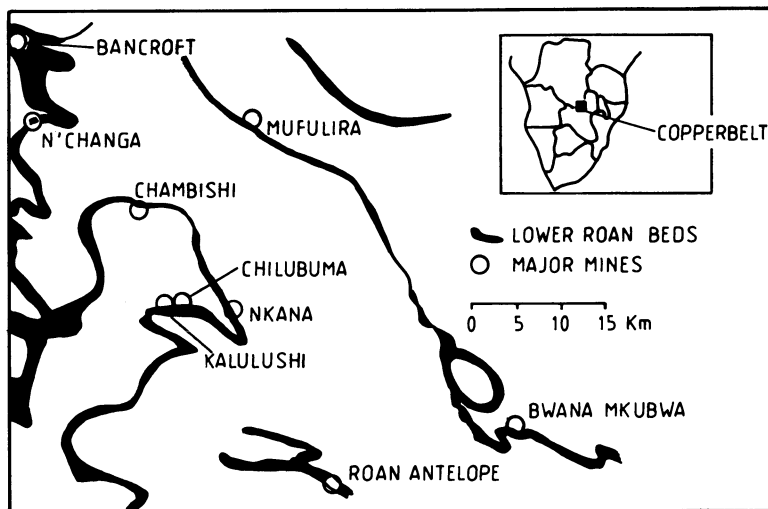
Fig. 13.18. Location of main orebodies of the Zambian Copperbelt (After Fleischer et al. 1976)

extremely irregular with hills and ridges of basement, and is marked by a basal conglomerate. Details of Copperbelt mineralisation can be found in the book edited by Mendelsohn (1961) and in Fleischer et al. (1976)

Arenite-Hosted Deposits

The Chibuluma arenite-hosted deposit lies on the south flank of the Chambishi-Nkama basin, and has reserves of approximately 22×10^6 tonnes at 4.7% Cu and 0.2% Co. The Lower Roan, from the base upwards, comprises: an extensively deformed basal conglomerate, up to 5 m thick, which flanks basement hills and gullies; aeolian feldspathic quartzite, 0–13 m thick, unconformably overlain by 3 to 15 m of arkosic sediments; the Ore Formation, up to 23 m thick, consisting of arkose overlain by feldspathic arenites; and the Hanging Wall Formation, consisting of arkose with interbedded argillite. The sequence is metamorphosed to greenschist facies but the rocks retain their sedimentary structures. The ore minerals are chalcopyrite, bornite, chalcocite, carollite and pyrite and follow the stratification of the host arenites. Vertical and lateral mineral zonations are present. From top to bottom the ore zone shows pyrite in albitic arenite to chalcopyrite-sericite arenite to Co-rich "sulphidite" (a term used to indicate beds exceptionally rich in sulphides). Laterally, from margin to centre, bornite and chalcopyrite occur in cross-bedded arkose, followed by chalcopyrite, carollite and pyrite in sericitic arkose and then pyritic feldspathic arenite.

The Mufulira mine opened in 1933, with initial reserves in the order of 280×10^6 tonnes at 3.5% Cu. The orebodies occur in three repeated sequences of the Lower Roan, which from the base upwards comprises: Foot Wall Formation, up to 150 m thick, consisting of a poorly developed boulder conglomerate, overlain by

feldspathic sandstone or greywacke, and characterised by a carbonate or anhydrite cement; the Ore Formation, 30 to 80 m thick, which is a sequence of three transgressive cycles of arenite-argillite-greywacke-dolomite-mottled sandstone, with the ore-bearing arenites containing fairly abundant anhydrite and dolomite; Hanging Wall Formation, 60 to 80 m thick, which is a sequence of anhydrite-rich argillaceous quartzite and dolomite. The mineralisation occurs in 21 distinct horizons, and ore minerals include chalcopyrite, bornite, pyrite, chalcocite and carollite. A mineral zonation is present: stratigraphically – from bottom upwards – chalcocite→ bornite→chalcopyrite→pyrite; and laterally, from low-grade pyrite-rich zones over basement highs, to chalcopyrite in the greywake, to high-grade chalcocite zones.

The arrangement of metal and sulphide zones appears to be related to the paleogeographic configuration as deduced from basement highs and the nature or facies of the host lithologies. In general from the paleoshore – oxygenated – towards deeper parts of the depositional basin – anoxic – sulphide zoning is: chalcocite→ bornite→chalcopyrite→pyrite. Models explaining the origin of this zonation are discussed in Chapter 3.

Shale-Hosted Deposits

Ore-shale deposits are confined to the west flank of the Kafue anticline. The Luanshya and the Rokana Cu-Co deposits are hosted mainly by shales. The Luanshya basin consists of an outlier of Katanga Sequence sediments folded into a synclinorium surrounded by basement rocks. The Lower Roan Foot Wall Formation consists of argillaceous feldspathic arenites, conglomerate, sandstone, arkose and argillite. The Ore Shale unit is also part of the Lower Roan Group, and contains nearly all the Cu mineralisation in the Luanshya basin. Initial reserves of the Luanshya deposits were in the order of 318×10^6 tonnes at approximately 2.8% Cu. The Ore Shale unit has a thickness ranging from 15 to 55 m. The Hanging Wall Formation consists of arkose and dark grey argillite. The orebodies comprise two Cu zones separated by a barren pyritic layer. Locally the mineralisation penetrates basement rocks, where the Ore Shale horizon rests directly on the underlying basement. Ore minerals are disseminated and include chalcocite, bornite, chalco-pyrite and pyrite. Covellite, digenite, carollite and pyrrhotite occur as accessory ore minerals. The gangue mineralogy, i.e. the components of the Ore Shale, are biotite, quartz, microcline and dolomite with minor quantities of calcite, chlorite, anhydrite, sericite, scapolite, tremolite and oligoclase. Mineral zoning, from near-paleoshore towards deeper basin environments, is chalcocite→bornite→chalco-pyrite→pyrite.

Mineral Exploration in the Copperbelt

Mineral exploration in the Copperbelt was at its peak during the 1960s and 1970s. Geochemical techniques – stream sediment sampling and soil sampling – were very successful in locating stratiform Cu mineralisation. In fact, some of the best case histories of classic geochemical exploration originated in the Copperbelt (Cornwall
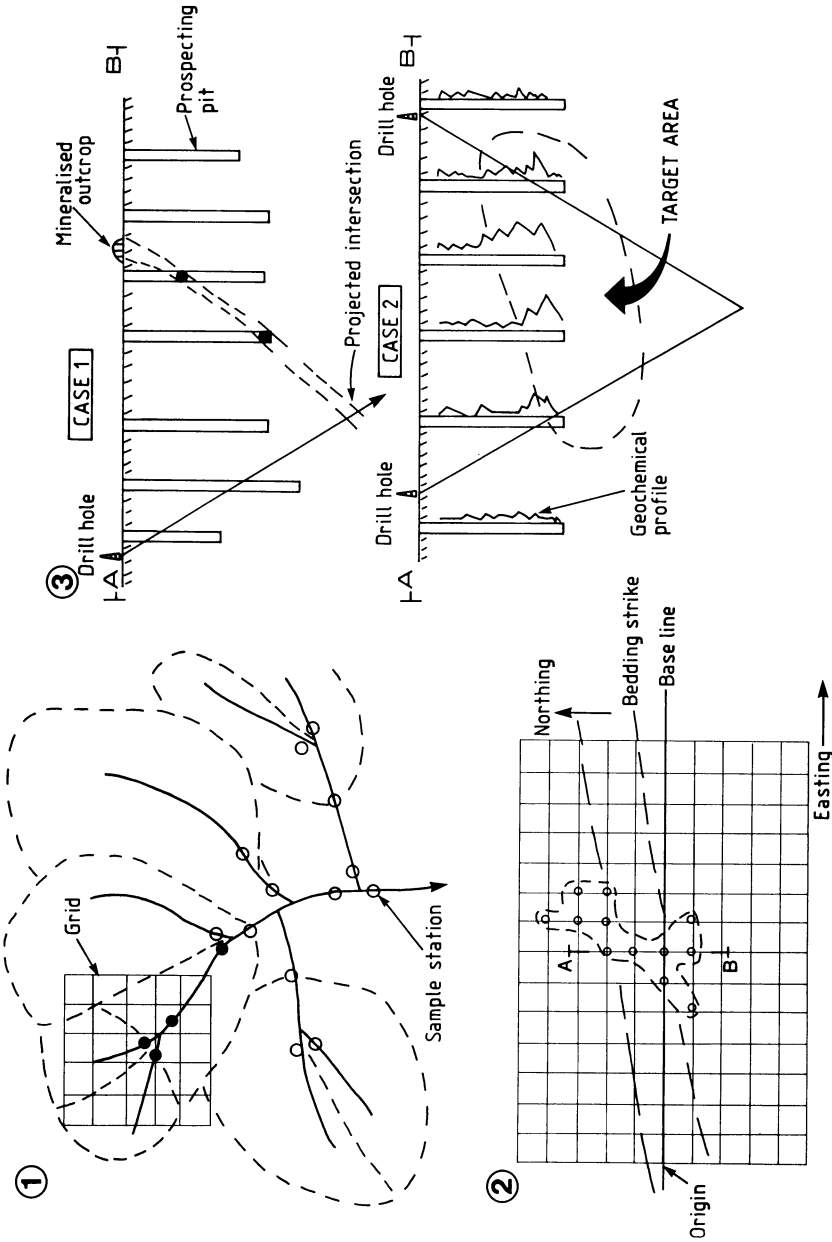
Fig. 13.19. Stages of Zambian Copperbelt-style mineral exploration. *1* Stream sediment sampling; *filled circles* indicate samples that returned anomalous metal values (i.e. Cu). *2* The area of interest is subsequently gridded and soil sampled. The soil-sampling grid is usually laid out so that sample lines run approximately at right angle to the regional strike. In *2* the *dashed line* indicates anomalous Cu contour. *3* Prospecting pits are excavated through the soil overburden to bedrock. In *case 1* the mineralised zone is detected in the pits and its down-dip projection tested by drilling. *In case 2* the soil overburden is deep and the pits do not reach to bedrock. Geochemical channel sampling is carried out and Cu values plotted along each pit; in this way, a target area may be delineated where geochemical values are greater, and later tested by drilling. Drawings are not to scale, but depth of pit may reach 25–35 m

1961; Rose et al. 1979, p.382–416), which provided ideal climatic, topographic and drainage conditions. Geological mapping – usually conducted in conjunction with the geochemical surveys – would be carried out, on a regional scale, during stream sediment sampling, while, along grid lines on a more detailed basis, during soil sampling. Both stream sediments and samples of soil – taken from the B-horizon – were sieved to minus 80 mesh and the minus fraction submitted for Cu analyses, which, before the advent of the Atomic Absorption Spectrometer (AAS), were commonly carried out in field-based laboratories by the colorimetric method. Lines of pits and/or trenches would be excavated across the anomalies in order to reach the C-zone or fresh bedrock. Pits and trenches were geologically logged and channel samples taken in order to determine the attitude and approximate Cu content of the ore horizon. Diamond drilling would follow to intersect the mineralised horizon below the zone of oxidation. Figure 13.19 illustrates the steps followed during an exploration programme in the Zambian Copperbelt.

13.7.5 Stratiform and Stratabound Cu Deposits of the Keweenawan Rift

The North American craton has a number of important Mid- to Late Proterozoic rift structures which host stratabound and stratiform base metal mineralisation. On the western margin of the North American cratonic area, rift structures with thick sedimentary and volcanic sequences have approximately east-west trends and host the Sullivan Pb-Zn deposit in British Columbia, and the Coppermine Cu deposit in the North West Territory (Canada). On the eastern side of the continent is a combined major gravity and magnetic anomaly which has been interpreted to represent a 600-km-wide rift zone, extending approximately 1600 km from Lake Superior to Kansas, and known as the Mid-Continent Rift System, or Keweenawan rift (Keller et al. 1983). The Keweenawan rift is filled by a succession of tholeiitic flood basalts, approximately 1600 m thick, with minor cogenetic rhyolitic and gabbroic intrusives and interbedded continental sandstone and shales. The Duluth intrusive complex, contemporaneous with the lavas, is emplaced along the unconformity at the base of the Keweenawan sequence.

In the Lake Superior region the Keweenawan rift hosts a number of mineral deposits which cover a wide spectrum from pre-early-rifting mineralisation, including Nb-U-REE and Cu-Mo porphyry types, associated with alkali and felsic intrusive complexes, to syn-late rifting stratiform and stratabound Cu mineralisation. A review of the mineral deposits of the Lake Superior region can be found in Sims (1976) and Norman (1978). Stratiform Cu mineralisation is hosted by carbonaceous shale horizons, deposited above thick piles of tholeiitic volcanic lavas, which in turn host stratabound Cu mineralisation. The White Pine Cu deposit is located near the southern shore of Lake Superior in northern Michigan, on the southeastern margin of the Keweenawan rift. Native Cu in amygdaloidal lavas was exploited by the Indians prior to recent mining, and in the late 19th and early 20th centuries mining operations exploited sandstone-hosted native Cu and Ag deposits. In 1921 operations ceased due to the apparent exhaustion of reserves, although the presence of disseminated Cu mineralisation had been detected but its significance

not realised. It was not until 1942 that the economic importance of the shale-hosted disseminated Cu mineralisation was appreciated.

The Keweenawan Group includes a Lower sedimentary sequence, a Middle volcanic sequence and an Upper sedimentary sequence. The stratigraphy of the latter two sequences consists of the Portage Lake Formation, the Copper Harbour Formation, the Nonesuch Shale Formation and the Freida Sandstone Formation. The Portage Lake Formation includes the thick sequence of flood basalts, locally overlain by rhyolitic lavas and pyroclastics. In the Porcupine mountains a volcanic centre gave rise to a thick pile of rhyolites, 15–20 km in diameter and about 1 km thick. The volcanics are interbedded with lenses of conglomerate and sandstone. Cu mineralisation occurs locally at the top of the Formation as native Cu in amygdales, within brecciated tops of the lava flows, or in quartz-carbonate veins and in breccias. The Copper Harbour Formation consists of 100 to 2000 m of grey-brown sandstone, conglomerate and siltstone. Native Cu is present in the conglomerate beds. In the White Pine area Cu mineralisation is confined to the basal sections (Parting Shale Member) of the Nonesuch Shale Formation. This Formation is approximately 180 m thick and consists of interbedded reddish, greenish and carbonaceous shale and siltstone, which grade laterally into sandstone units. There appears to be a correlation between the carbon content of the shales and the mineralisation, the highest grades being associated with the darkest sediments. The principal ore minerals are chalcocite, pyrite, native Cu, bornite, chalcopyrite and native Ag. Lesser amounts of covellite, digenite, sphalerite and galena also occur. Chalcocite is the main ore mineral and occurs as fine disseminations in shale and siltstone. Chalcocite also occurs in zoned ellipsoidal structures elongated in the bedding plane. These ellipsoidal structures have a core of hematite surrounded by chalcocite, followed by an outer zone of hematite. Native Cu which is locally abundant occurs in association with chalcocite.

There is a broad vertical and lateral zonation (Brown 1971, 1979). The vertical zoning, as postulated by Brown (1971, 1979), is characterised by a lower native Cu subzone in the clastic units of the Copper Harbour Formation. This zone changes abruptly upwards into a chalcocite-native Cu subzone in the Nonesuch Shale, followed by a chalcocite subzone which is in turn overlain by an extensive pyritic zone. On a regional scale, however, the mineralisation and zoning patterns appear to be transgressive to the bedding, even though in detail the mineralisation is confined to certain stratigraphic horizons. The top of the cupriferous zone varies laterally across the ore deposit, reaching a maximun height at the intersection of the White Pine fault with a sandstone paleohigh. There is an inverse relationship between the height of the top of the cupriferous zone and the concentration of Cu in the mineralised zone, and the Cu grades tend to decrease away from the White Pine fault, suggesting that the Fault acted as the main channel for Cu-bearing hydrothermal solutions.

According to Brown (1979), the genesis of the Keweenawan Cu deposits is due to the action of chloride-rich brines of various origins (basinal brines and/or magmatic ?) which leached metals from the basement rocks and the basaltic lavas, containing an average 120 ppm Cu. In their movement, the fluids encountered suitable conditions for the deposition of native Cu and chalcocite in the porous amygdaloi-

dal tops of the lava flows and in the reducing environments of the overlying sedimentary rocks. There are many similarities with the stratabound Cu deposits of the Irumide belt in Africa. The genetic model proposed by Borg and Maiden (1987) for Klein Aub could well be applicable to the stratabound Cu in the Keweenawan rift.

13.8 Mineral Deposits Related to Advanced Stages of Rifting – the Red Sea Deeps

Chapter 3 (Figs. 3.22 and 3.23) makes mention of the nature and geometry of the hydrothermal systems which are active today in the axial zone of the Red Sea rift. In this section we examine the hydrothermal deposit of the Atlantis II Deep, which has been extensively reported in the literature (Bischoff 1969; Degens and Ross 1969; Shanks and Bischoff 1977, 1980; Pottorf and Barnes 1983; Zierenberg and Shanks 1988). Details on the geological and tectonic evolution of the Red Sea rift system may be found in McKenzie et al. (1979), Gass (1979), Bonatti (1985), Bayer et al. (1989) and Bohannon (1989).

The Red Sea represents an ocean basin in its early stage of development. Spreading in the Gulf of Aden commenced in the Early Cretaceous and resulted in north-northwest movement of the Arabian shield. Left-lateral movement along the existing Red Sea-Suez fault system allowed the separation of Africa from the Arabian peninsula. The Red Sea extends for approximately 2000 km, along a north-northwest to south-southeast direction, cutting across Precambrian terranes of the African and Arabian plates to a triple junction, represented by the Gulf of Aden and the Afar depression (see Fig. 3.23). The Red Sea rift is bordered by uplifted margins of the Precambrian terranes, reaching up to 2000 m in elevation. The rift started its development during Early-Mid Eocene, by continental thinning above a mantle plume or a hot spot. The main graben-like structures, however, were developed in the early Miocene, which Bonhannon (1989) proposes to have taken place through crustal breakup on large detachment faults.

The Red Sea area is characterised by three main types of volcanism: alkaline, peralkaline and tholeiitic. Alkaline and peralkaline volcanism occurred mainly during the early phases of doming, uplift and rifting, and on land forms "the Trap series", which extends over an area of some 700000 km^2 and reaches a thickness of 3 km. The distribution of the volcanic rocks is somewhat asymmetric with respect to the rift axis, being concentrated on the Arabian side and in the Afar region. The reason for this asymmetry is explained by a shallower asthenosphere beneath the Arabian plate (Bayer et al. 1989). From the axial zone, broad flank areas on either side are covered by clastic graben sediments, evaporites and interbedded marine sediments of Miocene age. As previously mentioned, the Red Sea basin is subdivided, on the basis of sea-floor morphology and the nature of its crust, into northern, transitional, multi-deep and rift-valley regions. Oceanic crust is present in the latter region, the rest being underlain by transitional and thinned continental crust (Bonatti 1985). This, combined with the history of
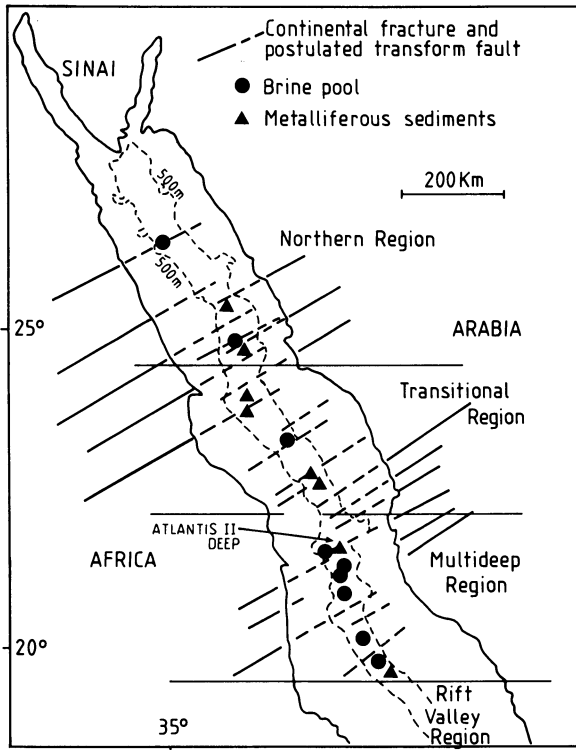
Fig. 13.20. Northern and central Red Sea with location of brine pools and metalliferous sediments. The pools are localised along the intersection of the rift valley with continental fracture lines and their possible continuation as transform faults (After Bignell 1975, in Sawkins 1990); subdivisions of Northern to Rift Valley regions are after Bonatti (1985)

sedimentation and volcanism, suggests propagation of the Red Sea rift in a northerly direction.

Most of the active geothermal brine pools are located at the intersection of transform faults and the axial zone of the rift. Some base metal deposits occur on shore and are probably situated along the on-land continuation of these transform faults (Fig. 13.20). Not all depressions or pools contain metal-rich sediments, but all are filled with brines. The brines exhibit considerable variations in their chemistry, temperature, and the mineralogy of the metalliferous sediments. Bischoff (1969) reported in detail the results of studies of the Red Sea hot brines and associated metal-rich sediments. Of the numerous hot brine pools discovered, the Atlantis II Deep is the only one with economic potential and is also the best studied. Ore reserves are given in Chapter 3 (Sect. 3.6.2). The Deep, located at approximately 21.5° N and 38° E longitude, is characterised by an upper and lower brine and variable thicknesses of metalliferous muds (see Chap. 3). A generalised cross-section of the Atlantis II Deep is shown in Fig. 13.21.

The metalliferous sediments in the Atlantis II pool are approximately 20–25 m thick, finely banded and brightly coloured. Bischoff (1969) recognised a number of facies: detrital, carbonate, Fe-montmorillonite, goethite, sulphide, manganosiderite and anhydrite. Pottorf and Barnes (1983) divide the metalliferous sediments into five lithostratigraphic facies: detrital-oxide-pyrite, lower sulphide
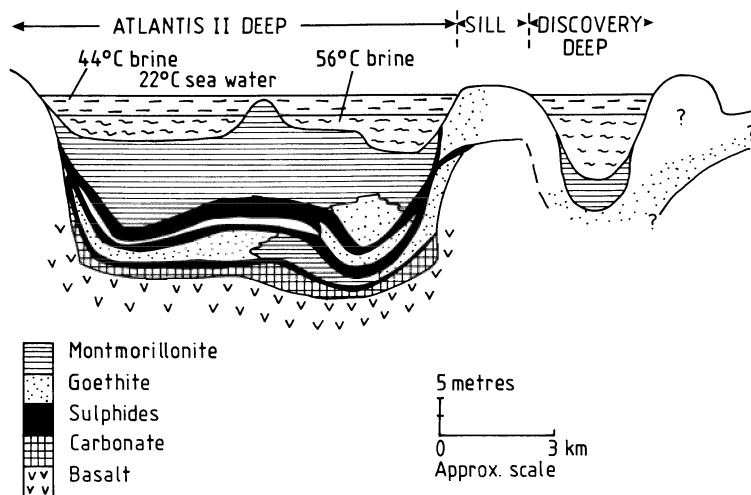
Fig. 13.21. Schematic cross-section of Atlantis II Deep (After Bischoff 1969; Sawkins 1990)

zone, central oxide zone, upper sulphide zone and the currently precipitating amorphous siliceous zone.

The floor of the metalliferous muds is formed by basaltic rocks. A basal detrital facies consists of unstratified and unconsolidated carbonate-rich sediment, approximately 2 m thick. Here sedimentation started about 28 000 years ago, and on top of this zone an aragonite-pteropod zone is recognised to be 13 000 years old. The main mineral is biogenic calcite with detrital quartz, feldspar and clay. Fossils are present and are represented by formaninifera and pteropods. Carbonate facies material consists of coarse, crystalline, buff-coloured rhodocrosite, manganosiderite, siderite with quartz, feldspar and halite. These carbonates may have formed by the replacement of the detrital carbonate by Fe and Mn. The sulphide facies consist of black homogeneous material, including mainly sphalerite, lesser chalcopyrite galena and pyrite and locally barite and anhydrite. The sulphide beds are rich in Fe, Cu, Zn, Cd, Pb, Au, Ag and Hg. There are at least three sulphide layers: a lower layer about 10 cm thick, a middle layer (50 cm) and an upper layer (2 m). The goethite facies can reach a thickness of 4 m and occurs between sulphide layers. The main mineral components are poorly crystalline goethite and amorphous limonite. It appears that the amorphous limonite is precipitated from the brines and form goethite on dehydration. The goethite layers are rich in Fe and Zn. Lepidocrocite and hematite are often mixed with goethite, whereas black crystalline magnetite is locally present. The Fe-montmorillonite facies, while representing the uppermost layer, is also present between the middle and upper sulphide zones. The Fe-montmorillonite layer varies in thickness from 12 to 15 m, is dark brown, finely bedded mud and consists of up to 90–96% by weight of interstitial brine. There is also minor sphalerite, goethite and manganosiderite. The anhydrite, or sulphate facies, is mainly developed as white massive beds of anhydrite up to 20 cm thick within the

Fe-montmorillonite and the sulphide facies. Locally present in the goethite facies are beds (15–50 cm thick) of manganite, which in places are associated with todorokite.

Both syngenetic and epigenetic types of mineralisation are present. Syngenetic mineralisation forms the main part of the basin with its bedded, laminated varicoloured metalliferous muds. Epigenetic mineralisation occurs in the southwestern part of the Deep and is represented by fissures filled with anhydrite, talc, smectite, pyrite, sphalerite and chalcopyrite. As outlined in Chapter 3, it is postulated that the origin of the Red Sea mineralisation is caused by sea water, which descends through fractures in the thick Miocene evaporites, becoming highly saline. These brines are then heated in the axial zone, leaching metals from the basaltic crust. The heated brine is convected upwards and starts cooling; metals are probably carried by chloride complexes, rather than sulphide complexes, because, it is thought, large amounts of Fe may preclude sulphide complexing (Pottorf and Barnes 1983). On the basis of thermodynamic data, precipitation of sulphides appears to occur at about 250°C. Precipitation of sulphides occurs in the lower parts of the pool, whilst Fe and Mn oxides are precipitated in the upper parts of the brine pool due to a more oxidised environment and mixing with normal sea water. The source of S is believed to be from reduction of sulphate. Shanks and Bischoff (1980) propose that sulphide deposition takes place during periods of maximum influx of the brines, so that the contrast in the composition of the various facies may be the result of variation in the rate of brine discharge and the rate of mixing with Red Sea bottom waters. In contrast to the brine pools, the hydrothermal fluids in the southwestern areas, where epigenetic mineralisation is formed, have salinities near that of sea water. The ore fluids in this case are not ponded in depressions, but the resulting mineralisation occurs as veins and chimney constructs and not as stratiform accumulations. The epigenetic mineralisation is dominated by sulphides, which is explained by higher temperatures of the discharging fluids. The epigenetic deposits are considered to be the proximal, while the stratiform syngenetic mineralisation would be the distal facies of the mineralising system (see Fig. 3.17 for a possible model).

13.9 Banded Iron Formations (BIF) of Proterozoic Age

The Proterozoic Banded Iron Formations (BIF) – such as those of the Transvaal-Griqualand West basin in South Africa, Lake Superior in North America, the Hamersley basin in Western Australia, Minas Gerais in Brazil, and the Aldan region in Siberia – are thought to have formed in shelf environments of rift-controlled basins along the margins of cratonic areas. The Proterozoic BIF are known as Superior type (from the BIF of Lake Superior) to distinguish them from BIF of Archean age, which are volcanic-associated and known as Algoma type. The latter type occurs at the end of mafic to felsic volcanic cycles and probably represents phases of exhalative activity related to the volcanism.

Various ideas on the origin of BIF are discussed in Chapter 5, and for the present purpose we adopt the views of Gross (1980, 1983), who regards BIF as chemically precipitated metalliferous sediments. Button (1976, 1981) considers the BIF in the context of basin geology and related mineral deposits. An issue of Economic Geology (1973) is devoted to BIF.

BIF are thinly bedded or laminated rocks containing at least 15% Fe, formed by alternating Fe-rich and quartz or chert-rich layers, bands or laminae, which in some instances can be correlated across hundreds of kilometres. BIF therefore contain quartz, magnetite, hematite, stilpnomelane, minnesotaite, riebeckite, grunerite, greenalite, carbonates (siderite, ankerite, ferrodolomite etc.) and sulphides (pyrrhotite, pyrite), usually occurring as monomineralic layers. Stilpnomelane may have originated from a precursor mineral derived from alteration of volcanic glass, as for example montmorillonite; magnetite could have originated from hematite through diagenetic processes, whereas riebeckite is thought to have derived from Na^+ metasomatism of the BIF (Button 1976).

13.9.1 The Mineral Deposits of the Transvaal-Griqualand Basins

The Transvaal Sequence is preserved in two structural subbasins: the Transvaal province in the east (Bushveld subbasin of Button 1981), forming the Transvaal Supergroup, and the Griqualand province in the west (Cape-Botswana subbasin of Button 1981), forming the Griqualand West Supergroup (Fig. 13.22). Details of the stratigraphy of these subbasins can be found in Button (1981, 1986) and Beukes (1986). The development of the Transvaal and Griqualand basins, which occurred between 2.4 and 2.1 Ga, comprise sedimentary successions subdivided into a lower volcanic and clastic units (Wolkberg and Campbell Groups, Transvaal and Griqualand respectively), a chemical sedimentary sequence (Chuniespoort and Griquatown Groups), and an upper clastic sequence (Pretoria and Posmasburg-Olifantshoek Groups). BIF and associated chemical sediments, such as chert, overlie carbonate rocks and occur at or near the top of the Chuniespoort and Griquatown Groups. It is important to note that late in the history of the Chuniespoort and Griquatown Groups, the southeastern margin of the Transvaal basin was uplifted and terrigenous clastic sediments prograded over the BIF. The sea retreated off the Kaapvaal craton and uplift with a major erosional period followed. The important consequence of this hiatus was the development of a karst topography by chemical weathering of the dolomites, resulting in the formation of supergene Fe and Mn enrichments.

A wide variety of mineral deposits are present in the Transvaal-Griqualand West basin. The most important include Fe and Mn, fluorite, Pb-Zn, crocidolite asbestos and Au in hydrothermal quartz veins. Button (1976) classified the Transvaal deposits into: (a) syngenetic chemical deposits (Mn in BIF, Kalahari field); (b) diagenetic and load metamorphic (crocidolite asbestos, Kuruman deposits); (c) metamorphic deposits (chrysotile asbestos); (d) supergene deposits (Mn in dolomite host, Mn in shale, hematite enrichment in BIF, Posmasburg-Sishen Fe and Mn fields); (e) low-temperature, carbonate-hosted hydrothermal
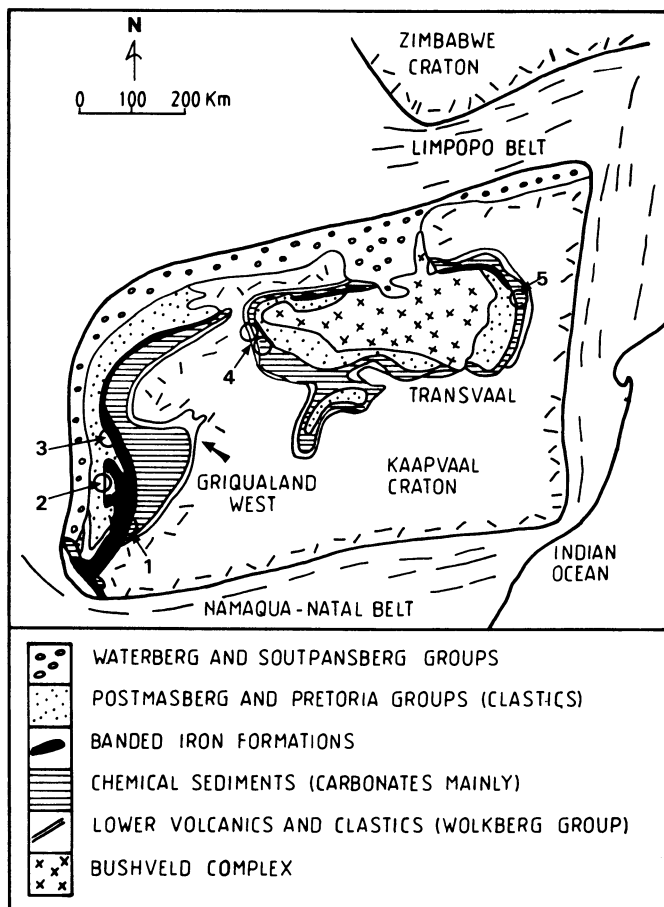
Fig. 13.22. Generalised stratigraphic and tectonic setting of the Transvaal and Griqualand West basins, showing distribution of BIF (Penge Iron Formation) and some major mineral deposits. *1* Pering Pb-Zn; *2* Western and Eastern Manganese belts; *3* Kalahari Manganese Field; *4* Zeerust Pb-Zn-F mineralisation in carbonate rocks; *5* Pilgrim's Rest-Sabi Au in hydrothermal quartz veins. See Fig. 13.16 for location of Kaapvaal craton in southern Africa

Pb-Zn and F; and (f) high-temperature hydrothermal Au in quartz vein lodes (Pilgrims Rest-Sabi goldfield). Except for the BIF and the syngenetic Mn mineralisation in (a), all other mineral deposits were formed during diagenetic, metamorphic and hydrothermal processes well after sedimentation had ceased. In this section we examine in some detail the Mn mineralisation of the Kalahari Field.

The Kalahari Mn Field

The Kalahari Mn field occurs about 100 km north of the Posmasburg Fe and Mn fields (see Fig. 13.22). Reserves stand at approximately 6×10^9 tonnes of ore at

greater than 28% Mn, making this field one of the world's largest resources of Mn. The field is entirely covered by Kalahari sand, except for one isolated outcrop of chemical sediments at Black Water (Voelwater Jasper, which overlies lavas of the Ongeluk Formation). The succession consists of dolomitic rocks overlain by a 450-m thick sequence of BIF and mudstone jasper (Asbesheuwels and Koegas subgroups respectively), overlain in turn by the Ongeluk volcanics. Above these lithologies is the Voelwater Formation, locally known as the Hotazel Formation, which is a well-developed BIF unit in which Mn occurs as three conformable layers. The major structural feature of the area is the Dimoten Syncline, and the orebodies are situated in the middle of this structure. There are three main mines: Wessels (underground), Hotazel and Mamatwan (open pits).

At Wessels all three Mn-bearing layers are present; at Hotazel the middle layer is discontinuous, whereas it is absent altogether at Mamatwan. The ore is finely laminated and composed of dull black semi- to non-crystalline braunite. Two types of braunite occur: braunite I ($3Mn_2O_3.MnSiO_3$) and braunite II [($7Mn.Fe)_2O_3.CaSiO_3$]. Other ore minerals include hausmanite (Mn_3O_4) and jacobsite ($MnO.Fe_2O_3$). The ore, in places, has small spherical accretions, interpreted as ooliths, which may be dolomitic in compositions but are replaced by Mn. Within the orebodies are thin (less than 1 cm) and regular hematite layers, and one of these layers is used by mine geologists as a grade line in the lower orebody. Best grades are in the basal parts of the lower and upper orebodies, although secondary enrichment occurs close to faults. Primary braunite I changes to braunite II as a fault is approached, and hausmanite is best developed next to the fault. These mineralogical changes are accompanied by concomitant changes in grade, which in places may increase by as much as 7%, to higher than 50% Mn, over a distance of a few metres. This fault-controlled epigenetic upgrading of the orebodies is particularly important at the structurally more complex Wessels mine, where up to three periods of faulting are present. There appears to be no correlation, however, between grade and any particular set of faults. South of Wessels the orebodies are of lower grade, but they come closer to the surface and therefore are amenable to open-cast mining as at Mamatwan and Hotazel. Supergene enrichment resulted in the development of secondary Mn minerals such as cryptomelane [$(K.H_2O)_2Mn_5O_{10}$] and todokorite [$(Mn,Ca,Mg)-Mn_3O_7.H_2O$]. Two bostonite dykes occur at Wessels, and one at Hotazel, but the only observed effect on the orebodies is the development of a narrow aureole of jacobsite around one of the dykes at Wessels. Locally, there are zones of skarn assemblages, which are attributed to burial metamorphism, and are characterised by sugilite (an attractive purple-coloured mineral, $(K,Na)(H_2O,Na)_2-(Fe^{3+},Na,Ti,Fe^{2+})_2(Li,Al,Fe^{3+})_3(Si_{12}O_{30})$, andradite, wollastonite, pectolite, vesuvianite and quartz.

The genesis of the Mn ore is thought to be the result of sedimentation of oolitic carbonate in a matrix of gelatinous Mn and Fe hydroxides and carbonates, and locally, hydrous silicates of Mg and Fe. The limits of the known Mn field presumably represent a part of the Griqualand West basin, in which conditions were conducive to the precipitation of Mn rather than Fe. Precisely what these conditions were and what caused them is not understood. During diagenesis,

crystallisation of the manganiferous gel formed braunite I, rhodocrosite, jacobsite and pyrolusite. At a later stage, perhaps during burial metamorphism, minerals like braunite II, hausmanite and those of the skarn assemblages were formed. Nevertheless, in order to form the economic Mn orebodies, it is believed that some form of enrichment (hypogene or supergene?) must have taken place. If a manganiferous gel did exist, then it is implied that a colloidal solution must have been active. The source of so much Mn is also problematical. It has been suggested that the source of both the Mn and Fe of the Voelwater Formation may, in some way, be connected with the underlying Ongeluk andesitic lavas, perhaps through fumarolic discharge. Beukes et al. (1982) draw attention to the association of the Mn deposits with jaspers and pillow lavas. They also point to the presence of hematite in hyaloclastites as being indicative of fumarolic-derived ferrous Fe, which was then rapidly oxidised and precipitated in proximity of the volcanic source. Divalent Mn ions, on the other hand, take much longer to oxidise than ferrous Fe, and are therefore deposited distally from the volcanic source.

References

Bahnemann K P (1986) A review of the geology of the Messina copper deposits, Northern Transvaal. In: Anhaeusser CR and Maske S (eds) Mineral deposits of Southern Africa, vol 2. Geol Soc S Afr, pp 1671–1688

Bailey D K (1978) Continental rifting and mantle degassing. In: Neumann E R, Ramberg I B (eds) Petrology and geochemistry of continental rifts. Proc NATO Adv Stud Inst. Reidel, Dordrecht, pp 1–14

Bailey D K (1983) The chemical and thermal evolution of rifts. Tectonophysics 94:585–598

Bailey D K (1984) Kimberlite: "the mantle sample" formed by ultrametasomatism. In: Kornprobst J (ed) Kimberlites and related rocks. Developments in petrology 11A. Elsevier, Amsterdam, pp 232–333

Bailey D K (1987) Mantle metasomatism – perspective and prospect In: Fitton J G, Upton B G J (eds) Alkaline Igneous Rocks. Geol Soc Spec Publ 30:1–14

Baker B H (1987) Outline of the petrology of the Kenya rift alkaline province. In: Fitton J G, Upton B G J (eds) Alkaline igneous rocks. Geol Soc Spec Publ 30:293–312

Bally A W, Snelson S (1980) Realms of subsidence. Can Soc Pet Geol Mem 6:9–94

Barberi F, Varet J (1978) The Afar rift junction. In: Neumann E R, Ramberg I B (eds) Petrology and geochemistry of continental rifts. Proc NATO Adv Stud Inst. Reidel, Dordrecht, pp 55–70

Barton J M, Roering C, Barton E S, Allsop H L, Van Reenen D D, Smit C A (1986) The Late Archean-Late Proterozoic evolution of the Kaapvaal craton and its possible relationships to the Witwatersrand basin. In: Abstr Geocongress '86 Johannesburg. Geol Soc S Afr, pp 15–18

Bayer H J, El-Isa Z, Hotzl H, Mechie J, Prodehil C, Saffarini G (1989) Large tectonic and lithospheric structures of the Red Sea region. J Afr Earth Sci 8:565–587

Behr H J, Ahrendt H, Porada H, Rohrs J, Weber K (1983) Upper Proterozoic playa and sabkha deposits in the Damara orogen, SWA/Namibia. Geol Soc S Afr Spec Publ 11:1–20

Bermingham P M, Fairhead J D, Stuart G W (1983) Gravity study of the central African rift system: a model of continental disruption. 2. The Darfur domal uplift and associated Cainozoic volcanism. Tectonophysics 94:205–222

Beukes N J (1986) The Transvaal sequence in Griqualand West. In: Anhaeusser C R, Maske S (eds) Mineral deposits of southern Africa, vol 1. Geol Soc S Afr, pp 1819–828

Beukes N J, Kleyenstuber A, Nel C (1982) Volcanogenic-sedimentary cycles in the Kalahari Manganese Field. Abstr Sedimentology '82. Geol Soc S Afr, pp 93–97

Bickle M J, Erikson K A (1982) Evolution and subsidence of early Precambrian sedimentary basins. Phil Trans R Soc Lond A305:225–247

Bignell R D (1975) Timing, distribution and origin of submarine mineralization in the Red Sea. Trans Inst Min Metall 84:B1–B6

Bischoff J L (1969) Red Sea geothermal brine deposits: their mineralogy, chemistry and genesis. In: Degens E T. Ross D A (eds) Hot Brines and recent heavy metal deposits in the Red Sea. Springer, Berlin, Heidelberg, New York, pp 368–401

Bizouard H, di Paola G M (1978) Mineralogy of the Tullu Moje active volcanic area (Arussi: Ethiopian rift valley). In: Neumann E R Ramberg I B (eds) Petrology and geochemistry of continental rifts. Proc NATO Adv Stud Inst. Reidel, Dordrectht, pp 79–86

Bohannon R G (1989) Style of extensional tectonism during rifting, Red Sea and Gulf of Aden. J Afr Earth Sci 8:589–602

Bonatti E (1985) Punctiform initiation of seafloor spreading in the Red Sea during transition from a continental to an oceanic rift. Nature (London) 316:33–37

Borg G (1988) The Koras-Sinclair-Ghanzi rift in southern Africa. Volcanism, sedimentation, age relationships and geophysical signature of a late middle Proterozoic rift system. Precambrian Res 38:75–90

Borg G, Maiden K J (1986) A preliminary appraisal of the tectonic and sedimentological environment of the Sinclair Sequence in the Klein Aub area, SWA/Namibia. Commun Geol Surv of SWA/Namibia 2:65–73

Borg G, Maiden K J (1987) Alteration of late Middle Proterozoic volcanics and its relation to stratabound copper-silver-gold mineralisation along the margin of the Kalahari Craton in SWA/ Namibia and Botswana. Geol Soc Spec Publ 33:347–354

Bott M H P ((1981) Crustal doming and the mechanism of continental rifting. Tectonophysics 73:1–8

Brown A C (1971) Zoning in the White Pine copper deposit, Michigan. Econ Geol 66:543–573

Brown A C (1979) Stratiform copper deposits: evidence for their post-sedimentary origin. Mineral Sci Eng 10:152–170

Browne S E, Fairhead J D (1983) Gravity study of the central African rift system: a model of continental disruption. 1. The Ngaoundere and Abu Gabra rifts. Tectonophysics 94:187–204

Burke K, Kield W S F, Kushky T (1985) Is the Ventersdorp rift system of Southern Africa related to a continental collision between the Kaapvaal and Zimbabwe cratons at 2.64 Ga ago? Tectonophysics 115:1–24

Button A (1976) Transvaal and Hamersley basins – Review of basin development and mineral deposits. Mineral Sci Eng 8:262–293

Button A (1981) The Transvaal Supergroup. In: Hunter D R (ed) Precambrian of the southern hemisphere, Chap 9. Elsevier, Amsterdam, pp 527–536

Button A (1986) The Transvaal sub-basin of the Transvaal sequence. In: Anhaeusser C R, Maske S (eds) Mineral deposits of southern Africa, vol 1. Geol Soc S Afr, pp 811–817

Clendenin C W, Charlesworth E G, Mashe S (1988) An Early Proterozoic three-stage rift system, Kaapvaal craton, South Africa. Tectonophysics 145:73–86

Cornwall F W (1961) Geochemistry (1). Chartered Exploration. In: Mendelsohn F (ed) The geology of the Northern Rhodesian Copperbelt, Chap 8. Macdonald, London, pp 187–205

Cox K G (1970) Tectonics and vulcanism of the Karroo period and their bearing on the postulated fragmentation of Gondwanaland. In: Clifford T N, Gass I G (eds) African magmatism and tectonics. Oliver & Boyd, London, pp 211–236

Degens E T, Ross D A (eds) (1969) Hot brines and recent heavy metal deposits in the Red Sea. Springer, Berlin, Heidelberg, New York, 600 pp

De Rito R F, Cozzarelli F A, Hodge D S (1983) Mechanisms of subsidence of ancient cratonic rift basins. Tectonophysics 94:141–168

Dewey J F (1982) Plate tectonics and the evolution of the British Isles. J Geol Soc London 139:371–412

Dickinson W R, Yarborough H (1976) Plate tectonic evolution of sedimentary basins. Am Assoc Petrol Geol Short Course Handb, pp 1–56

Economic Geology (ed) (1973) Precambrian Iron Formation of the world. Econ Geol 68

Fairhead J D, Green, C M (1989) Controls on rifting in Africa and regional tectonic model for the Nigeria and East Niger rift basins. J Afr Earth Sci 8:231–249

Finlow-Bates T (1979) Studies of the base metal sulfide deposits at McArthur River, Northern territory, Australia: II. The sulfide-S and organic-C relationships of the concordant deposits and their significance – A discussion. Econ Geol 74:1697–1699

Fitton J G, Upton B G J (eds) (1987) Alkaline Igneous Rocks. Geol Soc Spec Publ 30, 568 pp

Fleischer V D, Garlick W G, Haldane R (1976) Geology of the Zambian Copper Belt. In: Wolf K H (ed) Handbook of strata-bound and stratiform ore deposits, vol 6. Elsevier, Amsterdam, pp 223–352

Frostick L E, Renaut R W, Reid I, Tiercelin J-J (eds) (1986) Sedimentation in the African rifts. Geol Soc Spec Publ 25, 382 pp

Gass I G (1979) The evolution of volcanism in the junction area of the Red Sea, Gulf of Aden and Ethiopian rifts. Phil Trans R Soc London A267:369–381

Girdler R W (1983) Processes of planetary rifting as seen in the rifting and breakup of Africa. Tectonophysics 94:241–252

Gross G A (1980) A classification of iron formations based on depositional environments. Can Mineral 18:215–222

Gross G A (1983) Tectonic systems and the deposition of iron formation. Precambrian Res 20:171–187

Gulson B L, Perkins W G, Mizon K J (1983) Lead isotope studies bearing on the genesis of copper orebodies at Mount Isa, Queensland. Econ Geol 78:1466–1504

Hartnady C, Joubert P, Stowe C (1985) Proterozoic crustal evolution in southwestern Africa. Episodes 8:236–244

Hermance J F (1982) Magnetotelluric and geomagnetic deep-sounding studies in rifts and adjacent areas: constraints on physical processes in the crust and upper mantle. In: Palmason G (ed) Continental and oceanic rifts. Geodynamic series, vol 8. Am Geophys Un, pp 169–192

Hoffman P F (1987) Continental transform tectonics: Great Slave Lake shear zone (ca. 1.9 Ga), northwest Canada. Geology 15:785–788

Hoffman P F, Dewey J F, Burke K (1974) Aulacogens and their genetic relation to geosynclines, with a Proterozoic example from Great Slave Lake, Canada. In: Dott R H, Shaver R H (eds) Modern and ancient geosynclinal sedimentation. Soc Econ Paleontol Mineral Spec Publ 19:38–55

Hutchison C S (1983) Economic deposits and their tectonic setting. Macmillan, New York, 355 pp

Jacobsen J B E, McCarthy T S (1975) Possible late Karroo carbonatite and basalt intrusions at Messina, Transvaal. Trans Geol Soc S Afr 78:153–159

Jacobsen J B E, McCarthy T S (1976) An unsual hydrothermal copper deposit at Messina, South Africa. Econ Geol 71:117–130

Jacobsen J B E, McCarthy T S, Laing G J (1976) The copper-bearing breccia pipes of the Messina district, South Africa. Mineral Depos 11:33–45

Keller G R, Lidiak E G, Hinze W J, Braile L W (1983) The role of rifting in the tectonic development of the Midcontinent, USA. Tectonophysics 94:391–412

Lambert I B (1976) The McArthur zinc-lead-silver deposit: features, metallogenesis and comparisons with some other stratiform ores. In: Wolf K H (ed) Handbook of strata-bound and stratiform ore deposits, vol 6. Elsevier, Amsterdam, pp 535–585

Lambiase J J (1989) The framework of African rifting during the Phanerozoic. J Afr Earth Scie 8:183–190

Laznicka P (1981) Data on the world-wide distribution of stratiform and stratabound ore deposits. In: Wolf K H (ed) Handbook of strata-bound and stratiform ore deposits, vol 10. Elsevier, Amsterdam, pp 79–389

Le Bas M J (1971) Peralkaline volcanism, crustal swelling, and rifting. Nature (London) 229:3027–3031

Mathias B V, Clark G J (1975) Mount Isa copper and silver-lead-zinc orebodies – Isa and Hilton mines. In: Knight C L (ed) Economic Geology of Australia and Papua New Guinea. 1. Metals. Australas Inst Min Metall Monogr 5. Parkville, Victoria, pp 351–372

McCarthy T S, Jacobsen J B E (1976) The mineralizing fluids at the Artonvilla copper deposit: an example of a silica-deficient, alkaline hydrothermal system. Econ Geol 71:131–138

McConnell R B (1972) Geological development of the rift system of Eastern Africa. Geol Soc Am Bull 83:2549–2572

McGregor G J (1986) Geology of the Black Mountain ore body – Aggeneys. In: Abstr Geocongress '86 Johannesburg. Geol Soc S Afr, pp 1025–1028

McKenzie D (1978) Some remarks on the development of sedimentary basins. Earth Planet Sci Lett 40:25–32

McKenzie D P, Davies D, Molnau P (1979) Plate tectonic of the Red Sea and East Africa. Nature (London) 226:243–248

Mendelsohn F (Ed) (1961) The geology of the Northern Rhodesian Copperbelt. Macdonald, London, 523 pp

Milanovski E E (1983) Major stages of rifting evolution in the earth's history. Tectonophysics 94:599–607

Moore J M (1989) A comparative study of metamorphosed supracrustal rocks from the western Namaqualand Metamorphic Complex. Precambrian Res Unit, Univ Cape Town, Bull 37:370 pp

Morgan P, Baker B H (eds) (1983a) Processes of continental rifting. Tectonophysics Spec Issue 94, 680 pp

Morgan P, Baker B H (1983b) Introduction – processes of continental rifting. Tectonophysics 94:1–10

Murray W J (1975) McArthur River HYC lead-zinc and related deposits, Northern Territory. In: Knight C L (ed) Economic Geology of Australia and Papua New Guinea. 1. Metals. Australas Inst Min Metall Monogr 5. Parkville, Victoria, pp 329–339

Neumann E R, Ramberg I B (eds) (1978) Petrology and geochemistry of continental rifts. Proc NATO Adv Stud Inst 1. Reidel, Dordrecht, 296 pp

Norman D I (1978) Ore deposits related to the Keweenawan rift. In: Neumann E R, Ramberg I B (eds) Petrology and geochemistry of continental rifts. Reidel, Dordrecht, pp 245–253

Oreskes N, Einaudi M T (1990) Origin of rare-earth element-enriched hematite breccia at the Olympic Dam Cu-U-Au-Ag deposit, Roxby Downs, South Australia. Econ Geol 85:1–28

Palmason G (ed) (1982) Continental and oceanic rifts. Am Geophys Un Geodyn Ser 8:309 pp

Plimer I R (1986) Sediment-hosted exhalative Pb-Zn deposits. Products of contrasting ensialic rifting. Trans Geol Soc S Afr 89:57–73

Porada H (1983) Geodynamic model for the geosynclinal development of the Damara orogen, Namibia, South West Africa. In: Martin H, Eder F W (eds) Intracontinental Fold Belts. Springer, Berlin, Heidelberg, New York, pp 503–541

Pottorf R J, Barnes H L (1983) Mineralogy, geochemistry, and ore genesis of hydrothermal sediments from the Atlantis II Deep, Red Sea. Econ Geol Monogr 5:198–223

Pretorius D A (1976) Gold in the Proterozoic sediments of South Africa: systems, paradigms and models. In: Wolf K H (ed) Handbook of strata-bound and stratiform ore deposits, vol 7. Elsevier, Amsterdam, pp 29–88

Pretorius D A (1981) Gold and uranium in quartz-pebble conglomerates Econ Geol 75th Anniv Vol, pp 117–138

Reading H G (1986) African rift tectonics and sedimentation: an introduction. Geol Soc Spec Publ 25:3–8

Reeve J S, Cross K C, Smith R N, Oreskes N (1990) Olympic Dam copper-uranium-gold-silver deposit. In: Hughes F E (ed) Geology of the mineral deposits of Australia and Papua New Guinea, Vol 2. Australas Inst Min Metall Monogr 14. Parkville, Victoria, pp 1009–1036

Roberts, D E (1986) The Olympic Dam copper-uranium-gold deposit. In: 8th Aus Geol Convention Adelaide. Abstr, vol 15, pp 165–166

Roberts D E, Hudson G R T (1983) The Olympic Dam Copper-Uranium-Gold deposit, Roxby Downs, South Australia. Econ Geol 78:799– 822

Rose A W, Hawkes H E, Webb J S (1979) Geochemistry in Mineral Exploration. Academic Press, New York, London, 657 pp

Rozendaal A (1986) The Gamsberg zinc deposit, Namaqualand district In: Anhaeusser C R, Maske S (eds) Mineral Deposits of southern Africa, vol 2. Geol Soc S Afr, pp 1477–1488

Ruxton P (1986) Sedimentology, isotopic signature and ore genesis of the Klein Aub Copper Mine, South West Africa/Namibia. In: Anhaeusser C R, Maske S (eds) Mineral deposits of southern Africa, vol 2. Geol Soc S Afr, pp 1725–1738

Ryan B D, Kramers J D, Stacey J S, Deleveaux M, Barton J M, Fripp R E P (1983) Strontium and lead isotope studies and K/Rb ratio measurements relating to the origin and emplacement of the copper deposits near Messina, South Africa. Geol Soc S Afr Spec Publ 8:47–53

Ryan P J, Lawrence A L, Lipson R D, Moore J M, Paterson A, Stedman D P, Van Zyl D (1986) The Aggeneys base metal sulphide deposits, Namaqualand District. In: Anhaeusser C R, Maske S (eds) Mineral Deposits of southern Africa, vol 2. Geol Soc S Afr, pp 1447–1475

Rye D M, Williams N (1981) Studies of the base metal sulfide deposits at McArthur River, Northern Territory, Australia: III. The stable isotope geochemistry of the HYC, Ridge and Cooley deposits. Econ Geol 76:1–26

Sandiford M, Powell R (1986) Deep crustal metamorphism during continental extension: modern and ancient examples. Earth Planet Sci Lett 79:151–158

Sawkins F J (1977) Fluid inclusion studies of the Messina copper deposits, Transvaal, South Africa. Econ Geol 72:619–631

Sawkins F J (1982) Metallogenesis in relation to rifting. In: Palmason G (ed) Continental and oceanic rifts. Am Geophys Un Geodyn Ser 18:259–270

Sawkins F J (1989) Anorogenic felsic magmatism, rift sedimentation, and giant Proterozoic Pb-Zn deposits. Geology, 17:657–660

Sawkins F J (1990) Metal deposits in relation to plate tectonics, 2nd edn. Springer, Berlin, Heidelberg, New York, 461 pp

Sawkins J F, Rye D O (1979) Additional geochemical data on the Messina copper deposits, Transvaal, South Africa. Econ Geol 74:684–689

Shanks W C, Bischoff J L (1977) Ore transport and deposition in the Red Sea geothermal system: a geochemical model, Geochim Cosmoch Acta 41:1507–1519

Shanks W C, Bischoff J L (1980) Geochemistry, sulfur isotope composition, and accumulation rates of Red Sea geothermal deposits. Econ Geol 75:445–459

Sims P K (1976) Precambrian tectonics and mineral deposits, Lake Superior region. Econ Geol 71:1092–1127

Smith P (1986) The geology of the Broken Hill Pb-Ag-Zn-Cu deposit. In: Abstr Geocongress '86 Johannesburg. Geol Soc S Afr, pp 881–884

Solomon R J (1965) Investigation into sulfide mineralization of Mount Isa, Queensland. Econ Geol 60:737–765

Swager C P (1985) Syndeformational carbonate-replacement model for the copper mineralization at Mount Isa, northwest Queensland: a microstructural study. Econ Geol 80:107–125

Sykes L R (1979) Earthquakes and other processes within lithospheric plates and the reactivation of pre-existing zones of weakness. In: Strangway D W (ed) The continental crust and its mineral deposits. Geol Ass Can Spec Pap 20:215–238

Tankard A J, Jackson M P A, Erikson K A, Hobday D K, Hunter D R, Minter W E L ((1982) Crustal evolution of Southern Africa – 3.8 billion years of earth history. Springer, Berlin, Heidelberg, New York, 523 pp

Tiercelin J J, Thouin C, Kalala T, Mondeguer A (1989) Discovery of sublacustrine hydrothermal activity and associated massive sulfides and hydrocarbons in the north Tanganyika trough, East African rift. Geology 17:1053–1056

Tregoning T D (1977) The mineralised argillite and the significance of the breccia at Klein Aub Mine, South West Africa. BSc Honours Proj, Rhodes Univ, Grahamstown, 54 pp

Tregoning T D (1987) The tectono-metallogenesis during the Irunide and Pan African events in South West Africa/Namibia. MSc Thesis, Rhodes Univ, Grahamstown, 106 pp

Truswell J F (1977) The geological evolution of South Africa. Purnell, Cape Town, 218 pp

Walker R N, Logan R G, Binnekamp J G (1977) Recent geological advances concerning the HYC and associated deposits, McArthur River, Northern Territory. J Geol Soc Aus 24:365–380

White R, McKenzie D (1989) Magmatism at rift zones: the generation of volcanic continental margins and flood basalts. J Geophys Res 94:7685–7729

Wickham S M, Oxburgh E R (1985) Continental rifts as setting for regional metamorphism. Nature (London) 318:330–333

Wickham S M, Taylor H P (1987) Stable isotope constraints on the origin and depth of penetration of hydrothermal fluids associated with Hercynian regional metamorphism and crustal anatexis in the Pyrenees. Contrib Mineral Petrol 95:255–268

Wyllie P J (1980) The origin of kimberlite. J Geophys Res 85:6902–6910

Williams L A J (1982) Physical aspects of magmatism in continental rifts. In: Palmeson G (ed) Continental and oceanic rifts: Am Geophys Un Geodyn Ser 8:193–222

Williams N (1978a) Studies of the base metal sulfide deposits at McArthur River, Northern Territory, Australia: I. The Cooley and Ridge deposits. Econ Geol 73:1005–1035

Williams N (1978b) Studies of the base metal sulfide deposits at McArthur River, Northern Territory, Australia: II. The sulfide-S and organic-C relationships of the concordant deposits and their significance. Econ Geol 73:1036–1056

Willner A, Schreyer W, Moore J M (1990) Peraluminous metamorphic rocks from the Namaqualand Metamoprhic Complex (South Africa): Geochemical evidence for an exhalation-related sedimentary origin in a Mid-Proterozoic rift system. Chem Geol 81:221–240

Wilson M (1989) Igneous Petrogenesis. Unwin Hyman, London, 466 pp

Zierenberg R A, Shanks W A (1988) Isotopic studies of epigenetic features in metalliferous sediment, Atlantis II deep, Red Sea. Canad Mineral 26:737–753

Chapter 14

Stratabound Carbonate-Hosted Base Metal Deposits

14.1 Introduction

Stratabound carbonate-hosted Pb-Zn ± Cu deposits constitute a major source of Pb and Zn in North America and Europe, where this type of deposit is represented in the MacKenzie district in Canada, the Appalachian, Tri-State, southeast and southcentral Missouri (Viburnum Trend) and the upper Mississippi Valley districts in the USA, in the Alpine, Silesian, central Irish Plain and Pennine districts of Europe. Other important deposits also occur in southern Africa, North Africa and Russia (Fig. 14.1). The deposits of the Mississippi Valley have often been considered as classic examples of stratabound carbonate-hosted base metal sulphide deposits, and for this reason are often referred to as Mississippi Valley type, or MVT. While these deposits have a wide temporal geological distribution, they are most common in the Phanerozoic, from the Cambrian through to the Cretaceous. A number of deposits also occur in the carbonate sequences of Early Proterozoic age, such as those of the Transvaal basin in South Africa, mentioned briefly in the previous chapter (see Fig. 13.23). Important Pb-Zn deposits of Late-Proterozoic age are the Kabwe deposit in Zambia, and the world-famous Tsumeb and adjacent deposits in the Otavi Mountain Land in Namibia, to be discussed later in some detail. Other Proterozoic occurrences are present in the McArthur River basin and Dugald River in north Australia.
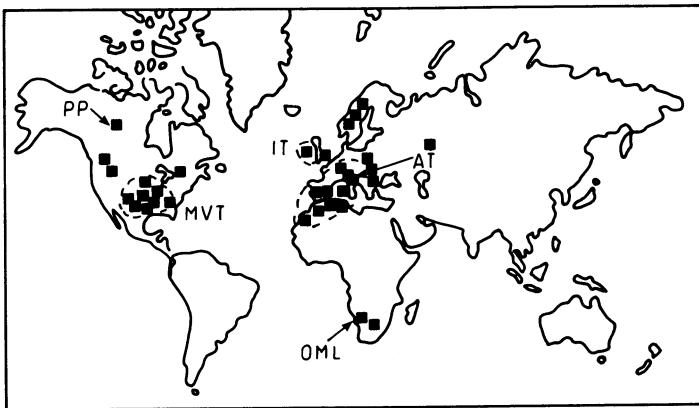
Fig. 14.1. Distribution of the main carbonate-hosted Pb-Zn deposits. *MVT* Mississippi Valley type in the USA; *PP* Pine Point; *IT* Irish-type; *AT* Alpine-type; *OML* Otavi Mountain Land, Namibia

Sangster (1983) classifies carbonate-hosted deposits on the basis of metal ratios (Zn/Zn + Pb). He distinguishes Pb-rich cratonal, Zn-Pb basinal and Zn-rich platformal deposits. Here, we adopt the classification used by Sawkins (1990), who subdivided carbonate-hosted base metal deposits into three main groups, namely: (1) Mississippi Valley type; (2) Alpine type; and (3) Irish type. These deposits do not appear to have any connection with magmatic activity, nor do they have a clear connection with rifting events; nevertheless Sawkins (1990) notes that there are instances in which a relationship to rift tectonics can be made. An example of this relationship is provided by the presence of carbonate-hosted Pb-Zn deposits along the coasts of the Red Sea (see Fig. 3.22). For this reason it is also considered possible that all gradations may exist from a Red Sea-type deposit to carbonate-hosted deposits on passive continental margins. Carbonate-hosted base metal deposits generally occur in shelf-facies sedimentary sequences along rifted passive margins or within intracratonic basins (Sawkins 1990). In some cases carbonate deposition was almost contemporaneous with tectonic activity and ore deposition, while in other instances the ore fluids acted on karst structures in post-tectonic times (Sangster 1983). The mineralisation exhibits features which range from typically hydrothermal to diagenetic in character, thus making its origin difficult to establish. Sangster (1983) maintains that the differences in the various carbonate-hosted deposits outweigh the similarities, making the attainment of a unifying genetic scheme virtually impossible. However, it must be pointed out that carbonate-hosted deposits are probably part of the larger family of sediment-hosted base metal sulphide deposits, including the "Red Bed" disseminated Cu sulphide mineralisation, sedimentary-exhalative massive sulphides (discussed in the previous chapter) and sandstone-Pb deposits (Bjorlykke and Sangster 1981). In view of these uncertainties, together with their unique character, we deal with carbonate-hosted deposits in a separate chapter, in which examples of Mississippi Valley-, Alpine- and Irish-type deposits, and those of the Otavi Mountain Land in Namibia, are discussed.

The most important features of the carbonate-hosted base metal deposits, discussed by Sverjensky (1986), are summarised as follows: (1) they occur in limestone or dolomitic rocks; (2) the ore is usually stratabound and consists of replacements and/or veins; (3) the chief ore minerals are galena, sphalerite, pyrite, marcasite and chalcopyrite, whereas gangue minerals are dolomite, calcite, fluorite, barite and quartz; (4) they are not associated with igneous rocks; (5) they occur in areas of mild deformation; (6) the mineralisation is often spatially associated with basement highs, with the ore being located within reef structures around these highs; (7) the mineralisation was probably formed at relatively shallow depths (1–1.5 km), and fluid inclusion studies indicate that the ore solutions were of low temperature (50–200°C) with a salinity range of between 10 to 30% wt. NaCl equivalent; (8) stable isotope data from the water of fluid inclusions suggest that it is similar to the water of pore fluids in sedimentary basins; also, the $\delta^{34}S$ per mill values indicate that the source of S could not have been magmatic; (9) finally there is always evidence that dissolution of the host carbonate rocks has taken place and is manifested by the presence of breccias and collapse structures.

A possible connection between the major Pb-Zn districts and areas containing petroleum and natural gas has been suggested (see, for example, Sverjensky 1984;

Oliver 1986; Chap. 3). In the USA the areas of carbonate-hosted Pb-Zn mineralisation occur along basin margins and there is almost complete lack of overlap with the petroliferous areas. This type of spatial arrangement may reflect differential movement of fluids in the sedimentary basins, with base metal-bearing brines moving over longer distances than the more viscous oils which require trapping in suitable structures. Mississippi oil-field brines contain appreciable amounts of Pb, Zn, Cu, Ag, Au, Co and Ni (Saunders and Swann 1990), while Sverjensky (1984) has shown that fluids with a composition similar to Mississippi oil-field brines could become an ore solution during migration towards the basin margins. S- and Pb-isotope systematics and fluid inclusion studies of galenas from the Viburnum Trend corroborate Sverjesnky's idea that MVT ore-forming brines originated from sedimentary basins and that they have similar composition to oil-field brines (Crocetti and Holland 1989). On the basis of Br^-/Cl^- and K^+/Na^+ values of fluid inclusions in cubic and octahedral galenas, respectively, Crocetti and Holland (1989) also show that the composition of oil-field brines was probably of marine-evaporite origin.

Comprehensive papers and reviews on the present topic can be found in Brown (1967), Sangster (1976), Anderson and Macqueen (1982), Kisvarsanyi et al. (1983) and Sverjensky (1986).

14.2 Mississippi Valley-Type Deposits (MVT)

As its name implies, the classic area for this mineralisation is the drainage basin of Mississippi river in the central USA, although similar deposits occur in the Appalachian district where the ore deposits are folded, and at Pine Point in the North West Territories in Canada. According to Callahan (1967), sedimentary environments such as reefs, facies changes, talus or breccias, and solution collapse structures situated below an unconformity, are the major locales for the MVT-mineralising fluids.

14.2.1 The Viburnum Trend, USA

The Viburnum Trend ore deposits contain the largest reserves of Pb and Zn in the USA, with approximately 800×10^6 tonnes at 7 % combined Pb + Zn. Significant amounts of Au, Ag and Cd are also present. Mining of Pb (Old Lead Belt) began in 1868, but there are reports of mining which date to the 18th century. An issue of Economic Geology (1977) is devoted to the Viburnum Trend.

The Viburnum Trend, southeast Missouri, is approximately 70 km long (Fig. 14.2) and lies near the southern edge of the central stable region of the North American craton. The dominant structural feature in the region is the Ozark Dome, composed of rhyolitic and granitic rocks of Precambrian age (ca. 1.4 Ga). The Dome constitutes an area of uplift which probably formed an island complex in the Cambrian seas. The stratigraphy in the region consists of six formations which are,

in ascending order: Lamotte Sandstone, Bonneterre Formation, Davis Formation, Derby-Doerun Dolomite, Potosi Dolomite and Eminence Dolomite. Late Cambrian sedimentation started with the deposition of the Lamotte Sandstone on a shallow stable platform constituted by a Precambrian basement. In the Viburnum Trend area these sediments have a shallow (ca. 6°) westward dip. The Lamotte Sandstone is a clean orthoquartzite, fine-grained and cross-bedded, porous and therefore permeable, with a maximum thickness of approximately 125 m. Shelf sedimentation continued with the conformably overlying Bonneterre Formation, about 90 m thick, which is the carbonate platform unit hosting the mineralisation. The impermeable Davis Shale Formation, which is 50 m thick, unconformably overlies the Bonneterre Formation and consists of alternating shales, carbonates, siltstones and some sandstones. Thin, irregularly bedded (Derby-Doerun dolomite) and massive bedded dolomitic rocks (Potosi and Eminence dolomites) follow upward in the sequence.

The ore-bearing Bonneterre Formation has been compared to the present-day carbonate platform in the Bahamas. The Formation is divided into four facies: (1) offshore or basin facies; (2) reef facies; (3) back-reef facies; and (4) shelf facies. The offshore facies is composed of micrite and shales of a low-energy environment; the reef facies is composed of stromatolite and algal material. Erosion surfaces, surge channels and inter-reef areas, filled with clastic carbonate and reef debris, are present. Oolitic material occurs in the front and back parts of the reef. The back-reef facies is made up of light-coloured (white rock) coarse and crystalline dolomite and burrowed lime mudstones and stromatolites are also common. The environment of deposition is probably represented by tidal flats. The reefs formed a paleoshore line along the Viburnum Trend and coalesced to form a linear barrier reef.

Mineralisation

The feature common to all mines in the Viburnum Trend is that they all occur in the Bonneterre Formation, although the mineralisation is not confined to a specific horizon within the Formation, but is generally controlled by the paleotopography of the Precambrian basement. The main mines of the Trend are Viburnum Nos. 27, 28, 29, Magmont, Buick, Brushy, Fletcher and Ozark (Fig. 14.2). The orebodies are aligned along a north-south trend more or less parallel to the paleoshore line. The Viburnum 27 Mine (Grundmann 1977) occurs adjacent to three basement highs which probably formed islands during the Cambrian. The mine had reserves of approximately $20-23 \times 10^6$ tonnes grading over 4% Pb, with minor quantities of Zn and Cu. The Bonneterre Formation is completely dolomitised in the mine area and most of the ore is associated with algal reefs, and more specifically with surge channels and troughs filled with clastic material. The contact between the reef and the channels, which vary from 1 to 10 m width, is characterised by numerous fractures which provided the pathway for the ore solutions. The ore minerals are galena, sphalerite and chalcopyrite, with a ratio of approximately 10:1:0.6, and lesser amounts of pyrite and marcasite. Gangue minerals are calcite and dolomite. The mineralisation occurs as disseminations and open-space fracture fillings. In the Ozark Mine (Mouat and Clendenin 1977) the mineralisation appears to be
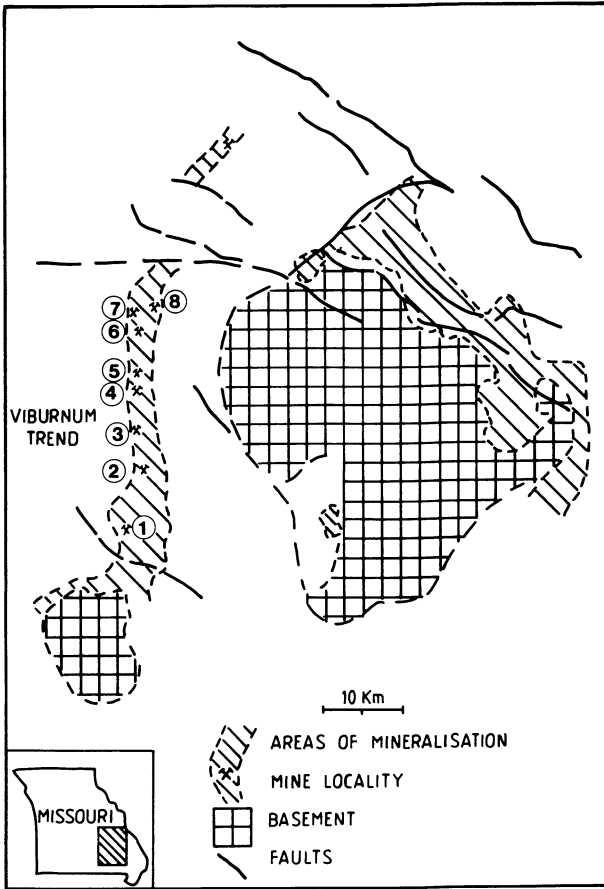
Fig. 14.2. The southeast Missouri Pb-Zn mining district. Deposits of the Viburnum Trend are: *1* Ozark Lead; *2* Fletcher Mine; *3* Brushy Creek Mine; *4* Buick Mine; *5* Magmont Mine; *6* No. 28; *7* No. 27; *8* No. 29 (After Kisvarsanyi 1977)

structurally and stratigraphically controlled. The ore is divided into four types: (1) bedded and disseminated; (2) breccia ore; (3) marginal break; and (4) fracture stockwork. The bedded and disseminated type, which is the most important, is localised along permeable horizons such as burrowed mudstone, along bedding planes, or lithological contacts. Breccia bodies are due to solution collapse and extend across the depositional strike of the sediments. Marginal breaks occur on both sides of collapse breccias, forming zones up to 50 m wide. Both solution and tensional structures are used as sites of deposition by the mineralising solutions. Fracture stockwork is commonly found below the collapse breccia, and the mineralisation occurs as veinlets and fracture fillings that cross-cut the strata. Dominant ore minerals are galena and sphalerite with a ratio of 6:1. Chalcopyrite is a minor constituent. In addition to Pb and Zn, other metals recovered from the concentrates are Ag, Cu and Cd.
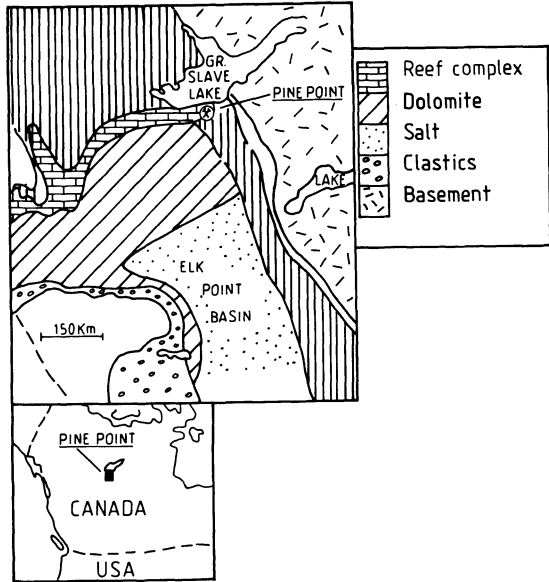
Fig. 14.3. Simplified geology of the Pine Point area (After Campbell 1967)

14.2.2 Pine Point, Canada

The Pine Point carbonate-hosted Pb-Zn deposit is located on the southern shore of the Great Slave Lake in the MacKenzie district of Canada's North West Territory (Beals and Jackson 1966; Campbell 1967; Skall 1975; Dixon 1979; Kyle 1981). In 1976 ore reserves at Pine Point were in the order of 65×10^6 tonnes grading 3% Pb and 7% Zn. The Pine Point mineralisation occurs at the north end of the Elk Point basin in rocks of Mid-Devonian age. The Canadian Shield outcrops approximately 100 km to the east and is cut by a number of northeast-trending faults, one of which, if projected below the Phanerozoic cover (Fig. 14.3), passes underneath the Pine Point deposit. The Elk Point basin was a large depository extending along the western side of the Canadian Shield, from North Dakota in the USA, across Saskatchewan, Alberta, and to the Great Slave Lake, where it is known as the MacKenzie basin.

Initial sedimentation in the MacKenzie basin began in the Early Paleozoic, but the main development of the sedimentary sequences was during Mid- to Late-Devonian. The mineralisation is hosted by the Mid-Devonian sequence, which consists of three main facies: evaporite, barrier carbonate and marine shale facies. The evaporite rocks (Muskeg sequence) consist of gypsum, anhydrite and shale, whereas the marine shale facies include bituminous limestone and the Buffalo River grey limestone and shale sequence. The barrier carbonate facies hosts the mineralisation, which is within a complex series of dolomitic rocks known as the Presqu'ile Barrier Complex (Fig. 14.4). The overlying rocks occur on a paleokarst surface and include mainly shale and limestone (Watt Mountain Formation and Amco Shale). It is important to note that in addition to the Pine Point Pb-Zn deposits, the Presqu'ile Barrier Complex also hosts substantial oil fields in northern Alberta.
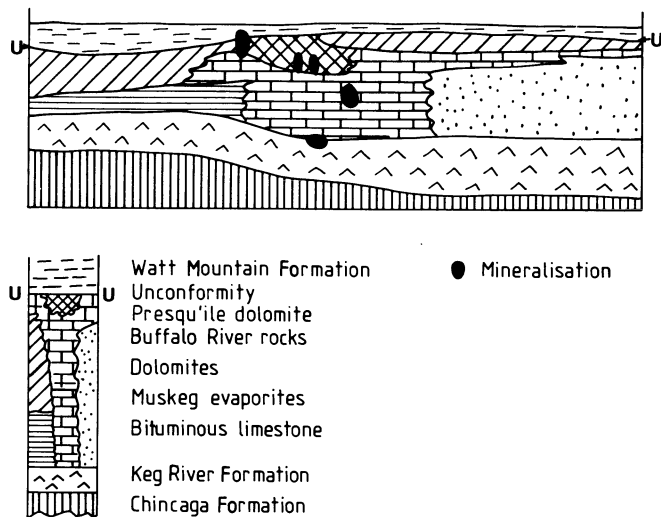
Fig. 14.4. Schematic cross-section across the Pine Point district, showing stratigraphic position of Pb-Zn orebodies; drawing not to scale (After Dixon 1979)

If one is to place constraints on models of ore genesis for the Pine Point mineralisation, it is essential to understand the geological history and evolution of the MacKenzie basin. Thus, the sequence of events believed to have taken place during and after the development of the barrier reef complex is summarised. At first a carbonate shoal was formed following the arching of the basement rocks and the overlying Lower Paleozoic sediments (Keg River Formation). This shoal formed an efficient barrier and resulted in the southern part of the basin becoming hypersaline due to an arid climate as well as a restricted recharge. Evaporites were deposited over a large area (Muskeg Formation), and Mg-rich brines may have caused early diagenetic dolomitisation of the barrier carbonates. The seaward side was to the north of the reef barrier, and on this side deeper water conditions existed and marine shales were deposited. A rise in the sea level resulted in the deposition of carbonates behind the barrier into the evaporite basin. Uplift followed, causing the development of karsting. Karsting was very important in establishing structures which facilitated the ingress and movement of the ore solutions. Karst structures included subsurface channels, solution cavities and collapse breccias. Renewed subsidence resulted in the deposition of tidal flat sediments, mostly shale and limestone (Watt Mountain Formation and Amco Shale).

The Pine Point district contains a number of deposits, all confined to the dolomitised rocks of the Presqu'ile sequence, locally called the Pine Point Group. Rocks of the Pine Point Group consist of fossiliferous coarse and fine dolomite and undolomitised limestone, interpreted as a barrier reef complex (Fig. 14.4). There are about 40 known orebodies in the district, varying in size from approximately 0.1×10^6 to 15×10^6 tonnes. According to their morphology the orebodies are divided into massive and tabular types. Massive orebodies, with a Pb/Zn ratio of 1:1.7, have

a restricted horizontal extent compared to their vertical dimension. This type of mineralisation is associated with collapse breccias and the development of solution cavities in the dolomite. Clasts in the breccias are locally cemented by sulphides and the gangue minerals have been identified as belonging to the overlying Watt Mountain Formation. Strata collapse is thought to be the result of subsurface drainage along dominant fractures due to karst development. The tabular orebodies, with a Pb/Zn ratio of about 1:2.6, are much smaller and generally conformable to bedding. The Pine Point deposits are characterised by a fairly simple ore and gangue mineralogy. Ore minerals include galena, crystalline and colloform sphalerite, minor pyrite, marcasite and pyrrhotite. Euhedral galena crystals are commonly enclosed in colloform sphalerite. There are also minor amounts of selenite, celestite, native S and bitumen. Gangue minerals are dolomite and calcite, which occur as coarse crystals filling cavities. Textural relationships indicate a complex paragenesis with several periods of galena and sphalerite deposition. The mineralisation is clearly significantly later than the host reef carbonates, because it extends into the strata deposited on top of the karst structures developed on the reef carbonates.

14.3 Alpine-Type Deposits

Carbonate-hosted Pb-Zn-Ba-F deposits occur in the eastern Alps, in a metallogenic district, shared by Austria, Italy and Yugoslavia. This district extends for approximately 450 km in an east-west direction and 250 km in a north-south direction. Four deposits, Bleiberg-Kreuth, Mezica, Raibl and Salafossa, account for most of the Pb and Zn production in the region. These deposits occur within carbonate sequences in the Ladinian stage of the Mid-Triassic (Maucher and Schneider 1967; Brigo et al. 1977; Brigo and Omenetto 1985). The deposits are spatially associated with the so-called Peri-Adriatic Line, a tectonic lineament active since the Paleozoic. Unfortunately the complexities – both geological and cultural – of this particular region have somewhat hampered the development of genetic models. Nevertheless, it appears that the main difference between the MVT deposits and the Alpine type is the timing of sulphide deposition relative to the host rocks. The Alpine deposits are characterised by two main mineralisation styles: stratiform and discordant. The carbonate host rocks consist mainly of shallow-water calc-arenite and oolitic limestones, with stromatolites, intraformational breccias and karst structures. Tuffaceous rocks occur in the footwall sequence of most orebodies and are considered important in terms of source of metals by the German-speaking geologists. A paleogeographic reconstruction (Fig. 14.5) shows that the Salafossa and Raibl deposits occur in a reef platform environment, whereas the Bleiberg and Mezica deposits occur in a back-reef lagoonal setting. At least five styles of mineralisation are present: (1) stratiform (syngenetic?) ores; (2) stratabound veins and fissure filling; (3) fault-related epigenetic ores; (4) ores in breccia networks; (5) orebodies in karst structures. The ore minerals are represented by galena, sphalerite, wurtzite, pyrite and marcasite. Wulfenite and descloizite are present at the Mezica
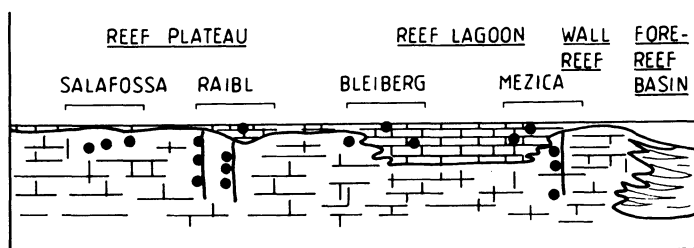
Fig. 14.5. Schematic representation of the paleogeographic setting of carbonate-hosted base metal deposits in the eastern Alps. *Filled circles* indicate ore deposits; drawing not to scale (After Brigo et al. 1977)

deposit. Gangue minerals include calcite, dolomite, barite, fluorite and quartz. Fluorite is currently mined at a number of localities in the Italian sector. In many instances ore and gangue minerals show typical sedimentary depositional structures, including rhythmic layering, graded bedding and load casts.

The Raibl Pb-Zn deposit, located within the Dolomia Metallifera, is characterised by filling of fissure and karst cavities which are spatially related to fault systems of Triassic age (Brigo and Omenetto 1985). The Raibl mineralisation is therefore epigenetic and consists of colloform sphalerite, galena, pyrite, marcasite and barite. The sphalerite contains significant amounts of Ge and Tl, while the galena is enriched in As, Sb and Tl, but is Ag-free. The Salafossa orebody is essentially a breccia pipe and is spatially associated with a fault in the Mid-Triassic Serla Dolomite.

14.4 Irish-Type Deposits

At least three major metal deposits – Zn-Pb at Navan, Pb-Zn-Ag-Ba at Silvermines, and Pb-Zn-Cu-Ag at Tynagh – as well as a number of lesser ones (Keel, Ballinalack, Abbeytown and Moate) occur in Lower Carboniferous carbonate rocks of shelf facies situated between the Caledonides and Hercynian belt in Ireland (Evans 1976; Dixon 1979; Sevastopulo 1981a, b; Boyce et al. 1983). The Irish deposits, which have been compared to the Australian McArthur River and Canadian Sullivan Pb-Zn deposits, are considered to be the result of submarine exhalations of hydrothermal fluids in fault-controlled basins (Boyce et al. 1983). This view is substantiated by the discovery of pyritic tubes resembling hydrothermal chimneys through which fluids are discharged (Larter et al. 1981).

All of the major Pb-Zn orebodies occur north of the Hercynian front, where deformation was minimal, and most of the structures associated with the mineralisation are related to the Caledonian event which took place following the collision of the North American and European plates. The Caledonian suture zone remained active well into the Lower Carboniferous, and probably controlled basin development. Most deposits are situated along east-northeast and northeast-

trending faults, and all appear to be associated with pre-Carboniferous basement inliers.

The stratigraphic succession indicates that a Devonian red-bed sequence was deposited in a deep basin in southern Ireland. This sequence gradually thinned northwards and was transgressed during the Lower Carboniferous by marine sandstones, overlain by interbedded limestone and calcareous shale, containing algal mats and occasional gypsum pseudomorphs. This lower stage succession is overlain by a widespread green mudstone marker horizon, bedded shelf limestone, in turn overlain by carbonate reef bank limestone consisting of mounds and sheet-like bodies of pale- to dark-grey porous bioclastic material. There are no known post-Devonian plutonic rocks, although Lower Carboniferous volcanic centres are present.

14.4.1 Mineral Deposits

Navan

The Navan Zn-Pb deposit is located 1.5 km west of the town of Navan. The mineralisation was discovered in 1969 during a followup on a geochemical anomaly. A drilling programme was carried out over I.P. anomalies and one of the holes intersected some 35 m of mineralised material. Approximately 80×10^6 tonnes of ore were delineated grading 10% Zn and 2.6% Pb. The orebody occurs in bioclastic and oolitic dolomitised limestones, unconformably overlain by deeper-water dark limestone. The mineralisation is located at the intersection of a reverse northeast-trending fault and a normal east-west-trending fault. This latter fault cuts the orebody and is cut by the unconformity. The main ore minerals are sphalerite and galena with minor pyrite and marcasite. Barite is also present. The ores, which are generally fine-grained, show bedding parallel laminations, but disseminated and fracture filling ores also occur.

Tynagh

This deposit was discovered in 1961 as a result of soil geochemistry and E.M. surveys. Subsequently, drilling outlined a primary orebody containing approximately 8.5×10^6 tonnes of 3% Pb, 3.2% Zn, 0.3% Cu and 34 g/t Ag, and a secondary orebody of 3.8×10^6 tonnes grading 9% Pb, 7.4% Zn, 0.6% Cu and 110 g/t Ag. The deposit is now worked out. The primary mineralisation occurs in carbonate reef-bank limestone which thins laterally into a banded hematite-chert unit. These rocks are overlain by argillaceous pyritic limestone. The mineralisation occurs in three orebodies, namely: (1) residual cavity fills of Tertiary age; (2) massive steeply dipping orebody close to the Tynagh Fault; (3) a bedded orebody. The ore minerals are sphalerite, argentiferous galena, chalcopyrite, tennantite, pyrite, marcasite and barite. Secondary minerals include cerussite, smithsonite, malachite, azurite, native Cu and Ag. Ore textures vary from fine bedding-parallel laminations to disseminations and fracture filling.
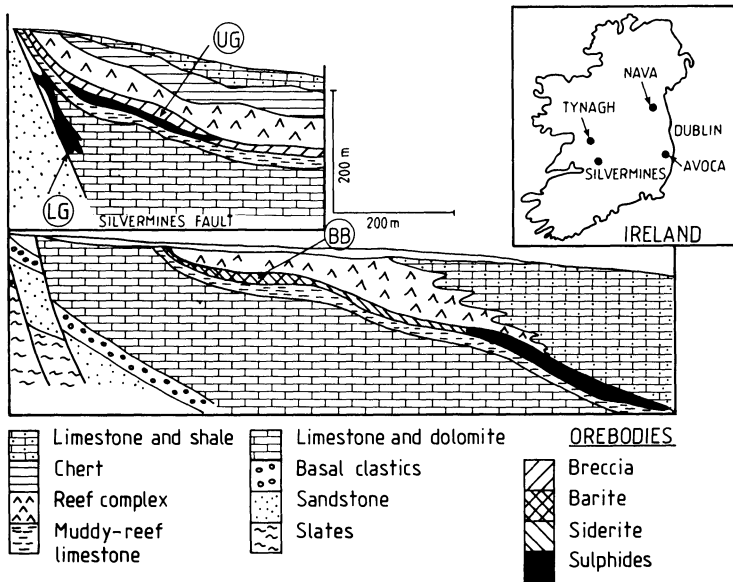
Fig. 14.6. Schematic cross-sections of Lower and Upper G orebodies (*LG* and *UG* respectively) and Ballynoe barite body (*BB*) at Silvermines. *Inset* shows location of main Irish base metal deposits (After Dixon 1979)

Silvermines

The Silvermines deposits are located south of the town of Nenagh. The district has a history of mining dating to the 17th century. In the 1960s geochemical and I.P surveys followed by drilling located a number of orebodies. The "upper G and B" orebodies combined contained approximately 13×10^6 tonnes grading 8.3% Zn, 2.4% Pb and 28 g/t Ag. The B orebody grades laterally into the Ballynoe barite deposit, where the fossil pyrite chimneys were discovered. The "lower G" orebody contained approximately 2×10^6 tonnes at 4.5% Pb, 3.4% Zn and 39 g/t Ag. Schematic cross-sections of the Silvermines orebodies are illustrated in Fig. 14.6. The ore mineralogy consists of sphalerite, galena, pyrite, marcasite and barite. The upper G and B orebodies consist of stratiform fine-grained massive sulphides with laminated and colloform textures. The lower G orebody consists of massive, coarse-grained sulphides with brecciated and open-space filling textures. The footwall limestone is dolomitised and brecciated, whereas the overlying bank carbonates contain disseminated mineralisation.

14.5 Models of Ore Genesis for the MVT, Alpine and Irish Types

There are a number of conceptual models that attempt to explain the origin of stratabound carbonate-hosted base metal deposits. As mentioned earlier, the timing of introduction of ore solutions in relation to the deposition of the host carbonates is
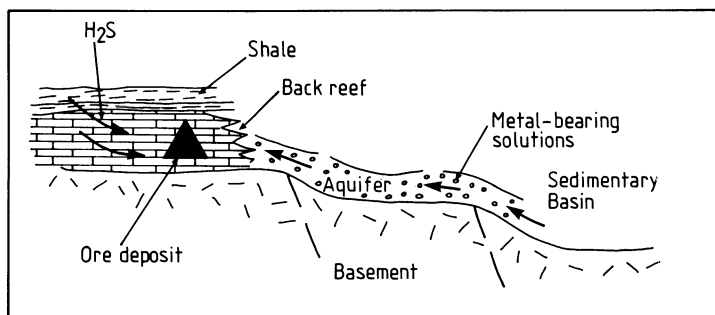
Fig. 14.7. Model to explain the origin of some carbonate-hosted base metal deposits. Pore and/or connate waters are squeezed out of a sedimentary basin during compaction and diagenesis. The fluids become metal-bearing solutions as they travel along an aquifer. Metals are precipitated at a favourable site of deposition, possibly as a result of encountering a reducing environment due to the presence of H_2S; drawing not to scale. This figure combines the models of Sverjensky (1986) and Anderson (1983)

one of the key issues – at least in the case of the Alpine deposits where, locally, ore textures suggest a syngenetic origin. Nevertheless, most models envisage an epigenetic origin for the mineralisation. One model looks at the formation of brines during compaction, dewatering and diagenesis of sediments in an evolving sedimentary basin. The brines include formation or connate waters, which would migrate from the centre towards the edges of the basin. Migration of brines towards basin margins is thought to occur under the influence of hydraulic gradients, which may be established in response to tectonic movements (Hearn et al. 1987). This model is schematically illustrated in Fig. 14.7 (see also Fig. 3.14). Migration of fluids is reputed to occur along great distances by mechanisms of tectonic expulsion, following continental collision. This would result in the focusing of the fluids along thrust faults (Duane and de Wit 1988). Another model envisages that hydrothermal fluids would move along faults and are discharged on the sea floor where they precipitate sulphides, sulphates and oxides (see, for example, Figs. 3.16 and 3.17). The origin of the fluids in this case is more problematical, and a geothermal gradient, perhaps enhanced by a heat source, must be assumed. Equally problematical in both these models is the origin of the metals and that of S. In the European deposits, peculiar submicroscopic spherical structures called "peloids" occur associated with the mineralisation. In fact, peloids are predominantly composed of Zn-rich carbonate, siderite, silica, pyrite, sphalerite and galena. Detailed studies by Kucha et al. (1990) indicate that these peloids are formed through bacterial activity, and the authors suggest that the same bacteria may be responsible for converting sulphates into native S. Kucha et al. (1990) conclude that the mechanism of peloid formation might be significant for the genesis of carbonate-hosted base metal deposits.

In all cases, however, it is clear that the carbonate host rocks play a dual role in that they constitute both physical and chemical traps. Features such as basin morphology, paleotopographic highs, erosional surfaces and paleoaquifers are of particular significance for the origin of these deposits. In the case of MVT and

Alpine types especially, basement highs play an important role in localising the mineralisation. Thus, the main controlling parameters must include (1) carbonate lithologies, which provide suitable sites of ore deposition, and (2) paleogeographic features, such as basement highs and unconformities. An important prerequisite for the formation of a hydrothermal ore deposit is the permeability of the host rocks, which must allow the passage of the ore solutions. Dissolution, brecciation (karsting) and dolomitisation of the host carbonates are therefore important in this respect. Dolomitisation, discussed in Chapter 4, and silicification are characteristic features of the deposits in question. The term "dolomite" refers to the mineral species with the general formula $CaMg(CO_3)_2$, and a rock with greater than 50 % dolomite is referred to as "dolostone". Dolostones are the favoured host rocks for the stratabound carbonate-hosted base metal deposits. Evaporite basins, if present, may be important sources of both Mg and S. Evaporation of sea water causes precipitation of gypsum ($CaSO_4 . 2H_2O$), resulting in the removal of Ca, and thereby increasing the Mg^{2+}/Ca^{2+} ratio and migration of Mg, which may induce dolomitisation. Hydrothermal dolomite, or late dolomite cement (LDC), however, is also thought to form from the migration and effervesence of CO_2-rich basinal fluids interacting with carbonate rocks (Leach et al. 1991). These authors studied fluid inclusions in LDC materials from the Ozark region (Mississippi Valley), where LDC is associated with sulphides in fractures and solution collapse structures.

Apart from dolomitisation, other alteration features associated with carbonate-hosted Pb-Zn deposits are silicification and K-alteration. The latter has been suggested by Hearn et al. (1987) on the basis of fluid inclusion studies of overgrowths on detrital K-feldspars and quartz grains in unmineralised rocks.

14.5.1 Karsting

This is an important process of ground preparation for the localisation of most carbonate-hosted mineral deposits. Karsting provides excellent conduits and receptacles for the introduction and movement of hydrothermal solutions, and the precipitation of ore materials, respectively. The process of karsting is due to the dissolution and transport of Ca carbonate by meteoric waters in terranes predominantly underlain by carbonate rocks. The term karst is derived from the Carso region in the Istria peninsula, a border area between Italy and Yugoslavia, where the phenomenon is especially well developed. Ca carbonate which is normally insoluble in pure water, becomes soluble in meteoric water enriched in CO_2, according to:

$$CaCO_3 + H_2O + CO_2 \rightarrow Ca^{2+} + 2HCO_3^-.$$
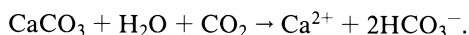
This reaction is responsible for the formation of caves, subterranean chambers and channels, created by the action of the CO_2-enriched meteoric waters along joints and fractures, which become progressively enlarged through the dissolution of the carbonate by the descending waters. In this way, a water solution is formed which contains the ions Ca^+ and HCO_3^-. On release of CO_2 (i.e. by evaporation), the above reaction is reversed and $CaCO_3$ precipitated to form the spectacular

stalactites (conical constructs hanging from the roof of a cave) and stalagmites (constructs rising from the floor), cascades and myriads of other forms. The deposits thus formed are known as speleothems (Esteban and Klappa 1983). In the Istria region entire drainage systems have gone underground, as, for example, in the Timavo and Postumia districts. In general, karsting phenomena operate in the vadose zone, but, in the specific case of carbonate-hosted base metal deposits, dissolution of the carbonate lithologies may also have been achieved by the action of hot waters in the vadose zone, perhaps with a contribution of basinal waters (Misiewicz 1988). It has been proposed that the term "hydrothermal karsting" be adopted to explain and describe the brecciation and open-space filling of carbonate rocks by ore-related brines (Ohle 1985). The idea is that ground preparation of the host carbonate rocks is the result not only of karsting but also of chemical brecciation and dissolution, or hydrothermal karsting. The latter would be aided during tectonic compression (Ohle 1985).

14.5.2 Nature and Temperature of Fluids, Source of Metals and Sulphur

Fluid inclusion studies of sphalerite and calcite in MVT deposits indicate that the fluids have temperatures in the order of 50 to 200°C, more commonly from 95 to 120°C. The fluids are Na-Ca-Cl sulphur-deficient brines, with salinities of approximately 20–30 wt% NaCl equivalent. Fluid inclusion studies of Irish-type deposits, however, indicate higher temperatures (approximately 150–260°C).

Pb isotope studies of Viburnum Trend deposits show an anomalous radiogenic character of Pb, and it is postulated that the metal was derived from the Lamotte Sandstone, with lesser amounts having been leached from the Precambrian basement rocks and perhaps the offshore facies of the Bonneterre Formation (see Chap. 2). At Pine Point, isotope studies suggest a sea-water origin for the S. The similarity in the isotopic composition of S of the sulphides with that of anhydrite from the Devonian evaporites in the Elk Point basin has led to the conclusion that sulphates in the evaporite sequence are reduced to H_2S or S by anaerobic bacteria, and that this S combines with the metals to precipitate the sulphide mineralisation (Sverjensky 1986). Though controversial, the weight of the evidence appears to favour chloride complexing and pH values less than neutral for the transport of Pb and Zn at low temperatures. The acidic pH is required if the reduced S model is accepted (Sverjensky 1986). Organic ligands have also been considered, as their presence has been ascertained in the brines of oil fields (Giordano 1985). At Pine Point the metals may have derived from the carbonaceous shale of the MacKenzie basin. Metals, possibly contained as adsorbed ions on clay minerals, or even organic matter, could have been released during burial diagenesis and introduced into highly saline pore fluids that are low in S. The low S content is possibly the result of fixing by Fe to form pyrite or marcasite during diagenesis. Movement of the metal-bearing brines occurs along permeable horizons – a sandstone unit, for example – and updip, towards the edges of the basin and the topographic highs, against which carbonate reefs are formed (Fig. 3.14). In this environment there may be an influx of H_2S derived either from organic material in the carbonates or

from overlying shales. The H_2S fluids mix with the metalliferous brines to precipitate sulphides in suitable traps within the carbonate lithologies. This concept is illustrated in Fig. 14.7. A recent model to explain Pb-Zn-Ba mineralisation in the carbonate rocks of Nova Scotia is advocated by Ravenhurst et al. (1989). In this model the authors envisage overpressured mineralising fluids escaping from deep within the basin, breaking through an evaporite seal. The fluids would move updip, towards the basin edge, to precipitate sulphides in a barrier reef on a basement high, and along active faults, where they could discharge as hot springs on the sea floor.

In summary the weight of evidence for the origin of the hydrothermal fluids favours connate (or formation) waters trapped in a sedimentary basin undergoing compaction. During compaction increasing lithostatic loading reduces the porosity and expells water towards regions of lower pressure (the margins of the basin). This process is essentially a mechanical one in that only pore fluids and low-temperature clay breakdown are involved. By contrast, metamorphic fluids derive from high-temperature devolitilisation reactions in which water, and other volatiles, bound in mineral lattices are released (Chap. 15). Hydrothermal fluids generated during basin dewatering have a low pH and high salinities, and they can leach metals from the sandstone and argillaceous layers (Pb and Zn respectively).

14.6 The Carbonate-Hosted Pb-Zn-Cu-Ag and V Deposits of the Otavi Mountain Land, Namibia

The carbonate-hosted mineral deposits of the Otavi Mountain Land present an interesting case of multistage processes of ore genesis. As explained later, the nature and character of these deposits suggest they are the result of a number of mineralising episodes. At least three episodes are recognised. The first involved low-temperature and high-salinity Cu-poor basinal fluids, which formed MVT deposits. The second episode appears to have involved Cu-rich fluids with higher temperatures and salinities. The third, and last, episode is related to recent weathering processes which resulted, locally, in the chemical re-distribution of the ores deposited during the first two episodes.

In this section we discuss the geology and mineralisation of the Otavi Mountain Land, and take a look at three of the most important representative deposits, namely: Tsumeb, Kombat and Berg Aukas. A discussion on the multistage aspects of their genesis concludes the chapter and introduces the reader to the topic of the following chapter.

The Otavi Mountain Land, covering approximately 10000 km^2, is a mineral province located on the eastern end of the Northern Carbonate Platform of the Damara orogen (see Chap. 7). In the Otavi Mountain Land there are over 600 occurrences of Cu-Pb-Zn mineralisation, some of which have associated Ag and V. The largest deposits in the area are Tsumeb, Kombat, Berg Aukas and Abenab (Innes and Chaplin 1986; Lombaard et al. 1986; Misiewicz 1988; Fig. 14.8). Tsumeb and Kombat are the only mines currently in operation. Tsumeb is the largest deposit
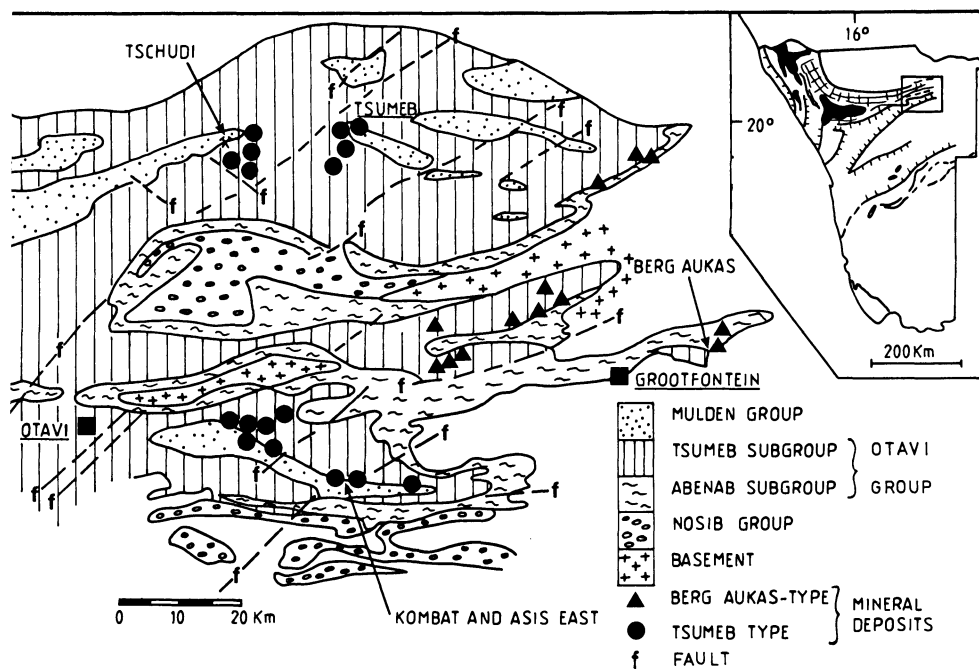
Fig. 14.8. Simplified geology of the Otavi Mountain Land and distribution of main base metal mineral deposits. Based on information provided by Tsumeb Corporation Ltd. *Inset* shows position of the Northern Carbonate Platform, paleorifts and basement highs (*black*) (see also Fig. 7.4, Chapter 7 and references therein). Otavi Mountain Land is outlined by the *small square*

Table 14.1. Approximate tonnage and grade for the Tsumeb, Kombat and Berg Aukas deposits. At Tsumeb other economically important commodities are Cd, Ge and As (After Misiewicz 1988)

Mine	Tonnes ($\times 10^6$)	Cu%	Pb%	Zn%	Ag g/t	V_2O_5
Tsumeb	27	4.3	10	3.66	> 100	–
Kombat	10	2.7	1.9	–	26	–
Berg Aukas	3.2	–	4.5	17	10	0.77

and world-renowned for the variety and beauty of its minerals. Tonnages and grades of Tsumeb, Kombat and Berg Aukas are given in Table 14.1.

The localisation of these carbonate-hosted deposits was largely controlled by karst structures, faults and shear zones as well as joints and fractures. Karst topography developed at two levels in the stratigraphy of the Mountain Land with both levels being marked by a disconformity. Information and data given in this section are taken from the authors above, mine geologists at Tsumeb and Kombat

and unpublished material from the present author's experience of the Otavi Mountain Land.

14.6.1 Geology, Structure and Metamorphism

Rocks of the Otavi Group were deposited in a miogeosynclinal environment. Overlying the Nosib Group, they also, in places, lie directly on pre-Damara basement rocks (Grootfontein Complex), and are overlain by the Mulden Group – a molasse-type sedimentary sequence. Basement lithologies include granitic rocks and a poorly exposed mafic layered complex (Grootfontein Mafic Body) in which a common rock type includes hornblende-pyroxene gabbro. It is significant that these mafic rocks locally contain phenocrysts of blue opaline quartz, thought to be the result of interaction with hydrothermal fluids. The Otavi Group is divided into the Abenab and Tsumeb Subgroups which are separated by a disconformity. The Abenab subgroup includes the Berg Aukas, Gauss and Auros Formations. The Berg Aukas Formation represents a transition facies from the coarse-grained clastic sediments of the Nosib Group to the predominantly carbonate depositional environment of the Otavi Group. Main lithologies include light grey to dark grey laminated dolomites with occasional stromatolitic horizons and interbedded arkose, greywacke and shale. The Gauss Formation is characterised by a thick succession of massive fine-grained dolomite, with oolitic cherts towards the top. The Auros Formation includes dark grey to black, thinly bedded limestone and olive-green shale, overlain by grey to white massive dolomite with distinctive marker horizons of stromatolites. The stromatolitic reefs are thought to have developed adjacent to cratonic areas prior to a period of crustal disturbance, erosion and the deposition of the Chuos Formation.

The Tsumeb Subgroup begins with the Chuos Formation, overlain by a thick (approximately 3000 m) sequence of limestone and dolomite, which is bedded and laminated to massive, locally intercalated with cherts, stromatolitic and oolitic beds. The rocks of the Tsumeb Subgroup are, from bottom to top, informally labelled T1 to T8, and subdivided into the Chuos, Maieberg, Elandshoek and Huttensberg Formations. The Chuos Formation (T1) consists predominantly of diamictites with lenses of dolomite and schist. Sorting of clasts is very poor and an individual clast may reach a diameter of 1 m. The clast population includes dolomite, limestone, quartzite, basement granite and gneiss. The origin of the Chuos Formation is controversial but it has been described as a tillite, a fluvioglacial deposit, debris or mass-flow deposit. Evidence from elsewhere, however, supports a depositional model involving continental to shallow glacio-marine conditions (Hoffmann 1990). The Maieberg Formation consists of a thick carbonate sequence containing the T2 and T3 zones. T2 includes laminated limestone and marl with abundant breccias and limestone conglomerates. The T3 zone consists of finely laminated grey dolomites. The Elandshoek Formation includes the T4 and T5 zones. T4 consists of massive light grey dolomite with oolitic and stromatolitic beds towards the top. It includes a stratabound zone of brecciation typified by a network of silica veinlets, subrounded blocks of dolomite within a matrix of silica and sparry calcite, This

breccia zone is regionally extensive and is considered as a paleoaquifer. Along the northern flank of the Otavi Syncline the T4 dolomites are intensely jointed and replaced by jasperoidal material. Zone T5 consists of light grey, thinly bedded dolomite with occasional oolitic lenses. The Huttenberg Formation includes zones T6, T7 and T8. Zone T6 is a light grey bedded dolomite with chert lenses and oolitic beds towards the top. Three stromatolitic horizons are well developed and used by local geologists as marker horizons. In the Tsumeb area the T6 zone also contains a 10-m-thick zone of alteration and brecciation, and it too is interpreted as a paleoaquifer (Lombaard et al. 1986). Zones T7 and T8 consist of sedimentary sequences of lagoonal facies, including algal beds, oolitic, pisolitic and fetid carbonates. At Tsumeb a prominent marker horizon, known as the Augen Marker, comprises calcite nodules which are interpreted as pseudomorphs after anhydrite (Lombaard et al. 1986).

The Mulden Group is a syn-tectonic molasse-type sedimentary sequence, deposited over a wide area covering the Northern Platform as far west as the Kaoko Belt towards the Atlantic coast (see Fig. 7.4). It disconformably overlies the Otavi Group rocks and is subdivided into the Tschudi and Kombat formations. The former includes red-brown to grey, massive to thinly bedded feldspathic sandstone, greywacke, argillite and conglomerates at the base. The Kombat Formation consists mainly of phyllite, arkose and pebbly sandstone near the base.

The regional structure of the Northern Platform and Otavi Mountain Land is characterised by east-west-trending F1 folds. A second folding phase (F2) resulted in northward-verging recumbent folds. Near Kombat, the southern limb of the Otavi Valley Syncline is locally overturned with northward thrusting. Mild compression along east-west trends resulted in the formation of doubly-plunging synclines. A number of north-east-trending faults and fractures occurs throughout the area, the most important being the Tsumeb West and Kombat West faults. These faults may be related to the major north-east-trending lineaments which characterise the Central Zone of the Damara orogen (Chap. 7).

The Otavi Mountain Land was affected by metamorphism ranging from lower greenschist facies in the Kombat area, to zeolite and prehnite-pumpellyite facies for the Mulden group rocks. The metamorphic gradient decreases northwards from the southern flank of the Otavi Valley Syncline, coinciding with decreasing deformation.

In the Tsumeb Syncline there is evidence for a paleokarst surface, which was probably formed during the hiatus before sedimentation of the Mulden Group commenced (Misiewicz 1988). In fact, the origin of the Tsumeb pipe (to be discussed later) is attributed to a chimney-like structure formed by dissolution of carbonate during this karsting event. The solution collapse of the Tsumeb pipe is thought to have occurred in the phreatic zone at the intersection of the karst structure with an aquifer (North Break Zone). Karst structures are also well developed at the top of the Abenab Subgroup, but their nature and timing are less well constrained. The mineralised Abenab breccia pipe is situated on the Abenab fault, which is a bedding-plane thrust along the contact between massive dolomite and laminated limestone. According to Misiewicz (1988), this pipe – one of many along the fault – post-dates the structure, so that solution brecciation must therefore have followed tectonism

Table 14.2. Karsting events in the Otavi Mountain Land (After Misiewicz 1988)

Karst event	Period	Remarks
I	Post-Huttemberg	Uplift prior to Mulden initiates karsting of the exposed surface. Possible hydrothermal karsting at Tsumeb.
II	Syn-tectonic	Faulting and fracturing at Abenab and Berg Aukas, provide loci for hydrothermal karsting.
III	Post-Damara	Oxidation and re-mobilisation of ore. Late-stage fluids move into fracture to form superficial enrichments.

in the area and a karst chimney formed by solution collapse, prior to the entry of the ore solutions. Karsting events in the Otavi Mountain Land are listed in Table 14.2.

14.6.2 Mineralisation

The distribution of carbonate-hosted hydrothermal mineral deposits in the Otavi Mountain Land is shown in Fig. 14.8. There are two broad types of mineralisation, namely: (1) Tsumeb-type and (2) Berg-Aukas type. The former (exemplified by the Tsumeb and Kombat deposits) is characterised by complex ores containing Cu, Pb, Zn, Ag, As, Ge, Cd and Ga. The ore minerals are generally disseminated in a variety of loci including pipes, solution breccias, shear zones, dilation fractures and breccias derived from hydraulic fracturing. The orebodies which are not stratabound are generally confined to the upper part of the Tsumeb Subgroup and have a close spatial relationship with the disconformity which separates the Tsumeb Subgroup from the Mulden Group. The most significant deposits are located close to northeast-trending fractures and faults regarded as re-activated basement structures. The Berg Aukas type is characterised by ores containing Pb, Zn and V, and is very similar to the Pb-rich members of the MVT deposits. They have little or no Cu, and although the sulphides are enriched in Ag, Ge, Ga and Cd, the abundance of these trace elements is typically much less than the sulphides of Tsumeb-type mineralisation. These deposits are generally confined to the Abenab Subgroup and the lower part of the Tsumeb Subgroup. Also, they have a close spatial relationship with the basal unconformity between the Abenab Subgroup and the Nosib Group, or basement rocks (Grootfontein High). The two principal deposits – Berg Aukas and Abenab – while occurring at different stratigraphic levels, lie at approximately equal distances above the unconformity. However, a number of Berg Aukas-type deposits occur above the Abenab-Tsumeb Subgroups disconformity and contain minor Cu. The mineralisation occurs in breccia bodies and may be stratabound or discordant. Brecciation and paleokarsting were important in the localisation of the orebodies.

14.6.3 Tsumeb

The Tsumeb polymetallic Pb-Cu-Zn-Ag orebody is a pipe-like structure, situated on the northern side of a doubly-plunging synform within dolomitic rocks of the upper Tsumeb Subgroup. Details of the Tsumeb deposit can be found in Lombaard et al. (1986). A cross-section of the Tsumeb orebody is shown in Fig. 14.9E. The orebody is defined by underground drilling and chip sampling. Approximately 500 000 tonnes of ore are mined a year by cut and fill methods. Ore reserves are calculated at a 2% Cu cut-off (or 4% Pb).

The Tsumeb pipe penetrates zones T8 to at least T5, and is defined by the distribution of mineralisation, dolomite breccia, feldspathic sandstone (formerly known as pseudo-aplite), alteration and arcuate fracturing. The feldspathic sandstone, found throughout the known vertical extent of the pipe (1716 m), is correlated with the Tschudi Formation which disconformably overlies the Otavi Group. The plunge of the pipe is approximately perpendicular to bedding in the lower levels and subparallel to bedding in the upper levels, and was controlled by the reaction of competent dolomites and incompetent limestones to folding. Thus, bedding slip was more pronounced in limestone lithologies of the upper levels, with the result that the pipe structure was dragged along the slips. For this reason the plan shape of the pipe is elliptical in undeformed areas and lensoid where bedding slip is prevalent.

Two main types of solution-collapse breccia occur in the pipe. One is attributed to solution by circulating meteoric water in folded, cleaved and fractured dolomite above and below a prominent zone of brecciation, known as North Break, and interpreted as a paleoaquifer. This channel eventually breached the basin floor in which deposition of Tschudi sediments was taking place, thus allowing the influx of unconsolidated arenaceous material to form the feldspathic sandstone. The second type of breccia resulted from subsequent solution activity associated with ascending hydrothermal fluids along fracture cleavages. The hydrothermal event induced arcuate collapse fractures in the breccia and adjoining bedded dolomite as well as alteration of the rocks. Hydrothermal alteration consists of calcitisation, which within the pipe extends upwards to about 570 m below the present surface, reaching a maximum intensity at approximately 1120 m depth. Below this level silicification becomes the predominant alteration type. Evidence indicates that regional deformation was active during the evolution of the pipe structure and the mineralising event was more or less synchronous with waning tectonic activity. The development and evolution of the Tsumeb pipe are illustrated in Fig. 14.9.

Mineralisation

The hypogene ores at Tsumeb are epigenetic, hydrothermal-replacement and fracture-filling type. The main ore minerals are galena, tennantite, sphalerite, chalcocite, bornite, pyrite and enargite. Lesser quantities of, and erratically distributed, sulphides and sulphosalts of Ge, Ga, V, Sn, and W are also present. Massive ore is concentrated at the periphery of the deposit, or as manto-like bodies in bedded dolomite. Disseminated and stringer ores occur in the deeper part of the
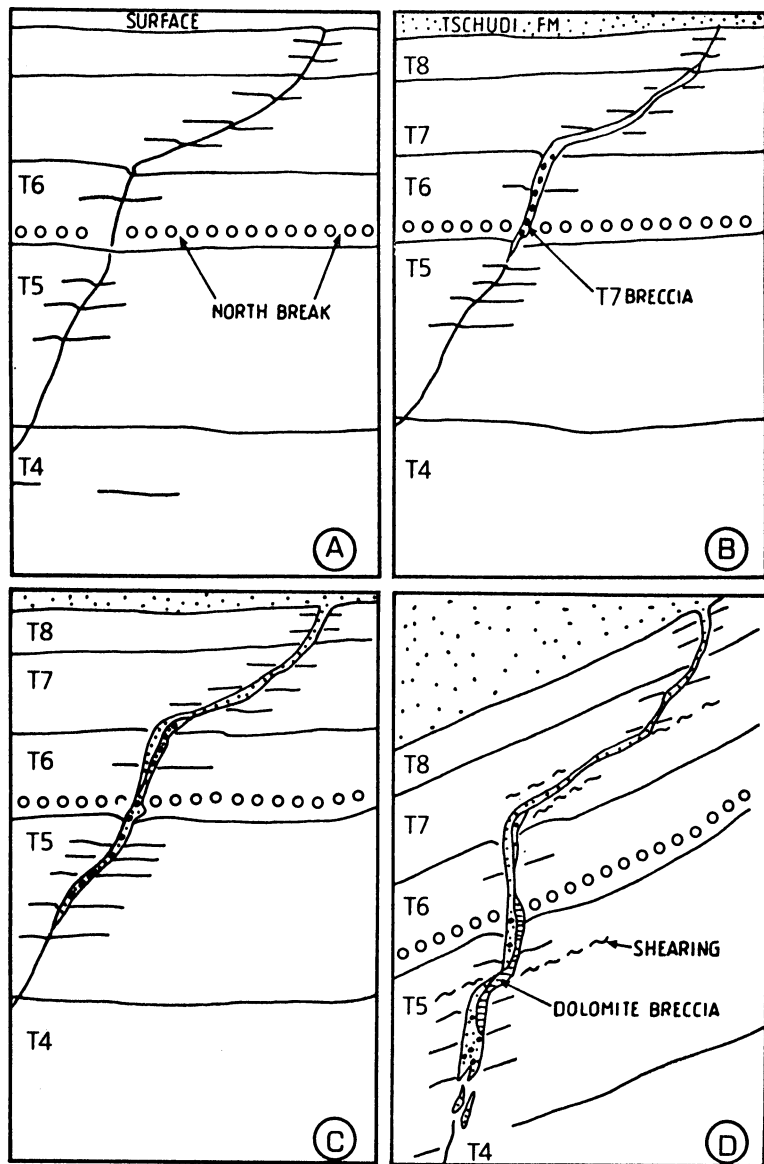
Fig. 14.9A–E

pipe. The manto sulphide bodies, which are of high grade, are thought to have formed by re-mobilisation of sulphides into tensional fractures during folding. Massive sulphides in the pipe display minor folding and textures indicative of deformation and partial annealing. Lombaard et al. (1986) report that the mineralisation was formed at a temperature range of 250–230°C and at about 700
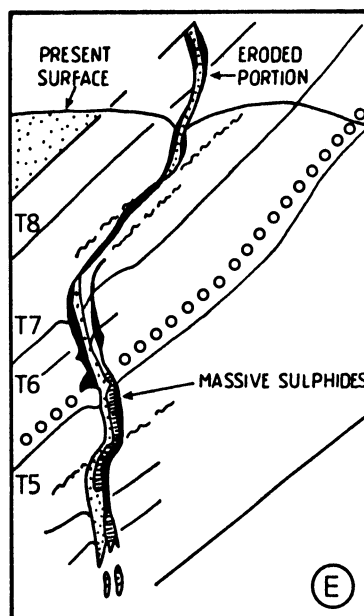
Fig. 14.9A–E. Schematic cross-sections depicting the possible evolution of the Tsumeb pipe and associated mineralisation. The model is after A.F. Lombaard, A. Gunzel, J. Innes and L. Kruger (Tsumeb Corporation Ltd. 1984, Mine handout). Drawings are not to scale; the pipe, however, is known to extend to a depth of more than 1700 m. **A** An incipient shear fracture being developed in carbonate lithologies of zones T4 to T8. In **B** dissolution of carbonate by circulating meteoric water occurred above the North Break aquifer. This resulted in a solution cavity which was infilled with dolomite fragments, mainly from the T7 zone. This formed a dark dolomite breccia. In **C** dissolution of carbonate material proceeded downward as well as upward, breaking through into a sedimentary basin in which unconsolidated sandy and arkosic material of the Tschudi Formation (Mulden Group) was being deposited. The Tschudi Formation material infilled the karst cavity above the North Break, while further down it mixed with constituents of the dark dolomite breccia. **D:** Regional folding and bedding plane shears modify the geometry of the pipe. Ingress of hydrothermal fluids occurred at approximately this time and resulted in alteration (calcitisation and silicification), dissolution, formation of collapse breccia (dolomite breccia), and arcuate fractures. **E:** Ore solutions ascended into the pipe resulting in sulphide deposition, which overprinted the last stages of rock alteration and deformation

bar pressure. The age of the deposit is approximately 580–550 Ma (Allsopp et al. 1981; Lombaard et al. 1986).

Secondary, oxidised ores are of economic importance to a depth of approximately 300 m, and again from 750 to 1160 m, in the zone of intersection between the North Break paleoaquifer and the pipe. At surface, the North Break is visible as a solution-collapse zone with a vanadiferous calcrete infill. The North Break is associated with Cu, Pb and V mineralisation, and characterised by silicification, calcitisation, ferrusiginisation and Mn oxides alteration. The supergene ore minerals include native Cu, native Ag, cuprite, azurite, malachite, cerussite, smithsonite, anglesite, duftite, chrysocolla and dioptase. More than 200 mineral species have been recorded, of which at least 30 are unique from this deposit. The
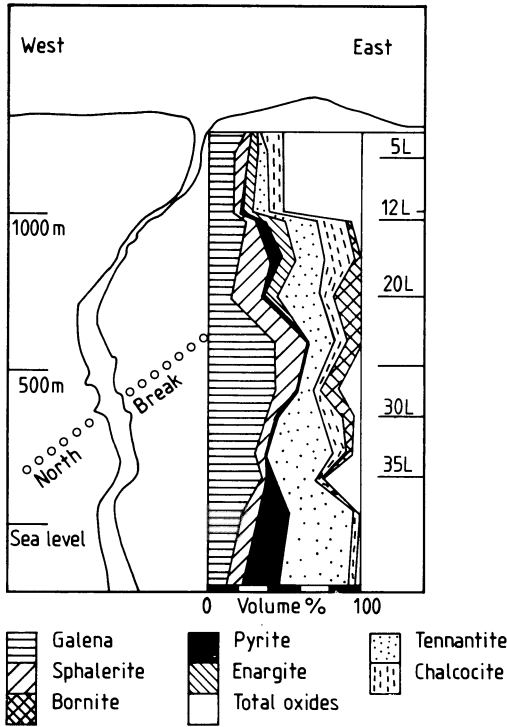
Fig. 14.10. Vertical mineral zonation in the Tsumeb pipe. Chalcocite includes the hypogene and supergene phases as well as digenite (After Lombaard et al. 1986)

feldspathic sandstone infill is also mineralised and locally calcitised. The orebody is vertically and laterally zoned with respect to metal abundance and ore mineralogy. The vertical distribution of the principal ore minerals is illustrated in Fig. 14.10. Ag is mainly associated with tennatite and increases in grade with depth at an approximate rate of 20–40 g/t per 1% Cu.

Other Mineral Prospects in the Tsumeb Area

A number of uneconomic or subeconomic prospects occur south and west of Tsumeb (Tsumeb-Uris belt) (Fig. 14.8), of which the most important are Tsumeb West, Domingo, Alt Bobos, Karavatu, Uris and Tschudi. The Tsumeb West pipe, located some 3 km from Tsumeb, is characterised by a similar feldspathic sandstone plug which is in part mineralised. Mineralisation in the Domingo prospect, on the southern flank of the Tsumeb Syncline, is associated with zones of calcitised chert and silicified oolitic dolomite in the T8 unit. Lenses of calcitised chert are conformable to bedding and contain disseminated chalcocite, bornite, galena and sphalerite. Limestone and dolomite lower down in the sequence (T7 unit) are dark in colour and thought to have been deposited in a back-reef environment. The "augen-marker" horizon in this sequence is interpreted as part of an evaporite deposit, in which, as mentioned previously, nodules represent anhydrite replaced by calcite.

The Alt Bobos prospect is located about 20 km west of Tsumeb along the southern flank of the Tschudi Syncline. Mineralisation consists of chalcocite and malachite and is associated with calcitised and Mn oxide-altered T8 dolomite. Close to Alt Bobos is the Karavatu prospect, in which conformable jasperoid horizons are enriched in Cu, Pb and V. Approximate grades of the deposit, as estimated from past mining activity, are 3–4% Cu, 7–8% Pb, and 3% V_2O_5. In the Uris area, a few kilometres west of Karavatu, mineralisation is associated with a calcitised pipe in T5 dolomite. This pipe, which does not have a feldspathic sandstone infill, extends to a depth of 300 m and was mined in the past. A recent drilling programme in this area has outlined 100000 tonnes of ore grading 2.5% Cu, with minor Pb, Zn and V. The Tschudi prospect – north of Uris – occurs in Mulden Group arenites (Tschudi Formation). The Tschudi Cu-Ag mineralisation consists of a stratabound body containing disseminated sulphides, vertically zoned from top to bottom in the following order: pyrite, chalcopyrite, bornite and chalcocite. The mineralisation is hosted in dark grey greywacke and arkose containing carbonaceous matter. The footwall rests on a basal conglomerate, locally infilling karst cavities developed in the underlying T8 zone dolomite. In places the sulphide mineralisation extends into the T8 dolomite in the vicinity of the karst structures. The Tschudi Cu-Ag deposit is thought to be of the Zambian Copperbelt type and to have originated from Cu-bearing fluids generated during compaction and diagenesis of sediments and subsequent upward replacement of early diagenetic pyrite. This would be reflected in the increasing upward Fe content of the sulphide zones from chalcocite at the footwall to pyrite in the hangingwall.

With the exception of the Tschudi Cu-Ag prospect, the carbonate-hosted deposits situated in the Tschudi Syncline are thought to have formed in stromato-
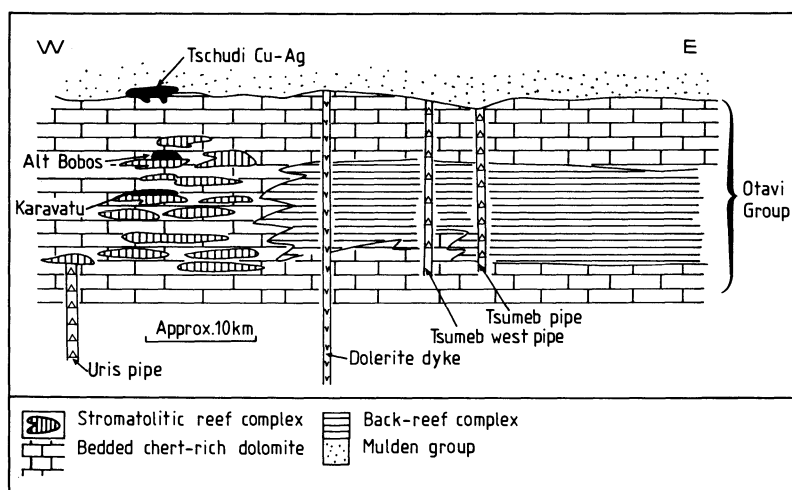
Fig. 14.11. Schematic section across the Tsumeb area showing the spatial relationship between mineralisation and facies changes in the carbonate rocks. Drawing is not to scale in the vertical dimension. Dyke emplacement is parallel to a regional lineament and/or fault zone in the basement; the same structure may have locally controlled facies variations and mineral deposition; cf Fig. 14.5

litic reef complexes west of a major back-reef complex in which the Tsumeb pipe is located. Figure 14.11 illustrates this relationship between carbonate facies and mineralisation in the Tsumeb-Uris belt.

14.6.4 Kombat

In the Otavi Valley, south of Tsumeb, are numerous carbonate-hosted mineral deposits including Baltika, Central, Auros, Kupferberg, Gross Otavi, Kombat and Guchab (Fig. 14.9). All occur along the northern limb of the Otavi Valley Syncline. The only producing deposit is Kombat, which includes at least five orebodies, namely: Asis East, Kombat East, Kombat Central, Kombat West and Asis West. A detailed account of the Kombat mineralisation can be found in Innes and Chaplin (1986).

The Kombat orebodies are developed in the T7 and T8 zones at and along the contact with shales and phyllites of the Mulden Group. The orebodies are generally associated with faults and fractures along this contact. As is the case for Tsumeb, feldspathic sandstone material from the Tschudi Formation is found associated with the mineralisation. The contact between the phyllites and dolomites dips 40 to 80° to the south, and the main ore-localising features are F1 monoclinal flexures – locally known as "roll structures" – which are characterised by fissures in the footwall dolomite. The fissures strike northeast and contain lenses and stringers of the feldspathic sandstone which was locally deposited along the phyllite-dolomite contact. A schematic cross-section of a Kombat orebody is illustrated in Fig. 14.12A, whereas a three-dimensional view of a roll structure and associated mineralisation is shown in Fig. 14.12B. The origin of these roll structures is not clear, but mine geologists have attributed them to flexuring, parasitic folding or to thrust tectonics (A. H. Maclaren pers. comm. 1990). Significantly, the area is cut by numerous northeast-trending faults, which parallel a major northeasterly fracture, thought to be related to an original rift shoulder. The Kombat West fault is post-mineralisation; there are, however, many subsidiary faults between this and the Asis East fault which may be pre-mineral and may have played a role in ground preparation, facilitating access of the ore solutions.

Mineralisation

Mineralisation occurs as fracture filling and as replacements in the dolomite and feldspathic sandstone rocks. A feature of the orebodies is their brecciated nature. The mineralisation consists of sulphide bodies and overlying Fe-Mn bodies. Primary sulphides include bornite, chalcopyrite, galena, tennantite and sphalerite. In the Asis West orebody, supergene sulphides are of economic importance and include chalcocite, cuprite, malachite, cersussite and mottramite. The sulphide orebodies are characterised by a fairly well-defined zonation; they are enriched in Cu in the centre and become Pb-, Zn- and pyrite-rich towards the periphery. Thus, a zonation of ore minerals, from the core towards the periphery, consists of bornite, chalcopyrite, galena, sphalerite and pyrite. Ag is associated with Cu and grades at

Fig. 14.12. A Idealised cross-section of a Kombat orebody, showing stratigraphic relationships and position of Fe-Mn and sulphide zones; drawing not to scale. B Block diagram illustrating "roll structure" and associated mineralisation; the structure is bound by later northeast-trending faults. Structural evidence indicates that the Fe-Mn deposition was probably taking place at the same time as early Mulden Group sedimentation, whereas sulphide deposition was in progress during the development of the roll structure which enhanced the movement of the hydrothermal fluids
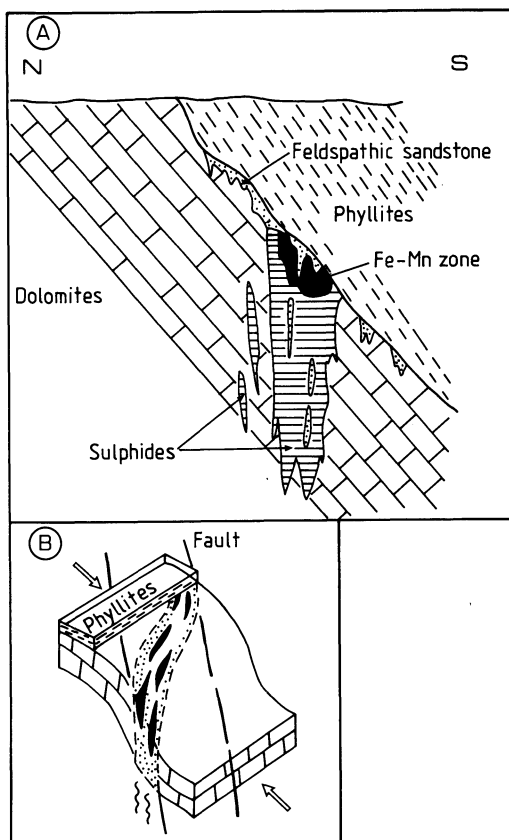
approximately 10 g/t for every 1% Cu. The ore is defined by a 1% Cu, or 3% Pb, cutoff. The average grade of ore mined in a rich zone at Asis West is 4.5 % Cu, 2.3% Pb, and 42 g/t Ag. Approximately 25 000 tonnes of ore are milled each month. Ore reserves are extremely difficult to determine because of the irregular shape of the orebodies, and for this reason, reserves are continuously calculated as new ore is delineated by underground drilling. Fans of boreholes are drilled every 15 m along drives in order to define the orebody.

The Fe-Mn bodies are generally separated from the sulphide ore by magnetite and hematite. The Fe-Mn ores have sharp boundaries and display pre-tectonic layering. They comprise oxide, silicate and carbonate facies as well as metasomatic borate and arsenate assemblages. The mineralogy of the Fe-Mn bodies is complex and some 48 Fe-Mn minerals have been identified. Some of the minerals present in the layered Fe-Mn ores include hausmannite, jacobsite, hematite, magnetite, barite, calcite, tephroite (Mn_2SiO_4), alleghanyite $[Mn_5(SiO_4)_2(OH)_2]$, pyrochroite $[Mn(OH)_2]$, mangonosite (MnO), galaxite $(MnAl_2O_4)$, glaucochroite $(CaMnSiO_4)$, spessartine, andradite and vesuvianite.

The Kombat orebodies are associated with hydrothermal alteration forming haloes up to 50 m away from the mineralisation. Alteration consists of calcitisation

and re-crystallisation of the dolomite lithology, with coarsening of the carbonate grains and local replacement by Mn oxides. Calcitisation is generally fracture-controlled and is an important exploration guide.

Fluid inclusion studies indicate a temperature of 300 °C for early sphalerite and a range of 280–200 °C for the main period of Cu mineralisation. On the basis of S-isotopic data (δ^{34}S = −0.8 per mill) and the presence of elements such as B, Li and Be, Innes and Chaplin (1986) propose a magmatic affinity for the Kombat mineralisation. Pb-isotope dating by Allsopp et al. (1981) reveals an age of 600–550 Ma for the mineralisation.

14.6.5 Berg Aukas

The Berg Aukas Zn-Pb-V deposit, located approximately 20 km east-northeast of the town of Grootfontein (Fig. 14.8), is important because it contains large resources of V. The deposit is hosted by the Light Grey Dolostone of the Gauss Formation of the Abenab Subgroup. Mineralisation, which is breccia-hosted, was deposited as open-space filling created by karsting, and consists of massive sulphides, including mainly sphalerite and galena. Other sulphides are pyrite, tennantite, enargite, chalcopyrite and renierite. Circulating meteoric waters during subsequent karst activity resulted in extensive oxidation and deposition of secondary, supergene minerals which include willemite, smithsonite, cerussite and descloizite [PbZn(VO)$_4$OH]. The deposit consists of three distinct orebodies, namely: a stratabound Northern Ore Horizon, a discordant Central Orebody and a stratabound Hanging Wall Ore Horizon (Misiewicz 1988).

The Northern Ore Horizon comprises three stratabound massive sulphide lenses (sphalerite and galena), of which the top portion is oxidised to willemite, cerussite and smithsonite. The ore is capped by dolomite breccia enriched in descloizite, and the ore lenses are characterised by sharp contacts with the host dolomite. Cavities of varying dimensions may occur within or adjacent to the ore, but are more common towards the hanging wall. Caliche sand and mud enriched in descloizite and ore material fill these cavities. The Central Orebody is a breccia pipe-like mineralised zone. The ore was extensively oxidised and enriched in vanadiferous muds and breccia, consisting of blocks of barren dolomite and partially oxidised sulphides mixed with vanadiferous caliche. The Hanging Wall Orebody is characterised by north-south-trending lenses of steeply dipping ore-filled fractures hosted in dolomitic rocks above the Northern Ore Horizon. Sphalerite is the dominant ore mineral and varies from an Fe-rich, fine-grained variety to an Fe-poor, honey-coloured, coarse-grained variety. Cd and Ge are present as traces in the sphalerite. Galena, which is more sporadically developed compared to sphalerite, also occurs in two forms, of which one is coarse-grained, while the other variety occurs intergrown with sphalerite. Ore textures indicate that the sulphide mineralisation is syn- to late-tectonic.

Fluid inclusion studies (Misiewicz 1988) indicate homogenisation temperatures ranging from 205° to 97 °C in sphalerite. Results of freezing experiments suggest brine compositions containing NaCl, MgCl, CaCl$_2$ and H$_2$O with a salinity of approximately 23 wt.% NaCl equivalent.

14.6.6 Models of Ore Genesis

A genetic model for the ore deposits of the Otavi Mountain Land must explain: (1) the origin of the metals; (2) the nature and origin of the mineralising fluids; and (3) substantial differences between the Berg Aukas type and Tsumeb type. The main differences needing explanation are: (a) the timing of the mineralisation as indicated by the stratigraphic levels (i.e. Berg Aukas-type below the Abenab disconformity and the Tsumeb type above it; (b) different ore mineral assemblages and metal associations; (c) high temperature range and low salinities for the Tsumeb type, and low temperature range and high salinities for the Berg Aukas type; (d) the Fe-Mn bodies associated with the Kombat deposits; and (e) distinct Pb-isotope signatures (Allsopp et al. 1981).

The Otavi deposits have often been considered by local geologists to be of Mississippi Valley-type affinity. Black shales, arkose and evaporites provide probable source rocks for MVT deposits, but it has been proposed that most rocks represent potential sources of metals, providing a large enough volume is taken into consideration. Since the genetic model for MVT deposits favoured by most workers involves basin dewatering, the eugeosynclinal sediments of the Swakop Group would seem a likely source, with the underlying Nosib Group – which contains evaporites – as a possible alternative, or additional, source. The large layered mafic intrusion east of Berg Aukas (Grootfontein Mafic Body) could also be considered as a source of metals, in particular Cu and V. A basin-dewatering model involves compaction, diagenesis and movement of fluids from the graben troughs along rift margins and towards basement highs, into karst cavities formed in carbonate rocks (see Fig. 14.7). This model seems to adequately explain most features of the Berg Aukas deposit and may be extended to include all of the Berg Aukas-type occurrences in the Otavi Mountain Land. However, the model fails to explain some important features of the Tsumeb-type mineral deposits, such as their Cu content, the presence of layered Fe-Mn bodies at Kombat and their isotopic and fluid inclusion characteristics (Pirajno and Joubert unpubl.data).

Pb isotope systematics for the Tsumeb and Berg Aukas types of deposits have been investigated by Allsopp et al. (1981) and Welke et al. (1983). Allsopp et al. explain linear Pb-isotopic trends as representing mixing of two or more components with distinct Pb-isotopic signatures. In the model of Allsopp et al. the primary component corresponds to the intersection of the two trends as shown in Fig. 14.13. The other components which mixed with the original one would have compositions along the linear trends displayed in the figure. The difference between the trends for the Tsumeb and Berg Aukas type (Fig. 14.13) may therefore be ascribed to movement of the hydrothermal solutions through different lithologies. Welke et al. interpret the observed trends in terms of a mixing model involving a common lower end member, but distinct upper end members for the two deposit types.

In this context a brief digression is warranted to explain the principles of Pb-isotope systematics and their role in the discrimination of deposit types and, consequently, as a tool in the exploration of hydrothermal mineral deposits. As discussed above and illustrated in Fig. 14.13, Allsopp et al. (1981) successfully discriminated between the Tsumeb and Berg Aukas types. Pb isotopic ratios can
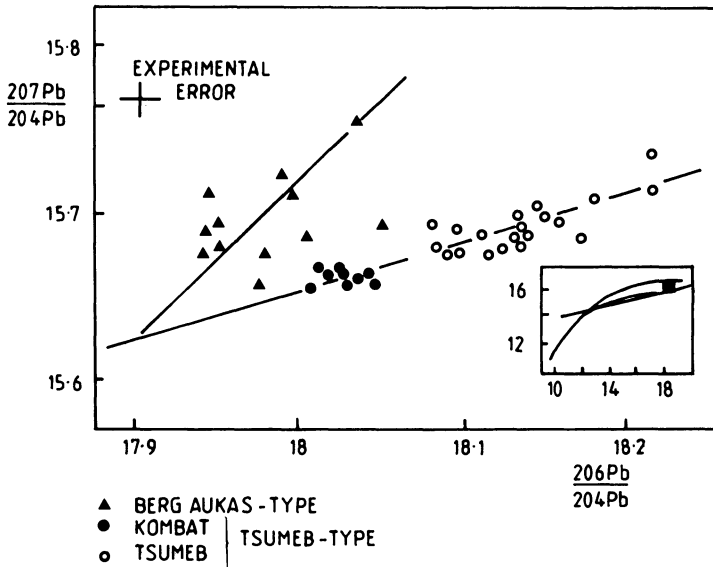
Fig. 14.13. Uranogenic Pb-isotope data from Tsumeb- and Berg Aukas-type deposits in the Otavi Mountain Land, shown on an enlarged scale; *inset* on the right illustrates the growth curve, related to U to Pb decay; the *black square* indicates the area of the enlarged diagram. Note the tight cluster displayed by the Kombat data, which suggests that this mineralisation is probably related to a different type of hydrothermal activity than that which operated at Tsumeb, although the Pb from both deposits had a common source (see also Fig. 14.14) (After Allsopp et al. 1981)

provide information not only on the age, but also on the origin of hydrothermal deposits. There are in nature four isotopes of Pb, namely: ^{208}Pb, ^{207}Pb, ^{206}Pb and ^{204}Pb. The first three are the products of the radioactive decay of ^{232}Th, ^{235}U and ^{236}U respectively. ^{204}Pb is non-radiogenic. The half-life of a radionuclide is a measure of the time it takes for half of the original nuclides to decay. Th and U, which have half-life rates comparable to the age of the Earth, are therefore suitable for dating purposes. It follows that a "growth curve" such as that shown in the inset of Fig. 14.13, represents the variation of the radiogenic Pb with time, the starting point being the primordial value as deduced from meteoritic measurements. Points that fall on the growth curve therefore indicate a single-stage evolution. However, the Pb-isotopic ratios from mineral deposits do not fall on the growth curve, because in most cases the Pb-bearing ores would have experienced more than one stage of evolution. In this case data points form a line which intersects the growth curve at two points. The lower intercept measures the age of the source rocks; the upper indicates the age of the mineralisation. Allsopp and coworkers, however, also point out that a linear trend can be obtained if there is mixing of two or more isotopic compositions. In other words, the hydrothermal solutions would have leached Pb from different sources with different Pb compositions related to the rocks with which the solutions interact. In this case a linear trend, such as that displayed by the Tsumeb Pb (Fig. 14.13), would indicate mixing in varying proportions of two end members.

Tsumeb and Kombat have high Cu contents compared to Berg Aukas, suggesting another mineralising fluid may have delivered Cu from a different source for the Tsumeb-type deposits. Fluid inclusion studies indicate that both at Tsumeb and Kombat deposition of sulphides occurred from weakly saline fluids (2–3 wt.% NaCl equivalent) and temperatures of approximately 250°C, and up to 300°C and 700–500 bar pressure. These temperature and salinity values are incompatible with a basin dewatering model, and contrast with the lower temperature and higher salinities of the fluids responsible for the Berg Aukas mineralisation, which are closer to fluids derived from the compaction and diagenesis of sediments in a basin. Also, and importantly, the Berg Aukas-type deposits tend to occur beneath the Abenab Subgroup-Tsumeb Subgroup unconformity, whilst the Tsumeb-type deposits all occur above this unconformity.

In view of these important differences, it is concluded that the two deposit types were formed during two distinct mineralising events, both in time and space. It can be postulated that the first event to take place was responsible for the Berg Aukas type, and involved fluids derived from basin dewatering. The ore fluids were of relatively low temperature in the range of 205 to 97°C, which is close to the range of MVT deposits. Movement of these fluids was probably along aquifers provided by clastic sedimentary horizons, breccias and contact zones.The fluids became enriched in Pb and Zn en route towards structural highs, where sulphide deposition took place in karst structures in carbonate rocks of the Abenab Subgroup. The second event took place at a later stage, and it involved Cu-rich, higher temperature and lower salinity fluids. The origin of these fluids is not known, but if one considers timing constraints, they would be compatible with an origin due to devolatilisation reactions during prograde metamorphism. The timing of the second mineralising event is constrained by isotopic dating of Pb from the Tsumeb and Kombat ores, which gives ages ranging from 600 to 550 Ma, whilst on the basis of the stratigraphic level the Tsumeb types must have formed after the Berg Aukas types. The second mineralising event is therefore postulated to be synchronous with the peak of metamorphism in the Damara orogen. Metamorphic mineral assemblages in the northern part of the Northern Zone (see Chap. 7) include chlorite + muscovite + quartz, whereas in the central and southern parts of the Northern Zone these assemblages include biotite. Thus, the "biotite-in" isograd occurs just south of the Otavi Mountain Land. This isograd represents the boundary of lower greenschist facies metamorphism, between 300 and 400°C (Winkler 1979). Prograde metamorphism of pelitic and silicate rocks involves dehydration reactions, and abundant fluids are believed to be produced in the range of low- to medium-grade metamorphism at temperatures of approximately 350 to 650°C (Etheridge et al. 1983). It is believed that large-scale hydrothermal convection cells form during regional metamorphism, a topic to be treated in some detail in the next chapter. Convection of metamorphic fluids can provide viable means for the leaching and transport of metals from large volumes of rocks. High-temperature metamorphic fluids would have moved along regional structures, such as graben faults, lineaments and shear zones. In some localities, focused fluid flow was discharged at the surface, or in structural traps, resulting in exhalative activity and the deposition of massive sulphides and the Fe-Mn bodies of Kombat. Innes and Chaplin (1986)
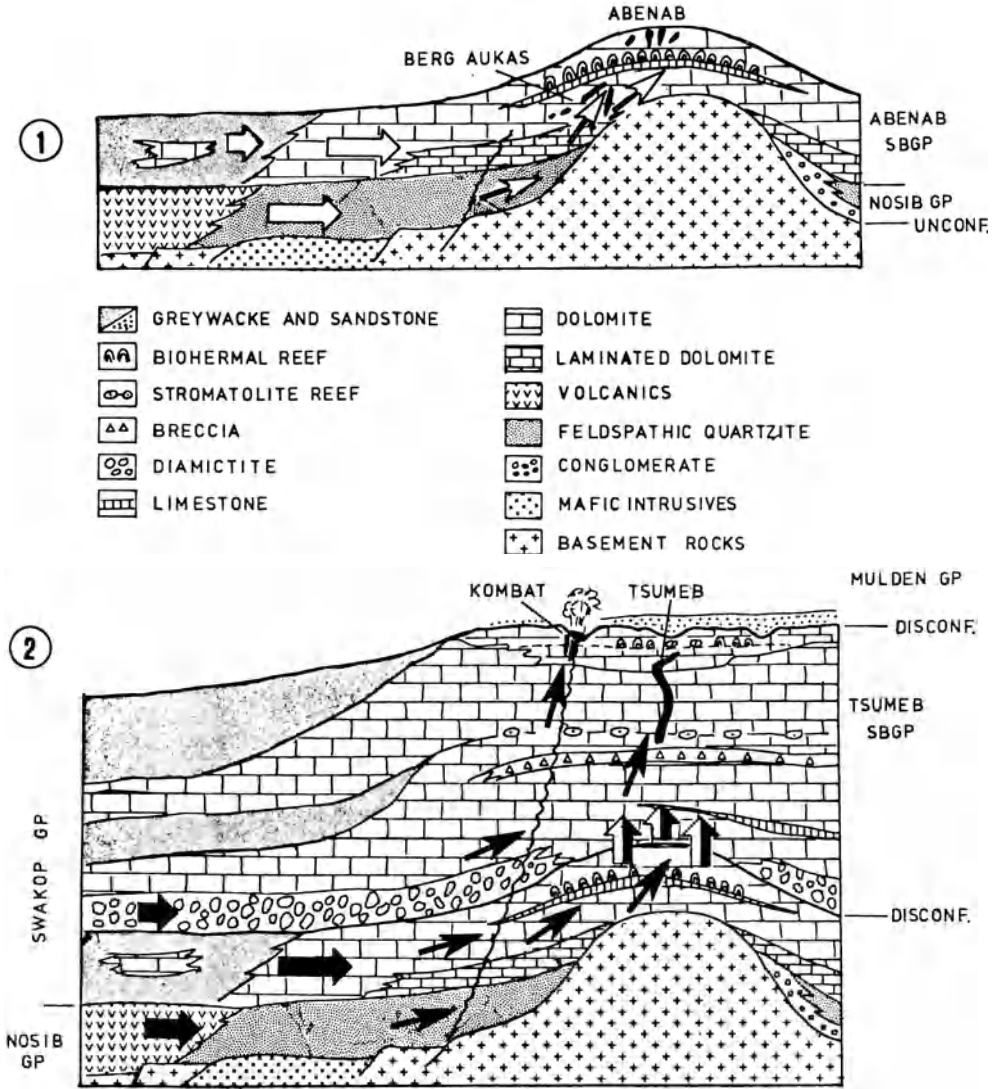
Fig. 14.14. Model illustrating the first two episodes of base metal mineralisation in the Otavi Mountain Land. The model, which is not to scale, shows an idealised, west-facing cross-section of the Otavi Mountain Land and the northern margin of the Northern Rift (refer to inset of Fig. 14.8), in which there is a change from miogeosynclinal (Otavi facies) to eugeosynclinal (Swakop facies) conditions. *1* The first episode which gave rise to the Pb-Zn-rich, Cu-poor Berg Aukas-type mineralisation. *White arrows* indicate flow of low-temperature and predominantly Pb-Zn-bearing basinal fluids. *2* The second episode which resulted in the emplacement of the Cu-rich Tsumeb-type mineralisation. *Black arrows* indicate flow of Cu-bearing fluids generated by metamorphic devolitilisation. Note the different hydrothermal character of Kombat (exhalative) and Tsumeb (pipe infill); this is confirmed by Pb isotope systematics (see also Fig. 14.13). Local "re-working" of mineralisation formed during the first event is indicated by *black + white arrows* (After Pirajno and Joubert, in prep)

give convincing evidence for the exhalative origin of these Fe-Mn bodies, their argument being based on the presence of layering in the bodies, presence of barite and the close similarity in the trace element content with the sea floor bedded Mn oxides. During the second mineralising event in the Otavi Mountain Land, the high-temperature fluids in places may have leached, or re-mobilised, metals from Berg Aukas-type deposits, resulting in the formation of Cu-bearing Berg Aukas-type mineralisation in areas situated above the Tsumeb-Abenab disconformity. This model of two-stage ore genesis is illustrated in Fig. 14.14.

The origin of the V mineralisation is probably not a result of hydrothermal activity, but rather of recent supergene processes. The element V is carried in solution in the oxidised weathering environment, and deposited when the solutions encounter a reducing environment, such as a sulphide body. Thus, the concentration of V mineralisation constitutes the third and final mineralising episode of the Otavi Mountain Land.

References

Allsopp H L, Welke H J, Hughes M J (1981) Shortening the odds in exploration. Nucl Act 24:8–12

Anderson G M (1983) Some geochemical aspects of sulfide precipitation in carbonate rocks. In: Kisvarsanyi G, Grant S K, Pratt W P, Koenig J W (eds) International conference on Mississippi Valley-type lead-zinc-deposits. Proc Vol. Univ Missouri, Rolla, pp 61–76

Anderson G M, Macqueen R W (1982) Ore deposits model – 6. Mississippi valley-type lead-zinc deposits. Geosci Can 9:108–117

Beals F W, Jackson S A (1966) Precipitation of lead-zinc ores in carbonate reservoirs as illustrated by Pine Point Ore Field, Canada. Trans Inst Min Metall 75:B278–B285

Bjorlykke A, Sangster D F (1981) An overview of sandstone lead deposits and their relation to red-bed copper and carbonate-hosted lead-zinc deposits. Econ Geol 75th Anniv Vol:179–213

Boyce A J, Anderton R, Russell M J (1983) Rapid subsidence and early Carboniferous base-metal mineralization in Ireland. Trans Inst Min Metall 92:B55–B66

Brigo L, Omenetto P (1985) Lithogeochemical observations on some ore-bearing Triassic sequences of the Italian southern Alps. Monograph series on mineral deposits, vol 25. Borntraeger, Berlin, pp 95–194

Brigo L, Kostelka L, Omenetto P, Schneider H J, Schroll E, Schulz O, Strucl I (1977) Comparative reflections on four Alpine Pb-Zn deposits. In: Klemm D D, Schneider H J (eds) Time- and strata-bound ore deposits. Springer, Berlin, Heidelberg, New York, pp 273–293

Brown J S (1967) (ed) Genesis of stratiform lead-zinc-barite-fluorite deposits. Econ Geol Monogr 3:443 pp

Callahan W H (1967) Some spatial and temporal aspects of the localization of Mississippi Valley-Appalachian type ore deposits. Econ Geol Monogr 3:14–19

Campbell N (1967) Tectonics, reefs and stratiform lead-zinc deposits of the Pine Point area, Canada. Econ Geol Monogr 3:59–70

Crocetti C A, Holland H D (1989) Sulphur-lead isotope systematics and the composition of fluid inclusions in galena from the Viburnum Trend, Missouri. Econ Geol 84:2196–2216

Dixon C J (1979) Atlas of economic mineral deposits. Chapman & Hall, London, 143 pp

Duane M J, de Witt M J (1988) Pb-Zn ore deposits of the northern Caledonides: products of continental-scale fluid mixing and tectonic expulsion during continental collision. Geology 16:999–1002

Economic Geology (ed) (1977) An issue devoted to the Viburnum Trend, Southeast Missouri. Econ Geol 72

Esteban M, Klappa C F (1983) Subaerial exposure. In: Scholle P A, Bedout D G, Moore C H (eds) Carbonate depositional environments. Mem Am Assoc Petroleum Geol 33:1–54

Etheridge M A, Wall V J, Vernon R H, (1983) The role of the fluid phase during regional metamorphism and deformation. J Metamorph Geol 1:205–226

Evans A M (1976) Genesis of Irish base metal deposits. In: Wolf K H (ed) Handbook of strata-bound and stratiform ore deposits, vol 6. Elsevier, Amsterdam, pp 231–256

Giordano T H (1985) A preliminary evaluation of organic ligands and metal-organic complexing in Mississippi Valley-type ore solutions. Econ Geol 80:96–106

Grundmann W H (1977) Geology of the Viburnum No. 27 Mine, Viburnum Trend, Southeast Missouri. Econ Geol 72:349–364

Hearn P P, Sutter J F, Belkin H E (1987) Evidence for Late-Paleozoic brine migration in Cambrian carbonate rocks of the central and southern Apalachians: Implications for Mississippi Valley-type sulfide mineralization. Geochim Cosmochim Acta 51:1323–1334

Hoffmann K H (1990) Sedimentary depositional history of the Damara Belt related to continental breakup, passive to active margin transition and foreland basin development. In: Abstr Geocongress '90 Cape Town. Geol Soc S Afr, pp 250–253

Innes J, Chaplin R C (1986) Ore bodies of the Kombat Mine, South West Africa/Namibia. In: Anhaeusser C R, Maske S (eds) Mineral deposits of southern Africa, vol 2. Geol Soc S Afr, pp 1789–1805

Kisvarsanyi G (1977) The role of the Precambrian igneous basement in the formation of the stratabound lead-zinc-copper deposits in southeast Missouri. Econ Geol 72:435–442

Kisvarsanyi G, Grant S K, Pratt W P, Koenig J W (eds) (1983) International Conference on Mississippi Valley-type lead-zinc Deposits. Proc Vol. Univ Missouri, Rolla, 603 pp

Kucha H, Van der Biest J, Viaene N A (1990) Peloids in strata-bound Zn-Pb deposits and their genetic importance. Mineral Depos 25:132–139

Kyle J R (1981) Geology of the Pine Point lead-zinc district. In: Wolf KH (ed) Handbook of strata-bound and stratiform ore deposits, vol 9. Elsevier, Amsterdam, pp 643–741

Larter R C L, Boyce A J, Russell M J (1981) Hydrothermal pyrite chimneys from the Ballynoe baryte deposit, Silvermines, County Tipperary, Ireland. Mineral Depos 16:309–318

Leach D L, Plumlee G S, Hofstra A H, Landis G P, Rowan E L, Viets J G (1991) Origin of late dolomite cement by CO_2-saturated deep basin brines: evidence from the Ozark region, central United States. Geology 19:348–351

Lombaard A F, Gunzel A, Innes J, Kruger T L (1986) The Tsumeb lead-copper-zinc-silver deposit, South West Africa/Namibia. In: Anhaeusser C R, Maske S (eds) Mineral deposits of southern Africa, vol 2. Geol Soc S Afr, pp 1761–1787

Maucher A, Schneider H J (1967) The Alpine lead-zinc ores. Econ Geol Monogr 3:71–89

Misiewicz J E (1988) The geology and metallogeny of the Otavi Mountain Land, Damara Orogen, SWA/Namibia, with particular reference to the Berg Aukas Zn-Pb-V deposit – A model of ore genesis. MSc Thesis, Rhodes Univ, Grahamstown, 143 pp

Mouat M M, Clendenin C W (1977) Geology of the Ozark Lead Company mine, Viburnum Trend, Southeast Missouri. Econ Geol 72:398–407

Ohle E L (1985) Breccias in Mississippi Vally-type deposits. Econ Geol 80:1736–1752

Oliver J (1986) Fluids expelled tectonically from orogenic belts: their role in hydrocarbon migration and other geological phenomena. Geology 14:99–102

Ravenhurst C E, Reynolds P H, Zentilli M, Krueger H W, Blenkinsop J (1989) Formation of Carboniferous Pb-Zn and barite mineralization from basin-derived fluids, Nova Scotia, Canada. Econ Geol 84:1471–1488

Sangster D F (1976) Carbonate-hosted lead-zinc deposits. In: Wolf K H (ed) Handbook of strata-bound and stratiform ore deposits, vol 6. Elsevier, Amsterdam, pp 447–456

Sangster D F (1983) Mississippi Valley-type deposits: a geological melange. In: Kisvarsanyi G, Grant S K, Pratt W P, Koenig J W (eds) International Conference on Mississippi Valley-type lead-zinc deposits. Proc Vol Univ Missouri, Rolla, pp 7–19

Saunders J A, Swann C T (1990) Trace-metal content of Mississippi oil field brines. J Geochem Explor 37:171–183

Sawkins F J (1990) Metal deposits in relation to plate tectonics, 2nd edn. Springer, Berlin, Heidelberg, New York, 461 pp

Sevastopulo G D (1981a) Economic geology. In: Holland C H (ed) A geology of Ireland. John Wiley & Sons, New York, pp 273–301

Sevastopulo G D (1981b) Hercynian structures. In: Holland C H (ed) A geology of Ireland. John Wiley & Sons, New York, pp 189–199

Skall H (1975) The paleoenvironment of the Pine Point lead-zinc district. Econ Geol 70:22–47

Sverjensky D A (1984) Oil field brines as ore forming solutions. Econ Geol 79:23–37

Sverjensky D A (1986) Genesis of mississipi valley-type lead-zinc deposits. Annu Rev Earth Planet Sci 14:177–199

Welke H J, Allsopp H L, Hughes M J (1983) Lead isotopic studies relating to the genesis of the base metal deposits in the Owambo basin, Namibia. Geol Soc S Afr Spec Publ 11:321

Winkler H G F (1979) Petrogenesis of metamorphic rocks, 5th edn. Springer, Berlin, Heidelberg, New York, 348 pp

Chapter 15

Crustal Hydrothermal Fluids
and Mesothermal Mineral Deposits

15.1 Introduction

In this chapter we examine a broad category of hydrothermal mineral deposits whose principal characteristic is their strong structural control, and whose genesis is attributed to the action of deep-circulating crustal fluids. The mineralisation is hosted in a variety of lithologies metamorphosed to lower-upper greenschist facies, and less commonly to lower amphibolite facies. In all cases, however, the mineralising events post-date peak metamorphism. The deposits are found within high strain zones in brittle (lower greenschist facies) to brittle-ductile structures (mid-upper greenschist facies). Nesbitt (1988) and Nesbitt and Muehlenbachs (1989) refer to these deposits, in which Au is the chief economic metal, as "mesothermal lode gold". In the literature these are also referred to as metamorphogenic or metamorphic vein deposits (Groves and Phillips 1987; Groves et al. 1987; Nesbitt and Muehlenbachs 1989), or solution-remobilisation ores (Boyle 1979, Guilbert and Park 1986). Here we adopt Nesbitt and Muehlenbachs' terminology and use for all of these deposits the general term mesothermal ore deposits. Within this broad category are included the mineralised quartz vein systems in Archean granite-greenstone terranes (Archean lode Au deposits), the quartz vein lode Ag deposits of Idaho (USA), the lode Au deposits of Pilgrim's Rest in South Africa and turbidite-hosted Au deposits. The latter are generally of Phanerozoic age, and examples are found in the Canadian Cordillera, Nova Scotia and Alaska in North America, Victoria in Australia, and Otago-Marlborough in New Zealand.

In the broad category of ore systems discussed in this chapter may also be included the unconformity-related U-Au deposits because they too appear to have been formed as a result of hydrothermal convection cells in the continental crust.

The origin of the hydrothermal solutions is contentious, and models – utilising isotope systematics, geochemical and petrological constraints – propose either magmatic, or metamorphic (including granulitisation processes), or a meteoric derivation or a combination of these. Many of the deposits – especially those of Archean age – have a spatial relationship to igneous rocks, while for others there is no clear connection with igneous activity. However, even in the former case the precise role of the igneous activity in the genesis of the mineralisation remains uncertain. Most geologists working on mesothermal mineralisation agree on its epigenetic nature, but volcano-exhalative models have also been proposed. In the final analysis, the weight of the evidence from field and laboratory data (see also later) indicates that metamorphic devolitilisation reactions were responsible for a

substantial component of the mineralising fluids. In fact, the best field evidence of fluid generation and flow during regional prograde metamorphism is the common presence of quartz and carbonate veining in the rocks of the metamorphic terranes hosting the mesothermal ore systems. In the Southern Alps of New Zealand it has been shown that these metamorphic quartz veinlets carry Au (Craw et al. 1987, Craw and Koons 1988). Deep-circulating meteoric waters probably did play an important role, particularly in Phanerozoic orogenic belts such as the New Zealand Southern Alps, just mentioned, and the Canadian Cordillera. The case for hydrothermal fluids of magmatic origin is less compelling, although, at least on a local scale, this is not ruled out.

Elements usually found in mesothermal lode deposits are Au, Ag, As, Sb, Hg, W, Mo, Te and B, in various economic ore combinations such as Au-Ag, Au-Te, Sb-W, Au-W, Au-Sb-W, Hg-Sb or U-Au-PGE (platinum group elements) and U-Ni-As, in the case of unconformity-related deposits. Less commonly, Pb-Zn and Cu may be present. The nature of the solutions, as deduced from fluid inclusion studies, is characterised by low salinities (up to 5 wt. % NaCl equivalent), high CO_2 content ($>$ 4 mol%) and near-neutral pH. Depositional conditions are characterised by a temperature range of approximately 200 to 450°C, but mainly between 250 and 350°C, at pressures of between 0.5 to 4 kbar. The styles of mineralisation include disseminations in shear zones, stratabound/stratiform replacements and massive to laminated quartz veins. Hydrothermal alteration generally includes carbonitisation, silicification, sulphidisation and alkali metasomatism. The ore-hosting structures are subsidiary shear zones or normal to reverse faults, which are always related to a major regional-scale structure such as a transcurrent fault or a crustal lineament or a thrust. Nesbitt and Muehlenbachs (1989), for example, draw attention to the close spatial association of mesothermal lode Hg, Sb and Au deposits of the Canadian Cordillera with right-lateral strike-slip fault systems. As is the case with most of these deposits, the mineralisation is not exactly on the fault structure but occurs on secondary or subsidiary faults or shear zones, although in some areas of the Cordillera Hg deposits do occur within the main strike-slip fault zone. This clearly suggests that both the main fault and its subsidiary structures have acted as conduits for the mineralising fluids. The fluids are channelled into these structures during the late stages of deformation and metamorphism of a tectonic cycle, in which temperature and pressure conditions, at or below the amphibolite facies transition, favoured the development of brittle to brittle-ductile structures (Groves et al. 1989). It is possible that mesothermal deposits may represent a part of an extensive mineralised system, whose vertical dimension is in the order of 10–15 km, extending from the ductile to the brittle domain (Fig. 15.1).

Nesbitt (1988) proposes that lode deposits in the continental crust form a continuum of at least three principal end members, namely: volcanic-hosted epithermal, sediment-hosted (Carlin-type) epithermal and mesothermal deposits. According to Nesbitt (1988), these reflect increasing depth and temperature of dominantly meteoric fluid circulation, and decreasing water/rock ratios, from shallow (1–2 km) for epithermal deposits, to deep (8–12 km) for mesothermal deposits. Using isotope systematics (particularly variations in δD) Nesbitt and Muehlenbachs (1989) recognise a major role for meteoric fluids in the Canadian
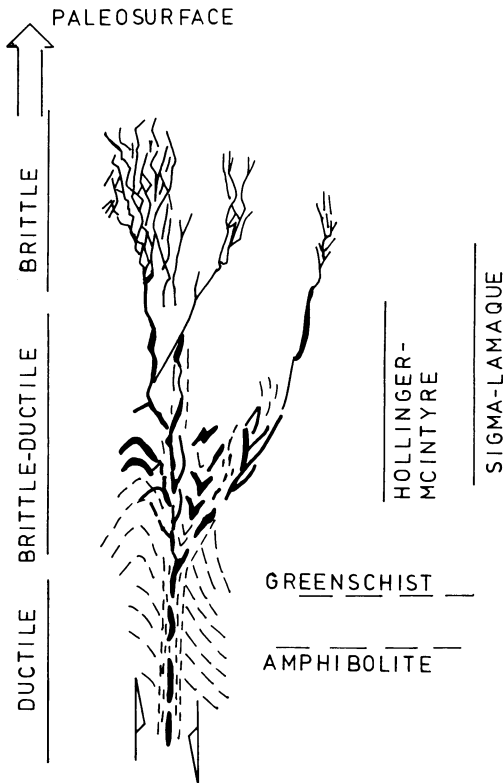
Fig. 15.1. Depositional model for Archean mesothermal Au lodes. Note changes in mineralisation styles from stockworks in the upper levels (brittle deformation) to quartz vein lodes in the lower levels (brittle-ductile deformation). Boudinaged veins occur in the area of ductile deformation in the amphibolite facies domain. This model is equally applicable to Phanerozoic mesothermal systems. The position of some lode systems discussed in the text are shown on the *right*. Drawing is not to scale; however, the total length of the system is considered to be approximately 10 km (see text) (After Colvine 1989)

Cordillera mesothermal deposits rather than metamorphic, although they also postulate that metamorphic fluids may participate in the overall mineralising event by mixing with the meteoric solutions. A similar idea is proposed by Craw and Koons (1989) and Craw et al. (1987) for the vein mineralisation in the Southern Alps of New Zealand. However, the role of meteoric fluids, if any, is less certain for the mesothermal lodes of Archean age.

Nesbitt et al. (1986) and more recently Barley et al. (1989) have also drawn attention to the similarities between Archean lode deposits and the mesothermal veins of Phanerozoic terranes (e.g. turbidite-hosted Au deposits). These similarities include (Barley et al. 1989): (1) host rock types; (2) metamorphic grade; (3) structural setting; (4) styles of mineralisation; (5) depositional physico-chemical conditions; (6) ore mineralogy and element association.

In the first part of this chapter we look at the origin of, nature and movement of fluids in the Earth's crust and in the metamorphic environment, the geometrical properties of shear zones, transport and movement of metals, and examine briefly the tectonic settings of mesothermal ore deposition. This is followed by a summary of Archean greenstone belt geology and a review of the theories of ore genesis for Archean lode deposits. Descriptions are given of some of the well known Archean lode Au deposits in South Africa, Western Australia and Canada, and the Phanerozoic mesothermal turbidite-hosted deposits in New Zealand and Alaska.

We conclude with a look at some special cases, such as unconformity-related U deposits, the Au deposits of the Central Zone of the Damara orogen in Namibia, and a controversial approach to explain the origin of the Au-U mineralisation in the Witwatersrand basin in South Africa.

15.2 Metamorphism and Fluid Generation

The concept that regional metamorphic processes may have been responsible for the generation of hydrothermal solutions and the mobilisation of metals was originally proposed by New Zealand geoscientists working on the Au-W-Sb lodes of the Haast Schists (see later) in the South Island (e.g. Mutch 1969; Williams 1974; Henley et al. 1976; Norris and Henley 1976). The origin of hydrothermal solutions derived from metamorphic fluids is introduced in Chapter 2, while a detailed discussion on the generation and movement of fluids in the crust during prograde regional metamorphism is given in Chapter 3 (Sect. 3.7). Here we look at more specific instances of metamorphic fluid generation, which result from the dehydration of minerals in mafic, carbonate and pelitic rocks, the formation of quartz veins, the mass transport and movement of metals in the metamorphic environment. Excluded from this are the more direct effects of diagenesis, bearing in mind, however, that contributions to hydrothermal solutions due to diagenetic changes (e.g. connate waters) may also be an important component of the ore-bearing fluids. The origin of hydrothermal solutions through diagenetic processes in sediments deposited in an evolving basin are discussed in Chapter 14. The boundary between diagenesis and low grade metamorphism is gradational and occurs at approximately 200°C, coinciding with the first appearance of muscovite (Phillips et al. 1990).

15.2.1 Metamorphic Devolitilisation Reactions

Fluid release curves for initially dry mafic rocks indicate first a hydration process, followed by dehydration which increase become steeper with increasing geothermal gradients as is also observed for the pelitic rocks (see Fig. 3.25). Near-surface hydration and oxidation of mafic rocks result from their equilibration with the hydrosphere (Fyfe et al. 1978). The hydrated minerals are zeolites (analcite, thomsonite), carbonates, chlorite and clays. With increasing temperature progressive dehydration reactions are as follows (Fyfe et al. 1978):

analcite $+ SiO_2$ = albite $+ H_2O$;

laumontite = wairakite $+ 2H_2O$;

2wairakite = prehnite $+$ kaolinite $+ 3SiO_2 + H_2O$;

and if CO_2 is present:

laumontite $+ CO_2$ = calcite $+$ kaolinite $+ 2SiO_2 + 2H_2O$.
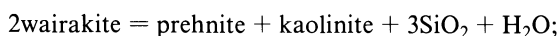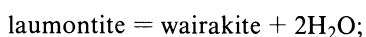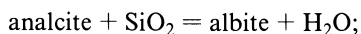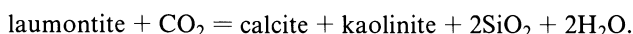
Greenschist facies mineral assemblages include quartz-chlorite-albite-epidote-calcite ± actinolite. This assemblage is developed by replacement of Fe-Mg minerals (chlorite-actinolite) and plagioclase. Muscovite and biotite may be formed if more potassic rocks are present (e.g. andesite). Fluids evolved from mafic rocks are generally H_2O-rich, with only limited development of CO_2, because of the stability of carbonate in the temperature and pressure range of mafic rock dehydration.

Breakdown of carbonate minerals during metamorphism results in the release of CO_2 and H_2O, with the amount of the latter being mostly dependent on the presence of impurities (clays, micas). Fyfe et al. (1978) investigated metamorphic reactions in carbonate rocks, and concluded that the presence of impurities in carbonate rocks have a very important effect for metamorphic reactions, and that they occur at temperatures less than those required for simple reactions, such as:

calcite + silica = wollastonite + CO_2,
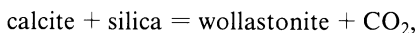
which takes place at temperatures greater than 600 °C. Dolomitic rocks dehydrate at much lower temperatures by reaction with quartz to produce clinopyroxene or actinolite with release of CO_2:

dolomite + $2SiO_2$ = diopside + $2CO_2$,
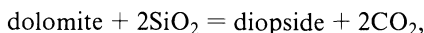
or, according to Winkler (1976):

5dolomite + 8quartz + H_2O = 1tremolite + 3calcite + $7CO_2$.
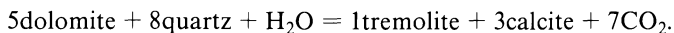
The inverse reaction may occur when CO_2 is infiltrated through calcitic marbles containing impurities (metamorphosed to calc-silicates) to produce dolomite + quartz. This type of reaction is postulated by Pirajno et al. (1990, 1991) to account for the regional-scale dolomitisation of marbles in the Central Zone of the Damara orogen (see later). In the reactions above the amount and rate of CO_2 release is a function of the composition of the mineral phases and temperature increase. The presence of impurities such as clay and mica minerals in the carbonate rocks is clearly important as they may provide the H_2O necessary for the decarbonation reactions.

Fyfe et al. (1978) propose three categories of carbonate sediments for the release of CO_2 to the fluid phase, namely:

1. Dolomitic marbles with quartz as the only impurity will release a CO_2-rich fluid at high metamorphic grades.
2. Carbonate rocks containing hydrated minerals as impurities will release H_2O-rich fluids.
3. Pelitic sediments with minor carbonates will tend to release H_2O-rich and CO_2-poor fluids.

Studies of prograde mineral reactions in carbonate rocks of the Vassalboro Formation, Maine (USA), by Ferry (1983) provided further and interesting insights into the mechanism and role of fluid/rock interactions, and related mass transfer of major elements. Ferry found that with increasing metamorphic grade there is a significant decrease in Na, K and C with concomitant depletion of these elements in the carbonate rocks. The mineral reactions that occurred during the prograde

metamorphism of the Vassalboro Formation produced CO_2-rich fluids, through the infiltration and interaction of the carbonate rocks with H_2O-rich fluids. The source of the infiltrating H_2O is unknown, but Ferry (1983) suggests that it may represent the product of dehydration reactions from adjacent sediments, or, it may have originated from nearby granitic rocks, or from deeper sources in the crust. Whatever the origin of the infiltrating H_2O, the important facet of Ferry's work is that Na, K and C were removed from the carbonate rocks, and CO_2 was produced by the interaction of large volumes of H_2O-rich fluids with the carbonate rock body.

Mineral reactions, fluid and heat transfer within areas enclosed by the chlorite and biotite isograds in metapelitic rocks of the Waterville formation, Maine, USA, were studied by Ferry (1984). He examined the mineral reactions leading to the formation of biotite, and found that they involve both hydration and devolitilisation resulting in widespread decarbonation and desulphidisation. The pressure and temperature conditions were found to be near 3.5 Kbar and 400°C, with the fluids being CO_2-H_2O-H_2S mixtures. The metapelites of the Waterville Formation are characterised by two main metamorphic zones: (1) a chlorite zone which contains muscovite, chlorite, quartz, albite, ankerite, siderite, calcite; and (2) a biotite zone containing biotite, muscovite, chlorite, quartz and plagioclase. No carbonate minerals are present. However, in the biotite zone a number of accessory minerals include ilmenite, pyrrhotite, or, pyrite + pyrrhotite. Chemical analyses show that the biotite zone metapelites contain less volatiles than the metapelites in the chlorite zone. There is no evidence of chemical changes in the system other than the loss of volatiles during the transition from the chlorite to the biotite zone. Therefore the metapelites of the Waterville Formation provide an example of isochemical metamorphism. Ferry's conclusions are that metamorphic reactions are not caused by changes in temperatures or fluid composition, but rather from addition or extraction of heat, and by interaction with fluids generated by metamorphism. The Waterville Formation metapelites were formed by infiltration and interaction with carbonate-bearing (average shale contains 4 to 12% carbonate) argillaceous rocks, resulting mainly in decarbonation.

15.2.2 Fluid Transport and Migration

Devolitilisation reactions provide abundant fluids resulting in high water/rock ratios (> 100), so that advective mass transport is likely to dominate during prograde regional metamorphism (Etheridge et al. 1983). Mass transport via a mobile fluid during metamorphism takes place through diffusion and infiltration. The former is believed to occur over small distances and is due to chemical gradients. An example of mass transport by diffusion is given by pressure solution which occurs during the development of cleavage (see Fig. 15.4). However, infiltration is considered to be far more important to explain the large scale metasomatic processes and associated vein formation. Infiltration of fluids is due to fluid movement along pressure and/or temperature gradients. Convective circulation of fluids over large distances in the metamorphic environment has been discussed by Etheridge et al. (1983), and is discussed in some detail in Chapter 3.

This circulation is permitted at the permeabilities present in the metamorphic environment. Hydraulic fracturing enhances the pressure gradients between fractures and wall rocks (Etheridge et al. 1984) and it is thought that fluid movement along the pressure gradient is much faster than the rate of diffusion by several orders of magnitude (Etheridge et al. 1984, Fig.3). Impermeable barriers breached by high-pressure fluids can become sealed through rapid precipitation of mineral phases and subsequent vein formation. The sealed barrier may be breached again if fluids reach a high enough pressure with renewed vein formation and perhaps sealing (see Chap. 3). This process can be repeated several times resulting in thick veins with complicated depositional histories of mineral phases (Fyfe et al. 1978). Movement of fluids carrying solutes is therefore a powerful mass transporter, and this is probably the primary cause for the large-scale metasomatism of Archean metamorphic systems and their associated veins, which may represent the channels through which precipitation of the solutes occurred (see later). Mass is transferred by the moving fluid from a source region to a site of precipitation or sink, along microfracture networks, foliation, cleavage, tensile fractures, faults and shear zones.

15.2.3 Shear Zones

The deformation systems with which mesothermal ore deposits are spatially associated include faults, fractures, bedding-controlled slip and dilation zones, brittle and brittle-ductile shear zones. The latter are especially important because they are the most common ore-hosting structures. It is therefore appropriate to consider briefly the geometry of shear zones and the formation of veins and related mineralisation (see following section). Details on the topic can be found in Ramsay (1980) and Hodgson (1989) whose work provided much of the information summarised here.

    Tectonic deformation processes cause strain in rock bodies. Strain – the change in the shape of a body as a result of applied stress – can be described in terms of three orthogonal axes: (1) principal maximum stress (σ_1); (2) intermediate stress (σ_2); and (3) minimum stress (σ_3). The change in the shape (deformation) of a body can occur by compression, for which $\sigma_1 > \sigma_2 = \sigma_3$ (pure shear), or by torsion or rotation, in which $\sigma_1 > \sigma_2 > \sigma_3$ (simple shear), a combination of the two, or by extension ($\sigma_3 > \sigma_1 = \sigma_2$). Failure by fracturing takes place at low mean stress and high strain rate. Fractures are developed parallel to the maximum principal stress σ_1. As stress increases and strain rate decreases tensile fracturing gives way to shear fracturing and eventually to ductile flow. The presence of pore fluids in rocks undergoing deformation is very important because it counteracts the effects of the confining pressure, and it also influences and promotes mineral reactions, which in turn affect the mechanical properties of the rocks (see Chap. 3). Ramsay (1980) classified shear zones into three types, namely: brittle, brittle-ductile and ductile. Recognition of these three types is essentially based on the type of markers' displacement across the shear zone. Thus, brittle shears are characterised by the abrupt offset of markers. In brittle-ductile shear zones external markers show both continuous and discontinu-

ous offsets along discrete slip surfaces, whereas rocks in ductile shears are mylonitic and external markers show continuous offsetting. It is clear that the character of shear zones reflects the temperature, pressure and fluid regime of the environment and the rheological properties of the rocks affected (Hodgson 1989). In terms of geometrical features Hodgson (1989) distinguishes internal features and external forms of shear zones. The former include microscopic to mesoscopic fabrics which can be recognised at the thin-section to hand-specimen scale. Cataclasites or rocks with cataclastic textures are characterised by non-foliated fragments produced by fracturing in the brittle regime. They form breccias, microbreccias and gouges, which through pseudotachylites (microbreccias cemented by frictionally produced glass), pass into mylonites. These are generally foliated fragments in a fine comminuted matrix and are further subdivided into protomylonites and ultramylonite. They are formed in the brittle-ductile to ductile regime. The external form of shear zones and shear zone systems are characterised by anastomosing patterns visible on hand specimen to map scale. The anastomosing geometry shows many fractures whose inclination towards the trend of the shear zone enables one to distinguish the following types: low-angle and high-angle Riedel shears (R), pressure or P shears, C shears and T shears. Shear zone systems often form intersecting sets or networks of planar deformed zones which wrap around areas of low deformation. Sets of subparallel shears in a system, which have an opposite sense of movement and are developed in the same stress regime, are called a conjugate system (Hodgson 1989).

15.2.4 Metamorphic Vein Systems and Vein Growth

Veins ranging in size from a few millimetres to several metres thick are commonly found in regions of low- to medium-grade metamorphism. Their presence is considered to be proof of the movement of fluids generated during metamorphism. Cox et al.(1986) consider that a regional metamorphic terrane is a large hydrothermal system, which can be likened to those developed in oceanic crust. In the metamorphic environment dissolution of material and mass transfer take place during deformation and metamorphism, so that hydrothermal convection cells are generated. The hydrothermal fluids can leach metals from large volumes of rocks and the fluids can either diffuse their solutes in a network of microcracks, or following transport by migration the fluid flow is focused through a small area, such as in dilatant sites. Precipitation of metals may then occur and a mineral deposit is formed (Cox et al. 1986). Focusing of fluids along faults and shear zones may locally enhance dissolution and mobilisation of material. Transport of metamorphic fluids and precipitation of solutes takes place in pre-existing rock porosity, or chemically, or mechanically developed sites (e.g. fractures or foliation). Thus, vein formation results from fracturing, which in turn is related to the dominant stress field in a given rock body. The development of hydraulic fractures as a result of high fluid pressure below impermeable zones is also discussed in Section 3.7.2. Here hydraulic fracturing is considered in terms of the predominant stress field. The stress state for hydraulic fracturing is given by:

$$P > \sigma_3 + T,$$
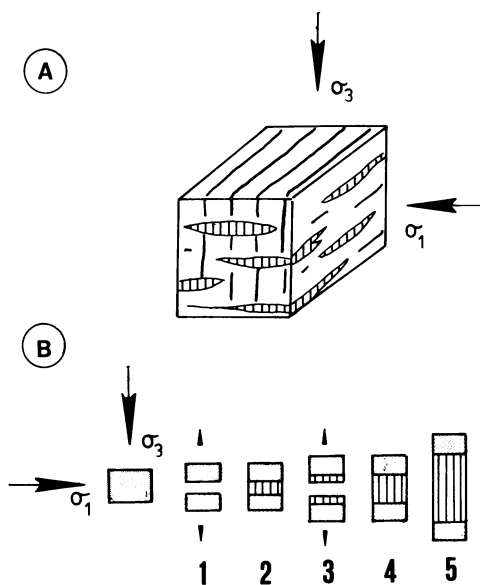
Fig. 15.2. A Metamorphic vein system resulting from fluids which migrate from cleavage zones perpendicular to σ_1 into tensile fractures perpendicular to σ_3, where solutes are precipitated to form veins. The vein material is precipitated by crack-seal mechanism as shown in **B** (after Etheridge et al. 1984). **B** Crack-seal mechanism and fibre growth parallel to σ_3. Hydraulic microfracturing and opening starts in *1*, solution and transfer of material occurs and mineral phases are deposited on the walls of the micro-fracture. In *2* sealing of the microfractures occurs; in *3* a new stage of micro-fracturing begins with opening and syntaxial growth of mineral phases taking place in *4*. The process is repeated in *5* (After Cox et al. 1986)

where σ_3 is the minimum principal stress and T is the tensile strength of the rocks. If σ_3 is vertical then a system of subhorizontal fractures (parallel to σ_1) would form. This concordant, more or less flat-lying system has been termed by Fyfe et al.(1978) "mineral flats", and they always occur below impermeable layers. If, on the other hand, σ_3 is horizontal, as in most extensional regimes, then vertical fractures would form (Fig. 3.26).

Metamorphic veins can be classified into at least two main types: (1) replacement type and (2) hydrothermal type. The former is generated by diffusion processes and precipitation of material into dilatancy sites constituted by small fractures. These veins are usually small and thin, although they can be abundant in a given unit area (Fyfe et al.1978). The second type is more important for the genesis of mineralised systems and is characterised by larger veins, formed by the migration of hydrothermal fluids along large-scale permeability paths, such as shear zones. In this case fluids migrate during deformation from the cleavage zones perpendicular to σ_1 into tensile fractures perpendicular to σ_3 (Fig. 15.2A). The fluid will deposit vein material into these fractures by a process of fibre growth (see later), in which the length of the fibres is parallel to σ_3 (Fig. 15.2B). The opening of the tensile fractures, fluid migration and mineral deposition can occur several times. The driving force for the movement of the fluids, according to Etheridge et al. (1984), is due to the difference between the fluid pressure in the rock and that in the tensile fractures.

Vein growth by a crack-seal mechanism (Ramsay 1980; Etheridge et al. 1984; Cox et al. 1986) occurs in metamorphic terranes. Crystals grow at rock-fluid interfaces from high pressure fluids within hydraulic fractures. Cox et al. (1986) consider two types of vein growth: simple and crack-seal. Simple vein growth is formed during continuous fracture opening accompanied by continuous crystallis-ation of mineral phases. This continuity would be due to constant high fluid

Fig. 15.3. Sequential development of "laddered ribbon" veins by a crack-seal mechanism. This figure depicts an actual example from the Hollinger mine (Ontario). *Stippled area* represents tourmaline; *clear area* is quartz; *dashes* represent schist; and *black areas* are late cross-cutting ladder veins (After Hodgson 1989)
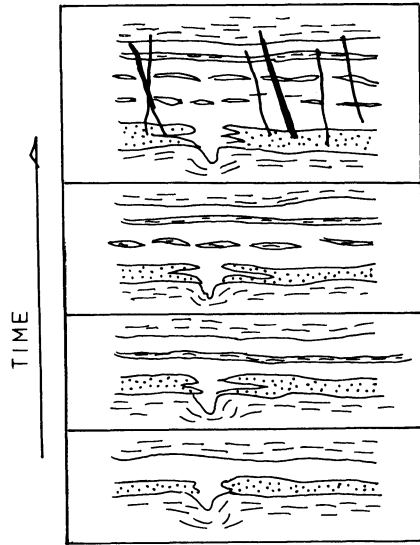
pressure which keeps the fracture open. The resulting textures are typically banded, crustified or comb-like. Variable fluid pressures lead to the collapse of the fracture, or alternatively fast mineral growth may result in the sealing of the fracture. Crack-seal vein growth is characterised by fibrous-like textures which are formed through a number of growth pulses related to an equal number of fracture opening events (Figs. 15.2B and 15.3).

In the structural environments considered, mineralisation may occur within shear zones, in the less deformed rocks between shears and in zones of dilation related to folds. Mineralisation in shear zones, especially Au, is characterised by a distribution along zones elongated in one direction (shoots). Ore shoots are often localised at the intersection of conjugate shears or other structural features. Veins within shears or fractures take different forms or styles according to the pressure and temperature regime and the nature of the fluids that produced them. Thus, there are crustiform and banded veins usually formed by open-space filling at low temperature and pressure (e.g. epithermal systems). Open-space filling produces massive or cockade textures. Breccia veins are typified by shattering of the host rocks and subsequent open-space filling. Mesothermal veins are characterised by a variety of forms such as sheeted veins and ribbon or laminated veins which are formed by the mechanism of crack-sealing (see above) and are common in mesothermal deposits. In terms of mineral orientation fibrous textures typify crack-seal veining with syntaxial and antitaxial growths. Syntaxial veins are formed by mineral grains in optical continuity with, and extending from those in the vein walls. Antitaxial veins, on the other hand, are formed by mineral grains different from those in the wall rocks, and they originate from cyclic cracking and sealing of vein material. Stretched crystal veins form as antitaxial veins in which, however, the crack-seal process occurs within the vein, resulting in one crystal stretching across from wall to wall and linking the parts of a crystal from both walls (Hodgson 1989).

15.2.5 Mass Transport and Movement of Metals

Mobilisation, migration and concentration of various elements can occur when a pile of rocks is subjected to heating, either because of regional metamorphism or by igneous intrusions. The precise mechanisms of mobilisation of elements from the rocks and the lattices of the mineral constituents are not clearly understood. Boyle (1979) favours diffusion as a viable process, whereby "atoms, ions and molecules migrate through rocks, natural solutions and gasses, as a result of differences in free energy (chemical potential) between any two points in these media". This diffusion according to Boyle (1979, p.399) may be due to migration of constituents, such as SiO_2, CO_2, Au, As, etc., along grain boundaries and microfractures, or pores in the rock. Migration of ions, hydrated ions or molecules can also occur through fluids or gases along the grain boundaries, fractures, foliation or other discontinuities in the rocks. Extremely slow diffusion is also believed to occur through the lattices of minerals. It is further pointed out that for migration of a constituent to occur a difference must exist in the chemical potential μ of the given constituent between its source and site of deposition. Thus, migration takes place where μ_1 (deposition site) $< \mu_2$ (source), and when $\mu_1 = \mu_2$ then equilibrium is attained and no migration takes place. The chemical potential is a function of the concentration C of the constituents, temperature (T) and pressure (P), and may be expressed thus (see also Sect. 2.1.6):

$$\mu = f(C,P,T).$$

Boyle (1979) introduced a qualitative index to express the migration capacity of an element, seen as a function of the energy required to mobilise it. Elements with high migration energies require a large energy input to mobilize them, and hence they have low migration capacity indexes. The opposite is valid for elements with low migration energies (high migration capacity index). The best example of an element with low migration energy and high migration capacity is of course Si. An arrangement of elements, from high to low migration capacities, is given in Table 15.1.

Etheridge et al. (1983) examined the microstructural evidence for mass transport via a fluid phase in the metamorphic environment. Arenaceous rocks of low metamorphic grade show spaced cleavage characterised by little modified quartz-rich domains separated by quartz-depleted and mica-rich domains (Fig. 15.4A). These authors reason that a substantial volume loss of up to 50% must have occurred, because the quartz-rich layers have remained unaltered, whereas the quartz-poor and mica-rich layers have undergone silica depletion, indicating linear

Table 15.1. Migration capacity of elements from high (left) to low (right) (After Boyle 1979)

Gangue elements:	Si, B, K, Na, Ca – Mn, Mg, Co, Fe – Ni, Al
Gaseous elements:	CO_2 – S – Se, As, Sb, Te
Metals:	Hg, Zn, Cd, Cu, Pb, Mo – Bi – Sn – W
Precious metals:	Ag, Au, Pt
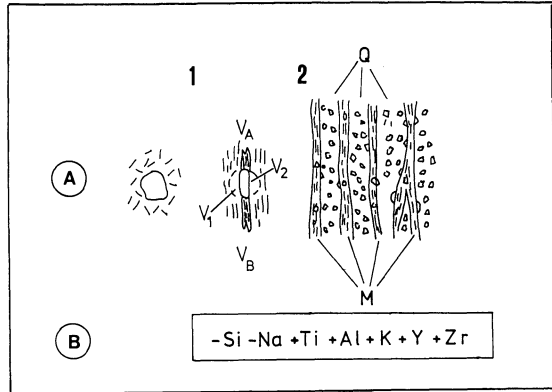
Fig. 15.4. A This figure shows the volume imbalance between dissolution sites (source) and precipitation sites (sink). At *1* a quartz grain is subject to pressure solution along faces parallel to cleavage; as a result, pressure fringes V_A and V_B form, so that $V_1 + V_2 = V_A + V_B$. At *2* cleavage development in low grade arenaceous rock shows quartz-rich domains *(Q)* and mica-rich domains *(M)*. Mass transfer occurs out of the M domains. This is quantified in **B**, in which the results of chemical analyses of Q and M domains indicate substantial loss, within the M domains, in Si and Na, and gain in Ti, Al, K, Y and Zr, assuming that the Q domains remain unaffected (After Etheridge et al. 1983)

zones of silica dissolution, since it is assumed that the original rock must have been all quartz-rich. Chemical analyses of the two types of domain indicate that the mass loss is accompanied by depletion in Na as well as Si, and enrichment in Ti, Al, K, Y and Zr (Fig. 15.4B). It is calculated that a fluid/rock ratio of about 10^3 can explain the inbalance between the two domains. At medium metamorphic grades (400–600° C) the evidence for mass transport is less obvious due to progressive destruction of the microstructures and an increase in grain size. At this metamorphic grade fluid inclusion studies show a large input of CO_2-rich fluids.

An interesting and instructive study is reported by Haack et al (1984) on mobilisation of metals from pelitic rocks during regional metamorphism. These workers emphasize that all common rocks normally contain enough metallic elements to generate ore deposits, providing that the metals can be extracted, mobilised and concentrated. They consider that regional metamorphism is a potential "ore maker", since large amounts of H_2O and CO_2 can be liberated as rocks undergo metamorphism. Haack et al. (1984) studied the mobility of elements such as Rb, Tl, Ba, Pb, Bi, Ag, Cd, Zn, Cu, S and Sr in the metapelites of the Damara orogen in Namibia. These rocks were metamorphosed at conditions ranging from the biotite isograd to anatexis. During metamorphism it is assumed that elements can be liberated by metamorphic reactions, providing that the new mineral phase cannot accomodate the freed elements into its lattice. Thus, the type and degree of metamorphic reaction would ultimately control the loss, or gain of a particular element. The result of this study indicate that in general the concentrations of Ba, Pb, Bi, Cu and Zn decrease with an increase in metamorphic grade, as measured by progressive loss of H_2O, quantified by the ratio H_2O^+/K_2O. This ratio – called the
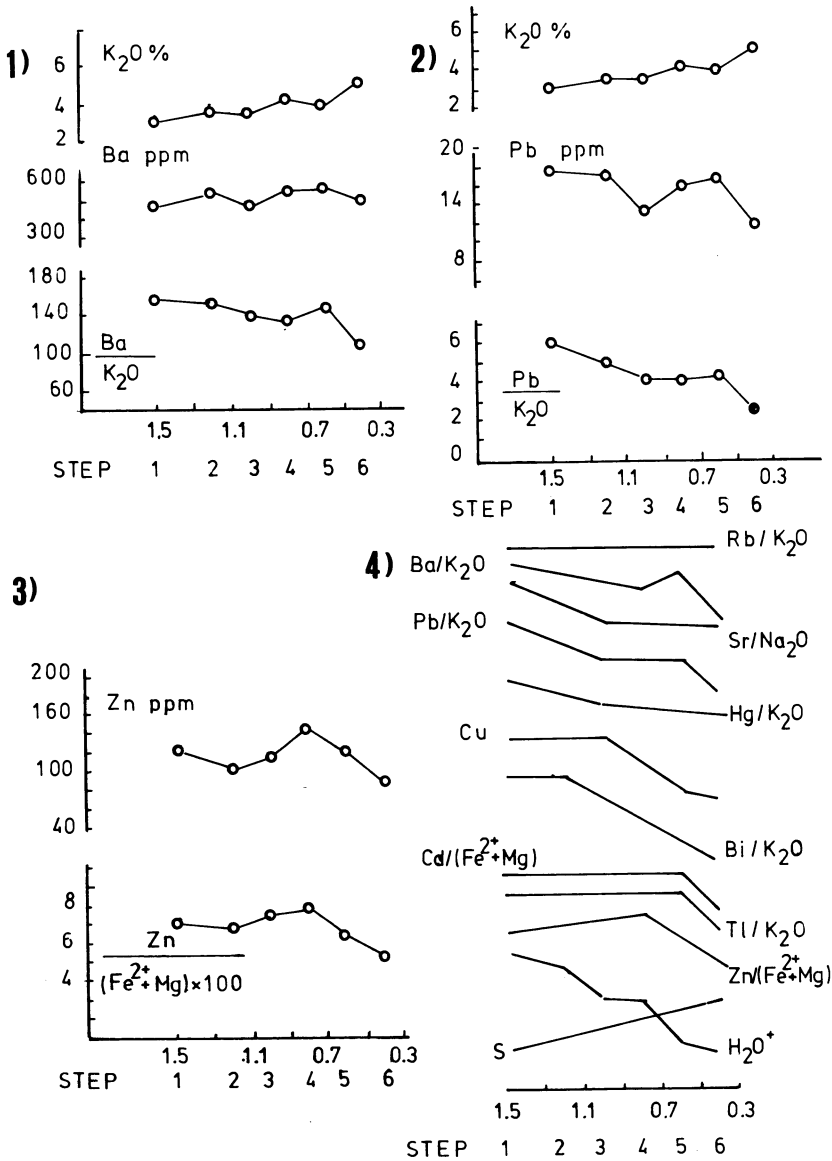
Fig. 15.5. Diagrams 1 to 3 show distribution patterns of Ba, Pb and Zn in relation to H_2O^+/K_2O ratios plotted along the abscissa. Diagram in 4 summarises the semi-quantitative pattern of element distribution in relation to this ratio. Steps 1 to 6 are discussed in the text (After Haack et al. 1984)

dehydration index – decreases in all prograde metamorphic reactions and is therefore considered a useful parameter. Figure 15.5 shows the distribution patterns of Ba, Pb, Zn as a function of the dehydration index defined above. In interpreting the diagram of Fig.15.5(1), Haack and his coworkers reasoned that Ba is normally

accomodated with K, and therefore in the first four steps these two elements run
sympathetically during dehydration. With increasing metamorphism K increases
while Ba first increases and then decreases. The trends of the Ba diagram in terms of
the prograde mineralogy are explained as follows. Reactions involving decompo-
sition of biotite to give staurolite, cordierite and garnet will result in loss of Ba
because these minerals have 8 to 180 times less Ba than the co-existing biotite. This is
shown by the increase at step 6 of the diagram [Fig. 15.5(1)]. As the amount of
cordierite and garnet increases, the capacity of the K-feldspar to contain Ba is
exhausted and Ba is further lost. These losses can be detected only if the element in
question (in this case Ba) is normalised with respect to the main element (K) which it
tends to replace (see bottom part of diagram).

Pb is known to replace K, Sr, Ba, and even Ca and Na. The ratio Pb/K_2O is
observed to decrease as K_2O increases, however the greater loss of Pb takes place at
steps 1 to 3 where K_2O is almost constant. Thus some Pb is clearly lost at this stage,
and further loss occurs in the last step at higher degrees of dehydration. The overall
interpretation of the Pb pattern is similar to that of Ba. Pb concentration in biotite is
higher then in co-existing garnets, so that when the latter increase, Pb is lost from the
rocks [Fig. 15.5(2)].

Zn replaces Fe^{2+} and Mg in octahedral sites in chlorite, hornblende and biotite.
In the diagram of Fig. 15.5(3) Zn is normalised to $Fe^{2+} + Mg$, showing a pattern of
Zn increase with the first step of prograde metamorphism; and then a sharp
decrease. The reason for this is probably due to the presence of magnetite and
staurolite which are minerals capable of incorporating Zn (up to 6200 ppm in
staurolite). The authors conclude that the highest Zn values indicate that this
element is not only derived by diffusion from the immediate surroundings at the
centimetre scale, but it may also be introduced by infiltrating metamorphic
solutions. Loss of Zn is conspicuous in the last two steps and is interpreted as due to
the decomposition of biotite and staurolite to form garnet, cordierite and K-feldspar
which are poor in Zn.

Table 15.2. Estimated concentrations and losses of elements in aluminous pelitic rocks during
prograde metamorphism (After Haack et al. 1984)

Element	Mean Concentration	Absolute loss (ppm)	Loss %	Yield per 1 km³ (t)	Concentration in solution (ppm)
Rb	137	0	0	0	–
Tl	0.79	0.156	20	406	50
Bi	0.376	0.323	86	840	14
Hg	0.016	0.007	44	19	0.3
Pb	23	7.4	32	19000	580
		6.2	27	16000	2140
Ba	597	106	18	280000	8190
Zn	120	13	11	0.34	1015
Cd	0.095	0.030	31	77	10
Cu	57	35	61	83×10^3	2400

Figure 15.5(4) gives the generalised patterns of elements lost during dehydration, and in Table 15.2 concentration, losses and yield of elements per km^3 during progressive metamorphism are given. From the values listed in Table 15.2 it can be deduced that the quantities of metals lost from pelitic rocks are indeed large, and from this metamorphic hydrothermal solutions may evolve.

15.2.6 Au in Hydrothermal Fluids

Because of the economic importance of Au in mesothermal ore systems, in this section we examine in some detail the solubility and transport of Au in hydrothermal fluids and its deposition in shear zones. We also have a brief look at the separation of precious metals from base metals in hydrothermal solutions. Aspects of these topics are also treated in Chapters 2 and 11.

The oxidation states of Au are 0, +1 (aurous) and +3 (auric). In hydrothermal fluids at high temperatures and pressures Au is present in the +1 state. The Au^+ ion is a soft electron acceptor with a large radius and therefore it preferentially interacts with soft ligands (Seward 1989, see also Chap. 2). The most stable interaction is with I^- ions, followed by Br^- and Cl^-. Other soft ligands, such as HS^-, also form stable complexes with Au^+. Seward (1989) emphasises that the $Au(HS)^-_2$ complex has a solubility 20 orders of magnitude greater than $AuCl^-_2$. Other elements commonly included in soft ligands are Ag, As, Hg and B. Most hard ligands, such as F^- and HCO^-_3, are not stable, or are insignificant in most hydrothermal fluids of high temperature and low oxidation potential. Seward (1973, 1984, 1989) concludes that the most significant ligands for Au complexing and transport are Cl^- at higher temperatures and HS^- at lower temperatures. A detailed review of this topic can be found in Seward (1991).

Henley (1973) investigated Au-chloride complexes at temperatures between 300 and 500 °C and found that higher solubilities exist at higher temperature and under oxidising conditions. Dissolution involves both oxidation and complex formation; and the reaction is:

$$Au + aHCl + bO_2 \rightarrow [Au\ complex] + cH_2O.$$
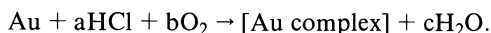
Solubilities increase with temperature from about 10 ppm at 300 °C to 500 and 1000 ppm at 500 °C at 1 and 2 kbar respectively, and Au deposition takes place mainly in response to decreasing temperature as a result of complex instability. Seward (1973) believes that sulphide complexes are more important and found little evidence for chloride complexing at 300–500 °C under near-neutral, reducing conditions. Seward's work shows that three thio-complexes are mainly involved. The complex $Au_2(HS)_2S^{2-}$ predominates in alkali solutions, the $Au(HS)^{2-}$ complex occurs in neutral solutions, while in acid solutions he concluded that the $Au(HS)_2^°$ complex is present. Later work (Seward 1984) indicates that in fact the $HAu(HS)_2^°$ complex does predominate in acid solutions, while an Au solubility maximum occurs in the near-neutral pH region. These features are illustrated in Fig. 15.6, which also demonstrates the increased Au solubility with increasing temperature, and the pH
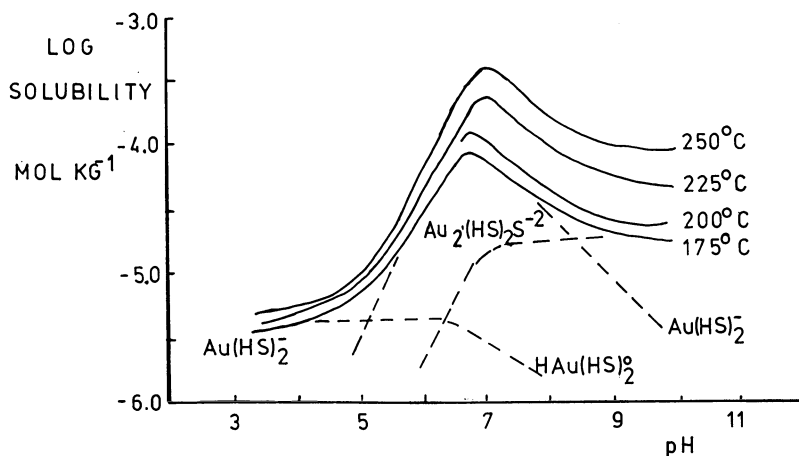
Fig. 15.6. Logarithm of Au solubility in sulphide solutions as a function of pH, temperature and complexes (pressure 1 kbar) (After Seward 1984)

regions in which particular complexes predominate. Some of the dissolution reactions may be written as follows:

$$Au^\circ + H_2S + HS^- \rightarrow Au(HS)_2^- + 1/2\ H_2$$

and

$$2Au^\circ + H_2S + 2HS^- \rightarrow Au_2(HS)_2S^{2-} + H_2.$$
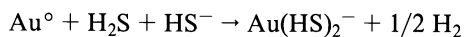
Seward (1984) concludes that Au is probably transported in hydrothermal solutions as both thio- and chloro-complexes, but thio-complexes are more important at temperature less than 400 °C. The common close association of Au with As and Sb suggests that arsenothio [$Au(AsS_2)^\circ$, $Au(AsS_3)^{2-}$] and antimonothio [$Au(Sb_2S_4)^-$] complexes may also be significant in the transport of Au in some hydrothermal solutions.

Deposition of Au, carried as sulphide complexes, may occur in response to decreasing temperatures during the ascent of a fluid, or from mixing with near-surface cooler waters. Precipitation may also be induced by any process which causes a decrease in the activity of reduced S. This can be achieved by boiling, precipitation of metal sulphides, dilution and oxidation (see Chap. 11). In addition, a decrease in pH accompanying oxidation of H_2S would also cause precipitation. Another effective mechanism of Au deposition involves its co-precipitation by colloidal As and Sb sulphide sols, which can give Au enrichments of up to seven orders of magnitude (Seward 1984). The effects of boiling occur by virtue of the partition of the volatile constituents (H_2S, CO_2, H_2 and CH_4) into the vapour phase. H_2 and CH_4 partition into the vapour phase more readily than H_2S and CO_2. CO_2 in turn transfers to steam more readily than H_2S (66 % and 51 % respectively) in the boiling interval of 290–280 °C (Seward 1989). The loss of volatiles changes the physico-chemical character of the solutions thus affecting the stability of Au complexes and consequently the solubility of the metal. Experimental work (Seward

1989) indicates that during boiling the solubility of Au first increases (at 285 °C) and then at 277 °C decreases and begins precipitating. From 277 to about 240 °C most of the Au in the solution is precipitated. Seward (1989) makes the interesting observation that if a hydrothermal solution cools slowly, then only about 65 % of the Au is precipitated and this would lead to a "geochemical anomaly" and not an ore deposit. By contrast, precipitation of Au in a boiling zone results in ore grade concentration of the metal in a relatively restricted area.

Fyfe and Kerrich (1984) suggest that other complexes based on CO may also be important for Au transport in the reduced state. This is in accord with both the low redox potential and the common Au-carbonate association in Archean mesothermal lode deposits. They report that initial experimental data indicate that Au is soluble in H_2O-CO_2-CO- and H_2O-CO_2-CO-Cl-dominated fluids. Deposition would be associated with decreasing temperature, a change in redox potential, or the breakdown of CO complexes in response to CO_2 fixation to form Fe, Mg and Ca carbonates. The authors also list a number of ligands, or complexing agents, that are sufficiently thermodynamically stable at high temperatures to be worthy of consideration as Au complexing agents. These include: CO, Cl^-, Br^-, NH_3, HS^-, S^{2-}, COS, HCN, CNS^- and AsH_3. It is also possible that different ligands are responsible for Au transport at different temperatures (Chap. 11).

Gold Deposition in Shear Zones

A study by Bonnemaison and Marcoux (1990) provides some interesting insights into the evolutionary sequence of Au deposition in shear zones. The authors developed their model on a study of a number of shear zone-hosted Au deposits from the Central Massif in France, and aurifereous quartz veins in Burkina-Faso and in Ghana. They recognised a number of distinct episodes, during which the element Au is introduced into the shear structure. At least five episodes, grouped into three stages – early, intermediate and late – are considered. The early stage, comprising episodes 1 and 2, is characterised by the deposition of Au-bearing sulphides. In episode 1, the hydrothermal fluids begin to flow into the evolving shear structure leaching, transporting metals and causing hydrothermal alteration. During this episode auriferous pyrrhotite is formed. The precise siting of the Au in the pyrrhotite lattice is not known, but the authors believe that it may occur as a diadochic substitution of Fe. In episode 2 strong silicification of the shear zone is accompanied by the deposition of arsenopyrite and the corresponding destruction of pyrrhotite. During this process Au is transferred as a solid solution into the arsenopyrite lattice. A distinct zonation is recognised in which As and Au increase from the core to the periphery of arsenopyrite crystals, with a concomitant decrease in Fe and Sb. During episode 2 although there is an overall upgrading of the Au concentration, this element is still not mineralogically expressed.

In the intermediate stages (episodes 3 and 4) Au appears in mineralogical form. During episode 3 the shear zone undergoes dilation and silica is deposited into the dilatant sites forming quartz veins. It is during episode 4 that there is a substantial concentration of Au while shearing continues, inducing cataclasis and recrystallisation of earlier-formed quartz veins, and resulting in the formation of "microsaccha-

roidal quartz". The hydrothermal fluids of this stage are enriched in Fe, Cu, Zn and Pb, and they move from the main body of the shear zone into the narrower receptacles created during this intermediated stage. These fluids destabilise the early aurifeorous sulphides (pyrrhotite and arsenopyrite) and, for the first time, native Au is precipitated. According to Bonnemaison and Marcoux (1990), in this way Au is reconcentrated into the microsaccharoidal quartz and in sulphides, and ore grades may be attained. At this stage native Au is found in several sulphides as discrete inclusions. Bonnemaiason and Marcoux report that the evidence of the early stage (episodes 1 and 2) is usually obliterated during the intermediate stage, making its recognition difficult. For example, the early formed pyrrhotite is only rarely preserved, and in most cases its presence can only be gauged by the occurrence of marcasite and pyrite which may have retained the lamellar structure of pyrrhotite. The intermediate stage is also characterised by a strong correlation of Au with Pb. This Au-Pb association may be a useful feature that can be exploited during exploration work.

The late stage (episode 5) is characterised by an extensional regime with the formation of dilatant openings into which late hydrothermal fluids move, enriched in Pb, Cu and Ag. This results in the recrystallisation of quartz (new quartz veins or stockwork zones), deposition of another generation of sulphides and newly formed sulphosalts, while Au is deposited as discrete native grains in fractures. In most cases this Au contains a high proportion of Ag, thus forming electrum with up to 20–60% Ag. Thus, the common occurrence of native Au within fractures of quartz veins is the expression of this latest mineralising stage. The grade of the mineralisation at this stage depends on the nature of the remobilised material formed during the previuos episodes. In this way, high grade ore may be formed from the remobilisation of episode 2 and/or 4 materials, while low grade ores are formed from the remobilisation of episode 1 and/or 3 materials (Bonnemaison and Marcoux 1990).

Separation of Precious Metals from Abundant Base Metals

If we assume that a large volume of hydrothermal fluid leaches Au out of a large volume of rock, take Au into solution and transport it to a suitable deposition site, it is then also reasonable to assume that greater amounts of the base metals – which are far more abundant than Au – will also be complexed, so that a base metal sulphide deposit should be formed rather than an Au deposit. The fact that this does not happen in either Archean or Phanerozoic mesothermal Au lode deposits indicates that a mechanism exists whereby Au is preferentially leached and transported, resulting in a separation between base metals and precious metals. Kerrich and Fryer (1981) address this problem, and theorise that if one considers metabasaltic rocks, assuming that they contain 2 ppb Au, and that 50% of the Au is taken into solution, as these rocks evolve 5% of water at the greenschist-amphibolite transition, the solute concentration can reach values comparable to the amount of Au reported in natural thermal waters. Fyfe and Kerrich (1984) show that average enrichment factors (average Au content of a deposit/background abundance) for lode Au deposits are approximately 10000 times, while corresponding enrichment factors for base metals in the same deposits vary from 0.1 to 10 times. This
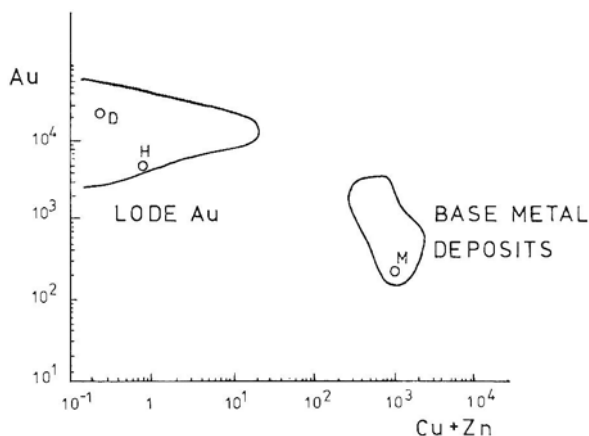
Fig. 15.7. Enrichment of Au as a function of Cu + Zn enrichment for lode Au deposits and base metal massive sulphides. Some of the deposits mentioned in text are shown: *H* Hollinger; *D* Dome; *M* Matagami (Chap. 11) (After Fyfe and Kerrich 1984)

represents an extreme separation of Au from the abundant soluble base metals. In contrast, Archean volcanogenic massive sulphide deposits show a remarkably uniform pattern of relative enrichment with Au, Ag, Cu and Zn all concentrated by factors of 200 to 2000 times background. However, the majority of Archean base metal massive sulphide deposits have lower absolute Au abundance than lode Au deposits (Fig. 15.7).

Well-known environments in which large quantities of fluids interact with large volumes of rock to produce a mineral deposit are mid-ocean ridges and areas of regional-scale prograde metamorphism. It is important to note that since sea water is trapped in the pore spaces, the pore fluids must have salinities close to sea water. As burial progresses the salinity of pore fluids will increase, and at low temperatures, some of these fluids will participate in hydration reactions. As a result the salinity of the remaining fluids will increase. These saline fluids are expelled during burial and compaction and they may form the hydrothermal solutions which are largely responsible for base metal deposits hosted in carbonate rocks (Chap. 14). Any further evolution of hydrothermal fluids will take place by dehydration reactions at higher temperatures. These are metamorphic fluids, which tend to have low chlorine contents and therefore low salinities. Fyfe and Kerrich (1984) – largely on the basis of geological and isotopic evidence – envisage that metamorphic fluids are the chief transporting agents for Au, while sea water is the main solvent for base metals. As mentioned previously, the character of fluids from which Au in veins precipitates are estimated to have temperatures of approximately 300 to 450°C, at lithostatic pressures, with significant CO_2 and salinity usually less than 3% NaCl equivalent. Fluids, from which base metal deposits are formed, have temperatures in the region of 250–300°C, at hydrostatic pressures and salinities of approximately 3–7 wt.% NaCl equivalent. During metamorphic dehydration reactions, both trace and abundant metals are available to the solutions, which initially are confined to grain boundaries and/or microfractures and foliations (metamorphic porosity). By contrast in thermally driven seawater convection systems, permeability is fracture-controlled so that the total volume of rock which is accessible to leaching is comparatively less.

In summary, the observed separation of precious metals from the abundant base metals in lode Au deposits may occur during metamorphic dehydration processes when the water/rock ratios are low and Cl availability is limited. These factors may result in limiting the uptake of abundant base metal into the solution, while the solubility of the rare precious metals is not constrained by limited fluid. Kerrich and Fryer (1981) note that water/rock ratios in submarine hydrothermal convective systems may be of the order of 10 to 100, which is 200 to 2000 times greater than for Au lode deposits, and Cl is present at about 1.9%. Under these conditions the solute abundances of base and precious metals are not constrained by solubility, or availability of halogens for complexing, and probably reflect background levels showing no large separation of elements in the hydrothermal deposit.

15.2.7 Oxygen and Hydrogen Isotope Systematics

The isotopic compositions of metamorphic waters is obtained from the isotopic values of whole rocks, mineral phases and fluid inclusions contained in quartz vein material in metamorphic rocks. The field of metamorphic waters is shown in Fig. 2.1, where it can be seen that these waters are $\delta^{18}O$-enriched and δD-depleted with respect to SMOW and the meteoric water line. The calculated field for metamorphic waters is δD 0 to -70 and $\delta^{18}O$ of $+3$ to $+20$ per mill (Sheppard 1986). In general metasediments have δD from -40 to -100 per mill, $\delta^{18}O$ of between $+8$ and $+26$, and $\delta^{18}O$ of $+3$ to $+14$ per mill. The range of these values in metamorphic rocks is probably related to the precursor rocks (Taylor 1979).

Below, we discuss two examples which serve to illustrate the use of hydrogen and oxygen isotope systematics in the understanding and interpretation of the source and evolution of fluids in the metamorphic environment. Kerrich (1986) reported on the isotope systematics of a number of mineral provinces in North and South America. The results of these studies, which focus on hydrogen and oxygen isotopes, indicate that for many of the mineralised localities, metamorphic or mixed metamorphic and meteoric fluids were responsible for the deposition and concentration of metals. These two cases – discussed in detail by Kerrich (1986) – are summarised below.

The first example is from the Grenville Front mylonitic zones which separate the Grenville high-grade gneisses from the low-grade sediments of the Southern Province. Two mylonitic zones, MZI and MZII, associated with the Grenville Front were investigated. MZI shows retrograde metamorphic reactions and has $\delta^{18}O$ values of $+7$ per mill for the associated fluids, with isotopic temperatures estimated at 420 to 490°C, which are in good agreement with the results of garnet-amphibole thermometry (540°C). MZII shows prograde metamorphic reactions and the $\delta^{18}O$ of quartz ranges from $+9.6$ to $+11.8$ per mill, with isotopic temperatures of 580 to 640°C, also in good agreement with garnet-biotite thermometry, and which gave a deformation temperature of around 600°C. Quartz-hematite veins, emplaced in fractures overprinting the deformation fabrics of MZI, have $\delta^{18}O$ (quartz) of -0.8 to -1.3 per mill. This quartz crystallised at temperatures of 200 to 350°C with fluids depleted in $\delta^{18}O$ (-8 to -14 per mill). In Kerrich's view the MZI and MZII were
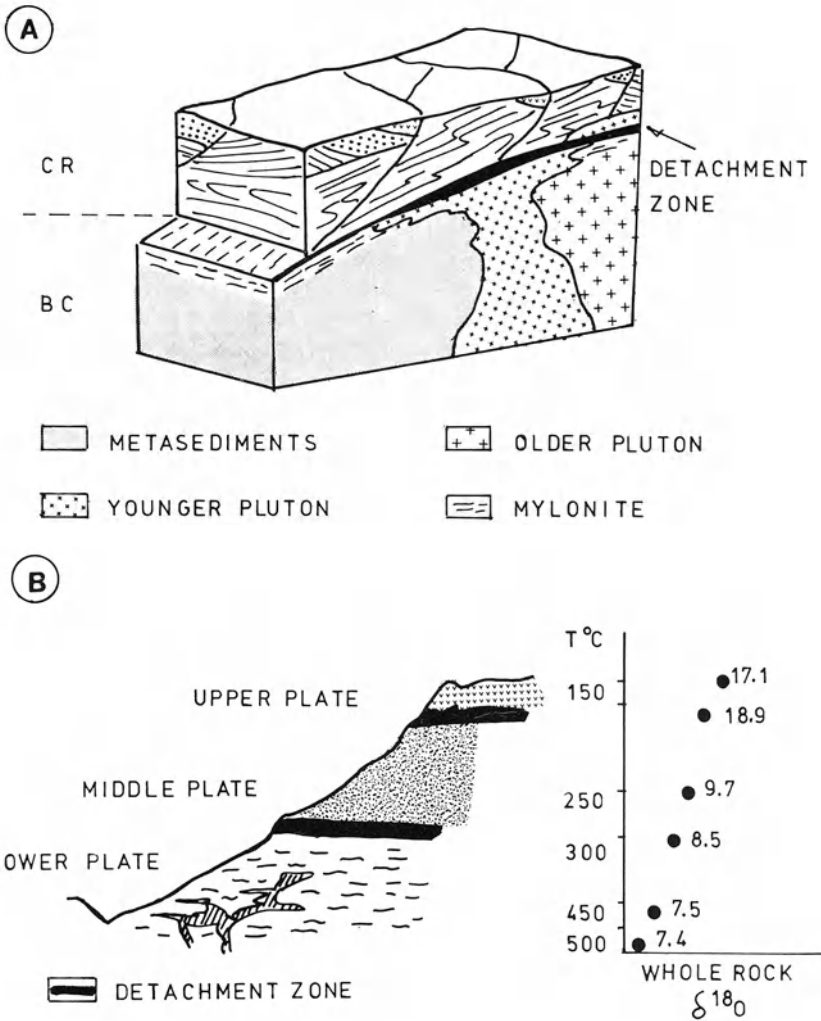
Fig. 15.8. **A** Block diagram showing domains of Cordilleran metamorphic core complexes. *CR* represents cover rocks; *BC* is basement complex (after Coney 1980). **B** Idealised cross-section of the Pichaco metamorphic core complex in Arizona; see text for details (After Kerrich 1986)

formed at high temperatures in the presence of metamorphic fluids (positive $\delta^{18}O$ values). The high grade rocks (gneisses) were tectonically placed into contact with low-grade rocks (metasediments) which had been subjected to brittle fracturing and had interacted with continental meteoric waters (negative $\delta^{18}O$ values).

The second example refers to a study of stable isotopes in the Picacho metamorphic core complex in Arizona, where Mn, Cu and Au mineralisation is present within breccia zones associated with detachment faults. These faults are low-angle structures that form the thrust boundaries between tectonic "plates"

(Coney 1980). There are three tectonic plates separated by two detachment fault zones (Fig. 15.8). The lower plate is formed by 1.4-Ga-old granitic rocks, generally undeformed, and overlain by the lower detachment fault, characterised by chloritic breccias. The lower plate becomes progressively more mylonitised towards the lower detachment fault. A 24-Ma-old granodiorite pluton intrudes the lower plate rocks and is itself affected by mylonitisation, thus establishing the age of thrusting at about or less than 24 Ma. Rocks of the middle plate are extensively brecciated and are probably part of the lower plate granitic rocks. The brecciated rocks of the middle plate are also fractured and propylitic alteration, characterised by minerals such as chlorite, epidote, quartz, albite, pyrite, carbonate and hematite, is spatially related to these fractures. Acid volcanics and sedimentary rocks of Miocene age form the allochthonous block or, upper plate (Fig. 15.8A). Isotopic data across an idealised section show a systematic increase in whole rock $\delta^{18}O$ with values ranging from +7.4 per mill (bottom) to +17.1 and +18.9 per mill at the top (Fig. 15.8B). The increase in $\delta^{18}O$ is accompanied by a temperature variation from 550 to 150°C at the top. Calculated fluid values range from $\delta^{18}O$ +3 to +7 per mill. The veined and hydrothermally altered rocks of the middle plate have higher $\delta^{18}O$ values for quartz (+12 per mill) and whole rock (+9.7 per mill) in relation to lower plate rocks, which have near-magmatic isotopic values. Thus the isotope systematics of the Picacho complex are interpreted in terms of expulsion of metamorphic fluids from lower crustal levels into rocks of the upper tectonic sections, accompanied by cooling. Sporadic ^{18}O-depleted mineral phases may be indicative of incursions of meteoric waters into the upper plate (Kerrich 1986).

15.3 Tectonic Settings

Orogenic and tectonic processes which favour large-scale generation and transport of hydrothermal fluids are subduction systems and collision orogens. Subduction of oceanic crust, release of fluids above a subducting slab, the role of collision tectonics and thrust faulting in the generation of fluids are introduced and discussed in Chapter 3.

Figure 15.9 illustrates the principal tectonic settings in which fluids are generated during convergent processes, which result in compression, deformation and prograde metamorphism of sedimentary wedges. Conceptual models of fluid generation and migration in these geotectonic environments have been investigated, among others, by Oliver (1986), Duane and de Witt (1988), Langseth and Moore (1990a, b) and Torgersen (1990).

In a subduction system, such as that depicted in Fig. 15.9A, the accretionary prims is subject to intense deformation. The prism comprises thick sedimentary packages, including turbidite-facies sequences, which by virtue of their depositional environment are sea-water-saturated. Subduction processes result in tectonisation, increasing temperature and pressure and the expulsion of sea water incorporated in the sediments as well as the water released from the dewatering of clays. Tectonic compaction of the accretionary prism commences near the oceanward portion,
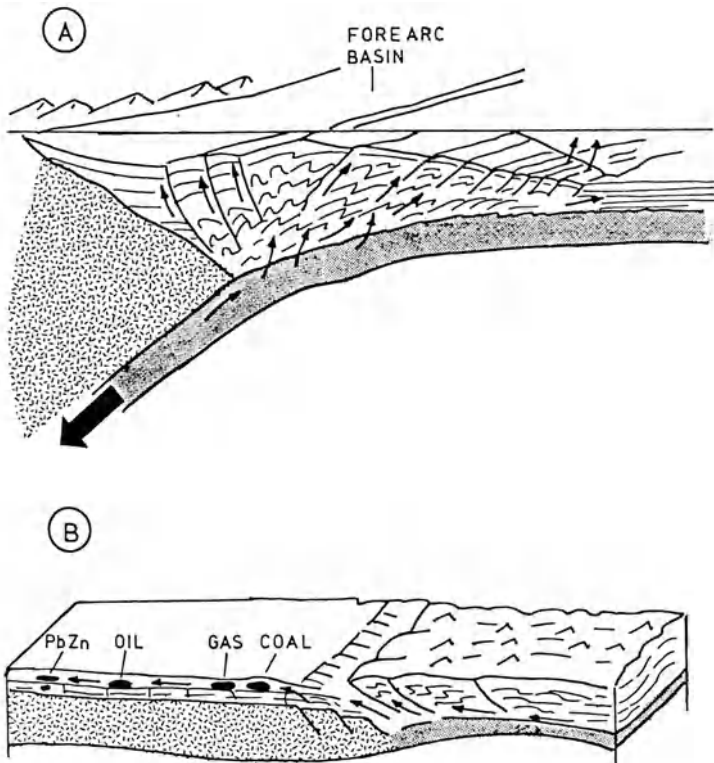
Fig. 15.9 A, B

where the fluids derived from the dewatering of the sediments, move along permeable beds and are expelled along thrusts and faults. Towards the trench – at the rear of the prism – fluids are generated at deeper levels by dehydration reactions. These fluids move along thrust faults and along the interface between the prism sediments and oceanic crust (basalt-sediment interface). As explained in Chapter 3, release of fluids also occurs in the underlying oceanic crust material and these may mix with those generated within the accretionary prism. Kerrich and Wyman (1990) in reviewing the geodynamic setting of mesothermal mineralisation note that, at least for Phanerozoic times, there is a distinct spatial association between mesothermal lode deposits and regional structures in allochthonous terranes which have accreted onto continental margins or island arcs. The common features (nature of fluids, structure, metal association) between Phanerozoic and Archean lode deposits suggest a common mechanism of ore deposition. Thus, Kerrich and Wyman (1990) developed a "transpressive accretion hypothesis", whereby the mesothermal lode mineralisation is the result of subduction-related crustal underplating and prograde metamorphism in subduction complexes.

Figure 15.9B, C illustrates the model in which fluids may be generated during collision of continental plates. These orogenic fluids are formed through processes
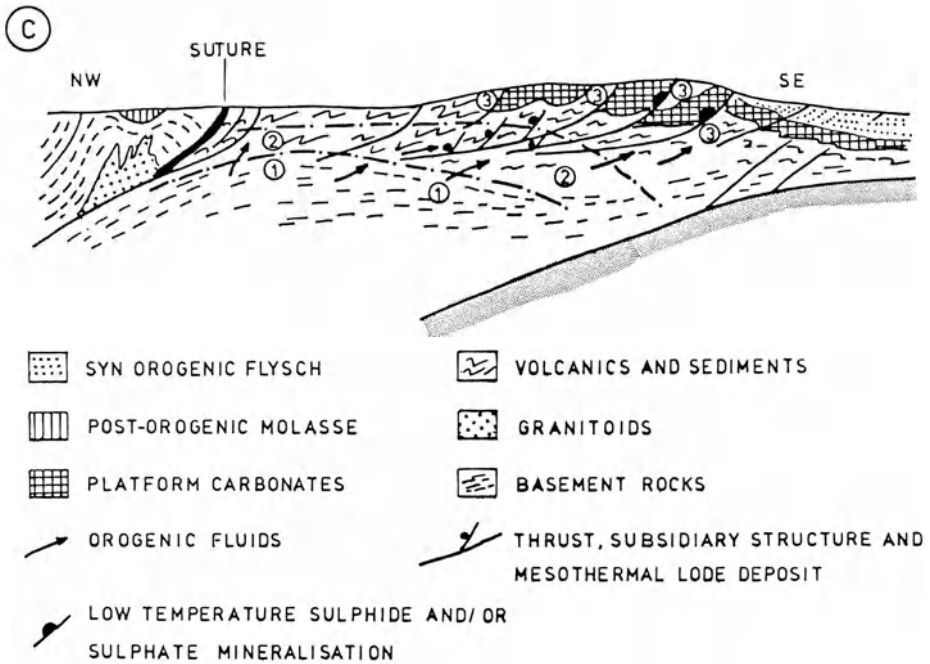
Fig. 15.9. A Subductions system showing accretionary prism. *Arrows* indicate paths of fluid movement. Dewatering of sediments predominates in the upper sectors and oceanward, while devolitisation reactions dominate at depth. Fluids are also derived from dehydration of oceanic crust (see Chap. 3). Drawing is not to scale (after Langseth and Moore 1990a, b). B Schematic representation of a collision orogen (as exemplified by the Appalachian belt) illustrating movement of orogenic fluids expelled from the sedimentary packages. Coal, gas, oil accumulations and base metal sulphides deposits are successively formed from the collision front towards the foreland as shown; drawing not to scale (after Oliver 1986). C Schematic representation of the eastern Alps orogen, which is the result of the collision between two continental plates: Noric and Austroalpine. Metamorphic zones in the collision zone are indicated by the dash-dot lines. *1* Amphibolite facies domain; *2* greenschist facies domain; *3* zone of mixing between metamorphic and meteoric fluids. Mesothermal lode deposits are formed along subsidiary shear zones branching off the main thrust faults. Further away in the carbonate platform low-temperature carbonate-hosted sulphide and sulphate deposits are formed (see Chap. 14); drawing is not to scale (After Frimmel 1990)

of tectonic burial, compression and prograde dehydration reactions in the collision zone. As collision proceeds the fluids, according to the model, are effectively "squeezed out" and expelled towards the foreland. The paths followed by the orogenic hydrothermal fluids are mainly along décollement zones and thrust faults. Oliver (1986) advocates a zoning from near the suture zone (collision area) towards the foreland as shown in 15.9B (see also Chap. 3). Using Oliver's model, Frimmel (1990) proposes that some fluids produced in the collision zone may facilitate thrusting and during their propagation or expulsion towards the fold belt (foreland), the orogenic fluids may remobilise metals from existing syngenetic deposits (15.9C). If the foreland contains platform sequences, such as evaporites and/or carbonate shelf sediments, these fluids would mix with

percolating meteoric waters, become oxidised and result in the precipitation of epigenetic sulphide and sulphate (e.g. barite) deposits in veins or pre-existing cavities (Chap. 14).

15.4 Archean Mesothermal Deposits

Mesothermal lode Au deposits of Archean granite-greenstone terranes are well known and are extensively mined in South Africa, Zimbabwe, Australia, Canada and Brazil, as well as other parts of the world where greenstone belts outcrop (see Fig. 5.2). These terranes are characterised by granitoids and gneissic rocks surrounding and intruding supracrustals (greenstone belts), which are dominated by early mafic-ultramafic and lesser felsic volcanics and later clastic sediments. The greenstone rocks show single-stage prograde metamorphism, generally greenschist facies, locally with zones of amphibolite facies developed adjacent to granitic rocks. In places there is good evidence of subhorizontal deformation and thrust tectonics.

In this section we examine the Archean greenstone terranes, related environments of Au mineralisation, and current theories of ore genesis; we then describe some of the well-known deposits from the Barberton and Murchison greenstone belts in South Africa, the Golden Mile of the Norseman-Wiluna belt in the Yilgarn Province in Western Australia and the unusual Hemlo deposit in the Abitibi greenstone belt in the Superior Province in Canada. A recent and comprehensive review of Archean mesothermal lode deposits can be found in Groves and Foster (1991).

15.4.1 The Archean Greenstone Belts

Models of Archean crustal evolution and developments of granite-greenstone terranes are reviewed in Chapter 5. Reviews and details on Archean geology and mineralisation can be found in Glover and Groves (1981). Here, we focus our attention on the geology of greenstone belts, as they are the main hosts of mesothermal Au lode deposits. Archean greenstone belts are the oldest volcano-sedimentary rock sequences which are preserved in shield areas, varying in age from approximately 3.5 to 2.3 Ga (Windley 1984). Their stratigraphy, general structure, igneous rock geochemistry and contained ore deposits are remarkably uniform, and this feature allows most greenstone belts to be treated as a single entity (Condie 1981). An idealised and simplified stratigraphic succession of a greenstone belt is shown in Fig. 15.10. This is broadly applicable to the well-studied belts of South Africa, Australia and Canada. With reference to this figure, a greenstone belt succession usually comprises three major sequences: (1) a lowermost ultramafic to mafic sequence; (2) a volcanic sequence dominated by mafic to felsic calc-alkaline units; and (3) an uppermost sedimentary sequence (Anhaeusser and Viljoen 1986). The ultramafic-mafic sequence comprises cyclic ultramafic to mafic volcanics and pyroclastics with some minor sedimentary rocks. This sequence is well known for
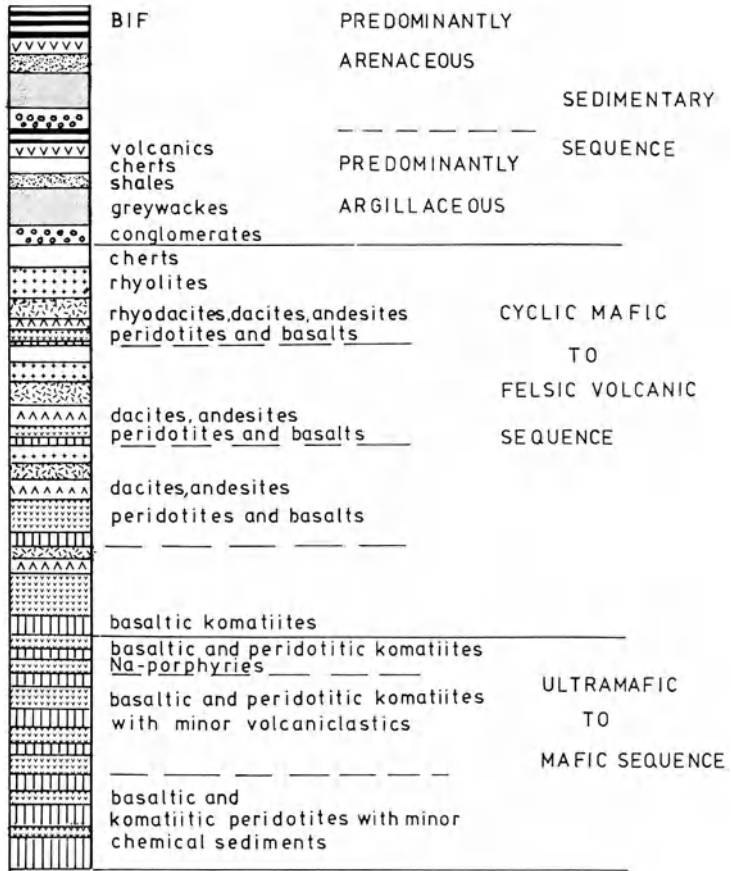
Fig. 15.10. Simplified volcano-sedimentary sequence typical of an Archean greenstone belt (After Anhaeusser and Viljoen 1986)

the common occurrence of basaltic and peridotitic komatiites first described by Viljoen and Viljoen (1969a). These rocks are characterised by MgO contents of between 8 and 40%), high Ni, Cr and low Fe and Ti. The volcanic sequence is dominated by cyclic mafic to felsic volcanics and pyroclastics with minor development of sedimentary rocks. The volcanics have a calc-alkaline chemistry, and the ratios of pyroclastics to lava flows increase with stratigraphic height, which means that the nature of volcanism becomes more acidic with time. Sediments, consisting mostly of chemically precipitated cherts, jaspers and BIF, generally mark the end of individual volcanic cycles. The uppermost sequence consists of alternating coarse to fine sedimentary assemblages with only minor development of volcanic rocks. These rocks ideally consist of a lower argillaceous, deep-water and an upper arenaceous shallow-water assemblages with BIF located at the tops of the cyclic units.

Platform-Phase and Rift-Phase Greenstones

Groves and Batt (1984), with reference to Western Australia mainly, have subdivided the greenstone belts into two major temporal categories, namely: (1) older greenstones, with supracrustals formed between 3.5 and 3.3 Ga and preserved in the Pilbara craton of Western Australia, the Barberton Mountain Land and in some parts of the Zimbabwe craton; (2) younger greenstones, much more common and best developed in the interval ca. 3 to 2.7 Ga, which form most of the Yilgarn craton of Western Australia, the Superior Province of Canada, the Zimbabwe craton and probably most of the Brazilian, Indian and Baltic shields. The authors describe platform-phase and rift-phase greenstones from both older and younger terranes and the differences in the tectonic styles have a direct influence on the genesis and style of their contained ore deposits.

Platform-phase greenstones are characterised by a tectonic pattern of roughly equally spaced granitoid batholiths with intervening greenstone belts, suggesting diapiric emplacement of the granites through greenstone slabs of constant thicknesses. Platform-phase greenstones have dominant basaltic rocks, poorly developed komatiite sequences and isolated felsic volcanic centres. The nature of the lower volcanic sequences suggest that they developed in shallow basins or platforms with no marginal relief (hence the name platform-phase greenstone). Although the basins were volcanically active, and presumably formed as a result of extensional tectonics, there appears to be no evidence for fault control on basin development. There is evidence to indicate that platform-phase volcanic sequences in the older terranes formed over an interval of 300 to 500 Ma, under shallow-water conditions, with vesicular basalts being well developed in the lower units. Distal sediments may represent volcanic ash re-worked in shallow water, while sediments derived from a basaltic source are rare, and turbidites and BIF are also rare or absent altogether. Silicified carbonates and evaporites are common. Platform-phase greenstones in the younger terranes formed over an interval of 100 to 300 Ma, under generally deeper water conditions, evaporites are rare, as are accretionary lapilli and vesicular basalts. Although felsic volcaniclastic sedimentary wedges were re-worked in shallow water, turbidites are well developed as a distal facies and BIF are common.

Rift-phase greenstones are characterised by linear tectonic patterns, and were developed on earlier platform-phase greenstones. The rift-phase greenstones of younger terranes are typified by linear fault-bounded basins, in the order of several hundred kilometres, and represent by far the most well-endowed Archean terranes in terms of mineral deposits. Rift-phase greenstones contain a complex stratigraphy of ultramafic-mafic sequences at the base, followed by mafic-felsic volcanics and volcaniclastic sediments. The volcaniclastic sediments were deposited both in terrestrial environments related to subaerial volcanic systems and in large submarine fans. Clastics include submarine mafic and ultramafic rocks, which suggest uplift and subaerial exposure of these early sequences. Komatiites are thicker and more extensively developed than in platform-phase greenstones. The type area in Western Australia is the Norseman-Wiluna belt of the Yilgarn Craton. This belt is characterised by thick extrusive peridotitic komatiites, intrusive komatiitic dunites,

sulphidic shales and abundant cherty sediments. Distal turbidites and thick non-vesicular basalts, indicative of deep-water conditions, occur in the central parts of the elongate basins. BIF are generally absent in rift-phase greenstones, while they are abundant in platform-phase greenstones. Rapid facies changes support the concept of fault-bounded basins and sedimentary facies suggest that parts of these basins were deep troughs. The occurrence of bimodal basalt-rhyolite volcanism provides evidence for a tensional tectonic setting and it is therefore likely that these rocks formed in an active extensional setting characterised by major crustal thinning. The Norseman-Wiluna belt is approximately 2.8 Ga old, and isotopic dating also indicates that the belt evolved in a much shorter time (ca. 100 Ma) than many platform-phase greenstone belts.

Groves and Batt (1984) believe that most greenstones were formed on a sialic continental basement, consisting of granitic gneisses and although direct evidence for a sialic basement is usually lacking, they cite various lines of reasoning to support this assumption. For example, the presence of calc-alkaline volcanics with geochemical characteristics similar to those erupted through continental crust, and the hiatus between volcanism and metamorphism which is suggestive of a thermal buffer such as continental crust. An alternative view is given by Smith et al. (1984) in which oxygen isotope systematics provide some evidence to show that komatiitic magmas in the Barberton Mountain Land were erupted in an oceanic setting. The $\delta^{18}O$ values of komatiites are around 5.7 per mill, which are similar to those of modern ocean-floor basalts, also indicating that the mantle source material of Archaen komatiites had the same isotopic composition as mantle material from which modern ocean ridge basalts are derived. These authors also show that alteration patterns in Archean pillow lavas are similar to those occurring today during alteration and metamorphism of submarine lavas. More recently, studies of Cretaceous komatiites from the island of Gorgona, off the coast of Colombia, have led to the proposal that komatiites may represent products of mantle plumes and that Archean komatiites could be overthrust fragments of oceanic plateaus (Storey et al. 1991).

It is therefore somewhat misleading to assume that all greenstones either represent oceanic crust or that they were deposited on a continental basement, as it is likely that both situations existed. If one returns to the model advocated by Windley (1984) – discussed in Chapter 5 – it can be seen that back arc extension, resulting in the formation of oceanic crust, could indeed be preserved as a greenstone belt such as the Barberton Mountain Land. Windley's model does not require continental basement as a prerequisite for greenstone formation.

Tectonic Evolution of Greenstone Belts

Perring et al. (1989) and Barley et al. (1989) compared the evolution of the greenstone sequences of the Norseman-Wiluna belt with those of younger orogenic belts formed at obliquely convergent plate boundaries. Their evolutionary model is based on a re-interpretation of the lithostratigraphic associations, structural and metamorphic history and the nature of the granitoid suites of the belt. Lithostratigraphic correlations indicate that the Norseman-Wiluna belt can be subdivided into

two sectors separated by the major Keith-Kilkenny lineament. East of this lineament (and east of the town of Kalgoorlie, home of the Golden Mile to be discussed later), tholeiitic rocks are intercalated with calc-alkaline volcanics erupted from subaerial centres. These rocks represent sequences with ages in excess of 2.9 Ga. West of the Keith-Kilkenny lineament, the successions are approximately 2.7 Ga in age and are characterised by Mg-rich basalts, tholeiites and komatiites intercalated with sulphidic and graphitic shales. The youngest units in the stratigraphy are rhyolitic volcanic and pyroclastics and feldspathic sedimentary rocks. These units are interpreted as having been deposited in graben structures. The association of mafic rocks, calc-alkaline volcanics and feldspathic sediments are compared to modern volcanic arc systems, whereas the Mg-basalts-komatiite-tholeiite association is compared to marine extensional basins. From the structural point of view the striking feature of the Norseman-Wiluna belt is the network of regional-scale north-northwest-trending fault systems, which divide the belt into a number of fairly well-defined domains. Importantly, zones of extensive carbonitisation are spatially associated with these fault systems. Deformation and metamorphism occurred some 50 Ma after the deposition of the supracrustal sequence.

Perring and coworkers subdivide the intrusive suites of the Norseman-Wiluna belt into "external" and "internal". They call external granitoids the expanse of granitic rocks which outcrop between individual greenstone belts. These granitoids are generally leucocratic and comprise biotite-bearing monzogranites, granodiorites and granites, locally with well-developed pegmatitic phases. The external granitoid are syn- to post-tectonic and have a restricted mineralogical and geochemical composition, which however does not appear to conform to either S or I types. External granitoids do not host Au mineralisation. The internal granitoids are by definition enclosed within the greenstone sequences and have variable compositions which range from tonalitic and granodioritic through monzogranite and syenogranite, quartz-syenite to trondhjemite. Porphyry dyke swarms and calc-alkaline lamprophyres are common and occur spatially associated with the internal granitoid plutons. Internal granitoids have mineralogical and geochemical characteristics close to I-type granites and to a lesser extent to A types. Au mineralisation is, in many instances, associated with the internal plutons, felsic to intermediate porphyries and calc-alkaline lamprophyres dykes.

Perring et al. (1989) and Barley et al. (1989) interpret the internal granitoids and associated porphyries as representing volcano-plutonic associations typical of volcanic arcs. The present-day juxtaposition of the tectono-stratigraphic associations discussed above is therefore modelled as being the result of westward subduction with development of an ensialic volcanic arc and back-arc basin geotectonic situations, in a manner not too dissimilar from the model of greenstone formation proposed by Windley (1984). If this scenario is feasible, even in its broad lines, then – the authors reason – it is possible that the Archean mesothermal lodes originated in much the same way as those of the Canadian Cordillera (Nesbitt and Muehlenbachs 1989).

Hodgson and Hamilton (1989) have also interpreted the geology of the Abitibi greenstone belt in Canada taking into consideration the main lithological assemblages and types of geological terranes. The history of the Abitibi belt can be

summarised as follows: quartzose sediments (greywacke) with intercalated koma-
tiites were formed in an extensional environment underlain by thinned crust
transitional between continental and oceanic. This assemblage – known as the
Bellecombe terrane – was deposited on the margin of a continental block. The
komatiitic and tholeiitic rocks occur in the lower part of older and younger volcanic
sequences and were formed in an oceanic crust setting. The calc-alkaline rocks of the
younger volcanic cycle were formed in an island-arc setting. Himalayan-type
collision is called upon to explain the main structural features of the Abitibi belt,
especially the geometry of D1 structures. These terranes were therefore tectonically
stacked during collision of a northward-moving continent, and its attached
sedimentary apron, against a volcanic arc, due to subduction of the intervening
oceanic crust.

Recent deep seismic reflection data obtained from seismic surveys carried out
across the Abitibi greenstone belt (Green et al. 1990) appear to confirm the notion
that horizontal tectonics, that is thrust and strike-slip faulting, played an important
role in the tectonic evolution of greenstone belts. According to the interpretation of
Green et al. (1990), the Abitibi belt is relatively shallow and characterised by
subhorizontal imbricated and thrust structures which overlie a reflective lower
crust. The latter is interpreted to be formed by layered felsic, mafic gneisses and
anorthosites, which in turn overlie the Moho discontinuity.

Studies in the Barberton greenstone belt by de Witt (1982, 1983) and Louw et al.
(1985) have revealed that tectonic stacking along original subhorizontal faults have
resulted in a sequence of thrust and nappe structures. The existence of these
structures in the Barberton greenstones is of considerable importance, firstly
because it implies that the stratigraphic thickness of the lowermost mafic-ultramafic
sequence (Onverwacht Group, see later) is substantially reduced from the original
estimates of 15 km by Viljoen and Viljoen (1969b), thus making these lithologies
comparable to oceanic crust. Secondly, it confirms that large-scale horizontal
tectonics occurred in the Archean further substantiating that plate tectonic
mechanisms, accretion and collision, played an important role in the geodynamic
evolution of greenstone belts. Thirdly, the presence of thrust faults is instrumental in
the channelling of hydrothermal fluids from deep sources and the generation of
mineral deposits spatially associated with these fault structures.

15.4.2 Metallogenesis

A brief review of Archean metallogenesis is given in Chapter 5. Groves and Batt
(1984) have proposed a model in which the differences in tectonic and deposi-
tional settings have a major influence on the development of metallogenic
associations within rift- and platform-phase greenstones of the younger and older
terranes.

These authors point out that volcanogenic Cu-Zn massive sulphide deposits are
preferentially developed and preserved in deeper water environments of the younger
greenstones, whereas subvolcanic Cu-Mo porphyry deposits are more common in
the subaerial environments of the older terranes. Syn-volcanic Ni-Cu deposits
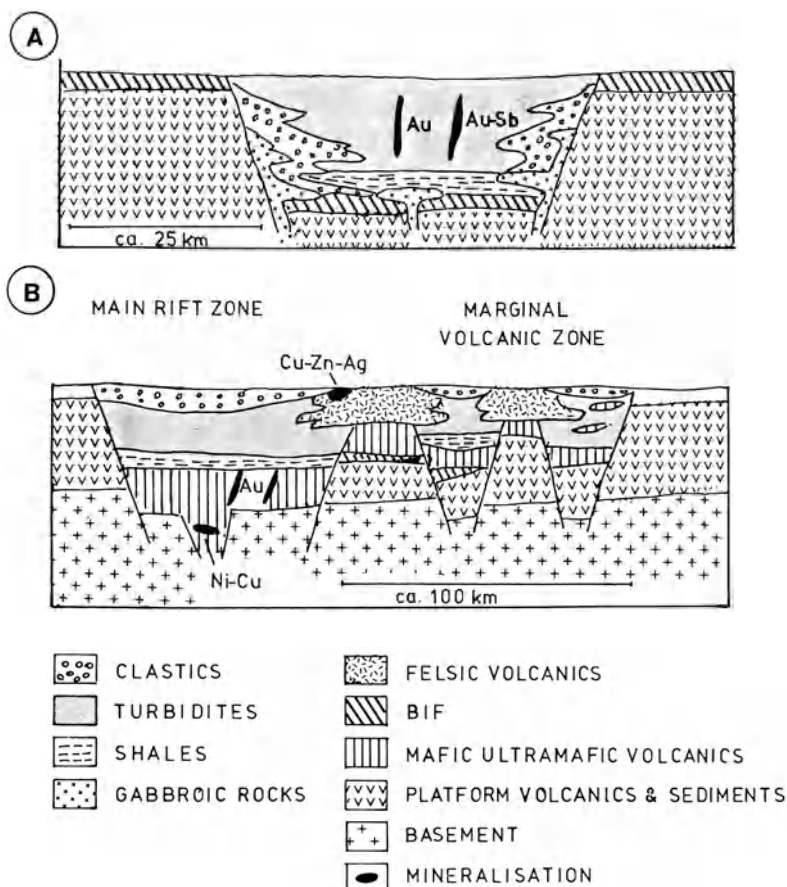
Fig. 15.11A, B. Rift-phase greenstones of A older and B younger terranes; see text for details. In B the main rift zone contains thick sequences of basalts, komatiites and clastic sediments. Magmatic Ni-Cu and mesothermal Au-Te deposits are predominantly volcanic-hosted. In the marginal volcanic zone are numerous calc-alkaline centres and mineralisation of the volcanogenic massive sulphide type predominates (see Chap. 11). Mesothermal vein lodes in the older rift-phase greenstones are sedimentary-hosted (After Groves and Batt 1984)

associated with komatiites are poorly developed in both older and younger platform-phase greenstones.

Rift-phase greenstones have a different expression in terranes of different ages, e.g. graben type in older terranes and true rift type in younger terranes. These differences, illustrated in Fig. 15.11, result in different metallogenic associations. In the older terranes the graben-like depositories are dominated by turbidites and proximal submarine fan accumulations, and the volcanic component is usually small. Mineralisation is poor and consists of sediment-hosted Au ± Sb ± As lodes. Rift-phase greenstones in younger terranes appear to represent greater extension and crustal thinning than in older terranes, and this environment is more conducive to the eruption of thick komatiitic sequences. The development of komatiites in the

lower parts of the rifts constitutes a favourable environment for the formation and preservation of syn-volcanic Ni-Cu deposits, as seen in the Norseman-Wiluna belt. Rapid subsidence and burial of mafic-ultramafic sequences within the rifts tends to preserve these rocks for later Au extraction by metamorphic fluids, while the re-activation of major faults may serve as channelways for the fluids migrating into suitable depositional sites.

Gold is perhaps by far the most important metal commodity of greenstone belts and types of Au mineralisation in Archean greenstones include stratabound-stratiform deposits, massive sulphides and mesothermal lodes. Stratabound-stratiform deposits are found in BIF, both carbonate and sulphide facies, but it is not clear whether BIF-hosted Au is syngenetic or epigenetic in origin. Au also occurs in sulphide minerals of volcanogenic massive sulphide deposits, which are of particular importance in the Superior Province in Canada (Chap. 11). However, the principal mode of Au occurrence in Archean granite-greenstone terranes is in quartz vein stockworks and mesothermal lode deposits, which are associated with faults and shear zones. There is often a spatial relationship between BIF-hosted and mesothermal lodes suggesting that they may be genetically linked.

15.4.3 Theories on the Genesis of Archean Mesothermal Au Deposits

In this section we examine the prevailing theories that have been proposed to explain the genesis of Archean mesothermal Au deposits. Archean mesothermal mineralisa-tion styles, as previously mentioned, vary from quartz veins in shear or fault zones, to quartz vein stockworks in igneous host rocks to stratabound and locally stratiform deposits in BIF and other Fe-rich sediments. These different styles have led to syngenetic, epigenetic and combined epigenetic-syngenetic theories.

A syngenetic theory was initially proposed by Fripp (1976) following his work on BIF-hosted Au in Zimbabwe. Fripp's model suggests that the mineralisation is the result of submarine hot spring activity. A similar model based on sea-floor hydrothermal actvity is also proposed by Paris et al. (1985). The epigenetic theories have their foundation on the fundamental observation that virtually all mesother-mal Au lodes are structurally controlled, although many syngeneticists claim that the mineralisation, initially syngenetic, was subsequently re-mobilised into favour-able structures during deformation events. One epigenetic view – metamorphic replacement model (e.g. Kerrich and Fyfe 1981; Fyfe and Kerrich 1984; Groves and Phillips 1987) – holds that the hydrothermal fluids were derived from devolitilisa-tion reactions during regional prograde metamorphism and subsequently focused into faults and shear zones. This model has substantial support particularly amongst Australian geoscientists. Another epigenetic model proposes that the hydrothermal fluids were of magmatic origin and related to granitic intrusions (Burrows et al. 1986; Wood et al. 1986; Burrows and Spooner 1989). A third model – lamprophyre-crust interaction (Rock and Groves 1988; Rock et al. 1989) – attempts to reconcile the two by adopting the view that fluids were formed in both the metamorphic and igneous environments, while yet another model attempts to reconcile epigenesis and syngenesis by suggesting that metamorphic fluids moved

along structural conduits to eventually debouch on the sea floor as hot springs (Kerrich and Fryer 1979). A model of mantle degassing and granulitisation is advocated by Fyon et al. (1989).

The Syngenetic Model

Fripp (1976) proposes a syngenetic origin for BIF-hosted Au-sulphide mineralisation. Fripp's theory is based on a comprehensive study of the distribution and nature of stratabound mineralisation in the BIF units in the greenstone belts of the Zimbabwean craton. The BIF-hosted Au-sulphide deposits show different characteristics, e.g. they are stratiform, from the obviously cross-cutting and therefore epigenetic quartz vein lodes. BIF – as oxide, silicate and carbonate facies in the greenstone sequences of Zimbabwe – occur in three distinct lithostratigraphic sequences: (1) within ultramafic and mafic rocks of the Sebakwian Group; (2) intercalated with calc-alkaline volcanics of the Bulawayian Group; and (3) intercalated within the sedimentary sequences of the Shamvaian Group. These Groups broadly correspond to the three major lithostratigraphic subdivisions of greenstone belts as outlined in Section 15.4.1. BIF units in the first two Groups are clearly volcanic-associated and conform to the Algoma type (see Chap. 5). Stratiform Au-sulphide deposits are more commonly found in the Sebakwian BIF, whereas fracture-controlled quartz lodes are more common in the lithologies of Bulawayan and Shamvaain age. Fripp (1976) proposes that during the Sebakwian high geothermal gradients promoted widespread and vigorous convective circulation of brines through the predominantly mafic greenstone pile, with leaching of Au, Fe, As, Si, S, Mn, Ti, Cu, Pb, Zn, Co and Ag. The brines discharged on the sea floor as hot springs, resulting in the formation of beds of BIF containing carbonate, Fe, S, SiO_2, As and trace metals including Au. In keeping with the general facies distribution of BIF with water depth, Fripp (1976) recognised three main categories of BIF-hosted Au deposits. Near shore, in shallow oxygenated waters, Fe oxides minerals predominated. The brines discharging in this area were characterised by near-neutral pH and temperatures of between 95 and 130°C, with less than 50 ppm Au. Mixing with sea water affected the solubility of Au and other components such as silica, Fe sulphides and carbonates. BIF formed in these shallow oxygenated waters contain chert, hematite, magnetite, Au-bearing sulphides and carbonate layers. In deeper water, the discharging brines, at temperatures between 130 and 205°C with a neutral to slightly acid pH, and higher Au contents (50 to 300 ppm) resulted in the precipitation of carbonates, Au and Fe-As sulphides. At water depths in excess of 200 m, in a predominantly reducing and alkaline environment, the hot springs would be very rich in Fe and sulphide components and contain only minor amounts of Au.

Paris et al. (1985) studied and identified cherts in the Barberton greenstone belt as being the product of silicification of a variety of rocks, such as pillow lavas, pyroclastics and sedimentary units. They found that the chert material is associated with silica-filled fractures, breccias and vein stockworks. These cherts are therefore interpreted as chemical precipitates (exhalites), which overlie the silicified and brecciated rocks. The cherts would have been precipitated from the discharging of a

sea water Si-rich geothermal system. The authors propose three stages in the development of the Barberton cherts. In the first stage, hydrothermal convection of sea water through oceanic crust layers 1 and 2 (see Chap. 12) takes place with leaching of Si and possibly also Au, Fe and Ba. In the second stage, the resulting brines move upward and penetrate, via fractures, into the overlying sediments (layer 1). During the third stage, the sediments, once sufficiently lithified, are brecciated and stockworks, breccias and pseudoconglomerates are formed. The Msauli Chert Unit in the Barberton greenstone belt is considered to be a good example of this silicification process. The close spatial association of Au mineralisation to the Zwartkoppie Chert Bar – Fairview and Sheba mines, Barberton greenstone belt (see later) – might be an indication of an exhalative origin for at least part of this mineralisation, which was possibly subsequently re-mobilised into structures to form epigenetic lodes during deformation events.

The Metamorphic Replacement Model

This is proposed by Groves and Phillips (1987) who base their model on the following observations. The vast majority of Au deposits occur in volcanic-dominated sequences, in greenschist facies domains and are hosted by Fe-rich rocks such as basalts, dolerites or BIF. Strong structural control is evident and ore deposition is commonly located in, or adjacent to, shear zones or faults, which in turn, are spatially associated with crustal-scale lineaments tens to hundreds of kilometres long. Structural and metamorphic studies indicate that Au mineralisation is essentially synchronous with regional prograde metamorphism. The authors also noted the remarkable down-plunge continuity of the ore zones relative to strike length and width. The lack of vertical zoning observed in many deposits suggest that the wall rocks were warm at the time of the mineralising event. Most Archean mesothermal Au deposits have distinctive alteration haloes with zones of K-mica ($\pm$ albite), ankerite-dolomite and Fe-sulphide alteration, surrounded by broader zones of carbonitisation. The BIF-hosted deposits, however, do not show the same degree of alteration. Au usually occurs as submicroscopic grains within Fe-sulphides in the alteration assemblage rather than within the penecontemporaneous to slightly later quartz veins, although there are exceptions to this. In any case the general association of the Au with sulphides, the Fe-rich nature of the host rocks and the lack of mobility of Fe are taken as evidence that Au deposition was related to sulphidisation of wall rocks. In fact, many Au deposits are believed to have formed as a result of sulphidisation of wall rock, and the contemporaneous deposition of Fe-sulphides and Au in those channelways which intersect Fe-rich lithologies within greenschist facies domains. In contrast to the syngenetic theory, Groves and Phillips contend that also stratabound, or locally stratiform, ores form as a result of sulphidisation adjacent to fractures in oxide facies BIF units (see Fig. 15.12). Interaction of Fe-rich host rocks and S-bearing soilutions would result in the formation of pyrite and the breakdown of sulphide complexes to precipitate Au (see also Chap. 11, Sect. 11.7.2). One of the possible reactions is (Phillips et al. 1984):

$$FeO + HAu(HS)_2 + 1/4O_2 \rightarrow FeS_2 + 3/2H_2O + Au.$$
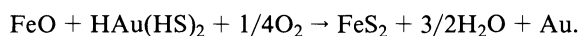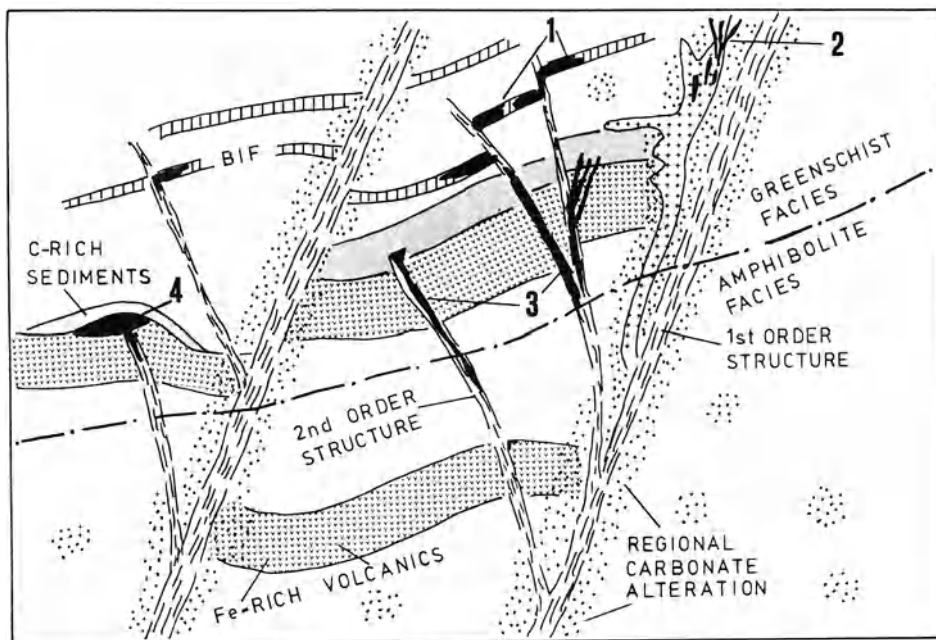
Fig. 15.12. Schematic representation of the metamorphic-replacement model of Groves and Phillips (1987). H_2O-CO_2 fluids gain access through first- and second-order structures, causing extensive carbonitisation (*dot pattern*) and the formation of mesothermal lodes above the greenschist-amphibolite facies transition. *1* Replacement BIF-hosted Au-sulphide deposit; *2* stockworks; *3* vein lodes; *4* Au-Te lodes. Drawing not to scale

A representation of the Groves and Phillips'model is shown in Fig. 15.12. In this model the source of the hydrothermal fluids was the dehydration and decarbonation of rocks above 450 °C during upper greenschist and amphibolite facies metamorphic conditions, deep within the greenstone pile, with high geothermal gradients, and in the absence of significant melting. This, however, raises the important question that if the fluids are of metamorphic origin, why is it that not all metamorphic terranes contain Au deposits? The possible answer, proposed by Groves and Phillips (1987), lies in the presence of Au in a form available to leaching in Archean mafic-ultramafic sequences (see later and Keays 1987), but a more critical factor is perhaps the low-pressure and high-temperature conditions of metamorphism of greenstone belts. Another facet of the metamorphic replacement model is that it allows the mesothermal Au deposits – initially formed at greenschist facies – to be overprinted by amphibolite facies metamorphism. This could be the case for the Big Bell (Western Australia) and Hemlo (Canada) Au deposits (Phillips 1985).

The metamorphic fluids evolved from grain reactions and therefore had effective contact with, and the ability to extract Au from a large volume of the greenstone rocks. The fluids were focused and channelled upward along faults and shear zones by means of mass-transfer processes such as seismic pumping, giving rise to high fluid/rock ratios. Seismic pumping as a mechanism of fluid transfer is discussed in

Chapter 3; here, it is briefly mentioned that seismic pumping occurs as a result of stress-induced dilatancy. Fluids are drawn in the source region of an earthquake before rupture and are expelled along a structural conduit when rupture occurs.

Fluid inclusion studies point to a certain homogeneity of the ore solutions. These were relatively reduced, H_2O-CO_2 fluids (ca. 75 mol% H_2O, 25 mol% CO_2) of low salinity (< 2 wt.% NaCl equivalent), of low density near-neutral to slightly alkaline with depositional temperatures of 300–450°C at 1–2 kbar.

Although Au deposits on the regional scale are associated with major lineaments – or first-order structures – they are generally localised within second-order structures, which occur as subsidiary structures to those of the first order. Second-order structures have lengths of 1 to 10 km and widths of centimetres to hundreds of metres. The question posed is why are first-order structures largely unmineralised, while the second-order structures host the majority of the deposits. According to Eisenlohr et al. (1989), there are two possible reasons: (1) there may be physico-chemical gradients between first- and second-order structures, such as temperature, which would be higher in the first-order structures, and therefore would cause migration of auriferous fluids into the second-order structures; (2) the Au source – as predicted by the metamorphic replacement model – was largely within greenstone belts and was tapped by the second-order structures while first-order structures tapped a mantle or lower crustal source.

Groves and Phillips (1987) do not believe that magmatic fluids, derived from felsic intrusions contributed significantly to the mesothermal mineralisation. They contend that the magmas and the mineralisation are both a consequence of the same thermal event, with magmas representing melting at deeper crustal levels. These magmas may have been selectively emplaced along crustal fractures which also localised earlier mantle degassing and controlled the formation of second-order structures, and the siting of the mineralisation. These authors consider the major source of Au to be komatiitic lavas and cite the work of Keays (1984; see also Keays 1987) in which it is suggested that high-Mg lavas are enriched in Au compared to the tholeiitic basalts. The reason for this is believed to be differences in the solubility and concentration of S in tholeiitic and komatiitic magmas and the presence of immiscible sulphides into which the precious metals tend to partition. Most mafic magmas are S-saturated, at or near the site of melting (source), so that they would lose most of the Au and other precious metals to immiscible sulphide liquids. As a result basaltic magmas are erupted with low Au contents. In contrast, komatiitic magmas represent higher degrees of melting at higher temperatures (ca. 1600°C) in which S solubility is enhanced, and they become S-saturated during late stage fractionation in high-level magma chambers, and also by assimilation of silica and S from crustal rocks. This enables the late formation of immiscible sulphides into which precious metals preferentially partition. Keays (1987) also suggests that the submarine eruption of komatiites facilitates liberation of Au during sea floor alteration and its concentration into interflow sediments and/or pillow margins. In the end, the high Mg-lavas have a good proportion of Au which is accessible to leaching by metamorphic fluids. These lavas are also an important source of S, which is available for leaching, thereby supplying reduced S species necessary for the transport of Au as a sulphide complex.

This scenario fits reasonably well with the metallogenic model of Groves and Batt (1984) in which greenstone belts containing thick sequences of komatiitic lavas, such as the rift-phase greenstones of younger terranes, have the highest potential for mesothermal Au lodes.

The Magmatic Model

This model is based on the close spatial relationship that many mesothermal Au deposits have with felsic igneous intrusions, particularly in the Abitibi subprovince in Canada. Advocates of the magmatic model are Wood et al. (1986), Burrows et al. (1986), Cameron and Hattori (1987), Burrows and Spooner (1987, 1989).

Wood et al. (1986) investigated the Hollinger-McIntyre deposits in the Abitibi belt in Ontario, and concluded that the epigenetic Au mineralisation resulted from magmatically derived fluids. The Hollinger-McIntyre system is within a suite of porphyry intrusions, and is one of the largest in the world, with total production and reserves of approximately 994 tonnes Au. The mineralisation consists of massive, white quartz veins and stringers with pyrite-ankerite and carbonate-sericite alteration envelopes. Approximately 95% of the total Au occurs in the altered wall rocks and adjacent to vein margins, and is believed to have been deposited in situ. Pyrite, scheelite, tourmaline, tellurides and minor Cu, Zn and Pb sulphides are associated with the Au mineralisation. Studies of primary fluid inclusions from vein material indicate either two-phase (liquid + vapour), or three-phase (two liquids + vapour) $H_2O + CO_2$-rich fluids, with a complete range of H_2O-CO_2 ratios indicating phase separation. An estimate of the primary fluid composition, before phase separation, shows that the fluid was dominantly H_2O (ca. 93 mol%) and that it contained six times as much dissolved CO_2 than equivalent NaCl (6 equivalent mol% CO_2 and ca. 1 equivalent mol% NaCl). This confirms the conclusion reached by Groves and Phillips (1987) that Archean Au-rich fluids were CO_2-rich and of low salinity. Wood et al. (1986) suggest that H_2O-CO_2 phase separation accompanied mineralisation and the average depositional temperature was approximately 300°C. The authors use fluid inclusion data as evidence of the magmatic derivation of the fluids. They point out that there is strong evidence (Burrows et al. 1986) to suggest that Au- and W-enriched MoS_2 mineralisation, with associated carbonate alteration, within the Archean Mink Lake sodic granodiorite stock in northwest Ontario was magmatically derived. Since the Hollinger-McIntyre fluid properties are essentially the same as the Mink Lake fluids, a magmatic origin for the former is postulated. The $\delta^{18}O$ values from the two deposits are also very similar and fall within the range +4 to +6 per mill, which is generally lower than the values recorded for metamorphic fluids (+5 to +25 per mill), although it must be borne in mind that there is a significant overlap between the magmatic and metamorphic fluid isotopic fields. Wood et al. (1986) also use ^{13}C isotope systematics from both Hollinger-McIntyre and the Mink Lake deposits to show that their values are statistically comparable (−2 to −4 per mill). Burrows et al. (1986) add to the Hollinger-McIntyre and Mink Lake deposits, ^{13}C data from the Golden Mile in Kalgoorlie and conclude that they are all statistically comparable, thus ruling out genesis by metamorphic fluids. They suggest that CO_2 derived by metamorphic decarbonation

is enriched in ^{13}C by 3 to 5 per mill relative to its starting material. Hence, the $\delta^{13}C$ values of CO_2 produced by metamorphic decomposition of sea-floor carbonates in greenstone belts is likely to be ca. $+3$ to $+7$ per mill greater than those observed in the above deposits.

Burrows and Spooner (1989) studied the mesothermal Au mineralisation in shear zones and igneous intrusions in Val d'Or and Timmins areas of the Abitibi subprovince. Igneous rocks include feldspar porphyries, syenites, monzonites, granodiorites and they are major host rocks of about 35% of the deposits. The Timmins (Porcupine) mining camp has produced some 1845 tonnes of Au up to 1981 from quartz-carbonate-pyrite veins hosted in a sequence of tholeiitic lava flows and breccias, with minor sedimentary units, intruded by post-tectonic quartz-feldspar porphyries. These porphyries are variably altered, ranging from nearly unaltered (quartz, oligoclase, hornblende) to a sheared quartz + carbonate + sericite rock. The porphyries, in turn, were intruded by albitite dykes which consist of carbonate, Na-plagioclase, chlorite, biotite, quartz and sericite. In places quartz + pyrite + Au stringers are entirely developed within the albitite dykes, and at one property (De Santis) the ore zones are restricted to altered (carbonate-sericite) albitites which emanate from a larger body at depth. At Lamaque 94% of the production was derived from intrusive granitic plugs in which mineralisation is present as veins and disseminations. One plug consists of concentric zones of diorite, quartz-diorite and granodiorite. Quartz-tourmaline-pyrite veins and stockworks occur in the altered granitic rocks. The Lamaque plugs appear to post-date the regional metamorphic event, which in turn was possibly caused by the intrusion of a larger parental body at depth, whose differentiation may have produced the Lamaque plugs. The Au content of these plugs is anomalous (mean of 18 ppb with peaks of 30 ppb) and, the authors note that there appears to be no correlation with Ag, Mo, B, W, As, Sb, Bi and CO_2.

Burrows and Spooner (1989) believe that cumulate-melt separation and differentiation provide a suitable mechanism to increase Au concentrations in the residual melts. Au would then partition into a magmatically derived fluid phase, so that this would have developed into the observed geometrical relationships and a style of mineralisation typical of stockwork-type intrusion-hosted deposit of island-arc settings.

The Au-Calc-Alkaline Lamprophyres Association and the Magmatic-Metamorphic Model

An interesting new model proposed by Rock and Groves (1988), Rock et al. (1988, 1989; see also Perring et al. 1989) attempts to reconcile the metamorphic-replacement, magmatic models as well as the meteoric model for the Phanerozoic mesothermal deposits of Nesbitt and Muehlenbachs (1989) mentioned in Section 15.1. The model of Rock and coworkers is based on the observation that a widespread space-time association exists between Archean mesothermal Au deposits and lamprophyres.

Rock (1987) provides a comprehensive overview of the nature and origin of lamprophyric rocks. Lamprophyres represent a diverse clan of ultramafic to mafic,

porphyritic, volatile-rich, alkaline igneous rocks, subdivided by Rock (1987) into five groups, namely: calc-alkaline, alkaline, ultramafic, lamproites and kimberlites. Rock et al. (1988) provide data to show that the lamprophyres contain from one to three orders of magnitude more Au than other common igneous rocks. Mean values for lamprophyres range from 1.6 to 99 ppb with a global average of 43 ppb (Rock et al. 1989). The authors believe that these high values are unlikely to represent secondary Au for a number of reasons including the fact that many samples analysed were petrographically fresh and that high Au also occurs in those lamprophyres which are nowhere associated with Au. Rock et al. (1989) offer at least four explanations for the high Au contents in lamprophyres: (1) lamprophyric melts are highly enriched in H_2O, CO_2, F, K, Ba, Rb etc., and minerals such as biotite, chlorite and carbonates, which are also present in the alteration haloes of Au deposits; (2) they are enriched in S, an element needed to complex Au; (3) lamprophyres occur in metasomatised mantle material at depths in excess of 150 km under volatile-rich conditions, which are ideal for concentrating Au; (4) the metasomatised mantle is thought to be formed by fluids rising from core-mantle areas, these fluids would produce an Au-enriched metasomatised mantle from which lamprohyric melts are generated.

However, although all lamprophyres groups are enriched in Au, the mesothermal Au-lamprophyre association is restricted to calc-alkaline lamprophyres, which are spatially, and perhaps genetically, associated with post-orogenic I-type granitoids. It must also be noted that the association of calc-alkaline lamprophyres with mesothermal Au deposits is by no means confined to the Archean but extends also to those of Phanerozoic age. The Au-calc-alkaline lamprophyres model "suggests that lamprophyres are part of large scale crust-mantle events in which they may contribute at least some Au, S and CO_2 to complex, crustal, metamorphic-hydrothermal systems" (Rock et al. 1989, p.620). In the model, lamprophyre melts, produced by partial melting of a Au-enriched metasomatised mantle, underplate the crust. From this, two end members are considered. In the first, the ascending lamprophyres interact with the crust to produce granitoid-porphyry magmas, in which case Au mineralisation could form according to the magmatic model. Because lamprophyres are both very hot and enriched in volatiles, they have an enhanced capacity to melt crustal material, although it must be borne in mind that lamprophyres are not the parental melts to all granitoids but only to the volumetrically smaller felsic stocks and dykes with which the mineralisation is associated. In the second case, the intrusion of lamprophyres would promote devolitilisation reactions and set up hydrothermal circulation in the crust, with Au being leached from the lamprophyric rocks, as well as the surrounding country rocks. Lamprophyre-derived fluids would mix with metamorphism-generated fluids. In this case the metamorphic-replacement model is satisfied. The authors also draw attention to the narrow temporal span of Au deposition, in which it appears that the auriferous fluids only enter the structural conduits during specific times, which – as they speculate – could coincide with the emplacement of the lamprophyric magmas. Clearly, all intermediate stages would exist between these two end members, implying that both the magmatic and metamorphic-replacement models are partly correct.

Wyman and Kerrich (1989) dispute the genetic relationship of lamprophyres with Au. They maintain that the anomalous Au present in these rocks is the result of secondary overprinting, and that a lack of correlation between Au and LREE in lamprohyres precludes mantle metasomatism as a main process for generating Au-rich melts. Thus, Wyman and Kerrich (1989) contend that the association between lamprohyric rocks and Au is the result of a common geotectonic setting, but otherwise represent distinct processes, with the Au-bearing hydrothermal systems being largely confined to continental crust regions.*
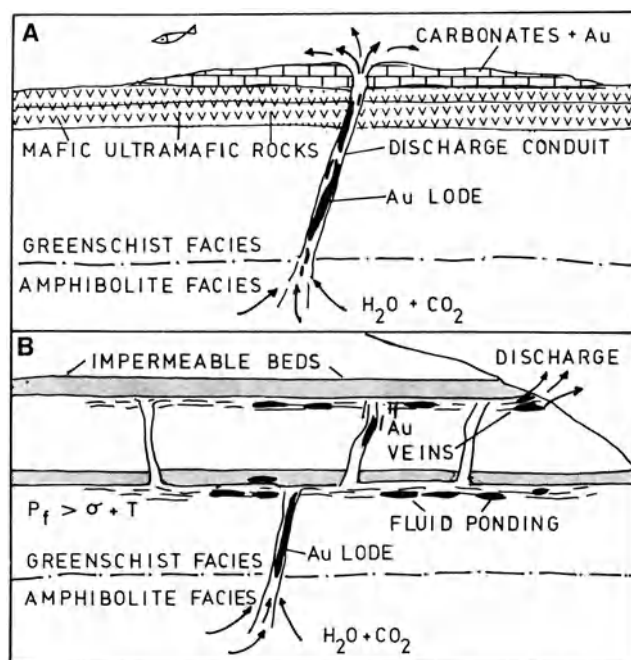
Fig. 15.13. Schematic representation of the epigenetic-syngenetic model of Kerrich and Fryer (1979). **A** Focusing and discharge of fluids at the sea floor; **B** focusing and ponding of fluids beneath impermeable barriers with lateral discharge; see text for details. Drawing not to scale

---

* Mueller et al. (1991; Econ Geol 86:780–809; see also Mueller and Groves 1991; Ore Geol Rev 6:291–331) recently reported the results of their studies of Sr isotope systematics of scheelites from the Archean Au deposits of the Yilgarn Block (Western Australia). On the basis of this work these authors have re-classified the Yilgarn Au deposits into two main genetic types, namely: (1) High temperature (450–650°C) skarn-like deposits characterised by a wall rock alteration assemblage of garnet-pyroxene-biotite and amphibole-biotite-calcite; (2) mesothermal (250–350°C) deposits characterised by biotite and/or sericite-ankerite-albite wall rock alteration.
The high temperature deposits are believed to have formed in the lower parts of the greenstone belts (10–15 km), whereas the mesothermal deposits would have formed in the upper parts (3–7 km). Mueller et al. (1991) further propose that the high temperature deposits are generated by magmatic hydrothermal fluids derived from granodiorite-granite plutons. They downgrade the role of both metamorphic and magmatic fluids for the genesis of the mesothermal deposits, suggesting that a meteoric component may have been present in the mineralising fluids.

Epigenetic-Syngenetic Model

Kerrich and Fryer (1979) studied the Au mesothermal systems of the Porcupine district in the Abitibi belt, and recognised at least two stages of Au metallogeny. One relates to the presence of Au in carbonate-chert chemical sediments, which occur in the lower mafic volcanic sequence. The other involves Au in hydrothermal quartz veins which clearly post-date deformation of the greenstone sequence. The model, shown in Fig. 15.13, proposes that metamorphic fluids are generated during burial and prograde metamorphism of the greenstone sequences, in much the same way as described earlier. At the greenschist-amphibolite transition – between 450 and 500° C – about 5% dehydration H_2O and other volatiles are released from the mafic rocks. Ambient conditions are such that the pressure of the metamorphic fluids, enhanced by thermal expansion of pore fluids, exceeds the lithostatic pressure. The fluid are focused along, and into structural conduits in which auriferous quartz vein lodes are formed. The authors reason that the residence time and accumulation of the metamorphic fluids in the crust are determined by rates of fluid generation and expulsion, and because the Archean geothermal gradients were high (ca. 90°C km^{-1}), fluid generation would have exceeded expulsion. This would have led to the ponding of the fluids beneath impermeable layers as shown in Fig. 15.13 (see also Figs. 3.26 and 3.27). When fluid pressure exceeds the sum of the horizontal stress plus the tensile strength of the rock (see formula in Sect. 15.2.3), subvertical hydraulic fracturing occurs, thus enabling the discharge of the fluids from the ponded reservoir. Hydraulic fractures tend to propagate towards the surface and the process of discharge and ponding may occur several times beneath successive impermeable lithologies in the sequence. Fluids may discharge laterally from the reservoir into permeable sediments (Fig. 15.13) to form Au-bearing quartz-albite-tourmaline veins at or near an unconformity, associated with stratiform carbonates. Kerrich and Fryer also envisage that the H_2O-CO_2-rich fluids can discharge onto the sea floor, resulting in the deposition of carbonate chemical sediments, and if enough Fe remains in solution, oxide facies BIF may replace the carbonate sediments.

Mantle Degassing and Granulitisation

Perring et al. (1989), referring to the Norseman-Wiluna belt (see Sect. 15.4.1), consider CO_2 mantle degassing as the major cause of carbonitisation along first-order structures. Au-mineralising events would take place in subsidiary (second order) structures, within which also porphyries and lamprophyres are emplaced. These authors consider deep-seated mantle activity, plutonism and metamorphic hydrothermal circulation as the combined complex processes that led to the development of mesothermal Au lode deposits (Perring et al. 1989, Fig. 4).

Fyon et al. (1989) propose a similar scenario which, however, is based on the observation that Au mineralisation was probably coeval with a shield-wide plutonic event which marked the final cratonisation of the Archean in the Superior province. This involved mantle diapirism and coupled crustal melting and tectonism, dated at between 2690 and 2673 Ma. The coeval introduction of Au and CO_2 into active zones of deformation and late plutonism suggests that these phenomena may be attributed to a common process. Geochronological data indicate contemporaneity

between granulite facies metamorphism at 2690 to 2640 Ma and the emplacement of Au, CO_2 and late plutonism. Fyon and coworkers, therefore, believe that lower crust granulite metamorphism was caused by underplating of the crust by mantle material, and that this event may have triggered the late plutonism in the Superior province.

The model suggests that hydrothermal H_2O-CO_2-rich fluids are generated in the upper mantle and in the crust by mantle degassing. Granulitisation of the lower crust would result from the influx of heat and volatiles, with CO_2-rich fluids accumulating in the lower crust, while H_2O would be taken up by the partial melts. The authors identify the lower crust as a very large reservoir capable of satisfying the Au budget, more specifically that portion which undergoes granulite metamorphism. They cite other studies (e.g. Sighinolfi and Santos 1976), which have shown significant depletion of Au in granulitic rocks. Two distinct processes would be involved in the extraction and transport of Au and CO_2 into the crust. One process involves the partitioning of the metal into magmas generated by anatexis of either mantle- or crust-derived material. Au is then transported to lower pressure and temperature regions, where it partitions into a magmatic fluid during the exsolution of an H_2O-CO_2-rich fluid phase. Magmas generated within or below the zone of granulitisation would have to be enriched in Au, since this is the region of the observed depletion in this metal. Such magmas have chemical characteristics reflecting either their mantle origin, or tend to be alkaline (potassic), if derived by small degrees of partial melting within the granulite zone. In fact, in the Abitibi belt there is evidence that alkaline magmas are temporally closest to Au mineralisation. The other process involves the presence of a CO_2-rich vapour phase throughout the zone of granutilisation. The presence of this CO_2-rich vapour phase provides a good medium for the transport of incompatible elements and some Au from the granulites. Access of the CO_2-rich fluids and silicate melts is through major structures, thus resulting in the regional spatial associations of the first-order structures, carbonitisation and Au deposits.

Conclusions

In all of the models discussed a key point is the timing of the geological processes, responsible for the generation of the fluids, and the actual emplacement of the Au mineralisation. Owing to the ancient age of the Archean deposits precise age dating is clearly difficult. Recent works, however, based on high-precision U-Pb dating as well as field evidence, seem to indicate that, at least in some cases, the mineralising events post-dated both metamorphism and magmatism. For example, in the Camflo mine in the Abitibi greenstone belt dating of magmatic zircon and titanite, and hydrothermal zircon and rutile showed a substantial gap in their ages (2680 $\pm$ 4 Ma and 2625 $\pm$ 7 Ma respectively) (Jemielita et al. 1990),. Similarly, from other areas in the Abitibi belt, Robert (1990) reports that hydrothermal minerals such as scheelite and rutile, display much younger ages (up to 55 million years) than the associated metamorphic and magmatic events. Robert (1990) concludes that these ages could only reflect deep crustal processes which continued long after metamorphism and magmatism in the upper crustal levels ceased. A confirmation of this view can be

found in the work of de Ronde et al. (1991). These authors provide new field, geochemical and U-Pb isotopic data from two porphyry intrusives in the Barberton greenstobe belt. Zircon dating from a porphyry at the Fairview mine (see later) reveals an age of 3126 ± 21 Ma. A mineralised shear zone crosscuts this porphyry and a hydrothermal rutile from the altered porphyry, which is associated with the Au mineralisation, gives an U-Pb age of 3084 ± 18 Ma. The porphyries are genetically related to the emplacement of the Kaapvaal tonalite pluton which took place at ca 3230 Ma. The authors conlcude that the Au mineralising fluids re-utilised shear zones some 150 Ma after the emplacement of the tonalite and its related porphyries along major thrusts (shear zones).

   In view of the above it is clear that the origin of Archean mesothermal lode Au deposits is still not satisfactorily resolved. The field is open to more research. Comparison and analogies with Phanerozoic mesothermal deposits and related tectonic regimes could help in the understanding of the Archean mesothermal deposits.

15.4.4 Mesothermal Au Deposits of the Barberton and Murchison Greenstone Belts, South Africa

Barberton

The Barberton greenstone belt is one of the best preserved and studied of the Archean volcano-sedimentary sequences in Africa. The belt, located in the eastern part of the Kaapvaal craton, comprises a wide variety of volcanic, plutonic and sedimentary rock types, which collectively form the Swaziland Supergroup, and is the type area for other greenstone sequences in the Kaapvaal craton. The Swaziland Supergroup is subdivided, from bottom to top, into the Onverwacht Group, Fig Tree Group, and the Moodies Group. Again, as previously mentioned (Sect. 15.4.1), these subdivisions correspond to the three main lithostratigraphic sequences of most greenstone belts, as shown in Fig. 15.10. Aspects of the stratigraphy and structure of the Barberton belt can be found in Anhaeusser (1976a, 1981, 1983), Anhaeusser and Wilson (1981) and Tankard et al. (1982).

   In the Barberton greenstone belt the most important mineral deposits are the occurrences of Au and chrysotile asbestos, while lesser deposits of Fe ore, Sn, talc, magnesite and barite have all been mined on a small scale. The Au deposits are of hydrothermal origin and occur in a wide range of lithologies including pyroclastics, volcanics, sediments and BIF. However, they are all characteristically associated with fracture, shear zone and fault systems. The majority of these Au deposits occur on the northwestern flank of the Barberton greenstone belt, where the combined influence of structure and granite intrusion appear to have been most favourable (Anhaeusser 1976b). Some Au occurrences are also located within the granitic rocks, but they are uncommon, and of little or no economic significance. From the 274 workings, for which records are available, an approximate total of 251 500 kg of Au and 8900 kg of Ag have been recovered, of which about 81% was derived from the Jamestown-Sheba Hills-Moodie Hills (Anhaeusser 1976a, b, 1984). The three
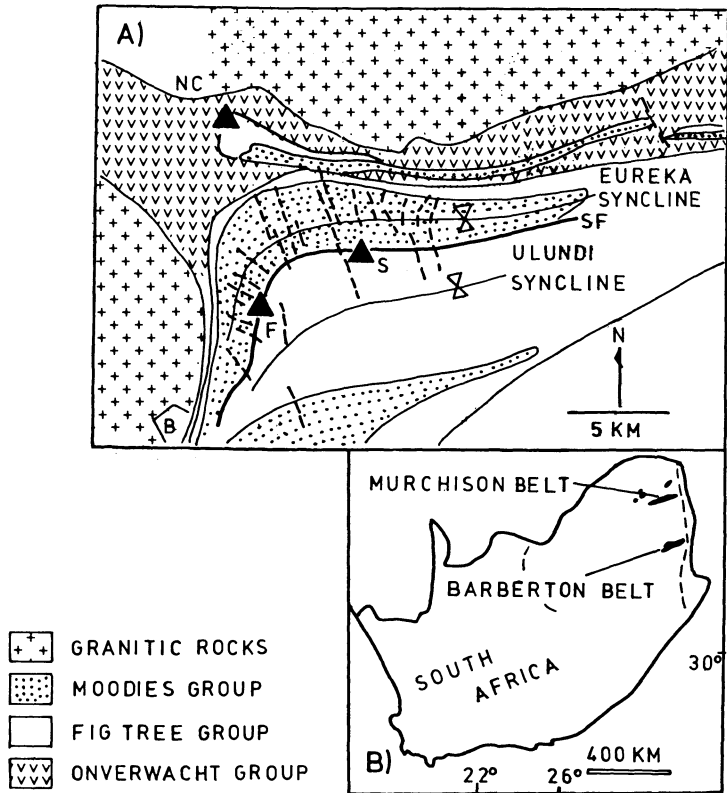
Fig. 15.14. A Simplified geological map of part of the Barberton greenstone belt (Sheba Hills area), showing position of Fairview *F*, Sheba *S* and New Consort *NC* mines; *SF* Sheba Fault; *B* Barberton. The Ulundi and Eureka synclines were refolded about a northwest axis; also note tensional fractures; see text for details (after Anhaeusser (1976b). B *Inset* map showing location of Barberton and Murchison greenstone belts

main Au deposits in the Barberton greenstone belt are Fairview, Sheba and New Consort (Fig. 15.14). Here, we briefly examine the first two.

The Fairview mine, situated approximately 6 km northeast of the town of Barberton in the Sheba Hills, is the largest single Au producer in South Africa outside the Witwatersrand goldfields. Between 1885 and 1983 approximately 50 000 kg of Au and 1628 kg of Ag have been produced from 5.05×10^6 tonnes of ore (Rossiter 1988). The mine area is located along the central and southwestern portions of the Eureka and Ulundi synclines. These structures comprise lithologies of all three lithostratigraphic groups, mentioned previously. The east-dipping Sheba Fault separates the Moodies Group rocks in the Eureka Syncline from isoclinally folded greywacke and shales of the Fig Tree Group and altered volcanics of the Onverwacht Group (Zwartkoppie Formation) (Fig. 15.15).

Au mineralisation is clearly epigenetic as it occupies fracture networks parallel and cross-cutting the strata. The mine sequence comprises, from bottom to top: talc-
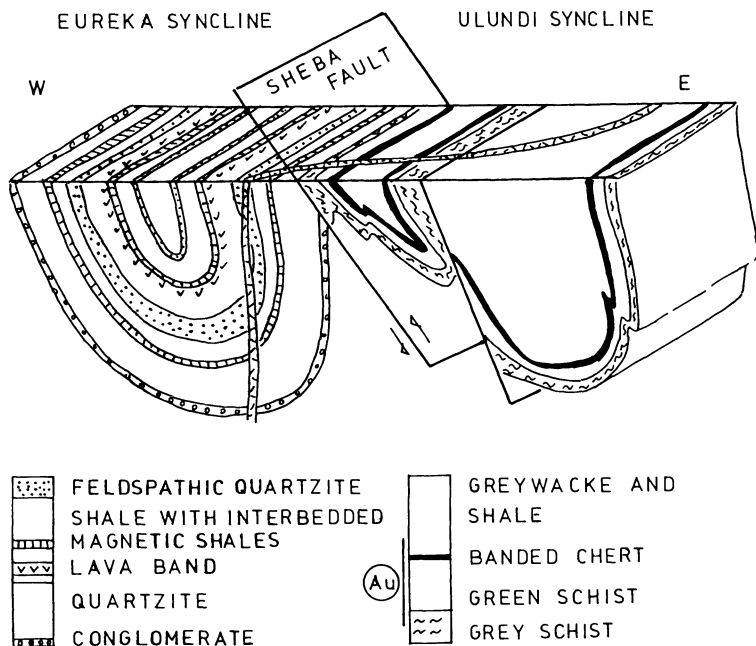
Fig. 15.15. Schematic representation of Eureka and Ulundi synclines separated by the Sheba Fault. Au mineralisation is associated with grey schist, green schist and chert units (Sheba Bar) of the Zwartkoppie Formation. This mineralisation mainly consists of Au-sulphides lodes, whereas fracture-related quartz lodes extends upward into Fig Tree rocks (Fairview mine geologists, written comm. 1986)

carbonate and quartz-carbonate schist (grey schist), overlain by fuchsitic quartz-carbonate schist (green schist), in turn overlain by a black to grey and white-banded chert, commonly capped by a thin unit containing spheroids which are interpreted as accretionary lapilli (Msauli Chert). These rocks form the Zwartkoppie Forma-tion and are followed by greywacke and shales of the Fig Tree Group. Pre-mineralisation feldspar-quartz porphyry dykes and post-mineralisation dolerite dykes are also present (Rossiter 1988). The structures associated with the Au mineralisation appear to have formed during two periods of deformation. The first was probably the formation of the the Ulundi and Eureka synclines, with development of shear zones and slaty cleavage. The second involved refolding of the synclines about a northwest axis, causing strike-slip movement along bedding and cleavage. This refolding event resulted in the formation of a radial tensional fracture pattern about the fold axis (Anhaeusser 1976a; Fig. 15.14). The Au mineralisation at Fairview comprises essentially two types. One consists of free-milling Au, with only minor associated pyrite and aresnopyrite, contained within pale-grey to blue-black quartz veins emplaced into the radial tensional fractures mentioned above, and which are developed in the brittle quartzite horizons of the Moodies Group. The quartz-filled fractures are orientated at right angles to the bedding and have dips varying from 60° to the vertical. The best quartz vein development is confined to the

quartzite units closest to the Sheba Fault, and is dissipated on penetrating the upper argillaceous units by bifurcating into numerous small veinlets. These auriferous quartz veins vary in thickness from 1 cm to 1.5 m and are typically 60 to 150 m long. Vertically they form sinuous pay-shoots, which may extend to approximately 600 m below surface. The second, and most important type of Au mineralisation occurs as sulphide reefs, developed within concordant and discordant fractures in the greywacke and shales of the lower Fig Tree Group, and the altered schists of the Onverwacht Group. The sulphide-bearing reefs are more persistent than the mineralised fractures in the Moodies quartzites, reaching strike lengths of up to 500 m and extending to depths of 1500 m. In addition to Au, the main ore minerals are pyrite and arsenopyrite with minor amounts of chalcopyrite, sphalerite, pyrrhotite, stibnite, native Sb, galena, enargite, pentlandite and niccolite. Quartz, calcite and sericite are the most common gangue minerals. Au is largely refractory, and it is estimated that approximately 50% occurs as inclusions in pyrite, 20% in arsenopyrite and associated minerals, and about 30% as free milling Au. Refractory Au is mineable to a cutoff grade of approximately 7 g/t, and is liberated by sulphide roasting. Mine geologists have noted that tenors drop sharply where the mineralised fractures pass from green schist to grey schist (S. Wiggett pers. comm. 1986).

The Sheba mine is situated approximately 5 km northeast of the Fairview mine, and it straddles the Sheba fault zone. The mineralised fractures and ore shoots at Sheba and Fairview merge into one other within the faulted, fractured and isoclinally folded Onverwacht (Zwartkoppie Formation) and Fig Tree groups in the Ulundi Syncline. Four main styles of mineralisation occur within the Sheba mine area (van der Berg 1984): (1) quartz-filled, north-dipping fractures in quartzite of the Moodies Group; (2) shears within greywacke and shales of the Fig Tree Group; (3) mineralisation within the Sheba Fault; (4) siliceous fracture networks. The last two are the economically most important. A type example of the mineralisation associated with the Sheba Fault was the very rich reef discovered by Edwin Bray in 1886 and known as the Golden Quarry. This Quarry is developed along a zone of brecciation in quartzites of the Moodies group on the footwall side of the Sheba Fault (Fig. 15.15), with the mineralisation being characterised by an elliptical pipe-like quartz stockwork orebody with associated carbonate alteration and disseminated sulphides. The trace of the Sheba Fault in the Golden Quarry is clearly visible as a zone of white cherty material commonly underlain by banded chert, known as Sheba Bar. This is a zone of intense silicification, which has been interpreted as the result of replacement by Si-rich fluids moving along a thrust plane, or, alternatively as a result of replacement by hydrothermal fluids formed by convecting sea water according to the model of Paris et al. (1985), previously discussed. The style of mineralisation which accounts for most of the Au production at the mine is represented by siliceous fracture networks which occur within the green schist of the Zwartkoppie Formation. As at Fairview this Formation consists of three units, which from bottom to top are: (1) carbonate-chlorite-talc – grey schist; (2) fuchsitic quartz-carbonate – green schist; and (3) alternating white chert layers and dark grey to black siliceous carbonate and siderite layers. The units of the Zwartkoppie Formation are clearly mafic or ultramafic rocks hydrothermally altered by fluids containing mainly K and CO_2.
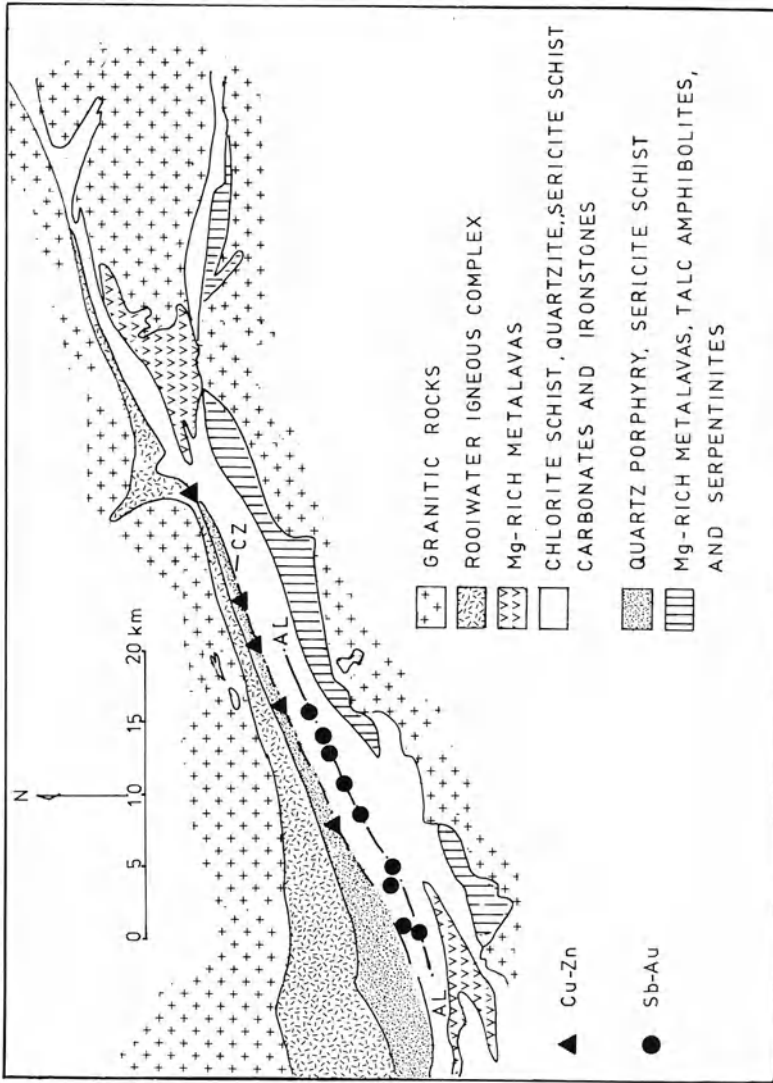
Fig. 15.16. Simplified geological map of part of the Murchison greenstone belt, showing location of main mineral deposits. *AL* Antimony Line; *CZ* Cu-Zn Line (After Viljoen et al. 1978)
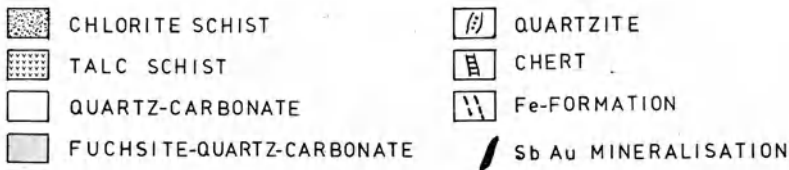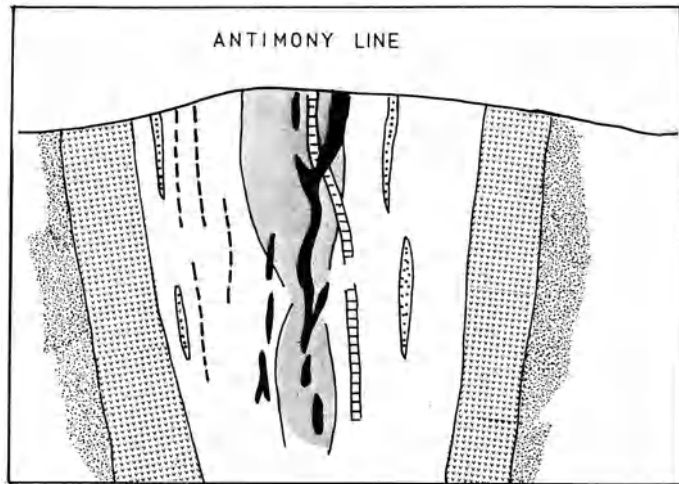
Fig. 15.17. Idealised cross-section of the Antimony Line. The width of the Line ranges from 5 to 130 m (After Muff and Saager 1979)

The fuchsitic green schist units commonly show fuchsite pseudomorphs after olivine or clinopyroxene "spinifex"-textured rocks. Most of the Au mineralisation is associated with the fuchsitic schist, and it occurs both as refractory in pyrite and lesser arsenopyrite, and as coarse free-milling Au.

Murchison

The Murchison greenstone belt is one of the narrow, east-northeast-trending belts of the Kaapvaal craton. The east-northeast linearity of these belts is attributed to the influence of major craton-scale lineaments, one of which is the Murchison Lineament. Aspects of the geology and mineralisation of the Murchison greenstone belt can be found in Viljoen et al. (1978), Viljoen (1979), Pearton (1978, 1979) and Muff and Saager (1979). The belt is characterised by an ultramafic assemblage along the southern flank, overlain to the north by mafic and felsic volcanics and volcaniclastic rocks. No extensive sedimentary sequences that may be considered the equivalent of the Moodie and Fig Tree groups of Barberton are present. The layered mafic Rooiwater Igneous Complex, along the northern flank of the belt, is believed to have been intruded at the time of the emplacement of the volcanic sequence (Fig. 15.16). Structurally, the most important features are the prominent east-northeast trends as delineated by large and small stratigraphic units, fold axes, cleavage and schistosity. This general trend is locally influenced by several cross

structures, the most important of which strike east-west. These intersecting trends have played an important role in localising mineralisation along the so-called Antimony Line, a linear zone within the mafic-felsic lithologies, along which a number of important Sb-Au deposits are situated. The distribution of the hydrothermal mineral deposits of the Murchison greenstone belt are shown in Fig. 15.16, and an idealised section across the Antimony Line is shown in Fig. 15.17.

The Antimony Line, a well-defined zone, extending for approximately 28 km and varying in thickness from approximately 5 to 130 m, consists of a central resistant siliceous carbonate zone, enveloped by a less resistant, poorly exposed, and variably developed talc-carbonate and talc schist. This central zone is subdivided into fuchsite-quartz-carbonate schist (green schist) and a more common quartz-carbonate schist (grey schist). Within the grey and green schists, pods and lenses of a chert-carbonate material occur. This rock ranges from massive, grey, siliceous carbonates to banded almost pure cherty material. It hosts the greater part of the Sb-Au mineralisation, which constitutes one of the most important sources of Sb in the world and is certainly the largest deposit of its kind in Archean terranes. Between the Alpha-Gravelotte and Monarch deposits the mineralisation occurs in thick carbonate masses along the Antimony Line, and is more specifically associated with the fuchsitic zones within these masses. A regional structural control of the mineralisation is suggested by the attitude of the orebodies, which individually have lensoid shapes. Grades are approximately 2% Sb and 2 g/t Au. Viljoen et al. (1978) have noted two types of mineralisation along the Antimony Line. One includes a finely crystalline variety which occurs within the cherty-carbonate zones and contains lenses of massive stibnite forming layers to irregular vein-like structures to scattered specks and films along foliation planes. A broad zonation is present in some of these ore lenses with a central core of stibnite grading outward to a peripheral zone containing berthierite ($FeSSb_2S_3$), with lesser amounts of pyrite, arsenopyrite, gersfordite (NiAsS) and ullmannite (NiSbS). The second type of mineralisation comprises coarsely crystalline stibnite associated with quartz and carbonate veins which tend to occur in fractures diverging from the main orebodies. This mineralisation appears to be a younger and re-mobilised variety localised by fracture systems, shear zones, foliation planes and saddle reef-like structures. Au occurs with both types and is found as inclusions in the larger stibnite aggregates, or within arsenopyrite.

As can be expected, the source and genesis of the Sb-Au mineralisation at Murchison are controversial. Evidence has been put forward to advocate both a syngenetic and an epigenetic origin. Viljoen et al. (1978) believe in an epigenetic origin and they list the following features in support of their views: (a) the talc-carbonate-fuchsitic and siliceous carbonate masses of the Antimony Line suggest a zonal pattern of hydrothermal alteration; (b) stibnite is rarely banded or layered, but generally irregular; (c) the cherty carbonates are commonly associated with shear zones and transgress the lithologies; (d) although Sb and carbonate are anomalously developed, the general features of the Murchison mineralisation conform to that of other mesothermal lode deposits in greenstone belts. A volcanic-exhalative model is supported by Muff and Saager (1979) who suggest, mainly on petrographic evidence, that the carbonate rocks were possibly formed during late

stages of volcanism, in which fumarolic activity resulted in the discharge of fluids carrying Si, CO_2, and base metals. These were responsible for the extensive carbonitisation, silicification and mineralisation. The Murchison elemental association (Sb-Au-Hg-W) is considered similar to the stratabound W, Hg and Sb deposits of Western Europe, including the Felbertal deposits in Austria described by Höll et al. (1972), which occur in submarine mafic volcanics and are believed to be of syngenetic origin. After their formation the syngenetic deposits would have suffered regional deformation and metamorphism which could have caused the reconstitution and, locally re-mobilisation, of the ores into suitable structures. The volcanic exhalative model would also account for the Cu-Zn Line (Fig. 15.17) along the southern contact zone of a quartz-porphyry assemblage situated along the southern margin of the Rooiwater Igneous Complex. Along this Line are several massive, commonly banded, pyritic lenses with locally abundant sphalerite and lesser chalcopyrite, and it is thought that these are all of volcanogenic affiliation, associated with the final phase of acid volcanicity which resulted in the emplacement of the quartz-porphyry (Viljoen et al. 1978).

15.4.5 The Golden Mile, Yilgarn Block, Western Australia

The Yilgarn Block, an Archean Craton in Western Australia (Gee 1979), contains more than 2000 Au occurrences, of which the Golden Mile of Kalgoorlie is responsible for more than 50% of the total production and is therefore considered to be a giant Au deposit (Phillips 1986). Several papers have been published on the Golden Mile (e.g. Woodall 1965; Travis et al. 1971; Tomich 1974, 1986), but the information provided in this section is mostly derived from the recent works of Phillips (1986) and Boulter et al. (1987).

The Golden Mile deposit has produced 1200 tonnes of Au from approximately 110×10^6 tonnes of ore, covers an area of 5 km^2, and is situated within the previously mentioned Norseman-Wiluna greenstone belt. The deposit is located within a 5-km belt of uplifted mafic and ultramafic rocks which extend in a north-south direction for approximately 100 km. This belt, interpreted to be a rift zone, is flanked by stratigraphically younger volcano-sedimentary sequences, and is characterised by north-northwesterly major faults with numerous subsidiary structures. The area was affected by regional metamorphism of upper greenschist facies, with most original rock textures being well preserved. The dominant structures in the deposit area are an asymmetric pair of folds, namely the Kalgooorlie anticline and syncline, and the Golden Mile strike fault. This fault separates the Golden Mile deposit into the Western and Eastern Lode Systems (Fig. 15.18). Numerous anastomosing ductile shear zones were formed synchronously with the folding event and provided the channelways for the mineralising fluids. Structural, and other evidence, suggest that the mineralisation was synchronous with progressive deformation. The main host for the Au mineralisation is the Golden Mile Dolerite, a concordant, 400- to 800-m thick differentiated mafic sill which was emplaced between the Black Flag Beds (base of sequence) and the Paringa Basalts (top of sequence). The Golden Mile Dolerite is divided into ten units, with units 1 and 10 forming its bottom and top-
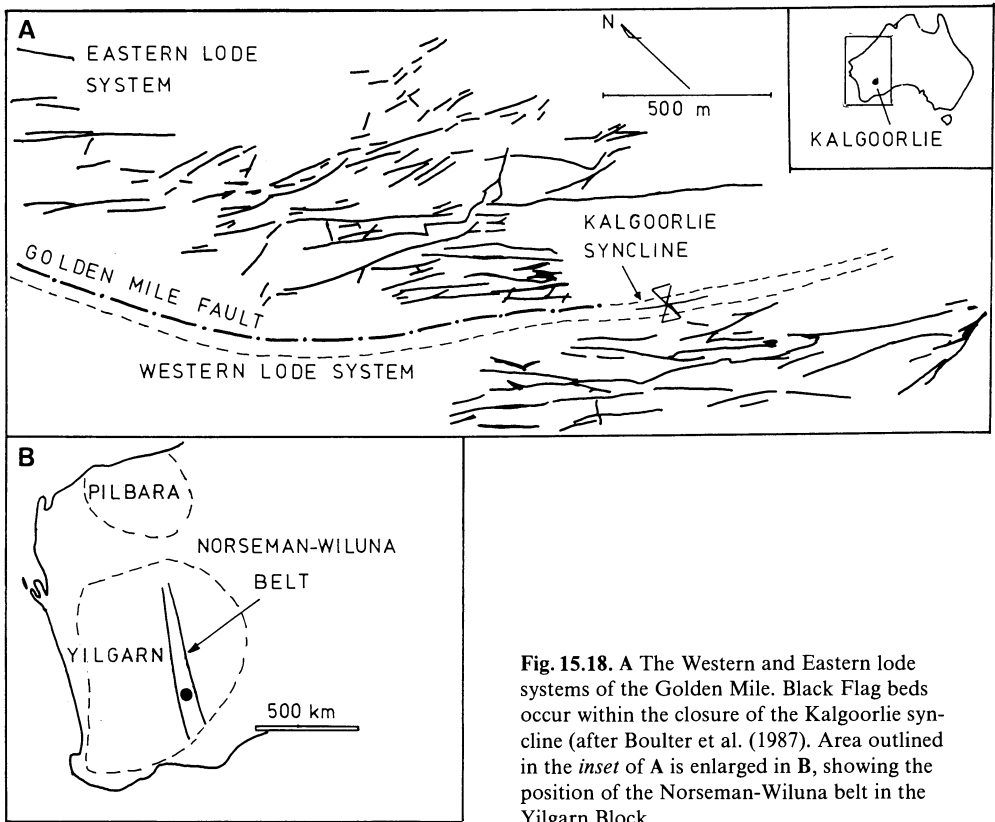
Fig. 15.18. A The Western and Eastern lode systems of the Golden Mile. Black Flag beds occur within the closure of the Kalgoorlie syncline (after Boulter et al. (1987). Area outlined in the *inset* of A is enlarged in B, showing the position of the Norseman-Wiluna belt in the Yilgarn Block

chilled margins respectively. In spite of metamorphism and hydrothermal alteration the main original igneous textures are well preserved, and it is these textural features which have allowed a reconstruction of the magmatic evolution of the sill. Regional metamorphism of the sill resulted in an upper greenschist assemblage consisting of albite + actinolite + chlorite + epidote + quartz.

There are three distinct styles of mineralisation: (1) Golden Mile style – responsible for some 70% of the production – with grades of 10–15 g/t Au, and characterised by narrow tabular lodes containing auriferous pyrite; (2) Oroya style – responsible for approximately 25% of the production – occurs adjacent or within carbonaceous sediments of the Paringa Basalt Formation and is characterised by having tellurides and high grades (up to 1500 g/t Au); (3) Charlotte style – about 5% of production – characterised by stratabound stockworks within a granophyric zone of the Golden Mile Dolerite, with grades of approximately 5 g/t Au. The Mount Charlotte lode system is geographically separated from the Golden Mile sensu stricto.

Interaction of the hydrothermal fluids with the Golden Mile Dolerite resulted in a series of reactions, in part controlled by the mineralogical changes of the original igneous layering. Some of these reactions are discussed in Chapter 4. Phillips (1986)

recognised three distinct alteration zones within the Golden Mile Dolerite, which overprint the metamorphic assemblages of the sill. Alteration assemblages reflect not only different degrees of alteration intensity, but also the Fe/Mg ratios of the host rocks, and the CO_2/H_2O ratios of the hydrothermal solutions (see Dubé et al. 1987). Throughout the Golden Mile, the outermost wall-rock alteration halo is the chlorite zone which, in the area studied by Phillips, is estimated to be at least 1 km wide and 3 km long. This zone is characterised by the assemblage chlorite $+$ calcite $\pm$ ankerite $\pm$ albite $\pm$ paragonite $\pm$ quartz $\pm$ magnetite $\pm$ siderite $\pm$ pyrite. This is followed by the carbonate zone, forming 100-m thick areas around the Eastern and Western Lode Systems, along strike lengths of up to 2 km. This zone, which parallels the stratigraphy and is influenced by the main ductile shear zones, is characterised by the assemblage ankerite $\pm$ quartz $\pm$ muscovite $\pm$ albite $\pm$ siderite $\pm$ pyrite. Within the carbonate alteration and controlled by ductile shear zones, are zones, 1 to 5 m thick, of pyritic alteration (pyrite zones) which contain the Au lodes. These are characterised by the assemblage pyrite $\pm$ quartz $\pm$ ankerite $\pm$ albite $\pm$ muscovite $\pm$ siderite $\pm$ dolomite $\pm$ tourmaline. Other sulphide minerals are chalcopyrite, arsenopyrite and minor pyrrhotite.

Studies of geochemical changes in the host rocks during the chlorite, carbonate and pyritic alteration indicate that CO_2, S, K, Rb, Si, B, Ba, W, Au were added, while there was a moderate loss of H_2O and Li. The geochemical nature of the alteration zones indicates that only one hydrothermal fluid was involved, whose introduction into the shear zone system post-dated the peak of regional metamorphism. It is concluded that the alteration-mineralisation event was probably part of a single and progressive episode, which began with pyrite $+$ Au, during a deformation stage of a transitional ductile regime, leading to a brittle regime, and the deposition of late veins containing telluride $+$ Au.

The giant size of the deposit is attributed to the large volume of hydrothermal fluids, the exceptional permeability of the host lithologies due to intense development of shear zones, and their Fe-rich character.

15.4.6 The Hemlo Au-Mo Deposit, Superior Province, Canada

The Hemlo Au-Mo deposit, discovered in 1982, is located near the northern shore of Lake Superior, Ontario. This deposit does not conform to the more common Archean lode type but it represents an unusual type of mineralisation which spans the range from mesothermal to epithermal (350 to 175°C, based on the thermal stability of some of its ore minerals). Details of the geology, geochemistry and mineralisation of the Hemlo deposit can be found in Cameron and Hattori (1985), Harris (1986, 1989), Hugon (1986), Kuhns et al. (1986), Valiant and Bradbrook (1986), Walford et al. (1986), Muir et al. (1988) and Corfu and Muir (1989). These works constitute the basis of this review.

The Hemlo deposit is located in the Archean Hemlo-Heron greenstone belt (Abitibi subprovince), which is a sequence of east-west-trending volcano-sedimentary units enclosed by granitic rocks (Muir 1982a, b; Fig. 15.19). Recent U-Pb zircon analyses have given ages ranging from 2.69 to 2.77 Ga (Corfu and Muir 1989). The
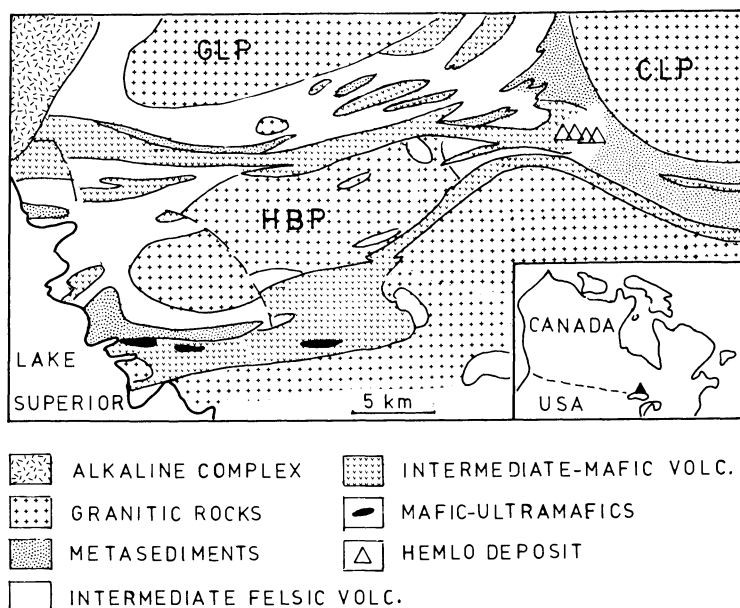
Fig. 15.19. Simplified geological map of part of the Hemlo-Heron greenstone belt, showing location of the Hemlo Au-Mo deposits. *GLP* Gowan Lake Pluton; *HBP* Heron Bay pluton; *CLP* Cedar Lake pluton (After Corfu and Muir 1989)

belt underwent at least two main deformation events which resulted in four generations of structures (Muir et al. 1988). Metamorphism ranges from greenschist facies in the eastern part of the belt, near Heron Bay, to amphibolite facies in the Hemlo area, where metamorphic assemblages consist of biotite + garnet + quartz + plagioclase ± muscovite ± kyanite ± sillimanite ± staurolite ± cordierite. However, this grade of metamorphism was possibly followed by metamorphic minerals of lower grades, in association with the development of low-temperature ore minerals such as cinnabar, realgar and orpiment.

The main ore zone of the deposit contains some 80×10^6 tonnes at approximately 8 g/t Au. In one of the orebodies (Golden Giant) the MoS_2 content reaches an average of 0.16%. In addition to Au and Mo the ore zone contains Sb, As, Hg, Tl, V and Ba. The deposit extends for approximately 3 km along the strike, with thicknesses of 3 to 45 m and a vertical extent of 1.3 km, and appears to be situated within a major ductile fault zone. Three mine properties are developed, which from east to west are: David Bell, Golden Giant and Page Williams (Fig. 15.20). The dominant type of mineralisation consists of a laminated quartzo-feldspathic rock, characterised by the presence of laminae of a green vanadian muscovite, 5–10 wt.% pyrite and up to 0.5% MoS_2 with grades of approximately 12 g/t Au. The mineralisation forms irregularly shaped tabular to lensoid orebodies (Fig. 15.20), characterised by the presence of abundant pyrite (average 8 wt.%), native Au accompanied by lesser amounts of aurostibite, molybdenite, sphalerite, arsenopyrite, stibnite, tetrahedrite, tennantite, realgar, cinnabar, V-Sb-W-bearing rutile, and
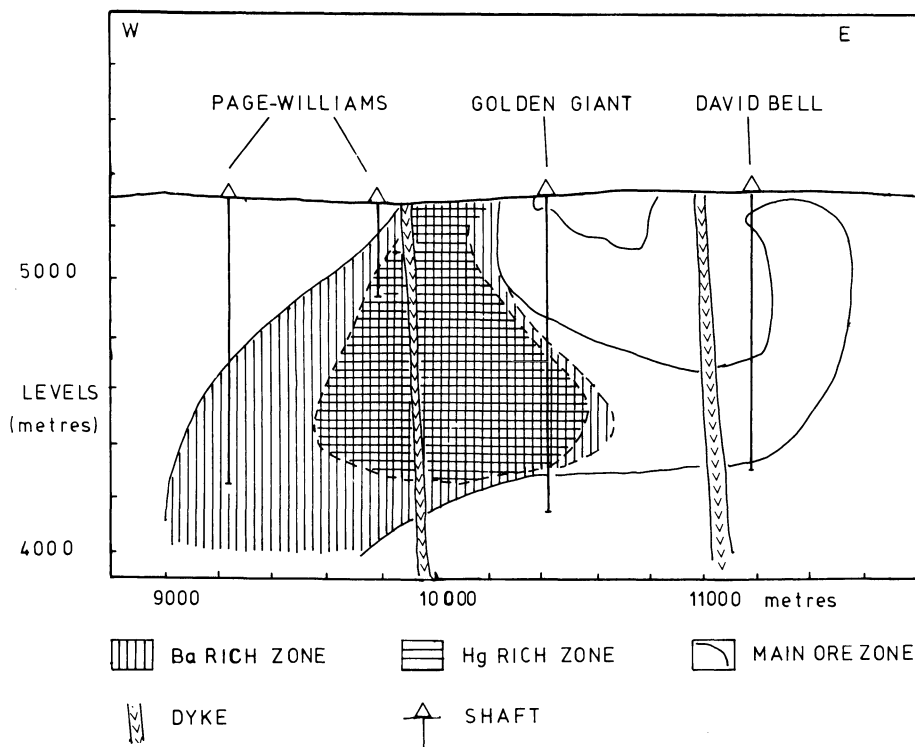
Fig. 15.20. Schematic longitudinal section showing outline of the Hemlo main ore zone and distribution of Ba- and Hg-rich areas (After Harris 1989)

a host of other ore minerals some of which have been recognised as new species, such as hemloite [(Ti,V,Fe,Al)$_{12}$(As,Sb)$_2$(O,OH)$_{24}$] (see Harris 1989). Native Au occurs as disseminated grains at grain boundaries of silicate minerals and only rarely as inclusions in sulphides. Microprobe analyses show that it is Hg-rich (up to 27 wt.%). Characteristically, sphalerite and tetrahedrite-tennantite also contain Hg in amounts of up to 29.5 and 18 wt.%, respectively. Common gangue minerals include quartz, muscovite, phlogopite, barian feldspar (microcline) and barite. Tourmaline (dravite variety) is present as an accessory gangue mineral and is essentially confined to the footwall rocks and in the areas of quartz veining.

The deposit is crudely zoned with a central As- and Hg-rich portion, within which are also deformed quartz veins and pods. These are enriched in realgar, stibnite, cinnabar and Tl-bearing minerals. Barite occurs as massive zones (up to 70 wt.%) extending from the central zone to the peripheral regions of the deposit, which are depleted in As and Hg minerals (Fig. 15.20). Microcline is also common, and contains up to 17 wt.% Ba. The host rocks in the eastern areas (David Bell) and in the upper levels are biotite schist and a quartz-feldspar porphyry, at depth these pass into muscovite-rich rocks and feldspathic rocks. Hydrothermal alteration is characterised by three main types: (1) pervasive potassic; (2) quartz-muscovite

alteration; and (3) calc-silicate alteration. Unusual at Hemlo is the relative deficiency of carbonate alteration compared to other Archean Au deposits. The Au-Mo mineralisation appears to be related to the potassic alteration of the host rocks as well as to areas of most intense deformation. There is also a close relationship between V and Au, while the precise relationship between Au and Mo is not clear, except that the presence of molybdenite is also indicative of the presence of Au. It appears that the early potassic alteration was associated with the influx of Au into the system, while later, the formation of quartz ($+$ microcline $+$ albite) veins was associated with an influx of Mo.

Because of its unusual features, the origin of the Hemlo deposit has been vigourously debated during its short history of scientific enquiry. A syn-volcanic origin was postulated first. The stratiform nature of portions of the ore zone has been used to suggest that the mineralisation was formed syngenetically and was only later deformed during orogenic events. The presence of muscovite and Al-rich minerals (e.g. kyanite) was interpreted to reflect argillic-type hydrothermal alteration. It was also suggested that the mineralising event may have been related to rifting, with circulation of hydrothermal solutions along growth faults and precipitation of Au-bearing material. The Au-As-Sb-Hg-Tl element association was also called upon to postulate a syngenetic origin for the mineralisation by comparing it with the sinters of the Taupo Volcanic Zone in New Zealand (Goldie 1985). Although by no means resolved, more recent studies indicate that the hydrothermal alteration-mineralisation is epigenetic, structurally controlled, and is probably related to stages of dextral shearing, and to K metasomatism. On the basis of U-Pb dating, it is estimated that the hydrothermal activity was episodic and occurred over a period of some 50 Ma (Corfu and Muir 1989).

15.5 Mesothermal Vein Deposits of Phanerozoic Age (Turbidite-Hosted Au)

Hydrothermal quartz vein lodes enriched in metals such as Au, Sb, W, Hg and As occur in many sedimentary terranes which have been subjected to compression, deformation and metamorphism. Some of these mesothermal lodes are also known in the literature as turbidite-hosted Au deposits (Keppie et al. 1986). The age of these mineralised sedimentary terranes ranges from Late Proterozoic to Tertiary, but as previously mentioned there are many similarities between these mesothermal occurrences and the Archean lodes discussed above. Occurrences of Proterozoic age which may be likened to the category of mesothermal vein lode deposits are the base metals and Ag deposits of the Coeur d'Alene district in Idaho (Leach et al. 1988), and the auriferous quartz vein lodes of Pilgrims' Rest in the eastern Transvaal (South Africa) (Ash and Tyler 1986; Tyler 1986). In Namibia, the Ondundu Au deposit of Late Proterozoic age is also considered to be a turbidite-hosted mesothermal lode type (Pirajno and Jacob, in press).

In this section we look at some examples of Phanerozoic mesothermal deposits such as those of the Ballarat Slate Belt in the Victorian goldfields, the lode systems in

GRANITIC ROCKS

GREENSTONE AXIS

ANTICLINE

FAULT

MINERAL DEPOSIT
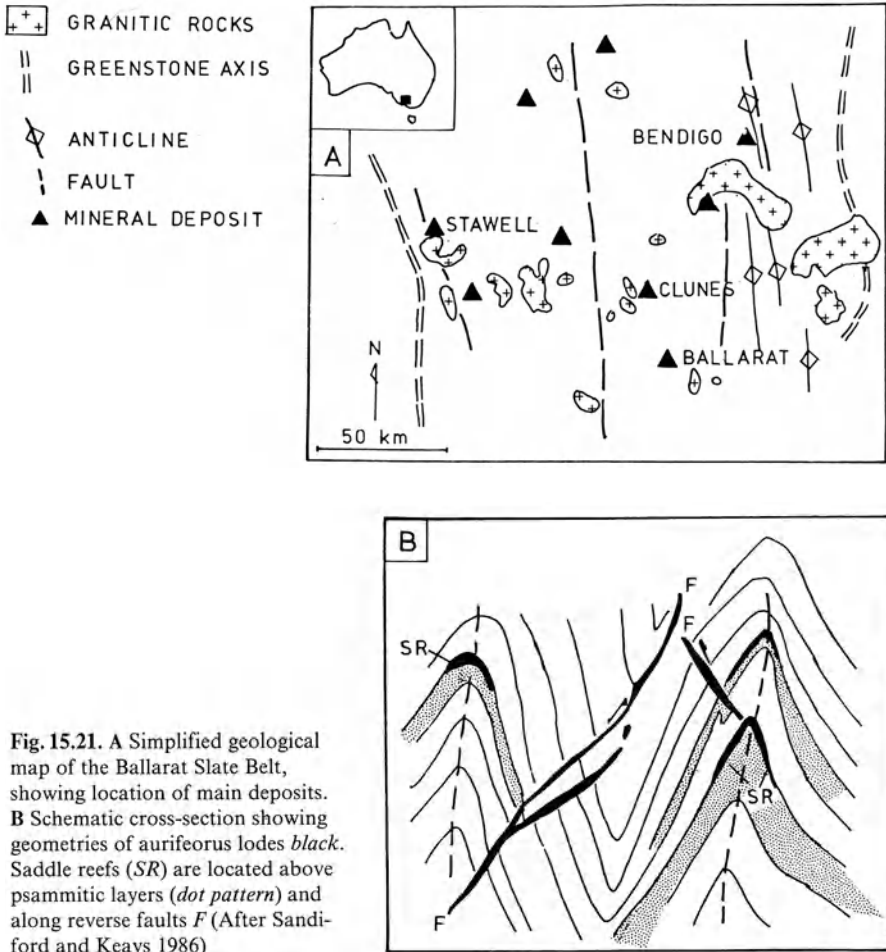
Fig. 15.21. A Simplified geological map of the Ballarat Slate Belt, showing location of main deposits. B Schematic cross-section showing geometries of aurifeorus lodes *black*. Saddle reefs (*SR*) are located above psammitic layers (*dot pattern*) and along reverse faults *F* (After Sandiford and Keays 1986)

Otago and in the Southern Alps of New Zealand and the Juneau gold belt in southeastern Alaska. Other mesothermal lode deposits, not discussed here, are those of Nova Scotia (Mawer 1986), the Canadian Cordillera, mentioned in Section 15.1 (Nesbitt and Muehlenbachs 1989), the California Mother Lode system (Landefeld and Silberman 1987; Weir and Kerrich 1987; Landefeld 1988), and the Au-W-Sb quartz lodes of the Reefton goldfields, hosted in turbidite rocks in the northwest of the South Island (New Zealand) (see also Chap. 7).

15.5.1 The Ballarat Slate Belt, Victoria, Australia

The goldfields of Victoria are situated within turbidite lithologies of Devonian age which are part of the Paleozoic Lachlan orogen, briefly mentioned in Chapter 5. They are of great importance from both the historical and geological viewpoints. The Victorian goldfields have given fame to a style of mineralisation known as

"saddle reefs", mention of which is made in virtually every textbook containing a chapter on mineralisation. In this section we examine briefly some specific aspects of this famous mineral province. The goldfields comprise a number of provinces which are roughly delimited by northerly-trending linear belts of greenstone rocks of Cambrian age (Fig. 15.21A). The Ballarat Slate Belt includes the Bendigo-Ballarat and Stawell provinces in the western portion of the Victorian goldfields (Sandiford and Keays 1986; Binns and Eames 1989; Watchorn and Wilson 1989). Here again there is debate as to the origin of the mineralisation. Everyone recognises the epigenetic nature of the mineralised lodes but not everyone agrees as to the origin of the hydrothermal fluids. A magmatic origin for the fluids is postulated by some (Watchorn and Wilson 1989), while others subscribe to the metamorphic model (Sandiford and Keays 1986). Indeed, it is difficult to separate metamorphism, deformation and igneous activity. Significant fluid fluxes can be derived from loss of water from dehydration of the sedimentary pile in response to a thermal anomaly (high geothermal gradients), the cause of which is heat whose origin must ultimately be magmatic. The argument then hinges on whether any of the mineralisation observed is actually connected with the cooling of discrete plutons. Structural studies in the Victorian goldfields (Tomlison et al. 1988) indicate the following sequence of events: (1) folding; (2) dyke emplacement; (3) reverse faulting; (4) quartz veining and alteration-mineralisation; (5) Au mineralisation; and last (6) emplace-ment of Mid-Devonian granitoids. The timing of the granite emplacement and cooling history is of crucial importance and by no means resolved.

The dominant mineralisation styles in the Bendigo-Ballarat province are shown in Fig. 15.21B. In this province auriferous saddle reefs typically occur above psammitic units and are associated with reverse strike-slip faults. In the Stawell area (Watchorn and Wilson 1989) two distinct types of shear zone-hosted mineralisation occur. One, found in the Magdala mine, is characterised by vein lodes emplaced on the western limb of a structure known as the Magdala anticline. The other, typified by the Wonga open pit, is characteriesd by a mineralised fracture system within the contact aureole of the Stawell granite.

At the Mgadala mine Au mineralisation occurs in: (a) laminated and massive quartz veins; (b) gash and stockwork systems; and (c) sulphide lodes. The miner-alisation and associated hydrothermal alteration are retrogressive with respect to, and post-date, deformation events (D1 to D6) and the peak of regional metamor-phism. D4 to D6 are zones of brittle-ductile deformation trending north-south, northwest and east-west, The prominent Stawell-Ararat fault is one of these zones (Fig. 15.21A). Laminated quartz veins consist of re-crystallised quartz laminae and thin carbonaceous material, chlorite and ilmenite-rich remnants of schist. There is abundance of laminated and massive quartz veins in the lode systems, most of which are sulphide-bearing. Au and arsenopyrite occur as inclusions in pyrrhotite and pyrite, and these sulphides, in turn, are intergrown with chlorite and stilpnomelane (Watchorn and Wilson 1989). Gash and stockwork vein systems cross-cut the lami-nated quartz and D4 ductile shear zones. They are restricted to dilatant areas, partic-ularly where there are changes in the strike and dip of the shear zones. Minor Au is present and it occurs within euhedra of arsenopyrite and pyrite which, in turn, occupy fractures. Sulphide lodes, containing up to 80% pyrrhotite, are parallel to foliation,

and this is interpreted to be of a syngenetic origin. Gold mineralisation occurs where the shear zones cut across the pyrrhotite concentrations. At the Wonga open pit, Au mineralisation is post-peak contact metamorphism and is contemporaneous with late stages cooling of the Stawell granite. Gold occurs in biotite-quartz-arsenopyrite lodes or in carbonate-sericite-arsenopyrite lodes, and the authors argue that the latter veins may have originated from magmatic fluids.

Binns and Eames (1989) carried out petrological and geochemical studies of the hydrothermally altered wall rocks at the Clunes deposit within the Bendigo-Ballarat province (Fig. 15.21A). They observed that the altered wall rocks are characteristically bleached due to the presence of carbonate porphyroblasts which surround the auriferous quartz veins. At Clunes these veins contain quartz, minor ankerite, chlorite and albite. Sulphides are rare but where present they include arsenopyrite, pyrite, and lesser galena, sphalerite and chalcopyrite. Carbonate porphyroblasts are well developed in the wall rocks near the lodes, although in detail there appears to be little correlation between their abundance and the distance from the veins.

Background pelites contain fine-grained phengite, chlorite, quartz, rutile-anatase granules and some graphite. Phyllites near the mineralised zones have a lustrous sheen, and have the same mineralogy, except for the presence of ankerite and siderite porphyroblasts, which cut across the cleavage. Minor siderite veinlets are also present. Background greywacke has abundant angular clasts of quartz, albite, rare K-feldspar, tourmaline and lithic particles – possibly chert – minor chlorite and muscovite. The altered greywackes show a spaced fabric oblique to bedding. Again, the characteristic feature is the presence of ankerite and siderite porphyroblasts, approximately 1 mm in size, and in amounts of up to 5%. The psammitic rocks also show greater geochemical variation compared to pelitic rocks. Pelitic rocks are enriched in CO_2 and As and depleted in S, while psammitic rocks are enriched in CO_2, As and K. The CO_2 and As enrichment is explained by the presence of the ankerite and siderite porphyroblasts and sulphide veinlets. The authors believe that both CO_2 and As were introduced late in the deformation history of the region. A peculiar feature is that the altered rocks have a bulk density lower than the unaltered rocks, and this is attributed to greater microporosity. The subdued geochemical and mineralogical character of the altered rocks with respect to the unaltered or background lithologies is probably due to near-equilibrium between fluids and wall rocks in a metamorphogenic environment.

It is of interest to note that the presence of porphyroblasts in the altered wall rocks is a common feature for most turbidite-hosted Au deposits. The Ondundu Au prospect in Namibia, referred to earlier, is characterised by abundant disseminations of carbonate porphyroblasts in the wall rocks, up to 1 or 2 m from the vein margins. These porphyroblasts range in size from less than 1 mm to approximately 5 mm. Unpublished work by the present author confirms the observations of Binns and Eames. At Ondundu, petrological work indicates that CO_2 could have derived from the devolitilisation reactions in pelitic rocks, with decarbonation and subsequent evolution of CO_2-rich fluids. If Fe is present in the wall rocks, then CO_2 would be fixed in the form of carbonate. As Binns and Eames rightly observe, the presence of carbonate porphyroblasts and the associated geochemical anomalies in As, can be utilised in the exploration for this type of deposit.

15.5.2 Hydrothermal Lode Systems of Otago-Marlborough and the Southern Alps, New Zealand

Scheelite, gold and stibnite mineralisation occurs in quartz vein lodes in the metamorphosed turbidite sequences of Otago, the Southern Alps and the Marlborough district. These sequences are part of the Torlesse and Caples terranes, which form a complex belt of schist (Haast Schist) displaced by the Alpine Fault (see Chap. 7 and Fig. 7.9) The mesothermal mineralisation of the Haast Schist provided the basis for the development of the metamorphic models of ore genesis mentioned above (e.g. Henley et al. 1976). Recent reviews on mineralised lodes of the Haast Schist can be found in Paterson (1986), Brathwaite (1988), Johnstone et al. (1990) and Brathwaite and Pirajno (in prep.). Williams (1974) provides details of individual lodes and lode fields. Although the production from these lodes was relatively small – approximately 10000 kg of Au and 3000 tonnes of scheelite (Paterson 1986; Brathwaite 1988) – larger quantities of Au were, and are currently being won from Tertiary and Quaternary placer deposits derived from the erosion of uplifted segments of mineralised schists. The placers of Otago and Westland, which are mainly fluvial, fluvio-glacial and beach deposits, have yielded approximately 500000 tonnes of Au since the second half of the 19th century. The South Island placers have had a long history of continuous reworking of auriferous conglomerate. In this context it is worth mentioning the concept of "giant placers" proposed by Henley and Adams (1979). According to these authors, giant placers are formed in response to tectonic uplifts of Au-bearing source terranes and consequent reworking of alluvial accumulations. The Otago, Westland, the Yukon and California placers would fall into this category, and it is possible that the larger and richer Witwatersrand paleoplacers, in South Africa, may have originated in this way.

The Haast Schist rocks include the Otago and Alpine schists and their displaced portion on the northwestern side of the Alpine Fault – the Marlborough schists. These rocks consist of metagreywacke, metapelite, with minor intercalations of mafic metavolcanics, pyroclastics and cherts. The metamorphic grade increases from prehnite-pumpellyite facies to greenschist facies (chlorite and biotite zones), to narrow bands of amphibolite facies metamorphism (garnet and garnet-oligoclase zones) along the Alpine Fault. It is worthy of mention here that this part of the world also provided the ground for classic studies of regional prograde metamorphism (e.g. Turner 1935; Hutton and Turner 1936; Bishop 1972). The Au-W-Sb mineralisation occurs in quartz lodes which tend to form major systems, or lode fields. In Otago these appear to be concentrated in a central area within textural zones III and IV (Bishop 1972) of greenschist facies rocks which have been exposed by uplift. In this area are the well-known Glenorchy and the Macraes Flat lode fields, described by Paterson and Rankin (1979) and Lee et al. (1989) respectively. The lodes are emplaced within crush or shear zones, which can be up to 350 m wide and 10 km long, as at Endeavour Inlet (Marlborough district), and are characterised by quartz veins, predominantly set in the hinge zone of recumbent folds (Paterson 1986). Individual lodes generally cut the deformation fabrics at a high angle, although at Macreas the lodes are subparallel to the main fabric of the host lithologies. The

thickness of the veins ranges from a few centimetres to approximately 6 m, but more commonly around 1–2 m. Veins are irregular and discontinuous, and arranged in zones of up to a few hundred metres in strike length.

At Glenorchy the mineralisation is mainly scheelite, contained in laminated and massive quartz with minor pyrite, arsenopyrite, sphalerite, rare Au, calcite, kaolinite, sphene and clinozoisite. Fluid inclusion studies by Paterson (1986) indicate that the fluids contained about 4 mol% CO_2 with salinites of approximately 6–7 wt.% NaCl equivalent. Trapping temperatures are estimated to have been at least 290°C. Hydrothermal alteration of wall rocks at Glenorchy consists of a
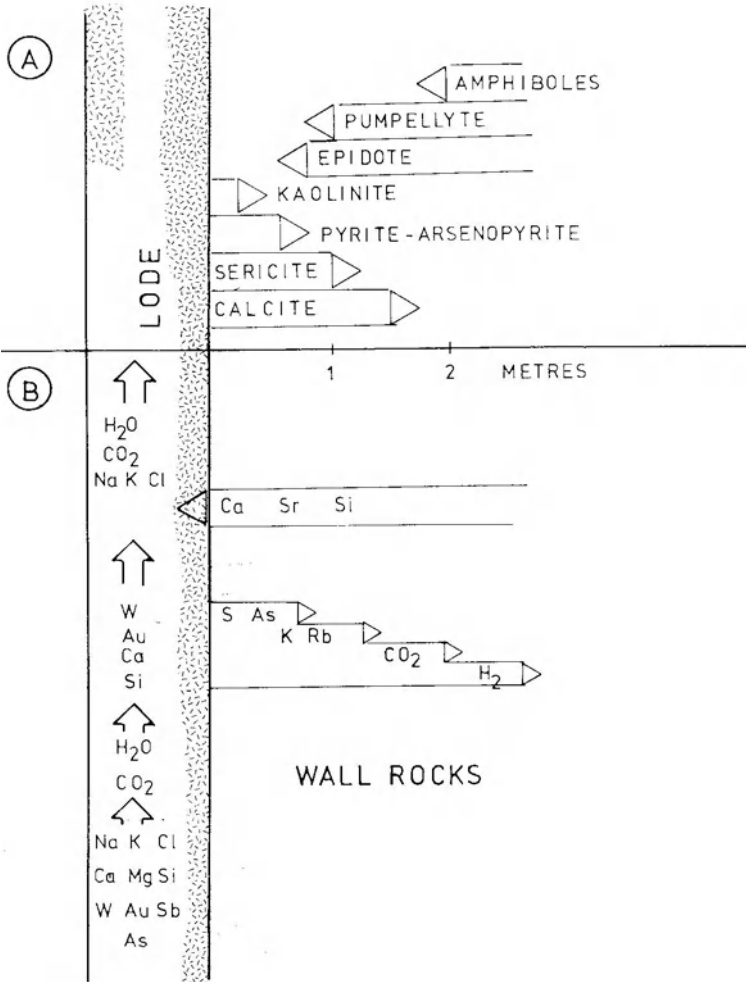
Fig. 15.22. A Distribution of alteration minerals from lode margins to wall rock. B Metasomatic exchange of elements between fluid conduit (lode vein) and wall rocks. Scale is the same for both A and B. This is an example from the Glenorchy scheelite deposit in New Zealand (After Paterson 1986)

change in colouration of the schist from grey to greenish and black, and there is a decrease, or loss, of some of the metamorphic minerals such as actinolite and epidote, while calcite, pyrite, arsenopyrite and kaolinite are added. Figure 15.22 illustrates these mineralogical and geochemical additions and subtractions, associated with the ingress of the hydrothermal fluids in the shear zone at Glenorchy.

The Round Hill Au-W deposit (Lee et al. 1989) is part of the Macraes Flat field. This deposit is characterised by Au-scheelite-arsenopyrite-pyrite within shear zone-hosted quartz veins. Lee and coworkers recognised three styles of mineralisation, namely: (1) fissure lode quartz veins and deformed stockworks within silicified shear zones; (2) low strain stockworks; and (3) disseminated sulphide and weak stockworks. The highest W and Au grades are associated with the first style and the estimated reserves of the deposit are 6.7×10^6 tonnes at 2.67 g/t Au, with a cutoff grade of 1 g/t Au.

The Endeavour Inlet Sb-Au deposit consists of a series of irregular quartz veins, arranged en echelon within a northeast-trending shear zone. The main feature of this deposit is that it is vertically zoned with an upper stibnite-rich zone grading down – approximately 200 m below – into an arsenopyrite-pyrite-marcasite-Au zone (Pirajno 1979).

In the Mount Cook region, thin quartz-calcite veinlets in the Alpine Schist contain traces of scheelite, sulphides and native Au. These occurrences have been studied by Craw et al. (1987), Craw and Koons (1988, 1989) and Johnstone et al. (1990). The mineralised localities are distributed close to the Alpine Fault and within amphibolite and greenschist facies domains (Fig.15.23C). Johnstone et al. (1990) have noted that older Au-bearing veins are confined to areas of greenschist facies, while younger veins containing base metals – mainly Cu – occur closer to the Fault and are restricted to amphibolite facies rocks. Gold, arsenopyrite and scheelite occur in quartz-calcite ± epidote ± actinolite veinlets which are from 1 to 10 cm thick and contain Au where they cut graphitic horizons. Craw et al. (1987) recognised at least three types of veinlets. One contains rhombohedral calcite and prismatic quartz crystals with minor chlorite. The second type, with Au and sulphides, consists of massive quartz-calcite veinlets in which the grain size of the mineral components is much smaller than in the first type. The wall rocks show some degree of hydrothermal alteration with arsenopyrite grains, biotite and chlorite. The third type of veins consists of open-space filling with quartz, platy calcite and adularia, and are associated with the second type. Fluid inclusions studies indicate that these three types represent precipitation products from fluids of different character. Type 1 veins were probably formed from H_2O-CO_2 fluids at 270°C and 2–3 km of depth; type 2 veins were formed from fluids with temperatures in excess of 320°C, which may have mixed with cooler and less saline fluids, while type 3 veins were formed from low salinity fluids which boiled at about 240°C.

On the basis of geological, fluid inclusion data and stable isotope systematics, Craw and coworkers have devised an interesting model (Fig. 15.23) to explain the Alpine Schist occurrences (see Craw and Koons 1989 for details). In their model, the authors take cognizance of the tectonic environment, in which the Southern Alps represent a major zone of collision between the Pacific and the Indo-Australian plates. This has resulted in considerable uplift, and the presence of a thermal
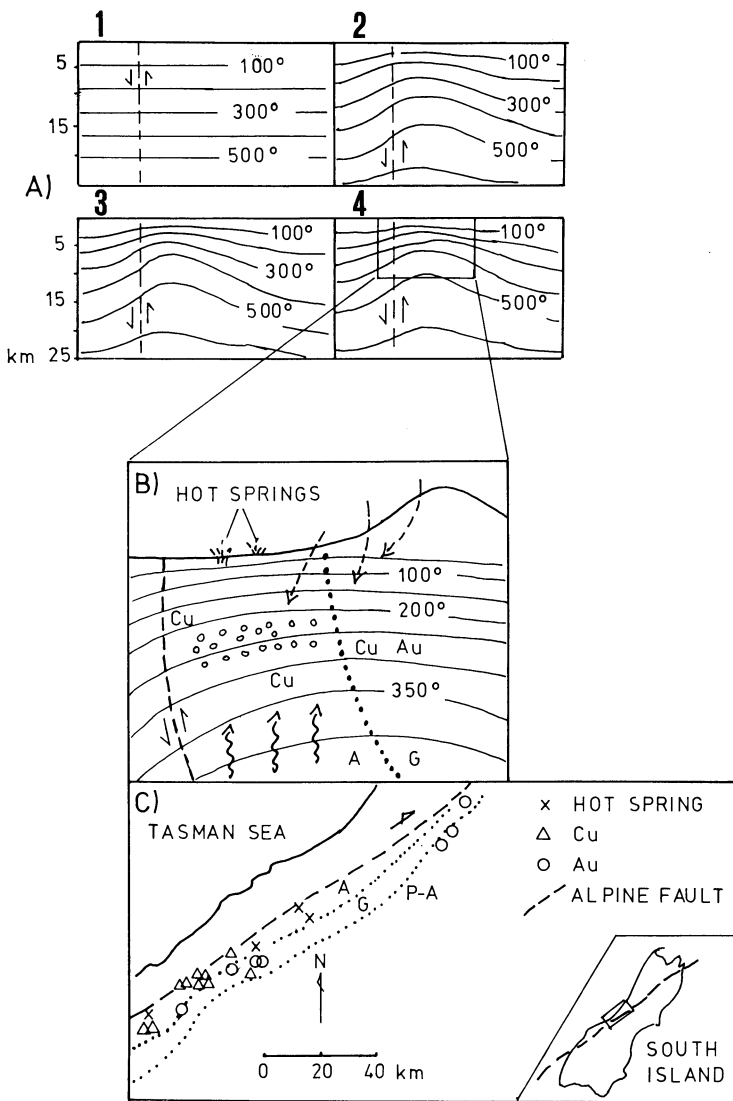
Fig. 15.23. A Modelled thermal profiles at t = 0 Ma *1*, t = 2 Ma *2*, t = 3 Ma *3* and t = 4 Ma *4*. After 4 Ma the 300 and 400 °C isotherms are raised to within 5–10 km of the surface on the upthrown block (*right hand side* of the fault, shown by *dashed lines*). Isothermal intervals are 100 °C. B Portion of thermal profiles (outlined in A) showing movement of metamorphic fluids (*wavy arrows*, H_2O-CO_2) and meteoric fluids (*dashed arrows*). Boiling zone illustrated by bubbles; dotted line represents the boundary between amphibolite facies *A* and greenschist facies *G* domains. Au and sulphides are preferentially precipitated within the greenschist facies domain, while Cu sulphides are deposited closer to the fault within amphibolite facies rocks. Cu sulphide assemblages of amphibolite facies include chalcopyrite + pyrrhotite, and chalcopyrite + pyrite as late veins; in the greenschist facies domain ore assemblages are mainly chalcopyrite + pyrite, bornite + hematite and Au + pyrrhotite or pyrite. C Map showing location of veinlet occurrences and hot springs. *A* Amphibolite facies; *G* greenschist facies; *P-A* pumpellyite-actinolite facies. A and B are after Craw and Koons (1988, 1989), C is after Craw and Koons (1988, 1989) and Johnstone et al. (1990)

anomaly, manifested by the numeorus CO_2-bearing hot springs which issue along and close to the Alpine Fault. The authors point out that during uplift – with rates greater than 3 mm yr^{-1} and continuing today – temperatures as high as 300°C can occur at depths of less than 5 km. This would constitute a very powerful heat engine, for which no igneous activity, at least in the immediate vicinity, is needed. This system is capable of activating hydrothermal convection for a longer time than shallow igneous intrusions, which tend to decay much more rapidly as heat sources. Another key facet of the model is that uplift occurs at a rate greater than that at which rocks cool by conduction. In this way a complex hydrothermal convective system develops at depths ranging from 1 to 6 km. In this system, rising and hot metamorphic fluids leach out Au and base metals (e.g. Cu), boil and mix in the upper levels with descending cool meteoric fluids. This hydrothermal activity results in the formation of various generations of veins and veinlets as discussed above. Type 1 veinlets would be the product of CO_2-rich metamorphic fluids. Type 2 veinlets result from mixing of these fluids with cooler metoric waters, while those of type 3 result from possible boiling as indicated by the presence of platy calcite and adularia. The earlier generations of quartz-calcite veinlets contain Au and scheelite, are probably the result of hot and reduced fluids of metamorphic origin, and are restricted to domains of greenschist facies. Greenschist facies rocks, in the opinion of the authors, are particularly ideal as a source of fluids because of their chlorite content, which would provide abundant H_2O on devolitilisation. The hydrothermal fluid thus formed is capable of leaching Au, As and W from the surrounding lithologies, some of which might include bands of metavolcanics and manganifer-ous cherts. In the original metamorphic model of Henley et al. (1976) these rocks may constitute protore lithologies for Au and W respectively. A later generation of veinlets, emplaced at shallower levels and closer to the Fault, contain mainly Cu sulphides, and result from cooler and more oxidised fluids (Fig. 15.23B).

The implications of the model of Craw and coworkers are important because it highlights the role of uplifted segments of crust at collision plate boundaries – past and present – in the localisation of mesothermal ore deposits and their derived placers. In these regions thermal anomalies are associated with the rise of isotherms (hot lower crust) due to rapid uplift, which in the Southern Alps is estimated at between 8 and 10 mm yr^{-1}. In the light of fluid inclusion and stable isotope data – as demonstrated by Craw and Koons (1988, 1989) – it is reasonable to assume that at least two sources of fluids are involved. One source is in that sector of the crust where sedimentary packages are being deformed and metamorphosed to release H_2O-CO_2-rich fluids. Waters of meteoric origin constitute the other source; they are able to penetrate deep into the crust due to the inherent intense deformation associated with the collisional boundaries. Thus, young mountain ranges, formed at collision boundaries, are prime targets for both mesothermal lodes and placer deposits. The major challenge facing the exploration geologist is to recognise these targets in older terranes, in situations where they may have been preserved from erosion.

15.5.3 The Juneau Gold Belt, Southeast Alaska

Mesothermal lode gold systems, known as the Juneau gold belt, or Alaska-Juneau and Treadwell systems, occur in southeast Alaska, from which approximately 217 000 kg Au have been won, representing about 75% of the total state production (Light et al. 1990). This brief review is derived from Goldfarb et al. (1988, 1989) and Light et al (1990).

The gold belt occurs along the western flank of the Coast batholith, is spatially associated with the north-northwest-trending Coast Range megalineament, and it comprises five major Au districts, which from northwest to southeast are: (1) Berners Bay; (2) Eagle River; (3) Alaska-Juneau and Treadwell; (4) Snettisham; (5) Windham Bay. The auriferous quartz lodes of the gold belt occur in an accretionary continental margin setting, in which regional metamorphism prograes eastward from prehnite-pumpellyite facies to greenschist facies, within which is the Coast Range Megalineament, to amphibolite facies towards the Coast batholith. The gold belt is situated within the greenschist facies domain (e.g. Treadwell system) and at the greenschist-amphibolote facies boundary (e.g. Alaska-Juneau system).

The belt is characterised by a sequence of Jurassic to Tertiary age, comprising volcanics and metasediments including carbonaceous phyllites, biotite schist, chlorite schist with minor marble and calc-silicates. In the Alaska-Juneau area the metasediments are intruded by numerous sills or lenses of amphibolites, ranging in size from a few centimetres up to 300 m wide and 3 km long. The metamorphic petrology of these mafic rocks is suggestive of protoliths of gabbroic composition. In the mineralised areas there are numerous faults which parallel the foliation or the compositional layering. The Au lodes post-date peak metamorphism, have K-Ar ages of approximately 55 Ma, and the mineralisation occurs as networks of fissure veins and stockwork systems. The Alaska-Juneau system extends along the strike for approximately 6 km to depths in excess of 700 m. The system consists of numerous quartz veins and veinlets usually less than 1 m thick and 50 m long, and containing less than 5% sulphides, which are represented by pyrrhotite, galena, pyrite, chalcopyrite, arsenopyrite with some intergrown Au. Native Ag, pyrargyrite and tetrahedrite are present in some localities. The veins are surrounded by broad haloes of hydrothermal alteration, characterised by Fe-carbonate $\pm$ biotite $\pm$ sericite $\pm$ pyrite $\pm$ tourmaline. A paragenetic study of one orebody indicates that Au is late with respect to the sulphides and the gangue (quartz + ankerite). At the Treadwell mine the mineralisation occurs as disseminations and stockworks within a fractured diorite body. The stockworks consist of 2–3-cm-thick quartz and calcite veinlets containing pyrite, chalcopyrite and Au. Around these veinlets the diorite is albitised and sulphidised. In the Berners Bay district fissure veins and stockworks cut a diorite intrusion and here too, the veins are less than 1 m thick with a few percent sulphides and a wallrock alteration characterised by sericite + albite + Fe-carbonate + pyrite, all within approximately 1 m of the veins.

Fluid inclusion studies have revealed that the ore fluids contained about 5 wt.% NaCl equivalent, with deposition of Au having occurred at temperatures above 250° C and at depths of less than 5 km. The ore fluids contained CO_2, CH_4, N_2 and H_2S. The presence of H_2S is regarded as important for the dissolution and transport of

Au as sulphide complexes, while CO_2 is believed to have derived from decarbonation of pelitic rocks during metamorphism.

15.6 Mineral Deposits Formed by Multistage Ore Genesis

In this section we consider three classes of mineral deposits, for which geological evidence indicates that they may have formed through multistage genetic processes, including metamorphic devolitilisation. In the first, we examine unconformity-related U deposits whose origin, although as yet not clear, may have involved several mineralising episodes, one of which could have been metamorphism. The second – of recent discovery – includes skarn-like and vein deposits containing Au, Cu, Bi and W, whose precise nature and origin are as yet to be determined, although geological evidence indicates that they may have formed through stages of metamorphism and magmatism. Third and last, we take a "metamorphic", if highly controversial, look at the conglomerate-hosted Au-U deposits of the Witwatersrand basin in South Africa.

15.6.1 Unconformity-Related U Deposits

The time-bound character of U mineralisation (Fig. 5.6) is a striking feature, whose precise reason is not known. If we consider only hydrothermal U concentrations in the Earth's crust, then the physico-chemical conditions for the dissolution, transport in solution and deposition of U must have been particularly favourable at least twice in the geological history of our planet. The first time between 1.8 and 1.2 Ga, when the majority of unconformity-related U deposits were formed, and the second time between the Permian and the Jurassic when sandstone-hosted (or roll front) U mineralisation was formed. Some of the constraints on the physico-chemical conditions of U transport and deposition are related to the geochemical cycle and behaviour of the lithophile element U. There are many works that deal with this topic, but for a short and comprehensive review the reader is referred to Nash et al. (1981). By and large, the chemical behaviour of U can be explained in terms of its two most common ions, the reduced form U^{6+} and the oxidised form U^{4+}. All U ions tend to combine with oxygen even in the reduced form (e.g. uraninite UO_2), and this tendency allows the U ions to form soluble complexes with anions such as CO_3^{2-}, PO_4^{-4}, SO_4^{-4} and AsO_4^{-3}. Therefore redox conditions are important in determining the environment of solution and precipitation of U-bearing minerals. In passing from its hexavalent state to the tetravalent state – oxidising to reducing conditions – and in the presence of metal ions, such as Na^+, K^+, Ca^{2+}, Cu^{2+}, the solubility of the uranyl complexes decreases and very complex U salts are precipitated (Nash et al. 1981).

Unconformity-related U deposits constitute a major source of U (Table 15.3). Most of these deposits occur in the Proterozoic terranes of the province of Saskatchewan in Canada and the Northern Territory in Australia. Works that

Table 15.3. Estimated reserves of unconformity-related U deposits in the East Alligator River area, Northern territory, Australia (After Hegge and Rowntree 1978; Wilde et al. 1989)

Deposit	10^6 Tonnes	U_3O_8 (%)	Tonnes U_3O_8
Jabiluka 1	1.3	0.25	3000
Jabiluka 2	52	0.39	207000
Ranger 1	37.7	0.27	100350
Nabarlek	0.4	2.37	9500

describe this class of U mineralisation include the collection of papers edited by Ferguson and Goleby (1980), Evans (1986), and the review by Marmont (1987). A special issue of Economic Geology (1978) is devoted to uranium geology, which includes a number of papers on this type of mineralisation.

Apart from their age, one of the chief characteristic of unconformity-related U deposits – as the name implies – is that they tend to occur close to a major unconformity. The mineralisation therefore is located both above and below a paleosurface, separating predominantly metasedimentary sequences of Proterozoic age, deposited on Archean basement. Evidence indicates that the unconformity acts as a redox front between oxidising (above) and reducing (below) domains (Wilde et al. 1989). Another important feature is that the mineralisation is spatially associated with fractures, reverse and normal faults.

In Canada, host lithologies include feldspathic gneisses, graphitic pelitic gneisses, biotite schist and metamorphic rocks resembling pegmatites and named anatexites. Minor intercalations of calc-silicates, amphibolites and marbles are present in the sequence. These rocks probably represent a sequence of basinal sediments of shelf and/or lagoonal facies with clastics and pelitic rocks. The unconformity at the top of the sequence is characterised by the presence of a regolith, up to 200 m thick, which consists of chloritic material, illite, kaolinite and hematite. This regolith is interpreted to be either a paleosol or a paleolateritic horizon. The Athabasca Group, of Upper Proterozoic age, overlies the regolith and is made up of hematite-rich sediments, mainly sandstone, siltstone and mudstone intercalated with conglomeratic beds. Some of the important Canadian deposits include Key Lake (Dahlkamp 1978), Rabbit Lake (Hoeve and Sibbald 1978) and McClean (Wallis et al. 1986). In the Alligator Rivers region in the Northern Territory (Australia), the mineralisation is hosted by the Cahill Formation, which is part of a thick Early Proterozoic sequence of metapelitic, metaevaporites and carbonate sediments, resting on the Nanambu Complex of Lower Proterozoic-Archean age. The metamorphic grade of these rocks ranges from amphibolite to granulite facies. The Cahill Formation is approximately 3000 m thick and is divided into two members: a lower member comprising Mg-rich marble, graphitic schist and gneisses and an upper member comprising quartz-biotite schist and gneiss. The Kombolgie Formation, of Mid-Proterozoic age (Carpentarian), unconformably overlies the Lower Proterozoic rocks and is the equivalent of the Athabasca Group rocks in Canada. The main Australian deposits are Koongarra, Ranger, Jabiluka
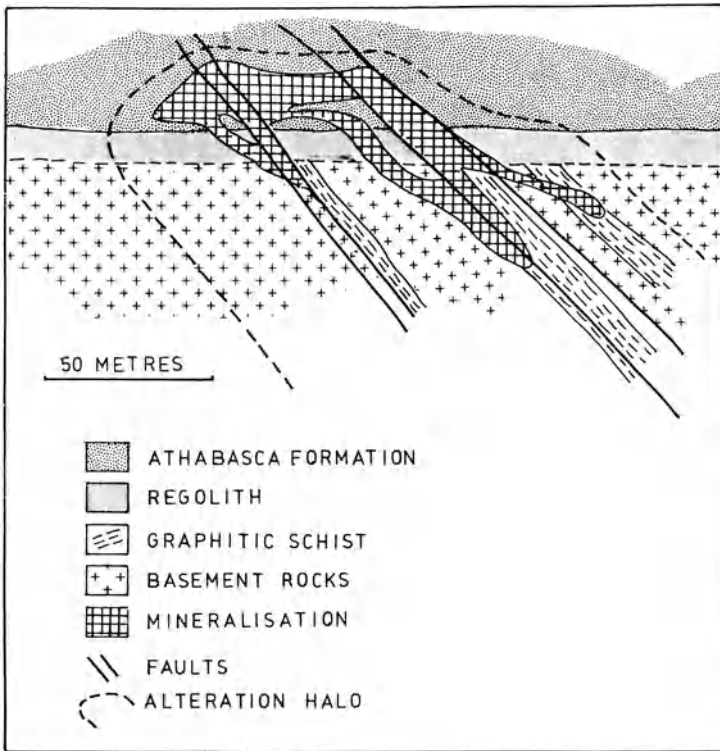
Fig. 15.24. Cross-section of an idealised unconformity-related U deposit in Canada (After Hoeve and Sibbald 1978)

and Nabarlek (see Table 15.3 for estimated U reserves). Details of their geology, mineralisation and alteration can be found in Hegge and Rowntree (1978), Wilde and Wall (1987), Wilde et al. (1989) and Nutt (1989).

Figure 15.24 illustrates an idealised cross-section of a Canadian unconformity-related U deposit. Mineralisation styles include pods, lenses, veins and fault breccias, which form orebodies whose geometry is generally wedge-like, tabular or elongate (Marmont 1987). The deposits are characterised by an element association which, in addition to U, also includes Ni, Co, Ag, Mo, As, Se, Te, Au and platinum group elements (PGE). The Jabiluka 2 orebody, for example, contains a reserve of 8100 kg of Au at an average grade of 10 g/t, with significant amounts of Pd (Wilde et al. 1989). Platinum is present in the Nabarek deposit, while Ni and As occur in appreciable quantities at Key Lake (Canada). The chief U minerals are uraninite and pitchblende, accompanied by other ore minerals such as pyrite, arsenopyrite, chalcopyrite, galena, molybdenite, rammelsbergite, gersfordite and millerite. Gold and PGE may occur as tellurides. Secondary minerals may also be present and include coffinite, uranophane, torbenite and autunite. Hydrothermal alteration is prominent and forms haloes of up to a few hundred metres around the orebodies (Fig. 15.24). Alteration consists of chloritisation, argillisation, dolomitisation and

silicification. It is important to point out that this hydrothermal alteration may extend into the rocks above the unconformity. Usually chlorite is the most abundant alteration mineral, but sericite, tourmaline, apatite and hematite are also part of the alteration assemblage. At Nabarlek, where the mineralisation is hosted by amphibolite and pelitic schist, hydrothermal alteration is very extensive – up to 1 km from the main mineralised conduit – and it consists of concentric haloes (Wilde and Wall 1987). The outer halo, which is clearly fracture-controlled, is defined by silicified and hornblende-deficient lithologies. In the amphibolite and schist rocks, hornblende is replaced by chlorite and sericite, biotite by chlorite and rutile and plagioclase by sericite. Other alteration minerals are quartz, dolomite and prehnite. The inner zones are characterised by removal of quartz, presence of pervasive hematite, clay-sized chlorite and sericite. Detailed studies of alteration mineralogy at Jabiluka by Nutt (1989) revealed that sericitic alteration preceded chloritisation, and that there are several types and generations of chlorite. The presence of this mineral is indicative of intense Mg metasomatism which is associated with the U mineralisation. This association is not clear but it is possible that chlorite may have lowered the pH of the solutions destabilising U carbonate or phosphorous U complexes causing precipitation of reduced U minerals. Mg metasomatism and the release of H^+ ions are therefore invoked as the main agents for causing chloritisation and a concomitant depletion in silica. Dolomite is thought to have provided much of the Mg needed to form the chlorite. The reaction, as proposed by Nutt (1989) is:

quartz + muscovite + K-feldspar + Mg^{2+} + H_2O →

Mg-chlorite + K^+ + H_4SiO_4 + H^+.
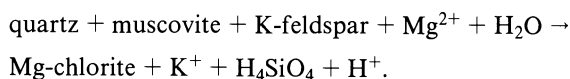
Fluid inclusion and isotopic studies (Pagel et al. 1980; Ypma and Fuzikawa 1980) indicate at least two types of fluids. One is of possible metamorphic origin (Cahill Formation) containing CO_2 and with homogenisation temperatures of approximately 350°C. The other (ore and alteration minerals) indicate highly saline fluids, containing 20–30 wt.% $CaCl_2$, 5–10 wt.% $MgCl_2$ and 10–20 wt.% NaCl. Homogenisation temperatures are estimated to range from 200 to 180°C. According to recent modelling by Wilde et al. (1989) the mineralising fluids are characterised by acidic and oxidising solutions with a high Cl content.

Genetic Models

Genetic models which attempt to explain the origin of unconformity-related U deposits regard the role of U-enriched lithologies (protore), such as the Archean basement, to be an important factor in processes of ore genesis. Two basic models are considered. In one, the source of the mineralising fluids is thought to be metamorphic or magmatic or a combination of both, while in the other, the fluids are believed to be of diagenetic or meteoric derivation. The available data suggest that the diagenetic-hydrothermal hypothesis is perhaps more likely. However, it must be remembered that the mineralisation event, or events, appear to extend over a large time span, during which tectonism metamorphism and magmatism took place. In the Alligator Rivers deposits, for example, U-Pb isotopic dating indicates
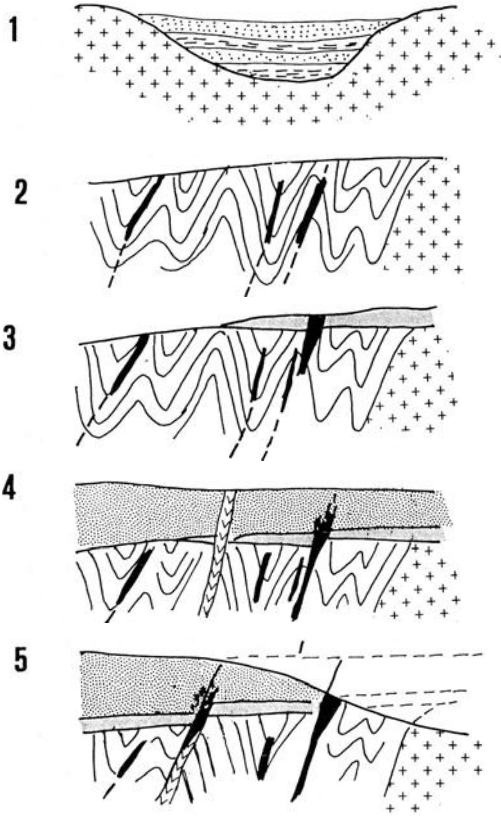
Fig. 15.25. Schematic representation of the development stages of unconformity-related U deposits, as exemplified by the Key Lake deposit in Canada. Stage 1 Sedimentation of U-rich sediments into a basin (ca. 2200–1900 Ma); stage 2 folding and metamorphism with formation of mesothermal vein U mineralisation (ca. 1900–1800 Ma); stage 3 uplift and erosion with formation of a regolith, weathering and leaching with re-concentration of U in structural traps (ca. 1800–1350 Ma); stage 4 sedimentation of cover rocks (Athabasca Formation), diagenetic processes, and dyke intrusion (ca. 1350–1000 Ma); continuing uplift and erosion accompanied by several cycles of U redistribution along structural traps above and below the unconformity (1000–200 Ma); stage 5 erosion and partial destruction of orebodies ca. 200 Ma to Recent). *Symbols* for Athabasca Formation, regolith and basement same as in Fig. 15.24; a dyke is indicated by *v's*; mineralisation is shown in *black*; drawings not to scale (After Hoeve and Sibbald 1978)

mineralisation ages ranging from 1737 $\pm$ 20 Ma to 1437 $\pm$ 40 Ma, metamorphism and magmatism have been dated from approximately 1900 to 1690 Ma, while the Kombolgie Formation has a Rb-Sr date of 1648 $\pm$ 29 Ma (Nutt 1989). Another important factor to bear in mind is that oxygen would have been required to move U in solution, and once in solution a reducing environment is needed to precipitate U. This redox front was probably present in the vicinity of the unconformity (e.g. graphitic schist). For these reasons a multistage genetic model is perhaps more feasible. A possible scenario of multistage ore genesis is illustrated in Fig. 15.25. The stages depicted in this figure can be summarised as follows. Mobilisation and pre-

concentration of uraninite occurred during deformation and metamorphism as vein-type deposits in both Archean basement and cover rocks of the Early Proterozoic. Uplift and erosion followed, with weathering and leaching occurring in places, and with re-deposition of U ore into structural traps within a regolith. Sedimentation above the unconformity (Athabasca and Kombolgie sequences) took place and was accompanied by generation of oxygenated diagenetic brines, which remobilised U and associated metals, carried them along structural zones and re-distributed the mineralisation at a redox front, represented by the unconformity.

15.6.2 Au Mineralisation in the Central Zone of the Damara Orogen, Namibia

The tectonic evolution of the Damara orogen and related hydrothermal mineralisation are discussed in some detail in Chapter 7 (Figs. 7.4 and 7.5). Attention is drawn to the possibility that a number of hydrothermal deposits, in the Damara Orogen, could have formed through a series of mineralising episodes related to fluids generated during deformation, metamorphism and granite emplacement. Although little laboratory data are available to constrain the timing and relationship between the variuos mineralising episodes, empirical geological evidence suggests that both metamorphism and magmatism may have played important roles (Pirajno et al. 1990, 1991).

Au and base metal mineralisation in the Central Zone of the orogen occurs in syngenetic massive sulphides associated with mafic volcanics, in shear-zone hosted deposits, turbidite-hosted deposits and mineralisation of skarn affinity. The latter is stratabound, marble-hosted, and contains Au with minor Cu, W and Bi. This deposit type is exemplified by the Navachab mine, discovered in 1985 and soon to come into production. This deposit, which, together with a number of similar types is located in the Karibib district, contains approximately 10×10^6 tonnes at an average grade of 2.8 g/t Au (Pirajno and Jacob, in press).

The known Au mineralisation of the Karibib district is generally located in major northeast-trending anticlinoria and hosted within marble units at different stratigraphic levels (Karibib and Okawayo Formations, Badenhorst 1987). Apart from the Navachab deposit, other Au occurrences in the district are Onguati, Brown Mountain, Otjimboyo and Habis (Pirajno et al. 1990; Pirajno and Jacob, in press). The geology of the Karibib district (Central Zone of the Damara Orogen) is characterised by 2000-Ma old granitic basement rocks, which are unconformably overlain by late-Proterozoic clastic sedimentary rocks of the Nosib Group. These, in turn, are overlain by the Chuos Formation mixtites, which – as mentioned in Chapter 7 – represent an important marker horizon within the Damara lithostratigraphy. The mixite rocks are followed upward by a thick sequence of alternating pelitic schist, calc-silicates layers and marbles. The sequence is subdivided into a number of formations, which from bottom to top are: Spes Bona Formation, Okawayo Formation, Oberwasser Formation, Karibib Formation, Onguati Formation and Kuiseb Formation (Badenhorst 1987). Intercalated within these sedimentary rocks, and at various levels, are lenses of orthoamphibolites. These orthoamphibolites are derived from the metamorphism of mafic volcanics,

including pillow lavas, vent agglomerates, ash-flow tuffs and bedded pyroclastics. The marble units, which host the Au mineralisation, are grouped into the stratigraphically lower Okawayo Formation and the upper Karibib Formation, each overlain and underlain by pelitic schist with calc-silicate bands. At least three major phases of deformation and low-pressure-high-temperature metamorphism affected the rocks in the Karibib district. Metamorphism is of amphibolite facies with temperatures of around 500°C and pressures of approximately 3.3 kb (Pirajno and Jacob, in press). There is field and petrological evidence that metamorphic fluid flow was responsible for regional-scale metasomatism of the marble layers, as is further explained later. The metamorphic fluid flow was probably caused by the dehydration and loss of H_2O from the pelitic rocks.

The Navachab deposit is hosted in marble and calc-silicate rocks of the Karibib and Okawayo Formations (Swakop Group). The mineralisation consists of millimetre to centimetre thick quartz veins, locally forming stockworks which, although deformed, are transgressive to the strata and to deformation fabrics. The vein margins are characterised by selvages of diopside, tremolite, garnet and phlogopite. Au occurs in free form and associated with native Bi, scheelite and sulphides, which include pyrite, pyrrhotite and chalcopyrite.

At Onguati and Brown Mountain hydrothermal vein mineralisation occurs at a higher stratigraphic level (Karibib Formation) than at Navachab. At these localities, and the nearby Western Workings, the mineralisation occurs as quartz veins in marble with spectacular pinch-and-swell structures. These veins can be up to 200 m long and 2 m thick. Gold is associated with sulphides which are represented by pyrrhotite, chalcopyrite, pyrite and arsenopyrite. This mineralisation is generally located within fractures in the vein material, along vein margins and as off-shoots into the marble wall rocks. The Au content ranges from 0.1 to 6 g/t but peak values of 80 g/t have been recorded locally. High Au values correlate with high concentrations of Cu (1000 ppm), Bi (300 ppm) and W (1400 ppm). This metal association is similar to that at Navachab, although the development of skarn assemblages is not the same because at Onguati anhydrous minerals (garnet and diopside) do not occur and this is taken to indicate a more distal facies. At Brown Mountain the mineralised quartz veins are much thinner and they tend to form stockwork zones. At this locality the main sulphide phases are pyrrhotite and arsenopyrite with minor chalcopyrite, Au is erratically distributed and attains values of up to 0.4 g/t. Pirajno et al. (1990, 1991) explain the different skarn mineralogy and the element associations in terms of a metal zonation from a proximal facies at Navachab, with Cu-Au-Bi-W and anhydrous skarn minerals, to As-Cu-Au plus a hydrous skarn mineralogy (tremolite) at Onguati and Brown Mountain-Western Workings. This zonation can be interpreted as a function of the distance from the source of the hydrothermal fluids and the level of erosion which has exposed the mineralised localities.

The mineralisation is spatially associated with extensive regional-selective skarn development (tremolite mainly) and dolomitisation of calcitic marble units. Dolomitisation is a later event, as it resulted in the destruction of the sedimentary structures, tectonic fabrics and the tremolite minerals. Ongoing studies in the region by the present author and coworkers suggest that the Navachab-type mineralisation

was formed through more than one stage of ore genesis. This involved the generation and movement of CO_2-rich metamorphic fluids, during phases of folding and prograde metamorphism of the volcano-sedimentary sequence of the Swakop Group. High-temperature prograde metamorphism marmorised the carbonate rocks and produced extensive zones of coarse- to fine-grained tremolite sheaves in impure calcareous units. As metamorphism progressed, CO_2-rich fluids, derived from devolitilisation reactions in the sedimentary pile, passed through the marble rocks inducing dolomitisation. According to Ferry (1984) pelitic rocks, apart from H_2O, may also contain up to 4–5% carbonates and devolitilisation causes decarbonation with loss of CO_2. Alternatively, decarbonation occurs when H_2O is flushed through the carbonate rocks with liberation of large quantities of CO_2. A possible reaction to account for the widespread dolomitisation and destruction of the tremolitic marbles is (Winkler 1976):

$$1\,tremolite + 3\,calcite + 7\,CO_2 \rightarrow 5\,dolomite + 8\,quartz + H_2O.$$
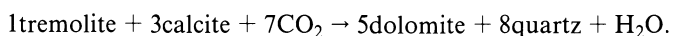
These fluids leached metals such as Au and Cu, out of protore lithologies (e.g. mafic volcanics or chemical sediments known to contain up to 900 ppb Au). At a later stage, syn- to post-tectonic emplacement of granitic rocks resulted in the inception of hydrothermal convection cells associated with the cooling plutons, and subsequent re-distribution of the mineralisation in the present skarn-like vein systems.

Metasomatism of marble rocks and skarn development as a result of fluids released during prograde regional metamorphism have been postulated by Yardley et al. (1991) for metapelitic and marble rocks of late Proterozoic age in western Ireland. The lithostratigraphy, deformation and metamorphism of this area are similar to those of the Karibib district. Studies of stable isotopic variations carried out by Yardley et al. (1991) corroborate their findings and lend support to the field and petrological evidence provided by Pirajno et al. (1990, 1991) for the Namibian situation.

15.6.3 The Possible Role of Metamorphic Fluids in the Origin of the Witwatersrand Goldfields, South Africa

The world-famous Witwatersrand goldfields would not normally be discussed in a book concerned with hydrothermal mineral deposits, owing to their, generally recognised, sedimentary (placer) origin. Results of recent investigations, however, have cast some doubts on the established sedimentary model, and in this section we take a brief look at a new, but controversial, theory for the origin of the Witwatersrand mineralisation.

Readers unfamiliar with the geology of the Witwatersrand area should consult Tankard et al. (1982), the many references therein and a special issue of the South African Journal of Geology (1990). For the present purpose, it is important to remark that the Witwatersrand fields are by far the largest producers in the world, with a total of approximately 40 000 tonnes of Au. The Witwatersrand Supergroup comprises a thick sequence of argillaceous, arenaceous and rudaceous rocks

subdivided into a Lower and Upper Witwatersrand. Most of the mineralisation is located in the conglomerates of the Upper Witwatersrand. The Witwatersrand element association is typified by Au-U-Fe-C, in the form of native Au, uraninite, pyrite and complex organic matter, whose mixture with uraninite is known as thucolite. In its long history of development of geological ideas, the Witwatersrand mineralisation seemed to have settled on to placer, or a modified-placer, origin for its Au and U mineralisation. The placer model is effectively well corroborated by sedimentological constraints, and is well championed and illustrated by W.E.L. Minter of the University of Cape Town (see Tankard et al. 1982). Also, as mentioned in Chapter 5, the form of pyrite (detrital or buckshot pyrite), and the reduced form of U, uraninite, have been used as evidence for an oxygen-deficient atmosphere during the Archean and Early Proterozoic. The source regions of the Au and U are widely debated and range from greenstone belt Au, to Au-enriched hydrothermally altered granites, to high level epithermal volcanic systems.

In a series of papers Phillips (1987, 1988), Phillips and Myers (1989) and Phillips et al. (1989, 1990) challenged the established placer theory for the Witwatersrand goldfields, presenting arguments for a possible role of fluids of metamorphic derivation for the origin of the Au and U mineralisation. However, the validity of these arguments is disputed by Minter (1989) and Reimer and Mossman (1990). Phillips and coworkers reason that since regional greenschist facies metamorphism affected the Witwatersrand sedimentary basin, hydrothermal fluids must have been generated and must have resulted in some fundamental changes in the mineralogy of the sedimentary packages. Indeed, evidence for metamorphic mineral assemblages is compelling, as shown by the presence and co-existence of pyrophyllite-chloritoid-chlorite-muscovite-quartz-rutile-tourmaline-pyrite in the argillaceous lithologies and the conglomerates of the Upper Witwatersrand. Phillips and coworkers, therefore, propose an epigenetic replacement model, whereby Au-S-bearing metamorphic fluids interacted and selectively replaced Fe-C-rich mineral phases, such as pisolites, ferricretes and carbon seams, accumulated by sedimentary processes in fluvial systems. This replacement would have preferentially occurred along unconformities, because they were the sites where Fe-C phases would have preferentially accumulated. These Fe-C rich lithologies are particularly concentrated along the basin margins, where stacked unconformities are situated. These sites are regarded as particularly favourable, because, according to the authors, this is where the hydrothermal fluid flow would have been most effective. The round pyrite grains, so typical of the Witwatersrand, are attributed to pyrite replacement of Fe pisolites on the unconformity surfaces by processes of sulfidisation during burial. The high Fe contents of these sedimentary traps favoured the destabilisation of sulphide-Au complexes and the precipitation of native Au and pyrite at these locales, whereas the association of C, U and hydrocarbons is attributed to redox controls (see section on unconformity-related U deposits). Original hydrocarbon material formed during diagenesis could have interacted with U-bearing fluids to precipitate uraninite. The authors argue, inter alia, that the metamorphic-replacement model eliminates the problem of the source area for both Au and U.

It is interesting to note that after more than 100 years of Witwatersrand geology, ideas on the genesis of the goldfields have turned full circle, from epigenetic models

to placer models and back to epigenesis. The lesson is that all models, conceptual or genetic, are far from perfect. Scientific enquiry thrives on the questioning of established ideas, and as new information is continuously gained, through the work of geoscientists from all over the world, old concepts must be re-appraised and new ones considered.

References

Anhaeusser C R (1976a) The geology of the Sheba Hills area of the Barberton Mountain Land, South Africa, with particular reference to the Eureka Syncline. Trans Geol Soc S Afr 79:253–280
Anhaeusser C R (1976b) The nature and ditsribution of Archean gold mineralization in Southern Africa. Minerals Sci Eng 8:46–84
Anhaeusser C R (1981) Barberton Excursion Guide Book. Geocongress '81 Geol Soc S Afr
Anhaeusser C R (ed) (1983) Contributions to the geology of the Barberton Mountain Land. National geodynamics programme. Geol Soc S Afr Spec Publ No 9
Anhaeusser C R (1984) The nature and distribution of Archaean gold mineralization in the Barberton Mountain Land. In: Abstr Archean Gold – Barberton Centenary Symp, Barberton
Anhaeusser C R, Viljoen M J (1986) Archean metallogeny of Southern Africa. In: Anhaeusser C R, Maske S (eds) Mineral Deposits of southern Africa, vol 1. Geol Soc S Afr, pp 33–42
Anhaeusser C R, Wilson J F (1981) The granitic-gneiss greenstone shield of Southern Africa. In: Hunter D R (ed) Precambrian in the southern hemisphere. Developments in Precambrian geology 2. Elsevier, Amsterdam, pp 423–499
Ash J P, Tyler N (1986) Preliminary investigation of fluid inclusions in the Pilgrim's Rest goldfield, Eastern Transvaal. Econ Geol Res Unit, Inf Circ 180, Univ Witwatersrand
Barley M E, Eisenlohr B N, Groves D I, Perring C S, Vearncombe J R (1989) Late Archean convergent margin tectonics and mineralization: a new look at the Norseman-Wiluna belt, Western Australia. Geology 17:826–829
Badenhorst F P (1987) Lithostratigraphy of the Damara Sequence in the Omaruru area of the northern Central Zone of the Damara orogen and a proposed correlation across the Omaruru Lineament. Comm Geol Surv SW Afr/Namibia 3:3–8
Binns R A, Eames J C (1989) Geochemistry of wall rocks at the Clunes gold deposit, Victoria. Econ Geol Monogr 6:310–3(19
Bishop D G (1972) Progressive metamorphism from the prehnite-pumpellyite to greenschist facies in the Dansey Pass area, New Zealand. Geol Soc Am Bull 83:3177–3(197
Boulter C A, Fotios M G, Phillips G N (1987) The Golden Mile, Kalgoorlie: a giant gold deposit localized in ductile shear zones by structurally induced infiltration of an auriferous metamorphic fluid. Econ Geol 82:1661–1678
Bonnemaison M, Marcoux E (1990) Auriferous mineralization in some shear zones: a three-stage model of metallogenesis. Mineral Depos 25:96–104
Boyle R W (1979) The geochemistry of gold and its deposits. Geol Surv Can Bull 280:584 pp
Brathwaite R L (1988) The tectonic setting and control of gold deposits in New Zealand. In: Bicentennial Gold '88. Geol Soc Aust Abstr Ser 22:191–196
Brathwaite R L, Pirajno F (in prep) Metallogenic Map of New Zealand. NZ Geol Surv Bull, Govt Printer
Burrows D R, Spooner E T C (1987) Generation of a magmatic H_2O-CO_2 fluid enriched in Mo Au and W within an Archean sodic granodiorite stock, Mink Lake, northwestern Ontario. Econ Geol 82:1931–1957
Burrows D R, Spooner E T C (1989) Relationships between Archean goldquartz vein-shear zone mineralization and igneous intrusions in the Val d'Or and Timmins areas, Abitibi Subprovince, Canada. Econ Geol Monogr 6:424–444
Burrows D R, Wood P C, Spooner E T C (1986) Carbon isotope evidence for a magmatic origin for Archean gold-quartz vein ore deposits. Nature (London) 321:851–854

Cameron E M, Hattori K (1985) The Hemlo gold deposit, Ontario: a geochemical and isotopic study. Geochim Cosmochim Acta 49:2041–2050

Cameron E M Hattori K (1987) Archean gold mineralization and oxidised hydrothermal fluids. Econ Geol 82:1177–1191

Colvine A C (1989) An empirical model for the formation of Archean gold deposits: products of final cratonization of the Superior Province, Canada. Econ Geol Monogr 6:37–53

Condie K C (1981) Archean greenstone belts. Elsevier, Amsterdam, 434 pp

Coney P J (1980) Cordilleran metamorphic core complexes: an overview. Mem Geol Soc Am 153:7–31

Corfu F, Muir T L (1989) The Hemlo-Heron Bay greenstone belt and Hemlo Au-Mo deposit, Superior Province, Ontario, Canada. 2. Timing of metamorphism, alteration and Au mineralization from titanite, rutile and monazite U-Pb geochronology. Chem Geol Isotope Geoscie Sec 79:201–223

Cox S F, Etheridge M A, Wall V J (1986) The role of fluids in syntectonic mass transport, and the location of metamorphic vein-type ore deposits. Ore Geol Rev 2:65–86

Craw D, Koons P O (1988) Tectonically induced gold mineralisation adjacent to major fault zones. In: Bicentennial Gold '88. Geol Soc Aust Abst Ser 22:338–343

Craw D, Koons P O (1989) Tectonically induced hydrothermal activity and gold mineralisation adjacent to major fault zones. Econ Geol Monogr 6:471–478

Craw D, Rattenbury M S, Johnstone R D (1987) Structural geology and vein mineralisation in the Callery River headwaters, Southern Alps, New Zealand. NZ J Geol Geophys 30:273–286

Dahlkamp F J (1978) Geologic appraisal of the Key Lake U-Ni deposits, Northern Saskatchewan. Econ Geol 73:1430–1449

De Ronde C E J, Kamo S, Davis D W, de Witt M J, Spooner E T C (1991) Field, geochemical and U-Pb isotopic constraints from hypabyssal felsic intrusions within the Barberton greenstone belt, South Africa: Implications for tectonics and the timing of gold mineralization. Precambrian Res 49:261–280

De Witt M J (1982) Gliding and overthrust nappe tectonics in the Barberton greenstone belt. J Struct Geol 4:117–136

De Witt M J (1983) Notes on a preliminary 1:25000 geological map of the southern part of the Barberton greenstone belt. Geol Soc S Afr Spec Publ 9:185–187

Duane M J, de Witt M J (1988) Pb-Zn ore deposits of the northern Caledonides: Products of continental-scale fluid mixing and tectonic expulsion during continental collision. Geology 16:999–1002

Dubé B, Guha J, Rocheleau M (1987) Alteration patterns related to gold mineralization and their relation to CO_2/H_2O ratios. Mineral Petrol 37:267–291

Economic Geology (ed) (1978) Special Issue devoted to Uranium Geology. Vol 73, 8

Eisenlhor B N, Groves D I Partington G A (1989) Crustal-scale shear zones and their significance to Archean gold mineralization in Western Australia. Mineral Depos 24:1–8

Etheridge M A, Wall V J, Vernon R H (1983) The role of the fluid phase during regional metamorphism and deformation. J Metamorph Geol 1:205–226

Etheridge M A, Wall V J, Cox F S, Vernon R H (1984) High fluid pressure during regional metamorphism and deformation: implications for mass transport and deformation mechanisms. J Geophys Res 89:4344–4388

Evans E L (ed) (1986) Uranium deposits of Canada. Can Inst Min Metall Spec Vol 33

Ferguson J, Goleby A B (eds) (1980) Uranium in the Pine Creek geosyncline. IAEA Vienna

Ferry J M (1983) regional metamorphism of the Vassalboro Formation, south-central Maine, USA: a case study of the role of fluid in metamorphic petrogenesis. J Geol Soc London 140:551–576

Ferry J M (1984) A biotite isograd in South-Central Maine, USA: mineral reactions, fluid transfer, and heat transfer. J Petrol 25:871–893

Frimmel H E (1990) Ore mineralization in platform sediments – passive or active continental margin features ? In: Abstr Geocongress '90 Cape Town. Geol Soc S Afr, pp 165–168

Fripp R E P (1976) Stratabound gold deposits in Archean banded iron formation, Rhodesia. Econ Geol 71:58–75

Fyfe W S, Kerrich R (1984) Gold: natural concentration processes. In: Foster R P (ed) Gold '82: The geology, geochemistry and genesis of gold deposits. Geol Soc Zimbabwe Spec Publ 1:199–127

Fyfe W S, Price N J, Thompson A B (1978) Fluids in the Earth's crust. Elsevier, Amsterdam, 383 pp

Fyon J A, Troop D G, Marmont S, Macdonald A J (1989) Introduction of gold into Archean crust, Superior Province, Ontario – Coupling between mantle-initiated magmatism and lower crustal thermal maturation. Econ Geol Monogr 6:479–490

Gee R D (1979) Structure and tectonic style of the Western Australian shield. Tectonophysics 58:327–369

Glover J E, Groves D I (eds) (1981) Archaean geology. In: 2nd Int Symp Geol Soc Aust Spec Publ 7, 515 pp

Goldfarb R J, Leach D L, Pickthorn W J, Paterson C J (1988) Origin of lode gold deposits of the Juneau gold belt, southeastern Alaska. Geology 16:440–443

Goldfarb R J, Leach D L, Rose S C, Landis G P (1989) Fluid inclusion geochemistry of gold-bearing quartz veins of the Juneau gold belt, southeastern Alaska: implications for ore genesis. Econ Geol Monogr 6:363–375

Goldie R (1985) The sinters of the Ohaki and Champagne pools, New Zealand: possible modern analogues of the Hemlo gold deposits, Northern Ontario. Geosci Can 12:60–64

Green D, Milkereit B, Mayrand L J, Ludden R, Hubert C, Jackson S L, Sutcliffe M, West G F, Verpaelst P, Simard A (1990) Deep structure of an Archaean greenstone terrane. Nature (London) 344:327–330

Groves D I, Batt W D (1984) Spatial and temporal variations of Archean metallogenic associations in terms of evolution of granite-greenstone terrains with particular emphasis on the Western Australian shield. In: Kröner A, Hanson G H, Goodwin A M (eds) Archaean Geochemistry. Springer, Berlin, Heidelberg, New York, pp 73–98

Groves D I, Phillips G N (1987) The genesis and tectonic control on Archean gold deposits – A metamorphic replacement model. Ore Geol Rev 2:287–322

Groves D I, Phillips G N, Ho S E, Houston S M, Standing C A (1987) Craton-scale distribution of Archean greenstone gold deposits; predictive capacity of the metamorphic model. Econ Geol 82:2045–2058

Groves D I, Barley M E, Ho S E (1989) Nature, genesis, and tectonic setting of mesothermal gold mineralization in the Yilgarn Block, Western Australia. Econ Geol Monogr 6:71–85

Groves D I, Foster R P (1991) Archaean lode gold deposits. In: Foster R P (ed) Gold metallogeny and exploration. Blackie, Glasgow, London, pp 63–103

Guilbert J M, Park C F (1986) The geology of ore deposits. Freeman, San Francisco, New York, 985 pp

Haack U, Heinrichs H, Bones N, Schneider A (1984) Loss of metals from pelites during regional metamorphism. Contrib Mineral Petrol 85:116–132

Harris D C (1986) Mineralogy and geochemistry of the main Hemlo gold deposit, Hemlo, Ontario, Canada. In: Macdonald A J (ed) Proc Gold '86, Montreal, pp 297–310

Harris D C (1989) The mineralogy and geochemistry of the Hemlo gold deposit, Ontario. Geol Surv Can Rep 38:88 pp

Hegge M R, Rowntree J C (1978) Geologic setting and concepts on the origin of uranium deposits in the East Alligator River region, N.T., Australia. Econ Geol 73:1420–1429

Henley R W (1973) solubility of gold in hydrothermal chloride solutions. Chem Geol 11:73–87

Henley R W, Adams J (1979) On the evolution of giant gold placers. Trans Inst Min Metall 88:B41–B50

Henley R W, Norris R J, Paterson C J (1976) Multistage ore genesis in the New Zealand geosyncline, a history of post-metamorphic lode emplacement. Mineral Depos 11:180–186

Hodgson C J (1989) The structure of shear-related, vein-type gold deposits: a review. Ore Geol Rev 4:231–273

Hodgson C J, Hamilton J V (1989) Gold mineralization in the Abitibi greenstone belt: End-stage results of Archean collisional tectonics? Econ Geol Monogr 6:86–100

Hoeve J, Sibbald T I I (1978) On the genesis of Rabbit Lake and other unconformity-type uranium deposit in Northern Saskatchewan, Canada Econ Geol 73:1450–1473

Höll R, Maucher A, Westenberger H (1972) Synsedimentary-diagenetic ore fabrics in the strata- and time-bound scheelite deposits of Kleinarltal and Felbertal in the Eastern Alps. Mineral Depos 7:217–226

Hugon H (1986) The Hemlo gold deposit, Ontario, Canada: A central portion of a large scale, wide zone of heterogeneous ductile shear. In: Macdonald A J (ed) Proc Gold '86, Montreal, pp 379–387

Hutton C O, Turner F J (1936) Metamorphic rocks in northwest Otago. Trans R Soc NZ 65:405–406

Jemielita R A, Davis D W, Krogh T E (1990) U-Pb evidence for Abitibi gold mineralization postdating greenstone magmatism and metamorphism .Nature (London) 346:831–834

Johnstone R D, Craw D, Rattenbury M S (1990) Southern Alps Cu-Au hydrothermal system, Westland, New Zealand. Mineral Depos 25:118–125

Keays R R (1984) Archean gold deposits and their source rocks: the upper mantle connection. In: Foster R P (ed) Gold '82: The geology, geochemistry and genesis of gold deposits. Geol Soc Zimbabwe Spec Publ 1:17–51

Keays R R (1987) Principles of mobilization (dissolution) of metals in mafic and ultramafic rocks. The role of immiscible magmatic sulphides in the generation of hydrothermal gold and volcanogenic massive sulphide deposits. Ore Geol Rev 2:47–63

Keppie D J, Boyle R W, Haynes S J (eds) (1986) Turbidite-hosted gold deposits. Geol Ass Can Spec Pap 32:186 pp

Kerrich R (1986) Fluid transport in lineaments. Phil Trans R Soc London Ser A 317:219–251

Kerrich R, Fryer B J (19790 Archaean precious-metal hydrothermal systems, Dome Mine, Abitibi greenstone belt. II. REE and oxygen isotope relations. Can J Earth Sci 16:440–458

Kerrich R, Fryer B J (1981) The separation of rare elements from abundant base metals in Archean lode gold deposits: implications of low water/rock source regions. Econ Geol 76:160–166

Kerrich R, Fyfe W S (1981) The gold-carbonate association: source of CO_2 and CO_2-fixation reactions in Archaean lode deposits. Chem Geol 33:265–294

Kerrich R, Wyman D (1990) Geodynamic setting of mesothermal gold deposits: An association with accretionary tectonic regimes. Geology 18:882–885

Kuhns R J, Kennedy P, Cooper P, Brown P, Mackie B, Kusins R, Friesen R, (1986) Geology and mineralization associated with the Golden Giant deposit, Hemlo, Ontario, Canada. In: Macdonald A J (ed) Proc Gold '86, Montreal, pp 327–339

Landefeld L A (1988) The geology of the Mother Lode Gold Belt, Sierra Nevada foothills metamorphic belt, California. In: Bicentennial Gold '88. Geol Soc Aus Abstr Series 22:167–172

Landefeld L A, Silberman M L (1987) Geology and geochemistry of the Mother Lode Gold Belt, California, compared with Archean lode gold deposits. In: Johnson J L (ed) Bulk mineable precious metal deposits of the Western U.S. Guidebook for field trips. Geol Soc Nev, Reno, pp 213–222

Langseth M G, Moore C J (1990a) Introduction to special section on the role of fluids in sediment accretion, deformation, diagenesis and metamorphism in subduction zones. J Geophys Res 95:8737–8741

Langseth M G, Moore C J (1990b) Fluids in accretionary prisms. EOS Am Geophys Un 71:245–247

Lee M C, Batt W D, Robinson P C (1989) The Round-Hill gold-scheelite deposit, Macraes Flat, Otago, New Zealand. Australas Inst Min Metall Monogr 13. Parkville, Victoria, pp 173–180

Leach D L, Landis G P, Hofstra A H (1988) Metamorphic origin of the Coeur d'Alene base- and precious metal-veins in the Belt Basin, Idaho and Montana. Geology, 16:122–125

Light T D, Brew D A, Ashley R P (1990) The Alaska-Juneau Treadwell lode gold systems, southeastern Alaska. US Geol Surv Bull 1857:D27–D36

Louw D R, Byerly G R, Ransom B, Land B, Nocita B W (1985) Stratigraphioc and sedimentological evidence bearing on structural repetition in early Archean rocks of the Barberton greenstone belt, South Africa. Precambrian Res 27:165–186

Marmont S (1987) Unconformity-type uranium deposits Ore deposit models 13. Geosci Can 14:219–229

Mawer C K (1986) The bedding-concordant gold-quartz veins of the Meguma Group, Nova Scotia. Geol Ass Can Spec Pap 32:135–148

Minter W E L (1989) Problems with the placer model for Witwatersrand gold (Comment on paper by Phillips et al (1988). Geology 16:1153–1154

Muff R, Saager R (1979) Metallogenic interpretations from a mineragraphic and geostatistic study of antimony ores of the Murchison greenstone belt. Geol Soc S Afr Spec Publ 5:167–179

Muir T L (1982a) Geology of the Hemlo area, District of Thunder Bay. Ont Geol Surv Rep 217:65 pp

Muir T L (1982b) Geology of the Heron Bay area, District of Thunder Bay. Ont Geol Surv Rep 218:89 pp

Muir T L, Elliott C G, Corfu F (1988) The tectono-stratigraphic setting of the Hemlo Au-Mo deposit, Ontario, Canada. In: Bicentennial Gold '88. Geol Soc Aust Abstr Series 23:95–97

Mutch A R (1969) The scheelite resources of the Glenorchy District, West Otago. NZ Geol Surv Rep 40:68 pp

Nash J T, Granger H C, Adams S S (1981) Geology and concepts of genesis of important types of uranium deposits. Econ Geol 75th Anniv Vol, pp 63–116

Nesbitt B E (1988) Gold deposit continuum: A genetic model for lode Au mineralization in the continental crust. Geology 16:1044–1048

Nesbitt B E, Muehlenbachs K (1989) Evidence for ore formation from evolved meteoric water. Econ Geol Monogr 6:553–563

Nesbitt B E, Murowchick J B, Muehlenbachs K (1986) Dual origin of lode gold deposits in the Canadian Cordillera. Geology 14:506–509

Norris R J, Henley R W (1976) Dewatering of a metamorphic pile. Geology 80:333–336

Nutt C J (1989) Chloritization and associated alteration at the Jabiluka unconformity-type uranium deposit, Northern Territory, Australia. Can Mineral 27:41–58

Oliver J (1986) Fluids expelled tectonically from orogenic belts: Their role in hydrocarbon migration and other geological phenomena. Geology 14:99–102

Pagel M, Poty B, Sheppard S M F (1980) Contribution to some Saskatchewan uranium deposits mainly from fluid inclusion and isotope data. In: Ferguson J, Goleby A B (eds) Uranium in the Pine Creek Geosyncline. IAEA, Vienna, pp 639–654

Paris I, Stanistreet I G, Hughes M J (1985) Cherts of the Barberton greenstone belt interpreted as products of submarine exhalative activity. J Geol 93:111–129

Paterson C J (1986) Controls on gold and tungsten mineralization in metamorphic-hydrothermal systems, Otago, New Zealand. Geol Ass Can Spec Pap 32:25–39

Paterson C J, Rankin P C (1979) Trace element distribution in the schist surrounding a quartz-scheelite lode, Glenorchy, New Zealand. NZ J Geol Geophys 22:329–338

Pearton T N (1978) The geology and geochemistry of the Monarch orebody and environs, Murchison Range, northeast Transvaal. Geol Soc S Afr Spec Publ 4:77–86

Pearton T N (1979) A geochemical investigation of the carbonate and associated rocks on the Monarch antimony mine, Murchison Range. Geol Soc S Afr Spec Publ 5:159–166

Perring C S, Barley M E, Cassidy K F, Groves D I, McNaughton N J, Rock N M S, Bettenay L F, Golding S D, Hallberg J A (1989) The association of linear orogenic belts, mantle-crust magmatism, and Archean gold mineralization in the eastern Yilgarn Block of Western Australia. Econ Geol Monogr 6:571–584

Phillips G N (1985) Interpretation of Big Bell/Hemlo-type gold deposits: Precursor, metamorphism, melting and genetic constraints. Trans Geol Soc S Afr 88:159–173

Phillips G N (1986) Geology and alteration in the Golden Mile, Kalgoorlie. Econ Geol 81:779–808

Phillips G N (1987) Metamorphism of the Witwatersrand gold fields: conditions during peak metamorphism. J Metamorph Geol 5:307–322

Phillips G N (1988) Widespread fluid infiltration during metamorphism of the Witwatersrand gold fields: generation of chloritoid and pyrophyllite. J Metamorph Geol 6:311–332

Phillips G N, Myers R E (1989) The Witwatersrand gold fields: Part II. An origin for Witwatersrand gold during metamorphism and associated alteration. Econ Geol Monogr 6:598–608

Phillips G N, Myers R E, Law J D M, Bailey A C, Cadle A B, Beneke S D, Giusti L (1989) The Witwatersrand gold fields: Part I. Postdepositional history, synsedimentary processes, and gold distribution. Econ Geol Monogr 6:585–597

Phillips G N, Law J D M, Myers R E (1990) The role of fluids in the evolution of the Witwatersrand basin. S Afr J Geol 93:54–69

Pirajno F (1979) Geology, geochemistry and mineralisation of the Endeavour Inlet antimony-gold prospect, Marlborough Sounds, New Zealand. NZ J Geol Geophys 22:227–237

Pirajno F, Jacob R E (in press) Gold mineralisation in the intracontinental branch of the Damara Orogen, Namibia: a preliminary survey. J Afr Earth Scie 13

Pirajno F, Jacob R E, Petzel V F W (1990) Marble-hosted sulphide and gold mineralisation at Onguati-Brown Mountain, Southern Central Zone of the Damara Orogen, Namibia. In: Abstr Geocongress '90 Cape Town. Geol Soc S Afr, pp 443–446

Pirajno F, Jacob R E, Petzel V W F (1991) Distal skarn-type gold mineralization in the Central Zone of the Damara orogen, Namibia. In: Ladeira E A (ed) Proc Brazil '91, Belo Horizonte. Balkema, Rotterdam, pp 95–100

Ramsay J G (1980) Shear zone geometry: a review. J Struct Geol 2:83–100

Reimer T O, Mossman D J (1990) The Witwatersrand controversy revisited. Econ Geol 85:337–343

Robert F (1990) Dating old gold deposits. Nature (London) 346:792–793

Rock N M S (1987) The nature and origin of lamprophyres: An overview. Geol Soc London Spec Publ 30:191–226

Rock N M S, Groves D I (1988) Do lamprophyres carry gold as well as diamonds? Nature (London) 332:253–255

Rock N M S, Groves D I, Perring C S (1988) Gold, porphyries and lamprophyres: a new genetic model. In: Bicentennial Gold '88. Geol Soc Aust Abstr Ser 22:307–312

Rock N M S, Groves D I, Perring C S, Golding S D (1989) Gold, lamprophyres, and porphyries: what does their association mean? Econ Geol Monogr 6:609–625

Rossiter R D (1988) The geology of Fairview gold mine, Barberton, South Africa. In: Bicentennial Gold '88. Geol Soc Aust Abstr Ser 23:116–118

Sandiford M, Keays R R (1986) Structural and tectonic constraints on the origin of gold deposits in the Ballarat Salte Belt, Victoria. Geol Ass Can Spec Pap 32:15–24

Seward T M (1973) Thio complexes of gold and the transport of gold in hydrothermal ore solutions. Geochim Cosmochim Acta 37:379–399

Seward T M (1984) The transport and deposition of gold in hydrothermal systems. In: Foster R P (ed) Gold '82. The geology, geochemistry and genesis of gold deposits. Geol Soc Zimbabwe Spec Publ 1:165–181

Seward T M (1989) The hydrothermal chemistry of gold and its implications for ore formation: boiling and conductive cooling as examples. Econ Geol Monogr 6:398–404

Seward T M (1991) The hydrothermal geochemistry of gold. In: Foster R P (ed) Gold metallogeny and exploration. Blackie, Glasgow, London, pp 137–62

Sheppard S M F (1986) Characterization and isotopic variations in natural waters. Reviews in mineralogy, vol 16. Min Soc Am, pp 165–183

Sighinolfi G P, Santos A M (1976) Geochemistry of gold in Archean granulite facies terranes. Chem Geol 17:113–123

Smith H S, O'Neil J R, Erlank A J (1984) Oxygen isotope compositions of minerals and rocks and chemical alteration patterns in pillow lavas from the Barberton greenstone belt, South Africa. In: Kröner A, Hansen G N, Goodwin A M (eds) Archaean Geochemistry. Springer, Berlin, Heidelberg, New York, pp 115–137

South African Journal of Geology (ed) (1990) Special issue on the origin and evolution of the Witwatersrand Basin and its mineralization. Econ Geol Res Unit, Dep Geol, Univ Witwatersrand, Johannesburg. S Afr J Geol 93, 1

Storey M, Mahoney J J, Kroenke L W, Saunders A D (1991) Are oceanic plateaus sites of komatiite formation? Geology 19:376–379

Tankard A J, Erikson K A, Hobday D R, Hunter D R, Minter W E L (1982) Crustal evolution of southern Africa – 3.8 billion years of earth history. Springer, Berlin, Heidelberg, 523 pp

Taylor H P (1979) Oxygen and hydrogen isotope relationships in hydrothermal mineral deposits. In: Barnes H L (ed) Geochemistry of hydrothermal ore deposits, 2nd edn. John Wiley & Sons, New York, pp 236–277

Tomich S A (1974) A new look at Kalgoorlie Golden Mile geology. Proc Australas Inst Min Metall 251:27–35

Tomich S A (1986) An outline of the economic geology of Kalgoorlie, Western Australia. Trans Geol Soc S Afr 89:35–55

Tomlison K M, Wilson C J L, Hazeldene R, Lohe E M (1988) Structural control on gold mineralization at Walhalla, Victoria. Aust J Earth Scie 35:421–444

Torgersen T (1990) Crustal scale fluid transport – magnitude and mechanisms. EOS Am Geophys Un 71:11–13

Travis G A, Woodall R, Bartram G D (1971) The geology of the Kalgoorlie goldfield. Geol Soc Aust Spec Publ 3:175–190

Turner F J (1935) Metamorphism of the Te Anau Series in the region northwest of Lake Wakatipu. Trans R Soc NZ 65:329–349

Tyler N (1986) The origin of gold mineralzation in the Pilgrim's Rest goldfield, Eastern Transvaal. Econ Geol Res Unit, Inf Circ 179 Univ Witwatersrand, Johannesburg

Valiant R I, Bradbrook C J (1986) Relationship between stratigraphy, faults and gold deposits, Page-Williams Mine, Ontario, Canada. In: Macdonald A J (Ed) Proc Gold '86, Montreal, pp 355–361

Van der Berg M A (1984) The geological setting of gold mineralisation at the Sheba Mine. In: Abstr Archean Gold. Barberton Centenary Symp, Barberton

Viljoen M J (1979) The geology and geochemistry of the Antimony Line in the United Jack complex, Murchison range. Geol Soc S Afr Spec Publ 5:133–158

Viljoen M J, Viljoen R P (1969a) The geology and geochemistry of the lower ultramafic unit of the Onverwacht group and a proposed new class of igneous rocks. Geol Soc S Afr Spec Publ 2:55–86

Viljoen M J, Viljoen R P (1969b) An introduction to the geology of the Barberton granite-greenstone terrain. Geol Soc S Afr Spec Publ 2:9–28

Viljoen M J, Van Vuuren C J J, Pearton T N, Minnitt R C A, Muff R, Cilliers P (1978) The regional geological setting of mineralization in the Murchison range with particular reference to antimony. Geol Soc S Afr Spec Publ 4:55–86

Walford P, Stephens J, Skrecky G, Barnett R (1986) The geology of the "A" zone, Page-Williams Mine, Hemlo, Ontario, Canada. In: Macdonald A J (ed) Proc Gold '86, Montreal, pp 362–378

Wallis R H, Saracoglu N, Brummer J J, Golightly J P (1986) The geology of the McClean uranium deposits, northern Saskatchewan In: Evans E L (ed) Uranium deposits of Canada. Can Inst Min Metall Spec Vol 33:193–217

Watchorn R B, Wilson C J L (1989) Structural setting of the gold mineralization at Stawell, Victoria, Australia. Econ Geol Monogr 6:292–309

Weir R H, Kerrich D M (1987) Mineralogic, fluid inclusion, and stable isotope studies of several gold mines in the Mother Lode, Tuolumne and Mariposa Counties, California. Econ Geol 82:328–344

Wilde A R, Wall V J (1987) Geology of the Nabarlek uranium deposit, Northern Territory, Australia. Econ Geol 82:1152–1168

Wilde A R, Bloom M S, Wall V J (1989) Transport and deposition of gold, uranium and platinum-group elements in unconformity-related uranium deposits. Econ Geol Monogr 6:637–660

Williams J G (1974) Economic Geology of New Zealand, 2nd edn. Australas Inst Min Metall Monogr 4. Parkville, Victoria, 490 pp

Windley B F (1984) The evolving continents. John Wiley & Sons, New York, 399 pp

Winkler H G F (1976) Petrogenesis of metamorphic rocks. 4th edn. Springer, Berlin, Heidelberg, New York, 334 pp

Wood P C, Burrows D R, Thomas A V, Spooner E T C (1986) The Hollinger-McIntyre Au-quartz vein system, Timmins, Ontario, Canada: geologic characteristics, fluid properties and light stable isotope geochemistry. In: MacDonald A J (ed) Proc Gold '86, Montreal, pp 56–80

Woodall R (1965) Structure of the Kalgoorlie goldfield. In: Modigan R T (ed) 8th Common Min Metall Cong Aust & NZ, vol 1. Australas Inst Min Metall, Parkville, Victoria, pp 71–79

Wyman D, Kerrich R (1989) Archean shoshonitic lamprophyres associated with Superior Province gold deposits: distribution, tectonic setting, noble metal abundances and significance for gold mineralization. Econ Geol Monogr 6:661–667

Ypma P J M, Fuzikawa K (1980) Fluid inclusion and oxygen isotope studies of the Nabarlek and Jabiluka uranium deposits, Northern Territory, Australia. In: Ferguson J, Goleby A B (eds) Uranium in the Pine Creek geosyncline. IAEA, Vienna, pp 375–395

Epilogue

In this book we have examined hydrothermal processes, the origin and nature of their products, i.e. their mineral deposits, the nature of the geological terranes and the geotectonic settings in which they occur. We have seen that these processes are essentially confined to the upper 10–15 km of the lithosphere. There are five major factors that govern hydrothermal processes and the mineral deposits that are formed by them, namely: (1) the energy source; (2) the source rock ; (3) the water (the solvent); (4) the channelways, sensu lato, which allow the movement of the solutions; and (5) the site of discharge and/or precipitation of solutes.

The ultimate energy source is the internal heat of the Earth. This is manifested by the upward movement of magmas, volcanic eruptions and by lithospheric plate motions. The tectonic setting, nature and composition of magmas dictate the nature, extent and duration of the heat source. Thus, a high-level pluton, such as a porphyry intrusion, constitutes a discrete heat source and, given enough available water, the resulting hydrothermal system is confined to the area of influence of the heat from the intrusion. On the other hand, in areas of crustal attenuation (continental rifting) a large and more diffuse heat source, such as a mantle diapir, results in high geothermal gradients over a large sector of the crust which may give rise to a number of diverse and overlapping hydrothermal systems. The same applies to mid-ocean ridges, where numerous magmatic plumes, more or less regularly distributed along the length of the oceanic rifts, transfer heat to relatively large sectors of lithosphere. Therefore, in areas of rifting, whether it be continental or oceanic, numerous and/or extensive massive sulphide and stratabound/stratiform sulphide disseminations occur, testifying to the presence of larger and more diffuse heat sources. Prograde regional metamorphism of collision zones results in wholesale dehydration of lithologies, leading to the generation of fluids and their migration through thick sections of the crust. Here, incursion of meteoric water may play an important role. Cool meteoric water can mix with the rising hot metamorphic fluids, resulting in the precipitation of solutes into the appropriate structural locales.

Source rocks provide the necessary solutes to form a hydrothermal solution. These solutes comprise elements such as S, Cl, Mg, Na, Ca, K, Cu, Pb, Zn, Au, As, Ag etc. The nature of the source rocks is clearly important in determining the type and abundance of solutes and ore elements. The availability of Cl, SO_2, H_2S, NH_4 etc. are just as important as the availability of metals, because many of these solutes, especially S and Cl, may act as ligands for metal complexes, thus enabling their transport in solution.

We know that Au mineralisation is common in the predominantly mafic Archean greenstones and in the mafic environments of ocean-floor subduction, such as the southwest Pacific with its volcanic-hosted epithermal Au and Au-rich porphyry systems. Mafic and ultramafic rocks thus seem to constitute a good source of Au. The volume of the source rocks which is available to leaching by hydrothermal solutions must be important but, again, the quantification of this parameter is not easy and still largely unknown owing, among other things, to the extreme complexity and variability of the geological terranes involved. It is reasonable to assume that if large volumes of rocks are affected by leaching, then the abundance of given elements need not be unusually high. This appears to be the case for metamorphic and mid-ocean ridge hydrothermal systems in which the fluids circulate through substantial volumes of lithosphere. However, many geoscientists feel that some specific lithologies are necessary for the supply of at least some ore elements. An often quoted example of "protore" lithologies is evaporite sequences, which would provide S, B, Cl, Na, Mg as well as metals such as W and Cu. Black shales are recognised to be a good source of U, Mo and Zn, whilst basaltic rocks supply abundant Cu. Other protores are less extensive. They may be represented by high concentrations of metals, such as Sn-rich alluvial deposits, which can be transformed into Sn-rich granitic rocks.

Metallic elements can be leached out of these protores and re-distributed elsewhere by the hydrothermal solutions. Although there is no direct proof that this phenomenon does take place, empirical evidence, and geochemical and isotopic tracing suggest that this possibility is real.

Water is the universal and most powerful solvent. Whatever the origin, its greatest abundance is within the uppermost layers of the Earth's crust, at or near the surface in fact, as oceanic, meteoric or ground water. The abundance, and indeed the role, of water exsolving from magmas, or of juvenile (not recycled) water in hydrothermal systems, must surely be subordinate to meteoric waters sensu lato. Consider, for example, the vast amount of ocean water that impregnates sediments accumulated in basins, or that which percolates down into the present-day lithosphere, and has percolated into the lithosphere throughout the geological ages. In addition, sea water is already endowed with abundant solutes – most notably NaCl – and, as such, once heated it becomes a powerful hydrothermal solution.

Permeability and the availability of channelways allow the flow of water and the migration of hydrothermal fluids in the lithosphere. Fluid flow enables the leaching out of different elements from different lithologies. Also, and equally important, fluid flow is towards regions of lower temperature and pressure, and this causes fundamental changes in the nature of the solutions and the resultant precipitation of the solutes, which are no longer stable in solution, under the continuously evolving physico-chemical conditions. Discharge, and/or a site of deposition, is where ore elements and minerals are precipitated. Hot spring discharges result in syngenetic accumulations which tend to form stratiform masses, ranging in size from a few hundred tonnes to several tens of millions of tonnes, of ore material. These mineral precipitates generally include silica (cherts), Fe and Mn oxides, and banded massive to disseminated sulphides. Subaerial discharges are markedly different from submarine hot springs. The former are generally sulphide-poor and silica- and/or

carbonate-rich, but may be enriched in a host of ore elements, most notably precious metals. Submarine hot springs, on the other hand, normally result in massive sulphide and sulphate deposition. The difference must lie primarily in the greater availability of halogens, such as Cl, which enable the complexing of metals.

Focused fluid flow through restricted channelways, such as faults or shear zones, results in mineral deposits whose shape is constrained by the geometry of the conduit. In this way epigenetic hydrothermal veins are formed. In terms of ore tonnage, they are normally of relatively small size compared to, say, sulphide disseminations in a porphyry system or a stratabound disseminated sulphide deposit. In a porphyry system, fluid flow is confined to numerous, fine and interconnecting fractures (stockwork), whereas in stratabound sulphide dissemina- tions the mineralising fluids diffuse through a network of microcracks and grain boundaries throughout an entire lithology. The size of these deposits, therefore, is correspondingly much larger and can be measured in hundreds or thousands of millions of tonnes of ore material.

Enhanced permeability of the lithosphere on a regional scale is very important for hydrothermal activity to occur. Surprisingly, this aspect is rarely considered by explorationists. As mentioned above, regional-scale permeability allows the infiltration of large quantities of water in regions of high heat flow and this allows hydrothermal processes to take place (e.g. mid ocean ridges). This tells us that, for hydrothermal activity to occur, large sectors of the lithosphere must break. Breakage of the lithosphere is greatest in areas of tectonic activity, namely at divergent and convergent plate boundaries. Uplift, hot spots, oceanic and continen- tal rifting, subduction zones, transcurrent faulting and zones of continental collision are the areas where hydrothermal activity takes place at all scales. It is in these areas, subjected to enormous stress, that the lithosphere breaks, thus allowing the influx of fluids from above and below.

The challenge facing exploration geologists is to recognise these areas in the geological record, and through the understanding of hydrothermal processes, to identify targets where significant mineral deposits might be present.

Appendix

International System (S.I.)

Length	millimetre	(mm)	0.001 m
	centimetre	(cm)	0.01 m
	metre	(m)	1
	kilometre	(km)	1000 m
Mass	gram	(g)	1
	kilogram	(kg)	1000 g
	tonne	(t)	1000 kg
Area	square metre or		
	centare	(ca)	$1m^2$
	hectare	(ha)	$10000\ m^2$
Volume	cubic centimetre	(cm^3)	$0.000001\ m^3$
	cubic metre	(m^3)	$1\ m^3$
	millilitre	(ml)	0.001 l
	litre	(l)	1 l
	kilolitre	(kl)	1000 l
Density	gram/cubic centimetre	(g/cm^3)	
	kilogram/cubic metre	(kg/m^3)	$1000\ g/1000000\ cm^3$
	tonne/cubic metre	(t/cm^3)	$1000\ kg/m^3$
Pressure	millibar	(mbar)	0.001 bar
	bar	(bar)	
	kilobar	(kb)	1000 bars
	pascal	(Pa)	1000 kilobar
	atmosphere	(atm)	1013.25 millibar
			or, 10.35 metre head of water
Temperature	degree Celsius	(°C)	
	degree Kelvin	(K)	°C + 273.15
Energy	Joule	(J)	

S.I. Unit Prefixes

n	nano	10^{-9}	0.000000001
μ	micron	10^{-6}	0.000001
m	milli	10^{-3}	0.001
c	centi	10^{-2}	0.01
		10^{-1}	0.1
		10°	1
		10^1	10
		10^2	100
k	kilo	10^3	1000
		10^4	10000
		10^5	100000
M	Mega	10^6	1000000
G	giga	10^9	1000000000

e.g. geological time:

1 ka = 1000 years
1 Ma = 1 million years
1 Ga = 1 billion years

e.g. wavelengths of the electromagnetic spectrum:

1 nm = 1 nanometre = 1 billionth of a metre
1 μm = 1 micrometre = 1 millionth of a metre

Some useful conversions

1 gram (g)	....	0.0322 ounces (troy)
		0.0353 ounces (avoirdupois)
		15.4 grains
1 kilogram (kg)	....	32.151 ounces (troy)
1 tonne (t)	....	1.102 short tons
		2204 pounds
1 litre (l)	....	0.220 U.S. gallons
		1.759 pints
		35.195 fluid ounces
1 centimetre (cm)	....	0.394 inches
1 metre (m)	....	3.28 feet; 1.093 yards
1 kilometre (km)	....	0.621 miles
1 square centimetre (cm²)	....	0.155 square inches
1 centare (m²)	....	10.76 square feet
1 hectare (ha)	....	2.471 acres
		1.16 morgen

@GEOLOGYBOOKS

1 cubic metre (m^3) .... 35.315 cubic feet
                                                       1.308 cubic yards
1 atmosphere (atm) .... 14.69 pound force/square inch
1 degree Celsius (°C) .... 0.555 (Fahrenheit $-$ 32)
1 Joule (J) .... 0.73 foot pound force

Ore Grades or Concentration of Elements in Unit Mass

1 part per billion (ppb) = 0.001 part per million (ppm)
100 ppb = 0.1 ppm
1000 ppb = 1 ppm
1 ppm = 1 gram per tonne (1 g/t) .... 0.583 pennyweight (dwt)/short ton
100 ppm = 0.01%
1000 ppm = 0.1%
10000 ppm = 1%
gram/cubic metre (g/m^3) .... 11.8 grains/cubic yard
                                                       0.49 dwt/cubic yard
1 metric carat (CM) = 0.2 g .... 3.08 grains

GEOLOGICAL SOCIETY OF AMERICA

GEOLOGIC from the Decade of Nor...

CENOZOIC

AGE (Ma)	MAGNETIC POLARITY	PERIOD	EPOCH	AGE	PICKS (Ma)
	C1	QUATER-NARY	HOLOCENE / PLEISTOCENE	CALABRIAN	0.01 / 1.6
	C2	NEOGENE	PLIOCENE L	PIACENZIAN	3.4
	C2A		PLIOCENE E	ZANCLEAN	5.3
5	C3A		MIOCENE	MESSINIAN	6.5
	C4 / C4A		MIOCENE L	TORTONIAN	
10	C5				11.2
	C5A		MIOCENE M	SERRAVALLIAN	15.1
15	C5B / C5C / C5D / C5E			LANGHIAN	16.6
20	C6 / C6A / C6B / C6C		MIOCENE E	BURDIGALIAN	21.8
	C7 / C7A			AQUITANIAN	23.7
25	C8 / C9	TERTIARY / PALEOGENE	OLIGOCENE L	CHATTIAN	
30	C10 / C11 / C12				30.0
35	C13		OLIGOCENE E	RUPELIAN	36.6
	C15 / C16 / C17		EOCENE L	PRIABONIAN	40.0
40	C18			BARTONIAN	43.6
45	C19 / C20		EOCENE M	LUTETIAN	
50	C21				52.0
55	C22 / C23 / C24		EOCENE E	YPRESIAN	57.8
60	C25 / C26		PALEOCENE L	THANETIAN	60.6
			SELANDIAN	UNNAMED	63.6
65	C27 / C28 / C29		PALEOCENE E	DANIAN	66.4

MESOZOIC

AGE (Ma)	MAGNETIC POLARITY	PERIOD	EPOCH	AGE	PICKS (Ma)
	C29 / C30 / C31 / C32	CRETACEOUS	LATE	MAASTRICHTIAN	66.4
70					74.5
80	C33			CAMPANIAN	
				SANTONIAN	84.0
				CONIACIAN	87.5
90				TURONIAN	88.5 / 91
				CENOMANIAN	97.5
100			EARLY	ALBIAN	
110					113
				APTIAN	119
120	M0 / M1 / M3 / M5		NEOCOMIAN	BARREMIAN	124
	M10			HAUTERIVIAN	131
130	M12 / M14 / M16			VALANGINIAN	138
140	M18 / M20			BERRIASIAN	144
150	M22 / M25	JURASSIC	LATE	TITHONIAN	152
	M29			KIMMERIDGIAN	156
160				OXFORDIAN	163
				CALLOVIAN	169
170			MIDDLE	BATHONIAN	176
180				BAJOCIAN	183
				AALENIAN	187
190			EARLY	TOARCIAN	193
				PLIENSBACHIAN	198
200				SINEMURIAN	204
210				HETTANGIAN	208
220		TRIASSIC	LATE	NORIAN	225
230				CARNIAN	230
			MIDDLE	LADINIAN	235
240				ANISIAN	240
			EARLY	SCYTHIAN	245

(left margin, vertical: RAPID POLARITY CHANGES)

@GEOLOGYBOOKS

Reproduced by permission of the *Geological Society of America*, Boulder, Colorado, USA

TIME SCALE
American Geology Project
© 1983, GSA

PALEOZOIC

AGE (Ma)	PERIOD	EPOCH	AGE	PICKS (Ma)	UNCERT. (m.y.)
260	PERMIAN	LATE	TATARIAN	245	20
			KAZANIAN	253	20
			UFIMIAN	258	24
			KUNGURIAN	263	22
		EARLY	ARTINSKIAN	268	12
280			SAKMARIAN		
			ASSELIAN		
300	CARBONIFEROUS	PENNSYLVANIAN / LATE	GZELIAN	286	12
			KASIMOVIAN	296	10
			MOSCOVIAN		
			BASHKIRIAN		
320				315	20
		MISSISSIPPIAN / EARLY	SERPUKHOVIAN	320	
340				333	22
			VISEAN		
360			TOURNAISIAN	352	8
	DEVONIAN	LATE	FAMMENIAN	360	10
			FRASNIAN	367	12
380		MIDDLE	GIVETIAN	374	18
			EIFELIAN	380	18
		EARLY	EMSIAN	387	28
400			SIEGENIAN	394	22
			GEDINNIAN	401	18
	SILURIAN	LATE	PRIDOLIAN	408	12
420			LUDLOVIAN	414	12
		EARLY	WENLOCKIAN	421	12
			LLANDOVERIAN	428	8
440	ORDOVICIAN	LATE	ASHGILLIAN	438	12
			CARADOCIAN	448	12
460		MIDDLE	LLANDEILAN	458	16
			LLANVIRNIAN	468	16
480		EARLY	ARENIGIAN	478	16
			TREMADOCIAN	488	20
500	CAMBRIAN	LATE	TREMPEALEAUAN	505	32
520			FRANCONIAN		
			DRESBACHIAN	523	36
		MIDDLE			
540				540	28
		EARLY			
560					
				570	

PRECAMBRIAN

AGE (Ma)	EON	ERA	BDY. AGES (Ma)
750	PROTEROZOIC	LATE	570
1000			900
1250		MIDDLE	
1500			1600
1750		EARLY	
2000			
2250			
2500			2500
2750	ARCHEAN	LATE	
3000			3000
3250		MIDDLE	3400
3500		EARLY	
3750			3800?

THE PERIODIC TABLE OF THE ELEMENTS

(Based on carbon-12)

@GEOLOGYBOOKS

n	1	2	3	4	5	6	7	8	9	10	11	12	13	14	15	16	17	18
1	1.00794 **H** 1																	4.0026 **He** 2
2	6.941 **Li** 3	9.0122 **Be** 4											10.811 **B** 5	12.011 **C** 6	14.0067 **N** 7	15.9994 **O** 8	18.9984 **F** 9	20.1797 **Ne** 10
3	22.9898 **Na** 11	24.3050 **Mg** 12											26.9815 **Al** 13	28.0855 **Si** 14	30.9738 **P** 15	32.066 **S** 16	35.4527 **Cl** 17	39.948 **Ar** 18
4	39.0983 **K** 19	40.078 **Ca** 20	44.9559 **Sc** 21	47.88 **Ti** 22	50.9415 **V** 23	51.9961 **Cr** 24	54.9381 **Mn** 25	55.847 **Fe** 26	58.9332 **Co** 27	58.69 **Ni** 28	63.546 **Cu** 29	65.39 **Zn** 30	69.723 **Ga** 31	72.61 **Ge** 32	74.9216 **As** 33	78.96 **Se** 34	79.904 **Br** 35	83.80 **Kr** 36
5	85.4678 **Rb** 37	87.62 **Sr** 38	88.9059 **Y** 39	91.224 **Zr** 40	92.9064 **Nb** 41	95.94 **Mo** 42	98.9063 **Tc** 43	101.07 **Ru** 44	102.9055 **Rh** 45	106.42 **Pd** 46	107.8682 **Ag** 47	112.411 **Cd** 48	114.82 **In** 49	118.710 **Sn** 50	121.75 **Sb** 51	127.60 **Te** 52	126.9045 **I** 53	131.29 **Xe** 54
6	132.9054 **Cs** 55	137.327 **Ba** 56	138.9055 **La** a 57	178.49 **Hf** 72	180.9479 **Ta** 73	183.85 **W** 74	186.207 **Re** 75	190.2 **Os** 76	192.22 **Ir** 77	195.08 **Pt** 78	196.9665 **Au** 79	200.59 **Hg** 80	204.3833 **Tl** 81	207.2 **Pb** 82	208.9804 **Bi** 83	208.9824 **Po** 84	209.9871 **At** 85	222.0176 **Rn** 86
7	223.0197 **Fr** 87	226.0254 **Ra** 88	227.0278 **Ac** b 89	261.1087 **Unq** 104	262.1138 **Unp** 105	263.1182 **Unh** 106	262.1229 **Uns** 107	**Uno** 108	**Une** 109									

a (n = 6)	140.115 **Ce** 58	140.9077 **Pr** 59	144.24 **Nd** 60	146.9151 **Pm** 61	150.36 **Sm** 62	151.965 **Eu** 63	157.25 **Gd** 64	158.9253 **Tb** 65	162.50 **Dy** 66	164.9303 **Ho** 67	167.26 **Er** 68	168.9342 **Tm** 69	173.04 **Yb** 70	174.967 **Lu** 71
b (n = 7)	232.0381 **Th** 90	231.0359 **Pa** 91	238.0289 **U** 92	237.0482 **Np** 93	244.0642 **Pu** 94	243.0614 **Am** 95	247.0703 **Cm** 96	247.0703 **Bk** 97	251.0786 **Cf** 98	252.0829 **Es** 99	257.0951 **Fm** 100	258.0986 **Md** 101	259.1009 **No** 102	260.1053 **Lr** 103

Reproduced by courtesy of *Inorganica Chimica Acta*

Subject Index

Page numbers in *italics* refer to citation in figures and/or tables

@GEOLOGYBOOKS